Theory of Nuclear Structure

TRIESTE LECTURES 1969

LECTURES PRESENTED
AT AN INTERNATIONAL
COURSE, TRIESTE,
7 JANUARY - 31 MARCH 1969
ORGANIZED
BY THE INTERNATIONAL
CENTRE FOR
THEORETICAL PHYSICS,
TRIESTE

INTERNATIONAL ATOMIC ENERGY AGENCY, VIENNA, 1970

THEORY OF NUCLEAR STRUCTURE:
TRIESTE LECTURES 1969

THEORY OF NUCLEAR STRUCTURE:
TRIESTE LECTURES 1969

LECTURES PRESENTED AT
AN INTERNATIONAL COURSE ON NUCLEAR THEORY
AT TRIESTE FROM 7 JANUARY TO 31 MARCH 1969
ORGANIZED BY THE
INTERNATIONAL CENTRE FOR THEORETICAL PHYSICS, TRIESTE

THE INTERNATIONAL CENTRE FOR THEORETICAL PHYSICS (ICTP) in Trieste was established by the International Atomic Energy Agency (IAEA) in 1964 under an agreement with the Italian Government, and with the assistance of the City and University of Trieste.

The IAEA and the United Nations Educational, Scientific and Cultural Organization (UNESCO) subsequently agreed to operate the Centre jointly from 1 January 1970.

Member States of both organizations participate in the work of the Centre, the main purpose of which is to foster, through training and research, the advancement of theoretical physics, with special regard to the needs of developing countries.

FOREWORD

The International Centre for Theoretical Physics has maintained an interdisciplinary character in its research and training program so far as different branches of theoretical physics are concerned. In pursuance of this aim the Centre has organized extended research courses with a comprehensive and synoptic coverage in varying disciplines. The first of these — on Plasma Physics — was held in 1964; the second in 1965 was concerned with the physics of particles; the third in 1966 covered nuclear theory; the fourth in 1967 dealt with condensed matter. The proceedings of all these courses were published by the International Atomic Energy Agency. The present volume records the proceedings of the fifth course, held from 7 January to 31 March 1969, which was concerned with the study of microscopic nuclear structure and the many-body approaches to nuclear theory.

The program of lectures was organized by Professor G. Alaga of Yugoslavia and Professor L. Fonda of Italy. The course itself and its program were originally conceived by the late Professor J. Sawicki who tragically died in an air crash in September 1968. We all missed his dynamic and passionate involvement with the subject. This book is dedicated to his memory.

Abdus Salam

EDITORIAL NOTE

CONTENTS

PART II : SELECTED TOPICS IN THE MANY-BODY DESCRIPTION
OF NUCLEI AND NUCLEAR REACTIONS

PART I

General Properties of Nucleon-Nucleon Interactions and Nuclear Structure

SECTION I

Nucleon-Nucleon Interactions

NUCLEON-NUCLEON INTERACTIONS

D.M. BRINK
Department of Theoretical Physics,
University of Oxford,
Oxford, United Kingdom

Abstract

NUCLEON-NUCLEON INTERACTIONS.
1. Introduction; 2. General symmetries of nuclear forces; 3. Nucleon-nucleon scattering;
4. Potential models.

1. INTRODUCTION

All microscopic models of nuclear structure assume that nuclei are composed of neutrons and protons, and that nuclear properties can be understood in terms of the interactions between nucleons. In this paper we discuss our present state of knowledge and understanding of the inter-nucleon interactions.

Physical laws satisfy a number of general symmetry principles which lead to well-known conservation laws such as those concerning the conservation of energy and momentum. In a nuclear system these symmetries place some restrictions on the form of the nucleon-nucleon interactions. Any model of internucleon interactions should satisfy these restrictions.

Soon after the development of accelerators in the early 1930s it was established that the forces between two protons are different from a pure Coulomb interaction, and that there is a strong interaction between neutrons and protons. Cross-sections for proton-proton and neutron-proton scattering were measured. Nucleon-nucleon scattering experiments have now been extended over a very wide range of energies and most of our quantitative information about the two-nucleon interaction comes from an analysis of these experiments.

In 1935, Yukawa made his fundamental assumption that the forces between nucleons are due to the exchange of mesons. The meson theory of nuclear forces has been developed and although there is no complete quantitative theory many qualitative features are now well understood Developments in elementary particle physics, especially the discovery of heavy mesons, have contributed to our understanding of the origin of nuclear forces.

For the purposes of investigating nuclear structure it is convenient to try to represent internucleon interactions by a potential. Various potential models for the two-nucleon interaction have been proposed and parameters in the models fitted using the results of nucleon-nucleon scattering experiments. It is interesting to know the extent to which the results of scattering experiments determine the potential.

If the potential energy V of a system of A nucleons can be written as $V = \sum_{i<j} v_{ij}$ where the term v_{ij} depends only on the co-ordinates of the i-th and j-th nucleons then one speaks of a two-body force. A contribution

$V_3 = \sum\limits_{i<j<k} v_{ijk}$ to the potential energy where each term v_{ijk} depends on the co-ordinates of three nucleons would be associated with a three-body force. In the same way one can conceive of 4-body or many-body forces. We can learn something about the two-body component of the nuclear force by studying the deuteron or nucleon-nucleon scattering. It is necessary to make experiments with more complex systems to obtain information about 3-body or many-body forces. Such experiments are difficult to interpret and at the moment we know almost nothing about the strength of the 3-body or many-body component of nuclear forces.

2. GENERAL SYMMETRIES OF NUCLEAR FORCES

We begin this section by listing the various symmetries and conservation laws which are important for nuclear forces.

i) Conservation of energy, momentum and angular momentum: These conservation laws are associated with symmetry operations of translations in time and space, and of rotations. They seem to hold exactly for nuclear systems.

ii) Galilei invariance: Nucleon-nucleon interactions should be invariant under Lorentz transformations. It is usual to discuss the structure of nuclei in a non-relativistic approximation. If this approximation is valid Lorentz invariance reduces to Galilei invariance. It requires that the interaction of two nucleons should not depend on the motion of their centre-of-mass.

iii) Conservation of parity: This conservation law is not exact. Parity is not conserved for so-called weak interactions, for example in β-decay, and weak interactions should give a small contribution to the force between nucleons. However, the "strong" part of the interaction between nucleons is expected to conserve parity and experiments testing parity selection rules suggest that the parity-violating part of the interaction is very small [1].

iv) Time reversal invariance: This symmetry leads to the principle of reciprocity in reactions. Experiments with nuclei show no evidence for violation of time reversal invariance [2].

v) Charge independence: Physically this hypothesis means that the forces between all pairs of nucleons are the same and that the masses of neutrons and protons are equal. In a mathematical formalism this is equivalent to saying that the Hamiltonian for a nuclear system can be written in terms of space and spin variables only and does not differentiate between neutrons and protons (i.e. it should be completely symmetric in these co-ordinates). Nucleon-nucleon interactions are not exactly charge-independent. The Coulomb interaction between protons violates charge independence, and there are probably small violations in the specially nuclear part of the forces between nucleons. Experiments suggest that these terms are small [3]. (The small mass difference between neutrons and protons also violates charge independence).

Charge independence in a two-nucleon system consisting of a neutron and a proton requires that the Hamiltonian should be invariant for inter-charge of the space and spin co-ordinates of the two-particles. This

exchange symmetry is important in the analysis of neutron-proton scattering.

Although some of the conservation laws mentioned above do not hold absolutely the parts of the internucleon interaction violating the laws seems to be small. The main features of nucleon-nucleon scattering, nuclear structure and reactions should be given by the parts of the nuclear force satisfying the conservation laws. The non-conserving parts of the interaction give rise to small perturbations which can be important for some specific effects.

<u>Unitarity:</u> This means that the equations for a nuclear system should conserve probability or that the nuclear Hamiltonian should be Hermitian. Unitarity restricts the general form of the nucleon-nucleon scattering.

3. NUCLEON-NUCLEON SCATTERING

Nucleon-nucleon scattering has been a subject of intensive study for many years, and most of our quantitative information about nuclear forces comes from analysis of two-nucleon scattering experiments. In these lectures we give a very brief review of the subject and for more detailed information, refer to books by Moravcsik [4] and Wilson [5], a review article by Signall [6] and original papers by MacGregor et al. [7] giving the most recent analysis of experimental data.

3.1. Consequences of conservation laws

The conservation laws listed in section 2 place restrictions on the general form of the nucleon-nucleon scattering amplitude which are important for the analysis and interpretation of scattering experiments. The general form of the scattering amplitude is discussed in the book of Moravcsik [4]. We outline the results in this section.

Galilei invariance and conservation of momentum require that the two-nucleon scattering amplitude depends only on their relative momenta $\hbar \vec{k}_i$ and $\hbar \vec{k}_f$ in the initial and final states.

Conservation of energy gives $|\vec{k}_i| = |\vec{k}_f| = k$.

The asymptotic form of the wave function for scattering from an initial spin state α to a final spin state β is

$$\psi_\beta^\alpha(\vec{r}) \sim \delta_{\alpha\beta} e^{ikz} + M_{\beta\alpha} e^{ikr}/r \qquad (3.1)$$

The scattering amplitude M is a 4×4 matrix acting on the spin co-ordinates of the two nucleons. (Each nucleon has spin $-\frac{1}{2}$, and the two nucleons together have 4 possible spin states).

If $\vec{k}_i$ and $\vec{k}_f$ are the wave vectors of relative motion in the initial and final states we can define a mutually perpendicular set of unit vectors

$$\vec{P} = \frac{\vec{k}_i + \vec{k}_f}{|\vec{k}_i + \vec{k}_f|} \; , \qquad \vec{K} = \frac{\vec{k}_i - \vec{k}_f}{|\vec{k}_i - \vec{k}_f|} \; , \qquad \vec{N} = \vec{P} \times \vec{K} \qquad (3.2)$$

And if $\vec{\sigma}_1$ are the Pauli spin matrices for the first nucleon then the 4 matrices

$$1, \quad \vec{\sigma}_1 \cdot \vec{P}, \quad \vec{\sigma}_1 \cdot \vec{K}, \quad \vec{\sigma}_1 \cdot \vec{N}$$

form a complete set of 2×2 matrices acting on the spin co-ordinates of the first nucleon. We denote these matrices by m_{10}, m_{21}, m_{12} and m_{13} to obtain a condensed notation. The direct products of matrices m_{1i} with the corresponding matrices m_{2j} for the second nucleon form a set of 16 independent 4×4 matrices $m_{1i} m_{2j}$ which act in the vector space of spin co-ordinates of the two nucleons. The most general amplitude M can be expressed as a linear combination of these 16 matrices with coefficients g_{ij} depending on $\vec{k}_i$ and $\vec{k}_f$

$$M = \sum_{jk} g_{jk}(\vec{k}_i, \vec{k}_f) \, m_{1j} \, m_{2k} \tag{3.3}$$

Each of the matrices $m_{1j} m_{2k}$ is a scalar for rotation of axes; hence, if M is rotationally invariant, the coefficients g_{jk} must be scalar functions of $\vec{k}_i$ and $\vec{k}_f$. Therefore g_{jk} can depend only on $k = |\vec{k}_i| = |\vec{k}_f|$ and the scattering angle θ defined by $\vec{k}_i \cdot \vec{k}_f = k^2 \cos \theta$, $(0 \le \theta \le \pi)$. The exchange symmetry requirement coming from charge independence gives $g_{jk} = g_{kj}$.

If we make an inversion of co-ordinates then $\vec{\sigma} \to \vec{\sigma}$, $\vec{k}_i \to -\vec{k}_i$, $\vec{k}_f \to -\vec{k}_f$, $\vec{P} \to -\vec{P}$, $\vec{K} \to -\vec{K}$, $\vec{N} \to \vec{N}$. The corresponding time reversal transformations are $\vec{\sigma} \to -\vec{\sigma}$, $\vec{k}_i \to -\vec{k}_f$, $\vec{k}_f \to -\vec{k}_i$, $\vec{P} \to -\vec{P}$, $\vec{K} \to \vec{K}$, $\vec{N} \to -\vec{N}$. The coefficients g_{jk} in Eq.(3.3) depend only on k and are invariant under time reversal and parity operations. The matrices m_{1i} and m_{2i} are either invariant or change sign under parity and time reversal. The transformation properties are shown in Table I. Requiring time reversal invariance and parity conservation excludes all terms $m_{1i} m_{2j}$ from expression (3.3) which are not invariant with respect to both operators. The most general amplitude matrix M consistent with all these restrictions is

$$M = a + ib(\vec{\sigma}_1 + \vec{\sigma}_2) \cdot \vec{N} + g(\vec{\sigma}_1 \cdot \vec{P})(\vec{\sigma}_2 \cdot \vec{P}) + h(\vec{\sigma}_1 \cdot \vec{K})(\vec{\sigma}_2 \cdot \vec{K}) + m(\vec{\sigma}_1 \cdot \vec{N})(\vec{\sigma}_2 \cdot \vec{N}) \tag{3.4}$$

where the 5 coefficients a, b, g, h, m are complex functions of k and σ_i. Hence we require 5 complex functions of energy and scattering angle to specify M completely. Unitarity gives 5 non-linear relations between these 5 complex functions [4].

TABLE I. TRANSFORMATION PROPERTIES

	$m_{\alpha 0} = 1$	$m_{\alpha 1} = \vec{\sigma}_\alpha \cdot \vec{P}$	$m_{\alpha 2} = \vec{\sigma}_\alpha \cdot \vec{K}$	$m_{\alpha 3} = \vec{\sigma}_\alpha \cdot \vec{N}$
Parity	+	-	-	+
Time reversal	+	+	⟋	+

We may conclude from this analysis that a measurement of the differential cross-section for nucleon-nucleon scattering (one real function of k and θ) can not by itself fix the 5 complex functions a, ..., m. A range of relatively complicated polarization experiments is needed. The different kinds of experiment are described by Moravcsik [4]. We only want to emphasize here that the necessity for performing complicated polarization experiments makes it difficult to determine the scattering amplitude M experimentally.

3.2. Partial-wave analysis

In an angular-momentum representation a state of relative motion of two nucleons can be written as $|k, \ell s j m_j, T, T_3\rangle$. The quantum number k is the magnitude of the wave vector of relative motion. The quantum numbers ℓ, s, j are the magnitudes of the relative orbital angular momentum, the total spin and the total angular momentum $(\vec{j} = \vec{\ell} + \vec{s})$, respectively, and m is the eigenvalue of j_z. The quantity T is the total isospin and $T_3 = (Z - N)/2$. Because of the generalized Pauli principle T = 1 states are anti-symmetric in space-spin co-ordinates, and T = 0 states are symmetric. In other words only states with T + s + 1 odd are allowed. The (p, p) and (n, n) systems have only T = 1 states, while both T = 0 and T = 1 states can occur for the (n, P) system. The first few allowed states are

$$T = 1 : \quad {}^1S_0 , \quad {}^3P_{0,1,2} \quad , {}^1D_2 , \ldots$$

$$T = 0 : \quad {}^3S_1 , \quad {}^1P_1 \quad , {}^3D_{1,2,3} , \ldots$$

One can specify the two-nucleon scattering amplitude by giving matrix elements of the scattering matrix S in the angular momentum representation.

$$\langle k, \ell s j, T | S | k, \ell' s' j, T \rangle \qquad (3.5)$$

The matrix elements of S are diagonal in k because of energy conservation, they are diagonal in j and independent of m because of conservation of angular momentum, and they are diagonal in T because of charge independence. The parity π of a state of relative motion is $\pi = (-1)^\ell$ and and conservation of parity requires that $\ell - \ell'$ is even. These restrictions together with the generalized Pauli principle give that s - s' is even and since s, s' = 0 or 1 it follows that s = s'.

In some cases there is only one state with a given j and T, e.g. ${}^1P_1$. Such a state is a simple state and has no off-diagonal matrix elements of S with other states. By unitarity the corresponding diagonal scattering matrix element is a complex number of modulus unity and can be represented by a phase shift $\delta_{\ell s j}$,

$$\langle k, \ell s j, T | S | k, \ell s j, T \rangle = \exp\{2i\delta_{\ell s j}(k)\} \qquad (3.6)$$

In other cases there are two states with the same j, and T but different $\ell = j \pm 1$. The corresponding scattering matrix is a 2×2 matrix $S_{\alpha\beta}$ where

$\alpha(\beta) = 1$ refers to the $\ell = j-1$ state and $\alpha(\beta) = 2$ to the $\ell = j+1$ state. The matrix $S_{\alpha\beta}$ is unitary $(S S^\dagger = S^\dagger S = 1)$ because of unitarity and symmetric $(S_{\alpha\beta} = S_{\beta\alpha})$ because of time reversal invariance. Three real parameters are needed to specify the components $S_{\alpha\beta}$. Two ways of introducing these parameters are by

a) $\quad S_{\alpha\beta} = \begin{pmatrix} \cos \epsilon & -\sin \epsilon \\ \sin \epsilon & \cos \epsilon \end{pmatrix} \begin{pmatrix} \exp 2 i \delta_- & 0 \\ 0 & \exp 2 i \delta_+ \end{pmatrix} \begin{pmatrix} \cos \epsilon & -\sin \epsilon \\ -\sin \epsilon & \cos \epsilon \end{pmatrix}$

b) $\quad S_{\alpha\beta} = \begin{pmatrix} \exp i \bar{\delta}_- & 0 \\ 0 & \exp i \bar{\delta}_+ \end{pmatrix} \begin{pmatrix} \cos 2 \bar{\epsilon} & \sin 2 \bar{\epsilon} \\ \sin 2 \bar{\epsilon} & \cos 2 \bar{\epsilon} \end{pmatrix} \begin{pmatrix} \exp i \bar{\delta}_- & 0 \\ 0 & \exp i \bar{\delta}_+ \end{pmatrix}$

In the representation (a) the quantities δ_- and δ_+ are eigenphases or Blatt and Biedenharn [8] phases. The quantities $\bar{\delta}_-$, $\bar{\delta}_+$ and $\bar{\epsilon}$ in the second representation (b) are called "bar" phases and mixing parameters. This representation was introduced by Stapp et al. [9] and is now used for almost all phase shift analyses of scattering experiments. It is more convenient than the eigenphase representation because Coulomb effects in (p, p) scattering can be allowed for more easily.

The Coulomb interaction between two protons is much weaker then the nuclear interaction, but it is important in proton-proton scattering because of its long range. The proton-proton S-matrix elements contain contributions from the nuclear and the Coulomb forces and the two contributions can only be separated in a simple way [9] if the WKB approximation is valid for the Coulomb field. Then the bar phase shifts can be written as a sum of nuclear and Coulomb parts, and charge independence means that the nuclear part of the bar phases and mixing parameters for (p, p) scattering are equal to the T = 1 bar phases for (n, p) scattering.

3.3. Results of phase shift analysis

A phase shift analysis of nucleon-nucleon scattering data relies on unitarity, invariance principles and the short range of the nuclear force. Phase shifts corresponding to a large relative orbited angular momentum ℓ are set at the values required by the one pion exchange model (cf. section 4) and phases with smaller ℓ are adjusted to give a best χ^2-fit to the experimental data. The pion-nucleon coupling constant is also taken as a parameter in the search procedure and the analysis gives a value for this quantity. There are over 2000 pieces of experimental data at energies below 350 MeV. The pion production threshold is at about 290 MeV and above this energy allowance must be made for a modification of the unitarity restriction. Most recent phase shifts are given by MacGregor et al. [7]. Signell evaluates the present stage of our knowledge of phase shifts in a recent review article [6]. Briefly the situation seems to be as follows:

i) The phase parameters for (p, p) scattering are well determined up to 350 MeV and even beyond. Assuming charge independence this gives the T = 1 part of the S-matrix.

ii) The (n, p) scattering data is not complete enough to be analysed by itself. If charge independence is assumed and T = 1 phase parameters are

taken from the analysis of (p, p) scattering data, then the (n, p) data can be analysed to give the T = 0 phase parameters. The T = 0 phases are less accurately determined than the T = 1 phases and the phase shifts in the $^3S_1$, $^3D_1$ states and the associated mixing parameter $\bar{\epsilon}$ are not well determined. Even the sign of $\bar{\epsilon}$ is uncertain at low energies.

iii) The best value of the OPE coupling constant is $g^2 = 14 \pm 2$ [7] in good agreement with the value found from pion-nucleon scattering experiments.

4. POTENTIAL MODELS

4.1. Isospin dependence

For the purposes of calculating nuclear properties it is convenient to try to represent the nucleon-nucleon interaction by a potential. Before discussing the general form of such a potential we look at different ways of representing the spin and isospin dependence in the case of a local central potential

$$V = U(r)\,(w + m\,P_m + b\,P_\sigma + h\,P_m\,P_\sigma) \qquad (4.1)$$

where $U(r)$ is a function of the relative separation of the two interacting nucleons. P_m and P_σ are orbital and spin exchange operators and w, m, b, h are constants. Introducing an isospin exchange operator P_τ and using the generalized Pauli principle

$$P_m\,P_\sigma\,P_\tau = -1 \qquad (4.2)$$

and the relations

$$P_m^2 = P_\sigma^2 = P_\tau^2 = 1$$

it is possible to write the interaction (4.1) as

$$V = U(r)\,(w + b\,P_\sigma - h\,P_\tau - m\,P_\sigma\,P_\tau) \qquad (4.3)$$

We may also use the relations

$$P_\sigma = \tfrac{1}{2}(1 + \vec{\sigma}_1 \cdot \vec{\sigma}_2)\,, \quad P_\tau = \tfrac{1}{2}(1 + \vec{\tau}_1 \cdot \vec{\tau}_2) \qquad (4.4)$$

to write the potential (4.1) as

$$V = U(r)\,(\alpha + \beta\,\vec{\sigma}_1 \cdot \vec{\sigma}_2 + \gamma\,\vec{\tau}_1 \cdot \vec{\tau}_2 + \delta\,(\vec{\sigma}_1 \cdot \vec{\sigma}_2)(\vec{\tau}_1 \cdot \vec{\tau}_2)) \qquad (4.5)$$

where $\alpha = w + \tfrac{1}{2}b - \tfrac{1}{2}h - \tfrac{1}{4}m$ etc. The three interactions (4.1), (4.3) and (4.5) are identical. In the form (4.1) V depends on space and spin coordinates only. The forms (4.3) and (4.5) show an explicit isospin de-

pendence. The relation (4.2) expressing the generalized Pauli principle allows one to write the same interaction in several different ways. It is always possible to write an expression for a charge-independent interaction in a way which does not show an explicit isospin dependence.

4.2. General form for the spin dependence of the two-nucleon potential

The most general form of the two-nucleon interaction potential consistent with the conservation laws listed in section 2 can be found by making a comparison with the general form (3.4) of the scattering amplitude M. We let $\vec{r}$, $\vec{p}$, $\vec{\ell}$ denote the relative position, momentum and angular momentum ($\vec{\ell} = \vec{r} \times \vec{p}$) of the two nucleons. The scalar quantities $\vec{\sigma} \cdot \vec{p}$, $\vec{\sigma} \cdot \vec{r}$, $\vec{\sigma} \cdot \vec{\ell}$ have the same transformation properties with respect to time reversal and parity as $\vec{\sigma} \cdot \vec{P}$, $\vec{\sigma} \cdot \vec{K}$, $\vec{\sigma} \cdot \vec{N}$ in sub-section 3.1. Hence the general form of V invariant, under rotation, parity, time reversal, and exchange symmetry is analogous to the form (3.4) of M:

$$V = \tfrac{1}{2} (V_1 + V_2 (\vec{\sigma}_1 + \vec{\sigma}_2) \cdot \vec{\ell} + V_3 (\vec{\sigma}_1 \cdot \vec{\ell})(\vec{\sigma}_2 \cdot \vec{\ell}) + V_4 (\vec{\sigma}_1 \cdot \vec{p})(\vec{\sigma}_2 \cdot \vec{p}) + V_5 (\vec{\sigma}_1 \cdot \vec{r})(\vec{\sigma}_2 \cdot \vec{r})$$

$$+ V_6 \, \vec{\sigma}_1 \cdot \vec{\sigma}_2) + \text{Hermitian conjugate} \qquad (4.6)$$

In Eq.(4.6) the V_i are general scalar functions of $\vec{r}$, $\vec{p}$ and $\vec{\ell}$ or, equivalently, general non-local scalar functions of the relative co-ordinate.

The term V_1 is a central force and $V_6 \vec{\sigma}_1 \cdot \vec{\sigma}_2$ is a spin-dependent central force. A tensor force is contained in a combination of the terms V_5 and V_6

$$V_T S_{12} = V_T \left(\frac{3}{r^2} (\vec{\sigma}_1 \cdot \vec{r})(\vec{\sigma}_2 \cdot \vec{r}) - \vec{\sigma}_1 \cdot \vec{\sigma}_2 \right) \qquad (4.7)$$

The term $V_2(\vec{\sigma}_1 + \vec{\sigma}_2) \cdot \vec{\ell} = \tfrac{1}{2} V_2 \vec{S} \cdot \vec{\ell}$ is a spin-orbit force and $V_3(\vec{\sigma}_1 \cdot \vec{\ell})(\vec{\sigma}_2 \cdot \vec{\ell})$ is a quadratic spin orbit force. One of the terms $V_1 \ldots V_6$ is redundant and can be expressed in terms of the other five. For a more complete discussion of the material outlined in this section the reader is referred to the review article by Okubo and Marshak [10].

The scattering amplitude for nucleon-nucleon scattering may be expressed by giving M in the form of Eq.(3.4) with five arbitrary functions of k and θ, a (k, θ), b(k, θ) .... Alternatively one may specify M by giving the phases and mixing parameters (3.5) as functions of k. In an analogous way Eq.(4.6) gives the potential V between two nucleons in terms of the functions V_i and general spin dependent terms. One may also specify the interaction by giving the potential in each partial wave state, that is, by giving the matrix elements

$$\langle r, \ell \, s \, j, \, T | V | r', \ell' \, s' \, j, \, T \rangle \qquad (4.8)$$

The matrix elements are diagonal in s, j and T because of exchange symmetry, rotational invariance and charge independence. Conservation of parity requires $\ell - \ell'$ to be even. For each j we may have s = 0, $\ell = \ell'$ s = 1, $\ell = \ell' = j$, j $\pm$ 1; s = 1, $\ell = j$, $\ell' = j-1$; that is, there are 4 diagonal

matrix elements in s, ℓ and j and one off-diagonal matrix element. Hence
we need five non-local functions of r to specify the interaction in each state
of angular momentum j. The values of T are limited by the requirement
of the generalized Pauli principle that $(-1)^{1+s+T} = -1$.

4.3. The radial part of the potential

The potential matrix elements (4.8) can be general non-local functions
$V(\vec{r}, \vec{r'})$ of the relative co-ordinate. In this section we give some special
examples of non-local scalar operators which have been used in potential
models of the nucleon-nucleon interaction. A non-local operator is an
integral operator

$$V\phi = \int V(\vec{r}, \vec{r'}) \, \phi(\vec{r'}) \, d^3\vec{r'} \tag{4.9}$$

and the function $V(\vec{r}, \vec{r'})$ is the matrix element $\langle \vec{r} | V | \vec{r'} \rangle$ of V in the co-
ordinate representation. If V is Hermitian then $V(\vec{r}, \vec{r'}) = V^*(\vec{r}, \vec{r'})$.
   i) A local potential is a special case with

$$V(\vec{r}, \vec{r'}) = v(\vec{r}) \, \delta(\vec{r} - \vec{r'})$$

$$V\phi = v(\vec{r}) \int \delta(\vec{r} - \vec{r'}) \, \phi(\vec{r'}) \, d^3\vec{r'} = v(\vec{r}) \, \phi(\vec{r}) \tag{4.10}$$

   ii) An orbital exchange local potential is a special case with

$$V(\vec{r}, \vec{r'}) = v(\vec{r}) \, \delta(\vec{r} + \vec{r'})$$

$$V\phi = v(\vec{r}) \int \delta(\vec{r} + \vec{r'}) \, \phi(\vec{r'}) \, d^3\vec{r'} = v(\vec{r}) \, \phi(-\vec{r}) = v(\vec{r}) \, P_m \, \phi(\vec{r})$$

The operator P_m exchanges $\vec{r}_1$ and $\vec{r}_2$. Hence $\vec{r} = \vec{r}_1 - \vec{r}_2 \rightarrow -\vec{r}$.
   iii) The potential $V(\vec{r}, \vec{r'}) = -\lambda f(r) \, f^*(r')$ where f(r) is a function of $r = |\vec{r}|$
only is separable and acts in relative s-states only. If

$$V_\ell(\vec{r}, \vec{r'}) = -\lambda f_\ell(r) \, f_\ell^*(r') \sum_m Y_{\ell m}(\theta, \phi) \, Y_{\ell m}^*(\theta', \phi')$$

then V_ℓ is separable and acts only in states with relative orbital angular
momentum ℓ.
   We may always write a non-local potential $V(\vec{r}, \vec{r'})$ as a function of
$W((\vec{r} + \vec{r'})/2), \vec{r} - \vec{r'})$. If $V(\vec{r}, \vec{r'})$ has a short range of non-locality the a
matrix element $\langle \phi | V | \psi \rangle$ can be evaluated approximately by expanding
$\phi(r)$ and $\psi(r')$ as a power series about the point $R = \frac{1}{2}(r + r')$. We have
$(\vec{r} - \vec{R}) = \frac{1}{2}(\vec{r} - \vec{r'})$ and $\vec{r'} - \vec{R} = \frac{1}{2}(\vec{r'} - \vec{r})$ so that

$$\phi(r) = \phi(R) + \tfrac{1}{2}(\vec{r}' - \vec{r}).\vec{\nabla}\,\phi(R) + \ldots$$

and similarly for $\psi(r')$. Substituting these expansions in the integral for the matrix element

$$\langle\phi|V|\psi\rangle = \langle\phi|V_0|\psi\rangle + \tfrac{1}{2}\langle\phi|\vec{P}^2 V_1 + V_1\,\vec{P}^2|\psi\rangle + \langle\phi|V_2\,\vec{\ell}^2|\psi\rangle + \ldots \qquad (4.10a)$$

one finds that

$$\langle\phi|V|\psi\rangle = \langle\phi|V_0|\psi\rangle + \tfrac{1}{2}\langle\phi|\vec{P}^2 V_1 + V_1\,\vec{P}^2|\psi\rangle + \langle\phi|V_2\vec{\ell}^2|\psi\rangle \qquad (4.10b)$$

where $V_0(R) = \int W(R,S)\,d^3s$ etc.

A potential of the form

$$V = V_0(r) + \tfrac{1}{2}(\vec{P}^2 V_1(r) + V_1(r)\vec{P}^2) + V_2(r)\vec{\ell}^2 + \ldots$$

is called a momentum-dependent or velocity-dependent potential. Equation (4.10b) shows that a non-local potential is approximately equivalent to a velocity-dependent potential.

4.4. Meson theory of nuclear forces

At present, there exists no complete quantitative theory of nuclear forces, but it is generally believed that the force between nucleons has its origin in meson exchange processes. The history of the development of meson theory is reviewed in Ref. [11], and there is information about the present states of the meson theory of nuclear forces in Ref. [12].

In boson exchange theories of nuclear forces the meson responsible for the interaction obeys Bose-Einstein statistics. The range, spin and isospin dependence of the exchange interaction depends on the properties of the boson producing the interaction. Bosons may be characterized by spin, isospin and intrinsic parity:

scalar boson   spin 0   parity +

pseudo-scalar boson   0   -   e.g. $\pi(T=1)$, $\eta(T=0)$.

vector boson   1   -   e.g. $\omega(T=0)$, $\rho(T=1)$.

One boson exchange (OBE) theories assume that the most important part of the two-nucleon force is due to exchange of a one boson at a time. If the interaction is calculated in lowest-order perturbation theory in a static model (fixed nucleons) the potentials are
for scalar bosons:

$$V = -f^2\hbar c(e^{-\mu r}/r) \qquad (4.11)$$

for pseudo-scalar bosons:

$$V = \tfrac{1}{3} f^2 \hbar c \left[\vec{\sigma}_1 \cdot \vec{\sigma}_2 + S_{12} \left(1 + \frac{3}{\mu r} + \frac{3}{(\mu r)^2} \right) \right] (e^{-\mu r}/r) \qquad (4.12)$$

for vector bosons:

$$V = V_\ell + V_t$$

$$V_\ell = f_\ell^2 \hbar c (e^{-\mu r}/r) \qquad (4.13)$$

$$V_t = f_t^2 \hbar c \left[\tfrac{2}{3} \vec{\sigma}_1 \cdot \vec{\sigma}_2 - \tfrac{1}{3} S_{12} \left(1 + \frac{3}{\mu r} + \frac{3}{(\mu r)^2} \right) \right] (e^{-\mu r}/r)$$

In these formulae the factors f are coupling constants and $\mu = mc/\hbar$ where m is the mass of the exchanged boson. The potentials should be multiplied by a factor 1 for a T = 0 boson and a factor $\vec{\tau}_1 \cdot \vec{\tau}_1$ for a T = 1 boson.

Vector boson exchange gives an interaction (4.13) with two coupling constants f_ℓ and f_t, because the spin of the boson may be polarized longitudinally or transversely with respect to its direction of emission. Each mode of polarization has its own coupling constant. We may write the various possible forms of a non-relativistic meson-nucleon interaction in terms of field operators ψ^+, ψ for the nucleons and ϕ for the mesons. They are

scalar $\psi^+ \psi \phi$

pseudo-scalar $\psi^+ \vec{\sigma} \psi \cdot \vec{\nabla} \phi$

vector, longitudinal coupling $\psi^+ \psi \vec{\nabla} \cdot \vec{\phi}$

    transverse coupling $\psi^+ \vec{\sigma} \psi \cdot \vec{\nabla} \times \vec{\phi}$

The characteristic range of a OBE interaction is $1/\mu = \hbar/mc$; it is inversely proportional to the boson mass. Hence the longest-range part of the two-nucleon interaction potential is due to pion exchange and has the pseudoscalar character (4.12).

Non-static and other corrections modify the potentials (4.11) (4.13) and in particular vector boson exchange gives rise to a spin-orbit force.

4.5. Uniqueness of the potential

Most of our quantitative information about nuclear forces comes from analysis of two-nucleon scattering experiments. This raises the question of the extent to which the two-nucleon scattering data determine the nucleon-nucleon potential. The scattering data do not determine the interaction potential uniquely. It is always possible to find an infinite number of different potentials which produce exactly the same phase shifts.

To see this result we consider the simple case of scattering of spinless particles by two different potentials V and $\overline{V}$. We suppose that

$$H = T + V, \quad \overline{H} = T + \overline{V} \text{ and } \overline{H} = U^\dagger H U$$

where U is a unitary operator which does not affect the scattering wave function at large distances. Then the phase shifts $\delta(k)$ as functions of k are identical for V and $\bar{V}$. We look in more detail at a specific example of an operator U with the required properties.

We put

$$U = 1 - 2P$$

where

$$P\phi = g(\vec{r}) \int g^*(\vec{r}') \phi(\vec{r}') \, d^3\vec{r}', \qquad \int |g(\vec{r})|^2 d^3\vec{r} = 1 \qquad (4.14)$$

and

$$g(r) = 0 \quad \text{if} \quad r > b \qquad (4.15)$$

Then P is a projection operator,

$$U^\dagger U = U^2 = (1 - 2P)^2 = (1 - 4P + 4P^2) = 1$$

and the operator U is unitary. Let $\phi(r)$ be a scattering solution of the Schrödinger equation $\bar{H}\phi = E\phi$, then $U\psi = \psi$ is a solution of the equation $H\psi = E\psi$ with the same energy.
At large distances

$$\phi(r) \simeq \sin(kr + \bar{\delta}(k)) \quad \text{and} \quad \psi(r) \simeq \sin(kr + \delta(k)) \qquad (4.16)$$

Using Eq. (4.14) we have

$$\psi(r) = \phi(r) - 2g(r) \int g^*(r') \phi(r') \, d^3 r'$$

$$= \phi(r), \text{ if } r > b, \text{ because of } (4.15). \qquad (4.17)$$

Combining Eqs (4.16) and (4.17) we see that $\bar{\delta}(k) = \delta(k)$. Thus, the potentials V and $\bar{V}$ have the same phase shifts. Another example of a unitary transformation U which leaves phase shifts invariant has been given by Baker [13]. Two potentials like V and $\bar{V}$ which have the same phase shifts differ in their off-energy-shell behaviour. The differences could show in systems of many nucleons but at present we do not know how important the off-shell behaviour of the nucleon-nucleon interaction is for the properties of nuclei.

4.6. Phenomenological potentials

The $^1S_0$ (T = 1) phase shift changes sign at 240 MeV laboratory energy. A purely attractive potential can never produce this effect, and it proves the existence of some repulsive component in the interaction. In early potential models this repulsive component was represented by a hard core

in the two-nucleon interaction potential. Hard-core potentials have been fitted to scattering data by Hamada, Johnston [14], a Yale group [15] and by Ried [16]. In these potentials the two nucleon interaction potentials become infinitely repulsive for internucleon separations less than a hard core radius r_c. "Soft-core" potentials have a strong repulsion at small internucleon separations which is mathematically less singular than the hard-core potentials. For example, a finite-core potential has been used by Bressel and Kerman [17], and a Yukawa core by Ried [16].

All the potentials mentioned so far are too singular to be used directly in nuclear-structure calculations. A separable potential fitted by Tabakin [18] gives quite a good fit to scattering data and is non-singular enough to be used in nuclear calculations. Velocity-dependent potentials have also been tried [19] but there is no such potential which gives a good fit to the scattering.

ACKNOWLEDGEMENTS

REFERENCES

[1] HAMILTON, W. D., Progress in Nuclear Physics 10 (1969) 3,
    OKUN, L. B., Comments on Nuclear and Particle Physics 1 (1967) 181.
[2] FITCH, V. R., Comments on Nuclear and Particle Physics 1 (1967) 47, 117 2 (1968) 63.
[3] HENLEY, E. M., in Isobaric Spin in Nuclear Physics (FOX, D. D., ROBSON, D., Eds) Academic Press (1966) 3.
[4] MORAVCSIK, M. J., The Two-Nucleon Interaction, OUP (1963).
[5] WILSON, R., The Nucleon-Nucleon Interaction, Interscience (1962).
[6] SIGNELL, P. S., Advances in Nuclear Phys. 2 (1969) 223.
[7] MACGREGOR, M. H., ARNDT, R. A., Phys. Rev. 173 (1968) 1272, 159 (1967) 1422, 154 (1967) 1549, 141 (1966) 873.
[8] BLATT, J. M., BIEDENHARN, L. C., Rev. mod. Phys. 24 (1952) 258.
[9] STAPP, H. P., YPSILANTIS, T. J., METROPOLIS, N., Phys. Rev. 105 (1957) 302.
[10] OKUBO, S., MARSHAK, R. E., Ann. Phys. 4 (1958) 166.
[11] BRINK, D. M., Nuclear forces, Pergamon (1966).
[12] FESHBACH, H., KERMAN, A. K., Comments on Nuclear and Particle Phys. 1 (1967) 132, 2 (1968) 22, 78.
[13] BAKER, G. A., Phys. Rev. 128 (1962) 1485.
[14] HAMADA, T., JOHNSTON, I. D., Nucl. Phys. 34 (1962) 382.
[15] LASSILA, K. E., HULL, M. H., Jr., RUPPEL, H. M., MACDONALD, F. A., BREIT, G., Phys. Rev. 126 (1962) 881.
[16] REID, R. V., to be published.
[17] BRESSEL, C. N., KERMAN, A. K., unpublished, quoted in BHARAGAVA, P. C., SPRUNG, D. W. L., Ann. Phys. 42 (1967) 222.
[18] TABAKIN, F., Ann. Phys. 30 (1964) 51.
[19] GREEN, A. M., Nucl. Phys. 33 (1962) 218.
    TABAKIN, F., DAVIES, K. T. R., Phys. Rev. 150 (1966) 793.

EXPERIMENTAL ASPECTS OF
NUCLEAR INTERACTION

I. ŠLAUS

Institute "Rudjer Bošković",

Zagreb, Yugoslavia

Abstract

EXPERIMENTAL ASPECTS OF NUCLEAR INTERACTION.

1. Introduction; 2. Basic features of nuclear interaction; 3. How accurate is our present knowledge of phase parameters? 4. Experimental problems in N-N scattering studies; 5. N-N potential models; 6. Some open problems in nuclear interaction studies.

1. INTRODUCTION

In 1953, Bethe estimated that in the preceding quarter of the century more man-hours of work had been devoted to the problem of nuclear force than to any other scientific problem in the history of mankind [Be 53]. Yet, the problem had not been solved and Goldberger stated in 1960: "There are few problems in modern theoretical physics which have attracted more attention than that of trying to determine the interaction between two nucleons. It is also true that scarcely has physics owed so little to so many ... In general, in surveying the field one is oppressed by the unvelievable confusion and conflict that exists. It is hard to believe that many of the authors are talking about the same problem, or, in fact, that they know what the proble is" [Go 60]. In the last ten years a significant progress has been achieved and summarizing the Nucleon-Nucleon Interaction Conference (Gainesville, 1967) Wolfstein concluded that an extremely impressive amount of information about nucleon-nucleon interaction had been accumulated, and "Furthermore, whereas before there were no potentials to fit the data other than purely phenomenlogical models requiring some 20 to 50 adjustable parameters, now it would appear that we have quite a number of potential models rooted in meson field theory that fit the data... Also, all of the meson theoretic models represent relatively minor variations of a common physical theme" [Gr 67].

The study of nuclear forces led to the discovery of the pion, and eventually resulted in the vast field of hadron physics. In 1935, Yukawa explained the short range of nuclear forces in terms of the exchange of a quantum having a finite mass of approximately 250 - 300 electron masses. A quantum of mass m_π is virtually emitted by a nucleon. During the time $\Delta t \sim \hbar/\Delta E \sim \hbar/m_\pi c^2$ the quantum can travel a distance $r_0 \sim c\,\Delta t \sim \hbar/m_\pi c$ and within that range be absorbed by another nucleon. The nuclear interaction at largest distances is represented by the exchange of the lightest quantum, specifically, by the exchange of one such quantum. The lightest particle that could be a nuclear-force quantum is a pion, which was discovered in 1947.

The crucial step in the development of the meson theory of nuclear forces was made in 1951 by Taketani, Nakamura and Sasaki [Ta 51], who

divided nuclear interaction into three regions: 1. classical (static) region;
$\mu r \gtrsim 1.5$, where $\mu = m_\pi c / \hbar$; 2. dynamic region, $0.7 \lesssim \mu r \lesssim 1.5$, and
3. phenomenological region, $\mu r \lesssim 0.7$, and who proposed an approach to
the nuclear-force problem from the outside of the nucleon. The outside
region is dominated by the one-pion-exchange processes (OPEP) and
should be treated on the basis of meson theory. As the distance between
two nucleons decreases, two-pion exchange processes (TPEP) and exchange
of heavier bosons contribute (region II), and finally at very short distances
the structure of elementary particles may become important (region III).
The inner region should be treated phenomenologically. The success in
understanding the inner region depends on the reliability of our knowledge
of the outside region. The basic philosophy of the Taketani approach is:
"We consider that the phenomenon of nuclear force is a rare example
which enables us to pick up the OPE phenomena purely.... the OPE tail
of nuclear force has a correspondence to the classical field, which makes
its treatment simple. On the contrary, it is difficult to study the pheno-
mena of absorption and emission of real pions, because these are involved
with big energy jump." [Ta 56]. The remarkable results of this approach
lie in establishing quantitatively the validity of OPEP in region I, and in
determining the value of the pion-nucleon coupling constant and the pseudo-
scalar nature of the pion.

The increasing number of experimentally established hadrons caused
many attempts to develop a classification of particles on the assumption
that some are more "elementary" than the others. In 1949 Fermi and
Yang tried to regard the pion as composed of a nucleon-antinucleon pair.
In 1956 Sakata proposed a model [Sa 56] in which hadrons are considered
to be composite particles of the fundamental particles: proton, neutron
and lambda, and their antiparticles. The quark model [Ge 64] considers
all hadrons to be composed of three quarks and three antiquarks. If this
model is correct, one can speculate that strong interaction should be
derived from the fundamental interaction between fundamental particles
(e.g. quarks?), and indeed the complexity of strong interaction might be
an indication that the interaction between pions and nucleons results from
the projection of the fundamental interactions (compare the interaction
between two atoms and the fundamental Coulomb force!). This model
"strong interaction" should be valid in the region where the structure of
elementary (i.e. composite) particles is not effective.

The development in the field of particle physics is reflected in the
formulation of the one-boson-exchange model (OBEM) [Ho 62, Sa 62,
Br 63, Sc 63, etc.]. The essence of this model is the assumption that
hadronic interactions are well determined by lowest-order processes
(i.e. diagrams involve no hadron closed polygon), specifically that the
nucleon-nucleon interaction is represented by the exchange of one boson.
In a more conservative version, one allows also the TPEC besides the
OPE and OBE contributions.

The nuclear force problem is not only the central theme in nuclear
physics, but also the organic link with particle physics.

In this review we shall discuss the experimental information deter-
mining the basic feature of nuclear interaction (section 2), the accuracy
of our present knowledge of phase parameters (section 3), experimental
problems in nucleon-nucleon (N-N) scattering studies (section 4), N-N
potential models (section 5), and some open problems in nuclear inter-

action: off-energy-shell interaction, neutron-neutron force, charge symmetry and charge independence.

2. BASIC FEATURES OF NUCLEAR INTERACTION

The very fact that nuclei exist implies the necessity for some N-N force, which at least in a certain region of relative N-N distances has to be attractive. The region where nuclear force should be attractive is of the order of the size of atomic nuclei $\sim 10^{-12}$ cm.

To keep the nucleons within the atomic nucleus, the nuclear potential should be at least 20-30 MeV deep.

Nuclear interaction certainly does not extend to large distances. If it is extended much beyond nuclear radius, it would manifest itself through the modification of the molecular behaviour. Indeed, nuclear force should have a very short range. This can be shown by comparing the binding energies of the lightest nuclei [Wi 33]. The binding energy of the lightest nuclei increases faster than linearly when the number of bonds increases. A large number of bonds per particle implies that particles are pulled closer together. The fact that the binding energy depends so strongly on the spacing between nucleons indicates that the range of nuclear force is of the same order of magnitude as the size of the lightest nuclei.

A comparison of the binding energies of deuteron and triton shows that nuclear force cannot have zero range. Thomas' theorem [Th 35] proves that the binding energy of the triton, even neglecting the neutron-neutron force, tends to infinity as the range of the neutron-proton (n-p) force tends to zero, and its strength is adjusted to give the correct deuteron binding energy. Thus, nuclear force has a short, but finite range.

The quadrupole moment of the deuteron demonstrates that nuclear force contains also a tensor term besides the central one.

Most of our knowledge about the N-N force comes from the study of N-N collisions. In scattering experiments one prepares two particles in certain states prior to scattering and subsequently measures the states of the particles after scattering. A nucleon has spin 1/2, and one can measure the differential cross-section, polarization components of the scattered and the recoil nucleons, and the correlation of two final-state spin directions. Besides, either projectile or target particles, or both, can be polarized yielding a total of 256 possible experiments at each angle for every energy. The symmetry properties of the two-nucleon system and the conservation of the number of particles severely restrict the number of experiments necessary to describe the N-N scattering completely, e.g. half of 256 observables are pseudo-scalars and hence vanish identically if parity is conserved. Indeed, only 5 experiments at each angle and for each energy, among which at least one should be with non-parallel planes e.g. $\sigma(\theta)$, $P(\theta)$, $D(\theta)$, C_{nn}, $R(\theta)$ or C_{kp} are enough to specify the N-N interaction on the energy shell completely [Pu 57]. For the proton-proton (p-p) system it is enough to measure the region $0 \leq \theta \leq \pi/2$, while for the n-p system one needs $0 \leq \theta \leq \pi$. Above the pion production threshold, a complete set of experiments contains 11 measurements [Sc 61].

The spin state of a two-nucleon system is determined by the expectation values of 16 independent matrices $O_n = \ell_1\ell_2$; $\ell_1\vec{\sigma}_2$; $\vec{\sigma}_1\ell_2$; $\vec{\sigma}_1\vec{\sigma}_2$. Sixteen initial states can be prepared $\langle O_n \rangle_i$ ($n = 1, 2, \ldots 16$) and in the final state 16 measurements of $\langle O_m \rangle_f$ ($m = 1, 2, \ldots 16$) are possible, yielding 256 experiments. The expectation value $\langle O_n \rangle_f = \langle \sigma_1^\alpha \sigma_2^\beta \rangle_f$ ($\alpha, \beta = 0, x, y, z$) can be expressed as

$$\langle \sigma_1^\alpha \sigma_2^\beta \rangle_f = \frac{1}{Tr\,\rho_f}\, Tr[\rho_f\,(\sigma_1^\alpha \sigma_2^\beta)_f] \tag{2.1}$$

where ρ_f is the final state density matrix, connected with the initial state density matrix $\rho_i = \sum_{n=1}^{16} \frac{1}{4} Tr(\rho_i)\langle O_n \rangle O_n$ by

$$\rho_f = M\rho_i M^* \tag{2.2}$$

Expression (2.1) becomes

$$\langle \sigma_1^\alpha \sigma_2^\beta \rangle_f = \frac{Tr(\rho_i)}{4\,Tr(\rho_f)} \sum_{n=1}^{16} \langle O_n \rangle_i\, Tr(M O_n M^* \sigma_1^\alpha \sigma_2^\beta) \tag{2.1'}$$

M is the 4×4 matrix which depends on the incident and outgoing momenta k and k', respectively, and on $\vec{\sigma}_1$ and $\vec{\sigma}_2$. Introducing $p = k + k'$, $q = k' - k$ and $n = k \times k'$, and assuming that the N-N interaction is invariant under space reflection, rotation, time reversal and assuming the validity of charge independence, the most general M matrix is

$$M = A + B(\sigma_1 n)(\sigma_2 n) + C(\sigma_1 + \sigma_2)n + E(\sigma_1 q)(\sigma_2 q) + F(\sigma_1 p)(\sigma_2 p) \tag{2.3}$$

A, B, C, E and F are complex functions of energy and angle. The unitarity requirement of the S matrix implies five relations between coefficients A, $\ldots$ F and leaves 5 independent real parameters to be determined for each angle and energy.

If parity is not conserved M also contains the terms $R(\sigma_1 - \sigma_2)p$ and $S[(\sigma_1 n)(\sigma_2 p) - (\sigma_1 p)(\sigma_2 n)]$.

If time reversal does not hold, the term $T[(\sigma_1 p)(\sigma_2 q) - (\sigma_1 q)(\sigma_2 p)]$ should be added.

If both parity and time reversal are violated two additional terms are $P(\sigma_1 - \sigma_2)q$ and $Q[(\sigma_1 q)(\sigma_2 n) - (\sigma_1 n)(\sigma_2 q)]$.

The connections between the formalism and the observables are:
Differential cross-section:

$$\sigma_0 \equiv \sigma(\theta) = \frac{Tr(\rho_f)}{Tr(\rho_i)} = \frac{1}{4} Tr(MM^*)$$

Spin expectation value after scattering of an unpolarized beam from an unpolarized target:

$$\sigma_0 \langle \vec{\sigma}_1 \rangle_f = \frac{1}{4} Tr(MM^*\vec{\sigma}_1) \tag{2.4}$$

After calculating the indicated trace in Eq. (2.4), one is left with functions of k and k', and the only axial vector one can form is $k \times k'$. Therefore, the scattering produces polarization perpendicular to the scattering plane. The spin direction can be rotated with the magnetic field (which also bends the trajectory of the charged particle, but at a different angle so that the overall effect is that the spin is turned with respect to the direction of particle motion). In this way one can obtain the beam with any desired orientation of polarization by scattering an unpolarized beam from a suitable target and using an appropriate magnet.

The differential cross-section for the scattering of a polarized beam on an unpolarized target is

$$\sigma(\theta) = \frac{1}{4}[Tr(MM^*) + \langle \sigma \rangle_i \, Tr(M\vec{\sigma}M^*)]$$

On the basis of time reversal and parity conservation we have $Tr(M\vec{\sigma}M^*) = Tr(MM^*\vec{\sigma})$ proportional to n, and the polarizing and the analysing powers of the nuclear process are equal.

Triple-scattering experiments determine the manner in which second scattering changes direction and magnitude of the polarization of the incident particle. First scattering serves as a polarizer and third scattering as an analyser.

Formula (2.1) gives

$$I\langle \sigma_1^\alpha \rangle_f = \frac{1}{4} Tr(MM^*\sigma_1^\alpha) + \sum_{\beta=1}^{3} \frac{1}{4} Tr(M\sigma_1^\beta M^*\sigma_1^\alpha) \langle \sigma_1^\beta \rangle_i \qquad (2.5)$$

with

$$I = \frac{1}{4} Tr(MM^*) + \sum_{\beta=1}^{3} \frac{1}{4} Tr(M\sigma_1^\beta M^*) \langle \sigma_1^\beta \rangle_i$$

The momenta of the incident and the scattered particle in the second scattering are denoted by k_2 and k'_2, respectively. It is convenient to introduce two co-ordinate systems: one, $n_2 = k_2 \times k'_2$, k_2 and $x_2 = n_2 \times k_2$, and the other, n_2, k'_2 and $s_2 = n_2 \times k'_2$.

Expression (2.5) can be written as

$$I \langle \sigma_1^\alpha \rangle_f = \sigma_{0(2)} \{[P_2 + D \langle \vec{\sigma} \rangle_i \cdot n_2] n_2 + [A \langle \sigma \rangle_i k_2 + R \langle \sigma \rangle_i (n_2 \times k_2)] s_2$$

$$+ [A' \langle \sigma \rangle_i k_2 + R' \langle \sigma \rangle_i (n_2 \times k_2)] k'_2\} \qquad (2.6)$$

The depolarization parameter, D, and the rotation parameter, A, can be measured by a simple succession of three scatterings. If the analysing plane is parallel to the second scattering plane, i.e. n_3 parallel to n_2, one measures $P_2 + D \langle \sigma \rangle_i \cdot n_2$ (see Fig. 1). If the beam is prepared with its polarization in direction x_2 (i.e. the polarizing plane perpendicular to the second scattering plane: n_1 perpendicular to n_2), and if the analysing plane is perpendicular to the second scattering plane and n_3 parallel to s_2, one measures R. Measurements of R', A and A' require
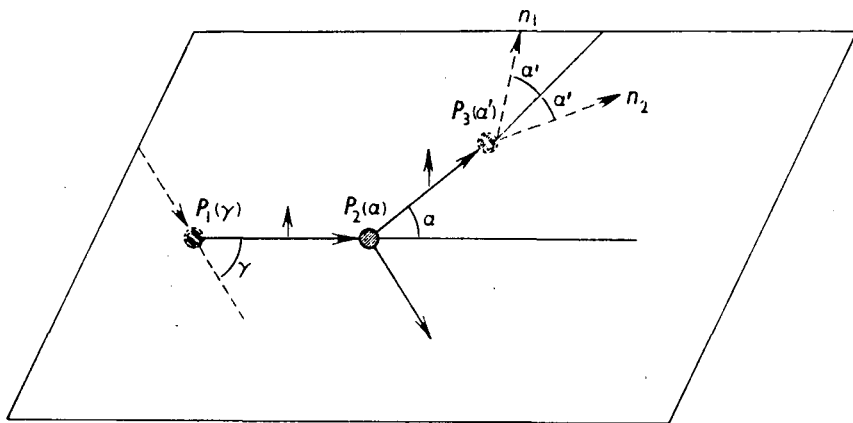
FIG.1. Scattering experiment.

the use of magnetic fields since scattering can neither produce nor detect
the polarization in the direction of motion. The measurement of A re-
quires the magnetic field between the first and the second scattering, and
n_3 should be parallel to s_2 (Fig. 2). Similarly, the measurement of R'
requires the magnetic field between the second and the third scattering,
(Fig. 3) and the measurement of A' two magnetic fields, one between
the first and the second, and the other between the second and the third
scattering.

From the invariance under time reversal it follows that A, R, A'
and R' are not independent and that the following relation holds

$$A + R' = (A' - R) \tan \theta / 2$$

The correlation between the polarization of the scattered and recoil
nucleon produced in the unpolarized-projectile-unpolarized-target scatter-
ing is

$$\sigma_0 \langle \sigma_1^\alpha \sigma_2^\beta \rangle_f = \frac{1}{4} \, \mathrm{Tr} \, (MM^* \, \sigma_1^\alpha \sigma_2^\beta)$$

Referring to the laboratory co-ordinate system k, k', n = k×k', s = n×k'
and k'' (momentum of the recoil nucleon) and t = n×k'', one defines

$$\sigma_0 \, C_{nn} = \frac{1}{4} \, \mathrm{Tr} \, (MM^* \, \sigma_1^n \sigma_2^n)$$

$$\sigma_0 \, C_{kp} = \frac{1}{4} \, \mathrm{Tr} \, (MM^* \, \sigma_1^s \sigma_2^t)$$

$$\sigma_0 \, C_{pp} = \frac{1}{4} \, \mathrm{Tr} \, (MM^* \, \sigma_1^{k'} \sigma_2^t)$$

(2.7)

$$\sigma_0 \, C_{kk} = \frac{1}{4} \, \mathrm{Tr} \, (MM^* \, \sigma_1^s \sigma_2^{-k''})$$

where $\sigma_2^{-k''} \equiv - \sigma_2 \cdot k''$. C_{nn} is measured when two analysing planes are
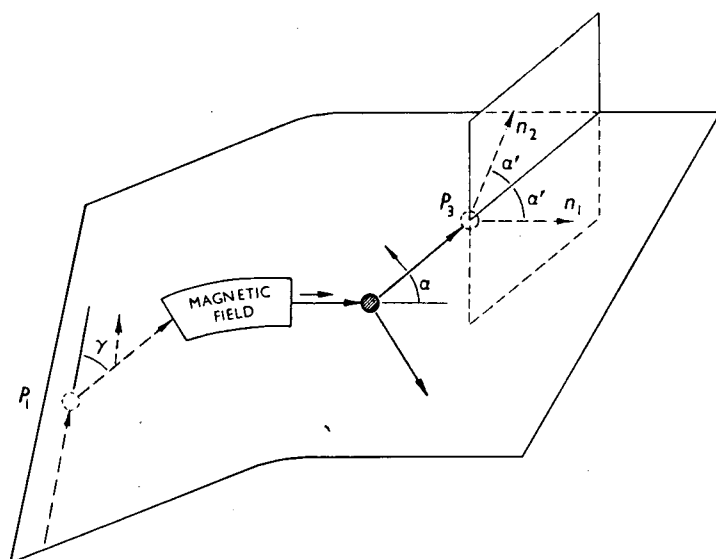
FIG.2.   Scattering experiment with magnetic field between first and second scattering.
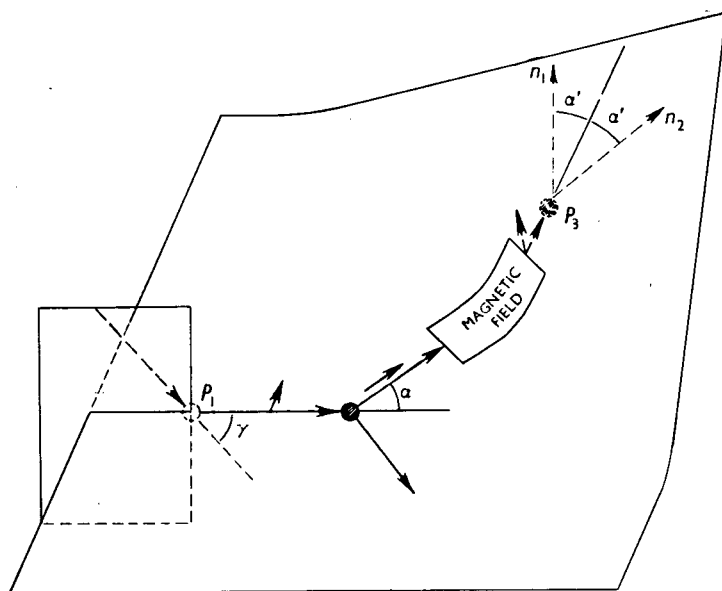
FIG.3.   Magnetic field after second scattering.

parallel to the first scattering plane, and C_{kp} is measured when two
analysing planes are mutually perpendicular and perpendicular to the
scattering plane (Fig. 4).   The measurements of C_{pp} and C_{kk} require
the use of magnetic fields.

    The correlation parameters $C_{\alpha\beta}$ can be determined also from experi-
ments using polarized projectiles and polarized targets.   The cross-
section $I_{\alpha\beta}$ for the polarized beam with polarization along the direction α
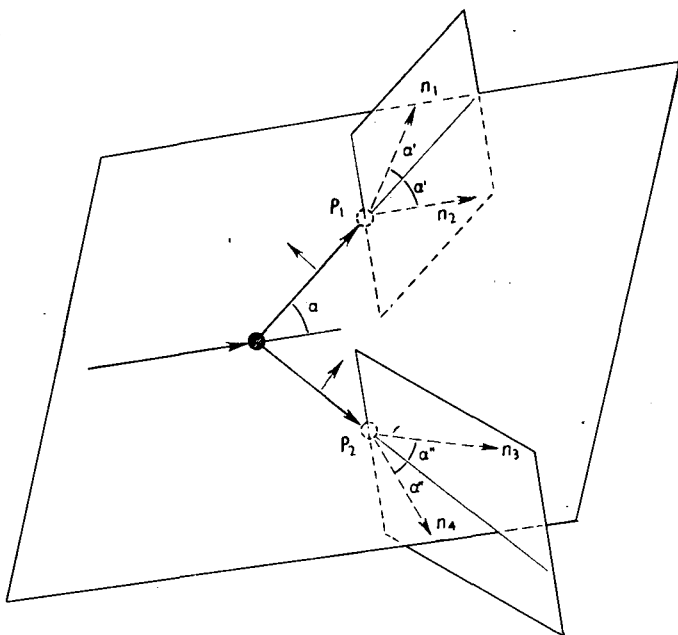
FIG.4.   Scattering experiment.

scattered from the polarized target with polarization along the direction β is from Eq.(2.1)'

$$I_{\alpha\beta} = \frac{1}{4} \, \text{Tr} \, (MM^*) + \frac{1}{4} \, \text{Tr} \, (M\sigma_1^\alpha M^*) \langle \sigma_1^\alpha \rangle_i + \frac{1}{4} \, \text{Tr} \, (M \sigma_2^\beta M^*) \langle \sigma_2^\beta \rangle_i$$

$$+ \frac{1}{4} \, \text{Tr} \, (M \sigma_1^\alpha \sigma_2^\beta M^*) \langle \sigma_1^\alpha \sigma_2^\beta \rangle_i \qquad\qquad (2.8)$$

and $\frac{1}{4} \, \text{Tr} \, (M\sigma_1^\alpha \sigma_2^\beta M^*) = \sigma_0 A_{\alpha\beta}$.   The coefficients $A_{\alpha\beta}$ are related to $C_{\alpha\beta}$, specifically:

$$A_{nn} = C_{nn} \qquad \text{and} \quad A_{xx} = \sin \theta \, C_{kp} + \cos^2 \frac{\theta}{2} \, C_{pp} + \sin^2 \frac{\theta}{2} \, C_{kk}$$

with $x = n \times k$.

   We shall not discuss higher rank spin-correlation parameters $C_{\alpha\beta\gamma}$. and $C_{\alpha\beta\gamma\delta}$ and refer the reader to Refs [Ho 68] and [Ja 68].

   The study of N-N collisions yields the following information:

   1. Nuclear force is a short-range force. The argument is based on the measurements of the angular distribution in n-p and p-p scattering. The isotropy of n-p scattering up to 10 MeV implies from $\hbar L = pb$ that the range b is $\sim 10^{-13}$ cm. From the angle and from the energy at which p-p scattering deviates from the Coulomb scattering, one estimates the range of the N-N force to be $\sim 10^{-13}$ cm.

   2. The n-p angular distribution from 30 to 300 MeV has a U-shape almost symmetric about a c.m. angle of 90° indicating that nuclear

forces in odd-parity states are weaker than those in even parity states (Serber-type force). The p-p angular distribution is, except for the Coulomb scattering part, isotropic up to ~400 MeV, and this cannot be explained if all partial waves in even states interfere constructively (i.e. equal sign for even-state phase shifts). Jastrow [Ja 51] assumed that the $^1S_0$ phase shift changes its sign as a result of the hard core. Thus the $^1S_0$ wave destructively interferes with other even-parity waves, resulting in an isotropic angular distribution. The direct confirmation that the $^1S_0$ phase shift decreases and becomes negative at about 250 MeV came from the energy-dependent phase-shift analysis.

The idea that nuclei might have a highly compact structure at small distances was raised by Rutherford already in 1927 [Ru 27], and was subsequently considered by Morse [Mo 36], Breit [Br 37], and others [Fe 41, Pa 48].

At present, there is no evidence against the assumption that the N-N interaction contains the repulsive inner region in all N-N states. However, evidence for the repulsive interaction is sound only for the $^1S_0$ state, it is probable that the $^3S_1$ state and may be even the ^3P state also contains the inner repulsion (the $^3S_1$ phase shift at higher energies, ~350 MeV, becomes negative). For other states, there is no evidence for or against, and one should mention that the impact parameters for D and F waves are 0.4 fm at as high energies as 3.2 GeV and 6.2 GeV, respectively.

Qualitatively, the effect of the repulsive core is to make the effective interaction weaker as the relative energy increases. Such an effect can be produced by the hard-core, soft-core or a velocity-dependent interaction. Indeed, for each hard-core potential model there exists a family of velocity-dependent potentials which equally give a good fit to the N-N scattering data. Hard-core, soft-core and velocity-dependent potential models which produce identical (or very similar, and thus from the experimental point of view, equivalent) phase parameters could be discriminated by investigating the off-energy-shell interaction (see Ref. [Ot 68]).

3. Nuclear forces are spin-dependent. The n-p system has a bound state, the deuteron. If one assumes that the n-p scattering can entirely be described by the parameters characterizing the ground state of the deuteron, for the zero-energy n-p cross-section one obtains values between 2.33 and 9.32 mb, depending on the value of the n-p effective range. The experimental cross-section is 20.36 ± 0.10 mb! The problem was solved by Wigner [Wi 36], who pointed out that the spins of n and p in the deuteron are correlated and, in fact, parallel, while the spins in the scattering experiment are uncorrelated. Thus, the cross-section is $(3/4)\sigma_t + (1/4)\sigma_s$, where t and s indicate triplet and singlet states, and only σ_t can be related to the properties of the deuteron. The experimentally determined zero energies σ_s and σ_t differ by almost an order of magnitude, which implies that the N-N force is spin-dependent.

4. The outer region of the N-N interaction is OPE. The static OPEP is

$$V_{static} \text{ (OPEP)} = \frac{f^2}{4\pi} \mu(\tau_1 \tau_2) \frac{e^{-x}}{x} \frac{1}{3} \left[(\sigma_1 \sigma_2) + S_{12} \left(1 + \frac{3}{x} + \frac{3}{x^2} \right) \right]. \quad (2.9)$$

where μ is the pion mass, $x = \mu r$, $f = g\mu/2M$, and M is the nucleon mass.

The proof that the outer region is dominated by OPE consists in including the OPEP in the phase-shift analysis for higher partial waves in much the same way as the Coulomb interaction is customarily included. In such a calculation the OPEP contribution has one free parameter: the nucleon-pion coupling constant. The modified phase-shift analysis [Cz 59, Gr 59] proves that phase shifts indeed approach δ(OPEP) as L and E increase. The coupling constant determined from the analysis is in agreement with that determined from pion-nucleon scattering. In addition, the phase shift solution for $L < L_0$ (for $L \geq L_0$ one uses OPEP) become unique if one uses OPEP.

The study of the deuteron by Iwadare et al. [Iw 56] established the validity of OPEP in 1956. Since the deuteron is a loosely bound structure, it is expected that its static properties depend very little upon the inner part of the potential. In the outer region ($x > 1$) the characteristic of OPEP is the dominant tensor feature and from the quadrupole moment they determined the coupling constant $f^2/4\pi = 0.065 - 0.09$. Glendenning and Kramers [Gl 62] showed that various potentials are consistent with the deuteron data providing the tail is described by OPEP. The predicted quadrupole moment and the D state probability turn out to be $2.80 \leq Q \leq 2.88 \times 10^{-27}$ cm^2 and $5.4 \leq P_D \leq 7.5\%$, respectively. The experimental value for Q is $2.80 \pm 0.01 \times 10^{-27}$ cm^2 (Wi 63), though the other analysis [Na 66] gave $2.7965 \pm 0.005 \times 10^{-27}$ cm^2.

5. Nuclear force contains the spin-orbit (LS) term. The measurement of the depolarization D ($\theta = 45° - 90°$) at 150 MeV was the clear evidence requiring the LS force, which had to reduce the large value of $\delta(^3P_0)$ at E = 150 MeV predicted by the OPEP tensor force. Hoshizaki and Machida [Ho 62a] investigated the non-static OPE and TPE contributions and found that the LS force due to TPE is weaker than phenomenologically needed in triplet odd states. It has been known for a long time (see, e.g. Ref. [Ro 48]) that the LS force can be derived from the exchange of the vector and/or the scalar meson. Since the experimental N-N scattering data at higher energies (100 - 300 MeV) indicated a rather strong LS force in region II, many authors attributed this force to the exchange of the scalar or vector bosons [Gu 59, Sa 60, Br 60]. It seems that the outer part of the LS force is mainly described by the OBEC (boson other than pion) though TPE can also contribute. The short range of the LS force seemed to be indicated by the fact that the splitting of ^3F_j phase shifts experimentally found is not of the LS type even at E = 310 MeV. However, if the range of the LS force is too short the polarization P(θ) at E $\sim$ 150 MeV is too small.

6. For singlet even L = 0, L = 2 and L = 4 phase shifts, phase-shift analysis yielded values which could not be explained by using the central potential only (the tensor and spin-orbit potentials vanish in singlet states). The static potential gave too large a value at 100 MeV for $\delta(^1D_2)$ and the disagreement became 40% at 300 MeV. The OPEP including the $(\mu/M)^2$ non-static correction [Ho 62a] is

$$V(OPEP) = \frac{f^2}{4\pi}\mu\,(\tau_1\;\tau_2\,)\,\frac{e^{-x}}{x}\left[\frac{1}{3}\left\{(\sigma_1\sigma_2) + S_{12}\left(1 + \frac{3}{x} + \frac{3}{x^2}\right)\right\}\right.$$

$$\pm\frac{1}{2}\left(\frac{\mu}{M}\right)^2\frac{1}{x^2}\left(1 + \frac{3}{x} + \frac{3}{x^2}\right)\left\{\frac{1}{2}\left[(\sigma_1\,L)(\sigma_2\,L) + (\sigma_2\,L)(\sigma_1\,L)\right]\right.$$

$$\left.\left. - (\sigma_1\sigma_2)L^2\right\}\right] \qquad\qquad\qquad (2.10)$$

The minus sign corresponds to the pseudo-scalar (pseudo-vector) coupling with the Lagrangian density

$$L = i\,\frac{f}{\mu}\,\bar{\psi}\,\tau_\alpha\,\gamma_5\,\gamma_\mu\,\psi\,\partial_\mu\,\phi_\alpha$$

and the plus sign corresponds to the pseudo-scalar (pseudo-vector) coupling with

$$L = ig\,\bar{\psi}\,\tau_\alpha\,\gamma_5\gamma\,\phi_\alpha$$

The first term in Eq.(2.10) is the well-known static OPEP, and the $(\mu/M)^2$ term is the so-called quadratic spin-orbit force, which does not vanish in singlet even states. Although the non-static term in OPEP provides the theoretical standard for the asymptotic behaviour and the order of magnitude, its sign and strength should be considered phenomenologically.

The inclusion of the quadratic spin-orbit term makes the problem of the range of the spin-orbit term less serious.

7. Nuclear forces are to a large extent charge independent (CI). The charge symmetry (CS) of nuclear forces was postulated by Heisenberg in 1932 [He 32] and the comparison between low-energy n-p and p-p scattering data led Breit [Br 36, Br 36a] to the suggestion of CI. Nuclear-structure data confirm the CI. The N-N scattering data also confirm that CI is valid within several percents. The validity of CI can be checked separately for low-L and high-L partial waves. The investigation of low-L states consists in varying non-OPEP phase shifts. T = 1 phase shifts obtained from the analysis of p-p data were used in n-p analysis and T = 0 phase shifts were determined by fitting the n-p data. T = 1 phase shifts were then released so as to obtain the best fit to the n-p data. The conclusion was that T = 1 phase shifts for p-p and n-p data were the same within experimental uncertainties (which, however, are not always small).

Very accurate and extensive data on p-p and n-p scattering around 210 MeV were used [Mi 68] to perform an energy-independent phase-shift analysis, and an attempt was made to determine whether the data require any charge splitting in the $^1S_0$ state. The n-p and p-p $^1S_0$ phase shifts were allowed to be independent and the splitting found was 3.3° ±4.5°. A similar analysis was performed by MacGregor et al. [Ma 68] resulting in 0.06° ±0.74°. Both results are consistent with no splitting, but the second limits the magnitude of any possible splitting to less than 0.8°, while the first allows as much splitting as 7.8°. The reason is that Signell et al. [Mi 68] compare $\delta(^1S_0)$ for p-p with $\delta(^1S_0)$ for n-p, while MacGregor

et al. [Ma 68] compare the $\delta(^1S_0)$ determined from p-p with that deter-
mined from p-p and n-p, and the rather inaccurate n-p data combined
with accurate p-p data cannot yield the result much different from $\delta(^1S_0)$
for p-p. The uncertainty in the n-p $^1S_0$ phase shift around 210 MeV is
10 times larger than in the p-p phase shift: $\delta(^1S_0)$ for p-p: 5.43 ± 0.44,
and for n-p 2.13 ± 4.50. Additional n-p data are needed.

The analysis of high L states consists in the study of OPEP phases.
The pion exchanged in n-p and p-p interactions is a neutral one, while
n-p can interact by exchanging either charged or neutral pions. The
masses of charged and neutral pions differ and, in principle, the coupling
constants might be different. To account for these differences, OPEP
should be written as

$$V(OPEP) = g_{0\pm}^2 W(m_{\pi\pm}, r) [\tau_1 \tau_2 - \tau_1^z \tau_2^z] + g_{00}^2 W(m_{\pi0}, r) \tau_1^z \tau_2^{z'} \qquad (2.11)$$

where g_{00} and $g_{0\pm}$ are the coupling constants for neutral and charged
pions, respectively. For the $T = 1$ p-p and n-n system $\tau_1 \tau_2 = 1$ and
$\tau_1^z \tau_2^z = 1$ yielding only the term due to neutral pion exchange. For the
$T = 1$ n-p system $\tau_1 \tau_2 = 1$, and $\tau_1^z \tau_2^z = -1$ yielding $2\delta(m_{\pi\pm}) - \delta(m_{\pi0})$. For
$T = 0$, $\tau_1 \tau_2 = -3$ and one has $-[2\delta(m_{\pi\pm}) + \delta(m_{\pi0})]$. The phase-parameter
analysis affords the possibility of determining g^2 and thus testing CI.
The YLAM analysis for p-p and $L \geq 5$ gave $g_{00}^2/4\pi \sim 13.5 \pm 0.9$,
YLANZM for n-p and $L \geq 5$ gave 14.5 ± 1.1 [Br 60a]. The
analysis AM VII [Ma 68a] yields 14.72 ± 0.83 from p-p data, and Y-IV
yields 15.99 ± 0.62 for p-p and 13.76 ± 0.74 for n-p data [Br 67]. The
coupling constant determined from charged pion-nucleon scattering is
14.636 ± 0.34. It should be mentioned that the values of the coupling
constant derived from the most recent Yale analysis of n-p and p-p data
differ by more than the uncertainties, while the older values as well
as the pion-nucleon scattering value are mutually compatible.

8. The study of N-N scattering gives information on the validity of
time reversal and parity conservation. There is a number of experiments
in nuclear-reaction studies which provide quite low upper limits for parity
non-conserving (PNC) and time reversal non-invariance (TRNI) terms
in the N-N interaction. It is desirable, however, to study the validity
of these basic conservation laws investigating N-N scattering (e.g. PNC
and TRNI interaction can be energy-dependent).

If PNC holds, then the differential cross-section for the scattering of
the polarized beam on the unpolarized target is

$$\sigma = \sigma_0 [1 + \langle \vec{\sigma} \rangle_i \vec{n} A_n + \langle \vec{\sigma} \rangle_i \vec{x} A_x + \langle \vec{\sigma} \rangle_i \vec{k} A_k] \qquad (2.12)$$

The spin expectation value after the scattering of the unpolarized beam
from the unpolarized target is

$$\langle \vec{\sigma} \rangle_f = P_n \vec{n} + P_s \vec{s} + P_k \vec{k}' \qquad (2.13)$$

and if PC holds then $P_s = P_{k'} = A_x = A_k = 0$, and if TR-invariant, then
$P_{n|} = A_n$.

We summarize some experimental information (see Ref.[Th 65]):

$P_n - A_n = 0.029 \pm 0.018$, at 30°, 210 MeV

$= 0.007 \pm 0.023$,   31°, 176 MeV

$= 0.011 \pm 0.022$,   50°, 179 MeV

$A_x = 0.008 \pm 0.033$, at 57°, 210 MeV

$= 0.02 \pm 0.04$,   45°, 315 MeV, from $p - {}^{12}C$ scattering.

The longitudinal polarization from $p + {}^9Be$ at 0°, 350 MeV is less than 4×10^{-3}.

The data on N-N scattering do not give any evidence for parity and/or time reversal violation. However, the upper limits for TRNI are smaller than those for PNC.

3.   HOW ACCURATE IS OUR PRESENT KNOWLEDGE OF PHASE PARAMETERS?

Experimental data on N-N scattering can be parametrized in terms of phase parameters: phase shifts and coupling parameters. The states of the two-nucleon system are:

T = 0, even triplets: ${}^3S_1$ and ${}^3D_1$, coupling parameter ϵ_1; ${}^3D_2$;

${}^3D_3$ and ${}^3G_3$, coupling parameter ϵ_3; ${}^3G_4$; ...

T = 0, odd singlets: ${}^1P_1$, ${}^1F_3$, ${}^1H_4$, ...

T = 1, even singlets: ${}^1S_0$, ${}^1D_2$, ${}^1G_4$, ...

T = 1, odd triplets: ${}^3P_0$; ${}^3P_1$; ${}^3P_2$ and ${}^3F_2$, coupling parameter ϵ_2, ...

Owing to the short range of nuclear forces, it is possible to describe the scattering in terms of a relatively small number of phase shifts.

The experimental accuracy determines to some extent the number of phases, e.g. better angular resolution requires more phase shifts. The relationship $L_{max}\hbar = bp$ indicates that $L_{max} = 2$ for 40 MeV, and 6 for 350 MeV. This semi-classical argument should not be taken literally, at least for low L, where the correspondence principle cannot be applied.

Below the pion threshold, the phase shifts are real. Above 400 - 500 MeV the total p-p cross-section appreciably differs from the total elastic p-p cross-section indicating the large contribution of meson production.

In 1957 Stapp, Ypsilantis and Metropolis performed the phase-shift analysis at 310 MeV where the most complete data exist. They obtained 5 sets of phase parameters [St 57]. The reduction of the ambiguity was achieved using the modified analysis which incorporated the OPEC. Only two of SYM solutions were consistent with the OPEP behaviour of large-L phase shifts. The phase-shift analysis was also performed for the 210 MeV

data and again led to the solutions similar to SYM and evidence was found
supporting SYM 1.

In 1960, the Yale group started the energy-dependent analysis including
the data from 9.7 to 345 MeV. The advantages of energy-dependent
analysis are:

1) Phase-shift analysis at one energy can yield many solutions, and
the theoretical guides for energy dependence can distinguish reasonable
from unreasonable solutions.

2) S wave dominates at low energy and higher L should appear succes-
sively as energy increases.

3) Experimental idiosyncrasis can be revealed.

The form of the energy dependence can be chosen so as to have enough
freedom to match the data (Yale approach) or to have a plausible form from
the theoretical standpoint (Livermore approach). Two approaches are
in practice quite close since both are flexible and both have some theo-
retical justification. The phase-shift form used in the Livermore analysis
is

$$\delta_\ell^{S,J} = \delta_{\ell 0}^{S,J}(T) + \sum_{i=1}^{N} \alpha_i(S,J) F_{\ell,i}(T) \tag{3.1}$$

where T is the kinetic laboratory energy, and α are the coefficients
searched for. For S waves, δ_{00} is taken from the effective-range theory,
and for other waves $\delta_{\ell 0}$ is taken from OPEP.

$$F_{\ell,i}(x_0) = (x_0 - 1) \int_0^1 Q\left(\frac{x_0 - x}{1 - x}\right) \frac{x^{i-1/2}}{1-x}\, dx$$

where $x_0 = 1 + 4\mu^2/MT$, μ is the pion mass, and Q is the Legendre function
of the second kind.

3.1. Proton-proton data below 400 MeV

The Livermore phase-shift analysis AM VII included 1084 data points
[Ma 68a]. A few small-angle data were omitted since they contained ob-
vious systematic errors. The criterion for the data selection was based
on self-consistency. All data from 1 to 400 MeV were considered, and
a subset of data was formed of those data having $\chi^2 \leq 1$ per data point.
This set consisted of 439 data and was considered to be a new basic set
for re-examining all data. This time all data with $\chi^2 < 1.55$ were in-
cluded forming a new basic set. This set was used to make a final selec-
tion which contained 839 data points. Thus, 245 data points were discarded
as "bad" data. Examples of data not included in the analysis are
a) $\sigma(\theta = 10° - 41°)$, E = 98 MeV, uncertainty 3% (Harwell 1960)
b) $P(\theta = 31° - 67°)$, E = 107 MeV, uncertainty 5% (Harvard 1958).

The phase shift solutions were obtained using 20, 23 and 30 free para-
meters in Eq. (3.1). The number of free parameters for each partial
wave and the total χ^2 are given in Table 3.1 (from AM VII).

Figure 5 shows some phase parameters from the solution AM-VII
together with the "corridor of errors" which increases at higher incident
energies.
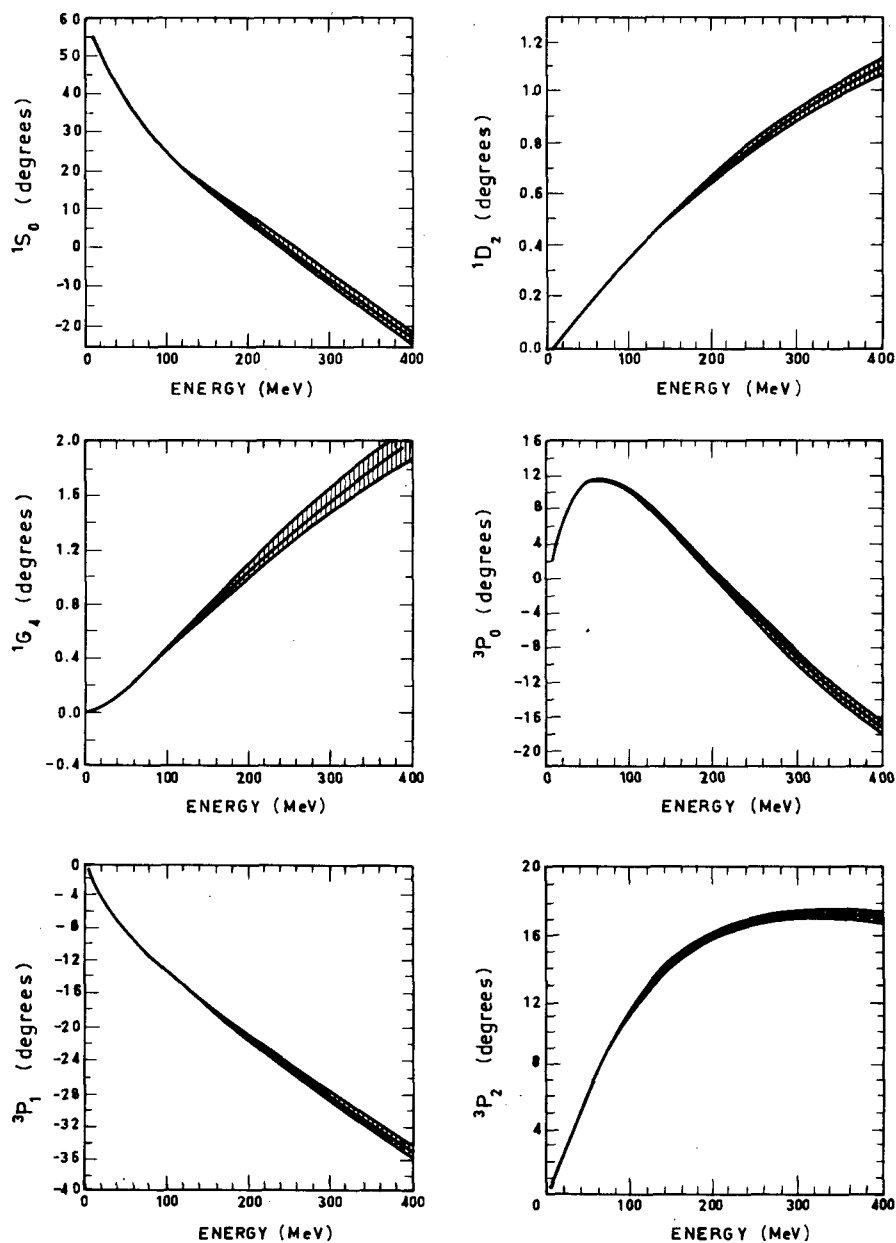
FIG.5.   Some phase parameters.

TABLE 3.1. NUMBER OF PARAMETERS FOR EACH
PARTIAL WAVE AND TOTAL χ^2

Number of parameters	30	23	20
χ^2	810	858	874
$^1S_0$	4	4	4
$^1D_2$	3	2	2
$^1G_4$	2	1	1
$^3P_0$	2	2	2
$^3P_1$	4	2	2
$^3P_2$	3	3	3
ϵ_2	3	2	2
$^3F_2$	2	1	1
$^3F_3$	2	1	1
$^3F_4$	1	1	1
ϵ_4	1	1	1
$^3H_4$	1	1	
$^3H_5$	1	1	
$^3H_6$	1	1	

TABLE 3.2. COMPARISON OF NEW AND OLD PHASE PARAMETERS

Phase parameters	$^1S_0$	$^1D_2$	ϵ_2
new	38.12 ± 0.47	1.81 ± 0.11	- 1.89 ± 0.14
old	37.50 ± 0.78	2.16 ± 0.27	- 2.27 ± 0.36

The Yale phase-shift analysis used 886 data and the results are given
in Ref. [Br 67] and go under the name Y-IV. The Y-IV represent a signi-
ficantly better fit than YRB1 (Ko) or YLAM, the earlier Yale analyses.
     The effect of the very accurate measurement at 49.4 MeV
[Ba 67] on the phase-shift analysis is shown in the analysis of Perring
[Pe 67]. Since the experimental accuracy of 0.5% represents an improve-
ment of an order of magnitude over the older data, a significantly more
accurate phase shift could be obtained (see Table 3.2). Perring concluded:
"The phase shifts are now so accurately known that there seems to be
no motive for further p-p experiments at 50 MeV2."

3.2. Proton-proton data, energies above 400 MeV

     Difficulties of the phase-shift analysis above 400 MeV are:
     1. Inelastic effects are important, e.g. at 660 MeV almost half of
         the scattering events are inelastic;

2. many partial waves have to be taken into account;

3. extensive elastic scattering data exist only at a few energies
   (e.g. 430 and 650 MeV) and inelastic data are quite poor.

The approach to the analysis consists of

a) estimating the imaginary part of the phase shifts from the data on pion production using the (3,3) resonance model for pion-production [Ma 58];

b) determining the real part of the phase shifts on the basis of the extrapolation of well-determined solutions below 400 MeV. This method was successfully used for the 600 MeV analysis [Ho 63, Ho 63a] and then extended up to 1 GeV [Ha 64].

Above 1 GeV the condition a) should be modified since the Mandelstam model is not valid there. The imaginary phase shifts were calculated on the basis of the OPE model for pion production with the use of unitarity [Am 67]. Thus at $E \gtrsim 1$ GeV a) should be replaced by a'):

a') The imaginary phase shifts with $L > L$ critical should be taken from the Amaldi model [Am 67].

An additional constraint can be taken:

c) The intermediate and long range part of nuclear force is represented by OBE.

The analyses at 1, 2 and 3 GeV have shown some validity of this approach [Ha 65, Ha 66].

The Livermore analysis AM-VIII [Ma 68b] included 599 data between 358 and 736 MeV coupled with the set of data representing the region below 400 MeV. The energy-dependent form (3.1) was used with 31 and 38 free parameters. Also the explicit inclusion of σ, ρ and ω exchange contribution was considered together with 20 and 25 free parameters. The result of the analysis indicates that the inclusion of OBE does not give any improvement. Also, the addition of more free parameters did not yield smaller χ^2.

Figure 6 shows some phase parameters from solution AM-VIII (taken from Ref. [Ma 68b]). The inelasticity part for all solutions was taken from the Amaldi model. Solutions 1 and 2 are with 31 and 38 free parameters, and 3 and 4 include OBE with 20 and 25 parameters, respectively. Also shown are analyses at specific energies. Solution 1 yields $\chi^2 = 1.3$ per data point. Some problems revealed by this analysis are:

i) The treatment of inelastic scattering is not satisfactory. The Amaldi model is valid around 1 GeV, and at 600 MeV predicts the total reaction cross-section which is one half of the experimental one.

ii) The experimental accuracy is poor. One needs 5% accurate triple-scattering data, and it seems that the effective target polarization is 20% wrong. An order-of-magnitude improvement of the present accuracy of data is needed if the analysis around 500-700 MeV is to be as accurate as those below 400 MeV.

TABLE 3.3. VALUES OF SOME PHASE SHIFTS

	$^1S_0$	$^1D_2$	$^3P_0$	Number of data	χ^2	$D(90°)$	$A_{xx}(70°)$
Solution 1	- 50.8	16.0	- 65.9	60	51.8	0.70	- 0.09
Solution 2	- 36.6	10.5	- 46.5	60	40.7	- 0.31	- 0.51
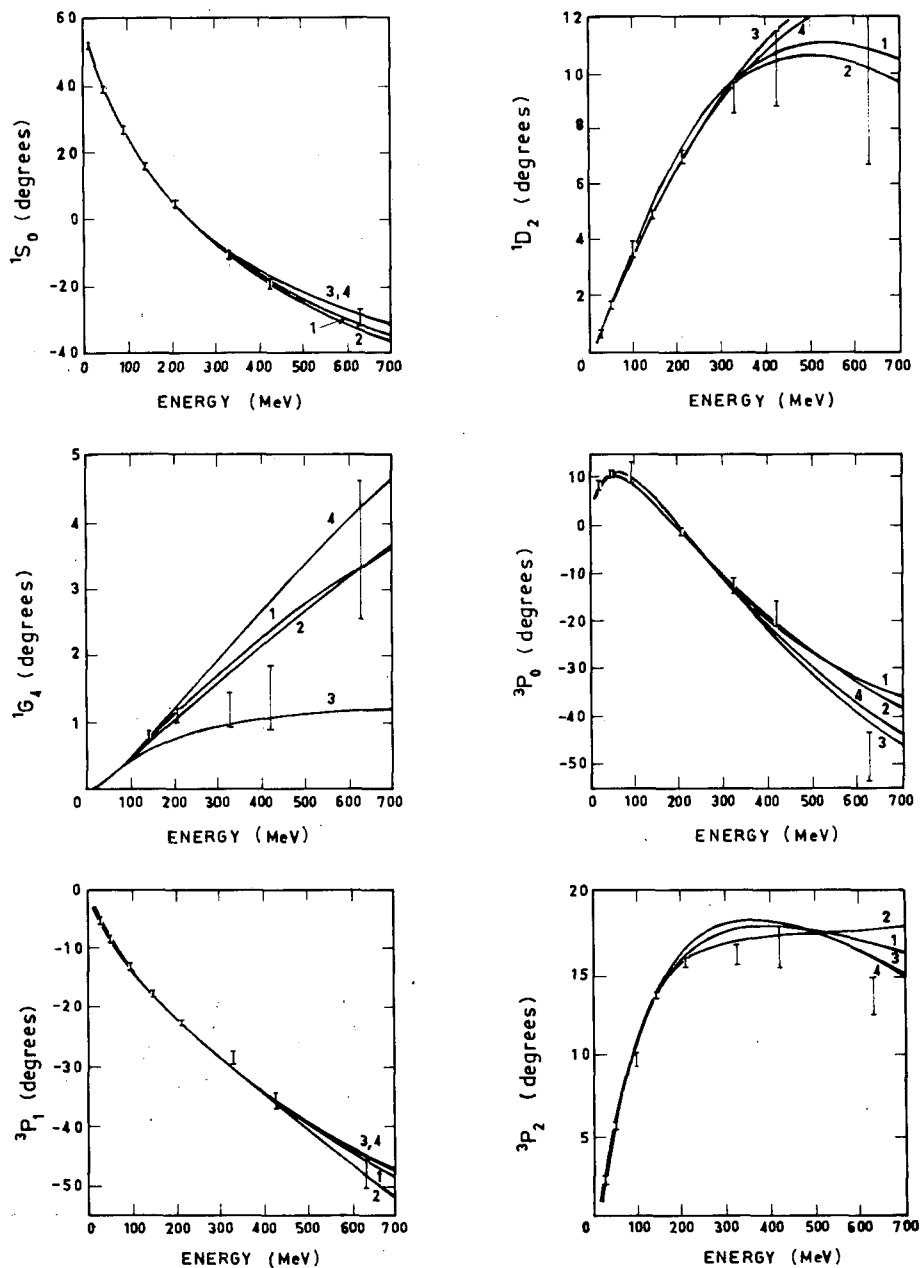
FIG. 6.   Some phase parameters of solution AM-VIII.

TABLE 3.4.   ANALYSIS OF p-p DATA AT 2 GeV AND 3 GeV

	2 GeV			2.85 GeV		
	Sol.1	Sol.2	Sol.3	Sol.1	Sol.2	Sol.3
$^1S_0$	- 73.3	- 105.1	- 70.0	- 66.8	- 136.5	- 120.0
$^1D_2$	- 27.9	29.2	- 19.0	- 45.5	44.3	46.0

The analysis [Ho 68] of 970 MeV data from Saclay and Birmingham yields two solutions. Further experiments are needed to discriminate the correct solution, and the most valuable measurements are D(90°) and $A_{xx}(70°)$. Table 3.3 shows the values of some phase shifts for these solutions together with the predicted D and A_{xx}. The analysis of p-p data at 2 GeV and 3 GeV also yield ambiguous solutions, which correspond to the solutions at 970 MeV. The results are given in Table 3.4.

The phase-shift analyses from 400 MeV to 3 GeV showed:

1. $\delta(^1S_0)$ decreases monotonically with energy even at as high energies as 0.6 to 2 GeV. Since the $^1S_0$ state does not suffer any serious inelastic effect, this monotonic decrease suggests that the repulsive core exists up to these energies.

2. $\delta(^1D_2)$ is strongly influenced by inelastic effects and one cannot deduce directly information on real potentials from its real phase shifts. However, solution 1 at 2 and 3 GeV is consistent with the hard core, and solution 2 is inconsistent. The two solutions could be discriminated by the measurements of C_{nn} and C_{kp} at 1.5 - 3 GeV.

3. The P-wave interval: $[\delta(^3P_0) - \delta(^3P_1)]/[\delta(^3P_1) - \delta(^3P_2)]$ in the 660 MeV phase-shift analysis is $(0.1 \sim - 0.1) \pm 0.4$ in agreement with LS type potentials (0.5) and in disagreement with tensor type potentials (-2.5). However, the potentials having besides the central and tensor also the LS term predict too large a $\delta(^3F_4)$ at 660 MeV. The reduction of the LS force on F waves can be achieved by the non-static quadratic LS.

3.3.   Neutron-proton data

Neutron-proton data are rather incomplete and considerably less accurate than p-p data. The phase-shift analysis can yield meaningful unique results only if one assumes CI and takes T = 1 phase shifts from p-p data. MacGregor et al. [Ma 68] attempted the analysis of 140 MeV n-p data only, but essentially found an infinite number of solutions.

The Livermore analysis of n-p data AM-IX [Ma 68] uses 912 n-p data in the 0 - 400 MeV interval, and 95 data in the 410 - 750 MeV interval and assumes T = 1 p-p phase shifts. Owing to scarcity of n-p data, no self-consistency criterion can be applied, and only a few obviously in-correct data were rejected. Examples of the data with large uncertainties, but nevertheless included in the analysis are:

P ($\theta = 21° - 101°$), E = 30 MeV, uncertainty 50%, Harwell 1965
R ($\theta = 42° - 84°$), E = 137 MeV, uncertainty 80%, Harvard 1962

After determining T = 0 phase parameters (T = 1, fixed from p-p), a
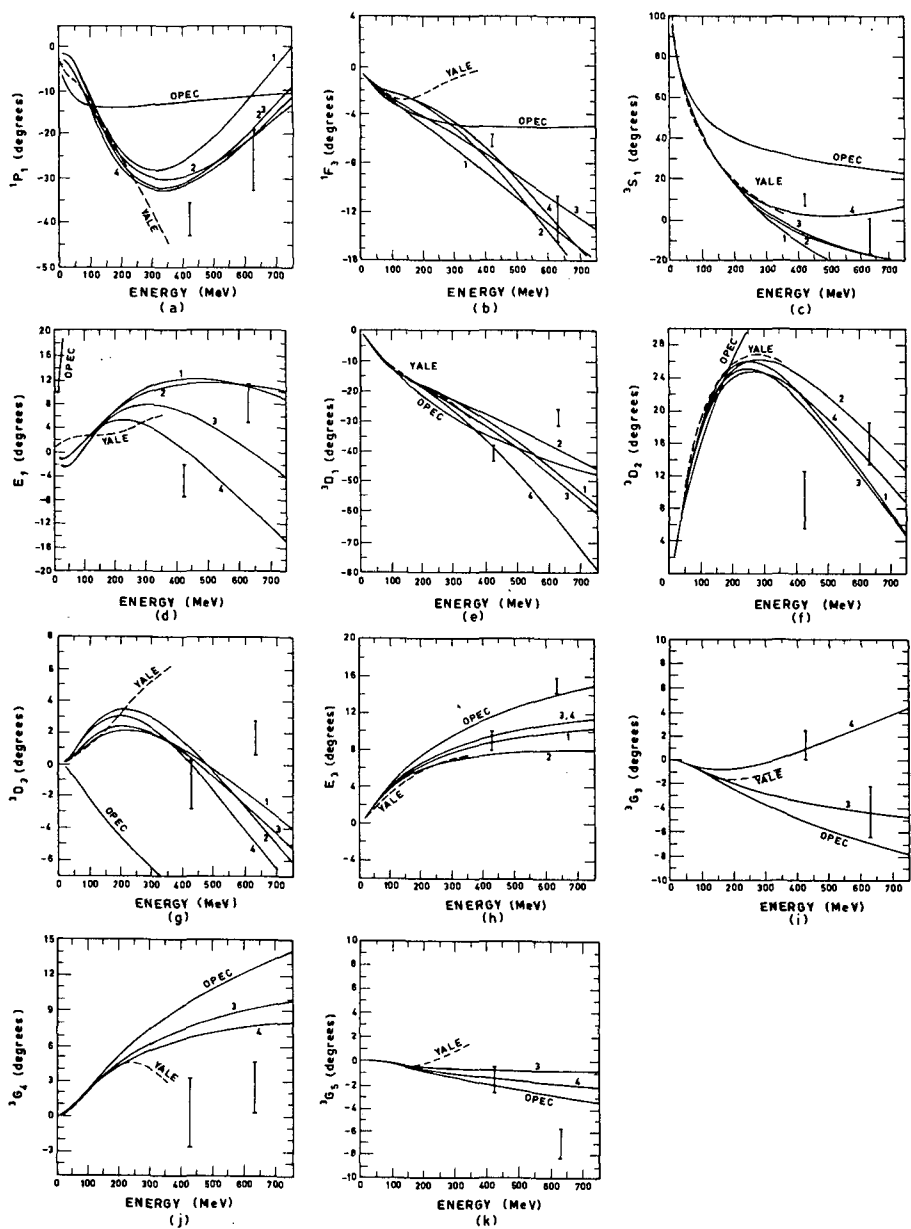
FIG. 7.   T = 0 energy-dependent solutions of AM-IX.

search was made releasing also T = 1 phase parameters, but both sets
were essentially identical, implying that n-p data are consistent with
p-p T = 1 phase shifts.

Energy-dependent analysis up to 750 MeV was performed using T = 1
p-p phase parameters and assuming T = 0 phases to be wholly elastic over
the entire energy region, since the isospin conservation prevents T = 0
phases to be coupled to (3.3) resonance that seems to dominate T = 1 in-
elastic scattering near the threshold.

The final data used in AM-IX consist of 901 n-p data from 14 to
730 MeV. Phase parameter solutions were obtained using 29, 22 and
19 parameters. The χ^2 values were 1134, 1172 and 1360, respectively,
and the preferable solution is the 22-parameter solution. Figure 7 shows
the T = 0 energy-dependent solutions of AM-IX.

The combined T = 1 phases from AM-VIII and T = 0 from AM-IX used
1147 p-p and 901 n-p data. χ^2 per data point was 1.34, when 53 pheno-
menological parameters were used to represent 14 free T = 1 and 11 free
T = 0 phases.
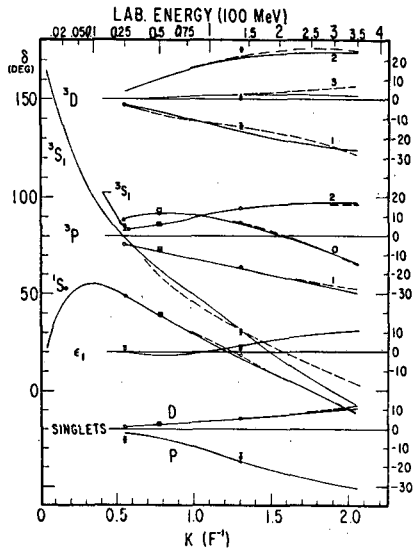
FIG.8.   Phase parameter solutions.

Figures 8 and 9 represent phase-parameter solutions obtained by
the Livermore (solid curves) and Yale (dashed) groups. The squares are
from the analysis of Hoshizaki (50 MeV) and circles are due to Perring
(25, 50 and 140 MeV). δ(S) has the ordinates on the left, and P and D on
the right. The ordinate scaling for ϵ, F and G is 4 times as large, and
for H is 8 times as large. The energy-dependent Livermore and Yale
analyses are, in general, in very good agreement except for ϵ_1 and $^1P_1$
at low energies. The Yale analysis fixed phases to be OPEP at low energies,
while the Livermore analysis has not such a restriction and the Livermore ϵ_1
and $^1P_1$ strongly deviates from their OPEP values. Thus, one can say
that there is nothing in the data that requires ϵ_1 and $^1P_1$ to have the OPEP
behaviour in 10-25 MeV range. However, the sign of the quadrupole moment
of the deuteron implies $\epsilon_1 > 0$ at very low energies contrary to the Livermore
result.
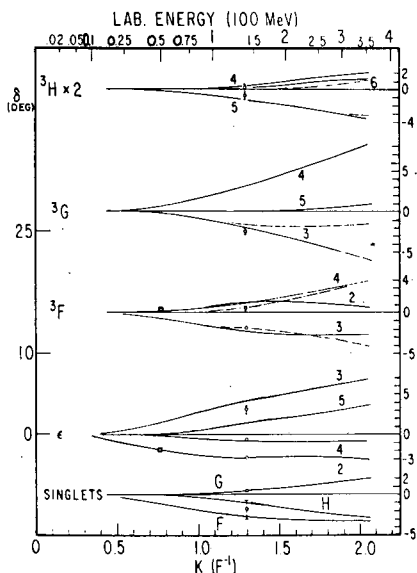
FIG.9.   Phase parameter solutions.

3.4. Conclusion of the phase shift analyses

The p-p T = 1 phase shifts up to 400 MeV are quite accurately known.
In the 400 - 750 MeV interval the accuracy of phase parameters is, at
least, an order of magnitude inferior, and because of the uncertainties
in the handling of inelasticities, might even be worse. The phase para-
meters in the interval 1 - 3 GeV are much worse.

The n-p data are insufficient and quite inaccurate, which is reflected
in large uncertainties in T = 0 phases even when CI is assumed. Even
at low energies 10 - 100 MeV n-p data are poor.[1] The knowledge of T = 0
phase parameters below 400 MeV is bad to fair, particularly poor is ϵ_1
and $^1P_1$. At energies above 400 MeV T = 0 phase parameters are very
badly known.

3.5. Low-energy p-p and n-p data

A number of very accurate p-p scattering experiments have been per-
formed in the energy region between 0.3 and 15 MeV.

a) Relative cross-sections have been measured to an accuracy of 1%
at six energies between 0.33766 and 0.40517 MeV at $\theta_{c.m.} = 90°$. The
destructive interference between Coulomb and nuclear forces causes a
pronounced minimum in $\sigma(90°)$ around 400 keV. The cross-section is

$$\sigma(90°) = \left(\frac{2e^2}{mv^2}\right)^2 \left[1 - \frac{2}{\eta} \sin\delta_0 \cdot \cos\epsilon + \frac{1}{\eta^2}\sin^2\delta_0\right] \qquad (3.2)$$

---

[1] An example is the $^1P_1$ phase at 25 MeV which is - 2.06 ± 2.66 (Livermore) or - 6.21 ± 1.28
(Perring [Pe 67]). OPEP is - 7.02. The crucial value is $\sigma(180°)/\sigma(90°)$. The present analyses had to
depend on the old measurement of $\sigma(\theta)$ at 27.2 MeV [Br 51].

where $\eta = e^2/\hbar v = 0.1581 \, (E_{MeV})^{-1/2}$, $\epsilon = \delta_0 - \eta \ln 2$ and in the vicinity of the minimum, $\eta = \delta$, $\cos \epsilon \cong 1$. Energy measurement determines the phase shift. A velocity measurement [Br 64] enabled a very accurate measurement of the energy, to an accuracy of 0.2 keV: E (min) = 382.43 ± 0.20 keV, compared with a previous accuracy of 1.5 keV. This accuracy permitted the determination of the phase shift to an accuracy of 0.01°, which implied that the shape parameter P in the effective range expansion can be determined to an accuracy of ± 0.02.

   b) Differential cross-sections have been measured at 13 angles at 1.397, 1.855, 2.425 and 3.037 MeV. An accuracy of 0.1 to 0.3% has been achieved [Kn 59, Kn 66].

   c) The angular distribution at 9.69 MeV, with an accuracy of 0.7% [Jo 59].

   d) A_{yy}/A_{xx} at 90° at four energies between 11.4 and 26.5 MeV [Ca 67].

   e) There also exist earlier angular distribution data which extend up to 4.2 MeV [Wo 53] and recent data at 6.141, 8.097 and 9.918 MeV [Sl 68], the accuracy of which has been questioned.

   To extract very accurate S phase shifts, one has to make certain assumptions about higher-L phase shifts. The analysis of data c) and d) [No 67] shows that i) higher phase shifts are small and consistent with their OPE values, in particular $\delta(^1D_2)$ is within 30% of its OPE; ii) one cannot obtain a unique solution of the 4-parameter (one S and three P) phase-shift analysis; iii) the quantities Δ_C, Δ_T and Δ_{LS} are linear combinations of $\delta_{1.0}$, $\delta_{1.1}$ and $\delta_{1.2}$ and in the Born approximation they are proportional to the matrix elements of the central, tensor and spin-orbit potentials. The analysis yields a very small $\Delta_{LS}/\Delta_T \sim 0.07 - 0.15$ which can be understood in terms of the short-range LS force; iv) if one fixes Δ_{LS}/Δ_T in the range 0.07 - 0.15 one can uniquely determine δ_0, Δ_C and Δ_T at 9.69 and 11.4 MeV.

   p-p scattering is not only influenced by nuclear forces but also by Coulomb forces, magnetic interaction and vacuum polarization (VP) effects. The VP potential falls off exponentially at large distances with a range corresponding to the Compton wavelength of an electron-positron pair (193 fm):

$$V_{vp}(r) = \frac{2\alpha e^2}{3\pi r} \int_1^\infty dx \, e^{-2K_e^r x} \left(\frac{1}{x^2} + \frac{1}{2x^4} \right) (x^2 - 1)^{1/2}$$

where $\alpha^{-1} = 137$ and $K_e^{-1} = 386.2$ fm.

   The magnetic interaction falls off as r^{-3} and they both influence a large number of L. The phase shifts in p-p scattering are defined by:

$$R_L(r) = \cos \delta_L^E \, S_L(r) + \sin \delta_L^E \, T_L(r), \qquad r \gg \frac{\hbar}{\mu c}$$

$$R_L(r) = \cos K_L F_L(r) + \sin K_L G_L(r), \qquad r \gg (2K_e)^{-1}$$

$$K_L = \delta_L^E + \tau_L$$

where τ_L is the phase shift produced by the electromagnetic potential with respect to the Coulomb functions F_L and G_L.

The effective-range expansion for p-p δ_0^E is

$$[C^2 k/(1 - \phi_0)][(1+\chi_0)\cot\delta_0^E - \tan\tau_0] + 2\eta\,k[h(\eta)+\ell_0(\eta)]$$

$$= -\frac{1}{a} + \frac{1}{2}r_0 k^2 - P r_0^3 k^4 + Q r_0^5 k^6 + \dots \qquad (3.3)$$

C^2, η and $h(\eta)$ are parameters which arise in a pure Coulomb problem, while χ_0, ϕ_0, τ_0 and ℓ_0 are non-Coulomb electromagnetic parameters.

The phase δ_0^E at 382.43 keV is $14.611 \pm 0.011°$.

The $^1S_0$ effective-range parameters extracted from the low-energy p-p data are given in Table 3.5.

The analysis of Slobodrian [Sl 68] differs from other analyses. In particular, it has employed the data e). The quadratic fit is very satisfactory. The fact that $P > 0$ is further evidence for OPEP since various potential models which include OPEP predict $P > 0$.

The analysis of the low-energy n-p data [No 63] gives: $a_{np} = -23.678 \pm 0.028$ fm; $r_{np} = 2.5166 \pm 0.1036$ fm if one takes into account the rather recent cross-section of Engelke et al. [En 63]. The analysis which does not include Engelke's data would yield $r_{np} = 2.7$ fm. This result has been essentially confirmed by Breit et al. [Br 65], but they have pointed out that $r_{np} = 2.7$ cannot be excluded. The number of errors has been considered [Br 65]: dynamic effects of molecular electrons in n-p scattering at energies above the epithermal region, the participation of molecular structure of hydrocarbons, etc. More experimental work is needed to settle r_{np}.

Czibok, Hrehuss and collaborators [Cz 69, Hr 69] measured $\sigma(\theta_p = 0°)/\sigma(30°)$ in n-p scattering at 2.5, 2.7 and 2.8 MeV and found 1.07 ± 0.02, 1.07 ± 0.02, and 1.033 ± 0.012, respectively. The anisotropy of the n-p angular distribution together with the fine-structure in energy dependence of both total and differential cross-sections observed for $E_n < 6$ MeV should be carefully investigated experimentally.

4.   EXPERIMENTAL PROBLEMS IN N-N SCATTERING STUDIES

4.1. Proton-proton scattering

Various types of accelerators produce protons with energies up to ten GeV region (70 GeV). The advent of high-intensity machines (SF cyclotrons) solves the problem of beam intensity. The beam-energy resolution is adequate for N-N scattering studies.

The energy of the incident particle has been measured by velocity (very low energy, accuracy 0.2 keV), time-of-flight (at 50 MeV achieved an accuracy of ~0.1%), magnetic and electric fields, and at higher energies by the range (which at $E \gtrsim 100$ MeV sometimes included errors as large as 1 - 2 MeV).

Polarized beams can be obtained by i) nuclear scattering and reactions, and ii) production of slow polarized protons in a special ion source and the subsequent acceleration to higher energies. Two most common errors in (particularly older) experiments involving polarized beams are: a) carbon was very often used as a polarizer, and the polarized beam also contained the inelastic component. When this effect was realized

TABLE 3.5. $^1S_0$ EFFECTIVE-RANGE PARAMETERS EXTRACTED FROM LOW-ENERGY p-p DATA

a (fm)	r_0 (fm) ·	P	Q	Fit	χ^2	References
- 7.804 ± 0.006	2.748 ± 0.008	0	0	linear	16.8	[He 67]
- 7.816 ± 0.007	2.810 ± 0.018	0.035 ± 0.009	0	quadratic	1.11	[He 67]
- 7.819 ± 0.009	2.820 ± 0.044	0.043 ± 0.034	0.008 ± 0.031	cubic	1.05	[He 67]
- 7.815 ± 0.004	2.799 ± 0.016	0.029 ± 0.012	0	quadratic		[Br 68]
- 7.7856 ± 0.0078	2.840 ± 0.009	0.072 ± 0.005	0.034 ± 0.004	cubic		[Sl 68]

some of the older data had to be renormalized by 2 - 3%; b) the alignment is the crucial point in polarization, triple-scattering and spin-correlation experiments. Significant progress has been achieved using the solenoid. Thus, the data obtained without the solenoid are subject to a larger systematic error.

At low energies the uncertainties in target thickness and in uniformity (except for a gas target) might contribute a large error. In the higher-energy region the hydrocarbon targets are the most common type and the elimination of p-C scattering is achieved by measuring p-p coincidences, by subtraction, or by energy discrimination. Liquid targets have also been used. The gas and liquid target assembly should be carefully designed in order to avoid scattering due to the container walls.

Remarkable progress has been achieved in producing polarized targets. To be useful for scattering experiments the polarized target should have the following features: i) Polarization should be maintained in the presence of the incident beam. Since, e.g. a beam of 10^{10} protons/s each losing 1 MeV in the target, dissipates approximately 1 mW, all the methods which use extremely low temperatures are ruled out. ii) The target material should be dense enough and relatively simple. The successful polarized target has been developed by the Saclay group: $La_2 Mg_3 (NO_3)_{12} \cdot 24 H_2O$ in which 1% La is replaced by Nd. The amount of hydrogen is only 3%, but a large polarization has been obtained $P_T \sim 20 - 60\%$. The following problems have been experienced with the present polarized targets: a) large systematic errors in the determination of target polarization (P_T), typically ±10%; b) non-uniformity in P_T — a difference as large as a factor of 2 from the centre to the edge of the target; c) radiation damage of the target which causes the decrease of P_T by a factor of 2 after 10^{12} protons/cm^2 exposure. It would still be advisable to use not only solid-state but also nuclear methods to determine P_T and to perform these P_T calibrations in time intervals small in comparison with the damage rate.

The advantage that polarized beams — polarized targets offer over the conventional techniques is best seen when one compares, e.g., the Tokyo measurement of C_{nn} at 52 MeV, 20 counts/h, random/true = 10%, $P^2 = 0.15$, with the Saclay measurement of A_{yy} at 26 MeV, with 10 counts/s, random/true = 0.1%, $P_B P_T = 0.45 - 0.15$ implying that the same statistical accuracy can be achieved during half an hour of the Saclay measurement as in one month of the Tokyo experiment.
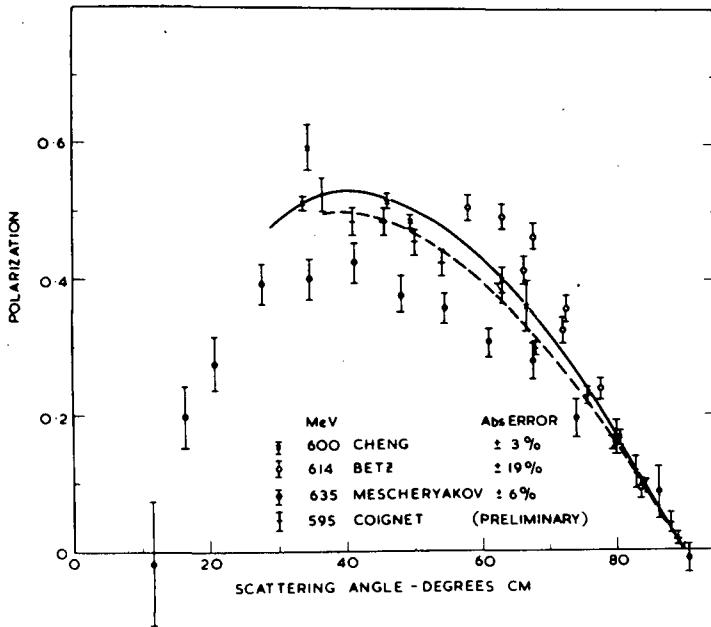
FIG.10.   p-p polarization near 600 MeV.

    A brief review of some experimental data is given as an illustration
of various experimental problems.
    Figure 10 shows the p-p polarization around 600 MeV, and Fig.11
around 700 MeV.   Betz and Dost used polarized targets and P_T was
determined using solid-state methods.   Ashgirey obtained a polarized
beam by scattering from hydrogen, and thus, no inelastic scattering
difficulties were present.   However, the same method used by Dost gave
a mean polarization by 15% lower than what was expected from p-p scatter-
ing at that energy.   Particularly bad agreement between various data is
at 600 MeV.
    Figure 12 shows the polarization in p-carbon scattering at 6° indicat-
ing that the measurement which used a carbon polarizer can contain
non-negligible uncertainties particularly above 350 MeV.
    The maximum polarization in p-p scattering as a function of energy
is shown in Fig.13.
    Figure 14 shows the data on C_{nn} at 600 MeV.   Dost used a polarized
target and a polarized beam produced by scattering from hydrogen.
Coignet also used a polarized target and a polarized beam produced by
p-C scattering.   The difference is 40%.

4.2.   Neutron-proton scattering (for an extensive discussion
       see also Ref.[Sl 68a])

    In the past ten years only half as many n-p data as p-p data have
been accumulated.   The experimental information on n-p scattering is
meagre, incomplete and often inaccurate.   The measurements of n-p
scattering are more difficult and more time consuming.   It should be
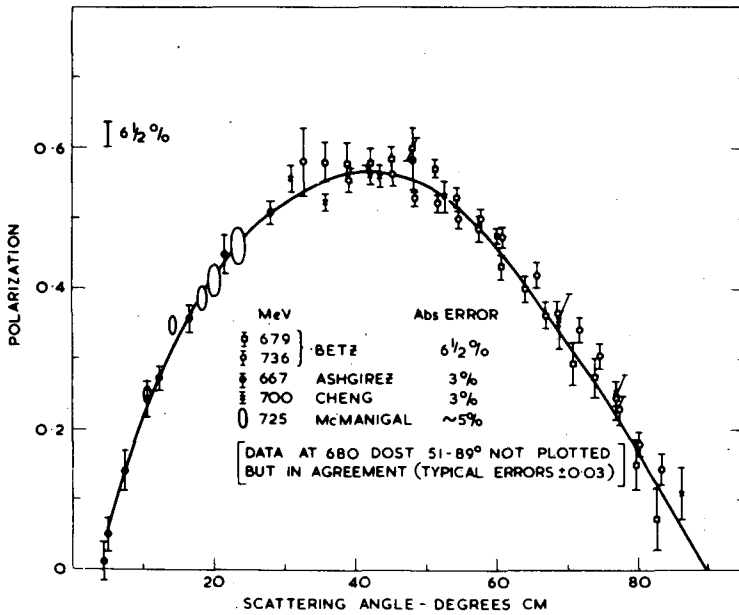
FIG.11.   p-p polarization near 700 MeV.
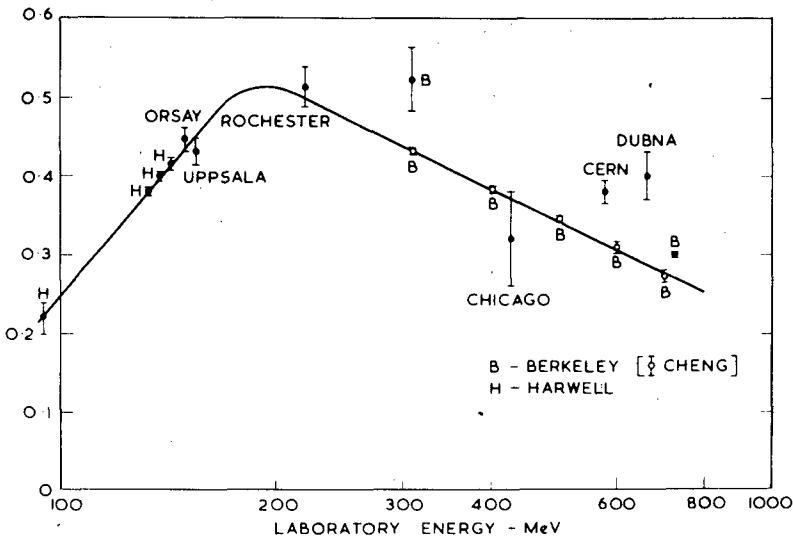
FIG.12.   Polarization in p-carbon scattering at 6° lab.

stressed that it is extremely important to perform accurate n-p scattering studies, and that many older measurements should be repeated with better techniques now available.

The development of intense charge particle beams has opened the possibility of producing neutrons of an arbitrary energy up to several GeV.
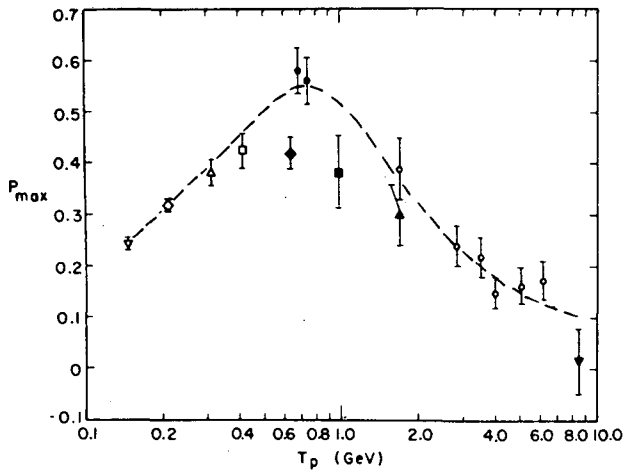
FIG.13.   Maximum polarization in p-p scattering as a function of energy.
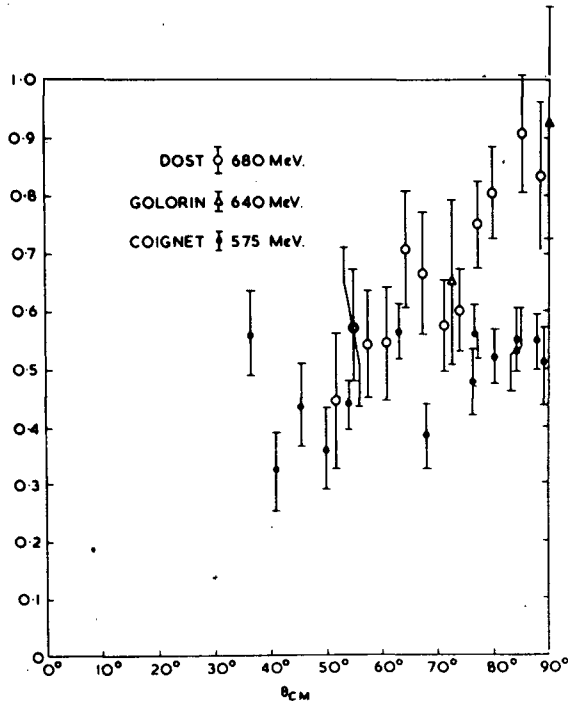
FIG.14.   Proton-proton scattering $\bar{C}_{nn}$ 600-700 MeV.

The problems to cope with are: i) the neutron-beam intensity which is
determined by the current the accelerator can supply to the target, by
the properties of the target, and by the cross-section for the particular
neutron producing reaction,   ii) the energy spectrum of the neutron beam.
Even at low energies (E_n < 30 MeV) the neutron beam is not monoenergetic

because of the energy loss and scattering of the charged particle producing neutrons, and the geometrical conditions. High-energy neutrons normally have a large energy spread (20-30%) and a low energy tail of intensity comparable with the main component. This low-energy tail can be eliminated by the time-of-flight condition, if the neutron energy is not too high ($E_n \lesssim 150$ MeV). Very useful reactions to produce "monoenergetic" neutrons in 100 MeV regions are D(p, n) and ^{7}Li(p, n).

The measurement of the energy and intensity of the neutron beam is typically one to two orders of magnitude worse than for proton beams.

Polarized neutron beams have been produced using various methods: i) neutrons from various reactions are already polarized. High polarization has been obtained; ii) unpolarized neutrons have been scattered from carbon, and typical polarizations obtained are up to $\sim 50\%$; however, the neutron energy resolution is quite poor and the intensity is rather low; iii) the D(p, n) reaction at 0° using polarized protons produces polarized neutrons. The difficulties are: polarization transfer below 250 MeV is low, typically 0.25 - 0.5 and the low-energy tail has the opposite polarization to the peak.

In view of difficulties related to the use of neutron beams many n-p scattering data have been accumulated using deuterium as a neutron target. The process $p + d \rightarrow p + n + p$ can yield reasonably meaningful p-n scattering data if one has ensured that the proton in the deuteron acted as a spectator during the scattering event. Such processes are called quasi-free scattering processes and have been indeed observed from very low energies (5 MeV incident energy) up. A quasi-free process can be treated in an impulse approximation which makes it possible to relate the experimental cross-section to the n-p data. This simple model can be improved in various ways: i) introducing double scattering corrections, ii) final state interaction, iii) the cross-section is actually related to the off-energy-shell matrix element and one should take this into account, iv) from the experimental point of view the scattering out of the scattering plane should be investigated since detectors often have a finite size. The effects i) - iv) can amount from a few percent (at $E \sim 200$ MeV) to an order of magnitude correction (at $E \sim 10$ MeV). The validity of models to treat quasi-free scattering has been investigated by comparing free and quasi-free p-p and n-p scattering. Figure 15 shows the difference ΔP between free p-p and quasi-free p-p polarization data against the opening angle between the counters. The data are compared with the final state interaction correction. Figure 16 shows n-p free and quasi-free polarization measurements at 140 MeV and the maxima differ by 20%, while the combined error is only 8%. Quasi-free and free p-p data compared in the region between 300-700 MeV show a disagreement of $\sim 10\%$.

The use of quasi-free scattering to obtain the n-p data can be summarized as follows: i) the impulse approximation model corrected for the final-state interaction can be used to extract n-p data if the energy is not low ($E > 100$), and if the final-state-interaction correction is small ($\lesssim 20\%$). Then the extracted n-p cross-sections are probably accurate to 10%; ii) the model is much better for polarization and triple-scattering data, since they involve the ratio of cross-sections. The extensive discussion of quasi-free processes and procedures to extract free-scattering data is found in [Cr 63, Ko 64, Sl 68b].
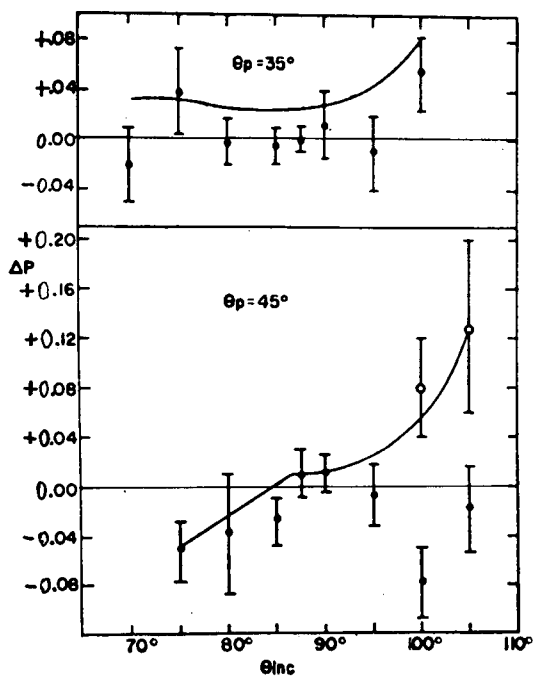
FIG.15.   ΔP difference between p-p and quasi-free polarization data against opening angle between counters.
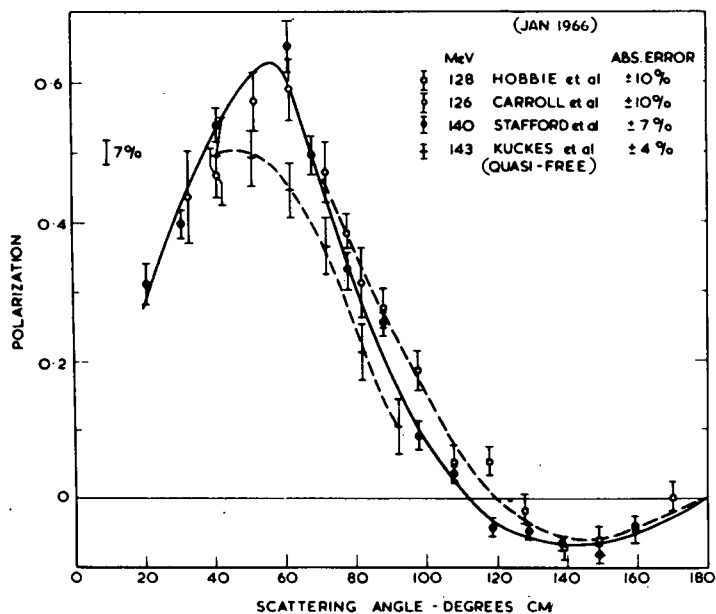
FIG.16.   n-p free and quasi-free polarization measurements.

5. N-N POTENTIAL MODELS

The most general non-relativistic N-N potential contains the central, tensor, spin-orbit and quadratic spin-orbit forces:

$$V = V_0(r) + (\sigma_1 \sigma_2)V_\sigma(r) + S_{12} V_T(r) + LS\, V_{LS}(r)$$

$$+ (\sigma_1 L)(\sigma_2 L) V_{QLS}(r) \tag{5.1}$$

V_0, V_σ, V_T and V_{QLS} have the OPEP tail, and the modification in the inner regions (II and III regions) is given by terms of the form $(1 + a(e^{-x}/x) + b(e^{-2x}/x^2))$ introduced by Hamada [Ha 62]. The outer part of V_{LS} should be given by OBEP or TPEP.

The quantitative nature of the potential in region II has been established fairly well [Ta 67]. The approach to understand region III depends on the reliability of our knowledge of region II.

In the following we summarize our present knowledge of the NN potential [Ta 67]:

Region II. $(0.7 < x < 1.5)$

Singlet even: $^1V_C^+$ is strongly attractive. Using the $\delta(^1S_0)$ below 50 MeV one can accurately determine the strength of the Hamada type $^1V_C^+$ potential, because other parts of the potential do not contribute.

The non-static V_{QLS} should be present to decrease $\delta(^1D_2)$, but it is difficult to separate the contribution of region I and region II to this potential.

Triplet odd: Tail of $^3V_{LS}^-$ is negative and the strength is about $^3V_{LS}^-$ $(x = 0.7) = -50$ MeV. Its range parameter $\sim 1/5.5$ determined by the mass of the vector boson. $^3V_C^-$ is weakly attractive: $^3V_C^-$ $(x = 1.0) = -3 - 5$ MeV. $^3V_T^-$ is positive, but weaker than OPEP.

Triplet even: Negative $^3V_T^+$ is weaker than OPEP. $^3V_C^+$ is strongly attractive. $^3V_{LS}^+$ is uncertain.

Singlet odd: Repulsive $^1V_C^-$ is weaker than OPEP.

Region III. $(x \lesssim 0.7)$

Singlet even: Repulsive core in $^1S_0$ and its radius is $x_c = 0.35 - 0.20$ (for $f^2/4\pi \approx 0.08 - 0.06$) for hard-core potentials. For the Gaussian soft core, its height is larger than 2 GeV.

Triplet odd: $^3V_{LS}^-$ is abruptly strong: $^3V_{LS}^-$ $(x = 0.5) < -200$ MeV. $^3V_C^-$ is not strongly attractive, but positive or weak. $^3V_C^-$ is not strongly positive, but negative or weak. The effective repulsive potential is necessary at short distances so as to cancel the attraction due to $^3V_{LS}^-$ in $^3P_2$ and $^3F_4$ states.

Triplet even: $^3V_C^+$ is strongly attractive, although $^3V_T^+$ is uncertain.

Singlet odd: Repulsion is probably strong.

A number of potential models has been developed:

i)   hard-core potentials: Hamada-Johnston (or Yale); $x_c = 0.343$

ii)   soft-core potentials: Bressel-Kerman Rouben [Br 69] when the soft
        core is the finite square well of radius $x_c = 0.4852$. Outside of the
        soft core the potential is of Hamada type. The height of the soft core
        is, e.g. 670 for $^1V_C^+$.
        soft (Yukawa) core: Reid [Re 68]. This type of the soft core produces
        quite a different wave function near $r = 0$ than the BKR potential, e.g.
        $\int_0^{0.8 \text{ fm}} u^2(r) dr$ for the ^3S wave function for the BKR potential differs from
        the Reid potential as much as the Reid potential prediction differs from
        the hard-core potential.

iii)   velocity dependent potentials

iv)   separable unlocal potentials, e.g. Tabakin [Ta 64] and Mongan [Mo 68]

v)   older potential model such as the Gammel-Thaler

vi)   OBEP models. The N-N data require the following mesons [Og 67]:
        a) $T = 0$, the scalar meson is required in all analyses. Its mass
        should be between 2 and 5 m_π and the coupling constant $g_s^2/4 = 1.2$ to 4.0.
        There is a relationship between m_s and g_s^2 and when m_s approaches
        the mass of the vector boson, g_s^2 increases since there is a large
        cancellation between vector and scalar mesons in OBE. There is no
        clear evidence regarding the existence of the $T = 0$ scalar boson. It
        could be a phenomenological substitute for the $\pi - \pi$ interaction in
        $T = 0$, $J = 0$ states.
        b) $T = 1$, the scalar meson indicated in the analysis of Bryan and
        Scott [Br 64a], but not in other analyses. There is no experimental
        evidence for the existence of such a boson.
        c) $T = 0$, the pseudoscalar boson is a well-known η, $m_\eta = 550$ MeV,
        and $g_\eta^2/4\pi$ from 4 to 12. Its significance in the N-N interaction is not
        very clear.
        d) $T = 1$, vector boson and $T = 0$ vector bosons are required by N-N
        data. Vector bosons ρ ($T = 1$), ω ($T = 0$) and ϕ ($T = 0$) are firmly
        established experimentally, masses 765, 753 and 1020 MeV, respec-
        tively, spin parity 1^-. The ρ and ω bosons play a crucial role, while
        the contribution of ϕ is not clear. Coupling constants $g_\omega^2/4$ 2 to 21.5,
        $f_\omega^2/4$ 0 to 3.1; f_ω/g_ω 0 to 1.2, $g_\rho^2/4\pi$ 0.31 to 2, $f_\rho^2/4\pi$ 1.8 to 7;
        f_ρ/g_ρ 1.5 to 3.5.
        e) The effect of 2^+ isoscalar and isovector bosons in the mass region
        1200 - 1500 MeV is not quite clear.

        Various potential models are compared in Table 5.1 with the results
of the phase-shift analysis of 71 p-p and 54 n-p data at 210 MeV.

        BKR and HJ give the best fit. Actually, HJ is inferior only in $^3P_2$
phase.

        The coupling parameter ϵ_1 is correlated with the ratio of central and
tensor potentials in $^3S_1 - ^3D_1$ and is a very important quantity in nuclear
physics (e.g. the binding energy of nuclear matter). The values of ϵ_1
are given in Table 5.2.

        The Green-Sawada [Gr 67a] and Brueckner-Gammel-Thaler potentials
which give better nuclear matter binding energy yield had $\epsilon_1 \sim -1.0$. Re-
sults for various potential models were compatible with the AM-IV phase-
shift analysis, but accurate n-p data used in Ref. [Mi 68] ruled out any
ϵ_1 smaller than 5.0.

TABLE 5.1. VARIOUS POTENTIAL MODELS AND RESULTS OF
PHASE-SHIFT ANALYSIS [Mi 68]

	Phase-shift analysis	BKR	HJ	Yale	Reid
χ^2	91	257	398	529	759

TABLE 5.2. VALUES OF ϵ_1 [Mi 68]

	Phase shift analysis [Mi 68]	AM-IV	BKR	HJ	Reid	Yale
ϵ_1	6.6 ± 0.7	2.91 ± 3.21	4.2	4.8	5.0	6.5

TABLE 5.3. VARIOUS POTENTIAL MODELS [No 67a] $\chi^2/648$

AM-IV	IRB (K_0) Yale	HJ	Yale potential	OBEM Scotti-Wong
1.38	1.94	3.08	3.91	2.53
Bryan-Scott	Reid	BKR	Tabakin	BGT
3.90	2.9	2.0	28	106

In Table 5.3, potential models were compared using a selected set of 648 p-p data in the 9-330 MeV region.

The Bryan-Scott potential was modified by including the latest $^1S_0$ Livermore phases. The value for Reid used 652 data and OPE for $J > 2$ [Yó 67]. The BKR potential is the best representation of the data. On the contrary, the Tabakin and BGT potentials are very poor.

6. SOME OPEN PROBLEMS IN NUCLEAR INTERACTION STUDIES

Our present understanding of nuclear interaction for the purpose of nuclear-physics studies is insufficient at least in the following:
 a) neutron-proton T = 0 phase parameters,
 b) N-N off-energy-shell interaction,
 c) neutron-neutron interaction and the degree of validity of CI and
  charge symmetry, and
 d) the importance of three-body, few-body and many-body forces.
We shall briefly review problems b) and c).

6.1. Off-energy-shell interaction

The properties of nuclear systems containing more than two particles depend upon the off-energy-shell interaction. The simplest processes to

measure off-energy-shell matrix elements are nucleon-nucleon brems-
strahlung (NNB) and three-body breakup processes. Information about
the off-energy-shell interaction has so far been extracted only from NNB:

$$N + N \rightarrow N + N + \gamma$$

The n-p B is expected to have the largest cross-section due to the dominant
E1 transition. The total electric dipole moment for the p-p system is
zero, and it remains zero if the recoil due to the gamma ray is neglected.
In this simple non-relativistic approximation E1 does not contribute to
ppB.

TABLE 6.1. $\sigma(30°, 30°)$ VALUES

| Energy (MeV) | Experimental value ($\mu b/sr^2$) | HJ [Ma 69] | | Bryan-Scott | | OBE |
		No Coulomb	With Coulomb	[Ma 69,	Br 67a]	[Ba 69]
3.2	$0.15 \, ^{+0.17}_{-0.15}$ [Si 68]	0.29	0.10			
10	0.42 [Jo 68]	0.58	0.44			
10.5	$0.5 \, ^{+0.7}_{-0.5}$ [Cr 68]	0.60	0.46			0.12
33.5	3.6 ± 1.1 [Sl 66]	1.47	1.32			
46	3.8 ± 0.7 [Sl 66]	2.06	1.89		1.91	
47.1	1.37 ± 0.29 [Ma 68c]	2.12	1.94			
48	2.68 ± 0.45 [Wa 66]	2.17	1.99			1.73
61.7	2.04 ± 0.24 [Ha 68]	2.90	2.66	3.24	2.63	2.60
65	2.34 ± 0.38 [Ma 69]	3.08	2.82			2.80
99	5.14 ± 0.22 [Sa 68]	5.03	4.75			5.27
158	10.2 ± 1.7 [Go 67]	8.46	8.12		8.06	9.4
204	13.0 ± 2.4 [Ro 67]	11.07	10.59	10.7	10.7	13.3

The results of measurements of ppB are summarized in Tables 6.1
and 6.2. Besides, there are data at E = 65 MeV: $\sigma(\theta_1 = \theta_2 = 25) = 2.21 \pm 0.35$;
$\sigma(\theta_1 = 25, \ \theta_2 = 35) = 1.98 \pm 0.23$; at 99 MeV $\sigma(\theta_1 = \theta_2 = 25) = 3.77 \pm 0.23$,
$\sigma(\theta_1 = \theta_2 = 40) = 18.83 \pm 1.15$; at 158 MeV $\sigma(\theta_1 = \theta_2 = 40) = 37$; at 200 MeV
$\sigma(\theta_1 = \theta_2 = 40) = 29.0 \pm 6.0 \ \mu b/sr^2$. Most of the measurements were done
by detecting two protons at angles θ_1 and θ_2 satisfying $\theta_1 + \theta_2 < \pi/2$. The
present status of experimental art is such that ppB cross-section measure-
ments could be done with an absolute accuracy of better than 5 - 10% (for
and extensive discussion see Ref. [Sl 68b]).

The npB data are meagre and inaccurate. There are some p-nucleus
B data which are in mutual disagreement and often give only the upper
limit. The reliable npB data are given in Table 6.3. Measurements of
npB are just becoming feasible. Accuracies of 20 - 30% can be achieved.

The NNB cross-section depends on processes in which the N-N inter-
action is followed or preceded by the emission of the gamma ray, and the

process in which the N-N interaction exists prior and after the emission of
the gamma ray (the so-called rescattering time). It is obvious that the
NNB cross-section depends on the off-energy-shell interaction. There is
no a priori reason that models which adequately represent on-the-energy-
shell interaction should adequately represent off-the-energy-shell inter-
action. NNB appears as a test for the NN interaction models, and speci-
fically as a criterion which can discriminate between models equivalent
on the energy shell.

Part of the NNB amplitude is model-independent, i.e. independent
of the off-energy-shell interaction. It is possible to write the ppB cross-
section as $(A/k\gamma) + B + O(k\gamma)$, where A and B are given in terms of matrix
elements for non-radiative corrections [Ny 67, He 68]. The model-
independent calculation accounts for 70% of measured ppB at 150 - 200 MeV

TABLE 6.2. $\sigma(35°, 35°)$ VALUES

Energy (MeV)	Experimental value ($\mu b/sr^2$)	HJ [Ma 69] No Coulomb	Bryan-Scott [Br 67a]	OBE [Ba 69]	Model independent [Ny 67]
20	1.3 ± 0.4 [Ba 68]	1.49	1.47	0.77	1.11
30	2.10 ± 0.28 [Th 67]	2.06	1.97	1.45	1.71
48	3.93 ± 0.57 [Wa 66]	3.26	2.93	2.93	3.0
52	3.6 ± 1.4 [Sa 68a]	(at 33°-33°)			
99	9.01 ± 0.33 [Sa 68]	7.27		7.88	
158	14.7 ± 2.5 [Go 67]	12.3	12.3	14.0	11.8
204	14.0 ± 2.7 [Ro 67]	16.4	16.4	20.4	15.3

The results of various calculations of ppB are shown in Tables 6.1
and 6.2.

Several calculations using HJ [Br 67a, Ma 69, Dr 68] are in very good
agreement: e.g. at E = 61.7 MeV $\sigma(30°, 30°)$ predictions are 2.98, 2.90
and 2.89 $\mu b/sr^2$, respectively. The inclusion of Coulomb forces is found
to reduce the cross-section (Table 6.1) by about 10% at 50 MeV, but much
more at very low energies. The calculation using the OBE model [Ba 69]
found only a 3% decrease when Coulomb forces were added at 60 MeV.

Table 6.1 reveals the difference between the hard-core potential and
the Bryan-Scott velocity-dependent potential. The calculations [Br 67a
and Ma 69] are not in agreement. One should favour Ref. [Ma 69] which
was able to reproduce elastic-scattering phases found by Bryan and Scott.

The comparison between various potential models cannot be done until
they are indeed equivalent on the energy shell. HJ gives a considerably
better fit to 25 - 50 MeV pp scattering data. In addition, there are gauge
corrections which have to be made for the velocity-dependent potential.

Calculations were done using the Tabakin potentials [Pe 67a, Ma 69],
and the result differs depending upon the values of ϵ_2. If one assumes
$\epsilon_2 = 0$ one obtains, e.g. at E = 61.7, $\sigma(30°, 30°)$, 2.2 $\mu b/sr^2$, and with
OPE for ϵ_2 one obtains 3.4 [Ma 69]. If one uses the Tabakin potentials
with the HJ for L > 2 one obtains 2.83 which is very close to 2.9 found
in Tables 6.1 for HJ.

Brown [Br 67a] investigated the re-scattering effects and found that it contributes 0.2% at 62 MeV and increases to 15% at 300 MeV. The re-scattering correction depends on the angle of gamma ray emission (θ_1 and θ_2 fixed).

All calculations give the quadrupole shape of the gamma angular distribution. This feature is model-independent. When $\theta_1 = \theta_2$ decreases a flattening of the angular distribution occurs as a consequence of going further off the energy shell.

TABLE 6.3. RESULTS OF npB CALCULATIONS

Energy (MeV)	(θ_p, θ_n)	Cross-section (μb/sr^2)	
		OBE	Experiment
10.5	30,30	24	
200	(30,30)	46	50 ± 15 [Br 68a]
200	(35,35)	60	55 ± 15 [Br 68a]
200	(37.5, 37.5)	92	110 ± 15 [Br 68a]

Energy (MeV)	θ_γ^{CM}	Cross-section $d\sigma/d\Omega_\gamma$ (μb/sr)	
		OBE	Experiment
200	60°	2.8	3.4 ± 1.0 [Ko 67]
200	108°	1.9	2.5 ± 0.8 [Ko 67]
200	147°	0.9	1.8 ± 0.5 [Ko 67]

NNB cross-sections were calculated using the OBE model in a fully relativistic and gauge-invariant manner [Ba 69]. The results are given in Tables 6.1 and 6.2. The exchange of scalar, pseudo-scalar and vector bosons with T = 0 and T = 1 were considered. The same model was used to calculate npB. The exchange of charged bosons and gauge invariance requires the inclusion of diagrams in which the photon is emitted from internal meson lines and from vertices if they contain gradient couplings. The typical npB angular distribution of gamma rays has the E1 shape. The coplanar npB symmetric cross-section decreases as E_{inc} decreases opposite to the result of Pearce et al. [Pe 67a]. The results of npB calculations are given in Table 6.3.

The total cross-section at 200 MeV is 35 ± 12 μb and the theoretical prediction is 30 μb [Ba 69].

More npB measurements are needed.

6.2. Neutron-neutron interaction

From the experimental viewpoint our understanding of the nn force is restricted to some attempts to determine the scattering length a_{nn}. The summary of various measurements using the D(n, p)2n reaction are given in Table 6.4.

The results extracted from studying more complex reactions are given in Table 6.5.

TABLE 6.4. VARIOUS MEASUREMENTS USING THE D(n, p)2n REACTION

Energy (MeV)	a_{nn} (fm)	Reference
14.4	- 22 ± 2	[Il 61]
14.4	- 21.7 ± 1	[Ce 64]
13.9	- 23.6 ± 2	[Vo 65]
22	- 17 < a_{nn} < - 15	[De 66]
13.9	- 14 ± 3	[Ba 67a]
14.1	- 22 ± 3	[Sh 68]
8 to 28	- 16.8 ± 1	[Bo 68]
14	- 20 - 23	[Bo 69]

TABLE 6.5. RESULTS FROM MORE COMPLEX REACTIONS

Reaction	Energy (MeV)	a_{nn} (fm)	Reference
$^3H(n, d)2n$	14.4	- 18 ± 3	[Aj 65]
	15.1	- 17 ± 2	[Fu 68]
$^3H(d, ^3He)2n$	22	- 22 (5°)	[Ma 69a]
		- 14 (8°)	
$^3H(^3H, \alpha)2n$	22	- 16 ± 3	[Gr 68]

None of these values is reliable (see Ref. [Sl 68b]). The reaction $\pi^- + d \rightarrow 2n + \gamma$ is a considerably better candidate to extract a_{nn}, since there is only one strong final-state interaction: n-n. The available data show some inconsistency: $a_{nn} = - 12 \pm 5$ fm [Sl 65], $- 16.9^{+4.4}_{-7.8}$ fm [Ry 64], $- 16.5 \pm 1.3$ fm [Ha 65a], $- 18.4 \pm 1.5$ fm [Ny 68] and $- 13.1^{-3.4}_{+2.4}$ [Ni 68]. In addition, there are theoretical uncertainties which optimists estimate to be ~ 1 fm.

The comparison procedure [Sl 68b] has been suggested to extract a_{nn} and, particularly, it has been recommended to use kinematically completely determined measurements in the comparative analyses. In a not very rigorous manner, the comparative procedure was applied to obtain a_{nn} by comparing $^3H(d, ^3He)2n$ and $^3He(d, ^3H)2p$ processes: -16.1 ± 1.0 [Ba 66] and D(n, p)2n and D(p, n)2p a_{nn}: $- 16.7^{+2.6}_{-3.0}$ fm [Sl 68c]. r_{nn} was also determined: 3.2 ± 1.6 fm [Ba 66], which is indeed stretching things too far!

Kinematically complete measurements were also performed for the D(n, 2n)p reaction at 14 MeV yielding $a_{nn} = - 24 \pm 4$ fm [Ni 65], $- 25 \pm 3$ fm [Pe 67b] and $- 18.8^{+5.6}_{-11.9}$ [Ho 68a] at 18.5 MeV $a_{nn} = - 16.4 \pm 2.9$ [Ze 69]. The study of the D(p, pp)n reaction gave for $a_{np} = - 23.9 \pm 0.8$ [Va 69] in agreement with the experimentally known a_{np} and, thus, there it is

possible to determine a_{nn} from the comparison procedure applied to complete experiments.

A comparison of p-p and n-p data indicates that CI is broken by ~3% as is expected from the mass difference between charged and neutral bosons. The question of charge-symmetry violation is opened. Radiative corrections to boson-nucleon vertices and π-η and ρ-ω-ϕ mixing could cause the charge-symmetry breakdown ~1% and the data do not exclude it. The comparison between a_{nn} and the nuclear part of a_{pp} reflects not only the departure from charge symmetry, but also the type of the N-N potential used to correct electromagnetic effects. Strictly speaking, electromagnetic and nuclear interaction effects cannot be separated completely, e.g. nuclear force depends on the masses of the boson and the splitting is believed to be of electromagnetic origin, and anomalous magnetic moments result from nuclear forces [He 67]. The predictions for nuclear effective range parameters using hard-core potentials are:

a = - 17.067 fm, r = 2.933, P = 0.02 [Ta 67],
a = - 16.7 fm [He 64], and for velocity-dependent potentials
a = - 19.3 fm [Si 64].

The present knowledge of the nn-interaction is inadequate and much more experimental and theoretical studies are required.

REFERENCES

[Aj 65]   AJDAČIĆ, CERINEO, LALOVIĆ, PAIĆ, ŠLAUS, TOMAŠ, Phys. Rev. Lett. 14 (1965) 442.
[Am 67]   AMALDI, BIANCASTELLI, FRANCAVIGLIA, Nuovo Cim. 47 (1967) 85.
[Ba 66]   BAUMGARTNER et al., Phys. Rev. Lett. 16 (1966) 105.
[Ba 67]   BATTY et al. in [Pe 67].
[Ba 67a]   BAR AVRAHAM, et al., Nucl. Phys. B1 (1967) 49.
[Ba 69]   BAIER, KÜHNELT, URBAN, (unpublished internal report).
[Be 53]   BETHE, H.A., Scient. Am. 189 (1953) 58.
[Bo 68]   BOND, A., Nucl. Phys. A120.(1968) 183.
[Bo 69]   BOUCHEZ, R., (private communication).
[Br 36]   BREIT, G., FEENBERG, E., Phys. Rev. 50 (1936) 850.
[BR 36a]   BREIT, CONDON, PRESENT, Phys. Rev. 50 (1936) 825.
[Br 37]   BREIT, G., Phys. Rev. 51 (1937) 248.
[Br 51]   BROLLEY, COON, FOWLER, Phys. Rev. 82 (1951) 190.
[Br 60]   BREIT, G., Phys. Rev. 120 (1960) 278.
[Br 60a]   BREIT, HULL, LASSILA, PYATT, Phys. Rev. 120 (1960) 2227.
[Br 63]   BRYAN, DISMUKE, RAMESAY, Nucl. Phys. 45 (1963) 353.
[Br 64]   BROLLEY, SEAGRAVE, BERRY, Phys. Rev. 135B (1964) 1119.
[Br 64a]   BRYAN, R.A., SCOTT, B.L., Phys. Rev. 135B (1964) 434.
[Br 65]   BREIT, SEAMON, FRIEDMAN, Progr. theor. Phys., Suppl. (1965) 449.
[Br 67]   BREIT, G., Rev. mod. Phys. 39 (1967) 560.
[Br 67a]   BROWN, V.., Phys. Lett. 25B (1967) 506.
[Br 68]   BROLLEY (private communication).
[Br 68a]   BRADY, YOUNG, BADRINATHAN, Phys. Rev. Lett. 20 (1968) 750.
[Br 69]   BRESSEL, KERMAN, ROUBEN, Nucl. Phys. A124 (1969) 624.
[Ca 67]   CATILLON et al., in Ref. [He 67].
[Ce 64]   CERINEO, ILAKOVAC, ŠLAUS, TOMAŠ, VALKOVIĆ, Phys. Rev. 133B (1964) 948.
[Cr 63]   CROMER, A.H., Phys. Rev. 129 (1963) 1680.
[Cr 68]   CRAWLEY, POWELL, NARASIMHA, Phys. Lett. 26B (1968) 576.

[Cz 59]   CZIFFRA, MacGREGOR, MORAVCSIK, STAPP, Phys. Rev. 114 (1959) 880.
[Cz 69]   CZIBOK (private communication).
[De 66]   DEBERTIN (private communication).
[Dr 68]   DRECHSEL, D., MAXIMON, L.C., Ann. Phys. 49 (1968) 403.
[En 63]   ENGELKE et al., Phys. Rev. 129 (1963) 324.
[Fe 41]   FERRETTI, B., Ricerca scient. 12 (1941) 993.
[Fu 68]   FUSCHINI (private communication).
[Ge 64]   GELL MANN, M., Phys. Lett. 8 (1964) 214.
[Gl 62]   GLENDENNING, N.K., KRAMERS, G., Phys. Rev. 126 (1962) 2159.
[Go 60]   GOLDBERGER, M.L., in Theoretical Physics (Proc. Midwestern Conf., April 1960) 50-63.
[Go 67]   GOTTSCHALK, SCHLAER, WANG, Nucl. Phys. A94 (1967) 491.
[Gr 59]   GRASHIN, A.F., JETP 36 (1959) 1717.
[Gr 68]   GROSS (private communication).
[Gr 67]   GREEN, A.E.S., MacGREGOR, M.H., WILSON, R., Rev. mod. Phys. 39 (1967) 498.
[Gr 67a]   GREEN, A.E.S., SAWADA, T., Rev. Mod. Phys. 39 (1967) 594.
[Gu 59]   GUPTA, S.N., Phys. Rev. Lett. 2 (1959) 124.
[Ha 64]   HAMA, Y., HOSHIZAKI, N., Progr. theor. Phys. 31 (1964) 615, 1162.
[Ha 65]   HAMA, Y., HOSHIZAKI, N., Progr. theor. Phys. 34 (1965) 584.
[Ha 65a]   HADDOCK et al., Phys. Rev. Lett. 14 (1965) 9.
[Ha 66]   HAMA, Y., Progr. theor. Phys. 35 (1966) 261.
[He 32]   HEISENBERG, W., Z. Physik 77 (1932) 1.
[He 64]   HELLER, SIGNELL, YODER, Phys. Rev. Lett. 13 (1964) 577.
[He 67]   HELLER, L., Rev. mod. Phys. 39 (1967) 584.
[He 68]   HELLER, L., Phys. Rev. 174 (1968) 1580.
[Ho 62]   HOSHIZAKI, OTSUKI, WATARI, YONEZAWA, Progr. theor. Phys. 27 (1962) 1199.
[Ha 62]   HAMADA, T., JOHNSTON, I.D., Nucl. Phys. 34 (1962) 382.
[Ho 62a]   HOSHIZAKI, N., MACHIDA S., Progr. theor. Phys. 27 (1962) 288.
[Ho 63]   HOSHIZAKI, N., MACHIDA, S., Progr. theor. Phys. 29 (1963) 49.
[Ho 63a]   HOSHIZAKI, N., Progr. theor. Phys. 29 (1963) 321.
[Ho 68]   HOSHIZAKI, N., Progr. theor. Phys. Suppl. 42 (1968) 107.
[Ho 68a]   HONECKER, R., GRÄSSLER, H., Nucl. Phys. A107 (1968) 81.
[Hr 69]   HREHUSS (private communication).
[Il 61]   ILAKOVAC, KUO, PETRAVIĆ, ŠLAUS, TOMAŠ, Phys. Rev. Lett. 6 (1961) 356.
[Iw 56]   IWADARE, OTSUKI, TAMAGAKI, WATARI, Progr. theor. Phys. Suppl. 3 (1956) 32.
[Ja 51]   JASTROW, R., Phys. Rev. 81 (1951) 165.
[Ja 68]   JANOUT, LEHAR, WINTERNITZ, Czech. J. Phys. B18 (1968) 8.
[Jo 59]   JOHNSTON, L.H., YOUNG, D.E., Phys. Rev. 116 (1959) 989.
[Jo 68]   JOSEPH, C. et al., Bull. Am. Phys. Soc. 13 (1968) 567.
[Kn 59]   KNECHT, MESSELT, BERNERS, NORTHCLIFFE, Phys. Rev. 114 (1959) 500.
[Kn 66]   KNECHT, DAHL, MESSELT, Phys. Rev. 148 (1966) 1031.
[Ko 64]   KOEHLER, THORNDIKE, CROMER, Phys. Rev. 134B (1964) 1030.
[Ko 67]   KOEHLER, ROTHE, THORNDIKE, Phys. Rev. Lett. 18 (1967) 933.
[Ma 58]   MANDELSTAM, S., Proc. Roy. Soc. A244 (1958) 491.
[Ma 68]   MacGREGOR, ARNDT, WRIGHT, Phys. Rev. 173 (1968) 1272.
[Ma 68a]   MacGREGOR, ARNDT, WRIGHT, Phys. Rev. 169 (1968) 1128.
[Ma 68b]   MacGREGOR, ARNDT, WRIGHT, Phys. Rev. 169 (1968) 1149.
[Ma 68c]   MASON, HALBERT, NORTHCLIFFE, Phys. Rev. 176 (1968) 1159.
[Ma 69]   MARKER, D., SIGNELL, P., preprint C00-1051-25.
[Ma 69a]   MALANIFY (private communication).
[Mi 68]   MILLER, SIGNELL, P., preprint (1968).
[Mo 36]   MORSE, FISK, SHIFF, Phys. Rev. 50 (1936) 748.
[Mo 68]   MONGAN, T.R., Phys. Rev. 175 (1968) 1260.
[Na 66]   NARUMI, H., WATANABE, T., Progr. theor. Phys. 35 (1966) 1154.
[Ni 65]   NIILER, A. (private communication).
[Ni 68]   NICHOLS, BUTLER, COHEN, JANUS, Phys. Lett. 27B (1968) 452.
[No 63]   NOYES, P.H., Phys. Rev. 130 (1963) 2025.
[No 67]   NOYES, H.P., LIPINSKI, H.M., SLAC preprint, see Ref. [He 67].
[No 67a]   NOYES, SIGNELL, YODER, WRIGHT, Phys. Rev. 159 (1967) 789.
[Ny 67]   NYMAN, E.M., Phys. Lett. 25B (1967) 135.

[Ny 68]   NYGREN (private communication).
[Og 67]   OGAWA, SAWADA, UEDA, WATARI, YONEZAWA, Progr. theor. Phys. Suppl. $\underline{39}$ (1967) 140.
[Ot 68]   OTSUKI, S., Progr. theor. Phys. Suppl. $\underline{42}$ (1968) 39.
[Pa 48]   PARZEN, G., SCHIFF, L.I., Phys. Rev. $\underline{74}$ (1948) 1564.
[Pe 67]   PERRING, J.K., Rev. mod. Phys. $\underline{39}$ (1967) 550.
[Pe 67a]   PEARCE, GALE, DUCK, Nucl. Phys. $\underline{B3}$ (1967) 241.
[Pe 67b]   PERRIN (private communication).
[Pu 57]   PUZIKOV, RYNDIN, SMORODINSKI, Nucl. Phys. $\underline{3}$ (1957) 436.
[Re 68]   REID, R.V., Jr., Ann. Phys. $\underline{50}$ (1968) 411.
[Ro 48]   ROSENFELD, L., Nuclear Forces, North Holland, Amsterdam 1948.
[Ro 67]   ROTHE, KOEHLER, THORNDIKE, Phys. Rev. $\underline{157}$ (1967) 1247.
[Ru 27]   RUTHERFORD, E., Phil. Mag. $\underline{4}$ (1927) 580.
[Ry 64]   RYAN, J.W., Phys. Rev. Lett. $\underline{12}$ (1964) 564.
[Sa 56]   SAKATA, S., Progr. theor. Phys. $\underline{16}$ (1956) 686.
[Sa 60]   SAKURAI, J.J., Phys. Rev. $\underline{119}$ (1960) 1784.
[Sa 62]   SAWADA, UEDA, WATARI, YONEZAWA, Progr. theor. Phys. $\underline{28}$ (1962) 991.
[Sa 68]   SANNES, TRISCHUK, STAIRS, Phys. Rev. Lett. $\underline{21}$ (1968) 1474.
[Sc 61]   SCHUMACHER, C.R., BETHE, H.A., Phys. Rev. $\underline{121}$ (1961) 1534.
[Sc 63]   SCOTTI, A., WONG, D.Y., Phys. Rev. Lett. $\underline{10}$ (1963) 142.
[Sh 68]   SHIRATO, S., KOORI, N., Nucl. Phys. $\underline{A120}$ (1968) 387.
[Si 64]   SIGNELL (private communication).
[Si 68]   SILVERSTEIN, E.A., KIBLER, K.G., Phys. Rev. Lett. $\underline{21}$ (1968) 922.
[Sl 65]   SLOAN (private communication).
[Sl 66]   ŠLAUS, VERBA, RICHARDSON, CARLSON, Van OERS, AUGUST, Phys. Rev. Lett. $\underline{17}$ (1966) 536.
[Sl 68]   SLOBODRIAN (private communication).
[Sl 68a]   ŠLAUS, I., PAIĆ, G., in the Ninth Latin-American School of Physics, Benjamin 1968.
[Sl 68b]   ŠLAUS, I., in Few Body Problems, Light Nuclei and Nuclear Interactions, Gordon and Breach,
           1968.
[Sl 68c]   SLOBODRIAN (private communication).
[St 57]   STAPP, YPSILANTIS, METROPOLIS, Phys. Rev. $\underline{105}$ (1957) 302.
[Ta 51]   TAKETANI, NAKAMURA, SASAKI, Progr. theor. Phys. $\underline{6}$ (1951) 581.
[Ta 56]   TAKETANI, M., Progr. theor. Phys. Suppl. No.3 (1956).
[Ta 64]   TABAKIN, F., Ann. Phys. $\underline{30}$ (1964) 51.
[Ta 67]   TAMAGAKI, R., WATARI, W., Progr. theor. Phys. Suppl. $\underline{39}$ (1967) 23.
[Th 35]   THOMAS, L.H., Phys. Rev. $\underline{47}$ (1935) 903.
[Th 65]   THORNDIKE, E.H., Phys. Rev. $\underline{138}$ (1965) 583.
[Va 69]   VALKOVIĆ, V. (private communication).
[Vo 65]   VOITOVETSKII, KARSUNSKII, PAZHIN, Nucl. Phys. $\underline{69}$ (1965) 513.
[Wa 66]   WARNER, R.E., Can. J. Phys. $\underline{44}$ (1966) 1225.
[Wi 33]   WIGNER, E.P., Phys. Rev. $\underline{43}$ (1933) 252.
[Wi 36]   WIGNER, E.P., never published this work, Ref. in BETHE, H.A., Rev. Mod. Phys. $\underline{8}$
           (1936) 193.
[Wi 63]   WILSON, R., The nucleon-nucleon interaction, Interscience Publishers (1963).
[Wo 53]   WORTHINGTON, McGRUER, FINDLEY, Phys. Rev. $\underline{90}$ (1953) 899.
[Yo 67]   YODER, N.R., SIGNELL, P., Bull. Am. Phys. Soc. $\underline{12}$ (1967) 50.
[Ze 69]   ZEITNITZ, MASCHUW, SUHR, Phys. Lett. $\underline{28B}$ (1969) 420.

SECTION II
Bulk Properties of Nuclei

NUCLEAR BINDING ENERGIES
AND DENSITIES

D.M. BRINK
Department of Theoretical Physics,
University of Oxford,
Oxford, United Kingdom

Abstract

NUCLEAR BINDING ENERGIES AND DENSITIES.
1. Introduction; 2. Saturation and nuclear matter; 3. Properties of nuclear matter ; 4. Binding energies of finite nuclei.

1.   INTRODUCTION

In these lectures we let $B(N, Z)$ denote the total binding energy of a nucleus with N neutrons and Z protons and $M(N, Z)$ denote the total atomic mass of the corresponding atom measured in energy units. Neglecting the electronic binding energy compared with the nuclear binding energy we have

$$M(N, Z) = ZM_H + NM_n - B(N, Z) \qquad (1.1)$$

where M_H is the mass of the hydrogen atom and M_n is the neutron mass. $W = - B(N, Z) = \langle KE + PE \rangle$ is the total energy of the nucleus excluding mass energy. Theoretical problems associated with nuclear binding energies include the following:

i)   To understand the variation of $B(N, Z)$ with N and Z,

ii)   To predict masses of yet unknown nuclei, and

iii) To predict limits of stability of nuclei against α- and β-decay, nucleon emission and fission.

Problems of nuclear binding energies and matter distributions are closely connected. We denote the nucleon density distribution by $\rho(r)$ normalized so that $\int \rho(r) d^3r = A$; $\rho_n(r)$ and $\rho_z(r)$ are the corresponding neutron and proton densities, $\rho = \rho_n + \rho_z$.

2.   SATURATION AND NUCLEAR MATTER

There are about 1270 nuclei whose masses are known [1]. The most remarkable aspect of the experimental masses is the approximate constancy of $B(N, Z)/A$. Except for nuclei with $A \lesssim 10$, B/A always lies between 7.4 and 8.8 MeV. Experiments measuring the charge and matter distributions in nuclei suggest that nuclear radii R are related to the atomic weight A by

$$R \simeq r_0 A^{1/3} \qquad (2.1)$$

where r_0 is a constant whose value depends on the precise definition of the

nuclear radius ($r_0 \simeq 1.1 \times 10^{-13}$ cm). Equation (2.1) shows that the nuclear volume is approximately proportional to A or, equivalently, the matter density is nearly constant in all nuclei. The approximately constant binding energy per nucleon, and constant matter density in nuclei led to the idea of nuclear matter.

The idea of nuclear matter was recognized by Heisenberg [2] and Majorana [3] in their first papers on nuclear structure. In 1933 Majorana [3] says that: "One finds at the centre of an atom a sort of matter which has the same property of uniform density as ordinary matter. Light and heavy nuclei are built up from this matter and the difference between them depends mainly on their different content of nuclear matter". The relation $R = r_0 A^{1/3}$ seems to have been suggested by Gamow [4] and the idea of nuclear matter may have originated in his α-particle model [5].

Stable even nuclei with $A < 30$ tend to have $N = Z$. This is a consequence of the approximate charge symmetry of nuclear forces {(n, n) forces equal (p, p) except for Coulomb effects}. On the other hand, stable heavy nuclei all have a large neutron excess. The Coulomb energy of a nucleus is proportional to Z^2/R or $Z^2/A^{1/3}$. It is rather small in light nuclei (~ 15 MeV in O^{16}), but increases as Z^2 and is very important in heavy nuclei (~ 600 MeV in lead). This energy is responsible for the neutron excess of heavy nuclei and for the instability of heavy nuclei against α-decay and fission. The Coulomb energy per nucleon is not a constant and does not have the saturation property of nuclear forces. When discussing the properties of nuclear matter it is the custom to neglect Coulomb forces and to add them only in finite nuclei.

3. PROPERTIES OF NUCLEAR MATTER

The total energy per nucleon $E = -B/A = W/A$ in nuclear matter depends on the nucleon density ρ and the neutron-proton difference $x = (N-Z)/A$, i.e. $E(\rho, x^2)$. In nuclear matter it is assumed that ρ and x are independent of position. E is a function of x^2 because of charge symmetry.

The equilibrium state of nuclear matter is found by minimizing E as a function of ρ and x. If the minimum occurs at $x = 0$ and $\rho = \rho_0$ then, near equilibrium, we have

$$E(\rho, x^2) = E_0 + \frac{1}{2} K\{(\rho - \rho_0)/\rho_0\}^2 + \beta x^2 \qquad (3.1)$$

At equilibrium nuclear matter is characterized by an equilibrium density ρ_0 and an energy per nucleon E_0. Deviations from equilibrium are characterized by a compressibility K and symmetry energy β. If R_0 is the radius of a large finite nucleus and ρ_0 is its density then

$$K = \rho_0^2 \frac{d^2E}{d\rho_0^2} = \frac{1}{9} R_0^2 \frac{d^2E}{dR_0^2} = \frac{1}{9} K' \qquad (3.2)$$

Some authors use $K' = R_0^2 (d^2E/dR_0^2)$ as a definition of compressibility. Values of the parameters E_0, ρ_0, K and β can not be found directly from

experiment because nuclear matter does not exist. Their values can only
be inferred by extrapolation from properties of finite nuclei. Most authors
give $E_0 \simeq 16$ MeV and $\beta \sim 25 - 30$ MeV. An equilibrium density $\rho_0 \simeq 0.22$ fm^{-3}
corresponds to a radius parameter (Eq.(2.1)) of $r_0 \simeq 1.1$ fm. The value of
the compressibility parameter K is very uncertain and could be anything
between 100 and 300 MeV.

3.1. Fermi theory [6]

The simplest model for nuclear matter is a model of non-interacting
nucleons moving in a uniform average potential. Each nucleon occupies a
plane-wave state with momentum $\vec{k}$. All states are occupied up to $k = k_f$ by
neutrons and protons (i.e. $\rho_n = \rho_z$ or $N = Z$). Under these conditions the
nucleon density is

$$\rho = \frac{2}{3\pi^2} k_f^3 \qquad (3.3)$$

If the radius is $R = r_0 A^{1/3}$, then $(r_0 k_f)^3 = 9\pi/8$ or $r_0 k_f = 1.51$. Hence if
$r_0 = 1.1$ fm, $k_f = 1.39$ fm^{-1}; $r_0 = 1.2$ fm corresponds to $k_f = 1.26$ fm. One may
calculate the symmetry energy β in Fermi theory by assuming different
values of k_f for neutrons and protons. The result is

$$\beta = \frac{1}{3} \epsilon_f, \text{ where } \epsilon_f = (\hbar^2 k_f^2 / 2 \, m) \simeq 40 \text{ MeV if } k_f = 1.39 \text{ fm}^{-1}$$

The average kinetic energy per nucleon in Fermi theory is

$$\langle KE \rangle / A = \frac{3}{10} (\hbar^2 k_f^2 / 2 \, m) = \frac{3}{5} \epsilon_f \simeq 24 \text{ MeV}$$

3.2. Landau theory [7, 8]

This theory extends the results of Fermi theory by including the effects
of nucleon-nucleon interactions. A very attractive feature is that the theory
is rather general, and the equations hold for many approximate descriptions
of nuclear matter. The relations we give have hold for Hartree-Fock
theories as well as many more general theories which give rise to some
effective nucleon-nucleon interaction in nuclear matter. Landau theory
supposes that the energy of the system is a function of the occupation
numbers n(k) of single-particle (or single quasi-particle) states. If the
quantities $\delta n(k)$ refer to deviations of these occupation numbers from their
equilibrium values then the change in energy is

$$\delta W = W_0 + \sum_k \epsilon(k, \alpha) \delta n(k, \alpha) + \frac{1}{2} \sum_{kk'\alpha\alpha'} \Phi(k\alpha, k'\alpha') \delta n(k, \alpha) \delta n(k', \alpha') \qquad (3.4)$$

The $\epsilon(k, \alpha)$ are single-particle energies and $\Phi(k\alpha, k'\alpha')$ represent effective
interactions, α stands for spin and isospin quantum numbers.

The velocity of a particle $v(k)$ is related to its single-particle energy by

$$v(k) = \frac{1}{\hbar} \frac{\partial \epsilon}{\partial k} \tag{3.5}$$

and one can define an effective mass by

$$m^*(k) = \hbar k / v(k) \tag{3.6}$$

The effective mass m^* depends on wave number k and has a value m_f^* at the Fermi level k_f. If we put

$$\epsilon_0 = \hbar^2 k_f^2 / 2 m_f^* \tag{3.7}$$

then ϵ_0 defines a characteristic energy for the system. The density of single-particle states ν_0 at the Fermi level is

$$\nu_0 = \frac{1}{2} [\partial \rho / \partial \epsilon(k)]_{k_f} = \frac{1}{2} \left(\frac{\partial \rho}{\partial k_f} \frac{\partial k}{\partial \epsilon_f} \right) = \frac{m^* k_f}{\hbar^2 \pi^2} = \frac{3}{4} \frac{\rho}{\epsilon_0} \tag{3.8}$$

Here ν_0 is the density of states for neutrons or protons and we assume $\rho_n = \rho_z$. Thus the characteristic energy ϵ_0 or the effective mass m_f determines the density of states at the Fermi level.

The effective interaction Φ depends on momentum, spin and isospin quantum numbers $(\vec{k}, \sigma, \tau) = (\vec{k}, \alpha)$

$$\Phi(\vec{k}\sigma\tau, \vec{k}'\sigma'\tau') = F + F'\tau\tau' + G\sigma\sigma' + G'\tau\tau'\sigma\sigma' \tag{3.9}$$

where F, G, F', G' depend on $\vec{k}$ and $\vec{k}'$. At the Fermi surface ($|k| = k_f$) they depend only on θ, the angle between $\vec{k}$ and $\vec{k}'$. Using the density of states ν_0 (Eq. 3.8) one can define dimensionless interaction constants by the relations

$$f = \nu_0 F, \quad g = \nu_0 G, \quad f' = \nu_0 F', \quad g' = \nu_0 G \tag{3.10}$$

These dimensionless coefficients depend on θ and can be expanded

$$f(\vec{k}, \vec{k}') = \sum f_\ell P_\ell (\cos \theta)$$

to give dimensionless interaction constants f_ℓ, g_ℓ, f'_ℓ, g'_ℓ.

Landau theory shows that the symmetry energy β, the compressibility K and the effective mass m_f^* are related to the residual interaction constants f_ℓ, etc. by

$$m_f^* = m \left(1 + \frac{2}{3} f_1 \right), \quad K = \frac{2}{3} \epsilon_0 (1 + 2f_0), \quad \beta = \frac{1}{3} \epsilon_0 (1 + 2 f'_0)$$

Single-particle energies $\epsilon(k)$, effective mass and residual interaction constants are also quantities which can be used to characterize properties of nuclear matter.

4. BINDING ENERGIES OF FINITE NUCLEI

4.1. Surface energy

We assume i) that the density of nucleons ρ_0 in the interior of the nucleus is a constant, and ii) that there is a surface layer of nucleons with a surface density σ which do not make their full contribution to the nuclear binding energy. Then the total interaction energy of the nucleus is

$$W = A E(\rho, x^2) + \sigma \, ax \, (\text{surface area}) \qquad (4.1)$$

where a is the binding energy defect per surface nucleon. For a nucleus with A nucleons and density ρ_0 the surface area is proportional to $A^{2/3}$. Hence

$$W = A E(\rho, x^2) + b_s \, f(\text{shape}) \, A^{2/3} \qquad (4.2)$$

For a sphere we take $f(\text{shape}) = 1$ and for an arbitrary shape f is defined as f(shape) = surface area/surface area of a sphere with same volume (see Ref. [9]). Always $f(\text{shape}) \geq 1$. The coefficient b_s is called the surface energy and may depend on the proton-neutron ratio x.

4.2. Coulomb energy

The Coulomb energy of a nucleus E has a direct term

$$E_c^{(\alpha)} = \frac{e^2}{2} \int \frac{\rho_z(\vec{r}_1) \, \rho_z(\vec{r}_2)}{|\vec{r}_1 - \vec{r}_2|} \, d^3\vec{r}_1 \, d^3\vec{r}_2 \qquad (4.3)$$

plus an exchange term. The origin of the exchange term is as follows: physically the Pauli principle introduces correlations in the nuclear wave function which give zero probability for two protons with the same spin to be at the same point in space. The effect of these correlations is to reduce the Coulomb energy. Mathematically in an independent particle model

$$E = \frac{1}{2} \sum_{\alpha\beta}' \left(\langle \alpha\beta | v_c | \alpha\beta \rangle - \langle \alpha\beta | v_c | \beta\alpha \rangle \right) \qquad (4.4)$$

where $\alpha = (\sigma, u)$ stand for the quantum numbers of a proton state. The sum in Eq. (4.4) is taken over all occupied proton states. The quantity σ stands for a spin quantum number of a proton state while u is an orbital quantum number. If each orbital state is occupied by two protons the spin sum in (4.4) can be calculated to give the result

$$E_c = \sum_{uu'}' \left(2\langle uu' | v_c | uu' \rangle - \langle uu' | v_c | u'u \rangle \right)$$

$$= E_c^{(\alpha)} - \frac{e^2}{4} \int \frac{|\rho(r_1, r_2)|^2}{|r_1 - r_2|} d^3r_1 \, d^3r_2$$

(4.5)

where the mixed density

$$\rho(r_1, r_2) = 2 \sum_u' \phi_u^*(r_1) \, \phi_u(r_2)$$

(4.6)

The exchange contribution always has the same sign so that $E_c < E_{cd}$. For a charge density distribution

$$\rho(r) = \text{const}, \ r < R_c, \ \rho(r) = 0, \ r > R_c$$

the direct contribution is

$$E_c^{(\alpha)} = \frac{3}{5} \frac{Z^2 e^2}{R_c}$$

Including a surface correction due to the finite surface thickness d and an approximate form for the exchange correction gives (see Refs [9] [12]).

$$E_c = \frac{3}{5} \frac{Ze^2}{R_c} \left[g - \frac{5\pi^2}{6} \left(\frac{d}{R_c} \right)^2 - \frac{0.76}{Z^{2/3}} \right]$$

(4.7)

The quantity g depends on the shape of the nucleus; $g = 1$ for a spherical shape and $g < 1$ for a deformed shape.

4.3. Mass formulae

A mass formula aims at accounting for the variations of nuclear binding energies with N and Z. From an analysis of available nuclear masses von Weizsäcker [10] and Bethe and Bacher [11] were able to identify four terms which accounted for the average variation of B(N, Z) with N and Z,

$$W = -B = A(E_0 + \beta x^2) + b_s A^{2/3} + \frac{3}{5} Z^2 e^2 / R_c$$

(4.8)

Typical values for the parameters (Preston [6]) are

$$E_0 = -15.835 \text{ MeV}, \ \beta = 23.20 \text{ MeV}, \ b_s = 18.33 \text{ MeV}, \ \frac{3}{5} \frac{e^2}{R_c} = 0.714 \text{ MeV}$$

We have discussed the origins of the four terms in the introduction to section 3 and in 4.1 and 4.2. A generalization of this formula to describe other shapes of the nucleus than the spherical shape is usually called a liquid-drop formula. It involves studying the shape functions f and g in formulae (4.2) and (4.7).

A liquid-drop formula does not include effects of the shell structure on binding energies. These effects have their origins in a single-particle model. Mass formulae including shell corrections have been discussed recently by Myers and Światecki [9] and by Nilsson [12].

Mass formulae are important for questions related to nuclear stability and have recently become very important for the study of fission and questions related to the existence of superheavy nuclei.

An approach to the study of nuclear masses which is based on arguments quite different from those leading to the liquid-drop formula has been used by Garvey and Kelson [13]. In a more recent article Garvey et al. [13] give some relations between masses of neighbouring nuclei:

$$M(N+2, Z-2) - M(N, Z) + M(N, Z-1) - M(N+1, Z-2) + M(N+1, Z) - M(N+2, Z-1) = 0$$

$$(4.9)$$

$$M(N+2, Z) - M(N, Z-2) + M(N+1, Z-2) - M(N+2, Z-1) + M(N, Z-1) - M(N+1, Z) = 0$$

$$(4.10)$$

Formula (4.9) gives relations between masses of nuclei with N, N+1, N+2 neutrons and Z, Z-1, Z-2 protons. Terms (1) and (6) in this formula refer to the masses of nuclei with the same number (N+2) of neutrons, but different numbers (Z-2 and Z-1) of protons. If the neutron configuration does not depend on the number of protons then the neutron-neutron (n, n) interaction in a nucleus with N+1 neutrons should cancel between these two terms. In the same way, the (n, n) interaction should cancel between terms (2) and (3), and between terms (4) and (5). By a similar argument, the proton-proton (p, p) interactions should cancel between the pairs of terms (1) and (4), (2) and (5), (3) and (6). Hence, all (n, n) and (p, p) interactions cancel in formula (4.9). In a rather crude shell model picture neutron-proton (n, p) interactions also cancel. All the nuclei in formula (4.9) consist of several neutrons and protons outside a core with N neutrons and Z-2 protons. The n-p interactions between core neutrons and protons all cancel if the core configuration is the same in each nucleus. Interactions between external neutrons and core protons cancel between the pairs of terms (1) and (6), (2) and (3), (4) and (5). Interactions between external protons and core neutrons cancel between the terms (1) and (4), (2) and (5), (3) and (6). The only terms containing both external neutrons and protons are (5) and (6). There the interaction of two neutrons with one proton cancels the interaction of one neutron with two protons. The cancellations are illustrated in the diagram (Fig. 1) in which the lines represent single-particle levels; circles represent neutrons and crosses protons. Formula (4.10) can be checked in a similar way.

Amongst known masses there are 621 tests of Eq.(4.9). The average deviation is 198 keV. Amongst 755 cases of Eq.(4.10) the average deviation
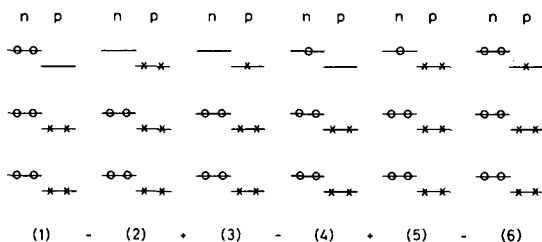
FIG.1.   Diagrams illustrating the cancellations in Eq.(4.9).

is 189 keV. This agreement is remarkably good in view of the rather crude arguments which are used to derive the formulae. The mass relations (4.9) and (4.10) can be looked on as recursion relations for the nuclear masses. These are solved by the formulae

$$M(N, Z) = g_1(N) + g_2(Z) + g_3(N+Z) \quad \text{for (4.9)}$$

$$M(N, Z) = f_1(N) + f_2(Z) + f_3(N-Z) \quad \text{for (4.10)}$$

where g_i and f_i are arbitrary functions. Garvey et al. [13] have constructed a mass table by fitting the g_i to known masses. They predict the masses of many unknown nuclei.

REFERENCES

[1]   MATTAUCH, J.H.E., THIELE, W., WAPSTRA, A.H., Nucl.Phys. 67 (1965) 32.
[2]   HEISENBERG, W., Z.Physik 77 (1932) 1; 80 (1933) 587.
[3]   MAJORANA, E., Z.Physik 82 (1933) 137.
[4]   GAMOW, G., Z.Physik 51 (1928) 204.
[5]   GAMOW, G., Proc.Roy.Soc. A126 (1928) 632.
[6]   PRESTON, M.A., Physics of Nucleus. Addison-Wesley (1962) Chapter 6.
[7]   LANDAU, L., Soviet Phys.JETP 30 (1956); 32 (1957) 59.
      NOZIÈRES, P., Le problème de N corps, Dunod (1962) Chapter 1.
[8]   MIGDAL, A.B., Theory of finite Fermi systems.
[9]   MYERS, W.D., ŚWIĄTECKI, W.J., Nucl.Phys. 81 (1966) 1.
[10] VON WEIZSÄCKER, C.F., Z.Physik 96 (1935) 431.
[11] BETHE, H.A., Rev.mod.Phys. 8 (1936) 82.
[12] NILSSON, S.G., Summer Inst.on Nucl.Physics, Cargèse (1968).
[13] GARVEY, G.T., KELSON, I., Phys.Rev.Lett. 16 (1967) 197.

BASIC CONCEPTS AND PROPERTIES OF COLLECTIVE MOTION AND THE SINGLE-PARTICLE STATES IN DEFORMED NUCLEI

Z. SZYMAŃSKI
Institute for Nuclear Research
Warsaw, Poland

Abstract

BASIC CONCEPTS AND PROPERTIES OF COLLECTIVE MOTION AND THE SINGLE-PARTICLE STATES IN DEFORMED NUCLEI.
1. Charge and matter distribution in nuclei; 2. Semi-empirical mass formula; 3. Individual nucleon motion in the non-spherical potential field; 4. Polarizability of the nuclear core. Methods for the determination of nuclear shape; 5. The onset of nuclear deformation. 6. Nuclear rotational motion; 7. Rotational spectra; 8. Rotational intensity rules; 9. Other applications of the rotational coupling scheme; 10. Further developments in the rotational coupling scheme. 11. Heavy nuclei. Fission; 12. Superheavy elements.

1. CHARGE AND MATTER DISTRIBUTIONS IN NUCLEI

Various methods are used to determine size and distribution of matter in nuclei. The electromagnetic interaction of charged particles with nuclei serves as the best tool for investigating the distribution of electric charge of the protons in the nucleus. On the other hand, the methods involving strongly interacting particles provide us with information on the distribution of nuclear matter. By comparing the differences between the two groups of methods one can, in principle, attempt to estimate the distributions of protons and neutrons separately. This chapter is not meant to give a review of the experimental methods used in the determination of nuclear size and density distributions (see Refs [1,2]). We shall rather confine ourselves to a short discussion of electron scattering. However, let us only mention that the measurements of μ-onic atoms, isotope shifts, X-ray fine structure, nuclear-particle scattering etc. provide us with very valuable information.

One of the most fruitful experiments is the elastic scattering of electrons by nuclei. The scattered electrons usually have relativistic energy so that their wave-length is

$$\lambdabar = \frac{\hbar c}{E} = \frac{197 \text{ fm}}{E \text{(MeV)}} \tag{1.1}$$

For low-energy electrons the scattering is mainly caused by the Coulomb field outside of the nucleus so that the scattering is that of a point charge. For energies of the order of 20 MeV, we begin to observe the finite-size effects of heavy nuclei, while for about 100 MeV the observation of the details of the nuclear charge distribution becomes possible.

In general, there is no simple relation between the scattering amplitude $f(\theta)$ and the density distribution of nuclear charge. The standard

phase-shift procedure involves usually more than one hundred partial waves that prove to be significant in the analysis. The formalism is developed in such a way that a certain expression for the nuclear electric charge density is assumed. Then, the electrostatic potential of the nucleus is derived by solving the Poisson's equation. Finally, the parameters of the expression for density are varied as to get the best fit in the differential cross-section for the elastically scattered electrons.

Let us discuss the relationship between the scattering amplitude $f(\theta)$ and the density of nuclear charge $\rho(r)$ in the Born approximation which is by no means valid in most physical situations in our case. The differential cross-section of a relativistic electron obeying the Dirac equation is

$$\frac{d\sigma}{d\Omega} = \frac{1}{\hbar^2 c^2} \, \text{ctg}^2 \frac{\theta}{2} \left| \int_0^\infty \sin(qr) \, V(r) \, r \, dr \right|^2 \tag{1.2}$$

where $\hbar q = 2\hbar k \sin(1/2)\theta$ is the momentum transfer. Using Poisson's equation

$$\Delta V(r) \equiv \frac{1}{r} \frac{d^2}{dr^2} (rV) = 4\pi e^2 \, Z \, \tilde{\rho}(r) \tag{1.3}$$

which relates the density per particle $\tilde{\rho}(r)$ to the potential $V(r)$ we finally get

$$\frac{d\sigma}{d\Omega} = \frac{Z^2 e^4 \cos^2 \frac{1}{2}\theta}{4 E^2 \sin^4 \frac{1}{2}\theta} \left| \frac{4\pi}{q} \int_0^\infty \sin(qr) \tilde{\rho}(r) \, r \, dr \right|^2 \tag{1.4}$$

The expression $d\sigma/d\Omega$ as plotted versus θ exhibits minima and maxima of the diffraction type. The difference between two successive minima or maxima can be used for the first rough estimate of the nuclear size: $\Delta(qR) \approx \pi$.

To obtain full information on $\tilde{\rho}(r)$ we should know the form factor

$$F(q) = \frac{4\pi}{q} \int_0^\infty \sin(qr) \tilde{\rho}(r) r \, dr \tag{1.5}$$

appearing in expression (1.4) in the whole region of q. However, the observation of $d\sigma/d\Omega$ is difficult both at small angles 0 and large q. Consequently, we do not know too much about $\rho(r)$ either for large distances r, or in the central part of the nucleus. This conclusion, which follows directly from the Born approximation, is also approximately valid in the more general case.

Figure 1-1 shows the example of the fit in the density parameters for the $d\sigma/d\Omega$ curve [3]. The most commonly used expression for the density $\rho(r)$ is the Fermi distribution

$$\rho(r) = \frac{\rho_0}{1 + \exp\left(\dfrac{r - R}{a}\right)} \tag{1.6}$$
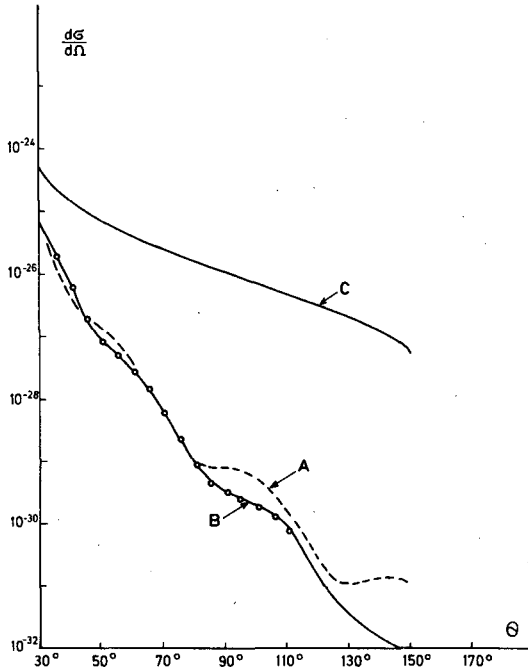
FIG.1-1. Differential cross-section for elastic scattering of 153-MeV electrons on Au. Curves A and B correspond to uniform density distribution and Fermi distribution, respectively. Curve C represents the scattering on a point charge.

where R is the half-way radius and a determines the surface thickness. The experiments on electron scattering give the best fit for

$$\rho_0 = 0.17 \text{ nucleons}/\text{fm}^3$$
$$a = 0.54 \text{ fm}$$

(1.7)

for all nuclei beyond oxygen. This result is also consistent with other measurements. We now use the normalization condition

$$A = \int \rho \, d\tau = \rho_0 \frac{4\pi}{3} R^3 \left(1 + \pi^2 \left(\frac{a}{R} \right)^2 + \dots \right)$$

(1.8)

so that $\rho(r) = A\tilde{\rho}(r)$, where $\tilde{\rho}(r)$ enters Eqs (1.3 - 1.5). This last equation can be obtained from the more general Fermi integral [1]:

$$F_n(k) = \int_0^\infty \frac{x^n \, dx}{1 + \exp(x - k)} = \frac{k^{n+1}}{n+1} + \frac{n\pi^2}{6} k^{n-1} + \dots$$

(1.9)

for large k.

From Eq.(1.8) and the estimates (1.7) we obtain

$$R = 1.12 \, A^{1/3} - 0.33 \, A^{-1/3} \qquad (1.10)$$

By calculating the mean square radius we get another convenient estimate of the nuclear size.

Finally, the Coulomb energy requires another type of the average:

$$\frac{1}{R_c} = \frac{5}{6} \frac{\int d^3 r_1 \int d^3 r_2 \dfrac{\rho(r_1)\,\rho(r_2)}{|\vec{r}_1 - \vec{r}_2|}}{\left\{\int d^3 r\, \rho(r)\right\}^2} \qquad (1.11)$$

The factor 5/6 appearing in this equation leads simply to the equality $R_c = R$ where R is the radius of a constant-density nucleus with a sharp surface. The calculation of the average (1.11) with the Fermi density (1.6) gives [3]

$$R_c = \frac{R}{1 - \dfrac{7}{6}\,\pi^2 \left(\dfrac{0.54}{1.12 \times 100}{}^{1/3}\right)^2} \approx 1.22 \, A^{1/3} \qquad (1.12)$$

Most of the conclusions derived from the analysis of various experiments have been summarized in Ref.[1]. It appears that the density of nucleons in the nucleus is approximately constant (A-independent). The radial distribution may be of the Fermi type, however, this is not too certain especially in the central part of the nucleus. The thickness of the surface region is approximately constant for most of the nuclei and much less than the half-way radius R. The latter quantity is roughly proportional to $A^{1/3}$. Most experiments seem to indicate that the neutron distribution is not very much different from proton distribution.

2.   SEMI-EMPIRICAL MASS FORMULA

An atomic nucleus is a system of many interacting nucleons. Its total energy and mass depend essentially on the motion of nucleons in the nucleus and on their interactions. Until a satisfactory theory for such a motion is developed we are bound to use simple semi-empirical expressions for the calculation of the total nuclear mass as a function of the neutron and proton numbers, Z and N. Various expressions for the nuclear mass have been suggested. Here, we shall use the expression of Myers and Świątecki [4] that is fairly complicated but reflects correctly most of the properties of the nuclear binding energy. The formula has the following structure

B(N, Z) = (volume energy) + (surface energy) + (Coulomb energy)
        + (pairing energy correction) + (shell energy correction)   (2.1)

where $B(N, Z)$ denotes the (negative) binding energy of the nucleus defined as the difference between the total nuclear mass $M(N, Z)$ and the sum of nucleon masses, times c^2

$$B(N, Z) = \left\{ M(N, Z) - N M_N - Z M_H \right\} C^2 \qquad (2.2)$$

Here M_N and M_H are masses of the neutron and of the hydrogen atom, respectively.

For nuclear matter, — an infinite medium filled uniformly with neutrons and protons, — we expect that the volume energy is the only term responsible for the existence of nuclear binding. As the nuclear density proves to be constant for the central part of most nuclei we can conclude that the main part of the volume energy is a negative constant. As neutrons and protons obey the Pauli principle, they should — roughly saying — populate the lowest available levels. We can then expect that the nuclear binding is most effective for $N = Z$. For $N - Z \neq 0$ correction terms should appear which first of all ought to weaken the binding and, secondly, should not depend on whether $Z > N$ or $Z < N$. In other words, if we introduce the nuclear asymmetry parameter $I = (N - Z)/(N + Z) = (N - Z)/A$ we can expect that to second order we obtain

$$\text{volume energy} = - a_1 (1 - \kappa_V I^2) A \qquad (2.3)$$

where a_i and κ_V are positive constants.

A nucleon located on the nuclear surface is less bound than those of the central part of the nucleus. This statement is valid provided the range of nuclear attractive forces is short compared to the size of the whole nucleus. The same situation prevails in the drop of an incompressible liquid and gives the explanation of the existence of surface tension. As the nuclear radius is proportional to $A^{1/3}$ we may write down the following expression for the surface energy:

$$\text{surface energy} = a_2 (1 - \kappa_S I^2) A^{2/3} f(\text{shape}) \qquad (2.4)$$

where we also have used the expansion in I^2. The last factor f in expression (2.4) accounts for the possibility of nuclear deformation: if the nucleus is deformed its surface increases. Using a general expression for the nuclear surface

$$R = R \left(1 + \sum_{\lambda \mu} \alpha_{\lambda \mu} Y_{\lambda \mu} \right) \qquad (2.5)$$

one can calculate the increase of nuclear surface caused by deformation. As the result of a purely geometrical calculation we obtain

$$f(\text{shape}) = 1 + \sum_{\lambda \mu} \frac{(\lambda - 1)(\lambda + 2)}{8 \pi} |\alpha_{\lambda \mu}|^2 \qquad (2.6)$$

This expression is valid to the second order in the "surface co-ordinates" $\alpha_{\lambda\mu}$. In the case of a simple quadrupole (axially symmetric distortion)

$$R = R_0(1 + \alpha\, P_2\,(\cos\,\vartheta)) \tag{2.7}$$

the above expression for f reduces to

$$f(\text{shape}) = 1 + \frac{2}{5}\,\alpha^2 \tag{2.8}$$

The Coulomb-energy term can be calculated from the integral

$$\frac{1}{2} \int \frac{\rho(\vec{r}_1)\,\rho(\vec{r}_2)}{|\vec{r}_1 - \vec{r}_2|}\, d^3 r_1\, d^3 r_2 \tag{2.9}$$

It can be easily seen that this term is of the order of $Z^2/A^{1/3}$. The integration can be carried out explicitly for a uniformly charged sphere. Then we get $(3/5)/(e^2/r)(Z^2/A^{1/3})$ where r_0 is the nuclear radius parameter $(R = r_0\, A^{1/3})$. If the nucleus is deformed this expression has to be corrected with another shape factor g(shape). The appropriate expression for g can be obtained in the second-order in the quantities $\alpha_{\lambda\mu}$ entering Eq.(2.5):

$$g(\text{shape}) = 1 - \sum_{\lambda\mu} \frac{5(\lambda-1)}{4\pi(2\lambda+1)}\,|\alpha_{\lambda\mu}|^2 \tag{2.10}$$

In the case when the nuclear shape is determined by Eq.(2.7) one gets

$$g(\text{shape}) = 1 - \frac{1}{5}\,\alpha^2 \tag{2.11}$$

We see from the above expressions that the distortion of the nucleus tends to diminish the (positive) Coulomb energy. As we have learned in the previous lecture, the nuclear surface is not sharply defined. This effect tends to diminish the value of the Coulomb energy. The corresponding correction goes actually beyond the simplest version of a liquid-drop model. If we denote by $\tilde{\rho}$ the modification of the density due to the diffuseness of the surface

$$\tilde{\rho} = \rho_{\text{diffuse}} - \rho_{\text{sharp}} \tag{2.12}$$

we can estimate the magnitude of the corresponding correction in the Coulomb energy. By choosing a co-ordinate n as varying in direction perpendicular to the nuclear surface we obtain

$$\Delta E_{\text{Coul.}} = \int \varphi\tilde{\rho}\, d\tau \approx \oint ds \int_{-\infty}^{+\infty} dn\, \varphi\, \tilde{\rho} \tag{2.13}$$

where φ is the electrostratic potential. The expansion of φ in powers of n gives

$$\Delta E_{Coul} = \oint ds \varphi(0) \int dn \, \tilde{\rho} + \oint ds \left(\frac{\partial \varphi}{\partial n}\right)_0 \int dn \, n \tilde{\rho} \qquad (2.14)$$

now the first term vanishes as $\int dn \, \tilde{\rho} = 0$, while the second term factorizes into two parts. The first part is proportional to the total nuclear charge. We see, therefore, that the effect is of the order of Z^2/A. The detailed calculation of Myers and Świątecki [4] gives

$$\Delta E_{Coul} = - \frac{\pi^2}{2} \frac{e^2}{r_0} \frac{Z^2}{A} \left(\frac{d}{r_0}\right)^2 \qquad (2.14)$$

Let us observe that this part of the Coulomb energy is independent of the nuclear shape.

The final expression for the Coulomb energy is therefore

$$\text{Coulomb energy} = \frac{Z^2}{A} c_3 \cdot g(\text{shape}) - c_4 \frac{Z^2}{A} \qquad (2.15)$$

The pairing-energy correction appearing in expression (2.1) corresponds to the well-known fact that even nuclei are more bound than odd-A ones, while the odd-A nuclei are more bound than odd nuclei. The relative differences turn out to decrease proportionally to $\sqrt{A}$. Thus we have

$$\text{Pairing energy correction} \equiv \delta = \begin{cases} -\Delta/\sqrt{A} & \text{for even nuclei} \\ 0 & \text{for odd-A nuclei} \\ \Delta/\sqrt{A} & \text{for odd nuclei} \end{cases} \qquad (2.16)$$

Finally the shell correction term has been added to the liquid-drop mass formula in order to account for the well-known fact that there exist nuclei with "magic" number of protons and/or neutrons for which the binding becomes especially strong. These numbers are

$Z = 2, 8, 20, 28, 50, 82$ and probably 114

$N = 2, 8, 20, 28, 50, 82, 126$ and probably 184

$$(2.17)$$

One can now attempt to write down an expression that gives a negative contribution for every Z or N equal to a magic number, while a positive one for Z and N in between. A convenient expression for the shell correction has been derived in Ref. [4] by assuming that it comes from the difference between a continuous spectrum of energy levels of a Fermi gas and the spectrum obtained by "bunching" the levels so as to obtain magic numbers. The shell-correction term obtained in such a way for a spherical nucleus has the form of a two-parameter quantity

$$S(N, Z) = C \left\{ \frac{F(N) + F(Z)}{(A/2)^{2/3}} \approx c A^{1/3} \right\} \tag{2.18}$$

with C and c being adjustable parameters. The function F is determined between each pair of two adjacent magic numbers M_{i-1} and M_i as

$$F(N) = \frac{3}{5} \frac{M_i^{5/3} - M_{i-1}^{5/3}}{M_i - M_{i-1}} (N - M_i) - \frac{3}{5} \left(N^{5/3} - M_{i-1}^{5/3} \right) \tag{2.19}$$

for

$$M_{i-1} \leq N \leq M_i$$

The expression of $F(Z)$ is analogous.

In the deformed nucleus the single-nucleon states depend on the distortion, and they may mix so that the bunching responsible for shell structure becomes less effective. Therefore, the shell energy term has to be corrected by the attenuating factor. The final expression for the shell correction becomes

$$\text{shell-energy correction} = S(N, Z) e^{-\overline{(\delta R)^2}/a^2} \tag{2.20}$$

where a is a new adjustable parameter and $\overline{(\delta R)^2}$ denotes the quantity $R(\vartheta, \varphi) - R_0$ squared and averaged over directions. It follows from relation (2.5) that

$$\overline{(\delta R)^2} = \frac{R_0^2}{4\pi} \sum_{\lambda\mu} |\alpha_{\lambda\mu}|^2 \tag{2.21}$$

while in the simpler case of Eq.(2.7)

$$\overline{(\delta R)^2} = R_0 \frac{1}{5} \alpha^2 \tag{2.22}$$

The final mass formula is then obtained by substituting expressions (2.3), (2.4), (2.15), (2.16) and (2.18) into Eq.(2.1).

Not all of the parameters of the mass formula have been treated as free. Let us first list those that have been taken as known from other sources: δ, and the magic numbers M_i have been treated as fixed. Also C_3 and C_4 are not independent as we treat r_0, e and d as known quantities. Finally a relation $\kappa_V = \kappa_S$ was assumed in Ref.[4]. The deformation parameter α has been determined analytically by minimization of $B(N, Z)$ with respect to α. The alternative way of determining α would consist of using the measured quadrupole moments Q of nuclei. The seven remaining parameters a_i, a_2, κ, C, c c_3 and a have been adjusted as to get best agreement in nuclear masses.

The results are

$$
\begin{aligned}
a_1 &= 15.677 \text{ MeV} \\
a_2 &= 18.56 \text{ MeV} \\
\kappa &= \kappa_V = \kappa_S = 1.79 \\
C_3 &= 0.717 \text{ MeV (this fixes } r_0 = 1.2049 \text{ fm and} \\
& \qquad C_4 = 1.21129 \text{ MeV)} \\
C &= 5.8 \text{ MeV} \\
c &= 0.26 \text{ MeV} \\
a/r_0 &= 0.27
\end{aligned}
\tag{2.23}
$$

The quantity Δ entering Eq.(2.16) was chosen to be equal to 11 MeV.

With these parameters it has been possible to fit about 1200 nuclear masses, some 240 quadrupole moments and some of 40 fission barriers. The results seem to agree remarkably well with the systematic trend in nuclear properties.

In the following, we shall try to report on some new developments that attempt to improve the mass formula and justify some of its coefficients. Various approaches have been considered. We shall only mention some of them. First of all, attempts have been made to calculate the coeffficients such as volume energy or surface energy from more basic theories. We shall not review them here as they are the topic of many other papers in these Proceedings. Let us only mention the interesting results obtained by Naqvi [5]. Using a nuclear version of a Thomas-Fermi model he was able to obtain reasonable estimates for surface and symmetry energy for nuclides with a very high neutron excess.

Another way has been tried by Myers who follows essentially the ideology of a liquid-drop model and manages to avoid its major shortcomings. The new effects included in his droplet model [6] are

1) the finite curvature of the surface ($\sim A^{1/3}$),
2) compressibility of nuclear matter,
3) difference between neutron and proton distributions, and
4) higher powers in $I^2 = [(N-Z)/A]^2$.

The importance of the new terms in the mass formula (as well as the old ones) can be seen best if we arrange different terms in an array ordered with respect to powers of both $A^{-1/3}$ and I^2 (Table I):

TABLE I.   ORDERS IN $A^{-1/3}$

A	$A^{2/3}$	$A^{1/3}$
$I^2 A$	$I^2 A^{2/3}$	
$I^4 A$		

Here the A term denotes volume energy, $I^2 A$ is the volume symmetry energy, $A^{2/3}$ corresponds to the surface energy. The last three terms $A^{1/3}$, $I^2 A^{2/3}$ and $I^4 A$ would then correspond to surface curvature correction, surface symmetry energy and the anharmonicity correction to symmetry

energy. As a result of a variational procedure used by Myers one sees
that there are also other contributions to the last three terms stemming
from another origin (for example, the difference between neutron and
proton distributions). The final expression for the nuclear binding energy

$$E = -a_1 A + a_2 A^{2/3} + \left(a_3 - \frac{2 a_2^2}{K}\right) A^{1/3}$$

$$+ \mathscr{J} I^2 A - \left(\frac{9 \mathscr{J}^2}{4 Q} - \frac{2 a_2 L}{K}\right) I^2 A^{2/3} \tag{2.24}$$

$$- \left(\frac{L^2}{2K} - \frac{1}{2} M\right) I^4 A$$

contains many new parameters such as K, a_3, Q, L, M that can either be
adjusted experimentally or calculated from a more basic approach. In
Ref.[6] these parameters are estimated from the Thomas-Fermi model.

3. INDIVIDUAL NUCLEON MOTION IN THE NON-SPHERICAL POTENTIAL
   FIELD

    In the previous chapter we saw that nuclear binding energies can be well
described by means of a simple mass formula justified partly on the basis of
the liquid-drop model of the nucleus. However, many nuclear properties,
especially those connected with nuclear ground state and low-energy excita-
tions may be very successfully represented by the individual nucleons moving
in an average field. It appears that for many purposes a spherically sym-
metric field is satisfactory. Nevertheless, the assumption of spherical
symmetry is not a basic one and does not have to be generally valid. In
fact, there are important situations with considerable deviations from
spherical symmetry of the nucleus itself and, therefore, of the nuclear
average potential, as well.
    Let us discuss the possible existence of regions of nuclides exhibiting
large distortions of spherical shape. A nucleon in the j-shell in the spherical
potential is characterized by the j- and m-quantum numbers. Several
nucleons moving near the equatorial plane in the nucleus will then tend to
produce distortion of the total field. We easily find that in such a distorted
field degeneracy with respect to the m-quantum number will be removed
and — in case of many shells lying close to each other the ℓ and j quantum
number will be mixed. The only quantum number remaining good is Ω,
the projection of the total angular momentum j on the symmetry axis of the
field (we use Ω instead of m). Owing to time-reversal invariance of the
Hamiltonian, the $\pm \Omega$ states will be degenerate. (We shall always assume
that $\Omega > 0$.) In the more general case of a non-axial field the single-particle
states will become mixtures of various Ω-states but the double degeneracy
will remain (Cramers degeneracy). We shall assume axial symmetry in
our considerations.
    We shall later see that nuclei with totally filled shells will remain
spherical while those lying far from closed shells will be the best candidates
for large distortions. Figure 3-1 illustrates the possible regions of large
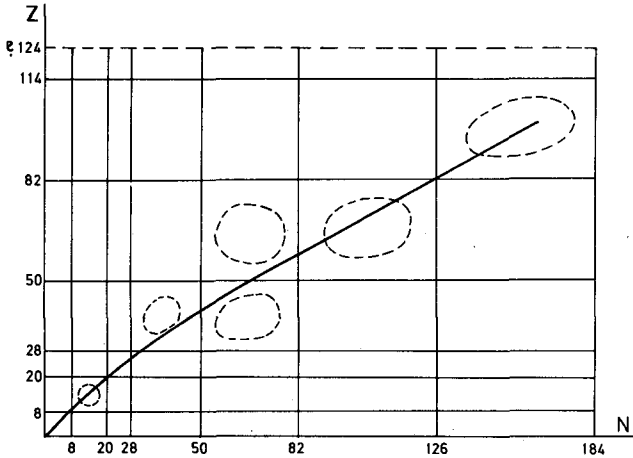
FIG.3-1. Possible regions of large deformations.

deformations. The fact that most of the known nuclei lie close to the stable nuclei "valley" limits the number of large deformed regions

1) Light-element region (A ~ 24)
2) Rare-Earth region (150 < A < 190)
3) Actinide region (A > 220).

However, one may also want to look for new deformed regions off the stability valley. The neutron-deficient region with both Z and N lying between 50 and 82 has been suggested [7] as one of the new candidates. Also such regions as the neutron-deficient region with 28 < (Z and N) < 50 or the neutron-rich region 28 < Z < 50 and 50 < N < 82 can be investigated.

A three-dimensional h.o. (harmonic oscillator) potential is the simplest potential to be used for the more detailed discussion of the eigenstate and eigenenergy properties in the deformed field. The one-particle Hamiltonian is

$$H_0 = T + M \left[\frac{\omega_x^2 x^2}{2} + \frac{\omega_y^2 y^2}{2} + \frac{\omega_z^2 z^2}{2} \right] \tag{3.1}$$

where T denotes the kinetic energy of a nucleon. Now, the dependence of the h.o. frequencies ω_x, ω_y, ω_z on deformation should be chosen in such a way that the effective "attractive power" of the potential is deformation-independent. This can be ensured by the requirement that the equipotential surfaces always enclose the same volume. This condition can be expressed simply by the relation

$$\omega_x \omega_y \omega_z = \overset{o}{\omega}_0^3 \tag{3.2}$$

where $\overset{o}{\omega}_0$ is a deformation-independent constant. It should be determined from the condition that the nucleus has a proper size. For this reason we have to calculate the average square radius of the nucleus

$$A\langle r^2 \rangle = \frac{\hbar}{M} \sum_{n_x n_y n_z} \left[\frac{1}{\omega_x} \left(n_x + \frac{1}{2} \right) + \frac{1}{\omega_y} \left(n_y + \frac{1}{2} \right) + \frac{1}{\omega_z} \left(n_z + \frac{1}{2} \right) \right]$$

(3.3)

$$\approx \frac{\hbar}{M \overset{\circ}{\omega}_0} \sum_p \left(N + \frac{3}{2} \right)_p$$

Since the number of particles in an N h.o. shell is $(N=1)(N+2)$ the quantity

$$\sum_p \left(N + \frac{3}{2} \right)_p = \sum_N \left(N + \frac{3}{2} \right) (N+1)(N+2)$$

(3.4)

is of the order of N^4, while the number of particles

$$A = \sum 1$$

(3.5)

is of the order of N^3. Thus, if we use the equation

$$\langle r^2 \rangle = \frac{3}{5} r_0^2 A^{2/3} = \frac{1}{A} \frac{\hbar}{M \overset{\circ}{\omega}_0} \sum_p \left(N + \frac{3}{2} \right)_p$$

(3.6)

we can see that $\hbar \overset{\circ}{\omega}_0$ has to be proportional to $A^{-1/3}$. The numerical value for actual nuclei is

$$\hbar \overset{\circ}{\omega}_0 \approx \frac{41}{A^{1/3}} \text{ MeV}$$

(3.7)

Now, in the axially symmetric a.h.o. (anisotropic h.o.) we can introduce a deformation parameter [8] ϵ:

$$\omega_x = \omega_y = \omega_\perp = \omega_0(\epsilon) \left(1 + \frac{1}{3} \epsilon \right) \omega_z = \omega_0(\epsilon) \left(1 - \frac{2}{3} \epsilon \right)$$

(3.8)

Then from the volume-conservation condition (3.2) we obtain

$$\omega_0(\epsilon) = \overset{\circ}{\omega}_0 \left(1 - \frac{1}{3} \epsilon^2 - \frac{2}{27} \epsilon^3 \right)^{-1/3} = \overset{\circ}{\omega}_0 \left(1 + \frac{1}{9} \epsilon^2 + \cdots \right)$$

(3.9)

The eigenstates and eigenenergies in the pure a.h.o. case can be written in a simple form. However, our aim is to add additional terms to our a.h.o. potential to get a more realistic model (Nilsson model [8]). In such a more general case it is convenient to use $\overset{\circ}{H}_0$ (= the isotropic part of the Hamiltonian (3.1)) as a diagonalization basis. In this case we have two simple possibilities for diagonalization:

1) Use of the original (x, y, z) co-ordinate system. Then we would have $\overset{0}{H}_0$ (= kinetic energy) plus a spherical part of the potential V. The non-spherical part of V remains then to be diagonalized.

2) Use of the fully "stretched" co-ordinates (x', y', z'). Then, in these co-ordinates the potential would become isotropic but the kinetic energy T would have a non-isotropic part.

It turns out that the most convenient method is to use "the stretched co-ordinates" which are only half stretched compared to case 2). Therefore we choose:

3) "the stretched co-ordinates" (dimensionless) defined by

$$\xi = x\sqrt{\frac{M\omega_\perp}{\hbar}}; \quad \eta = y\sqrt{\frac{M\omega_\perp}{\hbar}}; \quad \zeta = z\sqrt{\frac{M\omega_z}{\hbar}} \tag{3.10}$$

In these co-ordinates we have

$$H = H_\xi + H_\eta + H_\zeta \tag{3.11}$$

with

$$\left. \begin{aligned}
H_\xi &= \frac{1}{2}\,\hbar\,\omega_\perp\left(-\frac{\partial^2}{\partial\xi^2} + \xi^2\right) \\[2mm]
H_\eta &= \frac{1}{2}\,\hbar\,\omega_\perp\left(-\frac{\partial^2}{\partial\eta^2} + \eta^2\right) \\[2mm]
H_\zeta &= \frac{1}{2}\,\hbar\,\omega_z\left(-\frac{\partial^2}{\partial\zeta^2} + \zeta^2\right)
\end{aligned} \right\} \tag{3.12}$$

and

$$E = \hbar\omega_\perp\left(n_x + \frac{1}{2}\right) + \hbar\omega_\perp\left(n_y + \frac{1}{2}\right) + \hbar\omega_z\left(n_z + \frac{1}{2}\right) \tag{3.13}$$

Instead of the quantum numbers n_x, n_y, n_z, it is more convenient to use the total h.o. quantum number N and n_z together with the projection Λ of the orbital angular momentum $\vec{\ell}_t$ on the ζ - axis (where $\vec{\ell}_t$ is expressed by (ξ, η, ζ) co-ordinates instead of (x, y, z). In this way we obtain a Hamiltonian that separates into two parts: (i) a one-dimensional h.o. along ζ-axis and, (ii) a two-dimensional h.o. in the (ξ, η)- plane

$$H_\zeta \,|\, n_z \,\rangle = \hbar\,\omega_z\left(n_z + \frac{1}{2}\right) |\, n_z \,\rangle$$

$$H_\perp \,|\, n_\perp \Lambda \rangle = \hbar\omega_\perp(n_\perp + 1)\,|\, n_\perp \Lambda \rangle \tag{3.14}$$

$$(\ell_t)_\zeta \,|\, n_\perp \Lambda \rangle = \Lambda \,|\, n_\perp \Lambda \rangle$$

where

and

$$\left. \begin{aligned}
n_\perp &= n_x + n_y \\
H_\perp &= H_\xi = H_\eta
\end{aligned} \right\} \tag{3.15}$$

Including, furthermore, a spin-projection quantum number Σ we shall label the states by

$$\left| N\, n_z \Lambda \Omega \right\rangle = \left| n_z \right\rangle \left| n_\perp \Lambda \right\rangle \left| \Sigma \right\rangle \quad , \tag{3.16}$$

where

$$\left. \begin{array}{c} n_\perp + n_z = N \\ \Lambda + \Sigma = \Omega \end{array} \right\} \tag{3.17}$$

It is a property of the two-dimensional h.o. that the Λ-quantum number differs from n by an even integer

$$n_\perp - \Lambda = 0, 2, 4, 6, \cdots \tag{3.18}$$

One can prove this statement and obtain a convenient method of calculating matrix elements of various operators in the a.h.o. representation by using a very convenient set of creation and annihilation operations [9].

We first introduce familiar boson operators for creating and annihilating a single h.o. quantum:

$$\left. \begin{array}{l} \Gamma_x^+ = \dfrac{1}{\sqrt{2}}\left(\xi - \dfrac{\partial}{\partial \xi} \right) \quad \Gamma_x = \dfrac{1}{\sqrt{2}}\left(\xi + \dfrac{\partial}{\partial \xi} \right) \\[4mm] \Gamma_y^+ = \dfrac{1}{\sqrt{2}}\left(\eta - \dfrac{\partial}{\partial \eta} \right) \Gamma_y = \dfrac{1}{\sqrt{2}}\left(\eta + \dfrac{\partial}{\partial \eta} \right) \\[4mm] \Gamma_z^+ = \dfrac{1}{\sqrt{2}}\left(\zeta - \dfrac{\partial}{\partial \zeta} \right) \Gamma_z = \dfrac{1}{\sqrt{2}}\left(\zeta + \dfrac{\partial}{\partial \zeta} \right) \end{array} \right\} \tag{3.19}$$

Then usual conmutation relations hold

$$\left. \begin{array}{c} \left[\Gamma_x , \Gamma_x^+ \right] = 1 \text{ etc.} \\[4mm] \left[\Gamma_x , \Gamma_y \right] = \left[\Gamma_x , \Gamma_y^+ \right] = 0 \text{ etc.} \end{array} \right\} \tag{3.20}$$

while

For the one-dimensional motion in the ζ-direction we then get the standard h.o. representation:

$$H_\zeta = \hbar \omega_z \left(\Gamma_z^+ \Gamma_z + \dfrac{1}{2} \right) \tag{3.21}$$

with

$$\Gamma_z^+ |n_z\rangle = \sqrt{n_z + 1} \ | \ n_z + 1\rangle$$

$$\Gamma_z \ |n_z\rangle = \sqrt{n_z} \ |n_z - 1\rangle$$

(3.22)

In the (ξ, ζ)-plane it is more convenient to use S and R operators

$$S^+ = \frac{1}{\sqrt{2}} \left(\Gamma_x^+ - i \Gamma_y^+ \right) \quad R^+ = \frac{1}{\sqrt{2}} \left(\Gamma_x^+ + i \Gamma_y^+ \right)$$

$$S = \frac{1}{\sqrt{2}} \left(\Gamma_x + i \Gamma_y \right) \quad R = \frac{1}{\sqrt{2}} \left(\Gamma_x - i \Gamma_y \right)$$

(3.23)

Then we get

$$[S, S^+] = 1; \quad [R, R^+] = 1$$

$$[S, R] = [S, R^+] = [R, S^+] = 0$$

(3.24)

and

$$H_\perp = \hbar\omega_\perp (R^+ R + S^+ S + 1)$$

$$E_\perp = \hbar\omega_\perp (n_\perp + 1) = \hbar\omega_\perp (r + s + 1)$$

(3.25)

so that

$$r + s = n_\perp$$

(3.26)

Now, it is easy to show that

$$(\ell_t)_\zeta = R^+ R - S^+ S$$

(3.27)

and therefore

$$\Lambda = r - s$$

(3.28)

Here r and s denote quantum numbers associated with the two separated oscillators

$$R^+ |r\rangle = \sqrt{r+1} \ |r+1\rangle$$

$$R \ |r\rangle = \sqrt{r} \ |r-1\rangle$$

(3.29)

and

$$S^+ \mid s \rangle = \sqrt{s+1} \ \mid s+1 \rangle$$

$$S \mid s \rangle = \sqrt{s} \mid s-1 \rangle$$

(3.30)

From Eqs (3.26) and (3.28) we obtain

$$r = \frac{1}{2} (n_\perp + \Lambda)$$

$$s = \frac{1}{2} (n_\perp - \Lambda)$$

(3.31)

Since r and s are integers Eq.(3.18) is proved. Taking the normalization into account we obtain an expression for the h.o. states

$$\mid n_\perp \Lambda \rangle = \frac{1}{\sqrt{\left[\frac{1}{2} (n_\perp + \Lambda) \right]! \left[\frac{1}{2} (n_\perp - \Lambda) \right]!}} (S^+)^{\frac{n_\perp - \Lambda}{2}} (R^+)^{\frac{n_\perp + \Lambda}{2}} \mid 0 \rangle$$

(3.32)

The above representation can be used very conveniently in the calculation of various matrix elements. The physical operators are built of x, y, z co-ordinates or the corresponding momenta. By means of the above formalism we have to express them in terms of Γ_z, Γ_z^+, S, R, S^+ and R^+. Then the matrix elements are computed with Eqs (3.22), (3.29) and (3.30).

The a.h.o. oscillator potential has been used by S.G. Nilsson [8] as a basis for a more realistic model for the deformed single-particle field. We have seen that the nuclear-structure properties require the inclusion of a strong $\vec{\ell} \cdot \vec{s}$ coupling into the potential. It is convenient to write this term in the form $(\vec{\ell}_t \cdot \vec{s})$ using $\vec{\ell}_t$ rather than a real angular momentum $\vec{\ell}$; the difference between $\vec{\ell}_t$ and $\vec{\ell}$ is actually quite negligible [8]. Furthermore, the radial dependence of a realistic nuclear potential is different from that determined by h.o. The potential has to give more binding at the nuclear surface. In the h.o. potential there is no sharp surface but the addition of a term proportional to $\vec{\ell}_t^2$ with a negative coefficient will generally tend to produce the desired effect. The total Nilsson Hamiltonian has the form

$$H = H_0 + C \vec{\ell}_t \cdot \vec{s} + D \vec{\ell}_t^2$$

(3.33)

with H_0 given by Eq.(3.1).

Now the eigenstates and eigenvalues cannot be obtained in close form. Therefore, an isotropic h.o. is used as a basis of the representation (in ξ, η, ζ- variables)

$$\overset{\circ}{H}_0 = \frac{1}{2} \hbar \omega_0(\epsilon) \left(-\Delta_{(\xi, \eta, \zeta)} + \rho^2 \right)$$

(3.34)

where

$$\rho = \sqrt{\xi^2 + \eta^2 + \zeta^2} \qquad (3.35)$$

The $H - \overset{\circ}{H}_0$ part is then diagonalized.

The resulting Nilsson states are linear combinations of the eigenstates of $\overset{\circ}{H}_0$

$$\chi_\Omega = \sum_{\substack{\ell \Lambda \Sigma \\ (\Lambda + \Sigma = \Omega)}} a_{\ell \Lambda} R_{N\ell}(\rho) \, Y_{\ell \Lambda}(\vartheta_t, \varphi_t) \, \varphi_\Sigma \qquad (3.36)$$

where the coefficients $a_{\ell \Lambda}$ have been tabulated [8]. It is a great advantage of the stretched co-ordinates that the non-diagonal part $H - \overset{\circ}{H}_0$ does not involve the off-shell matrix elements (i.e. those for which $N' \neq N$).

It is also convenient to use another expansion for the Nilsson states

$$\chi_\Omega = \sum_{j\ell} c_j R_{N\ell} \, \mathcal{Y}_{j\Omega}^{\ell s} \qquad (3.37)$$

where

$$\mathcal{Y}_{j\Omega}^{\ell s} = \left[Y_{\ell \Lambda} \varphi_\Sigma \right]_{j\omega}$$

The new coefficients c_j are then related to the old ones by the relation

$$c_j = \sum_{\substack{\Lambda \Sigma \\ \Lambda + \Sigma = \Omega}} a_{\ell \Lambda} \langle \ell \tfrac{1}{2} \Lambda \Sigma | j \Omega \rangle \qquad (3.38)$$

We shall discuss the meaning of these coefficients later on.

Now, the results of the Nilsson procedure are very remarkable. Practically all the ground-state properties such as spins, level order etc. are fairly well understood in terms of the Nilsson model. Extensive discussions have been done starting with the classical work by Mottelson and

1340	$\frac{3}{2} - [512]$
1224	$\frac{3}{2} - [521]$
1031	$\frac{1}{2} - [510]$
637	$\frac{7}{2} - [514]$
399	$\frac{1}{2} - [521]$
351	$\frac{7}{2} + [633]$
0	$\frac{5}{2} - [512]$
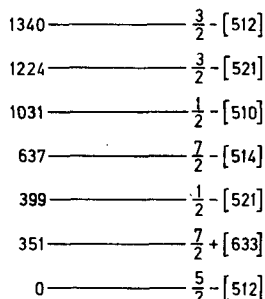
FIG. 3-2. Levels of $^{173}_{70}\text{Yb}_{103}$.

Nilsson [10]. Here, we shall give only one example of the level assignments by using an a. h. o. representation. The levels are shown on Figs. 3-2 (see Ref. [11]). All of them can be found in the Nilsson diagram of the eigenenergies plotted versus deformation ϵ.

4. POLARIZABILITY OF THE NUCLEAR CORE. METHODS FOR THE DETERMINATION OF NUCLEAR SHAPE

It is interesting to analyse the factors tending to change the shape of the nucleus. The closed-shell nuclear core obviously tends to restore spherical symmetry. On the other hand, a single nucleon moving in its individual orbit will produce a deviation from spherical distribution. Then by the interaction of the single outside nucleon with the nucleons in the core, a certain change of shape in the core may develop which might be a measure of the core distortion. We shall discuss the phenomena of this type by investigating the (E 2) interactions in the nucleus and the nuclear quadrupole movement. For a single nucleon moving in a j-shell we obtain

$$Q_p = - \frac{2j - 1}{2j + 2} \langle j | r^2 | j \rangle \tag{4.1}$$

for the mass quadrupole moment. Now we want to estimate to what extent nuclear core is deformed by the existence of the external nucleon. One possible way of handling the polarizability problem is to employ the self-consistency condition, i.e. to require that the distortion of the nuclear potential be equal to that of the nuclear-density distribution. Let us write down explicitly this condition for a three-dimensional a. h. o. [3]. We may use a Hamiltonian of the form

$$H = \frac{\vec{p}^2}{2M} + \frac{M}{2} \left(\omega_x^2 x^2 + \omega_y^2 y^2 + \omega_z^2 z^2 \right) \tag{4.2}$$

The self-consistency problem reduces then to the relations

$$\sum_j \langle x_j^2 \rangle : \sum_j \langle y_j^2 \rangle : \sum_j \langle z_j^2 \rangle = \omega_x^{-2} : \omega_y^{-2} : \omega_z^{-2} \tag{4.3}$$

Now, we may use the following notation

$$\sum_j \langle x_j^2 \rangle = \frac{\hbar}{M \omega_x} \sum_x ; \quad \sum_j \langle y_j^2 \rangle = \text{etc.} \tag{4.4}$$

where

$$\sum_x = \sum_j \left(n_x + \frac{1}{2} \right)_j ; \quad \sum_y = \dots \text{ etc.} \tag{4.5}$$

Then condition (4.3) reduces to

$$\omega_x : \omega_y : \omega_z = \sum_x^{-1} : \sum_y^{-1} : \sum_z^{-1} \tag{4.6}$$

However, using the volume-conservation condition (see chapter 3)

$$\omega_x \, \omega_y \, \omega_z = \overset{\circ}{\omega}_0^{\,3} \tag{4.7}$$

we may find that

$$\omega_x = \overset{\circ}{\omega}_0 \frac{\left(\sum_x \sum_y \sum_z \right)^{1/3}}{\sum_x} \; ; \quad \omega_y = \dots \text{ etc.} \tag{4.8}$$

Now, in Σ_x, Σ_y, Σ_z we may indicate separately the contributions from closed shells and those coming from the last particle. The former ones are equal for the x, y, z degrees of freedom, while the latter ones depend on the h.o. quantum numbers n_x, n_y, n_z. We have therefore

$$\sum_x = \frac{1}{3} \sum_0 + \left(n_x + \frac{1}{2} \right)$$

$$\sum_y = \frac{1}{3} \sum_0 + \left(n_y + \frac{1}{2} \right) \tag{4.9}$$

$$\sum_z = \frac{1}{3} \sum_0 + \left(n_z + \frac{1}{2} \right)$$

where

$$\sum_0 = 3 \sum_x = 3 \sum_y = 3 \sum_z \tag{4.10}$$
$$\quad\;\; \text{closed} \quad\;\; \text{closed} \quad\; \text{closed}$$
$$\quad\;\; \text{shells} \quad\;\;\; \text{shells} \quad\;\; \text{shells}$$

Now, let us calculate the total nuclear-mass quadrupole moment

$$Q = \sum_j \left\langle (2\,z^2 - x^2 - y^2) \right\rangle_j = \frac{\hbar^2}{M} \left(2\,\frac{\Sigma_z}{\omega_z} - \frac{\Sigma_x}{\omega_x} - \frac{\Sigma_y}{\omega_y} \right) \tag{4.11}$$

We then can separate the contributions from closed shells and those from the external nucleon

$$Q = \frac{\hbar}{M} \frac{1}{3} \sum_0 \left(\frac{2}{\omega_z} - \frac{1}{\omega_x} - \frac{1}{\omega_y} \right) + \frac{\hbar}{M} \left(\frac{2\,n_z + 1}{\omega_z} - \frac{n_x + \frac{1}{2}}{\omega_x} - \frac{n_y + \frac{1}{2}}{\omega_y} \right) \tag{4.12}$$

Using this equation we can show directly that both the terms appearing in Eq. (4.12) are equal to the first order. For this purpose, we have to use an approximation $\omega_x \approx \omega_y \approx \omega_z$ in the second term. We see that the induced mass quadrupole moment in the core is equal to that of the external nucleon. This seems to be a special property of an h.o. potential. If we introduce the core polarizability γ by the relation

$$Q_{core} = \gamma\, Q_p \tag{4.13}$$

we shall obtain $\gamma = 1$ for h.o.

Now, let us turn to the electric quadrupole moments, i.e. to quantities that are determined experimentally. For the total electric quadrupole moment we obtain

$$e\, Q^{(e)} = e_p\, Q_p + \frac{e\,Z}{A} Q_{core} = e_p\, Q_p + \frac{e\,Z}{A}\, \gamma\, Q_p \tag{4.14}$$

where

$$e_p = \begin{cases} e & \text{for a proton} \\ 0 & \text{for a neutron} \end{cases} \tag{4.15}$$

We can conclude that for light nuclei with $Z = (1/2)\, A$ we shall expect that a nucleus with one neutron outside the core will exhibit a quadrupole moment of the order of one half of the single particle unit (4.1), while in case of a proton the enhancement factor will be of the order of $3/2$. In heavier nuclei the situation seems to be more complicated. First of all, we have $Z < (1/2)\, A$, but, on the other hand, the nuclear potential differs more considerably from the h.o. one. In this case we may expect that the polarizability γ increases [12]. Roughly speaking, there is an approximate agreement between the results of this consideration and the experimental data. We may also expect that the same mechanism can be employed in the description of the (E2) electromagnetic transitions in the nuclei containing one single neutron or proton outside the core. In this case we should use the effective charge e_{eff} to account for the core contributions. From Eq. (4.14) we can see that

$$e_{eff} = e_p + \frac{e\,Z}{A}\, \gamma \tag{4.16}$$

Similar nuclear properties can be observed for the M1 transition and the nuclear magnetic moments [3].

We shall now discuss various experimental methods for the determination of the nuclear shape. First of all, we can state that the existence of rotational bands in nuclei is a qualitative indication of the existence of nuclear distortion. Similarly, the cross-section for the E2 Coulomb excitation may be seen to be proportional to the square of the intrinsic quadrupole moment Q_0. These considerations follow from the properties of the nuclear rotation and we shall analyse them later. Now, we shall limit ourselves to the more direct methods.

The simplest and most direct effect one could think of would be the shifting of the electronic energy levels in atoms caused by the non-spherical

distribution of the electric charge in the nucleus. This is usually referred to as the hfs (=hyperfine structure) in atoms. The classical expression for the Coulomb interaction between the electronic and nuclear charge has a well-known form:

$$E_{int} = \int \frac{\rho_N(\vec{\xi}) \, \rho_{e\ell}(\vec{r})}{|\vec{r} - \vec{\xi}|} \, d^3r \, d^3\xi \qquad (4.17)$$

where $\vec{\xi}$ and $\vec{r}$ are nuclear and electronic co-ordinates, respectively. Now we may expand the interaction operator $1/|\vec{r} - \vec{\xi}|$ in the region outside of nucleus

$$\frac{1}{|\vec{r} - \vec{\xi}|} = \sum_{\ell=0}^{\infty} \frac{\xi^\ell}{r^{\ell+1}} \, P_\ell(\cos \vartheta)$$

$$\qquad (4.18)$$

$$= \sum_{\ell=0}^{\infty} \frac{4\pi}{2\ell+1} \frac{\xi^\ell}{r^{\ell+1}} \sum_{\mu=-\ell}^{+\ell} Y_{\ell\mu}(\Omega_{\vec{\xi}}) \, Y_{\ell\mu}(\Omega_{\vec{r}})$$

The 1 = 0 part of this interaction when integrated over the nuclear co-ordinates is proportional to nuclear charge and gives the pure Coulomb part of the electrostatic potential of the nucleus. The 1 = 1 part vanishes and the 1 = 2 part appears to be proportional to the nuclear quadrupole moment Q

$$H^{(2)} = \frac{4\pi}{5} \sum_\mu \frac{\rho_{e\ell}(\vec{r})}{r^3} \, Y_{2\mu}(\Omega_{e\ell}) \int d^3\xi \, \xi^2 \, Y_{2\mu}(\Omega_{\vec{\xi}}) \sim \frac{1}{r^3} \, Y_{2\mu} Q \qquad (4.19)$$

Now we have to integrate it with the electronic wave functions in the coupling scheme

$$\vec{F} = \vec{\mathcal{J}} + \vec{I} \qquad (4.20)$$

where $\vec{F}$ is the spin (= total angular momentum) of the atom and $\vec{\mathcal{J}}$, $\vec{I}$ denote angular momenta of the electrons and the nucleus, respectively. The reduced matrix element of expression (4.19) is

$$\langle [I\mathcal{J}] \, F \, || \, H^{(2)} \, || \, [I\mathcal{J}] F \rangle$$

$$\qquad (4.21)$$

$$= (-1)^{I+\mathcal{J}+F} (2F+1) \left\{ \begin{matrix} \mathcal{J} \, F \, I \\ F \, \mathcal{J} \, 2 \end{matrix} \right\} \langle \mathcal{J} \, || \, H^{(2)} \, || \, \mathcal{J} \rangle$$

From this equation we can see the energy dependence on the total atomic spin F:

$$|I - \mathcal{J}| \leq F \leq I + \mathcal{J} \qquad (4.22)$$

We expect the electronic levels in atom to be split $(2I+1)$ or $(2\mathcal{J}+1)$ times and this explains the hfs in the atom [13]. The above calculation holds, of course, in first-order perturbation theory, providing the interaction is weak.

Very similar arguments can be used in the case when the external electric field with a non-vanishing gradient is employed to produce the interaction with the nuclear quadrupole moment.

Also, similar arguments are used when the experiments on μ-onic atoms are employed to look for information on nuclear shape. Here, the situation is more favourable since the μ-onic orbits are of a much smaller size (more than 200 times smaller) than the electronic ones. The μ-on is then a much more sensitive probe in the investigation of the non-sphericity of nuclear electric charge. The first-order perturbation theory is insufficient in this case and one has to diagonalize a matrix of the type of expression (4.20) with various I's and $\mathcal{J}$'s [14].

The methods described above are mainly based on the determination of the nuclear quadrupole moment Q. This quantity is obviously related with nuclear deformation. For a uniform distribution of nuclear density the relation between Q and the deformation parameter ϵ (see chapter 3) is

$$Q_0 = \frac{4}{5} Z R^2 \epsilon \left(1 + \frac{1}{3} \epsilon \right) \tag{4.23}$$

The existence of anomalous isotope shifts in some regions can also serve as a check for the nuclear deformation. The "standard unit" for the isotope shift is given [3] by considering the increase of the average square radius in the nucleus

$$\langle r^2 \rangle \approx \frac{3}{5} \left(r_0 A^{1/3} \right)^2 \tag{4.24}$$

From this we obtain

$$\delta \langle r^2 \rangle_{std} = \frac{2}{3} \langle r^2 \rangle \frac{\delta A}{A} \tag{4.25}$$

Fig. 4-1 illustrates the isotope shifts near the neutron number $N = 90$. Normally the values of $\delta \langle r^2 \rangle$ are of the order, or even lower than, $\delta \langle r^2 \rangle$ standard. However, in the $N = 90$ region, a sudden increase occurs. This behaviour can be understood in terms of nuclear deformation. The equation for the nuclear surface is

$$R = R_0 \left(1 - \frac{\beta^2}{4\pi} + \beta Y_{20} \right) \tag{4.26}$$

where the second term follows from the condition of volume conservation. Now, the increase of nuclear deformation causes the increase of the quantity $\langle r^2 \rangle$:

$$\langle r^2 \rangle \left(\frac{4}{3} \pi R_0^3 \right) = \int d\Omega \int_0^{R(\vartheta, \varphi)} dr \, r^4$$

$$= \frac{4\pi}{5} R_0^5 \left(1 + \frac{5}{4\pi} \beta^2 \right) \tag{4.27}$$
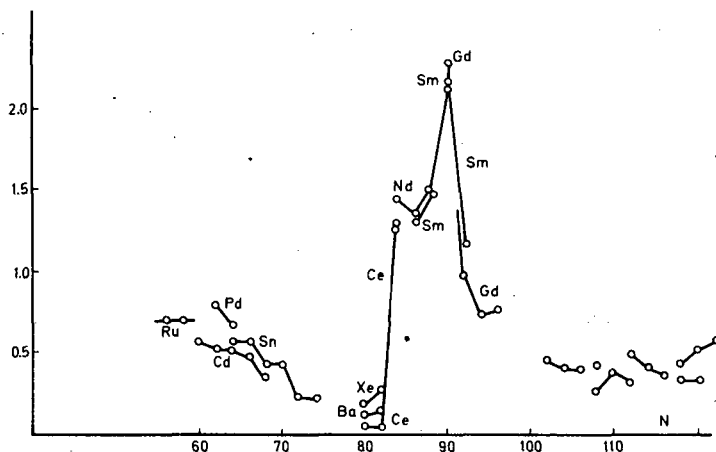
FIG.4-1. Isotope shifts near neutron number N = 90.

Hence

$$\langle r^2 \rangle = \left(1 + \frac{5}{4\pi}\beta^2\right)\langle r^2 \rangle_0 \tag{4.28}$$

Now, if we assume that in ^{150}Sm we have 0.032 for β^2, which comes from the zero-point vibration, while the corresponding quantity is 0.084 (as derived from the stable deformation) we get in ^{152}Sm

$$\frac{\delta\langle r^2 \rangle_{^{152}\text{Sm} - ^{150}\text{Sm}}}{\delta\langle r^2 \rangle_{\text{std}}} = \frac{15\,A}{8\pi}\,\delta(\beta^2) \tag{4.29}$$

This quantity is of the order of 2.4 which seems to be in a reasonable agreement with the observed value [3] (see Fig.4-1).

Some further methods of nuclear-shape determination and further references can be found in a review article, Ref.[15].

5.   THE ONSET OF NUCLEAR DEFORMATION

The considerations of this chapter will be partly based on a review article, Ref.[16]. They will mostly concern the discussion of various tendencies in nuclear motion responsible for the onset of nuclear deformation.

1) Energy of closed shells. This part of the total energy is the main contribution tending to stabilize the spherical shape. In the Nilsson model (see chapter 3) this tendency follows directly from the volume-conservation condition. The ϵ-dependence of this term is

$$\mathscr{E}_{\text{closed shells}} \sim \hbar\omega_0(\epsilon) \sim 1 + \frac{1}{9}\epsilon^2 \tag{5.1}$$

as follows from (3.9).

2) Energy of the nucleons outside of closed shells. As the single-particle orbits split in the deformed potential and some of them decrease rapidly with ϵ it is always more convenient for the nucleons to occupy the lower states at large deformation. Therefore, this term strongly tends to produce deformation. Roughly for small ϵ we have

$$\mathscr{E}_{\text{external nucleons}} \sim \epsilon \tag{5.2}$$

with a negative proportionality constant.

3) Short-range pairing forces acting between the nucleons. These forces tend to couple the nucleons in pairs with the total angular momentum $I = 0$. Such a coupling proves to be more effective in spherical nuclei than in deformed ones. Therefore, at small deformations, pairing force will rather strongly tend to restore spherical symmetry. At large deformations, however, pairing forces have the only result of washing out the little cusps in the energy curve coming from the intersections of various Nilsson levels. Thus, they are of minor influence for large ϵ. The total single-particle energy sum is modified in presence of pairing forces. The expression is

$$\mathscr{E} = \sum_{\nu} \epsilon_{\nu} \, 2v_{\nu}^2 - \Delta^2/G - G \sum_{\nu} v_{\nu}^4 \tag{5.3}$$

in standard notation.

4) Coulomb energy

$$\mathscr{E}(e) = \mathscr{E}(0) \cdot f(e) \tag{5.4}$$

where $\mathscr{E}(0)$ is the energy of a charged sphere while

$$f(e) = \frac{(1 - e^2)^{1/3}}{2e} \ln \frac{1 + e}{1 - e} \tag{5.5}$$

Here e denotes ellipsoidal excentricity and is connected with the deformation parameter ϵ by the relation

$$e = \sqrt{2\epsilon - \frac{1}{3}\epsilon^2} \Big/ \left(1 + \frac{1}{3}\epsilon\right) \tag{5.6}$$

Using the above relations we get for small ϵ

$$\mathscr{E}_{\text{Coul}} \sim 1 - \frac{4}{45}\epsilon^2 \tag{5.7}$$

We can conclude that the onset of deformation is a matter of a very detailed balance among many terms.

Mottelson and Nilsson [10] have performed the total energy calculation as a function of deformation including only terms of 1) and 2). Later on, following the Belyaev method [17], pairing and Coulomb terms have been

also included [18] with rather good agreement with experiment (see also Ref.[19]).

However, in the transition region between spherical and deformed nuclei (for example at N = 90, in the vicinity of the A = 150 nuclei or at Z = 88, in the vicinity of A = 220) it was very hard to obtain the balance between the four terms discussed above, and for some nuclei the total energy was strongly decreasing with deformation showing no minimum in the energy curve. As a remedy to this, artificial shifts, of the main h.o. shells were applied [18] which seems to be an unsatisfactory procedure. This serious difficulty has been solved by Gustafson et al. [20] who have noticed that the single-particle potential has to be improved in order to obtain the correct behaviour of the total energy as a function of the deformation. The $D\ell_t^2$ term (see chapter 3) with $D < 0$ leads to an artificial decrease at the distances between the main h.o. shells. This is indeed the case, because the average value of the operator $\vec{\ell}^2$ in the h.o. shell is not constant but increases with N. We have

$$\langle \vec{\ell}_t^2 \rangle_N = N(N+3)/2 \tag{5.8}$$

The original distance between the major h.o. shells is not an arbitrary constant but fixed by Eq.(3.7).

Therefore Gustafson et al. [20] suggested the replacement of the $D\vec{\ell}_t^2$ term in the Nilsson potential (3.33) by the term

$$D(\vec{\ell}_t^2 - \langle \vec{\ell}_t^2 \rangle_N) \tag{5.9}$$

Now, with the new term included the scheme of the single-particle levels has been calculated again with all the parameters re-adjusted, to obtain good agreement for the ground-state spins, energies of the low-lying states etc. Most probably, the new Nilsson scheme obtained in such a way gives also a better base for many other nuclear properties. As for the ground-state deformations in the transition region the obtained energy curves have now the correct behaviour (Fig.5-1).
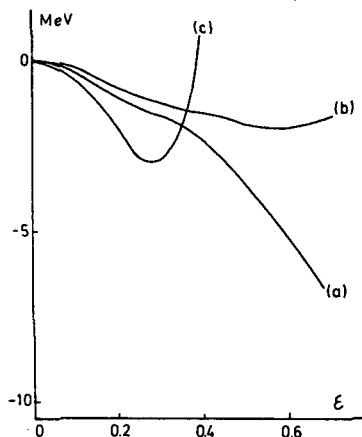
FIG.5-1. Total energy for the ^{152}Sm nucleus plotted versus deformation parameter ϵ. Curve (a) corresponds to the 1955 Nilsson potential without any modifications. Curve (b) includes the level shifts, in addition, Curve (c) corresponds to the new Nilsson potential. Pairing interactions have been included in all the three cases.
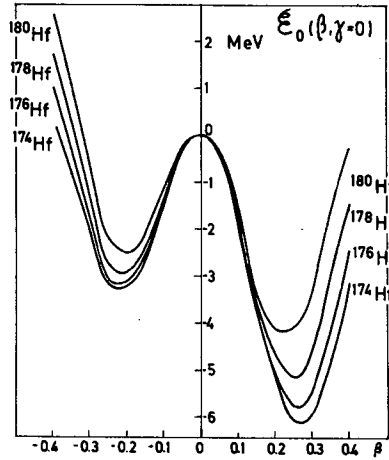
FIG. 5-2. Total-energy curves plotted for some nuclei for negative and positive values of the deformation parameter $\beta = \beta_2$. This figure is taken from Ref. [21].

The existence of higher than quadrupole components in the nuclear shape seems to be another important feature of the nuclear structure. Also the non-axial quadrupole deviations have been investigated [21]. Figures 5-2 and 5-3 show that for nuclei in the rare-earth region there is neither a big chance for the onset of an oblate shape, nor for the non-axial deviations [20]. As for the higher multipoles, the hexadecapole $\lambda = 4$, and perhaps some of the $\lambda = 6$ multipoles seem to play a role in nuclei. Including also a possibility of the octupole ($\lambda = 3$) term we may write the modified Nilsson Hamiltonian in the form

$$H = \frac{1}{2}\hbar\,\omega_0(\epsilon,\ \epsilon_4,\ \epsilon_6,\ \epsilon_3\ldots)\left\{-\Delta_\rho + \rho^2\right.$$

$$-\frac{2}{3}\rho^2\epsilon\,P_2(\cos\theta_t) + 2\epsilon_4\rho^2 P_4(\cos\theta_t)$$

$$+ 2\epsilon_6\,\rho^2\,P_6(\cos\theta_t) + 2\epsilon_3\,\rho^2\,P_3(\cos\theta_t) \tag{5.10}$$

$$\left.+ \frac{1}{3}\epsilon\left(2\frac{\partial^2}{\partial\zeta^2} - \frac{\partial^2}{\partial\xi^2} - \frac{\partial^2}{\partial\eta^2}\right)\right\} + C\vec{\ell}_t\cdot\vec{s} + D\left(\vec{\ell}_t^{\,2} - \langle\vec{\ell}_t^{\,2}\rangle_N\right)$$

Up to now, only ϵ_4 and partly ϵ_6 have been included in real calculations [22, 23]. It has been found that nuclei in both classical regions of deformation (rare earths and actinides) are unstable with respect to ϵ_4 and partly to ϵ_6. The equilibrium ϵ_4 are illustrated in Figs 5-4 and 5-5. The experimental values have been determined by Hendrie et al. [24] by the measurement of the inelastic scattering of alpha particles. The agreement seems to be remarkably good as there are no free parameters to be fitted.

$\mathcal{E}_0(\beta_0 \gamma)$
MeV
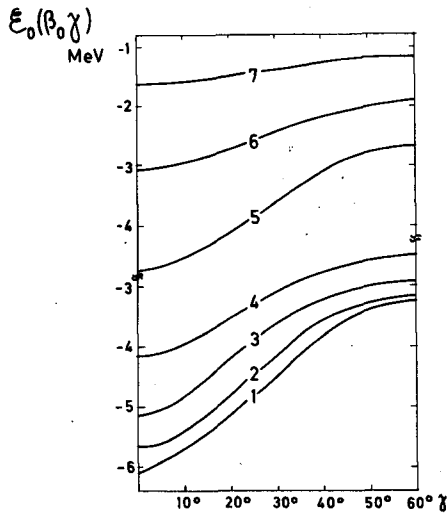
FIG. 5-3. Total energy plotted versus non-axial deformation parameter γ for some nuclei. Curves 1, 2....7 correspond to the following nuclei [174]Hf, [176]Hf, [178]Hf, [180]Hf, [156]Gd, [154]Gd, [152]Gd, respectively. This figure is taken from Ref. [21].
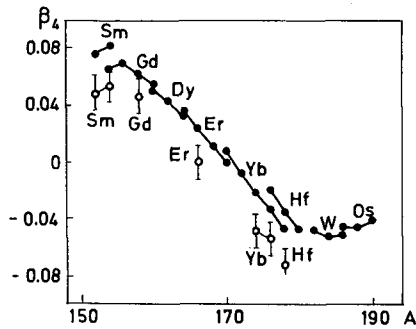
FIG. 5-4. The equilibrium hexadecapole deformation for nuclei in the rare earth region. Solid line with black circles refers to the theoretical results. Open circles correspond to the experimental values obtained by Hendrie et al. [24]. This figure is taken from Ref. [22].
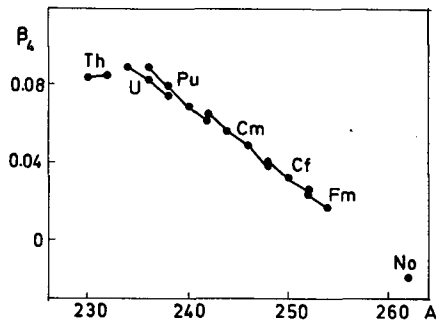
FIG. 5-5. Theoretical results for the equilibrium hexadecapole parameters for the actinide region. This figure is taken from Ref. [22].

6. NUCLEAR ROTATIONAL MOTION

So far we have been discussing only the motion of nucleons in the non-spherical well. The corresponding wave function χ (x¹) is not characterized by the total angular momentum quantum number I. The χ wave function depends therefore on the positions of the main nuclear axes with respect to the "laboratory frame" indirectly as the body-fixed co-ordinates x¹ refer to the nuclear axes. We may indicate this by writing explicitly χ (x¹ (α, β, γ)) where α, β, γ are variables that define the positions of nuclear axes in the original x-frame. The variables α, β, γ may be chosen for example as the familiar Euler angles of x¹-frame with respect to x-frame. Now, $\chi_\Omega(x¹(\alpha, \beta, \gamma))$ is obviously a degenerate state with respect to α, β, γ. We may take the wave packet

$$\Psi = \int \Phi(\alpha, \beta, \gamma) \chi_\Omega (x¹ (\alpha, \beta, \gamma)) \, d(\alpha, \beta, \gamma) \qquad (6.1)$$

Now, we may choose $\Phi(\alpha, \beta, \gamma)$ such as to obtain Ψ as an eigenstate of the total angular momentum $\vec{I}^2$ and its projection on the z-axis M.

In the following, we shall use a simpler approach by assuming that the two groups of the degrees of freedom are independent [3]:

$$\Psi_M^I \sim \Phi(\alpha, \beta, \gamma) \chi_\Omega (x¹) \qquad (6.2)$$

The function Φ must be a simultaneous eigenfunction of $\vec{I}^2$ and I_z. For an axially symmetric system also the projection of $\vec{I}$ on the nuclear symmetry axis, I_3, is a good quantum number and may be used simultaneously with $\vec{I}^2$ and I_z to label the states. This is possible as it turns out that each of the body-fixed projections I_1, I_2, I_3 of $\vec{I}$ commutes with each of the operators I_x, I_y, I_z:

$$[I_k, I_\alpha] = 0 \qquad (6.3)$$

for k = 1, 2, or 3 and α = x, y, or z.

These relations can easily be proved by observing that I_k is essentially a scalar product of $\vec{I}$ with a unit vector $\vec{e}$ (k) along the k-th axis

$$I_k = \vec{I} \cdot \vec{e}^{(k)} \qquad (6.4)$$

Relations (6.3) follow immediately after employing the well-known relations for the commutators of $\vec{I}$ with an arbitrary vector

$$[I_\alpha, v_\beta] = i \epsilon_{\alpha\beta\gamma} v_\gamma \qquad (6.5)$$

Similarly, we may prove the commutation relations among the I_1, I_2 and I_3 components

$$[I_k, I_\ell] = - i \epsilon_{k\ell m} I_m \qquad (6.6)$$

which differ from the ordinary relations for angular momenta by the
existence of a minus sign on the right-hand side of Eq.(6.6). Therefore
we have

$$(I_1 \mp i I_2)|IK\rangle = \sqrt{(I \mp K)(I \pm K + 1)} \; | \; I \; K \pm 1 \rangle \qquad (6.7)$$

while for the I_x and I_y components

$$(I_x \pm i \; I_y)|IM\rangle = \sqrt{(I \mp M)(I \pm M + 1)} \; |IM \pm 1\rangle \qquad (6.8)$$

We conclude that $\Phi(\alpha, \beta, \gamma)$ must be a simultaneous eigenfunction of the
operators $\vec{I}^2$, I_z and I_3

$$\vec{I}^2 \Phi = I(I+1) \Phi$$

$$\qquad\qquad\qquad\qquad\qquad\qquad (6.9)$$

$$I_z \Phi = M \Phi; \qquad I_3 \Phi = K \Phi$$

fulfilling simultaneously Eqs (6.7) and (6.8). It can be shown that the above
conditions are fulfilled by the well-known rotational $D^I_{MK}(\alpha, \beta, \gamma)$ wave function
of the symmetrical top. The same function is also defined as a transition
matrix for the spherical harmonics when they are rotated

$$Y_{\ell m}(\vartheta, \varphi) = \sum_{mm'} D^\ell_{mm'}(\alpha, \beta, \gamma) \; Y_{\ell m'}(\vartheta', \varphi') \qquad (6.10)$$

We shall assume that the properties of the D-functions are known [25].
We can then conclude that the structure of the wave function Ψ^I_{MK} is

$$\Psi^I_{MK} \sim D^I_{MK}(\alpha, \beta, \gamma) \; \chi_\Omega(x') \qquad (6.11)$$

The simple form (6.11) has to be modified in order to account for the
additional symmetry with respect to reflection on the plane perpendicular to
the symmetry axis. For an axially symmetric system this is equivalent
to the rotation R through 180° with respect to the axis perpendicular to the
symmetry axis. We shall choose the "2" axis for this purpose. Now, the
transformation R can be performed in two ways:

1) Rotation R_e of the "123" axes. The corresponding operator is then

$$R_e = e^{i\pi I_2} \qquad (6.12)$$

2) Rotation R_i of the intrinsic system

$$R_i = e^{i\pi \mathscr{I}_2} \qquad (6.13)$$

Here, $\mathcal{J}_2$ is the "2" projection of the intrinsic angular momentum $\vec{\mathcal{J}}$. Together with the collective part of the angular momentum $\vec{R}$ they form the total nuclear angular momentum

$$\vec{R} + \vec{\mathcal{J}} = \vec{I} \qquad (6.14)$$

Now it is clear that both ways 1) and 2) must give the same result so that

$$R_e^{-1} R_i = 1 \qquad (6.15)$$

This relation is not an identity but should rather be understood as a condition imposed on the wave function Ψ_{MK}^I. Let us examine more closely the result of this condition. We have

$$R_e D_{MK}^I = (-1)^{I-K} D_{M-K}^I \qquad (6.16)$$

as following from the properties of the D-functions. Let us now turn to R_1, assuming first that $\Omega \neq 0$. Then we have

$$e^{i\pi \mathcal{J}_2} \chi_\Omega = e^{i\pi \mathcal{J}_2} \sum_{\mathcal{J}} c_{\mathcal{J}} \chi_{\mathcal{J},\Omega} = \sum_{\mathcal{J}} c_{\mathcal{J}} (-1)^{\mathcal{J}+K} \chi_{\mathcal{J},-\Omega} \qquad (6.17)$$

where $\chi_{\mathcal{J},\Omega}$ is the eigenfunction of $\vec{\mathcal{J}}^2$ and $\mathcal{J}_3$. Now, we shall choose the phases of χ_Ω in such a way that $\chi_{-\Omega}$ is defined (for $\Omega > 0$) as

$$R_i \chi_\Omega = e^{i\pi \mathcal{J}_2} \chi_\Omega = \chi_{-\Omega} \qquad (6.18)$$

for $\Omega > 0$.

For half integer Ω or K we must observe that

$$R_e^2 = (-1)^{2I} \quad \text{and} \quad R_i^2 = (-1)^{2I} \qquad (6.19)$$

Employing the above relations we obtain (using also the normalization) for $K \neq 0$

$$\Psi_{MK}^I = \sqrt{\frac{2I+1}{16\pi^2}} \left\{ D_{MK}^I \chi_\Omega + (-1)^{I+K} D_{M-K}^I \chi_{-\Omega} \right\} \qquad (6.20)$$

Now both for $K \neq 0$ and $K = 0$ we must have

$$\Omega = K \qquad (6.21)$$

as result of the required rotational invariance with respect to the rotation

about the "3" axis, i.e. we assume that Ψ^I_{MK} should not change if we rotate the system about this axis; this gives

$$(I_3 - \mathscr{J}_3)\, \Psi^I_{MK} = 0 \tag{6.22}$$

so that (6.21) follows immediately. For $K \neq 0$ then (6.20) becomes

$$\Psi^I_{MK} = \sqrt{\frac{2I+1}{16\pi^2}} \left\{ D^I_{MK}\, \chi_K + (-1)^{I+K}\, D^I_{M-K}\, \chi_{-K} \right\} \tag{6.23}$$

for $K > 0$.

For $K = 0$ Eq. (6.16) still holds while for the intrinsic part $\chi_{K=0}$ we may write

$$R_i\, \chi_0 = r\, \chi_0 \tag{6.24}$$

where $r = \pm 1$ is a quantum number related to the operation R_i. In this case we obtain for a normalized wave function

$$\Psi^I_{M,K=0} = \sqrt{\frac{2I+1}{32\pi^2}}\, D^I_{M,0}\, \chi_0 \left(1 + (-1)^I r \right) \tag{6.25}$$

Now, we shall write the Hamiltonian for our system in the form

$$H = T_{rot} + H_{intr}(x') \tag{6.26}$$

where T_{rot} is rotational energy:

$$\begin{aligned}
T_{rot} &= \frac{\hbar^2 R_1^2}{2\mathscr{J}} + \frac{\hbar^2 R_2^2}{2\mathscr{J}} + \frac{\hbar^2 R_3^2}{2\mathscr{J}_3} \\
&= \frac{\hbar^2}{2\mathscr{J}}\, \vec{R}^2 + \left(\frac{\hbar^2}{2\mathscr{J}_3} - \frac{\hbar^2}{2\mathscr{J}} \right) R_3^2
\end{aligned} \tag{6.27}$$

where $\mathscr{J}$ and $\mathscr{J}_3$ are moments of inertia. The last term in Eq. (6.27) must vanish since $R_3 = I_3 - \mathscr{J}_3$ has always the eigenvalue equal to zero as a result of Eq. (6.21). We have not introduced any coupling between the two groups of the degrees of freedom in Eq. (6.26) as we assume that the coupling is very weak. The separation in the wave function Ψ in the form of expression (6.2) is only possible if the rotational motion is slow as compared to the intrinsic motion and if the deformation in $\chi(x')$ is well pronounced. Using expression (6.14) we may transform our Hamiltonian (6.26) in the form

$$H = H_0 + H_{RPC} + H'_{intr} \tag{6.28}$$

where

$$H_0 = \frac{\hbar^2}{2\mathscr{J}}\left(\vec{I}^2 - I_3^2\right) \tag{6.29}$$

$$H_{RPC} = -\frac{\hbar^2}{2\mathscr{J}}\left(I_+ \mathscr{J}_- + I_- \mathscr{J}_+\right) \tag{6.30}$$

$$H'_{intr} = H_{intr} + \frac{\hbar^2}{2\mathscr{J}}\left(\vec{\mathscr{J}}^2 - \mathscr{J}_3^2\right) \tag{6.31}$$

where $J_3 = I_3 = K$ and $I_\pm$, $\mathscr{J}_\pm$ operators are given by

$$\left.\begin{array}{l} I_\pm = I_1 \pm i I_2 \\[2mm] \mathscr{J}_\pm = \mathscr{J}_1 \pm i \mathscr{J}_2 \end{array}\right\} \tag{6.32}$$

We can see that H_0 is the part determining the rotational energy, H_{RPC} defines a rotation-particle coupling (although we have not introduced any primary coupling in expression (6.26)) and H'_{intr} corresponds to the motion of particles in a deformed rotating potential. The part H_{RPC} has the structure of a Coriolis coupling.

7. ROTATIONAL SPECTRA

In the last lecture we have formulated fundamental principles under-lying the structure of rotational motion in deformed nuclei. We have arrived at the form of the wave functions (6.23) or (6.25) and of the rota-tional Hamiltonian (6.28). Now, we shall turn our attention to the discus-sion of the main consequences of the above assumptions. In this lecture, we shall be mostly concerned with the rotational spectra of the even-even and odd-A nuclei.

The ground-state rotational band in an even nucleus is characterized by the wave function (6.25)

$$\Psi^I_{MK} = \sqrt{\frac{2I+1}{32\pi^2}}\, D^I_{M0}\, \chi_0\left(1 + r\,(-)^I\right) \tag{7.1}$$

The intrinsic wave function χ_0 is constructed from pairs of nucleons occupying pairwise the Nilsson orbitals $+K$ and $-K$. For two nucleons we have

$$\chi_0 = \sum_K C_K \left(\varphi_K(1)\varphi_{-K}(2) - \varphi_K(2)\varphi_{-K}(1)\right) \tag{7.2}$$

satisfying the antisymmetry requirement. We shall now investigate the properties of the function χ_0 with respect to rotation through 180° about

the "2"-axis. For this purpose we apply the operator (6.13). The result is

$$e^{i\pi \not j_2} \chi_0 = \sum_K C_K \left(- \varphi_{-K}(1) \varphi_K(2) + \varphi_{-K}(2) \varphi_K(1) \right) = \chi_0 \qquad (7.3)$$

This formula follows from the fact that for positive K we must have

$$e^{i\pi \not j_2} \varphi_{-K} = - \varphi_K; \qquad (K > 0) \qquad (7.4)$$

in accordance with relations (6.18) and (6.19). We conclude that r = +1 for the ground-state rotational band.

Slightly more general considerations have to be applied to rotational bands due to the vibrational K = 0 states, such as the β-vibrational state, i.e. Kπ = 0⁺ (π = parity), octupole vibration Kπ = 0⁻, etc. Essentially, K = 0 vibrations involve states built up from pairs of quasi-particles coupled to K = 0. The general structure of a two-body wave function can be expressed in the form of

$$\chi_0 = \sum_{\tau \tau' K} \langle \tau' K | M_\lambda | \tau K \rangle \left(\varphi_{\tau' K}(1) \varphi_{\tau -K}(2) - \varphi_{\tau' K}(2) \varphi_{\tau -K}(1) \right)$$

$$= \sum_{\tau \tau', K > 0} \langle \tau' K | M_\lambda | \tau K \rangle \left(\varphi_{\tau' K}(1) \varphi_{\tau -K}(2) - \varphi_{\tau' K}(2) \varphi_{\tau -K}(1) \right) \qquad (7.5)$$

$$+ \sum_{\tau \tau' K > 0} \langle \tau' - K | M_\lambda | \tau - K \rangle \left(\varphi_{\tau' -K}(1) \varphi_{\tau K}(2) - \varphi_{\tau' -K}(2) \varphi_{\tau K}(1) \right)$$

where M_λ is a tensor operator of rank λ. Now, there exists a definite relation between the matrix elements of M_λ when the sign of K is changed

$$\langle \tau' - K | M_\lambda | \tau - K \rangle = p(-1)^\lambda \langle \tau' K | M_\lambda | \tau K \rangle \qquad (7.6)$$

where p denotes a certain phase factor independent of multipolarity λ. The use of the operator R_i given by expression (6.13) in the wave function (7.5), taking account of relation (7.6) gives

$$R_i \chi_0 = - p(-1)^\lambda \chi_0 \qquad (7.7)$$

We can fix the phase p by considering the case λ = 0 for which M = 1 and the wave function reduces to (7.2); then p = -1 so that finally we obtain in expression (7.1)

$$r = (-1)^\lambda \qquad (7.8)$$

It follows immediately from the above value of r and Eq.(7.1) that for the ground-state and the vibrational Kπ = 0⁺ bands in even nuclei only even values

of the total nuclear angular momentum I can occur. On the other hand, the odd-parity rotational bands with $K\pi = 0^-$ (and the vibrational character) we have only odd I-values. Now looking at the Hamiltonian (6.29) and the wave function (7.1) we see that the following spectra of the rotational type can occur in even nuclei:

$$E = E_0 + \frac{\hbar^2}{2\mathscr{J}} I(I + 1) \qquad (7.9)$$

with

$I\pi = 0^+, 2^+, 4^+, \ldots$ for the ground state and even-parity $K = 0$ vibrations

and

$I\pi = 1^-, 3^-, 5^-, \ldots$ for the negative-parity $K = 0$ vibrations

The most direct verification of the validity of the rotational model and formula (7.9) consists of calculating the ratios of the excited-state energies observed in deformed nuclei. For example, in the ground-state band the energy ratios should be

$$\frac{E_4}{E_2} = \frac{10}{3}; \qquad \frac{E_6}{E_2} = 7; \text{ etc.} \qquad (7.10)$$

The agreement of these predictions with observation is remarkable, and the deviations occur at the boundaries of the deformed-nuclei regions where the rotational model itself is not so well founded.

As an illustration of the occurrence of rotational bands in even nuclei let us take the ^{238}U nucleus (Fig. 7-1). We can easily recognize the ground state rotational band as well as the other two $K = 0$ bands: 1) of positive parity (β-vibrational quadrupole states) and 2) of negative parity (octupole, $K = 0$ vibration). The fourth, highest band (a quadrupole γ-vibration) is characterized by $K\pi = 2^+$ quantum numbers. As $K \neq 0$ we have no restriction on the values of I for this band, and its wave function is given by Eq.(6.23) instead of Eq.(6.25). The levels presented in Fig. 7-1 have been obtained by Coulomb excitation [26]. Another example of a single band in the ^{170}Hf nucleus is given in Fig. 7-2. This band has been observed [27] due to the heavy ion excitation method. Heavy ions are able to transfer rather large units of angular momentum to the target nucleus and the multiple Coulomb excitation becomes possible. The occurrence of all the spins up to $I\pi = 18^+$
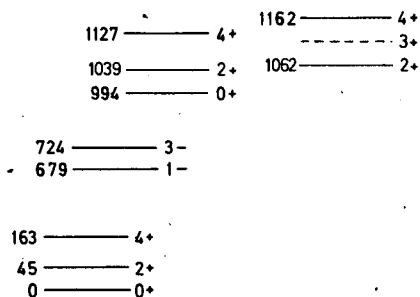
FIG. 7-1.   Rotational bands in ^{238}U.

```
     3761 ——————— 18+



     3147 ——————— 16+



     2564 ——————— 14+



     2013 ——————— 12+



     1503 ——————— 10+
```

FIG.7-2. Single band in ^{170}Hf nucleus.

```
     1041 ——————— 8+


     641 ——————— 6+

     321 ——————— 4+

     100 ——————— 2+
       0 ——————— 0+
              170
               72 Hf
```
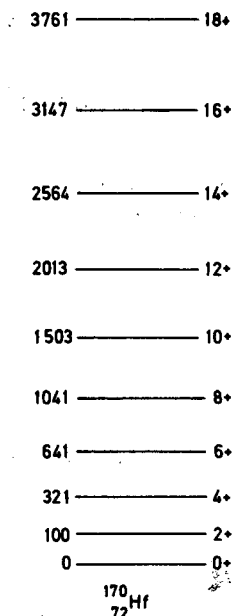
is quite impressive. Let us turn our attention to the odd-A nuclei. Here
we expect the existence of many single-particle states with half integer K,
which are essentially Nilsson orbitals. Each of these states generates a
rotational band with $I = K, K+1, K+2, \ldots$. Again the energy ratios in such
a band would be determined by the $I(I+1)$ rule following from relation (7.9).
There is one important deviation from this rule for $K = 1/2$. In this case,
there exists a non-zero contribution (diagonal) coming from the H_{RPC} part
(6.30) apart from the normal term which follows from H_0 given by relation
(6.29).

   The non-zero diagonal contribution derived from relation (6.30) is
possible, owing to the existence of the two terms in the wave function (6.23).
The interference terms in question are

$$-\frac{\hbar^2}{2\mathscr{I}}\frac{2I+1}{16\pi^2}\left\{\left\langle D^I_{MK}\chi_K\left|I_-\mathscr{J}_+\right|D^I_{M-K}\chi_{-K}\right\rangle\right.$$

$$\left.+\left\langle D^I_{M-K}\chi_{-K}\left|I_+\mathscr{J}_-\right|D^I_{MK}\chi_K\right\rangle\right\}(-)^{I+K}\qquad(7.11)$$

Now

$$\left\langle D^I_{MK}\chi_K\left|I_-\mathscr{J}_+\right|D^I_{M-K}\chi_{-K}\right\rangle$$

$$=\left\langle D^I_{MK}\left|I_-\right|D^I_{M-K}\right\rangle\left\langle\chi_K\left|\mathscr{J}_+\right|\chi_-\right\rangle\qquad(7.12)$$

$$=\frac{8\pi^2}{2I+1}\sqrt{(I+K)(I-K+1)}\,\delta_{K,-K+1}\left\langle\chi_K\left|\mathscr{J}_+\right|\chi_{-K}\right\rangle$$

The other element in expression (7.11) gives

$$\sqrt{(I+K)(I-K+1)} \; \frac{8\pi^2}{2I+1} \; \delta_{-K,\,K+1} \langle \chi_{-K} | \mathcal{J}_- | \chi_K \rangle \tag{7.13}$$

In the above calculations we have used Eq.(6.7). Now the application of the R_i (unitary) operator to the matrix elements appearing in (7.13) gives

$$\langle \chi_{-K} | \mathcal{J}_- | \chi_+ \rangle = \langle \chi_{-K} | R_i^+ \; (R_i \; \mathcal{J}_- R_i^{-1}) \; R_i | \chi_K \rangle \tag{7.14}$$

$$= \langle \chi_K | \mathcal{J}_+ | \chi_{-K} \rangle \tag{7.15}$$

Here we have employed the following relations

$$R_i \, \mathcal{J}_- R_i^{-1} = - \, \mathcal{J}_+$$

$$\langle \chi_{-K} | R_i^+ = - \langle \chi_K | \quad \text{for } K > 0 \tag{7.16}$$

Finally, the expectation value of the H_{RPC} operator (6.30) in the state (6.23) is obtained

$$\langle \Psi^I_{MK} | H_{RPC} | \Psi^I_{MK} \rangle = \left(I + \frac{1}{2}\right)(-)^{I+\frac{1}{2}} \delta_{K,\,\frac{1}{2}} \frac{a\hbar^2}{2\mathcal{J}} \tag{7.17}$$

as it is obvious that the term (7.13) and (7.14) are different from zero only if $K = 1/2$. In Eq.(7.17) there appears a parameter a, called the decoupling parameter:

$$a = - \langle \chi_K | \mathcal{J}_+ | \chi_{-K} \rangle \tag{7.18}$$

which depends only on the details on the intrinsic structure and can, for example, be calculated with Nilsson wave functions.

The total energy including the additional contribution (7.17) is

$$E = E_0 + \frac{\hbar^2}{2\mathcal{J}} \left[I(I+1) + \delta_{K,\,\frac{1}{2}} (-)^{I+\frac{1}{2}} \left(I + \frac{1}{2}\right) a \right] \tag{7.19}$$

Owing to the additional term in the $K = 1/2$ bands, the energy levels tend to bunch in pairs. It turns out that for $a < -1$ the level with $I = 3/2$ goes below the $I = 1/2$ level, whereas for $a > 1$ the $I = 5/2$ level goes below the $I = 3/2$ level.

As an example, let us see the level spectrum in the odd-A nucleus $^{165}_{67}$Ho (Fig.7-3). The ground-state band is built on a single-proton state labelled by the Nilsson quantum numbers 527 7/2 (see Eq.3.16)). The
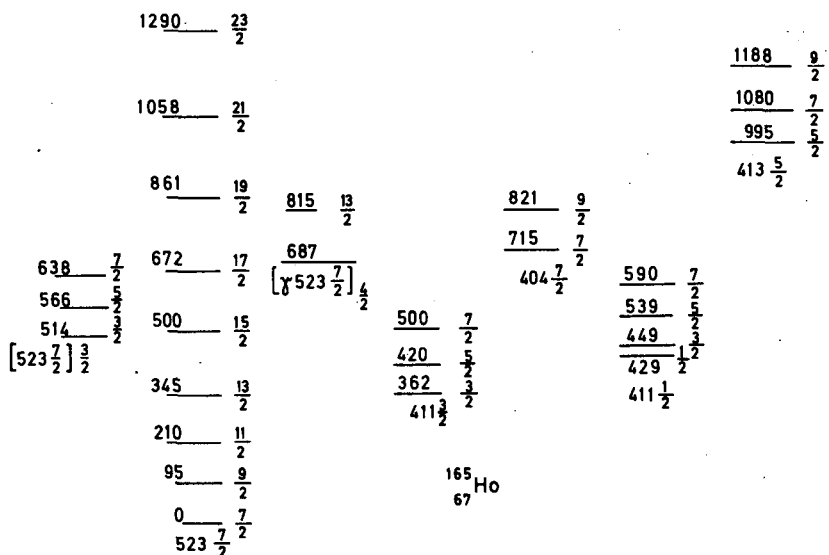
FIG.7-3. Level spectrum in $^{165}_{67}$Ho nucleus.

other single-particle states 411 3/2, 404 7/2, 411 1/2 and 413 5/2 have
also been observed and produce other rotational bands. In the K = 1/2 band
(411 1/2) the obvious deviation from the I(I+i) can be seen. They can be
well understood in terms of the generalized energy formula (7.19). We can
also turn our argument around and use expression (7.19) in order to fit
the two intrinsic parameters: moment of inertia, I, and decoupling para-
meter, a from the observed energies in the (411 1/2) band. In Fig.(7-3) we
can also see the two bands due to the two intrinsic states at 514 keV and
687 keV. The structure of these states is understood as a result of a
coupling of the single-particle state 523 7/2 to the quadrupole γ-vibration
with Kπ = 2$^+$. The two resulting K values equal to 11/2 and 3/2 follow from
the parallel and antiparallel coupling of K = 7/2 to K = 2. The above example
presented in Fig.7-3 has been taken from the lectures by S.G. Nilsson [28].
Many other examples in this paper have been taken from this reference.

8. ROTATIONAL INTENSITY RULES

Up to now, we have only been interested in discussing the positions of
the energy levels in various rotational bands. In this lecture we shall
consider another very important conclusion following directly from the
assumptions of the rotational motion: the rules governing various transitions
in nuclei. We shall discuss only the electromagnetic (gamma) transitions.
However, the rules are also valid in other cases such as, for example,
beta-decay transitions.

Let us take a gamma transition of multipolarity λ. The electromagnetic
operator for such a transition (E λ or M λ) is a tensor of the rank λ and
transforms with the D^λ matrices [25]:

$$\mathcal{M}(\lambda,\mu) = \sum_\nu D^\lambda_{\mu\nu}(\alpha,\beta,\gamma)\mathcal{M}'(\lambda,\nu) \qquad (8.1)$$

where $\mathcal{M}'(\lambda, \nu)$ denotes the operator referred to the body-fixed frame of reference determined by the Euler angles α, β, γ.

To calculate the transition probability we have first to start with a matrix element of $\mathcal{M}(\lambda, \mu)$ computed between two nuclear states: final $\Psi_{M_f K_f}^{I_f}$ and initial $\Psi_{M_i K_i}^{I_i}$. Using expression (6.23) for the wave functions and separating various parts of the operator (8.1) we obtain

$$M_{if} = \left\langle \Psi_{M_f K_f}^{I_f} \left| \mathcal{M}(\lambda, \mu) \right| \Psi_{M_i K_i}^{I_i} \right\rangle$$

$$= \frac{\sqrt{(2I_i+1)(2I_f+1)}}{16\pi^2} \sum_\nu \left\{ \left\langle D_{M_f K_f}^{I_f} \left| D_{\mu\nu}^\lambda \right| D_{M_i K_i}^{I_i} \right\rangle \left\langle K_f \left| \mathcal{M}'(\lambda\nu) \right| K_i \right\rangle \right.$$

$$+ (-1)^{I_i+K_i+I_f+K_f} \left\langle D_{M_f-K_f}^{I_f} \left| D_{\mu\nu}^\lambda \right| D_{M_i-K_i}^{I_i} \right\rangle \left\langle -K_f \left| \mathcal{M}'(\lambda\nu) \right| -K_i \right\rangle \qquad (8.2)$$

$$+ (-1)^{I_i+K_i} \left\langle D_{M_f K_f}^{I_f} \left| D_{\mu\nu}^\lambda \right| D_{M_i-K_i}^{I_i} \right\rangle \left\langle K_f \left| \mathcal{M}'(\lambda\nu) \right| -K_i \right\rangle$$

$$+ (-1)^{I_f+K_f} \left\langle D_{M_f-K_f}^{I_f} \left| D_{\mu\nu}^\lambda \right| D_{M_i K_i}^{I_i} \right\rangle \left\langle -K_f \left| \mathcal{M}'(\lambda\nu) \right| K_i \right\rangle \right\}$$

Using the relations

$$\left\langle D_{M_f K_f}^{I_f} \left| D_{\mu\nu}^\lambda \right| D_{M_i K_i}^{I_i} \right\rangle = \frac{8\pi^2}{2I_f+1} \left\langle I_i \lambda M_i \mu | I_f M_f \right\rangle \left\langle I_i \lambda K_i \nu | I_f K_f \right\rangle \qquad (8.3)$$

and

$$\left\langle -K_f \left| \mathcal{M}'(\lambda\nu) \right| -K_i \right\rangle = (-1)^{\lambda+K_i-K_f} \left\langle K_f \left| \mathcal{M}'(\lambda, \nu) \right| K_i \right\rangle \qquad (8.4)$$

(the first of these relations can be found in any textbook on angular momentum [25]; the second relation is obtained by expanding the states in terms of spherical orbitals and applying the Wigner-Eckart theorem) we come to the conclusion that the first and second terms in the curly bracket of Eq. (8.2) are equal. The third and fourth terms are equal by similar arguments. Thus we finally get by also employing relation (8.3)

$$M_{if} = \sqrt{\frac{2I_i+1}{2I_f+1}} \left\langle I_i \lambda M \mu | I_f M_f \right\rangle \left\{ \left\langle I_i \lambda K_i \nu | I_f K_f \right\rangle \right.$$

$$\times \left\langle K_f \left| \mathcal{M}'(\lambda\nu) \right| K_i \right\rangle + (-1)^{I_i+K_i} \left\langle I_i \lambda -K_i \nu | I_f K_f \right\rangle \qquad (8.5)$$

$$\times \left\langle K_f \left| \mathcal{M}'(\lambda\nu) \right| -K_i \right\rangle \right\}$$

We have omitted the summation over ν since always $\nu = K_f \mp K_i$.

In many cases of interest we have $\lambda < K_i + K_f$. Then the second term in expression (8.5) vanishes and we obtain

$$M_{if} = \sqrt{\frac{2I_i + 1}{2I_f + 1}} \langle I_i \lambda M_i \mu | I_f M_f \rangle \langle I_i \lambda K_i \nu | I_f K_f \rangle \langle K_f | \mathscr{M}'(\lambda \nu) | K_i \rangle \qquad (8.6)$$

Introducing the reduced matrix element by the Wigner-Eckart formula

$$\langle \Psi^{I_f}_{M_f K_f} | \mathscr{M}(\lambda \nu) | \Psi^{I_i}_{M_i K_i} \rangle \qquad (8.7)$$

$$= \frac{\langle I_i \lambda M_i \mu | I_f K_f \rangle}{\sqrt{2I_f + 1}} \langle \Psi^{I_f}_{K_f} || \mathscr{M}(\lambda) || \Psi^{I_i}_{K_i} \rangle$$

we can also write down relation (8.6) in the form

$$\langle \Psi^{I_f}_{K_f} || \mathscr{M}(\lambda) || \Psi^{I_i}_{K_i} \rangle \qquad (8.8)$$

$$= \sqrt{2I_i + 1} \langle I_i \lambda K_i \nu | I_f K_f \rangle \langle K_f | \mathscr{M}'(\lambda \nu) | K_i \rangle$$

In case of $K_i = 0$ an additional factor $\sqrt{2}$ occurs in this equation. The reduced transition probability $B(\lambda)$ is defined as

$$B(\lambda, I_i K_i \to I_f K_f) = \sum_{M_f(\mu)} |M_{if}|^2 \qquad (8.9)$$

or equivalently in terms of the reduced matrix element

$$B(\lambda, I_i K_i \to I_f K_f) = \frac{1}{2I_i + 1} \langle \Psi^{I_f}_{K_f} || \mathscr{M}(\lambda) || \Psi^{I_i}_{K_i} \rangle \qquad (8.10)$$

If Eq. (8.6) is valid we obtain from these definitions

$$B(\lambda, I_i K_i \to I_f K_f) = \langle I_i \lambda K_i \nu | I_f K_f \rangle^2 |\langle K_f | \mathscr{M}(\lambda, \nu) | K_i \rangle|^2 \qquad (8.11)$$

A remarkable property of the transitions follows from this formula. If we have two transitions from state $(I_i K_i)$ to the two members I_f and I'_f of the same rotational band the ratio of the corresponding $B(\lambda)$ turns out to be a purely geometrical factor

$$\frac{B(\lambda, I_i K_i \to I'_f K_f)}{B(\lambda, I_i K_i \to I_f K_f)} = \frac{\langle I_i \lambda K_i \nu | I'_f K_f \rangle^2}{\langle I_i \lambda K_i \nu | I_f K_f \rangle^2} \qquad (8.12)$$

determined by the sector-addition coefficients. Similar relations would hold for two transitions starting from two members of one initial rotational

band and ending on the same final state $I_f K_f$. Equations (8.12) are widely
known and used as the Alaga, Alder, Bohr and Mottelson intensity rules [29].

The most important conclusions following from the above consideration
are the following:

1) The branching ratios (8.12) may be used in order to determine
experimentally the K-value for a band given.

2) In case of $\lambda < |K_i - K_f|$ the transition becomes forbidden within the
framework of the scheme. As the wave functions (6.23) are only approximate
we shall expect the transition to occur in nature but retarded. This fact is
confirmed in many cases and known as the approximate K-selection rule.

3) The electric quadrupole transitions calculated between the states of
the same rotational band provide us with an additional important conclusion.
The E2 operator is

$$\mathcal{M}\,(E2,\,0) = e \sum_{\text{protons}} r_p^2 Y_{20}\,(\Omega_p) \tag{8.13}$$

We have written down only the $\mu = 0$ component, since the others will not
contribute. The B(E2) calculated in this case is

$$B(E2, I_i K \to I_f K) = \frac{5e^2}{16\pi} \left\langle I_i\, 2\, K0 \,\middle|\, I_f K \right\rangle^2 \; Q_0^2 \tag{8.14}$$

where Q_0 is the <u>static</u> intrinsic quadrupole moment calculated as the
expectation value of the operator

$$\left(\frac{16\pi}{5}\right)^{1/2} \sum_{\text{proton}} r_p^2 \, Y_{20}\,(\Omega_p)$$

with the intrinsic wave functions. In particular the Coulomb excitation of
the first excited 2^+ state is determined by

$$B(E2, 00 \to 20) = (5e^2/16\pi)\, Q_0^2 \tag{8.15}$$

Relations (8.15) or (8.14) have been used extensively in the determi-
nation of the intrinsic quadrupole moment Q_0 and, therefore, the nuclear
deformation (see Eq.(4.23)).

Let us now discuss briefly the magnetic properties of rotational nuclei.
The operator of the magnetic moment μ is composed of two parts, a collec-
tive one and single-particle one:

$$\vec{\mu} = \vec{\mu}_{\text{coll}} + \vec{\mu}_{\text{s.p.}} \tag{8.16}$$

where

$$\vec{\mu}_{\text{coll}} = g_R \vec{R} \tag{8.17}$$

$$\vec{\mu}_{\text{s.p.}} = \sum_j \left(g_\ell^{(j)} \vec{\ell}_j + g_s^{(j)} \vec{s}^{(j)} \right) \tag{8.18}$$

The appearance of $\vec{\mu}_{coll}$ in (8.16) is connected with the additional contribution to the magnetic moment due to the nuclear rotation. This contribution is proportional to the total collective angular momentum $\vec{R} = \vec{I} - \vec{J}$ (see Eq.(6.14)). For a single-particle state (J =j) we have

$$\mu_q = g_R I_q + (g_\ell \ell_q + g_s s_q) - g_R j_q \qquad (8.19)$$

where we have written μ as the q-th component of the first-order tensor (rank 1). Now, the matrix element of μ_q in the rotational-type state contains expressions like

$$\langle D^I_{MK} \chi_K | \mu_q | D^I_{MK} \chi_K \rangle$$

$$= \sum_{q'} \langle D^I_{MK} | D^1_{qq'} | D^I_{MK} \rangle \langle \chi_K | \mu'_{q'} | \chi_K \rangle \qquad (8.20)$$

$$= \frac{8\pi^2}{2I+1} \langle I1M0 | IM \rangle \langle I1 K0 | I K \rangle \langle \chi_K | \mu'_0 | \chi_K \rangle$$

Let us define a "single-particle" factor g_K by the relation

$$\langle \chi_K | \mu'_0 | \chi_K \rangle = g_K K$$

$$= g_\ell K + (g_s - g_\ell) \langle K | s_0 | K \rangle \qquad (8.21)$$

Working with the full wave function (6.23) we obtain finally

$$\mu = \langle \Psi^I_{MK} | \mu_q | \Psi^I_{MK} \rangle_{M=I}$$

$$= \left\{ g_R M + \langle I1M0 | IM \rangle \langle I1K0 | IK \rangle K (g_K - g_R) \right\}_{M=I} \qquad (8.22)$$

$$= g_R I + \frac{K^2}{I+1} (g_K - g_R)$$

This formula is valid in all cases except for K = 1/2. In the case of K = 1/2 there are additional cross terms similar to those in the energy formula (7.19) for the K = 1/2 bands. The complete formula is given below without derivation

$$\mu = g_R I + \frac{K^2}{I+1} \left(g_K - g_R \right) \left\{ 1 + \delta_{K,\frac{1}{2}} (-1)^{I+\frac{1}{2}} (2I+1) b_0 \right\} \qquad (8.23)$$

where b_0 is a quantity similar to the decoupling parameter (see Eq.(7.18)):

$$(g_K - g_R) \, b_0 = \langle \chi_K | (g_\ell \ell_t + g_s s_+ - g_R j_+) | \chi_{-K} \rangle \qquad (8.24)$$

We can expect that roughly the following estimate of the gyromagnetic ratio g_R is valid:

$$g_R \approx Z / A \qquad (8.25)$$

Let us finally turn to the discussion of the M1 transition in rotational nuclei. The corresponding operator is

$$\vec{\mathscr{M}} \, (M1, \mu) = \sqrt{\frac{3}{4\pi}} \, \frac{e\hbar}{2Mc} \left\{ g_R \vec{I} + \left(g_\ell \vec{\ell} + g_s \vec{s} \right) - g_R \vec{j} \right\} \qquad (8.26)$$

Now, employing the same procedure as before, we arrive at the expression for the reduced transition probability within a band

$$B \, (M1, I_i \, K \to I_f \, K) = \frac{3}{4\pi} \left(g_K - g_R \right)^2$$

$$\times \left(\frac{e\hbar}{2Mc} \right)^2 \langle I_i 1 K 0 \, | \, I_f K \rangle^2 \qquad (8.27)$$

valid in the case $K \neq \frac{1}{2}$.

For the case $K = \frac{1}{2}$ we have

$$B \left(MI, I_i \frac{1}{2} \to I_f \frac{1}{2} \right) = \frac{3}{4\pi} \left(g_K - g_R \right)^2 \left(\frac{e\hbar}{2Mc} \right)^2$$

$$\times \langle I_i 1 \frac{1}{2} 0 \, | I_f \frac{1}{2} \rangle^2 \left(1 + b_0 (-1)^{I_> + \frac{1}{2}} \right) \qquad (8.28)$$

where

$$I_> = \max \, (I_i, I_f)$$

The above formulae for the $B(Mi)$ and μ work very well in most of the deformed nuclei. As an example, let us choose the [169]Tm nucleus [30]. As its ground-state band is $K = 1/2$ we have to use the modified formulae containing b_0. Thus, we have to fit three parameters: b_0, g_R and g_K. Using three measured quantities to determine them, we can predict the other data and compare them with experiment. Table II illustrates the results [31]. The asterisk means that the value has been used to determine the parameters b_0, g_R, g_K.

TABLE II.   RESULTS FOR THE ^{169}Tm NUCLEUS

I	E	μ_I (eℏ/2Mc)		B(M1, I+1 → I) (eℏ/2Mc)^2	
		Experimental	Predicted	Experimental	Predicted
$\frac{1}{2}$	0	-0.229	*	0.055	0.045
$\frac{3}{2}$	8.4	+0.534	*	0.115	*
$\frac{5}{2}$	118.2	+0.64	+0.70	0.080	0.059
$\frac{7}{2}$	139.9	+1.37	+1.42	-	-

Most of the discussions in this chapter as well as in chapters 6 and 7 are taken from Ref.[3].

9.   OTHER APPLICATIONS OF THE ROTATIONAL COUPLING SCHEME

In this lecture we shall discuss two different topics. First of all, we shall describe a very interesting method of verifying the intrinsic structure in the nuclear deformed orbitals. It is often referred to as a method of "finger-prints". Then we shall return to the discussion of rotational spectra and complete it by a non-trivial case of odd-odd nuclei.

We have seen that the deformed single-nucleon orbitals in nuclei are very well understood in terms of an individual nucleon motion in the deformed nuclear potential (see chapter 3). In particular, the widely used Nilsson model [8, 10] has been employed to explain even very fine details of nuclear spectra. We have seen that the Nilsson deformed orbitals can be represented as superpositions of the spherical nuclear orbitals (see Eq.(3.37)). Now, it turns out that the investigation of the one-nucleon transfer reactions may provide us with a very interesting check of the intrinsic structure of the Nilsson orbitals. Our considerations will be based on the rotational coupling scheme as outlined in chapter 6. Let us consider a stripping reaction such as (d, p), (d, n), (t, d) etc. In such a process, an initial nucleus with angular momentum I_1 captures one nucleon with an angular momentum j and forms the final nucleus with a total angular momentum I_2. The cross-section for such a process may be written as [3].

$$d\sigma\left(\vec{I}_1 + \vec{j} \to \vec{I}_2\right) = \frac{1}{(2j+1)(2I_1+1)} \left\langle I_2 \left|\left| a^\dagger(j) \right|\right| I_1 \right\rangle^2 d\sigma_{s.p.}(+j) \qquad (9.1)$$

The second factor $\left\langle I_2 \left|\left| a^\dagger(j) \right|\right| I_1 \right\rangle^2$ is determined by the overlap between the two nuclear states after having added a(j)-nucleon to the initial nucleus. We shall limit ourselves to the discussion of this term without going into further details of the reaction process. The factor itself is proportional to the spectroscopic factor, which is discussed in many other papers in

these Proceedings (see papers by Cindro and Frahn). Formally the factor $\langle I_2 || a^+(j) || I_1 \rangle$ is a reduced matrix element of the tensor operator and can be shown, by the Wigner-Eckart theorem, to be proportional to the matrix element of the $a^+_{j\mu}$ creation operator calculated between the two rotational states (see Eq. 6.23))

$$\langle \Psi^{I_2}_{M_2 K_2} | a^{\dagger}_{jm} | \Psi^{I_1}_{M_1 K_1} \rangle \qquad \text{.} \qquad (9.2)$$

This matrix element can be evaluated by means of a procedure outlined in chapter 8 leading to the intensity rules. After a transformation to the intrinsic frame of reference the expression (9.2) is seen to be proportional to the element between the intrinsic states

$$\langle K_2 | g^{\dagger}_{jm} | K_1 \rangle \qquad (9.3)$$

The discussion becomes especially simple when the target nucleus is even-even (in the ground-state). Then the final state $| K_2 \rangle$ may be understood to be one-particle state (plus an even-even core) and can be expanded in terms of spherical orbitals

$$| K_2 \rangle = \sum_j c_{j\ell} | j\ell K_2 \rangle \qquad (9.4)$$

(Thus is exactly the expansion (3.37).)

Substituting relation (9.4) into the matrix element (9.3) we finally obtain

$$d\sigma \left((\vec{I}_1 = 0) + \vec{j} \to \vec{I}_2 \right) \sim (c_{j\ell}^{\;2})_{j = I_2} \qquad (9.5)$$

In the experiment various states I_2 are populated as the final states of the nucleus. If they belong to the same rotational band, Eq. (9.5) enables us to determine directly various coefficients $c_{j\ell}$ of the expansion (9.4). In this way we are in a position to check whether the coefficients $c_{j\ell}$ calculated correspond to reality. In the more refined version of the theory with pairing correlations included, the coefficient $c_{j\ell}^2$ appearing in Eq. (9.5) has to be completed by the standard coefficient u_j^2 characteristic of the theory with pairing forces. The coefficient u_j^2 determines the degree to which the j-th level is empty.

Similar considerations may be applied in the case of pick-up reactions such as (p, d), (n, d), (d, T) etc. Here, the roles of the initial and final states are interchanged and the coefficient u_j^2 has to be replaced by $v_j^2 = 1 - u_j^2$.

Various experiments of the type described above have been made [32]. A typical example is given [32, 28] in Table III. Of course, the experimental determinations have been normalized so that only the ratios of the coefficients are relevant. Nevertheless, the agreement of the Nilsson results with experiment is remarkable. This means, that in spite of the very great simplicity of the Nilsson potential (see chapter 3), its results

TABLE III.   COEFFICIENTS $c_{j\ell}^{2}$ OBTAINED FROM (d, p) EXPERIMENT

	Theory	^{169}Yb	^{171}Yb	^{173}Yb
5/2	0.01	0.02	0.03	0.03
7/2	0.79	0.72	0.66	0.61
9/2	0.14	0.18	0.17	0.18
11/2	0.06	0.09	0.14	0.18

are quite relevant to the real angular structure of the intrinsic single-
particle states in deformed nuclei.

Let us turn now our discussion to the spectra of odd-odd deformed
nuclei. The low-lying states are constructed from the individual states of
the odd proton and odd neutron lying outside the even core. Suppose that
the lowest states of the proton and the neutron are characterized by the
projection of the angular momenta Ω_p and Ω_n, respectively. We can expect
the existence of two rotational bands due to the two K-states with

$$K = \Omega_n + \Omega_p, \quad \text{or} \quad |\Omega_n - \Omega_p| \tag{9.6}$$

The splitting between the two bands depends mostly on the properties of
the residual neutron-proton interaction. An empirical rule discovered by
Gallagher and Moszkowski [33] states that out of the two configurations
(9.6) the lower one is characterized by the parallel spin projections

$$\Sigma_n + \Sigma_p$$

where the quantum number Σ has been defined in chapter 3 (see Eq. 3.17).
Pyatov [34] has shown theoretically that the Gallagher-Moszkowski rule can
be explained with the use of the short range spin-dependent neutron-proton
residual force. According to Pyatov, the only exception from this rule may
be expected for $\Omega_n = \Omega_p$ and opposite parities of the two states. In this case
the rule does not have to hold. Such a situation seems to be observed in
^{166}Ho where two bands [35] separated by very small energy (≈ 8 keV) exist.

Let us take $^{250}_{97}$Bk (Fig. 9-1) as an illustration of the level structure in an
odd-odd nucleus. One can see here various rotational bands [36-28] built
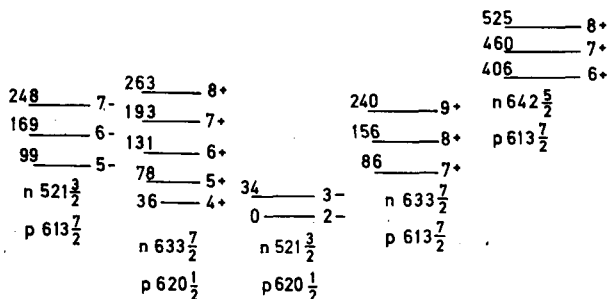
FIG. 9-1.   Level spectrum in an odd-odd nucleus ($^{250}_{97}$Bk).

on two-particle configurations. One can also see that the Gallagher-Moszkowski rule works in all the cases.

Now, let us discuss more closely an interesting special case of $\Omega_n = \Omega_p$. Then, according to expression (9.6) one of the bands is characterized by $K = 0$. The intrinsic wave function in this case may be constructed of the proton and neutron orbital in two ways:

$$\chi_0^{(\pm)} = \frac{1}{\sqrt{2}} \left\{ \chi_\Omega(p) \chi_{-\Omega}(n) \mp \chi_{-\Omega}(p) \chi_\Omega(n) \right\} \tag{9.7}$$

The two combinations have different behaviour with respect to rotation through 180° about "2"-axis:

$$R_i \chi_0^{(\pm)} = \pm \chi^{(\pm)} \tag{9.8}$$

According to considerations from chapter 6 we actually have here two different bands with the r quantum number equal +1 or -1. The two bands are described by two different rotational wave functions

$$\Psi_{M0}^{(+) I} = \sqrt{\frac{2I+1}{16\pi^2}} \chi_0^{(+)} \left(1 + (-)^I\right) D_{M0}^I \tag{9.9}$$

with $I = 0, 2, 4, \ldots$

and

$$\Psi_{M0}^{(-) I} = \sqrt{\frac{2I+1}{16\pi^2}} \chi_0^{(-)} \left(1 - (-)^I\right) D_{M0}^I \tag{9.10}$$

with $I = 1, 3, 5, \ldots$

As the intrinsic structure of the two bands differs there may be substantial differences between them (for example, the moments of inertia or energy positions may be different).

As an example of such a situation, let us consider the odd-odd nucleus ^{170}Tm. Its level spectrum has been observed experimentally [37]. The assignments for odd proton and neutron are $(411\frac{1}{2})$ and $(521\frac{1}{2})$, respectively. According to what we have said we should expect the existence of the three rotational low-lying bands in this nucleus:

1) The $K\pi = 1^-$ band from the parallel total projections:

$$\Omega_p + \Omega_n$$

2) The $K\pi = 0^-$ band with r = +1 and $I\pi = 0^-, 2^-, 4^-, \cdots$
3) The $K\pi = 0^-$ band with r = -1 and $I\pi = 1^-, 3^-, 5^-, \ldots$

The fact, that $\Omega_p = \Omega_n = 1/2$ causes further complication: the 1-band may be strongly coupled by the Coriolis interaction (6.30) to both the $K = 0$ bands. The matrix elements of the Coriolis interaction may be expressed by the decoupling parameters for the neighbouring odd-A nuclei exhibiting $(411\frac{1}{2})$-proton and $(521\frac{1}{2})$-neutron orbitals. The examination of
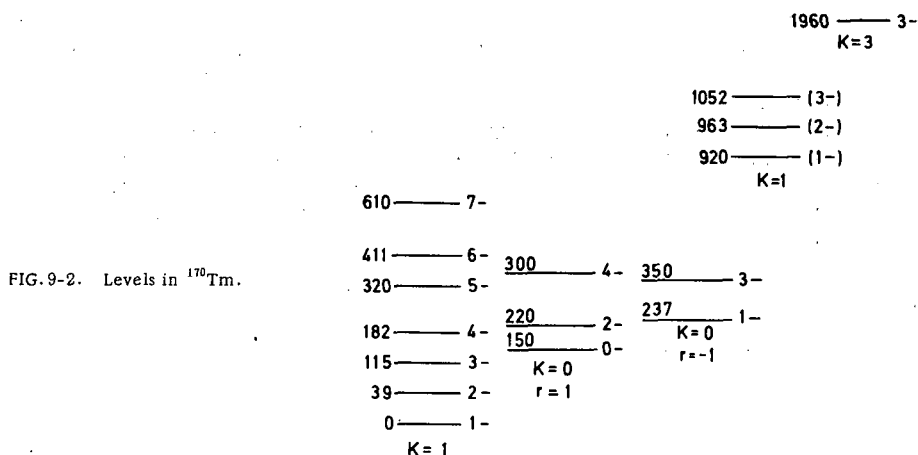
FIG.9-2. Levels in ^{170}Tm.

the decoupling parameters, however, shows that only the r = +1 band interacts strongly with the K = 1⁻ band. This causes small disturbances in the odd-spin part of the Kπ = 1⁻ band. The level scheme of ^{170}Tm is shown in Fig.9-2.

Apart from the three rotational bands discussed above one can see other bands or levels of different instrinsic structure.

10. FURTHER DEVELOPMENTS IN THE ROTATIONAL COUPLING SCHEME

In this chapter we shall discuss the deviations from the rotational coupling scheme as formulated in chapters 6-9. We shall see that there are some regular, systematic features in these deviations so that they can be well understood in terms of the corrections to the scheme itself. We shall treat the formalism developed up to now as a zero-order formulation. Now, we shall try to extend the theory to a kind of first order stage in order to explain the systematics of the observed deviations [3].

Let us start with the discussion of the rotational spectra. By examining numerous rotational spectra in deformed nuclei we can notice that the I(I + 1) rule (see Eq.(7.9)) holds only approximately. We may try to correct it by adding higher powers of I(I +1) to the energy expression

$$E = AI(I+1) - BI^2(I+1)^2 - CI^3(I+1)^3 - \ldots \qquad (10.1)$$

where $A = \hbar^2/2\mathcal{J}$. We have used the minus sign for the second and third term in (10.1) since then it turns out that they usually give a negative contribution (so that B > 0, C > 0). We can now treat A, B, C... as parameters and determine them from the energies of the first states in the rotational bands. In this way we generally get that:

A is of the order of several keV
B is of the order of several eV
C is of the order of several 10^{13} eV

However, this procedure does not seem to be too satisfactory since the positions of higher levels are poorly predicted from the knowledge of A, B and C. Therefore, expansion (10.1) may be understood only as an approximation of the first order.

The other method of parametrization consists of dropping higher-order terms B, C... and treating the A-coefficient (or else the moment of inertia J) as I-dependent. Let us take the *ground-state rotational band* in ^{170}Hf (Fig. 7-2) as an example. The distance between two neighbouring levels is

$$E_{I+2} - E_I = \frac{\hbar^2}{2J} (4I + 6) = \begin{cases} \dfrac{3\hbar^2}{J} & \text{for} \quad I = 0 \\[4mm] \dfrac{35\,\hbar^2}{J} & \text{for} \quad I = 16 \end{cases} \tag{10.2}$$

The corresponding two determinations of the moment of inertia J, in ^{170}Hf are $J \doteq 0.030\ \hbar^2\,\text{MeV}^{-1}$ and $J = 0.057\ \hbar^2\,\text{MeV}^{-1}$, respectively. We can see that the increase in the moment of inertia is quite considerable in the band.

Let us now briefly review the theories of the moments of inertia. The simplest assumption concerning the structure of nuclear rotation is a hydrodynamical picture (The irrotational flow of an inviscid and incompressible liquid). The estimates of the moment of inertia, J_{irr} obtained in this way are about 5 times too low than the observed ones. Let us now turn to the alternative description currently called the *cranking model* [38]. In this model, a slow classical rotation is applied to the whole nucleus. Then, the nuclear states are slightly modified owing to this rotation. The perturbation calculation with respect to angular velocity of the rotational motion Ω gives the energy to second order in Ω as

$$E = \frac{1}{2} J \Omega^2 \tag{10.3}$$

where the coefficient is identified as the moment of inertia. A final formula obtained for J in case of the independent particle motion in the nucleus is

$$J = 2\hbar^2 \sum_{\nu\mu} \frac{|\langle \nu | j_x | \mu \rangle|^2}{\epsilon_\nu - \epsilon_\mu} \tag{10.4}$$

with j_x being a projection of the particle angular momentum j on the axis perpendicular to the nuclear symmetry axis. The summation in Eq. (10.4) extends over all single-particle configurations μ and ν fulfilling the conditions $\epsilon_\nu > \epsilon_F$ and $\epsilon_\mu < \epsilon_F$ where ϵ_F denotes the Fermi energy. The calculation of J according to Eq. (10.4) for the independent particle motion gives as a result [39]

$$J \approx J_{\text{rigid}} \tag{10.5}$$

where J_{rigid} is the rigid-body moment of inertia of the nucleus. This

result overestimates the values of J with a factor of the order of two. The most satisfactory theory of moments of inertia seems to be based on the cranking model combined with the introduction of the short-range pairing interaction between nucleons in the nucleus [3, 40, 41]. The formula (10.4) is modified in this case

$$J = 2\hbar^2 \sum_{\nu\mu} \frac{(u_\nu v_\mu - v_\nu u_\mu)^2 |\langle \nu |j_x| \mu \rangle|^2}{E_\nu + E_\mu} \tag{10.6}$$

where v_μ^2 is the probability that the state μ is occupied, $u_\nu^2 = 1 - v_\nu^2$, and E_ν are the elementary excitations of the nucleus with pairing correlations present. The calculation of J based on Eq. (10.6) gives a quite good agreement with experiment [41]. Pairing correlations reducing the value of J by a factor about two create the nuclear state, the structure of which is very similar to the electron structure of the superconducting metal.

Let us now discuss the deviations in the intensity rules [3, 42]. Here again, by an examination of the experimental data, we come to the conclusion that the rotational intensity rules only hold approximately. In some cases such as the E1 transitions the rules described in chapter 8 become a very poor tool in the explanation of the measured intensities of various transitions. Let us consider a simple scheme as is to be faced in most of the typical intensity measurements. An initial state $|\Psi_{M_i K_i}^{I_i}\rangle$ decays to the two final states $|\Psi_{M_f K_f}^{I_f}\rangle$ and $|\Psi_{M_f K_f}^{I_f}\rangle$ belonging to the same rotational band. The branching ratio (i.e. the ratio of the intensities of the two transitions $I_i \to I_f$ and $I_i \to I_f'$) is given in the zero-order approximation by the formula (8.12). However, with more accurate experiments, systematic deviations from this rule have been observed. They can be understood in terms of possible admixtures in the wave functions $|\Psi_{MK}^I\rangle$ characterizing rotational bands. Let us see what kind of couplings cause the admixtures of the other K-bands to the band given. The type of admixture depends on the value of the other K-quantum numbers to be admixed. For example the $\Delta K = 1$ admixtures are caused by the familiar Coriolis-type coupling H_{RPC} (see Eq. (6.30))

$$h_{+1} I_- + h_{-1} I_+ \tag{10.7}$$

Here the operators $I_\pm$ acting on the D_{MK}^I part of the rotational wave function (6.23) change the value of K by unity. The operators $h_{\pm 1}$ act on the instrinsic part of the wave function (6.23). In this chapter we shall not be interested in the details of intrinsic motion and only attempt to obtain the explicit I-dependence due to the $I_\pm$ operators acting on the D_{MK}^I part. All we have to know about the $h_{\pm 1}$ operators is their properties with respect to Hermitian conjugation

$$h_{+1}^+ = h_{-1} \tag{10.8}$$

Now, for $\Delta K = 2$ or $\Delta K = 0$ we can write down expressions similar to expression (10.7)

$$h_{+2} I_-^2 + h_{-2} I_+^2 \quad \text{for} \quad \Delta K = 2 \tag{10.9}$$

and

$$h_0(I_1^2 + I_2^2) \quad \text{for} \quad \Delta K = 0 \tag{10.10}$$

Let us discuss the correction to rotational intensity rules in case of the E1 transitions acting between two rotational bands with $K_i = K_f + 1$. In this case the $\Delta K = 1$ admixtures to both final and initial states are relevant. We shall write the perturbed states in the form

$$|IMK\rangle = (1 + \epsilon_+ I_- + \epsilon_- I_+) |\Psi^I_{MK}\rangle \tag{10.11}$$

where $\epsilon_\pm$ are the operators creating the admixtures. They are defined by the first order perturbation theory

$$\langle K|\epsilon_\pm|K'\rangle = \frac{1}{E_K - E_{K'}} \langle K|h_\pm|K'\rangle \tag{10.12}$$

with

$$\epsilon_\pm^+ = - \epsilon_\mp \tag{10.13}$$

We shall not be interested in the particular form of the intrinsic matrix elements (10.12).

Now, to calculate the intensities we need the matrix element (see chapter 8)

$$\langle I_f M_f K_f | \mathscr{M}_{\lambda\mu} | I_i M_i K_i \rangle$$

$$= \sum_\nu \langle \Psi^{I_f}_{M_f K_f} | \left(1 - \epsilon_-^f I_+ + \epsilon_+^f I_-\right) D^\lambda_{\mu\nu} \mathscr{M}'_{\mu\nu} \tag{10.14}$$

$$\times \left(1 + \epsilon_-^i I_+ + \epsilon_+^i I_-\right) |\Psi^{I_i}_{M_i K_i}\rangle$$

In case of $K_i = K_f + 1$ only terms containing I_+ contribute to Eq.(10.14), apart from the zero-order terms. Therefore, we can drop the I_--terms in this case. We are then left with the corrections containing products of $I_+ D^\lambda_{\mu\nu}$ and $D^\lambda_{\mu\nu} I_+$ times some intrinsic operators. Expressing both of them by a commutator and an anticommutator

$$I_+ D^\lambda_{\mu\nu} = \frac{1}{2}\left[I_+, D^\lambda_{\mu\nu}\right] + \frac{1}{2}\left\{I_+, D^\lambda_{\mu\nu}\right\} \cdot$$

$$D^\lambda_{\mu\nu} I_+ = -\frac{1}{2}\left[I_+, D^\lambda_{\mu\nu}\right] + \frac{1}{2}\left\{I_+, D^\lambda_{\mu\nu}\right\} \tag{10.15}$$

we can rewrite the right-hand side of Eq.(10.14) in the form of

$$\sum_\nu \langle \Psi^{I_f}_{M_f K_f}| \left(\mathscr{M}'_{\lambda\mu} D^\lambda_{\mu\nu} + O_\nu \left[I_+, D^\lambda_{\mu\nu}\right]\right.$$

$$\left. + \tilde{O}_\nu \left\{I_+, D^\lambda_{\mu\nu}\right\}\right) | \Psi^{I_i}_{M_i K_i}\rangle \tag{10.16}$$

where O_ν and $\tilde{O}_\nu$ are the intrinsic operator constructed from the $\epsilon_\pm$ operators and the $\mathscr{M}'_{\lambda\nu}$. The zero-order term in expression (10.16) gives a non-vanishing contribution only if $\nu = -1$ in case of $K_i = K_f + 1$. The commutator term produces exactly the same type term containing $D^\lambda_{\mu\nu-1}$ and no I_f or I_i dependence. This can be seen from the relation

$$\left[I_+, D^\lambda_{\mu\nu} \right] = \sqrt{(\lambda+\nu)(\lambda-\nu+1)} \, D^\lambda_{\mu\,\nu-1} \tag{10.17}$$

in which we have to consider only the case of $\nu - 1 = -1$.

Therefore, the only non-trivial modification of the intensity rule can come from the anticommutator in expression (10.16). Now, owing to the relations

$$\left\{ I_{+1} D^\lambda_{\mu\nu} \right\} = I_+ D^\lambda_{\mu 0} + D^\lambda_{\mu 0} I_+ \tag{10.18}$$

$$\text{for } \nu = 0$$

and

$$\left[\vec{I}^2, D^1_{\mu-1} \right] = \frac{\sqrt{2}}{2} \, I_+ D^1_{\mu 0} + \frac{\sqrt{2}}{2} I_+ \tag{10.19}$$

$$+ \text{ (terms containing only } D^1_{\mu-1} \text{ times } I_0) \text{ (for } \lambda = 1)$$

we see that apart from the terms containing only $D^1_{\mu-1}$ (which can be incorporated in the zero-order term) expressions (10.18) and (10.19) give the same contribution to the matrix element (10.16). We can summarize the above considerations by saying that the operator of transition (10.16) is of the form

$$\tilde{M}_1 D^1_{\mu-1} + \tilde{M}_2 \left[\vec{I}^2, D^1_{\mu-1} \right] \tag{10.20}$$

in case of an E1 transition ($\lambda = 1$) in which $K_i = K_f + 1$. In expression (10.20) the operators $\tilde{M}_1$ and $\tilde{M}_2$ act on the intrinsic degrees of freedom. Instead of expressing them in terms of $\epsilon^i_\pm$ and $\epsilon^f_\pm$ as well as $\mathscr{M}'_{\lambda\nu}$ and calculating the matrix elements with the Nilsson wave functions we shall rather treat the matrix elements as parameters. Substituting expression (10.20) into Eq.(10.16) and calculating the matrix elements we obtain

$$\sum_\nu \left\langle \Psi^{I_f}_{M_f K_f} \left| \left(\tilde{M}_1 D^1_{\mu-1} + \tilde{M}_2 \left[\vec{I}^2 D^1_{\mu-1} \right] \right) \right| \Psi^{I_i}_{M_i K_i} \right\rangle \tag{10.21}$$

$$= (M_1 + M_2 \Delta) \left\langle I_i 1 K_i - 1 | I_f K_f \right\rangle \left\langle I_i | M_i \mu | I_f M_f \right\rangle$$

where M_1 and M_2 are parameters and

$$\Delta = I_f(I_f + 1) - I_i(I_i + 1) \tag{10.22}$$

The reduced transition probability following from the above matrix element is (see chapter 8)

$$B(E1, I_i K_i \rightarrow I_f K_f)_{K_f = K_i - 1}$$ (10.23)

$$= (M_1 + M_2 \Delta)^2 \langle I_i 1 K_i - 1 | I_f K_f \rangle^2$$

We see [42] that the square root of $B(E1)$ should be a linear function of Δ for all the transitions between the two bands [1]. Figure 10-1 taken from Ref. [42] illustrates this relation as applied to the particular case. Similar relations [42] can be deduced for other than $\Delta K = 1$ transitions (such as $\Delta K = 2$, $\Delta K = 0$ etc.). The very simple form of Eq.(10.23) has been obtained in a general case owing to the calculations by Michailov [43].
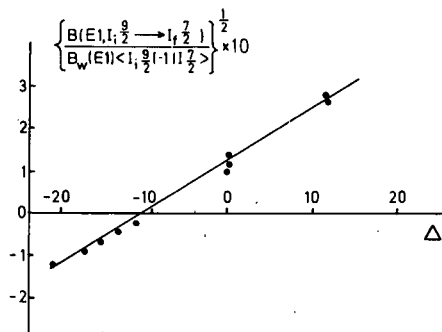
FIG.10-1.   Illustration of Eq.(10.23).

Let us now come back to the discussion of the deviations in the rotational spectra and try to see what can be deduced from the knowledge of the modified intensity rules. Comparison of Eq.(10.23) with experiment enables us to estimate the admixtures to the given rotational band. These admixtures also cause the deviations from the $I(I+1)$ rule in the band. In this way various contributions to the coefficient B from Eq.(10.1) can be calculated. Such contributions to the ground-state rotational band in the even nucleus coming from the other low-lying bands ($K = 2$, $K = 0$, etc.) have been calculated.

$$B = B_2 + B_0 + \cdots$$ (10.24)

Now, it turns out that B_0 and B_2 contribute only to 10-20% of the total B. The remaining part of the effect has to be explained by other reasons. There may be at least two effects able to explain this fact:

1) The centrifugal stretching of the nucleus, causing the increase of the effective moment of inertia J in the band.

2) The Coriolis-antipairing (CAP) effect. When the nucleus rotates the superconducting-type correlations in the nucleus are weakened so that the moment of inertia is rather described by Eqs (10.4) and (10.5) than by Eq.(10.6).

---

[1] $\sqrt{B(E1)}$ should be divided by the Clebsch-Gordan coefficient appearing in Eq.(10.23).

Variational-type calculations performed recently [44] seem to suggest that the CAP may be more important than centrifugal stretching in heavy nuclei.

11. HEAVY NUCLEI. FISSION

In this chapter we shall discuss the properties of heavy nuclei lying beyond lead. Nuclear fission is one of the most striking phenomena occurring in this domain. To explain the properties of nuclear fission we shall have to extend our knowledge of nuclear structure into the states of very highly distorted nuclei. Recently, very fascinating progress has been made which gives us more information on the properties of fissioning nuclei.

The nuclear liquid-drop model has been used almost exclusively in the investigation of the low-energy fission phenomena. In spite of its numerous successes, however, this approach must be considered far from satisfactory as it consists of a very crude simplification of a nuclear picture. First of all, the stable shape of a liquid drop is a sphere while most of the heavy fissioning nuclei are well known to be highly deformed in their equilibrium. Secondly, various properties of fission such as barrier height, spontaneous fission half-life and mass asymmetry have been observed as strongly dependent on the fine details of nuclear structure.

We have seen that the addition of a shell-structure correction to the liquid-drop mass formula (see chapter 2) improves the results very much. According to Myers and Świątecki [4] this approach can be also extended to the non-spherical deformation of the nucleus. Unfortunately, in the more detailed investigations of nuclear fission we need more of nuclear-structure information than that given by a schematic shell correction in the form derived in Ref. [4]. In principle, we can start from the other extreme point of view, i.e. we may try to apply the single-particle model of the deformed nuclei (cf. Lecture 3) and extrapolate its results into the region of the very large distortions. We shall see that this method has not been successful up to now, yet. Nevertheless we shall present its results shortly.

The starting point is the Hamiltonian (5.10) of the independent particles in the deformed field characterized by the deformation parameters $\epsilon_2, \epsilon_4, \epsilon_3, \epsilon_6 \ldots$. Now, we can solve the eigenvalue problem for a deformation given, for a single-particle energy. The sum of all single-particle energies gives us the total single-particle energy as a function of deformation. This quantity is modified (not very significantly) by the existence of pairing interactions (see chapter 5). The total nuclear energy $\mathscr{E}$ is then obtained by adding the Coulomb energy calculated for the deformed shape. Such a procedure has been developed by S.G. Nilsson et al. [20, 22, 23, 45] and seems to give excellent agreement with experiment in the vicinity of the nuclear equilibrium. However, at very large deformations the energy surface $\mathscr{E}(\epsilon_2, \epsilon_4, \ldots)$ shows an unnatural increase for large ϵ_2, so that no fission barrier is obtained [45]. This "disbehaviour" of $\mathscr{E}$ is most probably connected with the drawbacks of the single-particle potential (5.10). In particular, the $\vec{\ell}^2$ term (compare Eq.(5.9)) that has been added is suspected to cause the unphysical increase of the total energy with ϵ_2 [45]. This can be concluded from the fact that analogous calculations with a pure anisotropic h.o. potential (i.e. without the $\vec{\ell}^2$ term) show proper behaviour (decrease with ϵ_2 at very large ϵ_2).

To obtain the proper behaviour of the total energy surface we, there-
fore, have to come back to the idea of calculating the shell-structure
correction to the liquid-drop mass formula and investigate its deformation
dependence. On the other hand, we want to have a realistic model without
the simplifications of Myers and Świątecki made for the shell-structure
part of the calculation. Both the above requirements can be fulfilled by
the application of the method suggested by Structinsky [46]. The method
consists of the following procedure. First, the total energy $\mathscr{E}'$ is calcu-
lated as a sum of the single-particle energies (possibly including pairing
interaction). Then another quantity $\mathscr{E}''$ is calculated in the following
manner. We attach a definite width γ to each single-particle level e_ν, that
is, we replace a single discrete level e_ν by a continuous (say Gaussian)
distribution

$$\frac{1}{\gamma\sqrt{\pi}} \exp\left\{-\left(\frac{e-e_\nu}{\gamma}\right)^2\right\} \tag{11.1}$$

Then we sum up all the terms (11.1) coming from different e_ν and finally
integrate over the variable e. The quantity $\mathscr{E}''$ obtained in this way has the
meaning of the energy averaged over an energy range γ large enough as to
wash out the short-range fluctuations of the single-particle levels. If in the
same time γ is small as compared to the long-range fluctuations in the
spectrum the difference

$$\mathscr{E}_{\text{sh. corr.}} = \mathscr{E}' - \mathscr{E}'' \tag{11.2}$$

gives us the shell correction for which we were looking. This quantity
is then completed by the addition of the liquid-drop energy $\mathscr{E}_{\text{l.d.}}$ (see
chapter 2)

$$\mathscr{E}_{\text{tot}} = \mathscr{E}_{\text{l.d.}} + \mathscr{E}_{\text{sh. corr.}} \tag{11.3}$$

The total energy $\mathscr{E}_{\text{tot}}$ may be then calculated for every deformation
point $(\epsilon_2, \epsilon_4, \ldots)$ and the energy surface is then obtained.
    The Strutinsky procedure as described above has been applied to the
potential (5.10) by S.G. Nilsson et al. [47, 23]. Typical results of these
calculations are illustrated in Figs 11-1 and 11-2. Figure 11-1 gives the
shell correction calculated by the procedure described above and compared
with experiment. Then rather good agreement of the calculation with
experiment can be seen. Figure 11-2 gives the cross-section of the energy
surface along the "steepest-descent" patch (very roughly with ϵ_2).
    The interesting behaviour of this curve, showing two maxima is most
probably connected with recent fascinating development in fission physics
within last few years. The whole development was started by the discovery
made in Dubna [48] of the isomers of some nuclei (mostly odd-odd or odd-A
nuclei) that are characterized by a very short half-life for a spontaneous
fission. No electromagnetic decay of these states to the ground state was
observed. The existence of these states leads to the suggestion that they
may be bound states of the nucleus corresponding to the second well in
the potential energy curve as shown in Fig. 11-2. Strutinsky has first
suggested [46] the possibility of the existence of the secondary minima in the
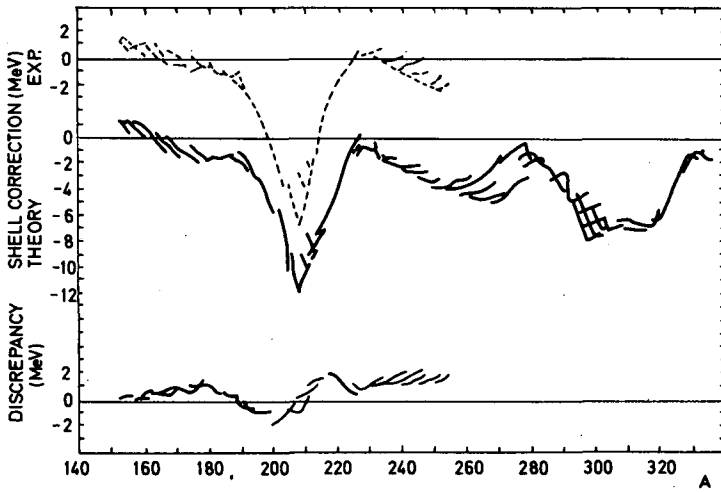
FIG.11-1.   Comparison of calculated shell correction with experimental values.
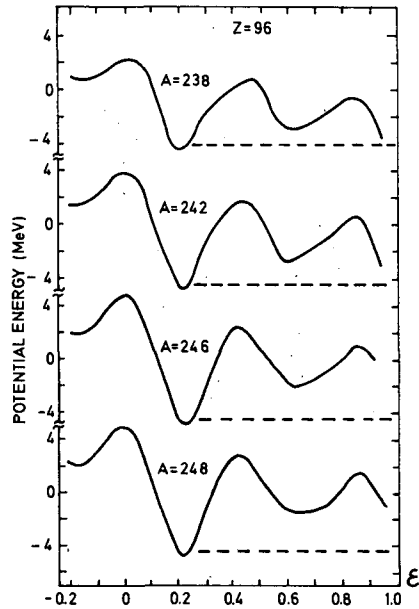
FIG.11-2.   Cross-section of energy surface along
the path of "steepest descent".

potential energy surface. For the new development in the research for the
spontaneously fissioning isomers see Refs [49, 50].

.The existence of the second well in the potential energy surface leads to
other interesting consequences that can be checked experimentally (and have
been observed, in fact). The additional structure in the curve of the cross-
section versus energy for fission induced by the sub-threshold neutrons is
one of the examples of the phenomenon of this type. Another example is
provided by the stripping-induced fission, (d, pf). The penetration function

in this case exhibits bumps when plotted versus energy transferred to the
nucleus. A more detailed discussion of these phenomena may be found in
Refs [51, 52].

12. SUPERHEAVY ELEMENTS

In the previous chapters we discussed the properties of deformed nuclei.
We have seen to what extent our knowledge of nuclear structure permits us
to explain the behaviour and various features of the nuclei. In the last
chapter we made an attempt to extrapolate our knowledge of the physics
involved into the region of very large distortions such as to be able to de-
scribe nuclear fission. We have seen that the results of such an investigation
were compatible with the new development in fission physics showing a
complicated structure of nuclear potential energy at large distortions. In
this chapter we shall try to make another extrapolation into the region of
superheavy nuclei characterized by proton number $Z \gtrsim 110$ and neutron
number $N \approx 184$.

There is a deep minimum in the nuclear binding energy in the region
of Pb (at A = 208) in excellent agreement with experiment. However, there
is another dip at $A \approx 300$ corresponding to Z lying around 110 to 124, showing
that nuclei in that region may also be relatively stable. The strong nuclear
binding observed from the theoretical curve in this region is connected with
the properties of the nuclear potential.

The calculations of Sobiczewski et al. [53] and Meldner [54] (see also
Refs [4, 23] and [47] show that for most of the reasonable potentials used
in the transuranic region and extrapolated towards the heavier nuclei, the
proton number Z = 114 and neutron number N = 184 appear to be magic.
Another semimagic number seems to occur at Z = 124, so that the whole
region between Z = 114 and Z = 124 is characterized by strong binding.

To decide whether there is any chance for nuclei in the above region to
stay stable for a time long enough we have to answer two principal questions:

1) What is the shape of the potential energy barrier against fission
(what is the height and width of the barrier)?

2) What would be the estimate of the life-time with respect to spontane-
ous fission? The answer to the second question depends on the answer to
the first question and on the knowledge of the effective inertial parameter B
corresponding to the collective nuclear motion in the fission channel. The
answer to the first question is that there exists a barrier about 8 MeV high,
with a rather narrow maximum at $\epsilon \approx 0.2$. This answer comes from the
calculation made [55, 23, 47] on the basis of the Nilsson model [8, 20]
based on the Strutinsky method [46], as described in the previous lecture.
The barrier calculated is shown in Fig. 12-1.

The answer to the second question is that the inertial parameter B
is of the order of

$$B \approx 900 \, \hbar^2 \, \text{MeV}^{-1} \qquad\qquad (12.1)$$

This rough estimate has been obtained as an average from the theo-
retical calculations [56] of the microscopic character based on the method
suggested by Bohr and Mottelson [3]. By examining the results of this
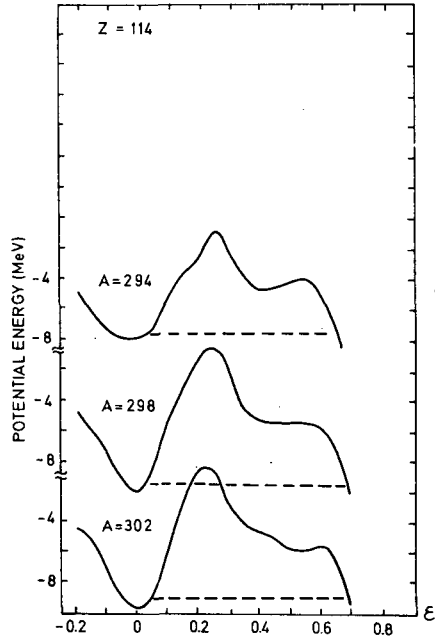
FIG.12-1. Calculation of potential energy based on the Nilsson model.

calculation we can expect that the inertial parameters B are of the order of 4 to 11 times larger than the B_{irr} obtained in the liquid-drop model. They are – very roughly speaking – linear functions of deformation and depend very sensitively on the strenght of the pairing force acting between the nucleons.

Combining our knowledge of the potential energy barrier with the estimates for B one can try to estimate the spontaneous fission half-life $\tau_{1/2}$ from the familiar WKB formula

$$\tau_{1/2} = n^{-1} e^{\frac{2}{\hbar} \int_{\epsilon_1}^{\epsilon_2} \sqrt{2B(E-V(\epsilon))} \, d\epsilon} \tag{12.2}$$

where n, the number of barrier assaults, can be estimated to be

$$n \approx 10^{21} \, s^{-1} \tag{12.3}$$

from the knowledge of the vibrational energy in heavy nuclei ($\hbar\omega \approx 1$ MeV).

To make a very rough estimate let us assume that the mass parameter B entering Eq.(12.2) is deformation-independent (which is not the case as we have seen above). Let us also assume that the variation of B with the mass number A is roughly given by the relation

$$B \sim A^{5/3} \tag{12.4}$$
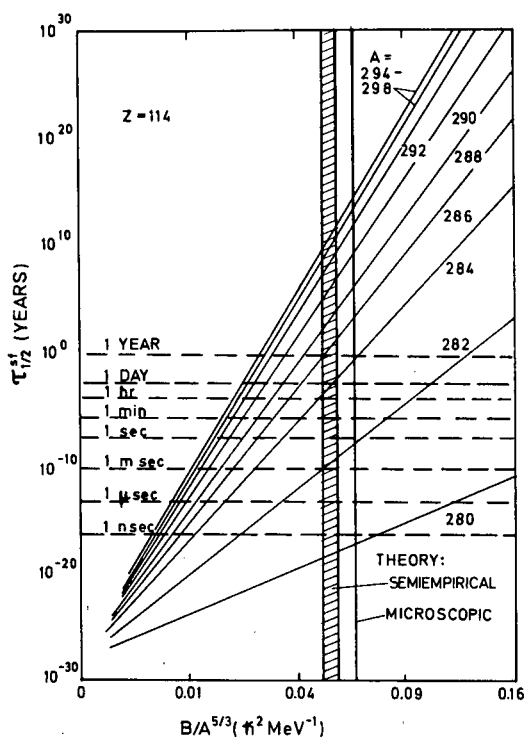
FIG.12-2.   Calculation of $\tau_{\frac{1}{2}}$ versus $\sqrt{B/A^{5/3}}$.

In this case it follows from Eq.(12.2) that the ln of half-life $\tau_{1/2}$ is a linear function of the square root of B divided by the square root of $A^{5/3}$ for various nuclei:

$$\ln \tau_{1/2} = \text{const.} \sqrt{B/A^{5/3}} \qquad\qquad (12.5)$$

where the proportionality constant depends on the height and width of the fission barrier of the individual nuclei. The results of such a calculation are shown [55] in Fig.12-2. The result is remarkable: nuclei with Z = 114 and N lying in the vicinity of 184 have a very large half-life with respect to spontaneous fission. Further calculations with the inclusion of the linear dependence of B on deformation [23] show that in the region of nuclei in the transuranic region, where $\tau_{1/2}$ is known experimentally, we may fail in the estimate of $\tau_{1/2}$ by 4 to 6 orders of magnitude. Nevertheless, even with such an error included we can still claim that the Z = 114 and N = 184 nuclei have $\tau_{1/2}$ greater than the age of the earth (10^9 years)!

Of course, the other decay modes may change our conclusion. First of all, the requirement of beta stability limits the number of stable nuclides to few isotopes for each element only. Secondly, the nuclei in this region are most probably all instable against alpha decay. Alpha and beta stability combined with spontaneous fission has been discussed by Nilsson, Thompson and Tsang [57]. The conclusion of this discussion is best summarized in Fig.12-3 (taken from Ref.[57], showing the lines of constant $\tau_{1/2}$ with respect to spontaneous fission (solid lines) and alpha decay (broken lines)

FIG.12-3. Lines with a constant $\tau_{\frac{1}{2}}$ with respect to fission and α-decay.
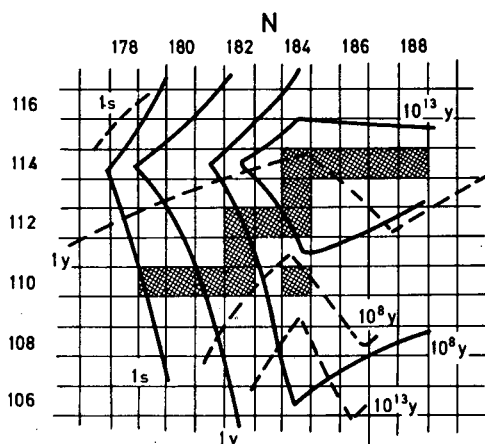
simultaneously. The squares corresponding to beta-stable nuclei are shaded. One can see from this figure that only one nuclide seems to exist that should be relatively stable with respect to all the decay modes. This is the $Z = 110$ and the $N = 184$ nucleus which should be called ekaplatinum according to its location in the Mendeleyev table. Its half-life is still comparable with the age of the earth so that it could be, in principle, looked for in the earth (possibly in the platinum ores). The experiments [58] started for this purpose have not yet brought positive results.

The double-magic nucleus $^{298}114$ or any other neighbouring nuclei should not be detectable in the earth according to the estimates of Ref. [57]. This seems to be in line with the negative results of the experiments made recently by Flerov's group in Dubna [59]. However, there are good chances that they may be produced artificially in the future with the help of heavy ions in heavy-ion accelerators.

Possibly, superheavy nuclei may also be observed in cosmic rays [60]. All nuclei with $Z > 83$ have been most probably produced in the r-process of neutron capture (for the description of this process see Ref. [61] commonly quoted as B^2FH) occurring probably in some exploding stars such as super-novae or quasars. Recently, very heavy nuclei have been detected in cosmic rays [62, 63]. Particles with $Z > 104$ or even heavier [63] seem to be seen.

REFERENCES

[1]   ELTON, L.R.B., Nuclear Sizes, Oxford University Press (1961).
[2]   HOFSTADTER, R., Nuclear and Nucleon Structure, Benjamin New York (1963).
[3]   BOHR, A., MOTTELSON, B., Lectures on Nuclear Structure and Energy Spectra, Monograph (to be published).
[4]   MYERS, W.D., ŚWIATECKI, W.J., Nucl.Phys. 81 (1966) 1 and UCRL – 11980 (preprint).
[5]   NAQVI, M.A., Unpublished contribution to Nuclear Structure, Symposium Dubna, July, 1968); see also DONELLY, I.J., NAQVI, M.A., Nucl.Phys. A100 (1967) 305.
[6]   MYERS, W.D., Ph.Thesis, preprint UCRL-18214 (1968).
[7]   ARSENIEV, MALOV, PASHKEVICH, SOBICZEWSKI, SOLOVIEV, Nucl.Phys.(1968).
[8]   NILSSON, S.G., Mat.-fys.Meddr. 29 No.16 (1955).
[9]   MOTTELSON, B., NILSSON, S.G., Nucl.Phys. 13 (1959) 281.
[10] MOTTELSON, B., NILSSON, S.G., Mat.fys.Meddr. 1 No.8 (1958).

[11]   REICH, C.W., BUNKER, M.E., in Nuclear Spectroscopy (Proc.16th Annual Conf.Moscow, Jan.1966).

[12]   SZYMAŃSKI, Z., Nucl.Phys. 11 (1959) 454.

[13]   TOWNES, C.H., Determination of Nuclear Quadrupole Moments, Encyclopedia of Physics, (Flügge,S., Ed.) 38 1 Springer (1958).

[14]   RABOY, TRAIL, BJORKLUND, EHRLICH, POWERS, TELEGDI, Nucl.Phys. 73 (1965) 353.

[15]   BÈS, D.R., SZYMAŃSKI, Sci.Prog.Oxf. 55 (1967) 187.

[16]   SZYMAŃSKI, Z., invited paper in Nuclear Structure, (Proc.Symp.Dubna, 1968), IAEA (Vienna, 1968) 405.

[17]   BELYAEV, S.T., Mat.fys.Meddr. 31 No.11 (1959).

[18]   BÈS, D.R., SZYMAŃSKI, Z., Nucl.Phys. 28 (1961) 42; SZYMAŃSKI, Z., ibid. 28 (1961) 63.

[19]   SOBICZEWSKI, A., Nucl.Phys. A93 (1967) 501 and A96 (1967) 258.

[20]   GUSTAFSON, LAMM, NILSSON, B., NILSSON, S.G., Ark.Fys. 36 (1967) 613.

[21]   ARSENIEV, MALOV, PASHKEVICH, SOLOVIEV, Preprint JINR. E4-3703, Dubna (1968).

[22]   MOLLER, NILSSON, B., NILSSON, S.G., SOBICZEWSKI, SZYMAŃSKI, WYCECH, Phys.Letts 26B (1968) 418.

[23]   NILSSON, S.G., TSANG, SOBICZEWSKI, SZYMAŃSKI, WYCECH, GUSTAFSON, LAMM, MÖLLER, NILSSON, B. (to be published).

[24]   HENDRIE, GLENDENNING, HARVEY, JARVIS, DUHM, SANDIROS, MAHOVEY, Phys.Letts 26B (1968) 127.

[25]   See, for example, the paper by RIMINI in these Proceedings or the book by EDMONDS, A.R., Angular Momentum in Quantum Mechanics, Princeton University Press (1957).

[26]   ELBEK, B., Determination of Nuclear Transition Probabilities by Coulomb Excitation. Thesis, Copenhagen (1963).

[27]   STEPHENS, LARK, DIAMOND, Nucl.Phys. 63 (1965) 1.

[28]   NILSSON, S.G., Deformed Nuclei, Lecture Course from Lectures in Theoretical Physics, Summerschool Colorado (1965).

[29]   ALAGA, ALDER, BOHR, MOTTELSON, Mat.fys.Meddr., Dan.Vid.Selsk. 29 No.9 (1955).

[30]   BOWMAN, de BOER, BOEHM, Nucl.Phys. 61 (1965) 682.

[31]   ROGERS, J., Ann.Rev.nucl.Sci. 15 (1965) 241.

[32]   BURKE, ZEIDMAN, ELBEK, HERSHIND, OLESEN, Mat.fys.Meddr., Dan.Vid.Selsk. 35 No.2 (1966); BURKE, D.G., ELBEK, B., ibid. 36 No.6 (1967); TJØM, P.O., ELBEK, B., ibid. 36 No.8 (1967); JASKÓŁA, NYBO, TJØM, ELBEK, Nucl.Phys. A96 (1967) 52.

[33]   GALLAGHER, C.J., MOSZKOWSKI, S.A., Phys.Rev. 111 (1958) 1282.

[34]   PYATOV, N.I., Izv.Akad.Nauk SSSR 27 (1963) 1436.

[35]   STRUBLE, KERN, SHELINE, Phys.Rev. 137B (1965) 772.

[36]   ASARO, MICHEL, THOMPSON, PERLMAN, C.r.Congr.Int.Phys.Nucl. 2, Paris (1964) 564.

[37]   RYDE, SYMONS, SZYMAŃSKI, Nucl.Phys. 80 (1966) 241; FRANSSON, RYDE, HERSKIND, SYMONS, TVETER, ibid. A106 (1968) 369; SHELINE, R.K. et al., Phys.Rev. 143 (1966) 857.

[38]   INGLIS, D.R., Phys.Rev. 96 (1954) 1059 and 97 (1955) 701.

[39]   BOHR, A., MOTTELSON, B.R., Mat.fys.Meddr.Dan.Vid.Selsk. 30 No. 1 (1955).

[40]   BELYAEV, S.T., ibid. 31 No.11 (1959).

[41]   NILSSON, S.G., PRIOR, O., ibid. 32 No. 16 (1960).

[42]   MOTTELSON, B.R., (Proc.Int.Conf.Tokyo, 1967) in Nuclear Structure, Suppl.J.Phys.Soc.Japan 24 (1968) 87.

[43]   MICHAILOV, Izv.Akad.Nauk USSR, Ser.Fiz. 30 (1966) 1334.

[44]   KRUMLINDE, J., NILSSON, S.G., in Nuclear Structure (Proc.Int.Conf.Tokyo 1967); KRUMLINDE, J., preprint, Nordita, June (1968); BÈS, LANDOWNE, MARISCO, preprint (1968).

[45]   NILSSON, S.G., Nucleonic Structure of Equilibrium and Fission Deformation, International School of Physics "Enrico Fermi", Varenna, Course 40 (1967).

[46]   STRUTINSKY, N.M., Yadern.Fiz. 3 (1966) 614, Nucl.Phys. A95 (1967) 420; Nucl.Phys. (1968) (in press).

[47]   NILSSON, S.G., Nuclear Structure, Fission and Superheavy Elements, Lectures delivered in Corgèse (1968) and preprint UCRL – 18355.

[48]   FLEROV, G.N., POLIKANOV, S.M., C.r. Corgèse du Congrès International de Physique Nucléaire, Paris (1964).

[49]   LARK,, N., SLETTEN, G., BJÄRNHOLM, S., Contribution No.90 to Nuclear Structure, Dubna (July 1968), Dubna publication D-3893,(Dubna, 1968).

[50]   POLIKANOV, S.M., Symposium in Nuclear Structure (Proc.Conf.Dubna, 1968) IAEA, Vienna (1968) 449.

[51]   STRUTINSKY, V.M., BJÄRNHOLM, S., ibid. 431.

[52] LYNN, J.E., ibid, 463.
[53] SOBICZEWSKI, GAREEV, KALINKIN, Phys.Letts 22 (1966) 500.
[54] MELDNER, H., Ark.Fys. 36 (1967) 593 (Lysehill Symposium, 1966).
[55] NILSSON, NIX, SOBICZEWSKI, SZYMAŃSKI, WYCECH, GUSTAFSON, MÖLLER, Nucl.Phys. A115
    .   (1968) 545.
[56] SOBICZEWSKI, SZYMAŃSKI, WYCECH, NILSSON, S.G., NIX, TSANG, GUSTAFSON, MÖLLER,
       NILSSON, B., Nucl.Physics (in press).
[57] NILSSON, THOMPSON, TSANG, Phys.Letts (in press).
[58] THOMPSON, ŚWIĄTECKI, BOWMAN, GATTI, MORETTO, JORED (to be published); GIORSO,
       SIKKELAND, NURMIA (to be published); THOMPSON, GATTI, MORETTO, BOWMAN, MICHEL (to be
       published);   seé also THOMPSON, S.G., review lecture delivered at the Conference in Miami (1968).
[59] FLEROV, G.N., Communication at the Soviet Conference on Nuclear Spectroscopy, Erevan
       (January 1969).
[60] SEEGER, FOWLER, W.A., CLAYTON, Astrophys.J. Suppl. 97 (1967) 121.
[61] BURBIDGE, E.M., BURBIDGE, G.R., FOWLER, W.A., HOYLE, F., Rev.Med.Phys. 29 (1957) 547.
[62] FOWLER, P.H., ADAMS, COWAN, KIDD, Proc.Roy.Soc. A301 (1967) 39.
[63] FOWLER, P.H., Private communication.

SECTION III

Application of Many-Body Theory

FUNDAMENTALS AND ELEMENTARY OUTLINE OF THE MANY-BODY THEORY OF NUCLEAR MATTER

J. DĄBROWSKI
Institute for Nuclear Research
Warsaw, Poland

Abstract

FUNDAMENTALS AND ELEMENTARY OUTLINE OF THE MANY-BODY THEORY OF NUCLEAR MATTER.
1. Introduction; 2. Nuclear matter; 3. Fermi gas; 4. Perturbation theory; 5. Second quantization;
6. Calculation of ΔE with the help of Wick's theorem; 7. Diagrams; 8. Linked-cluster theorem;
9. Momentum representation. Time integration; 10. Low-density approximation; 11. Hole self-energies;
12. Solution of the K-matrix equation; 13. The Brueckner-Gammel calculation; 14. The Q = 1
approximation; 15. Convergence of the theory; 16. Bethe's treatment of the three-body energy;
17. Review of nuclear-matter calculations.

1. INTRODUCTION

One of the main problems of nuclear theory is to deduce the properties of atomic nuclei starting from the description of the nucleus as a system of A interacting nucleons. In such a formulation of the problem we tacitly assume that we may eliminate from the description of the nucleus the mesonic field whose only effect is the inter-nucleon interaction. Furthermore, we shall assume that the interaction V between the nucleons inside of the nucleus is the sum of two-body interactions v_{ij}:

$$V = \sum v_{ij} \qquad (1.1)$$

where v_{ij} is the same as the interaction between two free or isolated nucleons, i.e. two nucleons outside the nucleus.

Now, the average distance between nucleons in nuclei is of the same order of magnitude (~2fm) as the range of v_{ij}, and it would not be easy to justify our assumptions a priori. Nevertheless we shall accept these assumptions for reasons of simplicity. By comparing the consequences of these assumptions with the observed properties of nuclei we shall try to justify the assumptions a posteriori.

The knowledge of the nucleon-nucleon interaction v_{ij} is of fundamental importance in the problem stated. As can be seen from Brink's paper [1] in these Proceedings, v_{ij} is a complicated interaction: it depends on spin, parity, angular momentum, possibly on velocity, and is strongly repulsive at small inter-nucleon distances. In spite of the tremendeous efforts of so many physicists, our knowledge of v_{ij} is not complete. We then face the first serious difficulty of not knowing exactly the input data of our problem. In this situation the calculation of nuclear properties should shed some light on the proper form of v_{ij}. And it really does, though the conclusions concerning v_{ij} are not easy to achieve, because the way from v_{ij} to nuclear properties is not a simple one.

To realize the difficulties encountered in solving the nuclear many-body problem, let us mention that a correct theory should explain two seemingly contradictory features of nuclei:

i) the shell structure, which indicates that, approximately, nucleons behave like independent particles in nuclei;

ii) strong nucleon-nucleon correlations, as exhibited by the high-energy nuclear photoeffect, π-meson absorption and other experiments indicating the presence of high-momentum nucleons in nuclei [2].

2.   NUCLEAR MATTER

In face of the difficulties posed by the nuclear many-body problem we shall first try to solve a simplified problem, i.e. the problem of nuclear matter. From Szymański's paper [3] we learn that atomic nuclei have a well-defined surface, and that their volume is proportional to the number of nucleons, A. We may picture the nucleus as a drop of practically incompressible nuclear matter, which does not appear in an infinite size only because of the Coulomb repulsion between the protons. We then define the hypothetical configuration of nucleons called nuclear matter by the following operations:

1) Switching off the Coulomb forces,
2) Switching off the surface effects,
3) Increasing the number of nucleons infinitely:

$$A \to \infty$$

We believe that the central part of sufficiently large nuclei is a good approximation of nuclear matter. This enables us to determine experimentally the parameters of nuclear matter [3]:

Equilibrium density:

$\rho = \dfrac{1}{\frac{4}{3}\pi r_0^3}$ (where the denominator is the volume per nucleon): $r_0 \cong 1.1$ fm.

Volume energy: $\epsilon_{vol} \cong [15\text{-}16]$ MeV.

Symmetry energy: $\epsilon_{sym} \cong [50\text{-}60]$ MeV.

The two energies produce together the energy of nuclear matter E

$$E/A = -\epsilon_{vol} + \tfrac{1}{2}\epsilon_{sym}\alpha^2$$

where the neutron excess parameter $\alpha = (N - Z)/A$. For the main part of our considerations we shall assume the number of neutrons N equal to the number of protons Z. Usually, by nuclear matter one understands a system with $N = Z = A/2$.

Compressibility: $K_0 = r_0^2(d^2/dr_0^2)/(E/A) \cong 70 - 300$ MeV,

measured at equilibrium density.

The main problem of the theory of nuclear matter is the calculation of the parameters r_0, ϵ_{vol}, ϵ_{sym}, K_0 only on the basis of our knowledge of the nuclear force v_{ij}. The general procedure is to compute E/A for several values of r_0. In this way one obtains a curve as shown in Fig.1. The value of r_0, for which the curve has a minimum, determines the equilibrium density, and the value of E/A at this point is equal to $-\epsilon_{vol}$. The curvature at the minimum determines K_0. If one wants to calculate ϵ_{sym}, one has to repeat the whole procedure for values $\alpha \neq 0$.
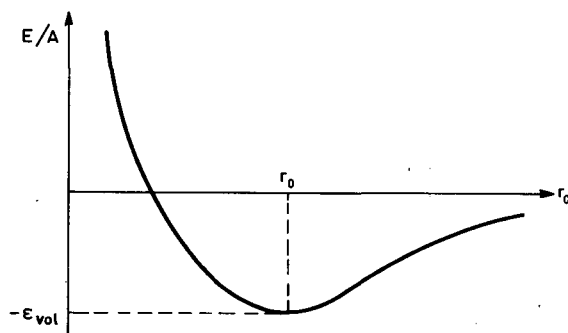
FIG.1.   E/A versus r_0.

Most important for the development of the theory of nuclear matter has been the work of K.A. Brueckner, supplemented subsequently by the work of other physicists, notably by J. Goldstone, N.M. Hugenholtz, and H.A. Bethe. This approach to the theory of nuclear matter, often called the Brueckner theory, will be the subject of these lectures.

The subject has been treated in several review articles and books (see, in particular, Refs [4-10]) among which the excellent review by Bell and Squires [5], the clear exposition by Day [8] and the review of the latest developments by Rajaraman and Bethe [9] are highly recommendable.

3.   FERMI GAS

The starting point for our theory is the system of non-interacting nucleons, i.e. the Fermi gas. The best way of treating an infinite system is to put the A nucleons into a cubic box of volume Ω. Eventually, we go to the limit $A \rightarrow \infty$, $\Omega \rightarrow \infty$ keeping the density $\rho = A/\Omega = $ const. It is assumed that for sufficiently large Ω the precise boundary conditions are unimportant, and we impose the most convenient periodicity conditions. The permitted states of the i-th nucleon (i = 1, ..., A) are then plane waves

$$\varphi_{\underset{\sim}{p}}(q_i) = \frac{1}{\sqrt{\Omega}} \, e^{i\vec{p}\cdot\vec{r}_i} \, \chi_s(\sigma_i)\xi_t(\tau_i) = \varphi_{\vec{p}}(\vec{r}) \, \chi_s(\sigma_i)\xi_t(\tau_i) \tag{3.1}$$

with momentum vectors

$$\vec{p} = (p_x, p_y, p_z) = \frac{2\pi}{\Omega^{1/3}}(n_x, n_y, n_z) \tag{3.2}$$

where n_x, n_y, n_z are positive or negative integers. We apply the notation

$$\underline{p} = \vec{p}, \ s, \ t, \quad q_i = \vec{r}_i, \ \sigma_i, \ \tau_i \tag{3.3}$$

where s, t are the third components of spin and isotopic spin of the nucleon, and σ_i, τ_i are the corresponding co-ordinates.

Since in the region $\Delta p_x \Delta p_y \Delta_z$ there are $\Delta n_x \Delta n_y \Delta n_z = (\Omega/2\pi)^3 \Delta p_x \Delta p_y \Delta p_z$ plane-wave states (without counting the spin and isotopic spin states), for sufficiently large Ω we make the replacement

$$\sum_{\vec{p}} \rightarrow \frac{\Omega}{(2\pi)^3} \int d\vec{p} \tag{3.4}$$

The wave function Φ of the whole system is a determinant constructed from the single-nucleon wave functions (3.1). In the ground state Φ_0 all states with momenta (in units of $\hbar$) $|\vec{p}| \leq k_F$ (k_F is the Fermi momentum) are occupied, each with four nucleons ($s = \pm\frac{1}{2}$, $t = \pm\frac{1}{2}$).

From now on we shall denote by $\vec{m}$ momenta for which $|\vec{m}| \leq k_F$, by $\vec{k}$ momenta for which $|\vec{k}| > k_F$, and by $\vec{p}$ any momenta ($p \gtrless k_F$).

A simple relation holds between k_F and ρ:

$$A = \sum_{\underline{m}} = 4 \sum_{\vec{m}} = 4 \frac{\Omega}{(2\pi)^3} \int d\vec{m} = 4 \frac{\Omega}{(2\pi)^3} \frac{4\pi}{3} k_F^3$$

and we get

$$k_F = \left(\frac{3\pi^2 \rho}{2}\right)^{1/3} = \left(\frac{9\pi}{8}\right)^{1/3} r_0^{-1} = 1.52 \ r_0^{-1} \tag{3.5}$$

The ground-state energy, E_0, is the sum of the single-nucleon kinetic energies

$$E_0 = 4 \sum_{\vec{m}} \frac{m^2}{2\mathscr{M}} = 4 \frac{\Omega}{(2\pi)^3} \int d\vec{m} \ \frac{m^2}{2\mathscr{M}} = 4 \frac{1}{2M} \frac{\Omega}{(2\pi)^3} 4\pi \frac{k_F^5}{5}$$

and with the help of relation (3.5) we obtain

$$E_0/A = \frac{3}{5} \epsilon(k_F) = \frac{3}{5} \frac{1}{2\mathscr{M}} \left(\frac{3\pi^2}{2}\right)^{2/3} \rho^{2/3} \tag{3.6}$$

where we have used the general notation

$$\epsilon(p) = p^2/2\mathscr{M} \tag{3.7}$$

for the kinetic energy of the $\vec{p}$ state.

In all our formulas we denote by $\mathcal{M}$ the mass of the nucleon divided by $\hbar^2$, i.e. $\mathcal{M} = 0.0241$ MeV^{-1} fm^{-2}.

Let us also write the expressions for the compressibility of our Fermi gas

$$K_0 = \frac{18}{5}\,\epsilon(k_F) \tag{3.8}$$

With $r_0 = 1.12$ fm we find

$$k_F = 1.35 \text{ fm}^{-1} \tag{3.9}$$

$$\epsilon(k_F) = 38 \text{ MeV} \tag{3.10}$$

$$E_0/A = 23 \text{ MeV} \tag{3.11}$$

$$K_0 = 138 \text{ MeV} \tag{3.12}$$

Since the experimental value of $E/A = -\epsilon_{vol}$ is about -16 MeV, we expect the contribution of the potential energy to E/A to be about -40 MeV. We see that the net value of E/A is a difference of a big kinetic part, E_0/A, and a big potential part. To obtain then ϵ_{vol} with an accuracy of 1 MeV we have to calculate the potential part with an accuracy of about 2-3%.

4. PERTURBATION THEORY

Let us denote by H the total Hamiltonian, by É the ground-state energy, and by Ψ_0 the ground-state wave function of a system of A nucleons. We have to solve the Schroedinger equation

$$(H - E)\Psi_0 = 0 \tag{4.1}$$

Now

$$H = H_0 + V$$

where H_0 is the kinetic energy of the system, and V is the interaction between the nucleons given in Eq.(1.1). From chapter 3 we know the solution of the ground-state problem for H_0:

$$(H_0 - E_0)\Phi_0 = 0 \tag{4.2}$$

From Eq.(4.1) we obtain

$$\langle \Phi_0 | H - E | \Psi_0 \rangle = 0$$

or, by applying Eq.(4.2)

$$\langle \Phi_0 | H_0 + V - E | \Psi_0 \rangle = \langle \Phi_0 | E_0 + V - E | \Psi_0 \rangle =$$

$$= (E_0 - E)\langle \Phi_0 | \Psi_0 \rangle + \langle \Phi_0 | V | \Psi_0 \rangle = 0$$

and thus we get

$$\Delta E = E - E_0 = \frac{\langle \Phi_0 | V | \Psi_0 \rangle}{\langle \Phi_0 | \Psi_0 \rangle} \tag{4.3}$$

To make the formula for ΔE practically useful we must work out a method of calculating Ψ_0. The method we are going to apply is the perturbation expansion. We shall simply assume that the perturbation expansion for ΔE is converging to the true value, although the problem of the applicability of the perturbation is not simple (see, e.g. Refs [11-13]).

Although we have a stationary problem the easiest way (but by no means the only one) of obtaining the proper form of the perturbation expansion is to apply the time-dependent approach, as has been shown by Goldstone [14]. (The essential ideas for the approach are due to Salam [15]). The basic idea in the time-dependent approach is to start off with a non-interacting system in the ground state Φ_0 at, say, $t = -\infty$, switch on the interaction slowly and smoothly (adiabatically) and wait till, say $t = 0$, when the interaction reaches its full strength, and when ϕ_0 evolves into the ground state of the interacting system, Ψ_0. The details of the switching-on are not important, and to be specific, we shall switch on very slowly, i.e. we replace the original time-independent V by

$$V \rightarrow V_\alpha = V e^{\alpha t} \big|_{\alpha \rightarrow +0} \tag{4.4}$$

We then solve the time-dependent Schroedinger equation (in the following considerations we put $\hbar = 1$)

$$[H_0 + V_\alpha] \Psi_0^\alpha(t) = i \frac{\partial}{\partial t} \Psi_0^\alpha(t) \tag{4.5}$$

with the initial condition

$$\Psi_0^\alpha(-\infty) = \Phi_0 \tag{4.6}$$

and expect that the ground-state wave function of interacting system, Ψ_0, is

$$\Psi_0 = \lim_{\alpha \rightarrow 0} \Psi_0^\alpha(0) \tag{4.7}$$

Goldstone [14] proves the correctness of this procedure in the sense that Ψ_0 given by Eq.(4.7) satisfies the Schroedinger equation (4.1) with E given by Eq.(4.3). That these Ψ_0 and E correspond to the real ground state, will simply be assumed here.

Most convenient for solving the Schroedinger equation (4.5) is the interaction representation which involves the following substitutions:

$$\hat{\Psi}_0^\alpha(t) = e^{iH_0 t} \Psi_0^\alpha(t) \tag{4.8}$$

$$\hat{V}_\alpha(t) = e^{iH_0} V_\alpha e^{-iH_0 t} \tag{4.9}$$

which change Eq.(4.5) to

$$i \frac{\partial}{\partial t} \hat{\Psi}_0^\alpha(t) = \hat{V}_\alpha(t) \hat{\Psi}_0^\alpha(t) \tag{4.10}$$

The initial condition is assumed in the form

$$\hat{\Psi}_0^\alpha(-\infty) = \Phi_0 \tag{4.11}$$

which differs from Eq.(4.6) only by an irrelevant phase factor.
    By integrating Eq.(4.10) we obtain

$$\hat{\Psi}_0^\alpha(t) = \Phi_0 - i \int_{-\infty}^{t} dt' \, \hat{V}_\alpha(t') \hat{\Psi}_0^\alpha(t') \tag{4.12}$$

    We solve this equation by iteration, and get $\hat{\Psi}_0^\alpha(t=0) = \Psi_0^\alpha(0)$. Taking
the limit $\alpha \to 0$, we obtain for Ψ_0, Eq.(4.7), the following result:

$$\Psi_0 = U \Phi_0 \tag{4.13}$$

where

$$U = \lim_{\alpha \to 0} \sum_{n=0}^{\infty} (-i)^n \int_{-\infty}^{0} dt_n \int_{-\infty}^{t_n} dt_{n-1} \cdots \int_{-\infty}^{t_2} dt_1 \hat{V}_\alpha(t_n) \cdots \hat{V}_\alpha(t_i) \tag{4.14}$$

Instead of $\hat{V}_\alpha(t)$ we shall use in the future $\hat{V}(t)$

$$\hat{V}(t) = e^{iH_0 t} \, V \, e^{-iH_0 t} \tag{4.15}$$

    The factors $e^{\alpha t}$ and the symbol $\lim_{\alpha \to 0}$ shall be not indicated explicitly
in Eq.(4.14). From now on we shall write simply

$$U = \sum_{n=0}^{\infty} (-i)^n \int_{-\infty}^{0} dt_n \cdots \int_{-\infty}^{t_2} dt_1 \hat{V}(t_n) \cdots \hat{V}(t_1) \tag{4.16}$$

and we shall understand that each time integration must be performed with
the "switching on" of the factor exp αt and that in the end the limit $\alpha \to 0$ must
be taken.
    Let us introduce the Dyson chronological-ordering operator P, defined
with respect to any operators $\Omega_i(t_i)$ by

$$P[\Omega_1(t_1) \cdots \Omega_k(t_k)] = \Omega_{p_1}(t_{p_1}) \cdots \Omega_{p_k}(t_k) \tag{4.17}$$

$$t_{p_1} \geq t_{p_2} \cdots \geq t_{p_k}$$

With the help of P we may put Eq.(4.16) in the more convenient form

$$U = \sum_{n=0}^{\infty} \frac{(-i)^n}{n!} \int_{-\infty}^{0} dt_1 \dots \int_{-\infty}^{0} dt_n P[\hat{V}(t_1)\dots\hat{V}(t_n)] \qquad (4.18)$$

This equation, together with Eq.(4.3), which may be written

$$\Delta E = \langle \Phi_0 | VU | \Phi_0 \rangle / \langle \Phi_0 | U | \Phi_0 \rangle \qquad (4.19)$$

form the basis of our perturbation theory.

5.   SECOND QUANTIZATION

Undoubtedly, we could calculate ΔE, Eq.(IV.19), with the Φ-functions in the form of Slater determinants. However, it is easy to imagine how complicated it would be to deal with Slater determinants in computing high-order terms. It is much simpler to introduce the occupation-number representation and the creation and annihilation operators, explained in the paper by Frahn [16] in these Proceedings. (A very neat presentation of the second-quantization formalism may be found in Ref.[17].)

A Φ-state of non-interacting nucleons will be specified by a set of occupation numbers N_p, where $N_p = 1$ if the single nucleon state p is occupied, i.e. it is present in Φ, and $N_p = 0$ otherwise. For instance, the ground state Φ_0 will be specified by $N_m = 1$ and $N_k = 0$:

$$\Phi_0 \rightarrow \underbrace{|1, 1, \dots N_{k_F}^{'} = 1,}_{p \le k_F} \underbrace{0, 0, \dots \rangle}_{p > k_F}$$

The annihilation operator a_p when acting on a state Φ with $N_p = 1$ produces a state with $N_p = 0$ (with a proper sign), i.e. a_p annihilates the nucleon in the p state. When $N_p = 0$ in the Φ state, then $a_p \Phi = 0$. The action of the creation operator $a_p^\dagger$ is the opposite one: it creates a nucleon in the p state. Important for us are the anticommutation relations:

$$a_p a_{p'}^\dagger + a_{p'}^\dagger a_p = [a_p, a_{p'}^\dagger] = \delta_{pp'}$$
$$[a_p, a_{p'}] = [a_p^\dagger, a_{p'}^\dagger] = 0 \qquad (5.1)$$

and the expression for V in the occupation-number representation

$$V = \tfrac{1}{2} \sum_{\substack{p_1 p_2 \\ p_3 p_4}} (p_1 p_2 | v | p_3 p_4) a_{p_1}^\dagger a_{p_2}^\dagger a_{p_4} a_{p_3} \qquad (5.2)$$

where

$$(p_1 p_2 | v | p_3 p_4) = \int dq_1 \int dq_2 \varphi_{p_1}^*(q_1) \varphi_{p_2}^*(q_2) v(q_1, q_2) \varphi_{p_3}(q_1) \varphi_{p_4}(q_2) \qquad (5.3)$$

With the help of the field operators

$$\varphi(q) = \sum_{\underline{p}} a_{\underline{p}}\, \varphi_{\underline{p}}(q); \quad \varphi^{\dagger}(q) = \sum_{\underline{p}} a_{\underline{p}}^{\dagger}\, \varphi_{\underline{p}}^{*}(q) \tag{5.4}$$

we may rewrite Eq.(5.2) as

$$V = \tfrac{1}{2}\int dq_1 dq_2\, \varphi^{\dagger}(q_1)\, \varphi^{\dagger}(q_2) v(q_1 q_2)\, \varphi(q_2)\, \varphi(q_1) \tag{5.5}$$

In the interaction representation we have

$$\hat{V}(t) = \tfrac{1}{2}\sum (\underline{p}_1\underline{p}_2\,|v|\,\underline{p}_3\underline{p}_4)\, \hat{a}_{\underline{p}_1}^{\dagger}(t)\hat{a}_{\underline{p}_2}^{\dagger}(t)\hat{a}_{\underline{p}_4}^{\dagger}(t)\hat{a}_{\underline{p}_3}^{\dagger}(t) \tag{5.6}$$

where

$$\hat{a}_{\underline{p}}(t) = e^{iH_0 t}\, a_{\underline{p}}\, e^{-iH_0 t} = e^{-i\epsilon(p)t}\, a_{\underline{p}} \tag{5.7}$$

$$\hat{a}_{\underline{p}}^{\dagger}(t) = e^{i\epsilon(p)t}\, a_{\underline{p}}^{\dagger}$$

where, e.g. the validity of the first equation becomes obvious if we let it act on a state with $N_{\underline{p}} = 1$. The anticommutation relations take the form

$$[\hat{a}_{\underline{p}}^{\dagger}(t),\ \hat{a}_{\underline{p}'}(t')] = \delta_{\underline{p}\underline{p}'}\, e^{i\epsilon(p)(t-t')} \tag{5.8}$$

with other anticommutators vanishing.

Similarly, we may write

$$\hat{V}(t) = \tfrac{1}{2}\int dq_1 \int dq_2\, \hat{\varphi}^{\dagger}(qt)\hat{\varphi}^{\dagger}(q't)v(qq')\hat{\varphi}(q't)\hat{\varphi}(qt) \tag{5.9}$$

where

$$\hat{\varphi}(qt) = \sum_{\underline{p}} \varphi_{\underline{p}}(q)\hat{a}_{\underline{p}}(t); \quad \hat{\varphi}^{\dagger}(qt) = \sum_{\underline{p}} \varphi_{\underline{p}}^{*}(q)\hat{a}_{\underline{p}}^{\dagger}(t) \tag{5.10}$$

While in the ground state Φ_0 there is a large number A of nucleons, in the important excited states there are only a few nucleons excited from their states in the Fermi sea to states above the Fermi level. It is then simpler to keep track of the excited nucleons only, and to consider Φ_0 as the vacuum in field theory. For this reason we introduce the b operators defined by

$$b_{\underline{k}} = a_{\underline{k}}^{\dagger}, \quad b_{\underline{m}} = a_{\underline{m}}^{\dagger}$$

$$b_{\underline{k}}^{\dagger} = a_{\underline{k}}^{\dagger}, \quad b_{\underline{m}}^{\dagger} = a_{\underline{m}} \tag{5.11}$$

We interpret $b_{\underline{m}}^{\dagger}$ as creation operator of a hole in the $\underline{m}$ state of the Fermi sea, and $b_{\underline{m}}$ as annihilation operator of the hole. Most important for us is the relation

$$b_{\underline{p}}|\Phi_0\rangle = 0 \qquad \qquad . \tag{5.12}$$

The anticommutation relations of the b's are the same as those of the a's. The only change occurs in the interaction representation where for $p \leq k_F$ we have instead of Eq.(5.7)

$$\hat{b}_{\underline{m}}(t) = e^{i\epsilon(m)t} b_{\underline{m}}$$
$$\hat{b}^{\dagger}_{\underline{m}}(t) = e^{i\epsilon(m)t} b^{\dagger}_{\underline{m}}$$

(5.13)

and instead of Eq.(5.9)

$$[\hat{b}^{\dagger}_{\underline{m}}(t), \hat{b}_{\underline{m}'}(t')] = \delta_{\underline{m}\,\underline{m}'} e^{-i\epsilon(m)(t-t')}$$

(5.14)

For the field operator $\hat{\varphi}$ we have now the expression

$$\hat{\varphi}(qt) = \sum_{\underline{m}} \varphi_{\underline{m}}(q)\hat{b}^{\dagger}_{\underline{m}}(t) + \sum_{\underline{k}} \varphi_{\underline{k}}(q)\hat{b}_{\underline{k}}(t)$$

(5.15)

6.   CALCULATION OF ΔE WITH THE HELP OF WICK'S THEOREM

With the help of Eq.(5.9) we may rewrite Eq.(4.19) for ΔE in the form

$$\Delta E = N/D$$

(6.1)

where

$$N = \sum_{n=0}^{\infty} \frac{1}{n!} N_n; \quad D = \sum_{n=0}^{\infty} \frac{1}{n!} D_n$$

(6.2)

where

$$N_n = \left(\frac{1}{i}\right)^n \langle \Phi_0 | \int_{-\infty}^{0} dt_1 \dots dt_n \, T[\hat{V}(0)\hat{V}(t_1) \dots \hat{V}(t_n)] | \Phi_0 \rangle$$

(6.3)

$$D_n = \left(\frac{1}{i}\right)^n \langle \Phi_0 | \int_{-\infty}^{0} dt_1 \dots dt_n \, T[\hat{V}(t_1) \dots \hat{V}(t_n)] | \Phi_0 \rangle$$

(6.4)

To simplify the considerations of this chapter we have replaced the Dyson chronological operator P in Eq.(4.18) by the Wick chronological operator T which is defined by the following equation (compare with Eq.(4.16)):

$$T[\Omega_1(t_1) \dots \Omega_k(t_k)] = \delta_P \, \Omega_{p_1}(t_{p_1}) \dots \Omega_{p_k}(t_{p_k})$$

(6.5)

$$t_{p_1} \geq t_{p_2} \dots \geq t_{p_k}$$

The Ω_i operators are supposed to be constructed with the help of the operators b of chapter 5. To convert $\Omega_1 \dots \Omega_k$ into $\Omega_{P_1} \dots \Omega_{P_k}$ we have to make Z_P interchanges $bb' \to b'b$, and we define δ_p as

$$\delta_p = \begin{cases} + 1 \text{ for even } Z_P \\ \\ - 1 \text{ for odd } Z_P \end{cases} \tag{6.6}$$

Since the $\hat{V}$ operators are sums of terms each of which contains four b operators, Eq.(5.6), we always have $\delta_p = +1$ in the T operator in Eqs (6.3), (6.4). Hence, in this case, $T \equiv P$.

If we express the $\hat{V}(t_i)$ operators in Eqs (6.3) (6.4) by means of the $\hat{\varphi}^\dagger(q_i t_i)$, $\hat{\varphi}(q_i t_i)$ operators, Eq.(5.9) we get

$$N_n^{\cdot} = \int_{-\infty}^0 dt_1 \dots dt_n \int dq_0 dq'_0 \dots dq_n dq'_n \left[\tfrac{1}{2} v(q_0 q'_0)\right]\left[\frac{1}{2i} v(q_1 q'_1)\right] \dots$$

$$\dots \left[\frac{1}{2i} v(q_n q'_n)\right]\Big\langle \Phi_0\Big| T \Big\{ \hat{\varphi}^\dagger(q_0 0) \hat{\varphi}^\dagger(q'_0 0) \hat{\varphi}(q'_0 0) \hat{\varphi}(q_0 0)$$

$$\times \hat{\varphi}^\dagger(q_1 t_1) \hat{\varphi}^\dagger(q'_1 t_1) \hat{\varphi}(q'_1 t_1) \hat{\varphi}(q_1 t_1) \dots \hat{\varphi}^\dagger(q_n t_n) \hat{\varphi}^\dagger(q'_n t_n) \times$$

$$\times \hat{\varphi}(q'_n t_n) \hat{\varphi}(q_n t_n)\Big\}\Big| \Phi_0\Big\rangle \tag{6.7}$$

$$D_n = \int_{-\infty}^0 dt_1 \dots dt_n \int dq_1 \dots dq'_n \left[\frac{1}{2i} v(q_1 q'_1)\right] \dots \left[\frac{1}{2i} v(q_n q'_n)\right] \times$$

$$\times \Big\langle \Phi_0\Big| T\Big\{\hat{\varphi}^\dagger(q_1 t_1) \dots \hat{\varphi}(q_n t_n)\Big\}\Big| \Phi_0\Big\rangle \tag{6.8}$$

We are faced here with the difficulty of T acting on the product of $\hat{\varphi}^\dagger(q_i t_i)$, $\hat{\varphi}(q'_i t_i)$, both taken at the same time. Since $[\hat{\varphi}^\dagger, \varphi] \neq 0$ the action of T is not defined. To avoid this difficulty we replace everywhere

$$\hat{\varphi}^\dagger(q_i t_i) \to \hat{\varphi}^\dagger(q_i t_i + \epsilon)[= \hat{\varphi}^\dagger(q_i t_i^\dagger)] \tag{6.9}$$

This makes the operation of T unambiguous. Eventually, we take the limit $\epsilon \to +0$. We shall keep this procedure in mind but, in general, shall not indicate it in our formulas.

To compute the expectation values appearing in Eqs (6.7), (6.8) we shall use Wick's theorem. To state this theorem we have to introduce the idea of a normal product and of a contraction.

The normal product of the operators b_p, $b_p^\dagger$, is a product of these operators in which all the creation operators $b_{p'}^\dagger$ appear on the left side of all the annihilation operators b_p. By N we denote the operator which changes any product of the b's and $b^\dagger$'s into a normal product, with a proper sign. We have

$$N\{ \ldots b_{\underline{p}} \ldots b_{\underline{p'}}^\mathsf{T} \ldots \} = \delta_P \{ \ldots b_{\underline{p'}}^\mathsf{T} \ldots b_{\underline{p}} \ldots \} \tag{6.10}$$

where δ_P is defined as before in Eq.(6.6).

The N operators obey the distribution law, and we have, e.g.

$$N\left\{ \hat{\varphi}(qt)\,\hat{\varphi}^\dagger(q't') \right\} = N\left\{ \left[\sum_{\underline{m}} \varphi_{\underline{m}}(q)\,\hat{b}_{\underline{m}}^\dagger(t) \right. \right.$$

$$+ \sum_{\underline{k}} \varphi_{\underline{k}}(q)\hat{b}_{\underline{k}}(t) \right]\left[\sum_{\underline{m'}} \varphi_{\underline{m'}}^*(q')\hat{b}_{\underline{m'}}(t') \right.$$

$$+ \left. \left. \sum_{\underline{k'}} \varphi_{\underline{k'}}^*(q')\hat{b}_{\underline{k'}}^\dagger(t') \right] \right\} = \sum_{\underline{m}}\sum_{\underline{m'}} \varphi_{\underline{m}}(q)\varphi_{\underline{m'}}^*(q')\hat{b}_{\underline{m}}^\dagger(t)\hat{b}_{\underline{m'}}(t')$$

$$+ \sum_{\underline{m}}\sum_{\underline{k'}} \varphi_{\underline{m}}(q)\varphi_{\underline{k'}}^*(q')\hat{b}_{\underline{m}}^\dagger(t)\,\hat{b}_{\underline{k'}}^\dagger(t')$$

$$+ \sum_{\underline{k}}\sum_{\underline{m'}} \varphi_{\underline{k}}(q)\varphi_{\underline{m'}}^*(q')\,\hat{b}_{\underline{k}}(t)\hat{b}_{\underline{m'}}(t')$$

$$- \sum_{\underline{k'}}\sum_{\underline{k}} \varphi_{\underline{k'}}^*(q')\varphi_{\underline{k}}(q)\hat{b}_{\underline{k}}^\dagger(t')\hat{b}_{\underline{k}}(t) \tag{6.11}$$

Let us notice that Eq.(5.12) implies that

$$\left\langle \Phi_0 \left| N\{ \hat{\varphi}(qt)\,\hat{\varphi}^\dagger(q't') \} \right| \Phi_0 \right\rangle = 0 \tag{6.12}$$

Similarly, the expectation values of the products of the $\hat{\varphi}$ and $\hat{\varphi}^\dagger$ operators appearing in Eqs (6.7), (6.8) would vanish if the products were put into a form of a normal product. It is then essential to know the difference between a time-ordered and normal product. For two operators Ω_1, Ω_2 we call this difference the contraction of Ω_1, Ω_2 and denote it by $\overline{\Omega_1\Omega_2}$

$$\overline{\Omega_1\Omega_2} = T(\Omega_1\Omega_2) - N(\Omega_1\Omega_2) \tag{6.13}$$

Most important for us is the contraction between $\hat{\varphi}$ and $\hat{\varphi}^\dagger$ which we shall denote by G and call the propagator of Green function. With the

help of Eq.(6.11) we easily obtain

$$G(qt, q't') = \langle \Phi_0 | T\{\hat{\varphi}(qt)\,\hat{\varphi}^\dagger(q't')\} | \Phi_0 \rangle = \overline{\hat{\varphi}(qt)\,\hat{\varphi}^\dagger(q't')}$$

$$= -\overline{\hat{\varphi}^\dagger(q't')\,\hat{\varphi}(qt)} = \theta(t-t') \sum_{\underline{k}} \varphi_{\underline{k}}(q)\varphi_{\underline{k}}^{*}(q')e^{-i\epsilon(\underline{k})(t-t')}$$

$$- \theta(t'-t) \sum_{\underline{m}} \varphi_{\underline{m}}(q)\,\varphi_{\underline{m}}^{*}(q')e^{-i\epsilon(\underline{m})(t-t')} \tag{6.14}$$

It is also easy to see that

$$\overline{\hat{\varphi}^\dagger\,\hat{\varphi}} = \overline{\hat{\varphi}\,\hat{\varphi}} = 0 \tag{6.15}$$

    In cases, like that of Eq.(6.14), when the contractions are c-numbers
(i.e. the Ω's are linear in the b's), let us define a normal product with
contraction

$$N\{\Omega_1\overline{\Omega_2\ldots\Omega_i\ldots\Omega_\ell}\ldots\Omega_n\ldots\Omega_r\} = \delta_P \overline{\Omega_2\Omega_1}\,\overline{\Omega_i\Omega_n} \ldots N\{\Omega_1 \ldots \Omega_r\} \tag{6.16}$$

where δ_P is again defined by Eq.(6.6) with Z_P being the number of inter-
changes necessary to go from the left-hand side order of the operators,
$\Omega_1\Omega_2\ldots\Omega_r$ to the right-hand side order, $\Omega_2\Omega_2\ldots\Omega_r$.
    Now, we are ready to state Wick's theorem for the operators $\Omega_i = \Omega_i(t_i)$
which are linear in the b's and $b^\dagger$'s

$$T\{\Omega_1\ldots\Omega_n\} = N\{\Omega_1\ldots\Omega_n\} + N\{\overline{\Omega_1\Omega_2}\ldots\Omega_n\} +$$

$$+ \ldots + N\{\Omega_1\overline{\Omega_2,\,,\,,\Omega_i}\ldots\Omega_n\} + \ldots + N\{\overline{\Omega_1\Omega_2}\ldots\overline{\Omega_i}\ldots\Omega_n\} + \ldots \tag{6.17}$$

On the right-hand side of Wick's theorem we have first the normal
product and then the sum extends over the normal products with all
possible contractions of the Ω's.
    For $n = 2$ the theorem reduces to the definition of contraction,
Eq.(6.13). For $n > 2$ one proves Wick's theorem by induction (see,
e.g. [18]).
    We are now in a position to calculate the perturbation expansion of
ΔE, term after term. Namely, to compute the expectation values in
Eqs (6.7), (6.8), we apply Wick's theorem. We notice that only those
normal products appearing in the theorem give non-vanishing contribution,
in which all the $\hat{\varphi}$'s and $\hat{\varphi}^\dagger$'s operators are contracted. This is so
because the expectation value with respect to Φ_0 of a normal product of
the $\hat{\varphi}$'s and $\hat{\varphi}^\dagger$'s vanishes (see Eq.(6.12). Even more: because of

Eq.(6.15), only those among the fully contracted terms contribute in which each $\hat{\varphi}$ is contracted with a $\hat{\varphi}^\dagger$. Hence N_n and D_n are simply sums of products of the G propagators, Eq.(6.14).

7. DIAGRAMS

Diagrams are an essential tool in analysing the perturbation series. To understand the present state of the theory of nuclear matter we have to spend some time on explaining the diagrammatic language in which physicists working on nuclear matter communicate nowadays.

Let us first compute the first terms of the perturbation expansion of ΔE, Eqs.(6.1-2, 7-8).

First order (n = 0)

Equation (6.8) gives

$$D_0 = 1 \tag{7.1}$$

and Eq.(6.7) gives

$$N_0 = \int dq_0 \int dq'_0\, I(q_0 q'_0) \tag{7.2}$$

where

$$I(q_0 q'_0) = \tfrac{1}{2} v(q_0 q'_0) \langle \Phi_0 | \, T\{ \hat{\varphi}^\dagger(q_0 0)\, \hat{\varphi}^\dagger(q'_0 0)\, \hat{\varphi}(q'_0 0)\, \hat{\varphi}(q_0 0)\} \, | \Phi_0 \rangle \tag{7.3}$$

By applying Wick's theorem we get

$$I(q_0 q'_0) = \tfrac{1}{2} v(q_0 q'_0) \Big\{ \langle \Phi_0 | N\{ \hat{\varphi}^\dagger(q_0 0)\, \hat{\varphi}^\dagger(q'_0 0)\, \hat{\varphi}(q'_0 0)\, \hat{\varphi}(q_0 0)\} \, | \Phi_0 \rangle$$

$$+ \, \langle \Phi_0 | N\{ \hat{\varphi}^\dagger(q_0 0)\, \hat{\varphi}^\dagger(q'_0 0)\, \hat{\varphi}(q'_0 0)\, \hat{\varphi}(q_0 0)\} \, | \Phi_0 \rangle \Big\}$$

$$= \tfrac{1}{2} v(q_0 q'_0) \{ G(q_0 0,\, q_0 0^\dagger) G(q'_0 0,\, q'_0 0^\dagger) - G(q'_0 0,\, q_0 0^\dagger) G(q_0 0,\, q'_0 0^\dagger) \}$$

$$\tag{7.3a}$$

where the $0^\dagger$ values of the time variable remind us of the procedure (6.9).

Second order (n = 1)

Here we get

$$D_1 = \int_{-\infty}^{0} dt_1 \int dq_1 \int dq'_1\, I(q_1,\, q'_1,\, t_1) \tag{7.4}$$

where

$$I(q_1 q_1' t_1) = \frac{1}{2i} v(q_1 q_1') \{ G(q_1 t_1, q_1 t_1^\dagger) G(q_1' t_1, q_1'\ t_1^\dagger) - G(q_1' t_1, q_1 t_1^\dagger) G(q_1 t_1, q_1' t_1') \}$$

(7.5)

and

$$N_1 = \int_{-\infty}^{0} dt_1 \int dq_0 \int dq_0' \int dq_1 \int dq_1'\ I(q_0 q_0'; q_1 q_1' t_1)$$

(7.6)

where

$$I(q_0 q_0'; q_1 q_1' t_1) = \left[\tfrac{1}{2} v(q_0 q_0') \right] \left[\frac{1}{2i} v(q_1 q_1') \right] \Big\langle \Phi_0 \Big| T\{ \hat{\varphi}^\dagger(q_0 0) \hat{\varphi}^\dagger(q_0' 0)$$

$$\times\ \hat{\varphi}(q_0' 0) \hat{\varphi}(q_0 0) \hat{\varphi}^\dagger(q_1 t_1) \hat{\varphi}^\dagger(q_1' t_1) \hat{\varphi}(q_1' t_1) \hat{\varphi}(q_1 t_1) \} \Big| \Phi_0 \Big\rangle.$$

(7.7)

The Wick's theorem applied to the last expectation values produces $4! = 24$ terms resulting from all possible contractions between the four $\hat{\varphi}^\dagger$'s and the four $\hat{\varphi}$'s. Thus we have

$$I(q_0 q_0'; q_1 q_1' t_1) = \sum_{\alpha=1}^{24} I_\alpha(q_0 q_0'; q_1 q_1' t_1)$$

(7.8)

Let us compute one of the 24 terms, e.g. the term

$$I_{\alpha 0}(qq_0'; q_1 q_1' t_1) = \left[\tfrac{1}{2} v(q_0 q_0') \right] \left[\frac{1}{2i} v(q_1 q_1') \right]$$

$$\times \Big\langle \Phi_0 \Big| N\{ \hat{\varphi}^\dagger(q_0 0) \hat{\varphi}^\dagger(q_0' 0) \hat{\varphi}(q_0' 0) \hat{\varphi}(q_0 0) \hat{\varphi}^\dagger(q_1 t_1) \hat{\varphi}^\dagger(q_1' t_1) \hat{\varphi}(q_1' t_1) \hat{\varphi}(q_1 t_1) \} \Big| \Phi_0 \Big\rangle$$

$$= + \left[\tfrac{1}{2} v(q_0 q_0') \right] \left[\frac{1}{2i} v(q_1 q_1') \right] G(q_0 0 q_1 t_1) G(q_1 t_1 q_0 0) G(q_0' 0 q_1' t_1) G(q_1' t_1; q_0' 0)$$

(7.9)

In a similar fashion we may compute all the remaining 23 terms. This kind of procedure, however, becomes unpleasant. Especially for higher n values it is difficult to keep control of all of the $(2n+2)!$ terms of N_n as well as of the $(2n)!$ terms of D_n. Fortunately, we are able to associate with all terms of the perturbation expansion proper pictures called diagrams which shall help us considerably in writing all the contributions to ΔE. At the same time, they will give us a better insight into the physical meaning of different terms of the perturbation expansion.

Let us start with N_0. We draw the t-axis going upwards and a horizontal axis for the q variables. With the first (direct) term of Eq.(7.5) we associate the diagram shown in Fig.2a, with the second (exchange) term the diagram in Fig.2b. The way of associating the parts of the diagram with the factors of $I(q_0 q_0')$ is indicated in Fig.2. The right sign of the direct and exchange part of $I(q_0 q_0')$ is obtained by associating a minus sign, (-1), with each closed loop. To get N_0 we have to integrate over q_0 and q_0'.

(a) N_0 (direct)   (b) N_0 (exchange)
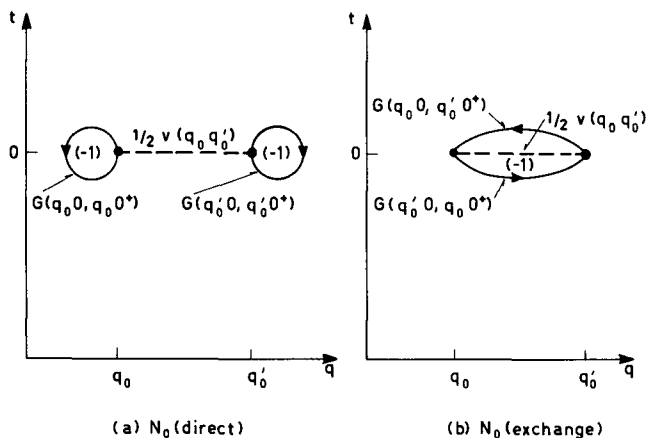
FIG.2.   (a) Diagram associated with the first (direct) term of Eq.(7.5);   (b) diagram associated with the second (exchange) term of Eq.(7.5).

(a) D_1 (direct)   (b) D_1 (exchange)
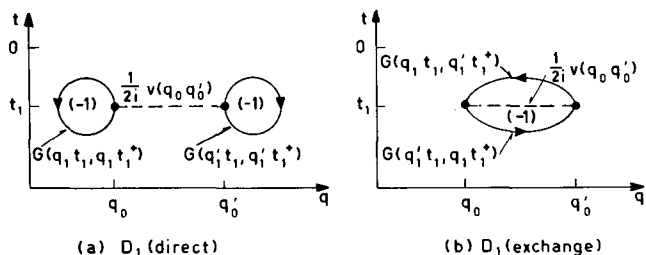
FIG.3.   Diagrams associated with D_1 (Eq.(7.5)).

The two diagrams associated with D_1, Eq.(7.5), are shown in Fig.3a-b. Notice the $(1/i)$ factor multiplying v. To the D_1 we have to integrate over q_1, q_1' and over t_1 from $-\infty$ to 0.

One of the 24 contributions to N_1, the contribution α_0, Eq.(7.9), is described by the diagram shown in Fig.4. To get $[N_1]_{\alpha_0}$ we have to integrate over $q_0 q_0' q_1 q_1'$ and t_1 from $-\infty$ to 0.

From now we shall not draw the horizontal q-axis. If necessary we shall indicate the q-co-ordinate at the ends of the dotted interaction lines (see Fig.5). Eventually, we shall not draw the time axis either, keeping in mind our convention of the time increasing upwards.
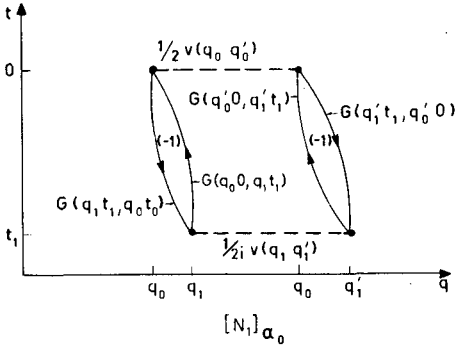
FIG.4.   Diagram depicting the contribution α_0 (Eq.(7.9)).   FIG.5.   An α-diagram without q-axis drawn.
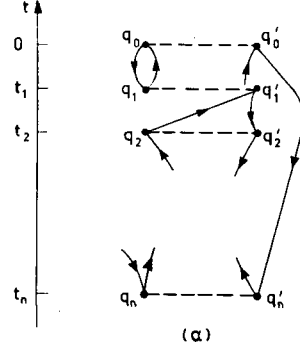
By now it should become obvious how to use the diagrams in com-
puting N_n and D_n. Namely in computing N_n we proceed as follows:

We draw $n+1$ horizontal broken interaction lines and join the ends
of these interaction lines by directed solid lines such that one line enters
and one line leaves each of every interaction line (Fig.5). There are
$(2n+2)!$ ways of doing it and thus we get $(2n+2)!$ diagrams. Each
diagram α $(\alpha = 1, ..., (2n+2)!)$ represents a contribution to N_n:

$$(N_n)_\alpha = \int_{-\infty}^{0} dt_1 ... \int_{-\infty}^{0} dt_n \int dq_0 ... \int dq_n' I_\alpha(q_0 q'_{0i} q_1 q'_1 t_{1i} ... q_n q'_n t_n)$$

(7.10)

and

$$N_n = \sum_{\alpha=1}^{(2n+2)!} (N_n)_\alpha$$

(7.11)

The integrand I_α is a product of the factors associated with all the
elements of the α diagram in the way shown in Table I.

In computing D_n we follow the same procedure except for the $t=0$
interaction line $q_0 \_ \_ \_ \_ \_ \_ \_ q'_0$ which does not occur in the D diagrams.
Consequently, there are $(2n)!$ diagrams contributing to D_n.
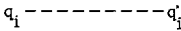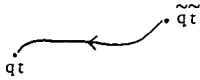
In Fig.6 all the $24N_1$ diagrams are shown.

Actually the number of diagrams which must be considered in calcu-
lating ΔE substantially reduced because of the linked-cluster theorem and
also because of momentum conservation.

8.   LINKED-CLUSTER THEOREM

We call the first four diagrams in Fig.6 disconnected (unlinked) be-
cause they are composed of two disconnected (unlinked) parts. If all
elements of a diagram are connected (by a nucleon line ⤳ or by an
interaction line $-----$) we call it a connected diagram. All the re-
maining 20 diagrams in Fig.6 are connected.

TABLE I.   RELATIONSHIP OF DIAGRAM ELEMENTS AND FACTORS IN I_α

Elements of a diagram	Factor in I_α
$q_i \text{-------} q_i'$	$\dfrac{1}{2i}\, v(q_i q_i')$ (with the i missing for the t = 0 interaction line ($\ell = 0$))
$q t \quad \widetilde{\widetilde{q\,t}}$	$G(qt,\ \widetilde{\widetilde{q\,t}})$
(loop)	(-1)
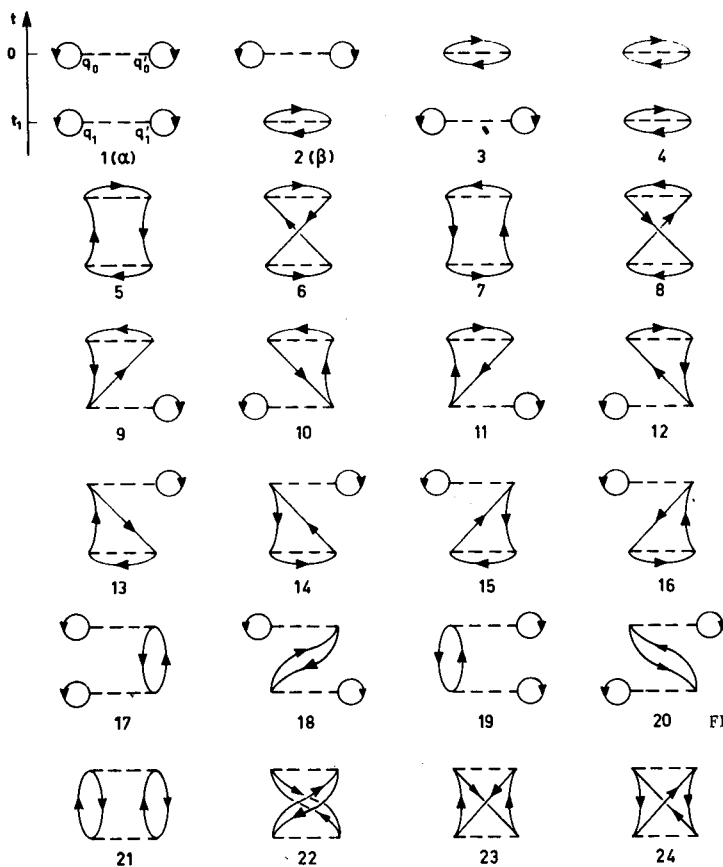
FIG. 6.   All N_1 diagrams (24).

Let us compute the contribution of the diagram α of Fig.6 to

N_1:

$$(N_1)_\alpha = \int_{-\infty}^{0} dt_1 \int dq_0 dq'_0 dq_1 dq'_1 \tfrac{1}{2} v(q_0 q'_0) \frac{1}{2i} v(q_1 q'_1) G(q_0 0 q_0 0) G(q'_0 0 q'_0 0)$$

$$\times G(q_1 t_1 q_1 t_1) G(q'_1 t_1 q'_1 t_1) = \left[\int dq_0 dq'_0 \tfrac{1}{2} v(q_0 q'_0) G(q_0 0 q_0 0) G(q'_0 0 q'_0 0) \right]$$

$$\times \left[\int_{-\infty}^{0} dt_1 \int dq_1 dq'_1 \frac{1}{2i} v(q_1 q'_1) G(q_1 t_1 q_1 t_1) G(q'_1 t_1 q'_1 t_1) \right]$$

$$= N_0 \text{(direct)} \times D_1 \text{(direct)}. \tag{8.1}$$

If we add a similar result for the contribution of the diagram β of Fig.6 we find:

$$(N_1)_\alpha + (N_1)_\beta = N_0 \text{(direct)} \times D_1 \text{(direct)} +$$

$$+ N_0 \text{(direct)} \times D_1 \text{(exchange)} = N_0 \text{(direct)}$$

$$\times [D_1 \text{(direct)} + D_1 \text{(exchange)}] = N_0 \text{(direct)} \times D_1 \tag{8.2}$$

If we add the contribution N_0 (direct) Fig.2a to it we obtain

$$N_0 \text{(direct)} + \frac{1}{1!} N_0 \text{(direct)} \times D_1 = N_0 \text{(direct)} \left[1 + \frac{1}{1!} D_1 \right] =$$

$$= N_0 \text{(direct)} \left[D_0 + \frac{1}{1!} D_1 \right] \tag{8.3}$$

Considering all those higher-order $(n > 1)$ contributions to N_n which are represented by disconnected diagrams having the disconnected $t = 0$ part o- - - - -o would lead us to the total contribution to N

$$N_0 \text{(direct)} \left[D_0 + \frac{1}{1!} D_1 + \frac{1}{2!} D_2 + \ldots \right] = N_0 \text{(direct)} \times D \tag{8.4}$$

Hence, the contribution to ΔE, Eq.(6.1), of all those diagrams which are composed of the $t = 0$ part o- - - - -o plus a disconnected remaining part, is given simply by

$$N_0 \text{(direct)} \times D/D = N_0 \text{(direct)} \tag{8.5}$$

The same argument holds for any connected diagram γ. If we consider together with this γ diagram all the disconnected diagrams composed of γ plus a part not connected with γ we find that the total contribution of all these diagrams to N is equal to the contribution to N of the γ diagram, N_γ, multiplied by D. This shows that in calculating ΔE we have to consider connected diagrams only and disregard in Eq.(6.1) the denominator D which is exactly cancelled by the omitted disconnected diagrams in the numerator N. We have then:

$$\Delta E = \langle \Phi_0 | V U | \Phi_0 \rangle_L \tag{8.6}$$

where the subscript L means that only connected or linked diagrams should be considered. This important linked-cluster theorem was demonstrated first by Brueckner in the first four orders of the perturbation expansion [19]. The first general proof was given by Goldstone [6].

As one can easily see the contribution of a linked diagram is proportional to Ω. We then obtain for ΔE - in fact for each separate term of our expansion — the desired result: $\Delta E \sim \Omega$.

Linked diagrams have the following two properties: (A) by interchanging $q_i \leftrightarrow q'_i$ (for $i \neq 0$) we get a distinct diagram which gives the same contribution; (B) by permuting the labels 1, ..., n of interactions we get a distinct diagram which gives the same contribution. Hence we shall restrict ourselves to diagrams which cannot be transformed into each other by means of (A) and (B) and shall drop the factor 1/2 for the interactions at $t \neq 0$ and the 1/n! factors in Eq.(6.2) for N_n. For instance in computing N_1 we shall consider only one of the diagrams 21, 22 and only one of the diagrams 23, 24 of Fig.6.

9. MOMENTUM REPRESENTATION. TIME INTEGRATION

The propagator $G(qt, q't')$ may be written, according to Eq.(6.14), in the form

$$G(qt, q't') = \sum_p \varphi_p(q) \varphi_p^*(q') G(\underline{p}, t-t') \tag{9.1}$$

where

$$G(\underline{p}, t-t') = e^{-i\epsilon(p)t-t'} \times \begin{cases} \theta(t-t') & \text{for } p > k_F \\ -\theta(t'-t) & \text{for } p \leq k_F \end{cases} \tag{9.2}$$

If we use the expression (9.1) for $G(qt, q't')$ in computing N_n, Eq.(7.10), the integration over the q variables may be performed, and as the result of this integration we obtain matrix elements of v, Eq.(5.3). Instead of the q integrals sums over $\underline{p}$'s appear. For instance, for the contribution to N_1 of the α_0 diagram, Eqs (7.6,9), we get

$$[N_1]_{\alpha_0} = \int_{-\infty}^{0} dt_1 \sum_{\underline{p}_1 \underline{p}_2 \underline{p}_3 \underline{p}_4} \left[\frac{1}{2} (\underline{p}_1 \underline{p}_2 | v | \underline{p}_3 \underline{p}_4) \right] \left[\frac{1}{2i} (\underline{p}_3 \underline{p}_4 | v | \underline{p}_1 \underline{p}_2) \times \right. \tag{9.3}$$

$$\left. \times G(\underline{p}_1, t_1-0) G(\underline{p}_2, t_1-0) G(\underline{p}_3, 0-t_1) G(\underline{p}_4, 0-t_1) \right]$$

FIG.7.   Diagram representing the contribution
to N_1 of the α_0-diagram.
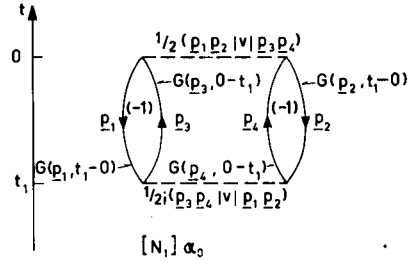
TABLE II.   RELATIONSHIP OF DIAGRAM ELEMENTS AND FACTORS
IN I_α IN MOMENTUM SPACE

	$\dfrac{1}{2i}(\underline{p}_2\,\underline{p}_4|v|\,\underline{p}_1\underline{p}_3)$. (with the i missing for the t = 0 interaction line)
	$G(\underline{p},\, t_j - t_i)$
	(-1)

This contribution may be represented by the diagram shown in Fig.7.
It looks exactly as the diagram in Fig.4. The only difference is, that in-
stead of attaching q values to the ends of interaction lines, now we attach
p values to each solid line. This is so because during a free propagation
of a nucleon its p value is conserved. The general rules for computing
the contribution of the new p diagrams, like that of Fig.7, are the same
as those explained in chapter 8, except for the following modifications:
    Equation (7.10) changes into

$$[N_n]_\alpha = \int\limits_{-\infty}^{0} dt_1 \ldots \int\limits_{-\infty}^{0} dt_n \sum_{\underline{p}_1\cdots\underline{p}_{2n+2}} I_\alpha(\underline{p}_1 \ldots p_{2n+2},\ t_1 \ldots t_n) \qquad (9.3')$$

and Table I is changed into Table II.
    Of course, the remarks concerning the factors 1/2, 1/n! for linked
diagrams made at the end of chapter 8 remain valid.
    It is important to notice that the interaction of two nucleons does not
change their total momentum, i.e. the matrix element

$$(\underline{p}_1\underline{p}_2|v|\underline{p}_3\underline{p}_4)$$

contains a factor $\delta_{\vec{p}_1+\vec{p}_2,\,\vec{p}_3+\vec{p}_4}$.

Now, the earliest interaction line of any diagram looks always like

$$\underset{\underline{p}_3}{\diagdown}\underset{\underline{p}_1}{\diagup} \qquad\qquad \underset{\underline{p}_4}{\diagdown}\underset{\underline{p}_2}{\diagup}$$

and because of the δ factor we have $\vec{p}_1 + \vec{p}_2 = \vec{p}_3 + \vec{p}_4$. We may proceed to later times, i.e. go upwards in the diagram and we find at any level of a diagram that the total momentum of the up-going lines is equal to the total momentum of the down-going lines. Or, to put it in a different way: the total momentum of the whole system, being zero in the Φ_0 state, remains zero at any stage of the interaction process. (Notice that because a down-going line represents a hole in the $\underline{p}$ state [see Eq.(9.2)] it contributes the momentum $-\vec{p}$ to the total momentum of the whole system.)

This momentum conservation substantially reduces the number of diagrams which give a non-vanishing contribution. For instance, all the 18 diagrams 5-20 of Fig.6 give a vanishing contribution.

We now want to perform the time integrations in Eq.(9.3'). After all, we should be able to eliminate the t variable which has been introduced artificially into our stationary problem. To do this, we have to apply the explicit form of $G(\underline{p}, t_j - t_i)$ of Eq.(9.2).

In the diagrams which we have drawn so far the relative positions of the t_i's were irrelevant (the only restriction was that $t_i < 0$ $(i = 1, ..., n)$), because, anyhow, in the calculation of the contributions represented by these diagrams, the integration $\int_{-\infty}^{0} dt_i$ was involved. These diagrams are called Feynman diagrams. However, the propagator $G(\underline{p}, t_j - t_i)$ has different form for positive and negative values of $t_j - t_i$, and consequently, performing the time integration, one has to consider separately each order of the times $t_1, t_2, ..., t_n$, or, in other words, one has to split the time intervals $0 > t_1 > -\infty$, ..., $0 > t_n > -\infty$ into $n!$ intervals in which the differences $t_j - t_i$ have definite signs. Each Feynman diagram for N_n gives the $n!$ distinct contributions, one for each possible order of $t_1, ..., t_n$. Diagrammatically, we shall represent these $n!$ contributions by the time-ordered or Goldstone diagrams, in which the relative positions of the t_i - s, i.e. of the interaction lines are significant. Now, for $t_j - t_i > 0$, $G(\underline{p}, t_j - t_i)$ differs from zero only for $p > k_F$, and for $t_j - t_i < 0$, $G(\underline{p}, t_j - t_i)$ differs from zero only for $p \leq k_F$. This means that in a Goldstone diagram a solid line going upwards (particle line) always represents the propagation of a nucleon with $p > k_F$ and a line going downwards (hole line) always represents the propagation of a hole with $p \leq k_F$. An example of how a Feynman diagram is equal to a sum of Goldstone diagrams is shown in Fig.8.

FEYNMAN DIAGRAM   GOLDSTONE   DIAGRAMS
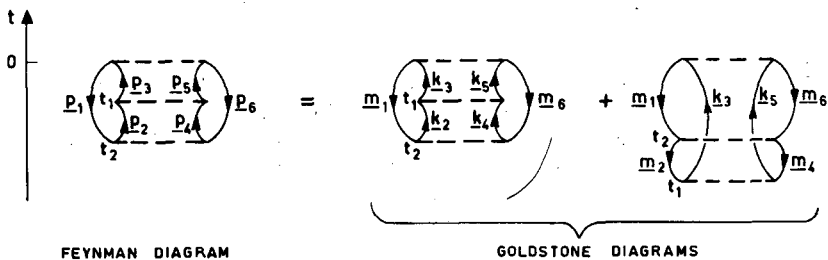
FIG.8.   Example showing how a Feynman diagram is equal to a sum of Goldstone diagrams.

Now we are ready to actually perform the time integration. Let us consider, e.g. the diagram $[N_1]_{\alpha_0}$ of Fig.4. This very simple Feynman diagram is identical to the Goldstone diagram since n = 1 and only one time order is possible. After the preceding discussion we may denote the nucleon lines of this diagram more precisely, as shown in Fig.9a.
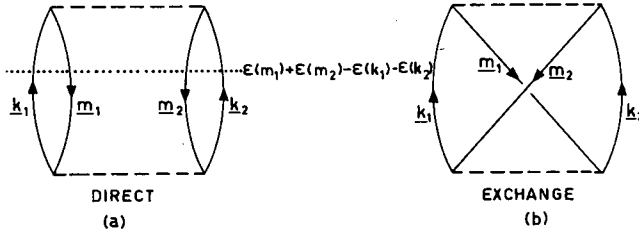
FIG.9.   Diagram describing the second-order term of the perturbation expansion of ΔE.

The contribution $[N_1]_{\alpha_0}$ is, according to Eqs (9.2, 3), (see also the remarks following Eq.(9.16)) given by

$$[N_1]_{\alpha=0} = \sum_{\underline{k}_1\underline{k}_2\underline{m}_1\underline{m}_2} \left[\frac{1}{2}(\underline{m}_1\underline{m}_2\,|v|\,\underline{k}_1\underline{k}_2)\right]\left[\frac{1}{i}(\underline{k}_1\underline{k}_2\,|v|\,\underline{m}_1\underline{m}_2)\right]$$

$$\times \lim_{\alpha\to0+}\int_{-\infty}^{0} dt_1 e^{\alpha t}\left[-e^{-i\epsilon(m_1)t_1}\right]\left[-e^{-i\epsilon(m_2)t_1}\right]\left[e^{i\epsilon(k_1)t_1}\right]\left[e^{i\epsilon(k_2)t_2}\right] \quad (9.4)$$

Notice that we dropped the 1/2 factor at the second v, and thus we do not have to consider separately the diagram 22 of Fig.6, as mentioned at the end of chapter 8. Notice also the minus sign for each hole line. The time integral gives

$$(-1)^2 \lim_{\alpha\to0^+} \left.\frac{e^{[i(\epsilon(k_1)+\epsilon(k_2)-\epsilon(m_1)-\epsilon(m_2))+\alpha]t}}{i(\epsilon(k_1)+\epsilon(k_2)-\epsilon(m_1)-\epsilon(m_2))+\alpha}\right|_{t=-\infty}^{t=0} =$$

$$= \frac{i}{\epsilon(m_1)+\epsilon(m_2)-\epsilon(k_1)-\epsilon(k_2)}$$

and for $[N_1]_{\alpha_0}$ we get

$$[N_1]_{\alpha_0} = \frac{1}{2}\sum_{\underline{k}_1\underline{k}_2\underline{m}_1\underline{m}_2} (m_1m_2\,|v|\,k_1k_2)(k_1k_2\,|v|\,m_1m_2)/(\epsilon(m_1)+\epsilon(m_2)-\epsilon(k_1)-\epsilon(k_2))$$

$$(9.4')$$

Proceeding in the same way with any Goldstone diagram we find that in general the time integration produces a factor

$$\frac{i}{\sum\limits_{\underline{m}} \epsilon(m) - \sum\limits_{\underline{k}} \epsilon(k)} \tag{9.5}$$

for each interval between two interaction lines, where the sum $\sum\limits_{m} \epsilon(m)$ runs over all hole lines and $\sum\limits_{k} \epsilon(k)$ over all particle lines present in the corresponding interval of the diagram. One may find all these lines by looking for the lines crossing any horizontal line drawn between the two adjacent lines (see Fig.9a). Let us notice that $\sum\limits_{\underline{m}} \epsilon(m) - \sum\limits_{\underline{k}} \epsilon(k)$ is equal to the negative excitation energy of the system in the interval. We see that the i factor in the numerator of (9.5) cancels the $1/i$ factor at each v for $t < 0$, and we may forget about the i factors altogether. As seen from Eq.(9.2) there is an extra (-1) factor for each hole line of a diagram, and we get altogether a $(-1)^h$ factor, where h is the number of hole lines of the diagram. Let us notice that we may ignore the loop $----\bigcirc m$ and its hole line in fixing the sign factor because it produces the factor $(-1)^{1+1} = +1$ (one minus for the loop and one minus for the hole line).

By applying these rules we are able to write expressions for all terms of the perturbation expansion of ΔE. For instance, let us write the second order term $(\Delta E)_2$. It is composed of only the two diagrams (a) and (b) of Fig.9. We obtain

$$[\Delta E]_2 = \frac{1}{2} \sum\limits_{\underline{k_1 k_2} \, \underline{m_1 m_2}} (\underline{m_1 m_2} | v | \underline{k_1 k_2}) \frac{1}{\epsilon(m_1) + \epsilon(m_2) - \epsilon(k_1) - \epsilon(k_2)}$$

$$\times [(\underline{k_1 k_2} | v | \underline{m_1 m_2}) - (\underline{k_1 k_2} | v | \underline{m_2 m_1})] \tag{9.6}$$

The last factor may be written shortly as

$$(\underline{k_1 k_2} | v | \underline{m_1 m_2} - \underline{m_2 m_1})$$

10. LOW-DENSITY APPROXIMATION

We shall not spend any time on discussing a straight application of the perturbation expansion in calculating the properties of nuclear matter, because all the attempts in this direction have failed. The reason for it is that a nucleon-nucleon interaction reproducing the two-body scattering data (the change of sign of $\delta(^1S_0)$ at about 200 MeV) is so singular at small distances that the perturbation series for ΔE is converging very slowly. This is best seen in the case of the often applied nuclear forces with a hard core, for which each term of the perturbation series (each matrix

element of v for that matter) is infinite. In this case it is obvious that to deal with finite quantities(instead of the infinite matrix elements of v) we have to perform a partial summation of properly selected diagrams. "Properly selected" means that: (i) we are able to calculate their sum, (ii) the sum is finite, and (iii) they are the physically most important diagrams.

We shall try to satisfy the three requirements by selecting those diagrams which are most important for low-density nuclear matter. As we shall see the requirements (i), (ii) will be satisfied. As far as the requirement (iii) is concerned, the situation does not look encouraging at first sight. Low density means that the average spacing between the particles of the system is large compared to the range of interaction. However, the average nucleon-nucleon distance between the nucleons in nuclear matter is about the same as the range of nuclear forces. At this stage, we might say that we consider the low-density limit only to be a convenient starting point in a systematic procedure in which terms of higher order in the density will be included in the next steps. Thus we have a well-defined procedure and we know − as we shall see − which diagrams to select at each step of the procedure. In fact, however, the situation seems to be much better. We shall discuss it later on in detail (see chapter 15), where we shall argue that the parameter determining the convergence of our procedure is, in fact, the ratio of the range of the short singular part of the forces to the average distance between nucleons, and this parameter is much smaller then unity.

The possibility of convergence in powers of the density ρ has been suggested by Hugenholtz [20]. According to Hugenholtz the dominant time-ordered diagrams at low density are those with the least number of hole lines, because each hole line introduces into ΔE an integration over momenta $m_i < k_F$ and a corresponding factor of the order of $k_F^3 \sim \rho$ (see Eq. 3.5). Since there are, at least, two hole lines in any diagram, in the low-density limit we have to select all the diagrams with two hole lines. The two hole lines produce a factor $\sim \rho^2$ in ΔE or a factor $\sim \rho$ in $\Delta E/A$ (notice that $\Delta E \sim \Omega$).
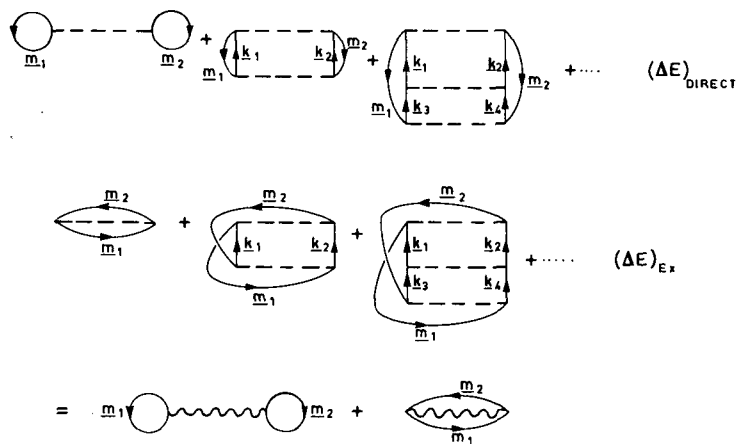
FIG.10.   Ladder diagrams.

The selected diagrams, called ladder diagrams, are shown in Fig.10.
Let us write the contribution of the direct diagrams (first line in Fig.10)
to ΔE

$$(\Delta E)_{direct} = \frac{1}{2} \sum_{\underline{m}_1 \underline{m}_2} \left\{ (\underline{m}_1 \underline{m}_2 | v | \underline{m}_1 \underline{m}_2) \right.$$

$$+ \sum_{\underline{k}_1 \underline{k}_2} (\underline{m}_1 \underline{m}_2 | v | \underline{k}_1 \underline{k}_2) \frac{1}{\epsilon(m_1) + \epsilon(m_2) - \epsilon(k_1) - \epsilon(k_2)} (\underline{k}_1 \underline{k}_2 | v | \underline{m}_1 \underline{m}_2)$$

$$+ \sum_{\underline{k}_1 \underline{k}_2 \underline{k}_3 \underline{k}_4} (\underline{m}_1 \underline{m}_2 | v | \underline{k}_1 \underline{k}_2) \frac{1}{\epsilon(m_1) + \epsilon(m_2) - \epsilon(k_1) - \epsilon(k_2)} (\underline{k}_1 \underline{k}_2 | v | \underline{k}_3 \underline{k}_4)$$

$$\left. \frac{1}{\epsilon(m_1) + \epsilon(m_2) - \epsilon(k_3) - \epsilon(k_4)} (\underline{k}_3 \underline{k}_4 | v | \underline{m}_1 \underline{m}_2) + \ldots \right\} \tag{10.1}$$

Let us introduce the K-matrix, defined by the equation

$$(\underline{p}_1' \underline{p}_2' | K(z) | \underline{p}_1 \underline{p}_2) = (\underline{p}_1' \underline{p}_2' | v | \underline{p}_1 \underline{p}_2) +$$

$$+ \sum_{\underline{k}_1 \underline{k}_2} (\underline{p}_1' \underline{p}_2' | v | \underline{k}_1, \underline{k}_2) \frac{1}{z - \epsilon(k_1) - \epsilon(k_2)} (\underline{k}_1 \underline{k}_2 | K(z) | \underline{p}_1 \underline{p}_2)$$

$$\tag{10.2}$$

Diagrammatically, this equation is shown in Fig.11 where the wavy line
represents the effective interaction K. Now, the sum of the infinite series
in the { } brackets, Eq.(10.1), is nothing else but an iterative solution of
Eq.(10.2) for $(\underline{m}_1 \underline{m}_2 | K(\epsilon(m_1) + \epsilon(m_2)) | \underline{m}_1 \underline{m}_2)$. If we proceed similarly
with $(\Delta E)_{EX}$ of Fig.10, we finally get the result

$$(\Delta E)_{\rho \to 0} = \frac{1}{2} \sum_{\underline{m}_1 \underline{m}_2} (\underline{m}_1 \underline{m}_2 | K(\epsilon(m_1) + \epsilon(m_2)) | \underline{m}_2 \underline{m}_1 - \underline{m}_1 \underline{m}_2) \tag{10.3}$$

which diagrammaticaly is shown in the last line of Fig.10.

If the parameter $z = \epsilon(p_1) + \epsilon(p_2)$ we say that $(\underline{p}_1' \underline{p}_2' | K(z) | \underline{p}_1 \underline{p}_2)$ is on
the energy shell. Otherwise we speak of the off energy shell elements of
the K-matrix. We see that the expression (10.3) for $(\Delta E)_{\rho \to 0}$ contains the
one-energy-shell elements of the K-matrix only.

Let us notice that Fig.10 contains all diagrams of the first and second
order in v, and thus, the corrections to ΔE, Eq.(10.3), start from the third-
order terms in v.
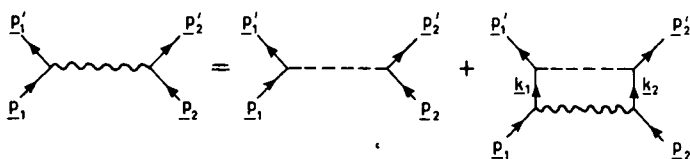
FIG.11.   Diagrams representing Eq.(10.2).

The whole perturbation series in v may be rearranged into a pertur-
bation series in K. We simply replace in all diagrams the broken inter-
action lines by the wavy K-lines, and drop those diagrams in which
consecutive K-lines appear joined by two particles lines, as, e.g. the
diagram (a) shown in Fig.12 (but not the diagram 12(b)). Consequently,
in the perturbation expansion in K there are no second-order contributions.
The z-value in K(z) in the rearranged perturbation series depends on the
place in which the wavy K-line appears in the diagram. This is a delicate
problem which we shall discuss later.

(a)   (b)
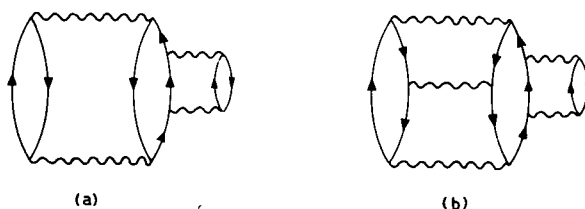
FIG.12.   Diagrams for perturbation series in K.

11. HOLE SELF-ENERGIES

No doubt, in any realistic theory of nuclear matter we have to go
beyond the low-density limit.
The next step in our systematic procedure which starts with the
ladder approximation (chapter 10) is to include all diagrams with three-
hole lines. Among the two-hole-line diagrams considered in chapter 10
there were diagrams of all orders in v. Similarly, among the three-hole
diagrams of our rearranged perturbation series there are diagrams of
all orders in K. We shall divide the three-hole-line diagrams into three
classes. Representatives of all the three classes may be already found
among the third-order diagrams in K. Typical third-order diagrams in
K are shown in Fig.13: the "hole-self-energy" diagram (a), the "hole-
hole-scattering" diagram (b), the particle-hole-scattering" diagram (c)
and the "particle-self-energy" diagram (d). In this chapter we shall dis-
cuss the class of three-hole-line diagrams represented by the "hole-self-
energy" diagram (a). The other two classes represented, respectively,
by the diagram (b) and by the diagrams (c), (d) of Fig.13 will be discussed
later, and we shall show that they are less important than the "hole-self-
energy" class.
Let us discuss now the z-value in the argument of the K-matrix,
represented by the middle wavy line of the diagram (a) of Fig.13. To do
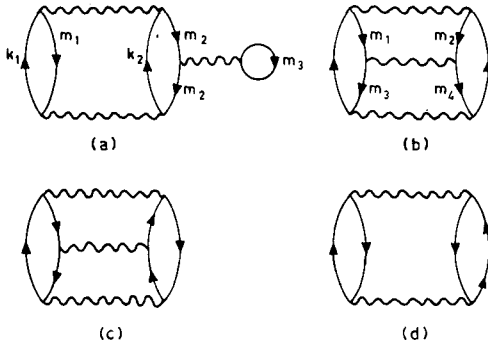
FIG.13.   Typical third-order diagrams in K.
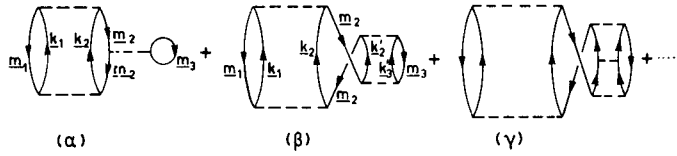
FIG.14.   Some of the v-diagrams the sum of which is represented by the (a) diagram of Fig.13.

it,we draw in Fig.14 some of the v-diagrams the sum of which is repre-sented by the (a) diagram of Fig.13. Their contribution to ΔE is givey by

$$
\sum_{\substack{m_1 m_2 \\ k_1 k_2}} \frac{|(\underline{k}_1 \underline{k}_2 | v | \underline{m}_1 \underline{m}_2)|^2}{[\epsilon(m_1) + \epsilon(m_2) - \epsilon(k_1) - G(k_2)]^2} \sum_{\underline{m}_3} \left\{ (\underline{m}_2 \underline{m}_3 | v | \underline{m}_2 \underline{m}_3) \right.
$$

$$
\left. + \sum_{\underline{k}'_2 \underline{k}'_3} \frac{(\underline{m}_2 \underline{m}_3 | v | \underline{k}'_2 \underline{k}'_3)(\underline{k}'_2 \underline{k}'_3 | v | \underline{m}_2 \underline{m}_3)}{\epsilon(m_1) + \epsilon(m_2) - \epsilon(k_1) - \epsilon(k_2) + \epsilon(m_2) + \epsilon(m_3) - \epsilon(k'_2) - \epsilon(k'_3)} + \dots \right\}
$$

$$
(11.1)
$$

Now, the series in the { } bracket is the iterative solution of Eq.(10.2) for $(\underline{m}_2 \underline{m}_3 | K(z) | \underline{m}_2 \underline{m}_3)$ for $z = \epsilon(m_1) + \epsilon(m_2) - \epsilon(k_1) - \epsilon(k_2) + \epsilon(m_2) + \epsilon(m_3)$. This is an off-energy-shell K-matrix with a negative shift off the energy shell equal to $\epsilon(m_1) + \epsilon(m_2) - \epsilon(k_1) - \epsilon(k_2)$, i.e. to the negative excitation of the rest of the system during the interaction between the m_1 and m_3 nucleons. This would complicate the calculation of "hole-self-energy" diagrams. However, Brueckner and Goldman [12] have noticed that there is another fourth-order diagram of the same type as the diagram (β) of Fig.14.which should be considered together with the(β)diagram. This diagram is shown in Fig.15. Its contribution is the same as that of the(β)diagram except for the energy denominator which is

$$
1/[\epsilon(m_1) + \epsilon(m_2) - \epsilon(k_1) - \epsilon(k_2)] [\epsilon(m_1) + \epsilon(m_2) - \epsilon(k_1) - \epsilon(k_2)
$$

$$
+ \epsilon(m_2) + \epsilon(m_3) - \epsilon(k'_2) - \epsilon(k'_3)] [\epsilon(m_2) + \epsilon(m_3) - \epsilon(k'_2) - \epsilon(k'_3)] \qquad (11.2)
$$

FIG.15.   Another fourth-order diagram of the same type
as the (β) diagram of Fig.14.
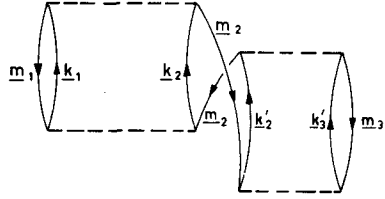
If we add this energy denominator to the energy denominator of the β
diagram (see Eq.(11.1)) we obtain

$$1/[\epsilon(m_1) + \epsilon(m_2) - \epsilon(k_1) - \epsilon(k_2)]^2 [\epsilon(m_2) + \epsilon(m_3) - \epsilon(k_2') - \epsilon(k_3')]$$

(11.3)

Similarly we may add two diagrams to the diagram (γ) of Fig.14 which
differ from the γ diagram only by the relative positions of the interaction
lines. And for the sum of all the three diagrams we get an energy denomi-
nator which is analogous to that of Eq.(11.3). Extending this procedure to
higher-order diagrams we find that for the sum of all these diagrams we
get instead of Eq.(11.1) an equation in which the series in the { } brackets
represents the on-energy-shell matrix $(\underline{m_2 m_3} | K(z = \epsilon(m_2) + \epsilon(m_3)) | \underline{m_2 m_3})$.
This result may be generalized to the following BBP theorem [22]
(see Ref.[23] for a simple proof): The contribution of the hole-self-
energy diagram of the third order in K, calculated with the on-energy-
shell K-matrix is equal to the sum of the contributions of the entire class
of three-hole-line diagrams shown in Fig.16. (The same applies to the
corresponding exchange diagrams.)
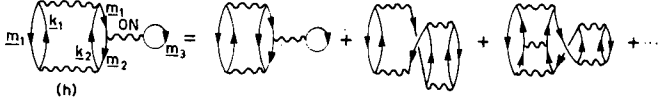
FIG. 16.   Hole-self-energy diagram of the third order in K.

We shall show now that the contribution to ΔE of the diagram (h) of
Fig.16, and of the corresponding exchange diagrams is automatically
included in the following expression for ΔE (compare Eq.(10.3)):

$$\Delta E = \tfrac{1}{2} \sum_{\underline{m_1 m_2}} (\underline{m_1 m_2} | K(e(m_1) + e(m_2)) | \underline{m_1 m_2} - \underline{m_2 m_1})$$

(11.4)

where

$$e(m_i) = \epsilon(m_i) + V(m_i)$$

(11.5)

where the single-hole potential V is given by

$$V(m_i) = \sum_{\underline{m_i'}} (\underline{m_i m_i'} | K(e(m_i) + e(m_i')) | \underline{m_i m_i'} - \underline{m_i' m_i})$$

(11.6)

To prove this relation, let us write the identity

$$(\underline{p}'_1 \underline{p}'_2 | K(z) | \underline{p}_1 \underline{p}_2) = (\underline{p}'_1 \underline{p}'_2) K(z_0) | \underline{p}_1 \underline{p}_2) +$$

$$+ \sum_{\underline{k}_1 \underline{k}_2} (\underline{p}'_1 \underline{p}'_2 | K(z_0) | \underline{k}_1 \underline{k}_2) \left\{ \frac{1}{z - \epsilon(k_1) - \epsilon(k_2)} \right. \tag{11.7}$$

$$\left. \frac{1}{z_0 - \epsilon(k_1) - \epsilon(k_2)} \right\} (\underline{k}_1 \underline{k}_2 | K(z) | \underline{p}_1 \underline{p}_2)$$

which follows directly from the K-matrix equation (10.2), and which may be looked upon as an integral equation for $K(z)$. First two terms of the iterative solution of this equation are

$$(\underline{p}'_1 \underline{p}'_2 | K(z) | \underline{p}_1 \underline{p}_2) = (\underline{p}'_1 \underline{p}'_2 | K(z_0) | \underline{p}_1 \underline{p}_2) + \sum_{\underline{k}_1 \underline{k}_2} (\underline{p}'_1 \underline{p}'_2 | K(z_0) | \underline{k}_1 \underline{k}_2)$$

$$\times \left\{ -\frac{z - z_0}{[z_0 - \epsilon(k_1) - \epsilon(k_2)]^2} + \ldots \right\} (\underline{k}_1 \underline{k}_2 | K(z_0) | \underline{p}_1 \underline{p}_2) + \ldots \tag{11.8}$$

where we have expanded the propagator difference in the { } brackets in powers of $z - z_0$.

Let us apply Eq.(11.8) for $z = e(m_1) + e(m_2)$ and $z_0 = \epsilon(m_1) + \epsilon(m_2)$ i.e. for

$$z - z_0 = V(m_1) + V(m_2) = \sum_{i=1}^{2} \sum_{\underline{m}_3} (\underline{m}_i \underline{m}_3 | K(e(m_i) + e(m_3)) | \underline{m}_i \underline{m}_3 - \underline{m}_3 \underline{m}_i) \tag{11.9}$$

If we introduce the expansion (11.8) into Eq. (11.4) we obtain, with an accuracy to terms of third order in K,

$$\Delta E = \frac{1}{2} \sum_{\underline{m}_1 \underline{m}_2} (\underline{m}_1 \underline{m}_2 | K(\epsilon_{m_1} + \epsilon_{m_2}) | \underline{m}_1 \underline{m}_2 - \underline{m}_2 \underline{m}_1)$$

$$-\frac{1}{2} \sum_{i=1}^{2} \sum_{\underline{m}_1 \underline{m}_2 \underline{m}_3 \underline{k}_1 \underline{k}_2} \left| (\underline{k}_1 \underline{k}_2 | K(\epsilon_{m_1} + \epsilon_{m_2}) | \underline{m}_1 \underline{m}_2 - \underline{m}_2 \underline{m}_1) \right|^2 \tag{11.10}$$

$$\times \frac{(\underline{m}_i \underline{m}_3 | K(\epsilon_{m_i} + \epsilon_{m_3}) | \underline{m}_i \underline{m}_3 - \underline{m}_3 \underline{m}_i)}{[\epsilon(m_1) + \epsilon(m_2) - \epsilon(k_1) - \epsilon(k_2)]^2}$$

The first term represents the contribution of the two diagrams in the last line of Fig.10, and the second term the contribution of the diagram (h) of Fig.16 and of the corresponding exchange diagrams for $i = 2$ and of the corresponding diagrams with bubble insertion in the m_1 line for $i = 1$.

It is obvious from our derivation of Eq.(11.10) that ΔE given by Eq.(11.4) contains more than the contribution of all two-hole-lines diagrams

and of the class of three-hole lines diagrams shown in Fig.16. A detailed discussion of this point is given in Refs [5] and [24-27].

From now on we shall denote by wavy lines the K(z) interaction with z expressed with the help of the hole energies e in place of the previous kinetic energies ϵ. To simplify our notation we shall simply write

$$(\underline{p}_1 \underline{p}_2 | K(e(m_1) + e(m_2)) | \underline{m}_1 \underline{m}_2) = (\underline{p}_1 \underline{p}_2 | K | \underline{m}_1 \underline{m}_2) \qquad (11.11)$$

in all cases where it is obvious that we use the on-energy-shell K-matrix.

Equations (11.4-6) together with the K-matrix equation (11.2) form the basic equations for our theory. They pose a self-consistency problem, because the equation for K contains the single-hole potentials $V(m_i)$ which in turn are expressed through the K matrix elements. Let us notice that Eqs (11.4-6) involve the on-energy-shell elements of the K-matrix only.

We may write Eq.(11.4) in the form familiar in Hartree-Fock theory

$$\Delta E = \tfrac{1}{2} \sum_{\underline{m}_i} V(m_1) \qquad (11.12)$$

where the famous factor $1/2$ prevents the two-body interaction from being counted twice.

12. SOLUTION OF THE K-MATRIX EQUATION

To simplify the presentation, we shall ignore from now on the spin and the isotopic spin of nucleons.

If we introduce the relative and the centre-of-mass momenta

$$\vec{p} = (\vec{p}_1 - \vec{p}_2)/2 \qquad \vec{p}_1 = \tfrac{1}{2}\vec{P} + \vec{p}$$

$$\vec{P} = \vec{p}_1 + \vec{p}_2 \qquad \vec{p}_2 = \tfrac{1}{2}\vec{P} - \vec{p} \qquad (12.1)$$

we have, because of momentum conservation

$$(\vec{p}_1' \, \vec{p}_2' | v | \vec{p}_1 \vec{p}_2) = \delta_{\vec{P}'\vec{P}} \, (\vec{p}' | v | \vec{p}) \qquad (12.2)$$

where

$$(\vec{p}' | v | \vec{p}) = \int d\vec{r} \, \varphi_{\vec{p}'}^*(\vec{r}) \, v \, \varphi_{\vec{p}}(\vec{r}) \qquad (12.3)$$

where $\vec{r} = \vec{r}_1 - \vec{r}_2$ is the relative co-ordinate of nucleons 1 and 2.

Similarly, we have

$$(\vec{p}_1' \, \vec{p}_2' | K(z) | \vec{p}_1 \vec{p}_2) = \delta_{\vec{P}'\vec{P}} \, (\vec{p}' | K(z)_{\vec{P}} | \vec{p}) \qquad (12.4a)$$

as one can verify easily by inspecting the iterative solution of the K-matrix equation.

In the relative and c.m. momenta, Eq.(10.2) for $(\vec{p}_1 \vec{p}_2 | K | \vec{m}_1 \vec{m}_2)$ (these are the only matrix elements which we need in the approximate theory derived in chapter 11) takes the form

$$(\vec{p} | K_{\vec{M}} | \vec{m}) = (\vec{p} | v | \vec{m}) + \sum_{\vec{k}} (\vec{p} | v | \vec{k}) \frac{Q(\vec{M}, \vec{k})}{z - \frac{1}{2}\epsilon(M) - 2\epsilon(k)} (\vec{k} | K_{\vec{M}} | \vec{m})$$

(12.4b)

where obviously $z = e(m_1) + e(m_2)$. In Eq.(12.4) we have indicated explicitly the range of summation over $\vec{k}$ by introducing $Q(\vec{M}, \vec{k})$ defined by

$$Q(\vec{M}, \vec{k}) = \begin{cases} 1 \text{ for } |\frac{1}{2}\vec{M} + \vec{k}| > k_F \text{ and } |\frac{1}{2}\vec{M} - \vec{k}| > k_F \\ \\ 0 \text{ otherwise} \end{cases}$$

(12.5)

The Pauli-principle operator Q takes care of the two nucleons with total momentum $\vec{M}$ in the intermediate state (with relative momentum $\vec{k}$) being outside the Fermi sea in which all states are occupied by other nucleons.

At this point it is useful to introduce the following notations:

$$(\vec{r} | \vec{p}) = \frac{1}{\sqrt{\Omega}} e^{i\vec{p}\cdot\vec{r}} = \varphi_{\vec{p}}(\vec{r})$$

(12.6)

$$\langle \vec{r} | \vec{R} \rangle = \left(\frac{1}{2\pi}\right)^{3/2} e^{i\vec{p}\cdot\vec{r}}$$

(12.7)

$$\langle \vec{p}' | v | \vec{p} \rangle = \frac{\Omega}{(2\pi)^3} (\vec{p}' | v | \vec{p})$$

(12.8)

$$\langle \vec{p}' | K_{\vec{p}'} | \vec{p} \rangle = \frac{\Omega}{(2\pi)^3} (\vec{p}' | K_{\vec{p}} | \vec{p})$$

(12.9)

Whereas the $(\vec{r} | \vec{p})$ functions are the plane waves normalized in the box of volume Ω, the $\langle \vec{r} | \vec{p} \rangle$ functions are plane waves normalized in the whole space $(\Omega \rightarrow \infty)$ according to

$$\int d\vec{r} \langle \vec{p}' | \vec{r} \rangle \langle \vec{r} | \vec{p} \rangle = \delta(\vec{p} - \vec{p}')$$

(12.10)

If we replace the sum over $\vec{k}$ in Eq.(12.4) by an integral, Eq.(3.4), we get

$$\langle \vec{p} | K_{\vec{M}} | \vec{m} \rangle = \langle \vec{p} | v | \vec{m} \rangle + \int d\vec{k} \langle \vec{p} | v | \vec{k} \rangle$$

(12.11)

$$\times \frac{Q(\vec{M}, \vec{k})}{z - \frac{1}{2}\epsilon(M) - 2\epsilon(k)} \langle \vec{k} | K_{\vec{M}} | \vec{m} \rangle$$

The standard way of solving Eq.(12.11) (a necessary one if v has a hare core) is to go over to configuration space. We introduce the two-body wave function $\Psi_{\vec{m}}^{\vec{M}}$ by the equation

$$\langle \vec{p} | K_{\vec{M}} | \vec{m} \rangle = \langle \vec{p} | v | \Psi_{\vec{m}}^{\vec{M}} \rangle \tag{12.12}$$

The wave function $\Psi_{\vec{m}}^{\vec{M}}$ describes the relative motion of two nucleons in nuclear matter, and depends on the relative as well as on the total momentum of the two nucleons. Eq.(12.11) may be written as the following equation for Ψ:

$$\langle \vec{p} | \Psi_{\vec{m}}^{\vec{M}} \rangle = \delta(\vec{p} - \vec{m}) + \frac{Q(\vec{M}, \vec{p})}{z - \frac{1}{2}\epsilon(M) - 2\epsilon(p)} \langle \vec{p} | v | \Psi_{\vec{m}}^{\vec{M}} \rangle \tag{12.13}$$

which multiplied by $\langle \vec{r} | \vec{p} \rangle$ and integrated over $\vec{p}$ gives the following equation for $\langle \vec{r} | \Psi_{\vec{m}}^{\vec{M}} \rangle = \Psi_{\vec{m}}^{\vec{M}}(\vec{r})$:

$$\Psi_{\vec{m}}^{\vec{M}}(\vec{r}) = \langle \vec{r} | \vec{m} \rangle + \int d\vec{p} \langle \vec{p} | \vec{r} \rangle \frac{Q(\vec{M}, \vec{p})}{z - \frac{1}{2}\epsilon(M) - 2\epsilon(p)}$$

$$\times \int d\vec{r}' \langle \vec{p} | \vec{r}' \rangle \langle \vec{r}' | v | \Psi_{\vec{m}}^{\vec{M}} \rangle \tag{12.14}$$

which may be written in the form

$$\Psi_{\vec{m}}^{\vec{M}}(\vec{r}) = \left(\frac{1}{2\pi}\right)^{3/2} e^{i\vec{m}\vec{r}} + \int d\vec{r}' \, G_{\vec{m}}^{\vec{M}}(\vec{r}, \vec{r}') v(\vec{r}') \Psi_{\vec{m}}^{\vec{M}}(\vec{r}') \tag{12.15}$$

where the Green function

$$G_{\vec{m}}^{\vec{M}}(\vec{r}, \vec{r}') = \left(\frac{1}{2\pi}\right)^{3} \int d\vec{p} \, e^{i\vec{p}\cdot(\vec{r} - \vec{r}')} \frac{Q(\vec{M}, \vec{p})}{z - \frac{1}{2}\epsilon(M) - 2\epsilon(p)} \tag{12.16}$$

The function $\Psi_{\vec{m}}^{\vec{M}}(\vec{r})$ has an important "healing property", i.e. it becomes asymptotically identical with $\langle \vec{r} | \vec{m} \rangle$. The interaction v changes the unperturbed wave function $\langle \vec{r} | \vec{m} \rangle$ at small values of r. This change (or "wound"), however, is quickly "healed" and Ψ_{m}^{M} approaches $\langle \vec{r} | \vec{m} \rangle$ within a "healing distance" [28].

We shall show this "healing property" first in the case of the low-density limit, i.e. for $z = \epsilon(m_1) + \epsilon(m_2)$. In this case Eq.(12.13) shows that except for the unperturbed relative momentum $\vec{m}$ the function $\Psi_{\vec{m}}^{\vec{M}}$ has only those Fourier components which correspond to the momenta of the two interacting nucleons outside the Fermi sea (because of the Q operator). In the unperturbed state the two nucleons are inside the Fermi sea, and their total energy is less than the total energy of the two nucleons outside

the Fermi sea. We then see that $\Psi_{\vec{m}}^{\vec{M}}$ has no Fourier components which would correspond to a state with a relative momentum different from the initial momentum $\vec{m}$ and with an energy equal to the initial energy. This obviously prevents any real scattering, i.e. $\Psi_{\vec{m}}^{\vec{M}}(\vec{r}) - \langle \vec{r} | \vec{m} \rangle$ decreases faster than $1/r$ with increasing r. Responsible for this "healing" is the exclusion principle operator Q.

In the case of the self-consistent theory we may ignore the Q operator, and still we have the healing. To see it let us notice that if we put

$$Q(\vec{M}, \vec{p}) = 1 \tag{12.17}$$

we may easily calculate G

$$G_{\vec{m}}^{\vec{M}}(\vec{r}, \vec{r}')_{nx} = - \mathcal{M} \frac{e^{-\gamma|\vec{r} - \vec{r}'|}}{4\pi |\vec{r} - \vec{r}'|} \tag{12.18}$$

where

$$\gamma = \sqrt{\frac{1}{4} M^2 - \mathcal{M} z} \tag{12.19}$$

Since $z = e(m_1) + e(m_2)$ is negative (as we shall see later) we have in Eq.(12.19), the square root of a positive number. The "nx" subscript at G stands for "no exclusion principle" ($Q = 1$). If we insert the G_{nx} into Eq.(12.15), we notice that for $r \to \infty$

$$\Psi_{\vec{m}}^{\vec{M}}(\vec{r}) - \langle \vec{r} | \vec{m} \rangle \sim e^{-\gamma r}/r \tag{12.20}$$

The negative sign of z is here responsible for this healing, i.e. the inclusion of the single-hole potentials into the single-hole energies.

Equation (12.15) for $\Psi_{\vec{m}}^{\vec{M}}$ may be solved directly with the present-day computers and this has been the standard procedure of Brueckner and his group [20]. One starts with an approximation for the Q operator. This operator introduces into the integrand in Eq.(12.16) a dependence on the angle between $\vec{p}$ and $\vec{M}$, and consequently the resulting Green function $G_{\vec{m}}^{\vec{M}}(\vec{r}, \vec{r}')$ is not merely a function of $|\vec{r} - \vec{r}'|$, i.e. $G_m^M(\vec{r}, \vec{r}')$ is not rotationally invariant ($\vec{M}$ introduces a distinguished direction). A partial-wave expansion of Ψ would lead to a system of coupled equations for different values of the orbital angular momentum ℓ [30]. To avoid this difficulty and to restore the rotational invariance we approximate $Q(\vec{M}, \vec{p})$ by its angle average

$$Q(\vec{M}, \vec{p}) \cong \bar{Q}(M, p) = \frac{1}{4\pi} \int d\hat{M} Q(\vec{M}, \vec{p}) \tag{12.21}$$

which may be computed easily with the result

$$\bar{Q}(M, p) = \begin{cases} 0 \text{ for } p < (k_F^2 - \frac{1}{4} M^2)^{1/2} \\ 1 \text{ for } p > \frac{1}{2} M + k_F \\ \left(\frac{1}{4} M^2 + p^2 - k_F^2\right)/pM \text{ otherwise} \end{cases} \tag{12.22}$$

It is shown in Ref.[31] that the approximation (12.21) is fairly accurate.

With the approximation (12.21) we may expand $G_{\vec{m}}^{\vec{M}}(\vec{r}, \vec{r}')$ Eq.(12.6), into spherical harmonics

$$G_{\vec{m}}^{\vec{M}}(\vec{r}, \vec{r}') = \sum_{\ell=0}^{\infty} (2\ell+1)G_\ell(r, r')Y_{\ell 0}(\hat{r}, \hat{r})\left(\frac{4\pi}{2\ell+1}\right)^{1/2} \tag{12.23}$$

where

$$G_\ell(r, r') = \left(\frac{1}{2\pi}\right)^3 4\pi \int dp p^2 \bar{Q}(M, p) \; \frac{j_\ell(pr)\, j_\ell(pr')}{z - \frac{\epsilon(M)}{2} - 2\epsilon(p)} \tag{12.24}$$

Similarly we expand Ψ and $\langle \vec{r}|\vec{m}\rangle$ into partial waves

$$\Psi_{\vec{m}}^{\vec{M}}(\vec{r}) = \left(\frac{1}{2\pi}\right)^{3/2}\sum_\ell \sqrt{(2\ell+1)4\pi}\; u_\ell(r)Y_{\ell 0}(\hat{m}\,\hat{r}) \tag{12.25}$$

$$\langle \vec{r}|\vec{m}\rangle = \left(\frac{1}{2\pi}\right)^{3/2}\sum_\ell \sqrt{4\pi(2\ell+1)}\; j_\ell(r m)Y_{\ell 0}(\hat{m}\,\hat{r}) \tag{12.26}$$

When all these expansions are introduced into Eq.(12.14) we get the following equations for the radial functions u_1:

$$u_\ell(r) = j_\ell(mr) + 4\pi\int dr' r'^2\, G_\ell(r, r')v(r')u_\ell(r') \tag{12.27}$$

We may now write $\langle \vec{p}|K_{\vec{M}}|\vec{m}\rangle$, Eq.(12.12), in terms of the functions u_ℓ for $\vec{p} = \vec{m}$, which is the only value of $\vec{p}$ which we need. We simply use the expansions (12.25) and (12.26) and get

$$\langle \vec{m}|K_{\vec{M}}|\vec{m}\rangle = \left(\frac{1}{2\pi}\right)^3\sum_\ell (2\ell+1)4\pi\int dr r^2 j_\ell(mr)v(r)u_\ell(r) \tag{12.28}$$

The whole problem of computing the K-matrix is thus reduced to the problem of solving Eqs.(12.27) for u_ℓ and of computing the integrals in Eq.(12.18). In fact, the problem is more complicated because the G_ℓ's in Eqs (12.27) depend on the value $z = e(m_1) + e(m_2)$, and the single-hole energies $e(m_i)$ may be determined only if we know the K-matrix, Eqs (12.5-6).

In practice one starts with any reasonable ansatz for $e(m_i) = e_0(m_i)$, computes the Green functions G_ℓ, Eq.(12.24), solves Eq.(12.27) for u_ℓ, computes the K-matrix, Eq.(12.18), and finally computes $e(m_i)$, Eqs (11.5-6), which we shall denote by $e_1(m_i)$. This we call the major iteration. We repeat now the major iteration with $e_1(m_i)$ as starting single-hole energies

and at the end of the second major iteration, obtain $e_2(m_i)$. We repeat the procedure till we get $e_n(m_i) = e_{n-1}(m_i)$ i.e. till self-consistency is achieved. At this moment we may compute the energy

$$E = E_0 + \Delta E = E_0 + \tfrac{1}{2} \sum_{\overrightarrow{m_i}} [e_n(m_i) - \epsilon(m_i)] \tag{12.29}$$

By repeating the hole calculation for different values of the density ρ we find the equilibrium density and binding energy (see Fig.1).

In actual calculations spin and isotopic spin of nucleons must be considered. The only complication appears then in the case of the states which are coupled in the presence of tensor forces. For example, the u functions in the $^3S_1$ and $^3D_1$ states satisfy coupled equations instead of two independent equations (12.27).

13. THE BRUECKNER-GAMMEL CALCULATION

The method described in chapter 12 has been applied first by Brueckner and Gammel [29] in 1958. Actually they have added single-particle potentials to the kinetic energies $\epsilon(k_i)$ in the intermediate states. However, we shall not discuss this delicate point here.

By applying the Brueckner-Gammel-Thaler potential (BGT) v, they obtained:

$$r_0 = 1.02 \text{ fm}, \quad \epsilon_{vol} = 15.2 \text{ MeV} \tag{13.1}$$

To see the importance of the hole-self-energy insertions the calculation was also done without these insertions ($z = \epsilon(m_1) + \epsilon(m_2)$ in the Green function) with the result: $r_0 = 0.98$ fm, $\epsilon_{vol} = 34.4$ MeV, which clearly indicates the importance of these insertions.

The healing property is best revealed by the behaviour of the ^1S state function, u_0, compared to $j_0(mr)$ for $m = 0.128$ fm (corresponding to two nucleons moving near the bottom of the Fermi sea), shown in Fig.17. We see that at a mean inter-particle distance $\sim 2 r_0$ the function u_0 which describes the relative motion of two nucleons in nuclear matter, is essentially identical with the function j_0 of two non-interacting nucleons.
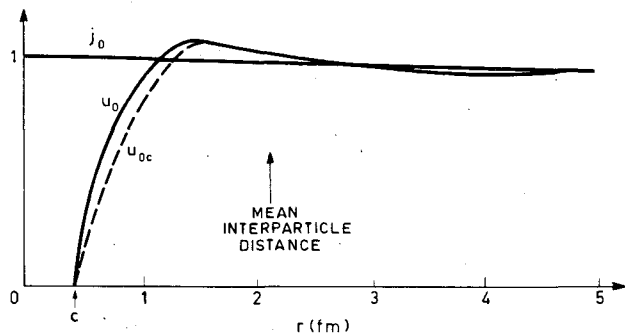
FIG.17. u_0 and u_{0C} versus r.

This explains the success of the shell-model approximation in which nucleons move independently. At the same time, there are strong nucleon-nucleon correlations within a distance of the order of the hard-core radius, c, in the nucleon-nucleon interaction. These correlations are necessary for the description of the high-energy reactions mentioned in chapter 1.
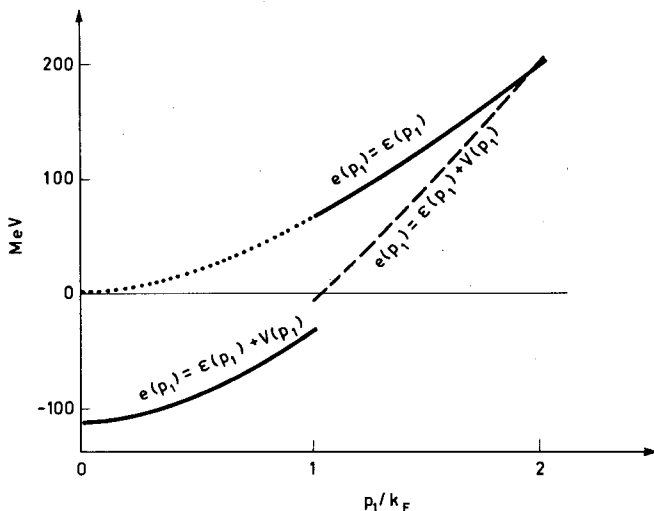
FIG.18.   Single-nucleon energy spectrum.

The curve u_{0c} in Fig.17 represents the u_0 function for a pure hard-core nucleon-nucleon interaction. We notice that the difference between u_0 and u_{0c} is very small: $\leq$ 15-20%. We may say then that the attractive part of v is weak in the sense that it does not change appreciably the two-nucleon wave function in nuclear matter (at equilibrium density).

Very important for our further considerations is the single-nucleon energy spectrum, shown in Fig.18. The value of the single-hole potential $V(m_1)$ at the bottom and at the top of the Fermi sea is, respectively: $V(0) \simeq -112$ MeV and $V(k_F) \simeq -70$ MeV.

If one approximates $V(m_1)$ by a quadratic function $-A + B m_1^2$, one may add $B m_1^2$ to $\epsilon(m_1)$. In this way one gets the following approximate expression:

$$e(p_1) \cong \begin{cases} \dfrac{p^2}{2\mathcal{M}^*} - A & \text{for } p \leq k_F \\[4mm] \dfrac{p^2}{2\mathcal{M}} & \text{for } p > k_F \end{cases} \qquad (13.2)$$

where the effective mass $\mathcal{M}^*$ is

$$\mathcal{M}^* \cong 0.7\,\mathcal{M} \qquad (13.3)$$

and

$$A \cong -112 \text{ MeV} \qquad (13.4)$$

As has been mentioned, Brueckner and Gammel included a single-particle potential into their definition of $e(k_1)$. Their $e(k_1)$ spectrum is represented by the broken curve in Fig.18. Notice that it practically coincides with the solid $\epsilon(k_1)$ curve for $k_1 \gtrsim 2k_F \cong 3 \text{ fm}^{-1}$. This is important since we shall show in the next chapter that most important in the calculation of the K-matrix is the range $3 \text{ fm}^{-1} \lesssim k_1 \lesssim 5 \text{ fm}^{-1}$ in the single-particle energy spectrum $e(k_1)$.

14. THE Q = 1 APPROXIMATION

The direct method of solving the K-matrix equation poses numerical problems which may only be mastered with large computers. To avoid these large computations, approximate methods of solving the K-matrix equation have been invented. They allow us to obtain approximate results in a simple way, and are extremely helpful in acquiring better insight into the theory.

The approximate method which we are going to discuss now amounts to the approximation

$$Q \cong 1 \tag{14.1}$$

in the K-matrix equation (10.2), i.e. to neglecting the Pauli principle in the intermediate states. Thus we allow nucleons to be excited also to the originally forbidden intermediate states whose energy spectrum is shown by the dotted line in Fig.18.

Let us explain why Eq.(14.1) is expected to be a reasonable approximation.

First of all the healing property is preserved in this approximation as has been explained in chapter 12. The second point is that the energy denominator in the K-matrix equation, which corresponds to the transitions to those originally forbidden states, is large because of the energy gap in the single-nucleon energies (the difference between the dotted and the solid curve for $p_1/k_F \lesssim 1$ in Fig.18). The third point is that — as we shall see — the range of important momenta in the intermediate states extends till $k_1 \sim 5 \text{ fm}^{-1}$ for which the volume in momentum space is much bigger than the volume $(4/3)\pi k_F^3$ corresponding to the forbidden states.

To get an idea about the error introduced by the approximation (14.1) let us quote the results obtained by Brueckner and Masterson [32] for the Brueckner-Gammel-Thaler two-body force. They find that the approximation (14.1) increases ϵ_{vol} by about 2 MeV and decreases r_0 by about 0.1 fm. (This is a rough estimate as it includes also the effect of the single-particle potential for the states above the Fermi sea. The last effect is probably responsible for the appreciable shift in r_0).

The approximation (14.1) has been used extensively by Bethe and his group [22] who call it the reference-spectrum method. By reference spectrum they mean the energy spectrum $e(p_1) = \epsilon(p_1)$ for $0 < p_1 < \infty$, i.e. the partly dotted and partly solid curve in Fig.18. The content of this chapter is mainly based on Ref.[22].

With the approximation $Q \cong 1$ we are able to calculate the Green function $G \cong G_{nx}$, Eq.(12.8), analytically. Let us note that $G_{\vec{m}}^{\vec{M}}(\vec{r}, \vec{r}')_{nx}$ does not depend explicitly on the total momentum $\vec{M}$, and we shall write simply $(G_{\vec{m}}(\vec{r}, \vec{r}')_{nx}$. However, there still remains in G_{nx} the dependence

on $z - (1/2) \epsilon(M)$ for $z = e(m_1) + e(m_2)$. We have $z - (1/2)\epsilon(M) = 2\epsilon(m)+V(m_1)+V(m_2)$ and this quantity depends on $\vec{M}$.

Since the G_{nx} satisfy the equation

$$(\Delta_{\vec{r}} - \gamma^2)G_{\vec{m}}(\vec{r}, \vec{r}')_{nx} = \mathcal{M} \delta(\vec{r} - \vec{r}') \tag{14.2}$$

we get — by acting on both sides of Eq.(12.16) with the operator $(\Delta_{\vec{r}} - \gamma^2)$ — the following differential equation for $\Psi_{\vec{m}}(\vec{r}) = \Psi_{\vec{m}}^{\vec{M}}(\vec{r})_{nx}$:

$$(\Delta_{\vec{r}} - \gamma^2)\zeta_{\vec{m}}(\vec{r}) = -\mathcal{M} v(r)\Psi_{\vec{m}}(\vec{r}) \tag{14.3}$$

where the difference function ζ is defined by:

$$\zeta_{\vec{m}}(\vec{r}) = \left(\frac{1}{2\pi}\right)^{3/2} e^{i\vec{m}\cdot\vec{r}} - \Psi_{\vec{m}}(\vec{r}) \tag{14.4}$$

The partial-wave expansions, Eqs (12.25-26), lead to the following system of differential equations:

$$\frac{1}{r}\left[\frac{d^2}{dr^2} - \frac{\ell(\ell+1)}{r^2} - \gamma^2\right]r\zeta_\ell(r) = -\mathcal{M} v(r)u_\ell(r) \tag{14.5}$$

where

$$\zeta_\ell(r) = j_\ell(m r) - u_\ell(r) \tag{14.6}$$

By solving Eqs (14.5), which are as easy to solve as ordinary Schrödinger equations for partial waves, we obtain $u_\ell(r)$ which we insert into Eq.(12.28) and get the approximate value of the K-matrix, $\langle \vec{m}|K|\vec{m}\rangle_{nx}$. To calculate the K-matrix, $\langle \vec{m}|K_{\vec{M}}|\vec{m}\rangle$, which satisfies the original "exact" Eq.(12.11), we apply the equation (compare Eq.(11.7)):

$$\langle \vec{m}|K_{\vec{M}}|\vec{m}\rangle = \langle \vec{m}|K|\vec{m}\rangle_{nx} + \int d\vec{p} \langle \vec{m}|K|\vec{p}\rangle_{nx}$$

$$\times \frac{Q(\vec{M}, \vec{p})-1}{z - \frac{1}{2}\epsilon(M) - 2\epsilon(p)} \langle \vec{p}|K_{\vec{M}}|\vec{m}\rangle \tag{14.7}$$

which may be solved by iteration.

Most powerful in discussing the qualitative features of the theory is the $Q = 1$ approximation. Let us discuss the most important S-wave. As we have noticed in chapter 13 the two-body wave function u_0 is well approximated by the two-body wave function u_{0c} for a pure hard-core potential v. This has been confirmed within the $Q = 1$ approximation in Ref.[22]. Now, for a pure hard-core interaction with the hard-core radius c we have from Eq.(14.5) for the S-wave

$$\left(\frac{d^2}{dr^2} - \gamma^2\right)r \zeta_{0c}(r) = 0 \quad \text{for } r > c \tag{14.8}$$

and

$$\zeta_{0c}(r) = j_0(mr) \qquad \text{for } r \leq c \qquad (14.9)$$

since $u_{0c}(r) \equiv 0$ for $r < c$. Equation (14.8) with the boundary conditions

$$\zeta_{0c}(r) \begin{cases} = j_0(mr) & \text{for } r = c \\ \to 0 & \text{for } r \to \infty \end{cases} \qquad (14.10)$$

has the solution

$$\zeta_{0c}(r) = cj_0(mc)e^{-\gamma(r-c)}/r \text{ for } r > c \qquad (14.11)$$

To get an average value of γ we put in Eq.(12.9)

$$z = \bar{z} = 2 \langle e \rangle_{av} \qquad (14.12)$$

$$\frac{1}{4}M^2 \cong \frac{1}{4} \langle M^2 \rangle_{av} = 0.3 \ k_F^2 \qquad (14.13)$$

To calculate $\langle e \rangle_{av}$, we notice, [33], that at the equilibrium density we should have (compare with Eq.(12.29)

$$-\epsilon_{vol} = \langle \tau \rangle_{av} + \tfrac{1}{2}(\langle e \rangle_{av} - \langle \tau \rangle_{av}) \qquad (14.14)$$

where $\langle J \rangle_{av} = E_0/A$ is the average kinetic energy. Thus, we have

$$\langle e \rangle_{av} = -(\langle \tau \rangle_{av} + 2\epsilon_{vol}) \qquad (14.15)$$

By inserting into Eqs (14.13) and (14.15) the empirical values of ϵ_{vol} and k_F (chapters 2,3) we obtain

$$\langle e \rangle_{av} = -53 \text{ MeV} \qquad (14.16)$$

and

$$\gamma \simeq \sqrt{\frac{1}{4} \langle M^2 \rangle_{av} - \mathcal{M}\bar{z}} \cong 1.7 \text{ fm}^{-1}, \ \gamma^{-1} \cong 0.6 \text{ fm}$$

The typical behaviour of ζ_{0c} is shown in Fig.19. The value of $\gamma^{-1} = 0.6$ fm is a measure of the healing distance which obviously is smaller than the average nucleon-nucleon spacing $\simeq 2r_0 \simeq 2$ fm.

We have mentioned before that most important in the calculation of the K-matrix are those intermediate states whose momenta k_i are with-

FIG.19.   Typical behaviour of ζ_{0c}.
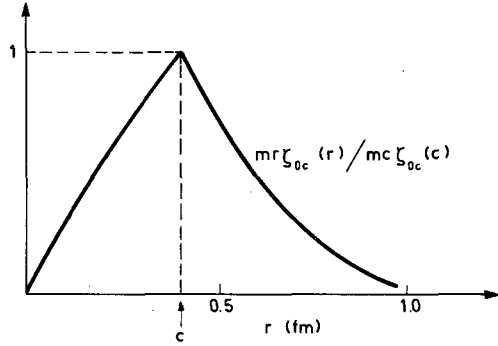
in the range 3 fm^{-1} $\lesssim k_i \lesssim$ 5 fm^{-1}. This may be made plausible in the following way.   First let us notice that, according to Eq.(12.11), most important are those relative momenta k in the intermediate states for which $\{Q/[\ z -(1/2)\epsilon(M) - 2\epsilon(k)]\} \langle \vec{k}|\vec{K}_{\vec{M}}|\vec{m} \rangle$ is large.   From Eq.(12.13) we have

$$\frac{Q(\vec{M}, \vec{p})}{z - \frac{1}{2}\epsilon(M) - 2\epsilon(p)} \langle \vec{p}|\vec{K}_M|\vec{m} \rangle = \langle \vec{p}|\Psi_{\vec{m}}^{\vec{M}} \rangle - \langle \vec{p}|\vec{m} \rangle$$

$$\cong \langle \vec{p}|\Psi_{\vec{m}}^{\vec{M}} \rangle_{nx} - \langle \vec{p}|\vec{m} \rangle = - \langle \vec{p}|\zeta_{\vec{m}} \rangle \tag{14.17}$$

where

$$\langle \vec{p}|\zeta_{\vec{m}} \rangle = \left(\frac{1}{2\pi}\right)^{3/2} \int d\vec{r}\, e^{-i\vec{p}\vec{r}}\, \zeta_{\vec{m}}(\vec{r}) \tag{14.18}$$

If we only keep the most important S-wave part of $\zeta_{\vec{m}}(\vec{r})$ we obtain

$$\langle \vec{p}|\zeta_{\vec{m}} \rangle \cong \frac{1}{2\pi^2}\frac{1}{p} \int dr(\sin pr)\, r\zeta_0(r) \tag{14.19}$$

Now, the fact that $\zeta_0 = \zeta_{0c}$ and Fig.19 indicate that the integral in Eq.(14.19) will be largest for sin pr having a maximum at r = c, i.e.   for

$$p = \frac{\pi}{2}/c \approx 4 \text{ fm}^{-1} \tag{14.20}$$

Since $\vec{p}_{1(2)} = (1/2)\vec{M} \pm \vec{p}$ and the average value of M/2 is about 0.7 fm^{-1}, Eq.(14.13), we may neglect the total momentum compared to $p = |\vec{p}_1 - \vec{p}_2|/2 \approx 4$ fm^{-1} and obtain for the single-particle momenta

$$p_1 \approx p_2 \approx 4 \text{ fm}^{-1} \tag{14.21}$$

We may state this result in the following way (see Eq.(14.17)): $K_{\vec{M}}$ acting on the nucleons in the Fermi sea excites them mostly to states around 4 fm^{-1}.

So far, we have not considered higher partial waves $(1 > 0)$ which, however, have very small difference functions ζ_ℓ, because for the relative momenta of two nucleons in the Fermi sea the centrifugal barrier is sufficiently strong to prevent the unperturbed function j_ℓ from differing appreciably from zero in the core region.

Obviously, for a pure hard-core potential we have the exact expression:

$$\zeta_{\vec{m}}(r) = \left(\frac{1}{2\pi}\right)^{3/2} e^{i\vec{m}\cdot\vec{r}} \quad \text{for } r \lesseqgtr c \tag{14.22}$$

in which, however, the S-wave part dominates.

15. CONVERGENCE OF THE THEORY

In chapter 10 we have outlined the general procedure of the theory. It consists in considering at each stage of the calculation all K-diagrams with a fixed number of hole lines. Within the $Q = 1$ approximation we are in a position to estimate quantitatively the convergence of this procedure. We shall add an extra K-interaction line to a given diagram and obtain a new diagram. We shall show that:

(i) if the new diagram differs from the original one by a larger number of particle lines and otherwise has the same number of hole lines then its contribution is essentially equal to that of the original diagram;

(ii) if the new diagram has one independent hole line more than the original diagram then its contribution is essentially smaller than the contribution of the original diagram (by a factor determining the convergence of our general procedure).

We shall follow here the arguments given by Day [8] and Rajaraman and Bethe [9]. We start with an arbitrary diagram which at some level has two particle lines $\vec{k}_1$, $\vec{k}_2$ as shown in Fig.20(0).

The blobs in the picture represent the upper and lower parts of the diagram.

(i) Adding particle lines. As an example let us consider a new diagram, Fig.20(i), obtained from the original (0) diagram by adding one K-interaction between lines $\vec{k}_1$ and $\vec{k}_2$. The new (i) diagram is of one order in

(0)   (I)   (II)
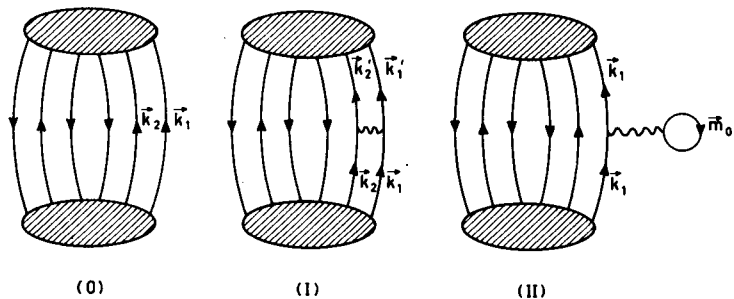
FIG.20. (0): arbitrary diagram with two particle lines;
         (i): the same as (0) + one K-interaction
         (ii): the same as (0) + a hole line

K higher than the original (0) diagram, but the number of hole lines is the same in both diagrams. Because of the additional K interaction in (i), the contribution of (i) is

$$\int d\vec{k}_{12}^{\,\prime} \; \frac{Q(\vec{k}_{12}, \vec{k}'_{12})}{z - \frac{1}{2}\epsilon(k_{12}) - 2\epsilon(k'_{12})} \langle \vec{k}'_{12} | K_{\vec{k}_{12}}(z) | \vec{k}_{12} \rangle \qquad (15.1)$$

times that of (0). In writing (15.1) we have exploited the momentum conservation $\vec{k}_{12} = \vec{k}'_{12}$. The value of z is equal to minus the excitation energy of the rest of the system (i.e., except for particles $\vec{k}_1$, $\vec{k}_2$) in the interval between the two blobs. Strictly speaking, the upper blob of (i) is different from the upper blob in (0) because the incoming lines $\vec{k}_1$, $\vec{k}_2$ have been changed to $\vec{k}'_1$, k'_2. To get a rough estimate we neglect this difference. Now, in the Q = 1 approximation (see Eq.(14.17)), the expression (15.1) is equal

$$- \int_{\bullet} d\vec{k}'_{12} \langle \vec{k}'_{12} | \zeta_{\vec{k}_{12}} \rangle = -(2\pi)^{3/2} \int d\vec{k}'_{12} \langle \vec{r} = 0 | \vec{k}'_{12} \rangle \langle \vec{k}'_{12} | \zeta_{\vec{k}_{12}} \rangle$$

$$= -(2\pi)^{3/2} \langle \vec{r} = 0 | \zeta_{\vec{k}_{12}} \rangle = -1 \qquad (15.2)$$

where we have used the fact that $(2\pi)^{3/2} \langle \vec{r} = 0 | \vec{k}'_{12} \rangle = 1$, Eq.(12.7), and also Eq.(14.22), valid for the hard-core nucleon-nucleon interaction. We come then to the conclusion

$$\frac{\text{contribution of (i)}}{\text{contribution of (0)}} \simeq -1 \qquad (15.3)$$

(ii) Adding a hole line. As an example let us consider a new diagram, Fig. 20(ii) obtained from the original (0) diagram by attaching a K interaction between $\vec{k}_1$ line and an additional $\vec{m}_0$ hole line (bubble). The contribution of (ii) is equal to the contribution of (0) times the factor

$$\sum_{m_0} \frac{1}{z - \epsilon(m_0) - \epsilon(k_1)} \; (\vec{m}_0 \vec{k}_1 | K | \vec{m}_0 \vec{k}_1)$$

$$\simeq A \; \frac{1}{z - \frac{1}{2}\epsilon(P_{10}) - 2\epsilon(p_{10})} \; \frac{(2\pi)^3}{\Omega} \langle \vec{p}_{10} | K | \vec{p}_{10} \rangle \qquad (15.4)$$

where we have replaced m_0 by an average value in the Fermi sea (we have then $\sum_{m_0} = A$), and where we have used the notation $\vec{P}_{10} = \vec{k}_1 + \vec{m}_0$, $\vec{p}_{10} = (\vec{k}_1 - \vec{m}_0)/2$. The precise value of z (connected with the excitation energy of the system in the interval between the two blobs) should not be

important. Similarly as in case (i) we may approximate expression (15.4) as

$$-(A/\Omega)(2\pi)^3 \left\langle \vec{p}_{10} | \zeta_{\vec{p}_{10}} \right\rangle = -\rho(2\pi)^{3/2} \int d\vec{r} \, e^{-i\vec{p}_{10}\cdot\vec{r}} \, \zeta_{\vec{p}_{10}}(\vec{r}) \tag{15.5}$$

According to Eq.(14.22), we have

$$(2\pi)^{3/2} e^{-i\vec{p}_{10}\cdot\vec{r}} \, \zeta_{\vec{p}_{10}}(\vec{r}) = 1 \quad \text{for } r \leq c \tag{15.6}$$

and the contribution to the integral in Eq.(15.5) of the core region

$$(2\pi)^{3/2} \int_{r<c} d\vec{r} \, e^{-i\vec{p}_{10}\cdot\vec{r}} \, \zeta_{\vec{p}_{10}}(\vec{r}) = \frac{4}{3}\pi c^3 \tag{15.7}$$

The contribution of the region outside the core is not so trivial, but the shape of ζ_{0c}, Fig.19, shows that the result should be of the same order as the core contribution. Rajaraman and Bethe's [9] estimate is about $(2 \times (4/3)\pi c^3$. Adding it to Eq.(15.7) we get

$$(2\pi)^{3/2} \int d\vec{r} \, e^{-i\vec{p}_{01}\cdot\vec{r}} \, \zeta_{\vec{p}_{01}}(\vec{r}) \simeq 4\pi c^3 \tag{15.8}$$

This estimate inserted into expression (15.5) leads to the conclusion

$$\frac{\text{contribution of (ii)}}{\text{contribution of (0)}} \simeq -3(c/r_0)^3 = -0.14 \tag{15.9}$$

where the last number is obtained for $c = 0.4$ fm, $r_0 = 1.1$ fm.

Equations (15.3) and (15.9) form the quantitative basis for our qualitative discussion of chapter 10 which led us to the general procedure of considering at each stage of the calculation all diagrams with a fixed number of hole lines. Equation (15.3) clearly indicates that the perturbation series in K is not converging, and what we have to do is to sum all diagrams with a given number of hole lines. The possibility of such a sum — which includes diagrams of all orders in K — being finite is connected with the fact that contributions of successive orders in K alternate in sign, Eq.(15.3). Crucial for the convergence of the procedure of grouping diagrams according to the number of hole lines is Eq.(15.9). It shows that by increasing the number of hole lines by one we reduce the magnitude of the corresponding contributions by a factor $\sim 3(c/r_0)$. This leads to an expansion in powers of the density because $3(c/r_0)^3 = \rho\mathscr{V}_c$, where the correlation volume $\mathscr{V}_c$ is determined predominantly by the core volume $(4/3)\pi c^3 (\mathscr{V}_c \cong 3(4/3)\pi c^3)$. The expansion parameter of the whole procedure, $3(c/r_0)^3 \cong 0.14$, is reasonably small.

Essential for our estimates is the hard core. This is the hard core which leads to $\Psi = 0$ and $\zeta = 1$ at small distances. Furthermore, we have

exploited the weakness of the attractive part of the nucleon-nucleon inter-
action. This weakness, which causes a rapid healing outside of the hard
core, allows us to approximate ζ by the pure hard core ζ_c and to obtain
the estimate (15.8).

16. BETHE'S TREATMENT OF THE THREE-BODY ENERGY

Among the three-hole-line diagrams only the class of the "hole-self-
energy" diagrams, Fig.13(a), has been included in our theory by the
proper definition of the hole energies, Eqs (11.5-6). Now, we want to
calculate the contribution of the two remaining classes of the three-hole-
line diagrams described at the beginning of chapter 11.
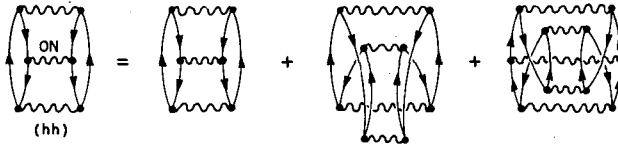
FIG.21. Sum of contributions of the entire class of "hole-hole" scattering diagrams equivalent to the
contribution of the third-order diagram (**b**) (from Fig.13).
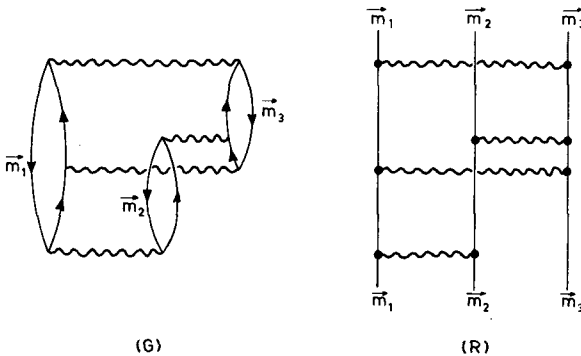
FIG.22.   A typical example of a fourth-order three-body diagram.

The "hole-hole scattering" class, represented by diagram (b) in Fig.13,
contains four hole lines but, because of momentum conservation, only three
of them are independent. This class is similar to the "hole-self-energy"
class in the sense that the contribution of the third-order diagram (b)
calculated with the K-interaction between the two holes on the energy shell
is equal to the sum of contributions of the entire class of "hole-hole
scattering" diagrams [8]. This is shown diagrammatically in Fig.21.

The contribution of the diagram 21(hh) is of the same order of magni-
tude as that of the self-energy-insertion diagram 16(h) except for a statisti-
cal factor $1/8$ and a phase-space factor $\sim 1/4$ [34]. Thus, the contribution
of the hole-hole scattering class should be about 32 times smaller than that
of the "hole-self-energy" class. Consequently, in our discussion, we shall
ignore the "hole-hole scattering" class.

We are left then with the class of the three hole lines diagrams represented in Fig.13 by diagrams (c) and (d). Diagrams belonging to this class we shall call three-body diagrams. Now, in any order in K there are such diagrams. A typical example of a fourth-order three-body diagram is shown in Fig.22. Thus we are faced with the very difficult problem of a partial summation of three-body diagrams in the perturbation series in K. An approximate solution of this problem has been found by Bethe [35], [36],[9]. (The possibility of such a solution was first noticed by Rajaraman [37].
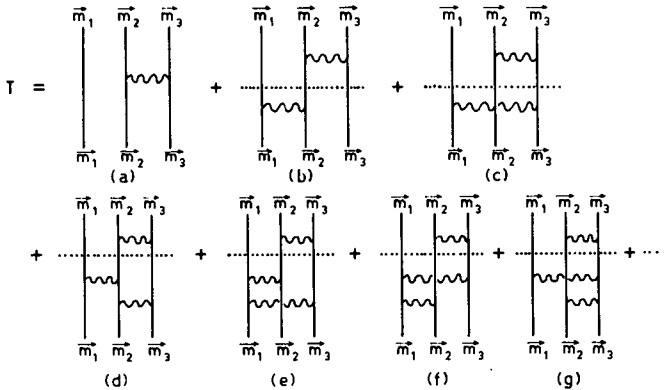
FIG.23. Some of the three-body diagrams.

The Rajaraman diagrams [37] are most helpful here. They are obtained by breaking all hole lines in the corresponding Goldstone diagrams. For example, the fourth-order Goldstone diagram (G) takes the form (R) of the corresponding Rajaraman diagram, Fig.22. Needless to say, except for initial and final states $\vec{m}_1$, $\vec{m}_2$, $\vec{m}_3$ all other states in the Rajaraman diagrams should be above the Fermi sea, and no two successive K-matrices should refer to the same pair of intermediate states.

Since the most important intermediate states momenta $p_i \simeq \pi/2c \simeq 4\,\mathrm{fm}^{-1}$, Eqs (14.20-21), whereas $m_i \lesssim k_F \simeq 1.4\,\mathrm{fm}^{-1}$, we shall approximate $\vec{m}_1$, $\vec{m}_2$, $\vec{m}_3$ by zero momenta. Furthermore, we shall apply the $Q = 1$ approximation.

Let us denote by T the sum of all the three-body diagrams. Some of them are shown in Fig.23. If we add to the diagrams of Fig.23 those obtained from them by cyclic permutations of $\vec{m}_1$, $\vec{m}_2$, $\vec{m}_3$ and all the exchange diagrams (one gets them by permuting, e.g. the bottom momenta $\vec{m}_1$, $\vec{m}_2$, $\vec{m}_3$, while keeping the upper ones fixed), we get all the diagrams of the third order in K. (To simplify the presentation we shall disregard the exchange diagrams.) Actually only the diagrams in the second line of Fig.23 are real three-body diagrams. The diagram 23(a) is simply the fundamental two-body diagram of our theory, and the diagrams 23 (b-c) vanish because of momentum conservation (before we introduce the $Q = 1$ approximation). Nevertheless, we include the first line of diagrams into our T to obtain simpler equations for T. Obviously, in computing the three-body energy we must subtract the contribution of the diagrams 23(a-c).

Now, the diagrams of Fig.23 look exactly as diagrams representing the scattering of three particles, and to perform the summation of these diagrams we apply the Faddeev [38] technique. We write

$$T = T^{(1)} + T^{(2)} + T^{(3)} \tag{16.1}$$

where $T^{(i)}$ is the sum of all those diagrams in which the i-th nucleon is the spectator of the last scattering. All the diagrams of Fig.23 belong to $T^{(1)}$. If we look at the parts of the diagrams (b), (d), (e) below the dotted lines we notice that they are the three first diagrams of $T^{(3)}$, whereas the parts below the dotted lines of diagrams (c), (f), (g) are the first three diagrams of T. Thus we are led to the following equation:

$$T^{(1)} = K_{23} + K_{23} \frac{1}{a} (T^{(2)} + T^{(3)}) \tag{16.2}$$

and to similar equations for $T^{(2)}$ and $T^{(3)}$. The denominator a is equal to minus the excitation energy of the intermediate state.

Similarly as we have introduced the two-body wave function, Eq.(12.12), we introduce now the three-body wave functions

$$T^{(1)} |\Phi\rangle = K_{23} |\psi^{(1)}\rangle, \text{ and cyclic permutations} \tag{16.3}$$

where $|\Phi\rangle$ is a three-nucleon plane-wave state with $\vec{m}_1 = \vec{m}_2 = \vec{m}_3 = 0$.

Equation (16.2) takes the form

$$|\psi^{(1)}\rangle = |\Phi\rangle + \frac{1}{a} K_{13} |\psi^{(2)}\rangle + \frac{1}{a} K_{12} |\psi^{(3)}\rangle \tag{16.4}$$

or

$$|\psi^{(1)} - \Phi\rangle = \frac{1}{a} K_{13} |\Phi\rangle + \frac{1}{a} K_{12} |\Phi\rangle$$

$$+ \frac{1}{a} K_{13} |\psi^{(2)} - \Phi\rangle + \frac{1}{a} K_{12} |\psi^{(3)} - \Phi\rangle \tag{16.5}$$

We proceed with these equations similarly as in chapter 12 with the K-matrix equation, namely, we go over to the configuration space. With the notations

$$\langle \vec{r}_1 \vec{r}_2 \vec{r}_3 | \psi^{(i)} \rangle = \psi^{(i)} (\vec{r}_1 \vec{r}_2 \vec{r}_3) = \psi^{(i)} \tag{16.6}$$

$$\langle \vec{r}_1 \vec{r}_2 \vec{r}_3 | \Phi \rangle = \langle \vec{r}_1 | \vec{m}_1 \rangle \langle \vec{r}_2 | \vec{m}_2 \rangle \langle \vec{r}_3 | \vec{m}_3 \rangle = \Phi \tag{16.7}$$

we may write Eq.(16.5) in configuration space

$$\psi^{(1)} - \Phi = \langle \vec{r}_1 \vec{r}_2 \vec{r}_3 | \frac{1}{a} K_{13} | \Phi \rangle + \ldots \tag{16.7a}$$

According to chapter 14 (see Eq.(14.17)) we have

$$\langle \vec{r}_1 \vec{r}_2 \vec{r}_3 | \frac{1}{a} K_{13} | \Phi \rangle = \langle \vec{r}_2 | \vec{m}_2 \rangle \langle \frac{\vec{r}_1 + \vec{r}_3}{2} | \vec{m}_1 + \vec{m}_3 \rangle$$

$$\times \langle \vec{r}_1 - \vec{r}_3 | \frac{1}{a} K_{13} | \frac{\vec{m}_1 - \vec{m}_3}{2} \rangle = - \zeta_0 (r_{13}) \Phi \approx - \zeta_{0c} (r_{13}) \Phi \equiv - \zeta (r_{13}) \Phi \tag{16.8}$$

Notice that all momenta $\vec{m}_i$ are zero, and the difference function reduces to its S-wave part. Notice also that when K_{13}/a acts on $|\Phi\rangle$ the

second nucleon is not excited and we may apply the estimate of the parameter $\gamma \simeq 1.7$ fm^{-1} of chapter 14.

The situation with the last two terms in Eq.(16.5) is much more difficult. The crudest approximation applied by Bethe amounts to putting

$$\langle \vec{r}_1 \vec{r}_2 \vec{r}_3 | \frac{1}{a} K_{13} | \Psi^{(2)} - \Phi \rangle \simeq -\widetilde{\zeta}(r_{13}) \langle \vec{r}_1 \vec{r}_2 \vec{r}_3 | \Psi^{(2)} - \Phi \rangle \qquad (16.9)$$

where $\widetilde{\zeta}$ differs from ζ only by the value of the γ parameter:

$$\widetilde{\gamma} \simeq 3.5 \text{ fm}^{-1}$$

To make approximation (16.9) plausible, let us notice that if we expand $|\Psi^{(2)} - \Phi \rangle$ into plane-wave state then the states $p_i \simeq \pi/2c$ dominate. On the other hand, we know how the operator K_{13}/a acts on a plane-wave state, Eq.(14.17). The larger value of γ is connected with the excitation of all the three nucleons at the moment of the K_{13} interaction. A more detailed discussion of the approximation (16.9) is given in the review article by Rajaraman and Bethe [9], who also described an improved and more complicated approximation than expression (16.9).

With the approximation (16.8-9), equation (16.7a) takes the form

$$\Phi - \Psi^{(1)} = \zeta(r_{13})\Phi + \zeta(r_{12})\Phi - \widetilde{\zeta}(r_{13})[\Phi - \Psi^{(2)}] - \widetilde{\zeta}(r_{12})[\Phi - \Psi^{(3)}] \qquad (16.10)$$

This equation together with analogous equations for $\Phi - \Psi^{(2)}$ and $\Phi - \Psi^{(3)}$ form a system of linear algebraic equations which may be solved immediately for $\Phi - \Psi^{(i)}$.

Let us consider the particular case where $r_{12} = r_{13} = r_{23} = r$ for which

$$\Phi - \Psi^{(i)} = \frac{2\zeta(r)}{1 + 2\widetilde{\zeta}(r)} \Phi \qquad (16.11)$$

The expansion of Eq.(16.11)

$$\Phi - \Psi^{(i)} = 2\zeta - 4\zeta\widetilde{\zeta} + 8\zeta\widetilde{\zeta}^2 - \dots \qquad (16.12)$$

corresponds to the expansion in powers of K.

However, for $\widetilde{\zeta}(r) > 1/2$ the geometric series (16.12) is diverging, although its sum is finite. (Notice that $\widetilde{\zeta}(r) = 1$ for $r < c$). Thus, we encounter once more the divergence of the perturbation expansion in powers of K.

To calculate the contribution of $T^{(1)}$ to the three-body energy we use not

$$\langle \Phi | T^{(1)} | \Phi \rangle = \langle \Phi | K_{23} | \Psi^{(1)} \rangle$$

but

$$\langle \Phi | K_{23} | \Psi^{(1)} - \Phi \rangle = \langle \Phi | K_{23} \frac{1}{a} K_{13} | \Phi \rangle$$

$$+ \langle \Phi | K_{23} \frac{1}{a} K_{12} | \Phi \rangle + \langle \Phi | K_{23} \frac{1}{a} K_{13} | \Psi^{(2)} - \Phi \rangle$$

$$+ \langle \Phi | K_{23} \frac{1}{a} K_{12} | \Psi^{(3)} - \Phi \rangle \qquad (16.13)$$

and in this way we get rid of the contribution of the diagram 23(a). To get rid of the diagrams 23(b-c) we drop the two first terms on the right side of Eq.(16.6) and get

$$\Delta E_3 = \sum_{\vec{m}_1 \vec{m}_2 \vec{m}_3} (\Phi | K_{23} \frac{1}{a} K_{12} | \Psi^{(3)} - \Phi) \qquad (16.14)$$

If we apply Eq.(16.8) to the factor $(\Phi | K_{23} \frac{1}{a})$ and approximate K_{12} by a function of r_{12}, we may reduce the expression (16.14) for ΔE_3 to a double integral over r_{23} and r_3. Details of the calculation may be found in Ref.[9].

The first numerical estimate by Bethe [35] was $\Delta E_3/A \approx 0.6$ MeV (for the soft-core potential of Wong [39], [40]). This result was supported by a simple variational estimate by Moszkowski [41] who obtained $\Delta E_3/A \approx 0.4$ MeV (for the same Wong potential). The calculation by Dahlblom [42] for the Reid hard-core potential [43] produced the result: $\Delta E_3/A \approx 1.1$ MeV for central interaction, and $\Delta E_3/A \approx -0.6$ MeV with tensor interaction taken into account (see also Ref.[44]).

All these results — which oscillate around zero — show that the total contribution of the three-body diagrams is very small. This result establishes the correctness of the following procedure: We calculate the K-matrix with self-consistent energies of the hole states and with pure kinetic energies of the intermediate particle states. We determine the energy of nuclear matter to first order in this K-matrix. The result thus obtained is expected to have an accuracy of about 1 MeV per nucleon. The remaining three-hole line diagrams, i.e. the three-body diagrams (and the hole-hole scattering diagrams) may be taken into account as a perturbative correction, e.g. in the fashion indicated by Bethe. (The four-body diagrams are expected to give a negligible contribution [44].)

17. REVIEW OF NUCLEAR MATTER CALCULATIONS

We want to present here the results of nuclear-matter calculations performed within the scheme outlined in chapters 11, 12, possibly including estimates of the small corrections discussed in chapter 16. However, right now, there are not many published calculations of this type, and thus our review will not be a long one. Unfortunately, in several of the calculations performed in the last few years, the single-particle energies of the excited states (with momenta above the Fermi level) have been treated in an erroneous way. These calculations shall not be mentioned here. Connected with these erroneous calculations were several estimates of the essential

increase in the binding energy due to the replacement of the hard-core potentials by the soft-core potentials. These estimates shall not be reviewed here, either. On the other hand, we shall include the computations of the type described in chapter 13 in our review, because the single-particle potential introduced in these computations does not affect the important range of intermediate states with momenta $p_1 \cong 4$ fm^{-1}, established in chapter 14.

TABLE III.   SUMMARY OF RESULTS OBTAINED BY VARIOUS AUTHORS

r_0(fm)	ϵ_{vol} (MeV)	ϵ_{sym}(MeV)	K_0 (MeV)	Potential	References
1.02	15.2	$56.0(1 - 0.67\alpha^2)$	172	BGT[†]	Brueckner, Gammel [29] Brueckner, Coon, Dąbrowski [46]
1.28	8.3	-	-	YALE[†]	Brueckner, Masterson [32]
0.92	14.3	-	119	BGT	Azziz [50]
1.13	8.3	-	105	HJ	Azziz [50]
~1.2	~8	-	-	REID HC	Sprung et al. [53]
~1.1	~10	-	-	REID SC	Sprung et al. [53]
0.98	15.47	-	-	OBEP	Ingber [51]
1.11	17.8	-	-	OBEP[†]	Ingber [51]

† with single-particle potential insertions

Let us now discuss the results shown in Table III. The results for the BGT potential, discussed in chapter 13, are in good agreement with the empirical values of the nuclear-matter parameters. However, after 1958, new results of nucleon-nucleon scattering have been accumulated. To get an improved fit to all these data Breit and his collaborators [47] have introduced the Yale potential which differs from the BGT potential by a larger core radius, a stronger odd-states repulsion, quadratic spin-orbit terms, and a weaker even-triplet central force. Essentially similar to the Yale potential is the Hamada-Johnston (HJ) potential [48] (see also Ref.[49] for corrections in the HJ potential).

Now, the calculation by Brueckner and Masterson [32], which was a slightly simplified version of the Brueckner and Gammel calculation, but performed with the Yale potential, yielded $\epsilon_{vol} = 8.3$ MeV, i.e. about 7 MeV short of the empirical value, and too low an equilibrium density. These results for ϵ_{vol} essentially agree with the recent results of Azziz [50] who has applied the reference spectrum approximation in solving the K-matrix equations. The higher equilibrium densities obtained by Azziz for both the BGT and HJ potentials are probably connected – at least partly – with the single-particle potential used in Ref.[29] (this is exhibited by the two results obtained by Ingber [51] and shown in Table III).

Azziz points out that the main reason for the lower binding energy given by the HJ interaction compared to BGT is the difference in the $^3S_1$-state contribution. Now, the fit to the $^3S_1$ phase shift is equally good in the case of both the BGT and HJ potentials. The two potentials differ mainly in their values of the mixing parameter ϵ_1 which measures the coupling between the $^3S_1$ and $^3D_1$ states resulting from the tensor force. The HJ potential produces bigger values of ϵ_1 than does the BGT potential, i.e., the HJ potential has a relatively stronger tensor part than the BGT potential. However, the ϵ_1 parameter was determined in the Yale phase-shift analysis [52] with a high uncertainty. Azziz suggests that one could probably use a HJ potential with the $^3S_1 + ^3D_1$ interaction replaced by the corresponding BGT interaction. The fit to the phase shifts would not be worse but one would probably get the right value of the binding energy of nuclear matter.

Let us state here the well-known property of tensor forces. The contribution of the tensor forces to the binding energy of nuclear matter is partly (spin-) averaged out and consequently a two-body interaction with a bigger central to tensor ratio gives stronger binding. Because of the averaging-out property the tensor force contribution to the nuclear binding is a second-order effect (in a perturbational approach), and becomes less important at higher densities, i.e. at higher values of k_F, where intermediate states are shifted up in energy and thus are less accessible to the two interacting nucleons. Consequently, tensor forces saturate at a comparatively lower density and shift the whole equilibrium towards a lower density (compare, e.g. the behaviour of the $^3S_1 + ^3D_1$ curve compared to the $^1S_0$ curve in Fig.24).

A very extensive calculation — still in progress — is that reported by Sprung [53]. The potential applied in this calculation is the Reid potential [43]. This potential has a different radial dependence in each nucleon-nucleon state. The hard-core radius of the original Reid potential has been
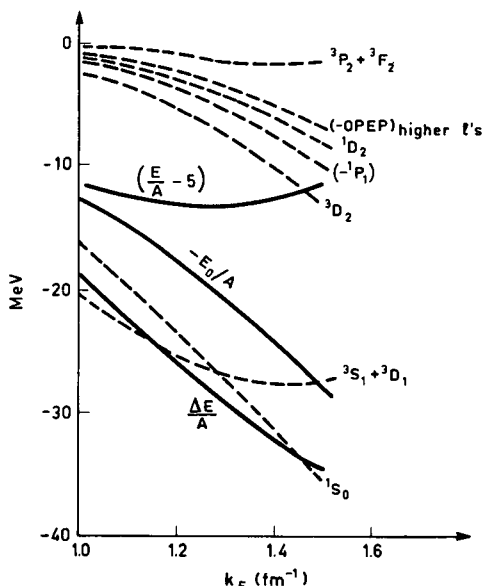
FIG.24.   Contributions of the different states in the case of the Reid HC potential.

$r_c = 0.42$ fm in all states except for the $^3S_1 + ^3D_1$ state for which $r_c = 0.52$ fm. This original hard-core potential (HC) has been modified later to fit the deuteron quadrupole moment. An other version of the potential (SC), with the hard-core being replaced by a soft core, has also been considered. The ratio of central-to-tensor force of the Reid potential is probably even smaller than in the HJ potential, and this certainly affects the calculated binding energy of nuclear matter. As the final results of the calculation has not been published yet, only approximate numbers are shown in Table III. They include corrections due to three-body diagrams. There is an uncertainty in the contribution of higher partial waves. The size and even the sign of this contribution depends on whether – within the phase-shift approximation ($Q \cong 1$ and $e(m_i) \cong \epsilon(m_i)$) – one applies the one-pion exchange potential (OPEP) or the phenomenologically determined phase shifts. One may hope to get with the calculated value of ϵ_{vol} as high as to about 12 MeV for the SC potential. The difference of about 2 MeV between the HC and SC potentials is not very large and more or less agrees with the estimate of Wong [40]. According to Sprung, the contributions of the interaction in many of the nucleon-nucleon states cancel approximately and one is left essentially with the contributions of the $^1S_0$, $^1D_2$, $^3S_1 + ^3D_1$ states only. The contributions of the different states in the case of the Reid HC potential is shown in Fig.24, taken from Ref.[53].

At this point one might express some concern whether a potential like the Reid potential – different in each nucleon-nucleon state – is a realistic representation of the nucleon-nucleon interation, or is it just a parametrization of phase shifts. The least one should do is to check how such a potential works in problems like the proton-proton bremsstrahlung, or triton ground state, or neutron-deuteron scattering where the knowledge of the off-energy shell scattering-matrix elements is necessary. On the other hand, in constructing the nucleon-nucleon potential one should probably try to use some theoretical guidance supplied by meson theory. This method of constructing the nucleon-nucleon potential has turned out to be very successful in recent years. The main progress here is connected with the possibility of approximating the multiple-pion exchange by an exchange of the observed resonance states of pions. In this way we obtain the so-called one-boson exchange potential (OBEP) [1]. As an example let us mention the work of Ingber [51] who considers the exchange of all known mesons with masses smaller than 1 BeV/c^2 plus the hypothetical σ meson. Altogether he uses 8 free parameters (some of the meson masses and coupling constants plus two cut-off parameters) and obtains an overall fit to the phase shifts of essentially the same quality as that obtained in the case of the Yale potential with about 80 free parameters. The characteristic features of this potential are: (i) a strong momentum dependence, (ii) a big central-to-tensor ratio. The results of nuclear matter calculation obtained by Ingber with his potential would be encouraging if it was not for the fact that his potential fails badly in reproducing two important low-energy data. Namely, Ingber's potential leads to the deuteron binding, $\epsilon_D = 8.09$ MeV, and to the deuteron quadrupole moment, $Q_D = 0.212$ fm^2. whereas the experimental values are: $\epsilon_D = 2.222$ MeV and $Q_D = 0.274$ fm^2. To say anything definite about the capability of OBEP of reproducing nuclear matter parameters we have to wait for results obtained with an OBEP fitted precisely to all the low-energy nucleon-nucleon data.

Right now the situation is such that, by applying a theory expected to work with an accuracy of about 1-2 MeV, we get a binding energy of nuclear matter about 5 MeV short of the empirical value.

What to do about the discrepancy? No doubt, we should try to exploit the possibility of choosing the proper form of two-body interaction. Here, however, we encounter the difficulty that even the phase shifts are not yet determined with sufficient precision. At the moment it would be most important to know more about the behaviour of the mixing parameter ϵ_1. At very low energy $\epsilon_1 \cong Q_D k^2$, and thus ϵ_1 must be positive. At energies higher than some 200 MeV all the phase-shift analyses indicate that $\epsilon_1 > 0$. However, the value of ϵ_1 is not determined unambiguously in the range of nucleon laboratory energies between about 25 and 100 MeV. This is just the range essential for nuclear-matter calculations where most heavily weighted are energies which correspond to a nucleon laboratory energy around 50 MeV. The recent Livermore phase-shift analysis [54] suggests a negative value of ϵ_1 in this range of energies. However, potentials like HJ or Yale produce a positive and increasing ϵ_1 in the whole energy range between 0 and 300 MeV. In nuclear-matter calculations a potential which would reproduce the oscillations of ϵ_1 around zero suggested in Ref.[54] would certainly give more binding since $\epsilon_1 = 0$ corresponds to pure central forces. One should point out that the momentum dependence of the OBEP should enable one to incorporate the tensor force in such a way that one would get the experimental value of Q_D and the oscillations of ϵ_1 around zero at intermediate energies. (In accordance with these remarks the potential of Mongan [55] is a promising candidate for nuclear-matter calculations since it has been fitted to the Livermore phase shifts. Since it is a separable potential, the numerical work would be comparatively simple.)

There is always another possible source of disagreement between the calculated and the empirically estimated values of the nuclear-matter parameters. We should be aware of the possibility that the basic assumption of the interaction between nucleons in nuclear matter being just the same two-body interaction as that between two free nucleons, might be wrong. Right now, the question to which extent the interaction between nucleons is changed by the presence of other nucleons in nuclear matter, is very much an open problem. Let us mention two recent estimates of the three-body forces in nuclear matter [56, 57] which come to opposite conclusions (see also Ref.[58] for an estimate of four-body forces).

REFERENCES

[1] BRINK, D.M., these Proceedings.

[2] BRUECKNER, K.A., EDEN, R.J., FRANCIS, N.C., Phys. Rev. 98 (1955) 1445.

[3] SZYMAŃSKI, Z., these Proceedings.

[4] BRUECKNER, K.A., The Many-Body Problem, Les Houches (1958) 47.

[5] BELL, J.S., SQUIRES, E.J., Phil. Mag. Suppl. 10 (1961) 211.

[6] PETSCHEK, A.G., Ann. Rev. Nucl. Sci. 14 (1964) 29.

[7] KUMAR, K., Perturbation Theory and the Nuclear Many-Body Problem, Amsterdam (1962).

[8] DAY, B.D., Rev. mod. Phys. 39 (1967) 719.

[9] RAJARAMAN, R., BETHE, H.A., Rev. mod. Phys. 39 (1967) 745.

[10] BRANDOW, B.H., Rev. mod. Phys. 39 (1967) 771.

[11] KOHN, W., LUTTINGER, J.M., Phys. Rev. 118 (1960) 41.

[12] LUTTINGER, J.M., WARD, J.C., Phys. Rev. 118 (1960) 1417.

[13] BAKER, G.A., Phys. Rev. 131 (1963) 1869.

[14] GOLDSTONE, J., Proc. Roy. Soc. A293 (1957) 267.

[15] SALAM, A., Progr. theor. Phys. 9 (1953) 553.

[16] FRAHN, W.E., these Proceedings.

[17] VILLARS, F., Proc. S.I.F., Course 23, New York-London (1963).

[18] BETHE, H.A., de HOFFMANN, F., Mesons and Fields 1, Evanston (1955).

[19] BRUECKNER, K.A., Phys. Rev. 100 (1955) 36.

[20] HUGENHOLTZ, N.M., Physica 23 (1957) 533.

[21] BRUECKNER, K.A., GOLDMAN, D.T., Phys. Rev. 117 (1960) 207.

[22] BETHE, H.A., BRANDOW, B.B., PETSCHEK, A.G., Phys. Rev. 129 (1963) 225.

[23] EASLEA, B.R., Physics Lett. 19 (1966) 662.

[24] KLEIN, A., PRANGE, R., Phys. Rev. 112 (1958) 994.

[25] THOULESS, D.J., Phys. Rev. 114 (1959) 1383.

[26] THOULESS, D.J., Phys. Rev. 116 (1959) 21.

[27] NUTTALL, J., Phys. Rev. 149 (1966) 755.

[28] GOMES, L.C., WALECKA, J.D., WEISSKOPF, V.F., Annls Phys. 3 (1958) 241.

[29] BRUECKNER, K.A., GAMMEL, J.L., Phys. Rev. 109 (1958) 1023.

[30] WERNER, E., Nucl. Phys. 10 (1959) 688.

[31] BROWN, G.E., SCHAPPART, G.T., WONG, C.W., Nucl. Phys. 56 (1964) 191.

[32] BRUECKNER, K.A., MASTERSON, K.S., Phys. Rev. 128 (1962) 2267.

[33] WEISSKOPF, V., Nucl. Phys. 3 (1957) 423.

[34] RAJARAMAN, R., Phys. Rev. 129 (1963) 265.

[35] BETHE, H.A., Phys. Rev. 138 (1965) B804.

[36] BETHE, H.A, Phys. Rev. 158 (1957) 941.

[37] RAJARAMAN, R., Phys. Rev. 131 (1963) 1244.

[38] FADDEEV, L.D., Zh. éxp. theor. Fiz. 39 (1960) 1459.

[39] WONG, C.W., Nucl. Phys. 56 (1964) 224.

[40] WONG, C.W., Nucl. Phys. 71 (1965) 385.

[41] MOSZKOWSKI, S.A., Phys. Rev. 140 (1965) B283.

[42] DAHLBLOM, T., Nucl. Phys. A114 (1967) 327.

[43] REID, R., Cornell Thesis, unpublished, and Phys. Rev.

[44] AKAISHI, Y., BANDO, H., KURIYAMA, A., NOGATA, S., Progr. theor. Phys. 40 (1968) 288.

[45] KURIYAMA, A., Progr. theor. Phys. 40 (1968) 301.

[46] BRUECKNER, K.A., COON, S.A., DĄBROWSKI, J., Phys. Rev. 168 (1968) 1184.

[47] LASSILA, K.E., HULL, M.H., Jr., RUPPEL, H.M., McDONALD, F.A., BREIT, G., Phys. Rev. 126 (1962) 881.

[48] HAMADA, T., JOHNSTON, J.D., Nucl. Phys. 34 (1962) 383.

[49] HAMADA, T., NAKAMURA, Y., TAMAGAKI, R., Progr. theor. Phys. 33 (1965) 769.

[50] AZZIZ, N., Nucl. Phys. 85 (1966) 15.

[51] INGBER, L., Phys. Rev. 174 (1968) 1250.

[52] HULL, M.H., Jr., LASSILA, K.E., RUPPEL, H.M., McDONALD, F.A., BREIT, G., Phys. Rev. 122 (1961) 1606.

[53] SPRUNG, D.W.L., in Proc. 3rd. Int. Conf. Winnipeg (1967) 37, and private communication.

[54] MacGREGOR, M.H., ARNDT, R.A., WRIGHT, R.M., Phys. Rev. 173 (1968) 1272.

[55] MONGAN, T.R., Phys. Rev. 175 (1968) 1260.

[56] BROWN, G.E., GREEN, A.M., GERACE, W.J., Nucl. Phys. A115 (1968) 435.

[57] McKELLER, B.H.J., RAJARAMAN, R., Phys. Rev. Lett. 21 (1968) 450.

[58] BROWN, G.E., GREEN, A.M., GERACE, W.J., NYMAN, E.M., Nucl. Phys. A118 (1968) 1.

SECTION IV

Phenomenological Aspects of Nuclear Structure
and Nuclear Reactions

SYMMETRY PROPERTIES OF
NUCLEAR VIBRATIONS

A. BOHR
Niels Bohr Institute,
Copenhagen, Denmark

Abstract

SYMMETRY PROPERTIES OF NUCLEAR VIBRATIONS.
   A brief survey of some problems in the field of nuclear vibrational modes, based on a collective description, is given.

A fundamental property of a physical system is the spectrum of vibrational eigenmodes. The vibrational modes represent oscillations about the equilibrium configuration, and may be described in terms of an amplitude a of displacement from equilibrium. For sufficiently small displacements, one expects harmonic motion corresponding to a Hamiltonian of the form

$$H = \tfrac{1}{2}C\dot{a}^2 + \tfrac{1}{2}Da^2 \qquad (1)$$

with eigenfrequency

$$\omega = \left(\frac{C}{D}\right)^{\frac{1}{2}} \qquad (2)$$

The vibrations can also be described in terms of the quanta of excitation. In this description, a vibration is a mode of excitation that can be repeated a large number of times. The vibrational states $|n\rangle$ are specified by the number of quanta, and the variables of immediate physical significance are, besides n, the operators $c^\dagger$ and c which increase and decrease the number of quanta. In the language of the quanta, harmonic vibrational motion corresponds to the absence of interaction between the quanta, which each possesses the energy $\hbar\omega$. Because of the finiteness of the zero-point motion, anharmonic effects may become of significance even for the lowest quantal states of vibrational motion.

The vibrational modes in classical systems represent pure motion, corresponding to quanta having only energy and momentum, or angular momentum. However, in quantal systems, one also encounters modes whose quanta possess electric charge and other similar attributes, which are not of kinematic nature. The aplitude a, though of basic significance for the description of the vibrational properties, can then no longer be visualized in the customary sense.

In the survey of the nuclear vibrations, we first consider modes with a classical analogue. An especially simple type corresponds to variations in the nuclear shape. For a nucleus with a spherical equilibrium, the quanta can be specified by the angular momentum λ and its projection μ on a fixed axis. The amplitude $a_{\lambda\mu}$ represents a density variation whose

angular dependence is proportional to $Y_{\lambda\mu}^*$, as follows from arguments of rotational invariance. For example, in the idealized case of a system with a sharp surface, the normal co-ordinates $a_{\lambda\mu}$ of the shape oscillations can be obtained from the expansion of the surface

$$R(\theta,\phi) = R_0\left(1 + \sum_{\lambda\mu} a_{\lambda\mu} Y_{\lambda\mu}^* (\theta,\phi)\right) \tag{3}$$

as is familiar from the theory of oscillations of a liquid drop. The parity of a quantum is $\pi = (-1)^\lambda$.

In the expansion (3), the terms with $\lambda = 1$ represent a displacement of the centre of mass. The lowest mode of shape oscillation is, therefore, of quadrupole type with $\lambda = 2$. This mode is a dominant feature in the low-energy nuclear spectra. Thus, all even-even nuclei have $I\pi = 0^+$ in the ground state, and the first excited state almost invariably has angular momentum and parity $I\pi = 2^+$ and can be associated with quadrupole shape deformations. This interpretation is based on the observed large matrix elements for exciting these states, which shows that we are dealing with a mode of excitation involving the coherent motion of a large number of nucleons. Moreover, the measured cross-sections for exciting the states in inelastic scattering processes can be rather well accounted for by assuming that the excitation is associated with a deformation of the nuclear equipotential surfaces of the form (3).

Strongly excited octupole modes ($\lambda = 3$) are also observed as a prominent feature of the low-energy nuclear spectra. Less evidence is so far available on vibrational modes of higher multipolarity.

As mentioned above, a basic property of a vibrational mode is the possibility of repeating the excitations. Because of experimental difficulties associated with the study of multiple excitations, the only evidence so far concerns the quadrupole mode. One finds that, indeed, the excitation can be repeated, but one observes major anharmonicity effects. The quantitative analysis of these phenomena is among the important areas of current development, but qualitatively, the anharmonicity can be simply understood in terms of the tendency of the nucleons outside closed shells to produce an ellipsoidal equilibrium shape. For configurations with relatively few such particles, the equilibrium remains spherical, but the stability decreases with the addition of particles in unfilled shells, as testified by the decreasing vibrational frequency. For nuclei with sufficiently many particles outside closed shells, the equilibrium shape is no longer spherical. The transition to a non-spherical equilibrium is revealed by the onset of rotational band structure in the nuclear spectra.

The observed stable nuclear deformations preserve axial symmetry, and the vibrations about such a deformed equilibrium can therefore be specified by the quantum number ν, representing the projection of angular momentum on the internal symmetry axis. The total angular momentum of a vibrational quantum is no longer a constant of the motion, but the shape vibrations can be classified by a quantum number λ representing the number of angular nodes in the density variation.

The best studied shape oscillations in the deformed nuclei are of quadrupole type ($\lambda = 2$); one observes $\nu = 0$ modes (β-vibrations) associated with density oscillations preserving axial symmetry as well as $\nu = \pm 2$ modes (γ-vibrations) representing excursions away from axial

symmetry. A shape deformation with $\lambda = 2$ and $\nu = \pm 1$ is equivalent to a rotation and therefore does not occur as a vibrational degree of freedom.

The rotational motion of the nucleus as a whole may affect the intrinsic motion through the Coriolis and centrifugal forces. Such Coriolis couplings are found to be especially important for the octupole modes in the deformed nuclei on which recently much new evidence has been obtained.

The occurrence of non-spherical equilibrium shapes in nuclei provides an instructive example of a violation of a symmetry possessed by the total Hamiltonian. The symmetry is restored by the inclusion of the collective rotational motion.

A new dimension to the nuclear vibrational spectra is provided by the occurrence of two types of nucleons, neutrons and protons.

The motion of neutrons and protons is strongly coupled, and the eigen-modes tend to represent oscillations in which the neutrons and protons move either in phase or in opposite phase. We can describe this symmetry in terms of the charge symmetry operation $\mathscr{R}_\tau$, which interchanges neutrons and protons. If we consider a nucleus with $N = Z$ and ignore the effect of the charge unsymmetric Coulomb forces and other electromagnetic inter-actions in modifying the nuclear wave function, the stationary states and the quanta of excitation can be labelled by the eigenvalue $r_\tau = \pm 1$ of $\mathscr{R}_\tau$.

The low-frequency shape oscillations discussed above represent symmetric motion of neutrons and protons, and the quanta have $r_\tau = +1$. The $r_\tau = -1$ modes represent a motion of neutrons against protons (polari-zation modes). The first collective mode of excitation to be identified in nuclei, the giant photoresonance, is of this type, and has $\lambda = 1$. In de-formed nuclei this mode is observed to split into two components with $\nu = 0$ and $\nu = \pm 1$, respectively.

If we are dealing with a nucleus with a large neutron excess, the ex-citations of neutrons and protons involve orbits with different single-particle quantum numbers ($nj\ell m$ in spherical, $Nn_z\Lambda K$ in deformed nuclei). The vibrational quanta can be decomposed in terms of single-particle ex-citations, and at this microscopic level the charge symmetry is therefore strongly broken. However, it may still be possible to characterize the collective properties of the vibrations, i.e. the associated oscillations in the average nuclear field and the multipole moments of long wavelength, by the charge-symmetry quantum number. Indeed, the available evidence as well as theoretical analyses suggest that, in this sense, the charge symmetry is approximately fulfilled also for the shape vibrations and polarization oscillations in heavy nuclei. For example, the inelastic scattering of α-particles and deuterons, which acts symmetrically on neutrons and protons, can excite the shape oscillations ($r_\tau \approx + 1$), but not the polarization mode ($r_\tau \approx - 1$).

Charge symmetry is part of a more general invariance, the charge independence or isospin symmetry. The variations in the nucleonic density can be expressed in terms of isoscalar ($\tau = 0$) and isovector ($\tau = 1'$) components. The charge-symmetry operation represents a rotation through the angle π, about an axis in isospace, perpendicular to the x-axis, and the quantum number r_τ is therefore

$$\hat{r}_\tau = (-1)^\tau \tag{4}$$

Thus, the charge-symmetric modes are isoscalar while the anti-symmetric modes are isovector.

The quanta of the polarization modes considered above have no charge and hence have the isospin component $\mu_\tau = 0$. The isovector modes involve additional components with $\mu_\tau = \pm 1$, whose properties are related to the $\tau = 1$, $\mu_\tau = 0$ modes by rotations in isospace. The $\mu_\tau = \pm 1$ excitations involve the transformation of a proton into a neutron, or vice versa, and represent modes of oscillation with no classical analogue.
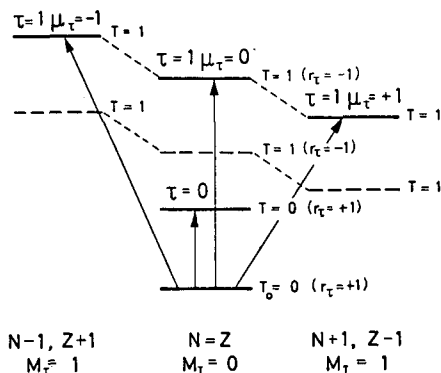
FIG. 1. The isospin structure of vibrational modes in a nucleus with N = Z and isospin $T_0 = 0$ in the ground state.
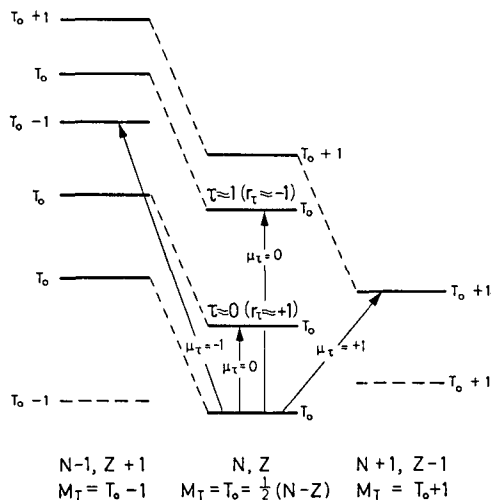
FIG. 2. Isospin structure for a nucleus with neutron excess.

The isospin structure of vibrational modes in a nucleus with N = Z and isospin $T_0 = 0$ in the ground state is indicated schematically in Fig. 1. Isobaric analogue states are connected with thin broken lines. The ground states of the adjacent nuclei and their analogue state in the target are indicated by dashed lines.

For a nucleus with neutron excess, the corresponding pattern is schematically illustrated in Fig. 2. The states are labelled by the total T quantum number and the excitations can be classified in terms of the isospin

change $\Delta T = T - T_0$. The target nucleus is fully aligned in isospace
($M_\tau = T_0$) and it is convenient first to focus attention on the excitations
with $\mu_\tau = \Delta T$, which lead to states remaining fully aligned in isospace.
The excitations to the isobaric analogue states ($\Delta T - \mu_\tau > 0$) can be obtained
from those to the fully aligned states by exploiting the rotational invariance
in isospace; the transition amplitudes are proportional to the vector
addition coefficient $\langle T_0\, T_0 \tau\, \mu_\tau / T T_0 + \mu_\tau \rangle$ and the transition probabilities
thus decrease approximately by a power of T_0, for each unit of $\Delta T - \mu_\tau$.
For small values of T_0, the excitation of an isovector mode would lead
to a multiplet with $\Delta T = -1, 0, 1$, with properties related by symmetry.
However, even for moderate values of the neutron excess, the strong
coupling between the isospins of target and vibration implies that tran-
sitions with different values of ΔT are no longer related in a simple manner.
The $\Delta T = 0$ modes are the ones considered above, whose collective pro-
perties can be approximately characterized by the charge-symmetry
quantum number r_τ.

The study of modes involving charge exchange is only in its infancy.
With the tools presently available we may soon learn a great deal more
about the isospin structure of the nuclear modes of excitation.

The total angular momentum of a vibrational mode consists of orbital
and spin components κ and σ, coupled to the resultant λ. The parity of a
quantum is determined by the orbital multipole order

$$\pi = (-1)^\kappa \tag{5}$$

and thus, for given (λ, π), we can have two different (κ, σ) components,
except for $\lambda = 0$,

$$
\begin{aligned}
\pi &= (-1)^\lambda \quad , \quad \kappa = \lambda, \quad \sigma = 0 \text{ or } 1 \\
\pi &= (-1)^{\lambda+1} \quad \kappa = \lambda \pm 1, \ \sigma = 1
\end{aligned}
\tag{6}
$$

If only central forces acted between nucleons, the orbital and spin
motion would be uncoupled, and the vibrational quanta would have definite
quantum numbers σ and κ (for a spherical nucleus). The spin-orbit inter-
action and tensor forces, however, imply a coupling between modes with
the two different sets of quantum numbers (κ, σ), for given (λ, π). These
non-central interactions affect the nuclear structure in a major way through
the spin-orbit coupling in the single-particle potential. Thus, for example,
vibrational modes may involve nucleonic orbits with $j = \ell + \frac{1}{2}$ with little
contribution from the spin-orbit partners with $j = \ell - \frac{1}{2}$. Such a dissymmetry
involves a complete violation of (κ, σ) symmetry at the microscopic level.
However, as for the charge symmetry referred to above, it may still be
possible to characterize the collective properties of the vibration by approxi-
mate quantum numbers κ and σ. For example, there is evidence that the
low-energy modes referred to as shape oscillations have $\sigma \approx 0$ as suggested
by the interpretation of these modes. The evidence comes from the obser-
vation that the nuclear field associated with these excitations is only weakly
spin-dependent.

Only rather little evidence is so far available concerning the occurrence
of vibrational modes with $\sigma \approx 1$. One may expect modes of spin-wave type,
by which a local excess of spin-up relative to spin-down propagates through

the nucleus; such modes are analogous to the polarization modes referred to above. Additional spin excitation modes may be associated with the presence of unsaturated spins in the nuclear ground state, and represent oscillations in the total spin and orbital angular momenta of the nucleus.

The spin and isospin symmetries, each representing an SU_2 invariance, can be combined to form an SU_4 invariance group, the supermultiplet symmetry of Wigner. For example, the giant dipole excitation with $\kappa = 1$ and $(\sigma, \tau) = (0, 1)$, together with corresponding spin-wave excitations with $\kappa = 1$ and $(\sigma, \tau) = (1, 0)$ and $(0, 1)$ would constitute a 15-dimensional representation of SU_4. (The $(\sigma, \tau) = (0, 0)$ dipole mode represents centre-of-mass motion, as mentioned above.)

Quite a new variety of vibrations occur when we consider the possibility of quanta possessing a non-vanishing nucleon number, α. The $\alpha = 0$ vibrational modes considered above involve variations in the nucleonic density, i.e. excitations of nucleons or particle-hole correlations. In the $\alpha = \pm 2$ modes, we are studying collective phenomena generated by particle-particle or hole-hole correlations. Correlations of this type are associated with the pairing effect, which is such a prominent feature of the low-energy nuclear spectra. In a spherical nucleus, this mode of pair vibration has $\lambda \pi = 0^+$, and the quanta of excitation involve a superposition of configurations $(j^2)_0$ with two nucleons in the same single-particle orbit, j.
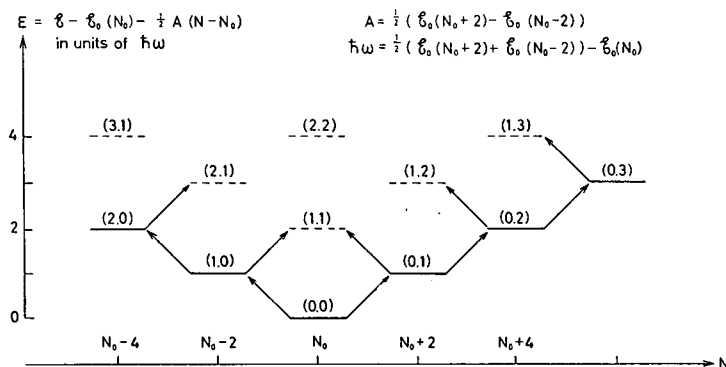
FIG. 3. Pattern of pair vibrations involving particles of one type (neutrons or protons).

The pattern of such pair vibrations involving particles of one type (neutrons or protons) is illustrated in Fig. 3. The excitations are based on the ground state of the nucleus with neutron number, N, assumed to represent a closed shell configuration. There are two modes with $\alpha = \pm 2$, and the states are labelled by ($n_\alpha = -2$, $n_\alpha = +2$), giving the number of quanta of each type. The states $(n_{-2}, 0)$ and $(0, n_2)$ represent the ground states of the nuclei with neutron number $N = N_0 - 2n_{-2}$ and $N = N_0 + 2n_2$, respectively. The energy E plotted in Fig. 3 is obtained from the total energy $\mathscr{E}$ by subtracting the ground-state energy $\mathscr{E}_0 (N_0)$ for $N = N_0$ and a linear term in N whose coefficient is so adjusted that $E(0, 0) = 0$ and $E(1, 0) = E(0, 1) = \hbar \omega$. The spectrum illustrated corresponds to the harmonic approximation, in which the interaction between the excitation quanta is neglected. The energy is then $E(n_2, n_{-2}) = (n_2 + n_{-2}) \hbar \omega$.

The vibrational amplitude a for the $\alpha = \pm 2$ oscillations is a measure of the pairing field (or pairing density), which represents the creation or

annihilation of two nucleons, at the space point considered. This field has no classical analogue, and a state with a finite average value of a does not possess a definite number of particles.

The collective oscillations of the pairing field are characterized by large excitation probabilities in two-nucleon transfer reactions, such as the (t, p) process by which two neutrons closely correlated in space are transferred to the target. Recently, collective modes with the properties expected for neutron pair vibrations have been found in the study of two-nucleon transfer reactions, and the subject is at present in rapid development.

The observed spectra show deviations from the harmonic approximation which one may attempt to describe in terms of effective interactions between the quanta. Such anharmonicity effects are expected to increase as more and more quanta are added to the closed-shell state. When many quanta are present, however, one may treat the pair correlation effect in terms of a static deformation of the pairing density. The problem is somewhat similar to the one encountered in the quadrupole vibrational spectrum of a spherical nucleus if we consider states with many quanta and large values of the angular momentum. Because of the centrifugal effect, the nuclear shape for such states possesses an average deformation, and one may obtain an approximate description by separating the motion into rotational motion and intrinsic motion with respect to the deformed shape.

Time does not permit a proper discussion of these phenomena, the study of which may shed new light on the nuclear pair-correlation phenomena which, in turn, is intimately related to the correlation effect for the electrons in the superconducting metal. New phenomena, which remain largely unexplored, are connected with the pairing modes involving neutron-proton correlations as well as the modes with non-vanishing angular momentum.

Although, in this brief survey, it has only been possible to touch upon a few topics, I hope to have conveyed an impression of the richness of the phenomena and the variety of patterns encountered in the exploration of the nuclear vibrational modes. The discussion has been based on a collective description, but one may also attempt to analyse the vibrational motion in terms of individual-particle components.

The main mechanism for generating the vibrational motion appears to be the coupling between the nucleonic excitations and the field they generate. On this basis, one can obtain an immediate qualitative explanation of many of the prominent features of the vibrations. As regards the quantitative analysis, one must recognize that we are dealing with properties of the nuclear material and thus of similar nature and subtlety as, for example, the estimate of the average nuclear density and potential.

The occurrence of collective motion and the relationship to underlying particle degrees of freedom is a general theme in many domains of quantal physics (plasma oscillations in an electron gas, π-mesons as nucleon-antinucleon correlations, etc.). In a finite system, such as the nucleus, there is no sharp distinction between excitations of individual nucleons (particle-hole configurations or two-quasiparticle configurations) and collective modes, and it has, therefore, been especially important to combine microscopic and macroscopic approaches.

BASIC CONCEPTS OF THE
SHELL MODEL AND SOME SIMPLE
EXCITATION MODES IN NUCLEI[†]

G. ALAGA
Institute "Rudjer Bošković"
Zagreb, Yugoslavia

Abstract

BASIC CONCEPTS OF THE SHELL MODEL AND SOME SIMPLE EXCITATION MODES IN NUCLEI.
1. The basic ideas of the shell model and the properties of single-particle states; 2. Simple features of some two-body and many-body systems.

1. THE BASIC IDEAS OF THE SHELL MODEL AND THE PROPERTIES OF SINGLE-PARTICLE STATES

In the courses given by D. Brink and I. Šlaus in these Proceedings we obtain much information on the present state of knowledge on free nucleon-nucleon interaction. In addition, the gross features of the nuclear many-body system such as binding energies and density distributions have been discussed from the macroscopic point of view (D. Brink, J. Németh and Z. Szymański, also in these Proceedings). Before turning to the discussion of the modes of excitations of nuclei it is instructive to review some of the consequences of the bulk properties.

The most significant and fascinating property of finite nuclei is the fact that the radii are proportional to $A^{1/3}$

$$R = r_0 A^{1/3} \tag{1}$$

with r_0 as the constant of proportionality. An immediate consequence is the fact that nuclear density is independent of the number of nucleons A. Another fact is that the nuclear density is rather small compared with that of closely packed nucleons. The estimate may be obtained as follows. Consider the hard core radius c = 0.5 fm as a distance of the closest approach of two nucleons. The ratio of nuclear density and that of closely packed nucleons is

$$\rho_N / \rho_{c.p} = \left(\frac{c}{2r_0}\right)^3 \sim 0.01 \tag{2}$$

taking $r_0 = 1.1$ fm. Thus we may further assume that nucleons move almost independently. Independent evidence may be obtained from neutron scattering experiments (Fig.1). Comparing the black-box cross-section to the measured one it is possible to conclude that the mean free path of neutrons

[†] These lecture notes were written by V.R. Pandharipande and L. Šips.
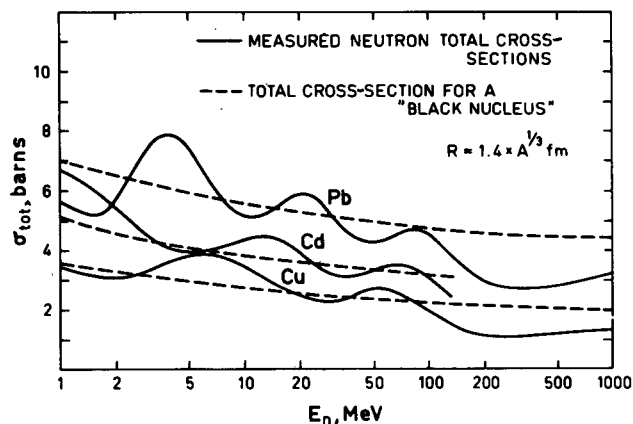
FIG.1.   Neutron-scattering cross sections.

in the nucleus is larger than the size of the nucleus. In a rough approxi-
mation we may then think of a nucleus as a degenerate Fermi gas. We
obtain for the density

$$\rho = \frac{A}{V} = \frac{2}{3\pi^2} k_F^3 = \frac{3}{4\pi r_0^3} \qquad . \tag{3}$$

which yields the relation

$$k_F = \left(\frac{9\pi}{8}\right)^{1/3} \frac{1}{r_0} \tag{4}$$

The kinetic energy of the most energetic nucleon is easily calculated
to be ($r_0 = 1.1$ fm)

$$T_F = \frac{\hbar^2 k_F^2}{2m} \sim 40 \text{ MeV}$$

To provide for the observed binding energy per nucleon (~ 8 MeV), the
average potential within which the nucleons are contained should have a
depth of about 50 MeV. Here Coulomb energy has not been taken into
account. The consequence of this is that in heavy nuclei the depth of the
nuclear potential as seen by protons is approximately 5 MeV deeper than
that seen by neutrons.

The excited state spectra in the Fermi gas model are independent of
the number of nucleons. The observed spectra, however, do show strong
dependence on A. Besides, the measured separation energy for the last
nucleon shows slight fluctuations (Fig.2). Similar fluctuations in the atomic
case (Fig.3) are much more pronounced and have been attributed to the
shell structure. Thus the shown fluctuations of the nuclear "ionization
potential" suggest the presence of the shell structure in nuclei. The
observed smallness of the fluctuations may be understood by comparing
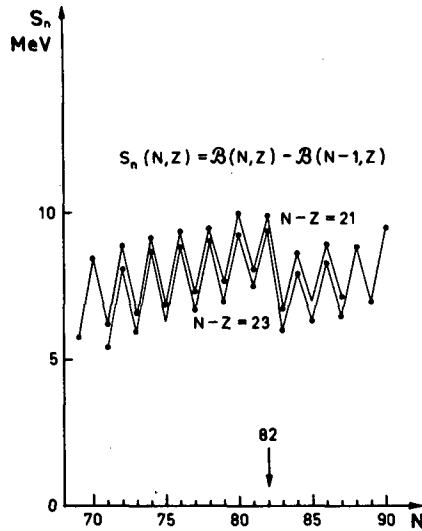
FIG.2.   Measurements of the separation energy.
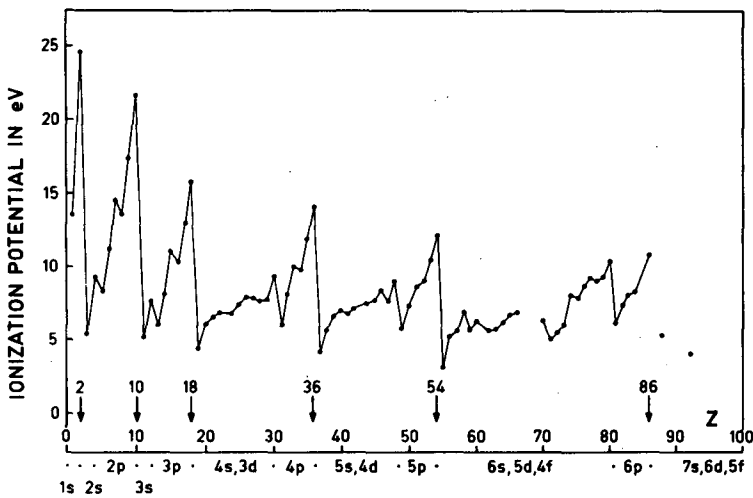
FIG.3.   Fluctuations of the ionization potential in atoms due to shell structure.

the strength of the binding in the H_2 molecule and the deuteron (Fig. 4).
Figure 4 shows that the binding energy, expressed in the characteristic unit
involving the size and the mass of the system $\hbar^2/Mr_c^2$, is by four orders of
magnitude larger in the H_2 molecule than in the deuteron. As a consequence
the wave function of the ground state of the H_2 molecule is well contained
within the range of the potential, whereas the deuteron radius is larger
than the range of the nuclear potential. Thus the observed smallness of
shell effects in the nuclear "ionization potential" can be attributed to the
relatively weak binding in nuclei.
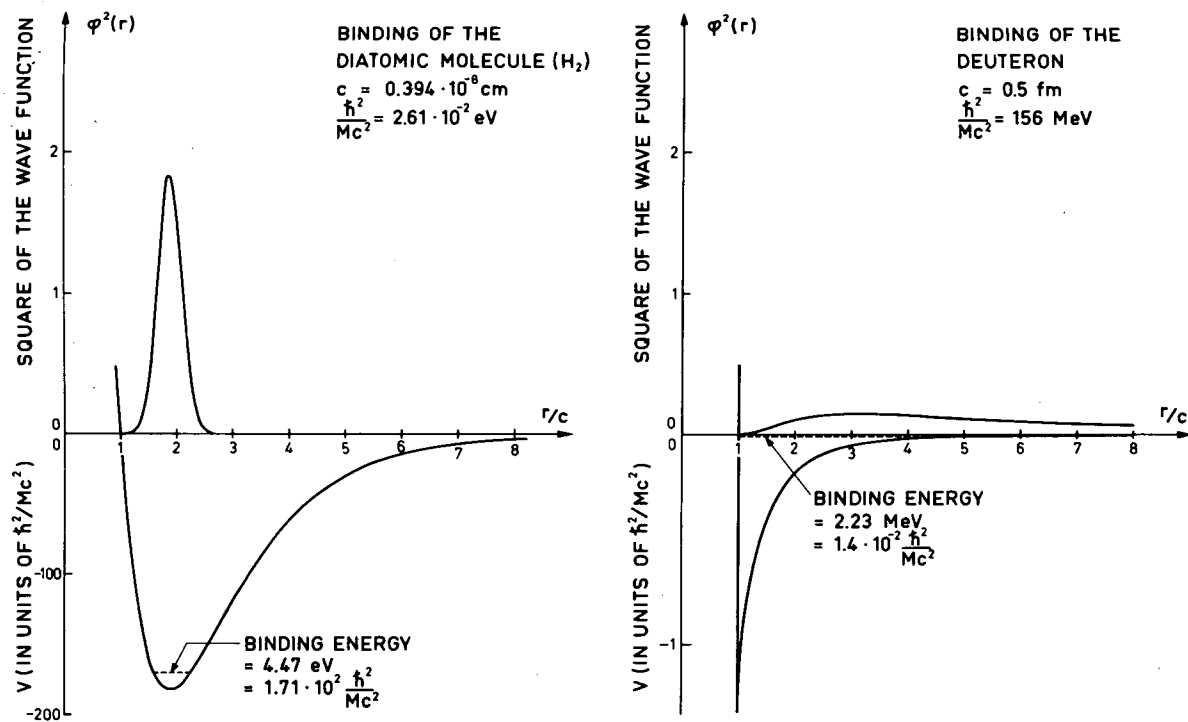
FIG. 4. Binding energy for the H_2 molecule and the deuteron.

Experimentally, the shell closures in nuclei are detected at the neutron N and proton P so-called magic numbers

$$2, 8, 20, 28, 50, 82, 126, 184^1 \dots$$

In the early days of the nuclear shell model, different types of average potentials, in which nucleons were put to move independently, were used. They range from harmonic oscillator to square well, wine bottle etc. However, none of these could provide for shell closures at the above mentioned magic numbers. The proper magic numbers were obtained independently by Goeppert-Meyer and by Haxel, Jensen and Suess adding a one-body spin-orbit term to the average field. The average potential felt by nucleons assumes the form

$$V(r) + U(r) \vec{\ell} \cdot \vec{s}$$

where $V(r)$ and $U(r)$ characterize the radial shape of the average potential and spin-orbit term, respectively. The origin of the spin-orbit term may be sought in the average of the two-body $\vec{L}_{12} \cdot \vec{S}_{12}$ term in the free nucleon-nucleon potential (see D. Brink, these Proceedings). The second-order tensor force may also contribute.

The range of the interaction is small compared with the observed thickness of the nuclear surface. Thus,one can state that the average potential will follow the nuclear density distribution and may be written as

$$V(r) = V_0\, f(r) = V_0\, \frac{1}{1 + \exp\left(\dfrac{r-R}{a}\right)} \qquad (5)$$

This form is known as the Woods-Saxon potential. Here $f(r)$ is the familiar function describing the nuclear-density distribution (see D. Brink, these Proceedings). For the $\vec{\ell} \cdot \vec{s}$ term we assume the form

$$V_{\ell s}(r) = (V_{\ell s})_0\, r_0^2 \frac{1}{r} \frac{\partial f(r)}{\partial r} \vec{\ell} \cdot \vec{s} \qquad (6)$$

The gradient form of the radial part can be understood intuitively, because the gradient of the potential defines the radial direction which, with the particle motion, can couple the pseudovector to the nuclear spin.

The experimentally observed spin-orbit splittings can be described, especially in the lead region, by the following expression[2]

$$\epsilon_{\ell s} = -20\, (\vec{\ell} \cdot \vec{s})\, A^{-2/3} \;\; \text{MeV} \qquad (7)$$

The evaluation of expression (7) gives, for example, the values shown in Table I.

---

[1]   In superheavy nuclei there seems to be an exception for P = 114 (see Z. Szymański: Lecture notes).

[2]   Estimates from the Hamada-Johnston potential give 30 MeV · $A^{-2/3}$ (See Bohr-Mottelson, Lectures on Nuclear Structure).

TABLE I.   EVALUATION OF EXPRESSION (7)

		$(\epsilon_{\ell s})_{calc}$ (MeV)	$(\epsilon_{\ell s})_{expt}$ (MeV)
^{15}O	$1p_{3/2} - 1p_{1/2}$	4.9	6.2
^{17}O	$1d_{5/2} - 1d_{3/2}$	7.6	5.08
^{207}Pb	$3p_{3/2} - 3p_{1/2}$	0.86	0.89
^{207}Pb	$2f_{1/2} - 2f_{5/2}$	2.0	1.77
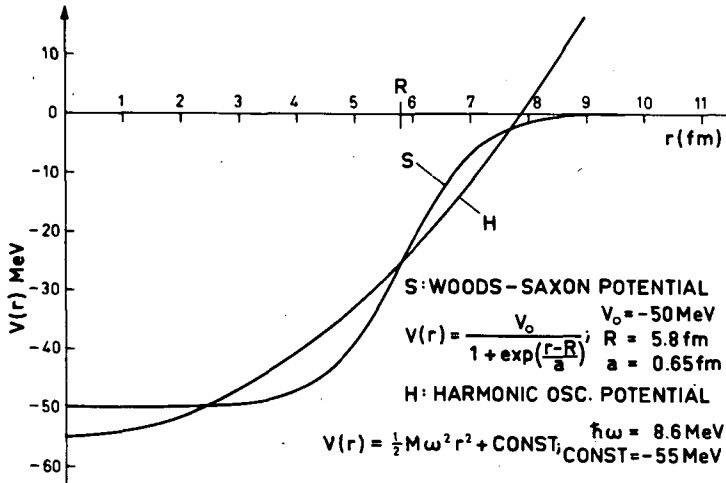
FIG.5.   Comparison of Woods-Saxon potential with harmonic-oscillator potential.

In an attempt to calculate systematically the single-particle levels and binding energies of the single-particle orbitals the potential

$$V(r) = V_0 \, f(r) + (V_{\ell s})_0 \; r_0^2 \, \frac{1}{r} \, \frac{\partial}{\partial r} \, f(r) \, \vec{\ell} \cdot \vec{s}$$

with the parameters ($R = r_0 \times A^{1/3}$)

$$r_0 = 1.27 \text{ fm}, \qquad a = 0.67 \text{ fm}$$

$$V_0 = \left[-51 + 33.1 \, \frac{N-Z}{A} \right] \text{ MeV}$$

$$(V_{\ell s})_0 = -0.439 \, V_0 = \left[21.9 - 14.5 \, \frac{N-Z}{A} \right] \text{ MeV}$$

can be used. The result for neutrons can be seen in Fig.5. The discrepancy of about 30% in the excitation energies of the single-particle orbitals may be attributed to the velocity dependence of the average potential.

The eigenfunctions of such a spherically symmetric potential have the quantum numbers n, ℓ and j and can be written as

$$\Psi^m_{n\ell j}(r, \theta, \phi) = R_{n\ell j}(r)\,\Phi^m_j(\theta, \phi) =$$

$$= R_{n\ell j}(r) \sum_{m_\ell m_s} \langle \ell\, m_\ell\, s\, m_s | j\, m \rangle \, Y^{m_\ell}_\ell(\theta, \phi)\, \kappa^{m_s}_s \tag{8}$$

$Y^{m_\ell}_\ell(\theta, \phi)$ are spherical harmonics, $\kappa^{m_s}_s$ is the spin function and $\langle a\alpha\, b\beta | c\gamma \rangle$ are vector coupling coefficients. The normalization of the wave function (8) is such that

$$\int_0^\infty R^2_{n\ell j}(r)\, r^2 dr = 1 \quad \text{and} \quad \int \Phi^{m*}_j(\theta, \phi)\, \Phi^{m'}_{j'}(\theta, \phi)\, d\Omega = \delta_{jj'}\, \delta_{mm'}$$

It is worth noting that the quantity $R^3_0 R^2_{n\ell j}(R_0)$ (R_0 is the nuclear radius) is fairly independent of the configuration, and for nucleons bound by 5-10 MeV assumes a value of ~1.4. Of course, the states calculated in the above average potential agree only qualitatively with the observed ones. In the following we shall try to find some of the reasons for the discrepancies.

A typical sequence of the single-particle orbitals of the shell-model potential is shown in Fig.6. It accounts for the closure of shells. The ground-state spins of the closed-shell nuclei are zero with positive parity and the general property of their excitation spectra is a large gap in energy between the ground and the first excited state. The cause of this gap in the spectrum is the fact that in order to form an excited state, we have to take a particle out of the closed shell and promote it to the next major shell which is well separated in energy. As an example of the closed-shell nucleus we shall take ^{208}Pb (Fig.7), which has been very extensively studied. The unperturbed energy of the lowest excited particle-hole state in ^{208}Pb is ~3.5 MeV. One finds (see Fig.7) that all of the excited states indeed occur above this energy except for the first excited 3$^-$ state, which we shall discuss in some detail later. The spins and parities of 3.47 4$^-$ and 5$^-$ state show that they may be formed by exciting a $p_{1/2}$ nucleon to the next $g_{9/2}$ orbital. The spins and parities of the low-lying states of the neighbouring odd-A nuclei ^{207}Tl, ^{209}Bi, ^{207}Pb and ^{209}Pb (shown in Fig.7) nicely follow the sequence predicted by the shell model. However, there are also some positive parity states in ^{209}Bi and ^{207}Pb which can readily be explained by the coupling of the particle (hole) to the 3$^-$ state of the ^{208}Pb core. As is seen in Fig.7 these states occur at about the energy of the ^{208}Pb 3$^-$ state. Thus, it seems that the energies, spins and parities of the low-lying levels can be well understood in terms of the simple shell model.

Besides energies, spins and parities one can also study the static magnetic and quadrupole moments of the shell-model states. In the spirit of the simple shell model the nucleon spins are coupled pairwise to the

spin-zero states. All even-even nuclei should therefore have (and they do)
0^+ ground states and have zero static moments. In odd-A nuclei the spin
and parity of the ground state are determined by the spin and parity of
the last unpaired nucleon. As a consequence the static moments in odd-A
nuclei should be given as those of the last nucleon. These moments can then
be calculated by using the single-particle wave function (8) obtained from
the shell-model Hamiltonian. For non-interacting point particles the
magnetic moment assumes the form (measured in nuclear magnetons)

$$\vec{\mu} = g_\ell \, \vec{\ell} + g_s \, \vec{s} \tag{9}$$
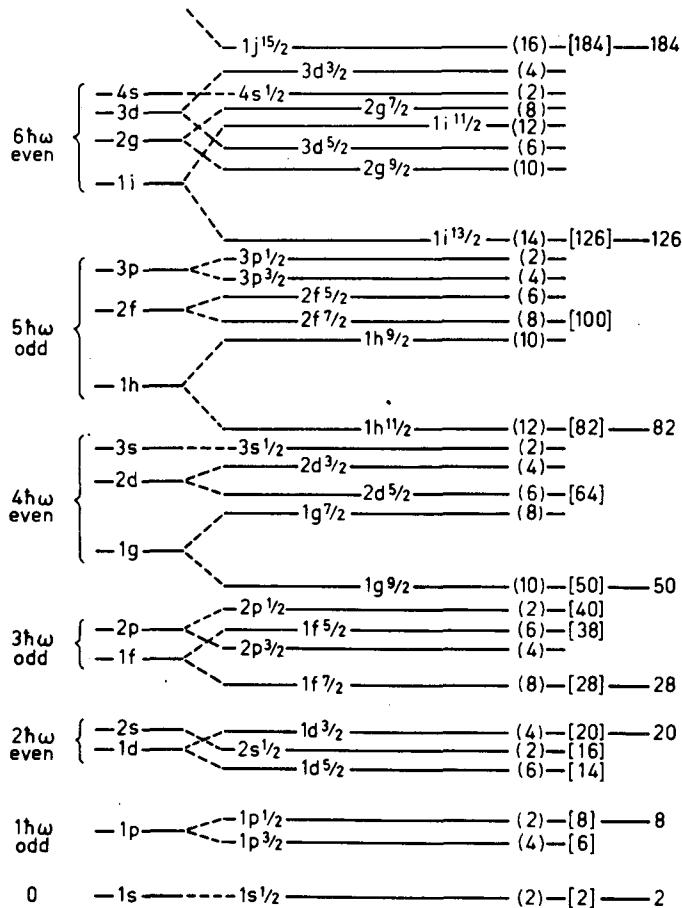
FIG.6. A typical sequence of single-particle orbitals in shell-model potential.

5.28 ——— 1⁻
5.25 — 5.13 ———
5.03 ———
4.97 ———
4.89 ——— 0⁺
4.69 ——— 3⁻
4.60 ——— 8⁺

4.53 ——— 3/2
4.35 ——— 1/2
4.29 ——— 5/2⁻
4.13 ——— 3/2⁻
4.05 ———

4.39 === 6⁺
4.37 === 4⁺
4.23 ———
4.13 ——— 2⁺

4.41 ——— 1/2⁻

3.64 ——— 5/2⁺
3.48 ——— 9⁻⁷/²
3.43 ——— h⁻¹₉/₂

3.71 ——— 5⁻
3.47 ——— 4⁻

3.64 ——— p₁/₂

3.19 ——— 5⁻

3.12 ——— p₃/₂

2.83 ——— f5/2

2.65 ——— 7/2⁺
2.61 ——— 5/2⁺
2.34 ——— t⁻¹₇/₂

2.62 ——— 3⁻

2.51 ——— d3/2
2.49 ——— g7/2

2.74 ——— 15/2, 13/2, 9/2, 5/2, 11/2, 7/2, 3/2
2.49 ===

2.01 ——— s1/2

1.67 ——— d⁻¹₅/₂
1.34 ——— h⁻¹₁₁/₂

1.64 ——— t⁻¹₁₃/₂

1.56 ——— d5/2
1.42 ——— j15/2

1.61 ——— l13/2

0.89 ——— p⁻¹₃/₂
0.57 ——— t⁻¹₅/₂
0.35 ——— d⁻¹₃/₂

0.79 ——— i11/2

0.90 ——— l7/2

0 ——— s⁻¹₁/₂
$^{207}_{81}$Tl$_{126}$

0 ——— p⁻¹₁/₂
$^{207}_{82}$Pb$_{125}$

0 ——— 0⁺
$^{208}_{82}$Pb$_{126}$

0 ——— g9/2
$^{209}_{82}$Pb$_{127}$

0 ——— h9/2
$^{209}_{83}$Bi$_{126}$

FIG. 7. ^{208}Pb as an example of a closed-shell nucleus.

where $g_\ell = 1$ for protons and $g_\ell = 0$ for neutrons. g_s are anomalous g factors of a proton and a neutron, 5.586 and -3.826, respectively. The evaluation gives

$$\mu = \langle jm = j | \vec{\mu} | jm = j \rangle = (j - 1/2)g_\ell + 1/2\, g_s \quad \text{for} \quad j = \ell + 1/2$$

$$= \frac{j}{j+1}[(j+3/2)g_\ell - 1/2\, g_s] \quad \text{for} \quad j = \ell - 1/2$$

(10)

These values are known as the Schmidt values.

The quadrupole tensor operator classically has the well-known form

$$Q_{ik} = \iiint (3x_i x_k - r^2 \delta_{ik})\rho(\vec{x})\, d\tau$$

What is measured is the Q_{zz} component of the quadrupole tensor which we may write

$$Q_{zz} = \iiint (3z^2 - r^2) \rho \, (\vec{x}) \, d\tau$$

and for a uniformly charged axially symmetric ellipsoid we have

$$Q_{zz} = Q \frac{2}{5} \, (c^2 - a^2) \tag{11}$$

Expression (11) is called the classical quadrupole moment, c and a are semiaxes of the ellipsoid, and Q is the total charge.

An analogous quantum-mechanical expression, divided by the charge and called the spectroscopic quadrupole moment, is

$$Q(J) = \frac{1}{e} \frac{16\pi}{5} \left\langle J\,M = J \,\middle|\, Q_2^0 \,\middle|\, J\,M = J \right\rangle = \sum_k \iiint \psi_J^{*} \, (3z_k^2 - r_k^2) \, \psi_J^J \, d\tau \tag{12}$$

The summation includes only proton co-ordinates. If we wish to know the value for any M it is simply calculated to be

$$Q(M) = \frac{3M^2 - J(J+1)}{J(2J-1)} \, Q(J)$$

The single-particle value calculated with the shell-model wave function is (for the last unpaired proton)

$$Q_p^j = - \frac{2j-1}{2j+2} \, \left\langle r^2 \right\rangle_{n\ell j} \approx - \frac{2j-1}{2j+2} \frac{3}{5} \, R_0^2 \quad \text{for} \quad j = \ell \pm 1/2 \tag{13}$$

$\left\langle r^2 \right\rangle_{n\ell j}$ denotes the mean value of r^2 using the wave function $R_{n\ell j}(r)$ and the last approximate equality is obtained by averaging r^2 over the uniformly charged sphere of the radius R_0. In explicit calculations, harmonic-oscillator wave functions are commonly used. One may immediately question the accuracy of such a calculation, but as we see in Fig. 8, the radial wave functions of a properly adjusted harmonic-oscillator well and the Woods-Saxon one are almost identical. The adjustment means the requirement that the root mean square of the radius of the last valence nucleon be equal to the nuclear radius.

Besides the static properties mentioned above one can investigate some of the dynamical ones such as transition probabilities for electromagnetic transitions. The interaction of the electromagnetic field with the nucleus is described by the coupling

$$H_\gamma = - \frac{1}{c} \int j_\mu (\vec{r}, t) \, A_\mu (\vec{r}, t) \, d\tau = \int (\rho V - \frac{1}{c} \vec{j} \cdot \vec{A}) \, d\tau \tag{14}$$
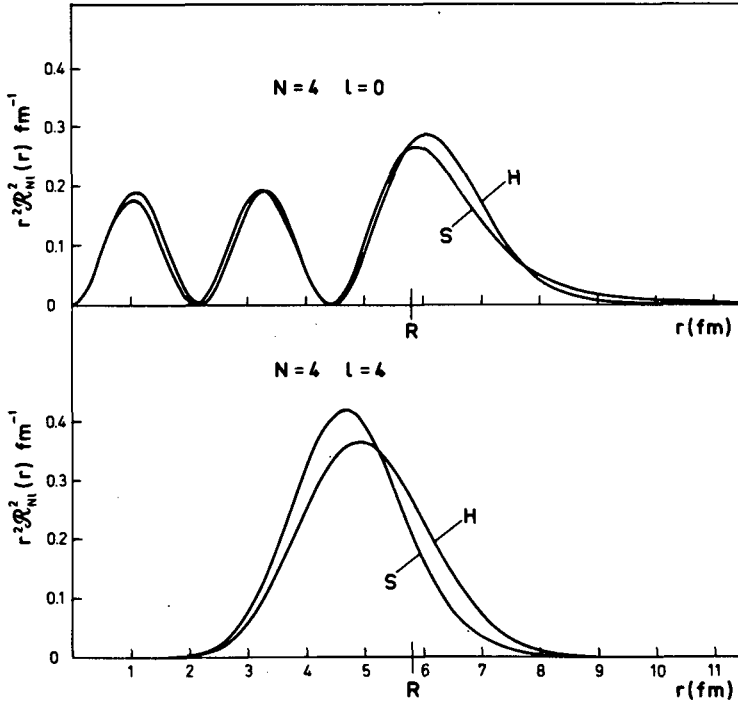
FIG.8.   Radial wave functions of a properly adjusted harmonic oscillator (H) and Woods-Saxon potential (S).

$A_\mu \equiv (\vec{A}, iV)$ is the electromagnetic four-vector potential and $j\mu \equiv (\vec{j}, ic\rho)$ the electromagnetic charge-current four-vector which satisfies the continuity equation

$$\nabla \cdot \vec{j} + \frac{\partial}{\partial t} \rho = 0 \qquad\qquad (15)$$

Equation (15) expresses the conservation of the electric charge. In the Coulomb gauge $V = 0$ possessing only transverse fields, the vector potential $\vec{A}$ satisfies

$$\Box A_\mu = \nabla \cdot \vec{A} = 0$$

Then the retarded plane-wave solution for the electric field $\vec{E}$ propagating in the z-direction can be written as

$$\vec{E} = a[\vec{e}\, e^{-i(\omega t - kz)} + c.c.] \qquad\qquad (16)$$

The amplitude a is a real number and $\vec{e}$ is the polarization vector. Expanding in multipoles[3] and assuming non-interacting point charges we obtain

$$\langle H_\gamma \rangle = -\frac{e}{2mc} \int \psi^* (\vec{p}\,\vec{A} + \vec{A}\,\vec{p})\,\psi\,d\tau - \mu \int \psi^*\,\vec{\sigma}\,\vec{H}\,\psi\,d\tau =$$

$$= \hbar\sqrt{2\pi}\,\left(\frac{\hbar\omega}{R}\right)^{1/2} \sum_{\ell\,\mu} (-i)^\ell \left[\frac{(2\ell+1)(\ell+1)}{\ell}\right]^{1/2} c_1^\mu \sum_m D_{m\mu}^\ell (z \to z')$$

$$\times \langle |\mu\, M_\ell^m - i\,E_\ell^m | \rangle \qquad (17)$$

where

$$M_\ell^m = \sum_r [\vec{\nabla}_r\, Y_\ell^m(\theta_r,\phi_r)\, j_\ell(k\,r_r)]\left[\frac{2}{\ell+1}\, g_\ell(r)\,\vec{L}_r + g_s(r)\,\vec{s}_r\right] \qquad (18)$$

and

$$E_\ell^m = \sum_r \frac{\ell}{2}\, [1 + \tau_3(r)]\, j_\ell(k\,r_r)\, Y_\ell^m(\theta_r,\phi_r) - k\, g_s(r)\,\vec{S}_r\vec{L}_r\, Y_\ell^m(\theta_r,\phi_r)\, j_\ell(k\,r_r) \qquad (19)$$

are the magnetic and the electric multipole operators, respectively. The second term in E_ℓ^m (19) is inversely proportional to the nucleon mass and can be neglected in the nuclear case, in contrast to the atomic case.

The expression for the transition probability can be calculated using Fermi's "golden rule"

$$W(k,\ell) = \frac{2\pi}{\hbar}\, |\langle H_\gamma \rangle|^2\, \rho(E) = \frac{8\pi}{\hbar}\, \frac{\ell+1}{\ell[(2\ell+1)!!]^2}\, k^{2\ell+1}\, B(\tau\ell) \qquad (20)$$

$B(\tau\ell)$ is the reduced transition probability of τ type and 2^ℓ pole radiation. It reads

$$B(\tau\ell) = \frac{1}{2I_i+1} \sum_{M_i M_f} |\langle I_f M_f | O_\ell^m(\tau) | I_i M_i \rangle|^2 \qquad (21)$$

The single-particle estimate for transition probabilities, to which we shall refer in the subsequent discussion, can be obtained as follows. Assume that only the valence particle participates and that its (or their, if there are more) radial wave function is constant within the nuclear volume.

---

[3] For details of multipole expansions see, e.g. Rose, Multipole Fields, or any advanced textbook.

For gamma rays of energy $\hbar\omega$ in MeV and the nuclear radius R_0 in fermis we obtain

$$W_E(k, \ell) \approx \frac{4.4(\ell+1)}{\ell[(2\ell+1)!!]^2} \left(\frac{3}{\ell+3}\right)^2 \left(\frac{\hbar\omega}{197}\right)^{2\ell+1} (r_0 A^{1/3})^{2\ell} \times 10^{21} \text{ s}^{-1} \tag{22}$$

$$W_M(k, \ell) \approx \frac{1.9(\ell+1)}{\ell[(2\ell+1)!!]^2} \left(\frac{3}{\ell+2}\right)^2 \left(\frac{\hbar\omega}{197}\right)^{2\ell+1} \left(\mu_p \ell - \frac{\ell}{\ell+1}\right)^2 (r_0 A^{1/3})^{2\ell-2} \times$$
$$\times 10^{21} \text{ s}^{-1} \tag{23}$$

Having the necessary expressions we are now ready to apply the simple shell model to real nuclei and compare its predictions with experimental findings.

As we mentioned earlier in ^{208}Pb, it has been observed that the 3^- state has the B(E3) value which is about 40 times larger than the single particle estimate. To explain such an enormous enhancement, one has to assume that this 3^- state is a superposition of many particle-hole excitations. The various components of this state must add their individual contributions and thus be coherent with respect to the E3 transition operator.

Recently it has been shown that the 3^- state really consists of many particle-hole excitations. The experiment was (p, p') resonance scattering through the isobaric analogue states of ^{209}Pb. The wave function of ^{209}Pb can be written as

$$\psi_k^m(^{209}\text{Pb}) = N_k^{m^+} | ^{208}\text{Pb}\rangle$$

$N_k^{m^+}$ is the operator which creates a neutron in the state k, m. The isobaric analogue state can be obtained by applying the isospin lowering operator

$$T_- = \sum_{J,M} P_J^{M^+} N_J^M \tag{24}$$

This gives

$$T_- \psi_k^m(^{209}\text{Pb}) = T_- N_k^{m^+}|^{208}\text{Pb}\rangle = \sum_{J,M} P_J^{M^+} N_J^M N_k^{m^+}|^{208}\text{Pb}\rangle$$

$$= P_k^{m^+}|^{208}\text{Pb}\rangle - \sum_{J,M} P_J^{M^+} N_k^{m^+} N_J^M |^{208}\text{Pb}\rangle \tag{25}$$

On inspecting Eq.(25) we see that the last term on the right-hand side represents the proton in the state J, M and a neutron particle-hole pair. The proton decay of this state then leaves the residual nucleus in the

excited neutron particle-hole state. It has been found experimentally
that the 3⁻ state at 2.61 MeV in ²⁰⁸Pb is populated through many analogue
resonances and thus should have the many particle-hole state character
we presumed earlier. However, the 4⁻ and 5⁻ state of ²⁰⁸Pb are popu-
lated mostly through one resonance, thus having the single particle-hole
state character.[4] Such a highly coherent collective 3⁻ state is generally
referred to as an octupole phonon state, and we shall discuss such states
in the next chapter.

    Looking at the spectra of odd-A nuclei near ²⁰⁸Pb (Fig.7) we found
that the low-lying states were those expected from the simple shell model.
We shall now compare their electromagnetic properties with the expectations
on the basis of the simple shell model. It has been found experimentally
that the magnetic moments of the closed-shell-plus-(minus)-one-nucleon
nuclei are generally smaller than the calculated ones (in magnitude) (Table II).

TABLE II. MAGNETIC MOMENTS OF NUCLEI WITH
CLOSED SHELLS PLUS (MINUS) ONE NUCLEON

Nucleus	Orbit	μ_{exp} (n.m.)	μ_{calc} (n.m.)
¹⁵O	$p_{1/2}^{-1}$	0.72	0.64
¹⁷O	$d_{5/2}$	-1.89	-1.91
¹⁷F	$d_{5/2}$	4.72	4.79
²⁰⁷Pb	$p_{1/2}^{-1}$	0.59	0.64
²⁰⁷Pb	$f_{5/2}^{-1}$	0.65 ± 0.05	1.37
²⁰⁹Bi	$h_{9/2}$	4.08	2.62

One could expect discrepancies because the particle (hole) outside the
closed shell will interact with the closed core and this part of the inter-
action has been left out in our simple shell-model picture. The remedy
for this discrepancy may be sought in polarization effects, which could
change the value of g_s as well as the form of the magnetic moment operator.
Note that the magnetic dipole operator is related to the magnetic-moment
operator (9) as

$$M(M1, \mu) = \left(\frac{3}{4\pi}\right)^{1/2} \frac{e\hbar}{2Mc} (\mu)_{\mu} \tag{26}$$

where $(\mu)_{\mu}$ denotes the spherical component μ of the vector $\vec{\mu}$ (9). It is
seen from the form of the M1 operator that it has allowed matrix elements
between the spin-orbit partners $j = \ell \pm 1/2$ only. Consider the spin-dependent

---
[4] For a detailed discussion see lectures by von Brentano (these Proceedings).

part of the central force $V_\sigma(r_{12})\vec{\sigma}_1 \cdot \vec{\sigma}_2$. Via this part of the central force an extra core nucleon can excite the $j = \ell \pm 1/2$ state of the core to the $j = \ell \mp 1/2$ state outside the core, causing thereby an admixture of the two states

$$\left|\ell+1/2, m\right\rangle \rightarrow \left|\ell+1/2, m\right\rangle - \frac{\langle V_\sigma \rangle}{\Delta\epsilon_{\ell s}} \; \sigma_{\text{ext}} \left\langle j = \ell-1/2, m\left|\vec{\sigma}\right|j = \ell +1/2, m\right\rangle$$

$$\times \left|\ell - 1/2, m\right\rangle \qquad (27)$$

σ_{ext} represents the spin of the external polarizing nucleon. As the magnetic moment thus generated is proportional to σ_{ext}, we can consider this polarization to be a renormalization of g_s by an amount

$$\delta g_s \approx - \frac{4\langle V_\sigma \rangle}{3\Delta\,\epsilon_{\ell s}} \; (g_s - g_\ell)\;(2j+1)\;\frac{2j-1}{2j} \qquad (28)$$

Here we have neglected the dependence of the polarizing field σ_{ext} on the position of the polarizing nucleon. However, there is another axial vector quantity which may be constructed, namely $(Y_2 \sigma_1)_1$, and it contains both position and spin coordinates of a nucleon. Such a term will cause a change in the magnetic moment operator

$$(\delta\mu)_\mu = \delta\,g_s (Y_2 \,\sigma_1)_{1,\,\mu} \qquad (29)$$

where the bracket on the right-hand side denotes the vector coupling. It is important to observe that the modification (29) can cause M1 transitions between $\Delta\ell = \pm 2$ states which transitions are 1-forbidden otherwise. In order to estimate the magnitude of δg_s and $\delta' g_s$, it is necessary to have two independent measurements. A tentative test may be made in the case of ^{207}Pb (Fig. 7) where the magnetic moments of $p_{1/2}^{-1}$ and $f_{5/2}^{-1}$ have been measured. From the observed E2/M1 ratio in the $f_{7/2}^{-1} - f_{5/2}^{-1}$ transition assuming the single-particle value with $e_{\text{eff}} = 0.9$ for the E2 component one obtains an M1 matrix element which is about half the single-particle one. From these one may consistently find $\delta g_s/g_s = -0.5$ and $\delta' g_s/g_s \sim 0.4$ yielding the correct M1 matrix element and

	exp	s.p.	corr.
$\mu(p_{1/2}^{-1})$	0.59	0.64	0.5
$\mu(f_{5/2}^{-1})$	0.65 ± 0.05	1.37	0.9

all in nuclear magnetons. The effective gyromagnetic ratios thus determined should be used in calculating the magnetic moments and transition probabilities with the shell-model wave functions. Unfortunately, at present, there are not too many cases involving different configurations known so that it is not possible to test the possible dependence of the effective gyromagnetic ratios on the configuration. From the start one could not expect them to be entirely configuration–independent.

There is yet another source of correction to the multipole operators and it comes from the velocity dependent interactions. In other words, the interaction will change the expression for the current used in the multipole expansion. An example of such an interaction is a two-body spin-orbit force

$$V_{so} = \frac{1}{2} \sum_{ik} V_{LS} (r_{ik}) (\vec{r}_i - \vec{r}_k) \times (\vec{p}_i - \vec{p}_k) \cdot \frac{1}{2} (\vec{\sigma}_i + \vec{\sigma}_k)$$

$$= \frac{1}{2} \sum_{ik} V_{LS} (r_{ik}) \vec{L}_{ik} \cdot \vec{S}_{ik} \tag{30}$$

Calculating the velocity of the kth particle

$$\vec{v}_k = \frac{i}{\hbar} [H, \vec{r}_k] = \frac{i}{\hbar} [H \vec{r}_k - \vec{r}_k H] = \frac{\vec{p}_k}{m} + \frac{i}{\hbar} [V, \vec{r}_k] \tag{31}$$

one immediately sees that the velocity dependence of the interaction will cause change in the velocity of particles, i.e. the relation between the momentum and the velocity is altered. In our example the commutator is readily evaluated to give

$$[\vec{L}_{ik} \cdot \vec{S}_{ik}, \vec{r}_s] = i\hbar \vec{S}_{ik} \times (\vec{r}_i - \vec{r}_k) [\delta_{ks} - \delta_{is}]$$

$$[V_{so}, \vec{r}_s] = -i\hbar \sum_k V_{LS} (r_{sk}) \vec{S}_{sk} \times (\vec{r}_s - \vec{r}_k)$$

Then, the final expression for the particle velocity reads

$$\vec{v}_s = \frac{\vec{p}_s}{m} - \sum_k V_{LS}(r_{sk}) (\vec{r}_s - \vec{r}_k) \times \vec{S}_{sk} \tag{32}$$

The new orbital angular momentum is thus

$$L'_s = \vec{r}'_s \times \vec{p}_s = \vec{L}_s - m \sum_k V_{LS} (r_{sk}) [\tau_3 (s) - \tau_3 (k)] \vec{r}_s \times [\vec{r}_s - \vec{r}_k) \times \vec{S}_{sk}] . \tag{33}$$

and the correction to the magnetic multipole operator is given by

$$\delta M_\ell^m = - \sum_k [\vec{\nabla}_k Y_\ell^m (\theta_k, \phi_k) j_\ell (k r_k) \frac{e\hbar}{(\ell+1)c} \tau_3 (k) \vec{r}_k \times [\vec{r}_s \times \vec{S}_k] V_{\ell s} (r_k) \tag{34}$$

$\tau_3(k)$ is the third component of the kth-particle isospin. The contribution to the static magnetic dipole moment is

$$\delta_\mu \approx - \frac{e\hbar}{c\sqrt{12\pi}} \, \vec{e}_1^{\,0} \tau_3 \left\langle V_{\ell s}(r) \, \vec{r} \times (\vec{\sigma} \times \vec{s}) \right\rangle \tag{35}$$

$$\delta_\mu \approx 0.15 \, \tau_3 \quad \begin{array}{c} \dfrac{2j-1}{2j+2} \\[2mm] \dfrac{-2j+3}{2j+3} \end{array} \quad \text{for} \quad \begin{array}{c} j = \ell + 1/2 \\[2mm] j = \ell - 1/2 \end{array} \text{, respectively.} \tag{36}$$

It is seen that the correction has different sign for protons and neutrons and is of the order of $1/10$ of the nuclear magneton. $\vec{e}_1^{\,0}$ is the zeroth component of the spherical tensor of rank one. Expression (35) can be cast into the form

$$\frac{1}{2} \, \vec{e}_1^{\,\mu} \cdot \vec{r} \times (\vec{r} \times \vec{\sigma}) = -\frac{1}{3} \, T_{12}^\mu \mu^2 - \frac{1}{3} \, r^2 \sigma_1^\mu \tag{37}$$

with

$$T_{J\lambda}^\mu = \sum_{m_s m_\lambda} \left\langle \lambda \, m_\lambda \, 1 \, m_s \big| J \mu \right\rangle Y_\lambda^{m_\lambda}(\theta, \phi) \sigma_1^{m_s}$$

Comparing the form of the correction term (37) with the polarization terms one can see that their form is the same. We should, therefore, say that taking the effective gyromagnetic ratios from the experiment we automatically include the above correction, too.

We shall now consider the static electric quadrupole moments and the E2 transition probabilities in nuclei having one valence nucleon outside the doubly closed shell. In the framework of the simple shell model the odd-N nuclei should not have any electric moments. However, it has been experimentally observed that such nuclei have both static and transition electric moments. Naturally, these moments are due to the polarization of the core which in turn causes a deformation of the core charge distribution. Also in the case of odd-Z nuclei the experimental moments are generally larger than those calculated from the simple shell model (13). One can hope to include the core polarization effects by attributing an effective charge to the valence nucleon:

$$(e_{eff})_{E2} = \frac{\left\langle I_f = j_f \| M(E2) \| I_i = j_i \right\rangle}{\left\langle j_f \| r^2 Y_2 \| j_i \right\rangle} = \frac{\text{experimental matrix element}}{\text{matrix element with } e = 1} \tag{38}$$

Such a procedure is meaningful if the effective charge obtained from the above definition does not depend critically on various j_i and j_f. It is,

TABLE III.   MEASURED B(E2) VALUES

Nucleus	$(\ell j)_i$	$(\ell j)_f$	$B(E2)_{sp}$ e^2 fm^4	$B(E2)_{exp}$ e^2 fm^4	e_{eff}/e
^{17}O	$s_{1/2}$	$d_{5/2}$	35	6.3	0.42
^{17}F	$s_{1/2}$	$d_{5/2}$	43	64	1.2
^{41}Sc	$p_{3/2}$	$f_{7/2}$	40	104	1.6
^{41}Ca	$p_{3/2}$	$f_{7/2}$	40	87	1.5
^{207}Pb	$f_{5/2}^{-1}$	$p_{1/2}^{-1}$	81	70	0.9
^{207}Pb	$p_{3/2}^{-1}$	$p_{1/2}^{-1}$	110	80	0.85
^{209}Pb	$s_{1/2}$	$d_{5/2}$	866	150	0.42

indeed, observed that the experimentally observed e_{eff} can be well approximated by the expression

$$(e_{eff})_{E2} \approx \frac{1}{2} e (1+\tau_3) + e'_{pol} \tag{39}$$

with $e'_{pol} \approx 0.5$ e. For example, the static quadrupole moment of the $5/2^+$ state in ^{17}O is experimentally found to be -0.026×10^{-24} cm^2, whereas the single-particle value calculated as if the last neutron were a proton is 0.066×10^{-24} cm^2. This would imply $e'_{pol} \approx 0.4$ e. In ^{209}Bi the $9/2^+$ ground state has $Q_{exp} = -0.4 \times 10^{-24}$ cm^2, while the calculated one is $Q_{sp} = -0.26 \times 10^{-24}$ cm^2 yielding $e'_{pol} \approx 0.6$ e. Table III shows measured B(E2) values (some of them).

A microscopic calculation of e_{eff} will be discussed by Rimini (these Proceedings), and note that the semiclassical treatment given by Z. Szymański also gave $e'_{pol} = 0.5$ e (these Proceedings).

In the same way we can discuss higher multipole transitions, for instance E3 and M4 (magnetic hexadecupole). It is of interest just to mention the M4 transition in ^{207}Pb depopulating the $(i_{13/2})^{-1}$ 1.64 MeV hole state going to the $f_{5/2}^{-1}$ 0.57 MeV hole state (see Fig. 7). It is retarded by a factor of 6 compared with the single-particle value. In ^{207}Tl (Fig. 7) the M4 transition from $h_{11/2}^{-1}$ at 1.34 MeV to $d_{3/2}^{-1}$ 0.35 MeV is also retarded by a factor of 7. Regarding the E3 transition, let us just quote the $j_{15/2}$ 1.42 MeV to $g_{9/2}$ ground-state transition in ^{209}Pb which is enhanced by a factor of about 20 over the single-particle value. It is clear that the concept of effective charge e_{eff} cannot account for such a large enhancement and therefore we must understand this in a different way. Detailed calculations (see the Cargese lecture notes by G. Alaga) explain this enhancement in terms of an admixture of the $j_{15/2}$ state and the 15/2 state obtained by coupling the $g_{9/2}$ particle to the 3^- state of the ^{208}Pb-core.

Information regarding the purity of the shell-model states around doubly closed shell nuclei can also be obtained from the data on beta decay.

The interaction responsible for beta decay can be written as a linear combination of the vector and axial vector current – current interaction. For each nucleon it can be written in the form (for a nucleus we have to sum over all nucleons)

$$H_\beta = \frac{1}{\sqrt{2}} \left[g_V \tau_\pm \, \gamma_4 \, \gamma_\mu \, \psi_{e^\pm}^\dagger \, \gamma_\mu \, (1+\gamma_5) \psi_\nu + g_A \tau_\pm \, \gamma_4 \gamma_5 \, \gamma_\mu \, \psi_{e^\pm}^\dagger \gamma_5 \, \gamma_\mu \, (1+\gamma_5) \psi_\nu + \text{H.A.} \right]$$

$$= \frac{1}{\sqrt{2}} \left\{ g_V \left[\tau_\pm \, \psi_{e^\pm}^* \, (1+\gamma_5) \, \psi_\nu - \vec{\alpha} \tau_\pm \, \psi_{e^\pm}^* \, \vec{\alpha} (1+\gamma_5) \psi_\nu \right] \right. \tag{40}$$

$$\left. + g_A \left[\vec{\sigma} \, \tau_\pm \, \psi_{e^\pm}^* \, \vec{\sigma} (1+\gamma_5) \, \psi_\nu - \gamma_5 \tau_\pm \, \psi_{e^\pm}^* \, \gamma_5 (1+\gamma_5) \psi_\nu \right] \right\}$$

where the upper and lower sign refer to β^+ and β^- decay, respectively. g_V and g_A are the coupling constants of the vector and the axial vector part of the interaction, respectively. The factor $1/\sqrt{2}$ guarantees the same definition of the coupling constants as before the parity non-conservation discovery. γ_μ, γ_4 and γ_5 are the usual Dirac matrices, while $\psi_e^\dagger$ and ψ_ν are the electron and neutrino field operators taken at the position of the transforming nucleon. The transition probability can be calculated in the perturbation theory. Proceeding along the same lines as in the electromagnetic multipole expansion, we expand in momentum transfer at the nuclear radius $\kappa R_0 = (1/\hbar)(p_e + p_\nu)R_0$ is of the order of $1/10$ for energies not higher than 10 MeV and therefore in the lowest approximation we can take $(\kappa R_0)^0$. The operators thus obtained are those corresponding to the allowed transitions. For the non-relativistic case we see from Eq.(40) that there are two possibilities $g_V \tau_\pm$ and $g_A \vec{\sigma} \tau_\pm$. Transitions caused by the operator $g_V \tau_\pm$ are called Fermi transitions and have the selection rules $\Delta J = 0, \Delta \ell = 0$ and $\Delta T = 0$. $g_A \vec{\sigma} \tau_\pm$ will cause the so-called Gamow-Teller transitions with the selection rules $\Delta J = 0, \pm 1$; $\Delta \ell = 0$ and $\Delta T = 0, \pm 1$. In the case of the nucleus the reduced transition probabilities may be defined (analogously to the electromagnetic case):

$$B(F: I T M_T \rightarrow I T M_T \pm 1) = \frac{g_V^2}{4\pi} \left| \left\langle I M T M_T \pm 1 \right| T_\pm = \sum_{i=1}^{A} \tau_\pm(i) \left| I M T M_T \right\rangle \right|^2 \tag{41}$$

and

$$B(GT: I_i T_i M_T \rightarrow I_f T_f M_T \pm 1) = \frac{g_V^2}{4\pi} \sum_{Mf\mu} \left| \left\langle I_f T_f M_T \pm 1 \right| \sum_i \tau_\pm(i) \sigma_\mu^1(i) \left| I_i T_i M_T \right\rangle \right|^2 \tag{42}$$

The transition operator for Fermi transitions is the component of the total isospin, the matrix elements will depend on the isospin quantum numbers of the states involved only. The observed Fermi-type transition rates provide a test of the goodness of the isospin quantum number for

nuclear states. On the other hand, Gamow-Teller matrix elements yield information regarding the coupling of the nucleon spins. One can see that the isovector part of the beta-current has a similar structure to the electromagnetic current. By rotational invariance in isospace, the Gamow-Teller operator is related to the isovector part of the spin contribution to the magnetic-dipole operator. Having such a relation one can expect that the effects we have discussed in connection with the renormalization of g_s will also affect the Gamow-Teller matrix elements. In the decay of $^{17}F - ^{17}O$ B(GT) is 15% smaller than the single particle value

$$B_{sp}(GT; = j_1 \to \ell \; j_2) = \frac{g_A^2}{4\pi} \begin{cases} \left(\dfrac{j_2 + 1}{j^2}\right)^{\pm 1} & \text{for} \quad j_1 = j_2 = \ell \pm 1/2 \quad \Delta j = 0 \\[3ex] \dfrac{2j_2 + 1}{\ell + 1/2} & \text{for} \quad \Delta j = 1 \end{cases}$$

This then implies the reduction of about 8% in the isovector contribution to the magnetic moments of these nuclei. It amounts to 0.2 nuclear magnetons, in disagreement with the necessary 0.1 n.m. required from the experiment.

Besides the information on the allowed transitions in the study of the decay $^{207}Tl - ^{207}Pb$, the analysis given by J. Damgaard and A. Winther (Nucl. Physics 54 (1964) 615) contains information on the forbidden beta-decay. In fact, the transitions are first-forbidden ones and the operators can be obtained by taking the first higher term in the momentum transfer expansion (c.f. above). In this transition an $s_{1/2}^{-1}$ proton decays into the $p_{1/2}^{-1}$ and $p_{3/2}^{-1}$ neutron. Knowing the experimental ft values defined as

$$\text{ft} = \frac{\text{const.}}{\sum |M|^2} \tag{43}$$

where the sum runs over the matrix elements with different transformation properties, and making use of vector-current conservation the authors find that for agreement to exist it is necessary to assume "effective β-charges" in analogy with the electromagnetic case. Those are then related rather directly to the effective values for g_V and g_A to be used in calculating the matrix elements with single-particle wave functions. The two sets of values found were

a $(g_V^{eff}/g_V) = 0.6$ $(g_A^{eff}/g_A) = 0.5$

b $(g_V^{eff}/g_V) = 0.3$ $(g_A^{eff}/g_A) = 0.7$

Of course, it would be highly desirable to have an independent check of these values. An experiment which they have proposed would be to measure the shape of the beta spectra. This has not been done as yet to the best of our knowledge.

There is yet another correction to the single-particle properties due to the presence of the short-range pairing correlations in nuclei. They have been left out in the averaging procedure, but can be approximately incorporated maintaining the single-particle picture though, of course, modified (pairing correlations are discussed in detail by Pal and in lectures on the HFB approach in these Proceedings).

The main feature of pairing correlations is the large matrix element for time-reversed pairs of particles $\langle k\text{-}k|V|k'\text{-}k'\rangle$ (k stands for a time-reversed state). Provided that the mean distance between the states is of the order of magnitude or smaller than the pairing matrix element, instead of the sharp Fermi surface, which is characteristic of the shell model and the Hartree-Fock potential, the scattering of pairs across will smear out the Fermi surface. At the price of conserving the number of particles only on the average, one performs the Bogoliubov-Valatin linear canonical transformation

$$\alpha_k = U_k\, a_k - V_k\, a_k^\dagger$$
$$\alpha_{-k} = U_k\, a_{-k} + V_k\, a_k^\dagger$$

(44)

replacing the particles a_k by new objects α_k for which then the single-particle picture again holds. These new objects are called quasi-particles and they have the probability amplitude V_k of being a particle and U_k of being a hole in the state k. Clearly, this will affect the transition matrix elements for electromagnetic transitions, beta-decay as well as the transfer reactions. In odd mass nuclei for the transition matrix element on the basis of relation (44) one easily derives the expression relating the quasi-particle to the particle matrix element.

$$\langle k_f|T_\lambda^\mu|k_i\rangle = (U_{k_i} U_{k_f} + (-)^T V_{k_i} V_{k_f})\,\langle k_f|T_\lambda^\mu|k_i\rangle$$

(45)

T_λ^μ is a tensor operator of rank λ and the phase factor $(-)^T$ is determined by the behaviour of T_λ^μ under time reversal. In the case of electromagnetic transitions the phase factor $(-)^T$ is +1 for the magnetic and -1 for the electric multipole operator. An immediate consequence is that the magnetic moment is not affected at all $(U_k^2 + V_k^2 = 1)$ by inclusion of pairing correlations, while magnetic transitions are changed only slightly. For strong pairing, the electric transitions are very much retarded, but, as the well-known E2 transitions are, in the majority of cases, of collective nature, it is very difficult to detect them. The same is true of E3 transitions, while E1 transitions between the low-lying states are hindered for other reasons. The pairing correlations have noticeably affected the calculated ft values for beta-decay.

It should be stressed that in almost doubly magic nuclei one does not expect a strong influence of pairing for large distances in energy between major shells.

From the analyses presented in this chapter it appears that we are
able to remedy the discrepancies between measured and calculated properties
of the nuclei around the doubly closed shells in terms of the effective
electromagnetic and beta-decay operators. Renormalization effects are
also expected in the reaction and inelastic scattering data (see the papers
by Agodi, von Brentano, Cindro, Dost and Frahn in these Proceedings).
All these renormalization effects have, in fact, been expected from the
beginning because the static average field, due to the averaging procedure,
definitely leaves out a certain amount of correlations among nucleons
(see the papers on Hartree-Fock and HFB approaches).

II. SIMPLE FEATURES OF SOME TWO-BODY AND MANY-BODY
SYSTEMS

After considering the nuclei having doubly closed shell plus or minus
one particle we can simply go on and generalize our considerations for
two particles or two holes outside the closed shells. In these calculations
one usually limits oneself to one major shell. To calculate the energies
and the wave functions of the coupled system, we can start with the
energies of the non-interacting system and assume the direct product
of the wave functions of the non-interacting system as the lowest approxi-
mation for the coupled or interacting system. In this way we obtain de-
generate ground states as well as excited states of the system. The ex-
periments clearly indicate that the states are not degenerate and so we
have to introduce residual interactions in order to remove the degeneracy.
This interaction cannot be taken simply as a free N-N interaction because
a part of this interaction has already been taken in creating the average
field. Therefore, our guide in choosing a residual interaction should be
the experimental evidence on degeneracy splitting and ordering of the
levels. Furthermore we have to pay attention to the truncation of the
configuration space. These points are extensively discussed by Pal,
Soper and Talmi (these Proceedings). As an illustration we shall take
a simple example of ^{206}Pb.

In ^{206}Pb we have two neutron holes distributed in the $3p_{1/2}$, $2f_{5/2}$,
$3p_{3/2}$ and $1j_{3/2}$ sub-shells. In the actual calculation done by True and
Ford[5] an attractive Gaussian two-body force acting in the singlet-even state
is assumed:

$$V(r) = V_0 \, e^{-r^2/\beta^2}$$

with

$$V_0 = -32.5 \text{ MeV} \quad \text{and} \quad \beta = 1.85 \text{ fm}$$

This potential has an effective range $V_{0s} = 2.65$ fm and a bound state
at zero energy. The harmonic-oscillator wave functions have been used and
the size parameter b adjusted so that the square root of the mean square

---

[5] TRUE, W.W., FORD, K.W., Phys. Rev. 109 (1958) 1675.
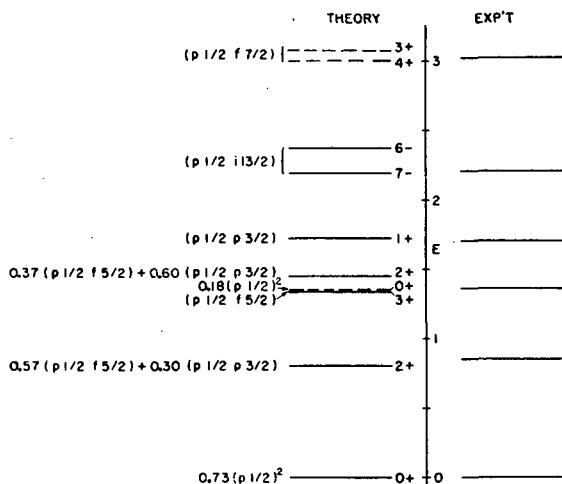
FIG.9. Comparison of calculated energy levels with observed ones.

radius of the valency nucleons equals the nuclear radius. For ^{206}Pb this
yields b = 2.33 fm. The energy matrix has been constructed in the valence
subshells and subsequently diagonalized.

In Fig.9 the calculated energy levels are compared with the observed
ones. The agreement for the energy levels appears to be quite satisfactory.
The 3$^-$ state which occurs at 2.6 MeV has not been predicted in the calcu-
lation. It is, as we have discussed in the previous chapter, a p-h excitation
of the ^{206}Pb core and hence cannot be described in a model considering
the excitations of valency nucleons in the major shell.

The transition probabilities are calculated using e_{eff} = 1.15. The
observed B(E2) for the $2_1^+ - 0^+$ transition can then be explained. However,
the ratio of the transitions from the second 2$^+$ to the first 2$^+$ and the
ground state is not in agreement with the experiment. The model pre-
dicts almost 100% transition to the first 2$^+$, whereas experimentally a
20% cross-over transition is observed. This is certainly an indication
of the fact that we are missing some degrees of freedom to account for
the discrepancy. Indeed, taking the quadrupole vibrational states in ^{208}Pb
and assuming a coupling between the calculated 2$^+$ states and the collective
modes of the core we obtain significant improvement. We may also
mention here the example of the 15/2$^-$ state at 1.42 MeV in ^{209}Pb (Fig.7).
It has a considerable admixture of the $g_{9/2}$ particle coupled to the 3$^-$
collective state of ^{208}Pb. The same is true of the 9/2$^+$ ^{209}Pb ground state.
Hence the E3 transition from the 15/2$^-$ state at 1.42 MeV to the ground
state of ^{209}Pb is enhanced by approximately a factor of twenty single
particle units.

Calculations in ^{206}Pb have also been carried out with different shapes
for the two-body potential (Yukawa potential, for example) and with slightly
different values for the other parameters. The results of such calcu-
lations agree well with each other. Thus the eigenfunctions calculated
by True and Ford can be considered typical examples of the results of
a simple shell-model calculation. Some of these eigenfunctions are listed
in Table IV.

TABLE IV.   EIGENFUNCTIONS DUE TO
SHELL-MODEL CALCULATION

		0^+ states		
Energy	$(p_{1/2})^2$	$(f_{5/2})^2$	$(p_{3/2})^2$	$(i_{13/2})^2$
0.011	0.8653	0.3077	0.3765	-0.1216
1.232	-0.4138	0.8755	0.1794	-0.1736

			2^+ states		
Energy	$(p_{1/2} f_{5/2})$	$(p_{1/2} p_{3/2})$	$(f_{5/2})^2$	$(p_{3/2} f_{5/2})$	$(p_{3/2})^2$
0.804	0.7229	-0.6017	0.2168	0.1509	0.2134
1.253	0.6538	0.7347	0.0016	0.0438	-0.1757

		4^+ states	
Energy	$(f_{5/2})^2$	$(p_{3/2} f_{5/2})$	$(p_{1/2} f_{7/2})$
1.705	0.6688	0.7021	-0.2444
1.963	0.7416	-0.6533	0.1526

It is interesting to consider the single-nucleon transfer reaction data
which give information on the large single-particle components in the wave
function. These experiments seem to give, for the ground state of ^{206}Pb,
$a_{1/2} = 0.91$ and $a_{3/2} = 0.34$. The True and Ford calculation is in good
agreement with these numbers.

The admixture in the first 2^+ state is such that all the contributions
to the ground state E2 transition moment have the same sign. In other
words, they add up coherently and enhance the E2 transition well above
the single-particle value. The transition matrix element from the second
2^+ state is retarded. Such a relation between the ground-state transitions
from the first and second 2^+ levels is similar to that observed in vibrational-
type spectra.

Most of the shell-model calculations use a simple phenomenological
residual interaction. The free nucleon-nucleon interaction seems to be
singular (see D. Brink's lecture notes) and thus cannot be treated by the
simple method described above. The problem of deriving the residual
interaction from the free nucleon-nucleon interaction are discussed by
Gmitro in these Proceedings. Secondly, it should also be noted that in
the above mentioned calculation the configuration space was restricted
to two-neutron holes in a single-major shell. Such a truncation is obviously

necessary in order to limit the size of the energy matrix. The parameters
of the effective residual interaction then depend on the size of the con-
figuration space. These problems are discussed in detail by Soper and
Talmi in these Proceedings. In general, the energy spectra can be ex-
plained by choosing a suitable effective residual interaction, and a few
dominant simple configurations account for the transfer reaction data.
However, the small neglected components may significantly affect the
electromagnetic transition probabilities. We consider some of these effects
by using an effective charge for the valence nucleons, but this may not
be sufficient as is demonstrated by the ground-state E2 transition from
the second 2^+ state in ^{206}Pb.

We have mentioned the difficulties in treating the two-valency par-
ticles outside the doubly closed shells. If we try to understand the
properties of nuclei far from the closed shells it is clear that the shell
model calculations become exceedingly difficult. So far exact diagonali-
zation has been carried out for five nucleons in the $d_{5/2}$ and $s_{1/2}$ sub-
shells. However, the problem may be partly overcome if one takes a
different starting point. We may turn to the experimental data and ask
the question: Which part and which features of the spectra of relatively
wide range of nuclei show only slight dependence on a particular nucleus?
Of the nuclei away from the closed shells we can make distinction at two
categories: deformed and spherical ones. The deformed nuclei, as a
most striking feature, exhibit rotational bands. These nuclei are discussed
in detail by Szymanśky in these Proceedings. We will briefly discuss
some regularities of the so-called spherical nuclei.

We have mentioned before that all even-even nuclei have ground state
spin and parity 0^+. With the exception of the closed-shell nuclei, the first
excited state of an even-even nucleus is invariably a 2^+ state. The energy
of this 2^+ state is not very sensitive to the particular nucleus except in
the case of isotopes and isotones nearest to the doubly closed shell. This
is also true of single closed-shell nuclei. A further striking feature of
this 2^+ state is that the ground-state E2 transition is enhanced above the
single-particle value by a factor of 3-10. Quite often in the energy region
of twice the excitation energy of the first 2^+ state we find states with spins
and parities $J^\pi = 0^+$, 2^+ and 4^+. These states decay to the first excited 2^+
states and the possible crossover transition from the second 2^+ state to
the 0^+ ground state is always found to be very small (2-3% of the main
transition). Such a pattern suggests that the lowest 2^+ state may be looked
upon as a quadrupole vibration of the nucleus. If accepted such an interpre-
tation predicts the above-mentioned 0^+, 2^+ and 4^+ states to be two-phonon
states of quadrupole vibrations. The observed selection rules for the E2
transitions confirm this description.

The energies of the 3^- states show an even weaker dependence on the
nuclear masses i.e. it varies as $\sim A^{1/3}$. The E3 transitions from these
states are also highly enhanced. We have quoted the 3^- state of ^{208}Pb
and its B(E3) is 40 times that of the single particle. Such states can be
classified as the octupole vibrational states.

The present status of the microscopic theory of vibrations will be
discussed by Pal in his course of lectures (these Proceedings). Phenomeno-
logically we can describe a_λ-pole vibration by a suitably chosen collective
co-ordinate α_λ. For a harmonic vibrator the Hamiltonian then assumes
the form

$$H = \frac{1}{2} B_\lambda \sum_{\mu=-\lambda}^{+\lambda} |\alpha_\lambda^\mu|^2 + \frac{1}{2} C_\lambda \sum_{\mu=-\lambda}^{+\lambda} |\alpha_\lambda^\mu|^2 \tag{46}$$

The eigenfrequencies and the energy of an N-phonon state is then obtained to be

$$\omega_\lambda = \sqrt{\frac{C_\lambda}{B_\lambda}} \quad \text{and} \quad E_N = \hbar\omega_\lambda\left(N_\lambda + \frac{2\lambda+1}{2}\right) \tag{47}$$

The spectra are sets of equidistant degenerate levels and there is a very simple $B(E\lambda)$ ratio rule

$$B(E\lambda; \ N_\lambda = 2, \ J_i \to N_\lambda = 1, \lambda) = 2B(E\lambda; \ N_\lambda = 1, \ \lambda \to N_\lambda = 0, 0) \tag{48}$$

The transition occurs only when $\Delta N_\lambda = \pm 1$. And also

$$B(E\lambda; \ N_\lambda = 1, \lambda \to N_\lambda = 0, 0) = \left(\frac{3}{4\pi} Ze \ R_0^\lambda\right)^2 \frac{\hbar}{2\sqrt{B_\lambda C_\lambda}} \tag{49}$$

if one assumes that the oscillating charge Ze has a constant average density within a radius R_0. Thus we see that the two parameters B_λ and C_λ characterize the spectra fully. A description of the symmetries of the vibrational problem can be found in A. Bohr's paper in these Proceedings.

Besides these collective modes associated with the enhanced electromagnetic transitions one could also observe the so-called pairing mode in two-nucleon transfer reactions. In the reactions

$$^{208}\text{Pb}(t, p)^{210}\text{Pb} \quad \text{and} \quad ^{208}\text{Pb}(p, t)^{206}\text{Pb}$$
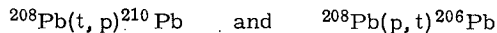
leading to the ground states of final nuclei, the cross-section is strongly enhanced as compared with the transition into the pure $|(j)^2 \ J = 0\rangle$ configuration. This enhancement indicates that the process is of collective nature, and, therefore, we may try to interpret the ground states of ^{210}Pb and ^{206}Pb as collective excitations of ^{208}Pb. The quanta of excitation of this so-called pairing mode will be characterized by the nucleon transfer number α. Thus $\alpha = +2$ is a pair-addition mode and $\alpha = -2$ corresponds to a pair-removal mode. The states are then labelled by (n_1, n_2) where n_1 is the number of pair addition mode quanta and n_2 the number of pair removal quanta.

The pairing mode may be associated with the fluctuations in Δ, the pairing-energy gap, around the equilibrium value. Its theory will be discussed by Ripka (these Proceedings). Analogously to the other vibrational modes the ratios of successive cross-sections in the following reactions should have the property

$$\sigma[(0, 0) \to (1, 0)] : \sigma[(1, 0) \to (2, 0)] : \sigma[(2, 0) \to (3, 0)] = 1 : 2 : 3$$

Experimentally for the reactions

$$^{208}Pb(p,t)^{206}Pb; \quad ^{206}Pb(p,t)^{204}Pb \quad and \quad ^{204}Pb(p,t)^{202}Pb$$
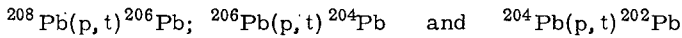
the ratio of the cross-section is $1:1.7+2.7$ ($\pm 20\%$) in good agreement with the vibrational formalism.

To obtain the energy associated with the pairing-mode quanta, we add a linear term in N

$$E' = E - E(^{208}Pb) + (N-126)\ 5.81\ MeV$$

Then

$$\hbar\omega_{\alpha=+2} = \hbar\omega_{\alpha=-2} = \hbar\omega_\alpha \tag{50}$$

and the energy of the state (n_1, n_2) is given by

$$E'_{(n_1, n_2)} = \hbar\omega_\alpha (n_1+n_2) \tag{51}$$

The energies of the 0^+ levels in the ^{208}Pb region are calculated and compared with the experimental levels in Fig.10.

Furthering the analogy it is to be expected that in the superfluid nuclei possessing non-zero static value for the pairing energy gap Δ one would observe pairing rotations. The ground-state energies of these nuclei would then lie on a parabola and this is demonstrated in the case of Sn isotopes in Fig.11.

We will now turn to experiments in order to see if our picture of harmonic vibrations is adequate. First we find that in all nuclei in which the two-quadrupole phonon triplet is experimentally identified, the 0^+, 2^+ and 4^+ levels are separated in energy by approximately 80 keV to 400 keV, and are not degenerate as predicted by the harmonic-vibrator model.
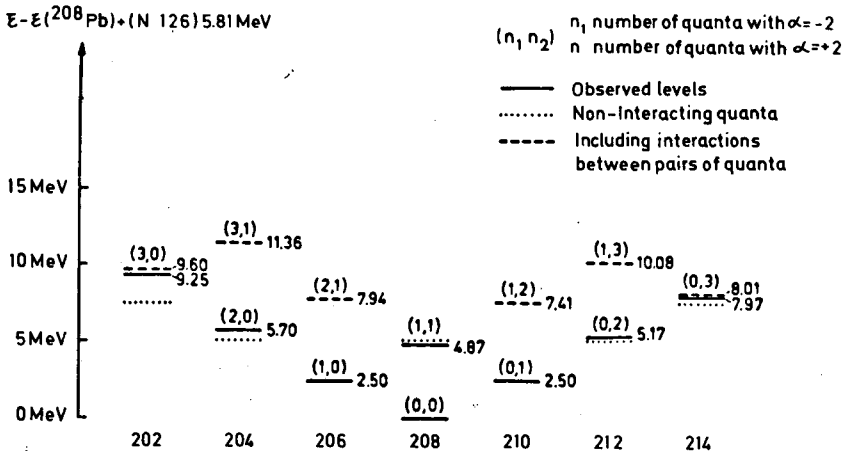
FIG.10.   Comparison of calculated energy of the 0^+ levels in the ^{208}Pb region with the experimental ones.

$E-E(^{114}Sn)+8.8(N-64)MeV$
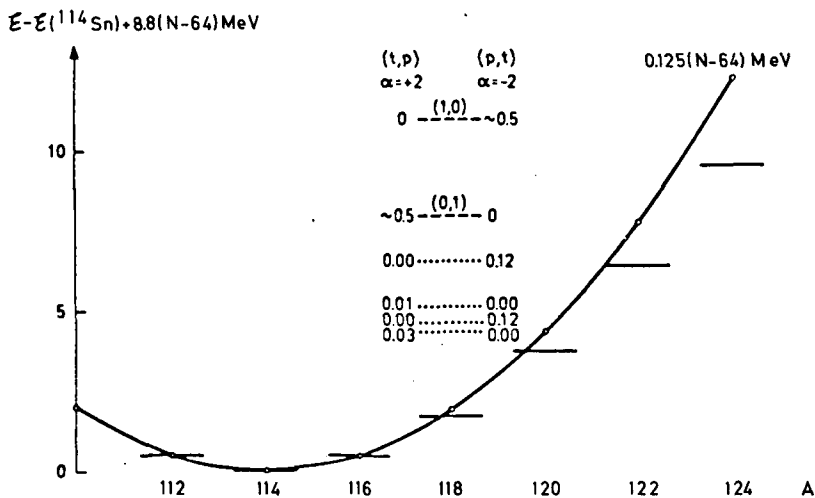
FIG.11.   Neutron pair excitations in Sn isotopes. The solid lines represent ground states.

This fact by itself points out the existence of quite appreciable anharmo-
nicities. Besides the energies, the transition intensities are also different
from the experimental ones. As has been mentioned earlier, the cross-
over transition from the second 2^+ state to the ground state is present and
is about 2-3% of the main transition. The harmonic-phonon picture also
predicts zero static quadrupole moment for the vibrational states. Experi-
mentally, however, we observe quite appreciable static quadrupole moments
for the first excited 2^+ states. In ^{114}Cd, for example, the first 2^+ state
has Q = -0.49 ± 0.25 eV.

One could try to explain the above-mentioned deviations from the
harmonic picture by taking the possible anharmonic terms into consider-
ation. However, the exact diagonalization, in states containing up to
seven phonons of the anharmonic terms, carried out by Sorensen (Phys.
Lett. 21 (1966) 683) in ^{114}Cd showed clearly that the large quadrupole
moment of the first excited 2^+ state could be obtained only at a price of
having a cross-over transition much larger than that observed
experimentally.

Secondly, from the experiments we find many other states not pre-
dicted by the vibrational model. These states usually occur in the energy
region of the two quadrupole phonon states. For example, in addition to
the 0^+, 2^+ and 4^+ states of the two phonon triplet, at 1.13, 1.21 and
1.38 MeV, we find a 0^+ and 2^+ state at 1.30 and 1.36 MeV, respectively,
in ^{114}Cd. In principle, in its microscopic description the phonon state
should contain a large number of small 1p-1h or 2 quasi-particle ampli-
tudes. Presumably, these other states, which are not explained by the
phonon model, contain large amplitudes of a few 1p-1h or two quasi-
particle excitations. These so-called two quasi-particle states can mix
with pure harmonic phonon states. Therefore, as a first improvement
over the phonon model we will consider the particle degrees of freedom
and their coupling with the phonon states. For example, in the treatment

of nuclei near the single closed shell, the single-closed-shell nuclei can be considered as vibrators and the particles (or holes) added (or taken from) the closed shell are considered explicitly and the two modes are coupled. Of course, similar calculations can be carried out near doubly closed shell nuclei. We will briefly discuss the calculations carried out for ^{114}Cd and ^{209}Bi.

The interaction of a particle with an average vibrational field, described by the surface oscillations, can be obtained as follows. We are interested in the difference $V(r, \theta, \phi(\alpha_\lambda^\mu \neq 0)) - V(r)$ between the vibrational and static case. Assuming that this difference is the same for all equipotential surfaces we write it for the sphere $r = R_0$ and expand around $\alpha_\lambda^\mu = 0$

$$V(R_0, \alpha_\lambda^\mu \neq 0) - V(R_0, \alpha_\mu^\lambda = 0) = V\left(\frac{R}{1 + \sum_{\lambda\mu} \alpha_\lambda^{\mu*} Y_\lambda^\mu}\right) - V(R_0)$$

$$= V(r) - r\frac{dV(r)}{dr}\sum_{\lambda\mu} \alpha_\lambda^{\mu*} Y_\lambda^\mu(\theta, \phi) + k'\left|\sum_{\lambda\mu} \alpha_\lambda^{\mu*} Y_\lambda^\mu(\theta, \phi)\right|^2 + \ldots \tag{52}$$

Keeping only terms linear in α expression (50) for a given multipole λ reads as

$$H_{int}^\lambda = -r\frac{dV(r)}{dr}\sideset{}{'}\sum_{\lambda\mu} \alpha_\lambda^{\mu*} Y_\lambda^\mu(\theta, \phi) \tag{53}$$

In the above expressions $V(r)$ is the spherically symmetric potential and θ and ϕ are particle co-ordinates.

As an example of full diagonalization we consider the case of ^{114}Cd. Here the vibrator is the Sn isotope to which the two proton holes in the $Z = 50$ shell are coupled. The energy matrix is constructed from all possible states up to three phonons and the two proton holes in the $Z = 28$ to $Z = 50$ shell. The coupling constant in H_{int}^λ Eq. (53) is adjusted to give best agreement with the spectra (Fig. 12). The wave functions obtained in the diagonalization are then used to calculate the electromagnetic properties and the strength distribution for particle transfer reactions. Thus these wave functions are subject to severer tests.

In the numerical comparison[6] an effective charge $e_{eff}^p = 2e^p$ and $e_{eff}^n = 2.9\ e^p$ have been used to obtain the B(E2) value for the first 2^+ to ground-state transition. The quadrupole moment of the first excited 2^+ state is then obtained as -0.33 eb, which agrees well with the experimental value -0.49 ± 0.25 eb. For calculating the M1 transition probabilities an effective gyromagnetic factor $g_s^{eff} = 0.7\ g_s^{free}$) was used. The results of this calculation are shown in Table V.

6 V. Lopac, M. Sc. thesis, Zagreb 1967.
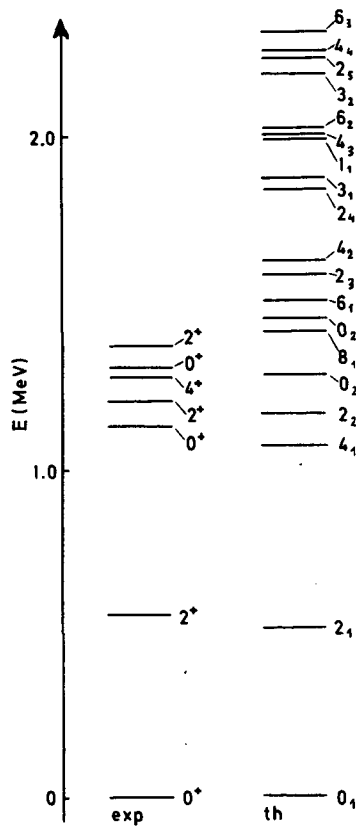
FIG.12. Comparison of theoretical spectrum with the experimental one for ^{114}Cd.

TABLE V.   M1 TRANSITION PROBABILITIES

Transition	B(E2)$_{calc}$ $e^2 b^2$	B(E2)$_{expt}$	B(M1)$_{calc}$
$2_1 - 0_1$	0.112	0.112	
$2_2 - 0_1$	0.003	0.002	
$2_3 - 0_1$	0.000	0.002	
$0_2 - 2_1$	0.067	0.090	
$2_2 - 0_2$	0.019	-	
$2_2 - 2_1$	0.134	0.138	0.137
$2_3 - 2_1$	0.021	0.019	0.483
$2_3 - 2_2$	0.007	-	0.204
$4_2 - 4_1$	0.003		1.474
$4_1 - 2_1$	0.170	0.203	

It is also interesting to compare the single-particle strengths for the transfer reactions. This comparison will test the particle component of the wave functions. The wave functions of the 0^+, 2_1^+ and 2_2^+ states are given below.

$$|0_1^+\rangle = 0.78 \left|(g_{9/2})_0^{-2}, 00\right\rangle + 0.42 \left|(g_{9/2})_2^{-2}, 12\right\rangle - 0.26 \left|(p_{3/2})_0^{-2}, 00\right\rangle$$

$$- 0.23 \left|(p_{1/2})_0^{-2}, 00\right\rangle + 0.17 \left|(g_{9/2})_0^{-2}, 20\right\rangle$$

$$|2_1^+\rangle = 0.67 \left|(g_{9/2})_0^{-2}, 12\right\rangle + 0.4 \left|(g_{9/2})_2^{-2}, 00\right\rangle + 0.28 \left|(g_{9/2})_2^{-2}, 24\right\rangle$$

$$+ 0.21 \left|(g_{9/2})_4^{-2}, 12\right\rangle - 0.21 \left|(p_{3/2})_0^{-2}, 12\right\rangle + 0.20 \left|(g_{9/2})_2^{-2}, 22\right\rangle$$

$$- 0.19 \left|(g_{9/2})_2^{-2}, 12\right\rangle - 0.18 \left|(p_{1/2})_0^{-2}, 12\right\rangle$$

$$|2_2^+\rangle = 0.536 \left|(g_{9/2})_0^{-2}, 22\right\rangle - 0.43 \left|(g_{9/2})_2^{-2}, 12\right\rangle$$

$$+ 0.27 \left|(g_{9/2})_2^{-2}, 20\right\rangle - 0.26 \left|(g_{9/2})_0^{-2}, 12\right\rangle$$

$$- 0.20 \left|(g_{9/2})_4^{-2}, 24\right\rangle + 0.19 \left|(p_{3/2})_0^{-2}, 12\right\rangle$$

The amount of $(g_{9/2})^{-2}$ configuration is large (85% in the ground state and 90% and 61% for the 2_1^+ and 2_2^+ states, respectively). These numbers are essentially in agreement with the experiment. It is also very interesting to observe that the final wave functions, which are linear combinations of states with different numbers of phonons, still preserve a vibrational-like pattern of B(E2)'s for certain states. Thus one could say that these states, although admixed, still behave like some new anharmonic-oscillator states.

There is yet another possible approach to this problem, namely that of perturbation theory. Of course, one has to pay much attention to the convergence and therefore choose proper cases. One such case – and there are probably many more – is offered by the observation of the septuplet of positive-parity levels, with spins ranging from 3/2 to 15/2, and with an energy spread of 250 keV in ^{209}Bi (Fig. 7). The lowest is the $3/2^+$ state at 2.49 MeV and the $15/2^+$ at 2.74 MeV is the highest. The centre of gravity of these levels lies at about 2.6 MeV which strongly suggests their nature to be of an $h_{9/2}$ proton coupled to the 3^- octupole state of the ^{208}Pb core. Indeed the calculations carried out by Mottelson, Paar and others (see Cargese lecture notes for details) fully support such an interpretation. In ^{207}Pb there is a doublet of levels, with $J^\pi = 5/2^+$ and $7/2^+$ at 2.61 and 2.65 MeV, respectively (Fig. 7), which can be explained as due to the coupling of the $p_{1/2}$ neutron hole with the octupole vibration. In both cases the perturbation expansion is well justified and provides an important tool in estimating the contributions from the closest levels. One may say that both approaches, the matrix diagonalization and the perturbation theory, are in a way complementary. While the full diagonalization is limited in the size of the energy matrix to be diagonalized and

therefore not appropriate to the investigation of the influence of many far distant levels, the perturbation approach in cases where it converges provides just such information.

There is as yet little evidence on vibrational states associated with higher multipoles. However, recently in an inelastic (p, p') experiment on Cd isotopes by M. Koike et al. (Nucl. Physics A 125 (1969) 161) it has been found that the reduced transition probability for $i = 4$ (electric hexa-decupole) transitions are 7 to 10 times the single-particle value. However, much more experimental data are needed before one draws definite conclusions.

Figures 1, 2, 3, 4, 5, 6, 8, 10 and 11 have been taken from A. Bohr and B.R. Mottelson, Lectures on Nuclear Structure; Fig. 9 from True, W.W., Ford, K.W. (Phys. Rev. 109 (1958) 1675); Fig. 12 from V. Lopac: M.Sc. Thesis, Zagreb, while Fig. 7 is due to the courtesy of N. Cindro.

SHELL-MODEL TECHNIQUES

J. M. SOPER
Theoretical Physics Division,
AERE, Harwell, United Kingdom

Abstract

SHELL-MODEL TECHNIQUES.
   1. Slater determinants (second-quantized wave functions); 2. The fractional parentage representation; 3. Calculation of one- and two-body matrix elements.

1. SLATER DETERMINANTS (SECOND-QUANTIZED WAVE FUNCTIONS)

A single Slater determinant is the simplest form of antisymmetric wave function. Completely equivalent to it is the function that consists of a single string of creation operators acting on the vacuum. We shall refer to wave functions of either of these forms simply as "determinants".

We shall use the following notation for determinants. We first define a "standard order" for the set of single-particle states $|n\ell j m\rangle$ that we are considering (assumed finite). We then need only indicate whether each state in the set is occupied or unoccupied in the determinant. This we do by means of a binary number, with as many digits as there are states in the space; for each state in the standard order a "1" in the corresponding position in the binary number denotes the state is occupied, "0" that it is .unoccupied. The notation is compact, and clearly suited to a computer, where a word of 64 bits can span a space amply large enough for most applications. This form is in fact used in the Argonne system of shell-model programs [1].

We shall here treat all-neutron systems, indicating (where it is not obvious) how neutron-proton systems can be included. We define a configuration as a distribution of the particles over the various shells $|n\ell j\rangle$ in which the choice of m-values within each shell is not specified.

Very few states of a many-body system (for which the total angular momentum J is a good quantum number) can be represented by a single determinant in the m-representation. Such a determinant has a precise value of M, but not of J. The exceptions are cases where the particular value of M can be obtained in only one way within a given configuration; such a unique state must be identical to a similarly unique state in the $|JM\rangle$ representation, and thus must have good J. The largest class of such states is that with the maximum possible M in a given configuration (we consider here only M ≥ 0). These states are always unique and have J = M. The most important examples are:
   (a) Closed shells, with J = M = 0, and
   (b) closed shells plus or minus one particle. If the extra (or missing) particle is in the $|n\ell j\rangle$ shell the determinants have J = j (note this is true for all M).

Other states of maximum M are less important physically than these, but of great importance in computation as we shall see below when we construct the states of good J in the general case.

States containing <u>two</u> particles (or holes) outside closed shells are not in general single determinants but linear combinations of two or more. Since each determinant is already antisymmetric, we have only to worry about forming states of good J; this is of course achieved with Clebsch-Gordan coefficients. As an example we consider the $J = 1$, $M = 1$ state of the configuration $j_1 = \frac{3}{2}$, $j_2 = \frac{1}{2}$. We have

$$\left| J = 1 \quad M = 1 \right\rangle = \sum_{m_1 m_2} C^{\frac{3}{2} \frac{1}{2} 1}_{m_1 m_2 1} \left| \frac{3}{2} m_1 \right\rangle \left| \frac{1}{2} m_2 \right\rangle$$

$$= \frac{\sqrt{3}}{2} \left| \frac{3}{2} \frac{3}{2} \right\rangle \left| \frac{1}{2} - \frac{1}{2} \right\rangle - \frac{1}{2} \left| \frac{3}{2} \frac{1}{2} \right\rangle \left| \frac{1}{2} \frac{1}{2} \right\rangle$$
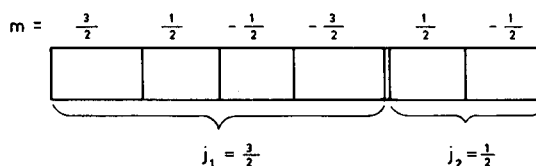
FIG.1.   "Standard order" for configuration $j_1 = \frac{3}{2}$, $j_2 = \frac{1}{2}$.

If we adopt the standard order A shown in Fig. 1 then the state we have written as $\left| \frac{3}{2} \frac{3}{2} \right\rangle \left| \frac{1}{2} - \frac{1}{2} \right\rangle$ represents the determinant (1 000 001) and the

$\left| \frac{3}{2} \frac{1}{2} \right\rangle \left| \frac{1}{2} \frac{1}{2} \right\rangle$ state is (010 010). The latter notation is preferable since the states are antisymmetrized.

States of good J for <u>more than two</u> particles are not so simple. We use the M-lowering operator:

$$J_- = \sum_i j^i_-$$

where J_- has the property

$$J_- \left| JM \right\rangle = \sqrt{(J + M)(J - M + 1)} \left| J M - 1 \right\rangle$$

and similarly for j_-. We operate on the <u>determinants,</u> with Σj^i_-, each term of which has the following effect. If the state i is unoccupied the term gives zero. If it is occupied, then j^i_- moves the 1 in that position one place to the right (in our form of standard order) and multiplies the resulting determinant by the appropriate factor. If the state on the right is already occupied or belongs to a different shell the result is again zero for that term.

We follow the procedure used in the Argonne shell-model program [1]. The steps are as follows:

(a) Choose a configuration.

(b) Construct the state of maximum M. This state will be unique, with $J = J_{max} = M_{max}$.

(c) Operate with J_- to give multiple of $|J_{max} \ M_{max}-1\rangle$.

Operate with Σj_-^i to give the appropriate linear combination of j-lowered determinants. Equate the two and normalize.

(d) All other linear combinations of these determinants which are normal and orthogonal to each other and to the combination found in (c) are eigenstates of J with $J = J_{max}-1$ and $M = M_{max}-1$. Find a complete set of these by Schmidt orthogonalization.

(e) Repeat (c) and (d), using all the vectors already found. For each successive M construct all the states belonging to $J>M$ by using J_- on their known M+1 components. Then fill out the space by Schmidt orthogonalization; the new vectors belong to $J = M$.

(f) It is possible to conserve seniority in this scheme. At each Schmidt orthogonalization (it can be shown) it will be possible to choose new vectors in which all the determinants have the same degree of pairing (a "pair" is defined as the occupation of both $|jm\rangle$ and $|j-m\rangle$ in a given shell; "degree of pairing" is simply the number of such pairs in the determinant). The resulting wave functions will then have good seniority (given by the number of impaired particles in the $M = J$ state) as will all functions subsequently derived from them by J_- operations.

As a (trivial) example we take the case of two particles considered above. The maximum M is 2 and hence we have

$$|2,2\rangle = (100\,010)$$

$$J_-|2,2\rangle = 2|2,1\rangle$$

$$= \sqrt{3}\,(010\,010) + (100\,001)$$

Hence

$$|2,1\rangle = \frac{\sqrt{3}}{2}(010\,010) + \frac{1}{2}(100\,001)$$

and hence

$$|1,1\rangle = -\frac{1}{2}(010\,010) + \frac{\sqrt{3}}{2}(100\,001)$$

This is the result which we had before.

Clearly, we had an arbitrary choice of phase here; in more complicated cases we will also have an arbitrary choice of orthogonal linear combinations in steps (d) and (e), though this will be reduced if we preserve seniority. Provided we are consistent, however, these choices will not affect any physical quantity, since we are here constructing a complete set of basis states in which to express operators and wave functions.

When both neutrons and protons are present the above operations can be carried out, treating the neutrons and protons as different particles

(i. e. counting the neutron and proton $|n\ell j\rangle$ shells as distinct). Then <u>within</u> each set of functions $|J, M=J\rangle$ we can classify according to the isospin T by using the isospin lowering operator T_- in the same way that we used J_-. We identify the state with the largest possible number of neutrons in this space of functions (maximum M_T); this will have $T = T_{max} = M_{T_{max}}$. Then we carry out the T_- and orthogonalizing operations exactly as before, <u>within the space</u> of functions $|J, M=J\rangle$. One small point has to be watched. In most "standard orders", corresponding neutron and proton states (which are connected by t_-) will not be next to each other (as they were in the case of j_- in the standard order we adopted). We must then remember that in moving a neutron to the corresponding proton state by means of t_- we must multiply the resulting determinant by $(-1)^r$ where r is the number of <u>occupied</u> states that we pass over in the transfer. This rule is of course an expression of the anticommutation law.

2.   THE FRACTIONAL PARENTAGE REPRESENTATION

Representation in terms of determinants is very simple in principle but very complicated in practice. To provide a basis for nuclei of mass 10 for example in L-S coupling (six particles in $1p_{\frac{3}{2}}$ and $1p_{\frac{1}{2}}$) we need to consider $(12!)/(6!)^2 = 924$ determinants. Clearly this representation becomes more suited to computers than human beings as soon as we leave the immediate neighbourhood of closed shells.

We use instead the technique of <u>fractional parentage</u>. We suppose that we <u>know</u> all the antisymmetric states of n-1 particles in a shell (we consider a single shell for the moment). Let these be $|j^{n-1} \bar{\alpha} \bar{J} \bar{M}\rangle \equiv \bar{\psi}$. If we simply vector couple to all of these states a nucleon labelled n in all possible ways we shall obtain a set of states

$$\left[\bar{\psi}(j^{n-1} \bar{\alpha} \bar{J})\ \phi(j)\right]^J_M = \sum_{\bar{M}m} C^{\bar{J}\,j\,J}_{\bar{M}m M} |j^{n-1} \bar{\alpha} \bar{J} \bar{M}\rangle |jm\rangle$$

where we denote the single-particle state by ϕ or $|jm\rangle$ and vector coupling by $[\quad]^J_M$. These states will <u>not</u> be antisymmetric for exchanges between particle n and the other particles, in general; only some subset of states will be totally antisymmetric, given by the linear combinations

$$|j^n \alpha J M\rangle = \sum_{\bar{J}\,\bar{\alpha}} a^\psi_{\bar{\psi}} \sum_{\bar{M}m} C^{\bar{J}jJ}_{\bar{M}m M} |j^{n-1} \bar{\alpha} \bar{J} \bar{M}\rangle |jm\rangle$$

$$= \sum_{\bar{\psi}} a^\psi_{\bar{\psi}} \left[\bar{\psi}(j^{n-1} \bar{\alpha} \bar{J})\ \phi(j)\right]^J_M$$

The coefficients $a^\psi_{\bar{\psi}}$ of this <u>projection</u> operation from the space of vector-coupled states to its totally antisymmetric subspace are called <u>coefficients of fractional parentage</u> (c. f. p.). They are extensively tabulated [2].

We have expressed the a. s. (antisymmetric) states of j^n in terms of the a. s. states of j^{n-1}; in turn we can express these if we wish in terms of

j^{n-2} and so on, to arrive at a complete expression for the j^n wave function which will be as complicated as (and equivalent to) its expression as a sum of Slater determinants. But nuclear physics consists essentially of matrix elements of one- and two-body operators, not of wave functions. For one-body operators we need never go beyond the first step in this reduction, for two-body operators we need only go as far as the second. In this way we find that we can immediately reduce the problem of finding n-body matrix elements to the simple problem of finding 2-body or 1-body matrix elements. This reduction is purely <u>geometric</u>.

(a)   Matrix elements of one-body operators

Operators corresponding to observable quantities in quantum mechanics must be <u>symmetric</u> in all particles (of a given type). The most general form of a one-body operator must therefore be $F = \sum_i f_i$ where the sum is taken over all particles. The f_i can in general be expressed as a sum of irreducible spherical tensors; we shall assume this has been done, and shall consider only one rank of tensor at a time. We therefore consider

$$\langle \psi | F_q^{(k)} | \psi' \rangle = \langle j^n \alpha J M | \sum_i f_{iq}^{(k)} | j^n \alpha' J' M' \rangle$$

Since the wave functions are totally antisymmetric it follows that each term in the sum will give a contribution of the same magnitude and sign (verify this). We therefore only consider the contribution of f_n and multiply the result by n. Applying also the Wigner-Eckart theorem gives

$$\langle \psi | F_q^{(k)} | \psi' \rangle = n \frac{C_{M' q M}^{J' k J}}{\sqrt{2J+1}} \langle j^n \alpha J || f_n^{(k)} || j^n \alpha' J' \rangle$$

We now use the fractional parentage expansion:

$$\langle \psi | F_q^{(k)} | \psi' \rangle = n \frac{C_{M' q M}^{J' k J}}{\sqrt{2J+1}} \sum_{\bar\psi \bar{\psi'}} a_{\bar\psi}^{\psi} a_{\bar{\psi'}}^{\psi'}$$

$$\times \langle [\overline{\psi}(\bar\alpha \bar J) \, \phi_n(j)]^J \, || f_n^{(k)} || [\overline{\psi'}(\bar\alpha' \bar{J'}) \, \phi_n(j)]^{J'} \rangle$$

The operator here acts only on the <u>second part</u> of the vector-coupled system, and we can therefore use the theorem [3]

$$\langle j_1 j_2 J || T^{(k)}(2) || j_1' j_2' J' \rangle = \delta_{j_1 j_1'} \sqrt{(2J+1)(2J'+1)}$$

$$\times W(j_2' k j_1 J; \, j_2 J') \langle j_2 || T^{(k)}(2) || j_2' \rangle$$

which gives us the final result

$$\langle \psi | F_q^{(k)} | \psi' \rangle = n \; \frac{C_{M' q M}^{J' k J}}{\sqrt{2J+1}} \sum_{\underline{\psi}} a_{\underline{\psi}}^{\psi} a_{\underline{\psi}}^{\psi'} \sqrt{(2J+1)(2J'+1)}$$

$$\times \; W(j k \bar{J} J; \; j J') \langle j || f^{(k)} || j \rangle$$

which expresses the n-body matrix element in terms of a one-body matrix element and geometrical factors.

(b) Two-body operators

We have defined the one-body c.f.p. above. The two-body c.f.p. are defined similarly

$$| j^n \alpha J M \rangle = \sum_{\tilde{\psi} \phi_2} a_{\tilde{\psi} \phi_2}^{\psi} \left[\tilde{\psi}(j^{n-2} \tilde{\alpha} \tilde{J}) \; \phi_2 (j^2 J_2) \right]_M^J$$

where $\tilde{\psi}$ is an a.s. state of the first $(n-2)$ particles and ϕ_2 is an a.s. state of particles $(n-1)$ and n. By exactly the same arguments that we used above, we have for the matrix elements of

$$G_q^{(k)} = \sum_{i < j} g_{ij, q}^{(k)} :$$

$$\langle \psi | G_q^{(k)} | \psi' \rangle = \frac{n(n-1)}{2} \; \frac{C_{M' q M}^{J' k J}}{\sqrt{2J+1}} \sum_{\tilde{\psi} \phi_2 \phi_2'} a_{\tilde{\psi} \phi_2}^{\psi} a_{\tilde{\psi} \phi_2}^{\psi'} \sqrt{(2J+1)(2J'+1)}$$

$$\times \; W(J_2' k \tilde{J} J; \; J_2 J') \langle J_2 || g_{n, n-1}^{(k)} || J_2' \rangle$$

In most cases of interest the two-body operator will be a scalar with $k = 0$. The result then reduces to the very simple one:

$$\langle J M | G_0^{(0)} | J M \rangle = \frac{n(n-1)}{2} \sum_{\tilde{\psi} \phi_2} a_{\tilde{\psi} \phi_2}^{\psi} a_{\tilde{\psi} \phi_2}^{\psi'} \langle J_2 M_2 | g^{(0)} | J_2 M_2 \rangle$$

(c) Relation between two- and one-body c.f.p.

There are many tables of one-particle c.f.p. There are few of two-particle c.f.p., which are necessarily more bulky. We therefore need to be

able to express the 2-body coefficients in terms of the one-body ones. We can write, using the one-particle breakdown twice in succession:

$$\psi(j^n \alpha\, J\, M) = \sum_{\bar\psi} a^\psi_{\bar\psi} \left[\bar\psi(\bar\alpha\,\bar J)\,\phi_n(j) \right]^J_M = \sum_{\bar\psi\tilde\psi} a^\psi_{\bar\psi}\, a^{\bar\psi}_{\tilde\psi} \left[[\tilde\psi(\tilde\alpha\,\tilde J)\,\phi_{n-1}(j)]^{\bar J}\,\phi_n(j) \right]^J_M$$

We now need to recouple the angular momenta in the last line to give the standard form for the two-body parentage expression, which involves ϕ_2. We use the recoupling coefficient:

$$\langle j_1 j_2(J_{12}),\ j_3;\ J \,|\, j_1,\ j_2 j_3(J_{23})\ ;\ J\rangle$$

$$= \sqrt{(2\,J_{12}+1)(2\,J_{23}+1)}\ \ W(j_1\,j_2\,J\,j_3;\ J_{12}\,J_{23})$$

which gives

$$\psi(j^n \alpha\, J\, M) = \sum_{\tilde\psi\,\tilde\psi\phi_2} a^\psi_{\bar\psi}\, a^{\bar\psi}_{\tilde\psi}\ \sqrt{(2\,\bar J+1)(2\,J_2+1)}\ W(\tilde J j\, J j;\ \bar J J_2) \left[\tilde\psi(\tilde\alpha\,\tilde J)\,\phi_2(J_2) \right]^J_M$$

and hence

$$a^\psi_{\tilde\psi\phi_2} = \sum_{\bar\psi} a^\psi_{\bar\psi}\, a^{\bar\psi}_{\tilde\psi}\ \sqrt{(2\,\bar J+1)(2 J_2+1)}\ W(\tilde J j\, J j;\ \bar J J_2)$$

3. CALCULATION OF ONE- AND TWO-BODY MATRIX ELEMENTS

The calculation of matrix elements of one-body operators is usually quite straightforward. The wave functions are vector-coupled combinations of spin and orbital angular momenta, and the operators can be written as combinations of irreducible spherical tensors in spin and orbital spaces. Once the split into these two spaces is complete, the spin parts can be evaluated using (for instance) Pauli matrices, and the orbital parts will reduce to integrals over products of spherical harmonics or to matrix elements of angular momentum operators, all of which are well-known. In general, there will also be radial integrals, which will be simple single integrals and easily evaluated for any chosen form of radial wave function.

Example:

The magnetic moment of a single neutron outside closed shells is given by

$$\mu = \langle s\,\ell\, j\, m = j \,|\, g_s\, s^{(1)}_0 \,|\, s\,\ell\, j\, m = j\rangle$$

where $g_s = -3.8256$ nuclear magnetons. Show that

$$\mu = g_s \, C_{j0j}^{j1j} \sqrt{\frac{3(2j+1)}{2}} \; W\left(\frac{1}{2} \, \ell \, 1 \, j; \, j \frac{1}{2}\right)$$

$$= g_s \, \frac{\frac{3}{4} + j(j+1) - \ell(\ell+1)}{2(j+1)}$$

$$= \frac{1}{2} \, g_s \left(\text{for } j = \ell + \frac{1}{2}\right)$$

and similarly calculate the single-particle ("Schmidt") moments for a single proton (with orbital contribution).

$$\text{or} = - \frac{j}{2(j+1)} \, g_s \left(\text{for } j = \ell - \frac{1}{2}\right)$$

Matrix elements of <u>two-body</u> operators may be a little more complicated from the angular momentum point of view. The most frequently encountered cases involve scalar operators, which can be written in terms of scalar products of spin and orbital operators; these two spaces can then be separated, by transforming the two-body wave functions from $j - j$ to $L-S$ coupling:

$$\langle (s\ell)j, (s\ell)j; \, J_2 M_2 | = \sum_{S_2 L_2} (2j+1) \, \sqrt{(2S_2+1)(2L_2+1)}$$

$$\times \begin{Bmatrix} s & \ell & j \\ s & \ell & j \\ S_2 & L_2 & J_2 \end{Bmatrix} \langle (s^2)S_2, \, (\ell^2)L_2; \, J_2 M_2 |$$

The general case has been treated by Elliott [4]; we here consider the most common example, in which the two-body operator represents (say) a two-body <u>central</u> interaction, in other words is a scalar both in space and spin. As in the one-body case we can deal easily with the spin part; the orbital part will involve the evaluation of

$$\langle \ell^2 L_2 | \, V(r_{12}) \, | \ell^2 L_2 \rangle$$

where $V(r_{12})$ is a scalar function of the distance r_{12}. We shall in fact consider here, not the one-shell case we have considered so far, but the general case where all the l-values involved may be different, i.e.

$$\langle \ell_1 \ell_2 L_2 | \, V(r_{12}) \, | \ell_3 \ell_4 L_2 \rangle$$

Our problem is that V is a function of r_{12} while the two-body wave function is a function of $\vec{r}_1$ and $\vec{r}_2$ separately. We deal first with the general

method, then with the simplified method that is possible when the radial
wave functions are those of a harmonic oscillator.

(a)   General method

We are faced with an integral over two wave functions (which are
essentially a product of functions of $\vec{r}_1$ and $\vec{r}_2$) and a potential (function of
r_{12}).   Our first method rewrites the function of r_{12} as a function of r_1 , r_2
and $\cos \omega_{12}$ where ω_{12} is the angle between $\vec{r}_1$ and $\vec{r}_2$.   Explicitly we write:

$$V(r_{12}) = \sum_k V_k(r_1, r_2) P_k(\cos \omega_{12})$$

where P_k is the Legendre polynomial of rank k.   Clearly we have

$$V_k(r_1, r_2) = \frac{2k+1}{2} \int V(r_{12}) P_k(\cos \omega_{12}) d(\cos \omega_{12})$$

since $\int P_k(z) P_{k'}(z) dz = 2 \delta_{kk'}/(2k+1)$.   If we define a renormalized spherical
harmonic as

$$C_q^{(k)}(\Omega) \equiv \sqrt{\frac{4\pi}{2k+1}} \; Y_{kq}(\Omega)$$

and treat it as a tensor operator of rank k, the spherical-harmonic addition
theorem can simply be written in the notation of a scalar product of tensor
operators

$$P_k(\cos \omega_{12}) = C^{(k)}(\Omega_1) \; C^{(k)}(\Omega_2)$$

Now the two-body wave function is a product of a radial and an angular
part, i.e.

$$\left| \ell_1 \ell_2 L_2 M_2 \right\rangle = \mathscr{R}_{\ell_1}(r_1) \mathscr{R}_{\ell_2}(r_2) \left[Y_{\ell_1}(\Omega_1) Y_{\ell_2}(\Omega_2) \right]_{M_2}^{L_2}$$

Hence putting the results together we see that

$$\left\langle \ell_1 \ell_2 L_2 M_2 \right| V(r_{12}) \left| \ell_3 \ell_4 L_2 M_2 \right\rangle = \sum_k f_k F_k$$

where F_k is a Slater Integral

$$F_k = \int\int \mathscr{R}_{n_1 \ell_1}^*(r_1) \mathscr{R}_{n_2 \ell_2}^*(r_2) \mathscr{R}_{n_3 \ell_3}(r_1) \mathscr{R}_{n_4 \ell_4}(r_2) V_k(r_1 r_2) r_1^2 dr_1 r_2^2 dr_2$$

and f_k is the matrix element of $C^{(k)}(1)\, C^{(k)}(2)$. Using the formula for a scalar product in a coupled system:

$$\langle j_1 j_2 J\, M \,|\, T^{(k)}(1)\; U^{(k)}(2)\,|\, j_1' j_2'\, J'\, M' \rangle = (-1)^k\, W(j_2 J k j_1'\,;\, j_1 j_2')$$

$$\times\, \langle j_1 \,||\, T^{(k)} \,||\, j_1' \rangle \, \langle j_2 \,||\, U^{(k)} \,||\, j_2' \rangle\, \delta_{JJ'}\, \delta_{MM'}$$

we have

$$f_k = (-1)^k\, W(\ell_1 L_2 k \ell_3\,;\, \ell_1 \ell_4)\, (\ell_1 \,||\, C^{(k)} \,||\, \ell_3)(\ell_2 \,||\, C^{(k)} \,||\, \ell_4)$$

Thus f_k is purely geometrical, depending only on the angular momentum quantum numbers; the F_k contain the physics expressed in the radial wave functions.

We can calculate the $(\ell \,||\, C^{(k)} \,||\, \ell')$ from the formulae for integrating three spherical harmonics of the same argument. We find

$$(\ell \,||\, C^{(k)} \,||\, \ell') = \sqrt{2\cdot\ell'+1}\; C^{\ell'\, k\, \ell}_{0\,0\,0}$$

(and therefore vanishes unless $\ell'+k+\ell$ is even; thus only all-even or all-odd k occur in the expansion. Also the triangular rule on ℓ, k and ℓ' limits the number of possible values of k, and hence the number of double integrals F_k that need to be evaluated, to a small value).

Example

Prove that $\delta(\vec{r}_1 - \vec{r}_2) = (1/r_1 r_2)\, \delta(r_1 - r_2)\, (1/2\pi)\, \delta(\cos\omega_{12} - 1)$ and hence for a δ-function $V(r_{12}) = \delta(\vec{r}_1 - \vec{r}_2)$ we have

$$V_k(r_1 r_2) = \frac{2k+1}{4\pi}\, \frac{\delta(r_1 - r_2)}{r_1 r_2}$$

and hence that $F_k = (2k+1)\, F_0$. Hence show that

$$\langle \ell_1 \ell_2 L_2 \,|\, \delta(\vec{r}_1 - \vec{r}_2)\,|\, \ell_1 \ell_2 L_2 \rangle = (2\ell_1 + 1)\left(C^{\ell_1 L \ell_2}_{0\,0\,0} \right)^2 F_0$$

plus an exchange term (evaluate). Hence plot a typical spectrum for ℓ^2 with δ-forces (no exchange needed for equivalent particles). See de Shalit and Talmi [3], p. 219.

<u>(b)   Method for harmonic oscillator wave functions</u>

Talmi has shown that it is possible to reduce the double Slater integrals to single integrals if the radial wave functions are those of a harmonic oscillator. Moshinsky and co-workers have developed (and computed)

expressions [5] for achieving this simplification directly. They transform the <u>wave-function</u> rather than the potential.

Oscillator wave functions for two particles arise from a potential Hamiltonian given by:

$$H_0 = \frac{1}{2}\frac{p_1^2}{m} + \frac{1}{2}m\omega^2 r_1^2 + \frac{1}{2}\frac{p_2^2}{m} + \frac{1}{2}m\omega^2 r_2^2$$

If we <u>define</u>

$$\vec{r} = \frac{1}{\sqrt{2}}(\vec{r}_1 - \vec{r}_2) \qquad \vec{R} = \frac{1}{\sqrt{2}}(\vec{r}_1 + \vec{r}_2)$$

$$\vec{p} = \frac{1}{\sqrt{2}}(\vec{p}_1 - \vec{p}_2) \qquad \vec{P} = \frac{1}{\sqrt{2}}(\vec{p}_1 + \vec{p}_2)$$

(Note these are <u>not quite the same</u> as the standard definitions of relative and centre-of-mass co-ordinate and momentum.) Then we have:

$$H_0 = \frac{1}{2}\frac{p^2}{m} + \frac{1}{2}m\omega^2 r^2 + \frac{1}{2}\frac{P^2}{m} + \frac{1}{2}m\omega^2 R^2$$

We have $\vec{\ell}_1$ and $\vec{\ell}_2$ as conserved angular momentum operators in the old Hamiltonian H_0. We similarly define $\vec{\ell} = \vec{r} \times \vec{p}$ and $\vec{L} = \vec{R} \times \vec{P}$ in the transformed Hamiltonian. A complete set of two-body wave functions can be written in terms of the former quantum numbers:

$$|n_1\ell_1 n_2\ell_2; L_2 M_2\rangle = \sum_{m_1 m_2} C^{\ell_1 \ell_2 L_2}_{m_1 m_2 M_2} \mathscr{R}_{n_1 \ell_1}(r_1) \mathscr{R}_{n_2 \ell_2}(r_2) Y_{\ell_1 m_1}(\omega_1) Y_{\ell_2 m_2}(\omega_2)$$

or in terms of the latter:

$$|n\ell NL; L_2 M_2\rangle = \sum_{mM} C^{\ell L L_2}_{mMM_2} \mathscr{R}_{n\ell}(r) \mathscr{R}_{NL}(R) Y_{\ell m}(\omega) Y_{LM}(\Omega)$$

We have of course the relationship

$$\vec{\ell}_1 + \vec{\ell}_2 = \vec{\ell} + \vec{L} = \vec{L}_2$$

The (real, orthogonal) transformation between these two complete sets can be written

$$|n_1\ell_1 n_2\ell_2 L_2 M_2'\rangle = \sum_{\substack{n\ell \\ NL}} |n\ell NL\, L_2 M_2\rangle\langle n\ell NL\, L_2|n_1\ell_1 n_2\ell_2 L_2\rangle$$

where the transformation coefficient is independent of M_2 of course. These coefficients $\langle n\ell\, NL\, L_2 | n_1\ell_1 n_2\ell_2 L_2 \rangle$ are called <u>Moshinsky brackets</u> and are extensively tabulated [5]. As well as having to obey the triangular relations implied by the angular momentum condition above, the brackets obey an <u>energy condition</u> – the number of energy quanta in the $n_1\ell_1 n_2\ell_2$ system must be the same as that in the $n\ell\, NL$ system. This gives the condition:

$$2n_1 + \ell_1 + 2n_2 + \ell_2 = 2n + \ell + 2N + L$$

To apply the method we first have to make the trivial but vital transformation from $V(r_{12})$ to $V(r)$ where $r = (1/\sqrt{2})\, r_{12}$. Having done this we then have

$$\langle n_1\ell_1 n_2\ell_2 L_2 M_2 |\, V\,(r)\, | n_3\ell_3 n_4\ell_4 L_2 M_2 \rangle$$

$$= \sum_{n\ell NL} \sum_{n'\ell'N'L'} \langle n_1\ell_1 n_2\ell_2 L_2 | n\ell NLL_2 \rangle \langle n'\,\ell'\,N'\,L'\,L_2 | n_3\ell_3 n_4\ell_4 L_2 \rangle$$

$$\times\ \langle n\ell NLL_2 M_2 | V(r) | n'\,\ell'\,N'\,L'\,L_2 M_2 \rangle$$

We take $V(r)$ to be a scalar, and it operates of course only on the relative co-ordinate, i.e. only on "part 1" of the coupled system. This gives a factor $\delta_{NN'}\cdot\delta_{LL'}\cdot\delta_{\ell\ell'}$ and the final result

$$\langle n_1\ell_1 n_2\ell_2 L_2 M_2 |\, V(r)\, | n_3\ell_3 n_4\ell_4 L_2 M_2 \rangle$$

$$= \sum_{nn'\ell} \sum_{NL} \langle n_1\ell_1 n_2\ell_2 L_2 | n\ell NLL_2 \rangle \langle n'\,\ell NLL_2 | n_3\ell_3 n_4\ell_4 L_2 \rangle$$

$$\times \int_0^\infty \mathscr{R}_{n\ell} V(r)\, \mathscr{R}_{n'\ell}(r)\, r^2 dr$$

involving the (tabulated) brackets and a simple single integral.

We can go one stage further. The $R_{n\ell}(r)$ are (polynomials of rank ℓ in $\underline{r}$) $\times \exp(-r^2/2)$ where we have expressed r in terms of units of $b = \sqrt{\hbar/m\omega}$, the oscillator length constant. All the integrals are therefore sums over integrals of the form

$$I_p = \frac{2}{\Gamma\left(p + \dfrac{3}{2}\right)} \int_0^\infty r^{2p}\, e^{-r^2}\, V(r)\, r^2 dr$$

(the normalization is such that $I_p = 1$ when $V(r) = 1$ everywhere). These are called <u>Talmi integrals</u>. We can now write

$$\int_0^\infty \mathscr{R}_{n\ell}(r)\, V(r)\, \mathscr{R}_{n'\ell'}(r)\, r^2 dr = \sum_p B(n\ell, n'\ell', p)\, I_p$$

where the B's can be tabulated once and for all. This has also been done [5].

Gaussian, Yukawa and Coulomb forces are all particularly easy to calculate with in this scheme, since the Talmi integrals can be performed analytically.

REFERENCES

[1]   COHEN, S., KURATH, D., LAWSON, R.D., MacFARLANE, M.H., SOGA, M., Meth.Comp.Phys. <u>6</u> (1966) 235.

[2]   EDMONDS, A.R., FLOWERS, B.H., Proc.Roy.Soc. <u>A214</u> (1952) 515.

[3]   See, e.g. DE SHALIT, A., TALMI, I. "Nuclear Shell Theory", Academic Press (New York and London) 1963.

[4]   ELLIOTT, J.P., Proc.Roy.Soc. <u>A218</u> (1953) 345.

[5]   BRODY, T.A., MOSHINSKY, M., "Tables of Transformation Brackets", Instituto di Fisica (Mexico) 1960.

BASIC EVIDENCE AND PROPERTIES
OF SINGLE-PARTICLE STATES IN NUCLEI

N. CINDRO†
Institute "Rudjer Bošković", Zagreb,
Yugoslavia

Abstract

BASIC EVIDENCE AND PROPERTIES OF SINGLE-PARTICLE STATES IN NUCLEI.
1. Introduction: the shell-model orbitals; 2. Information about single-particle orbitals: a critical evaluation; 3. Experimental evidence: 3.1. The lead region; 3.2. The calcium region; 3.3. Nuclei far from closed shells; 4. Conclusion.

1. INTRODUCTION: THE SHELL MODEL ORBITALS

This paper is meant as the experimental counterpart of Professor Alaga's paper on the foundations of the shell model. Hence, one could jokingly say that our task is to prove that what Prof. Alaga was saying up to now is experimentally correct and well founded. Now, with theoreticians this is always difficult; it would be much easier to prove that what they are saying is wrong. However, in this case our task is somewhat simplified in the sense that both Prof. Alaga and we are talking about a subject that seems to be well established, namely the shell model of the nucleus. We should, therefore, include in this paper not so much the evidence for this model – this evidence is well known and, anyway, it can be found in every nuclear physics textbook – but an evaluation of the state of art in crucial matters pertaining to the shell model: single-particle and single-hole levels, the fractioning of single-particle strength, the effect of core excitation and the way how we get at it. Of course, we shall not dwell on experimental methods. When we say "stripping reaction" we shall assume that we know what it is, and it is not necessary to know what experimental means are implied in its measurement.

In his paper, Alaga gives the theoretical foundations of the shell model (we shall use the names shell model and independent-particle-model interchangeably). The essence of his paper is the statement that it is now possible to understand why protons and neutrons are moving independently in something which can be called an average potential.

What does this mean? It means that we can take the nuclear Hamiltonian H and split it into two parts:

$$H = H_0 + \varkappa$$

where H_0 stands for an average potential and $\varkappa$ stands for everything which is not included in this average potential. Of course, we can do this with any Hamiltonian. The goodness of the shell model approach lies in the fact

---

† This work was completed in part while the author was at the Service de Physique Nucléaire à Basse Energie, CEN Saclay, France.

that H_0 contains already the essential features of the nuclear dynamics, i.e. that the wave function ψ obtained from

$$H_0 \psi = E_0 \psi$$

describes already, in zeroth approximation, the behaviour of the nucleus, whereas $\mathscr{v}$ can be treated as a relatively small perturbation.

Is this actually so? Namely, we are always speaking of the shell model; now, we know that a model is essentially a parametrization of data, i.e. a complex way of doing numerology, which is not necessarily related to the literal truth of nature. Is there some literal truth in the shell model? Rather than give an answer to the question posed in this way, we shall discuss the point how literally can we take the notion of neutrons and protons moving independently in unperturbed orbitals. Of course, when we say "orbitals" what we mean is motion with given angular momentum.

The facts of our knowledge of the nuclear shell model are, as a rule, highly inferential and come from a comparison with experiment of derived quantities such as energies and transition moments. We should like to have something more closely and directly demonstrating the literal truth – if any – of the independent-particle model.

A comprehensive survey of some experiments performed recently in order to elucidate this point was given by D.H. Wilkinson [1]. A direct way of probing the behaviour of a nucleon in the nucleus is to knock it out suddenly. If its motion is independent of that of other nucleons, the collision will be described by ordinary ballistics laws. The energy of the struck nucleon will be related in a simple way to its binding energy and the energy of the colliding particle: its momentum (mirrored by the angular distribution) will reflect the momentum distribution in the nucleus.

Let us consider a particle knock-out experiment in the 1p shell (^{4}He – ^{16}O region). In the zero-order independent-particle model, without any residual nucleon-nucleon interaction and spin-orbit coupling, we should expect two widely separated groups in the particle spectrum, corresponding, respectively, to knocking out particles from the 1p and 1s orbitals, the latter being more bound by about 15 - 20 MeV (Fig. 1a). We know, however, that this is a very rough approximation since we have to take into account the spin-orbit force (which splits the 1p orbital into two) and the residual nucleon-nucleon interaction, which, in turn, will split the pure 1s and 1p configurations by, perhaps, several MeV. In other words, the experimental spectrum will show several peaks, corresponding to the various states that can be left behind on a sudden removal of a nucleon, because of the different ways in which the residual interaction may act among the remaining nucleons (Fig. 1b).

Nevertheless, if the independent-particle picture is basically true, the effect of the spin-orbit and the residual interactions can change the picture only quantitatively, introducing states that cannot be reached by the primitive theory, without changing the general pattern. This pattern is shown in Fig. 1c.

The results of a real experiment are shown in Fig. 1d. It demonstrates strikingly the literal shell-structure of the nucleus. The spectrum is that of the ^{12}C (p, 2p) ^{11}B reaction at 160 MeV taken with about 3 MeV resolution [2]. It is very suggestive to take the two peaks as corresponding to, respectively, the 1p and 1s particles, the poor energy resolution having
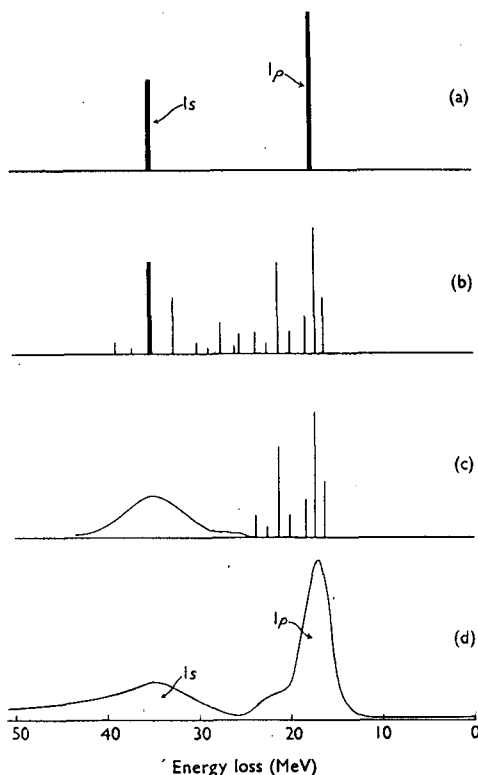
FIG.1. Energy spectra in the 1s-1p shell nuclei: various degrees of idealization (a, b, c) and experiment (d) (from Ref.[1]).

smeared out the fine-structure. As the binding energy of particles moving in an average field depends essentially on their size, the above result can be cross-checked by calculating the nuclear size through the use of a Saxon-Woods potential. The derived result agrees well with those obtained from electron scattering and Coulomb energy difference [3].

A more direct cross-check as to the nature of the peaks presented in Fig. 1d is given by the correlation experiments. As mentioned above, the correlation between the emerging particles, notably the angular distribution of the struck nucleon, will be determined by the momentum distribution in the nucleus itself. The momentum distributions for s and p particles are rather different, the former having a pronounced forward ($0°$) maximum, the latter having zero cross-section in the forward direction. Figure 2 shows data from the ^{12}C (e, e'p) ^{11}B experiment [4] performed in Frascati, where fixed-energy electrons, inelastically scattered at a fixed angle, were measured in coincidence with protons of fixed energy and variable angle of emission; in this way the momentum distribution of the struck nucleon could be measured. The particle energies were chosen so as to correspond to the maxima of the 1s and 1p peaks of Fig. 1, respectively. The lines (Fig. 2) show the expectation calculated on the basis of harmonic-oscillator 1s and 1p wave functions. The results wholly confirm the above orbital angular-momentum assignments for the two peaks.
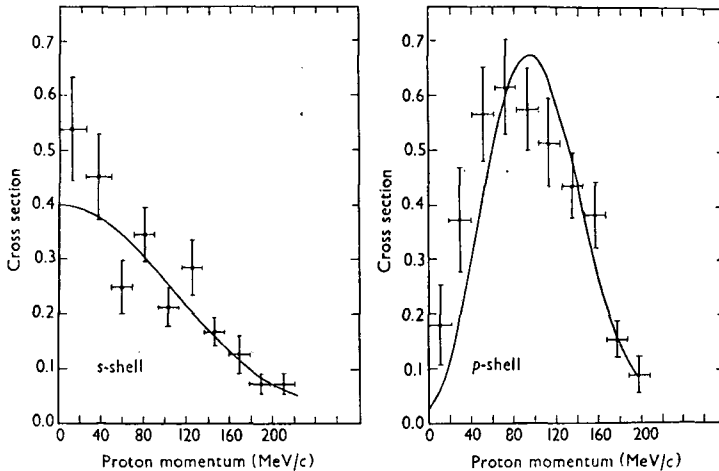
FIG.2.   Momentum distribution of the struck proton in the reaction ^{12}C (e, e' p) (from Ref.[4]).

These results, which examine directly the shell structure of a nucleus, leave no doubt that individual nucleons spend most of their time in motions which are roughly independent of the motion of neighbouring nucleons. At least, in light nuclei.

The transition to heavy nuclei is not trivial. To explore experimentally the deep-lying shells of heavy nuclei, one needs fine resolution, several hundred MeV particles, that are only becoming gradually available.

Thus we see that speaking of, e.g. 2f or 1g particles is not only a convenient way of classifying particles, but there is something more to it. By this we do not say that the shell model is an exact theory. What we are saying is that the independent-particle model is a good description of the essential features of nuclei, based on some good direct experimental evidence, and that the zeroth approximation contained in H_0 is applicable to solving nuclear problems. We should stress that this, alone, is not a minor achievement.

Let us see now what we know more about shell-model orbitals.

First an elementary fact: protons and neutrons move in separated orbitals. The p-p and n-n interactions are, furthermore, different. In fact, they differ by the Coulomb interaction. For heavier nuclei this should make, at first sight, quite a difference. Namely, from the stability of nuclei, it turns out that the highest filled orbits for protons and neutrons should be found at the same potential energy. If this were not the case, nuclei would be β-unstable. Hence one would expect the proton orbits to be wider spaced than the neutron ones. It is also plausible that the location of single particle states depends on the mass number A (size of the average potential well).

This problem was investigated by Cohen [5]. Contrary to what might be believed, the second effect (A dependence) is more important than the first. Figure 3 shows proton and neutron orbits in the region of 82 to 126. A remarkable similarity exists between the relative positions of the neutron and proton single-particle levels in the A = 208 region. This similarity is far greater than between neutron single-particle levels in, for example, ^{141}Ce and ^{207}Pb (right-hand side of Fig. 3), i.e. neutron levels correspond-
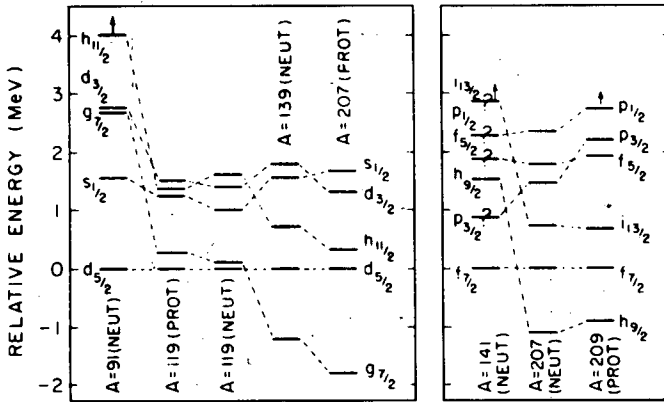
FIG.3.   Proton and neutron single-particle levels in the 82 - 126 particle region (from Ref.[5]).

ing to nuclei with different A.   The principal difference between the latter
is that the 1h$_{9/2}$ and 1i$_{13/2}$ orbitals move down with increasing A.   The
small upward shift of proton p-levels (ℓ = 1) can be explained tentatively
by assuming that particles of low angular momentum are near the centre,
where the Coulomb field is strongest, and shifts them up.

     A similar situation is shown on the left-hand side of Fig. 3 where the
50 - 82 single-particle levels are shown.   The similarity between single-
particle proton and neutron orbitals is remarkable (case of ^{119}Sb and ^{119}Sn)
while, e.g. single-particle orbitals for 50 neutrons and 50 protons, corres-
ponding to nuclei with A = 91 and A = 119 (^{91}Nb and ^{119}Sn) are very different.

     The same behaviour, although with less regularity, is shown for the
single-particle levels in the region of 20 - 50 particles.   Again the f and g
levels (ℓ = 3 and 4) shift down with respect to the p states with increasing A
(Fig. 4).

     The A-effect is, thus, more important in the location of single particle
levels than the effect of the Coulomb field.   Proton and neutron levels in
nuclei with close mass numbers (A) show a much stronger similarity than
expected at first sight.

2.   INFORMATION ABOUT SINGLE-PARTICLE ORBITALS: A CRITICAL
     EVALUATION

     After these preliminary remarks let us now answer the question of
how we learn about single-particle orbits.   We have seen the straight-
forward way.   However, the direct way is not always the simplest.   The
bulk of our information comes from the so-called transfer reactions.

     What is a transfer reaction?   It is a nuclear process in which a nucleon
or a cluster of nucleons is transferred from one nucleus to another without
considerably disturbing the rest of the nucleons.   Typical transfer reactions
are the so-called stripping [(d, p), (d, n), (^{3}He, d), (t, d), (α, ^{3}He), (α, t)] and
pick-up [(p, d), (n, d), (d, ^{3}He), (d, t), (^{3}He, α), (t, α) etc..] reactions.   In all
these reactions we add or subtract nucleons to the target nucleus and thus
we can learn something about the wave function of the nucleus.   Here we
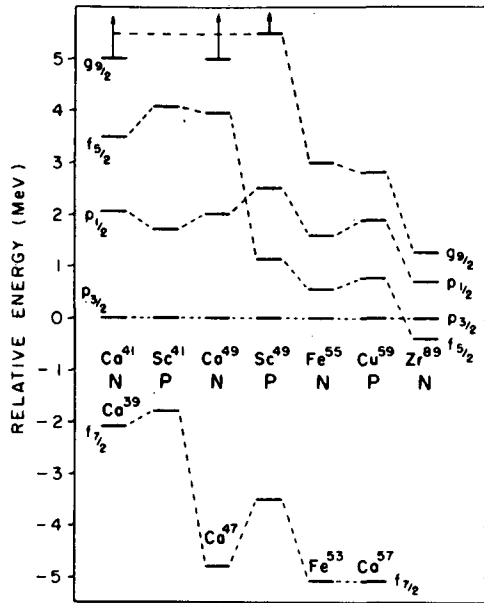
FIG.4.   Proton and neutron single-particle levels in the 20 - 50 particle region (from Ref.[5]).

have mentioned only single—nucleon transfer reactions. We shall, however, also utilize reactions in which more then one nucleon is transferred.

We shall assume, furthermore, that the mechanism of transfer reactions, – at least the mechanism of single—nucleon transfer, – is well described by the DWBA.

We shall not discuss here the DWBA; we shall rather examine some critical points in the physical basis of the DWBA and review the approximation involved. (For a detailed treatment, see, e.g. the article by W. Frahn in these Proceedings.)

The matrix element for a direct transition between an initial state i and a final state f is given by

$$T_{if} = \langle \phi_f | V | \psi_i \rangle \tag{1}$$

where ψ_i and ϕ_f are wave functions or the initial and final states and V is the interaction causing the transition.

The exact wave functions of nuclear systems are not available, nor do we know the exact interaction. It has been shown, however, that the exact expression (1) from the point of view of perturbation theory can be approximated by

$$T_{if} = \langle \chi_p^{(-)} | V | \chi_d^{(+)} \rangle \tag{2}$$

where

$$\chi_d^{(+)} = \psi_d^{(+)} (\vec{k}_d, \vec{R}) \, \phi_d(r) \, \chi_1^\mu (\vec{\sigma}_n, \vec{\sigma}_p) \, \Psi_{J_i}^{M_i} \tag{3a}$$

and

$$\chi_p^{(-)} = \psi_p^{(-)} (\vec{k}_p, \vec{r}_p') \chi_{1/2}^{\mu_p} \psi_{J_f}^{M_f} (A, \vec{r}_n, \vec{\sigma}_n) \tag{3b}$$

with

$$\vec{r} = \vec{r}_n - \vec{r}_p \qquad 2\vec{R} = \vec{r}_n + \vec{r}_p \qquad \vec{r}_p' = \vec{r}_p - \left(\frac{m_p}{m}\right)\vec{r}_m$$

where $\phi_d(r)$ is the internal wave function of the deuteron,
χ_1 its spin wave function (only S state, since D state is less than 10%),
ψ_{J_i}, ψ_{J_f} wave functions for the target and final nuclei and
$\chi_{1/2}$ proton spin-wave function.
$\psi_d^{(+)}$ and $\psi_p^{(-)}$ are elastic-scattering wave functions to be computed from the one-body interactions between the deuteron and the target and the proton and the target, respectively.

The next problem is the evaluation of expression (2). To compute the ingredients of this expression we shall have to make several approxima-tions. In writing expression (2) we have, however, already made some approximations:

    i) first, we have <u>factorized the wave functions for both the initial and the final state</u>. This implies weak coupling between the particle (outgoing and incoming) and the nuclear co-ordinates (the so-called sudden approximation);

    ii) second, we have tacitly assumed <u>that there will be only one collision by which the nucleon(s) is (are) removed from the target</u> (absence of so-called rearrangement stripping).

To calculate the components of the wave functions of Eqs (3a) and (3b) we introduce the distorted-wave approximation (DWA). We assume that the nucleus distorts the wave functions of the incoming and outgoing par-ticles and that this distortion is described by the optical model. Hence,

    iii) <u>the elastic-scattering wave functions $\psi_d^{(+)}$ and $\psi_p^{(-)}$ are substituted by the elastic-scattering wave functions</u> obtained from the optical model: Schrödinger differential equation.

Of the above approximations, the first and the third are crucial. Notably the third, which, by itself, need not be a bad approximation if it were not for the ambiguity in determining the parameters of the optical potential. Moreover, reasons connected with numerics of the integration of the optical functions may, e.g. force us to use zero-range forces, which is by itself a further approximation[1].

The difficulties caused by the radial part of the bound-state wave function are well known. This function is calculated from the Schrödinger type equation using a Saxon well with the binding energy of the transferred particle in the residual nucleus as an experimental parameter. This latter value is not always known and may introduce a serious error. This effect, however, could not be considered as an approximation, it is rather an imperfection of the method.

To recapitulate, the DWA analysis of transfer reactions gives two essential pieces of information concerning the shell-model orbitals:

    – the angular momentum of the orbit to which the transferred nucleon is stripped or picked-up;

---

[1] Surprisingly enough, this approximation does not seem to be too crucial in some aspects. In fact, finite-range DWA calculations were performed with no appreciable difference in the shape of the predicted angular distributions.

–ˈ the so-called spectroscopic factor S which tells us how well a state
is described by a single particle coupled to a core.

The angular momentum ℓ is a geometrical information which is deter-
mined from the kinematic conditions of the process. It is extracted from
the shape of the angular distributions and is not, in general, affected by
the above approximations. Hence DWA remains still a good tool for deter-
mining the angular momentum of the transferred particle.

The spectroscopic factor S remains the weakest point of the DWA ana-
lysis. This quantity is related to the expansion coefficients β_ℓ which give
the overlap between (a) the real wave function of the final state (residual
nucleus) and (b) a wave function constructed by vector-coupling the extra
nucleon in a spin-orbit state (j, ℓ) to the target nucleus [6]. If the final
state is in effect what we call a single-particle state, the overlap will be
large. Hence the spectroscopic factor tells us how well a state is described
by a single particle coupled to the core (see also chapter 4).

Most of our knowledge on shell filling comes from the obtained spectro-
scopic factors. It is therefore of utmost importance to keep in mind the
restrictions of the DWA. All the approximations we have mentioned – and
some that we have not – are present in the different codes we use to obtain
spectroscopic factors [7]. Knowing all this plus the fact that in the DWA
codes we use poor model wave functions it is more than surprising that we
obtain any consistent result.

Yet, we do obtain more or less consistent results which show that
there is a good physical basis to the DNA, namely the perturbation theory.
We believe that the "experimentally" obtained spectroscopic factors can
be trusted – if obtained correctly – to about 30 – 50%, the error being more
or less stochastic.

Qualitatively, thus, the most important fact stemming from the DWBA
analysis of transfer reactions is that the individual orbital angular
momentum of nuclear particles is a good quantum number. The informa-
tion about the spectroscopic factors should, however, be read very
carefully.

There are, of course, other methods to obtain information about single-
particle states, in particular using the ft values in β-decay. We shall,
however stop at this point and look at the experimental situation in a few
typical cases. We shall examine two regions: the Pb region of closed
shells Z = 82 and N = 126 and the Ca region of closed shells Z = N = 20.
Later we shall go away from closed shells, but let us first examine the Pb
and Ca region.

3.   EXPERIMENTAL EVIDENCE
3.1.   The lead region (Z = 82, N = 126)

The lead region: $^{208}Pb^{\pm}$ particle or hole. Physicists usually say that
^{208}Pb is a shell-model nucleus par excellence. Many would even say that
it is the only shell-model nucleus in the periodic table. In the sense that
a good shell-model nucleus is one for which the first term in the separation

$$H = H_0 + \mathbf{w}$$

presents a good approximation, ^{208}Pb is definitely good. On the other hand,
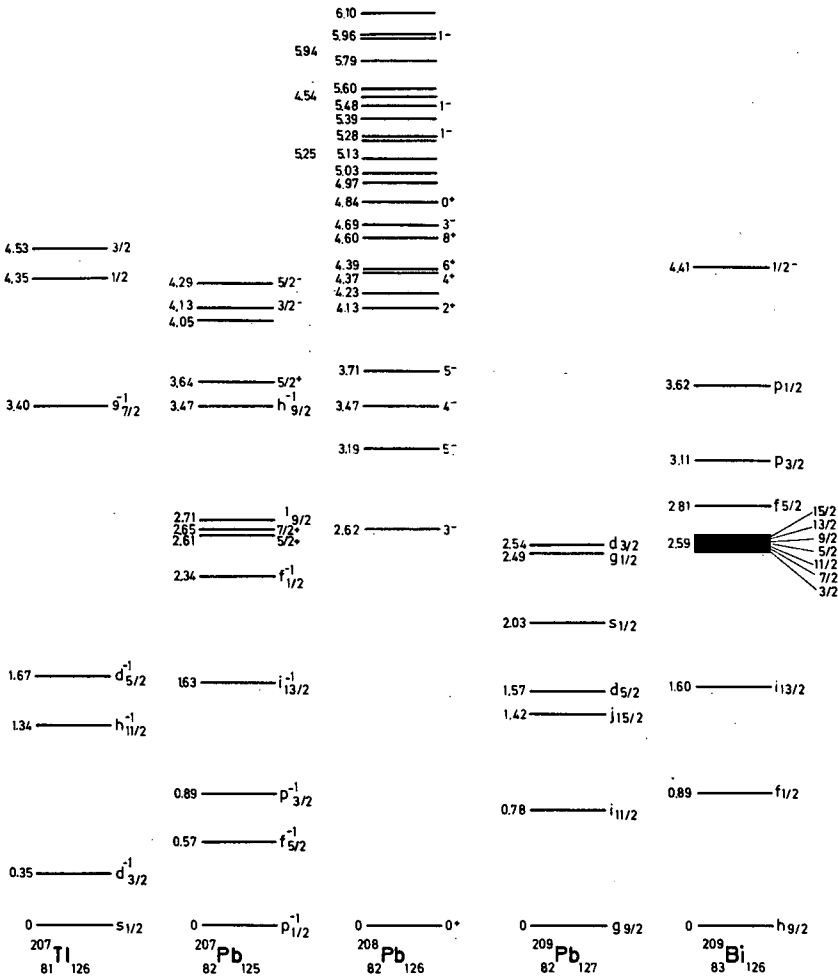
FIG.5.   Spectra around the Z = 82, N = 126 shells.

single-particle orbitals in ^{208}Pb are closely spaced allowing more con-
figuration mixing than expected for a good shell-model nucleus.

Let us examine the single-particle and single-hole levels in the Pb
region. They are shown in Fig.5.

This information is collected from various sources. We shall concen-
trate on more recent ones. The neutron single particles and single holes
around ^{208}Pb were recently studied by Muehllehner et al. [8] by means of
a combined study of (d, p) and (d, t) reactions. We consider ^{208}Pb a closed-
shell core; the (d, p) reactions will add neutrons on single-particle levels,
while the (d, t) reaction will pick up neutrons from existing levels. Hence
we should expect that the strongly excited levels in the, e.g. (d, p) reaction
will be single-particle levels. Figure 6 shows the experimental spectrum
of the ^{208}Pb (d, p)^{209}Pb reaction, while Fig.7 shows the corresponding (d, t)
spectrum. Both spectra have a common feature: a few isolated, strong
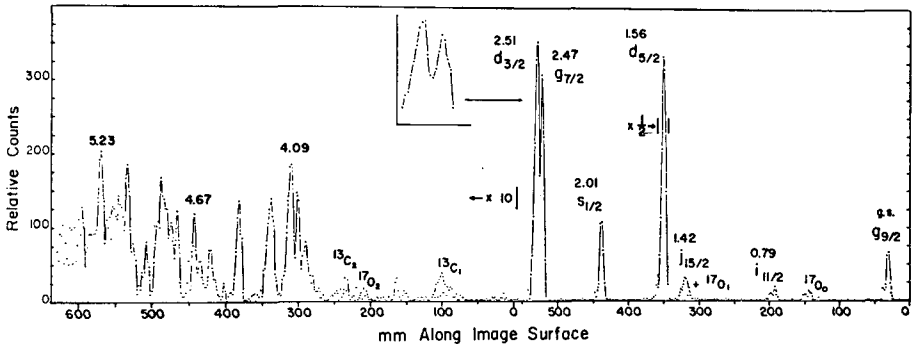
FIG.6.   The spectrum of the ²⁰⁸Pb(d,p)²⁰⁹Pb reaction (from Ref.[8]).
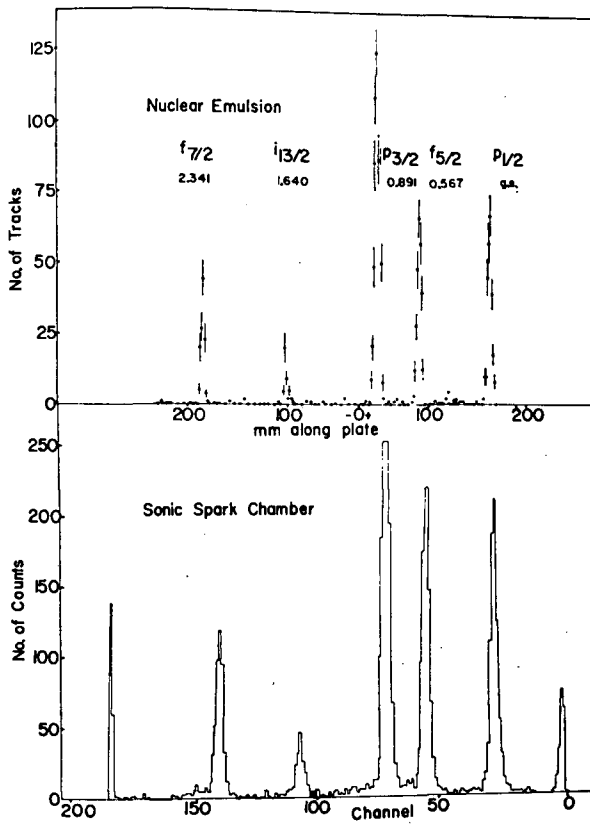
FIG.7.   The spectrum of the ²⁰⁸Pb(d,t)²⁰⁷Pb reaction (from Ref.[8]).

peaks and all the rest is much smaller. This is particularly visible in the
(d, p) reaction (Fig. 6), where the left-hand side of the spectrum has been
multiplied by 10.

TABLE Ia.   NEUTRON SINGLE-PARTICLE LEVELS IN ^{209}Pb EXCITED
BY THE ^{208}Pb(d, p)^{209}Pb REACTION (from Ref.[8]).

Level	Present work	Brady[a]	Cohen[b]	Harvey[c]
$p_{1/2}$	Q = -1.13 ± 0.01		-1.12	-1.10
$f_{5/2}$	E_x = 0.57	0.570	0.57	0.61
$p_{3/2}$	0.89	0.897	0.90	0.95
$i_{13/2}$	1.64	1.633	1.64	1.61
$f_{7/2}$	2.34	2.339	2.35	2.33
	3.23			
	3.33		3.38	
$h_{9/2}$	3.43		3.47	
	3.59			

[a] Brady, F.P., Peek, N.F., Warner, R.A., University of California, Davis, Report CNL-UCD 23
     (unpublished).
[b] Cohen, B.L., Mayo, S., Price, R.E., Nucl. Phys. 20 (1960) 360.
[c] Harvey, J.A., Can. J. Phys. 31 (1953) 278.

TABLE Ib.   NEUTRON SINGLE-HOLE LEVELS IN ^{207}Pb EXCITED BY
THE ^{208}Pb(d, t)^{207}Pb REACTION (from Ref.[8]).

Level	Present work	Mukherjee[a]	Erskine[b]	NDS[c]
$g_{9/2}$	Q = 1.70 ± 0.01	1.6	1.705 ± 0.015	...
$i_{11/2}$	E_x = 0.79	0.77	0..774	0.79
$j_{15/2}$	1.42	1.41	...	1.41
$d_{5/2}$	1.56	1.56	1.563	1.56
$s_{1/2}$	2.01	2.03	2.015	2.03
$g_{7/2}$	2.47	2.47	2.483	2.47
$d_{3/2}$	2.51	2.52	2.527	2.54

[a] Mukherjee, P., Cohen, B.L., Phys. Rev. 127 (1962) 1284.
[b] Erskine, J.R., Buechner, W.W., Bull. Am. phys. Soc. 7 (1962) 360.
[c] Nuclear Data Sheets, compiled by K. Way et al. (Printing and Publishing Office, National
     Academy of Sciences - National Research Council, Washington 25, D.C.) NRC 5-3-93 to
     5-3-94.

The energies of these levels are given in Tables Ia and Ib. To test
whether these levels correspond to single-particle levels, we perform the
usual DWBA analysis. Of course, we have already anticipated that they
will be close to one and written the single-particle configurations pertain-
ing to these energies. That this is more or less the case we see in
Tables IIa and IIb.

In fact, the spectroscopic factors for most of the levels are close to
unity in the (d, p) case and to (2j + 1) in the (d, t) case. (This difference
comes from the fact that the comparison for (d, t) cross-sections was done
using a formula which did not contain a (2j + 1) factor.) The values of the

TABLE IIa. SPECTROSCOPIC FACTORS FOR SINGLE-PARTICLE
STATES IN THE REACTION ^{208}Pb(d, t)^{207}Pb (from Ref.[8]).

Level	15.0 MeV	20.3 MeV	25.1 MeV
$g_{9/2}$	0.87	0.77	0.67
$i_{11/2}$	1.17	0.78	0.94
$j_{15/2}$	0.96	0.79	1.13
$d_{5/2}$	0.83	1.05	1.00
$s_{1/2}$	0.80	0.90	0.93
$g_{7/2}$	1.08	1.08	1.17
$d_{3/2}$	0.88	1.07	1.17

TABLE IIb. SPECTROSCOPIC FACTORS FOR SINGLE-HOLE STATES
IN THE REACTION ^{208}Pb(d, t)^{207}Pb. (from Ref.[8]).

Level	14.8 MeV	20.1 MeV	24.8 MeV
$p_{1/2}$	2.18	2.12	2.12
$f_{5/2}$	6.60	7.20	6.00
$p_{3/2}$	3.76	3.80	3.32
$i_{13/2}$	14.00	13.02	14.00
$f_{7/2}$	6.08	6.40	5.76
$h_{9/2}$		10.00	

spectroscopic factors are, however, interesting in another aspect. They
are, namely, incident-energy dependent, and, moreover, the value for the
$g_{3/2}$, g.s. configuration of ^{209}Pb is not quite unity. This, of course,
might show that there is something wrong with our picture of ^{209}Pb as an
inert ^{208}Pb core + neutron, but it is more likely showing the limitations of
the DWBA analysis and extracted spectroscopic factors.

Now we have a good idea of the single-particle neutron levels around Pb.
An important point is that the single-particle strength is not fractionated
and that the shell-model picture appears to work well in this region.

We have already seen the proton-particle states in Figs 3 and 5. The
situation is quite analogous to that of neutron particle states, except for
the fact that the shell-model orbitals involved are different. Detailed in-
formations on proton states can be found in the references listed in Ref.[9].

It would, of course, be wrong to conclude that the spectra of
(^{208}Pb $\pm$ 1p or 1h) consist of only single-particle or hole levels. In the same
way as coupling to the ground state, particles and holes can couple to some
strongly excited states of ^{208}Pb. As can be seen from Fig.5, the energy
spectra of ^{207}Pb or ^{209}Bi show more levels then observed in (d, t) or (^{3}He, d)
stripping. What is the nature of these levels?

In this respect it is very interesting to look at the manifold of levels
around 2.6 MeV in ^{209}Bi [11]. These levels are centred around the energy
of the 2.62 MeV 3$^-$ collective level in ^{208}Pb and are most conveniently
interpreted as the result of a coupling of the $h_{9/2}$ proton to the 3$^-$ level of

^{208}Pb. Angular—momentum coupling rules allow j values for the coupling of a $h_{9/2}$ particle to a 3⁻ level, ranging from $3/2^+$ to $15/2^+$. All these levels were found within 200 keV. Their spins were determined by the use of the $(2j+1)$ sum rule.

We see that even in the finest shell-model nuclei (^{208}Pb + a single particle or hole) the contribution of particles in the closed-shell core should be taken into account if we want to have an accurate description of physical reality. Naturally, this does not mean that the shell model is wrong; it means that it should be refined and that H_0, although it gives the essential features of the nuclear behaviour, does not give all of them.

Another example of the same kind is reported in Ref.[12], where single neutron—hole states of ^{207}Pb were excited in inelastic scattering of protons. Inelastic scattering of protons provides a good experimental test for the microscopic structure of levels. Now, the states at 0.570, 0.894, 1.633 and 2.33 MeV in ^{207}Pb were so far interpreted as practically pure single hole states corresponding to, respectively, the $2f_{5/2}$, $3p_{1/2}$, $i_{13/2}$ and $2f_{7/2}$ neutron holes in a ^{208}Pb core. As mentioned before, no definite evidence has been found from a transfer reaction leading to ^{207}Pb that the hole strength is split and that ^{208}Pb is not a good closed core.

What about other processes? The inelastic scattering on hole states gives the values of B(E2) for the $(2f_{5/2})^{-1} \rightarrow (3p_{1/2})^{-1}$ and $(3p_{3/2}^{-1}) \rightarrow (3p_{1/2}^{-1})$ transitions. These experimental values require an effective charge close to 1! Now, we know what effective charge (for a neutron) means: it is a way of parametrising the composite action of all the core particles.

Another fact which favours this interpretation is the angular distribution of inelastic protons: the DWBA gave a good fit only when considerable amounts of core polarization component was added to the single—hole wave function of these states.

Perhaps the most dramatic demonstration of the core + particle coupling in the lead region are the experiments by Stein et al. [13] which show that this description is valid even when the energies of both particle and core increase considerably. Stein et al. have investigated analogue states in ^{209}Bi by proton inelastic scattering on ^{208}Pb. The compound nucleus states formed in ^{209}Bi are analogues to the low—lying states in ^{209}Pb. As can be seen in Fig. 8, between 18 and 22 MeV bombarding energy new resonance behaviour is observed in the inelastic scattering to the 2.615 MeV 3⁻ level, totally missing in the ground state (elastic scattering). Now, if these resonances are isobaric analogues, they correspond to levels in ^{209}Pb between 4 and 6 MeV of excitation. A simple interpretation of the results would then be that the structure of these ^{209}Pb levels can be described as a ^{208}Pb core, excited to its 3⁻ state coupled to the odd neutron in one of its single-particle states. It is clear that the isobaric analogues of these levels would then be expected to decay strongly to the 3⁻ level in ^{208}Pb. In a simple-minded picture, we should expect 7 multiplets of levels, one for each of the 7 low—lying single-particle states. The location of each multiplet, obtained by simply adding 2.62 MeV to each single particle state is shown by arrows in Fig. 1. The agreement with the position of the resonances is remarkable.

It should, however, not be forgotten, and we should repeat again and again that although these examples show that the simple shell model description in the region of ^{208}Pb is not valid, the fact is that it fails only
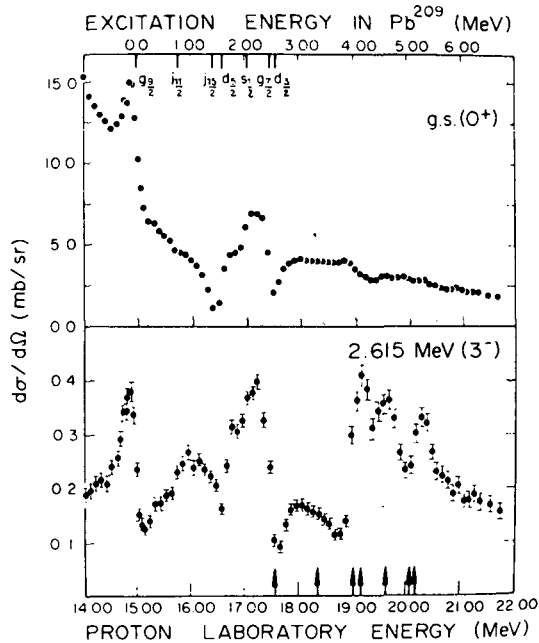
FIG. 8.   Excitation function of the ^{208}Pb (p, p) ^{208}Pb reaction in the elastic and inelastic channels (from Ref.[13]).

when applied to details; the main features of spectra are, nevertheless, well described.

The lead region: ^{208}Pb. Let us now turn to the microscopic description of the ^{208}Pb core in terms of the shell model.   Being a doubly closed shell, ^{208}Pb can be excited only by creating pairs of holes and particles.   The simplest way how to excite it would be to lift one single particle to the next orbital leaving a hole in the filled shell.   For neutron particle–hole pairs this would be a ($g_{9/2}$, $p_{1/2}^{-1}$) configuration, its unperturbed energy would be higher than 3 MeV.   For proton particle–hole pairs this would be a ($h_{9/2}$, $s_{1/2}^{-1}$) configuration; its unperturbed energy would be still higher. Now, the lowest excited state in ^{208}Pb the 3$^-$ state (which, by the way, could not be formed at all by these configurations because of its spin and. parity) lies at 2.62 MeV!

This has been explained as the result of a coherent action of many particle–hole configurations to form what we call a collective level.   For instance, the mentioned 3$^-$ state in ^{208}Pb would be a coherent mixture of 17 neutron and 14 proton particle–hole configurations [14].   We will leave the details of this description to other papers in these Proceedings.   Nevertheless, this gives us an indication as to the sense in which we should orient our experimental investigations, since our experimental methods should be adapted to the nature of levels which we want to investigate.   In particular, single particle–hole configurations should be investigated by stripping a single particle over an existing hole or vice-versa, more complex configuration by the transfer of several particles or holes, etc. ...

The levels of ^{208}Pb are shown in Fig. 5.   There are many of them, still more are found virtually day by day, and it is thus probably that very different configurations are present.

The easiest way to investigate the particle-hole structure of ^{208}Pb is by means of the ^{207}Pb (d, p)^{208}Pb reaction. What are the particle-hole levels bound to be excited by such a reaction? It is clear that only levels having configurations of the type [particle, $p^{-1}_{1/2}$]$_n$ will be excited. This reaction was investigated by Bardwick and Tickle [14] and earlier by other authors [15].

We shall discuss here the results of Ref.[14] where incident deuterons of 21.6 MeV and magnetic analysis were used. As mentioned above, we expect that configurations of the type (particle, $p^{-1}_{1/2}$) will be excited. On the other hand, collective levels like the 3$^-$ level at 2.62 MeV, consisting of <u>many</u> particle-hole configurations should be weakly or not at all excited. This latter conjecture is experimentally verified. What about the levels which <u>are</u> excited? If they are particle-hole configurations of the above type we should, naively, expect them to lie near the zero-order unperturbed energies of particle-hole configurations of the above type [particle, $p^{-1}_{1/2}$]. In the ideal case we should expect a few levels, split in two by J splitting effects since for each configuration two J values are allowed. The experimental situation is not too different, as seen in Table III. Table IV shows that the levels are not only clustered around the 0-order energy of the corresponding configuration, but also that their strength is not too frac- tionated. Let us take any example, for instance, the (i$_{11/2}$, p$^{-1}_{1/2}$) configura- tion. The zero order, unperturbed energy is expected at 4.21 MeV (Table III). Now, let us look for this configurations in Table IV. We see that at 4.22 MeV there is a strong level which exhausts practically all the strength of the i$_{11/2}$ configuration. (The values of the spectroscopic factors are twice as large since we start from a spin-1/2 nucleus and not from a

TABLE III. COMPARISON OF ZEROTH-ORDER ENERGIES OF NEUTRON SINGLE-PARTICLE SINGLE-HOLE CONFIGURATIONS WITH CORRES- PONDING, EXPERIMENTALLY DETERMINED CENTRES OF GRAVITY (from Ref.[14])

Configuration	Zeroth-order excitation energy[a] (MeV)	Experimental centre of gravity[b] (MeV)
$(3p_{1/2})^{-1} (2g_{9/2})$	3.44	3.39
$(3p_{1/2})^{-1} (1i_{11/2})$	4.21	4.25
$(3p_{1/2})^{-1} (1j_{15/2})$	4.85	4.77
$(3p_{1/2})^{-1} (3d_{5/2})$	5.00	5.00
$(3p_{1/2})^{-1} (4s_{1/2})$	5.47	5.28
$(3p_{1/2})^{-1} (2g_{7/2})$	5.91	5.94[c]
$(3p_{1/2})^{-1} (3d_{3/2})$	5.96	5.92[c]

[a] Absolute energy values are based on the difference of neutron-separation energies for ^{208}Pb and ^{209}Pb, respectively. The relative energies correspond to the spacing of the neutron single-particle states in ^{209}Pb.

[b] For levels based on the same configuration, the centre of gravity is defined as
$\sum_i E^i_x (2J+1) S_{\ell j} / \sum (2J+1) S_{\ell j}$, where E^i_x is the excitation energy.

[c] Based on the observed strength below 6.1 MeV, which does not fulfill the sum-rule prediction.

TABLE IV. SINGLE PARTICLE-HOLE LEVELS IN ^{208}Pb OBSERVED IN
THE REACTION ^{207}Pb(d, p)^{208}Pb (from Ref.[14])

E_x^a (MeV)	$(d\sigma/d\Omega)$ (mb/sr) (lab)	θ_{max} (deg) (lab)	l, j	(2J+1)S
0	1.3	10		
2.6	0.049	20		
3.19	2.2	30	$2g_{9/2}$	9.5
3.47	2.0	25	$2g_{9/2}$	8.7
3.73 ⎫ 3.76 ⎬	0.35	20	$2g_{9/2}$	1.9
4.22 ⎫ 4.28 ⎬	0.39	35	⎰ $1i_{11/2}$ ⎱ $2g_{9/2}$	23.2 0.59
4.61	· 0.13	45	$1j_{15/2}$	10.00
4.70	1.1	15	$3d_{5/2}$	1.5
4.83 ⎫ 4.86 ⎬	0.25	45	$1j_{15/2}$	20.00
4.98	2.0	15	$3d_{5/2}$	3.6
5.03	1.9	15	$3d_{5/2}$	2.6
5.12	1.0	15	$3d_{5/2}$	1.4
5.24	1.1	15	$3d_{5/2}$	1.3
5.28	2.2	30	$4s_{1/2}$	3.6
5.77 ⎫ 5.80 ⎬	0.46	35	$3d_{3/2}$	0.46
5.85	1.2	25	$2g_{7/2}$	3.1
5.89	1.5	30	$3d_{3/2}$	1.8
5.93	1.2	25	$3d_{3/2}$	1.4
5.96	2.5	25	$2g_{7/2}$	6.9
6.00	0.66	25	$2g_{7/2}$	1.7
6.05 ⎫ 6.07 ⎬	0.62	30	$3d_{3/2}$	0.67

a Excitation energies, except that of the first excited level which was obtained from Ref.[11]
   are taken from Mukherjee and Cohen, Ref.[15].

0−spin one). Or else, we can take the (4s$_{1/2}$, p$_{1/2}$) configuration. Its un−
perturbed energy is 5.47 MeV. Now, ^{208}Pb exhibits a level at 5.28 MeV.
We shall see later that its spin J$^{\pi}$ is in fact 1^{-}.

Of course, not all the levels are so well described (e.g. the d$_{3/2}$ or
g$_{7/2}$ particle configurations). However, when we take the experimentally
determined total strengths $\Sigma(2J+1)S_{\ell j}$ and compare it with sum rule
predictions we find an agreement that is more than satisfactory: in view of
what we know about DWBA it is astonishing (Table V). It is obvious that

TABLE V.   EXPERIMENT AND SUM-RULE PREDICTIONS IN THE
^{207}Pb(d, p)^{208}Pb REACTIONS (from Ref.[14]).

Shell-model state	$\Sigma(2J+1)S_j$ sum rule	$\Sigma(2J+1)S_j$ experiment
$2g_{9/2}$	20	20.7
$1i_{11/2}$	24	23.2
$1j_{15/2}$	32	30.0
$3d_{5/2}$	12	10.4
$4s_{1/2}$	4	3.6
$2g_{7/2}$	16	11.7
$3d_{3/2}$	8	4.3

we are missing some $2g_{7/2}$ and a $3d_{3/2}$ strength; they are probably at higher energies.

We could be even more exacting and ask for the J^π of some of these configurations.   Namely, we have obtained the ℓ of the transferred protons; however for each configuration, two J values are possible.   We can determine the J^π value of some of these levels by other methods, as in Ref.[16] which describes a search for 1$^-$ levels in ^{208}Pb.   The two configurations which can couple to $J^\pi = 1^-$ are the $(s_{1/2}, p_{1/2}^{-1})$ and $(d_{3/2}, p_{1/2}^{-1})$ configurations. These, as we have seen, should occur around 5 - 6 MeV.   In the pure neutron stripping ^{207}Pb (d, p) ^{208}Pb process we should also expect states with $J^\pi = 0^-$, 2$^-$, 3$^-$, 4$^-$, 5$^-$, 6$^-$, 7$^+$ or 8$^+$.

Now, all these states are expected to decay preferentially by gamma cascade transitions through the 3$^-$, 2.62 MeV level rather than by the cross-over transition.   On the contrary, 1$^-$ levels should decay by cross-over to the ground state.   Consequently, the presence of ground state cross-over transitions is a sign of a 1$^-$ level, since 1$^+$ or 2$^+$ levels are not expected to be excited in the ^{207}Pb (d, p) reaction.

The experiment has shown two cross-over ground-state transitions: one at 5.28 and the other about 5.96 MeV.   If we now turn to Table IV, we see that the energy found in Ref.[14] to correspond to the configuration $(4s_{1/2}, p_{1/2}^{-1})$ is exactly at 5.28 MeV while those corresponding to $(3d_{3/2}, p_{1/2}^{-1})$ are at 5.89 and 5.93 MeV.   A relative experimental error of 50 keV in determining the energy in the two experiments is not to be excluded, and the agreement should be considered satisfactory.   It is corroborated by other results [17].   Namely, particle-hole pairs can be created in ^{208}Pb in a number of ways.   A very useful way is through isobaric analogue resonances.

An isobaric analogue resonance formed by proton bombardment of a neutron closed-shell nucleus may be considered to be a superposition of a single-particle state and a set of 2 particle-1 hole states (Fig. 9).

If the resonance decays through the inelastic channel, a neutron particle-hole state is formed and since the particle and the hole are generally in different major shells, the state is of negative parity.   These states are bound and will decay by γ-transitions to lower-lying states:

$$1^- \longrightarrow \text{g.s. (E1)}$$
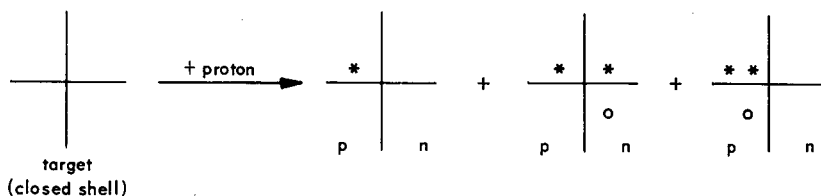
FIG.9. Isobaric analogue resonance formed by proton bombardment of a neutron closed-shell nucleus.

Higher angular momentum states will decay through the low-lying 2+ or 3+ states. Results obtained in this way [17] confirm the data of Ref.[16] on the spin and parity of the 5.27 and 5.94 states of ^{208}Pb.

Let us now return to transfer reactions. We have created particle-hole configurations by adding particles to an existing hole. We can proceed the other way round; we could dig holes and couple them to an existing particle. An example is the ^{209}Bi$(t, \alpha)^{208}$Pb [18]. The configurations which will be excited in this reaction differ from those excited in ^{207}Pb$(d, p)^{208}$Pb by the fact that the former are proton particle-hole configurations, and, in particular, configurations of the type (1h$_{9/2}$, proton hole). We expect, hence, configurations of the type (1h$_{9/2}$, s$_{1/2}^{-1}$)...(1h$_{9/2}$, d$_{5/2}^{-1}$). The results show that the ground state has a pure $\ell = 5$ angular distribution. Hence,

TABLE VI. EXPERIMENTAL AND THEORETICAL PROTON PICK-UP STRENGTHS FROM THE REACTION ^{209}Bi$(t, \alpha)^{208}$Pb (from Ref.[18])

E_x	J$^\pi$		$3s_{1/2}$	$2d_{3/2}$	$2d_{5/2}$	$1g_{7/2}$
		Exp.	0	≤ 0.10	≤ 0.07	≤ 0.28
2.62	3$^-$	Ref.[24]	0$^-$	0.15	0.006	0.014
		Ref.[19]				
		Exp.	0.06	< 0.09	< 0.06	< 0.28
3.20	5$^-$	Ref.[24]	0.11	0.04	0.009	0.004
		Ref.[19]	0.11	0.05	0.01	0.01
		Exp.	≤ 0.004	≤ 0.007	≤ 0.005	0.02
3.48	4$^-$	Ref.[24]				
		Ref.[19]	0.0002	0.0001	0.0001	0.00007
		Exp.	0.31	< 0.52	< 0.36	< 1.7
3.71	5$^-$	Ref.[24]	0.34	0.05	0.007	0.001
		Ref.[19]	0.25	0.03	0.003	0.0007
		Exp.	1.01	< 1.86	< 1.17	< 5.7
3.96	4, 5$^-$	Ref.[24]				
		Ref.[19]	0.68	0.03	0.0009	0.00003

E_x is given in MeV. The strengths are $S(9/2 \rightarrow j+J)$, where j is the hole configuration given on top of the table to the right and J the final-state spin. The particle configuration is always 1h$_{9/2}$, and the ^{209}Bi$(t,\alpha)^{208}$Pb ground-state S was put equal to 1. In case an ℓ-value was assigned from experiment, the corresponding strength is given as if no other ℓ-values contributed.

the ground state is a pure $h_{9/2}$ state. However, considerable configuration mixing is observed already in the first excited state, where transfers of $\ell = 2$ and 4 can be expected from the shell model: both are present, although $\ell = 2$ is predominant. The relative spectroscopic factors, normalized to the ground state as a pure $\ell = 5$ transition ($S = 1$), are shown in Table VI.

It seems, then, that negative-parity <u>proton</u> particle–hole levels in ^{208}Pb show relatively strong configuration mixing, in contrast to <u>neutron</u> particle–hole levels. The reasons for such a different behaviour are not obvious. Nevertheless, theoretical calculations [19] reproduce fairly well the gross structure of the proton particle–hole spectra (Fig. 10). The strongest transitions are concentrated in two regions:

a) near the unperturbed energy of $3s_{1/2}$ and $2d_{5/2}$ hole states
   ($E_x = 4 - 4.5$ MeV exc.), and
b) near the unperturbed energy of $1h_{11/2}$ and $2d_{5/2}$ hole states
   ($E_x = 5.5 - 6$ MeV exc.).

We should notice here that although the energies are close to the unperturbed ones, a strong configuration mixing is present. This just shows how poorly the energy spectrum indicates the nature of the wave function. Or, in other words, we could use almost any wave function to reproduce the experimental spectrum.
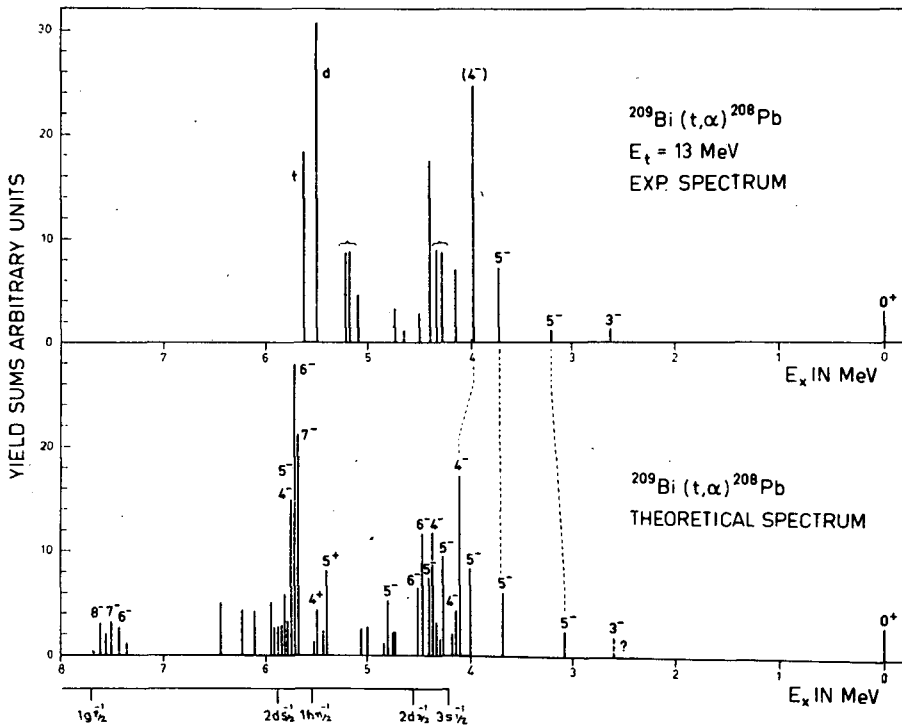
FIG. 10. Comparison between the experimental ^{209}Bi (t,α) ^{208}Pb yield sums (Ref.[18]) and yield sums calculated from the wave functions of Ref.[19] and the DW code JULIE.
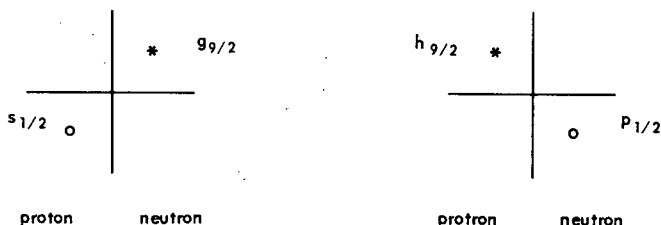
FIG.11.   Ground-state configurations of [208]Tl and [208]Bi.

   The lead region: [208]Tl and [208]Bi: These two nuclei are very similar
to [208]Pb, and can be used to test the validity of the independent-particle
model description in the [208]Pb region.   Either of these nuclei has a par-
ticular ground-state configuration (Fig.11).
   In principle, hence, these nuclei can be treated in the same way as
the excited states of [208]Pb.   Hence, we can study particle-hole configura-
tions by the stripping or pick-up of a particle.   Alford et al. [20] have
studied the levels of [208]Bi by both the pick-up reaction [209]Bi (d, t) and the
stripping reaction [207]Pb ([3]He, d).   [209]Bi is a $h_{9/2}$ proton particle state, and
[207]Pb its a $p_{1/2}$ neutron hole state, and we expect configurations of the type

$$\left\{\begin{array}{l} h_{9/2} \quad 3p_{1/2}^{-1}, \ 2f_{5/2}^{-1}, \ 3p_{3/2}^{-1}, \ i_{13/2}^{-1}, \ 2f_{7/2}^{-1} \ldots . \quad \text{for (d, t)} \\ \text{protons} \end{array}\right.$$

and

$$\left\{\begin{array}{l} p_{1/2}^{-1} \quad h_{9/2}, \ 2f_{7/2}, \ i_{13/2}, \ 2f_{5/2} \ \ldots \ldots \quad \text{for (}^{3}\text{He, d)} \\ \text{neutrons} \qquad\quad \text{proton particles} \end{array}\right.$$

to be excited.   Moreover, as both the [208]Pb (d, t) [207]Pb and [208]Pb ([3]He, d) [209]Bi
excite single hole single particle states with full spectroscopic strength,
we expect that the structure of the states in [208]Bi will be rather simple.
(except for the $h_{9/2}$ hole state, which in [207]Pb has been found to be badly
fragmented).   The data (Fig.12) show that there appears to be little con-
figuration mixing.   At least, the energies of the particle-hole J multiplets
cluster around the unperturbed values so that even an J attribution was
possible using the 2J + 1 rule.   This is visible especially for the (d, t)
reaction.
   The agreement between the two parts of the Fig.12 is actually more
than accidental.   Although in one case we have configurations of the type

$$p_{1/2}^{-1} \text{ hole } \otimes \text{ proton particles}$$

and in the other

$$h_{9/2} \text{ particle } \otimes \text{ neutron holes}$$

and hence we should have only one common configuration, ($h_{9/2}$, $p_{1/2}^{-1}$) it
happens that in [208]Pb proton particle states (Z = 82 - 126) practically
coincide with neutron hole states (N = 126 - 82), as seen from the labelling
above the figures (see also chapter 1, and Ref.[5]).
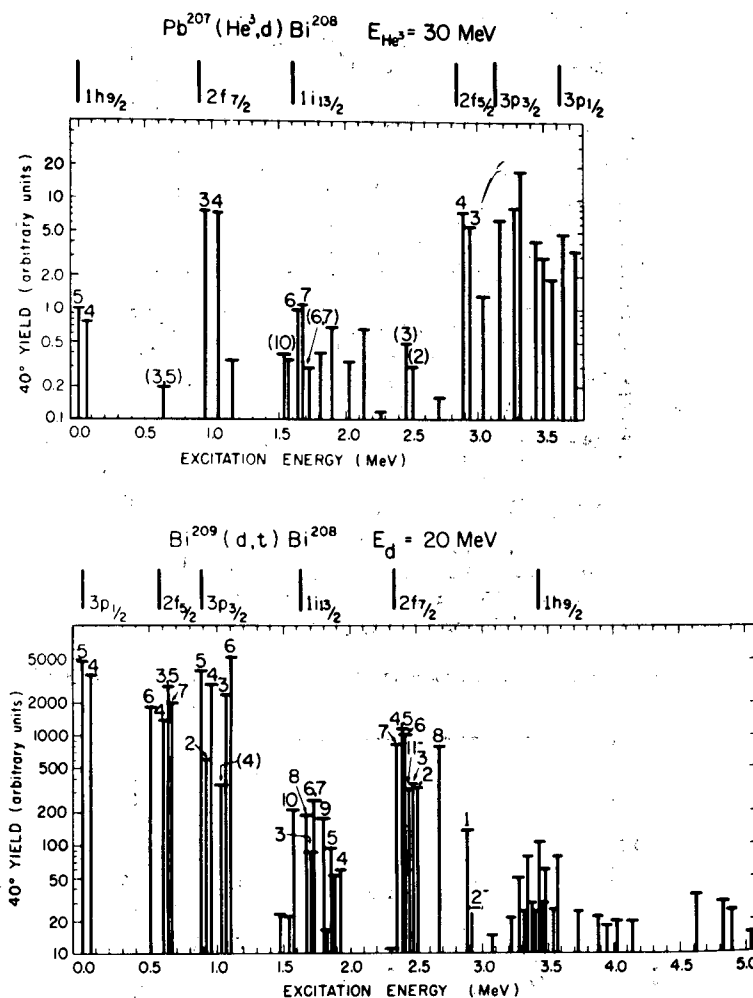
FIG.12.   Levels of 208Bi excited by the 207Pb (3He, d) 208Bi and 209Bi (d, t) 208Bi reactions (from Ref.[20]).

   Quite similar results were obtained earlier by Erskine [21] in the
209Bi (d, t) 208Bi reaction.   States found in Ref.[21] show a relatively simple
structure where one configuration usually predominates, (quite naturally,
the (d, t) reaction selects just such kind of levels.).   Figure 13 shows
a comparison between experimental and calculated triton spectra from the
(d, t) reaction.   In the experimental spectrum the groups are labelled in
sequence starting with 0 for the ground state.   In the calculated spectrum,
each group is labelled with its total angular momentum J.   The theory is
by Kim and Rassmussen.[22].   Again the overall agreement is very good,
and a more detailed comparison with Ref.[21] shows that several J^{π} values
are well reproduced.
   An overall comparison of theory and experimental data for 208Tl and
208Bi is given in Figs 14 and 15 taken from Ref.[22].
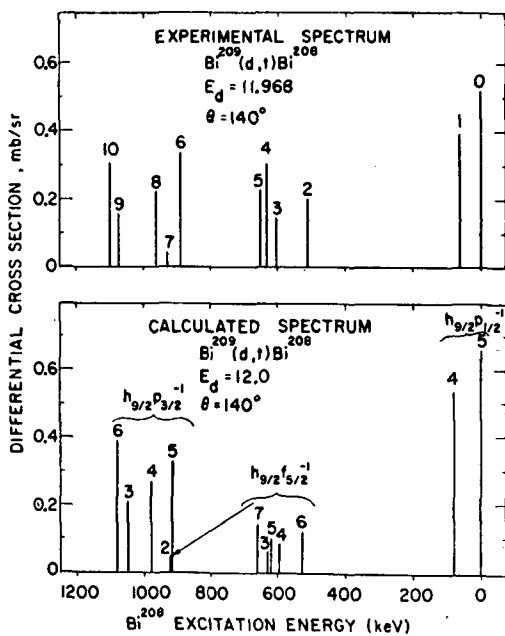
FIG.13.   Experimental and calculated spectrum of the reaction ^{209}Bi(d, t) ^{208}Bi (from Ref.[21]).
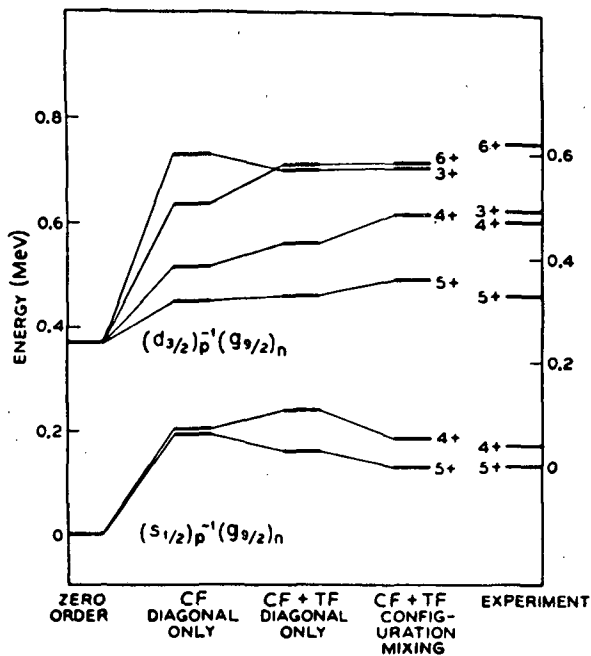
FIG.14.   Levels of ^{208}Tl calculated by different approximations and compared to experiment (from Ref.[21]).
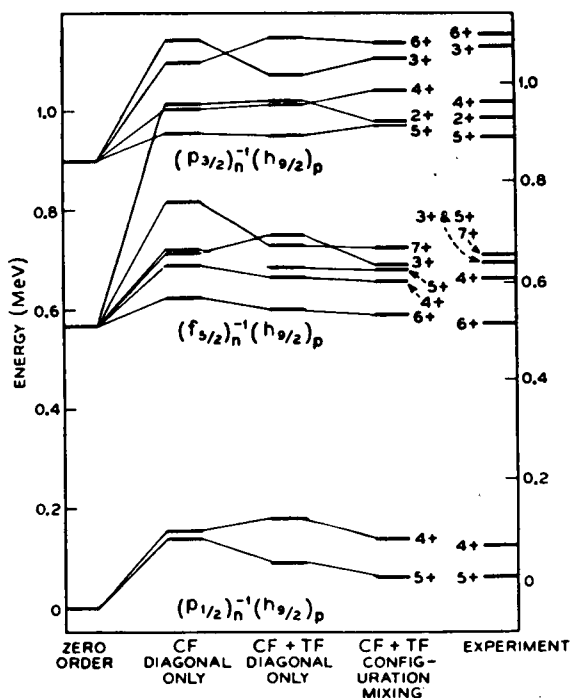
FIG.15. Levels of 208Bi calculated by different approximations and compared to experiment (from Ref.[22]).

At least for the low-lying states the agreement is almost spectacular.
The theory of Ref.[22] used a simple particle-hole calculation, where a
particle-hole state was created by taking a vector product of single-particle
and hole states, derived from the 208Pb core. The energy of the multiplets
was computed by determining the matrix element of the two-body interac-
tion operator, which comprised the particle-core and hole-core interactions
and, finally, the particle-hole interaction.

Table VII shows the configurational structure of 208Tl levels as cal-
culated by Kim and Rassmussen [22]. The calculated configurations
appear to be almost pure; the small amplitudes may be important in cal-
culating transition probabilities only.

At this point we should nevertheless be cautious. What we have seen
so far is that in the region of 208Pb, the essential features of the ground-
and low-lying excited levels are fairly well explained by a shell-model
208Pb core plus a particle or a hole. However, so far we have explained
only the energy of these states. Now, the energy is the physical quantity
easiest to reproduce theoretically. What about other quantities, like
transition moments, etc...? We have seen that there the simple shell
model fails, and the effects of the particles in the core should be taken
into consideration.

The lead region: complex configurations in 208Pb. Up to now we have
studied single particle-hole configurations of a various degree of com-
plexity in the spectrum of 208Pb and its isobars. Are there other types of

TABLE VII. CALCULATED EIGENFUNCTIONS FOR LOW-LYING [208]Tl STATES (from Ref.[22])

Eigenvalues (MeV)	Eigenfunctions								
	$s_{1/2}g_{9/2}$	$d_{3/2}g_{9/2}$	$s_{1/2}i_{11/2}$	$d_{3/2}i_{11/2}$	$s_{1/2}d_{5/2}$	$d_{3/2}d_{5/2}$	$s_{1/2}g_{7/2}$	$d_{3/2}g_{7/2}$	$d_{3/2}d_{3/2}$
J = 3									
0.695		0.9983			-0.0449	0.0226	0.0184	0.0218	-0.0018
J = 4									
0.183	0.9322	0.3613		-0.0058		0.0152	-0.0074	-0.0146	
0.616	-0.3613	0.9320		-0.0123		0.0114	-0.0136	0.0174	
1.516	0.0001	0.0124		0.9971		0.0007	-0.0700	-0.0259	
J = 5									
0.130	0.9538	-0.3001	-0.0022	0.0117				0.0089	
0.491	0.3000	0.9532	0.0336	0.0087				-0.0082	
0.832	-0.0121	-0.0323	0.9472	0.3178				0.0244	
1.277	-0.0102	0.0053	-0.3165	0.9474				-0.0453	
J = 6									
0.712		0.9993	-0.0307	0.0213					
0.951		0.0365	0.9249	-0.3785					
1.265		-0.0081	0.3790	0.9253					

configurations? If we are to take the particle-hole picture seriously, it is the 2p-2h configurations which come next in our hierarchy. It can be expected that these configurations will show up at somewhat higher energies. How to excite these configurations? For instance, by adding two particles to existing two holes.

An example is the reaction ^{206}Pb(t, p)^{208}Pb [23]. Because of the selective character of this reaction we should expect less states to be excited than, e.g. in ^{207}Pb(d, p). This is, in fact, true. The strongest transitions in ^{206}Pb(t, p)^{208}Pb are to the ground state, which obviously corresponds to filling two neutron holes and to the 3⁻ level at 2.62. Both of these levels are weakly excited in (d, p), the latter due to its collective character. Besides the ground and the 3⁻ states, many ^{208}Pb states between 5.5 - 6.1 MeV of excitation are also excited in the (t, p) reaction, as expected from a naive theory (Fig.16).
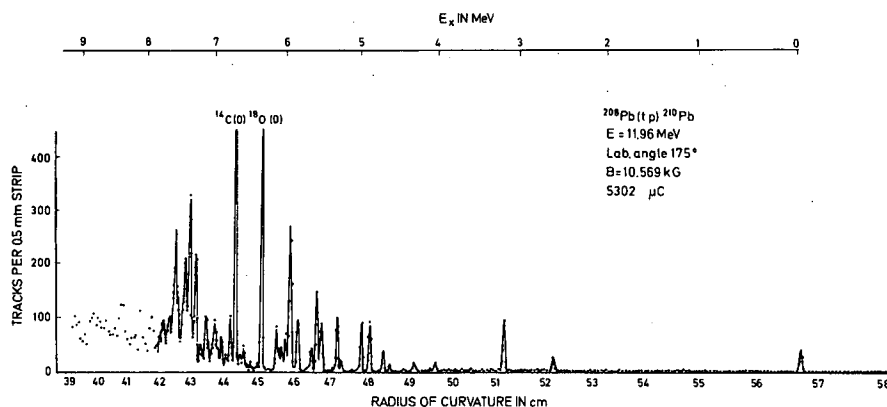
FIG.16.   The experimental spectrum of the ^{206}Pb(t, p)^{208}Pb reaction (from Ref.[23]).

The strong excitation of the 3⁻ state at 2.62 MeV deserves some comments. This fact can be explained by assuming that the g.s. of ^{206}Pb is not a pure 2-hole configuration.

In fact if ^{206}Pb(0) were a simple $(p_{1/2})^{-2}$ configuration, a low-lying 3⁻ state in ^{208}Pb could be formed by (t, p) only through components $(d_{5/2}, p_{1/2}^{-1})$ and $(g_{7/2}, p_{1/2}^{-1})$. Now both of these components should be small in 3⁻, according to calculations of Gillet et al. [24]. We should conclude that ^{206}Pb(0) contains additional hole components.

This is an example of how the details of the simple shell-model picture rapidly deteriorate when more than one particle or hole is added to a closed-shell core. While the ground state of ^{207}Pb was an almost pure $p_{1/2}^{-1}$ state, the ground state of ^{206}Pb contains additional hole components, different from $(p_{1/2})^{-2}$.

The lead region: ^{206}Pb and ^{210}Pb (nuclei away from closed shells): Let us now examine the situation 2, 4 and more particles or holes away from closed shells. A very extensive search of nuclei in the ^{208}Pb region was performed by the Copenhagen-Aldermaston groups, whose results we have quoted already. The simplest case - symmetrical to ^{208}Pb - are the ^{206}Pb and the ^{210}Pb nuclei. Spectra obtained from the (t, p) reaction leading to ^{209}Pb and ^{210}Pb are presented in Figs 16 and 17, respectively [25]. Now,
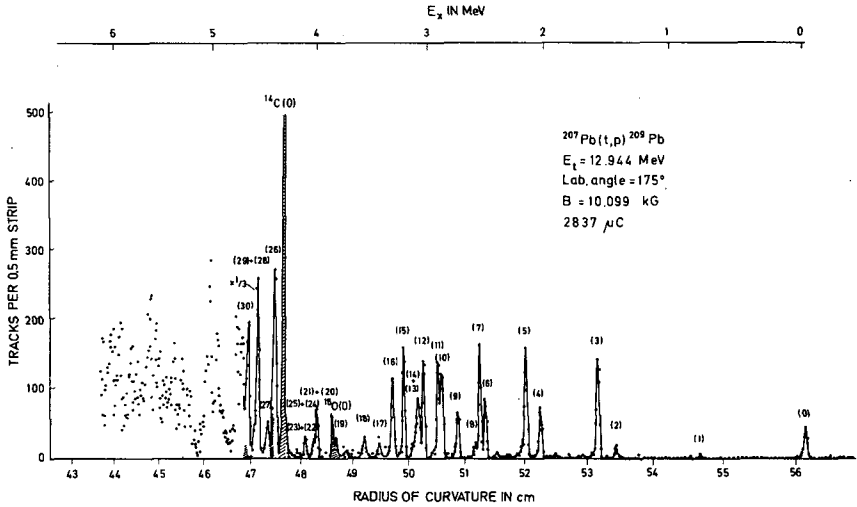
FIG. 17. Proton spectrum from the reaction ^{207}Pb (t, p) ^{209}Pb (from Ref. [25]).
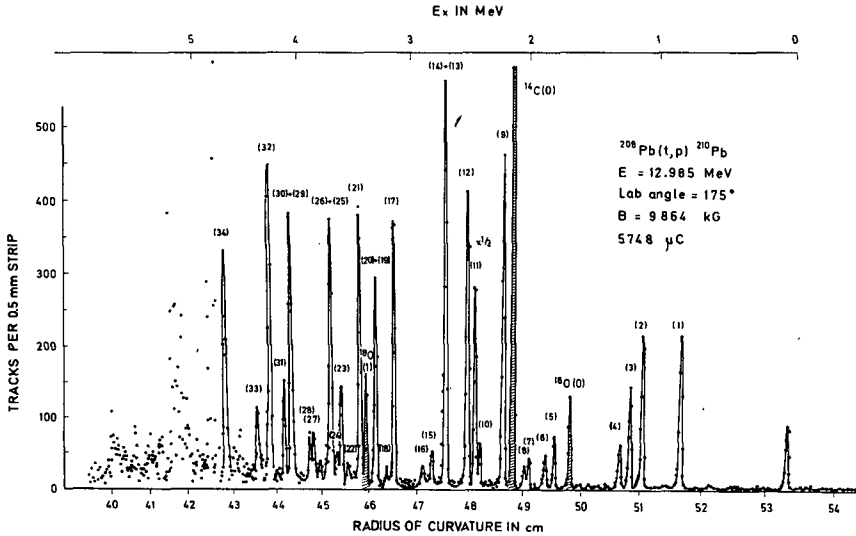
FIG. 18. Proton spectrum from the reaction ^{208}Pb (t, p) ^{210}Pb (from Ref. [25]).

the above reaction is by itself a very selective process. Furthermore, the
low-lying levels of ^{210}Pb are expected to be well described by two neutrons
out of the ^{208}Pb core, and (t, p) reactions are particularly suitable to study
them. Nevertheless, the comparison of Figs 17 and 18 shows how spectra
become more complicated when crossing from ^{209}Pb to ^{210}Pb. Actually,
the theory [26] describes the low-lying levels fairly well (up to ~1.5 MeV)
and all these levels have in fact large $(g_{9/2})^2$ components. Later on, there
is hardly any resemblance between theory and experiment (Fig. 19).

Levels of ^{210}**Pb**
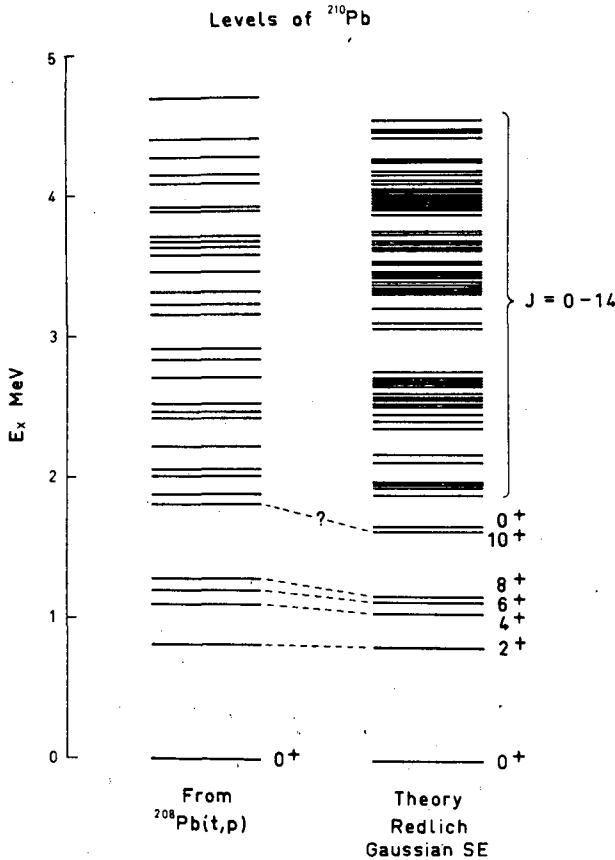
FIG.19. Calculated (from Ref.[26]) and experimental spectra of ^{210}Pb (from Ref.[25]).

The situation on the hole—side far away from ^{208}Pb (^{204,205,206}Pb) was also investigated by the Copenhagen—Aldermaston groups [27]. Figure 20 shows the density of states in ^{205}Pb obtained from the reaction ^{204}Pb(d, p) at excitation energies above 4 MeV. If we compare this with, e.g. (d, p) spectra on ^{208}Pb (see Fig. 6) the difference is more then striking.

A new phenomenon is the strong fractionation of single—particle strength shown in Fig. 21. Namely, the (d, p) reaction on ^{204}Pb starts filling up the almost filled 83 − 126 shells ($f_{5/2}$ and $p_{1/2}$ orbitals). At higher excitation energies (around 2. 5 MeV) the empty neutron orbital $g_{9/2}$ (127 and up) starts being filled. 'The cluster of levels at this energy have, in fact, all $\ell = 4$, which shows the heavy fractionating of the $g_{9/2}$ strength. This fractionating is interpreted as a consequence of the coupling of particle configurations to core excitation modes. Sum rules are, however, still valid, in particular for single particle states near the Fermi surface, as seen from Tables VIIIa and VIIIb. Table VIIIa shows the strength defined as $(2J + 1) S^{(+)}$ for the stripping ^{204}(d, p)^{205}Pb reaction and as $S^{(-)}$ for the pick-up ^{204}(d, t)^{203}Pb case. Near the Fermi surface (orbitals $3p_{1/2} - 2f_{5/2}$) the experimentally derived sum is in good agreement with the simple
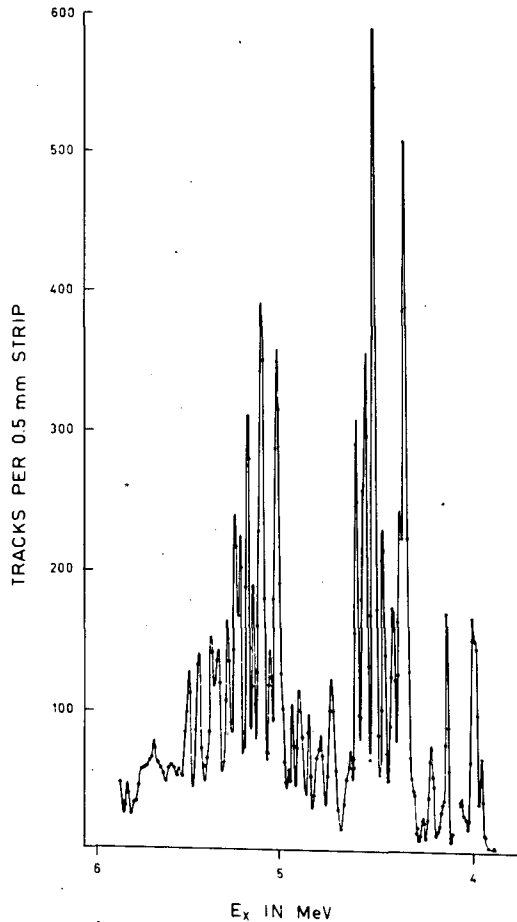
FIG.20. Proton spectrum from the reaction ^{204}Pb$(d, p)^{208}$Pb at excitation energies between 4 - 6 MeV; notice the large density of levels (from Ref.[27]).

(2J + 1) limit. Table VIIIb shows that near the Fermi surface, the experimentally derived quantities u^2(j) (see section 3.3) are in reasonable agreement with the results of the pairing model, in which the low-lying states in the odd-mass nuclei are one-quasi-particle states and no splitting of the strength occurs [27].

3.2. The Calcium Region

The Ca region, which is another region around doubly closed shell nuclei will be discussed in detail in a separate paper. We shall discuss it briefly, to point out the analogies – if any – with the Pb region.

The main spectroscopic feature of the Pb region was the fact that single-particle and hole states were excited in their full spectroscopic strength. In other words, the essential features of spectra in this region were described as a particle or a hole coupled to an inert, closed-shell
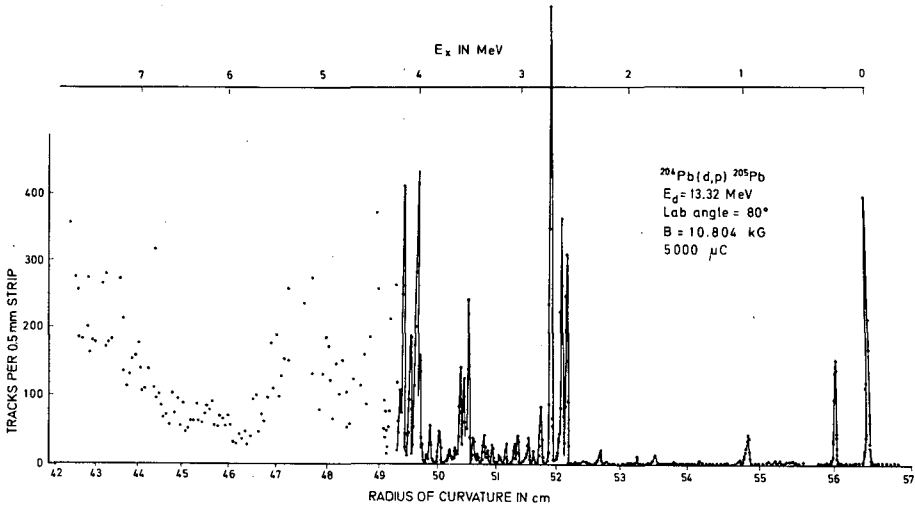
FIG.21.   Proton spectrum from the reaction ^{204}Pb(d, p)^{205}Pb (from Ref.[27]).

TABLE VIIIa.   THE REACTIONS ^{204}Pb(d, p)^{205}Pb AND ^{204}Pb(d, t)^{203}Pb: COMPARISON OF SUM RULES OF THE STRIPPING $(2j+1)S^{(+)}$ AND PICK-UP $(S^{(-)})$ STRENGTH TO THE $(2j+1)$ LIMIT (from Ref.[27]).

Configuration	$(2j+1)S^{(+)}(j)$	$S^{(-)}(j)$	Sum	$2j+1$
$3p_{1/2}$	1.4	0.8	2.2	2
$3p_{3/2}$	0.6	3.4[a]	4.0	4
$2f_{5/2}$	2.2	5.1	7.3	6
$1i_{13/2}$	1.3	7.2	8.5	14
$2f_{7/2}$	0.1	3.4	3.5	8
$2g_{9/2}$	5.4		5.4	10

a The $S^{(-)}$ was normalized to fulfil the sum rule

TABLE VIIIb.   THE EXPERIMENTALLY DERIVED OCCUPATION PARAMETERS $u^2(j)$ AROUND ^{204}Pb AND THE COMPARISON WITH THE PAIRING MODEL (from Ref.[27]).

Configuration	Experiment $u^2(j)$	Theory
$3p_{1/2}$	0.7	0.8
$3p_{3/2}$	0.15	0.1
$2f_{5/2}$	0.4	0.2
$1i_{13/2}$	0.1	0.02
$2f_{7/2}$	0.01	0.01

core. What happens in the Ca region? Let us take ^{40}Ca, although the belief exists that ^{48}Ca is a better example of a closed-shell nucleus.

First, about shell closure. It is a well known fact that ^{40}Ca is not a good closed-shell nucleus, i.e. that the ground state contains particles in the $f_{7/2}$ shell. This has been experimentally demonstrated by Glashausser et al. [28] who found $\ell = 3$ angular distributions in the deuteron spectra from the ^{40}Ca(p, d)^{39}Ca reaction. Now, the $\ell = 3$ neutrons could be picked-up only from particles in the $f_{7/2}$ shell. This result has been corroborated later by other authors.

Second, ^{40}Ca and other Ca isotopes show a series of low-lying positive-parity states which cannot be explained in terms of particle-hole configurations. Particles in ^{40}Ca fill up, in principle, the s-d shell. The next empty shell is the $f_{7/2}$ one and moreover, the shell above is again an odd ℓ-shell, while the first-positive parity orbital $g_{9/2}$ comes very high in energy. Hence to make a particle-hole configuration of positive parity one would need to couple the (s, d) holes with the $g_{9/2}$ particles or else dig up holes from very deep underneath the Fermi surface. As the lowest-lying levels in Ca isotopes are, as a rule, levels of positive parity, we should look for an explanation in terms of other, more complex configurations.

A third point which makes the difference between ^{40}Ca and ^{208}Pb region is the fractionating of the single-particle strength in ^{40}Ca(d, p) and (^{3}He, d) reactions. All this indicates that the crude shell-model description of ^{40}Ca is far from being satisfactory, and that all other particles in the core interact strongly and modify the simple shell-model description.

We shall briefly illustrate these points, leaving the detailed description of nuclei in this region to other papers.

The calcium region: ^{40}Ca ± particle - In the simplest shell model, states in ^{41}Ca should be pictured as an inert ^{40}Ca core plus a neutron in a single-particle level ($1f_{7/2}$, $2p_{3/2}$, $1f_{5/2}$ ....). These states are identified via the ^{40}Ca (d, p) reaction [29]. As we said before, the spectroscopic strength of these states was found to be fractionated, indicating that the simple picture does not contain sufficient degrees of freedom. The same is true for ^{43}Ca, where many more low-lying levels are found than could be predicted by the $(f_{7/2})^3$ configuration alone. Even when the three neutrons are allowed to occupy either the $1f_{7/2}$ or the $2p_{3/2}$ orbits the number of calculated levels is significantly lower then the number of experimental levels found below an excitation energy of, e.g. 3.5 MeV.

Another deviation from the simple shell model in ^{41}Ca is presented by the second excited state at 2.017 MeV which is a $3/2^+$ state. This J^π can be obtained only by promoting two particles in the $f_{7/2}$ orbital:

$$(1d_{3/2}^{-1}) \otimes (f_{7/2})^2$$

Now the first positive parity level of ^{41}Ca is 1.3 MeV lower then the 1st positive parity level in ^{40}Ca (the 0^+ at 3.35 MeV). Hence, to explain the excitation of these levels by (d, p), one should admit the presence of (2p, 2h) viz. (4p, 2h) configurations already in the ground state of ^{40}Ca and ^{42}Ca, respectively. These core excitations provide the extra degrees of freedom responsible for the fractionating of the single-particle strength.

Let us look now at the experimental situation. Table IX shows a survey of ^{41}Ca levels and the respective spectroscopic strengths [30]. The

TABLE IX. ^{41}Ca LEVELS AND SPECTROSCOPIC STRENGTH
(from Ref.[30]).

E (MeV)	Max. dσ/dΩ (mb/sr)	ℓ_n	C²S		C²S (^{3}He,α)	(2J+1)S (d, p)	dσ/dΩ (^{3}He, p) (mb/sr)	J$^\pi$
			ZR/L	FR/NL				
0.00	2.82	3	1.5	1.6	1.6	8.00	0.03	7/2$^-$
2.017	2.30	2	3.8	2.7	2.0	0.79	0.19	3/2$^+$
2.471	0.049	a			0.01	1.11		3/2$^-$
2.680	0.860	0	0.53	0.34	0.65	0.35		1/2$^+$
2.98	0.153	3	0.14	0.17	0.14			7/2$^-$, (5/2)$^-$
3.408	0.088	0	0.085	0.049	0.12	0.031	0.067	1/2$^+$
3.52	0.202	2	0.39	0.31	0.11			5/2$^+$, 3/2$^+$
3.740	0.180	2	0.36	0.28	0.26	0.28	0.18	3/2$^+$, 5/2$^+$
3.859	0.158	0	0.20	0.11	0.19	0.01		1/2$^+$
3.95	0.058	a						
4.105	0.364	2	0.85	0.71	0.13		0.51	5/2$^+$, 3/2$^+$
4.829	0.081	(2)	0.19	0.16	0.10	0.10	0.17	3/2$^+$, 5/2$^+$
5.49	0.058	a						
5.84	0.626	2	1.7	1.7	2.3		0.91	3/2$^+$
5.90	0.106	a						
6.04	0.097	a						
6.68	0.064	a						
6.82	0.139	0	0.93	0.85	0.54			1/2$^+$
7.13	0.123	3	0.15	0.20	0.37			7/2$^-$
7.41	0.104	a						

a Angular distribution with more than three data points was unobtainable.

fractionating is quite visible. The low-lying positive-parity states in ^{41}Ca
are of particular interest; especially the $\ell_n = 2$ state at 2.02 and the $\ell = 0$
state at 2.68 MeV. As mentioned above, these states can be readily identi-
fied as 2 particle-1 hole configurations, namely ^{42}Ca (g.s.) $\otimes \nu (1d^{-1}_{3/2})$;
^{42}Ca (g.s.) $\otimes \nu (2s^{-1}_{1/2})$ configurations. We see that states of complex con-
figuration are present rather low in the spectrum.

A quite similar situation exists in ^{43}Ca, where the lowest positive-
parity level is found already at 0.99 MeV (Table X). The experimental [30]
and calculated [31] spectroscopic strength C²S for the ^{42}Ca (p, d)^{41}Ca
reaction versus the excitation energy for $\ell_n = 0$ and $\ell_n = 2$ levels in ^{41}Ca is
shown in Fig.22. The agreement is, certainly, far from being satisfactory,
and a comparison with similar results in the lead region (see, e.g.
Tables IIa and IIb) clearly shows that simple shell-model descriptions are
less adequate in the Ca-region. Of course, some qualitative features of
the shell model are nevertheless valid as illustrated on Fig.23, which
shows a comparison of the spectroscopic strengths of levels in ^{43}Ca ob-
tained from the ^{42}Ca(d, p)^{43}Ca and ^{44}Ca(p, d)^{43}Ca reactions. The obvious

TABLE X. ^{43}Ca LEVELS AND SPECTROSCOPIC STRENGTHS
(from Ref.[30]).

E_x (MeV)	Max. $(d\sigma/d\Omega)$ (mb/sr)	ℓ_n	C^2S		$(2J+1)S$ (d,p)	J^π
			ZR/L	FR/NL		
0.00	6.26	3	3.6	3.8	5.5	$7/2^-$
0.373	0.224	3	0.13	0.15		$5/2^-$
0.594	0.545	1	0.10	0.10	0.21	$3/2^-$
0.992	3.23	2	3.6	2.5	0.52	$3/2^+$
1.395	0.141	2	0.22	0.16	(0.12)	$3/2^+$, $(5/2^+)$
1.680	0.074					$(11/2^-)$
1.959	2.20	0	0.80	0.62	0.13	$1/2^+$
2.050	0.531	1	0.16	0.18	3.0	$3/2^-$
2.252	0.234	2	0.42	0.28		$3/2^+$, $5/2^+$
2.69	0.258	2	0.53	0.36		$3/2^+$, $5/2^+$
2.87	0.266	2	0.49	0.37		$3/2^+$, $5/2^+$
3.05	0.523	0	0.33	0.22		$1/2^+$
3.28	0.255	3	0.22	0.28		$7/2^-$, $(5/2^-)$
3.60	0.045	$(1)^a$	0.01	0.02	0.24	$(3/2^-$, $1/2^-)$
3.92	0.218	(2)	0.58	0.40		$(3/2^+$, $5/2^+)$
4.20	0.266	(2)	1.2	0.75		$(3/2^+$, $5/2^+)$
4.46	0.308	(2)	0.80	0.53		$(3/2^+$, $5/2^+)$
7.97	0.179	2	0.80	1.1		$3/2^+$
8.59						
8.75						

a Parentheses indicate tentative assignment

feature is that the (p, d) strength is much larger for $\ell = 0$ and 2 transitions
while the (d, p) strength prevails for $\ell = 1$. The $\ell = 3$ strength is about
equally shared among (p, d) and (d, p) levels. In terms of a qualitative shell-
model picture, this means that neutrons in ^{43}Ca are still to be found in the
(s, d) shell (pick-up possibility) while the $f_{7/2}$ shell is half-filled (pick-up
and stripping equally possible). Extra core particles in ^{43}Ca are to be
found essentially in the $f_{7/2}$ shell, while the $\ell = 1$ $p_{3/2}$ and $p_{1/2}$ orbitals are
more or less empty (large stripping and small pick-up strengths).

    This evidence is corroborated by examining the ^{40}Ca plus hole case.
The splitting of hole strength in ^{39}K and ^{39}Ca is a well known fact. We shall
look for more direct evidence for the presence of core excitation in the low-
lying levels of ^{39}K or ^{39}Ca. In this respect ^{39}K and ^{39}Ca will present a
very favourable case since the strongly excited low lying core state (the
3$^-$ of ^{40}Ca at 3.73 MeV) has negative parity, and, each member of the core
multiplet will have parity opposite to that of the ground state. Hence, con-
figuration mixing of the ground state with the multiplet member of the same
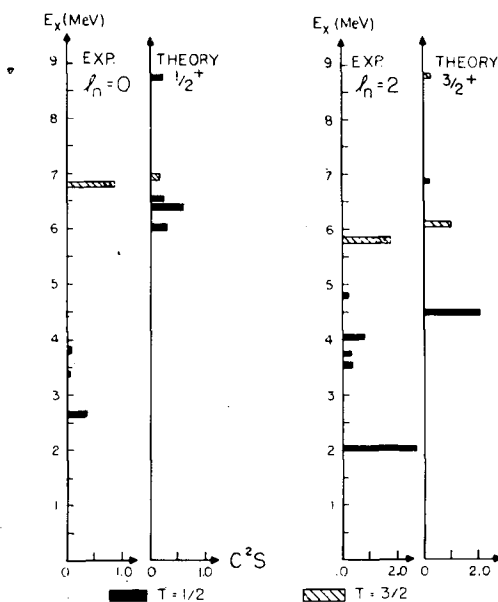
FIG.22.   The experimental (Ref.[30]) and calculated (Ref.[31]) spectroscopic strengths C²S from the
⁴²Ca(p,d)⁴¹Ca reaction for ℓ_n = 0 and ℓ_n = 2 levels in ⁴¹Ca (from Ref.[30]).

spin and parity (which results in a heavy loss of strength for the latter) will
not occur[2].

The quartet corresponding to the coupling of the $d_{3/2}$ proton hole to the
3⁻ level in ⁴⁰Ca was found by Lewis [32] by means of the (d,d') reaction.
The levels at 3.02, 4.12, 3.88 and 3.60 were found to be, respectively,
the 3/2⁻, 5/2⁻, 7/2⁻, 9/2⁻ members of the quartet resulting from $d_{3/2}$
proton-hole coupling to the 3⁻ level of ⁴⁰Ca. The angular distributions
were found to be identical, the cross-sections obeyed the 2j+1 rules,
while the centre of gravity of the four levels lay at 3.71 MeV.

We conclude that the inert, closed-shell core plus particle or hole
picture is hardly valid in the ⁴⁰Ca region. The evidence for shell non-
closure is overwhelming and the influence of the excitation of all the
particles in the core should be taken into account even in a first
approximation.

 The calcium region: positive-parity states – The most conclusive
evidence in this respect is the presence of low-lying positive parity states
in ⁴⁰Ca and other even Ca isotopes. In some isotopes, these levels were
found to make a rotational band like in ⁴⁰Ca, where the 0⁺, 2⁺ and (4⁺)
levels at 3.35, 3.90 and 5.27 MeV obey the I(I+1) rule. Recently,
Delaunay et al. [33] have found evidence for candidates for a fourth member
of the band (6⁺) around 7.3 MeV. Now, with particles in $f_{7/2}$, $p_{3/2}$, $p_{1/2}$
and $f_{5/2}$ orbitals the 0⁺ states in ⁴²,⁴⁴,⁴⁶Ca should appear at 5, 4.5 and
3.8 MeV, respectively, while experimentally they are found at 1.84, 1.89
and 2.43 MeV respectively. As the inclusion of other configurations could

_____

[2] A similar case occurs for ²⁰⁹Bi and ²⁰⁸Pb (see Physics Letters (1966) 579).
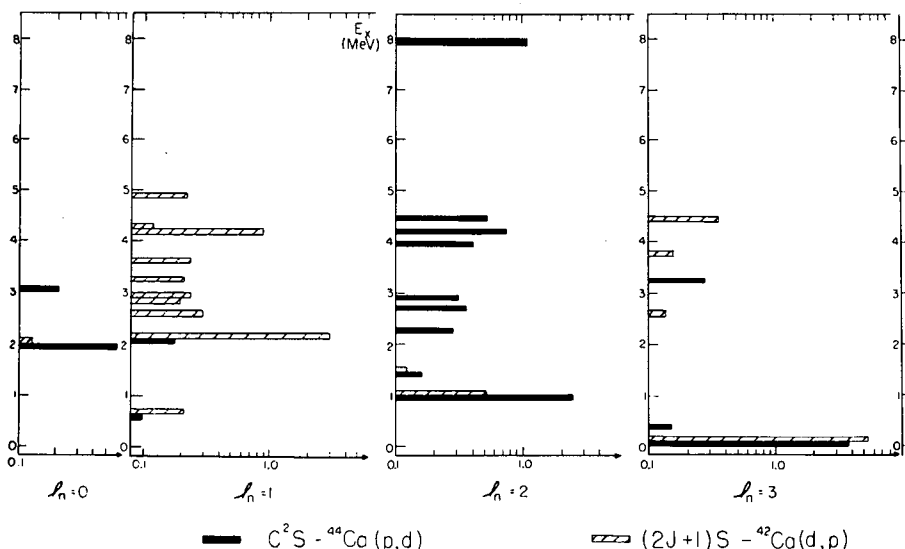
FIG.23. ^{43}Ca spectroscopic strength from ^{44}Ca(p, d) and ^{42}Ca(d,p) reactions (from Ref.[30]).

not mend the disagreement, we conclude that the first 0^+ states involve excitation of particles from the ^{40}Ca core into f-p orbits. Another argument in this respect is the strong E2 transition of these levels to the lower-lying positive-parity states.

The idea of introducing admixtures of deformed states in the low-lying levels of closed-shell nuclei was introduced by Brown [34] and followed by other authors [35] in order to explain the low-lying states of ^{16}O. Federman and Talmi [36], Bertsch [37], Gerace and Green [38] applied it to Ca isotopes with various degrees of success. Recently, Flowers and Skouras [39] calculated the deformed states by a variational procedure with no fitting of matrix elements to experimental energies.

At this point, one should ask several questions. First, why did they choose deformed states rather than spherical ones? Second, why many-particle many-hole configurations rather than 1 particle-1 hole, if one wishes to obtain low-energy excitations?

The answer to the first question is obvious: some deformed states have a lower energy then the spherical ones. It is sufficient to look at the Nilsson diagrams in order to see this.

The second question is more complex. Let us look at a system of four particles in a shell-model potential (Fig. 24). Let the energy difference between major shells be ϵ and ΔV the particle-particle or hole-hole interaction. We assume $|\Delta V| < |\epsilon|$ and we neglect particle-hole interactions. The energy of g.s. (a) is 0. Next we excite one particle. The excitation energy of the system (b) is $E = \epsilon + 0$. Next, we excite two particles (c). Now, the unperturbed energy of excitation 2ϵ is diminished by a particle-particle interaction $\Delta V: E(c) = 2\epsilon - \Delta V$. When we rise 3 particles (d) we have 3 interacting pairs and the total energy is $E(d): 3\epsilon - 3\Delta V$. For 4 particles we have $E(e) = 4\epsilon - 6\Delta V$, which might be lower than $E = \epsilon + 0$. Hence, under particular conditions, 4 particle-4 hole configurations might appear at lower energies than the 1 particle-1 hole ones.
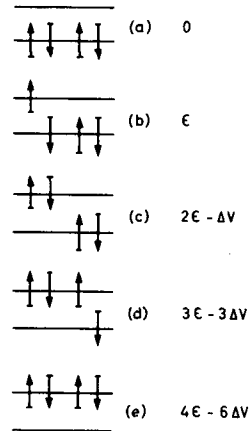
FIG.24.   Four particles in shell-model potential.

From this short survey of the Ca region, we see that the situation here is quite different from that in Pb and that we have to admit deviations from the simple shell-model picture even in a first-approximation description.

3.3. Nuclei far from closed shells

So far we have been looking at the vicinity of doubly-closed-shell nuclei. What about nuclei very far away from closed shells? Is the shell model still a good description there? In the simple shell model, the treatment of more than three particles outside of the closed shell becomes next to impossible. However, this is again simple in the pairing theory [40], provided that either the neutrons or the protons form a closed shell. We shall illustrate this for tin isotopes, $Z = 50$, $N = 66 \rightarrow 74$. The involved neutron sub-shells are:

$$d_{5/2}, \ g_{7/2}, \ s_{1/2}, \ d_{3/2}, \ h_{11/2} \,.$$

Cohen and Price [41] have shown that combining (d, p) and (d, t) reactions one can obtain useful information about single-particle levels. As is well known the cross-section for any stripping or pick-up reaction can be represented as the product of two factors, one containing the kinematics of the reaction, the other the nuclear structure information

$$\frac{d\sigma}{d\Omega} (d, p) = \frac{2I_f + 1}{2I_i + 1} \ P(\ell_n, Q, \theta). \ S(i, f)$$

$$\frac{d\sigma}{d\Omega} (d, t) = T(\ell_n, Q, \theta). \ S(i, f)$$

where P and T are functions which can be derived from the reaction theory and $S_{if} = S_{fi}$, the overlap of the initial and final states, can be obtained from nuclear-structure theory. We have chosen the (d, p) and (d, t) reactions as being experimentally simple.

From the French-Macfarlane rules one obtains for even-even targets and pure j^n configurations:

$$S = n \qquad \text{for } (d, t) \tag{4a}$$

$$S = 1 - \frac{n}{2j+1} \quad \text{for } (d, p) \tag{4b}$$

where n is the number of particles (neutrons) outside the closed shell. However, we know that the configurations are not pure, and we define an average occupation probability for a given orbital j, v_j^2 as

$$n = (2j+1) v_j^2$$

Thus, for even-even targets we can write the cross-section ($I_i = 0$, $I_f = j$).

$$\frac{d\sigma}{d\Omega} (d, p) = (2j+1) P \cdot u_j^{2 \, (i)}$$

$$\frac{d\sigma}{d\Omega} (d, t) = (2j+1) T \cdot v_j^{2 \, (i)}$$

It is obvious that the stripping cross-section will be proportional to the number of empty places, i.e. holes which can be filled, while the cross-section for pick-up will be proportional to the number of particles that can be taken out. Here $u_j^2 = 1 - v_j^2$; v_j^2 represents the fraction by which the sub-shell j is filled with particles. u_j^2 represents the fraction of unoccupied places, ·i.e. the number of holes, [actually, the number of holes is given by $(2j+1) \cdot u_j^2$].

How do we calculate v_j^2? We shall discuss a method proposed by Cohen and Price [41]. This method contains several approximations and simplifications and it is surprising that it works at all. Yet, it gives results that are not inconsistent. The reason, in our opinion, is that it contains a minimum number of simple physical assumptions and that hence it should work.

First we eliminate the Q-value dependence by the assumption

$$P (\ell_n, Q, \theta) = P'_{\ell_n} (\theta) F^{-Q}$$

$$T (\ell_n, Q, \theta) = T'_{\ell_n} (\theta) F^{Q}$$

where F is a factor close to 1.

This approximation is based on the experimental fact that stripping and pick-up reactions vary smoothly with Q (and, in general, with energy). This is already a first approximation in the calculation.

Next we take the ratio of cross-sections for two sub-shells of the same ℓ-value at the same angle, e.g. $d_{3/2}$ and $d_{5/2}$:

$$F^{(Q_{3/2} - Q_{5/2})} \left[\frac{d\sigma}{d\Omega} (d, p) \to d_{3/2} \right] \Big/ \left[\frac{d\sigma}{d\Omega} (d, p) \to d_{5/2} \right] = a = \frac{4}{6} \frac{u_{3/2}^2}{u_{5/2}^2}$$

TABLE XI. FILLING PARAMETERS $v_{3/2}^2$ AND $v_{5/2}^2$ (from Ref.[40])
CALCULATED FOR Sn ISOTOPES FOR A = 116 - 124.

A	Target mass	116	118	120	122	124
$v_{3/2}^2$	1.0	0.28	0.40	0.73	0.77	0.94
	1.12	0.26	0.36	0.60	0.66	0.76
	1.25	0.24	0.29	0.49	0.52	0.61
$v_{5/2}^2$	1.0	0.77	0.78	0.90	0.90	0.98
	1.12	0.78	0.80	0.87	0.87	0.94
	1.25	0.80	0.81	0.86	0.84	0.92

We do the same for (d, t):

$$F^{(Q_{5/2} - Q_{3/2})} \left[\frac{d\sigma}{d\Omega} (d, t) \to d_{3/2} \right] \bigg/ \left[\frac{d\sigma}{d\Omega} (d, t) \to d_{5/2} \right] = b = \frac{4}{6} \frac{v_{3/2}^2}{v_{5/2}^2}$$

We see that using v_j^2 and u_j^2, stripping and pick-up reactions can be treated
formally in the same way: a pick-up reaction is, essentially, the stripping
of a hole.

Now we have two equations with $u_{3/2}^2$, $u_{5/2}^2$, $v_{3/2}^2$ and $v_{5/2}^2$ since a and b,
the ratios, are experimental values. However, we also have a second pair
of equations, connecting the u^2 and the v^2 :

$$u_{3/2}^2 + v_{3/2}^2 = 1$$

and

$$u_{5/2}^2 = v_{5/2}^2 = 1$$

We have hence 4 equations with 4 unknowns and we can obtain the u^2's
and the v^2's. In the above procedure, however, we have facitly made a
second approximation, namely we have supposed that the shape of the
angular distribution for the two $\ell = 2$ levels is identical, which is not
always true. Nevertheless, the results as seen from Table XI, are not
completely unreasonable. For instance, both the $v_{3/2}^2$ and $v_{5/2}^2$ are slowly
increasing with increasing atomic number A, i.e. the sub-shells $d_{3/2}$
and $d_{5/2}$ are being gradually filled up. The $d_{5/2}$ orbital is filled first, as

$$\begin{array}{cc}
\underline{\hspace{3cm}} & h_{11/2} \\
\\
\underline{\hspace{3cm}} & d_{3/2} \\
\\
\underline{\hspace{3cm}} & s_{1/2} \\
\\
\underline{\hspace{3cm}} & g_{1/2} \\
\\
\underline{\hspace{3cm}} & d_{5/2}
\end{array}$$

expected from its lower energy. In a simple shell-model picture the $d_{5/2}$
orbital should have been filled already with 6 extra-core particles. In
practice, we find it almost filled with 16 particles (80%). The $d_{3/2}$ orbital
is more instructive. We should need 16 extra-core particles to start to fill
it up and 20 particles to fill it completely. In fact for ^{116}Sn it is almost
unfilled ($\sim 25\%$). For ^{120}Sn it is three-quarters filled, while for 4 more
particles (^{124}Sn) it is completely filled.

We see, hence, that even away from closed shells we can use simple
shell-model notions if we modify them in a proper way.

In the case when we do not have two sets of levels with identical angular
distributions (like, for example, the $g_{7/2}$ or $h_{11/2}$ levels), we have to make
further approximations. Even then the obtained results are not too
inconsistent.

The next information which we can obtain in this way is the unperturbed
single-particle energy. For doubly closed shells this information was
straightforward. Even when, owing to the interaction with the core, the
single-particle strength was fractioned, it was easy to obtain the spacing
of single-particle levels by taking the centre-of-gravity (a weighted
average) energy. Here this information is by no means straightforward
but it passes through the pairing theory. This theory relates the occupation
probabilities v_j^2 with the energies of the observed levels E_j and the energies
of the unperturbed single-particle levels ϵ_j through two empirical quantities:
the chemical potential λ and the pairing energy gap Δ:

$$v_j^2 = \frac{1}{2}\left[1 - \frac{e_j}{(1 - e_j^2)^{1/2}}\right] \tag{5}$$

where

$$e_j = (\epsilon_j - \lambda)/\Delta \tag{6}$$

TABLE XII. VALUES OF UNPERTURBED SINGLE-PARTICLE
ENERGIES FOR TIN ISOTOPES CALCULATED FROM THE v_j^2's OF
TABLE XI, USING THE PAIRING THEORY OF Ref.[40] (from Ref.[41])

Mass number		116	118	120	122	124	Nilsson K-S	Exp av
$s_{1/2}$	Exp	0.97	0.83	0.97	0.70	1.24	1.90	0.95
	E	1.65	1.72	1.57	1.40	1.37		
$d_{3/2}$	Exp	1.44	1.22	1.10	0.96	1.41	2.20	1.23
	E	2.45	2.12	1.87	1.85	1.94		
$d_{5/2}$	Exp	0	0	0	0	0	0	0
	E	0	0	0	0	0		
$g_{7/2}$	Exp	0.08	-0.33	-0.22			0.22	-0.16
	E	0.42	0.37	0.22				
$h_{11/2}$	Exp	1.34	1.22	1.54	1.22	1.75	2.80	1.41
	E	2.75	2.32	2.12	2.05	1.94		

Experimentally, Δ is a half of the pairing-energy gap [about 1.1 MeV] in this mass region. The relation between the observed level energy E_j and the unperturbed energy ϵ_j goes through the intermediate energies e_j:

$$E_j = \left[(1 - e_j^2)^{1/2} - (1 + e_{j-\epsilon}^2)^{1/2} \right]$$

where $e_{j-\epsilon}$ stands for the e_j value in the ground state. Solving Eq. (5) for e_j and using the relation between u_j^2 and v_j^2 we obtain:

$$e_j = \frac{u_j^2 - v_j^2}{2 (u_j v_j)^{1/2}}$$

and, using relation (6), ϵ_j.

The values of ϵ_j obtained from this equation are shown in Table XII. The determination of the single-particle energies for the various isotopes are reasonably consistent among themselves, although there are large fluctuations, as might be expected.

4. CONCLUSION

Let us conclude with some comments on what we mean by saying that a process or a state is well described by a certain model. We have seen, e.g. that the same model wave functions which give good energy spectra do not yield the transition probabilities etc. This point has been discussed extensively by De Shalit [42] and we refer the reader thereto.

A wave function of a system of A particles gives the complete information about the system, i.e. about the motion of all the particles. Usually, we do not need all this information. In fact, what we usually need are matrix elements of some one-body or two-body operators

$$F = \sum f_i \quad \text{or } G = \tfrac{1}{2} \sum g_{ij}$$

It can be shown, that, to calculate these matrix elements, one needs only a small part of the A-particle wave function, namely the single viz. two-particle density matrix. Hence it is clear that when we say that a certain set of model wave functions $\Phi_A (x_1 \ldots x_A)$ reproduces the experimental values of some F or G type operators, then what we mean at most is that the model wave function Φ_A and the real wave function Ψ_A yield the same density matrix $\rho_{ab} (x, x')$. Very little can be claimed as to the faithfulness with which Φ_A describes other types of correlations.

We can see now why some model wave functions give excellent results for some physical quantities, while failing completely to describe the others.

A few words should be said about the meaning of the concept of "overlap". A large overlap of two wave functions, say 90 or 95%, is usually taken as equivalent to these wave functions being equally valid. In fact, we have implicitly used this terminology in the description of the spectroscopic factor. We said that the spectroscopic factor was unity when the residual wave function had a maximum overlap with a wave function

constructed by vector coupling a single nucleon in a given orbital state ℓ, j to the ground-state target wave function. Such a statement should be carefully considered, since the validity of a wave function depends very much on the purpose for which it has been constructed. The trivial example is the case of the 1s wave functions in two harmonic oscillators with elastic constants k and 2k respectively, which have a 91% overlap since the bulk of both of them is concentrated around the origin. Nevertheless, if we use the two wave functions to determine a quantity at larger radii, the difference might well be all we were looking for.

It often has been repeated that the greatest discovery in nuclear physics in the last ten years is the evidence that the shell model is applicable to nuclei. This fact, at first difficult to understand, is now well understood and corroborated by convincing evidence. It was the scope of these lectures to illustrate the value and the limitations of this description. As to the value of the spectroscopic information obtained from, e.g. the analysis of transfer reactions, it is certainly correct to say that the most important facts stemming out from this analysis are (a) that the individual orbital angular momentum is a good quantum number and (b) that the orbital occupation parameters agree with our basic ideas of a shell-model description of nuclear states.

REFERENCES

[1]   WILKINSON, D.H., Comments on Particle and Nuclear Physics II 2 (1968) 48.
[2]   GOTTSCHALK, B., WANG, K.W., STRAUCH, K., · Nucl.Phys. A90, (1967) 83.
[3]   WILKINSON, D.H., MAFETHE, M.E., Nucl.Phys. 85,(1966) 97.
[4]   AMALDI, U., CAMPOS VENUTI, G., CORTELESSA, G., de SANCTIS, E., FRULLANI, S., LOMBARD, R., SALVADORI, P., Phys. Letters 25B, (1967) 24.
[5]   COHEN, B.L., Physics Letters 27B, (1968) 271.
[6]   See, e.g. GLENDENNING, N.K., Ann.Rev.Nucl.Sci. 13,(1963) 191.
[7]   The most widely used DWA code, JULIE, originated by BASSEL, R.H., DRISKO, R.M., SATCHLER, G.R., is still unpublished and available as an ORNL report.
[8]   MUEHLLEHNER, G. et al., Phys.Rev. 159,(1967) 1039.
[9]   WILDENTHAL, B.H. et al., Phys.Rev. Letters 19,(1967) 260.
[10]   HINDS, S. et al., Nucl.Phys. 83, (1966) 17.
[11]   HAFELE, J.C., WOODS, R., Phys. Letters 23,(1966) 579.
[12]   GLASHAUSSER, C. et al., Phys.Rev. Letters 21, (1968) 918.
[13]   STEIN, N. et al., Phys.Rev. Letters 20, (1968) 113.
[14]   BARDWICK, J., TICKLE, R., Phys.Rev. 161, (1967) 1217.
[15]   MUKHERJEE, P., COHEN, B.L., Phys.Rev. 127, (1968) 1284.
[16]   BALLINI, R. et al., Physics Letters 26B, (1968) 215.
[17]   CRAMER, J.G. et al., Phys.Rev. Letters 21, (1968) 298.
[18]   BJERREGAARD, J.H. et al., Nucl.Phys. A107, (1968) 241.
[19]   KUO, T.T. et al., Bull.Am.Phys.Soc. 12, (1967) 538.
[20]   ALFORD, W., Phys.Rev. Letters 21, (1968) 157.
[21]   ERSKINE, J.R., Phys.Rev. 135, (1964) B110.
[22]   KIM, V.E., RASMUSSEN, J.O., Phys.Rev. 135, (1964) B44.
[23]   BJERREGAARD, J.H. et al., Nucl.Phys. 89, (1966) 337.
[24]   GILLET, V. et al., Nucl.Phys. 88, (1966) 331.
[25]   BJERREGAARD, J.H. et al., Nucl.Phys. A113, (1968) 484.
[26]   REDLICH, W.G., Phys.Rev. 138B, (1965) 544.
[27]   BJERREGAARD, J.H. et al., Nucl.Phys. A94, (1967) 457.
[28]   GLASHAUSSER, C., KONDO, M., RICKEY, M.E., ROST, E., Physics Letters 14, (1965) 113.
[29]   BELOTE, T. et al., Phys.Rev. 139B, (1965) 80.
[30]   SMITH, S.M., BERNSTEIN, A.M., RICKEY, M.E., Nucl.Phys. A113, (1968) 303.

[31]   SARTORIS, G., ZAMICK, L., Phys.Rev. Letters 18, (1967) 292.
[32]   LEWIS, M.B., Phys. Letters 27B, (1968) 13.
[33]   DELAUNAY, J. et al., Contribution No.149, Dubna Symp. on Nuclear Structure, July (1968)
       Dubna publication D-3893.
[34]   BROWN, G.E., Proc.Int.Conf. Paris (1964), 1, (Dunod) 192.
[35]   BASSICHIS, W.H., RIPKA, G., Phys. Letters 15, (1965) 320.
[36]   FEDERMAN, P., TALMI, I., Phys. Letters 15, (1965) 165, 19, (1965) 490.
[37]   BERTSCH, G.F., Nucl.Phys. 89, (1966) 673.
[38]   GERACE, W.J., GREEN, A.M., Nucl.Phys. 93, (1967) 110.
[39]   FLOWERS, B.H., SKOURAS, L.D., Nucl.Phys. A116, (1968) 529.
[40]   KISSLINGER, L.S., SORENSEN, R.A., Rev.Mod.Phys. 35, (1963) 853.
[41]   COHEN, B.L., PRICE, R.E., Phys.Rev. 121, (1961) 1441.
[42]   De SHALIT, A., Nuclear Structure and Electromagnetic Interactions, (N. MacDonald, Ed.) (1965) 4.

CHARGE INDEPENDENCE IN NUCLEAR PHYSICS

L. FONDA
Istituto di Fisica Teorica, Università di Trieste
Trieste, Italy

Abstract

CHARGE INDEPENDENCE IN NUCLEAR PHYSICS.
1. Charge independence and isotopic spin; 2. Generalized Pauli principle; 3. Selection rules for nuclear reactions; 4. Electromagnetic transitions and β-decay; 5. Mass splittings; 6. Finite groups and charge independence; 7. The isotopic spin in heavy nuclei.

1. CHARGE INDEPENDENCE AND ISOTOPIC SPIN

Immediately after the discovery of the neutron in 1932, Heisenberg [1] put forward the idea that the nuclear force between a pair of protons is equal to the nuclear force between a pair of neutrons. In 1936, Breit and Feenberg [2] inferred from a comparison of the scattering of protons by protons and of protons by neutrons, that the nuclear force which acts between two protons is equal to that acting between a proton-neutron pair. These pioneering works paved the way to the introduction of a new symmetry in nuclear physics, i.e. to the so-called charge independence of the nuclear forces: the neutron and the proton are two states of a single entity, the nucleon. There are, of course, differences between these two particles, i.e. a small mass difference, different charges and magnetic moments, but one thinks that they can just be explained by the different role played by these particles in the interaction with the electromagnetic field.

There is great experimental evidence that nuclear forces are charge-symmetric, i.e. that the n-n and p-p interactions are the same, once having disposed of the Coulomb force in the p-p pair. This comes essentially from the equivalence of the spectra of mirror nuclei since for these nuclei the number of n-p bonds are the same. In Table I we show some examples[1]. To obtain an approximate estimate of the Coulomb part of the binding energy we have used the simple expression which is obtained for point protons uniformly distributed in a nucleus:

$$E_{Coulomb} \cong 0.61 \frac{Z(Z-1)}{A^{\frac{1}{3}}} \text{ MeV} \tag{1}$$

(we have used $r_0 = 1.41 \times 10^{-13}$ cm). The close equality of the net nuclear binding energies is striking.

The charge independence of nuclear forces, i.e. the fact that we actually have n-n = p-p = n-p for the nuclear forces of these pairs, is provided by the original work by Breit and Feenberg and by the equality of the nuclear binding energy of the so-called isomultiplets [3] that we now come to describe.

---

[1] The experimental binding energies of Table I and II are taken from MATTAUCH, J.H.E., THIELE, W., WAPSTRA, A.H., Nucl. Physics 67 (1965) 1.

TABLE I. BINDING ENERGIES (in MeV) OF SOME MIRROR NUCLEI

A	Z	Nucleus	Binding energy	Coulomb energy	Net nuclear binding energy
3 {	1	^{3}H	-8.48	0	-8.48
	2	^{3}He	-7.72	+0.85	-8.57
13 {	6	^{13}C	-97.11	+7.78	-104.89
	3	^{13}N	-94.11	10.89	-105.00
41 {	20	^{41}Ca	-350.4	+67.3	-417.7
	21	^{41}Sc	-343.1	+74.3	-417.4
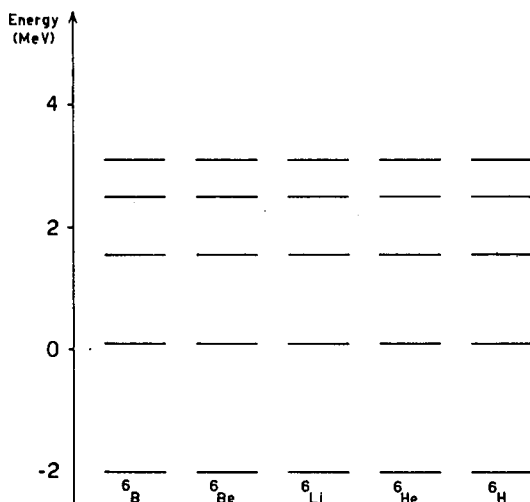
FIG. 1a.   Levels without exclusion principle.

Naively, one would think that, if the interaction between all nucleons is alike, all nuclei of same mass number A will have the same spectra and energy levels.   This is, however, not true because of the exclusion principle. In fact, some states which are compatible with the exclusion principle for a n-p pair, are incompatible for á n-n or for a p-p pair.   The states in question are those which are symmetric under the interchange of the two particles.   These states are perfectly permissible for a n-p pair. This kind of suppression is shown in Fig. 1 for the nuclei ^{6}H, ^{6}He, ^{6}Li, ^{6}Be and ^{6}B.   We see for example that the low-energy states of ^{6}B and ^{6}H are eliminated.   The experimental binding energies are, of course, not the same owing to the electrostatic force which tilts the levels in such a way that nuclei with fewer protons have lower energy.   However, after subtracting the Coulomb energy we get very close values for the net nuclear binding energy.   This is shown in Table II for some nuclei.   We have again
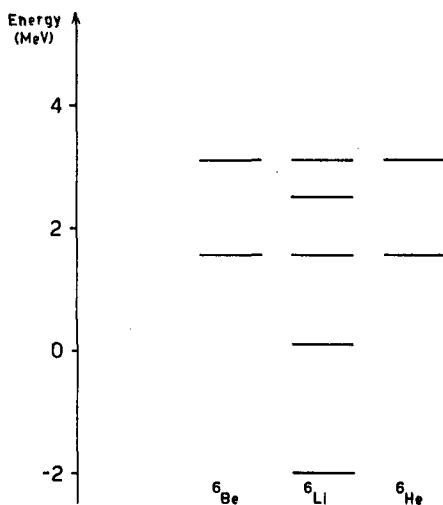
FIG. 1b. Allowed levels, without electrostatic energy.
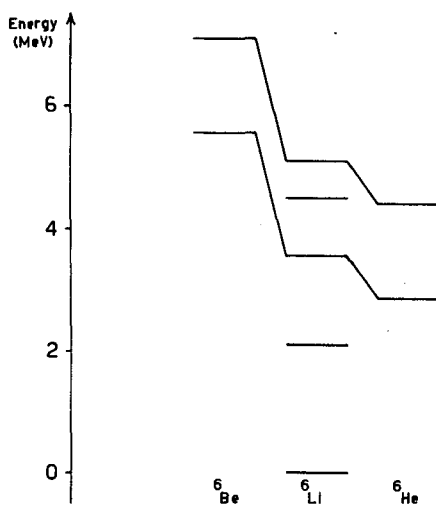
FIG. 1c. Allowed levels, with electrostatic energy.

used the simple-minded formula (1) in order to get a rough estimate of the Coulomb energy. We see from Tables I and II that nuclei arrange in multiplets of the same nuclear binding energy in much the same way as the spin multiplets in atomic spectroscopy. In the latter case the intro-duction of the concept of spin for the electron led to a concise mathematical

TABLE II. BINDING ENERGIES (in MeV) OF SOME I-TRIPLETS

A	Z	Nucleus	Binding energy	Coulomb energy	Net nuclear binding energy
6	2	^{6}He	-29.26	+0.67	-29.93
	3	^{6}Li* (3.56)	-28.43	+2.02	-30.45
	4	^{6}Be	-26.93	+4.03	-30.96
10	4	^{10}Be	-64.98	+3.40	-68.38
	5	^{10}B* (1.74)	-63.01	+5.66	-68.67
	6	^{10}C	-60.36	+8.49	-68.85
14	6	^{14}C	-105.3	+7.6	-112.9
	7	^{14}N* (2.32)	-102.3	+10.6	-112.9
	8	^{14}O	-98.7	+14.2	-112.9

formulation of the problem. In the same way, to express the hypotheses
of charge symmetry and charge independence in quantum-mechanical
language, one is led to the introduction of a new quantum number τ_3' for
the nucleon:

$$\tau_3' = +1 \quad \text{neutron}$$

$$\tau_3' = -1 \quad \text{proton}$$

This variable distinguishes between neutrons and protons just as the
electron spin variable distinguishes electrons with spin parallel or anti-
parallel to the z-axis. The corresponding operator can be written in
matrix form

$$\tau_3 = \begin{pmatrix} 1 & 0 \\ 0 & -1 \end{pmatrix} \tag{2}$$

In this representation the pure proton and the pure neutron state are, of
course, described by two-component wave functions:

$$\varphi_n = \begin{pmatrix} \psi_n \\ 0 \end{pmatrix} \qquad \varphi_p = \begin{pmatrix} 0 \\ \psi_p \end{pmatrix} \tag{3}$$

where ψ_n and ψ_p are wave functions of given spin. In this new two-
dimensional Hilbert space all operators will be a linear combination of
the 2 × 2 identity matrix and of the three matrices

$$\tau_1 = \begin{pmatrix} 0 & 1 \\ 1 & 0 \end{pmatrix} \quad \tau_2 = \begin{pmatrix} 0 & -i \\ i & 0 \end{pmatrix} \quad \tau_3 = \begin{pmatrix} 1 & 0 \\ 0 & -1 \end{pmatrix} \tag{4}$$

These matrices satisfy the commutation relations for spin $\frac{1}{2}$:

$$\{\tau_k , \tau_\ell\} = 2\delta_{k\ell}$$

We call $\vec{I} \equiv \frac{1}{2}\vec{\tau}$ the isotopic or isobaric spin of the nucleon. We say that the nucleon is a particle of isotopic spin $\frac{1}{2}$, it is an isospin doublet. For a system of A nucleons we define the total isotopic spin

$$\vec{I} = \sum_{k=1}^{A} \frac{1}{2}\vec{\tau}^{(k)} \tag{5}$$

where $\frac{1}{2}\vec{\tau}^{(k)}$ is the isospin of the k-th nucleon. We easily see that

$$[I_j, I_k] = i\,\epsilon_{jk\ell}\,I_\ell \tag{6}$$

That is, the I_j determine the algebra of the group SU(2) of the unimodular unitary 2×2 matrices. We can then proceed as in the case of angular momentum. We diagonalize $\vec{I}^2$ and I_3 together. To a given value of I we have $2I+1$ values of I_3 ranging from $-I$ to $+I$. These constitute an irreducible representation of the group SU(2). For I_3 we have:

$$I_3 = \frac{A}{2} - Z \tag{7}$$

We see that we can just use $\vec{I}^2$ and I_3 to identify a nucleus in a multiplet. In fact, once A is given we first fix a value $I(I+1)$ of the Casimir operator $\vec{I}^2$. According to the theory of angular momentum, I will be integer ($\geqq 0$) or half-integer (> 0) according to whether the number of nucleons is even or odd. In this way we have a multiplet of $2I+1$ isobar nuclei. The value of I_3 then identifies one of these in a one-to-one way according to Eq. (7). The $2I+1$ nuclei of the irreducible representation characterized by the value I for the isospin are then different states of a single entity. Of course, the nuclear binding energy, the spin J and the parity P is the same for all. Charge independence tells us that by jumping, in a given I-multiplet, from a value of I_3 to another possible value of this operator we get a particle (nucleus) which evolves in time in the same way as that from which we started. This means that the Hamiltonian commutes with I_+ and I_-

$$I_\pm = I_1 \pm i\,I_2 \tag{8}$$

which are the raising and lowering operators for the eigenvalues of I_3:

$$\begin{aligned}
I_+ \psi_I^{I_3} &= [\,(I - I_3)\,(I + I_3 + 1)\,]^{\frac{1}{2}}\;\psi_I^{I_3 + 1} \\
I_- \psi_I^{I_3} &= [\,(I + I_3)\,(I - I_3 + 1)\,]^{\frac{1}{2}}\;\psi_I^{I_3 - 1}
\end{aligned} \tag{9}$$

Since, on the other hand, H commutes also with I_3 (they can be simultaneously diagonalized) we obtain

$$[H, I_j] = 0 \tag{10}$$

and therefore also

$$[H, \vec{I}^2] = 0 \tag{11}$$

We say that H is an isospin scalar, an invariant under rotations in the so-called isotopic spin (or charge) space which is introduced by analogy with the ordinary three-dimensional space in which physical rotations operate. The unitary operator implementing a rotation in the charge space is, of course,

$$R_{\vec{n}}(\omega) = e^{i\vec{I}\cdot\vec{\omega}} \tag{12}$$

where $\vec{I}$ is the total isospin of the system given by Eq. (5) and $\vec{\omega} = \vec{n}\omega$. In particular, a rotation of 180° around the 1-axis corresponds to the substitution of all the protons of the considered nucleus by neutrons and ·vice versa. The invariance under this transformation is just the hypothesis of charge symmetry. We easily see that

$$R_1 (\pi) \psi_I^{I_3} \equiv e^{i I_1 \pi} \psi_I^{I_3} = i^{2I} \psi_I^{-I_3} \tag{13}$$

If $I_3 = 0$, i.e. for a self-conjugate nucleus (number of protons equal to the number of neutrons), we see that the nuclear wave function is eigenfunction of $R_1(\pi)$ for the eigenvalue $(-)^I$ (I is an integer in this case):

$$R_1 (\pi) \psi_I^{I_3 = 0} = (-)^I \psi_I^{I_3 = 0} \tag{14}$$

We say that the nucleus has "charge parity" $(-)^I$. Selection rules based on the application of Eq. (14) are then consequences of the weaker assumption of charge symmetry.

2.   GENERALIZED PAULI PRINCIPLE

The identity of the nucleons leads us to an investigation of the problem of the statistics obeyed of the nucleon. In nature identical particles obey either the Fermi-Dirac or the Bose-Einstein statistics [4]. Protons and neutrons are both fermions. A priori a nucleon could be either a fermion or a boson. However, since a neutron can transform into a proton via β-decay, it is possible to see that the nucleon is actually a fermion [5]. Consider, in fact, a system of a neutron and a proton in a scattering state ^3S of zero orbital angular momentum and spin 1. There are two linearly independent wave functions possible for the description of such a state:

$$\psi_s = \psi_{\ell=0}(r) \chi_{S=1} \psi_{I=1}^{I_3=0}$$
$$\psi_A = \psi_{\ell=0}(r) \chi_{S=1} \psi_{I=0}^{I_3=0} \tag{15}$$

the first being symmetric under interchange of all co-ordinates, i.e. under interchange of the two nucleons, the second being antisymmetric. For a system of two nucleons, $\psi_I^{I_3}$ is simply given in terms of the isotopic wave functions ξ of the two nucleons:

$$\text{triplet}\left\{\begin{array}{l}\psi_{I=1}^{I_3=1}=\xi^+(1)\,\xi^+(2)\\[2em]\psi_{I=1}^{I_3=0}=\frac{1}{\sqrt{2}}\,[\xi^+(1)\,\xi^-(2)+\xi^-(1)\,\xi^+(2)]\qquad(16t)\\[2em]\psi_{I=1}^{I_3=-1}=\xi^-(1)\,\xi^-(2)\end{array}\right.$$

$$\text{singlet}\qquad\psi_{I=0}^{I_3=0}=\frac{1}{\sqrt{2}}\,[\xi^+(1)\,\xi^-(2)-\xi^-(1)\,\xi^+(2)]\qquad(16s)$$

Here ξ^+ describes the neutron ($I_3=+\frac{1}{2}$), ξ^- the proton. Now, in a scattering state the system n-p can be transformed into the p-p system via β-decay. Since the β-interaction, like all physical observables (see below), is symmetrical for the interchange of the nucleons, ψ_S and ψ_A will retain their symmetry. But a p-p system must have a completely antisymmetric wave function, therefore the symmetric wave function ψ_S is ruled out: the nucleon is a fermion.

As anticipated above, all physical observables are symmetric under interchange of any pair of nucleons. For example, for the charge Z, kinetic energy K and Coulomb potential V_C we have

$$Z=\frac{A}{2}+I_3\qquad(17a)$$

$$K=\frac{A}{2}\,(m_n+m_p)\,c^2+(m_n-m_p)\,c^2\,I_3$$

$$-\frac{\hbar^2\,(m_p+m_n)}{4\,m_pm_n}\sum_{j=1}^{A}\Delta^{(j)}+\frac{\hbar^2\,(m_n-m_p)}{4\,m_pm_n}\sum_{j=1}^{A}\tau_3^{(j)}\Delta^{(j)}\qquad(17b)$$

$$V_C=\frac{e^2}{4}\sum_{k<j}^{1,A}\frac{(1-\tau_3^{(k)})\,(1-\tau_3^{(j)})}{r_{kj}}\qquad(17c)$$

where $\Delta^{(j)}$ is the Laplacian on the j-th particle and

$$\vec{r}_{kj}=\vec{r}_k-\vec{r}_j$$

3. SELECTION RULES FOR NUCLEAR REACTIONS

Charge symmetry alone is already able to forbid the occurrence of certain reactions. For example, we know that the self-conjugate nuclei ^{2}H, ^{4}He and ^{16}O have charge parity +1 while ^{14}N* (2.32) has charge parity -1. The reaction

$$^2\text{H}+{}^{16}\text{O}\longrightarrow{}^{14}\text{N*}\,(2.32)+{}^4\text{He}\qquad(18c)$$
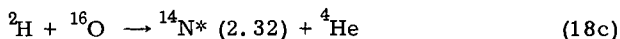
is then forbidden.   Analogously the fissions

$$^{10}B^* \; (6.5) \longrightarrow \; ^6Li + \, ^4He$$
$$\searrow \; ^8Be + \, ^2H \tag{19}$$
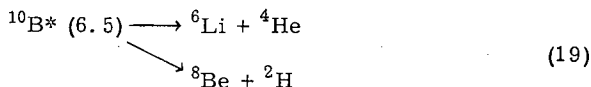
are also forbidden by charge symmetry.

If we assume the stronger hypothesis of charge independence we obtain selection rules as a consequence of conservation of the total I-spin. According to Eq. (11) I must be the same throughout the process.   For example the reaction

$$^6Li + \, ^4He \longrightarrow \, ^6Li^* \; (3.56) + \, ^4He \tag{20}$$
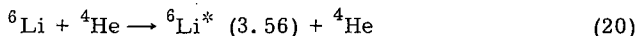
is forbidden since I is zero and one at the beginning and at the end, respectively ($^6Li^*$ (3.56) belongs to an I-triplet, see Table II).   On the other hand, from I-conservation we can get intensity rules. For example the ratio of the cross-sections for the two reactions

$$^2H + \, ^9Be \longrightarrow \, ^{10}B^* \; (1.74) + n$$
$$^2H + \, ^9Be \longrightarrow \, ^{10}Be + p \tag{21}$$
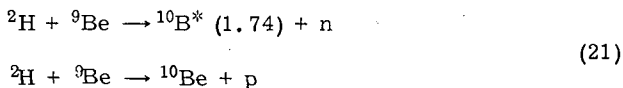
is equal to $\frac{1}{2}$.   This is seen by combining the isospin wave functions of the final products into a total I-spin eigenfunction:

$$\psi_{I_1}^{m_1} \psi_{I_2}^{m_2} = \sum_{I=|I_1-I_2|}^{I_1+I_2} C_{I_1 I_2} \; (I, \; m_1 + m_2; \; m_1, \; m_2) \; \psi_{I \; I_1 I_2}^{m_1+m_2} \tag{22}$$

Since the initial state is an I-doublet, only the term I = $\frac{1}{2}$ of Eq. (22) will contribute in constructing the scattering amplitude.   We see then that the scattering amplitude is proportional to $C_{1\frac{1}{2}} (\frac{1}{2}, \; \frac{1}{2}; \; 0, \; \frac{1}{2}) = -1/\sqrt{3}$ for the final state $^{10}B^*$ (1.74) = N and to $C_{1\frac{1}{2}} \; (\frac{1}{2}, \; \frac{1}{2}; \; 1, \; -\frac{1}{2}) = \sqrt{2/3}$ for the final state $^{10}Be + p$.   We finally get

$$\frac{\sigma \; (^{10}B^* + n)}{\sigma \; (^{10}Be + p)} = \frac{1}{2} \tag{23}$$

The above rules are approximate since the Coulomb interaction, which makes itself felt more and more on increasing the number of protons in the nucleus, while conserving I_3 (see relation (17c)), does not conserve I. The same is also true for the kinetic energy due to the $m_n - m_p$ mass difference (see Eq. (17b)) and to the β-decay interaction which makes the neutron decay according to $n \to p + e^- + \bar{\nu}$ while the proton is stable. As a consequence of the only approximate validity of charge independence we have for example that the reaction

$$^2H + \, ^{16}O \longrightarrow \, ^{14}N^* \; (2.32) + \, ^4He \tag{24}$$
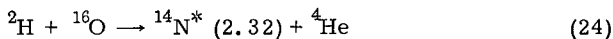
occurs experimentally while, being a $\Delta I = 1$ transition ($^{14}N^*$ (2.32) has $I = 1$, see Table II), it would be forbidden if isospin were strictly conserved. In the particular case of reaction (24) the reason for its occurrence lies in the fact that the compound nucleus ^{18}F which is formed as an intermediate step contains an isospin impurity of about 4 %. Impurities of this type always show up when the compound nucleus is formed in a highly excited state since in that case its wave function is strongly altered by the Coulomb force.

4. ELECTROMAGNETIC TRANSITIONS AND β-DECAY

If one takes into account the interaction of a nucleus with an electromagnetic field then clearly the I-spin is no longer conserved. We can, however, discuss certain selection rules concerning the change $\Delta I \equiv I_f - I_i$ of the I-spin in radiative reactions. The interaction of electromagnetic radiation with a system of nucleons is given by

$$H_{em} = \frac{1}{2m_p} \sum_{protons} \left[\left(\vec{p}_j - \frac{e}{c} \vec{A}(\vec{r}_j) \right)^2 - \vec{p}_j^{\,2} \right]$$

$$- \sum_{protons} \mu_p \vec{\sigma}^{(j)} \cdot \text{rot } \vec{A}(\vec{r}_j) - \sum_{neutrons} \mu_n \vec{\sigma}^{(j)} \cdot \text{rot } \vec{A}(\vec{r}_j) \tag{25}$$

where μ_p and μ_n are the magnetic moments of the proton and neutron, respectively. To first order in e , in the gauge div $\vec{A} = 0$ and after introduction of the isospin operators, we obtain

$$H_{em} = \mathcal{H}_s + \mathcal{H}_v$$

with

$$\mathcal{H}_s = - \frac{e}{2m_p c} \sum_{j=1}^{A} \vec{A}(\vec{r}_j) \cdot \vec{p}_j$$

$$- \frac{\mu_p + \mu_n}{2} \sum_{j=1}^{A} \vec{\sigma}^{(j)} \cdot \text{rot } \vec{A}(\vec{r}_j) \tag{26a}$$

$$\mathcal{H}_v = \frac{e}{2 m_p c} \sum_{j=1}^{A} \tau_3^{(j)} \vec{A}(\vec{r}_j) \cdot \vec{p}_j$$

$$+ \frac{\mu_p - \mu_n}{2} \sum_{j=1}^{A} \tau_3^{(j)} \vec{\sigma}^{(j)} \cdot \text{rot } \vec{A}(\vec{r}_j) \tag{26b}$$

$\mathcal{H}_s$ is an isoscalar, while $\mathcal{H}_v$ is an isovector; there follows as a simple application of the Wigner-Eckart theorem that to the first order in e:

$$\Delta I = 0 \qquad \text{for} \quad \mathcal{H}_s$$

$$\Delta I = 0, \pm 1 \quad \text{for} \quad \mathcal{H}_v \tag{27}$$

This selection rule can be used for the isospin assignment of an excited state. Let us, for example, suppose that we have a reaction of the type

$$\gamma + \text{nucleus} \longrightarrow \text{nucleus}^* \longrightarrow \text{nuclear fragments} \qquad (28a)$$
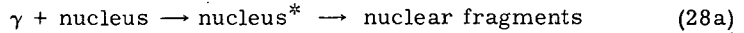
If the target nucleus has $I = \frac{1}{2}$, the I-spin of the excited state is either $\frac{1}{2}$ or $\frac{3}{2}$, and this can be understood by determining the I-spin of the final products since the second step of the reaction conserves I-spin. If the target nucleus is self-conjugate then it can be shown [6] that the excited states reached by the absorption of a slow photon, by means of an electric dipole transition, have an I-spin differing from that of the target nucleus by ±1:

$$I\,(\text{nucleus}^*) - I\,(\text{nucleus}) = \pm 1, \text{ for self-conjugate nuclei} \qquad (28b)$$

If consideration is given to the β-decay of nuclei, we have, of course, again breakdown of charge independence. Here we have both $\vec{I}^2$ and I_3 not conserved. The β-decay interaction is in general of the type

$$H^\beta = \tfrac{1}{2} \sum_{j=1}^{A} \left[D^{(j)} \tau_-^{(j)} + J^{(j)} \tau_+^{(j)} \right] \qquad (29)$$

where $\tau_\pm = \tau_1 + i\tau_2$ and $J^{(j)} = D^{(j)\dagger}$ from hermiticity. The first term describes β-disintegration while the second describes the process of inverse β-decay (e.g. $e^- + p \rightarrow n + \nu$). H^β behaves as an isovector so that, in general, we have the selection rule

$$\Delta I = 0, \pm 1$$
$$\Delta I_3 = \pm 1 \qquad (30)$$

For Fermi-type transitions we have the simplification that $D^{(j)}$ (and $J^{(j)}$) does not depend on j so that

$$H^\beta = D\,I_- + J\,I_+ \qquad (31)$$

Since $[I_\pm, \vec{I}^2] = 0$ we get

$$\left.\begin{array}{l} \Delta I = 0 \\[6pt] \Delta I_3 = \pm 1 \end{array}\right\} \quad \text{Fermi transitions} \qquad (32)$$

The Fermi transitions then shift the nucleus along the line which connects the members of an I-multiplet. The consideration of β-decay can then provide a tool to limit the assignment of I-spin of a nucleus if the I-spin of either the final or the initial state is known.

5.   MASS SPLITTINGS

As we have already pointed out, see in particular Fig. 1c, the Coulomb interaction among the protons gives rise to a splitting of the masses of the nuclei belonging to a multiplet of isotopic spin. Since the

electrostatic potential within a nucleus can hardly depend on the nucleon state, the dependence of the Coulomb-energy correction on I_3 should be almost the same for all I-multiplets. To understand the mechanism of the splitting, let us consider the Hamiltonian $H = K + V_C + V_N$, sum of the kinetic energy, of all Coulomb and of all nuclear interactions. K and V_C are given by (17b) and (17c). V_N is, of course, assumed to be an isoscalar. H is then in general the sum of a term H_s which is a scalar for rotations in the isospin space, a term H_v which behaves like an iso-vector and a term H_t which is the 33-component of a traceless isotensor. In particular, H_v and H_t have the form:

$$H_v = (m_n - m_p) c^2 I_3 + \frac{\hbar^2 (m_n - m_p)}{4 m_n m_p} \sum_{j=1}^{A} \tau_3^{(j)} \Delta^{(j)} - \frac{e^2}{4} \sum_{k<j}^{1,A} \frac{\tau_3^{(k)} + \tau_3^{(j)}}{r_{kj}} \quad (33)$$

$$H_t = \frac{e^2}{4} \sum_{k<j}^{1,A} \frac{\tau_3^{(k)} \tau_3^{(j)} - \frac{1}{3} \vec{\tau}^{(k)} \cdot \vec{\tau}^{(j)}}{r_{kj}}$$

The vector term H_v is the most important term of the interaction. It is responsible for the tilt in the energy lines connecting the members of an I-multiplet since its contribution is proportional to I_3. This can be seen by writing the matrix elements of H in the basis of the eigenstates $\psi_I^{I_3}$ of H_s, $\vec{I}^2$ and I_3:

$$(\psi_{I'}^{I_3}, H \psi_I^{I_3}) = \delta_{II'} E_s (I) + (\psi_{I'}^{I_3}, H_v \psi_I^{I_3}) + (\psi_{I'}^{I_3}, H_t \psi_I^{I_3}) \quad (34)$$

where $E_s (I)$ is the unperturbed energy. We have kept the eigenvalue of I_3 fixed since this remains a good quantum number. Both H_v and H_t are non-diagonal since they do not commute with $\vec{I}^2$. It is, however, easy to see that in the process of diagonalization we obtain contributions at least of the order e^4 or $(m_p - m_n)^2$ from the off-diagonal elements, so that in first approximation we can disregard them. From the Wigner-Eckart theorem we then obtain

$$(\psi_I^{I_3}, H \psi_I^{I_3}) = E_s (I) + E_v (I) \cdot I_3 + E_t (I) [I_3^2 - \frac{1}{3} I (I + 1)] \quad (35)$$

As anticipated the dependence of the energy corrections on I_3 is the same for all I, in the first approximation. We see that in the first approxi-mation, the masses of an I-multiplet lie on the parabola (35). Since any set of three or fewer points may always be joined by a parabola, the relation (35) has no relevance for $I \leq 1$. However, for $I > 1$ it can be used to predict the masses of the members of the I-multiplet if, at least, three of them are known. One can apply these reasonings, for example, to the nuclear quadruplets such as ^{17}N, $^{17}O^*$, $^{17}F^*$, ^{17}Ne and ^{13}B, $^{13}C^*$, $^{13}N^*$, ^{13}O. However, multiplets with $I \geq 3/2$ either occur at high energy where there are many levels, or contain very unstable nuclei so that the identification of their members becomes rather difficult.

6.   FINITE GROUPS AND CHARGE INDEPENDENCE

Equations (10) and (11) are the result of the hypothesis of charge
independence once we have assumed the formalism of angular momentum
or, which is just the same, of the continuous group SU(2) for the description
of the isotopic spin. We would, however, like to stress that charge inde-
pendence does not necessarily imply the use of a continuous group of trans-
formations. Finite groups may in fact be taken into consideration. In
particular, one can proceed as follows [7].

For the continuous group, using the expression (7) for I_3, we see that
a finite rotation through an angle ϕ around the 3-axis is implemented by
the operator

$$R_3 (\phi) = e^{i \phi (\frac{A}{2} - Z)} \tag{36a}$$

For the finite groups, one chooses the axis of largest symmetry to be
the 3-axis. If this is an n-fold axis one then requires the validity of
Eq. (36a) for all these rotations:

$$R_3 (\frac{2\pi}{n}) = e^{i \frac{2\pi}{n} (\frac{A}{2} - Z)} \tag{36b}$$

Eq. (36b) is the generalization of Eq. (7), and of course defines $A/2 - Z$
only modulo n. One next considers, as in the case of the continuous
group SU(2), an ℓ-dimensional irreducible representation of the considered
finite group. It will accommodate a multiplet of ℓ objects each one of
them belonging to an eigenvalue of (36b). The invariance of the Hamil-
tonian H under this rotation implies, for example, that in any reaction the
product of the eigenvalues of $R_3 (2\pi/n)$ for initial and final states must be
equal:

$$\sum_{\text{all fragments}} \left(\frac{A_j}{2} - Z_j\right) = \text{const} \; [\text{mod} \, n] \tag{37}$$

This is the generalization of the I_3 conservation law for SU(2). The redu-
cible representations furnished by the initial and final states must contain
a common irreducible representation of the finite group: this is the
analogue of conservation of total isotopic spin I. On the other hand, the
fact that the members of a multiplet have the same energy, spin and parity,
implies that H commutes with all the elements of the finite group, i.e.
also with the finite rotations defined by the given group around any
other axis.

Consideration has been given by Case, Karplus and Yang to the tetra-
hedral, octahedral and icosahedral groups. While the tetrahedral group
has representations such that the possible assignment of isobar nuclei to
a multiplet are again those implied by SU(2), for the other two finite groups
we have some irreducible representations which can accomodate nuclei
whose charges differ by two units. Up to now the existing experimental
information excludes the existence of such multiplets, and we can there-
fore safely rely on the formalism of the continuous group SU(2) in order
to describe the isospin properties of nuclei.

7.   THE ISOTOPIC SPIN IN HEAVY NUCLEI

The fact that H_v and H_t are rather small when the neutron-proton mass difference and the Coulomb force can be disregarded, makes the isotopic spin a useful quantum number for the classification of the levels of light nuclei.   Since for heavy nuclei the contribution of electrostatic forces become important, the considerations based on the isotopic spin concept should become less accurate with increasing proton number Z. Lane and Soper [8] have however argued on theoretical grounds that, at least for the ground state of heavy nuclei, the isospin is still a good quantum number and that, surprisingly, its "purity" even increases with mass number A (for nuclei near the stability line).   The reason why this is so is rather trivial.   It is true that in the part of the nucleus which contains an equal number of neutrons and protons (core) there is some mixing of states of different I.   However the neutrons outside the core, being neutral particles, build up pure eigenstates of I.   Since as A increases there is a more rapid increase of the neutron excess for nuclei in nature, i.e. near the stability line, the isospin impurity of the ground state correspondingly decreases.   The isospin purity for heavy nuclei is therefore of a rather artificial nature arising by virtue of the excess neutrons, irrespective of the existence of possible large isospin asymmetry between neutrons and protons in the core.   It is not surprising that, as pointed out by Lane and Soper, it is not possible to devise any experiments to really test the isospin purity as such in heavy nuclei.   As a consequence, the isotopic spin, even though quite pure, is a useless quantum number in heavy nuclei.

REFERENCES

[1] HEISENBERG, W., Z. Physik 77 (1932) 1.
[2] BREIT, G., FEENBERG, E., Phys. Rev. 50 (1936) 850.
[3] WIGNER, E.P., in R.A. Welch Foundation Conferences on Chemical Research (Proc. Conf. November 1957) Houston (Texas).
[4] See for example, FONDA, L., GHIRARDI, C.G., "Introduction to the Concept of Symmetry in Quantum Theories", M. Dekker, New York (in press).
[5] CASSEN, B., CONDON, E.U., Phys. Rev. 50 (1936) 846, SACHS, R.G., "Nuclear Theory", Addison-Wesley, Cambridge (1953) 159.
[6] See for example, NISHIJIMA, K., "Fundamental Particles", Benjamin, New York (1963) 73. For more material on electric and magnetic transitions and for an up-to-date bibliography, see TEMMER, G.M., in Fundamentals in Nuclear Theory, Lectures Int. Course Trieste, 1966, IAEA, Vienna (1967) 163.
[7] CASE, K.M., KARPLUS, R., YANG, C.N., Phys. Rev. 101 (1956) 874.
[8] LANE, A.M., SOPER, J.M., Physics Lett. 1 (1962) 28 and Nucl. Physics 37 (1962) 663.

STRUCTURE INFORMATION FROM
DIRECT NUCLEAR REACTIONS

W. E. FRAHN
Physics Department, University of Cape Town,
South Africa

Abstract

STRUCTURE INFORMATION FROM DIRECT NUCLEAR REACTIONS.
    1. Introduction; 2. Theory of direct reactions; 3. Calculation of reduced cross-sections;
4. Calculation of spectroscopic factors; 5. Comparison with experiment.

1. INTRODUCTION

A great deal of our knowledge about nuclear structure is derived from
the study of nuclear reactions. Elastic scattering other than resonant
scattering tells us mostly about overall or average properties of nuclei
while reactions probe detailed microscopic features of the nuclear many-
body system. In particular, direct reactions which affect only a small
number of nuclear degrees of freedom are ideally suited for studying low-
lying excited states that are characterized by simple elementary exci-
tations. Moreover, there often is a very specific connection between a
given type of level and the direct reaction by which it is strongly excited.
Thus different kinds of direct reactions usually probe different modes of
excitation. For example, an important feature of a reaction is whether
single-particle contributions enter coherently or incoherently into the
reaction amplitude. The reaction will then strongly excite collective
and single-particle modes, respectively. The former is the case in in-
elastic scattering and certain types of two-nucleon transfer reactions,
while the latter occurs in one-nucleon transfer reactions. In these
lectures we shall restrict ourselves mainly to one- and two-nucleon
transfer processes and describe the methods by which structure in-
formation is obtained from measured differential cross-sections.

The theory of direct reactions shows that it is possible in many
cases to write a differential reaction cross-section as a product of two
factors,

$$\frac{d\sigma}{d\Omega} = S\sigma(\theta) \tag{1}$$

where $\sigma(\theta)$ describes the shape of the angular distribution as a function of
scattering angle, while S measures the absolute magnitude of the cross-
section. In many important cases one finds that the shape function is
rather insensitive to the details of nuclear structure, so that the structure
information about the initial and final nuclear states is carried by the
magnitude factor S, called the spectroscopic factor. Usually this in-
formation is extracted from absolute differential cross-section measure-

ments by calculating the angular distribution $\sigma(\theta)$ in a suitable approximation, such as the distorted-wave Born approximation (DWBA); the factor S is then determined by normalization to the experimental data. The results are to be compared with values calculated from appropriate nuclear models.

After a survey of the different kinds of one- and two-nucleon transfer processes we describe the DWBA theory of direct reactions. From a discussion of the approximations and uncertainties involved in this method the reliability of the extracted spectroscopic factors will be estimated. Next we give a brief description of how these factors are calculated in various nuclear models. Finally we discuss typical examples from several regions of the nuclear periodic table.

For a general background we refer to the reviews by Austern [1], Bayman [2], Glendenning [3] and Satchler [4].

We shall confine ourselves to direct reactions of the type A(a,b)B, with two nuclei in the initial state and two nuclei in the final state. In

TABLE I. ONE-NUCLEON TRANSFER REACTIONS[†]

Mass number of particles $\underline{a}$ and $\underline{b}$	stripping		pickup	
	neutron	proton	neutron	proton
1 and 2	(d, p)	(d, n)[*]	(p, d)[*]	(n, d)
2 and 3	(t, d)	(^{3}He, d)[*]	(d, t)[*]	(d, ^{3}He)
3 and 4	(α, ^{3}He)	(α, t)[*]	(^{3}He, α)[*]	(t, α)

[†] Reactions with [*] can excite states with isospin $T = T_z - \frac{1}{2}$, $T_z + \frac{1}{2}$

TABLE II. TWO-NUCLEON TRANSFER REACTIONS[a]

Transferred "particle"[b]	Isospin change ΔT	stripping		pickup	
^{2}n or ^{2}He	1	(t, p)	(^{3}He, n)[††]	(p, t)[††]	(n, ^{3}He)
d or ^{2}H	0,1	(t, n)[†]	(^{3}He, p)[†]	(n, t)[†]	(p, ^{3}He)[†]
d	0	(α, d)		(d, α)	

[a] Reactions with [†] can excite states with isospin $T = T_z$, $T_z + 1$ in ^{2}H transfer, those with [††] can excite states with isospin $T = T_z$, $T_z + 1$, $T_z + 2$, if $T_z \geq 1$)

[b] ^{2}n = di-neutron, ^{2}He = di-proton, d = triplet deuteron (g.s.), ^{2}H = singlet deuteron

particular we consider transfer reactions in which the particles a and b differ by one or two nucleons. If a is heavier than b we speak of stripping, the inverse process is called pickup. The various kinds of one- and two-nucleon transfer reactions are listed in Tables I and II (Schiffer [5]).

2. THEORY OF DIRECT REACTIONS

2.1. The distorted-wave Born approximation

For a reaction of the type A(a, b)B we write the total Hamiltonian as

$$H = H_\alpha + K_\alpha + \mathcal{U}_\alpha = H_\beta + K_\beta + \mathcal{U}_\beta \tag{2}$$

where $\alpha = (a, A)$ and $\beta = (b, B)$ specify the initial and final channels, respectively, and where $H_\alpha = H_a + H_A$ is the internal Hamiltonian, K_α the kinetic energy operator in channel α, and $\mathcal{U}_\alpha$ the interaction operator between a and A. The total wave functions Ψ are solutions of the Schroedinger equation

$$H\Psi = E\Psi \tag{3}$$

belonging to the total energy E, while the internal wave functions $\phi_\alpha(\xi_\alpha) = \phi_a(\xi_a)\phi_A(\xi_A)$ satisfy

$$H_\alpha\phi_\alpha = (E - E_\alpha)\phi_\alpha \tag{4}$$

where $E_\alpha = (\hbar^2/2\mu_a)k_a^2$ is the relative kinetic energy of (a, A), k_a denotes the channel wave number and μ_a is the reduced mass in channel α. Thus the Q-value of the reaction is given by $Q = E_\beta - E_\alpha$. The ξ_α are the internal co-ordinates of nuclei A and a. An exact expression for the reaction amplitude is

$$T_{\alpha\beta} = \left\langle e^{i\vec{k}_\beta \cdot \vec{r}_\beta}\phi_\beta \middle| \mathcal{U}_\beta \middle| \Psi_\alpha^{(+)} \right\rangle \tag{5}$$

where $\Psi_\alpha^{(+)}$ is that solution of Eq.(3) which behaves asymptotically as an incoming free-particle wave in channel α plus outgoing spherical waves in all channels β. If we separate from the full interaction operator $\mathcal{U}_\beta$ an average interaction $\mathcal{U}_\beta$ ("optical potential") which is independent of the internal co-ordinates,

$$\mathcal{U}_\beta(\xi_\beta, \vec{r}_\beta) = U_\beta(\vec{r}_\beta) + u_\beta(\xi_\beta, \vec{r}_\beta) \tag{6}$$

we can use the Gell-Mann-Goldberger relation to write

$$T_{\alpha\beta} = \left\langle \chi_\beta^{(-)}\phi_\beta \middle| U_\beta \middle| \phi_\alpha e^{i\vec{k}_a \cdot \vec{r}_\alpha} \right\rangle + \left\langle \chi_\beta^{(-)}\phi_\beta \middle| u_\beta \middle| \Psi_\alpha^{(+)} \right\rangle \tag{7}$$

where χ_α is a solution of the one-particle equation

$$(K_\alpha + U_\alpha)\chi_\alpha = E_\alpha \chi_\alpha \tag{8}$$

The solutions $\chi^{(+)}$ with outgoing-wave boundary conditions describe the elastic scattering of (a, A) by the potential U_α and are called distorted waves; the solutions $\chi^{(-)}$ are the time-reversed scattering wave functions, $\chi^{(-)}(\vec{k}, \vec{r}) = [\chi^{(+)}(-\vec{k}, \vec{r})]^*$. The first term in expression (7) is the amplitude for elastic scattering in channel α, while the second term is the actual reaction amplitude which we will denote by T_{ab}. The differential cross section for the reaction A(a, b)B is then given by

$$\frac{d\sigma}{d\Omega} = \frac{\mu_a \mu_b}{(2\pi\hbar^2)^2} \frac{k_b}{k_a} \sum_{av} |T_{ab}|^2 \tag{9}$$

where $\sum_{av}$ denotes a sum over final and an average over initial spin projections.

All of our subsequent discussion will be based upon the distorted-wave Born approximation in the "post-interaction" form (Satchler [4])

$$\Psi_\alpha^{(+)} \to \phi_\alpha(\xi_\alpha)\chi_\alpha^{(+)}(\vec{k}_a, \vec{r}_\alpha) \tag{10}$$

in which the reaction amplitude becomes

$$T_{ab} = \langle \chi_\beta^{(-)}(\vec{k}_b, \vec{r}_\beta)\phi_\beta(\xi_\beta) | u_\beta(\xi_\beta, \vec{r}_\beta) | \phi_\alpha(\xi_\alpha)\chi_\alpha^{(+)}(\vec{k}_a, \vec{r}_\alpha) \rangle \tag{11}$$

We shall confine ourselves to transfer processes, specifically stripping reactions with $a = b + x$, $B = A + x$, where x is the stripped "particle" (Fig.1). Then the full interaction in the final state consists of two parts,

$$\mathscr{U}_\beta = V_{bx} + V_{bA} \tag{12}$$

so that

$$u_\beta = \mathscr{U}_\beta - U_\beta = V_{bx} + (V_{bA} - U_{bB}) \tag{13}$$

where $U_{bB} = U_\beta$ is the optical potential that distorts the waves in the final state. A vital step further is to make the "stripping approximation" which consists in the assumption that the nucleus A remains an inert "core" whose configuration does not change during the transfer process, so that $V_{bA} \approx U_{bA} \approx U_{bB}$. By this approximation it becomes possible to separate structure effects from kinematic effects. If we write $\phi_\alpha = \phi_a \phi_A$ and $\phi_\beta = \phi_b \phi_B$ the transition amplitude becomes

$$T_{ab} = \mathscr{J} \int d\vec{r}_a \int d\vec{r}_b \chi_b^{(-)*}(\vec{k}_b, \vec{r}_b) \langle \phi_b \phi_B | V_{bx} | \phi_A \phi_a \rangle \chi_a^{(+)}(\vec{k}_a, \vec{r}_a) \tag{14}$$

where $\mathscr{J}$ is the Jacobian of the transformation from the channel co-ordinates $\vec{r}_\alpha = \vec{r}_{xA}$, $\vec{r}_\beta = \vec{r}_{bx}$ to the relative co-ordinates $\vec{r}_a$, $\vec{r}_b$ (Fig.2).

We now consider separately one-nucleon and two-nucleon transfer reactions in which x is a single nucleon and a two-nucleon system, respectively.
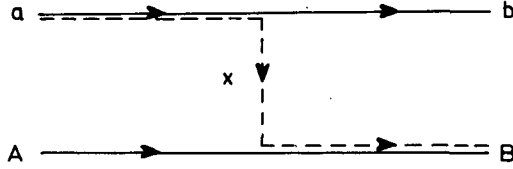
FIG.1. Diagram of a stripping reaction
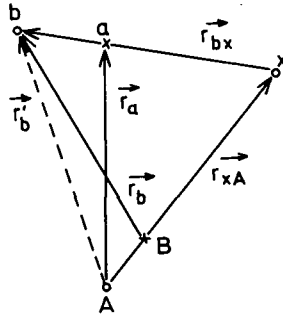
FIG.2. Co-ordinates of the stripping reaction A(a, b)B with a = b + x and B = A + x

2.2. One-nucleon transfer reactions

Here we denote the channel co-ordinates by $\vec{r} \equiv \vec{r}_{xA}$ and $\vec{\rho} \equiv \vec{r}_{bx}$. To evaluate the matrix element in expression (14) we first expand the wave function of the residual nucleus B in a complete set of states of the core A plus one nucleon,

$$\phi_B \equiv \phi_{J_B T_B}^{M_B T_{zB}}(\xi_A, \sigma\tau, \vec{r})$$

$$= \sum_{n\ell j} \left(J_A, n\ell j \mid\mid J_B \right) \left(T_A, \tfrac{1}{2} \mid\mid T_B \right) \left[\Psi_{n\ell j\frac{1}{2}}(\sigma\tau, \vec{r}) \phi_{J_A T_A}(\xi_A) \right]_{J_B T_B}^{M_B T_{zB}} \qquad (15)$$

where the bracket denotes vector coupling with respect to spin and isospin and the quantities $(\mid\mid)$ are single-particle coefficients of fractional parentage (c.f.p.). The wave function Ψ of the captured nucleon we separate into spin-isospin, orbital and radial parts:

$$\Psi_{n\ell j\frac{1}{2}}^{m j t_z}(\sigma\tau, \vec{r}) = u_{n\ell}(r)[i^\ell Y_\ell(\hat{r})\phi_{\frac{1}{2}\frac{1}{2}}(\sigma\tau)]_{j\frac{1}{2}}^{m j t_z} \qquad (16)$$

Next we make a similar expansion of the wave function of the incoming particle a in states of particle b plus one nucleon. Here we assume for simplicity that particle b and the nucleon are in an S-state of relative motion within a. Thus,

$$\phi_a \equiv \phi_{j_a t_a}^{m_a t_{za}}(\xi_b, \sigma\tau, \rho)$$

$$= (j_b, \tfrac{1}{2}|\} j_a)(t_b, \tfrac{1}{2}|\} t_a)\theta_a(\rho)[\phi_{j_b t_b}(\xi_b)\phi_{\frac{1}{2}\frac{1}{2}}(\sigma\tau)]_{j_a t_a}^{m_a t_{za}} \qquad (17)$$

where $\theta_a(\rho)$ is the radial wave function of particle a. Further we assume that the interaction is a scalar in ρ, $V_{bx} = V(\rho)$. Inserting expressions (15), (16), and (17) in Eq.(14) and integrating over the internal co-ordinates ξ_A, ξ_b and σ, τ yields

$$T_{ab} = \sum_{n\ell j} \sum_{m m_s m_j} \langle J_A M_A, jm_j | J_B M_B \rangle \langle \ell m, \tfrac{1}{2}m_s | jm_j \rangle \langle j_b m_b, \tfrac{1}{2}m_s | j_a m_a \rangle$$

$$\times \left(\frac{a}{2}\right)^{\frac{1}{2}} (2\ell+1)^{\frac{1}{2}} C_T S_{n\ell j}^{\frac{1}{2}} B_{n\ell}^m \qquad (18)$$

where

$$B_{n\ell}^m(\vec{k}_b, \vec{k}_a)$$

$$= (2\ell+1)^{-\frac{1}{2}} \int d\vec{r} \int d\vec{\rho}\, \chi_b^{(-)*}(\vec{k}_b, \vec{r}_b) u_{n\ell}(r)[i^\ell Y_\ell^m(\hat{r})]^* V(\rho)\theta_a(\rho)\chi_a^{(+)}(\vec{k}_a, \vec{r}_a) \qquad (19)$$

with $\vec{r}_b = \vec{\rho} + (A/B)\vec{r}$ and $\vec{r}_a = \vec{r} + (b/a)\vec{\rho}$,

$$S_{n\ell j}^{\frac{1}{2}} = (A+1)^{\frac{1}{2}}(J_A, n\ell j |\} J_B)(T_A, \tfrac{1}{2}|\} T_B) \qquad (20)$$

and

$$C_T = \langle T_A T_{zA}, \tfrac{1}{2}t_z | T_B T_{zB} \rangle \qquad (21)$$

The factor $[a(A+1)]^{\frac{1}{2}}$ arises from antisymmetrization of the target (A) and projectile (a) wave functions. Further, the projectile mass number has been restricted to $a \leq 4$, so that $(j_b, \tfrac{1}{2}|\} j_a)(t_b, \tfrac{1}{2}|\} t_a)\langle t_b t_{zb}, \tfrac{1}{2}t_z | t_a t_{za} \rangle = \pm 1/\sqrt{2}$.

After forming $|T_{ab}|^2$ and carrying out the sums over projection quantum numbers we find that the differential cross-section is proportional to

$$\sum_{\ell j m} \left| \sum_n S_{n\ell j}^{\frac{1}{2}} B_{n\ell}^m \right|^2 \qquad (22)$$

i.e., incoherent with respect to the orbital and spin quantum numbers, but coherent with respect to the principal quantum number of the captured nucleon. However, it is usually assumed that only a single value of n contributes. With this assumption we drop the index n and find [3]

$$\frac{d\sigma}{d\Omega} = \sum_\ell S_\ell \sigma_\ell(\theta) \tag{23}$$

where

$$\sigma_\ell(\theta) = \frac{\mu_a \mu_b}{(2\pi \hbar^2)^2} \frac{k_b}{k_a} \frac{2J_B+1}{2J_A+1} \frac{a}{4} C_T^2 \sum_m |B_\ell^m|^2 \tag{24}$$

In this form the differential cross-section, for a given orbital angular momentum transfer ℓ, is factored into a shape function $\sigma_\ell(\theta)$, determined by the kinematic amplitude B_ℓ^m, and a spectroscopic factor

$$S_\ell = \sum_j S_{\ell_j} \tag{25}$$

proportional to the square of the single-particle c.f.p. For the inverse pickup reaction B(b, a)A the only change in (24) is to replace the factor

$$\frac{k_b}{k_a} \frac{2J_B+1}{2J_A+1} \quad \text{by} \quad \frac{k_a}{k_b} \frac{2j_a+1}{2j_b+1} \tag{26}$$

2.3. Two-nucleon transfer reactions

In this case the internal co-ordinates ξ_x of the transferred system comprise the spin σ_1, σ_2, isospin τ_1, τ_2, and the relative co-ordinates $\vec{x} = \vec{r}_1 - \vec{r}_2$ of the two nucleons. The channel co-ordinates we again denote by $\vec{\rho}$ and $\vec{r} = \frac{1}{2}(\vec{r}_1 + \vec{r}_2)$. We follow closely the method developed by Glendenning [3, 6]. First the wave function of the residual nucleus B is expanded in states of the core A plus two nucleons,

$$\phi_B \equiv \phi_{J_B T_B}^{M_B T_{zB}} (\xi_A, \sigma_1 \sigma_2 \tau_1 \tau_2 \vec{x}, \vec{r})$$

$$= \sum_{LSJT, \gamma} \beta_{LSJT}^\gamma [\psi_{LSJT}^\gamma (\sigma_1 \sigma_2 \tau_1 \tau_2 \vec{x}, \vec{r}) \phi_{J_A T_A} (\xi_A)]_{J_B T_B}^{M_B T_{zB}} \tag{27}$$

where γ stands for the set of quantum numbers necessary to specify the states of the two-nucleon system in addition to its orbital (L), spin (S), isospin (T) and total angular momentum (J). The wave function ψ of the captured nucleons can be separated into spin-isospin and orbital parts,

$$\psi_{LSJT}^{\gamma M_J T_z} (\sigma_1 \sigma_2 \tau_1 \tau_2 \vec{x}, \vec{r}) = [\phi_L^\gamma (\vec{x}, \vec{r}) \phi_{ST} (\sigma_1 \sigma_2 \tau_1 \tau_2)]_{JT}^{M_J T_z} \tag{28}$$

Now it is desirable to separate the dependence on the relative co-ordinate $\vec{x}$ and the c.m. co-ordinate $\vec{r}$ of the two nucleons in the orbital wave function $\phi_L^\gamma(\vec{x}, \vec{r})$. This is possible if we use harmonic-oscillator wave functions. Then ϕ_L^γ, which can be constructed by coupling the single-particle orbital angular momenta ℓ_1 and ℓ_2 to L, may be written in terms of coupled functions of the relative and c.m. co-ordinates of the pair by means of a Talmi transformation,

$$\phi_L^{\gamma M}(\vec{x}, \vec{r}) \equiv [\phi_{n_1\ell_1}(\vec{r_1})\phi_{n_2\ell_2}(\vec{r_2})]_L^M$$

$$= \sum_{n\lambda, n\Lambda} \langle n\lambda, N\Lambda; L | n_1\ell_1, n_2\ell_2; L \rangle [\phi_{n\lambda}(\vec{x})\phi_{N\Lambda}(\vec{r})]_L^M \qquad (29)$$

Here, γ stands for $(n_1\ell_1, n_2\ell_2)$, λ and Λ are the orbital angular momenta of the relative and c.m. motions, respectively, while n and N are the corresponding principal quantum numbers. The coefficients in expression (29) are the Brody-Moshinsky brackets, and we have

$$\phi_{n\lambda}^{m_\lambda}(\vec{x}) = u_{n\lambda}(x)i^\lambda Y_\lambda^{m_\lambda}(\hat{x}), \quad \phi_{N\Lambda}^{M_\Lambda}(\vec{r}) = u_{N\Lambda}(r)i^\Lambda Y_\Lambda^{M_\Lambda}(\hat{r}) \qquad (30)$$

where $u_{n\lambda}$ and $u_{N\Lambda}$ are radial harmonic-oscillator eigenfunctions.

Next we expand the wave function of the projectile a in states of particle b plus two nucleons. Again we assume that particle b and the two-nucleon system are in an S-state of relative motion, so that

$$\phi_a \equiv \phi_{j_a t_a}^{m_a t_{za}}(\xi_b, \sigma_1\sigma_2\tau_1\tau_2\vec{x}, \rho)$$

$$= \varphi_a(\vec{x}, \rho)[\phi_{j_b t_b}(\xi_b)\phi_{ST}(\sigma_1\sigma_2\tau_1\tau_2)]_{j_a t_a}^{m_a t_{za}} \qquad (31)$$

where φ_a is the orbital part of the projectile wave function. This also implies that $\lambda = 0$ and $\Lambda = L$ in Eqs (29) and (30). If we assume a Gaussian form of φ_a, we can further separate the dependence on $\vec{x}$ and ρ,

$$\varphi_a(\vec{x}, \rho) = \chi_a(x)\theta_a(\rho) \qquad (32)$$

The interaction is again assumed to be spin-isospin independent and scalar, $V_{bx} = V(\rho)$.

With these ingredients the transition amplitude can be written in the form

$$T_{ab} = \sum_{NLSJT} \sum_{MM_SM_J} \langle J_A M_A, JM_J | J_B M_B \rangle \langle LM, SM_S | JM_J \rangle \qquad (33)$$

$$\times \langle j_b m_b, SM_S | j_a m_a \rangle (2L+1)^{\frac{1}{2}} C_T^b G_{ST} G_{NLSJT} B_{NL}^M$$

where the kinematic amplitude

$$B_{NL}^{M}(\vec{k}_b, \vec{k}_a)$$

$$= (2L+1)^{-\frac{1}{2}} \int d\vec{r} \int d\vec{\rho}\, \chi^{(-)*}(\vec{k}_b, \vec{r}_b) u_{NL}(r) [i^L\, Y_L^M(\hat{r})]^* V(\rho)\theta_u(\rho)\chi_u^{(+)}(\vec{k}_a, \vec{r}_a) \qquad (34)$$

has the same form as Eq.(19) for one-nucleon transfer.
    The structure factor is defined as

$$G_{NLSJT} = g \sum_{\gamma} \beta_{LSJT}^{\gamma}\, \Omega_n \langle n0, NL;\ L | n_1\ell_1, n_2\ell_2;\ L \rangle \qquad (35)$$

where

$$\Omega_n = \int_0^{\infty} u_{n0}(x)\chi_a(x) x^2\, dx \qquad (36)$$

and g = 1 if $(n_1\ell_1 j_1) = (n_2\ell_2 j_2)$, otherwise g = $\sqrt{2}$. The statistical factor
arising from antisymmetrization is included in the definition of β_{LSJT}^{γ}.
The isospin-coupling coefficient C_T is defined as in Eq.(21), while b_{ST}
comes from the overlap of the spin-isospin functions of particles a and b
and is given by

$$b_{ST} = \begin{cases} \delta_{S0}\,\delta_{T1} & \text{for (t, p) or } (^3\text{He, n}) \\[2mm] \frac{1}{2}(\delta_{S0}\delta_{T1} + \delta_{S1}\delta_{T0}) & \text{for (t, n) or } (^3\text{He, p}) \\[2mm] \delta_{S1}\,\delta_{T0} & \text{for } (\alpha, \text{d}). \end{cases} \qquad (37)$$

In the case of the (α, d) reaction the amplitude (33) contains another over-
lap factor Ω_d from the overlap of the deuteron with the corresponding part
of the α-particle wave function.
    Finally, the differential cross-section for two-nucleon stripping
becomes

$$\frac{d\sigma}{d\Omega} = \frac{\mu_a\mu_b}{(2\pi\hbar^2)^2} \frac{k_b}{k_a} \frac{2J_B + 1}{2J_A + 1} \Omega_d^2$$

$$\times \sum_{LSJTM} (C_T b_{ST})^2 \left| \sum_N G_{NLSJT}\, B_{NL}^M \right|^2 \qquad (38)$$

The cross-section for pickup is again obtained from Eq.(38) by the replacement (26).

Note that there is again incoherence with respect to L, S, J, T and M, but coherence with respect to the radial quantum number N. However, in contrast with the situation for one-nucleon transfer, the coherence in N is essential because the c.m. motion of a nucleon pair is described by more than one radial state. It is, therefore, in general no longer possible to factorize the two-nucleon transfer cross-section into a structure factor and a kinematic factor.

The use of harmonic oscillator wave functions has the disadvantage that the function $u_{NL}(r)$ does not have the right asymptotic behaviour which should be that of the solution of the free Schroedinger equation with negative energy corresponding to the separation energy ϵ_B of the two nucleons from nucleus B. We therefore have to match the interior harmonic-oscillator function to a spherical Hankel function at a matching radius R_N,

$$u_{NL}(r) \propto r^L e^{-\frac{1}{2}\nu r^2}, \quad r \lesssim R_N$$

$$u_{NL}(r) \propto -i^L h_L^{(1)}(i\kappa r), \quad r \gtrsim R_N \tag{39}$$

where $\kappa^2 = (4m^*/\hbar^2)\epsilon_B$, with $2m^*$ equal to the mass of the transferred nucleon pair.

Suppose now that, because of strong absorption, the contribution to the transfer amplitude B_{NL}^M from the nuclear interior can be neglected. Since $u_{NL}(r)$ at large r carries a sign factor $(-)^{N-1}$ we can write

$$B_{NL}^M = (-)^{N-1} W_{NL}(\nu, \kappa) \tilde{B}_L^M \tag{40}$$

where $\tilde{B}_L^M$ is the same amplitude as B_{NL}^M but with $u_{NL}(r)$ replaced by $-i^L h_L^{(1)}(i\kappa r)$. The quantity $W_{NL}(\nu, \kappa)$ is determined by the matching condition at $r = R_N$. In this case it is possible to write the cross-section (38) in the factored form

$$\frac{d\sigma}{d\Omega} = \sum_L S_L \sigma_L(\theta) \tag{41}$$

where

$$S_L = \sum_{SJT} (C_T b_{ST})^2 \left| \sum_N (-)^N W_{NL} G_{NLSJT} \right|^2 \tag{42}$$

is the spectroscopic factor, and $\sigma_L(\theta)$ is a reduced cross-section defined by

$$\sigma_L(\theta) = \frac{\mu_a \mu_b}{(2\pi\hbar^2)^2} \frac{k_b}{k_a} \frac{2J_B + 1}{2J_A + 1} \Omega_d^2 \sum_M |\tilde{B}_L^M|^2 \tag{43}$$

3. CALCULATION OF REDUCED CROSS-SECTIONS

In the preceding section the concept of spectroscopic factor in transfer reactions was introduced through the overlap integral between the wave functions of the final and initial nuclei. In stripping reactions it measures the probability with which the particular configuration of target nucleus plus transferred particles occurs in the final state wave function. For one-nucleon transfer processes, in particular the (d, p) stripping reaction, the spectroscopic factor was first defined by Macfarlane and French [7], who also explored in a comprehensive survey the usefulness of this quantity as a tool in nuclear spectroscopy. Since then, the majority of transfer reaction analyses has aimed at extracting spectroscopic factors as reliably as possible from measured differential cross sections by means of a suitable reaction theory (usually the DWBA), and then comparing the resulting values with those calculated from specific nuclear models. We shall now deal with the first problem, the extraction of spectroscopic factors from experimental data.

Let us assume there is no coherence so that the differential cross-section can be written in the factored form (23) or (24). Once the value of the orbital angular momentum transfer ℓ is ascertained from the shape of the angular distribution, the value of S_ℓ can be determined by normalization of the reduced cross-section $\sigma_\ell(\theta)$ to the data, usually at the peak cross-section. This is possible if absolute measurements are available, otherwise only relative spectroscopic factors can be obtained. The normalization method is open to uncertainties from two sources, (i) experimental errors in the transfer as well as the corresponding elastic differential cross-sections, and (ii) approximations in the calculation of the reduced cross-section. Experimental errors are usually considerably smaller than the theoretical ones, though they may amount to as much as 15%. The main uncertainties in determining S_ℓ arise from approximations in calculating the kinematic amplitude B_ℓ^m.

First of all, how good is the basic DWBA assumption (10)? This is difficult to estimate, except possibly by comparison with extensive coupled-channels calculations. Such calculations indicate [1, 4] that the DWBA is sufficiently accurate above some tens of MeV. However, several further approximations have been made to obtain the kinematic amplitudes in the form (19) or (34).

(i)   Interference from compound-nucleus formation is neglected. Part of its effect is taken into account summarily through the imaginary part of the optical potentials.

(ii) Antisymmetrization of the total wave function [8] is disregarded except for statistical factors that are incorporated in the definition of S_ℓ.

(iii) By the "stripping approximation", which neglects the term $V_{bA} - U_{bB}$ in Eq.(13), one disregards excitations of the core A. This is considered justifiable in stripping onto closed-shell nuclei but is doubtful in other cases.

(iv) The interaction V_{bx} is usually assumed central and spin-independent, excluding in particular tensor forces. One often goes a step further and makes the zero-range approximation,

$$D(\rho) \equiv V(\rho)\theta_a(\rho) = D_a\delta(\rho) \tag{44}$$

which considerably simplifies the calculation of B_{ℓ}^{m} by reducing the six-dimensional integral in relation (19) or (34) to the three-dimensional form

$$B_{\ell}^{m}(\vec{k}_b, \vec{k}_a) = \frac{D_0}{(2\ell+1)^{\frac{1}{2}}} \int d\vec{r}\, \chi_b^{(-)*}(\vec{k}_b, \frac{A}{B}\vec{r})\, u_{\ell}(r)[i^{\ell} Y_{\ell}^{m}(\hat{r})]^{*}\chi_a^{(+)}(\vec{k}_a, \vec{r}) \qquad (45)$$

The constant D_0 is determined by the volume integral

$$D_0 = \int d\vec{\rho}\, V(\rho)\theta_a(\rho) \qquad (46)$$

which in the case of the (d, p) reaction can be calculated from the Schroedinger equation for the internal deuteron wave function. Its value depends on the deuteron binding energy and on the form of $\theta_a(\rho)$, and can vary between $1.0-1.7 \times 10^4$ MeV^2 fm^3 [4]. Finite-range effects were first studied by Austern et al.[9]. Since then, finite-range DWBA calculations have been performed in increasing numbers. It became clear that finite-range effects reduce the amount of stripping that occurs in the nuclear interior. In a zero-range calculation this can be simulated approximately by a lower cutoff in the radial integral.

(v)   The assumption that, within particle a, particle b and the transferred system x are in an S state of relative motion neglects, for instance, the D-state component of the deuteron wave function. Johnson [10] has shown that the D-state contribution has an appreciable effect on the angular distribution of (d, p) and (p, d) reactions.

(vi) If particles a and/or b contain more than two nucleons there are additional uncertainties regarding their wave functions. For three-nucleon systems, Bassel [11] has calculated the normalization factors by which the reduced zero-range cross-sections of (t, d), (^{3}He, d) and their inverse processes should be multiplied to take account of the overlap between the three-particle and deuteron wave functions. Assuming Irving-Gunn wave functions for the former and Hulthén wave functions for the latter, Bassel finds the values given in Table III.

(vii) The distorted waves χ_a and χ_b are calculated as scattering solutions of the Schroedinger equation (8) for which the optical potentials U_a and U_b have to be determined by analysis of the elastic scattering in both the initial (a + A) and final (b + B) channels. A major source of uncertainty is the fact that this cannot be done unambiguously. For composite particles especially, several different sets of optical potentials generate the same scattering [12], for instance those whose well depth V_0 and radius R are related by $V_0 R^n$ = const. $(2 \lesssim n \lesssim 3)$. Because of strong absorption in the interior of the nucleus, elastic scattering is sensitive only to the surface part of the potential. However, since the radial integrals for transfer are somewhat more sensitive to the interior wave functions it is sometimes possible to distinguish between different well depths by fitting transfer cross-sections. It is found that this selects those potentials that satisfy Rook's criterion [13], $V_0 \cong a.50$ MeV, where a is the mass number of

TABLE III.   BASSEL NORMALIZATION FACTORS* [11]

stripping		pickup	
(t, d)	(^{3}He, d)	(d, t)	(d, ^{3}He)
	3.84		2.56
5.06		3.33	
	4.42		2.95

*
For proton transfers the upper values are calculated without, the lower with
inclusion of the Coulomb interaction between the proton and the deuteron

the projectile. On the other hand, both elastic and transfer cross-
sections are rather insensitive to the form of the imaginary part of the
optical potentials which makes it difficult to distinguish between volume
and surface absorption.

(viii) Elastic cross-sections are also rather insensitive to the spin-orbit
interaction except at large angles. Moreover, transfer cross-sections
too do not depend much on the spin-orbit part of the distorting
potentials. For instance, the shapes of (d, p) angular distributions are
mainly determined by ℓ, except for the Lee-Schiffer j-dependence [13]
which distinguishes the $p_{1/2}$ cross-section from that for $p_{3/2}$ by a
pronounced dip near $\theta = 100°$, whose origin is however not yet clear.
Another j-dependence was found in (p, d) reactions [14].

(ix) Optical potentials are energy-dependent. The major part of this, at
least for the real potentials, is due to non-locality of the average
nuclear field. Although the asymptotic wave functions of a non-local
potential must be the same as for the "equivalent" local potential
that generates the same elastic scattering, the non-local wave function
in the nuclear interior is smaller by typically 15% (Perey effect [15]).
Therefore, the effect of non-locality, in the so-called local energy
approximation [16], is to reduce the contribution to the transition
matrix elements from the nuclear interior [17, 18]. This can again
be simulated approximately by a lower cutoff in the radial integrals [19].

(x) If the nuclei A and B are deformed, one can use in the initial and final
channels generalized optical potentials which include the collective
co-ordinates. Then the incident and outgoing particles can excite low-
lying rotational levels in the target and residual nuclei. Lukyanov
and Petkov [20] have shown that this leads to multi-step contributions
to the stripping amplitude. However one may doubt whether calculating
multi-step processes in first-order DWBA is a consistent procedure.

(xi) The functions $u_\ell(r)$ in (19) and $u_{NL}(r)$ in (34) were introduced as the
radial wave functions of the captured particles. More generally,

these functions are to be defined by the overlap integral between the initial and final nuclear states, e.g. for one-nucleon transfer by

$$\int d\xi_A \phi^{M_B T_{zB}}_{J_B T_B}{}^* (\xi_A, \sigma\tau, \vec{r}) \phi^{M_A T_{zA}}_{J_A T_A}(\xi_A)$$

$$= \sum_{n\ell j} (J_A, n\ell j \| J_B)(T_A, \tfrac{1}{2} \| T_B)\langle J_A M_A, jm | J_B M_B\rangle$$

$$\times \langle T_A T_{zA}, \tfrac{1}{2} t_z | T_B T_{zB}\rangle \psi^{mt_z}_{n\ell j \frac{1}{2}}{}^* (\sigma\tau, \vec{r}) \qquad (47)$$

The normalized radial part of $\psi_j(\sigma\tau, \vec{r})$, viz. $u_\ell(r)$, defines the "form factor" of the transfer reaction. It is an <u>assumption</u> that this form factor is equal to the radial part of a single-particle shell model eigenstate in a central potential. This assumption has been made in most DWBA calculations so far. Then $u_\ell(r)$ is calculated as an eigenfunction of a finite well, usually of Woods-Saxon form. However, this procedure leads to an ambiguity with regard to the eigen-energy corresponding to this eigenfunction. If one chooses as the eigenenergy the observed separation energy ("separation energy prescription" [21]), the spectroscopic factors turn out too large in some cases. Better agreement with experiment is then obtained by adjusting the well depth such that the eigenenergy is equal to the binding energy of the shell-model single-particle level $n\ell j$ ("effective-binding-energy prescription" [14]). However, in this case $u_\ell(r)$ has not the correct asymptotic tail. In any case the spectroscopic factors depend quite sensitively on the eigenenergy and thus on the shape of the form factor, so that a better procedure for its calculation has to be found.

(xii) Actually, as Austern [22] has emphasized, the assumption that $u_\ell(r)$ is a radial single-particle wave function is not more than a guess at the shape of the form factor which is correct only for stripping by a closed-shell target nucleus. In general it is necessary to determine the form factor by calculating the overlap $\langle \phi_A, \phi_B \rangle$ from nuclear-structure theories. Berggren [23] and Pinkston and Satchler [24] have derived an exact equation satisfied by the form factor. Recently, Prakash and Austern [25] developed a general method of solving the form factor equation of Pinkston and Satchler. The results of their "structure-stripping" calculations show that the spectroscopic factors obtained from the usual separation energy prescription can be in error by as much as 50%.

In view of the many approximations and uncertainties one may ask whether reliable spectroscopic factors can be extracted at all by means of the DWBA method. This question was investigated by Lee et al.[26] who tested the reliability of the DWBA in the $^{40}Ca(d, p)^{41}Ca$ reaction, and by Smith [27] in the $^{90}Zr(d, p)^{91}$ reaction. Lee et al. assumed that ^{40}Ca is a good closed-shall nucleus so that the final states in ^{41}Ca are pure single-particle states for which the spectroscopic factors are known

($S_\ell = 1$). The parameters for elastic scattering d+ ^{40}Ca at the same energies
(7-12 MeV) were known, those for p+ ^{41}Ca were extrapolated. The calcu-
lations included spin-orbit coupling in the distorting potentials and a
finite range of the n-p interaction. The neutron was assumed to be cap-
tured into a shell model orbit which is an eigenstate of a Woods-Saxon
well. Comparison of the finite-range results with those for zero range
plus a lower cutoff showed that the latter procedure does not lead to a
consistent set of spectroscopic factors. For the finite-range calculation,
a detailed study of the variations in the potential parameters led to the
conclusion that absolute spectroscopic factors can be determined with an
uncertainty of not more than 20%. Relative spectroscopic factors were
found to be less subject to the uncertainties in the potentials and should
be more accurate than the absolute values. Smith's study [27] of the
ambiguities in the elastic scattering parameters led to a less optimistic
estimate. He found that absolute spectroscopic factors may vary by more
than a factor 2 over the range of acceptable elastic scattering parameters.
However, relative values for transitions with different ℓ (S_{ℓ_1}/S_{ℓ_2}) should
be about twice as dependable than the absolute ones.

Many of the uncertainties in the nuclear parameters are absent, or
at least greatly reduced, in transfer reactions at low energies, below the
Coulomb barrier, where the relative motion depends almost entirely upon
the Coulomb interaction. The determination of reliable spectroscopic
factors by such "sub-Coulomb stripping" experiments has been advocated
by Goldfarb [28], especially for heavier projectiles [29,30]. For the (d, p)
reaction this expectation is borne out for instance by the results of the
Heidelberg group (reported in the seminar lectures by Dost [31] and
von Brentano [32] in these Proceedings).

In the case of transfer processes between strongly absorbed composite
particles it is possible to make further approximations which greatly
simplify the DWBA expression for the reduced cross-sections. The so-
called diffraction models of transfer reactions [33,34] exploit the insensi-
tivity, due to strong absorption, of the reaction amplitude to the nuclear
interior. A more general formulation can be based on the localization of
the radial transfer integrals in orbital angular momentum space. This
leads to very simple closed expressions for the reduced cross-sections
which display the typical kinematic features common to all transfer angular
distributions [35-40]. Although this formalism is an approximation to the
DWBA theory, it is, at least, free of the ambiguities in the elastic scattering
parameters, because it describes the distortion directly in terms of
parameterized elastic scattering phase shifts and so avoids the intermediary
step of constructing optical potentials.

An alternative method of determining spectroscopic factors is based on
their relation to the reduced widths $\gamma^2_{n\ell j}$ for capture of a nucleon into the
state $n\ell j$, in units of the "single-particle width" $\gamma^2_{n\ell j}$ (s.p.),

$$S_{n\ell j} = \frac{\gamma^2_{n\ell j}}{\gamma^2_{n\ell j} \text{ (s. p.)}} \tag{48}$$

where

$$\gamma^2_{n\ell j} \text{ (s.p.)} = \frac{\hbar^2}{2ma_c}[u_{n\ell j}(a_c)]^2 \tag{49}$$

and a_c is the channel radius as defined in R-matrix theory. The reduced width for neutron capture can be obtained from an analysis of isobaric analogue resonances in (p, p) scattering. This method has been advocated by Robson [41, 42] who points out its advantages compared with the determination of $S_{n\ell j}$ from (d, p) measurements.

More detailed structure information can be derived from experiments that go beyond the measurement of differential cross-sections, such as polarization and angular correlation between the outgoing particle and de-excitation γ-rays [3, 43]. A discussion of these important sources of spectroscopic information is outside the scope of these lectures. Also, the significance for nuclear structure of reactions other than those of the type A(a,b)B, such as the important quasi-free proton scattering (p, 2p) [44], can only be mentioned here.

4. CALCULATION OF SPECTROSCOPIC FACTORS

Direct reactions can be roughly defined as processes in which only a few of the total number of nucleons take an active part. Accordingly it is assumed that the majority of nucleons remain passive during the interaction, i.e., occupy the same configuration in the initial and final nucleus. In other words, the passive nucleons form an inert core to which particles can be added in a stripping process, or from which particles can be removed in a pickup reaction. The spectroscopic factor is a measure of the validity of this picture in actual transfer reactions. Its values clearly depend upon the structure of the "core" and upon the nature of the configurations in which the transferred particles are added or removed. Therefore, theoretical calculations of spectroscopic factors can be based on each of the different models by which nuclear structure is described.

4.1. Shell model

Let us first consider one-nucleon transfer reactions. In the simplest shell-model calculations one assumes that the passive nucleons occupy a pure shell-model configuration to which a single nucleon is added in one of the empty single-particle orbitals (stripping), or from which a single nucleon is removed out of one of the occupied single-particle orbitals (pickup). The latter process is equivalent to the addition of a single hole in one of the occupied single-particle states. In this picture the spectroscopic factor for stripping is proportional to the squared coefficient of fractional parentage (c.f.p.) between the initial and final configurations. For the present, let us disregard isospin. Then we have from Eq.(20)

$$S_{n\ell j} = (N+1)(J_A, n\ell j \| J_B)^2 \tag{50}$$

where $N+1$ is the total number of nucleons in the system which are of the same type as the transferred particle (neutrons, say). This factor arises from the antisymmetrization of the transferred particle with respect to the N equivalent ones in the target nucleus. It is easily shown (see, for example, Ref.[2]) that this antisymmetrization in effect extends

only over equivalent nucleons in unfilled shells. Thus, for a nucleus with several closed and several open shells of neutrons (say), $N+1$ is the total number of neutrons in open shells only. This property is automatically taken care of if we express the c.f.p. in occupation number representation [45, 46].

Suppose the initial and final nuclei are in shell-model configurations $j^N \alpha J_A$ and $j^{N+1} \beta J_B$, respectively. Then we have the relation (see lectures by Rimini [47])

$$(j^N \alpha J_A, n\ell j |\} j^{N+1} \beta J_B) = \frac{(-)^{N+1}}{\sqrt{N+1}} \frac{\langle j^{N+1} \beta J_B || n_{n\ell j}^\dagger || j^N \alpha J_A \rangle}{\sqrt{2J_B+1}} \tag{51}$$

where α and β are additional quantum numbers (such as seniority, etc.) that may be necessary for complete specification of the initial and final states, respectively, and $n_{n\ell j}^\dagger$ is a creation operator of a neutron in the single-particle state $n\ell j$. Thus, the spectroscopic factor becomes

$$S_{n\ell j} = |\langle 0| \varphi_{J_B}^{(\beta)M_B}(N+1)[\varphi_{J_A}^{\dagger(\alpha)}(N)n_{n\ell j}^\dagger]_{J_B}^{M_B} |0\rangle|^2$$

$$= (N+1)(j^N \alpha J_A, n\ell j |\} j^{N+1} \beta J_B)^2 = \frac{\langle j^{N+1} \beta J_B || n_{n\ell j}^\dagger || j^N \alpha J_A \rangle^2}{2J_B+1} \tag{52}$$

where the creation (field) operators $\varphi^\dagger$ are defined by

$$\phi_{J_B}^{(\beta)M_B}(1,2\ldots N+1) \equiv \varphi_{J_B}^{\dagger(\beta)M_B}(N+1)|0\rangle \tag{53}$$

$$\phi_{J_A}^{(\alpha)M_A}(1,2\ldots N) \equiv \varphi_{J_A}^{\dagger(\alpha)M_A}(N)|0\rangle$$

and $|0\rangle$ is the particle vacuum.

In the shell model, therefore, the calculation of spectroscopic factors reduces essentially a computation of c.f.p. Bayman and Landé [48] have calculated extensive tables of identical fermion (and boson) c.f.p., using an elegant group-theoretical method. This method is based on the fact that the set of totally antisymmetric functions $\phi_{J_B}^{(\beta)M_B}(j^{N+1}, 1\ldots N+1)$ carries the irreducible representation $\underbrace{[1, 1, \ldots 1]}_{N+1}$ of the special unitary group $SU(2j+1)$. Since the set of functions $[\phi_{J_A}^{(\alpha)}(j^N, 1\ldots N)\psi_j(j, N+1)]_{J_B}^{M_B}$ carries the product representation

$$\underbrace{[1,1\ldots1]}_{N} \otimes [1] = \underbrace{[1,1\ldots1]}_{N+1} \oplus \underbrace{[2,1\ldots1]}_{N}$$

the problem consists in reducing this product representation. This is done by calculating the matrix of the Casimir operator of $SU(2j+1)$ in the basis $[\Psi\psi]_j^M$ and diagonalizing it. The c.f.p. are the eigenvectors which correspond to the eigenvalues associated with the representation $\underbrace{[1,\ldots.1]}_{N+1}$. Actually, since the c.f.p. connect eigenstates of seniority, which carry irreducible representations of the symplectic group $Sp(2j+1)$, the Casimir operators of $SU(2j+1)$ and $Sp(2j+1)$ are diagonalized simultaneously.

Consider the case of the lowest seniority states, i.e., those in which all even particles are coupled to zero. Then the c.f.p. have the following simple explicit form

$$(j^N J_A = 0, j \,|\} \, j^{N+1} J_B = j) = \left[\frac{2j+1-N}{(N+1)(2j+1)}\right]^{\frac{1}{2}}, \text{ for even } N \tag{54}$$

$$(j^N J_A = j, j \,|\} \, j^{N+1} J_B = 0) = 1, \text{ for odd } N$$

hence

$$S_j(N \leftrightarrow N+1) = \begin{cases} 1 - \dfrac{N}{2j+1}, & \text{for even } N \\[3mm] N+1, & \text{for odd } N \end{cases} \tag{55}$$

In general, for wave functions of mixed configurations the calculation of spectroscopic factors is carried out by means of Racah recoupling techniques. (As an example, see the calculations of Cohen and Kurath[70] for the 1p shell to be discussed in section 5.)

4.2. Sum rules

The spectroscopic factor for stripping $N \to N+1$ is equal to that for the pickup $N+1 \to N$,

$$S_{n\ell j}(N+1 \to N) = (N+1)(j^N \alpha J_A, n\ell j \,|\} \, j^{N+1} \beta J_B)^2 \tag{56}$$

From the orthonormality property of the c.f.p. [47],

$$\sum_{\alpha J_A} (j^N \alpha J_A, n\ell j \,|\} \, j^{N+1} \beta J_B)^2 = 1 \tag{57}$$

we find

$$\sum_{\alpha J_A} S_{n\ell j}(N+1 \to N) = N+1 \tag{58}$$

Since here βJ_B is the target state and αJ_A the final state, this means that the sum of the pickup spectroscopic factors over all final states $(n\ell j)$ equals the number of neutrons in the target. This is the simplest example

of sum rules satisfied by the spectroscopic factors of one-nucleon transfer reactions [7], which provide very useful checks in analyses of experimental data. We now derive more general sum rules using the occupation number representation of the spectroscopic factors [2]. First consider <u>stripping</u> $A(a, a-1)A+1$. Then

$$
S_{n\ell j}(\alpha J_A \to \beta J_{A+1}) = \left| \langle 0 | \varphi_{J_{A+1}}^{(\beta)M_{A+1}} [\varphi_{J_A}^{\dagger(\alpha)} n_{n\ell j}^\dagger]_{J_{A+1}}^{M_{A+1}} | 0 \rangle \right|^2 \tag{59}
$$

Now let us calculate the average number of $(n\ell j)$ neutron <u>holes</u> in the target A. This quantity is the expectation value of the neutron hole number operator

$$
\sum_{m=-j}^{j} n_{n\ell j}^m n_{n\ell j}^{\dagger m} \tag{60}
$$

in the target state $\varphi_{J_A}^{\dagger(\alpha)M_A}|0\rangle$

$$
\bar{n}_A(j^{-1}) = \langle 0 | \varphi_{J_A}^{(\alpha)M_A} \sum_m n_m n_m^\dagger \varphi_{J_A}^{\dagger(\alpha)M_A} | 0 \rangle \tag{61}
$$

(where we used a simplified notation for the particle operators). Inserting

$$
1 = \sum_{\beta J_{A+1}M_{A+1}} \varphi_{J_{A+1}}^{\dagger(\beta)M_{A+1}}|0\rangle\langle 0|\varphi_{J_{A+1}}^{(\beta)M_{A+1}}
$$

between n_m and $n_m^\dagger$ gives

$$
\bar{n}_A(j^{-1}) = \sum_{\beta J_{A+1}M_{A+1}m} \langle 0|\varphi_{J_A}^{(\alpha)M_A} n_m \varphi_{J_{A+1}}^{\dagger(\beta)M_{A+1}}|0\rangle\langle 0|\varphi_{J_{A+1}}^{(\beta)M_{A+1}} n_m^\dagger \varphi_{J_A}^{\dagger(\alpha)M_A}|0\rangle
$$

$$
= \sum_{\beta J_{A+1}M_{A+1}m} \left| \langle 0|\varphi_{J_{A+1}}^{(\beta)M_{A+1}} n_m^\dagger \varphi_{J_A}^{\dagger M_A}|0\rangle \right|^2 \tag{62}
$$

Now we use

$$
n_{n\ell j}^{\dagger m} \varphi_{J_A}^{\dagger(\alpha)M_A} = \sum_{J'_{A+1}} \langle jm, J_A M_A | J'_{A+1} M'_{A+1}\rangle [n_{n\ell j}^\dagger \varphi_{J_A}^{\dagger(\alpha)}]_{J'_{A+1}}^{M'_{A+1}} \tag{63}
$$

and get

$$\bar{n}_A(j^{-1}) = \sum_{\beta J_{A+1}} |\langle 0| \varphi_{J_{A+1}}^{(\beta)M_{A+1}} [n_{n\ell j}^{\dagger} \varphi_{J_A}^{\dagger(\alpha)}]_{J_{A+1}}^{M_{A+1}} |0\rangle|^2$$

$$\times \sum_{mM_{A+1}} \langle jm, J_A M_A | J_{A+1} M_{A+1} \rangle^2 \qquad (64)$$

or

$$\bar{n}_A(j^{-1}) = \sum_{\beta J_{A+1}} \frac{2J_{A+1}+1}{2J_A+1} S_{n\ell j}(\alpha J_A \rightarrow \beta J_{A+1}). \qquad (65)$$

In particular, for an even-even target with $J_A = 0$, $J_{A+1} = j$ we have

$$\bar{n}_A(j^{-1}) = (2j+1) \sum_{\beta} S_{n\ell j}(\alpha 0 \rightarrow \beta j). \qquad (66)$$

This means: the number of $(n\ell j)$ neutron holes in the target can be determined by measuring the stripping to all final states with the same $n\ell j$ (i.e., in practice, all final states with the same j and parity $\pi = (-)^{\ell}$).

Next we consider <u>pickup</u> from the same target, $A(a, a+1)A-1$. Then we have already seen that

$$S_{n\ell j}(\alpha J_A \rightarrow \gamma J_{A-1}) = S_{n\ell j}(\gamma J_{A-1} \rightarrow \alpha J_A)$$

$$= |\langle 0| \varphi_{J_A}^{(\alpha)M_A} [\varphi_{J_{A-1}}^{\dagger(\gamma)} n_{n\ell j}^{\dagger}]_{J_A}^{M_A} |0\rangle|^2 \qquad (67)$$

Now let us calculate the average number of $(n\ell j)$ neutron <u>particles</u> in the target A. This is the expectation value of the particle number operator

$$\sum_{m=-j}^{j} n_{n\ell j}^{\dagger m} n_{n\ell l}^{m}$$

in the target state,

$$\bar{n}_A(j) = \langle 0| \varphi_{J_A}^{(\alpha)M_A} \sum_{m} n_m^{\dagger} n_m \varphi_{J_A}^{\dagger(\alpha)M_A} |0\rangle$$

$$= \sum_{\gamma J_{A-1} M_{A-1} m} |\langle 0| \varphi_{J_A}^{(\alpha)M_A} n_m^{\dagger} \varphi_{J_{A-1}}^{\dagger(\gamma)M_{A-1}} |0\rangle|^2 \qquad (68)$$

Using

$$n^\dagger_{n\ell j, m}\varphi^{\dagger(\gamma)M_{A-1}}_{J_{A-1}} = \sum_{J'_A} \langle jm, J_{A-1} M_{A-1} | J'_A M'_A \rangle [n^\dagger_{n\ell j} \varphi^{\dagger(\gamma)}_{J_{A-1}}]^{M'_A}_{J'_A} \tag{69}$$

we find

$$\bar{n}_A(j) = \sum_{\gamma J_{A-1}} S_{n\ell j}(\alpha J_A \to \gamma J_{A-1}) \tag{70}$$

Again, for an even-even target with $J_A = 0$, $J_{A-1} = j$ we have

$$\bar{n}_A(j) = \sum_{\gamma} S_{n\ell j}(\alpha 0 \to \gamma j) \tag{71}$$

Therefore, the number of $(n\ell j)$ particles in the target can be determined by measuring the pickup leading to all final states with the same $(n\ell j)$. Clearly we must have

$$\bar{n}_A(j) + \bar{n}_A(j^{-1}) = 2j + 1 \tag{72}$$

Application of these sum rules in actual experiments requires that all states of given $(n\ell j)$ are excited and identified. This is often difficult (i) because the strength is usually spread over a number of levels in a certain energy range and (ii) because transfer angular distributions identify mainly the ℓ-value and are rather insensitive to the j-value except in special cases [13, 14].

More detailed sum rules can be derived [49] when the isospin of the target and final nucleus is taken into account. Consider a neutron pickup reaction on a target with isospin $T_A = T_{z,A}$. This reaction can excite states in the final nucleus with $T_{A-1} = T_A - \frac{1}{2} \equiv T_<$, but also states with $T_{A-1} = T_A + \frac{1}{2} \equiv T_>$. Let us now, in Eq.(71), distinguish between final states with $T_<$ and $T_>$,

$$\bar{n}_A(j) = \sum_{J_{A-1} T_{A-1}} S_{n\ell j}(J_A T_A \to J_{A-1} T_{A-1})$$

$$= \sum_{J_{A-1}} S_{n\ell j}(J_A T_A \to J_A T_<) + \sum_{J_{A-1}} S_{n\ell j}(J_A T_A \to J_{A-1} T_>) \equiv \mathscr{S}^<_j + \mathscr{S}^>_j \tag{73}$$

Now $\mathscr{S}^>_j$ for neutron pickup is proportional to the corresponding quantity for proton pickup, with a proportionality factor $(2T_A + 1)^{-1}$, for instance,

$$\mathscr{S}_j(p, d) = \frac{1}{2T_A + 1} \mathscr{S}_j(n, d) \tag{74}$$

Since in the proton pickup reaction only $T_>$ states can be excited, we must have $\mathscr{S}_j^>(n, d) = \bar{p}_A(j)$, where $\bar{p}_A(j)$ is the average number of protons in the target. Thus,

$$\mathscr{S}_j^>(p, d) = \frac{1}{2T_A + 1} \bar{p}_A(j) \qquad \qquad (75)$$

and we have the sum rules

$$\bar{n}_A(j) = \mathscr{S}_j^< + \mathscr{S}_j^>, \quad \bar{p}_A(j) = (2T_A + 1)\mathscr{S}_j^<$$

$$\bar{a}(j) = \mathscr{S}_j^< + 2(T_A + 1)\mathscr{S}_j^> \qquad \qquad (76)$$

where $\bar{a}_A(j)$ is the average number of nucleons in the state $(n\ell j)$.

Therefore, by measuring the neutron pickup strengths to final states with $T_<$ and $T_>$ separately, one can obtain the average number of neutrons and of protons in the target. Similarly, by measuring the proton stripping strengths to final states with $T_<$ and $T_>$ separately, one can determine both the average number of proton holes and of neutron holes in the target.

4.3. Pairing force model

We now turn to nuclei in the so-called vibrational region. These are spherical nuclei with several nucleons outside closed shells. Shell-model calculations for such nuclei would be very large. However, a much simpler description can be given when the short-range part of the residual interaction between nucleons is approximated by the so-called pairing force

$$\mathbb{H}_{pair} = -G \sum_{\substack{jj' \\ m>0, m'>0}} a_j^{\dagger m} \tilde{a}_j^{\dagger m} a_{j'}^{m'} \tilde{a}_{j'}^{m'} \qquad \qquad (77)$$

where G is the strength of the pairing interaction and $\tilde{a}_j^{\dagger m}$, $\tilde{a}_j^m$ are spherical creation and destruction operators (see [50]). This interaction describes perfect isotropic scattering of two paired particles from any state with $(m', -m')$ to any other state with $(m, -m)$. It therefore produces a mixing of shell-model configurations such that a given particle may be found in more than one shell; in other words, shells may be only partially occupied.

The ground state of the Hamiltonian (77) for an even-even nucleus is given by the BCS (Bardeen-Cooper-Schrieffer) wave function

$$|BCS\rangle = \prod_{j, m>0} (u_j + v_j a_j^{\dagger m} \tilde{a}_j^{\dagger m})|0\rangle \qquad \qquad (78)$$

where v_j and u_j are the probability amplitudes for occupation and non-occupation of the level j by a pair, respectively. Since v_j^2 is the probability of finding a zero-coupled j-pair in the ground state we have the condition

$$u_j^2 + v_j^2 = 1 \qquad (79)$$

The elementary excitations of the system are called BCS quasiparticles. Their creation and destruction operators, $\alpha_j^{\dagger m}$ and α_j^m are related to the particle operators by the Bogoliubov-Valatin transformation

$$\alpha_j^{\dagger m} = u_j a_j^{\dagger m} - v_j \tilde{a}_j^m$$

$$\alpha_j^m = v_j a_j^{\dagger m} + u_j \tilde{a}_j^m \qquad (80)$$

Since the state (BCS $\rangle$ is not an eigenstate of the particle-number operator $\mathbb{N}$, it does not correspond to a definite number of particles. However, we require that the expectation value of the number operator in $|BCS\rangle$, which is given by $2 \sum_j v_j^2$, equals the actual particle number

$$\langle BCS | \mathbb{N} | BCS \rangle = 2 \sum_j v_j^2 = N \qquad (81)$$

The probability amplitudes u_j and v_j are determined by minimizing the Hamiltonian

$$\mathbb{H} - \lambda \mathbb{N} \qquad (82)$$

where λ is a Lagrange multiplier. The result is

$$v_j^2 = \tfrac{1}{2} \left(1 - \frac{\epsilon_j - \lambda}{E_j} \right) \qquad (83)$$

where ϵ_j is the single-particle energy, E_j the single-quasiparticle energy

$$E_j = [(\epsilon_j - \lambda)^2 + \Delta^2]^{\frac{1}{2}} \qquad (84)$$

λ the chemical potential, and Δ is one-half the energy gap,

$$\Delta = G \sum_j (j + \tfrac{1}{2}) u_j v_j \qquad (85)$$

In a more general treatment one starts from the full nuclear Hamiltonian, rather than assuming the schematic pairing force (77), and transforms directly to quasiparticles by means of the Bogoliubov transformation (80). The coefficients u_j and v_j are then again determined by

BCS-type equations, but instead of the constant strength parameter G they contain the matrix elements of the full residual interaction and the gap parameter Δ_j becomes j-dependent.

After this sketchy introduction (for more details see the papers by Arvieu [51] and Pal [52] in these Proceedings) let us return to the spectroscopic factors. We are still considering one-nucleon transfer. Now we describe the ground state of an even-even vibrational nucleus approximately by $|BCS\rangle$ and that of a neighbouring odd nucleus by a one-quasiparticle state $\alpha_j^{\dagger m}|BCS\rangle$. Since these states are similar to those of the seniority scheme we may expect a simple generalization of the result (55) for the spectroscopic factors of stripping and pickup from the lowest seniority states, which we write in the form

$$. \quad S_j(0 \to j) = 1 - \frac{\bar{n}_A(j)}{2j+1} = \frac{\bar{n}_A(j^{-1})}{2j+1} \quad \text{(stripping)}$$

$$\tag{86}$$

$$S_j(0 \to j) = \bar{n}_A(j) \qquad \qquad \text{(pickup)}$$

In the BCS approach the average number of neutrons in the (even) target is $\bar{n}_A(j) = (2j+1)v_j^2$, and the average number of neutron holes is $\bar{n}_A(j^{-1}) = (2j+1) - \bar{n}_A(j) = (2j+1)u_j^2$. We therefore expect [53] that

$$S_j(0 \to j) = u_j^2 \qquad \text{(stripping)}$$

$$\tag{87}$$

$$S_j(0 \to j) = (2j+1)v_j^2 \quad \text{(pickup)}$$

Let us now confirm this result by a more detailed calculation [54, 2]. We denote the spectroscopic factors for stripping and pickup by a superscript (+1) and (-1), respectively. From Eq.(59) we have for stripping a neutron onto an even-even target

$$S_j^{(+1)}(0 \to j) = \left| \left\langle 0 \left| \varphi_j^m [n_j^\dagger \varphi_0^\dagger]_j^m \right| 0 \right\rangle \right|^2 \tag{88}$$

where now

$$\varphi_0^{\dagger 0}|0\rangle = |BCS\rangle, \quad \langle 0|\varphi_j^m = \langle BCS|\alpha_j^m$$

and

$$[n_j^\dagger \varphi_0^\dagger]_j^m |0\rangle = n_j^{\dagger m}|BCS\rangle$$

Thus

$$S_j^{(+1)}(0 \to j) = \left| \langle BCS|\alpha_j^m n_j^{\dagger m}|BCS\rangle \right|^2 \tag{89}$$

Here we insert the expression for $n_j^{\dagger m}$ in terms of quasiparticle operators, obtained by inverting Eq.(80),

$$\langle BCS | \alpha_j^m \, n_j^{\dagger m} | BCS \rangle = \langle BCS | \alpha_j^m (u_j \alpha_j^{\dagger m} + v_j \tilde{\alpha}_j^m) | BCS \rangle$$

$$= u_j \langle BCS | \alpha_j^m \alpha_j^{\dagger m} | BCS \rangle = u_j \langle \alpha_j^{\dagger m} BCS | \alpha_j^{\dagger m} \, BCS \rangle = u_j \tag{90}$$

since $\tilde{\alpha}_j^m | BCS \rangle = 0$ by definition. Hence

$$S_j^{(+1)}(0 \to j) = u_j^2 \tag{91}$$

Similarly, for pickup of a neutron from an even-even target (Eq.(67))

$$S_j^{(-1)}(0 \to j) = \left| \langle 0 | \wp_0^0 [n_j^\dagger \wp_j^\dagger]_0^0 | 0 \rangle \right|^2 \tag{92}$$

where

$$\langle 0 | \wp_0^0 = \langle BCS |, \quad \wp_j^{\dagger m} | 0 \rangle = \alpha_j^{\dagger m} | BCS \rangle$$

and

$$[n_j^\dagger \wp_j^\dagger]_0^0 | 0 \rangle = [n_j^\dagger \alpha_j^\dagger]_0^0 | BCS \rangle$$

Thus

$$S_j^{(-1)}(0 \to j) = \left| \langle BCS | [n_j^\dagger \alpha_j^\dagger]_0^0 | BCS \rangle \right|^2 \tag{93}$$

Now,

$$\langle BCS | [n_j^\dagger \alpha_j^\dagger]_0^0 | BCS \rangle = \sum_m \langle jm, j-m | 00 \rangle \langle BCS | n_j^{\dagger m} \alpha_j^{\dagger m} | BCS \rangle$$

$$= \sum_m \frac{(-)^{j-m}}{(2j+1)^{\frac{1}{2}}} \langle BCS | (U_j \alpha_j^{\dagger m} + v_j \tilde{\alpha}_j^m) \alpha_j^{\dagger m} | BCS \rangle$$

$$= \sum_m \frac{(-)^{j-m}}{(2j+1)^{\frac{1}{2}}} v_j \langle BCS | \tilde{\alpha}_j^m \alpha_j^{\dagger -m} | BCS \rangle$$

$$= \frac{v_j}{(2j+1)^{\frac{1}{2}}} \langle BCS | \sum_m \alpha_j^{-m} \alpha_j^{\dagger -m} | BCS \rangle = v_j (2j+1)^{\frac{1}{2}}$$

Hence

$$S_j^{(-1)}(0 \to j) = (2j+1)v_j^2 \tag{94}$$

This means: stripping onto an even-even target nucleus measures the "emptiness" u_j^2 of the level j, while pickup from an even-even target measures the "fullness" v_j^2 of the level, with respect to zero-coupled pairs. Again the sum rule (72) is valid,

$$\bar{n}_A(j) + \bar{n}_A(j^{-1}) = (2j+1)v_j^2 + (2j+1)u_j^2 = 2j+1 \tag{95}$$

The description of the ground states of even and odd vibrational nuclei by $|BCS\rangle$ and $\alpha_j^{\dagger m}|BCS\rangle$, i.e., by zero-quasiparticle and one-quasiparticle configurations of BCS-theory, respectively, is a very approximate one. If one uses a more realistic two-body interaction than the schematic pairing force, and introduces Bogoliubov quasiparticles (QP) by the transformation (80), the residual QP-interaction causes mixing of pure QP configurations. When the QP configuration mixing is limited (i) by truncating the space of active shell-model orbits and (ii) by restricting the number of excited QP's, one speaks of Quasiparticle Tamm-Dancoff (QTD) calculations. In recent years such calculations have been carried out with increasing size (as to the number of QP excitations) and complexity (projecting out spurious states, going from simple phenomenological to "realistic" two-body forces, taking into account core excitation by renormalization of the residual force, etc.). This work, which includes the calculation of spectroscopic factors for both one-nucleon and two-nucleon transfer reactions, was done mainly by the Pittsburgh [55-57], Orsay [58] and Trieste [59-63] groups. We shall return to it in section 5.

4.4. Two-nucleon transfer reactions

4.4.1. Definition of spectroscopic factor

For these reactions we defined in section 2.4, following Glendenning [3, 6], the structure factor (Eq.(35))

$$G_{NLSJT} = g \sum_\gamma \beta_{LSJT}^\gamma \, \Omega_n \, \langle n0, NL; L | n_1 \ell_1, n_2 \ell_2; L\rangle$$

Here the spectroscopic amplitude β_{LSJT}^γ is defined by the expansion (27). For a stripping reaction it is given by the overlap between the wave function of the final nucleus B and the wave function describing the ground state of nucleus A plus two neutrons in the state (γ, LSJT):

$$\beta_{LSJT}^\gamma =$$

$$\binom{A+2}{2} \int d\xi_A \int d\vec{r}_1 \int d\vec{r}_2 [\psi_{(LS)JT}^{\chi*} (\vec{r}_1 \vec{r}_2) \phi_{J_A T_A}^* (\xi_A)]_{J_B T_B} \, \phi_{J_B T_B} (\xi_A, \vec{r}_1 \vec{r}_2) \tag{96}$$

(where for simplicity we do not write the spin and isospin variables and the projection quantum numbers). Equation (96) includes the statistical factor arising from antisymmetrization, A being the number of nucleons in the target. The quantity $(\beta_{LSJT}^{\gamma})^2$ is the spectroscopic factor for the two-nucleon transfer reaction. It can be calculated from Eq.(96) if the wave functions ϕ_A and ϕ_B are given by a nuclear model.

4.4.2. Shell model

Consider first the shell model, and let us assume for simplicity that the target A is a closed-shell nucleus with ground state wave function $\phi_0(\xi_A)$. Then the states of the final nucleus B will be a product of $\phi_0(\xi_A)$ times a mixture of shell-model configurations of the two nucleons in levels above the closed shells of A,

$$\phi_{J_B T_B}(\xi_A, \vec{r}_1 \vec{r}_2) = \phi_0(\xi_A) \sum_{j_1 j_2} C_{J_B T_B}^{(j_1 j_2)} \psi_{(j_1 j_2) J_B T_B}(\vec{r}_1 \vec{r}_2) \tag{97}$$

To compare with Eq.(96) we transform from j-j coupling to L-S coupling. This transformation is given by

$$\psi_{(j_1 j_2)JT} = \sum_{LS} \begin{bmatrix} \ell_1 & \frac{1}{2} & j_1 \\ \ell_2 & \frac{1}{2} & j_2 \\ L & S & J \end{bmatrix} \psi_{(LS)JT} \tag{98}$$

where

$$\begin{bmatrix} \ell_1 & \frac{1}{2} & j_1 \\ \ell_2 & \frac{1}{2} & j_2 \\ L & S & J \end{bmatrix} \equiv \hat{L}\,\hat{S}\,\hat{j}_1\hat{j}_2 \begin{Bmatrix} \ell_1 & \frac{1}{2} & j_1 \\ \ell_2 & \frac{1}{2} & j_2 \\ L & S & J \end{Bmatrix} \tag{99}$$

Here, $\hat{L} \equiv (2L+1)^{\frac{1}{2}}$ etc., and the curly bracket is a 9-j symbol (see Ref.[47]). This gives

$$\beta_{LSJT}^{\gamma} = C_{J_B T_B}^{(j_1 j_2)} \begin{bmatrix} \ell_1 & \frac{1}{2} & j_1 \\ \ell_2 & \frac{1}{2} & j_2 \\ L & S & J \end{bmatrix} \delta_{JJ_B} \delta_{TT_B} \tag{100}$$

in terms of the mixture coefficients $C_{J_B T_B}^{(j_1 j_2)}$. Note that the configurations $\gamma = (j_1 j_2)$ enter <u>coherently</u> into the structure factor G. Therefore, we cannot

in general determine the wave function of B from experiment; we can only test whether an assumed model wave function is compatible with the data.

Consider now the case where A and B are both even-even nuclei, and let us assume that two neutrons are added to or removed from a given shell j. Then the ground states are connected by a two-particle c.f.p. (see Ref. [47]),

$$|j^{N+2}0\rangle = \sum_{v,J} (j^N vJ; (j^2)J | \} j^{N+2}0) |j^N vJ, (j^2)J, 0\rangle \qquad (101)$$

Here N (not to be confused with the principal quantum number N in the structure factor!) is the (even) number of neutrons in A, and v is the seniority. Again we transform the configuration $(j^2)J$ to L-S coupling by means of relations (98) and (99), and obtain

$$\beta^{\gamma}_{LSJ}(j^N vJ \longleftrightarrow j^{N+2}0) =$$
$$\binom{N+2}{2}^{\frac{1}{2}} (j^N vJ; (j^2)J |\} j^{N+2}0) \begin{bmatrix} \ell & \frac{1}{2} & j \\ \ell & \frac{1}{2} & j \\ L & S & J \end{bmatrix} \qquad (102)$$

In occupation-number representation, the two-particle c.f.p. has the form (see Ref. [47])

$$(j^N vJ; (j^2)J |\} j^{N+2}0) = \binom{N+2}{2}^{-\frac{1}{2}} \langle j^{N+2}0 || A^\dagger(jjJ) || j^N vJ\rangle \qquad (103)$$

where $A^\dagger$ is the two-particle creation operator (see Ref. [50])

$$A^\dagger(j_1 j_2 JM) = \frac{1}{(1+\delta_{j_1 j_2})^{\frac{1}{2}}} [a^\dagger_{j_1} a^\dagger_{j_2}]^M_J \qquad (104)$$

Hence

$$\beta^{\gamma}_{LSJ} = B(Jjj) \begin{bmatrix} \ell & \frac{1}{2} & j \\ \ell & \frac{1}{2} & j \\ L & S & J \end{bmatrix} \qquad (105)$$

where

$$B(Jjj) \equiv \langle j^{N+2}0 || A^\dagger(jjJ) || j^N vJ\rangle \qquad (106)$$

4.4.3. Pairing force model

It was first pointed out by Yoshida [64], in the framework of the pairing force model, that the two-neutron transfer reactions (t, p) and (p, t) are of special importance for studying pairing correlations. The (t, p) reaction, for example, will strongly excite those levels in the final nucleus in which the correlation between the two neutrons has a strong overlap with the correlation that existed between the two neutrons in the projectile.

By a straightforward generalization of Eq.(105) we have

$$\beta^{\gamma}_{LSJ} = B(Jj_1 j_2) \begin{bmatrix} \ell_1 & \frac{1}{2} & j_1 \\ \ell_2 & \frac{1}{2} & j_2 \\ L & S & J \end{bmatrix} \tag{107}$$

where

$$B(Jj_1 j_2) = \sum_{MM_A} \langle J_A M_A, JM | J_B M_B \rangle \langle \phi_{J_B}^{M_B} | A^\dagger (j_1 j_2 JM) | \phi_{J_A}^{M_A} \rangle \tag{108}$$

To calculate this quantity in the pairing force model we must first write the two-particle creation operator $A^\dagger$ in terms of quasi-particle operators, using Eq.(80). The result is

$$A^\dagger (j_1 j_2 JM) = \frac{1}{(1+\delta_{j_1 j_2})^{\frac{1}{2}}} \sum_{m_1 m_2} \langle j_1 m_1, j_2 m_2 | JM \rangle$$

$$\times \left[u_{j_1} u_{j_2} \alpha_{j_1}^{\dagger m_1} \alpha_{j_2}^{\dagger m_2} + v_{j_1} v_{j_2} \tilde{\alpha}_{j_1}^{m_1} \tilde{\alpha}_{j_2}^{m_2} + u_{j_1} v_{j_2} \alpha_{j_1}^{\dagger m_1} \tilde{\alpha}_{j_2}^{m_2} \right.$$

$$\left. - v_{j_1} u_{j_2} \alpha_{j_2}^{\dagger m_2} \tilde{\alpha}_{j_1}^{m_1} + \delta_{j_1 j_2} (-)^{j_1 - m_1} \delta_{-m_1 m_2} v_{j_1} u_{j_2} \right] \tag{109}$$

. We only quote Yoshida's results [64] for the most important simple cases:

(i) Both nuclei A and B are in 0-QP states (this applies to transition between ground states of even nuclei):

$$B(0jj) = (j + \tfrac{1}{2})^{\frac{1}{2}} u_{j_A} v_{j_B} \tag{110}$$

(ii) The parent nucleus B is in a 0-QP state, and the daughter nucleus A in a 2-QP state of configuration $(j_1 j_2)J$ (this applies to pickup from an even target B):

$$B(Jj_1 j_2) = -(2J+1)^{\frac{1}{2}} v_{j_1 B} v_{j_2 B} \tag{111}$$

(iii) The parent nucleus B is in a 2-QP state with configuration $(j_1 j_2)J$,
 .   and the daughter nucleus A in a 0-QP state (this applies to stripping
    from an even target A):

$$B(Jj_1 j_2) = u_{j_1 A} u_{j_2 A} \tag{112}$$

(Note that the subscripts A or B of the amplitudes u_j, v_j are necessary
because these quantities differ from neighbouring even nuclei).

    We can now easily see that the pairing correlations strongly enhance
that the (t,p) and (p,t) cross-sections in case (i). Then we have $S = 0$, $J = L$,
and the cross-section is proportional to

$$\left| \sum_j (2j+1) u_{j_A} v_{j_B} \right|^2 \approx \left| \sum_j (2j+1) u_j v_j \right|^2 = \left(\frac{2\Delta}{G} \right)^2 \tag{113}$$

using the gap equation (85). On the other hand, for a pure shell-model
configuration, we have $(2\Delta/G)^2 \leq j + \frac{1}{2}$, so that

$$\begin{array}{c} \text{Enhancement factor} \\ \text{due to pairing correlations} \end{array} \geq \left[\frac{2\Delta}{G(j+\frac{1}{2})} \right]^2 \tag{114}$$

which is about 10 for the Sn isotopes.

    Expressions (110)-(112) are obtained in the independent BCS-quasi-
particle model (IQM). If the residual interaction between quasiparticles
is taken into account, these results are changed due to mixing of QP-
configurations. The effect of quadrupole-quadrupole (Q-Q) forces has
been studied by Lin [65]. Extensive calculations for mixed 0-QP, 2-QP
and 4-QP configurations (i.e., in the so-called quasiparticle second
Tamm-Dancoff approximation, QSTD) have been made by the Trieste
group, using both phenomenological (Gaussian and Q-Q) [66] and realistic
(Tabakin) forces [67, 62]. It is found that the spectroscopic factors for
two-neutron transfer reactions are rather sensitive to the number of QP
excitations and to the nature of the residual interaction.

5.   COMPARISON WITH EXPERIMENT

    The amount of experimental information on transfer reactions is so
vast that we cannot attempt anything like a comprehensive survey. We
therefore select a few typical experiments which have been analysed in
some detail. In particular we prefer systematic studies that cover a range
of nuclei in those regions of the nuclear periodic table which are believed
to be specially amenable to analysis by transfer reaction theory. One of
the basic assumptions of the simple DWBA treatment is the presence of
an inert "core" of nucleons which acts as a spectator during the transfer
process and whose only function is to provide an average field that (i)
binds the particles to be captured or removed, and (ii) distorts the wave

functions in the initial and final channels. The best approximation of such a core would be a doubly closed shell nucleus. We shall therefore mainly look at experiments on nuclei in the vicinity of what are believed to be good closed shells. Since one- and two-nucleon transfer reactions probe different modes of excitation we consider them separately.

5.1. One-nucleon transfer reactions

5.1.1. The 1p shell

A systematic study of the (d, p) reaction with 12-MeV deuterons on all stable nuclei in the 1p shell ($6 \leq A \leq 14$) has been made by Schiffer et al.[68]. Angular distributions, over nearly the full range of angles, for transitions leading to the ground and low-lying excited states of the final nuclei were measured and their absolute values determined with an estimated accuracy of about 15%.

The results were compared with DWBA calculations. Because of the ambiguities in optical-model parameters derived from elastic-scattering data (see section 3.(vii)) a fixed average set of parameters (eight in each channel) was used, which was obtained by forming arithmetic means of previously determined parameter sets for deuteron and proton elastic scattering. Calculations were made with the JULIE code [69] using several approximations: zero range with and without lower cutoff, and with form factors calculated in local energy approximation. The shape of the angular distributions was fitted satisfactorily at forward angles, especially near the peak cross-section. However, considerable discrepancies were found at backward angles. In particular, the rather prominent j-dependence in the data at large angles could not be reproduced by the DWBA calculations although reasonable spin-orbit forces were included. At the peak cross-sections the uncertainty due to the different approximations used was estimated to be about 15%.

The actual analysis was carried out in zero-range approximation with a lower cutoff at 4 fm. Spectroscopic factors, for $\ell = 1$ transitions, were obtained from the expression

$$S_{\ell = 1} = \frac{(d\sigma / d\Omega)_{exp} \text{ (peak)}}{1.65 \, \frac{2J_B + 1}{2J_A + 1} \, \sigma_{JULIE} \text{ (peak)}} \tag{115}$$

where 1.65 is a normalization factor that results from the use of Hulthén wave functions for the deuteron.

Shell-model calculation of spectroscopic factors for stripping and pickup in the 1p shell was made by Cohen and Kurath [70]. These authors calculate

$$S_{n\ell j} (\alpha J_A T_A \rightarrow \beta J_B T_B) = (A + 1) \left| (\alpha J_A T_A ; n\ell j \,|\} \beta J_B T_B) \right|^2 \tag{116}$$

for $n\ell j = 1p_{3/2}$ and $1p_{1/2}$, where $A+1$ is the number of active 1p nucleons, and the c.f.p. are defined by

$$
\phi_{J_B T_B}^{(\beta)} (1 \ldots A+1) =
$$

$$
\sum_{(\alpha) J_A T_A} (\alpha J_A T_A; n\ell j \,|\} \beta J_B T_B) \left[\phi_{J_A T_A}^{(\alpha)} (1 \ldots A) \psi_{n\ell j \frac{1}{2}} (A) \right]_{J_B T_B}^{(\beta)} \tag{117}
$$

The wave functions are mixed shell model configuration wave functions for effective interactions in the 1p shell which were deduced by fitting energy levels. Also calculated are the summed spectroscopic factors. It is found that about 99% of the total strength is exhausted by the low-lying states calculated. The summation for pickup gives (see Eq.(70))

$$
\sum_{(\gamma) J_{A-1} T_{A-1}} S_{n\ell j} (\alpha J_A T_A \rightarrow \gamma J_{A-1} T_{A-1}) = \bar{n}_A (j) \tag{118}
$$

the number of $n\ell j$ nucleons in the target nucleus. As an example, the predicted filling of the $1p_{3/2}$ level in the ground state of the target nuclei is shown in Fig.3. Comparison with the values expected from the jj and LS coupling limits shows the degree to which the coupling is intermediate between these limits.

The spectroscopic factors extracted by means of relation (115) are compared with the predictions of Cohen and Kurath in Fig.4. The upper part of this figure also shows a comparison of the experimental and theoretical peak cross-sections. Except for the ground-state transition in the $^{12}C(d, p)^{13}C$ reaction, the agreement is surprisingly good. Since no systematic variation of the ratio S(exp)/S(theor) with the reaction Q-value, and thus with the reaction kinematics, is found, the DWBA results appear to be reliable and the agreement with the shell-model calculation seems genuine.

5.1.2. The Ca isotopes ($1f_{7/2}$ neutron shell)

Although ^{40}Ca is a doubly-magic nucleus the classic study of the $^{40}Ca(d, p)^{41}Ca$ reaction by Lee et al.[26], in which the reliability of the DWBA was tested (see section 3.), showed that the pure-configuration picture for ^{41}Ca is not valid. Table IV gives the spectroscopic factors for the low-lying states in ^{41}Ca seen by Lee et al., which were extracted by means of a finite-range calculation including spin-orbit coupling. Not only are the spectroscopic factors for the $7^-/2$ and $1^-/2$ states significantly below unity, but the $p_{3/2}$ single-particle strength is spread over two levels. Further investigations showed that $\ell = 2$ and $\ell = 0$ transitions occur in addition to the $\ell = 3$ ground state transitions. This led to the conclusion that the ground state of ^{40}Ca, and that of other even Ca isotopes, contain

admixtures of core-excited 2p-2h components. The ground-state wave
functions can be written as

$$^{40+2n}Ca(0) = a(1f_{7/2})^{2n} + b(1d_{3/2}, 2s_{1/2})^{-2}(1f_{7/2})^{2n+2} \qquad (119)$$

The mixing coefficient b was found to decrease rapidly with increasing n;
in particular, ^{48}Ca appears to be a much better closed-shell nucleus than
^{40}Ca.
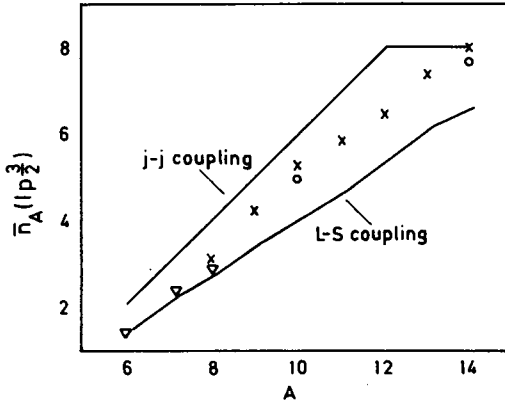
FIG.3. The number of $1p_{3/2}$ nucleons in the target ground states, calculated from Eq.(118). The triangles,
dots and crosses refer to different effective interactions. The lines connect values expected in the j-j
coupling or L-S coupling limits (Cohen and Kurath [70]).
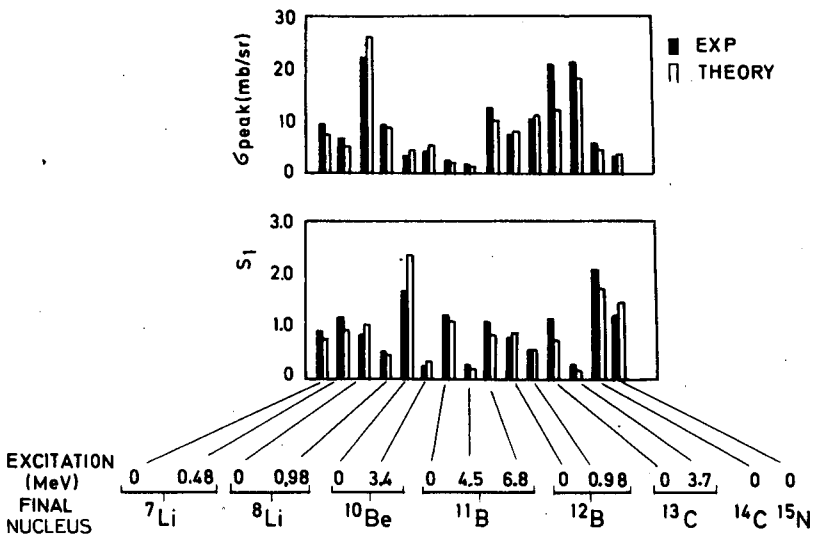
FIG.4. Comparison of experimental and calculated peak cross-sections and spectroscopic factors in the 1p
shell (Schiffer et al. [68])

TABLE IV.   SPECTROSCOPIC FACTORS FOR
LOW-LYING STATES IN ^{41}Ca EXTRACTED FROM
THE ^{40}Ca(d, p) ^{41}Ca REACTION BY LEE et al. [26]

E*(MeV)	j^{π}	S
0	$\frac{7-}{2}$	0.86 ± 0.07
1.95	$\frac{3-}{2}$	0.72 ± 0.12 ⎫
2.47	$\frac{3-}{2}$	0.32 ± 0.04 ⎬ 1.04 ± 0.13
3.95	$\frac{1-}{2}$	0.78 ± 0.04

TABLE V.   COMPARISON OF NORMALIZED
EXPERIMENTAL AND THEORETICAL VALUES OF
THE TOTAL STRENGTH OF $\ell = 3$ GROUND-STATE
TRANSITIONS IN THE EVEN Ca ISOTOPES
(From Ref. [71].)

Final state	$(2j+1)S(exp)$	$(2j+1)S(theor)$
^{41}Ca(0)	6.54	8
^{43}Ca(0)	4.89	6
^{45}Ca(0)	3.37	4
^{47}Ca(0)	2.00	2

A recent systematic study of the (d, p) reaction on the even Ca isotopes
was made by the MIT-Copenhagen-Aldermaston collaboration at 7 MeV [71]
and 10 MeV [72], who also review the earlier work in this region.   The
angular distributions were analysed in DWBA (JULIE code, zero-range,
no cutoff).   Table V gives the best extracted spectroscopic strengths of
the $\ell = 3$ ground state transitions, normalized such that $(2j+1)S = 2$ for
^{47}Ca(0), in comparison with the theoretically expected values.

The experimental values, believed to be accurate to about $\pm 10\%$,
fall considerably below the predicted shell-model ones.   This indicates
that shell closure is quite imperfect especially in the lighter isotopes
with A = 40, 42 and 44.

Similar results are obtained for the Z = 20 proton shell.   A recent study
of the (t, α) proton pickup reaction on the even Ca isotopes [73] shows
that $\ell = 3$ transitions occur in all cases except ^{48}Ca.   This indicates that
$1f_{7/2}$ protons are present in their ground states and suggests an admixture

of $(1d_{3/2})^{-2}$ $(1f_{7/2})^2$ two-particle two-hole components. This is corroborated by the occurrence of $\ell = 2$ transitions in the (^{3}He, d) proton-stripping reaction on all even Ca isotopes, except ^{48}Ca, which can be interpreted as stripping of protons onto the partially unfilled $1d_{3/2}$ orbital [74].

A mixed-configuration shell-model calculation of the Ca-even isotopes has been performed recently by Bayman and Hintz [75]. They include the following active single-particle states:

$$2s_{1/2} , 1d_{3/2} , 1f_{7/2} , 2p_{3/2} , 2p_{1/2} , 1f_{5/2}$$

The neutron-neutron interaction is approximated by a simple pairing force.

In Fig.5 the calculated ground-state occupation probabilities v_j^2 are compared with summed experimental spectroscopic factors, to which they are related by Eq.(86). This shows that the data are consistent with the pairing calculation and indicates to which extent deviations from unperturbed shell model values occur.
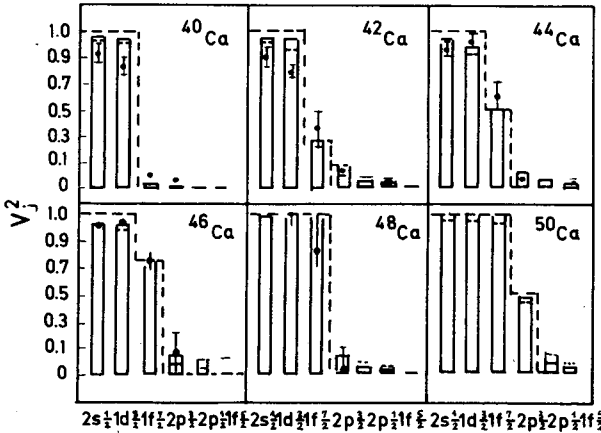
FIG.5.   Average ground-state occupation probabilities v_j^2 for the even Ca isotopes for single-particle states indicated. Rectangular bars are results of pairing-force calculations for G = 20/A, dotted lines are for G = 27/A. Dashed lines show unperturbed shell model values. Black points are experimental values from single-nucleon transfer data. (From Ref. [75]).

5.1.3. The Sn isotopes

The tin isotopes are prototypes of so-called vibrational nuclei, in which 12-24 neutrons populate the active levels

$$2d_{5/2} , 1g_{7/2} , 3s_{1/2} , 2d_{3/2} , 1h_{11/2}$$

above what is assumed to be a doubly closed 50-50 core. They are, therefore ideally suited for testing the pairing force model (see section 4.3.).

The classic investigation in this region is the work of Cohen and Price [53] who studied the (d, p) and (d, t) reactions on the isotopes ^{116}Sn - ^{124}Sn. No detailed fits of the angular ·distributions by means of a reaction theory were made, but the ℓ-values of the transitions were determined by the shape of the (d, p) cross-sections. This fixes the value of j, except for $\ell = 3$, in which case the cross-sections for $2d_{5/2}$ and $2d_{3/2}$ are distinguished by their Q-values. The analysis is based on the expressions for the spectroscopic factors in the simple pairing force model (Eqs (91) and (94)).

<div align="center">
even target nuclei   odd target nuclei

(ground-state transition)
</div>

$$(d, p): \quad S_j(0 \to j) = u^2_{j, A} \qquad , \quad S_j(j \to 0) = (2j+1)v^2_{j, B} \qquad (120a)$$

$$(d, t): \quad S_j(0 \to j) = (2j+1)v^2_{j, A} \quad , \quad S(j \to 0) = u^2_{j, B} \qquad (120b)$$

where $u^2_{j, A}$, $v^2_{j, A}$ refer to the target nucleus and $u^2_{j, B}$, $v^2_{j, B}$ to the residual nucleus. The cross-section ratios between the (d, p) reactions (odd A-1 → even A) and (even A → odd A+1), together with the condition $u^2_{j, A} + v^2_{j, A} = 1$, determines the probabilities $u^2_{j, A}$ and $v^2_{j, A}$. Similar relations for the (d, t) reaction give an independent check on these values. The results were compared with the pairing-force calculations of Kisslinger and Sørensen [78], and fairly satisfactory agreement was found.
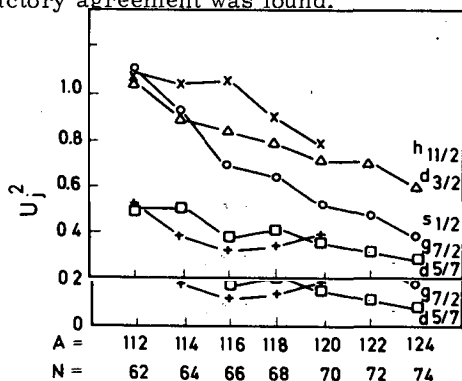
FIG. 6.   "Emptiness" u^2_j of the active levels in the even Sn isotopes. (From Ref. [79]).

In a more recent study by Schneid et al. [79] the earlier work was extended by including the isotopes of mass number 112, 114 and 115, and the energy resolution was improved by a factor two. The data were analysed by means of the DWBA, and the u^2_j, v^2_j were obtained from summed spectroscopic factors. The results for the "emptiness" u^2_j are given in Fig. 6. As expected, all active levels are gradually filled with increasing number of neutron pairs.

These results, as well as those for the (p, d) reaction on ^{117}Sn and ^{118}Sn by Yagi et al. [80], were found to be in fair agreement with calculations by Yoshida [81] which include quadrupole-quadrupole and
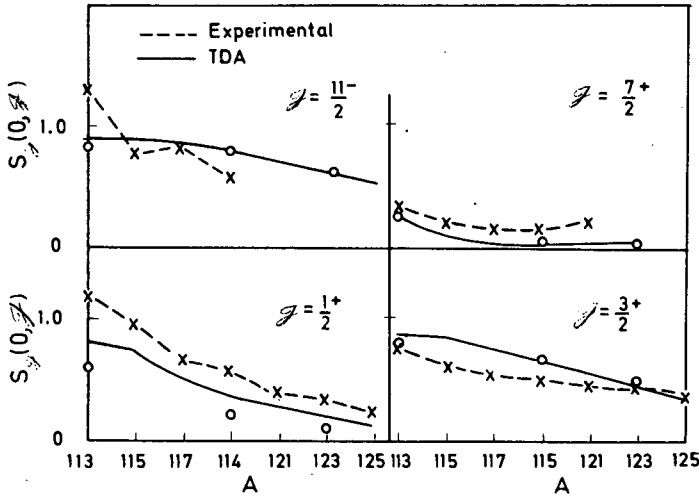
FIG.7.   Spectroscopic factors $S_{\mathscr{J}}(0,\mathscr{J})$ for (d, p) reactions leading to the lowest state in the odd-mass Sn isotopes of spin $\mathscr{J}$.   The solid lines connect results of the Tamm-Dancoff calculation (TDA).   The crosses connected by dashed lines are experimental values from Ref.[79].   Circles correspond to calculations with a different set of shell-model parameters.   (From Ref.[55].)
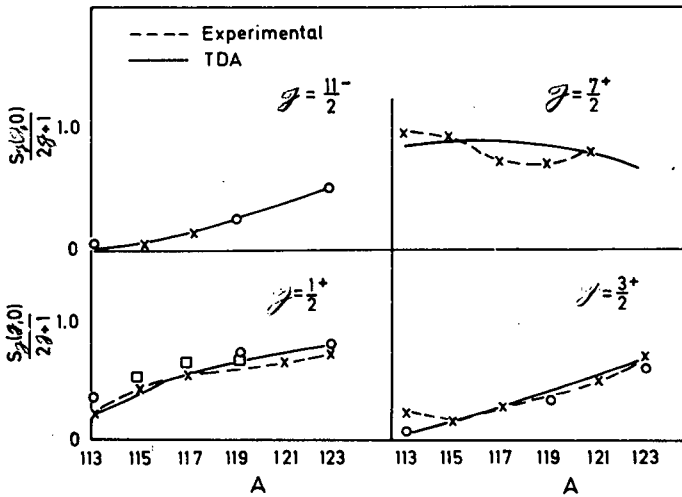
FIG.8.   Spectroscopic factors $S_{\mathscr{J}}(\mathscr{J}, 0)/(2\mathscr{J}+1)$.   The solid lines connect results of the Tamm-Dancoff calculation (TDA).   The crosses connected by dashed lines are experimental values from (d, t) reactions on the even Sn isotopes, squares are experimental values from (d. p) experiments on the odd-mass targets with A =115, 117 and 119.   Circles correspond to calculations with a different set of shell-model parameters.   (From Ref.[55].)

octupole-octupole interactions in addition to the pairing force.   More sophisticated calculations, in various forms of the Quasiparticle Tamm-Dancoff approximation (see section 4.4.3.) have been made recently [55-57], [59-63].   Kuo et al.[55] take for the ground state of the even isotopes the BCS ground state, and for the states of the odd isotopes the eigenfunctions
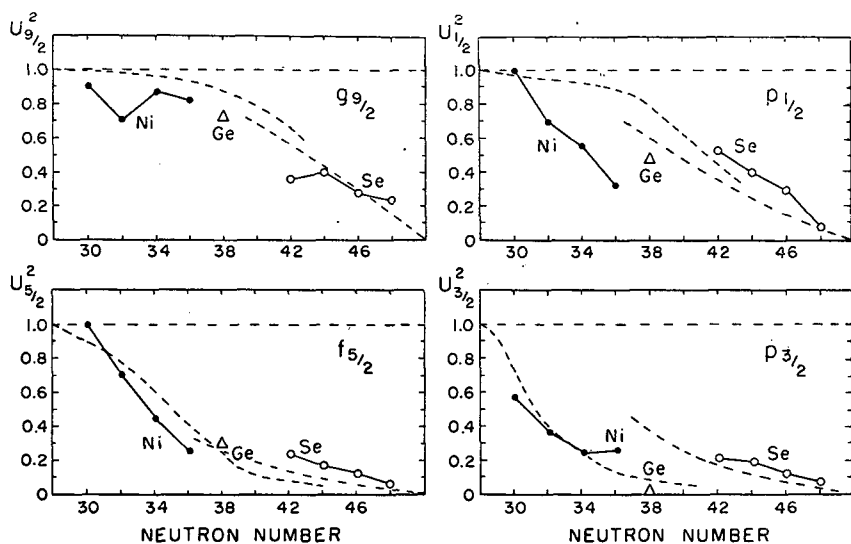
FIG.9.   Behaviour of u_j^2 in 28-50 shells.
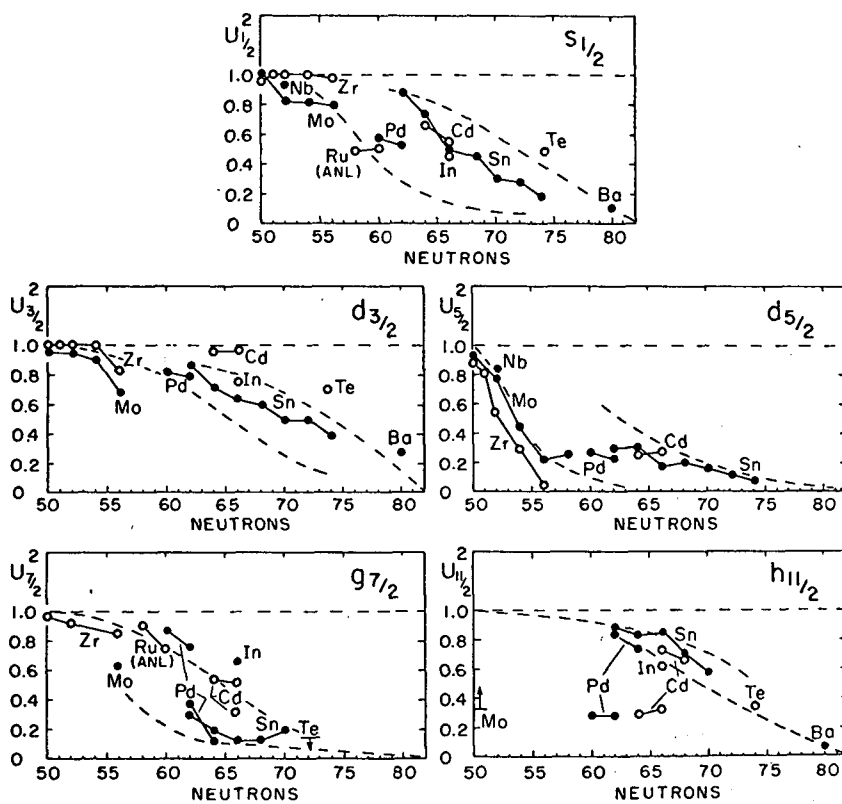
FIG.10.   Behaviour of u_j^2 in 50-82 shells.

of the (1QP) Tamm-Dancoff calculation. The spectroscopic factors for the (d, p) and (d, t) reactions on even target nuclei are then given by [54]

$$S_{\ell}(0, \ell) = u_p^2 \left| \psi_1^{(i)}(\ell) \right|^2 \tag{121a}$$

$$S_{\ell}(\ell, 0) = (2\ell + 1) v_p^2 \left| \psi_1^{(i)}(\ell) \right|^2 \tag{121b}$$

respectively, where $\left| \psi_1^{(i)}(\ell) \right|^2$ is the amount of 1QP state p admixed to the ith eigenstate of the odd isotope, and $j_p = \ell$. The spectroscopic factor (121b) applies also to a (d, p) reaction on an odd target with the final nucleus in its ground state. Figures 7 and 8 show a comparison of the calculated values (121) with the experimental ones of Schneid et al. The agreement is quite satisfactory.

A survey of the systematics of single-quasiparticle states in spherical nuclei through entire major shells was recently given by Cohen [82]. The behaviour of the "emptiness" u_j^2 in the 28-50 and 50-82 shells is shown in Figs 9 and 10, respectively. With few exceptions, the agreement is fairly good.
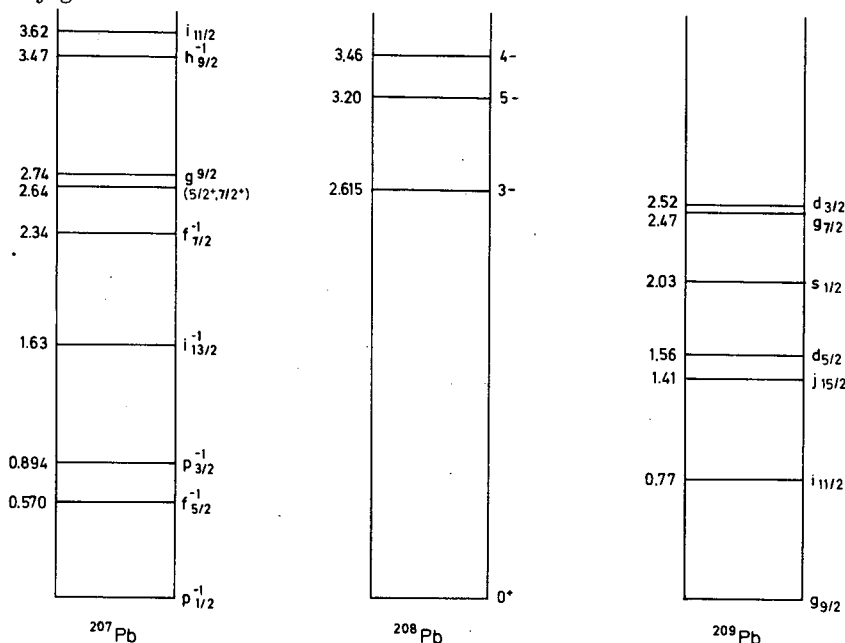
FIG.11.   Low-lying states near ^{208}Pb

5.1.4. The Pb region

This seems to be a region of happiness for the nuclear shell model. Recent thorough investigations have shown that the ground state of ^{208}Pb is a very good closed shell for both neutrons and protons. Evidence for this comes from neutron stripping and pickup reactions on ^{208}Pb, leading to single-particle states in ^{209}Pb and to single-hole states in ^{207}Pb, respectively. The low-lying levels in these nuclei are shown in Fig.11.

TABLE VI.   SPECTROSCOPIC FACTORS FOR SINGLE -PARTICLE
STATES IN ^{209}Pb

State	E_x (MeV)	(d, p) [83]			(t, d) [85]	(p, p) analogue [86]
		15.0 MeV	20.3 MeV	25.1 MeV		
$2g_{9/2}$	0	0.87	0.77	0.67	0.93	0.97
$1i_{11/2}$	0.79	1.17	0.78	0.94	1.05	
$1j_{15/2}$	1.42	0.96	0.79	1.13	0.51	
$3d_{5/2}$	1.56	0.83	1.05	1.00	0.86	0.85
$4s_{1/2}$	2.01	0.80	0.90	0.93	0.86	0.90
$2g_{7/2}$	2.47	1.08	1.08	1.17	0.90	0.84
$3d_{3/2}$	2.51	0.88	1.07	1.17	0.83	0.86

Muehllehner et al.[83] studied the reactions ^{208}Pb(d, p) ^{209}Pb and
^{208}Pb(d, t) ^{207}Pb at E_d = 15, 20 and 25 MeV; the reaction ^{208}Pb(p, d) ^{207}Pb
was studied by Whitten et al.[84] at E_p = 20 and 22 MeV, and the reaction
^{208}Pb(t, d)^{207}Pb by Igo et al.[85]. The resulting spectroscopic factors for
the single-particle states in ^{209}Pb are shown in Table VI, together with
values obtained from analysis [86] of isobaric analogue resonances in
(p, p) scattering (see section 3).

   With only two exceptions (the (d, p) reaction at 25.1 MeV to the ground
state, and the (t, d) reaction to the $1j_{15/2}$ state) these results show that
the low-lying levels in ^{209}Pb are pure, unfragmented single-particle
states.

   Table VII gives the spectroscopic factors for ^{207}Pb. Again there is
good evidence that the low-lying levels in ^{207}Pb (with the exception of
the $2f_{7/2}$ level) are pure single-neutron hole states. Similar evidence
is being obtained for the proton-particle states in ^{209}Bi and for the
proton-hole states in ^{207}Tl (see [87]).

   Other aspects of nuclear states in the Pb region are discussed in
the papers by Alaga [88] and Cindro [89] in these Proceedings.

5.2. Two-nucleon transfer reactions

   We have seen (section 4.4.) that two-nucleon transfer reactions depend
sensitively upon the nature of the correlations between the transferred
nucleons. Of particular importance are the two-neutron stripping and
pickup processes, especially (t, p) and (p, t), in which zero-coupled pairs

TABLE VII.   SPECTROSCOPIC FACTORS FOR SINGLE-HOLE STATES IN ^{207}Pb

State	E_x (MeV)	S_j (theoretical)	(p, d) [84] E_p =20.00 MeV (absolute)	(p, d) [84] E_p =22.00 MeV (relative), $S(3p_{3/2})\approx4$	(d, t) [83] E_d =14.8 MeV	(d, t) [83] E_d = 20.1 MeV	(d, t) [83] E_d = 24.8 MeV
$3p_{1/2}$	0	2	2.19	2.16	2.18	2.12	2.12
$2f_{5/2}$	0.57	6	6.00	5.82	6.60	7.20	6.00
$3p_{3/2}$	0.89	4	4.04	(4.00)	3.76	3.80	3.32
$1i_{13/2}$	1.64	14	14.3	12.7	14.00	13.02	14.00
$2f_{7/2}$	2.34	8	6.35	5.75	6.08	6.40	5.76
$1h_{9/2}$	$\begin{cases}3.43\\3.59\end{cases}$	10			10.00	10.00	10.00

are transferred. Since the addition or removal of zero-coupled pairs has little effect on the collective motions in the initial and final nuclei, we expect strongly enhanced cross-sections for pair transfer between states which have similar collective motions.

Recently there have been many experiments that confirm the collective enhancement of two-nucleon transfer reactions. The data of (t, p) and (p, t) reactions with $L = 0$ on the Ca isotopes of mass number 40-48 at $E_t = 10$-12 MeV [90] were analysed by Bayman and Hintz [75]. These authors calculated spectroscopic amplitudes for two-neutron transfer using mixed neutron configurations and approximating the neutron-neutron interaction by a simple pairing force. The good agreement obtained with the ratios of observed (t, p) and (p, t) cross-sections for ground state transitions indicates that the ground states of the Ca isotopes are characterized by simple pairing degrees of freedom. However, the transitions to some of the excited $0^\dagger$ states are predicted too large so that these states must involve more complicated degrees of freedom.

Detailed tests of the two-nucleon-transfer reaction theory have been carried out in the lead region. Glendenning [91] has analysed the data of Reynolds et al.[92] for the $^{208}Pb(t, p)^{206}Pb$ reaction, using the shell model wave functions of True and Ford [93]. A more extensive analysis along the same lines of this reaction has been made recently by Bromley and co-workers [94], who found excellent agreement for the shapes of the angular distributions, for the relative cross-sections for states up to 3 MeV excitation energy, and for the energy dependence of the cross-sections.

Two-nucleon transfer reactions are of special importance for the study of a new type of collective modes of excitation, the so-called pairing vibrations. The theoretical concepts have recently been discussed by Bohr [95], and the experimental situation was surveyed by Nathan [96]. Different aspects of these important and exciting developments are dealt with in other papers at this Course (Bohr [97], Alaga [88], Ripka [98] in these Proceedings).

REFERENCES

[1] AUSTERN, N., in Selected topics in nuclear theory (Proc. Summer School, Czechoslovakia, 1962) IAEA, Vienna (1963) 17.

[2] BAYMAN, B.F., in "Many-body problems and other selected topics in theoretical physics", Gordon and Breach, New York (1966) 441.

[3] GLENDENNING, N.K., A. Rev. nucl. Sci. 13 (1963) 191.

[4] SATCHLER, G.R., in "Lectures in Theoretical Physics, 8C-Nuclear Structure Physics", Boulder (1966), University of Colorado Press 73.

[5] SCHIFFER, J.P., in Nuclear Structure (Proc. Int. Conf. Tokyo 1967, Physical Society of Japan, Tokyo (1968) 319.

[6] GLENDENNING, N.K., Phys. Rev. 187B (1965) 102.

[7] MACFARLANE, M.H., FRENCH, J.B., Rev. mod. Phys. 32 (1960) 567.

[8] TOBOCMAN, W., Theory of Direct Nuclear Reactions, Oxford University Press London (1961).

[9] AUSTERN, N., DRISKO, R.M., HALBERT, E.C., SATCHLER, G.R., Phys. Rev. 133B (1964) 3.

[10] JOHNSON, R.C., Nucl. Phys. A 90 (1967) 289; JOHNSON, R.C., SANTOS, F.D., Phys. Rev. Lett. 19 (1967) 364.

[11] BASSEL, R.H., Phys. Rev. 149 (1966) 791.

[12] DRISKO, R.M., SATCHLER, G.R., BASSEL, R.H., Phys. Lett. 5 (1963) 347.

[13] LEE, L.L., Jr., SCHIFFER, J.P., Phys. Rev. Lett. 12 (1964) 108.

[14] SHERR, R., ROST, E., RICKEY, M.E., Phys. Rev. Lett. 12 (1964) 420.

[15] PEREY, F.G., in Direct Interactions and Nuclear Reaction Mechanisms, (Proc. Conf. Padua, 1962) Gordon and Breach, New York (1963) 125.

[16] PEREY, F.G., SAXON, D.S., Phys. Lett. 10 (1964) 107.

[17] BUTTLE, P.J.A., GOLDFARB, L.J.B., Proc. Phys. Soc. (London) 83 (1964) 701.

[18] BENCZE, G., ZIMANY, J., Phys. Lett. 9 (1964) 246.

[19] DICKENS, J.K., DRISKO, R.M., PEREY, F.G., SATCHLER, G.R., Phys. Lett. 15 (1965) 337.

[20] LUKYANOV, V.K., PETKOV, I.Ž., Soviet J. nucl. Phys. 6 (1968) 720; Phys. Lett. 28B (1969) 368.

[21] BUCK, B., HODGSON, P.E., Phil. Mag. 6 (1961) 1371.

[22] AUSTERN, N., in Nuclear Structure, (Proc. Int. Conf., Tokyo 1967) Physical Society of Japan (Tokyo 1968) 269.

[23] BERGGREN, T., Nucl. Phys. 72 (1965) 337.

[24] PINKSTON, W.T., SATCHLER, G.R., Nucl. Phys. 72 (1965) 641.

[25] PRAKASH, A., AUSTERN, N., Ann. Phys. (N.Y.) 51 (1969) 418.

[26] LEE, L.L., Jr., SCHIFFER, J.P., ZEIDMAN, B., SATCHLER, G.R., DRISKO, R.M., BASSEL, R.H., Phys. Rev. 136B (1964) 971.

[27] SMITH, W.R., Phys. Rev. 137B (1965) 913.

[28] GOLDFARB, L.J.B., Nucl. Phys. 72 (1965) 537.

[29] GOLDFARB, L.J.B., PARRY, E., Nucl. Phys. A 116 (1968) 289.

[30] GOLDFARB, L.J.B., STEED, J.W., Nucl. Phys. A 116 (1968) 321.

[31] DOST, M., Trieste, 1969 (not published in these Proceedings).

[32] von BRENTANO, P., Trieste, 1969 (these Proceedings).

[33] DAR, A., Phys. Lett. 7 (1963) 339; Nucl. Phys. 55 (1964) 305.

[34] HENLEY, E.M., YU, D.U.L., Phys. Rev. 133B (1964) 1445; ibid. 135B (1964) 1152.

[35] FRAHN, W.E., VENTER, R.H., Nucl. Phys. 59 (1964) 651.

[36] DAR, A., Phys. Rev. 139B (1965) 1193; Nucl. Phys. 82 (1966) 354.

[37] HAHNE, F.J.W., Nucl. Phys. 80 (1966) 113.

[38] FRAHN, W.E., in Fundamentals in Nuclear Theory (Proc. Int. Course, Trieste 1966), IAEA (Vienna, 1967) 3.

[39] VARMA, S., Nucl. Phys. A 106 (1968) 233.

[40] FRAHN, W.E., SHARAF, M.A., ICTP preprint IC/69/21 (1969) and Nucl. Phys. (to be published).

[41] ROBSON, D., Rev. nucl. Sci. 16 (1966) 119.

[42] THOMPSON, W.J., ADAMS, J.L., ROBSON, D., Phys. Rev. 173 (1968) 975.

[43] GOLDFARB, L.J.B., in "Lectures in Theoretical Physics, 8C-Nuclear-Structure Physics", Boulder (1966) University of Colorado Press, 445.

[44] JACOB, G., MARIS, Th.A.J., Rev. mod. Phys. 38 (1966) 121.

[45] BRINK, D.M., SATCHLER, G.R., Nuovo Cim. 4 (1956) 549.

[46] MACFARLANE, M.H., in "Lectures in Theoretical Physics, 8C-Nuclear-Structure Physics", Boulder (1966), University of Colorado Press, 583.

[47] RIMINI, A., Trieste, 1969 (these Proceedings).

[48] BAYMAN, B.F., LANDÉ, A., Nucl. Phys. 77 (1966) 1.

[49] FRENCH, J.B., MACFARLANE, M.H., Nucl. Phys. 26 (1961) 168.

[50] FRAHN, W.E., Lectures on occupation number representation, Course on Nuclear Theory, ICTP, Trieste, 1969 (not published in these Proceedings).

[51] ARVIEU, R., Trieste, 1969 (these Proceedings).

[52] PAL, M.K., Trieste, 1969 (these Proceedings).

[53] COHEN, B.L., PRICE, R.E., Phys. Rev. 121 (1961) 1441.

[54] YOSHIDA, S., Phys. Rev. 123 (1961) 2122.

[55] KUO, T.T.S., BARANGER, E., BARANGER, M., Nucl. Phys. 79 (1966) 513.

[56] BARANGER, E., KUO, T.T.S., Nucl. Phys. A 97 (1967) 289.

[57] CLEMENT, D.M., BARANGER, E.U., Nucl. Phys. A 120 (1968) 25.

[58] ARVIEU, R., BARANGER, E., VÉNÉRONI, M., BARANGER, M., GILLET, V., Phys. Lett. 4 (1963) 119.

[59] ALZETTA, R., SAWICKI, J., Phys. Rev. 173 (1968) 1185.

[60] ALZETTA, R., Nuovo Cim. 58B (1968) 323.

[61] SAWICKI, J., Nuovo Cim., Suppl. 6 (1968) 696.

[62] ALZETTA, R., GAMBHIR, Y.K., GMITRO, M., RIMINI, A., SAWICKI, J., WEBER, T., ICTP, Trieste, preprint IC/68/83, to be published in Phys. Rev.

[63] ALZETTA, R., RIMINI, A., WEBER, T., GMITRO, M., SAWICKI, J., ICTP, Trieste, preprint IC/69/2, to be published in Phys. Rev.

[64] YOSHIDA, S., Nucl. Phys. 33 (1962) 685.

[65] LIN, C.L., Progr. theor. Phys. 36 (1966) 251.

[66] GYARMATI, B., SAWICKI, J., Nucl. Phys. A 111 (1968) 609.

[67] GYARMATI, B., SAWICKI, J., Phys. Rev. 169 (1968) 966.

[68] SCHIFFER, J.P., MORRISON, G.C., SIEMSSEN, R.H., ZEIDMAN, B., Phys. Rev. 164 (1967) 1274.

[69] BASSEL, R.H., DRISKO, R.M., SATCHLER, G.R., Oak Ridge National Laboratory Report No. ORNL-3240.

[70] COHEN, S., KURATH, D., Nucl. Phys. 73 (1965) 1, ibid. A 101 (1967) 1.

[71] BELOTE, T.A., DORENBUSCH, W.E., RAPAPORT, J., Nucl. Phys. A 120 (1968) 401.

[72] ANDERSEN, S.A., HANSEN, O., CHAPMAN, R., HINDS, S., Nucl. Phys. A 120 (1968) 421.

[73] SANTO, R., STOCK, R., BJERREGAARD, J.H., HANSEN, O., NATHAN, O., CHAPMAN, R., HINDS, S., Nucl. Phys. A 118 (1968) 409.

[74] SANTO, R., in Proc. Conf. German Physical Society (Karlsruhe 1968), B.G. Teubner, Stuttgart (1968) 62.

[75] BAYMAN, B.F., HINTZ, N.M., Phys. Rev. 172 (1968) 1113.

[76] SHERR, R., BAYMAN, B., ROST, E., RICKEY, M.E., HOOT, C.G., Phys. Rev. 139B (1965) 1272.

[77] SHERR, R., in "Lectures in Theoretical Physics. 8C -Nuclear-Structure Physics", Boulder 1966, University of Colorado Press 1.

[78] KISSLINGER, L.S., SØRENSEN, R.A., Mat. Fys. Medd. Dan. Vid. Selsk. 32 (1960) 9.

[79] SCHNEID, E.J., PRAKASH, A., COHEN, B.L., Phys. Rev. 156 (1967) 1316.

[80] YAGI, K., SAJI, Y., ISHIMATSU, T., ISHISAKI, Y., MATOBA, M., NAKAJIMA, Y., HUANG, C.Y., Nucl. Phys. A 111 (1968) 129.

[81] YOSHIDA, S., Nucl. Phys. 38 (1962) 380.

[82] COHEN, B.L., Dubna Symposium on Nuclear Structure, IAEA, Vienna 1968, 3.

[83] MUEHLLEHNER, G., POLTORAK, A.S., PARKINSON, W.C., BASSEL, R.H., Phys. Rev. 159 (1967) 1039.

[84] WHITTEN, C.A., Jr., STEIN, N., HOLLAND, G.E., BROMLEY, D.A., in Nuclear Structure, (Proc. Int. Conf. Tokyo, 1967) Physical Society of Japan (Tokyo 1968) 702; BROMLEY, D.A., ibid. 250

[85] IGO, G.J., BARNES, P.D., FLYNN, E.R., ARMSTRONG, D.D., Los Alamos, to be published (see B.L. Cohen [82]).

[86] ZAIDI, S.A.A. DARMODJ, S., Phys. Rev. Lett. 19 (1967) 1446.

[87] BROMLEY, D.A., WENESER, J., Comm. nucl. Part. Phys. 2 (1968) 151.

[88] ALAGA, G., Trieste, 1969 (these Proceedings).

[89] CINDRO, N., Trieste, 1969 (these Proceedings).

[90] BJERREGAARD, J.H., HANSEN, O., NATHAN, O., CHAPMAN, R., HINDS, S., MIDDLETON, R., Nucl. Phys. A 103 (1967) 33.

[91] GLENDENNING, N.K., Phys. Rev. 156 (1967) 1344.

[92] REYNOLDS, G.M., MAXWELL, J.R., HINTZ, N.M., Phys. Rev. 153 (1967) 1283.

[93] TRUE, W.W., FORD, K.W., Phys. Rev. 109 (1958) 1675.

[94] HOLLAND, G.E., STEIN, N., WHITTEN, C.A. Jr., BROMLEY, D.A., in Nuclear structure, (Proc. Int. Conf. Tokyo 1967) Physical Society of Japan (Tokyo, 1968) 703; BROMLEY, D.A., ibid., 250.

[95] BOHR, A., in Nuclear Structure (Proc. Symp. Dubna 1968), IAEA, Vienna (1968) 179.

[96] NATHAN, O., in Nuclear Structure (Proc. Symp. Dubna 1968), IAEA, Vienna (1968) 191.

[97] BOHR, A., Trieste, 1969 (these Proceedings).

[98] RIPKA, G., Trieste, 1969 (these Proceedings).

SPECTROSCOPIC INFORMATION
FROM NUCLEAR REACTIONS

P. von BRENTANO, M. DOST, H.L. HARNEY
Max-Planck-Institut für Kernphysik,
Heidelberg, Federal Republic of Germany

Abstract

SPECTROSCOPIC INFORMATION FROM NUCLEAR REACTIONS.
    1. Introduction; 2. Spectroscopy with the sub-Coulomb stripping reaction; 3. Inelastic p-scattering via analogue resonances; 4. Conclusion.

1. INTRODUCTION

In this lecture we will discuss the problem of extracting nuclear structure information from nuclear reactions using two examples, namely the (d, p) stripping reactions below the Coulomb barrier and the (pp') reactions via isobaric analogue resonances (IAR) in heavy nuclei.

In the analysis of the cross-section of a particular reaction one must first consider the various reaction mechanisms or reaction modes which can contribute to the measured cross-section. For low-energy reactions the important modes are 1) the resonance reactions; here, one has first to consider statistical fluctuations and doorway resonances as the IAR, and 2) the class of the direct reactions and there one distinguishes between simple reactions and more complicated ones involving, e.g. target excitation [3] or resonances in entrance and exit channels [31]. It is obvious that one can obtain useful information mainly from reactions which are dominated by one particular reaction mode only. Still, in general, the problem of various reaction modes is quite serious because in the cross-section there are interference terms between the various modes, and thus even a reaction mode with a small amplitude can largely influence the cross-section.

For the reactions to be considered in this paper the analysis proceeds in two steps: 1) one parametrizes the cross-section with a small set of unambiguously determined reaction widths G and g. These parameters are model independent. 2) From the reaction widths G and g one can derive spectroscopic factors S by using additional information on the wave functions inside the nucleus.

2. SPECTROSCOPY WITH THE SUB-COULOMB STRIPPING REACTION

The cross-section of the one-step (d, p) stripping reaction $I_1 + d \xrightarrow{j} I_2 + p$ is usually decomposed [1] into a single-particle cross-section $\sigma_{\ell j}^{s.p.}$ and a spectroscopic factor $S_{I_1 j}^{I_2}$

$$\frac{d\sigma}{d\Omega} (I_1 \rightarrow I_2, \theta) = \frac{2 I_2 + 1}{2 I_1 + 1} \sum_j \frac{1}{2j + 1} \; S_{I_1 j}^{I_2} \; \sigma_{\ell j}^{s.p.} (\theta) \tag{1}$$
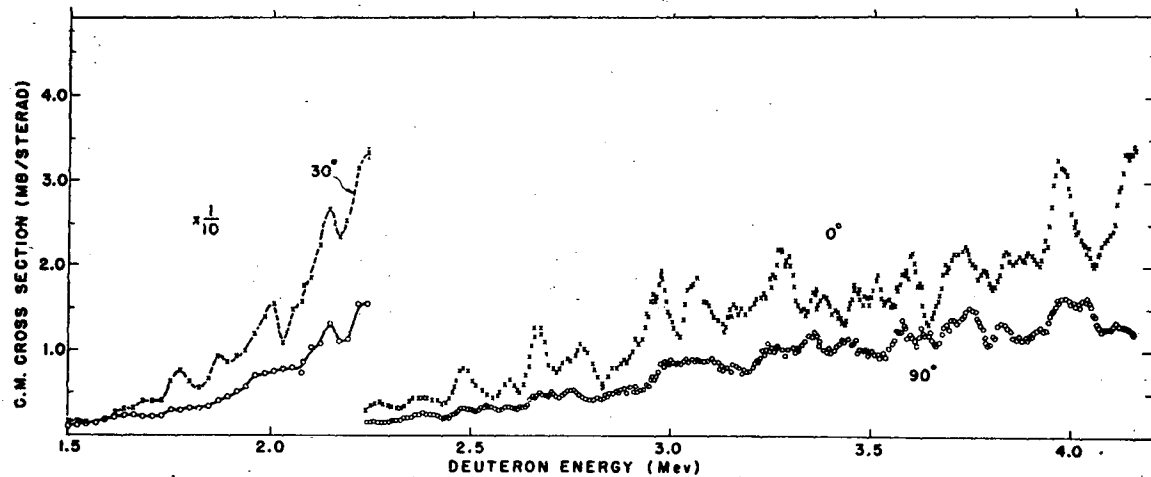
FIG. 1.   Excitation function of ^{40}Ca (d, p) ^{41}Ca showing statistical fluctuations which interfere with the direct process. From Lee and Schiffer, Ref. [29].

where

$$(S_{I_1j}^{I_2})^{\frac{1}{2}} = \langle I_2 M_2 | (a_j^+ \otimes I_1)_{I_2 M_2} \rangle (-1)^{+I_2 - j - I_1} \qquad (2)$$

In Eq. (1) all angular and energy dependences are contained in the single-particle cross-sections, which are, however, assumed to be independent of the spins I_1, I_2 and the nuclear structure of the states I_1 and I_2. The nuclear-structure information is then contained in the spectroscopic factors $S_{I_1j}^{I_2}$. The spectroscopic usefulness of expression (1) depends on two conditions:

(1) Is the factorization valid? For this, at least, rearrangements in the core and polarizing interactions in the initial and final channels have to be neglected. This means that the reaction must be a one-step-process, and contributions from statistical reactions must be negligible. A case where these contributions are important is shown in Fig. 1.

(2) How accurately can $\sigma_{\ell j}^{s,p}$ either be taken from experiment or be calculated theoretically?

We want to discuss the second point first and rely on the validity of a DWBA-description of the process. Thus, we ask only how well the ingredients to the single-particle amplitude in DWBA-approximation [2], i.e.

$$\sigma_{\ell j}^{s,p} = \frac{m_d m_p}{(2\pi \hbar^2)^2} \frac{k_p}{k_d} \frac{1}{3} \sum_{m, \mu_p, \mu_d} |\langle \chi_p^{(-)} (\vec{r}_p, \mu_p) \Phi_{\ell j}^m (\vec{r}_n) | V_{np} | \chi_d^{(+)} (\vec{r}_d, \mu_d) \rangle |^2 \qquad (3)$$

can be taken from experiment or be calculated. Although this is merely concerned with the applicability of a given theory and, therefore, hardly seems to be an ambitious question we will learn about some serius restrictions.

In Eq. (3), $\chi_p^{(-)}$, $\chi_d^{(+)}$ are the elastic scattering functions for the proton and deuteron, respectively, which we take for simplicity relative to an infinitely heavy target or residual nucleus. The scattering functions $\chi_p^{(-)}$ and $\chi_d^{(+)}$ are usually calculated from optical potentials that fit the elastic-scattering angular distributions for the appropriate targets and energies. However, elastic scattering only determines the asymptotic behaviour of the wave functions, i.e. the phase shifts which, in turn, can be reproduced by various different potentials (sometimes referred to as potential "families"). Thus the integration in Eq. (3) extends over the nuclear interior, where $\chi_p^{(-)}$, $\chi_d^{(+)}$ are not uniquely known from scattering experiments, and therefore introduces some ambiguity into the calculation of $\sigma_{\ell j}^{s,p}$. The function $\Phi_{\ell j}^m$ in Eq. (3) is called "the wave function of the transferred neutron" and it is defined by $\Phi_{\ell j} = \phi_{\ell j}^m \cdot \mathcal{Y}_{\ell jm}$ and

$$\langle I_2 M_2 | \psi^\dagger (\vec{r}_n) | I_1 M_1 \rangle = g (\vec{r}_n, \sigma_n)$$

$$\qquad (4)$$

$$= \sum_{\ell, j, m} (I_1 M_1 j m | I_2 M_2) \mathcal{Y}_{\ell jm} (\vec{r}_n, \vec{\sigma}_n) (S_{I_1j}^{I_2})^{\frac{1}{2}} \phi_{\ell j} (r_n)$$

where $\psi^\dagger (\vec{r}_n)$ creates a neutron at the location $\vec{r}_n$ and

$$\langle \Phi_{\ell j}^m (r) | \Phi_{\ell j}^m (r) \rangle = 1$$

In this equation, $S_{I_1 j}^{I_2}$ is the spectroscopic factor and $|I_1 M_1\rangle$, $|I_2 M_2\rangle$ are the true wave-functions of the initial and final states. The form factor $\phi_{\ell j}$ is also implicitly appearing in the formal definition of the spectroscopic factor given in Eq. (2). In principle, $\phi_{\ell j}$ is defined by Eq. (4). However, this equation does not give a practical method for obtaining it. Instead, one can use the "separation-energy method" by Pinkstone and Satchler [4]. In their method $\phi_{\ell j}$ is approximated by the eigenfunction $\phi_{\ell j}^{mod}$ of a single neutron in a real well, having the experimental separation energy E_B. The wave function $\phi_{\ell j}^{mod}$ obviously depends on E_B and the potential parameters, namely the r.m.s radius $\langle R_n^2 \rangle$ and the diffuseness a. It has been shown [5] that the dependence on the diffuseness a is rather weak if the r.m.s radius is kept fixed.

It seems that one can avoid the problems of the optical model wave function in the nuclear interior by the relative method, which is directly based on Eqs (1) and (2): one does not calculate $\sigma_{\ell j}^{s.p.}$ from an arbitrary model, but rather takes it from the experiment on a neighbouring nucleus whose spectroscopic factors are believed to be known. An example for this method is given in column 3 of Table I, where the spectroscopic factors from the ^{207}Pb(d, p) measurement of Bardwick and Tickle [7] are compared with sum rule limits. The $\sigma_{\ell j}^{s.p.}$ values were taken from the ^{208}Pb (d, p) cross-sections as shown in Fig. 2 under the assumption of pure single-neutron configurations in ^{209}Pb. The agreement, however, turns out to be not quite satisfactory (up to about 45% deviation). Part of this discrepancy certainly comes from the fact that the authors did not correct for the differences in binding energy which enter into the $\sigma_{\ell j}^{s.p.}$ via the $\phi_{\ell j}$ function. To do this they would have to calculate the $\sigma_{\ell j}^{s.p.}$, i.e. they would have to do a full DWBA-calculation.

The relative method has, however, a limited range of application, because $\sigma_{\ell j}^{s.p.}$ depends on two independent energies E_d and E_B or E_d and E_p. Thus, the relative method can work only if the corresponding configurations

TABLE I.   COMPARISON OF THE SPECTROSCOPIC FACTORS

$S^* = \left\{ \dfrac{2J}{2} S_{\frac{1}{2}J}^{J-\frac{1}{2}} + \dfrac{2J+2}{2} S_{\frac{1}{2}J}^{J+\frac{1}{2}} \right\}$ from the ^{207}Pb(d, p) ^{208}Pb reaction obtained

by the relative method [7] and the sub-Coulomb stripping [6] with sum rule limits.

Configuration		Dost and Hering[a] S^*		Bardwick and Tickle[b] S^*		Sum Rule S^*
$d_{\frac{3}{2}}$	$p_{\frac{1}{2}}^{-1}$	3.68	(-8%)	2.15	(-46%)	4
$g_{\frac{7}{2}}$	$p_{\frac{1}{2}}^{-1}$	8.33	(+4%)	5.85	(-27%)	8
$s_{\frac{1}{2}}$	$p_{\frac{1}{2}}^{-1}$	2.30	(+15%)	1.8	(-10%)	2
$d_{\frac{5}{2}}$	$p_{\frac{1}{2}}^{-1}$	5.99	(-)	5.2	(-13%)	6
$g_{\frac{9}{2}}$	$p_{\frac{1}{2}}^{-1}$	11.38	(+14%)	10.4	(+3%)	10

[a] Ref. [6]

[b] Ref. [7]
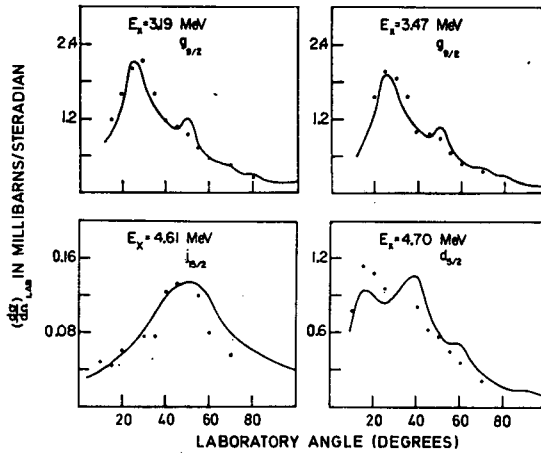
FIG. 2. ^{207}Pb(d, p) ^{208}Pb angular distribution [7] at E_d = 21.6 MeV together with fits according to the "relative method" using single-particle cross-sections $\sigma^{s.p.}_{\ell j}$ obtained from the ^{208}Pb(d, p) ^{209}Pb experiment. From Bardwick and Tickle, Ref. [7].

in the neighbouring nuclei have nearly the same excitation energy E_B and if none of them is spread out very much.

At this point we must emphasize that DWBA-analyses successfully fitting the sum rules are by now quite common; a typical example is the analysis of ^{40}Ca(d, p) by Lee and Schiffer [29]. But in this paper we want to consider reactions which are simpler because their analysis requires less additional information on the wave functions inside the nucleus.

Another way to avoid these problems is to use deuteron beams with energies below the Coulomb barrier as shown, e.g. in Refs [6, 8 - 12, 21]. In this case the contributions to the radial integral (3) entirely come from the surface region around the nucleus (see Fig. 3). The form factor $(S^{I_2}_{I_1 j})^{\frac{1}{2}} \phi_{\ell j}$ has there its asymptotic form

$$(S^{I_2}_{I_1,j})^{\frac{1}{2}} \phi^m_{\ell j} (\vec{r}_n) = C^{I_2}_{I_1,j} h^{(1)}_\ell (i k_B r_n) \mathscr{Y}_{\ell j m} (\vec{r}_n)$$

$$= (S^{I_2}_{I_1,j})^{\frac{1}{2}} C^{s.p.}_{\ell j} h^{(1)}_\ell (i k_B r_n) \mathscr{Y}_{\ell j m} (\vec{r}_n)$$
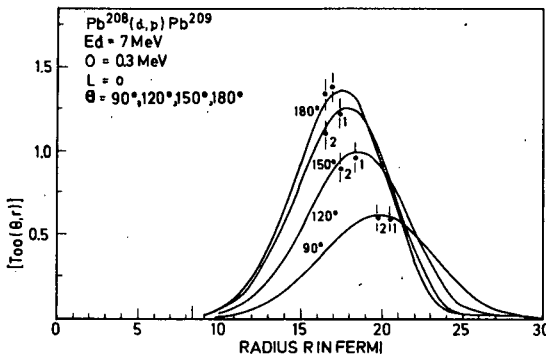
FIG. 3. Radial distribution of the integrand in Eq. (3) in a pure Coulomb stripping case for various reaction angles. From Goldfarb, Ref. [8].

We introduce Coulomb functions $\psi_p^{(-)\,\text{Coul}}$, $\psi_d^{(+)\,\text{Coul}}$ for the optical model wave functions $\chi_p^{(-)}$, $\chi_d^{(+)}$ in Eq. (3), we use a zero-range-interaction $V_{np} = \overline{V}_{np}\,\delta\,(\vec{r}_n - \vec{r}_p)$ and perform the summations over μ_p, μ_d. (In contrast to $\chi_p^{(-)}$ and $\chi_d^{(+)}$ the functions $\psi_p^{(-)\,\text{Coul}}$ and $\psi_d^{(+)\,\text{Coul}}$ shall not contain the spinors for proton and deuteron, respectively.) One then obtains from Eqs (2) and (3)

$$\frac{d\sigma}{d\Omega} = \pi\,\chi^2\,\frac{2\,I_2+1}{2\,I_1+1}\sum_j\,\frac{1}{(2j+1)}\,(G_{I_1,\,j}^{I_2})^2\,\widetilde{\sigma}_{\ell j}^{\,\text{s.p.}}$$

where

$$\widetilde{\sigma}_{\ell j}^{\,\text{s.p.}} = \frac{1}{2\pi}\,\frac{m_p\,m_d\,k_p k_d}{(2\pi\hbar^2)^2}\,A$$

$$A = \sum_{m,\mu_n}\left| \langle \psi_p^{(-)\text{Coul}}(\vec{r})\,h_\ell^{(1)}(i\,k_B r)\sum_{m_\ell}\,(\ell m_\ell\,\tfrac{1}{2}\,\mu_n|jm)\,Y_\ell^{m_\ell}(\hat{r})\,|\,\psi_d^{(+)\text{Coul}}(r)\rangle\right|^2$$

and $G_{I_1,\,j}^{I_2}$ contains $\overline{V}_{np}$, the value $\phi_d\,(0)$ of the internal deuteron wave function at the origin and the normalization $C_{I_1,\,j}^{I_2}$ of the neutron wave function:

$$G_{I_1,\,j}^{I_2} = \overline{V}_{np}\,\phi_d\,(0)\,C_{I_1,\,j}^{I_2}$$

There are only known functions in $\widetilde{\sigma}_{\ell j}^{\,\text{s.p.}}$, so $G_{I_1,\,j}^{I_2}$ is the quantity which one measures when doing a (dp) sub-Coulomb-experiment. The first two factors in G are common to all stripping experiments, the last factor contains the spectroscopic information.

    There are close analogies between G^2 and the partial width Γ in resonance reactions, it even has the proper dimension and this is the reason why we call G a reaction width. From $G_{I_1,\,j}^{I_2}$ we get the normalization $C_{I_1,\,j}^{I_2}$ of the asymptotic neutron wave function with the accuracy to which the constant $\overline{V}_{np}\,\phi_d\,(0)$ is known.. The quantity $C_{I_1,\,j}^{I_2}$ can be reduced to the spectroscopic factor according to

$$C_{I_1,\,j}^{I_2} = C_{\ell j}^{\text{s.p.}}\,(S_{I_1,\,j}^{I_2})^{\frac{1}{2}}$$

only if the asymptotic normalization $C_j^{\text{s.p.}}$ of the single-particle wave function $\phi_{\ell j}^{\text{s.p.}}$ is known. Though $\phi_{\ell,\,j}^{\text{s.p.}}$ is defined through Eq. (4) by using the physical wave functions of the target and residual nuclei only, it has in all practical cases to be approximated by a single particle shell model wave function. Thus the normalization $C_{I_1,\,j}^{I_2}$ can be measured directly while the spectroscopic factor $S_{I_1,\,j}^{I_2}$ cannot be extracted without the use of a potential model and, hence, will depend on the parameters discussed above. Numerical examples may be found in Refs [12] and [22]. A rather interesting extension of these ideas is quasi-Coulomb stripping [11]. In this case we still postulate that only the asymptotic parts of $\chi_p^{(-)}$, $\chi_d^{(+)}$ and $\phi_{\ell j}$ enter into the integral of Eq. (3) but we do not postulate that ψ_p and ψ_d are Coulomb waves. This extension is meaningful because the asymptotic part of the χ's is determined by the elastic-scattering phase shifts only and can thus be uniquely measured.
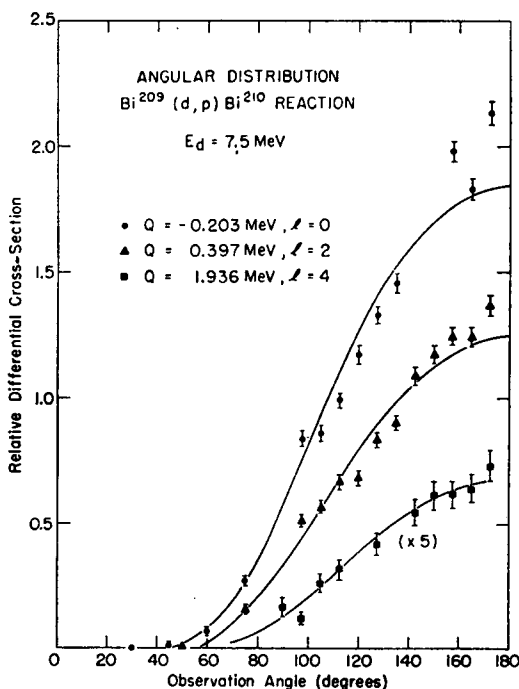
FIG. 4. Typical Coulomb-stripping angular distribution with DWBA-fit. From Erskine, Buechner and Enge. Ref. [10].

From an experimental point of view Fig. 5 shows that the cross-section is much more favourable in this case and thus, it is this reaction which is most often used.

Summing up we want to emphasize the following points on "quasi Coulomb stripping":

(1) Typical differential cross-sections are of the order of 100 $\mu b/sr$, so such experiments are quite feasible with spectrographs, especially with spectrographs having large solid angles.

(2) The angular distributions have a broad maximum at 180° irrespective of the orbital angular momentum ℓ as shown in Fig. 4. However, one can determine ℓ-values either at high energies, where it is easy to distinguish them as shown, e. g., in Fig. 2 or by an ingenious method of Hering et al. [9] using the excitation functions.

(3) The DWBA gives excellent fits to the excitation functions (Fig. 5) and angular distributions (Fig. 4) with a proportionality factor G^2 as the only free parameter. This excellent agreement is a real test and great success of the DWBA-theory and removes some doubts as to the effects of the polarization of the deuteron in sub-Coulomb stripping (see Ref. [12]).

(4) From the comparison the theoretical and experimental cross-section the parameter G^2 is unambiguously determined. The normalization C^2 of the asymptotic part of the neutron wave function $\phi_{\ell j}$ can be derived with the precision to which the univeral factor $\overline{V}_{np} \phi_d (0)$ is known.
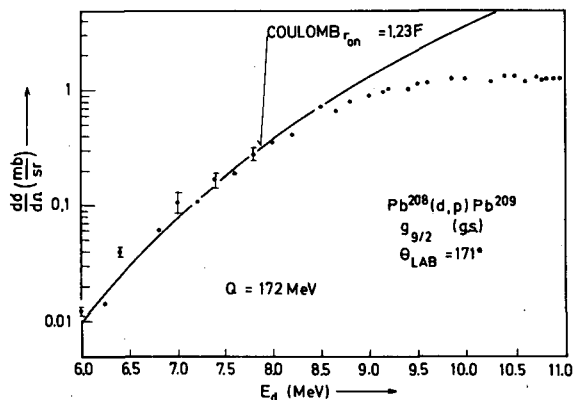
FIG. 5.   Typical Coulomb stripping excitation function with a DWBA-fit using pure Coulomb functions
(from Ref. [13]).   The region around 10 - 11 MeV is the region of quasi-Coulomb stripping.   From Hering
and Dost, Refs [6, 9].
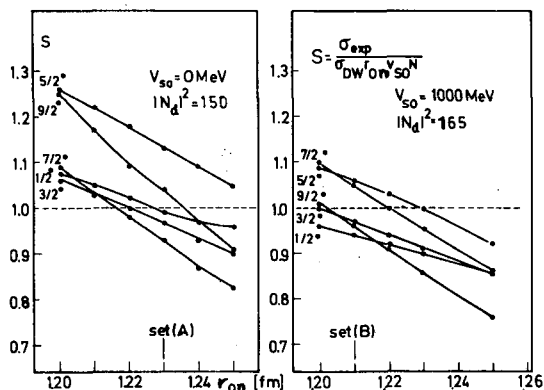
FIG. 6.   Dependence of the spectroscopic factors on the bound state radius $\langle R_n^2 \rangle$ for a given normalization C.
The separation energy method is used and the normalization C and the diffuseness a are kept fixed.   Dost and
Hering, Ref. [22].

(5) As can be seen from Eq. (4) one can unambiguously relate S to C^2
     if the shape of the form factor ϕ is known from a nuclear-structure
     calculation.   If this shape is calculated from the separation-energy
     method then the r. m. s. radius of the neutron potential R_n^2 must
     be known.   As shown in Fig. 6, S depends rather sensitively on R_n^2.

(6) As the bombarding energy for a quasi-Coulomb stripping experi-
     ment is rather low, contributions form statistical reactions be-
     come important in light to medium nuclei.   This is shown for
     example in Fig. 1.   Thus quasi-Coulomb stripping is primarily
     interesting for heavy nuclei.

(7) At the low bombarding energies the elastic cross-section dominates
     all inelastic cross-sections and thus two-step-processes as the
     excitation of an inelastic level with subsequent stripping become
     completely negligible.   This is again a valuable aspect of quasi-
     Coulomb stripping.

(8) The success of the DWBA for quasi-Coulomb stripping also shows
that the DWBA properly predicts the dependence of the cross-
section on the bombarding energy and the Q-value of the reaction.
Thus the DWBA method gives reliable ratios of spectroscopic
factors. If a complete spectrum is measured, one can then apply
sum rules to obtain absolute spectroscopic factors from the relative
ones, and this is the usual method.

3. INELASTIC P-SCATTERING VIA ANALOGUE RESONANCES

As an example of resonance spectroscopy we discuss the spectroscopic
information which one can obtain from the proton decay of isobaric analogue
resonances in heavy nuclei. The scattering matrix element describing an
isolated resonance is given by a Breit-Wigner expression:

$$\langle S_{cc'} \rangle = S_{cc'}^{D} - i \frac{g_c \, g_{c'}}{E - E_0^J + \frac{1}{2} \Gamma^J} \tag{5}$$

where the background scattering term $S_{cc'}^{D}$ is nearly energy-independent.
The indices c, c' stand for the quantum numbers which specify the channels.
The transition amplitudes g_c and $g_{c'}$ are complex numbers: $g_c = \exp(i\delta_c)\Gamma_c^{\frac{1}{2}}$,
where $\Gamma_c^{\frac{1}{2}}$ is a real number, whose sign is not necessarily positive. For
channel energies below the Coulomb-barrier, δ_c is the Coulomb phase-shift.
The IAR's in heavy nuclei have a fine structure and the brackets $\langle \ \rangle$ in
Eq. (5) denote an average over an interval which is large compared to the
width of the fluctuations and small compared to the total resonance with Γ^J.
The non-averaged matrix element is then $S_{cc'} = \langle S_{cd'} \rangle + S_{cc'}^{f\ell}$, thus
one obtains a simple picture only if $\langle |S_{cc'}^{f\ell}|^2 \rangle \ll |\langle S_{cc'} \rangle|^2$, because in this
case the fluctuating part can be neglected. This is usually possible for
strong IAR in (p, p_0) and (p, p') in heavy nuclei above about A =140. Under
this assumption and if one can also neglect the direct part $S_{cc'}^{D}$ one obtains
an explicit expression for the differential cross-section from Eq. (5). For
the reaction sequence $I_0 + p \xrightarrow{j_0} J \xrightarrow{j} I + p'$ one gets [14,15] the cross-
section formulae (6).
In Eq. (6) we have assumed that $I_0 = 0$, $j_0 = J$, and that $I_0, J, I, j, \bar{j}$ are
the spins of the target, resonance, final state and the transferred particles
respectively:

$$\frac{d\sigma}{d\Omega} = \frac{1}{2} \sum_{M, \mu', \mu} | A (M, \mu', \mu) |^2 \tag{6a}$$

where

$$A(M', \mu', \mu) = -i \, \pi^{\frac{1}{2}} \lambdabar \, \frac{g_{0j}^{J}}{E - E_0^J + \frac{i}{2} \Gamma^J} \, (2\ell + 1)^{\frac{1}{2}}$$

$$\times \sum_{j} g_{Ij}^{J} \sum_{M_J, m_j, m} (\ell \, 0 \, \tfrac{1}{2} \, \mu \,|\, J \, M_J) \, (I \, M \, j \, m_j \,|\, J \, M_J)$$

$$\times (\ell \, m \, \tfrac{1}{2} \, \mu' \,|\, j \, m_j) \, Y_{\ell m}(\theta, \phi)$$

This may be written

$$\frac{d\sigma}{d\Omega} = \pi \lambdabar^2 \frac{\Gamma_{0I}^J}{(E - E_0^J)^2 + (\Gamma^J/2)^2} \sum_{L=0, 2, 4, \ldots} P_L (\cos \theta)$$

$$\times \sum_{j, \vec{j}} B(j, \vec{j}, L) (\Gamma_{Ij}^J \; \Gamma_{I\vec{j}}^J)^{\frac{1}{2}} \cos (\delta_{Ij}^J - \delta_{I\vec{j}}^J)$$

where the $B(j, \vec{j}, L)$ are geometrical coefficients [15]. The Γ_{Ij}^J are widths for the decay $J \xrightarrow{j} I$; and Γ_{0j}^J is the elastic-scattering width.

The expression for the integrated cross-section is particularly simple

$$\int \frac{d\sigma}{d\Omega} \, d\Omega = \frac{1}{2} \pi \lambdabar^2 (2 J + 1) \frac{\Gamma_{0J}^J \sum_{i} \Gamma_{Ij}^J}{(E - E_0^J)^2 + (\Gamma^J/2)^2} \tag{7}$$

In Fig. 7 we show some typical excitation functions. It is seen that there are clearly cases, as, e.g. the excitation function to the ^{208}Pb(4^-) state, where the direct reaction mode can be neglected and the resonance has a Lorenz-shape as given by Eq. (7). But there are other cases, as e.g. the ^{208}Pb(3^-) states, where the direct amplitude must be taken care of.

It is obvious from Eq. (7) that from a measurement of the elastic and inelastic scattering one can directly determine the widths Γ^J, Γ_{0j}^J and the
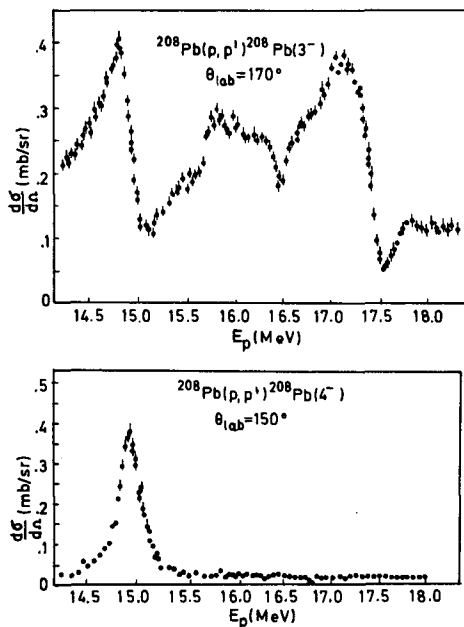
FIG. 7. Excitation functions of ^{208}Pb(p, p')^{208}Pb. The resonance at E_p = 14.91 MeV is the analogue of the $g_{\frac{9}{2}}$ g.s. of ^{209}Pb. From Zaidi et al., Ref. [23].

integrated width $\sum_j \Gamma_{Ij}^J$. Such a determination is unique and unambiguous and can be done if one can neglect competing reaction modes as the fluctu- ating and direct ones. If the phases δ_c are known, e.g. if they are Coulomb phases and if the number of widths Γ_{Ij}^J which contribute to the angular distribution is small, then one can also obtain the individual $(\Gamma_{Ij}^I)^{\frac{1}{2}}$ from a fit to the angular distribution [14-16]. While in one-nucleon transfer
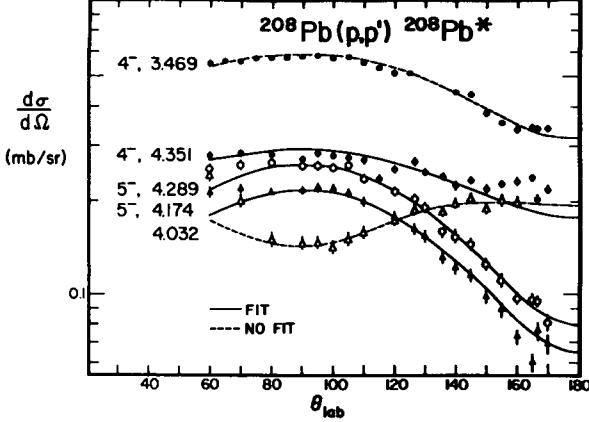
FIG. 8. Angular distributions for the ^{208}Pb(p, p') ^{208}Pb (E_x, I) leading to different final states measured on top of the g$\frac{9}{2}$ resonance at $E_p = 14.91$ MeV shown in Fig. 7. The fit is made using the Legendre polynomials P_0, P_2 and P_4. From Richard et al., Ref. [24].

reactions and in the integrated resonance cross-section the widths $(\Gamma_{Ij}^J)^{\frac{1}{2}}$ corresponding to different transferred angular momenta j add incoherently, they add coherently in the angular distribution and one can thus determine also the relative signs of the widths $(\Gamma_{Ij}^J)^{\frac{1}{2}}$. From a set of such widths $(\Gamma_{Ij}^J)^{\frac{1}{2}}$ for a given final state I one then can obtain an expansion of this state in various configurations as has been shown e.g. by Bondorf et al. [14] and Heusler et al. [15]. Some typical angular distributions measured on top of the g$\frac{9}{2}$ resonance in ^{209}Bi are shown in Fig. 8. The fits are made with the Legendre polynomials P_0, P_2 and P_4 which completely describe the angular distribution.

The spectroscopic use of the (p, p') reaction via IAR, comes from the fact that the analogue state and the parent state are both members of an isobaric multiplet and thus have the same internal structure. For a more complete discussion of the resonance reactions via IAR we refer to the Tallahassee conference on isospin [34] and to an article by G.M. Temmer [33]. The proton width $(\Gamma_{Ij}^J)^{\frac{1}{2}}$ of the IAR with spin J is proportional to the neutron width $G_{I,j}^J$ connecting the parent state J with the final state I. A schematic illustration of this relation is given in Fig. 9.

$$(\Gamma_{Ij}^J)^{\frac{1}{2}} = (\Gamma_j^{\text{s.p.}})^{\frac{1}{2}} G_{Ij}^J / G_j^{\text{s.p.}}$$

$$= (\Gamma_j^{\text{s.p.}})^{\frac{1}{2}} (S_{Ij}^J)^{\frac{1}{2}} \tag{8}$$

$$= (\Gamma_j^{\text{s.p.}})^{\frac{1}{2}} \langle J | (a_j^+ \otimes I)_J \rangle (-1)^{(J-j-I)}$$

TABLE II. COMPARISON OF THE INTEGRATED WIDTH $\sum_{\alpha I} \Gamma^J_{\alpha I j} (E_0)$ (CORRECTED FOR THE CHANNEL ENERGY ACCORDING TO Eq. (9) FROM THE DECAY OF THE $g_{9/2}$ RESONANCE [24] INTO STATES IN ^{208}Pb WITH THE SINGLE-PARTICLE WIDTH $(2j+1)$ $\Gamma^{s.p.}_j$ OBTAINED FROM THE DECAY [28,30] OF THE 0^+ GROUND-STATE ANALOGUE IN ^{208}Bi TO THE SINGLE-HOLE STATES IN ^{207}Pb.

Number of states with $\Gamma_{p'} > 2$ keV	E^{min} to E^{max} (MeV)	$\sum_{\alpha I} \Gamma^J_{\alpha I j}$	Assigned configurations		$(2j+1)\, \Gamma^{s.p.}_j \, (E^{s.p.}_j)$	$\tilde{E}_{exp}$ (MeV)	$E^{s.p.}_j$ (MeV)
3	3.0 - 3.8	55.8 keV	$g_{9/2}$	$p^-_{1/2}$	57.2	3.375	3.430
5	3.8 - 4.15	25 keV	$g_{9/2}$	$f^-_{5/2}$	33	3.994	4.000
6	4.15 - 4.8	62.4 keV	$g_{9/2}$	$p^-_{3/2}$	56	4.37	4.324
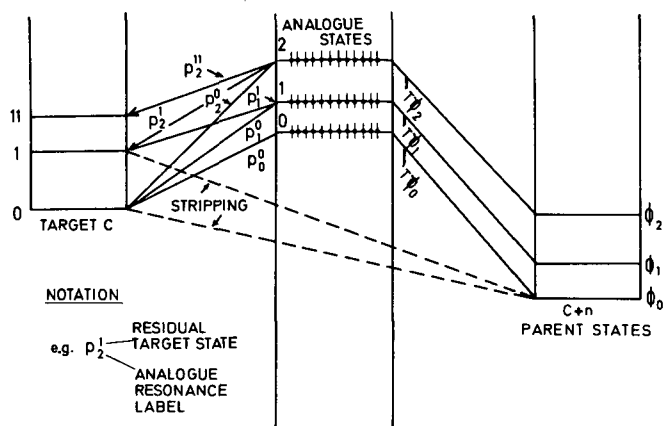
FIG. 9.   Relation of the compound nucleus (C+p) and corresponding parent states in the nucleus (C+n) to states in the nucleus C.

As is seen in Eq. 8 the study of IAR gives the same spectroscopic factors, which we would get from stripping and pick-up reactions on a target in an excited state if such an experiment were possible. The possibility of doing it via the (p, p') reaction is the main reason for the study of the resonant (p, p') reaction.   The factorization of the width Γ_{Ij}^{J} into a spectroscopic factor S and a single-particle width $\Gamma_{j}^{s.p.}$ is the reason for the strong selectivity of the resonant (p, p') reaction.   A beautiful example of this selective excitation is shown in the spectra (Fig. 10) obtained from the ^{208}Pb(p, p')^{208}Pb reaction measured at energies corresponding to various IAR in ^{209}Bi. Indeed, different groups of neutron particle-hole states are excited in different resonances.

The relation (8) is obviously only valid if the resonance decays in one step $J \xrightarrow{1} I$.   It is not valid if the final state is reached by a two-step reaction. Such more complicated reactions apparently exist as shown by Hamburger [17] who observed the isospin-forbidden excitation of analogue resonances in (d, p) stripping reactions.   An example is shown in Fig. 11.   Since the excitation of the IAR is isospin-forbidden in this case, Tamura [31] has suggested that the reaction must be interpreted as an elastic or inelastic resonance reaction followed by a pick-up reaction: ^{208}Pb + p $\rightarrow$ ^{209}Bi $\rightarrow$ ^{208}Pb + p $\rightarrow$ ^{207}Pb + d.

For the quantitative determination of spectroscopic factors S one must know the single particle decay width $\Gamma_{j}^{s.p.}$, which is the width of an isobaric analogue of a single-particle state.   Again one can try a relative method and obtain the single-particle widths from the resonance scattering on a neighbouring nucleus where the spectroscopic factor is known.   In Table II we give a comparison of the summed decay strengths of the $g_{\frac{9}{2}}$ IAR in ^{208}Pb + p to the sum rule limits derived from the decay of the 0^{+} g. s. analog resonance in ^{207}Bi + p.   In Fig. 12 we show a comparison of a set of integrated widths with theoretical widths obtained from the wave functions by Kuo and Brown [27].   Single-particle widths obtained by the relative method were used.   In making these comparisons one has to correct for the energy dependence of the single-particle with $\Gamma_{j}^{s.p.}$.

In the cases where the channel energy is below the Coulomb barrier, this correction is usually done by using Coulomb penetration factors as
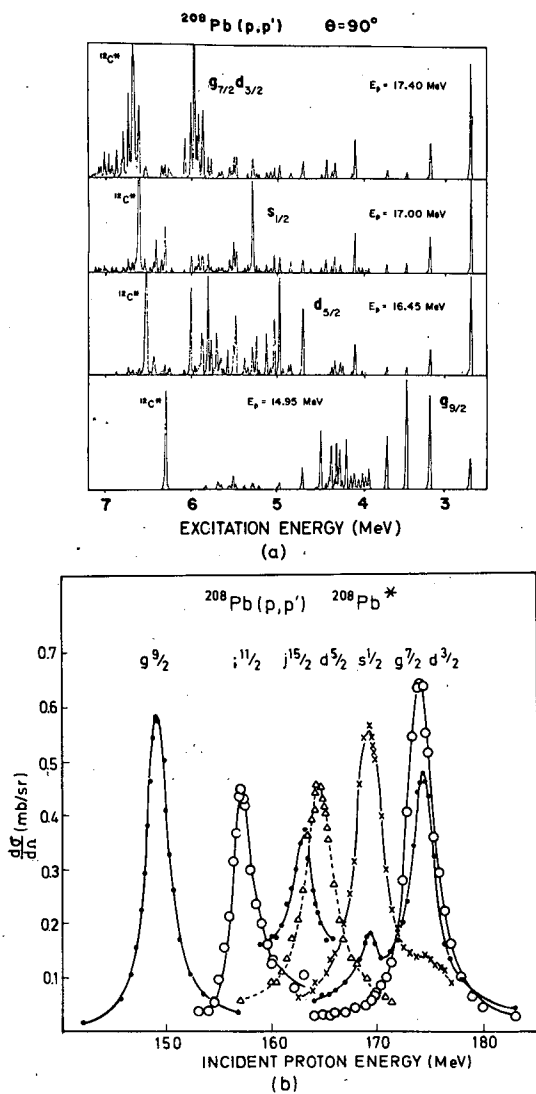
FIG. 10.   Inelastic proton spectra from ^{208}Pb at four bombarding energies corresponding to successive single-particle analogue states in ^{209}Pb.   We emphasize the selective character of the reaction: a given level is strongly excited in one resonance only.   From Moore et al., Ref. [25], and Brentano et al., Ref. [32].

shown in Eq. (9)

$$\Gamma_{\ell j}^{s.p.} = \frac{P_\ell (E_p, R_0)}{P_\ell (E_p{}', R_0)} \; \Gamma^{s.p.}(E_p{}')$$ (9)

where

$$R_0 \approx 1.4 \; A^{\frac{1}{3}} \; fm$$
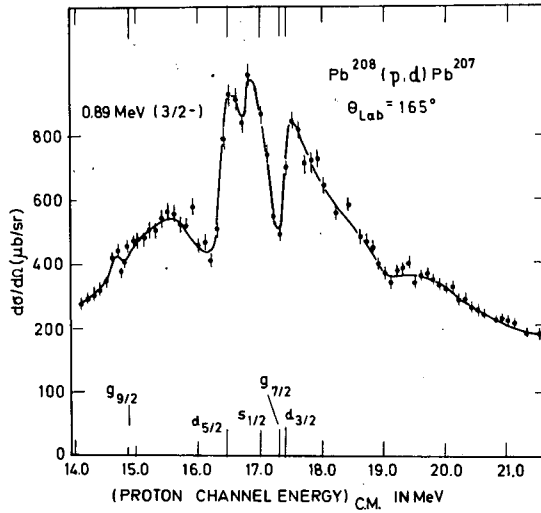
FIG. 11. Excitation function of ^{208}Pb(p, d) ^{207}Pb. This is an example of a resonance reaction followed by a direct excitation as discussed in the text. From Stein et al., Ref. [26].
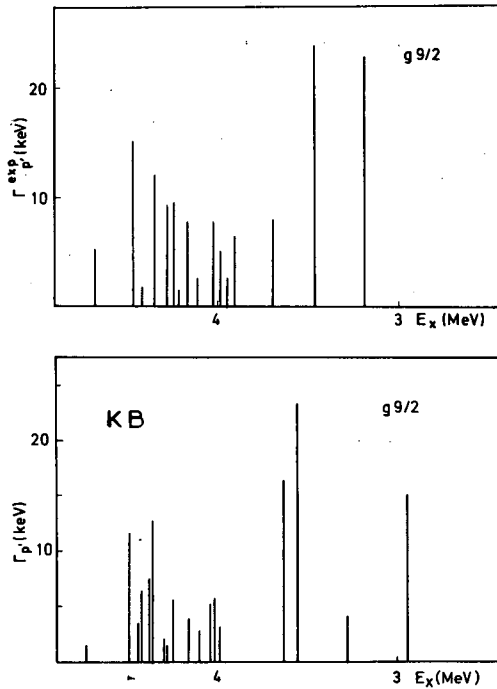
FIG. 12. The upper figure gives the width $\sum_{j}\Gamma_{\Gamma j}^{\frac{9}{2}}$ from the decay of the $g\frac{9}{2}$ resonance in ^{209}Bi to various states in ^{208}Pb obtained from angular distributions of ^{208}Pb (p, p:) shown in Fig. 8. Also shown is a calculation of these widths using the wave functions of excited states in ^{208}Pb by Kuo and Brown [26] and single-particle widths obtained by the relative method as discussed in the caption to Table II. From Richard et al., Ref. [27].

This procedure is, however, only approximate because the energy dependence on the bound-state wave function is not included. For the calculation of $\Gamma_j^{s.p.}$ different theories [18] all result with an expression which is up to minor corrections [19] equivalent to [20]

$$g_{\ell j}^{s.p.} = \exp\left(i\eta_{\ell j}\right)\left\langle\phi_{\ell j}^{(n)}(r)\left|V_c(r) - \Delta_c\right|\chi_{\ell j}^{(p)}(r)\right\rangle(\pi/\tau_0)^{\frac{1}{2}} \qquad (10)$$

Here, $\phi_{\ell j}^{(n)}$ is the single-particle neutron wave function for the parent state J; $\chi_{\ell j}^{(p)}$ is the optical-model proton wave function in the decay channel I + p having the (complex) scattering phase shift $\eta_{\ell j}$ and being normalized to a δ-function:

$$\left\langle\chi_{\ell j}^{(p)}(E)\left|\chi_{\ell j}^{P}(E')\right.\right\rangle = \delta(E - E') \qquad (11)$$

$V_c(r)$ is the Coulomb potential acting on the outgoing proton, Δ_c is the Coulomb-energy difference minus the proton-neutron mass difference, and it is known from the energies of the analogue state and its parent state. T_0 is the isospin of the state I. In general, the calculation of $g_{s.p.}$ again requires additional knowledge about potential parameters, as shown in Eq. (10). While a careful analysis of the proton scattering will determine many of these parameters the radii of the neutron potential and the proton potential are less well determined. The s. p. Coulomb potential depends on the charge radius, which can be taken from electron scattering. An example [19] of a comparison between spectroscopic factors from elastic scattering and (d, p) reactions on the same target is shown in Table III.

In analogy to the situation in the stripping reactions considerable simplification occurs in the calculation of $g_{s.p.}$ if the channel energy is

TABLE III.   COMPARISON OF SPECTROSCOPIC FACTORS S_{dp} FROM THE EXPERIMENTS ^{140}Ce (d, p) AND ^{138}Ba(d, p) WITH SPECTROSCOPIC FACTORS OBTAINED FROM THE ANALYSIS OF ELASTIC-RESONANCE SCATTERING VIA IAR ON THE SAME TARGETS [9]

Target	E_{res} (MeV)	E_x (MeV)	ℓj	$\mathscr{S}_{pp}$	$\mathscr{S}_{dp}$
^{138}Ba	10.02	0	$f_{\frac{7}{2}}$	0.94	0.76
$T_0 = 13$	10.65	0.64	$p_{\frac{3}{2}}$	0.40	0.49
	11.11	1.08	$p_{\frac{1}{2}}$	0.37	0.42
	11.46	1.43	$f_{\frac{5}{2}}$	0.28	0.24
	11.73	1.71	$f_{\frac{5}{2}}$	0.23	0.24
	9.75	0	$f_{\frac{7}{2}}$	0.86	0.89
^{140}Ce	10.40	0.65	$p_{\frac{3}{2}}$	0.42	0.42
$T_0 = 12$	10.88	1.13	$p_{\frac{1}{2}}$	0.28	0.38
	11.25	1.50	$f_{\frac{3}{2}}$	0.27	0.30
	11.49	1.74	$f_{\frac{5}{2}}$	0.25	0.38

well below the Coulomb barrier. In this case the integral in Eq. (10) be-
comes nearly independent of the proton parameters [19] because the
contributions of the nuclear interior become negligible. This case clearly
corresponds to the sub-Coulomb stripping and similar conclusions may be
drawn. Unfortunately the sub-Coulomb case does not seem to be realized
very often. In particular, in contrast to the situation in the (d, p) reaction
where one is free to choose the incident energy, the bombarding energy
for the production of a particular IAR is fixed and thus a consideration of
the non-sub-Coulomb case cannot be avoided.

4. CONCLUSION

We have discussed the problem of spectroscopic information from
resonant (pp') reactions which proceed via IAR and from "quasi-Coulomb"
(d, p) stripping reactions. In both cases the cross-section can be directly
and unambiguously analysed in terms of a set of reaction widths, if only
one reaction mode contributes to it, or if the contributions to the cross-
section from other reaction modes can be suitably taken into account. It is
these widths which a nuclear-reaction theory and a nuclear-structure theory
should try to calculate directly. However, a much more easily interpretable
parameter for nuclear-structure physics is the spectroscopic factor. There
are, as we have discussed, good theories for obtaining the spectroscopic
factors S from the reaction width g and G but additional knowledge on the
form factor and on the optical model wave functions inside the nucleus is
needed to make the calculation of S unique. The ratios of spectroscopic
factors are usually less dependent on the potential parameters and can thus
be determined quite reliably from these reactions. By the use of sum rules
one can obtain also absolute spectroscopic factors.

REFERENCES

[1] BOHR, A., MOTTELSON, B.R., Nuclear Structure; W.A. Benjamin Inc., New York (to be published).
[2] e.g. GLENDENNING, N.K., A. Rev. nucl. Sci. 13 (1963) 191.
[3] AUSTERN, N., Nuclear Structure (Proc. Int. Conf. Tokyo, 1967) Supplement to J. phys. Soc.
    Japan 24 (1968).
[4] PINKSTON, W.T., SATCHLER, G.R., Nucl. Phys. 72 (1965) 641.
[5] SHARPEY-SCHAFER, J.F., Phys. Lett. 26B (1968) 652.
[6] DOST, M., HERING, W.R., Phys. Lett. 26B (1968) 443; HERING, W.R., ACHTERATH, A.D.,
    DOST, M., Phys. Lett. 26B (1968) 568.
[7] BARDWICK, J., TICKLE, R., Phys. Rev. 161 (1967) 1217.
[8] GOLDFARB, L.J.B., in Lectures in Theoretical Physics, 8-C, University of Colorado Press (1966).
[9] HERING, W.R., DOST, M., Nucl. Phys. A111 (1968) 561.
[10] ERSKINE, J.R., BUECHNER, W.W., ENGE, H.A., Phys. Rev. 128 (1962) 720.
[11] GIBSON, F.P., KERMAN, A.K., Phys. Rev. 145 (1966) 758.
[12] RAPAPORT, J., KERMAN, A.K., Nucl. Phys. A119 (1968) 641.
[13] DOST, M., Diplomarbeit, Heidelberg, 1965 (unpublished).

[14] BONDORF, J. P., v. BRENTANO. P., RICHARD, P., Phys. Lett. 27B (1968) 5.

[15] HEUSLER, A., HARNEY, H. L., WURM, J. P. (submitted to Nuclear Physics).

[16] WURM, J. P., HEUSLER, A., v. BRENTANO, P., Nucl. Phys. A128 (1969) 433.

[17] HAMBURGER, E. W., Phys. Rev. Lett. 19 (1967) 36.

[18] e. g. WEIDENMÜLLER, H. A., invited paper given at the Second Conference on Nuclear Isospin at Asilomar (1969) and Refs given there.

[19] HARNEY, H. L., Nucl. Phys. A119 (1968) 591.

[20] BUND, G. W., BLAIR, J. S., Tokyo-Conference (see Ref.[3]), Contributed Paper 8.95.

[21] ZEH, H. D., Nucl. Phys. 75 (1966) 423.

[22] DOST, M., HERING, W. R., Z. Naturf. 219 (1966) 1015.

[23] ZAIDI, S. A. A., PARISH, J. L., KULLECK, J. G., MOORE, C. F., Phys. Rev. 165 (1968) 1312.

[24] RICHARD, P., WEITKAMP, W. G., WHARTON, W., WIEMAN, H., v. BRENTANO, P., Phys. Lett. 26 (1967) 8.

[25] MOORE, C. F., KULLECK, J. G., v. BRENTANO, P., RICKEY, F., Phys. Rev. 164 (1967) 1559.

[26] STEIN, N., COFFIN, J. P., WHITTEN, C. A., BROMLEY, D. A., Phys. Rev. Lett. 21 (1968) 1456.

[27] KUO, T., BROWN, G. E. (private communication).

[28] RICHARD, P., v. BRENTANO, P., WEIMAN, H., WHARTON, W., WEITKAMP, W. G., McDONALD, W. W., SPALDING, D. (submitted to Phys. Rev.)

[29] LEE, L. L., SCHIFFER, J. P., Phys. Rev. 107 (1957) 1340.

[30] LENZ, G. H., TEMMER, G. M., Nucl. Phys. A112 (1968) 625.

[31] TAMURA, T., Nuclear Structure,(Proc. Int. Conf., Tokyo 1967) Suppl. to J. phys. Soc. Japan 24 (1968).

[32] v. BRENTANO, P., DAWSON, W. K., MOORE, C. F., RICHARD, P., WHARTON, W., WIEMAN. H., Phys. Lett. 26B (1968) 666.

[33] TEMMER, G. M., in Fundamentals in Nuclear Theory (Int. Course Trieste. IAEA) 1966 Vienna (1967) 163.

[34] Isospin in Nuclear Physics (FOX, J. D., ROBSON, D., Eds) Academic Press, New York (1966).

PART II

Selected Topics in the Many-Body Description
of Nuclei and Nuclear Reactions

SECTION I

Nuclear Structure

HARTREE-FOCK CALCULATIONS
FOR LIGHT NUCLEI

M. BOUTEN
Centre d'Etude de l'Energie Nucléaire,
Mol-Donk, Belgium

Abstract

HARTREE-FOCK CALCULATIONS FOR LIGHT NUCLEI.
    1. Introduction; 2. Hartree-Fock equations; 3. Solution of the Hartree-Fock equations; 4. Results of
Hartree-Fock equations; 5. Projection operations; 6. Projected Hartree-Fock calculations for $4 \leq A \leq 12$;
7. Results of projected Hartree-Fock calculations for nuclei with $4 \leq A \leq 12$; 8. Collective moments and
transitions. Form factors for high-energy electron scattering.

1. INTRODUCTION

In recent years, Hartree-Fock (HF) calculations have become very
fashionable in nuclear-structure studies. The first calculation appears
to have been made by Nesbet and Ullah [1] for the ground state of ^{16}O.
Soon afterwards, an extensive investigation of most nuclei in the 1s-0d
shell was carried out by Levinson's group at the Weizmann institute,
using an approximation of the usual HF-method. In these calculations only
the particles outside the ^{16}O-core were taken into account, and their orbitals
were restricted to one major oscillator shell. These calculations can best
be looked upon as a HF-approximation to a standard shell-model calculation.
A good review of this work has been given by Ripka [2]. Complete HF-
calculations in which all particles are considered, were made by Baranger
and co-workers for spherical nuclei, and soon afterwards also by many other
people. The aim of these more general calculations is the same as in atomic
physics: starting from the two-body nucleon-nucleon force, one tries to
construct the self-consistent field of the shell model. In this picture, HF-
calculations are only a first step in a complete calculation. Configuration
mixing should be considered afterwards in the HF-basis. This has not been
done so far.
    The basic assumption of the shell model is that the nucleons in the nucleus
behave very much like independent particles, moving in a field created by
the presence of the other nucleons. In practical shell-model calculations,
this average field is chosen in a fairly arbitrary way, containing several ·
parameters which are then adjusted for each nucleus to reproduce good fits
to the experimental data. For example, it is customary to choose a harmonic
oscillator potential, the width of which is adjusted to the experimental
radius, and a one-body spin-orbit force, the strength of which is adjusted
in order to obtain a best fit to the experimental energy spectrum. In this
way, it is clear that part of the success of the shell model is obtained from
the adjustable parameters. In a better theory, one should start from
the nuclear Hamiltonian and construct the shell-model potential from it.
This is the usual procedure in atomic physics where the HF-method is
used to construct the average field. The reason why this method has not

been taken over into nuclear physics up to recently is that realistic inter-
actions between nucleons contain an infinitely repulsive core. This implies
that matrix elements of such an interaction between independently moving
particles become infinite. In recent years, a modification of the HF-method
has been developed for singular potentials. Also, some almost realistic
interactions have been obtained which do not possess a hard core [3,4].

In the next section, a derivation of the HF-equations is given starting
from Schrödinger's variational principle, assuming that the nuclear Hamil-
tonian is not singular. In section 3, we describe the approximations which
are usually made to find actual solutions of the HF-equations, and in sec-
tion 4 we describe some selected results obtained in HF-calculations.
This section is very short indeed compared to the large number of HF-
calculations in the literature. It is mainly given here as an illustration
of what comes out of a HF-calculation; more results are described by
J.P. Svenne in his lectures (these Proceedings).

The main emphasis of these lectures is on the last four sections. Sec-
tion 5 shows when and how an angular momentum projection can be carried
out without too much labour. In section 6, we describe how projected
Hartree-Fock calculations can be made in an approximate way for nuclei
with $4 \leq A \leq 12$. Results for energies and wave functions of such calcula-
tions are described in section 7. Finally, in section 8, these wave func-
tions are tested by calculating several physical quantities, and it is shown
that the enhanced matrix elements of collective moments and transitions
are systematically reproduced.

2. HARTREE-FOCK EQUATIONS

There exist several ways for deriving the HF-equations (see Baranger's
Varenna notes 1967 [5]). Here we will follow the conventional method [6],
which is based on Schrödinger's variational principle for the energy.

A system of A independently moving fermions is described by a Slater
determinant

$$\Phi(1,2..A) = \frac{1}{\sqrt{A!}} \begin{vmatrix} f_1(1) & f_1(2)... & f_1(A) \\ f_2(1) & f_2(2)... & f_2(A) \\ \\ f_A(1) & f_A(2)... & f_A(A) \end{vmatrix} \tag{1}$$

The Slater determinant Φ which is a vector of the Hilbert space of A-particle
states is constructed with A functions f_1, $f_2 \ldots f_A$ which are vectors of the
one-particle Hilbert space. These one-particle functions will be called
orbitals. Without any loss of generality, we may assume that the orbitals
f_1, $f_2 \ldots f_A$ in Φ are orthonormal. Indeed, the Slater determinant Φ depends
only on the A-dimensional subspace of the one-particle Hilbert space which
is spanned by the orbitals $f_1, f_2 \ldots f_A$ and not on the particular basis chosen
in this subspace. This is easily seen since a linear transformation of the
orbitals among themselves leaves Φ unchanged but for a factor. The subspace
spanned by the orbitals $f_1, f_2 \ldots f_A$ will be denoted by $\{f_1 f_2 \ldots f_A\}$. The ortho-

normality of the orbitals f_i has as a consequence that the Slater determinant Φ is automatically normalized.

In the HF-method, one looks for the best choice of the normalized Slater determinant Φ in the sense that it minimize the expectation value of the Hamiltonian H

$$\delta \langle \Phi | H | \Phi \rangle = 0 \qquad (2)$$

or

$$\langle \delta\Phi | H | \Phi \rangle + \langle \Phi | H | \delta\Phi \rangle = 0$$

This must be satisfied for any small variation $|\delta\Phi\rangle$ which keeps $|\Phi\rangle$ normalized, or, as one easily checks, for any small variation $|\delta\Phi\rangle$ which is orthogonal to $|\Phi\rangle$. Replacing then $|\delta\Phi\rangle$ by $|i\delta\Phi\rangle$ one obtains

$$- i \langle \delta\Phi | H | \Phi \rangle + i \langle \Phi | H | \delta\Phi \rangle = 0$$

The last two equations lead to the conditions

$$\langle \delta\Phi | H | \Phi \rangle = 0$$
$$\langle \Phi | H | \delta\Phi \rangle = 0 \qquad (3)$$

Since H is Hermitian, these two equations are equivalent so that it suffices to require the first one to be satisfied.

For the Slater determinant which satisfies Eqs (3), we use the following notation. The orthonormalized orbitals which occur in Φ will be labelled u_λ or $u_\mu (\lambda, \mu = 1, 2 .. A)$ and are called occupied orbitals. In the space orthogonal to $\{u_1, u_2 ... u_A\}$ we also choose an orthonormal basis, the vectors of which will be labelled by u_σ or u_τ $(\sigma, \tau > A)$ and which are called unoccupied orbitals. The whole set of occupied and unoccupied orbitals form a complete basis in the one-particle Hilbert space.

To a variation $\delta u_1, \delta u_2 ... \delta u_A$ of the orbitals, there corresponds a variation of the Slater determinant

$$\Phi = \frac{1}{\sqrt{A!}} \, |u_1 u_2 ... u_A|$$

which is given by

$$\delta\Phi = \frac{1}{\sqrt{A!}} \, |u_1 + \delta u_1 \ \ u_2 + \delta u_2 . \ ... u_A + \delta u_A| - \frac{1}{\sqrt{A!}} |u_1 u_2 ... u_A|$$

To first order in the variation this equals

$$\delta\Phi = \sum_{\lambda=1}^{A} \frac{1}{\sqrt{A!}} \, |u_1 u_2 ... \delta u_\lambda .... u_A|$$

The Slater determinant on the right-hand side of the last equation is obtained from Φ by replacing the orbital u_λ by δu_λ. Let us expand δu_λ in the complete basis (u_μ, u_σ)

$$\delta u_\lambda = \sum_{\mu=1}^{A} \eta_\mu^\lambda u_\mu + \sum_{\sigma > A} \eta_\sigma^\lambda u_\sigma$$

where the η's are small complex numbers. Introducing this in $\delta\Phi$ yields

$$\delta\Phi = \sum_{\lambda=1}^{A} \sum_{\mu=1}^{A} \eta_\mu^\lambda \Phi_\lambda^\mu + \sum_{\lambda=1}^{A} \sum_{\sigma > A} \eta_\sigma^\lambda \Phi_\lambda^\sigma$$

where Φ_λ^μ and Φ_λ^σ are the Slater determinants obtained from Φ by replacing the orbital u_λ by u_μ and u_σ, respectively. Obviously $\Phi_\lambda^\mu = \delta_{\lambda\mu}\Phi$. The Φ_λ^σ are one-particle-one-hole states. The orthogonality condition $\langle \delta\Phi | \Phi \rangle = 0$ requires now $\sum_{\lambda=1}^{A} \eta_\lambda^\lambda = 0$ so that we finally obtain

$$\delta\Phi = \sum_{\lambda=1}^{A} \sum_{\sigma > A} \eta_\sigma^\lambda \Phi_\lambda^\sigma \tag{4}$$

The condition (3) now becomes

$$\sum_{\lambda=1}^{A} \sum_{\sigma > A} \eta_\sigma^{\lambda*} \langle \Phi_\lambda^\sigma | H | \Phi \rangle = 0 \tag{5}$$

Since the η_σ^λ are arbitrary, we obtain the Brillouin condition

$$\langle \Phi_\lambda^\sigma | H | \Phi \rangle = 0 \qquad \text{for all } \lambda \le A, \sigma > A \tag{6}$$

which means that the Hamiltonian has no matrix elements between the HF-state Φ and the one-particle-one-hole states Φ_λ^σ.

We now assume that the Hamiltonian H consists of a one-body and a two-body part

$$H = H_1 + H_2 = \sum_{i=1}^{A} H_1(i) + \frac{1}{2} \sum_{i \ne j = 1}^{A} H_2(i, j) \tag{7}$$

Usually, H_1 is just the kinetic energy and H_2 the two-body interaction. The Brillouin condition (6) can now easily be transformed into a condition on the orbitals u_λ. Using the notation $|\lambda\rangle$ for u_λ, one immediately obtains from relation (6)

$$\langle \sigma | H_1 | \lambda \rangle + \sum_{\mu=1}^{A} \langle \sigma\mu | H_2(1 - P) | \lambda\mu \rangle = 0 \qquad \text{for all } \lambda \le A, \sigma > A \tag{8}$$

Here P is the permutation operator for two particles. This is called the Hartree-Fock condition. It is usually written in a different form as

$$\langle \sigma | h | \lambda \rangle = 0 \quad \text{for all} \ \lambda \leqq A, \ \sigma > A \tag{9}$$

where h is called the Hartree-Fock Hamiltonian defined by its matrix elements between any two one-particle states as

$$\langle a | h | b \rangle \equiv \langle a | H_1 | b \rangle + \sum_{\mu=1}^{A} \langle a\mu | H_2(1 - P) | b\mu \rangle \tag{10}$$

The HF-Hamiltonian h is a one-body operator which depends on the A occupied orbitals $u_1, u_2 \ldots u_A$ or, more exactly, on the subspace $\{u_1, u_2 \ldots u_A\}$ spanned by the occupied orbitals. To make this dependence more explicit, we will therefore often use the notation $h\{u_1 \ldots u_A\}$. The HF-condition (9) thus requires that the A orbitals $u_1 \ldots u_A$ must be such that the operator $h\{u_1 \ldots u_A\}$ constructed with them, has no matrix elements between occupied and unoccupied orbitals. The condition (9) can be written as a set of A coupled operator equations

$$h\{u_1 \ldots u_A\} u_\lambda = \sum_{\mu=1}^{A} e_{\lambda\mu} u_\mu \quad (\lambda = 1, 2 \ldots A) \tag{11}$$

where the $e_{\lambda\mu}$ form an eigenvalue matrix.

It is easy to check that if the set of functions $u_1, u_2 \ldots u_A$ satisfies the HF-condition (9) or (11), then any unitary linear combination of these functions also satisfies the HF-condition. This must obviously be so from the remark at the beginning of this section, since the new orbitals would build exactly the same Slater determinant Φ, so that condition (2) remains satisfied. This freedom in the choice of the orbitals u_λ can now be used to introduce an additional condition on the orbitals which determines them in a unique way, without, however, changing the Slater determinant Φ. We choose that particular basis in the subspace $\{u_1 u_2 \ldots u_A\}$ for which the eigenvalue matrix $e_{\lambda\mu}$ becomes diagonal. This is always possible because the $e_{\lambda\mu}$ form a Hermitian matrix (or because h is a Hermitian operator). In this way, one obtains the canonical form of the HF-equations

$$h\{u_1 \ldots u_A\} u_\lambda = \epsilon_\lambda u_\lambda \quad (\lambda = 1, 2 \ldots A) \tag{12}$$

These equations form a non-linear eigenvalue problem, the unknown orbitals u_λ occurring also in the definition of the HF-Hamiltonian h. The u_λ must be eigenfunctions of the operator h which itself is constructed by means of the u_λ. This is called the self-consistency condition.

Remarks

(1) If the one-body term in the Hamiltonian H contains only the kinetic energy operator $\sum_i T(i)$, the HF-Hamiltonian h takes the form $h = T + U$,

where U is called the HF-potential. Equations (12) then have the form of
a set of A single-particle Schrödinger equations for particles moving in the
common potential well U. This gives a connection to the shell-model
potential.

(2) If by Φ_λ we denote the Slater determinant of (A - 1) particles ob-
tained from Φ by taking away the orbital u_λ, and similarly, by Φ^σ, the
Slater determinant of (A + 1) particles obtained from Φ by adding the orbital·
u_σ, one easily calculates

$$\langle \Phi_\lambda | H_{A-1} | \Phi_\lambda \rangle = \langle \Phi | H_A | \Phi \rangle - \epsilon_\lambda$$

$$\langle \Phi^\sigma | H_{A+1} | \Phi^\sigma \rangle = \langle \Phi | H_A | \Phi \rangle + \epsilon_\sigma \tag{13}$$

where

$$H_A = \sum_{i=1}^{A} H_1(i) + \tfrac{1}{2} \sum_{i \neq j = 1}^{A} H_2(i, j) \tag{14}$$

This shows that, if Φ_λ, Φ and Φ^σ are good approximations for physical
states in the (A - 1), A and (A + 1)-particle nuclei, the ϵ_λ and ϵ_σ are good
approximations for the separation energy of a single nucleon.

(3) The subsidiary condition imposed on the occupied orbitals in deriving
Eqs (12) still leaves some arbitrariness in the definition of h since a one-
body operator can always be written in many different ways as a sum of a
one-body and a two-body operator. The kinetic energy operator can, for
example, be written as a sum of a one-body and a two-body operator

$$\sum_{i=1}^{A} T(i) = x \sum_{i=1}^{A} T(i) + (1 - x) \frac{1}{2(A - 1)} \sum_{i \neq j = 1}^{A} [T(i) + T(j)]$$

where x is an arbitrary real number. The canonical HF-equations will be
changed to a form which, for $x \neq 1$, does no longer have a simple physical
meaning, but which may be easier in practical numerical calculations (e.g.
with x = 0). The single-particle energies and the orbitals will, as a rule,
also be changed, but the Slater determinant Φ must obviously remain the
same. One should also notice that for $x \neq 1$, the new two-body operator
depends on the number of particles A which implies that a simple relation
of the type (13) is no longer valid (since the new operators H_{A-1}, H_A and
H_{A+1} are not related as those defined by (14)).

3. SOLUTION OF THE HF EQUATIONS

For definiteness, we will write the Hamiltonian in this section as
H = T + V where T is the kinetic energy and V is a two-body interaction
energy. The usual symmetry properties of V will be assumed throughout
this section. The HF-Hamiltonian will be written as h = T + U.

The HF-equations (12), being only a condition for the stationarity
of the energy, have very many solutions. In fact, it is easy to show

that there are always an infinite number of solutions of Eqs (12). The difficulty consists in finding the solution which gives the lowest energy.

Let us first show that any set of A plane waves with wave vectors $\vec{k}_1 \vec{k}_2 \dots \vec{k}_A$ forms a solution of Eqs (12). In the usual way, we take a large cube with periodic boundary conditions as normalization volume, so that the plane waves can be normalized $\langle \vec{k}_i | \vec{k}_j \rangle = \delta_{ij}$. We will show that

$$\langle \vec{k}_i | h \{\vec{k}_1 \vec{k}_2 \dots \vec{k}_A\} | \vec{k}_j \rangle = \epsilon_i \delta_{ij} \quad \text{for all } i \text{ and } j \tag{15}$$

which will prove that the plane waves $|\vec{k}_1\rangle |\vec{k}_2\rangle \dots |\vec{k}_A\rangle$ form a solution of Eqs (12). Using definition (10), the left-hand side of expression (15) can be rewritten as

$$\langle \vec{k}_i | T | \vec{k}_j \rangle + \sum_{\lambda=1}^{A} \langle \vec{k}_i \vec{k}_\lambda | V(1-P) | \vec{k}_j \vec{k}_\lambda \rangle$$

which equals

$$\frac{\hbar^2 k_i^2}{2m} \delta_{ij} + \delta_{ij} \sum_{\lambda=1}^{A} \langle \vec{k}_i \vec{k}_\lambda | V(1-P) | \vec{k}_i \vec{k}_\lambda \rangle$$

because V commutes with the total momentum (or is translationally invariant). This has the form of the right-hand side of expression (15) with

$$\epsilon_i = \frac{\hbar^2 k_i^2}{2m} + \sum_{\lambda=1}^{A} \langle \vec{k}_i \vec{k}_\lambda | V(1-P) | \vec{k}_i \vec{k}_\lambda \rangle$$

This proves that any set of A plane waves forms a solution of the HF-equations (12). Since we are interested in finding the lowest solution (lowest total energy), we calculate the total energy

$$\langle \Phi | H | \Phi \rangle = \sum_{\lambda=1}^{A} \frac{\hbar^2 k_\lambda^2}{2m} + \frac{1}{2} \sum_{\lambda \neq \mu = 1}^{A} \langle \vec{k}_\lambda \vec{k}_\mu | V(1-P) | \vec{k}_\lambda \vec{k}_\mu \rangle$$

Among all plane wave solutions, we then expect to find the lowest HF-solution by taking the A plane waves with lowest kinetic energy. One usually assumes that this solution will also be the lowest solution among all HF-solutions in the case of infinite systems like infinite nuclear matter. There is, however, no proof for this, and Overhauser [7] has shown that one may obtain a lower energy solution also in the case of infinite systems for special types of interactions.

In the case of finite nuclei, it is obvious that the plane wave solution will not be the lowest one, since the particles are interacting only very little when they are smeared out over all space. How can we find a lower energy solution and especially the lowest one? In practical calculations,

an iteration procedure is used to find a solution of the HF-equations, which
you may hope will be the lowest one. One makes a guess for the occupied
orbitals (call them $u_\lambda^{(1)}$), one calculates $h\{u_\lambda^{(1)}\}$ by means of definition (10)
and finds its eigenvalues and eigenfunctions. Let us call its lowest A
eigenfunctions $u_1^{(2)}$, $u_2^{(2)}$ ... $u_A^{(2)}$. These are now chosen to construct $h\{u_\lambda^{(2)}\}$.
This new operator is again diagonalized, its lowest A eigenfunctions chosen,
and one continues in the same manner until self-consistency is obtained,
i.e. until the u_λ in two consecutive steps of the iteration remain unchanged.

The reason for choosing the lowest eigenfunctions of $h\{u_\lambda\}$ at each step
of the iteration is that one hopes that this set will give the lowest total
energy $\langle \Phi | H | \Phi \rangle$ at each step of the iteration. This choice is not necessary
to find a solution of Eqs (12), but one hopes that it will help to find the lowest
solution.

The iteration procedure described above is still a formidable work.
In all practical calculations the problem has been simplified in either of
two different ways:

1.   Truncation of the one-particle Hilbert space

In most HF-calculations for light nuclei, one has taken the subspace
spanned by the lowest four harmonic oscillator shells 0s, 0p, 1s-0d, 1p-0f.
This is an eighty-dimensional subspace. If we call $|i\rangle$ $(i = 1, ...80)$ an
orthonormal basis in this subspace, the HF-orbitals u_λ are then determined
by their expansion coefficients X_i^λ

$$u_\lambda = \sum_{i=1}^{80} X_i^\lambda |i\rangle \tag{16}$$

and the HF-Hamiltonian $h\{u_1 u_2 ... u_A\}$ is replaced by an eighty-dimensional
matrix:

$$\langle i|h|j\rangle = \langle i|T|j\rangle + \sum_{\lambda=1}^{A} \sum_{k=1}^{80} \sum_{\ell=1}^{80} X_k^{\lambda*} \langle ik|V(1-P)|j\ell\rangle X_\ell^\lambda \tag{17}$$

The HF-equations (12) are then replaced by the matrix equation

$$\sum_{j=1}^{80} \langle i|h|j\rangle X_j^\lambda = \epsilon_\lambda X_i^\lambda \quad (i = 1, ...80) \tag{18}$$

Thus the X^λ are the different eigenvectors of the matrix (17). One again
proceeds by iteration. Making an initial guess for the A occupied eigen-
vectors (call them $X^{\lambda(1)}$), one calculates $\langle i|h^{(1)}|j\rangle$ by means of ex-
pression (17) and diagonalizes it. Calling the lowest A eigenvectors $X^{\lambda(2)}$ one
calculates again $\langle i|h^{(2)}|j\rangle$ by means of expression (17) and continues until
self-consistency is achieved. This iteration procedure is obviously much
simpler than the general iteration procedure sketched before because dia-
gonalizing a finite matrix is very much simpler than finding the lowest A
eigenfunctions of a general one-body operator.

If the dimension of the subspace is large, however, the numerical labour remains very large. For example, in the case of the finite eighty-dimensional space considered above, there are $(80 \times 81)/2 = 3240$ matrix elements to be calculated at each step of the iteration. Each matrix element, calculated by means of expression (17), contains a sum of $A \times 80 \times 80 = 6400 \times A$ matrix elements[1] of V. This large numerical problem can be simplified by the second approximation called the symmetry restriction.

2. Symmetry restriction

Suppose that our initial guess of the HF-orbitals $u_\lambda^{(1)}$ has a certain symmetry. For the sake of definiteness, let us suppose that each $u_\lambda^{(1)}$ has a definite parity $Iu_\lambda^{(1)} = \epsilon_\lambda^{(1)} u_\lambda^{(1)}$. Then the HF-Hamiltonian constructed with the $u_\lambda^{(1)}$ will commute with the parity operator $[h\{u_\lambda^{(1)}\}, I] = 0$. To show this, we only have to prove that $[U\{u_\lambda^{(1)}\}, I] = 0$. For general single-particle states $|a\rangle$ and $|b\rangle$ one has

$$\langle a | I^\dagger U I | b \rangle = \langle Ia | U | Ib \rangle$$

$$= \sum_{\lambda=1}^{A} \langle Ia, u_\lambda^{(1)} | V(1-P) | Ib, u_\lambda^{(1)} \rangle$$

from the definition of U. Transforming both bra and ket by the unitary operator I gives (since $[I, V] = 0$)

$$= \sum_{\lambda=1}^{A} \langle a, Iu_\lambda^{(1)} | V(1-P) | b, Iu_\lambda^{(1)} \rangle$$

$$= \sum_{\lambda=1}^{A} |\epsilon_\lambda^{(1)}|^2 \langle a, u_\lambda^{(1)} | V(1-P) | b, u_\lambda^{(1)} \rangle = \langle a | U | b \rangle$$

Since $|a\rangle$ and $|b\rangle$ are general single-particle states, one has the operator relation

$$I^\dagger U \{u_\lambda^{(1)}\} I = U \{u_\lambda^{(1)}\}$$

or

$$[I, U \{u_\lambda^{(1)}\}] = 0$$

The above proof only shows that if the probability density for finding the nucleons is symmetric under inversion through the origin, then the potential created by this mass distribution will also be symmetric.

---

[1] From expressions (17) and (18) one sees that the labour involved in a HF-calculation depends very little on the number of particles A, contrary to what is the case in the usual shell-model calculations, but mainly on the dimension of the one-particle subspace.

Now, since $[I, U\{u_\lambda^{(1)}\}] = 0$, the eigenfunctions of $h\{u_\lambda^{(1)}\}$ will have definite parity

$$I u_\lambda^{(2)} = \epsilon_\lambda^{(2)} u_\lambda^{(2)}$$

In other words, the symmetry of the initial guess is conserved during the iteration, and the iteration procedure will eventually converge towards a solution having the same symmetry property. If the initial guess has a definite parity, the iteration procedure will always converge towards a solution with a definite parity. A symmetry (like parity) which is conserved during the iteration procedure is called a consistent symmetry.

There are two aspects of consistent symmetries:

i)   Starting from a guess with definite parity, one will obtain a solution with definite parity. This means that if the lowest HF-solution does not have definite parity (i.e. if the HF-Hamiltonian has no inversion symmetry) one will never be able to obtain the lowest HF-solution if one starts from a guess with definite parity. If one wants the lowest HF-solution, one should start from a guess without symmetry.

ii)   On the other hand, a consistent symmetry simplifies the numerical work considerably. Consider, for example, again the case of the eighty-dimensional subspace and take the oscillator functions as basic states.

$$(|0s\rangle, \quad |1s\rangle, \quad |0d\rangle) \equiv |i\rangle \qquad (i = 1, \ldots 28)$$

$$(|0p\rangle, \quad |1p\rangle, \quad |0f\rangle) \equiv |i\rangle \qquad (i = 29, \ldots 80)$$

An initial guess with definite parity means that the $u_\lambda^{(1)}$ $(\lambda = 1, 2, \ldots, A)$ have the following expansion:

for even parity: $$u_\lambda^{(1)} = \sum_{i=1}^{28} X_i^\lambda |i\rangle$$

for odd parity: $$u_\lambda^{(1)} = \sum_{i=29}^{80} X_i^\lambda |i\rangle$$

The matrix $\langle i | h\{u_\lambda^{(1)}\} | j\rangle$ reduces to the following form:

and each matrix element (17) now contains at most $A \times (52)^2$ matrix elements of V. Thus the simplification is threefold:

(a) there are less matrix elements $\langle i|h|j \rangle$,
(b) each matrix element contains less elements of V in its sum, and
(c) smaller matrices are to be diagonalized

We shall later see that there is a fourth simplification if one has to make an angular-momentum projection.

Thus, although one may lose the lowest solution of the HF-equations by starting from a guess with consistent symmetry, this has been done in all practical calculations in order to simplify the numerical labour.

TABLE I. NUMBER OF TERMS IN BASIC-STATE EXPANSION

π	m	τ	Number of terms in the expansion
+	±5/2	±1/2	1
+	±3/2	±1/2	2
+	±1/2	±1/2	4
-	±7/2	±1/2	1
-	±5/2	±1/2	2
-	±3/2	±1/2	4
-	±1/2	±1/2	6

Other consistent symmetries are axial symmetry (orbitals are eigenfunctions of j_z) and axial symmetry in isospace (orbitals are eigenfunctions of t_3). To see how strongly these symmetries simplify the numerical work, let us consider the above example again. The orbitals are now eigenfunctions of I, j_z and t_3 with eigenvalues π, m and τ, respectively. Table I shows how many terms there are in their expansion in basic states. Also, the matrix $\langle i|h\{u_\lambda\}|j \rangle$ is reduced very much. It contains along the diagonal

4 submatrices of dimension 6
8   "   "   4
8   "   "   2
8   "   "   1

The total number of matrix elements $\langle i|h|j \rangle$ which are non-zero has consequently decreased from 3240 to 196 and every matrix element itself is now a sum of at most A × 36 terms (instead of A × 6400). The simplification in calculating the matrix $\langle i|h|j \rangle$ is more than a factor 2000. One sees how much you gain in numerical labour if one runs the risk of losing the lowest solution. In many cases, however, one has found as lowest solution a solution having a higher symmetry than the symmetry of the initial guess and so you may hope that the symmetry restriction will not affect the accuracy of the method.

It is interesting now to know whether one can still further simplify the calculation by starting from a guess with a still larger symmetry than the ones considered so far. Instead of talking about the symmetry of the orbitals, it is somewhat easier to talk about the symmetry of the HF

Hamiltonian which is, of course, the same thing. We have then seen that the assumption of axial symmetry, inversion symmetry and t_3-symmetry simplify the calculation considerably. May we, for example, not assume that h be spherically symmetric? The answer is in some cases "yes", in most cases "no". Of course, we can always start from an initial guess for h, having spherical symmetry, but the calculation is simplified only if the symmetry is conserved during the iteration. Assume, for example, for a nucleus like ^{5}He, that $h^{(1)}$ be spherically symmetric. Its lowest eigenfunctions are then

s-orbital :   4 times degenerate

p-orbital :   12 times degenerate

So the next $h^{(2)}$ will be constructed with four s-orbitals and one p-orbital and cannot be any longer spherically symmetric. On the other hand, for ^{16}O the next $h^{(2)}$ will be constructed with four s-orbitals and twelve p-orbitals and will again be spherically symmetric. Thus, spherical symmetry is a consistent symmetry for ^{16}O, but not for ^{5}He. The question then is: for what nuclei will a certain group be a consistent symmetry group? The answer to this question is not known in general. One can, however, answer the inverse question (at least, partly). For what nuclei will a certain group not be a consistent symmetry group? This will then exclude several symmetries as being non-consistent for a given nucleus, and one may try some of the remaining groups and find out whether it is consistent or not by doing the iteration.

The answer to the question "For what A-values is a given group G certainly not a consistent symmetry group?" is based on the following theorem:

If O is a unitary symmetry operator for the total Hamiltonian H and if $\{u_1 u_2 \ldots u_A\}$ is an invariant space under O, then O is also a symmetry operator for $h\{u_1 u_2 \ldots u_A\}$. More formally,

if $[O, H] = 0$

if $Ou_\lambda = \sum_{\mu=1}^{A} O_{\lambda\mu} u_\mu$ $(\lambda = 1, 2, \ldots A)$

then $[O, h\{u_1 \ldots u_A\}] = 0$

The proof is exactly the same as that given previously for the inversion operator (see Ref.[8]).

The theorem is also immediately extended to a group G of unitary operators: if $[G, H] = 0$ and $\{u_1 \ldots u_A\}$ is invariant under all operators of G, then $[G, h\{u_1 \ldots u_A\}] = 0$.

From the previous theorem we immediately have the trivial consequence that if G is a symmetry group for h, it is certainly necessary that in the one-particle Hilbert space there exists a subspace of dimension A which is invariant under G. In this way, at least, one can start with an initial guess $u_\lambda^{(1)}$ having the symmetry of the group G. There is no guarantee

that this symmetry will be conserved during the iteration[2] but, at least, values of A with the property that no invariant subspace of dimension A exists cannot have G as a consistent symmetry group. One is thus led to study the dimensions of the invariant subspaces in the one-particle Hilbert space for the different groups G. For R_3 one finds, for example, only even-dimensional subspaces and for the isospin group SU_2 only a two-dimensional subspace. If G is the product group $R_3 \otimes SU_2$, the invariant subspaces have dimensions which are multiples of four. Thus for nuclei with $A \neq 4n$, $R_3 \otimes SU_2$ is certainly not a possible symmetry group.

All this does not seem very useful. However, in the special case of a group G for which all irreducible invariant subspaces have the same dimension d, G is a consistent symmetry for all A which are multiples of d. A trivial application of this are the Abelian groups considered previously (I, j_z, t_3) which are consistent symmetries for all values of A. A non-trivial example is the two-dimensional rotation reflection group which has only irreducible subspaces of dimension two in the one-particle Hilbert space, and the isospin group SU_2 which also has only two-dimensional irreducible subspaces. As a result, the product of the two-dimensional rotation reflection group and SU_2 has only irreducible subspaces of dimension four and is a consistent symmetry for $A = 4n$. To show that the above statement is true, let us start from an initial guess $h^{(1)}$, commuting with G. It follows that the eigenvalues of $h^{(1)}$ will have degeneracy d, and the A particles will just fill the lowest A/d levels. This space is invariant under G and so $h^{(2)}$ will commute with G from the above theorem. Thus G is conserved as a summetry group during the iteration procedure and is thus a consistent symmetry.

For more details about these matters we refer to Ref.[8] . Most calculations so far have been done either for spherical nuclei (^{16}O, ^{40}Ca) where spherical symmetry is a consistent symmetry, or for Z = N (even) nuclei (A = 4n) for which the product of the two-dimensional rotation reflection group and SU_2 is a consistent symmetry group. The reason, of course, is that this simplifies the numerical work very much. As stated above, one may lose the lowest HF-solution. A typical example of this is ^{12}C, for which spherical symmetry turns out to be consistent, but the resulting HF-solution is not the lowest one. Starting from a guess without spherical symmetry, one finds a solution which is 14 MeV lower [9] .

4.   RESULTS OF HF CALCULATIONS

In this section, we shall describe a typical HF-calculation for light nuclei. We choose the calculation which in our opinion, is the best one done so far. Many other calculations about which we shall not talk have been done by other people, but our main purpose is to go on rather quickly to some HF-calculations with angular momentum projection in the next lectures.

Kerman, Svenne and Villars [10] have made a HF-calculation for the spherical nuclei ^{16}O and ^{40}Ca using the Tabakin interaction [3] . They have

---

[2] If one does not keep to the prescription that at each step of the iteration the lowest A orbitals should be filled, it is always possible to choose the orbitals such that the symmetry of the initial guess is conserved. However, one should not expect to find a low-lying HF-solution in this way.

simplified the HF-equations by assuming rotation inversion and time reversal symmetry as well as t_3-symmetry and by expanding the orbitals in spherical oscillator functions. The occupied orbitals are thus written as

$$u_\lambda = \sum_{n=0}^{N} X_n^\lambda |n \ \ell \ j \ m \ \tau\rangle \tag{19}$$

and they have truncated the space at $N = 4$. The X_n^λ are real and identical for different orbitals corresponding to the same $\ell \, j$-value.

Moreover, they optimize the total energy with respect to the oscillator parameter b by plotting the HF-energy as a function of b.

We describe their results for ^{16}O in some detail here. They find that the expansion coefficients X_n^λ decrease very rapidly with n so that the truncation at $N = 4$ is justified. The single-particle spectrum ϵ_λ is shown below (we plot only the neutron states):

ϵ_λ			ϵ_x
10.74	——————	$d_{3/2}$	0.93
6.12	——————	$s_{1/2}$	-3.28
2.31	——————	$d_{5/2}$	-4.15
-9.45	——————	$p_{1/2}$	-15.65
-19.65	——————	$p_{3/2}$	-21.81
-48.72	——————	$s_{1/2}$	?

and the experimental single-particle energies ϵ_x are given on the right. Comparison with experiment is based on relations (13) where Φ^o and Φ_λ are interpreted as states of ^{17}O and ^{15}O respectively. One sees that the lowest orbital is very deep, much deeper than is possible in a local potential which would have only three bound states. The comparison with the experimental single-particle energies is qualitatively good, but there are some discrepancies in the details. For example, the unoccupied orbitals $d_{5/2}$ and $s_{1/2}$ are not bound in contradiction to the experimental situation. We shall see that this comes out for many HF-calculations, an explanation will be given further on.

The spin-orbit splitting (e.g. between $d_{3/2}$ and $d_{5/2}$) is too large. A possible explanation of this was suggested by Elliott [11]. He found that the spin-orbit splitting is very sensitive to the size of the nucleus, the spin-orbit splitting decreasing as the size increases. Kerman et al. did calculate the radius for ^{16}O and found it about 10% too small. Thus the too large spin-orbit splitting may be related to the too small radius.

The total energy $\langle \Phi | H | \Phi \rangle$ is equal to -38.5 MeV, compared to the experimental value $E_x = -127$ MeV. To improve the agreement, Kerman and Pal [12] calculated the second-order correction to the total energy

$$\Delta E^{(2)} = \sum_{\lambda, \mu} \cdot \sum_{\sigma, \tau} \frac{\left| \langle u_\lambda u_\mu | V(1-P) | u_\sigma u_\tau \rangle \right|^2}{\epsilon_\lambda + \epsilon_\mu - \epsilon_\sigma - \epsilon_\tau} \tag{20}$$

They find

$$\Delta E^{(2)} \cong -69 \text{ MeV}$$

so that the total energy equals -107.5 MeV, which agrees satisfactorily with the experiment. The fact that the second-order contribution is very large does not mean that the convergence of the perturbation theory is bad. In fact, one must compare $\Delta E^{(2)}$ with the first-order potential energy $\langle \Phi | V | \Phi \rangle$ which equals about -350 MeV and so

$$\frac{\Delta E^{(2)}}{\langle \Phi | V | \Phi \rangle} < 0.20$$

Bassichis, Kerman and Svenne [9] extended these calculations to all Z = N (even) nuclei with A ≤ 40. They simplified the HF-problem by:

(i) Truncating the one-particle Hilbert space to the eighty-dimensional subspace spanned by the oscillator functions, 0s, 0p, 1s-0d, 1p-0f, and
(ii) restricting themselves to solutions with the symmetry of the two-dimensional rotation reflection group, good parity, time reversal and charge independence.

The occupied orbitals are then written as

$$u_\lambda = \sum_{n\ell j} X^\lambda_{n\ell j} | n \ell j m \tau \rangle \qquad \text{with } (-)^\ell \text{ fixed}$$

The $X^\lambda_{n\ell j}$ are real and are independent of m and τ for fixed nℓj.

The nuclei ^{4}He, ^{16}O and ^{40}Ca are found to be spherical and will not be discussed any more. The single-particle energies ϵ_λ for ^{8}Be, ^{12}C and ^{20}Ne are shown in Fig.1. The levels below the dashed line are the occupied ones. One finds a gap between occupied and unoccupied orbitals. This gap was discovered by Levinson in restricted HF-calculations within the s-d shell, where it shows up much more clearly. In HF-calculations, where all particles are taken into account, one also finds energy gaps between the "major shells" of the shell model and in the whole energy diagram; the Levinson gap is less conspicuous than in HF-calculations within one major shell.

As in the case of ^{16}O, it is again found that the unoccupied orbitals in ^{8}Be and ^{12}C have a positive single-particle energy, in contradiction to experimental bound nuclei ^{9}Be and ^{13}C and the single-particle 3/2$^+$ state in ^{20}Ne is only just bound, compared to a well bound ^{21}Ne nucleus. The
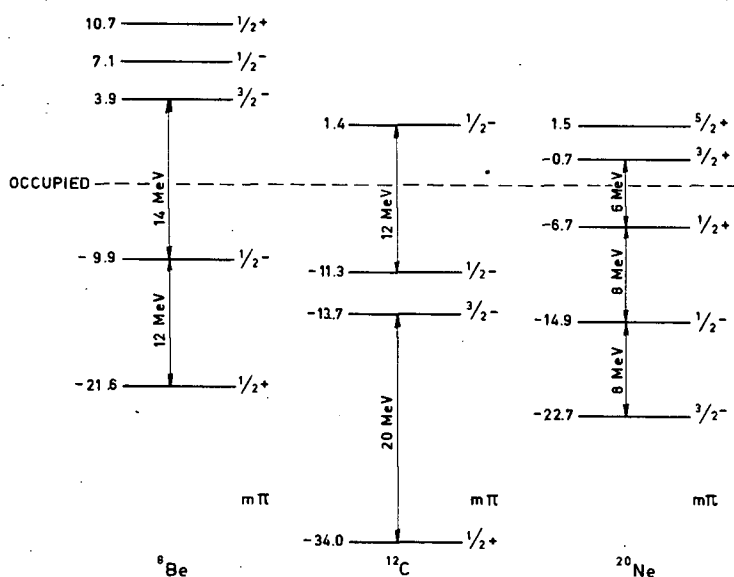
FIG. 1.   Single-particle energies ϵ_λ for ^{8}Be, ^{12}C and ^{20}Ne.

explanation of this discrepancy is probably the following. It is known from Levinson's work that the gap between occupied and unoccupied orbitals is considerably larger for Z = N (even) nuclei (^{8}Be, ^{12}C, ^{16}O, ^{20}Ne) than for the neighbouring odd nuclei. So it is to be expected that configuration admixtures will be more important for the odd nuclei, resulting in a larger correlation energy which will make the odd nuclei bound.

Bassichis et al. find the following values for the expansion coefficients of the orbitals:

^{8}Be:

$$u(1/2^+) = -0.96 \,|0s\,1/2\rangle - 0.20\,|0d\,5/2\rangle - 0.02\,|1s\,1/2\rangle + 0.18\,|0d\,3/2\rangle$$

$$u(1/2^-) = 0.85\,|0p\,3/2\rangle - 0.50\,|0p\,1/2\rangle + 0.13\,|0f\,7/2\rangle - 0.01\,|1p\,3/2\rangle$$

$$-0.11\,|0f\,5/2\rangle + 0.03\,|1p\,1/2\rangle$$

It is interesting to rewrite these coefficients in a L-S coupling basis $|n\,\ell\,m_\ell\,m_s\rangle$:
This becomes

$$u(1/2^+) = -0.96\,|0s\,0\,1/2\rangle - 0.27\,|0d\,0\,1/2\rangle + \underline{0.013}\,|0d\,1\,-1/2\rangle$$

$$-0.02\,|1s\,0\,1/2\rangle$$

$$u(1/2^-) = 0.98\,|0p\,0\,1/2\rangle + \underline{0.08}\,|0p\,1\,-1/2\rangle + \ldots$$

The remarkable thing is that $u(1/2^+)$ and $u(1/2^-)$ are to a very good approximation eigenfunctions of ℓ_z with eigenvalue zero. This is just what one obtains if one makes a HF-calculation starting from a central interaction. We see that spin-orbit and tensor forces play a very negligible role in determining the HF-orbitals for ^{8}Be.

If one does the same thing for ^{12}C and for ^{20}Ne, one finds for $\underline{^{12}C}$: the negative parity orbitals become

$$u(3/2^-) = 0.99 \,|0\,p\,1\ 1/2\rangle + \ldots$$

$$u(1/2^-) = -0.98 \,|0\,p\,1\ -1/2\rangle \ \underline{-0.18} \,|0\,p\,0\ 1/2\rangle + \ldots$$

and for $\underline{^{20}Ne}$ the highest occupied orbital becomes

$$u(1/2^{+\prime}) = 0.03 \,|0\,s\,0\ 1/2\rangle \dotplus 0.86 \,|0\,d\,0\ 1/2\rangle - \underline{0.30} \,|0\,d\,1\ -1/2\rangle$$

$$+ 0.40 \,|1\,s\,0\ 1/2\rangle$$

So you again find that u_λ are approximately eigenfunctions of ℓ_z for ^{12}C but with a larger admixture of different ℓ_z values and for ^{20}Ne this is still worse. Spin-orbit and tensor forces become more and more effective in determining the HF-orbitals as one goes to heavier nuclei. For light nuclei, as ^{8}Be, they can be neglected.

The total energies $\langle\Phi|H|\Phi\rangle$ obtained by Bassichis et al. again deviate strongly from the experimental energies. However, since the nuclei turn out to be deformed (except for ^{4}He, ^{16}O and ^{40}Ca), Φ is not an eigenfunction of the total angular momentum J^2 and can consequently not be associated with a particular physical state. One can, however, expand Φ in eigenstates of J^2:

$$\Phi = \sum_J \Psi_J \tag{21}$$

and associate Ψ_J with the lowest physical state with angular momentum J. The energy for this state is then $E_J = \langle\Psi_J|H|\Psi_J\rangle / \langle\Psi_J|\Psi_J\rangle$. To calculate E_J from a given $\langle\Phi|H|\Phi\rangle$ Bassichis et al. postulate that the E_J are related as in a rotational band

$$E_J = E_0 + B\,J(J+1) \tag{22}$$

One then has

$$\langle\Phi|H|\Phi\rangle = \sum_J \langle\Psi_J|H|\Psi_J\rangle = E_0 + B\,\langle\Phi|J^2|\Phi\rangle \tag{23}$$

Calculating both $\langle \Phi | H | \Phi \rangle$ and $\langle \Phi | J^2 | \Phi \rangle$, one can obtain E_0 if one knows B. Theoretical methods for calculating B are very unsuccessful. Therefore Bassichis et al. have taken B from the experimental knowledge of the lowest excited 2^+ state. They get, e.g. for ^{20}Ne,

$$\langle \Phi | H | \Phi \rangle \quad = -51.8 \text{ MeV}$$

$$E_0 \quad\quad\quad = -56.0 \text{ MeV}$$

whereas $\quad\quad\quad E_x \quad\quad\quad = -179.2 \text{ MeV} .$

In the same way as for ^{16}O, they calculate the second-order correction $\Delta E^{(2)}$ for the energy by means of Eq.(20). In this way, the agreement with experiment is substantially improved. For example for ^{20}Ne, they find

$$E_0 + \Delta E^{(2)} \quad = -150.5 \text{ MeV}$$

There seems, however, to be no justification for using the standard perturbation-theory formula (20) for deformed nuclei. For ^{16}O, the HF-determinant Φ can be considered to be an approximation to the exact eigenfunction of H. Splitting H into

$$H = \sum_i h(i) + \left\{ \frac{1}{2} \sum_{i \neq j} V_{ij} - \sum_i U(i) \right\} \tag{24}$$

where $h(i)$ is the HF-Hamiltonian, one can use standard perturbation theory. In the case of deformed nuclei, Φ is a very poor approximation for the real eigenstates of H, but Ψ_J is probably a good approximation. However, while Φ is an eigenfunction of $\sum_i h(i)$, Ψ_J is not. So using Ψ_J as an approximation for the real states, one should split up the total Hamiltonian H in a different way:

$$H = H_0 + H_1$$

where $H_0 \Psi_J = E_J \Psi_J$. It is, however, not easy to find a simple expression for H_0.

Another quantity which is calculated is the intrinsic quadrupole moment

$$Q_{intr.} \equiv \left\langle \Phi \left| \sqrt{\frac{16\pi}{5}} \sum_p r^2 Y_{20} \right| \Phi \right\rangle \tag{25}$$

The sign of $Q_{intr.}$ indicates whether Φ is prolate or oblate. Bassichis et al. found that only ^{12}C and ^{28}Si are oblate; all the other nuclei are prolate. To compare with experimental quadrupole moments or B(E2)'s, one has to postulate some relation between $Q_{intr.}$ and observable quantities (in the same way as for the energies E_J). If we postulate the rotational model relation

$$B(E2; 2 \to 0) = \frac{1}{16\pi} |Q_{intr.}|^2 . \tag{26}$$

we find, e.g. for ^{12}C, B(E2; 2 → 0) = 5.2 fm^4, compared to an experimental value of 8.4 fm^4. We have already remarked above that the calculated radii are about 10% too small. A larger radius will obviously increase $Q_{intr.}$ and, consequently, also B(E$_2$; 2 → 0), giving a better fit to the experimental result.

In the next section, we shall show how one can perform calculations with the function Ψ_J directly without having to postulate any relations between intrinsic and observable quantities which are not very well satisfied for light nuclei [13].

To conclude this section, we want to compare some properties of the HF-potential with what one expects from it on the basis of the standard shell-model calculations. Kurath's [14] intermediate-coupling calculation in the p-shell used a shell-model potential

$$U_{SM} = U_{oscillator} + \zeta \, \vec{\ell} \cdot \vec{s}$$

Treating ζ as an adjustable parameter, Kurath found best fits to the experimental spectra if ζ increased through the shell. Also, in the s-d shell, a larger spin-orbit splitting is needed at the end of the shell than at the beginning. Let us see if this comes out here.

$$^{16}O : \epsilon (d\,3/2) - \epsilon (d\,5/2) = 8.4 \text{ MeV}$$

$$^{40}Ca : \epsilon (d\,3/2) - \epsilon (d\,5/2) = 13.3 \text{ MeV}$$

Another property of the shell-model potential in the s-d shell is the so called s-d inversion. In ^{17}O, the s-orbital is known to lie below the centre of gravity of the d-orbitals whereas in ^{39}Ca the s-orbital is lying above. In the HF-calculation, the s-orbital lies above the centre of gravity of the d-orbitals both in ^{16}O and ^{40}Ca, so the inversion is not found. It is maybe interesting to remark that Baranger and Muthukrishnan [15] did find the s-d inversion in a HF-calculation using the central Yamaguchi potential.

5. PROJECTION OPERATORS

In general, the HF-determinant Φ is not an eigenfunction of J^2 and cannot be interpreted as an approximate description of a particular physical state. In this case, it is usual to regard Φ as an "intrinsic state" in the same sense as in the Nilsson model. Insofar as this intrinsic state is sufficiently stable, the real physical states are then associated with different rotational states of the intrinsic state Φ. The way of obtaining wave functions for the rotational states from a knowledge of Φ is not well known. The best way, so far, seems to be by means of projection operators for the angular momentum. For simplicity we shall assume that Φ is already an eigenfunction of J$_z$ with eigenvalue K:

$$J_z \Phi = K \Phi \tag{27}$$

(this is so if the HF-potential is axially symmetric). Expanding Φ into eigenfunctions of J^2

$$\Phi = \sum_J \Psi_{JK} \tag{28}$$

we obtain the function Ψ_{JK} from Φ by means of a projection operator P_J

$$\Psi_{JK} = P_J \Phi \tag{29}$$

An expression of P_J is, for example,

$$P_J = \prod_{J_i \neq J} \left\{ \frac{J_{op}^2 - J_i(J_i+1)}{J(J+1) - J_i(J_i+1)} \right\} \tag{30}$$

where J_{op}^2 is the quantum-mechanical operator for the total angular momentum. That is, P_J is an infinite product of operators, one for each value of $J_i = 0, 1, 2, \ldots$, with the exception of J. Expression (30) is, however, very difficult to work with, in general. A more useful expression for P_J is based on some properties of the rotation matrices

$$P_{J_k} = \frac{2J+1}{8\pi^2} \int d\Omega \, D_{KK}^{J*}(\Omega) \, R_\Omega \tag{31}$$

Here Ω is a shorthand notation for the three Euler angles $\Omega = (\varphi, \theta, \psi)$

and

$$\int d\Omega = \int_0^{2\pi} d\varphi \int_0^{\pi} \sin\theta \, d\theta \int_0^{2\pi} d\psi \tag{32}$$

The operator R_Ω is the rotation operator [6]

$$R_\Omega = e^{-i\varphi J_z} \, e^{-i\theta J_y} \, e^{-i\psi J_z} \tag{33}$$

and the function $D_{KK'}^J(\Omega)$ are the representation matrices

$$D_{KK'}^J(\Omega) = \langle JK | R_\Omega | JK' \rangle = e^{-iK\varphi} d_{KK'}^J(\theta) \, e^{-iK'\psi} \tag{34}$$

It is easily seen, by using standard properties of the D-functions, that the operator P_J defined by Eq.(31) is a projection operator for the angular momentum J. The operator P_J is a Hermitian projection operator which means that

$$P_J^\dagger = P_J$$

$$P_J^2 = P_J$$

Useful operators are the related operators

$$P_{JM} = \frac{2J+1}{8\pi^2} \int d\Omega D_{MK}^{J*}(\Omega) R_\Omega \qquad (35)$$

which construct the "partner-functions" Ψ_{JM} of Ψ_{JK}. The operators P_{JM} are, however, neither Hermitian nor projection operators.

The energy E_J corresponding to the projected state Ψ_{JK} can now be expressed as follows, using the fact that the Hamiltonian is a scalar, or

$$[H, P_J] = 0$$

One has

$$E_J = \frac{\langle \Psi_{JK} | H | \Psi_{JK} \rangle}{\langle \Psi_{JK} | \Psi_{JK} \rangle}$$

$$= \frac{\langle \Phi | H P_J | \Phi \rangle}{\langle \Phi | P_J | \Phi \rangle}$$

$$= \frac{\int D_{KK}^{J*}(\Omega) \langle \Phi | H R_\Omega | \Phi \rangle d\Omega}{\int D_{KK}^{J*}(\Omega) \langle \Phi | R_\Omega | \Phi \rangle d\Omega}$$

Using Eqs (27) and (34) one can easily carry out the integration over φ and ψ (this is the advantage of assuming Eq.(27)), so that

$$E_J = \frac{\int_0^\pi \sin\theta \, d\theta \, d_{KK}^J(\theta) \, h(\theta)}{\int_0^\pi \sin\theta \, d\theta \, d_{KK}^J(\theta) \, n(\theta)} \qquad (36)$$

where

$$h(\theta) = \langle \Phi | H \, e^{-i\theta J_y} | \Phi \rangle$$

$$n(\theta) = \langle \Phi | e^{-i\theta J_y} | \Phi \rangle \qquad (37)$$

Before describing how the functions $h(\theta)$ and $n(\theta)$ can be calculated, we should like to make some remarks about the interpretation of the functions $P_J \Phi$ as rotational states. Peierls and Yoccoz [16] introduced the projection operators as a quantum-mechanical description of the rotation of the intrinsic state Φ. They posed themselves the following problem:

Since $[H, R_\Omega] = 0$, it means that

$$\langle \Phi \mid H \mid \Phi \rangle = \langle R_\Omega \Phi \mid H \mid R_\Omega \Phi \rangle$$

for all Ω. So let us try to find the best superposition of these "degenerate functions" $R_\Omega \Phi$

$$\Psi = \int f(\Omega) R_\Omega \Phi$$

in the sense that

$$\delta \frac{\langle \Psi \mid H \mid \Psi \rangle}{\langle \Psi \mid \Psi \rangle} = 0$$

The answer to this problem is

$$f(\Omega) = D^{J*}_{MK}(\Omega)$$

The function Ψ is a superposition of the intrinsic function Φ rotated through different angles Ω. To see that it may correspond to a rotational state, consider the case that Φ is very strongly deformed so that both $n(\theta)$ and $h(\theta)$ go rapidly to zero as θ increases. In this case we can approximate the $d^J_{KK}(\theta)$ function in expression (36) by the first terms of its Taylor expansion

$$d^J_{KK}(\theta) \cong 1 - \frac{\theta^2}{4} [J(J+1) - K^2] + \dots \tag{38}$$

This expression can easily be obtained from the defining equation (34) by expanding the exponential

$$d^J_{KK}(\theta) = \langle JK \mid e^{-i\theta J_y} \mid JK \rangle$$

$$\cong \langle JK \mid 1 - \frac{\theta^2}{2} J^2_y \mid JK \rangle$$

$$= 1 - \frac{\theta^2}{2} \left\langle JK \left| \frac{J^2_x + J^2_y}{2} \right| JK \right\rangle$$

$$= 1 - \frac{\theta^2}{4} \langle JK \mid J^2 - J^2_z \mid JK \rangle$$

where we have used the obvious relations

$$\langle JK \mid J_y \mid JK \rangle = 0$$

$$\langle JK \mid J^2_x \mid JK \rangle = \langle JK \mid J^2_y \mid JK \rangle$$

Introducing the expansion (38) into expression (36) we obtain

$$E_J \cong \frac{\int_0^\pi h(\theta)\sin\theta\,d\theta - \frac{1}{4}[J(J+1)-K^2]\int_0^\pi \theta^2 h(\theta)\sin\theta\,d\theta}{\int_0^\pi n(\theta)\sin\theta\,d\theta - \frac{1}{4}[J(J+1)-K^2]\int_0^\pi \theta^2 n(\theta)\sin\theta\,d\theta}$$

Since the second term, both in the numerator and the denominator, is small compared to the first term [from the assumption for $n(\theta)$ and $h(\theta)$] one has

$$E_J \cong \frac{\int h(\theta)}{\int n(\theta)} + \frac{1}{4}[J(J+1)-K^2]\frac{\int h(\theta)\int \theta^2 n(\theta) - \int \theta^2 h(\theta)\int n(\theta)}{\left[\int n(\theta)\right]^2}$$

where we used the shorthand notation

$$\int f(\theta) \equiv \int_0^\pi f(\theta)\sin\theta\,d\theta$$

Thus, the energies E_J are related as in the rotational model

$$E_J = A + B[J(J+1)-K^2] + \ldots .$$

In the same limit of strong deformation, we also find that the same relations are valid between B(E2) values and the "intrinsic quadrupole moment" $Q_{intr.}$ in (25) as in the rotational model. One is then justified in saying that the functions $P_J \Phi$ correspond to rotational states of the intrinsic state Φ. This is, in fact, not surprising because, if Φ is strongly deformed, it defines a direction in space and this is, from the uncertainty principle, only possible if Φ contains very many angular momentum states which are related among themselves as having the same internal structure, or, in other words, only if Φ contains a "rotational band". Projecting out states with a definite J will then produce the rotational states which are contained in Φ. On the other hand, if Φ does not contain rotational states, P_J will still project states with definite J but the wave functions $P_J \Phi$ will not be related as rotational states. The operator P_J has nothing to do with "rotating the system Φ", but if Φ contains a rotational band, P_J will project the rotational states out.

A simple example showing clearly that a state $P_J \Phi$ does not always mean a rotational state of the intrinsic state Φ, is given by the LS-coupling shell-model wave functions for ^{6}Li. In the shell model one takes the configuration $(0s)^4 (0p)^2$ which for the most symmetric partition [4,2] can couple to L = 0 and L = 2. These shell-model functions can be written as L-projections from an "intrinsic state" Φ^0, which can be taken as a simple Slater determinant

$$\Phi^0 = \det \left| (0s)^4 (0p0)^{n+} (0p0)^{p+} \right|$$

Here n+ means a neutron state with spin $+\frac{1}{2}$, etc... One has

$$\Psi_{L=0} = P_{L=0} \Phi^0$$

$$\Psi_{L=2} = P_{L=2} \Phi^0$$

One easily calculates $\langle \Phi^0 | Q_{20} | \Phi^0 \rangle = \dfrac{2\sqrt{5}}{\sqrt{4\pi}} b^2$ where b is the oscillator length parameter. Thus Φ^0 is a prolate state and one might be inclined to say that $\Psi_{L=0}$ and $\Psi_{L=2}$ correspond to rotations of a cigar-shaped ^{6}Li. However, these same LS-coupling wave functions can also be written as

$$\Psi_{L=0} = P_{L=0} \Phi'$$

$$\Psi_{L=2} = P_{L=2} \Phi'$$

where Φ' is another Slater determinant

$$\Phi' = |(0 s)^4 (0 p 1)^{n+} (0 p -1)^{p+}|$$

and one easily calculates $\langle \Phi' | Q_{20} | \Phi' \rangle = \dfrac{\sqrt{5}}{\sqrt{4\pi}} b^2$, so that $\Psi_{L=0}$ and $\Psi_{L=2}$ could just as well be interpreted as "rotational states of a pancake-shaped ^{6}Li".

In fact, any wave function with a definite J can always be written as a J-projection from an infinite number of different intrinsic states. It is only possible to talk about rotational states if you have a large set of functions with different J-values, which are related among themselves as in the rotational model and an equivalent way of saying this is that they all can be obtained by angular momentum projection from a strongly deformed intrinsic state.

Let us now return to formula (37) and see how $h(\theta)$ and $n(\theta)$ can be calculated. If these functions are known, a simple integration yields the projected energies E_J.

5.1. Approximate method

In the case of strongly deformed Φ, the functions $n(\theta)$ and $h(\theta)$ go rapidly to zero as θ increases. For small values of θ, one has

$$n(\theta) \cong \langle \Phi | 1 - \frac{\theta^2}{2} J_y^2 | \Phi \rangle$$

$$h(\theta) \cong \langle \Phi | H (1 - \frac{\theta^2}{2} J_y^2) | \Phi \rangle$$

up to third order in θ.

An expression for $n(\theta)$ and $h(\theta)$ which is correct for small values of θ and which goes rapidly to zero as θ increases is

$$\tilde{n}(\theta) = \exp \left[- \frac{\theta^2}{2} \langle \Phi | J_y^2 | \Phi \rangle \right]$$

$$\tilde{h}(\theta) = \langle \Phi | H | \Phi \rangle \exp \left[- \frac{\theta^2}{2} \frac{\langle \Phi | H J_y^2 | \Phi \rangle}{\langle \Phi | H | \Phi \rangle} \right]$$

$$(39)$$

Lamme and Boeker [17] have tested this approximation for the light nuclei of ^8Be, ^{12}C, ^{16}O. They find that the energies calculated by using these approximate expressions differ from the exact results only by a few per cent. As is to be expected, they find that the agreement improves as Φ becomes more deformed.

Verhaar [18] has remarked that in the case K = 0, the functions $n(\theta)$ and $h(\theta)$ may become large again for $\theta = \pi$. The method can easily be adapted to include this case.

5.2. Exact method

Let us first consider how to calculate $n(\theta) = \langle \Phi | e^{-i\theta J_y} | \Phi \rangle$ where Φ is the normalized Slater determinant

$$\Phi = \frac{1}{\sqrt{A!}} \det |u_1 u_2 \ldots u_A|$$

Then $e^{-i\theta J_y}\Phi$ is also a Slater determinant which we denote with a bar above, $\bar\Phi$. We write

$$\bar\Phi = \frac{1}{\sqrt{A!}} \det |\bar u_1 \bar u_2 \ldots \bar u_A|$$

where $\bar u_\lambda = e^{-i\theta J_y} u_\lambda$. So $n(\theta)$ is the overlap of the two Slater determinants Φ and $\bar\Phi$. It is well known [19] that this equals the determinant of the overlap matrix O defined by its matrix elements

$$O_{\lambda\mu} = \langle u_\lambda | \bar u_\mu \rangle = \langle u_\lambda | e^{-i\theta J_y} | u_\mu \rangle \qquad (40)$$

thus

$$n(\theta) = \det O \qquad (41)$$

To calculate the matrix elements $O_{\lambda\mu}$, one expands the orbitals u_λ and u_μ into eigenfunctions of j^2 (this is just the form in which the orbitals are obtained in actual HF-calculations)

$$u_\lambda = \sum_i X_i^\lambda |i \, j_i m_\lambda\rangle$$

$$u_\mu = \sum_i X_i^\mu |i \, j_i m_\mu\rangle \qquad (42)$$

where m_λ and m_μ are fixed, since we are considering only the case of axial symmetry here. (Extension to non-axially symmetric HF-solutions is straightforward, but more tedious). One immediately obtains

$$O_{\lambda\mu} = \sum_i \sum_{i'} X_i^{\lambda *} X_{i'}^\mu d_{m_\lambda m_\mu}^{j_i}(\theta) \, \delta_{j_i j_{i'}} \, \delta_{ii'} \qquad (43)$$

This is simple to calculate if the number of terms in the sum is small.
Introducing these functions in the overlap matrix O, it is easy to calculate
the determinant of O if either A is very small or if the matrix O is reduced
to a simple form. The latter happens if the orbitals u_λ have some symmetry,
commuting with the rotation operators. At this stage then, we see how the
symmetry restriction described in section 3 also simplifies the calculation
of $n(\theta)$ and consequently of the angular momentum projection. The symmetry
restriction has as a consequence that the number of terms in the expansion
(42) is much smaller and consequently simplifies the calculation of $O_{\lambda\mu}$.
On the other hand, the symmetry restriction also has as a consequence a
reduction of the matrix O. To illustrate how simple the calculation of $n(\theta)$
may become in special cases, we again consider the LS-coupling shell-model
wave function of ^{6}Li already considered above. In this case,

$$\Phi = \frac{1}{\sqrt{6!}} \quad \det\left|(0\ s)^{n+}(0\ s)^{n-}(0\ s)^{p+}(0\ s)^{p-}(0\ p\ 0)^{n+}(0\ p\ 0)^{p+}\right|$$

where the superscripts n+, p-, etc.., describe the spin-isospin quantum
numbers, neutron with spin $+\frac{1}{2}$, proton with spin $-\frac{1}{2}$ etc. Since we consider
an L-projection here (and not a J-projection) the overlap matrix O is defined
as

$$O_{\lambda\mu} = \langle u_\lambda | e^{-i\theta \ell_y} | u_\mu \rangle$$

This gives

$$O = \begin{vmatrix} 1 & & & & & \\ & 1 & & & & \\ & & 1 & & & \\ & & & 1 & & \\ & & & & \cos\theta & \\ & & & & & \cos\theta \end{vmatrix}$$

i.e. a diagonal matrix, due to the symmetry of the orbitals (which are
eigenfunctions of I, s_z and t_3). We have used the special expressions for
d-functions

$$d^0_{00}(\theta) = 1$$

$$d^1_{00}(\theta) = \cos\theta$$

It follows that

$$n(\theta) = \det O = \cos^2\theta$$

To calculate $h(\theta)$ we must calculate matrix elements of both one-body
and two-body operators between Φ and $\overline{\Phi}$.

$$h(\theta) = t(\theta) + v(\theta) \tag{44}$$

where

$$t(\theta) = \left\langle \Phi \left| \sum_i T(i) \right| \bar{\Phi} \right\rangle$$

$$v(\theta) = \left\langle \Phi \left| \sum_{i<j} V(i,j) \right| \bar{\Phi} \right\rangle . \tag{45}$$

We first consider the one-body operator part $t(\theta)$. One has, because of the antisymmetry of the Slater determinants

$$\left\langle \Phi \left| \sum_i T(i) \right| \bar{\Phi} \right\rangle = A \left\langle \Phi \left| T(i) \right| \bar{\Phi} \right\rangle \tag{46}$$

Expanding Φ and $\bar{\Phi}$ with respect to the first particle

$$\Phi = \frac{1}{\sqrt{A}} \sum_{\lambda=1}^{A} (-)^{\lambda+1} u_\lambda(1) \, \Phi_\lambda(2, 3, \dots A)$$

$$\bar{\Phi} = \frac{1}{\sqrt{A}} \sum_{\lambda=1}^{A} (-)^{\lambda+1} \bar{u}_\lambda(1) \, \bar{\Phi}_\lambda(2, 3, \dots A)$$

where

$$\Phi_\lambda(2, 3, \dots A) = \frac{1}{\sqrt{(A-1)!}} \det \left| u_1 u_2 \dots u_{\lambda-1} u_{\lambda+1} \dots u_A \right|$$

and introducing this into Eq.(45), we obtain

$$t(\theta) = \sum_{\lambda,\mu=1}^{A} (-)^{\lambda+\mu} \langle u_\lambda | T | \bar{u}_\mu \rangle \langle \Phi_\lambda | \bar{\Phi}_\mu \rangle \tag{47}$$

Now $\langle \Phi_\lambda | \bar{\Phi}_\mu \rangle$ is again equal to the determinant of the overlap matrix corresponding to the orbitals of Φ_λ and Φ_μ. This is just the sub-matrix of O obtained by erasing row λ and column μ. This is easily calculated in the same way as $n(\theta)$. The matrix element $\langle u_\lambda | T | \bar{u}_\mu \rangle$ is further calculated by introducing the expansion (42) yielding

$$\langle u_\lambda | T | \bar{u}_\mu \rangle = \sum_{i,i'} X_i^{\lambda *} X_{i'}^\mu \langle i j_i m_\lambda | T | i' j_i m_\lambda \rangle \, \delta_{j_i j_{i'}} \, d_{m_\lambda m_\mu}^{j_i}(\theta) \tag{48}$$

which again is quite simple if the number of terms in the expansion (42) is small. In the above example of ^{6}Li one obtains in this way (because O is diagonal)

$$t(\theta) = \sum_\lambda \langle u_\lambda | T | \bar{u}_\lambda \rangle \langle \Phi_\lambda | \bar{\Phi}_\lambda \rangle$$

$$= 4 \langle 0s | T | 0s \rangle \cos^2 \theta + 2 \langle 0p | T | 0p \rangle \cos^2\theta$$

For the two-body part $v(\theta)$ one proceeds exactly in the same way, expanding Φ and $\overline{\Phi}$ in determinants of particles 1 and 2. This gives

$$v(\theta) = \sum_{\lambda < \mu}\sum_{\nu < \rho} (-)^{\lambda+\mu+\nu+\rho} \langle \Phi_{\lambda\mu} | \overline{\Phi}_{\nu\rho} \rangle \langle u_\lambda u_\mu | V(1-P) | \overline{u_\nu u_\rho} \rangle \tag{49}$$

where

$$\Phi_{\lambda\mu} = \frac{1}{\sqrt{(A-2)!}} \det | u_1 \cdots u_{\lambda-1} u_{\lambda+1} \cdots u_{\mu-1} u_{\mu+1} \cdots u_A |$$

The matrix element $\langle u_\lambda u_\mu | V(1-P) | \overline{u_\nu u_\rho} \rangle$ is again easily calculated by introducing the expansion (42) and coupling the two particles to a definite J. This gives

$$\langle u_\lambda u_\mu | V(1-P) | \overline{u_\nu u_\rho} \rangle = \sum_{pqrs} X_p^{\lambda *} X_q^{\mu *} X_r^\nu X_s^\rho$$

$$\times \sum_J C(j_p j_q J m_\lambda m_\mu) C(j_r j_s J m_\nu m_\rho) d^J_{m_\lambda + m_\mu, m_\nu + m_\rho}(\theta)$$

$$\times \langle p j_p; q j_q | V(1-P) | r j_r; s j_s \rangle_J \tag{50}$$

This formula shows clearly that the labour of such a calculation increases very rapidly with the number of terms in the expansion (42). In the next section, we describe an approximate projected Hartree-Fock calculation for the light nuclei with $4 \leq A \leq 12$ for which it is possible to give some good arguments for choosing a special form for the orbitals such that the overlap matrix O is very much reduced and the number of terms in the expansion (42) of the orbitals is small.

6.   PROJECTED HARTREE-FOCK CALCULATIONS FOR $4 \leq A \leq 12$

It has been said in the introduction that the main objective of HF-calculations in nuclei is the calculation of the shell-model potential and its eigenfunctions, starting from the nuclear Hamiltonian. In this way, the adjustable parameters are eliminated. However, one may also hope that HF-calculations may solve in a satisfactory way the old problem of collective moments and transitions. It is well known that even in very light p-shell nuclei, electric quadrupole moments and transitions are often a factor two larger and faster, respectively, than the shell-model values. Several suggestions have been made of how to improve the shell-model functions in order to reproduce the experimental collective quantities. The simplest of these suggestions is Nilsson's model in which the shell-model potential is allowed to deform. The deformation is treated as a new adjustable parameter and, in solving the problem of collective quantities, it sharpens the problem of the adjustable parameters. We know, however, that the HF-potential has a definite size and a definite deformation which are calculated starting from the nuclear Hamiltonian. So we can calculate whether this deformation is the one needed to reproduce the collective quantities.

To do so, it is necessary to calculate matrix elements of collective quantities with projected functions.

In this section we describe an approximate projected HF-calculation for the nuclei $4 \leq A \leq 12$. These are the simplest nuclei to calculate and, on the other hand, they are already sufficiently heavy to show the problem of collective quantities in a clear way.

We start from the Hamiltonian for the internal energy

$$H = \sum_{i=1}^{A} T(i) - T_{c.m.} + \frac{1}{2} \sum_{i \neq j} V(i, j) \qquad (51)$$

where $T_{c.m.}$ is the kinetic energy of the centre of mass which is subtracted. As nucleon-nucleon interaction we choose an interaction of the Volkov type [20]

$$V(1,2) = \left\{ -V_0 \exp\left[-\left(\frac{r_{12}}{a}\right)^2\right] + V_0' \exp\left[-\left(\frac{r_{12}}{a'}\right)^2\right] \right\} (1 - M + M P_x) \qquad (52)$$

Volkov [20] has studied potentials of this type to be used in HF-calculations for p-shell nuclei. The parameters V_0, a, V_0' and a' are chosen so as to fit approximately:

   i) low-energy two-body scattering data;
   ii) the binding energy and radius of ^{4}He.

The exchange mixture contains only Wigner and Majorana components; M is chosen so as to fit approximately the binding energy and radius of ^{16}O.

TABLE II. VOLKOV AND BRINK PARAMETERS

	V_0	a	V_0'	a'	M
Volkov	83.34	1.60	144.86	0.82	0.60
Brink	60	1.80	60	1.01	0.65

We have used two sets of values for the parameters and label them by "Volkov" and "Brink", respectively. The last set was used by Brink [21] in some variational calculations with α-particle type wave functions. The interaction (52) is purely central and independent of spin and isospin co-ordinates. The eigenfunctions of the Hamiltonian (51) can immediately be classified by Wigner's supermultiplet theory [22]. The lowest energy eigenfunctions belong to the most symmetric partition [f] and are eigenfunctions of both orbital (L) and spin (S) angular momentum separately, as well as of the total isospin T. How can the use of such a Hamiltonian in nuclear HF-calculations be justified? In particular, can a HF-calculation with a purely central Hamiltonian have and physical value?

There are some arguments why spin orbit forces can probably be neglected for the nuclei $4 \leq A \leq 12$, at least, in first approximation. From intermediate coupling shell-model calculations [23] it is well known that

the partition quantum number [f] is very good for nuclei with $4 \leq A \leq 9$ and for the heavier p-shell nuclei it is still a fairly good quantum number. The lowest partition [f] contains the following L-values:

A	[f]	L
5	[41]	1
6	[42]	0, 2
7	[43]	1, 3 ·
8	[44]	0, 2, 4
9	[441]	1, 2, 3, 4
10	[442]	0, 2, 4; 2, 3, 4
11	[443]	1, 2, 3, 4
12	[444]	0, 2, 4

With the exception of A = 9, 10, 11, all the other nuclei correspond to partitions whose L-values increase by steps of two. This means that a spin-orbit force has no off-diagonal matrix elements, mixing different L-values. As a result, if [f] is a good quantum number, L is also a good quantum number for A = 5, 6, 7, 8, 12. Spin-orbit forces then only play a role in lifting the degeneracy in J, without changing the wave functions, and can be neglected in a calculation of the wave functions. For the nuclei A = 9, 10, 11, the L-mixing due to the spin-orbit force can easily be taken into account afterwards by perturbation theory. The way to do this will be described in subsection 7.4 in the case of ^{9}Be. It is to be expected, however, that the results are less good for the heavier nuclei, since [f] is becoming a less good quantum number.

Another possible justification for the neglect of the non-central forces follows from the HF-calculations of Bassichis et al. [9] described in section 4. There we have seen that the HF-orbitals for ^{8}Be obtained in a calculation with the realistic Tabakin force are essentially identical with those obtained in a calculation with a central force, and this is still approximately so in ^{12}C. The non-central forces are thus of very little effect in determining the HF orbitals in light nuclei. We neglect them because this simplifies the calculation considerably.

Faessler [24] has made HF-calculations for ^{8}Be and ^{12}C starting from Volkov's interaction in a truncated Hilbert space (0 s, 0 p, 1 s, 0 d, 1 p, 0 f). As a result he finds the following Slater determinant:

$$\text{for } ^8\text{Be:} \quad \Phi = \frac{1}{\sqrt{8!}} \det \left| \psi_0^4 \, \varphi_0^4 \right|$$

$$\text{for } ^{12}\text{C:} \quad \Phi = \frac{1}{\sqrt{12!}} \det \left| \psi_0^4 \, \varphi_1^4 \, \varphi_{-1}^4 \right| \tag{53}$$

with

$$\psi_0 = \big|\, 0\,s\,0\big\rangle + \alpha \big|\, 1\,s\,0\big\rangle + \beta \big|\, 0\,d\,0\big\rangle$$

$$\varphi_0 = \big|\, 0\,p\,0\big\rangle + \gamma \big|\, 1\,p\,0\big\rangle + \delta \big|\, 0\,f\,0\big\rangle$$

$$\varphi_{\pm1} = \big|\, 0\,p\,\pm1\big\rangle + \epsilon \big|\, 1\,p\,\pm1\big\rangle + \zeta \big|\, 0\,f\,\pm1\big\rangle \qquad \qquad (54)$$

where $\alpha, \beta, \gamma, \delta, \epsilon, \zeta$ are some numerical coefficients. The expansion of the orbitals contains only three terms. On the other hand, one easily sees that $S^2 \Phi = 0$, so that $J = L$. Taking an L-projection $P_L\Phi$, one has to calculate the overlap matrix $O_{\lambda\mu} = \big\langle u_\lambda \big| \exp(-i\theta\,\ell_y)\big| u_\mu \big\rangle$ which turns out to be very much reduced because of parity, spin and isospin selection rules. Thus both conditions for carrying out the angular momentum projection without much labour are fulfilled.

Instead of proceeding in two steps as described in the previous sections, viz.

    i) solve the HF equations, resulting in finding Φ,
    ii) calculate with projected function $P_J \Phi$

one can try to do both operations at once. This then means that one asks for the best function of the form $P_J \Phi$ (where Φ is a Slater determinant) in the sense that

$$\delta \, \frac{\big\langle P_J\Phi \big| H \big| P_J\Phi \big\rangle}{\big\langle P_J\Phi \big| P_J\Phi \big\rangle} = 0 \qquad\qquad (55)$$

This method will be called the projected Hartree-Fock (PHF) method (the projection being carried out before the Slater determinant is obtained). The previously described method will now be called the HFP-method (the projection being carried out after the HF-determinant is obtained). The condition (55) leads to a very complicated set of equations for the HF-orbitals u_λ, and there is no hope of solving these. In section 3, it was shown how the complicated HF-equations can be simplified in order to find the solution of a standard HF-problem. Since the equations corresponding to the PHF-problem are more difficult, one must obviously also resort to some simplifying approximations.

An approximation procedure for a PHF-calculation with the Hamiltonian (51) for the nuclei $4 \leq A \leq 12$ is suggested in the following way. If we used this Hamiltonian in a standard shell-model calculation, we should just get the Elliott SU_3-functions [25] as shell-model wave functions. This follows from the fact that both [f] and L are exact quantum numbers and there is only one function with a definite L in the lowest partition (except for mass 10 for which some L-values occur twice). Now Elliott has shown that the SU_3-functions can be written as an L-projection from an intrinsic function Φ^0. In all nuclei with $4 \leq A \leq 12$ it turns out that it is always possible to choose a single Slater determinant for the intrinsic functions. For the consecutive mass numbers, one has

^{5}He Φ^0 = det $\left| (0 \, s \, 0)^4 \, (0 \, p \, 0)^{n+} \right|$

^{6}Li Φ^0 = det $\left| (0 \, s \, 0)^4 \, (0 \, p \, 0)^{n+} (0 \, p \, 0)^{p+} \right|$

^{7}Li Φ^0 = det $\left| (0 \, s \, 0)^4 (0 \, p \, 0)^{n+} (0 \, p \, 0)^{p+} (0 \, p \, 0)^{n-} \right|$

^{8}Be Φ^0 = det $\left| (0 \, s \, 0)^4 \, (0 \, p \, 0)^4 \right|$

^{9}Be Φ^0 = det $\left| (0 \, s \, 0)^4 \, (0 \, p \, 0)^4 \, (0 \, p \, 1)^{n+} \right|$

^{10}B $\Phi^0_{K=0}$ = det $\left| (0 \, s \, 0)^4 (0 \, p \, 0)^4 \, (0 \, p \, 1)^{n+} (0 \, p \, -1)^{p+} \right|$

                  $\Phi^0_{K=2}$ = det $\left| (0 \, s \, 0)^4 (0 \, p \, 0)^4 \, (0 \, p \, -1)^{n+} (0 \, p \, 1)^{p+} \right|$

^{11}B Φ^0 = det $\left| (0 \, s \, 0)^4 \, (0 \, p \, 1)^4 (0 \, p \, -1)^{n+} \, (0 \, p \, -1)^{p+} (0 \, p \, -1)^{n-} \right|$

^{12}C Φ^0 = det $\left| (0 \, s \, 0)^4 \, (0 \, p \, 1)^4 (0 \, p \, -1)^4 \right|$ (56)

In the case A = 10, there are two intrinsic states [25], respectively, with K = 0 and K = 2. It is immediately clear that the intrinsic functions belong to the most symmetric partition, except for the K = 0 intrinsic state of A = 10. In fact, an intrinsic state belonging to the partition [442] would be

$$\det \left| (0 \, s \, 0)^4 \, (0 \, p \, 0)^4 (0 \, p \, 1)^{n+} (0 \, p \, -1)^{p+} \right| + \det \left| (0 \, s \, 0)^4 (0 \, p \, 0)^4 (0 \, p \, -1)^{n+} (0 \, p \, 1)^{p+} \right|$$

One can, however, easily show that both determinants give the same contribution when an even L-value is projected out and an opposite contribution if an odd L-value is projected out. This shows that one can take just one of these determinants as intrinsic state.

Now, at the beginning of this section, we have pointed out that the main objective of HF-calculations was to eliminate the adjustable parameters, like, e.g., the size of the orbitals. If we should now take as trial functions just the shell-model function

$$\Psi^0_L = P^*_L \Phi^0 \tag{57}$$

with Φ^0 given by (56) and treat the oscillator parameter as a variational parameter to be determined such that

$$E^0_L(b) = \frac{\langle \Psi^0_L | H | \Psi^0_L \rangle}{\langle \Psi^0_L | \Psi^0_L \rangle} \tag{58}$$

becomes minimum, we would have eliminated the adjustable size parameter. The procedure could be looked upon as an approximation to the PHF-problem.

In the same way, we could consider different values for the oscillator parameters along the z-axis (symmetry axis $b_{\parallel}$) and along the x- and y-axes (symmetry plane $b_{\perp}$). This means that one would use as trial function

$$\Psi_L = P_L \Phi \tag{59}$$

where Φ is given by expressions (56) in which the following replacements are made:

$$0 \, s \, 0 \longrightarrow \chi_{000}(b_\perp, b_\parallel)$$

$$0 \, p \, 0 \longrightarrow \chi_{001}(b_\perp', b_\parallel')$$

$$0 \, p \pm 1 \longrightarrow \chi_{1, \pm 1, 0}(b_\perp'', b_\parallel'') \tag{60}$$

where $\chi \, (b_\perp, b_\parallel)$ are eigenfunctions of the axially symmetric deformed harmonic-oscillator potential. In this way, the deformation of the orbitals would be calculated. This would obviously be a better approximation to the PHF-problem.

Variational calculations of this type, but without angular-momentum projection have been carried out by Volkov [20]. His calculations can be looked upon as an approximation to a standard HF-calculation. Volkov found it very difficult to carry out the angular momentum projection. The reason is quite clear, since the orbitals (60) contain an infinite number of terms in their expansion in eigenfunctions of ℓ^2. If, however, we truncate this expansion after a few terms, e.g.,

$$\chi_{000}(b_\perp, b_\parallel) \cong |0 \, s \, 0\rangle + \alpha|1 \, s \, 0\rangle + \beta|0 \, d \, 0\rangle + \ldots$$

$$\chi_{001}(b_\perp', b_\parallel') \cong |0 \, p \, 0\rangle + \gamma|1 \, p \, 0\rangle + \delta|0 \, f \, 0\rangle + \ldots$$

$$\chi_{1, \pm 1, 0}(b_\perp'', b_\parallel'') \cong |0 \, p \pm 1\rangle + \epsilon|1 \, p \pm 1\rangle + \zeta|0 \, f \pm 1\rangle + \ldots \tag{61}$$

we know that the angular momentum projection is quite easy. Now, if $b_\perp$ and $b_\parallel$ are both not very different from the length parameter b in the spherical-oscillator functions $|n \, \ell \, m\rangle$, the expansion will have converged and the truncation will not change the physical meaning of the orbitals. Moreover, we see that the orbitals which we obtain in this way have exactly the same structure as those in relations (54) obtained in a standard HF-calculation with the same interaction for ^{8}Be and ^{12}C. So we may be confident that our approximation procedure to the PHF-problem is fairly accurate.

To summarize, we calculate the following energy:

$$E_L(\alpha, \beta, \gamma, \delta, \epsilon, \zeta; b) = \frac{\langle P_L \Phi | H | P_L \Phi \rangle}{\langle P_L \Phi | P_L \Phi \rangle} \tag{62}$$

where Φ is given by the Slater determinants in expressions (56) in which the one-particle functions $(0 \, s \, 0)$, $(0 \, p \, 0)$, $(0 \, p \pm 1)$ are replaced by the truncated expansions (61) of the deformed oscillator functions $\chi_{000} \chi_{001} \chi_{1 \pm 1 \, 0}$. The parameters $\alpha, \beta, \gamma, \delta, \epsilon, \zeta, b$ are treated as variational parameters, to be determined by the minimum condition for the energy E_L.

It is to be remarked that the energy $E_L^0(b)$ is obtained from $E_L(\alpha, \beta, \gamma, \delta, \epsilon, \zeta, b)$ by putting all parameters $\alpha = \beta = \gamma = \delta = \epsilon = \zeta = 0$. The trial function Ψ_L contains the shell-model function as a special case. Values for the parameters

α β γ δ ϵ ζ different from zero mean admixtures of higher configurations in the shell-model wave function.

7.   RESULTS OF PHF CALCULATIONS FOR NUCLEI WITH $4 \leq A \leq 12$

7.1.   Energies for the ground states (Volkov force)

In Fig. 2 are plotted the binding energies obtained for the ground states of the nuclei $4 \leq A \leq 12$, and compared with the experimental binding energies which were corrected for Coulomb energies.   The general behaviour
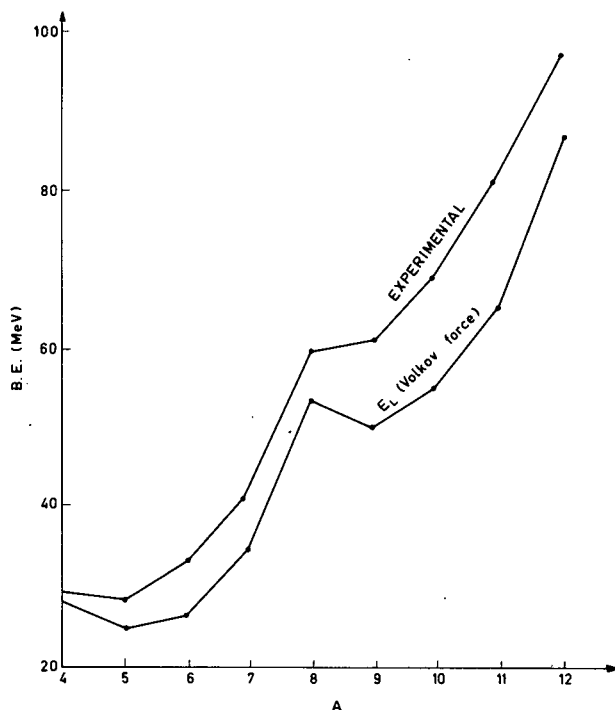
FIG. 2.   Experimental and calculated binding energies as a function of the mass number A.

of the calculated energies agrees quite well with the experimental binding energies, there being a cusp in the energy curve at A = 8.   The details, however, show some discrepancies, the main one being a large dip both at A = 5, 6 and at A = 9.   In fact, both A = 6 and A = 9 would not be bound in contradiction with the experimental situation.   A similar result was found by Volkov [20] and by Bassichis et al. [9] in their HF-calculations, as we have discussed in section 4.   The explanation suggested there also applies for the present calculation.

In this calculation, all nuclei with $A \leq 10$ are prolate whereas A = 11 and 12 are oblate.   This is not a result of our calculation but was in fact assumed when writing down the determinants Φ^0 in expressions (56).   In

general, it is possible to take another expression for Φ^0 (the "lowest weight" state of the SU_3-classification instead of the "highest weight" state). In expressions (56) we have chosen that which turned out to be a single Slater determinant. For some nuclei, A = 6 and A = 10, it is possible to write also an oblate Slater determinant from which the LS-coupling shell-model can be projected out. These are

$$A = 6 \quad \Phi' = \det \left| (0\,s)^4 \, (0\,p\,1)^{n+} \, (0\,p-1)^{p+} \right|$$

$$A = 10 \quad \Phi' = \det \left| (0\,s)^4 \, (0\,p\,1)^3 \, (0\,p-1)^3 \right| \tag{63}$$

and $P_L \Phi^0 \equiv P_L \Phi'$ up to a multiplying constant. If the replacement (61) is carried through and expression (62) is minimized one finds that for both A = 6 and A = 10 the prolate minimum is lower by one or two MeV, respectively. This is in contrast with Volkov's result (without projection) who found the oblate solution to be lower for $9 \le A \le 12$. This is, anyway, not an important problem because both the oblate and the prolate solutions have a very large overlap when a sharp L is projected out.

TABLE III. ENERGIES OF GROUND STATES

A	SM	HF	HFP	PHF	ΔE
4	-27.9	-27.9	-27.9	-28.0	0.1
5	-18.4	-20.7	-20.9	-21.4	3
6	-19.3	-21.3	-23.8	-25.3	6
7	-25.5	-29.7	-33.1	-34.5	9
8	-39.6	-46.5	-52.6	-54.3	14.7

In Table III we compare the energies for $4 \le A \le 8$ obtained from different variational methods:

1. SM: shell-model approximation (58);
2. HF: approximate Hartree-Fock. Trial function Φ given by expressions (56) in which the replacement (61) is made and $\alpha, \beta, \gamma, \delta, \epsilon, \zeta, b$ are treated as variational parameters;
3. HFP: L-projection from HF
4. PHF: approximate PHF (62)

In the last column $\Delta E = E_L^0 - E_L$ is the energy gained by introducing the parameters $\alpha, \beta, \gamma, \delta, \epsilon, \zeta$ in the shell-model function. The very large values show the importance of the admixtures of higher configurations in the shell-model function. The energy ΔE can also be called "deformation energy", since it is the energy gain due to the deformation of the orbitals.

The energy gain (HFP-PHF) is quite small. We shall see further that the deformation of the ground state in the PHF-method is somewhat larger

than in the HFP-method and this larger deformation brings about a better agreement for the collective quantities.

7.2. Excited states (Volkov force)

Since the Hamiltonian is purely central, one obviously cannot expect a detailed agreement with the energies of excited states. Table IV gives the calculated excitation energies, compared with some experimental "mean values", E_X, i.e., the mean for different J-values.

TABLE IV.   ENERGIES OF EXCITED STATES

A	L	E_L	E_X
6	2	3.78	3.74
7	3	6.41	5.69
8	2	3.55	2.90
8	4	12.36	11.4
9	2	2.0	2.43 (?)
9	3	7.0	6.66 (?)
9	4	10.1	?
11	2	1.64	?
11	3	5.90	?
12	2	3.0	4.43
12	4	10.0	?

It is interesting to see how well the energies E_L satisfy the rotational band relation. In the pure shell-model, Racah [26] has shown that a central force leads to a pure $L(L+1)$ spectrum in the p-shell

$$E_L^0 = E_0 + B\,L(L+1)$$

In Fig. 3 we have plotted both E_L^0 and E_L as a function of $L(L+1)$ for A = 9 and A = 11. For E_L, one finds a considerable distortion of the rotational band, the state with L = 3 lying about 2 MeV too high.

Another interesting problem which can be treated by the PHF-method is the occurrence of non-normal parity states in the low-energy spectrum. In ^{9}Be, there is a $1/2^+$ level at 1.7 MeV and a $5/2^+$ level at 3.03 MeV. Using the procedure described in the previous section, these levels would be described on the LS-coupling shell-model by the functions

$$P_L \det \left| (0\,s\,0)^4 (0\,p\,0)^4 (1\,s\,0 - \sqrt{2}\ 0\,d\,0)^{n+} \right|$$

with L = 0 and 2. Using the replacement (61), it would be natural to replace the last orbital $(1\,s\,0) - 2(0\,d\,0)$ by the truncated expansion of
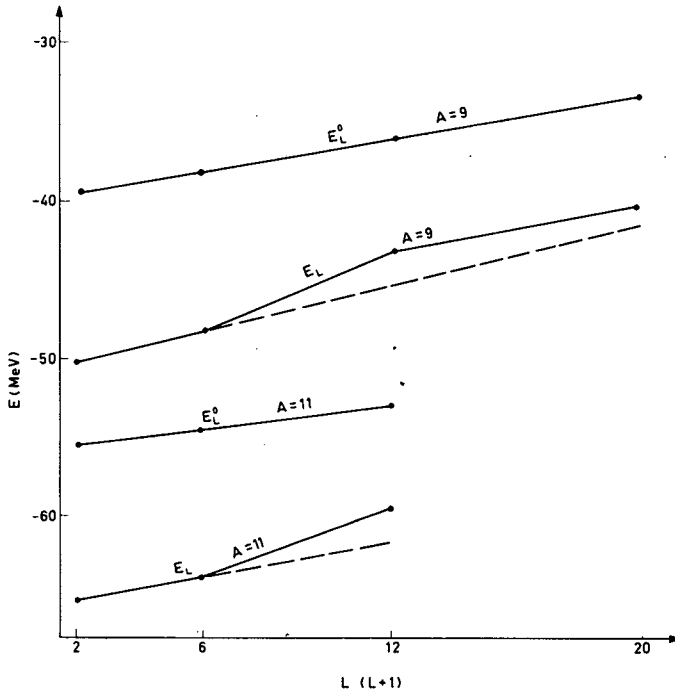
FIG. 3.   Plot of the energies E_L^0 and E_L as a function of $L(L+1)$.

TABLE V.   LEVELS AND ENERGIES

L	E_L^0	E_L	$E_L^0 - E_L$
1^-	-38.9	-49.7	10.8
2^-	-37.5	-47.7	10.2
3^-	-35.4	-42.6	7.2
4^-	-32.5	-39.6	7.1
0^+	-28.9	-45.4	16.5
2^+	-28.8	-43.0	14.2

$\chi_{002}(b_\perp, b_\parallel)$.   Because of computer limitations this has not been done. The energies found are listed in Table V, where we have also repeated the energies of the negative parity band.   One sees that the even parity states lie well above the odd parity states in the shell-model approximation (E_L^0) but drop down low between the odd parity states when the states are allowed to deform.   A very large gain in energy (16.5 MeV) is found, for the 0^+ level, although the outer orbital was not allowed to adjust its deformation to that of the other orbitals.   An extra gain may be expected if the outer orbital is allowed to deform so that the experimental value of 1.7 MeV is quite well attainable.

7.3. Wave functions, size and deformation

The parameters α, γ and ϵ will be called size parameters since they admix an oscillator function with the same angular part to the lowest oscillator functions 0 s and 0 p. In first order, this amounts only to a change in the length parameter of the 0 s and 0 p oscillator functions. From b, α, γ and ϵ one can thus calculate an effective length parameter for the inner (ψ_0) and outer $(\varphi_0, \varphi_{\pm 1})$ orbitals. Qualitatively, the same result is found for the behaviour of these effective length parameters, as was found by Volkov [20] : the size of the inner orbitals increases with A, the size of the outer orbitals decreases with A. At A = 12, inner and outer orbitals have about the same length parameters.
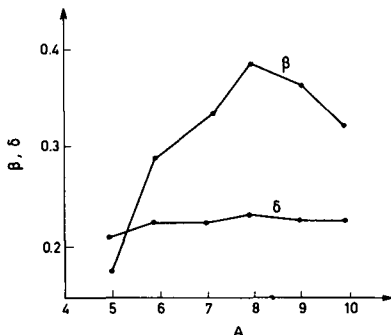
FIG.4.   Deformation parameters β and δ as a function of mass number A.

The parameters β, δ, ζ, on the other hand, admix oscillator functions having a different angular part. These parts can be admixed by the quadrupole deformation of the potential. Thus β, δ and ζ can be called deformation parameters. The values of β and δ for the ground states are given in Fig.4 for the prolate solutions $5 \leq A \leq 10$. The deformation becomes maximum at A = 8. One sees that β changes very much over the shell, whereas δ remains almost constant. Also surprising is that $\beta > \delta$. For a given prolate deformation (i.e. one definite $b_\perp$, $b_\parallel$) one finds that the expansion coefficients of χ_{000} and χ_{001} satisfy $\beta < \delta$. So $\beta > \delta$ means that the HF potential is more deformed for the inner orbital ψ_0 than for the outer orbital φ_0. It also means that there are more admixtures of configurations in which the [4] He core is excited. To have an idea of how much these admixtures take up of the total wave function, we give the decomposition of the ground state of [7] Li: ·

65.7% lowest configuration $(0 s)^4 (0 p)^3$
24%   configurations in which only s-particles are excited,
6.8%   configurations in which only p-particles are excited,
3.5%   configurations in which both s- and p-particles are excited.

This large deformation of the inner orbitals seems surprising in view of the great stability of the α-particle. One can, however, understand it in a qualitative way as follows [27] . The orbital φ_0 has a deformed mass distribution even when the parameter $\delta = 0$, whereas the orbital ψ_0 has a spherical mass distribution when $\beta = 0$. For the values β and δ obtained in the PHF-calculation, the orbital φ_0 still has a more deformed mass distribution than ψ_0 , although the harmonic well for which φ_0 is an approxi-

mate eigenfunction is less deformed than that of ψ_0. If we consider ^{8}Be as an example, an outer particle (with orbital φ_0) feels an average potential produced by four inner particles (orbital ψ_0) and by three outer particles, whereas an inner particle feels an average potential produced by three inner particles and by four outer particles. Since the outer particles have a more deformed mass distribution, it is quite natural that the inner particles feel a more deformed potential or $\beta > \delta$. In the same way, one understands the behaviour of β when the number of particles increases. As more particles with orbital φ_0 are added, the potential felt by the inner particles becomes more deformed and β increases. When the orbital φ_0 is completely filled, and the next particle is added (^{9}Be) in the orbital φ_1, which has an oblate deformation, the potential felt by the inner particles becomes less deformed and β decreases again.

To conclude this section, we remark that as a result of these PHF-calculations one invariably finds β and δ larger for the ground state than for the excited states. In fact, β and δ decrease monotonically as L increases within a "rotational band". This is exactly the opposite of what one expects for a rotational band from the centrifugal force. This result is probably an indication of the fact that the states $P_L\Phi$ are not very real rotational states yet in these light nuclei.

7.4. Influence of a one-body spin-orbit force

We now consider the influence on the PHF-wave functions of adding a one-body spin-orbit force

$$V_{s.o.} = -\zeta \sum_i \vec{\ell}_i \cdot \vec{s}_i \qquad (64)$$

to the central Hamiltonian (51) considered so far. From intermediate coupling shell-model calculations, it is known that the strength ζ of the spin-orbit force increases throughout the 0 p-shell, being quite weak for the nuclei with A < 10. For these nuclei, a perturbation treatment of $V_{s.o.}$ is certainly justified.

As has been remarked before, the introduction of a one-body spin-orbit force in the total Hamiltonian has no effect on the PHF-wave functions for the nuclei $4 \leq A \leq 8$. For these nuclei, the most symmetric partition [4, A-4] contains only values of the total orbital angular momentum L which increase by steps of two. If we restrict ourselves to functions belonging to the lowest partition (which is a good approximation if $V_{s.o.}$ is weak), the spin-orbit force will not change the wave functions for these nuclei since it can only mix L-values which, at most, differ by one unit. The only effect for the nuclei $4 \leq A \leq 8$ would be to lift the degeneracy of the energy, without affecting the wave functions, at all. In the case of the nuclei A = 9, 10 and 11, the lowest partition [4, 4, A-8] contains values of L which differ by one unit only, and these will be mixed even by a weak spin-orbit force. In the following, we restrict ourselves to the ^{9}Be case which is probably the only case for which a perturbation treatment of $V_{s.o.}$ is allowed. Since the strength of the spin-orbit force is not well known, we will treat ζ as a parameter as is done in intermediate coupling calculations [14]. From previous shell-model calculations, we expect ζ to be smaller than 3 MeV.

Having obtained the PHF-energies E_L and wave functions Ψ_L as described in the previous section, we now construct eigenfunctions of the total angular momentum J by coupling orbital and spin angular momenta

$$|\,L\,S\,J\,M\rangle = \langle\phi\,|\,P_L\,|\,\phi\rangle^{-\frac{1}{2}}\sum_{\mu} C\,(L\,S\,J;\,M-\mu,\mu)\,P_{LM-\mu}\,\Phi\,(S,\mu) \tag{65}$$

where $P_{LM-\mu}$ is the operator defined by (35) and $\Phi(S,\mu)$ is obtained from Φ by means of step operators for the spin (μ being the projection of the spin S on the z-axis). The factor $\langle\phi\,|\,P_L\,|\,\phi\rangle^{-\frac{1}{2}}$ is a normalization factor. We then set up the matrix of the total Hamiltonian $H-\zeta\sum\vec{\ell}\cdot\vec{s}$ within the space of functions with the same J. The matrix elements of the one-body spin-orbit force between two PHF functions is calculated by means of the formula

$$\left\langle L\,S\,J\,M\,\left|\,\sum_i\vec{\ell}_i\cdot\vec{s}_i\,\right|\,L'\,S\,J\,M\right\rangle = (-)^{L+L'+S+J+1}\,\frac{(2L+1)\,(2L'+1)}{2}$$

$$\times\sqrt{\frac{(S+1)(2S+1)}{S\,\langle\phi\,P_L\,\phi\rangle\langle\phi\,P_{L'}\,\phi\rangle}}\;\begin{Bmatrix} L & S & J \\ S & L' & 1 \end{Bmatrix}\sum_{\lambda=1}^{A}\sum_{\lambda'=1}^{A}(-)^{\lambda+\lambda'}\,\delta(\sigma_\lambda|\sigma_{\lambda'})\,\delta(\tau_\lambda|\tau_{\lambda'})\,S_z(\lambda)$$

$$\times\sum_{n\ell}\sum_{n'\ell'}X_{n\ell}^{\lambda*}X_{n'\ell'}^{\lambda'}\,\delta_{nn'}\delta_{\ell\ell'}\,\sqrt{\ell(\ell+1)(2\ell+1)}\sum_{\mathscr{L}}(-)^{\ell-\mathscr{L}}(2\mathscr{L}+1)$$

$$\times\begin{pmatrix} \mathscr{L} & \ell & L \\ K-m_\lambda & m_\lambda & -K \end{pmatrix}\begin{pmatrix} \mathscr{L} & \ell & L' \\ K-m_{\lambda'} & m_{\lambda'} & -K \end{pmatrix}\begin{Bmatrix} L' & L & 1 \\ \ell & \ell & \mathscr{L} \end{Bmatrix}$$

$$\times\int_0^\pi\sin\theta\;d\theta\;d^{\mathscr{L}}_{K-m_\lambda,\,K-m_{\lambda'}}(\theta)\qquad\det O_{\lambda\lambda'} \tag{66}$$

where $X_{n\ell}^\lambda$ are the expansion coefficients (54) of the occupied orbitals

$$u_\lambda = \sum_{n\ell}X_{n\ell}^\lambda\,|\,n\,\ell\,m_\lambda\,\sigma_\lambda\,\tau_\lambda\rangle$$

and $\det O_{\lambda\lambda'}$ is the determinant of the matrix, obtained from the overlap matrix O by erasing row λ and column λ'. The label K is the eigenvalue of L_z corresponding to the Slater determinant Φ. Formula (66) will be derived in the Appendix.

The matrix of the total Hamiltonian is then diagonalized for several values of ζ between 0 and 3 MeV. The resulting energies E_J are plotted as a function of ζ in Fig. 5. It is to be noticed that, for this figure, Brink's force [21] has been used in the central Hamiltonian (51). From now on, in this paper, all results that will be given were calculated with Brink's interaction. The reason for this sudden change is the following. In our original work, we used Volkov's force so that we have more complete results for the energies with Volkov's interaction. Later on, we found out that Brink's less attractive force gave a better quantitative agreement with
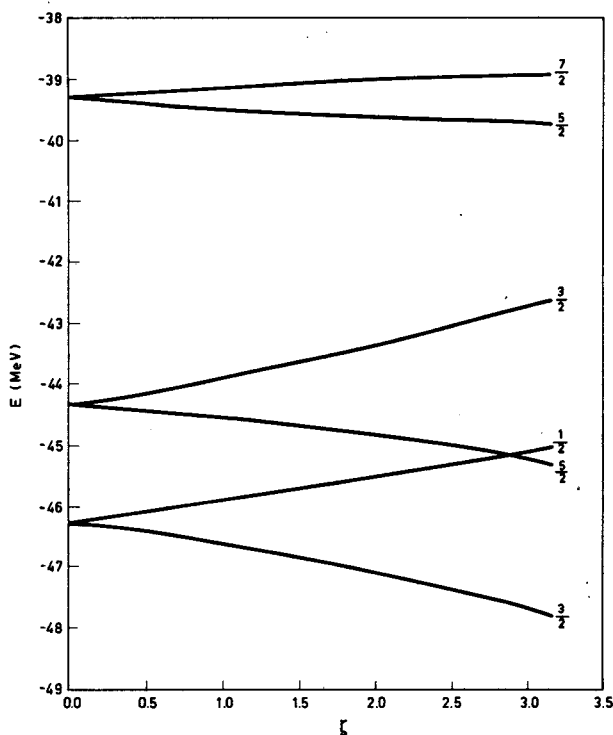
FIG. 5.   Energy of low-lying levels of ^{9}Be as a function of the spin-orbit strength ζ.

the experimental sizes and deformations in light nuclei. We did, however, not repeat all energy calculations with Brink's force, but only those which were necessary for obtaining the wave functions needed for the calculations described in the next section.

The dependence of E_J on ζ is very similar to that of the intermediate coupling calculations of Kurath [14]. The lowest $5/2^-$ level is found at an excitation energy in rough agreement with the experimental value over the whole range of ζ-values between 0 and 3 MeV. The lowest $7/2^-$ level is everywhere too high. The other calculated levels have not been observed experimentally. Hence, it is difficult to determine the best value of ζ from a comparison of the calculated and experimental energy spectra. In the next section, we shall determine ζ from a comparison of the calculated and experimental value for the magnetic moment of the ground state.

The eigenfunctions $\Psi(J)$ for the lowest $J = 3/2$ and $J = 5/2$ levels are given in Table VI. The following notation is used

$$\Psi(J) = x_- \left| L = J-1/2, S, J \right\rangle + x_+ \left| L = J+1/2, S, J \right\rangle \tag{67}$$

The wave functions for the second $3/2^-$ and $5/2^-$ level are obtained from the orthogonality condition. For $J = 1/2$, there is only one L-value:
$\Psi (J = 1/2) = \left| L = 1, S, J \right\rangle$.

TABLE VI. EXPANSION COEFFICIENTS OF THE FUNCTIONS $\Psi(J)$
AS DEFINED IN EQ. (67)

J		x_-	x_+
	0	1	0
	0.5	0.9908	-0.1354
	1	0.9729	-0.2311
3/2	1.5	0.9548	-0.2972
	2	0.9391	-0.3437
	2.5	0.9260	-0.3775
	3	0.9152	-0.4030
	0	1	0
	0.5	0.9992	-0.0411
	1	0.9966	-0.0820
5/2	1.5	0.9925	-0.1221
	2	0.9870	-0.1609
	2.5	0.9802	-0.1978
	3	0.9725	-0.2327

8. COLLECTIVE MOMENTS AND TRANSITIONS. FORM FACTORS FOR HIGH-ENERGY ELECTRON SCATTERING

The PHF-functions obtained in the way described above have a strongly deformed intrinsic state, and one may ask whether the electromagnetic collective E2-moments and transitions can be explained. If so, this would mean that the problem of the collective quantities in the shell model has its origin in the fact that the shell-model potential was not calculated but chosen incorrectly. That this is indeed so will be seen by calculating several collective quantities in ^{7}Li and ^{9}Be. Similar calculations performed for ^{6}Li and ^{12}C lead to the same conclusions [28, 29].

Before considering collective quantities, one may, however, wonder whether the large admixtures of higher configurations have not disturbed the agreement which existed between the shell-model predictions and experimental magnetic dipole moments and transitions. That this is not so can be seen as follows. The magnetic dipole operator

$$\mu = \sum_p \ell_z + \mu_p \sum_p \sigma_z + \mu_n \sum_n \sigma_z$$

consists of an orbital and a spin part. The spin part can be rewritten as follows:

$$\mu_{\text{spin part}} = \frac{\mu_p + \mu_n}{2} \sum_i \sigma_z + \frac{\mu_p - \mu_n}{2} \sum_i \sigma_z \tau_3$$

where the sums run now over all nucleons. The new operators $\sum \sigma_z$ and $\sum \sigma_z \tau_3$ are, however, infinitesimal operators of the group SU_4. The matrix elements of these operators are, consequently, completely determined by the transformation properties of the PHF-functions under the group SU_4 and not by the detailed structure of the functions (in the same way that the matrix elements of L_+, e.g., between functions which have definite transformation properties under rotations are determined by these transformation properties). This means that the spin part of the magnetic-moment operator is exactly the same for the PHF as for the shell-model LS-coupling functions. The orbital part, on the other hand, is usually much smaller and has no matrix elements between different shell-model configurations. This means that the change is only of second order in the variational parameters. The total change is quite small (the above argument is obviously also applicable to allowed β-transitions, the operators $\sum \tau$ and $\sum \sigma \tau$ being infinitesimal operators of SU_4).
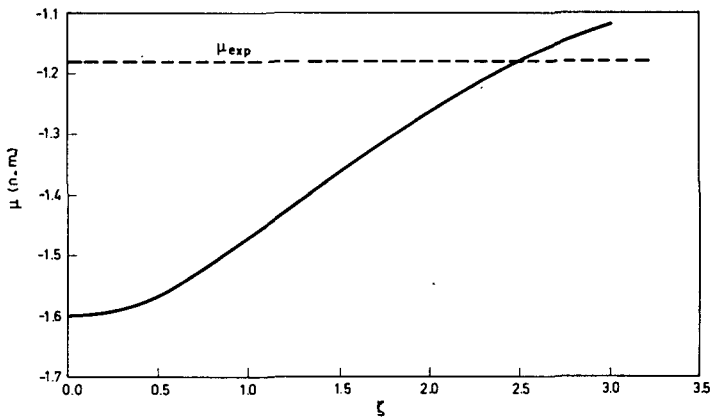
FIG.6. Magnetic dipole moment as a function of the spin-orbit strength ζ in ^{9}Be.

The above argument is not directly valid for ^{9}Be since the spin-orbit force disturbs the SU_4-symmetry. However, the actual calculation of μ gives also in this case a very similar result for the PHF and for the shell-model wave functions. One finds that μ depends very sensitively on the spin-orbit strength (Fig.6). The experimental value $\mu_{exp} = -1.18$ n.m. can then be used to determine the best value for ζ. This gives $\zeta \sim 2.5$ MeV.

For the calculation of collective moments and transitions, or for longitudinal form factors for electron scattering, one has to calculate matrix elements between PHF functions of operators of the form

$$T^r_\rho = \sum_p t^r_\rho = \sum_i t^r_\rho \left(\frac{1 + \tau_3}{2} \right) \tag{68}$$

where the sum $\sum_p$ runs over the protons only. The operator t^r_ρ is a one-body tensor operator of rank r and is independent of spin co-ordinates. In the same way as for the derivation of formula (66), one obtains the formula

$$\langle L\,S\,J\,\|T^r\|\,L'\,S\,J'\rangle = (-)^{S+J'}\,\frac{(2L+1)(2L'+1)}{2}\,\sqrt{\frac{(2J+1)(2J'+1)}{\langle\Phi|P_L|\Phi\rangle\langle\Phi|P_{L'}|\Phi\rangle}}$$

$$\times\begin{Bmatrix}L & S & J\\ J' & r & L'\end{Bmatrix}\sum_{\lambda=1}^{A}\sum_{\lambda'=1}^{A}(-)^{\lambda+\lambda'}\,\delta(\sigma_\lambda|\sigma_{\lambda'})\,\delta(\tau_\lambda|\tau_{\lambda'})\,\frac{1+\tau_3(\lambda)}{2}\sum_{n\ell}\sum_{n'\ell'}X^{\lambda*}_{n\ell}X^{\lambda'}_{n'\ell'}$$

$$\times\langle n\,\ell\,\|t^r\|\,n'\ell'\rangle\sum_{\mathscr{S}}(-)^{\ell-\mathscr{S}}(2\mathscr{S}+1)\begin{pmatrix}\mathscr{S} & \ell & L\\ K-m_\lambda & m_\lambda & -K\end{pmatrix}\begin{pmatrix}\mathscr{S} & \ell' & L'\\ K-m_{\lambda'} & m_{\lambda'} & -K\end{pmatrix}$$

$$\times\begin{Bmatrix}L & L' & r\\ \ell' & \ell & \mathscr{S}\end{Bmatrix}\int_0^\pi\sin\theta\,d\theta\,d^{\mathscr{S}}_{K-m_\lambda,\,K-m_{\lambda'}}(\theta)\quad\det O_{\lambda\lambda'}\qquad\qquad(69)$$

The reduced matrix element here is that defined by Racah

$$\langle J\,M|T^r_\rho|J'\,M'\rangle = (-)^{J-M}\begin{pmatrix}J & r & J'\\ -M & \rho & M'\end{pmatrix}\langle J\|T^r\|J'\rangle$$

The collective quantities which we consider first are the static quadrupole moments of the ground state. The quadrupole moment of ^{7}Li is known fairly well [30]: $Q = (-4.0 \pm 0.5)$ fm^2. The shell model in LS-coupling gives $Q = -3/5\,b^2$ where b is the oscillator-length parameter. Using the reasonable value b = 1.73 fm, one obtains $Q_{S.M.} = -1.8$ fm^2 which is smaller than the experimental value by a factor of two. The calculation with the PHF-function yields -3.91 fm^2.

It may be useful to notice at this point that the quadrupole moment of ^{7}Li is negative although the intrinsic state is prolate, i.e. has a positive intrinsic quadrupole moment. The Bohr-Mottelson relation between the intrinsic moment $Q_{intr.}$ and the quadrupole moment Q_J in a rotational state with spin J is

$$Q_J = \frac{3K^2 - J(J+1)}{(J+1)(2J+3)}Q_{intr.}\qquad\qquad(70)$$

The ground-state spin of most nuclei has J = K and since J ≥ 1 (in order to have $Q_J \neq 0$) one finds that Q_J and $Q_{intr.}$ have the same sign. However, in the case K = 1/2, the ground state may have J = 3/2 because of the decoupling parameter, and in this case Q_J and $Q_{intr.}$ have different signs. This then should be the picture of ^{7}Li in the rotational model.

The value of $Q_{intr.}$ calculated with the intrinsic state Φ turns out to be 17.88 fm^2. Using Eq.(70) this yields $Q_J = -3.58$ fm^2 for the ground state of ^{7}Li compared to the value -3.91 fm^2 obtained in the exact calculation. This shows the type of error made by using the Bohr-Mottelson relations.

The quadrupole moment of ^{9}Be is not well known experimentally, the quoted values [31] ranging between 2 fm^2 and more than 6 fm^2. The shell-model in intermediate coupling gives values between 1.8 fm^2 and 3 fm^2. The value calculated with the PHF-function $\Psi(J)$ in Eq.(67) is shown as a function of ζ in Fig.7. The value obtained is considerably larger than in the shell model. The quadrupole moment increases rapidly with ζ,
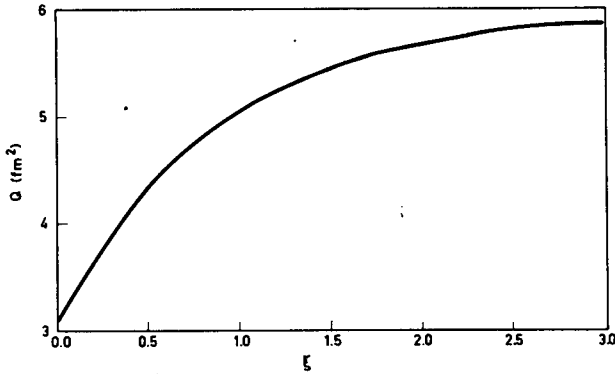
FIG. 7.   Electric quadrupole moment as a function of the spin-orbit strength ζ in ^{9}Be.

reaching an almost stationary value when ζ lies between 2 and 3 MeV. This suggests a quadrupole moment between 5.5 fm^2 and 6 fm^2, in rough agreement with the value $Q = 5.26$ fm^2 obtained from atomic beam h.f.s. [32]. It will be seen further on that this value is also consistent with the high energy electron scattering data.

Detailed and very accurate information about nuclei is obtained from high-energy electron-scattering experiments. It is commonly believed that the cross-section for scattering of high-energy electrons from light nuclei may be calculated in first-order Born approximation [33]:

$$\frac{d\sigma}{d\Omega} = \sigma_{\text{Mott}}(\theta)\left[\,|F_L(q)|^2 + \left(\frac{1}{2} + \text{tg}^2\frac{\theta}{2}\right)|F_T(q)|^2\right]$$

Here $\sigma_{\text{Mott}}(\theta)$ is the cross-section for scattering from a point nucleus in which the whole charge is concentrated. The functions $F_L(q)$ and $F_T(q)$ are called, respectively, the longitudinal and transverse form factors and are functions of the momentum transfer $q = |\vec{k}_i - \vec{k}_f|$ only where $\vec{k}_i$ and $\vec{k}_f$ are the wave vectors of the incoming and of the outgoing electron, respectively. By doing measurements at different initial electron energies and at different scattering angles, one can obtain $|F_L(q)|^2$ and $|F_T(q)|^2$ separately. We will concentrate here on the longitudinal form factors which are easier to calculate and which are usually better known experimentally.

The longitudinal form factor $F_L(q)$ is defined by

$$|F_L(q)|^2 = \frac{1}{Z^2}\frac{1}{2J_i+1}\sum_{M_iM_f}\left|\left\langle J_fM_f\left|\sum_p e^{i\vec{q}\cdot\vec{r}}\right|J_iM_i\right\rangle\right|^2 \qquad (71)$$

where the sum $\sum_p$ runs over the Z protons only. According to whether the final state J_f is equal or not to the initial state J_i, this formula defines the longitudinal form factor for elastic or inelastic scattering. Expanding the plane wave $\exp(i\vec{q}\cdot\vec{r})$ in multipoles, only a few terms will remain from angular-momentum and parity conservation.

We obtain

$$|F_L(q)|^2 = \sum_{\cdot\lambda} |F_{L,\lambda}(q)|^2 \tag{72}$$

where

$$|F_{L,\lambda}(q)|^2 = \frac{|\langle J_f\|M_\lambda(q)\|J_i\rangle|^2}{2J_i + 1} \tag{73}$$

with

$$M_{\lambda\mu}(q) = \frac{\sqrt{4\pi}}{Z}\sum_P j_\lambda(qr)\,\mathcal{Y}_{\lambda\mu}(\theta,\varphi) \tag{74}$$

If the parity of the initial and final states is the same, only even values of λ remain in Eq. (72).

For small values of momentum transfer, one has

$$j_0(qr) \sim 1 - \frac{q^2 r^2}{6}$$
$$j_2(qr) \sim \frac{q^2 r^2}{15} \tag{75}$$

Introducing this into Eq. (74), one obtains for small values of momentum transfer

$$F_{L,\lambda=0} \sim 1 - \frac{q^2}{6}\langle r^2\rangle$$
$$|F_{L,\lambda=2}|^2 \sim \frac{4\pi q^4}{225\,Z^2}\frac{|\langle J_f\|\sum_P r^2\mathcal{Y}_2\|J_i\rangle|^2}{2J_i+1} \tag{76}$$

Here $\langle r^2\rangle$ is the square of the r.m.s. radius of the charge distribution, and the reduced matrix element of $\sum_P r^2\mathcal{Y}_{2\mu}$ is related to the quadrupole moment in the case of elastic scattering and to the reduced E2-transition probability in the case of inelastic scattering. The last equation can be rewritten (always for small q)

$$|F_{L,\lambda=2}|^2 \sim \frac{q^4}{36\,Z^2}\frac{(J+1)(2J+3)}{5J(2J-1)}Q^2 \qquad \text{for } i = f$$
$$\sim \frac{4\pi q^4}{225\,Z^2}B(E2;\ J_i \rightarrow J_f) \qquad \text{for } i \neq f \tag{77}$$

This shows that the quadrupole part of the longitudinal form factor will be enhanced considerably compared to the shell-model predictions. As

an example, we consider a few longitudinal form factors which were deter-
mined quite accurately.

The cross-section for scattering of high-energy electrons from ^{7}Li
was measured by Suelzle, Yearian and Crannell [34], up to high momentum
transfers of $q^2 \lesssim 7$ fm^{-2}. In fact, electrons which were scattered elastically
could not be separated from those which were scattered inelastically with
excitation of the low-lying $1/2^-$ level at 0.478 MeV. The measured cross-
section is the sum of the elastic and inelastic cross-sections. From their
measurements, together with a previous determination [35] of the trans-
verse form factor $F_T(q)$, Suelzle et al. were able to determine the square
of the longitudinal form factor, which is again equal to the sum of the squares
of the elastic and the inelastic form factors

$$\left| F_L(q) \right|^2 = \left| F_L^{el}(q) \right|^2 + \left| F_L^{inel}(q) \right|^2 \tag{78}$$

Since $J_i = 3/2$ for the ground state, one has

$$\left| F_L^{el}(q) \right|^2 = \left| F_{L,\lambda=0}^{el}(q) \right|^2 + \left| F_{L,\lambda=2}^{el}(q) \right|^2 \tag{79}$$

and since $J_f = 1/2$ for the inelastic part, one has

$$\left| F_L^{inel}(q) \right|^2 = \left| F_{L,\lambda=2}^{inel}(q) \right|^2 \tag{80}$$

In the supermultiplet theory, the states $J = 3/2$ and $J = 1/2$ form a spin
doublet with $L = 1$ and $S = 1/2$. From this, there follows a relation between
the quadrupole part of the elastic and the inelastic form factors. One easily
calculates

$$\frac{\left| \left\langle L=1\ S=1/2\ J=3/2 \left\| \sum_P j_2 \mathcal{Y}_2 \right\| L=1\ S=1/2\ J=1/2 \right\rangle \right|^2}{\left| \left\langle L=1\ S=1/2\ J=3/2 \left\| \sum_P j_2 \mathcal{Y}_2 \right\| L=1\ S=1/2\ J=3/2 \right\rangle \right|^2} = \frac{\left\{ \begin{matrix} 1 & 1/2 & 3/2 \\ 1/2 & 2 & 1 \end{matrix} \right\}^2}{2 \left\{ \begin{matrix} 1 & 1/2 & 3/2 \\ 3/2 & 2 & 1 \end{matrix} \right\}^2}$$

The right-hand side turns out to be equal to unity. One, thus, has

$$\left| F_L(q) \right|^2 = \left| F_{L,\lambda=0}^{el}(q) \right|^2 + 2 \left| F_{L,\lambda=2}^{el}(q) \right|^2 \tag{81}.$$

The matrix elements are calculated by means of Eq.(69) and the result is
compared with the experimental data in Fig. 8. The very good agreement
gives experimental confirmation for the calculated value of the quadrupole
moment $Q = -3.91$ fm^2. The monopole part $F_{L,\lambda=0}^{el}$ becomes negligible com-
pared to the quadrupole part for $q^2 \gtrsim 4$ fm^{-2}, and a large discrepancy would
have been obtained for these momentum transfers with the pure shell-model
wave functions.
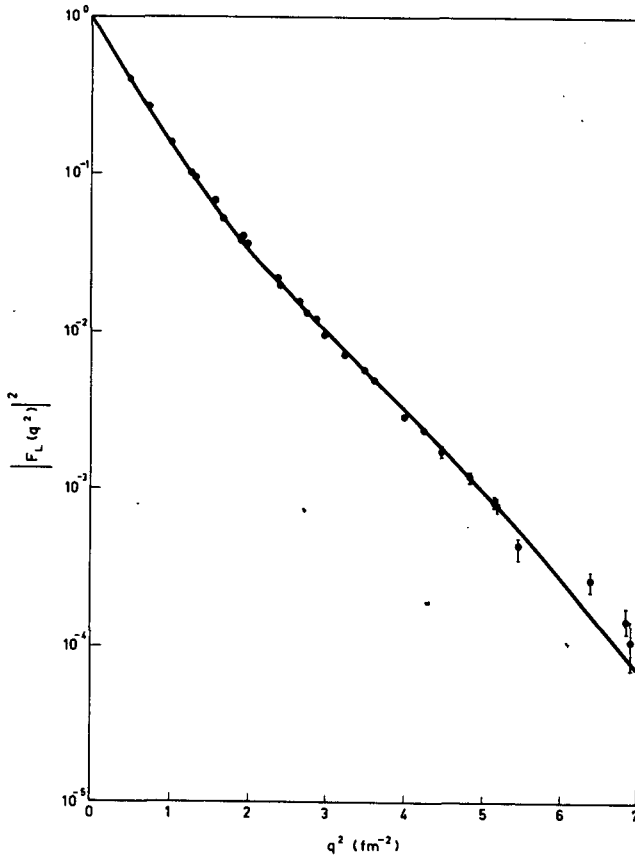
FIG. 8. Sum of elastic and inelastic (0.478 MeV level) longitudinal form factors in ^{7}Li.

As a second example, we consider the elastic form factor for ^{9}Be determined by several experimental groups [31,36]. Since the ground state has J = 3/2, there is again a monopole and a quadrupole contribution, and an eventual fit would support the calculated value of the quadrupole moment. The calculated form factor is shown in Fig. 9 for two values of the spin-orbit strength ζ = 0 and ζ = 2.5 MeV. For this latter case which is suggested from the value of the magnetic moment, the monopole and quadrupole contribution are drawn separately. The agreement is satisfactory over the whole range of q^{2}-values if the Meyer-Berkhout et al. [36] data are used in the region 2.5 fm^{-2} < q^{2} < 5 fm^{-2}. No equally good fit can be obtained for any value of the spin-orbit strength if the Bernheim et al. [31] data are used. A re-measurement would be needed to decide between the two experimental groups.

The inelastic form factor to the 5/2^{-} level at 2.43 MeV in ^{9}Be was determined by the Orsay group [37,31]. The form factor calculated with the PHF-functions is shown in Fig. 10 for ζ = 0 and ζ = 2.5 MeV. The agreement is very satisfactory although there appears again a discrepancy with the Bernheim et al. data in the same region of momentum transfers as in the case of elastic scattering.
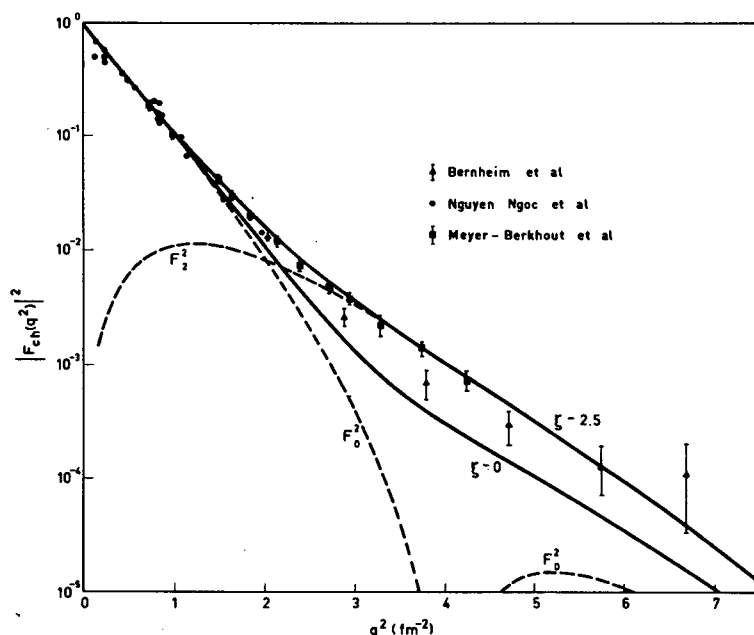
FIG.9.   Charge form factor for ^{9}Be, both for $\zeta = 0$ and $\zeta = 2.5$ MeV. The monopole and quadrupole contributions are shown separately (dashed curves) in the case $\zeta = 2.5$ MeV.
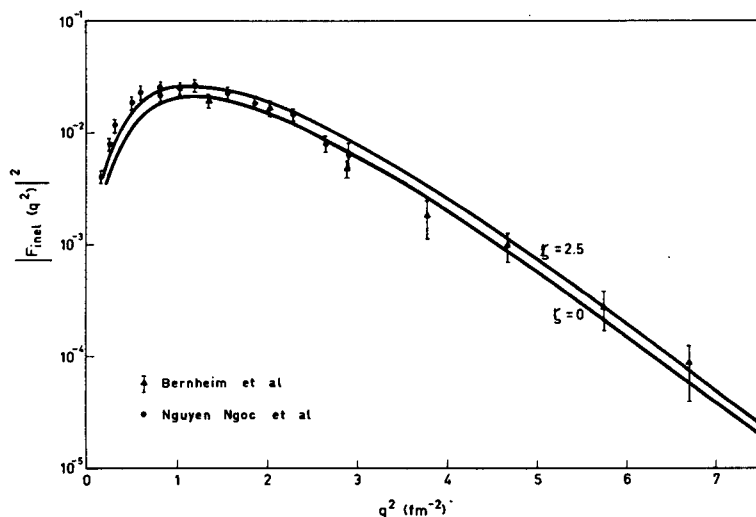
FIG.10. Inelastic form factor for excitation of the 5/2$^-$ level at 2.43 MeV in ^{9}Be, both for $\zeta = 0$ and $\zeta = 2.5$ MeV.

At the end of this section, we may conclude that the PHF-functions represent a considerable improvement compared to the usual shell-model functions in the sense that collective moments and transitions are reproduced

in a satisfactory way. The improvement is obtained by a considerable amount of excited configurations. Standard shell-model calculations cannot take these configurations into account because of computational limitations. They are, however, easily incorporated through a HF-calculation.

APPENDIX

To derive Eq.(66), we first decouple orbital and spin parts

$$\langle L S J | \sum \vec{\ell} \cdot \vec{s} | L' S J \rangle = (-)^{L'+S+J} \begin{Bmatrix} L & S & J \\ S & L' & 1 \end{Bmatrix} \frac{\langle L L, S S | \sum \ell_z s_z | L' L S S \rangle}{\begin{pmatrix} L & 1 & L' \\ -L & 0 & L \end{pmatrix} \begin{pmatrix} S & 1 & S \\ -S & 0 & S \end{pmatrix}}$$

where we have assumed $L' \geq L$. We now calculate the matrix element in the numerator. The functions $| L M S S \rangle$ are given by

$$| L M S S \rangle = \frac{2L+1}{8\pi^2 \langle \Phi | P_L | \Phi \rangle^{\frac{1}{2}}} \int d\Omega \ D_{MK}^{L*}(\Omega) \ R_\Omega \Phi(S, S)$$

where R_Ω rotates the spatial co-ordinates only. Using the group properties of the rotation operators and matrices, we easily obtain

$$\langle L L S S | \sum \ell_z s_z | L' L S S \rangle = \frac{C(L', L; L\, 0)}{\sqrt{\langle \Phi P_L \Phi \rangle \langle \Phi P_{L'} \Phi \rangle}} \sum_\mu C(L' 1 L; K - \mu, \mu)$$

$$\frac{2L'+1}{8\pi^2} \int d\Omega \ D_{K-\mu,K}^{L'\, *}(\Omega) \left\langle \Phi(S, S) \left| \sum_i \ell_\mu S_z R_\Omega \right| \Phi(S, S) \right\rangle$$

Performing the integration over the Euler angles φ and ψ yields

$$\langle L L S S | \sum \ell_z s_z | L' L S S \rangle = \frac{C(L', L; L\, 0)}{\sqrt{\langle \Phi P_L \Phi \rangle \langle \Phi P_{L'} \Phi \rangle}} \sum_\mu C(L' 1 L; K - \mu, \mu)$$

$$\frac{2L'+1}{2} \int_0^\pi \sin\theta \ d\theta \ d_{K-\mu,K}^{L'}(\theta) \left\langle \Phi(S S) \left| \sum_i \ell_\mu s_z e^{-i\theta L_y} \right| \Phi(S S) \right\rangle$$

We now use formula (47) for a general one-body operator between two Slater determinants, as well as the relations

$$\langle u_\lambda | \ell_\mu S_z | \bar{u}_{\lambda'} \rangle = \delta(\sigma_\lambda | \sigma_{\lambda'}) \ \delta(\tau_\lambda | \tau_{\lambda'}) \ s_z(\lambda) \sum_{n\ell} \sum_{n'\ell'} X_{n\ell}^{\lambda *} X_{n'\ell'}^{\lambda'}$$

$$\times \ d_{m_\lambda-\mu, m_{\lambda'}}^{\ell'}(\theta) \ \langle n \ell m_\lambda | \ell_\mu | n' \ell' m_\lambda - \mu \rangle$$

$$\langle n \ell m_\lambda | \ell_\mu | n' \ell' m_\lambda - \mu \rangle = \delta_{nn'} \ \delta_{\ell\ell'} C(\ell, \ell; m_\lambda - \mu, \mu) \sqrt{\ell(\ell+1)}$$

to obtain

$$\langle LLSS|\sum \ell_z S_z|L'LSS\rangle = \frac{C(L'1L;L0)}{\sqrt{\langle \Phi P_L \Phi\rangle\langle \Phi P_{L'}\Phi\rangle}} \frac{2L'+1}{2}\sum_{\lambda=1}^{A}\sum_{\lambda'=1}^{A}(-)^{\lambda+\lambda'}$$

$$\times\, \delta(\sigma_\lambda|\sigma_{\lambda'})\,\delta(\tau_\lambda|\tau_{\lambda'})\,s_z(\lambda)\sum_{n\ell}\sum_{n'\ell'}X_{n\ell}^{\lambda*}X_{n'\ell'}^{\lambda'}\,\delta_{nn'}\,\delta_{\ell\ell'}\,\sqrt{\ell(\ell+1)}$$

$$\times\int_0^\pi \sin\theta\,d\theta\,\det O_{\lambda\lambda'}\sum_\mu C(L',L;K-\mu,\mu)\,C(\ell,\ell;m_\lambda-\mu,\mu)\,d_{K-\mu,K}^{L'}\,d_{m_\lambda-\mu,m_{\lambda'}}^{\ell}.$$

The sum $\sum_\mu$ can be reduced to a simpler form by using properties of the d-functions and the Clebsch-Gordan coefficients yielding

$$\sum_\mu \ldots = \sum_{\mathscr{J}}(-)^{L+1-K}\sqrt{(2L+1)(2\mathscr{J}+1)}\;C(L'\ell\mathscr{J};-K,m'_\lambda)$$

$$\times\,C(L\mathscr{J}\ell;K,m_\lambda-K)\begin{Bmatrix} L & L' & 1 \\ \ell & \ell & \mathscr{J} \end{Bmatrix}d_{m_\lambda-K,m_{\lambda'}-K}^{\mathscr{J}}(\theta)$$

Introducing this into the previous formula, rewriting all Clebsch-Gordan coefficients as 3j-symbols and making use of the explicit expression

$$\begin{pmatrix} S & 1 & S \\ -S & 0 & S \end{pmatrix} = \sqrt{\frac{S}{(S+1)(2S+1)}}$$

one immediately gets (66).

REFERENCES

[1] ULLAH, N., NESBET, R., Nucl. Phys. 39 (1962) 239.
[2] RIPKA, G., in Advances in Nuclear Physics, 1(1968).
[3] TABAKIN, F., Ann. Phys. 30 (1964) 51.
[4] ELLIOTT, J.P. et al., Nucl. Phys. A121 (1968) 241.
[5] BARANGER, M., Varenna lectures (1967).
[6] MESSIAH, A., Mécanique Quantique 2, Dunod, Paris.
[7] OVERHAUSER, A.W., Phys. Rev. Letts 4 (1960) 415.
[8] BOUTEN, M., VAN LEUVEN, P., Physica (1967) 461.
[9] BASSICHIS, W., KERMAN, A., SVENNE, J., Phys. Rev. 160 (1967) 746.
[10] KERMAN, A., SVENNE, J., VILLARS, F., Phys. Rev. 147 (1966) 710.
[11] ELLIOTT, J.P., Nuclear Structure, Herceg Novi Lectures (1966).
[12] KERMAN, A., PAL, M., Phys. Rev. 162 (1967) 970.
[13] BOUTEN, M., VAN LEUVEN, P., DEPUYDT, H., Nucl. Phys. A94 (1967) 687.
[14] KURATH, D., Phys. Rev. 101 (1956) 216.
[15] MUTHUKRISHNAN, R., BARANGER, M., Phys. Lett. 18 (1965) 160.
[16] PEIERLS, R., YOCCOZ, J., Proc. Phys. Soc. 70 (1957) 381.
[17] LAMME, H., BOEKER, E., Nucl. Phys. A111 (1968) 492.
[18] VERHAAR, B.J, Nucl. Phys. 45 (1963) 129.

[19] LÖWDIN, P.O., Phys. Rev. 97 (1955) 1474.

[20] VOLKOV, A.B., Nucl. Phys. 74 (1965) 33.

[21] BRINK, D., Varenna lectures (1965).

[22] WIGNER, E.P., Phys. Rev. 51 (1937) 106.

[23] BARKER, F., Nucl. Phys. 83 (1966) 418.

[24] FAESSLER, A., Nuclear Many-Body Problems, Herceg Novi Lectures (1967).

[25] ELLIOTT, J.P., Proc. Roy. Soc. A245 (1958) 562.

[26] RACAH, G., L. Farkas Memorial Volume, Research Council, Israel (1951).

[27] MANNING, M.R., Ph.D. thesis, McMaster University (1967).

[28] BOUTEN, M., BOUTEN, M.C., VAN LEUVEN, P., Nucl. Phys. A102 (1967) 322; Phys. Lett. 26B (1968) 191.

[29] BOUTEN, M., VAN LEUVEN, P., Ann. Phys. 43 (1967) 421.

[30] Nuclear Moments, Appendix 1 to Nuclear Data Sheets (1965).

[31] BERNHEIM, M., STOVALL, T., VINCIGUERRA, D., Nucl. Phys. A97 (1967) 480.

[32] BLACHMAN, A.G., LURIO, A., Phys. Rev. 153 (1967) 164.

[33] BISHOP, G., Congr. Int. Phys. Nucl., Paris (1964) 343.

[34] SUELZLE, L., YEARIAN, M., CRANNELL, H., Phys. Rev. 162 (1967) 992.

[35] RAND, R., FROSCH, R., YEARIAN, M., Phys. Rev. 144B (1966) 856.

[36] MEYER-BERKHOUT, U., FORD, K., GREEN, A., Ann. Phys. 8 (1959) 119.

[37] NGUYEN NGOC, H., HORS, M., PEREZ-Y-JORBA, J., Nucl. Phys. 42 (1962) 62.

HARTREE-FOCK CALCULATIONS
IN DEFORMED LIGHT AND
MEDIUM-LIGHT NUCLEI

J.P. SVENNE
Institut de Physique Nucléaire
Orsay, France

Abstract

HARTREE-FOCK CALCULATIONS IN DEFORMED LIGHT AND MEDIUM-LIGHT NUCLEI.
1. Introduction; 2. Justification of the inert core; 3. Some details of the calculations; 4. Results of the s-d shell; 5. Projection of rotational states; 6. Results in the 2p-1f shells; 7. Major-shell-mixing unrestricted HF calculations.

1. INTRODUCTION

The Hartree-Fock (HF) method [1] is a systematic method of seeking approximate solutions to the many-body problem. In the case of the nucleus, the nature of the system and of the two-body interaction is such that even with the rather drastic assumptions underlying the HF method, the problem is still very difficult. Therefore, further approximations are made and various types of HF calculations have been and are being carried out by different groups. These may be classified according to the nature of the interaction used and to the kinds of symmetry properties assumed a priori, as follows:

Interactions	Symmetries
1) Effective, phenomenological: e.g. Rosenfeld	a) Inert core $\begin{cases} \text{axial} \\ \text{triaxial} \end{cases}$
2) Semi-phenomenological: e.g. Green, Baranger, Nestor-p^2 forces Brink-sums of Gaussians	b) Spherical c) No inert core $\begin{cases} \text{axial} \\ \text{triaxial} \end{cases}$
3) Semi-realistic: e.g. Tabakin-non-local	d) Parity mixing
4) Realistic, no hard core: e.g. Ried Bressel, Levy	
5) Realistic, hard core (BHF): e.g. Hamada-Johnston Yale	

For example, the MIT group [2] (Kerman, Villars, Bassichis, Svenne) work with emphasis on 3b, 3c, 3d (and aim for 4b, c). Baranger's group [3] (Davies, Krieger, Mathukrishnan, Tarbutton) have mainly worked on 1b and 2b

(but recent work [4] on BHF, 5b). Bouten discusses 2c in his contribution to these Proceedings, and Lande's lectures (not published in these Proceedings) mainly treat 5b.

In my papers, I shall mostly deal with the simplest and oldest type of HF calculations [5]: 1a. But first of all, we should explain what we mean by an "inert core" and how it affects the HF equation.

2.   JUSTIFICATION OF THE INERT CORE

To start with, let us say a few words about the self-consistent symmetries of the HF solution; these are symmetries which, once they are present at any stage of the iteration, remain so throughout all subsequent iterations. It is also possible to impose symmetry properties on the HF wave function by introducing external constraints. One such constraint is the inert core.

In may be possible to find a "core" of particles which can be assumed to remain invariant (inert) under the variations implicit in the HF method. If so, the HF self-consistency problem need be solved only for the few extra particles outside the core (e.g. for nuclei in the 2 s - 1 d shell, ^{16}O is usually taken as the core; then a nucleus such as ^{24}Mg is treated as the ^{16}O core plus 4 neutrons and 4 protons).

The matrix element of the single-particle (s.p.) Hamiltonian is [1]

$$\langle \alpha | h | \beta \rangle = \langle \alpha | t | \beta \rangle + \sum_{\lambda} \langle \alpha \lambda | v_A | \beta \lambda \rangle = \epsilon_\alpha \delta_{\alpha\beta} \tag{1}$$

and the ground-state energy E_0 is given by

$$E_0 = \sum_{\lambda} \langle \lambda | t | \lambda \rangle + \frac{1}{2} \sum_{\lambda\mu} \langle \lambda\mu | v_A | \lambda\mu \rangle \tag{2}$$

Here λ and μ run over all the occupied states.

Let C be the number of particles in the core, and let us rewrite Eq.(1) as

$$\langle \alpha | t | \beta \rangle + \sum_{\lambda=1}^{C} \langle \alpha \lambda | v_A | \beta \lambda \rangle + \sum_{\lambda=C+1}^{A} \langle \alpha \lambda | v_A | \rho \lambda \rangle = \epsilon_\alpha \delta_{\alpha\beta} \tag{3}$$

Assume that we have the HF solution for the core, with s.p. eigenvalues e_α:

$$\langle \alpha | t | \beta \rangle + \sum_{\lambda=1}^{C} \langle \alpha \lambda | v_A | \rho \lambda \rangle = e_\alpha \delta_{\alpha\beta} \tag{4}$$

If we assume that the wave functions of the core are not changed by the addition of the particles outside, we may substitute Eq.(4) into Eq.(3):

$$e_\alpha \delta_{\alpha\beta} + \sum_{\lambda=C+1}^{A} \langle \alpha \lambda | v_A | \beta \lambda \rangle = \epsilon_\alpha \delta_{\alpha\beta} \tag{5}$$

This is the HF equation in the restricted space outside the core. From Eq.(2) we have

$$E_0 = \sum_{\lambda=1}^{C} \langle \lambda | t | \lambda \rangle + \frac{1}{2} \sum_{\lambda,\mu=1}^{C} \langle \lambda\mu | v_A | \lambda\mu \rangle$$

$$+ \sum_{\lambda=C+1}^{A} \langle \lambda | t | \lambda \rangle + \frac{1}{2} \sum_{\lambda,\mu=C+1}^{A} \langle \lambda\mu | v_A | \lambda\mu \rangle + \sum_{\lambda=C+1}^{A} \sum_{\mu=1}^{C} \langle \lambda\mu | v_A | \lambda\mu \rangle \tag{6}$$

The sum of the first two terms is the ground state energy of the core $E_0(C)$. Using Eq.(4), the sum of the third and last terms gives

$$\sum_{\lambda=C+1}^{A} e_\lambda$$

where e_λ is the s.p. energy of a particle in the core.

Therefore,

$$E_0 = E_0(C) + \sum_{\lambda=C+1}^{A} e_\lambda + \frac{1}{2} \sum_{\lambda,\mu=C+1}^{A} \langle \lambda\mu | v_A | \lambda\mu \rangle \tag{7}$$

Equations (5) and (7) now represent the HF problem for the "valence" particles outside the inert core. This is a greatly simplified problem since we now have only $n = A - C$ particles to deal with rather than all A. Generally, the e_α are taken as the experimental s.p. energies appropriate for the core (in the s-d shell case, taken from the ^{17}O spectrum), though ideally, they should be the result of the HF calculation for the core nucleus. $E_0(C)$ is taken as the experimental binding energy of the core; in fact, usually one only calculates the energy of the nucleus relative to the core:

$$E_0 - E_0(C) = \sum_{\lambda=1}^{n} e_\lambda + \frac{1}{2} \sum_{\lambda,\mu=1}^{n} \langle \lambda\mu | v_A | \lambda\mu \rangle = \frac{1}{2} \sum_{\lambda=1}^{n} (e_\lambda + \epsilon_\lambda) \tag{8}$$

A further drastically simplifying assumption is usually made in these restricted HF calculations: the s.p. wave functions $|\alpha\rangle$ are taken as sums over spherical harmonic oscillator functions $|n\ell jm\rangle$

$$|\alpha\rangle = \sum C^\alpha_{n\ell jm} |n\ell jm\rangle \tag{9}$$

But in this case this sum is restricted to run over only one major shell of the harmonic oscillator, i.e. that shell which is outside the closed-shell of the inert core.

The main justification of all these assumptions is that they make the calculations very much easier and faster; therefore, they were the earliest type of HF calculations that had been done. In addition, an external justifi-

cation is provided by the work of Redlich, Kurath and Pičman [6]. They find that the wave functions obtained from intermediate-coupling shell-model calculations are very similar to those obtained by projecting states of good angular momentum from the intrinsic states obtained by filling a deformed harmonic-oscillator well. Such intrinsic states are essentially calculated in the way discussed here when the HF wavefunctions are taken as sums (on ℓ, j and m) of spherical oscillator functions in one major shell.

Of course, errors are introduced by these assumptions. In particular, it is not possible in this way to obtain the correct absolute magnitude of the deformations, since the deformation of the extra-core orbitals induces polarizations of the core, which is not accounted for here. However, the systematics of the deformation are well described, as are other details of the structure of the HF solution and excitation spectra built on it, as we shall see.

Since there is an inert core assumed in these calculations and the s.p. energies e_α are taken from experiment, there is not much sense in choosing the most realistic force possible. Any deficiency in the force or in the way it is treated can be "swept under the rug" by being taken up in the s.p. energies or the strength of the force. Therefore, simple effective interactions are used here (which have the further advantage of making the calculations still easier). The most popular one in 2s - 1d shell calculations is the Rosenfeld [7] force:

$$V(r_{12}) = \frac{V_0}{3} \left(\vec{\tau}_1 \cdot \vec{\tau}_2 \right) \left(0.3 + 0.7\, \vec{\sigma}_1 \cdot \vec{\sigma}_2 \right) e^{-r_{12}^2/\mu^2} \tag{10}$$

A possible way of estimating the error induced by the inert-core assumption could be by the following perturbation approach:

Suppose the wave-functions in the core are changed by the presence of the extra particles in such a way that Eq. (4) is to be replaced by:

$$\langle \alpha | t | \beta \rangle + \sum_{\lambda=1}^{c} \langle \alpha \lambda | v_A | \beta \lambda \rangle = e_\alpha \delta_{\alpha\beta} + \langle \alpha | \delta h^{(1)} | \beta \rangle$$

Then Eq. (5) has the additional term $\langle \alpha | \delta h^{(1)} | \beta \rangle$ and we may calculate its effect (assuming it to be small) by first-order perturbation theory. The modified eigenvalues $\epsilon_{\tilde{\alpha}}$ and eigenvectors $|\tilde{\alpha}\rangle$ are then

$$\epsilon_{\tilde{\alpha}} = \epsilon_\alpha + \langle \alpha | \delta h^{(1)} | \alpha \rangle + \sum_{\lambda=1}^{n} \left[\langle \alpha\tilde{\lambda} | v_A | \alpha\tilde{\lambda} \rangle - \langle \alpha\lambda | v_A | \alpha\lambda \rangle \right]$$

$$|\tilde{\alpha}\rangle = |\alpha\rangle + \sum_{\beta \neq \alpha} \frac{|\beta\rangle \langle \beta | \delta h^{(1)} | \alpha \rangle}{\epsilon_\beta - \epsilon_\alpha} + \sum_{\beta \neq \alpha} \frac{|\beta\rangle \left[\langle \beta\tilde{\lambda} | v_A | \alpha\tilde{\lambda} \rangle - \langle \beta\lambda | v_A | \alpha\lambda \rangle \right]}{\epsilon_\beta - \epsilon_\alpha}$$

The extra term in these equations comes from the self-consistency, the fact that h itself depends on its eigenvectors. It may be evaluated using the first two terms of the second equation, as:

$$\langle \alpha\tilde{\lambda} | v_A | \beta\tilde{\lambda} \rangle - \langle \alpha\lambda | v_A | \beta\lambda \rangle$$

$$= \sum_{\gamma \neq \lambda} \frac{\langle \alpha\lambda | v_A | \beta\gamma \rangle \langle \gamma | \delta h^{(1)} | \lambda \rangle}{\epsilon_\gamma - \epsilon_\lambda} + \sum_{\gamma \neq \lambda} \frac{\langle \lambda | \delta h^{(1)} | \gamma \rangle \langle \alpha\gamma | v_A | \beta\lambda \rangle}{\epsilon_\gamma - \epsilon_\lambda}$$

This correction due to modification of the core has never been calculated and, in fact, it is not clear if the perturbation $\delta h^{(1)}$ would be small enough to make this approach valid.

3.   SOME DETAILS OF THE CALCULATION

Most of the discussion of HF calculations given here to date have been quite abstract. I thought it might be instructive to go into a little more detail of how one actually proceeds in the simple case of the s-d shell. The spherical oscillator basis states in the 2s-1d shell are:

(n ℓ j m)		(n ℓ j -m)	
1d 5/2	1/2	1d 5/2	-1/2
2s 1/2	1/2	2s 1/2	-1/2
1d 3/2	1/2	1d 3/2	-1/2
1d 5/2	-3/2	1d 5/2	3/2
1d 3/2	-3/2	1d 3/2	3/2
1d 5/2	5/2	1d 5/2	-5/2

Each of these states can hold one neutron and one proton, in all 24 single-particle states are available. Thus, if the sum in Eq.(9) is taken as completely unrestricted (within the shell, of course), the HF single-particle Hamiltonian h is a 24×24 matrix. In practice, the problem is reduced significantly by the use of symmetry properties under which the HF matrix breaks down into a number of uncoupled sub-matrices:

$$h = \begin{pmatrix} \Box & & 0 \\ & \Box & \\ & & \Box \\ 0 & & \ddots \end{pmatrix}$$

The two most common symmetries which have been applied to all calculations to date are time-reversal invariance and isotopic spin conservation. Time reversal invariance implies that the oscillator state $| n\ell j m \rangle$ and its time-reverse

$$(-)^{\ell+j-m} | n\ell j -m \rangle$$

are not mixed in Eq.(9). That is the reason why I wrote the basis in the
two columns above – the states in one column do not couple with those in
the other. Isotopic-spin conservation implies that neutron wavefunctions
do not couple with proton functions. These symmetries reduce the HF
matrix to 4 decoupled 6 × 6 matrices. In fact, for N = Z, even-even nuclei
(for which these symmetries are exact if the Coulomb force is neglected)
all 4 matrices are identical and all HF s.p. levels become four-fold de-
generate, corresponding to the states: $|\lambda, p\rangle$ for protons, its time-reverse
$|\bar{\lambda}, p\rangle$ and $|\lambda, n\rangle$, $|\bar{\lambda}, n\rangle$ for neutrons. Then only one 6 × 6 matrix need be
diagonalized.

Since all states of the s-d shell have the same parity, the HF orbitals
automatically have good parity. However, if axial symmetry is also
assumed, the 6 × 6 matrix breaks down even further, since then states of
different m are uncoupled. Then the HF matrix breaks down into a 3 × 3
matrix for m = 1/2, a 2 × 2 for m = 3/2 and a 1 × 1 for m = 5/2.

With the choice of symmetry taken care of, the actual solution of the
HF equation proceeds as follows: First we write Eq.(5) in the oscillator
basis[1]

$$(n|h|n') = e_n \delta_{nn'} + \sum_{\lambda pp'} C_p^\lambda (np|v_A|n'p') C_{p'}^\lambda \qquad (11a)$$

and

$$\sum_{n'} (n|h|n') C_{n'}^\lambda = \epsilon_\alpha C_n^\alpha \qquad (11b)$$

Now, the two-body interaction appears only in terms of its matrix elements
between the oscillator states $(np|v_A|n'p')$. These are calculated at the start
for the interaction chosen (e.g. Eq.(10)) for all states (n, p, n', p') in the
s-d shell and are sotred in the program.

Then one selects some initial set of coefficients C_n^α. This selection
requires some care. Since Eqs (11) are non-linear, they may possess
several solutions, and some may be missed by improper selection of the
starting point. The simplest initial choice is $C_n^\alpha = \delta_{n\alpha}$, i.e. the initial states
$|\alpha\rangle$ are simply the spherical harmonic-oscillator states. There is a danger
in this, however. In the case of such nuclei as ^{28}Si, where it is possible
completely to fill one j-subshell (the d 5/2 shell for ^{28}Si) it is rigorously
true that the spherical solution is a self-consistent one. This means that
if one starts with spherical-oscillator functions, the wave functions will
remain spherical throughout the iteration process. But this is not the
lowest self-consistent solution, there are deformed ones at lower energy.
A better choice is suggested by the observation that the deformed HF orbitals
resemble those of particles in a deformed oscillator well. Therefore one
can start by making an initial guess for the HF Hamiltonian:

$$(n|h^{(0)}|n') = A_n \delta_{nn'} - B(n|n^2 Y_{20}|n')$$

---

[1] Here n, p, etc. stand for the full set of quantum numbers needed to specify the harmonic-oscillator
state: (n ℓ j m).

and diagonalizing this to get the initial wave functions C_n^α. This enables one to explore regions of widely different deformations. However, this still does not permit a search for triaxial solutions.

After the initial wave functions have been chosen, the HF Hamiltonian (11a) is calculated. This involves a sum over the occupied states λ outside the core (e.g. in ^{20}Ne, a sum of 4 terms) and for each λ a sum on all (p,p') in the s-d shell basis ($6 \times 6 = 36$ terms). This calculation proceeds quite rapidly once the matrix elements $(np|v_A|n'p')$ have been evaluated beforehand. The Hamiltonian matrix $(n|h|n')$ is then diagonalized (Eq.(11b)) to yield a new set of wave functions C_n^α with which $(n|h|n')$ is re-calculated. This cycle is repeated until the total energy (Eq.8)) does not vary significantly from one iteration to the next.

4. RESULTS IN THE s-d SHELL

We shall not present the results here in great detail since they can be found in the literature [5, 8, 9]. We shall, however, discuss some of their characteristic features. The calculations have been done on all N = Z, even-even nuclei in the s-d shell, as well as some other, both even and odd, nuclei near the beginning of the shell. The calculated binding energies are generally reasonably good (which is not surprising because the s.p. energies and strength of interaction are chosen to get reasonable binding) but quadrupole moments are generally too small by about a factor of 2. This is because of the neglect of the core polarization, as mentioned earlier. However, the correct systematics of the deformation are observed; Q is positive in the beginning of the shell and changes sign mid-shell, at about ^{28}Si.

The most striking feature of the results is seen in the spectrum of single-particle energies obtained (Fig. 1). One sees immediately that the Fermi level − the height to which the s.p. levels are occupied − is approximately constant, and, furthermore, that there is a large gap of 7-8 MeV between occupied and unoccupied levels. Such a gap is not evident in other models for deformed nuclei, such as the Nilsson model [10]. The HF wave functions are quite similar to Nilsson functions but the spectrum of s.p. levels differs by the presence of this gap.

It can be seen as essentially due to the non-locality of the HF field, as we shall see below. Its presence is an indication of the stability of the HF solution since it would take a large amount of energy to move a particle from the occupied states into one of the unoccupied ones.

A guide to an understanding of the gap is given by a simple solvable model introduced by Bar-Touv and Levinson [11]. An effective two-body interaction, such as the Rosenfeld force (Eq.(10), can be written as a radial function times a general exchange mixture:

$$v(r) = (W + BP_\sigma = HP_\tau + MP_\kappa) \, f(r) \tag{12}$$

Here W, B, H, and M are the Wigner, Bartlett, Heisenberg, and Majorana exchange forces, respectively and P_σ, P_τ, P_κ are the spin-, isospin-, and space-exchange operators, respectively. The idea of Ref. [11] is that the gross features of the HF solution come from the long-range part of this
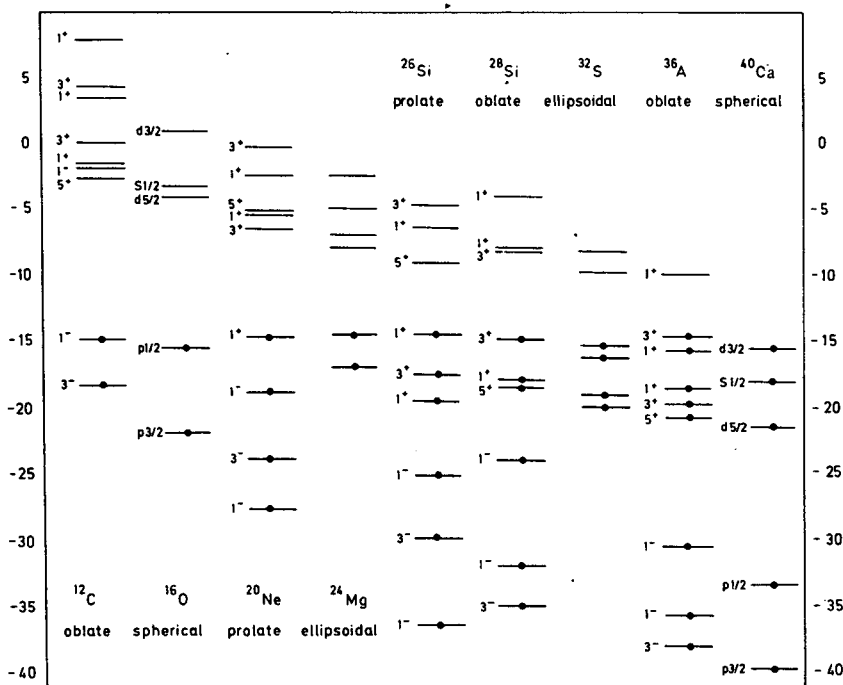
FIG.1.   Spectrum of the HF orbits of lowest-energy solutions of even-even N = Z nuclei between ^{12}C and ^{40}Ca. The levels are fourfold degenerate, and occupied orbits are marked with a dot. The additional symmetry of each solution is indicated and also the shape (prelate or oblate) of the axially symmetric solutions. The axially symmetric solutions are labelled by (2k)"; e.g. 3 means ak = 3/2 orbit of the 2s-1d shell and 1 means ak = 1/2 orbit of the p shell. For spherical and axially symmetric solutions the 1 p and 2s-1d shell orbits are shown. For ellipsoidal solutions only 2s-1d shell orbits are shown (figure taken from Ref.[1], Ripka).

interaction, therefore an infinite-range force is chosen, i.e. f(r) = 1. Then the HF equation is exactly solvable and the result (for N = Z, even-even) is that all the occupied orbitals are degenerate and lie at an energy

$$e_\lambda = \frac{Sn}{4} - G \qquad (13a)$$

and the unoccupied orbitals are degenerate at an energy

$$e_\alpha = \frac{Sn}{4} \qquad (13b)$$

Both are measured with respect to the inert core, − n is the number of particles outside the core, − and:

$$S = 4W + 2B - 2H - M$$
$$G = W + 2B - 2H - 4M \qquad (13c)$$

Thus, there is a constant (n-independent) gap G between the occupied and unoccupied shells, providing G > 0. The constancy of the Fermi level is due

to a saturation condition, $S = 0$, which holds for the Rosenfeld force used in the calculation for Fig. 1. From the form of G, we see that a strong attractive Majorana component $(M < 0)$ will ensure a large gap. In fact, most reasonable exchange mixtures used do have a strong $M < 0$.

To see that the gap is connected with the non-locality of the HF field, we write the HF equation in co-ordinate space. For a local, central force of the form (12), it is,

$$- \frac{\nabla^2}{2m} \psi_\alpha(\vec{r}) + S U_L(\vec{r}) \psi_\alpha(\vec{r}) - G \int U_{NL}(\vec{r}, \vec{r}') \psi_\alpha(\vec{r}') d\vec{r}'$$

$$= \epsilon_\alpha \varphi_\alpha(\vec{r}) \tag{14}$$

where

$$U_L(\vec{r}) = \int d\vec{r}' \sum_\lambda |\psi_\lambda(\vec{r}')|^2 f(|\vec{r} - \vec{r}'|)$$

comes from the direct term in Eq. (1) and the non-local part

$$U_{NL}(\vec{r}, \vec{r}') = \sum_\lambda \psi_\lambda(\vec{r}) \psi_\lambda(\vec{r}') f(|\vec{r} - \vec{r}'|)$$

comes from the exchange term. In other words, G is simply the strength of the non-local term. If G is large, the non-locality is large.

5. PROJECTION OF ROTATIONAL STATES

The solution of the HF problem for a deformed nucleus, in which s. p. states of different j are allowed to mix in Eq. (9) lead to a deformed intrinsic state for the nucleus. This state, however, does not have good angular momentum. It is therefore not the true ground state, but a mixture of the ground state with a number of low-lying levels associated with the same intrinsic state.

To compare to experimental levels obtained in nuclear spectroscopy, we must extract from the HF wave function states of good total angular momentum J. In this, one usually follows the projection method of Peierls and Yoccoz [12]. If the deformed intrinsic state is axially symmetric with projection K of J_Z on the intrinsic symmetry axis, a state of good total J and projection M is obtained from the integral

$$|\Psi_{MK}^J\rangle = \frac{2J+1}{8\pi^2 \sqrt{N_{JK}}} \int d\Omega \, D_{MK}^{J*}(\Omega) R(\Omega) |\Psi_K\rangle \tag{15}$$

Here $R(\Omega)$ is the rotation operator for a rotation defined by Ω, $D_{MK}^J(\Omega)$ are its representation matrices [13]

$$D_{MK}^J(\Omega) = \langle JM | R(\Omega) | JK \rangle$$

and N_{JK} is a normalization constant.

The energies E_J of the states of a rotational band projected in this way are then[2]:

$$E_J = \langle \Psi_{MK}^J | H | \Psi_{MK}^J \rangle$$

$$= \frac{\int_0^\pi \sin \beta \, d\beta \ d_{KK}^J(\beta) \langle \Psi_K | e^{-i\beta J_y} H | \Psi_K \rangle}{\int_0^\pi \sin \beta \, d\beta \ d_{KK}^J(\beta) \langle \Psi_K | e^{-i\beta J_y} | \Psi_K \rangle} \qquad (16)$$

We will not discuss in detail the projection method since it is quite complicated and discussed in Bouten's paper in these Proceedings (or, see Ripka, Ref.[1]). One can see from the expression above the origin of the difficulties in the projection method, i.e. the evaluation of the rather complicated matrix elements

$$\langle \varphi_K | e^{-i\beta J_y} | \Psi_K \rangle$$

and

$$\langle \Psi_K | e^{-i\beta J_y} H | \Psi_K \rangle$$

Since Ψ_K is an $n \times n$ determinant, the projection has been possible to date [2] only for a rather small number of particles. (Nuclei in the beginning of the s-d shell [2], and very light nuclei (Bouten's paper).)

A limiting case of Eq.(16) is the strong-coupling limit, when the matrix elements

$$\langle \Psi_K | e^{-i\beta J_y} | \Psi_K \rangle$$

and

$$\langle \Psi_K | e^{-i\beta J_y} H | \Psi_K \rangle$$

contribute significantly only near the values $\beta = 0$ and $\beta = \pi$. Then $E_J = A J (J+1)$, the well-known rotational spectrum. In actual calculations, these matrix elements do, in fact, peak rather strongly at $\beta = 0$ and $\beta = \pi$, therefore the projected spectra resemble rotational ones. Figure 2 shows some projected HF spectra. The agreement with experiment is worst for the ^{28}Si nucleus. A possible reason for this is the fact that ^{28}Si has two deformed HF minima, one oblate and one prolate, nearly degenerate in energy. The low-energy spectrum must then be influenced by some sort of interaction of these two possible structures. In the other nuclei shown, the projected spectra are in quite reasonable agreement with the experimental ones.

---

[2] Here $d_{MK'}^J$ (β) are the reduced rotation matrices [13].
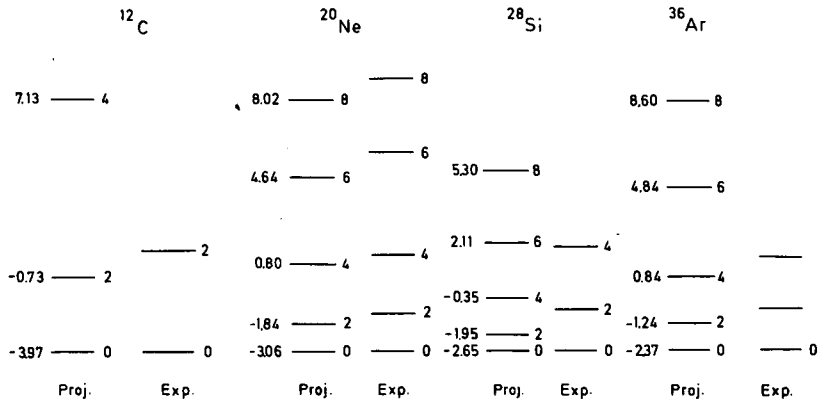
FIG.2. Projected HF spectra of ^{12}C, ^{20}Ne, ^{28}Si, and ^{36}Ar. The oblate solution of ^{28}Si was used. The projected spectra are drawn to the left of the experimental spectra for each nucleus. The number on the right of each level is the spin of the level. The number on the left of the projected levels is the difference Δ_j between the energy of the projected level and the HF energy of the intrinsic state (figure taken from Ref.[1], Ripka).

6.   RESULTS IN THE 2p-1f SHELL

Two possible extensions of the s-d shell HF calculations suggest themselves (and here finally we get to some of the author's work); namely, extension to other major shells, and extension to include mixing of several major shells.

The 2p-1f shell is the next major shell after the 2s-1d shell. It is known that nuclei in the beginning of this shell do not exhibit the characteristic large deformations of the s-d shell case. It was of interest, therefore, to perform calculations on the f-p shell, taking ^{40}Ca as the inert core. This is at once more difficult, since there are more oscillator states, and more dubious since ^{40}Ca is known to be not nearly as good a closed shell as ^{16}O. However, Parikh and the author [14], have carried out calculations of this type for a large number of nuclei in the f-p shell, using the effective interaction due to Shakin et al. [15]. Somewhat to our surprise, we found that the structure of the HF calculations for these nuclei did not look strikingly different from that in the s-d shell. They had the same large positive quadrupole moments[3], with a change of sign around the middle of the shell. One significant difference was observed as is evident in Fig.3: the gap between occupied and unoccupied states is much smaller, about 1 to 2 MeV. As a result, these nuclei are not nearly so stable against excitation of particles as in the s-d shell. An estimate of the effect of pairing excitations was made in Ref.[14], where it is shown that in these nuclei an important role may be played by excitations of the pairing-vibration type.

7.   MAJOR-SHELL-MIXING UNRESTRICTED HF CALCULATIONS

Another extension of the deformed HF calculation is to eliminate the inert core and let all particles of the nucleus move in variational orbits.

---

[3] Except for the Ca isotopes, dominated by the spherical ^{40}Ca core and the fact that ^{48}Ca is also spherical (closed $f_{7/2}$ neutron shell).

FIG.3.   Proton single-particle H.F. levels for the prolate, axial solutions of $N = Z$ nuclei. The levels are labelled by the value of k and on each level are given the dominant terms in their oscillator expansion.   The thin lines connect levels of the same k and approximately same structure.   Significant changes in structure of the levels from one nucleus to the next are indicated (figure taken from Ref.[14]).

FIG.4.   The Hartree-Fock energy with the angular-momentum correction and the second-order correction compared to the observed binding energies (after Coulomb subtraction).   The effect of assuming a constant (independent of A) for Hartree-Fock hole energies [Eq.(14)] could explain the systematic deviation of the corrected results from experiment (figure taken from Ref.[2], Bassichis, Kerman and Svenne).

That is, we return to a solution of the full equation (1), where λ runs over all A particles of the nucleus. Obviously, we can no longer confine ourselves to harmonic-oscillator wave functions in one shell, and the basis needed in Eq.(9) becomes much larger, the sum running over all $n \ell j$ and m.

Bassichis, Kerman and Svenne [16] have carried out such calculations for nuclei in the 1p and 2s-1d shell using the non-local Tabakin [17] two-body interaction. For reasons of computer storage, axial symmetry was assumed (i.e. no sum on m in Eq.(9)) and the basis was restricted to the first 4 major shells of the harmonic oscillator: 1s, 1p, 2s-1d and 2p-1f shells. The qualitative features of the results are essentially the same as for the single-shell calculations: large gaps and large deformations (away from closed shells) are found. However, the quadrupole moments are increased in magnitude and in much better agreement with observed values. Also, it is possible now to make meaningful comparisons of the total binding energy (Fig.4) with experimental values.

REFERENCES

[1] VILLARS, F., Proceedings of the International School of Physics "Enrico Fermi", Course 23, (WEISSKOPF, N.F., Ed.), Academic Press Inc., New York (1963); BARANGER, M.; Cargese Lectures in Theoretical Physics (W.A. Benjamin, Inc., New York (1963).
     RIPKA, G., Advances in Nuclear Physics 1 (1968) and the contribution by Bouten in these Proceedings.
[2] KERMAN, A.K., SVENNE, J.P., VILLARS, F.M.H., Phys.Rev. 147 (1966) 710.
     BASSICHIS, W.H., KERMAN, A.K., SVENNE, J.P., Phys.Rev. 160 (1967) 746.
[3,4] MATHUKRISHNAN, R., BARANGER, M., Phys.Letters 18 (1965) 160.
     DAVIES, K.T.R., KRIEGER, S.J., BARANGER, M., Nucl.Phys. 84 (1966) 545.
     TARBUTTON, R.M., DAVIES, K.T.R., Nucl.Phys. A120 (1968) 1.
     DAVIES, K.T.R., BARANGER, M., TARBUTTON, R.M., KUO, T.T.S., Phys.Rev. 177 (1969) 1519.
[5] KELSON, I., Phys.Rev. 132 (1963) 2189.
[6] REDLICH, M.G., Phys.Rev. 110 (1958) 468.
     KURATH, D., PIČMAN, L., Nucl.Phys. 10 (1959) 313.
[7] ROSENFELD, L., Nuclear Forces, North-Holland Publishing Co., Amsterdam (1948) 233.
[8] KELSON, I., LEVINSON, C.A., Phys.Rev. 134 (1964) B269.
     BAR-TOUV, J., KELSON, I., Phys.Rev. 138B (1965) 1035.
     RIPKA, G., Ref.[1].
[9] GUNYE, M.R., Nucl.Phys. A120 (1968) 691.
     GUNYE, M.R., WARKE, C.S., Phys.Rev. 156 (1967) 1087; 159 (1967) 885, 164 (1967) 1264.
[10] NILSSON, S.G., Kgl.Danske Vid.Selsk.Mat.fys.Meddr. 29 16 (1955).
[11] BAR-TOUV, J., LEVINSON, C.A., Phys.Rev. 153 (1967) 1099.
[12] PEIERTS, R.E., YOCCOZ, J., Proc.Phys.Soc. (London) A70 (1957) 381.
[13] EDMONDS, A.R., Angular Momentum in Quantum Mechanics, Princeton Univ.Press, Princeton, N.J. (1957) 53.
[14] PARIKH, J.C., SVENNE, J.P., Phys.Rev. 174 (1968) 1343.
[15] SHAKIN, C.M., WAGHMARE, Y.R., TOMASELLI, M., HULL, M.H., Jr., Phys. Rev. 161 (1967) 1015.
[16] BASSICHIS, et al., Ref.[2].
[17] TABAKIN, F., Ann.Phys. (N.Y.) 30 (1964) 51.

PAIRING VIBRATIONS AND
TWO-PARTICLE TWO-HOLE ADMIXTURES

G. RIPKA, R. PADJEN*
Service de Physique Théorique,
Centre d'Etudes Nucléaires de Saclay,
Gif-sur-Yvette, France

Abstract

PAIRING VIBRATIONS AND TWO-PARTICLE TWO-HOLE ADMIXTURES.
   1. Time-dependent Hartree-Bogolyubov theory; 2. The generator-co-ordinate method; 3. Two-particle two-hole admixtures in 2s-1d shell nuclei.

INTRODUCTION

This paper treats the pairing mode of vibration of normal systems and the two-particle two-hole admixtures to the Hartree-Fock states of 2s-1d shell nuclei. The two subjects are only formally related in that they both involve correlations due to the motion of two particles. The recent attention [1] which has been given to pairing vibrations is due to the selectivity of (p, t) and (t, p) reactions which excite preferentially a few states of the residual nucleus, namely those states which are called pairing vibrations. The theory of pairing vibrations and a measure of their collectivity with respect to (p, t) and (t, p) reactions have been formulated by Bes and Broglia [2]. There is a strong formal similarity between R.P.A. vibrations, which we shall call "normal vibrations" and pairing vibrations. In fact, to each of the innumerable ways of deriving the R.P.A. equations there is an analogous way of deriving the equations of pairing vibrations. In the first chapter, we shall derive both pairing and normal vibrations at the same time by considering time-dependent Hartree-Bogolyubov theory. This approach stresses the reaction mechanism by which these vibrations are excited. In the second chapter, we shall derive the same equations by a generator-co-ordinate method. This method, which was initially used by Jancovici and Schiff [3] to derive the normal R.P.A. vibrations, is very instructive, and its wide range of applications [4] has not yet been exhausted. In the last chapter, we shall discuss the methods and results of the calculations of two-particle, two-hole admixtures to the Hartree-Fock states of N = Z even-even nuclei.

The reader will find a review of the theory of pairing vibrations which includes the diagram expansion of two-body Green functions and the interdependence of normal and pairing vibrations in Ref. [5].

1. TIME-DEPENDENT HARTREE-BOGOLYUBOV THEORY

Consider the wave function $| \Psi(t) \rangle$ of a target nucleus which is bombarded by either protons or tritons. Let $| \Psi_0, \text{'A} \rangle$ be the ground state of the target nucleus A. During the reaction, the target nucleus may either

---

* On leave of absence from Institute "RudjerBošković", Zagreb, Yugoslavia

i) stay in its ground state $|\Psi_0\rangle$,

ii) be excited by an inelastic collision to some excited state $|N, A\rangle$,

iii) capture a pair of neutrons in which case it makes the transition to a state $|N, A + 2\rangle$ of the nucleus $A + 2$, which has two extra neutrons, or

iv) lose a pair of neutrons in which case it makes the transition to a state $|N, A - 2\rangle$ of the nucleus $A - 2$, which has two neutrons less.

We shall neglect the other processes. The wave function $|\Psi(t)\rangle$ of the target nucleus will then have amplitudes in all the states considered above:

$$|\psi(t)\rangle = e^{-iE_0 t}|\psi_0\rangle + \sum_N \alpha_N e^{-iE_N(A)t}|N,A\rangle$$

$$+ \sum_N \beta_N e^{-iE_N(A+2)t}|N,A+2\rangle + \sum_N \gamma_N e^{-iE_N(A+2)t}|N,A+2\rangle \qquad (1)$$

The states $|N, A\rangle$, $|N, A + 2\rangle$ and $|N, A - 2\rangle$ are eigenstates of the nuclear Hamiltonian H:

$$H|\psi_0\rangle = E_0|\psi_0\rangle$$

$$H|N,A\rangle = E_N(A)|N,A\rangle \qquad (2)$$

$$H|N,A \pm 2\rangle = E_N(A \pm 2)|N,A \pm 2\rangle$$

It is convenient to introduce the frequencies ($\hbar = 1$):

$$\omega_N = E_N(A) - E_0$$

$$\omega_N(A+2) = E_N(A+2) - E_0 \qquad (3)$$

$$\omega_N(A-2) = E_0 - E_N(A-2)$$

The coefficients α_N, β_N and γ_N depend on the reaction mechanism, and their explicit calculation will not be needed.

The theory of pairing vibrations is based on two basic hypotheses:

1) During the reaction, that is, at each time t, the wave function $|\Psi(t)\rangle$ remains a quasi-particle vacuum.

2) The amplitudes α, β and γ are small compared to unity.

A quasi-particle vacuum is entirely determined by the normal and abnormal density matrices ρ_{ij} and K_{ij}. These are defined by

$$\rho_{ij}(t) = \langle\psi(t)|b_j^\dagger b_i|\psi(t)\rangle$$

$$K_{ij}(t) = \langle\psi(t)|b_j b_i|\psi(t)\rangle \qquad (4)$$

The operators b_i and $b_i^\dagger$ are nucleon destruction and creation operators. It may be shown [6] that a necessary and sufficient condition for $|\Psi(t)\rangle$ to be a quasi-particle vacuum is that the density matrices ρ and K satisfy the matrix equations

$$\rho = \rho^\dagger \qquad\qquad K + \tilde{K} = 0$$

$$\rho^2 + KK^\dagger = \rho \tag{5}$$

$$\rho K = K\bar{\rho}$$

Let us then calculate the density matrices ρ and K of the state (1); we obtain by neglecting quadratic terms in α, β and γ:

$$\rho_{ij}(t) = \rho_{ij}^{(o)} + \sum_N \alpha_N\, e^{-i\omega_N t}\, \langle\psi_o | b_j^\dagger b_i | N,A\rangle + \sum_N \alpha_N^*\, e^{+i\omega_N t}\, \langle N,A | b_j^\dagger b_i | \psi_o\rangle$$

$$= \rho_{ij}^{(o)} + \rho_{ij}^{(1)}(t) \tag{6}$$

where

$$\rho_{ij}^o = \langle\psi_o | b_j^\dagger b_i | \psi_o\rangle \tag{7}$$

and

$$K_{ij}(t) = K_{ij}^{(o)} + \sum_N \beta_N\, e^{-i\omega_N(A+2)t}\, \langle\psi_o | b_j b_i | N,A+2\rangle$$

$$+ \sum_N \gamma_N^*\, e^{-i\omega_N(A-2)t}\, \langle N,A-2 | b_j b_i | \psi_o\rangle \tag{8}$$

$$= K_{ij}^{(o)} + K_{ij}^{(1)}(t) \tag{9}$$

where

$$K_{ij}^{(o)} = \langle\psi_o | b_j b_i | \psi_o\rangle \tag{10}$$

We shall discuss here only those nuclei which have normal ground states and for which $K_{ij}^{(0)} = 0$. A quasi-particle vacuum $|\Psi_0\rangle$ whose abnormal density matrix $K^{(0)}$ vanishes reduces to a simple independent-particle state made up of A orbits α. We shall distinguish the orbits which are occupied in the state $|\Psi_0\rangle$; we call them hole orbits and denote them by Greek indices $\alpha, \beta \ldots$ etc. We call the other orbits particle orbits and denote them
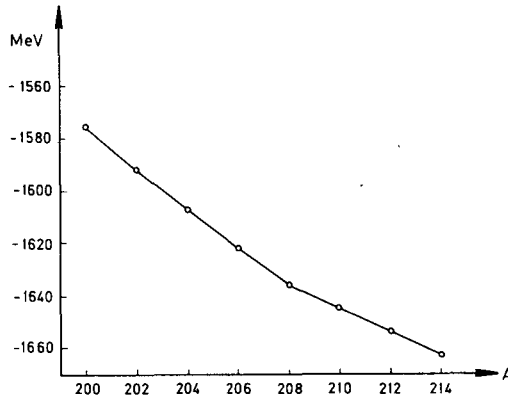
FIG.1.   Binding energies of Pb isotopes plotted against the mass number A.

by Roman letters i, j, ... In an independent-particle state $|\Psi_0\rangle$ the occupied orbits may be chosen so as to diagonalize the density matrix; thus for a normal system we may choose

$$\rho_{\alpha\beta}^{(o)} = \delta_{\alpha\beta} \qquad \rho_{\alpha i}^{(o)} = \rho_{ij}^{(o)} = 0$$

$$K_{\alpha\beta}^{(o)} = K_{\alpha i}^{(o)} = K_{ij}^{(o)} = 0 \tag{11}$$

Recalling that $\rho^{(1)}$ and $K^{(1)}$ are first-order quantities (in α_N, β_N and γ_N) with respect to $\rho^{(0)}$, it is easily verified that to first order Eqs (5) imply that

$$\rho_{\alpha\beta}^{(1)} = \rho_{ij}^{(1)} = 0$$

$$K_{i\alpha}^{(1)} = 0 \tag{12}$$

This means that the only non-vanishing elements of the matrix $\rho^{(1)}$ are the particle-hole elements $\rho_{i\alpha}^{(1)}$ and $\rho_{\alpha i}^{(1)}$, and that the only non-vanishing elements of the matrix $K^{(1)}$ are the particle-particle and hole-hole elements $K_{ij}^{(1)}$ and $K_{\alpha\beta}^{(1)}$, respectively.

   It is clear then that the two basic hypotheses made concerning the state $|\Psi(t)\rangle$ strongly limit the states described by the present theory. Indeed, the excited states $|N, A\rangle$ of the nucleus A must have only particle-hole and hole-particle configurations, and the states $|N, A\pm 2\rangle$ of the A ± 2 nucleus must have only two-particle and two-hole configurations. The theory does allow for ground-state correlations which are second- and higher-order effects.

   We have so far considered only the kinematics of the reaction. Let us now consider the dynamics. The density matrices $\rho(t)$ and $K(t)$ are given by the Schrödinger equation

$$i \frac{d}{dt} \rho_{ij}(t) = \langle \psi(t) | [b_j^\dagger b_i, H] | \psi(t) \rangle \tag{13}$$

$$i \frac{d}{dt} K_{ij}(t) = \langle \psi(t) | [b_j b_i, H] | \psi(t) \rangle$$

[ ] is a commutator. We use the Hamiltonian

$$H = \sum_{mn} \langle m | t | n \rangle \, b_m^\dagger b_n + \frac{1}{4} \sum_{rsmn} \langle rs | v | mn \rangle \, b_r^\dagger b_s^\dagger b_n b_m \tag{14}$$

where t is the kinetic-energy operator, and v is the two-body interaction. When $|\Psi(t)\rangle$ is a quasi-particle vacuum, the right-hand sides of Eqs (13) are easily evaluated by using Wick's theorem. The result is

$$i \frac{d}{dt} \rho_{ij}(t) = \sum_{s} \left[(t_{is} + U_{is}) \rho_{sj} - \rho_{is}(t_{sj} + U_{sj}) + K_{js}^* \Delta_{si} - K_{is} \Delta_{sj}^* \right] \tag{15}$$

$$i \frac{d}{dt} K_{ij}(t) = \sum_{s} \left[(t_{is} + U_{is}) K_{sj} - (t_{js} + U_{js}) K_{si} - \rho_{js} \Delta_{si} + \rho_{is} \Delta_{sj} \right] + \Delta_{ji} \tag{16}$$

We have written these equations in terms of the usual Hartree-Fock and pairing fields U_{is} and Δ_{is} which are defined by

$$U_{is} = \sum_{mn} \langle im | v | sn \rangle \, \rho_{nm} \tag{17}$$

$$\Delta_{is} = \frac{1}{2} \sum_{mn}' \langle is | v | mn \rangle \, K_{nm}$$

In the lowest order, Eq. (15) gives the usual time-independent Hartree-Fock equation for $|\Psi_0\rangle$, i.e.

$$i \frac{d}{dt} \rho^{(o)} = [t + U^{(o)}, \rho^{(o)}] = 0 \tag{18}$$

so that $t + U^{(0)}$ and $\rho^{(0)}$ may be diagonalized simultaneously. We shall use the following Hartree-Fock representation:

$$t_{ij} + U_{ij}^{(o)} = \varepsilon_i \delta_{ij}$$

$$t_{\alpha\beta} + U_{\alpha\beta}^{(o)} = \varepsilon_\alpha \delta_{\alpha\beta} \tag{19}$$

$$t_{i\alpha} + U_{i\alpha}^{(o)} = 0$$

The ϵ_j and ϵ_α are the energies of the Hartree-Fock orbits, and $U_{ij}^{(0)}$ is the static Hartree-Fock field

$$U_{ij}^{(0)} = \sum_{mn} \langle im|v|jn \rangle \, \rho_{nm}^{(0)} = \sum_{\alpha=1}^{A} \langle i\alpha|v|j\alpha \rangle \tag{20}$$

If we substitute the expressions of $\rho^{(0)}$ and $U^{(0)}$ in Eqs (15) and (16), and keep only first-order terms in $K^{(1)}$ and $\rho^{(1)}$, the following set of equations is obtained:

$$i \frac{d}{dt} \rho_{i\alpha}^{(1)} = (\epsilon_i - \epsilon_\alpha) \, \rho_{i\alpha}^{(1)} + \sum_{j\beta} \left[\langle i\beta|v|\alpha j \rangle \, \rho_{j\beta}^{(1)} + \langle ij|v|\alpha\beta \rangle \, \rho_{\beta j}^{(1)} \right] \tag{21}$$

$$i \frac{d}{dt} \rho_{\alpha i}^{(1)} = (\epsilon_\alpha - \epsilon_i) \, \rho_{\alpha i}^{(1)} - \sum_{j\beta} \left[\langle \alpha j|v|i\beta \rangle \, \rho_{\beta j}^{(1)} + \langle \alpha\beta|v|ij \rangle \, \rho_{j\beta}^{(1)} \right]$$

$$i \frac{d}{dt} K_{ij}^{(1)} = (\epsilon_i + \epsilon_j) \, K_{ij}^{(1)} + \frac{1}{2} \sum_{k\ell} \langle ij|v|k\ell \rangle \, K_{k\ell}^{(1)} + \frac{1}{2} \sum_{\alpha\beta} \langle ij|v|\alpha\beta \rangle \, K_{\alpha\beta}^{(1)} \tag{22}$$

$$i \frac{d}{dt} K_{\alpha\beta}^{(1)} = (\epsilon_\alpha + \epsilon_\beta) \, K_{\alpha\beta}^{(1)} - \frac{1}{2} \sum_{\gamma\delta} \langle \alpha\beta|v|\gamma\delta \rangle \, K_{\gamma\delta}^{(1)} - \frac{1}{2} \sum_{ij} \langle \alpha\beta|v|ij \rangle \, K_{ij}^{(1)}$$

Thus, in a normal system the equations for $\rho^{(1)}$ and $K^{(1)}$ are completely uncoupled to first order. Equations (21) are the familiar equations of time-dependent Hartree-Fock theory. They lead to the R.P.A. equations. If we had put $\beta_N = \gamma_N = 0$ in Eq. (1) and thus considered only inelastic processes, we would have obtained Eq. (21) and normal R.P.A. vibrations. If we had put $\alpha_N = 0$ and considered only transfer processes, we would have obtained Eq. (22) and pairing vibrations. To first order, that is, when only one vibration is present, normal and pairing vibrations are independent modes. In second-order processes, such as ground-state correlations, this is no longer true and the theory needs to be corrected for the interdependence of pairing and normal modes of vibration [5].

Equations (22) admit solutions of the form (8). Substituting expression (8) into Eq. (22) we obtain a set of linear equations for the amplitudes

$$x_{ij}^{N} = \langle \psi_o|b_j b_i|N,A+2 \rangle$$
$$x_{\alpha\beta}^{N} = \langle \psi_o|b_\beta b_\alpha|N,A+2 \rangle \tag{23}$$

i.e.

$$\omega_N(A+2)X^N_{ij} = (\varepsilon_i + \varepsilon_j)X^N_{ij} + \frac{1}{2}\sum_{k\ell} \langle ij|v|k\ell\rangle X^N_{k\ell} + \frac{1}{2}\sum_{\alpha\beta} \langle ij|v|\alpha\beta\rangle X^N_{\alpha\beta}$$

$$\omega_N(A+2)X^N_{\alpha\beta} = (\varepsilon_\alpha + \varepsilon_\beta)X^N_{\alpha\beta} - \frac{1}{2}\sum_{\gamma\delta} \langle \alpha\beta|v|\gamma\delta\rangle X^N_{\gamma\delta} - \frac{1}{2}\sum_{ij} \langle \alpha\beta|v|ij\rangle X^N_{ij} \tag{24}$$

We also obtain a set of linear equations for the amplitudes

$$Y^N_{ij} = \langle N,A-2|b_j b_i|\psi_o\rangle$$

$$Y^N_{\alpha\beta} = \langle N,A-2|b_\beta b_\alpha|\psi_o\rangle \tag{25}$$

namely

$$\omega_N(A-2)\, Y^N_{ij} = (\varepsilon_i + \varepsilon_j)\, Y^N_{ij} + \frac{1}{2}\sum_{k\ell} \langle ij|v|k\ell\rangle Y^N_{k\ell} + \frac{1}{2}\sum_{\alpha\beta} \langle ij|v|\alpha\beta\rangle\, Y^N_{\alpha\beta}$$

$$\omega_N(A-2)\, Y^N_{\alpha\beta} = (\varepsilon_\alpha + \varepsilon_\beta)\, Y^N_{\alpha\beta} - \frac{1}{2}\sum_{\gamma\delta} \langle ij|v|\gamma\delta\rangle Y^N_{\gamma\delta} - \frac{1}{2}\sum_{ij} \langle \alpha\beta|v|ij\rangle\, Y^N_{ij} \tag{26}$$

The amplitudes X^N_{ij} and $X^N_{\alpha\beta}$ are the amplitudes of a pairing vibrational mode N of the nucleus A which is excited by a (t, p) reaction. It corresponds to states of the A + 2 nucleus. The amplitudes Y^N_{ij} and $Y^N_{\alpha\beta}$ are the amplitudes of a pairing vibrational mode N of the same nucleus A, which is excited by a (p, t) reaction. It corresponds to states of the A - 2 nucleus. The pairing vibrations X^N and Y^N bear, respectively, the quantum number $\alpha = +2$ and -2 introduced by Bohr and Mottelson [1].

Finally Eqs (21) admit solutions of the form (6). Substituting expression (6) in Eq. (21) a set of linear equations is obtained for the amplitudes

$$Z^N_{i\alpha} = \langle \psi_o|b_i b^\dagger_\alpha|N,A\rangle$$

$$Z^N_{\alpha i} = \langle \psi_o|b^\dagger_i b_\alpha|N,A\rangle \tag{27}$$

i.e.

$$\left\{ \begin{aligned} \omega_N\, Z^N_{i\alpha} &= (\varepsilon_i - \varepsilon_\alpha)Z^N_{i\alpha} + \sum_{\beta j} \left[\langle \alpha j|v|i\beta\rangle Z^N_{j\beta} + \langle \alpha\beta|v|ij\rangle Z^N_{\beta j}\right] \\ \omega_N\, Z^N_{\alpha i} &= (\varepsilon_\alpha - \varepsilon_i)Z^N_{\alpha i} - \sum_{\beta j} \left[\langle \alpha j|v|i\beta\rangle Z^N_{\beta j} + \langle \alpha\beta|v|ij\rangle Z^N_{j\beta}\right] \end{aligned} \right. \tag{28}$$

Equations (28) are the familiar R.P.A. equations of which there is ample account in the literature [7].

In Eqs (24) and (26) the indices (i, j) and (α, β) always occur in pairs. Each pair (i, j) forms a two-particle configuration and each pair (α, β) forms a two-hole configuration. Since the configurations (i, j) and (j, i) are the same we use the convention

$$i > j, \ \alpha > \beta$$

Equations (24) and (26) may then be cast in matrix form. Each two-particle configuration is labelled by one index p, and each two-hole configuration is labelled by one index h. Let us assume that there are n_p and n_h two-particle and two-hole configurations, respectively. The amplitudes X_p^N, X_h^N, Y_p^N and Y_h^N are then seen to be the solutions of the following eigenvalue matrix equation:

$$S \, V^N \ = \ \omega_N \, \nu \, V^N \tag{29}$$

The eigenvector V^N is a column vector of dimension $n_p + n_h$:

$$V \ = \ \begin{pmatrix} V_p^N \\ V_h^N \end{pmatrix} \tag{30}$$

The matrix S is a hermitian matrix which can be written as:

$$S \ = \ \begin{pmatrix} A_{pp'} & B_{ph} \\ B_{hp} & C_{hh'} \end{pmatrix} \tag{31}$$

where

$$A_{pp'} \equiv A_{ij,k\ell} \ = \ \delta_{ik} \, \delta_{j\ell} (\varepsilon_i + \varepsilon_j) + \langle ij|v|k\ell \rangle$$

$$B_{ph} \equiv B_{ij,\alpha\beta} \ = \ \langle ij|v|\alpha\beta \rangle$$

$$B_{hp} \equiv B_{\alpha\beta,ij} \ = \ \langle \alpha\beta|v|ij \rangle \tag{31a}$$

$$C_{hh'} \equiv C_{\alpha\beta,\gamma\delta} \ = \ -\delta_{\alpha\gamma} \, \delta_{\beta\delta} (\varepsilon_\alpha + \varepsilon_\beta) + \langle \alpha\beta|v|\gamma\delta \rangle$$

Finally ν **is the matrix**

$$\nu \ = \ \begin{pmatrix} 1 & 0 \\ 0 & -1 \end{pmatrix} \tag{32}$$

$$\nu_{pp'} \ = \ \delta_{pp'} \, , \ \nu_{ph} \ = \ \nu_{hp} \ = \ 0 \, , \ \nu_{hh'} \ = \ -\delta_{hh'}$$

and ω_N **is the eigenvalue.**

The eigenvalue problem (29) is similar to the one encountered in the R. P. A.   The R. P. A. eigenvalue problem is a special case of the problem (29) in which $n_p = n_h$ and A = C.   In spite of the difference $n_p = n_h$ between the eigenvalue problem (29) and the R. P. A. equations, most of the properties of the solutions of Eq. (29) are similar to the ones of the R. P. A. equations.   The latter equations have been proven by Bloch [6].   We shall only list the properties of the solutions of the eigenvalue problem (29) since the proofs are the same as in Ref. [6].

1.   If ω_N is an eigenvalue, ω_N^* is also an eigenvalue.
2.   The norm of a vector defined as

$$(V^{N^*}, \nu\, V^N) = \sum_{p=1}^{n_p} V_p^{N^*} V_p^N - \sum_{h=1}^{n_h} V_h^{N^*} V_h^N$$

   belonging to a complex eigenvalue is zero.
3.   If two eigenvalues ω_N and ω_M are such that $\omega_N^* \neq \omega_M$ then the scalar product

$$(V^{N^*}, \nu\, V^M) = \sum_{p=1}^{n_p} V_p^{N^*} V_p^N - \sum_{h=1}^{n_h} V_h^{M^*} V_h^M = 0$$

4.   If ω_N is a real non-degenerate eigenvalue, the norm $(V^{N^*}, \nu V^N)$ of the corresponding eigenvector is different from zero.
5.   The vectors V^N which have a non-vanishing norm $(V^{N^*}, \nu V^N)$ are linearly independent.

In the next part we shall show that a complex eigenvalue is associated with an instability of the system with respect to the formation of BCS pairs.

In the limit of vanishing matrix elements v = 0 it is easy to check that there are n_p vectors V^N with positive norm   and which can be normalized to +1, and n_h vectors with negative norm and which can be normalized to -1. We assume that this remains true as the interaction is switched on, so long as no complex eigenvalues occur.   Then we identify the n_p vectors with positive norm to the X^N amplitudes which are therefore normalized to +1:

$$\sum_{i > j} X_{ij}^{M^*} X_{ij}^N - \sum_{\alpha > \beta} X_{\alpha\beta}^{M^*} \cdot X_{\alpha\beta}^N = \delta_{NM} \qquad (33)$$

and we identify the n_h vectors with negative norm to the Y^N amplitudes which are therefore normalized to -1:

$$\sum_{i > j} Y_{ij}^{N^*} Y_{ij}^M - \sum_{\alpha > \beta} Y_{\alpha\beta}^{N^*} Y_{\alpha\beta}^M = -\delta_{NM} \qquad (33a)$$

The eigenvalues of the positive norm vectors X^N are identified with $\omega_N (A + 2) = E_N (A + 2) - E_0$ and the eigenvalues of the negative norm vectors Y^N are identified with $\omega_N (A - 2) = E_0 - E_N (A - 2)$.

The inverse closure relation is

$$\mathbb{1} = \sum_{N=1}^{n_p} x^N x^{N^*} \nu - \sum_{N=1}^{n_h} y^N y^{N^*} \nu \qquad (34)$$

where $\mathbb{1}$ is the unit matrix.

2. THE GENERATOR-CO-ORDINATE METHOD

It was shown by Jancovici and Schiff [3] how the generator-co-ordinate method can be used to derive the R.P.A. vibrations. We shall derive the pairing vibrations by this method. In so doing, we shall derive a stability condition for a system against the formation of BCS pairs, relate this condition to the complex eigenvalues of the eigenvalue problem (29), and obtain explicit expressions for the ground-state energy and wave function of a system with zero-point pairing vibrations. The generator-co-ordinate method, illustrated in this lecture, has a wide range of applications [4], namely in the α-particle model, and it is an interesting and useful approach to the problem of small oscillations of a system about its equilibrium state.

A BCS state is usually written thus

$$|\text{B.C.S.}\rangle = \prod_{m > 0} (u_m + v_m b_m^\dagger b_{\bar{m}}^\dagger) |0\rangle \qquad (35)$$

where m and $\bar{m}$ are time-reversed states. We shall consider independent-particle states $|\Psi_0\rangle$ composed of even numbers of neutrons and protons such that for each occupied (hole) orbit α the time-reversal orbit $\bar{\alpha}$ is also occupied.

The state $|\Phi_0\rangle$ may therefore be written

$$|\Phi_0\rangle = \prod_\alpha (b_\alpha^\dagger b_{\bar{\alpha}}^\dagger) |0\rangle \qquad (36)$$

where $|0\rangle$ is the real vacuum and where the product is limited to the $A/2$ occupied orbits α. We shall consider BCS states which differ little from the independent-particle state (36) in which case it is more convenient to write the BCS state (35) in an equivalent form as an operator acting on $|\Phi_0\rangle$

$$|\Phi(x,y)\rangle = \prod_i (1 + x_i^* b_i^\dagger b_{\bar{i}}^\dagger) \prod_\alpha (1 + y_\alpha^* b_{\bar{\alpha}} b_\alpha) |\Phi_0\rangle$$

$$= \exp\left[\sum_i x_i^* b_i^\dagger b_{\bar{i}}^\dagger + \sum_\alpha y_\alpha^* b_{\bar{\alpha}} b_\alpha \right] |\Phi_0\rangle \qquad (37)$$

where the states i are the empty particle orbits. The state $|\Phi(x,y)\rangle$ is not normalized. In fact,

$$\langle \Phi(x,y) | \Phi(x,y) \rangle = \prod_i (1+|x_i|^2) \prod_\alpha (1+|y_\alpha|^2)$$

$$\langle \Phi(x,y) | \Phi_o \rangle = 1 \tag{38}$$

The parametrization $x_i^* = v_i/u_i$ and $y_\alpha^* = u_\alpha/v_\alpha$ is introduced for convenience.

The BCS theory consists in determining the coefficients x_i and y_α which minimize the energy

$$\frac{\langle \Phi(x,y) | H - \lambda N | \Phi(x,y) \rangle}{\langle \Phi(x,y) | \Phi(x,y) \rangle} = E - \lambda n \tag{39}$$

But we now show that the wave function (37) as such is of no use to us because whenever the eigenvalue problem (29) has real roots the energy (33) has a local minimum for $x_i = y_\alpha = 0$ in which case the BCS state (37) reduces to the independent-particle state $|\Phi_0\rangle$. Let us expand the energy (39) up to second order in x_i and y_α, using the exponential form (31) for $|\Phi(x,y)\rangle$

$$\frac{\langle \Phi(x,y) | H - \lambda N | \Phi(x,y) \rangle}{\langle \Phi(x,y) | \Phi(x,y) \rangle} = E_o - \lambda n$$

$$+ \sum_{ij} x_i (A_{ij} - 2\lambda \delta_{ij}) x_j^* + \sum_{\alpha\beta} y_\alpha (C_{\beta\alpha} + 2\lambda \delta_{\alpha\beta}) y_\beta^*$$

$$+ \sum_{i\alpha} (x_i B_{i\alpha} y_\alpha + y_\alpha^* B_{\alpha i} x_i^*) \tag{40}$$

Here A, B and C are the matrices (31a). A more compact form is obtained by expressing the parameters x_i and y_α as a column vector

$$V = \begin{pmatrix} x_i^* \\ y_\alpha \end{pmatrix} \tag{41}$$

The energy (40) becomes

$$E - \lambda n = E_0 - \lambda n + (V^*, S V) - 2\lambda (V^*, \nu V) \tag{42}$$

where $E_0 - \lambda n = \langle \Phi_0 | H - \lambda N | \Phi_0 \rangle$. The matrices S and ν are defined by Eqs (31) and (32). If the coefficients x_i and y_α are chosen such as to keep

the expectation value of the particle number equal to n, the vector V has
vanishing norm; indeed,if

$$\frac{\langle \Phi(x,y) | N | \Phi(x,y) \rangle}{\langle \Phi(x,y) | \Phi(x,y) \rangle} = n + 2(V^*, \nu V) = n$$

it follows that

$$(V^*, \nu V) = 0$$

In such a case the energy $E - \lambda n > E_0 - \lambda n$ whenever the matrix S is positive-
definite

$$(V^*, S V) > 0$$

If ω_N is a complex eigenvalue of the eigenvalue problem (29), the corresponding
eigenvector V^N has vanishing norm and hence

$$(V^{N^*}, S V) = \omega_N (V^{N^*}, \nu V^N) = 0$$

Thus, whenever there exists a complex eigenvalue ω_N, by choosing $V = V^N$
we can make the energy stationary up to second order. Whether the energy
is a minimum or not in that case depends on higher orders; if the energy
was a quadratic expression of the coefficients x_i and y_α it would in fact be
a maximum and the system would be unstable against the formation of BCS
pairs. When the eigenvalues are all real, the closure relation (34) allows
us to write the matrix S in terms of the eigenvectors and eigenvalues of the
eigenvalue problem (29). We then find two equivalent equations for the
energy

$$E - \lambda n = E_o - \lambda n + \sum_N \omega_{N(A+2)} |(x^{N^*}, \nu v)|^2 - \sum_N \omega_{N(A-2)} |(y^{N^*}, \nu v)|^2 - 2\lambda(v^*, \nu v)$$

$$= E_o - \lambda n + \sum_N{}' [\omega_{N(A+2)} - 2\lambda] |(x^{N^*}, \nu v)|^2 - \sum_M [\omega_{M(A-2)} - 2\lambda] |(y^{N^*}, \nu v)|^2 \tag{43}$$

The stability condition for a vector V of vanishing norm is

$$\omega_N(A+2) > \omega_N(A-2) \tag{44}$$

Let $E_0(A \pm 2)$ be the ground-state energies of the $A \pm 2$ systems. The
condition (44) then reads

$$E_o - E_o(A-2) < E_o(A+2) - E_o \tag{45}$$

Figure 1 shows the binding energies of lead isotopes. The discontinuity in the slope of the binding energy curve strikingly suggests the stability of ^{208}Pb against pairing correlations.

If the vector V does not have a vanishing norm, the system is stable provided λ is chosen so as to satisfy the inequalities

$$\omega_N(A-2) \quad < \quad 2\lambda \quad < \quad \omega_N(A+2) \tag{46}$$

Although the BCS wave function (37) is not as such an improvement for a normal system, a superposition of such wave functions may well be one, such that we consider the wave function

$$|\psi\rangle = \int dx dy \, f(x,y) \, |\Phi(x,y)\rangle$$

$$= \int dx dy \, f(x,y) \, \exp\left[\sum_i x_i^* b_i^\dagger b_{\bar{i}}^\dagger + \sum_\alpha y_\alpha^* b_{\bar{\alpha}} b_\alpha \right] |\Phi_0\rangle \tag{47}$$

The integrals in Eq. (47) are multi-dimensional integrals over the entire complex planes of each variable x_i and y_α

$$dx \, dy = \prod_i d(Re \, x_i) \, d(Im \, x_i) \prod_\alpha d(Re \, y_\alpha) \, d(Im \, y_\alpha)$$

$f(x,y)$ is a weight function expected to be peaked about the static-equilibrium values $x_i = y_\alpha = 0$. We determine the weight function f by minimizing the energy

$$E - \lambda n = \frac{\langle \psi | H - \lambda N | \psi \rangle}{\langle \psi | \psi \rangle} \tag{48}$$

with respect to infinitesimal variations of the weight function f. This leads to the equation

$$\int dx' \, dy' \left[\langle \Phi(x,y) | H - \lambda N | \Phi(x',y') \rangle - (E-\lambda n) \, \langle \Phi(x,y) | \Phi(x',y') \rangle \right] f(x',y') = 0 \tag{49}$$

which must be satisfied for all values of x_i and y_α. We can solve Eq. (49) if we make two approximations which should be compared to the two basic hypotheses made in the first chapter concerning the time-dependent state (1).

1. The overlap kernel $\langle \Phi(x,y) | \Phi(x',y') \rangle$ is approximated by a Gaussian function

$$\langle \Phi(x,y) | \Phi(x',y') \rangle = \prod_i (1+x_i x_i'^*) \prod_\alpha (1+y_\alpha y_\alpha'^*)$$

$$\simeq \exp\left[\sum_i x_i x_i'^* + \sum_\alpha y_\alpha y_\alpha'^* \right] \tag{50}$$

2. A quadratic approximation is sufficient for the Hamiltonian kernel

$$\frac{\langle \Phi(x,y)|H-\lambda N|\Phi(x',y')\rangle}{\langle \Phi(x,y)|\Phi(x',y')\rangle} = E_o - \lambda n$$

$$+ \sum_{ij} x_i(A_{ij} - 2\lambda\delta_{ij}) x_j'^* + \sum_{\alpha\beta} y_\alpha (C_{\beta\alpha} + 2\lambda\delta_{\alpha\beta}) y_\beta'^* \qquad (51)$$

$$+ \sum_{i\alpha} (x_i B_{i\alpha} y_\alpha + y_\alpha'^* B_{\alpha i} x_i'^*)$$

When the approximations (50) and (51) are substituted in Eq.(49), the resulting equation is equivalent to a differential equation for the function

$$G(x,y) = \int dx'\, dy'\, \exp\left[\sum_i x_i x_i'^* + \sum_\alpha y_\alpha y_\alpha'^*\right] f(x',y') \qquad (52)$$

i.e.

$$\left[\sum_{ij} x_i(A_{ij} - 2\lambda\delta_{ij})\frac{\partial}{\partial x_j} + \sum_{\alpha\beta} y_\alpha(C_{\beta\alpha} + 2\lambda\delta_{\alpha\beta})\frac{\partial}{\partial y_\beta}\right.$$

$$\left. + \sum_{i\alpha}\left(x_i B_{i\alpha} y_\alpha + B_{\alpha i}\frac{\partial}{\partial x_i}\frac{\partial}{\partial y_\alpha}\right) + E_o - E\right] G(x,y) = 0 \qquad (53)$$

Equation (53) is an equation for coupled oscillators. The uncoupled modes of oscillation are found by expressing the matrices A, B and C in terms of the eigenvectors of the eigenvalue problem (29). Indeed we can define the operators:

$$B_N^\dagger = \sum_i X_i^N x_i - \sum_\alpha X_\alpha^N \frac{\partial}{\partial y_\alpha}$$

$$B_N = \sum_i X_i^{N^*}\frac{\partial}{\partial x_i} - \sum_\alpha X_\alpha^{N^*} y_\alpha$$

$$C_N^\dagger = \sum_i Y_i^{N^*}\frac{\partial}{\partial x_i} - \sum_\beta Y_\beta^{N^*} y_\beta \qquad (54)$$

$$C_N = \sum_i Y_i^N x_i - \sum_\alpha Y_\alpha^N \frac{\partial}{\partial y_\alpha}$$

$$N = 2\sum_i x_i \frac{\partial}{\partial x_i} - 2\sum_\alpha y_\alpha \frac{\partial}{\partial y_\alpha}$$

and express Eq. (53) in terms of these:

$$\left[\sum_N \omega_N(A+2)B_N^\dagger B_N - \sum_N \omega_N(A-2)C_N^\dagger C_N + E_o + \Delta E - E - \mathcal{N} \right] G(x,y) = 0 \quad (55)$$

where

$$\Delta E = - \sum_{N,\alpha} \omega_N(A+2) |X_\alpha^N|^2 + \sum_{N,1} \omega_N(A-2) |Y_1^N|^2 \quad (56)$$

It is easy to check that the operators $B_N^\dagger$, $C_N^\dagger$, B_N and C_N obey the commutation rules of raising and lowering operators of a harmonic oscillator

$$[B_N, B_M^\dagger] = \delta_{NM} \qquad [C_N, C_M^\dagger] = \delta_{NM}$$

$$[B_N, C_N^\dagger] = [B_N, C_M] = 0 \qquad (57)$$

The operator $\mathcal{N}$ obeys the following commutation rules:

$$[\mathcal{N}, B_N^\dagger] = 2B_N^\dagger \qquad [\mathcal{N}, B_N] = -2B_N$$

$$[\mathcal{N}, C_N^\dagger] = -2C_N^\dagger \qquad [\mathcal{N}, C_N] = 2C_N \qquad (58)$$

The operator $\mathcal{N}$ commutes with the Hamiltonian operator acting on $G(x,y)$ in Eq. (55), so that they may be simultaneously diagonalized. Thus, a function $G(x,y)$ may be found which simultaneously safisfies the eigenvalue equations

$$\left[\sum_N \omega_N(A+2)B_N^\dagger B_N + \sum_N \omega_N(A-2)C_N^\dagger C_N + E_o + \Delta E \right] G(x,y) = EG(x,y) \quad (59)$$

$$\mathcal{N}G(x,y) = \alpha G(x,y) \qquad (60)$$

Equation (59) is an equation of uncoupled oscillators. The ground state $G_0(x,y)$ containing zero quanta of excitation is, therefore, the solution of the equations

$$B_N G_o(x,y) = C_N G_o(x,y) = 0 \qquad (61)$$

and it has an energy

$$E = E_o + \Delta E \qquad (62)$$

Thus, ΔE defined in Eq. (56) is the ground-state correlation energy due to zero-point pairing vibrations. It is easy to see that for a normal system $\Delta E < 0$. We thus improve the energy by using the trial wave function (47). The same correlation energy is obtained by an appropriate summation of diagrams [5]. It is easy to check that the function

$$G_o(x,y) = \exp\left(\sum_{i\alpha} x_i y_\alpha \, K_{i\alpha} \right) \tag{63}$$

will satisfy Eq. (61). The matrix $K_{i\alpha}$ is the solution of the compatible set of linear equations

$$x_\alpha^{N^*} = \sum_i{}' x_i^{N^*} K_{i\alpha} \qquad Y_i^M = \sum_\alpha K_{i\alpha} Y_\alpha^M \tag{64}$$

When the function $G(x, y)$ is known, the weight function $f(x, y)$ may be calculated with the help of the identity [3]:

$$G(x,y) = \left(\tfrac{1}{\pi}\right)^M \int \exp\left[\sum_i x_i x_i'^* + \sum_\alpha y_\alpha y_\alpha'^* - \sum_i |x_i'|^2 - \sum_\alpha |y_\alpha'|^2 \right] G(x',y') \tag{65}$$

which may be used to invert Eq. (52):

$$f(x,y) = \left(\tfrac{1}{\pi}\right)^M \exp\left[-\sum_i |x_i|^2 - \sum_\alpha |y_\alpha|^2 \right] G(x,y) \tag{66}$$

The number M is equal to the total number of complex variables x_i and y_α. The identity (65) may be used to obtain an expression for the state $|\Psi\rangle$. Using the identity (65) and Eq. (66), Eq. (47) reads

$$|\psi\rangle = G(b_i^\dagger \, b_{\bar{i}}^\dagger, \, b_{\bar{\alpha}} b_\alpha) \, |\Phi_o\rangle \tag{67}$$

where $G(b_i^\dagger b_{\bar{i}}^\dagger, b_{\bar{\alpha}} b_\alpha)$ is the function $G(x, y)$ in which each x_i and y_α is replaced, respectively, by the operators $b_i^\dagger b_{\bar{i}}^\dagger$ and $b_{\bar{\alpha}} b_\alpha$. Thus, an explicit expression for the trial wave function $|\Psi\rangle$ is obtained; in particular the ground state $|\Psi_0\rangle$ containing no quanta of vibrations is obtained using Eq. (63)

$$|\psi_o\rangle = \exp\left[\sum_{i\alpha} K_{i\alpha} \, b_i^\dagger b_{\bar{i}}^\dagger b_{\bar{\alpha}} b_\alpha \right] |\Phi_o\rangle \tag{68}$$

By expanding the exponential (68) we obtain the ground state with its zero-point vibrations in terms of two-particle two-hole, four-particle four-hole, etc., configurations built on the independent-particle state $|\Phi\rangle$.

The function $G(x,y)$ corresponding to the excited states with one or more quanta may be obtained by applying the raising operators B_N^+ and C_N^+ to the ground-state function (63).

We must finally answer the question: what is the extra operator $\mathscr{N}$? The reader will be satisfied to learn that it acts as the particle-number operator. This is apparent from the following equation which is easy to verify

$$\frac{\langle\psi|N|\psi\rangle}{\langle\psi|\psi\rangle} \;=\; n \;+\; \frac{\int dxdy\; f^*(x,y)\; \mathscr{N}G(x,y)}{\int dxdy\; f^*(x,y)\; G(x,y)}$$

$$=\; n \;+\; \alpha \tag{69}$$

The mean value of the number of particles is $n + \alpha$, and, furthermore, the mean value of the number of particles is stationary with respect to variations of the weight function $f(x,y)$. It is easy to check that $\mathscr{N}\, G_0(x,y) = 0$ so that in the ground state the mean value of the particle number is n, as is also obvious from Eq. (68). For each vibration B_N^+, the particle number is increased by 2, and for each vibration C_N^+ the particle number decreases by 2. Thus the eigenvalue α of the operator $\mathscr{N}$ is just the particle number quantum number α of pairing vibrations introduced by Bohr and Mottelson [1].

3.   TWO-PARTICLE TWO-HOLE ADMIXTURES IN 2s-1d SHELL NUCLEI

The Hartree-Fock theory has been extensively applied to 2s-1d shell nuclei, and it is quite successful in explaining the rotational properties of nuclei close to ^{20}Ne and ^{24}Mg. But the Hartree-Fock calculations fail to predict the nuclear properties of ^{28}Si and ^{32}S [8]. Strongly deformed states are predicted for ^{28}Si, and experimental data do not confirm this. A stable spherical equilibrium shape is not obtained for ^{32}S. It is, therefore, interesting to study the admixtures of two-particle two-hole configurations to the Hartree-Fock state. They are the simplest admixtures which one can consider since Hartree-Fock states are stable against particle-hole excitations. A full calculation of two-particle two-hole (2p-2h) admixtures has not yet been done, curiously enough. Some partial attempts have been made [9] which neither include all the configurations nor treat the many-body problem correctly. We shall first consider the problems which must be solved before diagonalizing the (2p-2h) admixtures and discuss the results of such calculations. We shall for simplicity consider the even-even N = Z nuclei, since generalizations are trivial. These nuclei are described by an independent-particle wave function $|\Phi_0\rangle$ which is time-reversal invariant, and the orbits of which have four-fold degeneracy [10]. The wave function $|\Phi_0\rangle$ has thus zero total isospin (see Fig. 2).

We wish to improve the wave function $|\Phi_0\rangle$ by adding to it 2p-2h configurations. We thus consider the wave function

$$|\psi\rangle \;=\; a_o|\Phi_o\rangle \;+\; \sum_{i>j}\sum_{\alpha>\beta} c(ij,\alpha\beta)b_i^+b_j^+b_\beta b_\alpha|\Phi_o\rangle \tag{70}$$
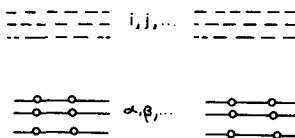
FIG.2.   Filled and empty orbits of an even-even N = Z nucleus represented by the state $|\Phi_0\rangle$.
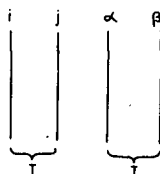
FIG.3.   Graphical representation of a two-particle two-hole configuration built on the independent-particle state $|\Phi_0\rangle$ shown in Fig.2.

The orbits i, j, ... are empty particle orbits and the orbits $\alpha, \beta, ...$ are filled hole orbits as shown in Fig. 2 (see Figs 2 and 3).

Since the isospin of the state $|\Phi_0\rangle$ is zero, there are two kinds of 2p-2h configurations, i.e. those in which each pair of particles (and holes) is coupled to isospin T = 0 or T = 1. A pairing force would produce 2p-2h configurations composed of T = 1 pairs. T = 0 pairing has also been considered [11].

The coupling of isospins is done in the usual way: a pair of nucleons with isospin (T, M_T) is created by the operator

$$A^\dagger_{T,M_T}(i,j) = \epsilon(i,j) \sum_{\tau_1 \tau_2} \begin{bmatrix} 1/2 & 1/2 & T \\ \tau_1 & \tau_2 & M_T \end{bmatrix} b^\dagger_{i,\tau_1} b^\dagger_{j,\tau_2} \tag{71}$$

where the labels i and j denote all the quantum numbers of the orbits except the isospin quantum number.

The pair of nucleons (71) is normalized if $\epsilon(i, j)$ is chosen such that

$$\epsilon(i,j) = 1 \qquad \text{if} \qquad i \neq j$$

$$= \frac{1}{\sqrt{2}} \qquad \text{if} \qquad i = j \quad \text{and} \quad T = 0 \tag{72}$$

$$= 0 \qquad \text{if} \qquad i = j \quad \text{and} \quad T = 1$$

and $A^\dagger_T(i, j) = (-)^T A^\dagger_T(j, i)$.

A coupled and normalized 2p-2h configuration is constructed as follows:

$$|i,j;\alpha,\beta;T\rangle = \epsilon(i,j)\epsilon(\alpha,\beta) \frac{1}{\sqrt{2T+1}} \sum_{M_T} A^\dagger_{TM_T}(i,j) A_{TM_T}(\alpha,\beta) |\Phi_0\rangle \tag{73}$$

The index T denotes the isospin 0 and 1 of each pair of nucleons; the total isospin of the 2p-2h configuration (73) is zero. The expansion of the state (70) with respect to the coupled and normalized basis (73) is

$$|\psi\rangle = a_0|\Phi_0\rangle + \sum_{i \geq j} \sum_{\alpha \geq \beta} C(i,j;\alpha,\beta;T)|i,j;\alpha,\beta;T\rangle \qquad (74)$$

Finally, a further reduction of the 2p-2h configuration space is obtained by the fact that $|\Phi_0\rangle$ is time-reversal invariant. Let us denote by a bar a time-reversed orbit. For example, if an orbit α is expanded on a shell-model basis $|n\ell jm\rangle$ with real coefficients $d^\alpha_{n\ell jm}$

$$|\alpha\rangle = \sum_{n\ell jm} d^\alpha_{n\ell jm} |n\ell jm\rangle \qquad (75)$$

then with the Condon-and-Shortley phase convention the time-reversed orbit is

$$|\bar\alpha\rangle = \sum_{n\ell jm} d^\alpha_{n\ell jm} (-)^{\ell+j-m} |n\ell j-m\rangle \qquad (76)$$

The time-reversed 2p-2h configuration (73) is $|\bar i\bar j, \bar\alpha\bar\beta,T\rangle$, so that the configurations $|ij, \alpha\beta, T\rangle$ in the expansion (74) may be replaced by the configurations

$$\frac{1}{\sqrt{2}} (|ij,\alpha\beta,T\rangle + |\bar i\bar j,\bar\alpha\bar\beta,T\rangle) \qquad (77)$$

with the exception of the configurations $|i\bar i, \alpha\bar\alpha, T\rangle$ which are time-reversal invariant and which should be included as such. Care must be taken when using configurations (77), so as not to count them twice.

One may be tempted to obtain the components a_0 and $C(ij, \alpha\beta, T)$ of the wave function (74) by simple diagonalization of the nuclear or shell-model Hamiltonian H between the state $|\Phi_0\rangle$ and the 2p-2h configurations. This is in fact an incorrect way to proceed for two reasons:

1. The ground state and the two-particle two-hole states are not treated on equal footing.

2. Spurious effects arise because $|\Phi_0\rangle$ is not an eigenstate of the angular momentum operator.

The correct procedure is the following:

1. One should first diagonalize the two-particle two-hole configurations alone, excluding the state $|\Phi_0\rangle$. Let us denote each two-particle two-hole configuration (ij, $\alpha\beta$, T) by one index λ. Let there be n two-particle two-hole configurations. The diagonalization of these configurations leads to the solution of the equations

$$\sum_{\lambda'=1}^{n} \langle \lambda | \hat{H} | \lambda' \rangle \, x_{\lambda'}^{N} = \omega_N \, x_{\lambda}^{N} \qquad \sum_{\lambda=1}^{n} |x_{\lambda}^{N}|^2 = 1$$

where $\hat{H}$ is the Hamiltonian used and where X_λ^N and ω_N are the eigenvectors and eigenvalues resulting from the diagonalization of the two-particle two-hole configurations. The ω_N obtained are then the energies of the two-particle two-hole states relative to the ground state. It may be asked: why not include the state $|\Phi_0\rangle$ in the matrix to be diagonalized since the Hamiltonian will certainly mix the state $|\Phi_0\rangle$ and the two-particle two-hole configurations?

The answer is that the energy of the two-particle two-hole states is ω_N, and that the admixture to the ground state must be calculated after the diagonalization is performed. This may be shown by the method of the linked-cluster expansion of the ground-state energy, a subject outside the scope of this paper. The physical justification is as follows: if one included the state $|\Phi_0\rangle$ in the diagonalization the lowest eigenvalue would correspond to the lowering of the energy of the ground state due to two-particle two-hole virtual excitations. But the two-particle two-hole states are lowered by the same amount owing to the same excitations [16]. Such a lowering would not be taken into account in the diagonalization. Thus the ground state and the two-particle two-hole states would not be treated on the same footing, and the distance between the ground state and the two-particle two-hole states would be over-estimated. These effects are corrected in the linked-cluster expansion by the elimination of unlinked diagrams.

The lowering ΔE of the ground-state energy may be calculated in the following way. Let

$$V_{o\lambda} = \langle \Phi_o | \hat{H} | \lambda \rangle$$

be the matrix element linking the state $|\Phi_0\rangle$ to the two-particle two-hole configuration λ. Then ΔE is given in terms of the ω_N and X_λ^N by the expression

$$\Delta E = - \sum_{N=1}^{n} \sum_{\lambda=1}^{n} \frac{|x_\lambda^N \, V_{o\lambda}|^2}{\omega_N}$$

The amplitude of a two-particle two-hole configuration on the ground state is given by

$$c_\lambda = \sum_{N=1}^{n} \sum_{\lambda'=1}^{n} \frac{V_{o\lambda'} \, x_{\lambda'}^{N} \, x_{\lambda}^{N*}}{\omega_N}$$

2. The diagonalization of two-particle two-hole configurations is further complicated by the fact that $|\Phi_0\rangle$ is a deformed state and hence not an eigenstate of $\vec{J}^2$, the total angular momentum. It is useful to consider the diagonalization of H as a variational procedure. Indeed the lowest eigenvalue is equal to the minimum energy which can be obtained with a wave function of

the form (74). It is well known [10] that an energy gain is obtained by projecting $|\Phi_0\rangle$ onto a state of zero angular momentum. The projected state $P_{J=0}|\Phi_0\rangle$ differs from $|\Phi_0\rangle$ by 2p-2h, 4p-4h etc. admixtures. Clearly we do not wish to include in $|\Psi\rangle$ the 2p-2h admixtures which are due to angular momentum projection because then the 2p-2h admixtures would depend entirely on what angular momentum J the state $|\Psi\rangle$ is projected on and the meaning of an intrinsic state would be lost. Whenever the state $|\Psi\rangle$ is well deformed so that its projected states $P_J|\Psi\rangle$ have a rotational spectrum

$$\frac{\langle\Psi|P_J H|\Psi\rangle}{\langle\Psi|\Psi\rangle} = E_o + AJ(J+1) \qquad (78)$$

it is better to diagonalize not H but the Hamiltonian

$$\hat{H} = H - A\vec{J}^2 \qquad (79)$$

where A is given by the Skyrme formula [13]

$$A = \frac{\langle\Psi|H\vec{J}^2|\Psi\rangle - \langle\Psi|H|\Psi\rangle\langle\Psi|\vec{J}^2|\Psi\rangle}{\langle\Psi|\vec{J}^4|\Psi\rangle - \langle\Psi|\vec{J}^2|\Psi\rangle^2} \qquad (80)$$

This method is justified because when Eq. (78) is satisfied, the state $|\Psi\rangle$ and the projected states $P_J|\Psi\rangle$ all have the same mean value of $\hat{H}$ so that no energy gain due to angular momentum projection is obtained by diagonalizing $\hat{H}$ [12].

Figure 4 shows the results of diagonalizing the Hamiltonian (79) between all the 2p-2h configurations belonging to the 2s-1d shell for ^{28}Si as a function of A:

$$\langle\Psi|H|\Psi\rangle = \langle\Phi_o|H|\Phi_o\rangle + \Delta E \qquad (81)$$

ΔE is the gain in energy due to the 2p-2h admixtures to the state $|\Phi_0\rangle$. Figure 4 shows the gain in energy ΔE, the mean value $\langle\Psi|\vec{J}^2|\Psi\rangle$ of angular momentum, and the strength $\sum_\lambda C_\lambda^2$ of two-particle two-hole admixtures, resulting from the diagonalization of $H - A\vec{J}^2$, all plotted against A. The vertical line gives the zero-order value of A, i.e.

$$A_o = \frac{\langle\Phi_o|H\vec{J}^2|\Phi_o\rangle - \langle\Phi_o|H|\Phi_o\rangle\langle\Phi_o|\vec{J}^2|\Phi_o\rangle}{\langle\Phi_o|\vec{J}^4|\Phi_o\rangle - \langle\Phi_o|\vec{J}^2|\Phi_o\rangle^2} \qquad (82)$$

We expect that the actual value of A calculated with expression (80) is not very different from the value (81) since the 2p-2h admixtures are small.
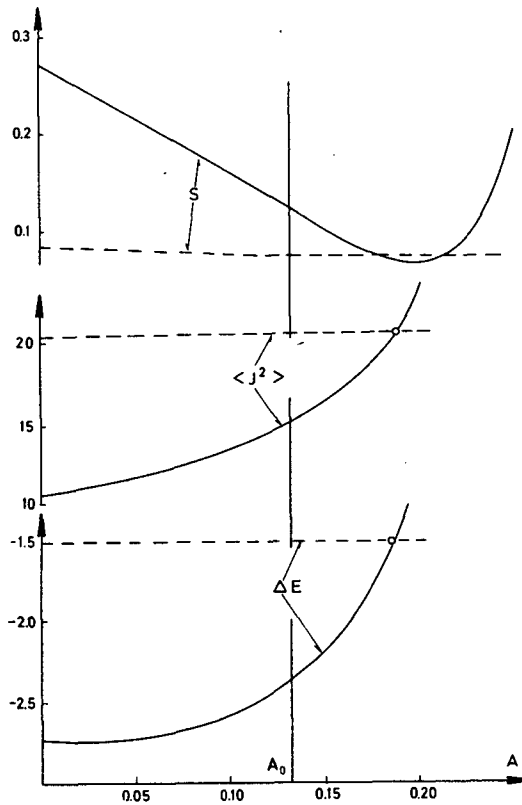
FIG. 4. Variation of the energy gain ΔE, the mean value $\langle J^2 \rangle$ of the angular momentum operator and of the total 2p-2h strength $S = \sum_\lambda |C_\lambda|^2$, with the moment of inertia parameter A. The full lines show the results of diagonalizing $H - A\vec{J}^2$ among all the 2s-1d shell 2p-2h configurations. The dashed lines show the result of diagonalizing $H - A\vec{J}^2$ after the spurious state $\vec{J}^2 |\Phi_0\rangle$ is eliminated from the 2p-2h configuration space. The vertical line is the zero order value A_0 obtained by the Skyrme formula of the moment of inertia parameter. This calculation is for ^{28}Si with an oblate deformation and using a Rosenfeld force.

It may then be expected that using value (81) in the Hamiltonian $\hat{H} = H - A\vec{J}^2$ is a sufficient approximation. But as seen in Fig. 4, ΔE and $\langle \Psi | \vec{J}^2 | \Psi \rangle$ are rapidly varying functions of A around the value A_0 so that the choice of A is very critical and the zero-order value (82) is dangerous to use in order to evaluate 2p-2h admixtures. This makes the use of the Hamiltonian (79) awkward since it requires a precise evaluation of A using the exact expression (80) which is quite difficult (in fact, the rapid variation of ΔE and $\langle \vec{J}^2 \rangle$ with A has been exploited for a precise determination of A_0 [14]).

It is possible to overcome the above difficulties by using another method. This consists in eliminating from the 2p-2h configurations the spurious state $\vec{J}^2 |\Phi_0\rangle$. This spurious state is due to a rotation of the state $|\Phi_0\rangle$

$$ e^{-i\beta J_y} |\Phi_0\rangle \;=\; |\Phi_0\rangle - i\beta J_y |\Phi_0\rangle - \frac{\beta^2}{2} J_y^2 |\Phi_0\rangle + \ldots \qquad (83) $$

The component $J_y|\Phi_0\rangle$ is a p-h state which does not produce admixtures
to $|\Phi_0\rangle$ because of the ellipsoidal symmetry of $|\Phi_0\rangle$. An examination of
the expression of the energy of a projected state [10] will show that for
nuclei with a large mean value $\langle\vec{J}^2\rangle$ only small angles β contribute to the
gain in energy due to the projection. Thus, for those nuclei the elimination
of the state $\vec{J}^2|\Phi_0\rangle$ from the 2p-2h configurations will effectively eliminate
in the diagonalization of H the gain in energy due to angular momentum pro-
jection. For nuclei which are weakly deformed and for which $\langle\vec{J}^2\rangle$ is small,
the gain in energy due to projection is small so that a straightforward
diagonalization of H becomes justified. In fact, weakly deformed nuclei do
not satisfy Eq.(78) so that the use of the Skyrme formula (80) and of the
Hamiltonian (79) is no longer justified, even as a first approximation. Thus,
instead of diagonalizing $H - A\vec{J}^2$, a method which requires a precise deter-
mination of A and has no justification in the case of weakly deformed nuclei,
one may use an alternative method, namely the diagonalization of H and the
elimination of the spurious state $\vec{J}^2|\Phi_0\rangle$ from the 2p-2h configurations. We
can check this method by diagonalizing $H - A\vec{J}^2$ and seeing whether after
eliminating the spurious state the result is independent of A. The dotted
lines of Fig.4 show that this is indeed the case. Furthermore, for a well-
deformed nucleus, the point at which the dashed line crosses the full line
is an estimate of A, because for this value no energy gain of $\hat{H}$ is expected
by projecting angular momentum. It is satisfying that the dashed and full
lines of ΔE and $\langle\vec{J}^2\rangle$ cross for the same value of A. The 2p-2h strength
is close to a maximum at this value of A, and the 2p-2h admixtures are
therefore smallest there. The vertical line on Fig.4 indicates the value
of A_0. It is seen that $A > A_0$ so that the 2p-2h admixtures decrease the moment
of inertia as expected.

The actual values of the moment of inertia parameters A_0 and A depend
on the equilibrium deformation. A convenient way to see how the equilibrium
deformation is affected by 2p-2h admixtures is to use Nilsson orbits [15]
which are parametrized by a single deformation parameter δ. When the
orbits are restricted to 2s-1d shell configurations the asymptotic Nilsson
orbits are obtained for $\delta \to \pm\infty$. The single-particle energies and the para-
meters of the Rosenfeld Gaussian force used are those of Ref.[10].

Figure 5 shows the values of the unperturbed energy $E_0 = \langle\Phi_0|H|\Phi_0\rangle$
and of the perturbed energy $E_0 + \Delta E$ plotted against the deformation parameter
δ for ^{20}Ne, ^{28}Si and ^{32}S. It is seen that the 2p-2h admixtures, restricted
to 2s-1d shell configurations do not alter the equilibrium deformation of ^{20}Ne,
for which the 2p-2h admixtures are small.

The 2p-2h admixtures make ^{32}S spherical which is in better agreement
with experimental data. The total 2p-2h strength, defined as $\sum_\lambda|C_\lambda|^2$ is equal
to 0.3 in ^{32}S. For ^{28}Si the 2p-2h admixtures considerably reduce the energy
gain due to deformation, but not enough (with a Rosenfeld force) to make
^{28}Si spherical.

With Hartree-Fock wave functions a Rosenfeld force behaves like a
monopole plus a quadrupole-quadrupole force [10]. It is interesting to note
that in the 2s-1d shell the 2p-2h admixtures which it produces are quite
different from those of a pairing force. At zero deformation, the strength
of the 2p-2h configurations (73) with T = 1 account for only 13% and 17%
of the total 2p-2h strength in ^{32}S and ^{28}Si respectively. Of this T = 1 strength,
however, about 80% is due to time-reversal invariant configurations $|i\bar{i},\alpha\bar{\alpha},T\rangle$
which a pairing force would produce. Most of the total 2p-2h strength is due
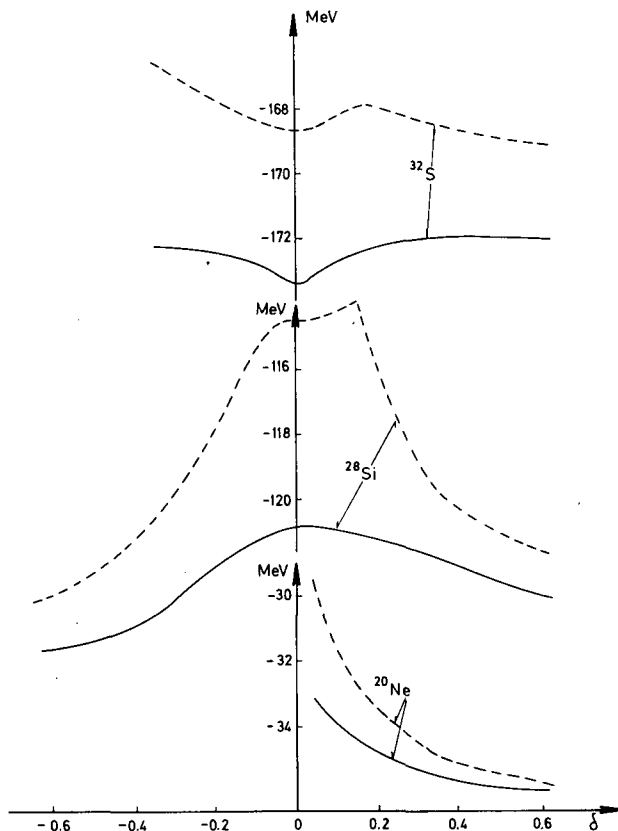
FIG.5.   Unperturbed energies $E_0 = \langle \Phi_0 | H | \Phi_0 \rangle$ (dashed lines) and perturbed energies $E_0 + \Delta E$ of ^{32}S, ^{20}Ne and ^{28}Si plotted against the deformation parameter δ of the Nilsson orbits. The energies are measured relative to the ^{16}O ground-state energy. This calculation was made by using a Rosenfeld force.

to 2p-2h configurations (73) with T = 0, but of this strength only about 30% is due to time-reversal pairs which a T = 0 pairing force[11] would produce.

The effects of 2p-2h admixtures which are excited from one major shell to the next are not yet investigated. They may be quite different because they depend on the odd moments of the interaction V which play no role within one major shell.

Finally it should be pointed out that the state $J^2 | \Phi_0 \rangle$ is not the only 2p-2h spurious state. There are also spurious states of the type $J_+ b_i^\dagger b_\alpha | \Phi_0 \rangle$ and $J_- b_i^\dagger b_\alpha | \Phi_0 \rangle$ which are rotated particle-hole configurations. It may be necessary to eliminate these states in cases where particle-hole configurations play an important role.

REFERENCES

[1] BOHR, A., in Nuclear Structure (Proc.Symp.Dubna, 1968), IAEA, Vienna (1968) 179;
      NATHAN, O., ibid., 191.
[2] BES, D.R., BROGLIA, R.A., Nucl.Phys. 80 (1966) 289;
      BROGLIA, R.A., RIEDEL, C., Nucl.Phys. A92 (1967) 145;

GLENDENNING, N.K., Phys.Rev. 137B (1965) 102;
see also: KLEBER, M., Z.Phys. 210 (1968) 251.

[3] JANCOVICI, B., SCHIFF, D.H., Nucl.Phys. 58 (1964) 678.

[4] BRINK, D.M., WEIGUNY, A., Nucl.Phys. A120 (1968) 59;
VI, H., BIEDERHARN, L.C., Phys.Letts 27B (1968) 608.

[5] RIPKA, G., PADJEN, R., Pairing vibrations of normal systems, submitted to Nucl.Phys.

[6] BLOCH, C., Lectures on the Many Body Problem, Tata Institute, Bombay (1964).

[7] THOULESS, D.J., The Quantum Mechanics of Many Body Systems, Academic Press, New York and London (1961);
GILLET, V., Many Body description of Nuclear Structure and Reactions, Course 36, International School of Physics "Enrico Fermi" (BLOCH, C., Ed.), Academic Press, New York and London (1966);
BARANGER, M., Cargèse Lectures in Theoretical Physics, W.A. Benjamin, New York and Amsterdam (1963);
BROWN, G.E., Unified Theory of Nuclear Models and Forces, North Holland Publishing Company, Amsterdam (1967).

[8] RIPKA, G., in Structure of Light and Medium Mass Nuclei, Proc.3rd Symp. Kansas University, April 1968.

[9] PAL, M.K., STAMP, A.P., Nucl.Phys. A99 (1967) 228.

[10] RIPKA, G., Advances in Nuclear Physics 1 (BARANGER, VOGT, Eds) Plenum Press (1968).

[11] CHEN, H.T., GOSWAMI, A., Phys.Letts 24B (1967) 257;
GOSWAMI, A., KISSLINGER, L.S., Phys.Rev. 140B (1965) 26.

[12] RIPKA, G., International School of Les Houches (de WITT, GILLET, Eds), Gordon and Breach, New York (1969).

[13] SKYRME, T.H.R., Proc. Phys.Soc. (London) A70 (1957) 433.

[14] LEVINSON, C.A., Phys.Rev. 132 (1963) 2184.

[15] NILSSON, S.G., Kgl. Danske Videnskab.Selskab.Mat.Fys.Medd. 29 (1955) 16.

[16] ELLIS, P.J., ZAMICK, L., Comparison of various approximations for the ground state of ^{16}O (to be published).

SECTION II
Microscopic Nuclear Spectroscopy

SIMPLE SHELL MODEL
AND EFFECTIVE NUCLEAR FORCES

I. ·TALMI
The Weizmann Institute of Science,
Rehovoth, Israel

Abstract

SIMPLE SHELL MODEL AND EFFECTIVE NUCLEAR FORCES.
  1. Introduction; How effective interactions can be determined; 2. Identical valence nucleons. Is there an energy gap? 3. Binding energies I. Are magic nuclei tightly bound? 4. Binding energies II. Proton-neutron interactions are important. 5. Coupling of neutrons and protons. Spin gaps. 6. Configuration mixing; hidden and explicit.

1. INTRODUCTION. HOW EFFECTIVE INTERACTIONS CAN BE DETERMINED

In the contributions to these Proceedings, rather sophisticated theories of nuclear structure are discussed. My paper is, however, rather simple, the formalism is not new and I hope that you are familiar with it. Let me state right at the beginning that I am going to consider spherical nuclei only and will not discuss at all strongly deformed nuclei exhibiting rotational spectra. The problem of n strongly interacting particles is indeed very difficult and a simplified model cannot be expected to give a correct description of all nuclear phenomena. The only virtue of the approach which I am going to describe is that it leads to significant agreements with some experimental data. This is not always the case with more sophisticated theories where so many assumptions should be introduced that it is hardly possible to make a prediction. The approach which I shall describe is drastically simple, but enables quantitative predictions. It may be described, so to say, as "poor, but honest".

As the announcement suggests, I am using a "straightforward approach" to the nuclear shell model. The shell model has such a phenomenal success in explaining and predicting a vast amount of nuclear data [1]. Almost all successful predictions are, however, qualitative. The present approach is an attempt to obtain from the shell model significant quantitative predictions. To do so, it is necessary to take the shell model seriously and consider very simple configurations for the nucleons outside closed shells (which should be considered as certain orbits completely filled). Sometimes it is even assumed that these "valence nucleons" are in a pure (jj-coupling) configuration. There are many objections to such simple-minded assumptions. It is argued that the very strong interaction between nucleons leads to strong configuration mixings. In fact, in view of the hard core in the nuclear potential followed by the very strong attraction, it could be argued that the shell model, which assumes independent motion of the nucleons, would not be a good approximation. Once it is realized that independent-particle wave functions are only model wave functions, it is possible to understand, at least in principle, why the shell model is so successful.

Also in the present approach, we shall consider simple configurations as model wave functions and try to find out what quantitative predictions can be made on the basis of the shell model.

The single-particle shell model should first be supplemented by some "residual" interactions between nucleons. Otherwise, even the wave functions of the valence nucleons are not specified [2]. In principle, the nuclear interaction to be used with shell-model wave functions should be very different from the interaction between free nucleons. The real wave functions have short-range correlations due to the hard-core and strong attraction. If we can transform the problem so as to be able to use wave functions of independent nucleons, the resulting effective interaction should be modified by the effect of the short range correlations. Thus, we expect the effective interaction to have no hard core and be much less violent in mixing configurations. How can this non-local interaction be determined? Using methods of many-body theory, one can calculate it from the interaction between free nucleons. This is a rather involved procedure which, however, can give nice qualitative results [3]. The trouble with this method is that one has to use special intuition to know which terms should be included and which terms, though large, should not be included.

In another approach, some simple-minded phenomenological interaction is being used. Popular choices nowadays are the "pairing" or the "pairing + quadrupole" interactions. Since the choice of interaction is so drastically limited, the question arises how it is possible to obtain agreement with experiments. This is usually achieved by making the space of wave functions as large as necessary. It is, therefore, difficult to expect that such a procedure will give quantitative agreement with experiment. The alternative phenomenological approach to finding the effective interaction for the shell model is to look at the experimental data rather than at the papers of other people. In this paper, I would like to show how this procedure is used and what we have learned from experiment. In particular, I would like to show that the well-known pairing interaction is a rather poor approximation to the effective nuclear interaction.

We try to use simple shell-model wave functions and determine the matrix elements of the effective interaction from experiment. To obtain less matrix elements than the number of data, we have to impose some restriction on the effective interaction. We consider only two-body effective interactions. This is certainly the simplest assumption and we can see whether it is justified. There are also some indications from many-body theory that this should be so although the arguments are not conclusive. Thus, we try to see whether nuclear energies can be calculated using shell-model wave functions and effective two-body interactions. Even with the most general two-body interaction, there must be some relations between the experimental data. These relations follow from the fact that for two-body interactions, matrix elements in the n-particle configuration are linear combinations of matrix elements in two-particle configurations. We have now a consistency check on our assumptions: we see whether these relations are obeyed by the experimental data. If they are, it means that a set of two-body matrix elements can be used for the calculation of a larger number of nuclear energies. We determine the values of these matrix elements which best reproduce the experimental data (in a least-square fit). These matrix elements can now be used for further calculations. If the agreement between the calculated and experimental energies is good

we conclude that the shell-model configuration assignments make sense. This means that these wave functions can be used to calculate energies with the matrix elements of the effective interaction determined in this way. As mentioned before, the relation between these model wave functions and the real wave functions is rather involved. In some cases, it can be shown that even wave functions which contain large mixing with other con-figurations can still lead to simple-minded model wave functions [4]. In general, as will be discussed later, the more experimental data available the more meaningful are the shell-model wave functions obtained by this approach.

To illustrate the method, let us consider a well known case [5,6]. It was the first successful application and is still the "best typical example". Consider the ground state configuration of $^{40}_{19}K_{21}$. The 21st neutron is expec-ted to be in the $1f_{7/2}$ orbit outside the closed shells with 20 neutrons. There are 11 protons in the (s, d) shell. If we assume pure jj-coupling, which may seem stupid, we expect closed $1d_{5/2}$ and $2s_{1/2}$ orbits and 3 protons in the $1d_{3/2}$ orbit. There are four states of this $d_{3/2}^3 f_{7/2}$ configuration with spins J=2, 3, 4, 5. The energies of these states are given, apart from a constant term, by the interaction energies of the three $d_{3/2}$ protons with the $f_{7/2}$ neutron. The interaction energies in this configuration are linear combinations of the matrix elements in the $d_{3/2}$-proton - $f_{7/2}$-neutron configuration expected in $^{38}_{17}Cl_{21}$. Thus, the spacings between the ^{40}K levels should be linear combinations of the spacings between the ^{38}Cl levels (with spins J=2, 3, 4, 5) and vice versa. The ^{40}K levels were known earlier and from them the ^{38}Cl levels were predicted [5] and later found to be in excellent agreement with experiment (Fig. 1).

The expression of the ^{40}K interaction energies in terms of the ^{38}Cl ones can be easily carried out by using coefficients of fractional percentage (c.f.p.). Noting, however, that in ^{40}K there is a $d_{3/2}$ proton hole - $f_{7/2}$ neutron configuration, we can use a general relation due to Pandya between particle-particle and particle-hole spectra [6]:

$$V(j^{2j}\,j'J) = const. - \sum_{J'} (2J'+1) \left\{ \begin{matrix} jj'J \\ jj'J' \end{matrix} \right\} V(jj'J) \qquad (1)$$

As emphasized by expression (1), the calculation of the ^{38}Cl spectrum does not involve any detailed assumption on the two-body effective interaction. It may be central or include tensor forces and spin-orbit force, it may be local or non-local. The only assumptions made are pure jj-coupling and two-body interactions. There are no adjustable parameters in this calculation. It makes use only of the geometry of recoupling angular momenta. The good agreement obtained is quite striking and shows that this simple model (which implies good jj-coupling also in e.g. $^{37}_{17}Cl_{20}$). makes rather much sense for energy calculations.

In view of the excellent agreement of the calculated energies, it should be recalled that the magnetic moment of the ^{40}K ground state does not agree at all with the value calculated from a $d_{3/2}$ proton hole and $f_{7/2}$ neutron. Also the magnetic moments of ^{39}K and ^{41}Ca do not agree with the single nucleon values (Schmidt values). This again emphasizes the fact that the shell-model wave functions cannot be the real wave functions. The good agreement obtained shows that the admixtures of other states in the real wave functions have a simple effect on the energies. The effect of these
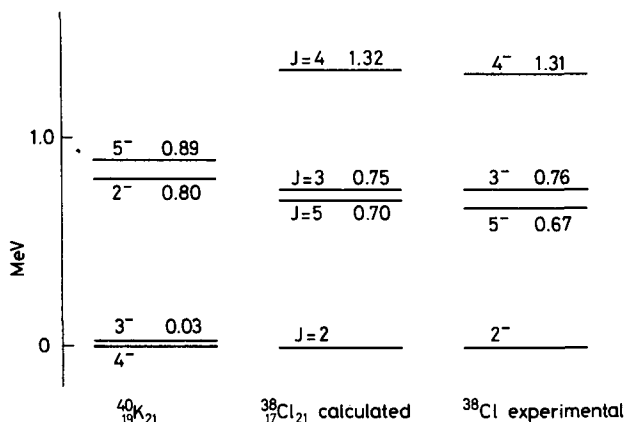
FIG. 1. Related configurations in ^{38}Cl and ^{40}K.

admixtures can be obtained by using with the simple shell-model wave functions a modified or renormalized interaction between the nucleons. This is the effective two-body interaction determined by the ^{40}K and ^{38}Cl energy levels.

The case of electromagnetic moments and transitions is not so clear. It may happen that in some cases the effect of the admixtures in the real wave functions can be reproduced by using renormalized or effective electromagnetic single-nucleon operators (or effective charges) with shell-model wave functions. For example, the ^{40}K magnetic moment can be accurately reproduced with the observed ^{39}K and ^{41}Ca magnetic moments (the ^{41}Ca magnetic moment was very accurately predicted from ^{39}K, ^{40}K and other K isotopes [7]). This, however, may be not so in other cases (e.g. the ^{37}Cl and ^{39}K magnetic moments are different). Transition probabilities are, in general, very sensitive to small changes in the wave functions while energies are stationary at the correct eigenstates.

2. IDENTICAL VALENCE NUCLEONS. IS THERE AN ENERGY GAP?

Let us now consider the simpler case of one kind of identical nucleons outside closed shells. We consider the j^n configuration of <u>either</u> protons or neutrons outside closed shells. The lowest j of interest is j = 5/2 which we will now take up. In order to make the discussion more concrete, let us consider the $1d_{5/2}$ neutron orbit in oxygen isotopes. This is an oversimplification of the actual situation in oxygen but it is useful to first look at it in this way. In ^{17}O we have one $d_{5/2}$ neutron. In ^{18}O the $d_{5/2}^2$ configuration can have states with J = 0, 2, 4 and in ^{19}O the $d_{5/2}^3$ configuration has states with J = 3/2, 5/2, 9/2 allowed by the Pauli principle. The $d_{5/2}^4$ neutron configuration is that of two holes, $d_{5/2}^{-2}$, and should have the same spectrum as the $d_{5/2}^2$ configuration.

The $d_{5/2}^3$ energies should be linear combinations of the matrix elements in the two-nucleon configuration. These latter quantities are simply the energies in the $d_{5/2}^2$ configuration (there are no two different states with the same value of J). The coefficients of the linear combinations can be found by using the appropriate c.f.p. In this simple case, however, we can use an elegant method due to Racah which will be useful later.

    The energies in all $(d_{5/2})^n$ configurations are linear combinations of V_0, V_2 and V_4 where $V_j = \langle (d_{5/2})^2 J \mid V \mid (d_{5/2})^2 J \rangle$. Within these configurations we can use for energy calculations any two-body interaction that will have in the $(d_{5/2})^2$ configuration the same eigenvalues V_0, V_2 and V_4. In the present case, there are only three parameters which fully characterize the effective interaction, no matter how complicated it looks. For our convenience, we can choose a simple two-body interaction with known eigenvalues in any state of any $(5/2)^n$ configuration. Let us look at the two-body operator

$$V'_{12} = a + b\, 2(j_1 \cdot j_2) + c\, q_{12} \tag{2}$$

where q_{12} is the seniority operator or the pairing interaction which has the eigenvalue $2j + 1$ in the $J = 0$ state and the eigenvalue 0 in all other states of the j^2 configuration. The eigenvalue of the operator (2) in a state of the j^n configuration with given J and seniority v is simply

$$\sum_{i<k}^{n} V'_{ik} = \sum_{i<k}^{n} a + b\left(\left(\sum_i^n j_i \right)^2 - \sum_i^n j_i^2 \right) + c \sum_{i<k}^{n} q_{ik} \tag{3}$$

$$= \frac{n(n-1)}{2}\, a + [J(J+1) - nj(j+1)]\, b + \frac{n-v}{2}\, (2j+3-n-v)\, c$$

We can adjust the constants a, b and c so that the eigenvalues of the operator (2) will be V_0, V_2 and V_4. With the constants thus determined we can calculate all energies using Eq.(3).

    Putting $n = 2$ in Eq. (3) and recalling that $v = 0$ for the $J = 0$ state while $v = 2$ for $J = 2$ and $J = 4$, we obtain

$$V_0 = a - \frac{35}{2}\, b + 6c \qquad\qquad a = \frac{1}{28}\,(5V_2 + 23V_4)$$

$$V_2 = a - \frac{23}{2}\, b \qquad\text{or}\qquad b = \frac{1}{14}\,(V_4 - V_2) \tag{4}$$

$$V_4 = a + \frac{5}{2}\, b \qquad\qquad c = \frac{1}{6}\, V_0 - \frac{1}{42}\,(10V_2 - 3V_4)$$

In the case of interest here, we obtain for the $(5/2)^3$ energies the following results

$$
\begin{array}{llll}
J = 5/2 & v = 1 & 3a - \dfrac{35}{2}\, b + 4c & \\[2mm]
J = 3/2 & v = 3 & 3a - \dfrac{45}{2}\, b & \quad(5) \\[2mm]
J = 9/2 & v = 3 & 3a - \dfrac{3}{2}\, b &
\end{array}
$$

If we take V_0, V_2 and V_4 from the $(d_{5/2})^2$ spectrum, we can thus calculate the energies of the $(d_{5/2})^3$ configuration.

    Before comparing with experiment the predictions based on the available data, let us look at a special case. If the pairing interaction is a good approximation to the effective interaction we have $a=b=0$ and only c

is different from zero. In that case, the v = 2, J = 2 and J = 4 levels are degenerate and lie above the v = 0 J = 0 ground state of the $(5/2)^2$ configuration. This spacing is 6c and is called the "energy gap". This gap is also found in the $(5/2)^3$ configuration. There, the v = 3, J = 3/2 and J = 9/2 levels should be degenerate and lie 4c (two thirds of the energy gap) above the v = 1, J = 5/2 ground state.

   In O^{18} the ground state has J = 0; 1.98 MeV above it there is a J = 2 level and 3.55 MeV above it there is a J = 4 level. Let us take these to be the $(1d_{5/2})^2$ levels. The 2 MeV 0-2 separation is indeed large but this is not an energy gap in the sense of the pairing theory! That would require the J = 2 and J = 4 levels to be degenerate whereas their spacing is almost as large as the 0-2 separation. The failure of the pairing theory is even more pronounced in O^{19}. There the ground state has indeed J = 5/2, but only 0.1 MeV above it there is a J = 3/2 level. This cannot be the $d_{3/2}$ level (which is at about 5 MeV excitation in O^{17}) as shown by its very small stripping width. It has also a very small M1-transition rate to the ground states whereas the corresponding matrix element for a spin flip is very large. On the other hand, the M1-operator within a j^n configuration of identical nucleons has the form $\sum gj_i$ = gJ and vanishing matrix elements between any orthogonal states [7]. Thus, there is no trace of an energy gap in ^{19}O. The J = 9/2 level which should be degenerate with the J = 3/2 level has now been found at 2.77 MeV.

   Since the pairing theory fails here we should check whether this failure is due to the arbitrary and too restrictive choice of interaction. Can the oxygen spectra be calculated at all by using a two-body interaction? Using the ^{18}O level spacings we can calculate the constants b and c which determine the ^{19}O spectrum. We obtain from (4) b = 0.11 MeV and c = -0.22 MeV. Using these values we obtain from the results (5) that the J = 3/2 level should lie -5b-4c = 0.33 MeV above the J = 5/2 ground state. The spacing between the J = 9/2 and J = 3/2 levels should be 21b = 3/2 $(V_4 - V_2)$ =2.35 MeV, putting the predicted position of the J = 9/2 level at 2.7 MeV. In some papers on the pairing theory a special reason is given for the fact that the J = 2 level is lower than other v = 2 levels. In papers where the authors worry about low-lying v = 3 levels in odd nuclei, another reason is given to explain this fact. If we just use $(d_{5/2})^n$ configurations with effective interactions suggested by the experimental data, we obtain rather good agreement. In the present approach, the fact that the J = 2 level is lower than the J = 4 <u>implies</u> the near degeneracy of the J = 5/2, v = 1 and J = 3/2, v = 3 levels.

   The more detailed description of the oxygen isotopes must include neutrons in the low-lying $2s_{1/2}$ orbit and also highly deformed states obtained by proton excitation [8]. A much clearer case seems to be the $(2d_{5/2})^n$ neutron configurations in zirconium isotopes [9] (Fig.2). In ^{92}Zr, with the $(d_{5/2})^2$ neutron configuration, the J = 2 and J = 4 levels are at 0.93 and 1.49 MeV, respectively. In the complementary $(d_{5/2})^4$ configuration in ^{94}Zr they are at 0.92 and 1.47 MeV. The calculated position of the J = 3/2 state in ^{93}Zr from either ^{92}Zr or ^{94}Zr is 0.26 MeV above the J = 5/2 ground state. Experimentally, it is at 0.27 MeV. The J = 9/2 level should be at 1.10 MeV above the ground state. In a recent publication [10], a level at 1.17 MeV was established in ^{93}Zr, and it was suggested that this is the J = 9/2 level of the $(d_{5/2})^3$ configuration. Another relevant feature is a highly attenuated M1-matrix element between the J = 3/2 state and the ground
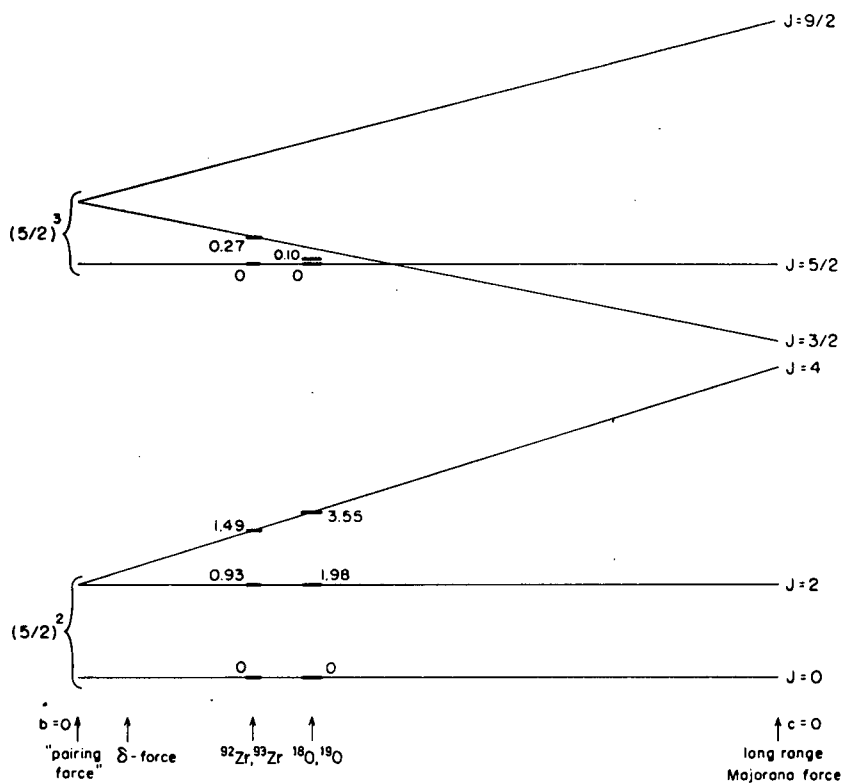
FIG.2.   Energies of $d_{5/2}^n$ configurations.

state [11]. The magnetic moment of the J = 3/2 state in ^{93}Zr was not
measured but in ^{95}Mo there are corresponding states. In the J = 5/2 ground
state of ^{95}Mo   g = -0.364 ± 0.001 was measured whereas in the first excited
J = 3/2 state the experimental result is g = -0.36 ± 0.04 [11].

     The occurrence of low-lying v = 3 J = j-1 states is not a unique feature
of the $(d_{5/2})^3$ configuration. In the $(1f_{7/2})^3$ and $(1f_{7/2})^5$ proton and neutron
configurations we see low lying J = 5/2 levels (^{43}Ca, ^{45}Ca, ^{51}V and ^{53}Mn [12]).
Such 5/2⁻ states show no stripping and have very small M1 transition
strengths to the 7/2⁻ ground states. Also in the neutron $(1g_{9/2})^7$ neutron
configuration in ^{85}Sr and in the $(1g_{9/2})^3$ proton configuration in ^{93}Tc we see
a very low-lying v = 3 J = 7/2 state [13]. The occurrence of such states is
strong evidence against the simple minded pairing theory. Such states
are predicted by using effective interactions determined from neighbouring
nuclei and furnish one of the successes of the approach presented here.

     In a j = 5/2 orbit with identical nucleons any two-body interaction is
diagonal in the seniority scheme as follows from the representation (2) of
any such interaction. This is really a simple case since there are no two
states with the same value of J in any $(5/2)^n$ configuration. For j = 7/2
this is no longer the case as in $(7/2)^4$ there are two states with J = 2 and
two states with J = 4. Still, in $(7/2)^4$ configuration, any two-body interaction
is diagonal in the seniority scheme. As a result, the $(7/2)^4$ levels with
seniorities v = 0 (J = 0) and v = 2 (J = 2, 4, 6) should have the same spacings
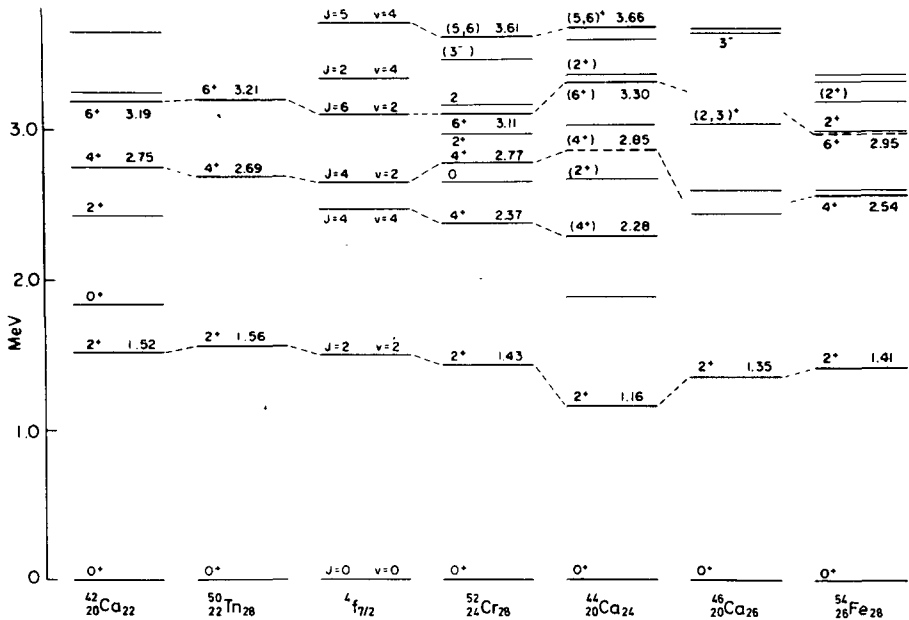
FIG. 3.   Energies of $1f_{7/2}^n$ configurations (even nuclei).

as in the $(7/2)^2$ configuration (Fig. 3). We see that this is roughly so in the $1f_{7/2}$ proton and neutron shells. We also see that the $(f_{7/2})^2$ matrix element taken from experiment lead to a rather low-lying v = 4 J = 4 level [14]. Such a level is actually observed in ^{44}Ca and ^{52}Cr. Using these values of the $(f_{7/2})^2$ matrix elements we can calculate the $(1f_{7/2})^3$ spectrum or the equivalent $(1f_{7/2})^5$ spectrum (Fig. 4). The low-lying J = 5/2 level is nicely reproduced as well as some other levels. It is clear that there are obvious perturbations, to be discussed later, but the general trend is good.

The ^{51}V nucleus is of particular interest because it shows a clear $(1f_{7/2})^3$ spectrum which can be calculated from $(1f_{7/2})^2$ matrix elements. The Coulomb excitations from the ground state to the J = 5/2, 3/2, 11/2 and 9/2 levels were measured. The B(E2)-values are considerably bigger than the $(1f_{7/2})^3$ estimate with the real E2-operator. However, the ratios between the E2-transition matrix elements agree well with those predicted from $(7/2)^3$ wave functions [15]. It seems that if the $f_{7/2}$ protons polarize the ^{48}Ca core, the individual polarizations are independent so that the E2-transitions can be obtained from $(1f_{7/2})^3$ wave functions using effective or renormalized E2 operators. The effective E2-operator determined in this way can be used to calculate the static quadrupole moment of the ^{51}V ground state giving the value Q = -0.058e $\times$ 10^{-24} cm^2. This agrees very well with the recently measured value [16] of Q = (-0.052 ± 0.010)e $\times$ 10^{-24} cm^2. The enhancement of the renormalized E2-operator corresponds to using the free E2-operator and harmonic-oscillator wave functions with an effective charge e_{eff} = 1.61 e.

The question whether seniority is a good quantum number for identical nucleon configurations becomes meaningful only for j $\geq$ 9/2. For j $\leq$ 7/2 any two-body interaction is diagonal in the seniority scheme. We have
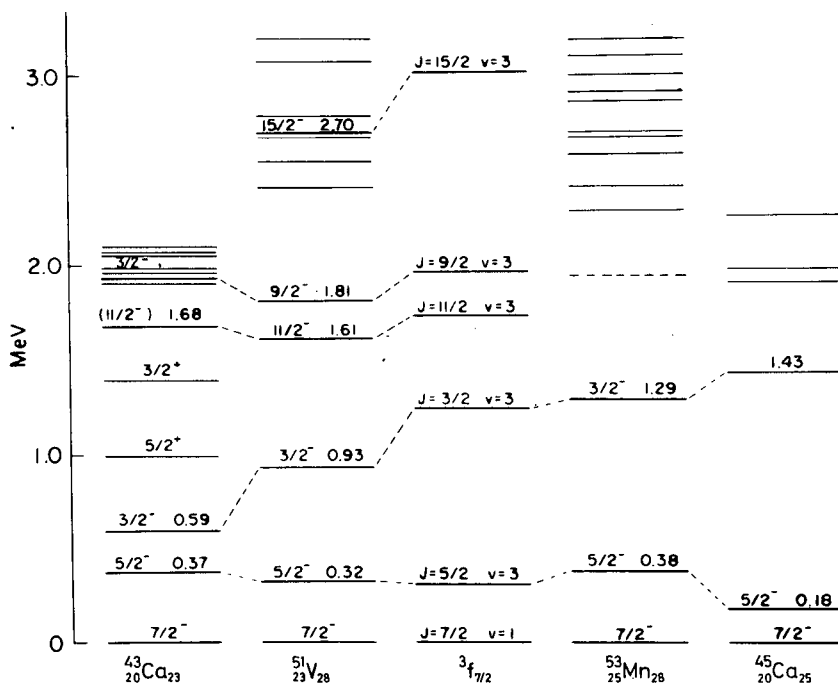
FIG.4.   Energies of 1f$_{7/2}$ configurations (odd nuclei).

some information about the proton $1g_{9/2}$ orbit which will be discussed later.
The resulting effective two-body interaction turns out to be diagonal in the
seniority scheme.   All matrix elements which are non-diagonal are pro-
portional to [13, 17]

$$\left\langle g_{9/2}^3 \ v=1 \ J=9/2 \ \Big| \ \sum V_{ik} \ \Big| g_{9/2}^3 \ v=3 \ J=9/2 \right\rangle$$

$$= \frac{1}{20\sqrt{429}} \ (65V_2 - 315V_4 + 403V_6 - 153V_8)$$

(6)

This matrix element turns out to be about 0.03 MeV whereas typical spacings
between states connected by it are of order 1 MeV.   Thus, the two-body
effective interaction between identical nucleons is diagonal in the seniority
scheme.   It shares this property with the pairing interaction but it is other-
wise considerably different from it.

3.   BINDING ENERGIES I.   ARE MAGIC NUCLEI TIGHTLY BOUND?

Another feature of the pairing interaction is the variation in binding
energy between odd and even nuclei.   Unlike the energy gap, this is a real
effect but it does not at all imply that the pairing interaction has any
validity.   As we shall see, this feature is a direct consequence of the seniori-
ty scheme for a very large class of interactions.   In fact, this was pointed
out long before the pairing theory was applied to nuclei [18,19].   It is
clear that the simple two-body interaction (2) cannot be used for j > 5/2

since it has only three free parameters. However, a modification of it can still be used to calculate binding energies. We first consider binding energies of nuclei with only one kind of nucleons outside closed shells.

As mentioned above, the interaction energy of any state in the j^n configuration is a linear combination of the two-nucleon matrix elements $V_J = \langle j^2 J |V| j^2 J \rangle$. In the case of identical nucleons, there are $(2j+1)/2$ of these, namely, $V_0, V_2 \ldots V_{2j-1}$. The interaction energy in the states with lowest seniority, $v = 0$ $J = 0$ for n-ever and $v = 1$ $J = j$ for n odd, has an even simpler expansion. It is a linear combination of only two parameters, V_0 and the average interaction in all states with seniority $v = 2$ defined by

$$\bar{V}_2 = \sum_{J > 0, \text{ even}}^{2j-1} (2J+1) V_J \Big/ \sum_{J > 0, \text{ even}}^{2j-1} (2J+1)$$

$$= \frac{1}{(j+1)(2j-1)} \sum_{J > 0, \text{ even}}^{2j-1} (2J+1) V_J \tag{7}$$

This property holds, in general, for the average interaction energy of all states with the same seniority v in the j^n configuration. There is just one state with $v = 0$ or $v = 1$ in any given j^n configuration.

Thus, we can use for the calculation of interaction energies in ground states any simple interaction that will reproduce correctly V_0 and $\bar{V}_2$. If we put $c = 0$ in (2) we obtain such an interaction. In the simplified interaction

$$V'_{12} = x + y \, q_{12} \tag{8}$$

we can fix the constants x and y to satisfy

$$x + (2j+1) y = V_0 \qquad x = \bar{V}_2 \tag{9}$$

The interaction (8) with the constants (9) has the same eigenvalue $\bar{V}_2$ for all states with seniority v, and in larger configurations will have similar degeneracies. It can still be used to calculate average interaction energies and, in particular, the interaction energies in ground states. In fact, we obtain

$$\langle j^n v J | \sum_{i<k}^{n} V'_{ik} | j^n v J \rangle = \bar{V}_2 \frac{n(n-1)}{2} + \frac{V_0 - \bar{V}_2}{2j+1} \frac{n-v}{2} (2j+3-n-v)$$

$$= \frac{n(n-1)}{2} \frac{2(j+1)\bar{V}_2 - V_0}{2j+1} + \frac{n-v}{2} \frac{2(j+1)}{2j+1} (V_0 - \bar{V}_2) + \frac{v(v-1)}{2} \frac{V_0 - \bar{V}_2}{2j+1} \tag{10}$$

For the states with $v = 0$ or $v = 1$ the last term in Eq.(10) vanishes and the interaction energy in ground states can be written as

$$\langle j^n \text{ g.s.} | \sum_{i<k}^{n} V_{ik} | j^n \text{ g.s.} \rangle = \langle j^n \text{g.s.} | \sum_{i<k}^{n} V_{ik} | j^n \text{ g.s.} \rangle$$

$$= \frac{n(n-1)}{2} \alpha + \left[\frac{n}{2} \right] \beta \tag{11}$$

In Eq. (11) the interaction parameters are

$$\alpha = \frac{2(j+1)\,\overline{V_2} - V_0}{2j+1} \qquad\qquad \beta = \frac{2(j+1)}{2j+1}\,(V_0 - \overline{V_2}) \qquad (12)$$

and $[n/2]$ is the step function which is equal to $n/2$ for even n and to $(n-1)/2$ for odd n.

    Expression (11), in spite of its simplicity, is not an empirical relation. It follows from the structure of wave functions in the seniority scheme. It holds for any two-body interaction which may be arbitrarily complex. In the ground states all the possible diversities in the possible two-body interactions give rise only to two numbers, α and β. In particular, the occurrence of the pairing term in Eq. (11), with the coefficient β, is a result of the seniority scheme and not of the pairing interaction. Different interactions give rise to different values of α and β, and we shall see soon some actual examples. If the interaction V_{ik} (not V'_{ik}) is diagonal in the seniority scheme, expression (11) is its eigenvalue in the ground state. If it is not, this is the diagonal matrix element while the ground state energy will be modified by the effect of states with seniorities 3, 5 or 4. As mentioned above, in actual nuclei, such modifications are negligible.

    We can now use nuclear binding energies to determine the α and β of the effective interaction. The binding energy of a nucleus with various j^n configurations outside closed shells has a constant term which is the energy of the closed shells. We, therefore, subtract from the binding energies considered the binding energy of the nucleus with the same closed shells and no j-nucleons. The remainder includes the kinetic energy of the j-nucleons and their interaction with the closed shells, in addition to the interaction energy within the j^n configuration. The kinetic energy of a j-nucleon as well as its interaction with closed shells is a scalar quantity independent of the projection m of j. Thus, the contribution of these terms is simply the sum of n equal single nucleon energies nC. Thus we obtain the result [18]

$$\text{B. E. } (j^n) - \text{B. E. } (n=0) = nC + \frac{n(n-1)}{2}\,\alpha + \left\lfloor \frac{n}{2} \right\rfloor \beta \qquad (13)$$

Using given binding energies we can look for values of C, α and β which will reproduce them as accurately as possible. A result of such a fit in the $1f_{7/2}$ shell is given in Table I.

    The values of C, α and β determined in this way are
C = 8.42±0.08, α = -0.23±0.01, β = 3.23±0.20 MeV for $1f_{7/2}$ neutrons
C = 9.69±0.05, α = -0.79±0.01, β = 3.15±0.13 MeV for $1f_{7/2}$ protons
The signs of these parameters are determined by taking binding energies as positive numbers. The single nucleon energy C is different for the protons and for the neutrons not only because of the Coulomb energy but also due to the interaction in the two cases being with different closed shells (those of ^{40}Ca and of ^{48}Ca respectively). The interaction parameters α and β for the protons include also the electrostatic repulsion and are indeed less attractive than the corresponding neutron parameters.

    The parameter β turns out to be rather large and attractive. This is so also in all other cases considered sor far [20]. The pairing term which contains it gives rise to a pronounced odd-even effect in binding energies. Looking at expressions (12) we see that the pairing term should

TABLE I. BINDING ENERGIES IN PROTON AND NEUTRON $1f_{7/2}^n$ CONFIGURATIONS IN MeV

Nucleus	Binding energy		Nucleus	Binding energy	
	experimental	calculated		experimental	calculated
$^{41}_{20}Ca_{21}$	8.36	8.42	$^{49}_{21}Sc_{28}$	9.62	9.69
$^{42}_{20}Ca_{22}$	19.83	19.84	$^{50}_{22}Ti_{28}$	21.78	21.75
$^{43}_{20}Ca_{23}$	27.76	27.81	$^{51}_{23}V_{28}$	29.83	29.86
$^{44}_{20}Ca_{24}$	38.90	38.79	$^{52}_{24}Cr_{28}$	40.34	40.34
$^{45}_{20}Ca_{25}$	46.32	46.31	$^{53}_{25}Mn_{28}$	46.91	46.88
$^{46}_{20}Ca_{26}$	56.72	56.83	$^{54}_{26}Fe_{28}$	55.75	55.78
$^{47}_{20}Ca_{27}$	64.00	63.90	$^{55}_{27}Co_{28}$	60.81	60.74
$^{48}_{20}Ca_{28}$	73.94	73.98	$^{56}_{28}Ni_{28}$	68.01	68.06

Note: The binding energy of ^{40}Ca was subtracted from the binding energies of the Ca isotopes. The binding energy of ^{48}Ca was subtracted from the binding energies of nuclei with proton configurations.

be large and attractive as long as the centre of mass of the v = 2 levels is considerably above the v = 0 J = 0 states. Thus, the odd-even effect is not at all related to the "energy gap". This effect will be present even if the v = 2 level will be spread out evenly; the J = 2 level, with its lower statistical weight, may even coincide with the ground state. The values of $V_0 - V_2$ obtained from the binding energies in Table I agree with the values calculated from the actual level spacings in Fig. 3.

The sign of α is opposite to that of β and it is therefore repulsive. This feature is common to all cases considered and due to the saturation properties of the nuclear interaction [20]. The quadratic term is always attractive for ordinary potential interactions being zero for a zero range force (δ-potential). A repulsive α can arise only from exchange forces or non-local interactions, like the pairing interaction (or a P_2 force). As we shall see later, the existence of an attractive symmetry energy, when both valence protons and valence neutrons are present, gives rise to the repulsive quadratic term.

FIG.5.   Neutron separation energies of calcium isotopes.
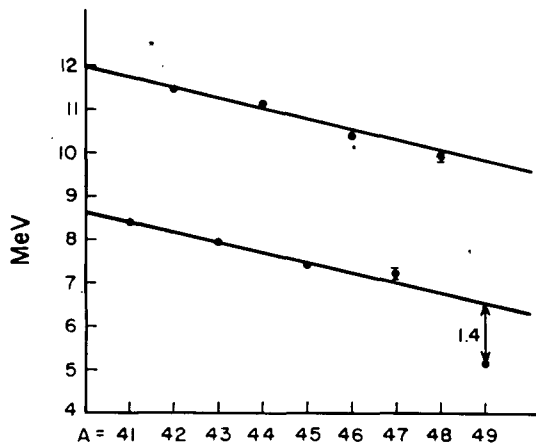
The form (13) of the binding energy gives rise to a very simple expression for the separation energies. These should lie on two straight lines, one for odd and the other for even nuclei. In Fig.5 we see neutron separation energies in calcium isotopes. The separation between the lines is due to the pairing term. The downward slope of the lines demonstrates the fact that α is repulsive.

The expression (13) with a repulsive parameter α has an interesting consequence [20]. Nuclei with magic proton or neutron numbers are not more tightly bound than their preceding even-even nuclei. When a magic nucleus is approached, the separation energy goes actually down as seen in Fig.5. This behaviour should be contrasted with the ionization energies of atoms which have high peaks at closed shells (noble-gas atoms). There, the plot is for neutral atoms so that the increase in the central charge more than compensates the additional repulsion of the electrons. Forgetting that the interaction between electrons is repulsive, some people think there should be similarity between closed electron shells and closed nucleon shells. The feature which is common to both cases is the large drop in the separation energy beyond a magic number. This drop, due to increased kinetic energy of the new shell, is clearly seen in Fig.5. Thus, nuclei

beyond a magic nucleus are less bound. Since stability is relative and is determined by two nuclei, this feature gives magic nuclei extra stability abundance, etc. Those who insist on similarity with atoms draw an average line through the points. This way they divide the drop into a rise before the magic number and a drop beyond it. They then increase the differences from the average with some weight function to make them look like in the atomic case. Such misrepresentations of the data give the erroneous impression about the extra large binding energies of magic nuclei.

The saturation properties of nuclear energies as well as the behaviour of the symmetry energy are much more pronounced than effects of nuclear shell structure. They do not stop at the beginning of a new shell although the actual numbers may undergo a change. Hence, we would not expect the repulsive part of the interaction between identical nucleons to be limited to a single j-orbit. When we consider two such nucleons in different j and j' orbits we expect them to repel each other on the average (the attractive pairing energy is not present in this case). Precisely, we consider the average interaction energy

$$
\begin{aligned}
\overline{V}_{jj'} &= \frac{1}{2} \left\langle j^2(0)\, j'\ J = 1 \ \Big|\ \sum_{i=1,2} V_{i3}\ \Big|\ j^2(0)\, j'\ J = j' \right\rangle = \\
&= \frac{1}{2} \left\langle j,\, j'^2(0)\ J = j \ \Big|\ \sum_{i=2,3} V_{1i}\ \Big|\ j,\, j'^2(0)\ J = j \right\rangle = \\
&= \sum_{J=|j-j'|} (2J+1)\langle jj'J|V|jj'J\rangle \Big/ \sum_{J=|j-j'|}(2J+1) = \\
&= \frac{11}{(2j+1)(2j'+1)} \sum_{J} (2J+1)\, V(jj'J)
\end{aligned}
\tag{14}
$$

In all cases considered so far the average interaction (14) turns out to be repulsive. Its absolute value is not very large; of the order of α for nucleons within the same orbit. Some of the individual V(jj'J) may be even attractive, though small, but the average value (14) is always repulsive.

It may happen that an overall attractive potential interaction may furnish not too bad an approximation of the effective interaction in the j^2 configuration. The resulting parameter α although attractive may be rather small (it vanishes for a zero-range potential). However, when several j-nucleons are considered the quadratic term becomes very important. Such a potential interaction will certainly be a poor approximation for the jj' configuration of identical nucleons. The average interaction (14) will then be attractive contrary to the experimental facts.

4.   BINDING ENERGIES II. PROTON-NEUTRON INTERACTIONS ARE
      IMPORTANT

Let us now consider both protons and neutrons outside closed shells. First let us look at both in the same j^n configuration. States are now characterized also by the total isospin T which is taken to be a good quantum

number (assuming charge independent interactions between nucleons apart
from the electrostatic repulsion between protons). The seniority scheme
can be defined as in the case of identical nucleons. The quantum numbers
which characterize states are now the seniority v and reduced isospin t.
A state in the j^n configuration with a given T, J, v and t is obtained from a
state in the j^v configuration (which has no pairs coupled to J=0) with the
same J and with T=t to which $(n-v)/2$ pairs with J=0 (and T=1) were added
and the resulting wave function property antisymmetrized.

The validity of the seniority scheme in the present case, apart from
the case of T=n/2 (which was considered above), is not at all assured. For
J=3/2 any two-body (charge-independent) interaction is diagonal in the
seniority scheme. For $j \geq 5/2$ this may not be so and whatever experimental
evidence we have indicates that the seniority is not a good quantum number.
In fact, it is even difficult to find nuclei where the j^n configuration gives a
good description of nuclear states. We shall nevertheless use the seniority
scheme in the following discussion. It may still be a good approximation
for ground-state energies and certainly exhibits the essential features of
the effective nuclear interaction.

We thus consider the states with lowest seniorities in j^n configurations
with protons and neutrons. For n even there is one such state for every
value of T = n/2, (n/2)- 2, ...; it has the quantum numbers J=0, v=0, t=0.
In even-even nuclei, such a state exists for the lowest value of the isospin
T and is the ground state. In odd-odd nuclei, such a state has a higher
value of T and is usually higher up. We shall discuss these nuclei later.
For odd n there is one state with lowest seniority for every value of allowed
isospin T with the quantum numbers J=j v=1 t=1/2. The interaction energies
of these states are linear combinations of only three parameters. These
are V_0 and $\overline{V}_2$ defined above, and the average interaction energy in the T=0
states of the j^2 configuration. This average interaction in the states with
J=1, 3, ..., 2j is defined by

$$\overline{V}_1 = \sum_{\substack{J \text{ odd}}}^{2j} (2J+1) V_J \bigg/ \sum_{\substack{J \text{ odd}}}^{2j} (2J+1) = \frac{1}{(j+1)(2j+1)} \sum_{\substack{J \text{ odd}}}^{2j} (2J+1) V_J \tag{15}$$

Any two-body interaction which reproduces the actual values of V_0, $\overline{V}_2$
and $\overline{V}_1$ can be used for the calculation of ground-state interaction energies.

In analogy with relation (8) we introduce the interaction

$$V'_{12} = x + y \, q_{12} + z2 \, (t_1 \cdot t_2) \tag{16}$$

which has in the j^n configuration the eigenvalues

$$\frac{n(n-1)}{2} x + y \left[\frac{n-v}{4} (4j+8-n-v) - T(T+1) + t(t+1) \right] + \left[T(T+1) - \frac{3}{2} n \right] z \tag{17}$$

We can now choose the free parameters x, y and z so that the averages of
the interaction (16) in the j^2 configuration will be V_0; $\overline{V}_2$ and $\overline{V}_1$. As seen
from expression (17), this interaction has large degeneracies, and the
averages coincide with the actual eigenvalues. Thus, we use the expression
(17) with n=2 and obtain

$$x + (2j+1) y + \frac{1}{2} z = V_0 \qquad\qquad x = (3\overline{V_2} + \overline{V_1})/4$$

$$x \qquad\qquad + \frac{1}{2} z = \overline{V_2} \qquad \text{or} \qquad y = (V_0 - \overline{V_2})/(2j+1) \qquad (18)$$

$$x \qquad\qquad - \frac{3}{2} z = \overline{V_1} \qquad\qquad z = (\overline{V_2} - \overline{V_1})/2$$

We can rewrite expression (17) as

$$\frac{n(n-1)}{2} (x - \frac{1}{2} y) + (z-y) \left[T(T+1) - \frac{3}{4} n \right] + y \frac{n-v}{4} (4j+4) +$$

$$+ y \left[t(t+1) - \frac{3}{4} v + \frac{v(v-1)}{4} \right] \qquad (19)$$

For $v=0$, $t=0$ or $v=1$ $t=1/2$, the last term in expression (19) vanishes and the expression simplifies to [19].

$$\langle j^n T, g.s. | \sum_{} V_{ik} | j^n T, g.s. \rangle = \langle j^n T, g.s. | \sum_{} V'_{ik} | j^n T, g.s. \rangle$$

$$= \frac{n(n-1)}{2} \alpha + \left[\frac{n}{2} \right] \beta + \left[T(T+1) - \frac{3}{4} n \right] \gamma \qquad (20)$$

The interaction parameters which appear in expression (20) are obtained from expressions (18) and (19) to be

$$\alpha = \frac{(6j+5) \overline{V_2} + (2j+1) \overline{V_1} - 2V_0}{4(2j+1)}$$

$$\beta = \frac{2(j+1)}{2j+1} (V_0 - \overline{V_2}) \qquad (21)$$

$$\gamma = \frac{(2j+3) \overline{V_2} - (2j+1) \overline{V_1} - 2V_0}{2(2j+1)}$$

Expression (20) for the interaction energy has a quadratic term, a pairing term and a term which depends on the isospin. The value of α turns out to be rather small in all cases considered. The pairing term is the same as in the case of identical nucleons, the value of β in formulas (21) is the same as in expression (12). The last term in expression (20) is the well known <u>symmetry energy</u>. In actual nuclei γ is big and repulsive and as a result, the higher the value of T, the smaller the binding energy. The sign of γ is determined by the fact that in the j^2 configuration, both the J=0 state and the average position of the T=0 levels with odd J are lower than the average position of the v=2 T=1 levels (with $J > 0$, even). This feature of the effective interaction is a result of the fact that in the interaction between free nucleons the T=0 forces are more attractive than the T=1 forces. For identical nucleons, $T = n/2$, the symmetry energy becomes $(\gamma/2) [n(n-1)/2]$ which is a repulsive quadratic term as discussed above. When there are both protons and neutrons present this repulsion between identical nucleons is more than compensated by the <u>attraction</u> between

protons and neutrons. For equal numbers of protons and neutrons and
T = 0, the symmetry-energy term yields the maximum attraction $-(3/4)n\gamma$.

The comparison of expression (20) with experiment is not as good as
in the case of identical nucleons, with the exception of the $1d_{3/2}$ shell
between ^{32}S and ^{40}Ca. However, simple relations that can be obtained from
expression (20) for binding energy differences are found to agree extremely
well with experiment [21]. We shall not present here a detailed discussion
of these but would like to point out an important exception. If odd-odd
nuclei with N=Z are included, the relations are significantly violated. For
other odd-odd nuclei, the relations hold very well. From expression (19)
we can only find out the average interaction energies of groups of states
with the same seniority quantum numbers. If N and Z are odd there is no
state with J = 0, v=0, t=0 for the lowest isospin value T=(N-Z)/2. For this
value of T there are states with v=2 t=1 and J > 0, even, and states with
v=2 t=0 and J odd. The positions of the centres-of-mass of these two groups
are determined by the last term in expression (19) i.e. by the amount of
pairing. As γ is attractive, the centre of mass of the v=2 t=1 levels lies
below the centre of mass of the v=2 t=0 states. In fact, ground states of
odd-odd nuclei with N > Z have even values of J.

If both N and Z are odd and N=Z, there are only states with odd values
of J (v=2 t=0) with T =(1/2)(N-Z) = 0. In many odd-odd nuclei with N=Z, the
ground states have T=0 and odd J. As is seen from the last term in ex-
pression (19), these states have, on the average, less pairing energy than
the t=1 states in N > Z odd-odd nuclei. Thus, ground states of N=Z odd-
odd nuclei have less interaction energy than ground states of other odd-odd
nuclei and cannot satisfy the Garvey-Kelson relations with them. This can
also be seen from the fact that in all N=Z odd-odd nuclei, the J=0 state is
rather low-lying even though it has a higher value of isospin T=1. In fact,
from ^{38}K on, the J=0 is actually the ground state of N=Z odd-odd nuclei.
This situation is not easy to understand from the Hartree-Fock point of view.
The interaction between a proton and a neutron would be expected to be
much stronger when they are in the same orbit.

The interaction between protons and neutrons in different orbits is also
strong and attractive. States with protons in the j orbit and neutrons in the
j' orbit have definite isospin if (and only if) the neutron j-orbit is completely
filled. In that case, the j-proton j'-neutron interaction is given by

$$\frac{1}{2} \left[\langle jj' \ T=0 \ J | V | jj' \ T=0 \ J \rangle + \langle jj' \ T=1 \ J | V | jj' \ T=1 \ J \rangle \right] \qquad (22)$$

The T=0 matrix element in expression (22) is attractive, and its absolute
value is larger than that of the T=1 matrix element. Thus, even if the latter
is repulsive the total matrix element (22) is attractive. As an example,
the matrix elements of the effective interaction between $1p_{1/2}$ protons and
$1d_{5/2}$ neutrons were determined to be [7]:

$1p_{1/2}$ proton - $1d_{5/2}$ neutron $\qquad$ J = 2 $\qquad$ 1.75 $\qquad$ J = 3 $\qquad$ 1.60 MeV.

These matrix elements are rather large and, according to the convention
used above, they are attractive. On the other hand, two identical nucleons
in these orbits repel each other on the average, the matrix elements being

$1p_{1/2}$-$1d_{5/2}$ $\ $ T = 1 $\qquad$ J = 2 $\qquad$ -0.49 $\qquad$ J = 3 $\qquad$ 0.07 MeV

We see that the forces that give rise to the attractive central potential of the shell model are the proton-neutron interactions. As we add to the nucleus nucleons of one kind, the potential well for the other kind of nucleons becomes deeper but also its form is changed. The spacings between single-nucleon orbits and even their order are changed as a result of changing the occupation numbers of nucleons. As an example, let us look at a case in which the addition of two protons changes the order of single-neutron levels which are in two different major shells [22]. In $^{13}_{6}C_7$ the neutron $1p_{1/2}$ orbit is the lowest, the $2s_{1/2}$ level lying 3.09 MeV above it. When going from $^{13}_{6}C_7$ to $^{11}_{4}Be_7$ two $1p_{3/2}$ protons (coupled to J=0) are removed. One would expect that the interaction of a $1p_{3/2}$ proton with a $1p_{1/2}$ neutron is stronger than its interaction with a $2s_{1/2}$ neutron (this feature appears in many cases). We can find out about these interactions by looking at $^{12}_{5}B_7$. A graphical solution which gives the order and spacing of the neutron $1p_{1/2}$ and $2s_{1/2}$ orbits in ^{11}Be is illustrated in Fig.6. We see here the ^{13}C spacing compared to the spacing between the centres of mass of the $p_{3/2}^{-1}$ $p_{1/2}$ levels (with 1^+ and 2^+) and the $p_{3/2}^{-1} s_{1/2}$ levels (with 1^- and 2^-) in $^{12}_{5}B_7$.
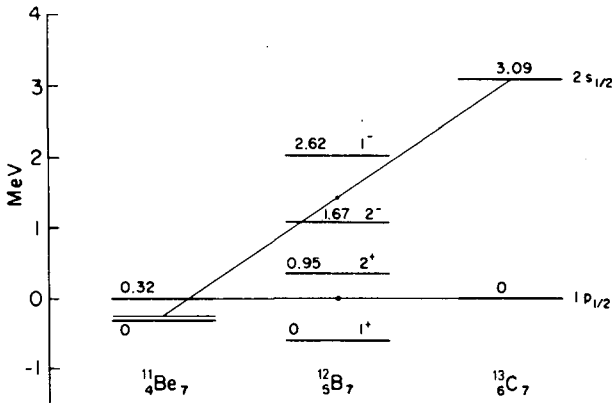
FIG.6.   Order of levels in ^{11}Be.

According to expression (14), the difference between the ^{11}Be and ^{13}C spacings should be twice the difference between the ^{12}B and ^{13}C spacings. The result is that the ground state of ^{11}Be should be $1^+/2$ in which the odd neutron is in the $2s_{1/2}$ orbit. The $1p_{1/2}$ should be 0.2 MeV above it. This prediction was confirmed by experiment, the $1^-/2$ level was found at 0.32 MeV above the $1^+/2$ ground state of ^{11}Be.

5.   COUPLING OF PROTONS AND NEUTRONS. SPIN GAPS.

In the last section we saw certain important properties of the average proton-neutron interaction. We shall look now at this interaction in more detail and reach certain conclusions about its effects. As mentioned above, within a j^n configuration this interaction is not diagonal in the seniority scheme. If we look at nuclei between ^{40}Ca and ^{56}Ni we can see whether $(1f_{7/2})^n$ configurations can account for the experimental data. The situation is not too clear at the moment. Certain spectra come out reasonably well but in some others there are very large deviations [23]. It is possible to check, for instance, whether the spectra of $^{42}_{21}Sc_{21}$ and $^{48}_{21}Sc_{27}$ can be related by

the Pandya relation. The agreement is satisfactory [24] and the resulting two-body matrix elements do not make seniority a good quantum number. This is clearly demonstrated by looking at the relative positions of the $v=2$ $t=1$ levels, with $J=2, 4, 6$, in both cases. In ^{42}Sc the $J=6$ level is about 1.7 MeV above the $J=2$ level (and 0.5 MeV above the $J=4$ level). If the effective interaction were diagonal in the seniority scheme the order and spacings of these levels should be the same in the particle-hole spectrum. Actually, the ground state of ^{48}Sc has $J=6$, the $J=4$ level is above it and the $J=2$ level is higher than both. We shall come back later to this shell.

Let us now consider the case with the j^n proton configuration and j'^n neutron configuration. The neutron j orbit is assumed completely filled so that the states would have a definite isospin $T=(1/2)(2j+1+m-n)$ in the absence of electrostatic interactions. It is possible to construct states of this system in the following way. We start with eigenstates of the j^n configuration with definite spin J_p and other quantum numbers α_p, if necessary. Similarly, we look at eigenstates with definite α_n, J_n in the j'^m configuration. We now construct a state with a definite total spin by coupling the states with given J_p and J_n. The states constructed in this way

$$\left| j^n(\alpha_p \, J_p) \, j'^m(\alpha_n \, J_n) \, JM \right\rangle \tag{23}$$

form a complete set of wave functions for this system. In this scheme the interaction energy within the j^n configuration is diagonal, and the same is true for the j'^m comfiguration. However, apart from the cases $j=1/2$ or $j'=1/2$, (see Ref. [9]), the j proton - j' neutron interaction energy is non-diagonal in the scheme (23). It has, in general, non-vanishing matrix elements connecting states with the same J but with different values of J_p and J_n.

Thus, it is impossible to characterize eigenstates of such configurations by the total proton spin and total neutron spin. The spins J_p and J_n are not, in general, good quantum numbers. The question whether the wave functions (23) may or may not be good approximations can be answered only by looking at the magnitude of the non-diagonal elements compared to the separation between the unperturbed levels which they connect. In some cases, where all two-body matrix elements are known, like the $(1d_{3/2})^n$ protons - $(1f_{7/2})^m$ neutron configurations, there is a quantitative answer. The admixtures of states with different J_p and J_n (within the same shell-model configuration) is present also for both m and n even. Such admixtures are larger for odd-even nuclei since there are low-lying states (with $v=3$) in the odd configuration.

The approximation of definite J_p and J_n is much worse in actual odd-odd nuclei. The non-diagonal matrix elements of the interaction play a very important role because of the proximity of several unperturbed states. This is the reason why it is difficult to give any rules for spins of odd-odd nuclei based on the approximation (23). In $^{42}_{19}K_{23}$ all states of the ground configuration have $J_p=3/2$. The state (23) with the lowest diagonal element has $J_n=7/2$ and $J=3$ (unlike ^{40}K where the ground state has $J=4$). However, the state with $J_n=5/2$ is only 0.37 MeV above the $J_n=7/2$ state in the $f^3_{7/2}$ configuration. After the diagonalization of the energy matrices (in which there are no adjustable parameters) it turns out that the lowest state has $J=2$ as experimentally observed. It has about <u>equal</u> admixtures of the states with $J_n=7/2$ and the state with $J_n=5/2$.

It should be pointed out that, in particular, the centre-of-mass theorem [25] holds only for the diagonal matrix elements in the scheme (23). This theorem implies, for n even,

$$\sum_{J=|J_p-J_n|}^{J_p+J_n} (2J+1) \left\langle j^n (J_p) j'^m (J_n) J \left| \sum V \right| j^n (J_p) j'^m (J_n) J \right\rangle \Big/ \sum (2J+1)$$

$$-\left\langle j^n (J_p=0) j'^m (J_n) J=J_n \left| \sum V \right| j^n(0) j'^m (J_n) J=J_n \right\rangle = \qquad (24)$$

$$= \left\langle j^n J_p \left| \sum V \right| j^n J_p \right\rangle - \left\langle j^n J_p = 0 \left| \sum V \right| j^n J_p = 0 \right\rangle .$$

If non-diagonal matrix elements of the proton-neutron interaction are indeed negligible, Eq.(24) is a statement relating the positions of centres of mass of the multiplets with definite J_n and various values of J_p to be spacings of states with the corresponding J_p in the j^n configuration. In actual nuclei, unless $j' = 1/2$ (and $m = 1$), we expect admixtures of multiplets and large deviations from the centre-of-mass theorem.

In heavier nuclei, the separation between higher values of J_p in the j^2 configuration (and higher even configurations) become rather small. The relative energies of states with such values of J_p are, therefore, largely determined by the proton-neutron interaction. The properties of the latter interaction give rise to the occurrence of high-spin isometric states. Let us consider the isomerism in ^{93}Mo where there is one $2d_{5/2}$ neutron outside closed shells and, for simplicity, we take the proton configuration to be $(1g_{9/2})^2$. The J=4 level in ^{92}Mo is 0.79 MeV above the J=2 level, the J=6 - J=4 spacing is only 0.33 MeV whereas the J=8 - J=6 separation is even smaller, 0.14 MeV. The $1g_{9/2}$ proton - $2d_{5/2}$ neutron interaction can be determined from the $^{92}_{41}$Nb$_{51}$ levels [26]. The ground state of ^{92}Nb has J=7 and otherother levels are at 0.135 MeV (J=2), 0.286 MeV (J=5), 0.357 MeV (J=3), 0.479 MeV (J=4) and at 0.500 MeV (J=6). Assuming, for simplicity, that these are due to the $g_{9/2} d_{5/2}$ configuration, we can write down the energy matrices of ^{93}Mo in the scheme (23) and diagonalize them. The results are in very good agreement with the experimental levels [27]. In particular, the J = 21/2 level is isomeric since there is a "spin gap" between it and the lower level with J = 13/2. The J = 15/2, J = 17/2 and J = 19/2 levels are all above the J = 21/2 level.

The occurrence of this spin gap can be traced to a simple property of the proton-neutron interaction. That interaction is very strong in the state with <u>maximum</u> spin of the two nucleons: J' = 7. In fact, in this case, it is the strongest interaction and much stronger than in the state with one less unit of spin J' = 6. The maximum amount of proton-neutron couplings with J' = 7 occurs in the state of ^{93}Mo where all spins are aligned as much as possible, i.e. $J_p = 8$, J = 21/2. The states with lower spin J, based either on $J_p = 8$ or $J_p = 6$, have less couplings J' = 7 (and have J' = 6 couplings instead). Thus, the J = 19/2 state (with $J_p = 8$) is higher than the J = 21/2 state, but even the states with J = 17/2 and J = 15/2, with $J_p = 6$ components, are higher. These states remain higher even if the non-diagonal elements are taken into account. The small J = 8 - J = 6 spacing does not balance the deficiency of these states in J' = 7 couplings (the other strong coupling, for J' = 2, does not occur for J ≳ 15/2). The J = 13/2

state, with its component having $J_p = 4$, is lower than the $J = 21/2$ level due to the 0.5 MeV separation between the $J_p = 8$ and $J_p = 4$ levels of ^{92}Mo.

A similar case of isomerism is found in $^{211}_{84}$Po$_{127}$ with the $(1h_{9/2})^2 \, 2g_{9/2}$ configuration [28]. The ^{210}Po spectrum shows the $(h_{9/2})^2$ levels to be $J = 0$ (g.s.) $J = 2$ (1.180 MeV), $J = 4$ (1.425 MeV), $J = 6$ (1.471 MeV) and $J = 8$ ($\sim$ 1.510 MeV). The $1h_{9/2}$ proton - $2g_{9/2}$ neutron interaction can be determined from the $^{210}_{83}$Bi$_{127}$ levels. These are in MeV: $J = 1$ (g.s.) $J = 0$ (0.047) $j = 9$ (0.268) $J = 2$ (0.820) $J = 3$ (0.347) $J = 5$ (0.433) $J = 7$ (0.433) $J = 4$ (0.501) $J = 6$ (0.547), and $J = 8$ (0.581). The situation is similar to that in ^{93}Mo. The strong proton-neutron interaction in the $J' = 9$ state (as compared to the $J' = 8$, $J' = 7$ and $J' = 6$ couplings) causes a spin gap between the state with maximum spin $J = 25/2$ (with $J_p = 8$) and other states. As found experimentally, the $J = 25/2$ state is isomeric since the $J = 23/2$, $J = 21/2$ and $J = 19/2$ levels are calculated to be above it. The $J = 17/2$ and $J = 15/2$ levels are somewhat lower but still very close to the $J = 25/2$ level. The very close spacings of the higher spin levels in j^2 configuration makes the proton-neutron interaction the dominant factor which determines the energies of states. This leads to isomeric states also in even-even nuclei like ^{212}Po. There is a spin gap in the $(1h_{9/2})^2 \, (2g_{9/2})^2$ configuration between the level with maximum spin $J = 16$ ($J_p = 8$ and $J_n = 8$) and other levels [28]. The $J = 15$, $J = 14$, $J = 13$ and $J = 11$ levels are calculated to lie above it while the $J = 12$ level although lower, is very close to it. This gives rise to the observed isomerism of the $J = 16$ level.

Let us make use of the $(h_{9/2})^2 \, (g_{9/2})^2$ configuration in ^{212}Po to illustrate an important feature. The higher the excitation energy, the more ways there are of distributing it between the nucleons. This effect is clearly seen even in the calculated spectrum of this simple configuration. Between the ground state and 0.8 MeV excitation there are only 2 levels. Between 0.8 MeV and 1.6 MeV there are nine. There are 20 levels between 1.6 MeV and 2.4 MeV and more than a hundred between 2.4 and 3.2 MeV. It is practically impossible to prepare a drawing with all these levels. In Fig.7 the same effect is seen in the calculated spectrum of ^{92}Zr. The large number of levels arise from rather simple shell-model configurations involving $1g_{9/2}$ protons and $2d_{5/2}$ neutrons [29].

The strong interaction between a proton and a neutron in the state with maximum spin is seen also when they are in the same orbit. In the $1f_{7/2}$ shell, as seen in ^{42}Sc, the state with $J' = 7$ is low-lying and is much slower than the $J' = 6$ level. As a result, a spin gap is obtained in the $(1f_{7/2})^3$ configuration with $T = 1/2$. In the $^{53}_{26}$Fe$_{27}$ spectrum, which agrees well with the Bayman, McCullen and Zamick calculations, the level with maximum spin allowed by the Pauli principle has $J = 19/2$ (at 3.04 MeV). In it there is maximum coupling to $J' = 7$ and it is indeed lower than the $J = 17/2$, $J = 15/2$ and $J = 13/2$ levels. It decays with a 2.5 min life-time [30] to the $J = 11/2$ level (at 2.34 MeV) which cascades through the $J = 9/2$ level (1.33 MeV) to the $J = 7/2$ ground state.

6.   CONFIGURATION MIXING; HIDDEN AND EXPLICIT

As mentioned before, configuration interaction lies at the foundation of the effective-interaction approach. If the interaction between free nucleons has a hard core, arbitrarily high shell-model configurations must

TALMI
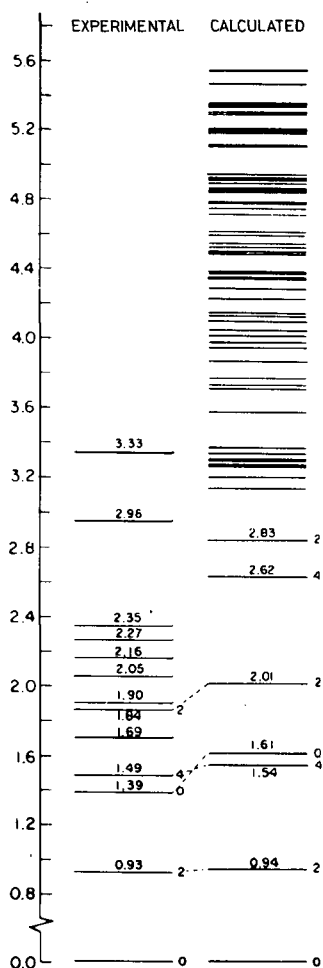
FIG.7. Levels arising from simple shell-model configurations (^{92}Zr).

be present in the real wave function of the nucleus. We assume, however, that the effect of such configuration mixing on the energies can be fully replaced by a modification or renormalization of the two-body interaction. If this assumption is valid, we can calculate nuclear energies by using simple shell-model wave functions and an effective two-body interaction between nucleons. We have seen several examples in which energies could actually be calculated consistently in this way. There are other cases, however, in which even the energy cannot be calculated in this way. In such cases, we have to enlarge the space of wave functions and include several configurations in the calculation.

The main difficulty in extending the approach described above is the large number of matrix elements which appear in the calculation. When several configurations are considered we have, in addition to the diagonal elements within each configuration also a large number of non-diagonal matrix elements. To determine these matrix elements, many more experimental data should be made available for the analysis. In several cases

it was found possible to determine diagonal and non-diagonal matrix elements from the experimental data and obtain good agreement between calculated and experimental energies. Some of these cases will now be described.

A rather simple case is offered by the proton configurations in the Zr region where the 50 neutrons occupy closed shells [13, 29, 31]. In ^{89}Y the $\frac{1}{2}^-$ ground state is taken to be due to a $2p_{1/2}$ proton. The $1g_{9/2}$ single-proton state is about 0.9 MeV above it. In ^{90}Zr the first excited state is a 0^+ level, 1.75 MeV above the 0^+ ground state. The other positive parity levels have $J = 2$ (2.18 MeV), $J = 4$ (3.08 MeV), $J = 6$ (3.45 MeV) and $J = 8$ (3.60 MeV). These latter levels are taken to be due to the $1g_{9/2}^2$ configuration. This configuration must be admixed with $2p_{1/2}^2$ to give the two 0^+ states [32]. The small 0-2 separation (0.43 MeV) is a clear indication which is supported by the detailed analysis of the energies of other nuclei with 50 neutrons. This case is simple since there is only one non-ciagonal element connecting the $J = 0$ states of the $g_{9/2}^2$ and the $p_{1/2}^2$ configurations.

A nice demonstration of the validity of this description is furnished by the ^{92}Mo spectrum. The lowest states must belong to the $p_{1/2}^2 g_{9/2}^2$ configuration which are, however, admixed to corresponding states of the higher $g_{9/2}^4$ configuration. The seniority is found to be a good quantum number for the $g_{9/2}^n$ configurations by inserting the $J = 2, 4, 6, 8$ spacings from ^{90}Zr into expression (6). Therefore, only the $v = 0$ ($J = 0$) and $v = 2$ ($J = 2, 4, 6, 8$) states of the $g_{9/2}^4$ configuration (but not the $v = 4$ states) can be admixed to the corresponding states of the $p_{1/2}^2 g_{9/2}^2$ configuration. Moreover, the non-diagonal elements between $v = 2$ states are independent of J. As a result, the spacings of the $J = 2, 4, 6, 8$ levels in ^{92}Mo are expected to be equal to those of ^{90}Zr [13]. Experimentally, the 2^+ level in ^{92}Mo is 1.54 MeV above the 0^+ ground state and the other levels are at 2.33 MeV (4^+), 2.66 MeV (6^+) and 2.80 MeV (8^+). The spacings do indeed agree which strongly supports the configuration assignments. Large configuration admixtures were obtained in this analysis (60% $p_{1/2}^2$ configuration and 40% $g_{9/2}^2$ configuration in the ^{90}Zr ground state). Still, the resulting behaviour of the energies beyond ^{90}Zr is so regular that it would be difficult to find evidence for configuration mixing in these energies. This effect is discussed in great detail by Professor Soper in these Proceedings. He considers "pseudonium" nuclei [4]. Here only the Zr region example will be presented. It was mentioned in Ref. [3] that "it is worth-while to notice that the lower $J = 9/2$ states in Fig. 3 [of that paper] after being shifted by configuration interaction, still lie fairly well on a straight line (with the exception of ^{77}Sr). Assuming that this really reproduces the experimental spacings, this feature could lead to the simple, yet wrong conclusion that these $J = 9/2$ states belong to pure configurations, say $p_{1/2}^2 g_{9/2}^{n-2}$. In other words, taking the $9/2^+$ states to belong to effective $p_{1/2}^2 g_{9/2}^{n-2}$ configurations, their energies could be well reproduced by effective two-body forces which have the same matrix elements in the nuclei considered. This is true in spite of the fact that the perturbing configurations, i.e. the $g_{9/2}^n$ configurations, are rather low-lying. This example demonstrates clearly that shell-model wave functions may well include considerable admixtures of other configurations". It was not realized at that time that this effect may show up for excited states as well.

Let us now see whether nuclei from ^{91}Nb on could be treated as having pure $p_{1/2}^2 g_{9/2}^{n-2}$ configurations in spite of the $g_{9/2}^n$ admixtures (30% in ^{91}Nb and less in the others) that they actually have 33). Let us first consider

binding energies calculated with configuration mixing and try to fit them
with the formula (13) of a pure j^n configuration (the $p_{1/2}^2$ protons form a
closed shell and can be ingored). The agreement between the exactly calcu-
lated binding energies and the results of using formula (13) is very good.
The coefficients of the result (13) obtained in this way include the effects
of the configuration mixings and are indeed different from the correspond-
ing values of the unperturbed $g_{9/2}^n$ configurations obtained by the detailed
analysis:

	C	α	β	
Unperturbed	5.430	-0.622	2.396	MeV
Effective	5.250	-0.632	2.710	MeV

From the change in the value of β we can compute the change in $V_0 - \overline{V_2}$
which gives directly the effective 0-2 separation to be 1.482 MeV (the
unperturbed value is 1.20 MeV). This prediction, based on the assumption
of a pure configuration, should be compared with the values calculated
exactly taking into account configuration mixing. These values are:

$n' = n-2$	2	4	6	8	predicted from pure configurations
0-2 separation in MeV	1.557	1.478	1.438	1.413	1.482

Again the agreement is rather good, the deviations are less than 0.08 MeV.
As mentioned before, the J = 2, 4, 6, 8 spacings are not changed by the con-
figuration mixing. For odd nuclei we can compute from the effective value
of β the spacing between the v = 1 J = 9/2 ground state and any v = 3 state.
We obtain the following results comparing detailed to effective calculations

$n' = n-2$	3	5	7	predicted from pure configurations
9/2-7/2 separa- tion in MeV	0.683	0.623	0.499	0.648

Also here the agreement, although worse, is still reasonably good.
    It can be shown that if the effect of configuration mixing in this example
can be treated in second-order perturbation theory it is equivalent to a
modification of the two-body interaction. Here, however, we have rather
large admixtures (up to 30% in the present case and even much larger mix-
tures in other fictitious cases [4]) and still this feature is rather well ob-
tained. This is remarkable indeed and may be an indication why the simple
minded shell model works so well. This phenomenon is mainly due to the
fact that the perturbing configuration is obtained by exciting two nucleons
from the ground configuration. In infinite nuclear matter this is the only
possible kind of admixtures because of momentum conservation. In finite
nuclei, however, angular momentum can be conserved even if only one
nucleon is excited to another orbit. The effect of mixing of configurations
differing by the orbit of one nucleon is not equivalent to a two-body inter-
action. In some cases, it may lead to a modification of the single-nucleon
orbitals and nuclear deformations [20]. Here we shall mention cases where
such configuration mixing was considered in detail.

It was mentioned above that in the $1f_{7/2}$ shell of identical nucleons there are definite deviations from the pure $1f_{7/2}^n$ description. The next orbit which should be considered is the $2p_{3/2}$ orbit which in ^{41}Ca is only 2 MeV above the ground state. A detailed analysis using both $1f_{7/2}$ and $2p_{3/2}$ orbits was carried out giving much better agreement with the data [34]. In particular, the positions of the $3/2^-$ states in ^{43}Ca and ^{45}Ca came out close to the experimental values (0.6 and 1.4 MeV, respectively). In pure $1f_{7/2}^n$ configurations the position of these levels above the $5/2^-$ ground states should be the same. Thus, the configuration mixing in this case <u>cannot</u> be well replaced by a modification of the two-body interaction in pure $1f_{7/2}^n$ configurations. The whole purpose of the analysis was to explain the <u>deviations</u> from the simple picture.

Another case in which the description in terms of pure jj-coupling configurations is not good enough in the 1p shell [35]. In the beginning of the shell, the description in terms of $1p_{3/2}^n$ configurations (of protons and neutrons) is rather poor. Towards the end of the shell, beyond ^{12}C, the description in terms of $1p_{1/2}^n$ configuration is better [7]. Taking into account both the $1p_{3/2}$ and $1p_{1/2}$ orbits (intermediate coupling) gives much better agreement with the experimental data. In particular, the matrix elements of the effective interaction determined in this way are equivalent to those obtained from central and non-central forces. The contribution of tensor forces is essential to the explanation of the large ft-value of the ^{14}C beta decay [36]. It is nice that the matrix elements of the effective interaction determined from the energies cause the necessary cancellation in the beta-decay matrix elements.

The last example is furnished by the spectra of the nickel isotopes. The energy levels look as if they were due to a "vibrational" spectrum. Although there is strong evidence against such an interpretation, the regularities observed are rather striking. The position of the first excited 2^+ level is about the same in all isotopes from ^{58}Ni to ^{64}Ni. The positions of other levels, with J = 2, J = 4 and J = 0 are at about twice the 0-2 separation. The position of the 2^+ state in itself clearly indicates that no single configuration could account for it, since the available neutron orbits are $2p_{3/2}$, $1f_{5/2}$ and $2p_{1/2}$. A detailed analysis of all levels including configuration interaction revealed large admixtures of the various configurations [37].

It turns out that the matrix elements of the effective interaction determined from the nickel isotopes are very similar to those obtained in other, simpler, cases. The matrix elements within each configuration (e.g. $2f_{5/2}^n$) are very similar to those obtained for a pure configuration (e.g. attractive pairing term and repulsive quadratic term). There is also an average repulsion between neutrons in different orbits.

The non-diagonal matrix elements between nucleon pairs in different orbits turn out to be large and attractive (in the zirconium region only the size but not the sign of the non-diagonal element could be determined). They are considerably larger than most other non-diagonal matrix elements and give rise to a scheme in which generalized seniority is a good quantum number. This means that the main admixtures to any given state are those states in which neutron pairs with J = 0 go into other orbits.

The large and attractive matrix elements between J = 0 pairs are similar to those suggested by the pairing theory. Although there are definite quantitative differences, these are not very important. If, however, one tries to use the pairing theory to account for the J = 0 levels, the agreement

obtained is very poor. The reason is that the average repulsion between identical nucleons in different orbits plays a very important role in the energy matrices. This repulsion is completely mission from the pairing interaction, and it is not surprising that no quantitative results could be obtained without it.

The detailed calculations involving the $1f_{5/2}$, $2p_{3/2}$ and $2p_{1/2}$ neutron orbits give a good description of the spectra of the nickel isotopes. It is not clear whether all transition probabilities can be explained, even when using effective single-nucleon operators. This is not very different from the simpler cases mentioned above. In spite of the good agreement, it is not clear how the simple features of the spectra arise. The "vibrational" structure of the spectrum appears in several other cases where there are only (or mostly)identical nucleons outside closed shells (like the tin isotopes). What is missing is a simple approximation which will exhibit the simple features of the energy levels. This is necessary also from a practical point of view. In the tin isotopes there are many single-nucleon orbits, and a detailed calculation would be extremely difficult. But more interesting is the theoretical problem of obtaining a physical insight into the structure of such nuclei. It is not easy to have a physical picture of the outcome of diagonalizing huge matrices. It would be very nice to have a simple approximation to explain the rather simple results obtained from the detailed and complicated calculations.

REFERENCES

[1] The evidence for magic numbers and the shell model is given by MAYER, M.G., JENSEN, J.H.D., Elementary Theory of Nuclear Shell Structure, John Wiley and Sons, New York (1955).
[2] The formulae given here are to be found in: DE-SHALIT, A., TALMI, I., Nuclear Shell Theory Academic Press, New York (1963).
[3] KUO, T.T.S., BROWN, G.E., Nucl. Phys. 85 (1966) 40.
[4] COHEN, S., LAWSON, R.D., SOPER, J.M., Phys. Letts 21 (1966) 306; LAWSON, R.D., SOPER, J.M., in Proc. Int. Nuclear Physics Conf. (Gatlinburg, 1966) Academic Press, New York (1967) 511, as well as the contribution by Professor Soper in these Proceedings).
[5] GOLDSTEIN, S., TALMI, I., Phys. Rev. 102 (1956) 589.
[6] PANDYA, S.P., Phys. Rev. 103 (1956) 956.
[7] TALMI, I., UNNA, I., A.Rev. nucl. Sci. 10 (1960) 353.
[8] BROWN, G.E., in Proc. of the Congr. Intern. de Physique Nucléaire, 1, Paris (1964) 129; ENGELAND, T., Nucl. Phys. 72 (1965) 68; FEDERMAN, P., TALMI, I., Phys. Letts 15 (1965) 165.
[9] TALMI, I., Phys. Rev. 126 (1962) 2116.
[10] ARAD, B., BOULTER, J., PRESTWICH, W.V., FRITZE, K., to be published.
[11] PRESTWICH, W.V., ARAD, B., BOULTER, J., FRITZE, K., Can. J. Phys. 46 (1968), 2321; Da R. ANDRADE, P., MACIEL, A., ROGERS, J.D., WIRTH, J., ZAWISLAK, F.C., Nucl. Phys. 77 (1966) 298.
[12] LAWSON, R.D., URETSKY, J.L., Phys. Rev. 106 (1957), 1369; TALMI, I., Ref. [18] and in Proc. 1957 Rehovoth Conf. Nuclear Structure North Holland, Amsterdam (1958) 31; SCHWAGER, J.E., Phys. Rev. 121 (1961) 569.
[13] TALMI,I., UNNA, I., Nucl. Phys. 19 (1960) 225.
[14] TALMI, I., Phys. Rev. 126 (1962) 1096.
[15] TALMI, I., Phys. Letts 25B (1967) 313.
[16] CHILDS, W.J., Phys. Rev. 156 (1967) 71.
[17] FRENCH, J.B., Nucl. Phys. 15 (1960) 393.
[18] TALMI, I., Phys.Rev. 107 (1957) 326.
[19] TALMI, I., THIEBERGER, R., Phys. Rev. 103 (1956) 718.
[20] TALMI, I., Rev. mod. Phys. 34 (1962) 704.

[21] GARVEY, G.T., KELSON, I., Phys. Rev. Letts 16 (1966) 197; GARVEY, G.T., GERACE, W.J., JAFFE, R.L., TALMI, I., KELSON, I., Rev. Mod. Phys. (In press).

[22] TALMI, I., UNNA, I., Phys. Rev. Letts 4 (1960) 469.

[23] McCULLEN, J.L., BAYMAN, B.F., ZAMICK, L., Phys. Rev. 134B (1964) 515.

[24] SCHWARZ, J.J., Phys. Rev. Letts 18 (1967) 174.

[25] LAWSON, R.D., URETSKY, J.L., Phys. Rev. 108 (1957) 1300.

[26] SHELINE, R.K., WATSON, C., HAMBURGER, W.E., Phys. Letts 8 (1964) 121; SWEET, R.F., BHATT, K.H., BALL, J B., Phys. Letts 8 (1964) 131.

[27] AUERBACH, N., TALMI, I., Phys. Letts 9 (1964) 153.

[28] AUERBACH, N., TALMI, I., Phys. Letts 10 (1964) 297.

[29] AUERBACH, N., TALMI, I., Nucl. Phys. 64 (1965) 458.

[30] ESKOLA, K., Phys. Letts 23 (1966) 471.

[31] COHEN, S., LAWSON, R.D., MACFARLANE, M.H., SOGA, M., Phys. Letts 10 (1964) 195.

[32] FORD, K.W., Phys. Rev. 98 (1955) 1516; BAYMAN, B.F., REINER, A.S., SHELINE, R.K., Phys. Rev. 115 (1959) 1627.

[33] This example as well as the following related discussion of the Ca isotopes were presented by the author in a lecture at the Gordon Research Conference on Nuclear Structure, 29 July - 2 August, 1968.

[34] ENGELAND, T., OSNES, E., Phys. Letts 15 (1965) 924; FEDERMAN, P., TALMI, I., Phys. Letts 22 (1966) 469.

[35] AMIT, D., KATZ, A., Nucl. Phys. 58 (1964) 388; COHEN, S., KURATH, D., Nucl. Phys. 73 (1965) 1.

[36] JANCOVICI, B., TALMI, I., Phys. Rev. 95 (1954) 289.

[37] AUERBACH, N., Nucl. Phys. 76 (1966) 321 and Phys. Letts 21 (1966) 57; COHEN, S., LAWSON, R.D., MACFARLANE, M.H., PANDYA, S.P., SOGA, M., Phys. Rev. 160 (1967) 903.

PSEUDONUCLEI AND THE SHELL MODEL

J. M. SOPER
Theoretical Physics Division
AERE Harwell,
Great Britain

Abstract

PSEUDONUCLEI AND THE SHELL MODEL. 1. Introduction; 2. The pseudonium isotopes; 3. A proton-neutron system; 4. Summary.

1. INTRODUCTION

Models have always been, and will always be, an essential part of nuclear physics. We may hope that with the foreseeable increase of computer power we might (if we wished) solve, more or less exactly, the problems of two, three, four, or even five bodies. But an N-body wave-function, a function of (3N-6) variables (at least), will always remain beyond our reach for values of N greater than five. At the other end of the scale we can probably achieve any desired degree of accuracy in calculating the properties of infinite nuclear matter. Even in the heaviest real nuclei, however, about half of the nucleons lie in the nuclear surface, so that we are very far from this ideal situation. Nuclei are therefore essentially "many-body", but also essentially finite; we can never know an "exact" nuclear wave-function, and cannot escape the use of models.

Since we do not have exact solutions to compare with, model wave-functions must be justified indirectly. We can try to justify our models theoretically, by starting from the equations that govern the many-body system and proceeding through a series of approximations, each of which has to be separately justified, to the model solution. This task has occupied much of the attention of nuclear theorists for many years now, but while the course of such a chain of reasoning has been outlined, and some of the links forged, the whole is neither complete nor quantitative.

We can also appeal to experiment. It is, of course, an essential property for a good model to agree with a wide range of experimental results. Many of our current nuclear models are very successful in this respect, and it is tempting to claim that this agreement constitutes not only a necessary test of the model but also a justification of it. It creates a presumption that the model wave-functions are in some sense close to the true ones. In a real nucleus, in the absence of the sort of theoretical chain referred to above, this presumption is impossible to prove and difficult to rebut. One tends to be led by the weight of the evidence (which for a successful model will be overwhelmingly favourable) and to dismiss as aberrant the handful of experimental results that disagree with the theory. Can we do this? Or can a theory that is both physically reasonable and also in excellent agreement with the vast majority of experimental data turn out to be based on wave-functions that are very far from

the true ones? I shall describe here some experiments on this theme
that were made by S. Cohen, R.D. Lawson and the author [7].

The model that we choose to examine is the j-j coupling shell model.
As Talmi [2] emphasizes elsewhere in this volume, this model in its
simplest form is remarkably successful in fitting a very large range of
nuclear properties in many parts of the periodic table. This success
might lead us to suppose that in these regions the simple wave-functions
of the model are necessarily "true" in some sense. Apart from pointing
to the occasional discrepancies with experiment, we can make little
useful comment on this hypothesis if it is applied to a real nucleus or
range of nuclei, because we cannot know the "true" wave-functions. How-
ever, we can, in a sense, "build our own" nuclei and investigate their
properties using a simple model. In shell-model terms, we can construct
wave-functions which contain configuration admixtures. This must be
done in a physically reasonable manner, for example by diagonalizing
the matrix of some Hamiltonian operator within some set of configurations
lying close together in energy. We say that these wave-functions represent
"pseudo-nuclei". We can then calculate the matrix elements of operators
representing physically observable quantities between these wave-functions.
These quantities correspond to experimental data in real nuclei − we call
them "results of pseudo-experiments". Then, taking account only of these
pseudo-data (and not of our knowledge of the true wave-function) we try
to find the simplest model assumptions that will give a reasonable fit to
the properties of the system. On the one hand, we can compare the quality
of the overall fit to that obtained in real situations. On the other hand,
we can compare simple wave-functions that give a good fit (assuming that
we find some) with the true wave-functions that we are privileged to know.
We may then be in a position to comment on the degree of confidence that
we can reasonably place in the "truth" of simple model wave-functions
that give a very good fit to a large body of data.

2. THE PSEUDONIUM ISOTOPES

These are very simple pseudo-nuclei in which only neutrons play an
active role. They consist of a completely inert core with only two valence
shells outside it − a $1d_{3/2}$ and a $1f_{7/2}$. No other shells play any active
part. We fill these two levels with neutrons, adding them one by one. The
neutrons are bound by the central potential well due to the core (which
we take to be a harmonic-oscillator potential) and are allowed to inter-
act among themselves through a two-body potential, which we take to
have a simple central Yukawa form with a range parameter

$$a = 0.94 \, b$$

where b is the usual harmonic-oscillator size parameter, and with spin-
singlet and spin-triplet strengths

$$V_0 = 30 \text{ MeV} \quad ; \quad V_1 = -10 \text{ MeV}$$

If we take our 1d shell to lie far below our 1f shell we shall get the usual
shell-closing effect; each of our first four neutrons will go into the 1d

level which will then be full. The next eight neutrons will then form a
fairly pure $1f_{7/2}$ shell. As long as the shell gap is large compared with
typical off-diagonal elements of the residual interaction this purity will
persist. If we reduce the shell gap until it is comparable with the re-
sidual interaction we shall get substantial configuration mixing, of
course. If we reduce it to zero the mixing will, indeed, become very
large. It is this last system that we shall study, and we shall look, in
particular, at the last eight particles to go into the pair of levels (which
we have made degenerate in energy). We shall call the systems with
four to twelve neutrons the pseudonium isotopes ^{40}Ps to ^{48}Ps. There is
an analogy here, of course, with the calcium isotopes, but in re-naming
the systems we wish to emphasize the fact that our calculations are com-
pletely self-contained, and that we are not concerned with reproducing
in detail the properties of any real nuclear system.

The pseudo-nuclear wave functions were calculated, and the pseudo-
experimental results deduced from them using the Argonne system of
shell-model programs [3]. It rapidly becomes clear when we inspect
this mass of pseudo-data that the main features of the spectra and other
properties of these systems are just those which we would expect if we
were filling a pure $1f_{7/2}$ shell with neutrons. If we look at the wave-
functions, of course, we can see that this is, indeed, very far from the
truth. The wave-function of ^{40}Ps contains only 9% of pure-closed-shell
wave-function. The other 91% consist of various excitations out of the
$1d_{3/2}$ "core" into the 1f shell. To describe this nucleus as a closed shell
would therefore seem pitifully inadequate to anyone with a knowledge of
the "true" wave-function. We emphasize again, however, that in real
life (which is the situation we are simulating) we have no such privileged
knowledge. A similar situation occurs in ^{41}Ps where 17% of the wave
function is one-particle-outside-closed-shell in character. We are going
to assume this to be 100% in our simple pure $1f_{7/2}$ model. As we go
through the shell the overlaps improve until we reach 100% at the end of
the shell, where the d-shell is forced to be closed because all available
states are full. Overlaps for the ground states are given in the last
column of Table I.

The simple pure $1f_{7/2}$-shell model predicts 31 states of various
J-values as we go through the shell; we reckon all energies relative to
the ground state of ^{40}Ps. Our pseudo-nuclei have, of course, many more
levels than this, but extra levels of "correct" parity do not intrude until
we are quite high in energy and the low-lying spectrum looks like that
of $f_{7/2}^n$. As in real life, therefore, we fit the lowest levels and ignore
the higher-lying ones. We have five parameters with which to fit our 31
data. For once the matrix-element parametrization is an economical
one and we use the parameters

$$E_J = \langle f_{\frac{7}{2}}^2 \ J \mid V \mid \ f_{\frac{7}{2}}^2 J \rangle$$

for J = 0, 2, 4, 6 together with ϵ, the bindings of a single nucleon to the
^{40}Ps core, to characterize completely the most general two-body inter-
action within the $f_{7/2}$ shell.

The quality of the fit obtained can be expressed in various ways.
The root-mean-square deviation of the theoretical energies from the
pseudo-experimental ones is 16.1 keV, which compares well with most
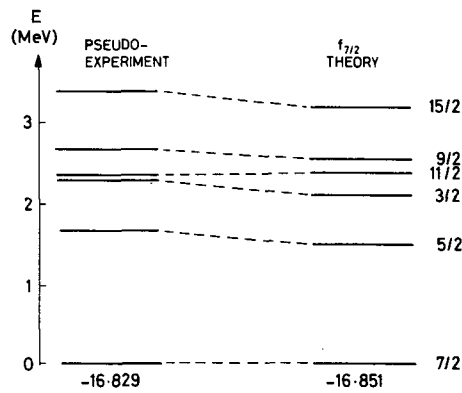
FIG.1.   The spectrum of pseudonium 43.

TABLE I. OVERLAP FOR GROUND STATES

	Pseudo-experiment (MeV)	$f_{7/2}$ theory (MeV)	Percentage of $d^4 f^n$ in wave-function
^{41}Ps	- 3.47	- 3.57	17.3
^{42}Ps	-11.66	-11.66	34.1
^{43}Ps	-16.83	-16.85	55.0
^{44}Ps	-26.56 ·	-26.57	65.8
^{45}Ps	-33.46	-33.38	85.4
^{46}Ps	-44.62	-44.71	88.0
^{47}Ps	-53.13	-53.15	100.0
^{48}Ps	-65.66	-66.11	100.0

TABLE II. MAGNETIC DIPOLE AND ELECTRIC QUADRUPOLE MOMENTS OF GROUND STATES

	Magnetic moment		Quadrupole moment	
	Pseudo-experiment	$f_{7/2}$ theory	Pseudo-experiment	$f_{7/2}$ theory
^{41}Ps	-1.895	-1.913	-1.32	-3
^{43}Ps	-1.909	-1.913	-0.11	-1
^{45}Ps	-1.913	-1.913	+1.29	+1
^{47}Ps	-1.913	-1.913	+3.00	+3

such fits in real nuclei. A typical fit to a spectrum is shown in Fig.1, the spectrum of ^{43}Ps. It should be remembered that the scales are "absolute" – we are not simply measuring energies from the ground state, but the total binding energy of each state. A third comparison is given in Table I where we show the fit to the ground-state binding energies. The last column lists the percentage overlap between the "theoretical" and and "real" wave functions.

Clearly the fit is very good – very surprisingly good – by any standards. It is, of course, well known that some effects of configuration mixing on the energy can be "mopped up" by the use of an effective interaction. The mopping up of this degree of admixture is quite startling, however.

We turn to the other properties of the levels in our search for signs of the presence of configuration mixing. The magnetic dipole and electric quadrupole moments of the ground states are shown in Table II.

The $f_{7/2}$ prediction for the magnetic moment is just the Schmidt moment throughout the shell. We see that the deviations from this value are quite negligible, even in ^{41}Ps; in real nuclei the uncertainties due to exchange-current effects are larger than this. As we might expect, the quadrupole moment predictions are much less close. In calculating quadrupole moments for neutrons we have to endow them with an effective charge. We have taken this to be one (in some arbitrary units) in setting up the pseudo-data. In real life we would have to determine this parameter by a fit to the data; we have not attempted this here (to do so for these four states would multiply the values in the last column by 0.72). Though the fit is not quantitative it is qualitatively reasonably good; in a real nucleus collective effects would undoubtedly introduce considerably more uncertainty than this.

So far we have looked at expectation values, and it may well be argued that a much more sensitive test of wave functions is afforded by transitions. These depend upon two rather than one single wave-function, with phase and amplitude relationships between them that might well be badly upset by the presence of configuration mixing. The simplest example is that of M1-transitions. The simple pure $f_{7/2}$ theory predicts that these should all vanish (the operator is simply [4] proportional to $\vec{J}$). There are ten possible M1-transitions in these pseudo-nuclei. For seven of them the value of $(2J_f + 1) (4\pi/3)B(M1)$ is less than 0.005. For one it is 0.01, for another it is 0.07. Only for one transition of the ten, the $9/2^-$ to $11/2^-$ transition in ^{43}Ps is the value at all appreciable at 0.69. For comparison purposes the "single-particle" value (calculated for the diagonal single-particle $7/2^-$ state) is 37.64, so that even in this case the inhibition is very great.

We might expect from the behaviour of the quadrupole moments that the E2-transitions would be appreciably less well predicted than this. We look first at what we expect to be an especially sensitive situation. At the mid-point of a shell of identical particles all E2-transitions vanish, unless they change seniority. The reason for this is most easily seen in the quasi-spin formalism [5]. The Wigner-Eckart theorem in quasi-spin space tells us that the matrix element of an operator of rank 1 in the space (such as the E2-operator) has a matrix element at the middle of the shell (where the quasi-spin magnetic quantum number is zero) proportional to the Clebsch-Gordan coefficient $(S_f 100| S_f 1S_i 0)$. This vanishes

FIG.2. Number of holes in $f_{7/2}$; --- pseudo-experiment, —— $f_{7/2}$ theory.
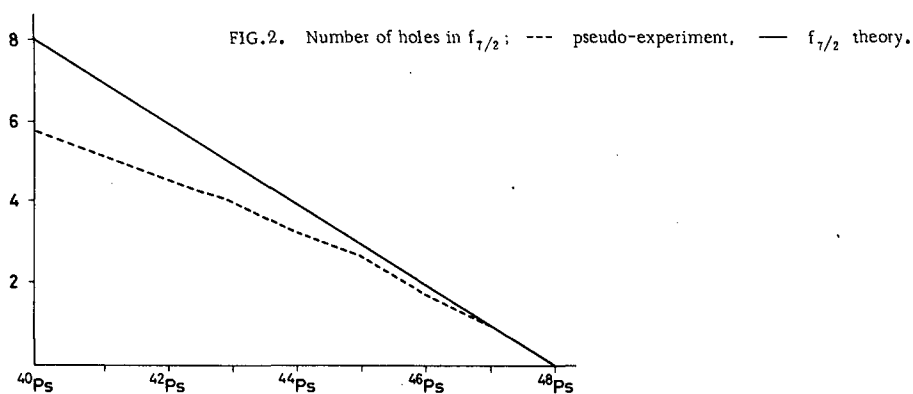
TABLE III. VALUES OF $(2 J_f + 1) (16 \pi/5 b^4) B (E2)$ IN ^{44}Ps

$J_i^{Vi} \longrightarrow J_f^{Vf}$		Pseudo-experiment	$f_{7/2}$ theory
2^2	0^0	105.87	102.83
2^2	4^2	4.63	0
2^2	4^4	179.61	204.66
2^4	0^0	0.02	0
2^4	4^2	37.38	50.38
2^4	4^4	0.11	0
4^2	5^4	186.65	144.00
4^4	5^4	0.14	0
4^2	6^2	3.12	0
4^4	6^2	196.12	246.87
5^4	6^2	144.59	122.76
8^4	6^2	227.02	249.76

TABLE IV. E2-TRANSITION STRENGTH IN ^{42}P

$J_i \longrightarrow J_f$		Pseudo-experiment	$f_{7/2}$ theory
2	0	123	77
4	2	24	138
6	4	9	91

unless $S_i + S_f + 1$ is even, and since the quasi-spins S_i and S_f are integral
they must differ by unity. This in turn means that the seniority must
change by two units in a non-vanishing transition.

The values of $(2J_f + 1)(16\pi/5b^4)B(E2)$ in ^{44}Ps are given in Table III.
Again we have not taken advantage of a potential freedom by fitting an
effective charge but have simply used the same one which we used in
setting up the pseudo-data. The fit is excellent. Not only is the selec-
tion rule reproduced to a remarkable degree in that the transitions pre-
dicted to vanish are indeed very small, but the fit to the large transitions
is also very good.

There are some sixty pieces of pseudo-data on electromagnetic
moments and transitions in the whole shell. Of these the only numbers
showing substantial disagreement with the simple $f_{7/2}$ predictions were
the three E2-transition strengths in ^{42}Ps given in Table IV.

We emphasize that these three numbers are the sole evidence
available to us from the data so far that we are dealing with anything
substantially different from a pure shell. We may reflect on the fre-
quency with which such isolated disagreements among otherwise well-
fitted data are encountered in real nuclei, and on the many "outside"
influences suffered by E2-transitions that might well mask a disagree-
ment of this size, or to which this disagreement might be attributed in
real life.

We look finally at stripping and pickup. Such experiments should be
particularly sensitive to configuration mixing, since they measure es-
sentially the single-particle nature (for a specific ℓ-value) of one state
relative to another. As an example we look at stripping of $f_{7/2}$ particles
onto the ground states of the even nuclei, going to the $7/2^-$ states of the
next odd nuclei. Since there is only one $7/2^-$ state (the ground state) for
each odd mass number in the shell in the simple pure $f_{7/2}$ model, the
stripping strength should all be concentrated here. The strength itself
should be proportional to the number of holes in the target nucleus; in-
deed the quantity $8 \Sigma S_{7/2}$ measures the number of $f_{7/2}$ holes in the target
nucleus and should drop from eight in ^{40}Ps to zero in ^{48}Ps on the simple
theory.

The odd pseudo-nuclei, of course, contain many $J = 7/2^-$ states to
which we can strip with f-waves. However, when we come to do the
pseudo-experiment we find that in all cases more than 98% of the strip-
ping strength goes to the ground state of the final nucleus, in close
accord with the simple theory. We can measure the quantity $8 \Sigma S_{7/2}$,
and this is plotted in Fig.2. This is a measure of the number of $f_{7/2}$
holes present in the target nucleus and obviously at the beginning of the
shell this number falls below the value eight predicted by the $f_{7/2}$ theory.
The plot is, however, quite close to being a straight line with mass
number, and the discrepancy would only be detectable if absolute spec-
troscopic factors could be reliably measured to better than 25%; the
achievement of this accuracy by DWBA is at the very limit of what is
possible. It would be quite in line with current practice to normalize the
^{40}Ps (d,p)^{41}Ps spectroscopic factor to some value close to unity since
it is essentially a single-particle reaction, in which event the broken
line in Fig.2 would lie very close indeed to the theoretical one.

We see in all this that the configuration mixing introduced here,
though very large, is of such a nature as to be virtually undetectable by

the experiments which we have discussed so far. While the admixtures in any given state may be very large, it appears that the relations between states, whether of a state with itself (expectation values) or with other states in the same nucleus (transition probabilities) or in neighbouring nuclei (stripping and pickup), are preserved very well in most cases. A similar situation that has been discussed [6] is the preservation of isobaric analogue relations between states that can have highly mixed isobaric spin.

Clearly, the only type of experiment that can give unequivocal evidence of strong configuration mixing is a stripping or pickup experiment that would have a null result if the closed-shell hypothesis were true. Only two such experiments exist in our system, the pickup of $f_{7/2}$ particles from ^{40}Ps and the stripping of $d_{3/2}$ particles into the same system. These pseudo-experiments would indicate the presence of 2.2 $f_{7/2}$ particles and 2.2 $d_{3/2}$ holes in this "closed-shell" system, showing that something is seriously wrong. In practice, we could probably only rely on such an experiment to about 50% accuracy, but this would be ample in this case. Such experiments would give us the only existing clue to the real situation.

The extreme insensitivity of the usual run of nuclear properties to this type of configuration mixing is, at least, partly due to the fact that the excitations out of the closed shell are almost entirely of pairs coupled to $J = 0$. If we ignore the "blocking" effect of such pairs on the nucleons already present, arising from the Pauli principle, such excitations will not affect the matrix elements of tensor operators of non-zero rank. Of course, the effects of antisymmetry in the open shell are not negligible in general, but they appear to be small for the types of experiment considered here; for the magnetic moment, for example, because the expectation value depends only on the seniority and not on the number of particles present (the operator is a quasi-spin scalar), the presence of additional zero-coupled pairs makes no difference at all even when the Pauli principle is applied. The strong favouring of zero-coupled pairs, is, of course, a feature of the forces between identical particles.

The main message of this work is the demonstration of this insensitivity, but it is interesting to explore various side-issues. One of these is the relation of the effective potential that we can deduce from the E_J ($J = 0, 2, 4, 6$) to the "primitive" potential that we assumed at the outset. The details are of no interest in this imaginary situation, but two general points emerge:

(a) Whereas the primitive interaction contained only a central potential, the effective interaction within the $1f_{7/2}$ shell turned out to have very substantial amounts of tensor and two-body spin-orbit potential in it.

(b) The main modification to the central potential itself was a considerable weakening of the odd-state interaction; it seems reasonable to suppose that if we had started with an odd-state potential that had been less attractive it would have changed sign and become repulsive. The reason for these movements is the following. When we allow excitations from the core into our shell we make no difference to the energy at the end of the shell where the excitations are forbidden by the Pauli principle. We do, however, produce an appreciable decrease in energy at the beginning of the shell. Because of the nature of the forces, nucleons settle in states of maximum possible orbital symmetry and therefore at the

beginning of a shell only experience the even-state potentials. At the end of the shell this is no longer possible; the Pauli principle forces the nucleons to occupy odd states of motion as well as the even ones. Thus, when we come to fit the whole shell we first find that the even-state effective potential has to be more attractive to fit the increased binding energies at the beginning of the shell. This by itself would lead to too much binding at the end of the shell (where the correction due to core excitation is zero), and hence the odd-state interaction has to be less attractive or even repulsive to compensate. It is interesting to notice that a repulsive central-odd potential is observed in fits to real nuclei, in contrast to that in the two-nucleon problem which is attractive; this behaviour exactly parallels what we have found here.

The behaviour of the matrix elements E_J themselves is much less complicated than that of the potentials. In going from the matrix elements calculated with the primitive interaction to the effective matrix elements found in the fit we find:

(a) all the E_J are multiplied by a constant factor of 1.24;

(b) in addition, the value of E_0 has been made even more attractive (i.e. something like a pairing potential has been added). Clearly local potentials (of finite range) are not particularly well suited to describe this phenomenon, which is related to the excitation of zero-coupled pairs.

3. A PROTON-NEUTRON SYSTEM

It might reasonably be objected that the results of the previous section, while startling, would not often be realizable in real nuclei. The reason is that in many cases where this type of configuration mixing might be important, excitation of protons would also take place; in light and medium-weight nuclei at any rate the excited protons and neutrons would occupy the same shells and we would have neutron-proton pairs with $T = 0$ possible which would preferentially couple to non-zero J-values. One might reasonably expect this type of excitation to have much more effect on the nuclear properties and therefore to be much more detectable than the type considered above. This has been investigated by S. Cohen, R.D. Lawson and the author [1].

The system we chose to study consisted of neutrons and protons in a $1p_{\frac{1}{2}}$ shell and a $1d_{\frac{3}{2}}$ shell. These two levels were assumed degenerate as before. The levels can hold up to twelve particles, which are allowed to interact through a central potential V_{TS}:

$$V_{01} = -50 \text{ MeV}$$
$$V_{10} = -30 \text{ MeV}$$
$$V_{00} = 30 \text{ MeV}$$
$$V_{11} = -10 \text{ MeV}$$

We again wish to test whether the low-lying even-parity states of the pseudo-nuclei with N from 4 to 12 can be represented at all reasonably by an assumed simple pure $1d_{3/2}$ shell. Again the assumption is far from the truth; the ground-state wave function of the N = 4 system is only 32.3%

TABLE V. GROUND-STATE BINDING ENERGIES AND OVERLAPS
BETWEEN STATES

N - 4	J	T	Pseudo-experiment (MeV)	$d_{3/2}$ theory (MeV)	Percent $p^4 d^{N-4}$
1	3/2	1/2	- 7.3	- 7.14	38.2
2	0	1	- 18.89	- 18.22	41.4
2	3	0	- 19.02	- 18.82	49.1
3	3/2	3/2	- 26.32	- 26.57	80.2
3	3/2	1/2	- 33.22	- 32.93	54.3
4	0	2	- 38.90	- 38.85	94.8
4	2	1	- 44.59	- 44.67	84.4
4	0	0	- 51.47	- 51.58	60.7
5	3/2	3/2	- 59.25	- 59.01	97.8
5	3/2	1/2	- 65.05	- 65.37	88.4
6	0	1	- 82.91	- 83.09	96.7
6	3	0	- 83.90	- 83.69	100.0
7	3/2	1/2	-104.68	-104.45	100.0
8	0	0	-129.72	-129.74	100.0

a closed-shell wave function, that of the N = 5 system is only 38.2% closed-shell-plus-one and so on (see Table V).

There are now 29 pieces of pseudo-data in the energy spectra, and we again have five parameters, the four E_{JT} :

$$E_{JT} = \langle (d_{3/2})^2 \, JT \, | \, V_{eff} \, | \, (d_{3/2})^2 \, JT \rangle$$

with J = 0, 2 (T = 1) and J = 1, 3 (T = 0), and the quantity ϵ, the binding energy of a $d_{3/2}$ nucleon to the "closed $p_{1/2}$-core". The situation is thus very similar indeed to the pseudonium case above.

The least-squares fit to the 29 energy levels gave an r.m.s. deviation of 390 keV. This is less good than we obtained before but still good compared to real shell-model calculations when neutrons and protons are both present. We noted earlier, for instance, that Cohen and Kurath [7] in the p-shell had fitted 35 data with 13 parameters and obtained r.m.s. deviations of 430 keV. This was a potential fit; a two-body matrix-element fit of the same data had 17 parameters and had 400 keV deviations. We have only five parameters.

We show the ground-state binding energies we obtain, together with the overlaps between the states of the "simple theory" and those of the pseudo-nuclei in Table V. The fit to excited states is of comparable quality.

Finally we again show an example of a fitted spectrum in Fig.3. This time we choose the N - 4 = 4 nucleus. The fit is clearly very good. The inclusion of protons in the problem has thus made no qualitative change, at least as far as the energies are concerned.
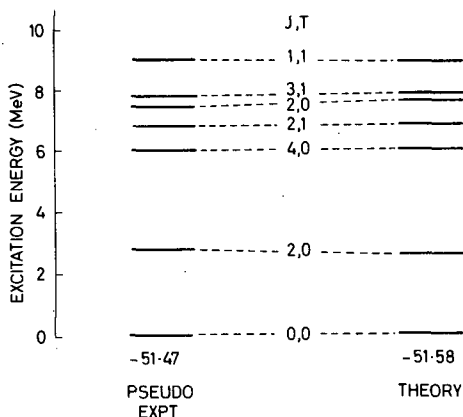
FIG.3. N=8 pseudonucleus.

We next look at the evidence from static moments. These are listed for N-4 = 4 in Table VI.

Again the fit is excellent; there is no clue here to the poorness of the assumption of pure $d_{3/2}$ wave-functions. The agreement is non-trivial since, for example, the second 2^+ state (here called $J = 2^2$) has an overlap with the pure $p^4 d^4$ state of only 24.4%.

Even the transitions tell the same story. We list some M1-transitions in Table VII.

The E2-transitions in the nucleus (N = 8) in the middle of the shell show an effect similar to those in ^{44}Ps. This is shown in Table VIII. The "$d_{3/2}$ theory" here uses an effective charge $\alpha = -0.112$ which was obtained by fitting the quadrupole moments of all states in the shell. This was an isoscalar effect; the proton charge was taken to be $(1 + \alpha)$, the neutron charge α. Varying the two charges independently produced almost exactly the same effective charges as the one-parameter fit. The quadrupole moments listed in Table VI happen to be independent of α.

Again the worst fitted data concerned the electric quadrupole properties of the N = 6 pseudo-nuclei. Here the $d_{3/2}$ theory gave - 2.17 for the quadrupole moment of the J = 3, T = 0 state (- 1.37 by pseudo-experiment) and 4.96 for the (3,0) to (1,0) E2-transition strength (observed 2.21). These cases are the only instances in some 100 electromagnetic data where the error in the matrix element exceeds about 40% (excluding very small numbers and zero, of course). Most errors are much smaller than this.

In these proton-neutron nuclei we can, of course, observe beta-decay. Some log (ft) for transitions within our N = 8 system are shown in Table IX. Perhaps surprisingly, the quality of the fit shown by these numbers is comparable to that of the E2-data rather than that of the M1 as might have been expected. The overall fit, however, is still very good; where the theory predicts a transition should vanish, the observed log (ft) is unusually large for an allowed transition, and the other trends are followed well. The only mildly serious discrepancy is in the (1,1) to (0,0) transition. Just as in the E2-case we would in real life have attributed such discrepancies as there were to weak collective effects, so here we would undoubtedly have invoked the mixing of $j = \ell + \frac{1}{2}$ and $j = \ell - \frac{1}{2}$ orbitals.

TABLE VI. STATIC MOMENTS FOR N - 4 = 4

J	T	Magnetic moments		Quadrupole moments	
		Pseudo-experiment	$d_{3/2}$ theory	Pseudo-experiment	$d_{3/2}$ theory
2	1	0.859	0.848	0.000	0.000
3	1	1.255	1.272	-2.519	-2.800
1	1	0.380	0.424	1.080	1.120
2	0	0.848	0.848	0.098	0.000 .
4	0	1.695	1.697	0.000	0.000
2^2	0	0.849	0.848	-0.075	0.000

TABLE VII. SOME M1-TRANSITIONS

N	J_i	T_i	J_f	T_f	Pseudo-experiment	$d_{3/2}$ theory
7	5/2	1/2	7/2	1/2	2.956	3.191
7	5/2	1/2	3/2	1/2	0.577	0.652
7	1/2	1/2	3/2	1/2	0.336	0.465
8	3	1	2	1	2.286	2.443
8	1	1	2	1	2.654	2.792
9	5/2	1/2	7/2	1/2	3.045	3.191
9	5/2	1/2	3/2	1/2	0.630	0.652
9	1/2	1/2	3/2	1/2	0.503	0.465

The beta-decay matrix elements are known to be particularly sensitive to this and it would be more than adequate to explain (with a small configuration admixture) the observed variations.

Finally we look at stripping. As an example we take the spectroscopic factors observed in stripping on the ground state of the N = 7 nucleus (J_i = 3/2, T_i = 1/2) and going to the various states of the N = 8 system we have been studying in some detail. These are listed in Table X. This is very good agreement, of course, which one would like to obtain for any theory in real life. The sum rule gives a value close to 4 for $1/8 \sum_f (2J_f + 1) (2T_f + 1) S_f$ which measures the number of $d_{3/2}$ holes in

the target nucleus. The $d_{3/2}$ theory gives 5, of course. To detect this, one would again have to be able to measure and extract correctly absolute spectroscopic factors to within 20%.

TABLE VIII. E2-TRANSITIONS IN THE N = 8 NUCLEUS IN THE
MIDDLE OF THE SHELL

J_i	T_i	J_f	T_f	Pseudo-experiment	$d_{3/2}$ theory
3	1	2	1	19.706	16.521
3	1	1	1	6.963	8.232
2	1	1	1	9.089	7.081
4	0	2^1	0	26.496	21.241
4	0	2^2	0	0.324	0
2^1	0	0	0	17.152	14.161
2^2	0	0	0	0.029	0

TABLE IX. SOME Log (ft) FOR TRANSITIONS WITHIN THE N = 8
SYSTEM

J_i	T_i	J_f	T_f	Pseudo-experiment	$d_{3/2}$ theory
0	2	1	1	3.27	3.00
1	1	0	0	4.64	5.27
1	1	2^1	0	7.12	∞
1	1	2^2	0	3.60	3.55
2	1	2^1	0	3.97	4.10
2	1	2^2	0	5.89	∞
3	1	2^1	0	∞	∞
3	1	2^1	0	3.91	4.01
3	1	2^2	0	4.02	3.99

We, thus, once more come to the conclusion that even in this system
with neutrons and protons both present the general run of nuclear physics
experiments gives no clue at all to the large configuration admixtures.
Only by performing null-expectation experiments can one obtain information
that is reasonably unequivocal, and again the only two that suggest them-
selves are $d_{3/2}$ pickup on the N = 4 system (which would show 1.48 such
nucleons present where theory says there should be none) or $p_{1/2}$ stripping
on any of these systems which would reveal the presence of holes in the
closed shell (e.g. 0.84 in the N = 8 system). In a real nucleus, I should

TABLE X. SPECTROSCOPIC FACTORS OBSERVED IN STRIPPING

J_f	T_f	Pseudo-experiment	$d_{3/2}$ theory
0	0	4.26	4.00
2^1	0	2.03	2.40
2^2	0	0.0004	0
1	1	0.20	0.27
2	1	0.79	1.07
3	1	0.17	0.27

emphasize that things would still not necessarily be simple; in a stripping experiment, for instance, one would have to convince oneself that an observed p-strength did not come from a smaller admixture of a higher p-state in the final nucleus rather than from 1p-holes in the target. It would often be necessary to distinguish between (say) $d_{3/2}$ and $d_{5/2}$, a difficult art as yet in its infancy. Even these apparently clear-cut experiments will therefore often have some degree of ambiguity.

We observe (somewhat surprisingly) that the neutron-proton systems are fitted (on the whole) just as well as the neutron-only ones. As we suggested at the beginning of this section, we might reasonably have expected the fit to be worse, since the preferred pairing for a neutron and proton is a $J = 1$ state. Such an excitation would at first sight be expected to affect the matrix elements of operators rather strongly.

A qualitative account of what seems to be happening is the following. We ignore, for the moment, the Pauli principle in the open shell, and treat the (excited-closed-shell) and (open-shell) systems separately. We then find by exact diagonalization that the lowest excited state of the closed shell has quantum numbers $J = 0$, $T = 0$. In real life, of course, this corresponds to the fact that the first excited state of a doubly-magic nucleus has generally $J = 0$ and $T = 0$ in spite of the repulsion between this state and the ground state. Thus, in lowest order, the main admixture to the core is simply this $J = 0$, $T = 0$ state. This, of course, contains large amounts of pairing of excited neutrons and protons to $J = 1$, but these are then coupled to the $J = 1$ hole state they leave behind to give a total $J = 0$ state. It is this total J-value of the excited core that is important in this no-Pauli-principle approximation, since any such $J = 0$ state of the core will give no contribution to the matrix elements of operators of non-zero tensor rank. Of course, this is only a very rough approximation to the real situation when all the effects are put in, but the main consequences seem to persist.

4. SUMMARY

We have here surveyed in some detail the work of Cohen, Lawson and the author which suggests that it is possible for the shell model to

swallow and to digest large configuration-mixing effects without showing any signs that it has done so. This points, I believe, very forcibly to the moral that one often learns very little from the experiment that agrees with the theory; it is the experiment that disagrees that is the important one. In any system all such experiments should be considered together and an explanation sought of the whole body of apparently discordant information; the fact that the overwhelming bulk of data agrees with a simple theory may not be particularly relevant to this search, and may even prove a psychological hindrance. Of course, in real life this is a counsel of perfection. In practice, there are many effects from "outside" the model considered that may cause plausible discrepancies in the fit, and since (by hypothesis) the discrepancies are few we will probably have too many explanations rather than not enough.

The effect on the effective parameters of absorbing admixtures might (if large enough) invalidate the comparison with many-body theory, introducing renormalizations that could vary from shell to shell in an unknown way. If they are as difficult to detect experimentally as our results suggest (and the difficulties encountered in our "clean" nuclei will be magnified tremendously in real systems) the only recourse may be to calculate from first principles, by taking the many-body calculation through a configuration-mixing calculation right to the bitter end of comparison with data. It may be, in other words, that many-body theorists may have to learn to do their own shell-model calculations.

Finally, I should perhaps make one point clear. We do not at any time claim that other forms of configuration mixing are concealed by the use of effective interactions and over-simple wave-functions. Calculations similar to those described here, but for $1f_{7/2}$ and $2p_{3/2}$ have been carried out by our group and (independently) by Engel and Unna [8]. In such a case, where the two degenerate levels have the same parity, and single-particle excitations can be admixed, a one-level fit to the pseudo-data gives poor results. This situation is familiar in real nuclei, where (for example) the nuclei of masses 16 to 20 are much better described by the shell model as $(d_{5/2} s_{1/2})^n$ than as $(d_{5/2})^n$ alone, proving that the addition of a second shell of the same parity can alter predictions significantly. This does not affect our basic thesis, of course, which is that some forms of admixture are very well concealed, but the difference between the two cases serves to indicate the situations where we should be most careful; we should, in particular, be especially critical when we examine the credentials of a closed shell at which a complete change of parity occurs.

REFERENCES

[1] COHEN, S., LAWSON, R.D., SOPER, J.M., Physics Letts 21 (1966) 306; see also Review by LAWSON, R.D. in Nuclear Physics (Proc. Conf. Gatlinburg, 1966) (BECKER, R.L. et al., Eds), Academic Press, New York (1967).

[2] TALMI, I., these Proceedings.

[3] COHEN, S., LAWSON, R.D., MACFARLANE, M.H., SOGA, M., Meth. comp. Physic 6 (1966) 235.

[4] DE-SHALIT, A., TALMI, I., Nuclear Shell Theory, Academic Press, New York (1963).

[5] LAWSON, R.D., MACFARLANE, M.H., Nucl. Phys. 66 (1965) 80.

[6] LANE, A.M., SOPER, J.M., Nucl. Phys. 37 (1962) 506,
    LANE, A.M., SOPER, J.M., Nucl. Phys. 37 (1962) 663,

[7] COHEN, S., KURATH, D., Nucl. Phys. 73 (1965) 1.

[8] ENGEL, M.Y., UNNA, I., Physics Letts 28B (1968) 12.

SOME TECHNIQUES AND APPROXIMATIONS
IN THE NUCLEAR SHELL MODEL

R. ARVIEU
Institut de Physique Nucléaire,
Orsay, France

Abstract

SOME TECHNIQUES AND APPROXIMATIONS IN THE NUCLEAR SHELL MODEL.
1. Introduction; 2. The model; 3. Seniority; 4. Tensorial character of operators and consequences; 5. The quasi-particle method for scalar interactions; 6. Generalized seniority breaking of two-body interactions; 7. Influence of the symmetry-breaking terms; 7. Summary.

1. INTRODUCTION

The aim of this paper is to develop and to discuss some of the techniques which are in use in the nuclear shell model. We shall not discuss the problem of extracting the ingredients of the shell model, i.e. the single-particle energies or wave functions, from the two-body interaction. These problems are considered, for example, in the papers dealing with the Hartree-Fock method. We shall rather concentrate on the problem of the shell model itself which is the N-body problem of finding some solutions, exact or approximate, of the shell-model Hamiltonian and the properties of eigenvalues and eigenfunctions resulting from such a calculation. Ultimately, one has to compare the theoretical results with the experiment. This last problem will not be discussed in this paper. We shall just require that the model to be dealt with contains the proper features to obtain qualitative agreement with experiment. This model is presented mainly as a tool to help one to understand the techniques developed to find the exact solutions or the approximations which can be employed instead of these solutions. The model which we shall study first, consists of a system of N identical particles occupying a degenerate subset of a spherically symmetric shell-model potential and interacting through a surface delta interaction. This interaction was first introduced by Green and Moszkowski [1] as a generalization of a pairing force. Its symmetry properties with respect to the quasi-spin transformations have been investigated [2], it was shown, for example, that the interaction contains a scalar part plus a part which varies only linearly with the number of particles. In such a case, it is very easy to understand the Bogolyubov-Valatin canonical transformation or what is more generally called the quasi-particle method [3]. This interaction cannot be used in an academic model only. As a matter of fact, it has also been applied to the description of the single-closed-shell nuclei [4] and it has been used successfully in various regions of the periodic table: closed-shell nuclei [5], medium nuclei [6] and deformed nuclei [7] as well. In some cases, the kind of agreement obtained with experiment is of the same order as that which results when a much more realistic interaction is used instead of the SDI. It can be asserted then that the SDI contains some of the essential features needed in shell-model

calculations. Therefore, it is justified to study the shell-model techniques by using such a simple two-body interaction.

In the following we shall first present the two-body interaction itself, and give some properties of the two- and of the three-particle systems. We shall then discuss the representation in which the SDI is diagonal: the generalized seniority representation. Besides, we shall also describe an other way of introducing the seniority quantum number. The generalized seniority representation, or, in other words, the quasi-spin scheme, can also be used to classify the operators. The electromagnetic properties of odd and of even systems will be studied in this respect; we shall also show how the BCS method can be very simply understood as a rotation performed in the quasi-spin space.

It is very interesting to compare other interactions with the SDI. We shall re-formulate this question more generally in this way: it is very interesting to compare the symmetry properties of any interaction to those of the SDI.

This comparison is carried out by performing an expansion of a general two-body interaction in terms of irreducible tensors under the quasi-spin space rotation. We measure tentatively the strength of each of these tensors in order to evaluate the symmetry breaking. This breaking is also measured in two other different ways. First, by a direct expansion of the exact wave functions, obtained by diagonalizing the entire Hamiltonian, in terms of wave functions of fixed generalized seniority. Secondly, by projecting these wave functions onto subspaces having a fixed number of broken pairs according to a method recently proposed by Lorazo [7 - 8]. From a comparison between these various ways of appraising the symmetry breaking we can deduce many informations, in particular, specify much better than before the conditions of applicability of the BCS method.

The contents of these lectures is a review of several papers and theses published in the last three years in collaboration with O. Bohigas, B. Lorazo, S. Moszkowski and C. Quesne. A similar résumé has also been given in the 1968 Cargese session [9].

2.   THE MODEL

2.1. Single-particle energies

Our aim is to describe the properties of a system of N identical nucleons interacting in a set of r single-particle levels in j-j coupling. Our first assumption is that this set of levels is completely degenerate in energy. Let a, b, ... r be the indices denoting these levels. Each of these indices denotes the complete set of quantum numbers which define a single-particle state except the magnetic quantum number m, i.e.

$$a = n_a \text{ (radial quantum number)},$$
$$\ell_a \text{ (orbital angular momentum)},$$
$$j_a \text{ (total angular momentum)}.$$

In some cases, the symbol j_a will be used instead of a to denote each individual state.

The nuclei for which such a description is relevant should only contain identical nucleons. Of course, this applies only to the valence nucleons,

i.e. those located outside a closed-shell core. The type of nuclei belonging to this class of single-closed-shell nuclei are the oxygen isotopes, the Ni, Sn, Pb isotopes, and also all the isotones N = 50, 82 and 126, for example $^{211}_{85}(126n)$ At.

Note that the number of valence particles (or valence holes) in these nuclei ranges from 2 (^{18}O, ^{58}Ni, ^{206}Pb, ^{210}Pb) to 16 (^{116}Sn). Those nuclei were first considered by Kisslinger and Sorensen [10].

In our model, the set of single-particle levels is the set located between two major shells. For example, in the case of Ni isotopes, the set is 1f 5/2, 2p 3/2 and 2p 1/2.

The assumption of degenerate single-particle levels is certainly not true for ^{16}O. It is, however, a much better approximation for the heavy Sn isotopes where the three sub-shells: 3s 1/2, 2d 3/2, 1h 11/2 are not very far apart from each other in energy. The same is also true for the Ni region.

We are aware of the fact that the approximation of taking only valence neutrons or protons is certainly not valid for all nuclei which we have considered. It has, indeed, been an important discovery to realize that a closed-shell core can be excited rather easily, i.e. that some low-lying states must be due to many-particle and many-hole configurations, like the first excited 0$^+$ states [12] in ^{16}O. The occurrence of such states at low energy in all the single-closed-shell nuclei is a possibility which must be considered seriously. Some recent calculations by Wong and Davies have been undertaken in this spirit for ^{56}Ni and ^{58}Ni where there is little doubt that these excitations play a great role. This is, however, not the case for the nuclei around ^{208}Pb. Indeed, in that region the shell-model description in terms of like nucleons works pretty well at low energy to the best of our knowledge. We must then underline that one drawback of our model is that it has certainly not the same degree of validity for all the single-closed-shell nuclei occurring in the periodic table.

The degeneracy of the single-particle energies is not a very serious restriction. This assumption is made here in order that the generalized seniority quantum number be a good quantum number so that each eigenstate of our interaction is a basis vector of an irreducible representation of the quasi-spin group.

2.2. The two-body interaction

As was said at the beginning, the two-body interaction which will be assumed to act between our identical particles is a surface delta interaction [1].

This interaction is a delta interaction acting only at the surface of a nucleus. Let us consider a two-body matrix element of this interaction between two particles states.
Let

$$\langle am_a \, bm_b \, | W | \, cm_c \, dm_d \rangle \tag{1}$$

be such a two-particle non-antisymmetric matrix element.

Let us perform the classical separation of radial and angular variables both for the two-body interaction and for each single-particle state. If the

two-body interaction is a general central force such a separation is carried out by expanding the force into Legendre polynomials:

$$W_{12} = \sum_K v_K(r_1, r_2) P_K(\cos \Omega_{12}) \tag{2}$$

where Ω_{12} is the angle between the directions of particles 1 and 2. On the other hand, P_K can be expanded as

$$P_K(\cos \Omega_{12}) = \sum_q C_q^K(\Omega_{12}) (-1)^q C_{-q}^K(\Omega_2) \tag{3}$$

C_q^K is a modified spherical harmonics

$$C_q^K = \left(\frac{4\pi}{2K+1}\right)^{\frac{1}{2}} Y_q^K \tag{4}$$

The expansion of a δ-force is

$$\delta(\vec{r}_1 - \vec{r}_2) = \frac{1}{4\pi r_1^2} \delta(r_1 - r_2) \sum_K (2K+1)(C^K(\Omega_1) C^K(\Omega_2)) \tag{5}$$

i.e.

$$v_K \delta(r_1, r_2) = \frac{\delta(r_1 - r_2)}{r_1^2} \frac{2K+1}{4\pi} \tag{6}$$

The v_K corresponding to a SDI is then

$$v_K^{SDI} = \frac{\delta(r_1 - r_2)}{r_1^2} \delta(r_1 - R_0) \frac{2K+1}{4\pi} \tag{7}$$

where R_0 is the radius of the nucleus.

Let us introduce the Slater integral

$$f_K(a\,b\,c\,d) = \int \int R_a(r_1) R_b(r_2) v_K(r_1, r_2) R_c(r_2) R_d(r_1) r_1^2 r_2^2 dr_1 dr_2 \tag{8}$$

We have, of course, for a delta interaction

$$f_K = (2K+1) f_0 \tag{9}$$

and besides for a SDI

$$f_0(a\,b\,c\,d) = \frac{1}{4\pi} [R_a(R_0) R_b(R_0) R_c(R_0) R_d(R_0)] \times R_0^2 \tag{10}$$

We shall assume as an approximation that the amplitudes of all the radial wave functions are equal at the surface of the nucleus; $f_0(a\,b\,c\,d)$ is, then, independent of the single-particle states $a\,b\,c\,d$.

Under these conditions the only dependence on the states is an angular one. We have indeed

$$\langle am_a\, bm_b | W_{SDI} | cm_c dm_d \rangle = f_0 \langle am_a\, bm_b | \sum_K (2K+1) P_K | cm_c dm_d \rangle \quad (11)$$

The calculation of the second factor on the right-hand side of Eq.(11) is a very classical one.

With a little algebra, this result can be expressed in terms of Clebsch–Gordan coefficients only. As a result, let us give only the matrix elements in which the two particles are coupled to J in the initial and final states.

The two-particle wave functions are taken here to be normalized and anti-symmetric. For this type of matrix element it is convenient to use the notation introduced by Baranger [15]:

$$G(a\,b\,c\,d\,J) = -\tfrac{1}{2} [(1+\delta_{ab})(1+\delta_{cd})]^{\frac{1}{2}} \langle abJM | W | cdJM \rangle \quad (12)$$

We have then:

$$G(a\,b\,c\,d\,J) = \frac{G}{4} h_J(ab) h_J(cd)(-1)^{\ell_a+\ell_c} [1+(-1)^{\ell_c+\ell_d+J}] \quad (13)$$

we have used here the notation

$$h_J(ab) = \sqrt{2j_b+1} \langle j_b J -\tfrac{1}{2}\, 0 | j_a -\tfrac{1}{2} \rangle \quad (14)$$

On the other hand, we include in the factor G the radial dependence as well as the strength of the interaction.

The last factor in Eq.(13) ensures that the force is effective only in states of natural parity. This is due to the zero-range character of the interaction. Indeed, such an interaction can act only in spatially symmetric states and is equal to zero, otherwise. For identical particles this state is the singlet state and $J = L$. Since $(-1)^{\ell_1+\ell_2} = (-1)^L$ where ℓ_1 and ℓ_2 are the orbital angular momenta of the particles we have $(-1)^{\ell_1+\ell_2+J} = +1$. For $J = 0$ the G's take the simple form

$$G(a\,a\,b\,b\,0) = \frac{G}{2} (-1)^{\ell_a+\ell_b} \sqrt{2\Omega_a} \sqrt{2\Omega_b} \quad (15)$$

Note also that the G's are separable quantities in the indices ab and cd. This separability which holds for all J's will introduce some simplifications in the two-particle spectrum as we shall see; it does not hold true for a usual delta interaction because of the presence of the Slater integral.

2.3. Two-particle spectrum

Let us consider two particles in our degenerate set of levels. Let us diagonalize the interaction in the complete two-particle basis. We have then, by using a single index to denote a two-particle state,

$$\langle \alpha | W | \beta \rangle = W_\alpha W_\beta \quad (16)$$

The eigenvalue problem is then written, if φ_α denotes the weight of the state α, as

$$\sum_\beta W_\alpha W_\beta \varphi_\beta = \epsilon \varphi_\alpha \tag{17}$$

A solution of this equation is $\epsilon = 0$ and

$$\sum_\alpha W_\alpha \varphi_\alpha = 0 \tag{18}$$

Another solution is

$$\epsilon = \sum_\alpha W_\alpha^2 \,; \qquad \varphi_\alpha = W_\alpha \tag{19}$$

The solution with $\epsilon \neq 0$ is unique; on the other hand, the φ's satisfying Eq.(17) span a vector space which has the dimension of the two-particle space minus one. For different values of J the result is exactly the same. Therefore the eigenvalues of W_{SDI} are either zero or

$$\epsilon_J = \tfrac{1}{2} \sum_{ab} (h_J(ab))^2 \tag{20}$$

where we have put $G = 1$ in Eq.(13). Since the interaction has to be attractive, ϵ_J is negative. Thus, the SDI for each total angular momentum is effective only for a single state. The weight of each two-particle state is simply equal to $h_J(ab)$.

$$|\psi_{JM}\rangle = C^t \sum_{ab} (-1)^{\ell_a} h_J(ab) |(j_a j_b) JM\rangle \tag{21}$$

Let us now consider the electric 2^J-pole operator:

$$Q_i(JM) = e_i r_i^J C_M^J(\Omega_i) \tag{22}$$

The matrix elements of the operator (22) are thus just those of C_M^J, up to a multiplicative term depending on the radial co-ordinates. This fact suggests that there is a connection between the wave function (21) and the operator (22). This relation which is easy to prove [2] means that $Q(JM)$ connects only the ground state with the single state of angular momentum J, which "feels" the interaction as shown in Fig. 1.

In some way, the lowest state for each angular momentum looks like a collective state with respect to the electromagnetic field. We can see here that our model already contains some physics since it can reproduce some general features of spherical nuclei: low-lying 0^+ state, and a sequence of levels occurring in the order of increasing angular momentum, each lowest being a collective one.
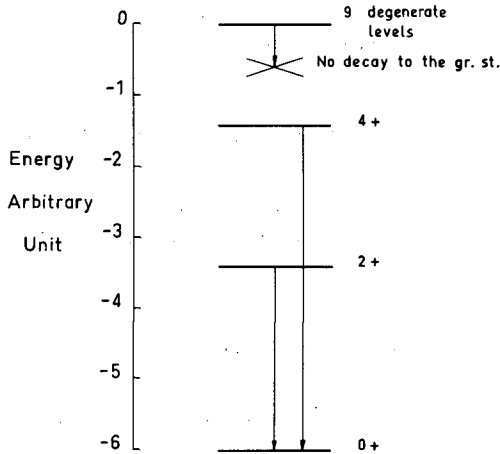
FIG.1.   Spectrum of $(1/2 \ 3/2 \ 5/2)^2$ configuration in the case of a pure SDI and zero-single-particle
splitting.   The only states decaying to the ground state are the first 2^+ and 4^+.

2.4.   Spectrum of three particles

We now want to discuss the properties of the SDI for a higher number
of particles.   For this purpose we shall use the formalism of second-
quantization.   Let $a^\dagger_{im_i}$ and a_{im_i} be the creation and annihilation operators
of one particle in the orbit i, respectively.   Let us define the operator
associated with the creation of two particles coupled to an angular
momentum J:

$$A^\dagger (ab \ JM) = \sum_{m_a m_b} \langle j_a j_b m_a m_b | JM \rangle \ a^\dagger_{am_b} a^\dagger_{bm_b} \qquad (23)$$

This can also be written as a tensor product:

$$[a^\dagger_a \times a^\dagger_b]^J_M \qquad (24)$$

It has the symmetry property

$$A^\dagger (b a \ J M) = (-1)^{j_a - j_b + J} \ A^\dagger (a b \ J M) \qquad (25)$$

For $J = 0$ we use the shorter notation

$$A^\dagger_0 a = A^\dagger (a a \ 0 \ 0) \qquad (26)$$

We now look for a possible extension of the property of the two-particle
system to three particles.   Let

$$\mathscr{A}^\dagger(JM) = \sum_{ab} (-1)^{\ell_a} h_J (ab) A^\dagger(ab \ JM) \qquad (27)$$

These operators generate all the low-lying collective states of the
interaction for each.

We now want to consider the three-particle case. Let us construct a particular subset of three-particle states:

$$\left| J_a \, jm \right\rangle = C^t \sum_{Mm_a} \left\langle J \, j_a \, M \, m_a \, \middle| \, jm \right\rangle \mathscr{A}^\dagger(JM) \, a^\dagger_{am_a} \left| 0 \right\rangle \tag{28}$$

where $\left| 0 \right\rangle$ is the vacuum for the operators a.

C. Quesne [14] has shown that the subspace (28) is left invariant by the SDI, i.e.

$$W_{SDI} \left| J_a \, jm \right\rangle = \sum_{J'a'} \left\langle J_a \, jm \, \middle| \, W_{SDI} \, \middle| \, J'_{a'}, jm \right\rangle \left| J'_{a'} \, jm \right\rangle \tag{29}$$

If we now consider a state $\left| \psi_{jm} \right\rangle$ which is orthogonal to this subspace it satisfies:

$$\left\langle 0 \middle| a_a \mathscr{A}(JM) \middle| \psi_{jm} \right\rangle = 0 \tag{30}$$

for all values of a and J. Therefore we have:

$$\mathscr{A}(JM) \left| \psi_{jm} \right\rangle = 0 \tag{31}$$

From Eq.(31) it follows that

$$W_{SDI} \left| \psi_{jm} \right\rangle = 0 \tag{32}$$

Indeed by using the second quantization the SDI is written as

$$W_{SDI} = -\frac{G}{4} \sum_{JM} \sum_{ab} (-1)^{\ell_a} h_J(ab) A^\dagger(ab \, JM) \sum_{cd} (-1)^{\ell_c} h_J(cd) A(c \, d \, J \, M) \tag{33}$$

$$= -\frac{G}{4} \sum_{JM} \mathscr{A}^\dagger(JM) \mathscr{A}(JM) \tag{34}$$

Equation (32) obviously derives from relations (34) and (31). Thus, there exist some eigenstates in which the strength of the interaction is concentrated, like the states $\mathscr{A}^\dagger(JM) \left| 0 \right\rangle$ for two particles. These states can be obtained by diagonalizing W in the subspace of the states defined by expression (28). Among these states it is possible to show that the set

$$\left| 0 \, am_a \right\rangle = C^t a^\dagger_{am_a} \mathscr{A}^\dagger(0 \, 0) \left| 0 \right\rangle \tag{35}$$

provides some exact eigenstates for three particles. These states are called states of generalized seniority one. The explanation of the occurrence of these states will be made clearer later on. As far as the other states are concerned, we have not been able to discover simple expressions. These states must then be obtained numerically.
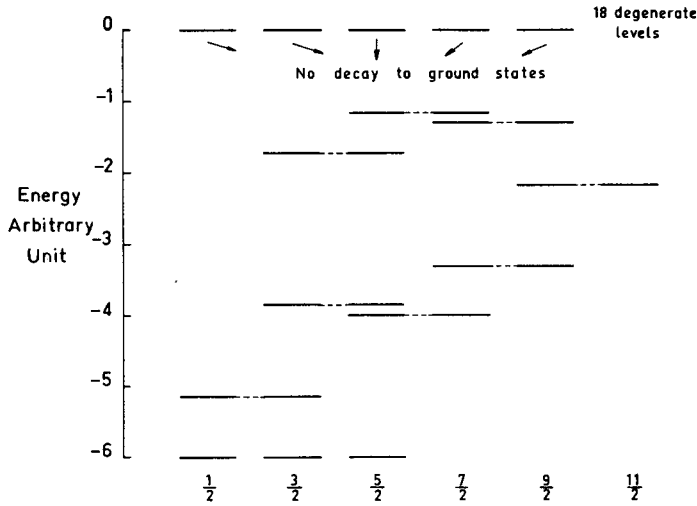
FIG.2. Spectrum of $(1/2 \; 3/2 \; 5/2)^3$ configuration in the case of a pure S D I and zero-single-particle splitting. The states at zero energy cannot decay to the ground-state levels. In this case the total spin of the three particles is a good quantum number which explains the two-fold degeneracies.

It is very gratifying to discover still that most of the states do not feel the interaction at all and are thus at zero energy. A typical spectrum is shown in Fig.2.

As to the electromagnetic transitions, some very interesting properties may be seen [14]. Let us consider a transition between a seniority-one state and any other state. We see that

$$\langle \psi_{jm} | Q(kq)\mathscr{A}^{\dagger}(0\,0)\, c_{\alpha}^{+} \, | \, 0 \rangle = \langle \psi_{jm} \, | \mathscr{A}^{\dagger}(0\,0)\, Q\,(kq)\, c_{\alpha}^{+} \, | \, 0 \rangle$$

$$+ \; 2\,(-1)^k \, \langle \psi_{jm} \, | \mathscr{A}^{\dagger}(kq)\, c_{\alpha}^{\dagger} \, | \, 0 \rangle \tag{36}$$

For all the states at zero energy the conjugate of the relations (31) implies that each term on the right-hand side of Eq.(36) is strictly zero.

We have, therefore, a very complete analogy with the two-particle state. At low energy, we obtain a set of levels which are very similar to the neighbouring even nucleus; these states have important electromagnetic transition states. This feature is also found in the experimental properties of odd nuclei.

3. SENIORITY

In this chapter we shall develop some of the mathematics necessary to understand the properties of the SDI, in particular, and of general interest in nuclear-shell-model studies. We shall discuss the two seniority quantum numbers which help to provide a complete classification of the states and operators. We defer the discussion of the operators for a while

and begin by applying this concept to a classification of shell-model states. The general references for this chapter are Refs [13, 16-19].

3.1. Single j-shell

3.1.1. Classification of the states of a $(j)^N$ configuration.

Let us first consider the case of identical particles occupying only a single j-shell. Here, there is only one possible two-particle state which has zero angular momentum, i.e. the state

$$\left| (j)^2_0 \right> = \frac{1}{\sqrt{2}} A^\dagger_0 \left| 0 \right> \tag{37}$$

all the other states having two particles; a non-zero angular momentum can be thought of as obtained from Eq. (37) by first destroying the pair in a zero total angular momentum and then creating a new pair which is not coupled to $J = 0$ as

$$\left| (j)^2_J \right> = \frac{1}{\sqrt{2}} A^\dagger_J \left| 0 \right> \tag{37bis}$$

More generally, we can try to construct the wave functions corresponding to a larger number of particles. For three particles a possible basis is

$$\left\{ a^+ \times \left| (j)^2_J \right> \right\}^{\mathcal{J}}_m \tag{38}$$

$$= \sum_{Mm} \left< JjMm \left| \mathcal{J}\mathcal{M} \right> a^+_m A^+_{JM} \left| 0 \right> = \left| (j)^2_J, j, \mathcal{J} \right>$$

It can be seen that, in general, these states are not independent; two states differing by the intermediate angular momentum J are not orthogonal and the number of these states exceeds, in general, the correct number of states allowed by the Pauli principle.

For example, if $j = 5/2$, and if we restrict J to 0 and 2, according to relation (38) the possible values of $\mathcal{J}$ are $5/2$ and $1/2, 3/2, 5/2, 7/2, 9/2$, The Pauli principle allows only $\mathcal{J} = 3/2, 5/2$, and $9/2$. Therefore, since all the states (38) are completely anti-symmetric the states having $\mathcal{J} = 1/2$ and $7/2$ must vanish completely. On the other hand, states having $\mathcal{J} = 5/2$ and $J = 0$ or $J = 2$ must be proportional. These results can be derived by calculating the matrix of the scalar products of these states. One can verify for example that their norm vanishes identically for $\mathcal{J} = 1/2$ and $7/2$.

At the end we are left with the states having $J = 0$, $\mathcal{J} = 5/2$; $J = 2$, $\mathcal{J} = 3/2$ and $9/2$; they are orthogonal and independent.

This procedure can be carried on for all values of j and $\mathcal{J}$. Let us mention the most important results:

For each j, the value $\mathcal{J} = j$ is always possible. For the lowest values of j, i.e. $j \leq 7/2$, there is only a single state for each value of $\mathcal{J}$. In these cases, one can always use the index J to label a state; for example:

if $j = \dfrac{7}{2}$, $J = 2$, $\mathscr{J} = \dfrac{3}{2}$, $\dfrac{5}{2}$, $\dfrac{9}{2}$, $\dfrac{11}{2}$

$J = 4$, $\mathscr{J} = \dfrac{13}{2}$.

From $j = 9/2$ on, for a given $\mathscr{J}$ two states may appear (as far as I know this is true only up to $j = 13/2$, for higher j there may be more than two states). In the latter case, $j = 9/2$, this happens only for $\mathscr{J} = 9/2$. We can then construct two orthogonal linear combinations of two states (38) which are not colinear. One can take the following two states

$$\left| (j)_0^2, \ j, \ \mathscr{J} = j \right\rangle \tag{39}$$

$$\lambda \left| (j)_0^2, \ j, \ J = j \right\rangle + \mu \left| (j)_2^2, \ j, \ J = j \right\rangle \tag{40}$$

where λ and μ have to be chosen such that these states are orthogonal.

For higher j, $j = 11/2$, for example, the same thing also happens for $\mathscr{J} = 9/2$, $11/2$ and $15/2$. Then we must consider some particular linear combination of $J = 0$, 2 and 4, as for example:

$$\left| \left(\frac{11}{2} \right)_2^2, \ \frac{11}{2}, \ \frac{9}{2} \ \right\rangle \tag{41}$$

$$\lambda \left| \left(\frac{11}{2} \right)_2^2, \ \frac{11}{2}, \ \frac{9}{2} \ \right\rangle + \mu \left| \left(\frac{11}{2} \right)_4^2, \ \frac{11}{2}, \frac{9}{2} \ \right\rangle \tag{42}$$

with different values of λ and μ as in expression (40). In other words, it is necessary to introduce additional quantum numbers.

The classification of the states can be continued along these lines; we have seen the essential steps but, in addition, we shall consider the case of four particles. We can then try to use the states which have been constructed. For example we can construct the states:

$$(A_0^\dagger)^2 |0\rangle \text{ which has } J = 0 \tag{43}$$

and

$$A_0^\dagger A_{JM}^\dagger \ |0\rangle \tag{44}$$

These states are properly anti-symmetric, they can be normalized and they are orthogonal. However, by just counting the number of states allowed by the Pauli principle, it is seen that they do not form a complete basis. There exist some other states which cannot be written along these lines. For example, in Eqs (43) and (44) the only possible values of J are 0 or the even values up to $2j - 1$. But there exist states, for four particles, which have odd values for their total angular momentum, or which have an even value higher than $2j - 1$, the upper limit in expression (44).

On the other hand, as for three particles, some values of the total angular momentum can appear several times. Therefore, we must look for an other construction, for example like

$$[A_{j'}^\dagger \times A_{j''}^\dagger]_M^J \ |0\rangle \tag{45}$$

The same as for states (38), these states are not orthogonal and are not orthogonal to states (43) and (44); moreover, they form a redundant basis. A Schmidt orthogonalization procedure has therefore still to be carried out. We are, therefore, led to some linear combinations

$$\lambda (A_0^\dagger)^2 |0\rangle + \mu (A_0^\dagger)(A_{JM}^\dagger) |0\rangle$$

$$+ \sum_{J'J''} \nu(J'J'') [A_{J'}^\dagger \times A_{J''}^\dagger]_M^J |0\rangle \equiv B_{JM}^{\alpha\dagger} |0\rangle \tag{46}$$

which satisfy the expected orthonormalization properties, in particular, they should be orthogonal to the states (43) and (44). Of course, the first term is present only for $J = 0$.

The label α is put here as an additional quantum number to distinguish states having, possibly, the same J.

More generally, one can introduce the states

$$(A_0^\dagger)^{N/2} |0\rangle \tag{47}$$

$$(A_0^\dagger)^{\frac{N-2}{2}} (A_{JM}^\dagger) |0\rangle \tag{48}$$

$$(A_0^\dagger)^{\frac{N-4}{2}} (B_{JM}^{\alpha\dagger}) |0\rangle \tag{49}$$

if N is even, and

$$\cdot a_{jm}^\dagger (A_0^\dagger)^{\frac{N-1}{2}} |0\rangle \tag{50}$$

if N is odd. These states are formed with the pair operator $A_0^\dagger$ which appears to some power. The seniority relative to a single j-orbital can be now defined as the number of unpaired particles. Thus the preceding states have, respectively, seniorities 0, 2, 4 and 1. Clearly, higher seniority can be obtained. We shall use the quantum number v to denote this additional quantum number. The state (39) has v = 1, the states (40), (41) and (42) have v = 3. Let us now introduce this quantum number more formally.

3.1.2. The quasi-spin scheme [19]

Let us build up the following three operators related to the orbit j:

$$S_+ = \frac{1}{2} \sum_m (-1)^{j+m} a_{-m}^\dagger a_m^\dagger \tag{51}$$

$$S_- = \frac{1}{2} \sum_m (-1)^{j+m} a_m a_{-m} \tag{52}$$

$$S_0 = \frac{1}{2} (N - \Omega) \tag{53}$$

where $N = \sum_m a^\dagger_m a_m$ is the number-of-particles operator in this subshell.

These operators are seen to satisfy the commutation relations of an angular momentum:

$$[S_+, S_-] = 2S_0, \quad [S_0, S_\pm] = \pm S_\pm \tag{54}$$

This angular momentum has been called the quasi-spin operator [19]. Let S^2_{op} be its square, $S(S+1)$ its eigenvalues. It is convenient to write this eigenvalue as

$$S = \frac{\Omega - v}{2} \tag{55}$$

where $\Omega = j + \frac{1}{2}$.

One sees that

$$A^\dagger_0 = \sum_m \langle jj - mm | 00 \rangle a^\dagger_{-m} a^\dagger_m = \sum_m \frac{(-1)^{j+m}}{\sqrt{2\Omega}} a^\dagger_{-m} a^\dagger_m = \sqrt{\frac{2}{\Omega}} S_+ \tag{56}$$

All the products $(A^\dagger_0)^p$ which appear in Eqs (47 – 50), with various values of p, commute with S^2_{op}.

The N-particle states can be classified according to the eigenvalues of S^2 and S_0 let

$$|\alpha S S_0\rangle \quad \text{or also} \quad |\alpha (j)^N v\rangle \tag{57}$$

be such a state where α denotes the additional labels necessary to specify the states. Given a value of $S_0 = (N - \Omega)/2$ means that the value of the number of particles is specified. The states for which $S_0 = -S$ have thus $(N - \Omega)/2 = -(\Omega - v)/2$ or $N = v$, they satisfy

$$S_- |\alpha S - S\rangle = 0 \tag{58}$$

Let us consider the 4-particle case $v = 4$; because of Eqs (58) and (56), the states $|\alpha S - S\rangle$ are thus orthogonal to the states (43) and (44) and, then, identical with the states (46).

On the other hand, one has

$$S^2_{op} (A^\dagger_0)^{\frac{N}{2}} |0\rangle = (A^\dagger_0)^{\frac{N}{2}} S^2 |0\rangle = (A^\dagger_0)^{\frac{N}{2}} (S_+ S_- + S^2_0 - S_0 |0\rangle = \frac{\Omega}{2} \left(\frac{\Omega}{2} + 1\right) (A^\dagger_0)^{\frac{N}{2}} |0\rangle \tag{59}$$

i.e. the states (47) have $S = \Omega/2$ or $v = 0$. By calculating the eigenvalue of S^2 for the states (48) – (50) it can be seen that the quantum number v defined by Eq. (55) is identical with the seniority quantum number.

From this study it is clear that the seniority quantum number can be used to classify the states. It has the advantage of connecting the wave functions of adjacent nuclei. Also in Eqs (47) to (50) the number of states is independent of N, which is a very important property of the seniority scheme. For more details about this scheme the reader should see Ref. [13].

3.2. Case of several orbitals

If we consider the case of several orbits we find two ways of generaliz-
ing seniority [16]. Let us now put as a superscript to the quasi-spin opera-
tors an index to denote the subshell which they refer to, S_+^i, for example,
and let v_i be the +1 quasi-spin component, and seniority relative to the
subshell i. For each subshell these operators and quantum numbers are
defined. We have two ways of adding them.
a.   The sum of the seniority quantum numbers relative to each orbit

$$v = \sum_i v_i \tag{60}$$

can be expected to generalize the seniority quantum number conveniently.
In this way seniority–zero states of N particles are all the states

$$\left| (j_a)_0^{n_a} v_a = 0, \ (j_b)_0^{n_b} v_b = 0 \ldots \ldots, \ (j_r)_0^{n_r} v_r = 0 \right\rangle \tag{61}$$

or any linear combination of them. For each of these states we have

$$n_a + n_b + \ldots \ldots \ldots + n_r = N \tag{62}$$

This definition does not take account of the weights of the configuration
mixing; it gives, for different values of the number of particles, different
numbers of states having the same seniority. For example, in the case of
three subshells 2p 1/2, 2p 3/2, 1f 5/2 we have 3 states of v = 0 for N = 2,
for N = 4 we obtain 5 states and for N = 6, 6 states. The same is true for
other values of v; there we must use the basis

$$\left| (j_a)^{n_a} v_a, \ (j_b)^{n_b} v_b, \ldots \ldots, \ (j_r)^{n_r} v_r \right\rangle \tag{63}$$

for which

$$v_a + v_b + \ldots \ldots \ldots + v_r = v. \tag{64}$$

Of course, states having a different v, or simply a different value of v_i
for the subshell i, are orthogonal. This classification can certainly be
used to construct a complete basis; it is inconvenient in that no connection
is drawn between the wave functions of adjacent nuclei. It can, anyway,
be used very successfully in some cases, for example, for a pairing force.
Indeed, if we consider a pairing Hamiltonian

$$H = \sum_i \epsilon_i a_{im_i}^\dagger a_{im_i} - \frac{G}{4} \sum_{ik} (-1)^{j_i + m_i + j_k + m_k} a_{i-m_i}^\dagger a_{im_i}^\dagger a_{km_k} a_{k-m_k} \tag{65}$$

None of these terms can break a pair. This means that this Hamiltonian
commutes with all the S_{op}^{i2}. Thus, the eigenvalue problem of the pairing
Hamiltonian must be solved inside each subspace having a given seniority.
b.   We can also use a representation in which the quasi-spins of each orbit
are vectorially coupled, i.e. we define a generalized quasi-spin operator as:

$$S_{\pm} = \sum_i (-1)^{\ell_i} S_{\pm}^i \quad \text{and} \quad S_0 = \sum_i S_0^i \quad \text{and} \quad \Omega = \sum_j (j + \tfrac{1}{2}) \tag{66}$$

Since two different $S_{0\pm}^i$ commute, these operators obey the same commutation relations as in Eq. (54). Everything that has been said before can now be repeated with the following differences:

Since the relation

$$S_{op}^2 (S_+)^{\frac{N}{2}} |0\rangle = \frac{\Omega}{2} \left(\frac{\Omega}{2} + 1 \right) (S_+)^{\frac{N}{2}} |0\rangle \tag{67}$$

holds true independently of whether S refers to a sum of orbits or to a simple orbit, we have $v_g = 0$. We must call a generalized seniority-zero state any state of the form

$$(S_+)^{\frac{N}{2}} = \left(\sum_i (-1)^{\ell_i} \sqrt{\frac{\Omega_i}{2}} A_0^i \right)^{\frac{N}{2}} |0\rangle \tag{68}$$

Here the generalized seniority quantum number v_g is related to the total quasi-spin eigenvalue by

$$S = \frac{\Omega - v_g}{2} \tag{69}$$

This quantum number refers now to the number of unpaired particles of the type shown in Eq. (68). Therefore (65) has $v_g = 0$. Let us construct states having a higher seniority:

$$a_{jm}^\dagger (S_+)^{\frac{N-1}{2}} |0\rangle \quad \text{has } v_g = 1 \tag{70}$$

These states are analogous to states (50). On the other hand, the states

$$\sum_{ab} \lambda_{ab} A^\dagger (ab\, JM) (S_+)^{\frac{N-1}{2}} |0\rangle \tag{71}$$

have $v_g = 2$, independently of λ provided that $J \neq 0$. If $J = 0$ they have $v_g = 2$ provided λ satisfies

$$\langle 0 | S_- \sum_a \lambda_{aa} A^\dagger (aa\, 00) |0\rangle = 0 \tag{72}$$

or also

$$\sum_a (-1)^{\ell_a} \sqrt{\Omega_a}\, \lambda_{aa} = 0 \tag{73}$$

If λ is arbitrary the state (71) has not a well defined seniority. Let us call

$B_{JM}^{\alpha\dagger}$ any operator creating a four-particle state which is orthogonal to the $v_g = 0$ state and to the $v_g = 2$ states; of course, it then satisfies

$$S_- B_{JM}^{\alpha\dagger} \, | \, 0 \, \rangle = 0 \tag{74}$$

and, therefore, has $v_g = N = 4$.

If we consider now the states

$$(S_+)^{\frac{N-4}{2}} \, B_{JM}^{\alpha\dagger} \, | \, 0 \, \rangle \tag{75}$$

their number is just the number of seniority-four states.

The only difference to the single-j-shell case which is worth mentioning is that for $J = 0$ we may have seniority-two states. The number of these states is equal to the number of orthogonal states which satisfy condition (70), i.e. to the number of single-particle levels minus one. It is possible now to use a mixed representation where both quantum numbers are used. It is easy to see immediately that the answer is positive. Indeed, by just looking at relations (68), (69), (70) and (71), we see that

$$v_g = 0 \quad \text{means that} \quad v = 0 \tag{76}$$

$$v_g = 2 \quad \text{means} \qquad v = 0 \quad \text{if} \quad J = 0 \tag{77}$$

$$v = 2 \quad \text{if} \quad J \neq 0 \tag{78}$$

$$v_g = 1 \quad \text{means} \qquad v = 1 \tag{79}$$

On the other hand, if we consider the definition of the operators $B_{JM}^{\alpha+}$ we see that they have only to create states which are orthogonal to the $v_g = 0$ and $v_g = 2$ states for four particles. Since the seniority basis defined in the preceding paragraph is an orthogonal basis, but, on the other hand, the space of states having $v = 0$ or $v = 2$ is not exhausted by the $v_g = 0$ and $v_g = 2$ states (just by counting states) it is seen that some of the states generated by the operator $B_{JM}^{\alpha+}$ can be chosen to have either $v = 0$ (if $J = 0$), $v = 2$, or $v = 4$.

In other words, given a subspace having v_g fixed we can expand it in terms of subspaces having also good v as follows:

$$\mathscr{E}_{vg} = \sum_v \mathscr{E}_{vg}^v \tag{80}$$

In expressions (76) – (78) we have seen that:

$$\mathscr{E}_0 = \mathscr{E}_0^0, \quad \mathscr{E}_2 = \mathscr{E}_2^2 \text{ if } J \neq 0, \quad \mathscr{E}_2 = \mathscr{E}_2^0 \text{ if } J = 0$$

$$\mathscr{E}_4 = \mathscr{E}_4^0 + \mathscr{E}_4^2 + \mathscr{E}_4^4$$

If we put between parentheses the dimension of each subspace we obtain for the case of $1/2 \ \ 3/2 \ \ 5/2$ levels the decomposition

$$\mathscr{E}_4(6) = \mathscr{E}_4^0(2) + \mathscr{E}_4^4(4) \tag{81}$$

$$\mathscr{E}_6(5) = \mathscr{E}_6^0(1) + \mathscr{E}_6^4(3) + \mathscr{E}_6^6(1) \tag{82}$$

Similarly, we can expand the spaces having good v into subspaces having a good v_g.

For example if $N = 6$, we obtain

$$\mathscr{E}^0 (6) = \mathscr{E}^0_0 (1) + \mathscr{E}^0_2 (2) + \mathscr{E}^0_4 (1) \tag{83}$$

Remarks

In this chapter we have seen how a complete basis of state can be constructed. We have defined two schemes which do not exclude each other. In the generalized seniority representation one uses subspaces of the space having fixed seniority (in the first meaning). Which of these subspaces is more useful cannot be said beforehand; this problem will be considered in a further chapter. It must be underlined that each of these quantum numbers does not lead to a complete classification of the states; for example, in the $(j)^N$ -case both cases (41) and (42) have $v = 3$, on the other hand, all the states satisfying condition (73) have $v_g = 2$. Additional quantum numbers must be found, but this problem will not be examined here.

4. TENSORIAL CHARACTER OF OPERATORS AND CONSEQUENCES

4.1. Tensorial character of the creation and destruction operators

It has been noted by Lawson and MacFarlane [20] that the angular momentum-like commutation relations of S_+, S_- and S_0 can be used to calculate many matrix elements in the seniority scheme. As pointed out in the preceding chapter the method can be used in the case of a single j-shell as well as in the case of mixed orbitals. In the following we shall consider the most general case.

First one notices that the couple of operators

$$a^\dagger_{jm} \quad \text{and} \quad (-1)^{j+m} a_{j-m} \tag{84}$$

behaves like a spinor under the transformation induced by the quasi-spin generators. Indeed, one has, for example for $a^\dagger_{jm}$,

$$[S_+, a^\dagger_{jm}] = 0; \quad [S_-, a^\dagger_{jm}] = (-1)^{j+m} a_{j-m}$$

$$[S_0, a^\dagger_{jm}] = \tfrac{1}{2} a^\dagger_{jm} \tag{85}$$

and the corresponding Hermitian conjugate relationships for a_{jm}. It is seen there that the operators (84) carry a double tensor character.

(a) Each of them is a spherical tensor of rank j and component m with respect to ordinary rotations.

(b) They are, respectively, the two components of a spinor with respect to the transformations in the quasi-spin space.

It would be more convenient to show this tensorial character explicitly as follows:

$$\mathscr{S}^{j\frac{1}{2}}_{m\frac{1}{2}} = a^\dagger_{jm} \tag{86}$$

$$\mathscr{S}^{j\frac{1}{2}}_{m-\frac{1}{2}} = (-1)^{j+m} a_{j-m} \tag{87}$$

Note that any linear combination of these two operators like

$$d^\dagger_{jm} = u_j a^\dagger_{jm} + (-1)^{j+m} v_j a_{j-m} \tag{88}$$

such as the one introduced by the Bogolyubov–Valatin canonical transformation, has a proper jm tensorial character, but, on the other hand, it corresponds to a combination of the spinor components.

This remark has two very interesting applications. Let us mention the first one.

Any product of creation and annihilation operators is a product of tensor of rank $1/2$ in the quasi spin space and of tensors of rank j_1, j_2, j_3 etc. ... in the ordinary space. In general, such products are not irreducible tensors, but can be expanded in terms of irreducible tensors by using the well known techniques developed for the coupling of angular momenta. For example:

$$a^\dagger_{j_1 m_1} a^\dagger_{j_2 m_2} = \mathscr{S}^{j_1 \frac{1}{2}}_{m_1 \frac{1}{2}} \mathscr{S}^{j_2 \frac{1}{2}}_{m_2 \frac{1}{2}} = \sum_{JM} \langle j_1 j_2 m_1 m_2 | JM \rangle \times \sum_{SS_0} \langle \tfrac{1}{2}\tfrac{1}{2}\tfrac{1}{2}\tfrac{1}{2} | SS_0 \rangle [\mathscr{S}^{j_1 \frac{1}{2}}$$

$$\times \mathscr{S}^{j_2 \frac{1}{2}}]^{J \ S}_{M \ S_0} \tag{89}$$

It is seen that the possible values of S are $S = 1$, $S_0 = 1$. If we were considering, instead, the product $a^\dagger_{j_1 m_1} (-1)^{j_2 m_2} a_{j_2 m_2}$ we would obtain the Clebsch–Gordan coefficient $\langle \tfrac{1}{2}\tfrac{1}{2}\tfrac{1}{2}\tfrac{1}{2} | SS_0 \rangle$ and S could then take two values $S = 0$ or 1 while $S_0 = 0$. On the other hand, we, obviously, must have

$$|j_1 - j_2| \le J \le j_1 + j_2 \tag{90}$$

Such products of operators, as can be seen in Professor Frahn's contribution to these Proceedings, are very common. In general, it is seen that they can be reduced to sums of irreducible tensors. On the other hand, the value of S_0 is unique. Indeed, let us take x creations and y annihilations; we have then

$$\underbrace{a^\dagger a^\dagger \ldots\ldots\ldots a^\dagger}_{x} \quad \underbrace{a \ a \ldots\ldots\ldots a}_{y} \tag{91}$$

Each $a^\dagger$ from (85) will give $1/2$, while each a will give $-1/2$, therefore the total value of S_0 is

$$S_0 = \frac{x-y}{2} \tag{92}$$

If an operator conserves the number of particles we have $S_0 = 0$. Let us then in a few examples consider the character of the most interesting physical operators.

4.2.   Tensorial character of the single-particle Hamiltonian and single-particle operators

As stated above we have in general $S = 0$ or 1, $S_0 = 0$. Thus, in general, none of the operators

$$V(abJM) = \sum_{m_a m_b} \langle j_a j_b m_a m_b | JM \rangle a^\dagger_{am_a} (-1)^{j_b + m_b} a_{b-m_b} \tag{93}$$

is an irreducible tensor operator in the quasi-spin space.

We can, however, carry out the decomposition into irreducible tensors:

$$V(abJM) = V_0^0(abJM) + V_0^1(ab\,JM) \; . \tag{94}$$

We find that the scalar part is

$$V_0^0(ab\,JM) = V(ab\,JM) + (-1)^{\ell_a + \ell_b + j_a + j_b + J}\, V(ba\,JM) \tag{95}$$

$$V_0^0(abJM) \equiv S_{0M}^{0J}(ab) \tag{96}$$

In Eq. (96) we have used a notation similar to that introduced in Eq. (89). On the other hand, the vector part is

$$V_0^1(abJM) = V(ab\,JM) - (-1)^{\ell_a + \ell_b + j_a + j_b + J}\, V(ba\,JM)$$

$$= S_0^1{}_M^J(ab) \tag{97}$$

If $J = 0$ it is seen that

$$V_0^0 = 0 \tag{98}$$

$$V_0^1 = V(aa\,00) = \frac{1}{\sqrt{2\Omega_a}} \sum_{m_a} a_{am_a}^\dagger a_{am_a} = \frac{1}{\sqrt{2\Omega_a}}\, \hat{N}_a \tag{99}$$

Any single-particle operator, which is of the form $\sum_a \epsilon_a \hat{N}_a$, is thus a vector in the quasi-spin space. Note that if $\epsilon_a = c^{te} = \epsilon$ we have

$$\sum_a \epsilon_a \hat{N}_a = \epsilon \hat{N} = \epsilon(2S_0 + \Omega) \tag{100}$$

On the other hand, if $a = b$ one has

$$V(aa\,JM) = V_0^0 \quad \text{if} \quad J \text{ is odd} \tag{101}$$

$$V(aa\,JM) = V_0^1 \quad \text{if} \quad J \text{ is even} \tag{102}$$

Within a single j-shell, all the spherical tensors of odd rank are pure scalars while those of even rank are pure vectors.

4.3. Tensor character of the operators creating two particles

By taking $V_0^1(ab\,J\,M)$ and applying S_+ and S_-, we generate an operator associated with two creations or two annihilations, i.e.

$$[S_+,\, V(abJM)] = (-1)^{\ell_b}\, A^\dagger(ab\,JM) \tag{103}$$

$$[S_+,\, V(ba\,JM)] = (-1)^{\ell_a}A^+(ba\,JM) = (-1)^{\ell_a + j_a - j_b + J}A^\dagger(abJM) \tag{104}$$

$$[S_+,\, V_0^1(ab\,JM)] = 2\,(-1)^{\ell_b}A^+(ab\,JM) \tag{105}$$

This means that V_0^1, $A^{\dagger}$ and A, with the same argument abJM, form the components of a vector. It is more convenient to take the three following operators as components of a vector:

$$\mathscr{S}_{M1}^{J\,1} = A^+ (ab\,JM) \tag{106}$$

$$\mathscr{S}_{M0}^{J\,1} = \delta_{ab}\,\delta_{J0}\,\delta_{M0}(-1)^{\ell_a}\sqrt{\Omega}_a + \frac{(-1)^{\ell_b}}{\sqrt{2}}\,V_0^1(ab\,JM) \tag{107}$$

$$\mathscr{S}_{M-1}^{J\,1} = -(-1)^{\ell_a+\ell_b+J+M}A\,(ab\,JM) \tag{108}$$

4.7. Tensor character of the interactions

By using the preceding methods one can now show that any two-particle interaction operator can be expanded as a sum of three terms:

$$W = y_0^0 + y_0^1 + y_0^2 \tag{109}$$

This results directly from the fact that W contains four operators each of which is a tensor of rank $1/2$.

We shall carry out this expansion later on for a general two-particle Hamiltonian; first, we shall study it for the S D I and the pairing force.

4.4.1. Tensor expansion of a pairing force

The pairing force is written as

$$W_{pair} = -G\,S_+\,S_- \tag{110}$$

It is immediately seen that

$$W_{pair} = -G\left[\frac{2}{3}\,S^2 + S_0 - \sqrt{\frac{2}{3}}\,(\vec{S}\times\vec{S})_0^2\right] \tag{111}$$

The last expression is obtained by considering $\vec{S}$ to be an angular momentum.

The scalar S^2 and the tensor $(\vec{S}\times\vec{S})_0^2$ can, of course, be expressed in terms of the three components of $\vec{S}$. One has, for example,

$$(\vec{S}\times\vec{S})_0^2 = \sum_q \langle 11\,q\,-q\,|\,20\rangle\,S_q^1 S_{-q}^1 = -\tfrac{1}{2}\langle 111-1\,|\,20\rangle\,[S_+S_- + S_-S_+]$$

$$+ \langle 11\,00\,|\,20\rangle\,(S_0^1)^2 \tag{112}$$

This operator[1] is a sum of a two-body operator, plus a single-body operator, plus a constant term. Indeed, S_+S_- is a two-body operator, but $S_-S_+ = S_+S_- - 2S_0$ is a sum of a two-body plus a single-body operator and $(S_0^1)^2 = (\hat{N} - \Omega)^2/4$ contains also a constant plus a one-body plus a two-body operator.

---

[1] The factor $-\tfrac{1}{2}$ comes from the relations $S_{\pm1}^1 = \mp\dfrac{1}{\sqrt{2}}\,[S_x \pm iS_y]$.

Note also that we can write

$$-\sqrt{\frac{2}{3}}\,(\vec{S}\times\vec{S})_0^2 = \frac{1}{3}\,S^2 - S_0^2 \tag{113}$$

Therefore

$$W_{pair} = -G\,[S^2 + S_0 - S_0^2] \tag{114}$$

$$= -G\left[S^2 - \frac{\Omega}{2}\left(\frac{\Omega}{2}+1\right)+\frac{N}{2}\,(\Omega+1)-\frac{N^2}{4}\right]. \tag{115}$$

The largest eigenvalue of S^2 is $\Omega/2$, then the ground-state energy of W_{pair} is

$$W_{pair} = -G\left[\frac{N}{2}\,(\Omega+1)-\frac{N^2}{4}\right] \tag{116}$$

Note that the presence of the terms S_0^2 introduces a quadratic dependence of the ground-state energy on N.

4.4.2. Tensor expansion of the SDI

A delta force is known to be identical (for like particles only) to a singlet force. We can write

$$\delta_{12} = -\tfrac{1}{3}\,(\sigma_1 \cdot \sigma_2)\,\delta_{12} \tag{117}$$

which means that a triplet force vanishes identically. We can thus replace the tensor expansion of δ_{12}, Eq. (5), by a tensor expansion of $(\sigma_1 \cdot \sigma_2)\,\delta_{12}$:

$$4\pi\,\delta_{12} = -\tfrac{1}{3}\,{\sum_{K\lambda}}'\,(-1)^{K+1+\lambda}\,(2K+1)\,(T_{K\lambda}(1)\cdot T_{K\lambda}(2)) \tag{118}$$

where $T_{K\lambda}$ is the tensor product

$$T_{K\lambda}^{\mu}(1) = [C^K(\Omega_1)\times\sigma^1(1)]_{\mu}^{\lambda} \tag{119}$$

The SDI contains two terms which are expressed as functions of these $T_{K\lambda}^{\mu}$:

$$W_{SDI} = -4\pi\,G\,\sum_{i<j}\delta\,(\Omega_{ij})$$

$$= \frac{G}{6}\,{\sum_{K\lambda}}'\,(-1)^{K+1+\lambda}\,(2K+1)\left[\left(\sum_i T_{K\lambda}(i)\cdot\sum_j T_{K\lambda}(j)\right)-\sum_i (T_{K\lambda}(i)\cdot T_{K\lambda}(i))\right] \tag{120}$$

This expansion turns out to be just the expansion of the SDI into a scalar term (the first one) and a vector term (the second) which happens to be proportional to $\hat{N}$.

To see this we first consider a general one-particle operator, which is a spherical tensor t_q^K, in second quantization,

$$t_q^K = \sum_{am_a} \sum_{bm_b} \langle am_a | t_q^K | bm_b \rangle a_{am_a}^\dagger a_{bm_b} \tag{121}$$

We first use the Wigner–Eckart theorem which allows us to introduce a V operator

$$t_q^K = \sum_{ab} \frac{\langle j_a \| t^K \| j_b \rangle}{\sqrt{(2K+1)}} V(abKq) \tag{122}$$

$$= t_{q\,0}^{K\,0} + t_{q\,0}^{K\,1} \tag{123}$$

In the second line we have expanded this operator into irreducible tensors according to expansion (94). This is done by replacing V by $V^1 + V^0$. We see that we now must consider the operator

$$t_q'^K = \sum_{ab} (-1)^{\ell_a + \ell_b + j_a + j_b + K} \frac{\langle j_a \| t^K \| j_b \rangle}{\sqrt{2K+1}} V(ba\,Kq) \tag{124}$$

We have thus

$$t_{q\,0}^{K\,0} = t_q^K + t_q'^K \tag{125}$$

$$t_{q\,0}^{K\,1} = t_q^K - t_q'^K \tag{126}$$

Interchanging the summation indices in $t_q'^K$ and adding we obtain the two coefficients;

$$\left[\langle j_a \| t^K \| j_b \rangle \pm (-1)^{\ell_a + \ell_b + j_a + j_b + K} \langle j_b \| t^K \| j_a \rangle \right] \tag{127}$$

respectively, for $t_{q\,0}^{K\,0}$ and $t_{q\,0}^{K\,1}$.

The tensorial character of t_q^K depends then on the relationship between $\langle j_a \| t^K \| j_b \rangle$ and $\langle j_b \| t^K \| j_a \rangle$. This relationship, in turn, depends on the behaviour of the operator t^K under the time-reversal operation. If the operator t^K changes of sign under time reversal we have

$$\langle j_a \| t^K \| j_b \rangle = (-1)^{j_a + j_b + K + \ell_a + \ell_b} \langle j_b \| t^K \| j_a \rangle \tag{128}$$

This is the case for $t^K \equiv T_{K\lambda}$, then such an operator is a pure scalar. If the operator t^K is invariant under time reversal we have

$$\langle j_a \| t^K \| j_b \rangle = -(-1)^{j_a + j_b + K + \ell_a + \ell_b} \langle j_b \| t^K \| j_a \rangle \tag{129}$$

Such an operator is then a pure vector.

From this we conclude that $\sum\limits_{i} T_{K\lambda}^{\mu}(i)$ is an operator scalar under the quasi-spin transformations, and so the first part of our statement concerning expansion (120) is shown.

The proof that the second term of expression (120) is proportional to N will not be given here. It can be seen in Ref. [2]. This self-energy term turns out to be:

$$-\frac{G}{6} \sum_{K\lambda} (-1)^{K+\lambda+1} (2K+1) \sum_{i} (T_{K\lambda}(i) \cdot T_{K\lambda}(i)) \tag{130}$$

$$= -\tfrac{1}{2} G\Omega \hat{N} = -G\Omega S_0 - \tfrac{1}{2} G\Omega^2 \tag{131}$$

The S D I can now be written as the sum of a scalar term and a vector term

$$W_{SDI} = y_0^0 (SDI) + y_0^1 (SDI) \tag{132}$$

with

$$y_0^1 (SDI) = -G\Omega S_0 \tag{133}$$

and

$$y_0^0 (SDI) = \text{first term of expression } (120) -\tfrac{1}{2} G\Omega^2 \tag{134}$$

We have thus found two interactions which are diagonal in the generalized quasi-spin representations.

4.4.3. Invariance properties of other two-body forces.

Any two-body interaction can be expanded in terms of spherical tensors. Expansion (2) is an example. From what has been said in the preceding case it is clear that the tensorial character of an interaction depends on the invariance property of its spherical tensors with respect to time-reversal transformations.

We can write

$$W = \sum_{i<j} W_{ij} = \sum_{i<j} \sum_{K} (T_1^K(1) \cdot T_2^K(2)) f_K(1, 2) \tag{135}$$

where T_1^K and T_2^K are spherical tensors. An expansion similar to expansion (120) can be performed. Then, if T_1^K and T_2^K both change sign in time reversal the first term will be a quasi-spin scalar. The following interactions can be seen to fulfill this statement [18].

* the spin-spin force. The derivation is then entirely the same as in the preceding section. It is also the same reasoning for an ordinary δ force,

** the tensor operator $S_{12} = [(\sigma_1 \cdot r)(\sigma_2 \cdot r) - \tfrac{1}{3}(\sigma_1\sigma_2) r^2]/r^2 \tag{136}$
which can be written.

$$S_{12} = -\sqrt{\frac{10}{9}} (\sigma_1 \cdot T_{21}(2)) \tag{137}$$

*** and similarly the quadratic spin-orbit operator.

These statements are not true for:
* a central interaction (except for the zero-range case)
** a spin-orbit interaction.

An important part of the two-body force has thus the property

$$y_0^2 \equiv 0 \tag{138}$$

These interactions contain, besides a scalar term, a second term which is a one-body operator and a vector term, but they have no second-order tensor. Since the shell-model Hamiltonian in realistic cases always contains single-particle energies, i.e. according to expression (99) an additional vector term, we find that for the interactions having $y_0^2 = 0$ the shell-model Hamiltonian is given by:

$$
\begin{aligned}
H_{\text{shell model}} \; &= y_0^0 \; (0+1+2\text{-body operator}) \\
&+ y_0^1 \; (0+1\text{-body operator})
\end{aligned}
\tag{139}
$$

4.5. Matrix elements of operators

Let T_q^k be a second-quantized operator which is also an irreducible tensor of rank k in the quasi-spin space. From what was said before we know that this operator changes the number of particles by 2q. Let us take its matrix elements in a generalized seniority representation by using the Wigner-Eckart theorem:

$$\langle \alpha SS_0 | T_q^K | \alpha'S'S_0' \rangle = \frac{\langle \alpha S \| T^K \| \alpha'S' \rangle}{\sqrt{2S+1}} \langle S'KS_0' q \mid SS_0 \rangle \tag{140}$$

From this theorem it is seen that the entire dependence on the number of particles is contained in a Clebsch-Gordan coefficient since $S_0 = (N-\Omega)/2$. The reduced matrix element does not depend on N any more, it can be calculated by taking the lowest possible values of N on the left-hand side of Eq.(140). Of course, if $K = 0$, the matrix elements are independent of N. Let $S = (\Omega - v_g)/2$ and $S' = (\Omega - v_g')/2$. By using the rules for the coupling of angular momenta one finds that

$$|\Delta v_g| \leq 2K \tag{141}$$

A vector term changes thus v_g by two units, a tensor by four units.

4.6. Spectrum of the SDI

The SDI for degenerate single-particle energies is now seen to be diagonal in a representation in which S_{op}^2 is diagonal (or in a representation in which the generalized seniority quantum number is diagonal). To obtain its eigenvalues we must find the eigenvalue spectrum of y_0^0. This problem has not yet been solved analytically and I do not know whether this is possible or not. It is certainly a good problem for those who are interested in group theory. The procedure which we have followed is quite empirical: to obtain the spectrum of the SDI for values of the generalized seniority

quantum number equal to 2 or 3 one must diagonalize y_0^0 in the space of configurations of $N = 2$ or $N = 3$ particles. For $N = 2$ we have already analytic formulas. To obtain the spectrum of $v_g = 4$, one uses the spectrum of $N = 4$ and substract the $v_g = 0$ and $v_g = 2$ levels, the energies of which are known from the preceding case, etc.... Until now this process has been carried out up to $v_g = 6$ for the set of levels 1/2 3/2 5/2. For the set of single-particle energies which are of physical interest we have calculated the spectra [22] corresponding to $v_g = 1$ and $v_g = 3$. It is interesting to obtain the eigenvalues of y_0^0 for large values of v_g as one has very little information, in general, on their position.
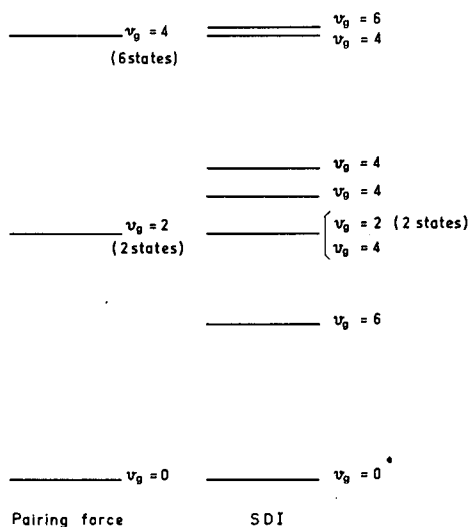
FIG.3. Relative position of the low lying 0^+ states for $(1/2\ 3/2\ 5/2)^6$ configuration in the case of a SDI and a pairing force of the same strength. The pairing force has its levels ordered according to increasing v_g. On the other hand, the SDI has some high seniority levels at low energy.

Lorazo [8] in Orsay has carried out the calculation for $N = 6$ and $v_g = 6$ (for the 0^+ states). He found that the first excited state has $v_g = 6$ which is quite surprising. This lowering of the large v_g is also seen in the $N = 5$ case for $v_g = 5$. It is then very challenging to understand this feature (see Fig.3).

As an other remark let us consider the binding energy of the ground state. Clearly y_0^0 always gives the same contribution whatever N may be. The energy shift of the ground state and of the whole spectrum is given by the N-dependent terms of y_0^1 or y_0^2. This shift is given by expression (116) for the pairing force, and by Eq.(131) for the SDI.

4.7. Electromagnetic properties of the eigenstates

By using the techniques developed previously we can now understand the electromagnetic properties of the eigenstates of the SDI. Let us apply $Q(\lambda\mu)$ the electric-multipole operator of order 2^λ on the ground state of a nucleus with $v_g = 0$ and 2 particles

$$Q(\lambda\mu)(S_+)|0\rangle = [Q(\lambda\mu),\ S_+]|0\rangle \tag{142}$$

By writing $Q(\lambda\mu)$ in the form (122) we obtain

$$[Q(\lambda\mu), S_+] = \left[\sum_{ab} \frac{\langle a\|q^\lambda\|b\rangle}{\sqrt{2\lambda+1}} V(ab\lambda\mu), S_+\right] \tag{143}$$

$$= -\sum_{ab} \frac{\langle a\|q^\lambda\|b\rangle}{\sqrt{2\lambda+1}} (-1)^{\ell_b} A^\dagger(ab\lambda\mu) \tag{144}$$

$$= C^t \sum_{ab} \frac{h_\lambda(ab)}{\sqrt{2\lambda+1}} (-1)^{\ell_b} A^\dagger(ab\lambda\mu) = C^t \mathscr{A}^\dagger(\lambda\mu)$$

We identify here

$$\langle a\|q^\lambda\|b\rangle = C^t h_\lambda(ab) \tag{145}$$

by assuming all the radial matrix elements to be equal. We have under these conditions:

$$\langle \alpha v_g = 2|Q(\lambda\mu)|v_g = 0\rangle = C^t\langle\alpha v_g = 2|\alpha_0 v_g = 2\rangle = C^t\delta_{\alpha\alpha_0} \tag{146}$$

where α_0 is the collective state

$$|\alpha_0 v_g = 2\rangle = \mathscr{A}^\dagger(\lambda\mu)|0\rangle \tag{147}$$

Equation (146) proves, for each λ, that only the collective state carries all the electromagnetic strength to the ground state for $N = 2$. To show that it applies also to a more general N, we must remind that $Q(2\mu)$ is time-reversal invariant; therefore, because of Eq.(129), it is a quasi-spin vector. Let us then apply the Wigner–Eckart theorem

$$\langle \alpha v_g = 2S_0|Q(\lambda\mu)|v_g = 0S_0\rangle = \frac{\langle\alpha v_g = 2\|Q(\lambda\mu)\|v_g = 0\rangle}{\sqrt{\Omega-1}}$$

$$\times \left\langle \frac{\Omega}{2} 1 \frac{N-\Omega}{2} 0 \Big| \frac{\Omega-2}{2} \frac{N-\Omega}{2}\right\rangle \tag{148}$$

The reduced matrix element appearing in Eq.(148) can be calculated by considering the case $N = 2$, this is enough to proof that the left-hand side of Eq.(148) is zero if α is different from α_0. Of course, the magnitude of the matrix element corresponding to α_0 depends on N through the Clebsch–Gordan coefficient.

Since there is a single state which exhausts all the electromagnetic quadrupole sum rule this suggests a strong similarity of our model with the vibrational model, the collective 2^+ state playing for each nucleus the role of the "one-phonon state", the non-collective states being in some way the intrinsic states. This is not only true for the quadrupole vibration, but for any 2^λ-pole vibration. We now want to see whether this analogy can be pushed further ahead, and if there exist some two-phonon states.

Let us construct the state:

$$[Q(2) \times Q(2)]_M^I |v_g = 0\rangle \tag{149}$$

The operator $[Q \times Q]^I$ is not an irreducible tensor under quasi-spin transformations, it is still a sum of a scalar plus a vector plus a tensor. In other words, the state (149) has not a well defined generalized seniority but it is a sum of $v_g = 0$ (for $I = 0$ only), $v_g = 2$ (for the proper values of I) and $v_g = 4$. Because of this there cannot exist a pure two-phonon state, the first 2^+ must be coupled to $v_g = 2$ and to $v_g = 4$ states, as well, by the electromagnetic operator.

Expanding $[Q \times Q]^I$ in tensors we now have

$$[Q \times Q]_M^I = [Q \times Q]_{M,0}^{I,\,0} + [Q \times Q]_{M,0}^{I,\,1} + [Q \times Q]_{M,0}^{I,2} \tag{150}$$

The problem with which we are now faced is to examine whether the states

$$\mathcal{N}_I^{-\frac{1}{2}} [Q \times Q]_{M,0}^{1,1 \text{ or } 2} \, \big| v_g = 0 \big\rangle \tag{151}$$

are eigenstates of W_{SDI} which belong to the subspace $\big| v_g = 2 \big\rangle$ or $\big| v_g = 4 \big\rangle$ for the possible values of $I : I \leq 4$. In Eq. (151) $\mathcal{N}_I^{-\frac{1}{2}}$ is the norm of each of these states.

This problem has been answered numerically. We have calculated the overlaps

$$x_I = \mathcal{N}_I^{-\frac{1}{2}} \big\langle \alpha \, v_g = 4 \, IM \, \big| \, [Q(2) \times Q(2)]_M^I \, \big| v_g = 0 \big\rangle_N \tag{152}$$

of the states (149) with all the eigenstates which come out from the exact diagonalization of W_{SDI} : $\big| \alpha v_g = 4 IM \big\rangle$. In this case, the dependence on the number of particles can be extracted very easily, it is only necessary to calculate this overlap for $N = 4$.

We present here the results[2] for $\left(\dfrac{1}{2} \dfrac{3}{2} \dfrac{5}{2} \right)^4$, a more complete discussion can be found in Ref. [23].

In this case there are 58 states having $J \leq 4$. Our results show that among the $v_g = 4$ states the first 2^+ and the first 4^+ have a very strong overlap with our state (151), while the second $v_g = 4$ 0^+ state presents also such a large overlap according to the following table:

I	x_I^2
0	0.95
2	0.95
4	0.99

The two-phonon approximation is seen to be very good as far as the properties of the wave functions are concerned. However, the energies do not follow any simple rule, they are not twice the excitation energy of the first 2^+. Let us now consider the case of the odd-nuclei system. The wave functions of the seniority-one levels are given by

$$a_{jm}^\dagger (S_+)^{\frac{N-1}{2}} \big| 0 \big\rangle \tag{153}$$

---

[2] If 2_1 denotes the first 2_+, the quantity x_1 is such that

$$x_1^2 = \frac{B(E2\ 2_1 \to \alpha\, v_g = 4IM)}{\sum_\beta (BE\ 2\, 2_1 \to \beta\, v_g = 4IM)}$$

We now want to see whether there are among the states of seniority three also some states which are collective. By analogy with the weak-coupling model of the nucleus we construct the states:

$$[Q(2) \times a_j^\dagger]_m^{\mathcal{L}} \, (S_+)^{\frac{N-1}{2}} \, |0\rangle \tag{154}$$

They are constructed in the same way as the one-phonon-plus-one-particle states.

As before, these states do not have a well defined generalized seniority, they can be linear combinations of $v_g = 1$ and $v_g = 3$. We can also look at the projection of the shell-model state which results from an exact diagonalization onto the part of state (154) which has $v_g = 3$ and which is properly normalized. This part is seen to be quite important for very few states [14].

We thus see that the SDI has some very interesting features. The interaction and the electromagnetic transition operators are effective only for a few number of states. This scheme is also a very approximated one, if one uses a slightly more sophisticated model, for example, by smearing out the interaction over the surface, and by introducing single-particle energies splitting, all these features will be affected. We must expect, for example, that the quadrupole sum rule of all the electromagnetic transitions which go to the ground state will not be condensed in a single-state anymore. This is really what happens when such a calculation is carried out [23]. But anyway the general trends of the solution should be the same as the one which we have studied.

5. THE QUASI-PARTICLE METHOD FOR SCALAR INTERACTIONS

In this section we apply the quasi-particle method to those interactions which are, like the surface delta interaction or the pairing force, diagonal in the generalized seniority representation. We can do that with the hope that afterwards we shall understand these approximations much better since we have a soluble model. There we can compare the results of the approximations with the exact results and see what we are doing.

As a general remark let us consider the set of all the wave functions which have the same v_g and the same set of quantum numbers except the number of particles. Let us, for example, consider the set of $v_g = 0$ states:

$$|0\rangle, \ S_+|0\rangle, \ S_+^2|0\rangle, \ \ldots\ldots, \ (S_+)^{\frac{N}{2}} \, |0\rangle \ldots \ldots (S_+)^\Omega \, |0\rangle \tag{155}$$

or the set of $v_g = 4$ states, generated by an operator $B_{JM}^{\alpha\dagger}$ which satisfies Eq. (74):

$$B_{JM}^{\alpha\dagger}|0\rangle, \ S_+ B_{JM}^{\alpha\dagger}|0\rangle, \ (S_+)^2 B_{JM}^{\alpha\dagger}|0\rangle \ldots \ldots (S_+)^{\Omega-2} B_{JM}^{\alpha\dagger}|0\rangle \tag{156}$$

Of course, any of the state (155) is an eigenstate of the SDI and the operator $B_{JM}^{\alpha\dagger}$ can always be chosen in such a way that all states of Eq. (156) are eigenstates of W_{SDI}. Let $E_0(N)$ the ground-state energy, $\epsilon_{\alpha J}$ the excitation energy of the states $B_{JM}^{\alpha\dagger}|0\rangle$ so that the absolute energy of the more general state of Eq. (156) satisfies

$$E_{\alpha J} = E_0(N) + \epsilon_{\alpha J} \tag{157}$$

Let us now consider the Hamiltonian deduced from H by subtracting the dependence on N

$$\mathscr{H} = H - E_0(N) \tag{158}$$

The reasoning can be used for a pairing force, for a SDI, as well as for any interaction or Hamiltonian which is diagonal in a v_g representation. In the case of the pairing force we have

$$\mathscr{H} = - G \left(S^2 - \frac{\Omega}{2} \left(\frac{\Omega}{2} + 1 \right) \right) \tag{159}$$

just because of Eq. (115).
On the other hand, we have for the SDI, because of Eq. (134)

$$\mathscr{H} = y_0^0 \,(\text{SDI}) + \tfrac{1}{2} G \Omega^2 \tag{160}$$

Note that in both of these cases these terms are not simply equal to the scalar parts of the interactions but contain some other terms due to the existence of the special terms y_0^1 or y_0^2 corresponding to these forces. But now we are sure that we have for any N

$$\mathscr{H} \, | v_g = 0 \rangle = 0 \tag{161}$$

Of course, the states (155) and (156) are also eigenstates of $\mathscr{H}$, but they have now the same energy. Any linear combination of them will have the same property. In particular, if we consider a given value of $N = N_0$ and choose a combination of, for example, the states (156)

$$| \Psi_{N_0}^\alpha \rangle = \sum_N C_{NN_0} B_{JM}^{\alpha\dagger} (S_+)^{\frac{N}{2}-2} \, |0\rangle \tag{162}$$

which satisfies

$$\langle \Psi_{N_0}^\alpha \, | \, \hat{N} \, | \Psi_{N_0}^\alpha \rangle = N_0 \tag{163}$$

by properly choosing the coefficients C_{NN_0}, it will have also the same eigenvalue

$$\mathscr{H} | \Psi_{N_0}^\alpha \rangle = \epsilon_{\alpha J} | \Psi_{N_0}^\alpha \rangle \tag{164}$$

Moreover, if P_{N_0} denotes the projection operator on the space with $\hat{N} = N_0$ we have

$$P_{N_0} | \Psi_{N_0}^\alpha \rangle = C_{NN_0} B_{JM}^{\alpha\dagger} (S_+)^{\frac{N_0}{2}-2} \, |0\rangle \tag{165}$$

This is just, within a normalization constant, an eigenstate of $\mathscr{H}$ for $N = N_0$.

Let us now show that the Bogolyubov–Valatin canonical transformation is just such an operation; a rotation in the quasi-spin space. Note that we have taken as the axis of quantization the axis where S_0 is diagonal, this corresponds to having a fixed number of particles. But we can choose any

other axis of quantization as well, for example, that corresponding to the operator

$$S_0^! = \cos\theta \, S_0 + \sin\theta \, \frac{S_+ + S_-}{2} \tag{166}$$

where θ is a parameter.
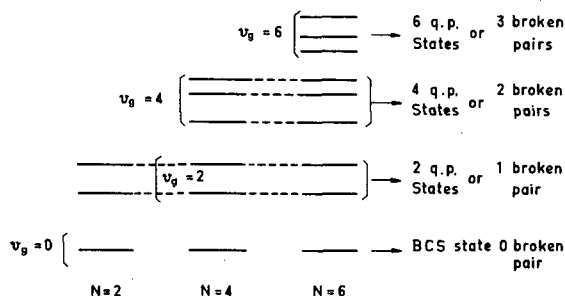
FIG.4.   Schematic illustration of the spectrum of $\mathcal{H} = H - E_0(N)$ where H is a generalized seniority-conserving Hamiltonian. States belonging to the same representations in different nuclei are degenerate. A rotation in the quasi-spin-space mixes all the states of the same representation according to Eq.(187). The resulting states are called zero-quasi-particle states (the BCS wave function), and respectively 2, 4, 6 etc... quasi-particle states.

We have performed here a rotation of our axis and we could use the representation where S^2 and $S_0^!$ are diagonal. This is just what is done in the Bogolyubov–Valatin method. See the schematic explanation in Fig.4. Let us define a quasi-particle creation operator by

$$d_{jm}^\dagger = \bar{u}_j \, a_{jm}^\dagger + \bar{v}_j \, (-1)^{j+m} \, a_{j-m} \tag{167}$$

and let d_{jm} be the associated annihilation operator. The operation defined in relation (167) combines a $\frac{1}{2}\frac{1}{2}$ tensor with a $\frac{1}{2} - \frac{1}{2}$ tensor in the quasi-spin space. Moreover, it satisfies

$$\bar{u}_j^2 + \bar{v}_j^2 = 1 \tag{168}$$

in order to satisfy the anticommutation relations. Therefore, this transformation is a rotation through a certain angle carried out by the quasi-spin generators.

We know that we have $a_{jm}^\dagger |0\rangle = 0$ and $d_{jm} |\bar{0}\rangle = 0$ where $|\bar{0}\rangle$ is the vacuum for the operators d_{jm}. The rotation which is identical to the Bogolyubov–Valatin canonical transformation can be found to be a rotation around the y-axis in the quasi-spin space of an angle θ_j related to $\bar{u}_j$ and $\bar{v}_j$ by

$$\bar{u}_j = \cos\tfrac{1}{2}\theta_j \, , \quad \bar{v}_j = \sin\tfrac{1}{2}\theta_j \tag{169}$$

The operator generating the rotation is just

$$U_j = \exp\left(i\,(-1)^{\ell_j}\,\theta_j\,S_y^j\right) \tag{170}$$

It satisfies

$$d^\dagger_{jm} = U_j \, a^\dagger_{jm} \, U^{-1}_j \tag{171}$$

$$d_{jm} = U_j \, a_{jm} \, U^{-1}_j \tag{172}$$

but each $a^\dagger_{jm}$ has to be rotated, therefore the total transformation is

$$U = \prod_j U_j = U_a U_b \ldots U_r \tag{173}$$

or

$$U = \exp \left(i \sum_j (-1)^{\ell_j} \theta_j S^j_y \right) \tag{174}$$

This is a product of rotations, it preserves the seniority quantum number but not the generalized seniority quantum number. If we want such a transformation to preserve this number we must impose:

$$\theta_j = C^t \text{ independent of } j \tag{175}$$

then:

$$U = \exp (i \theta S_y) \tag{176}$$

and thus we have for the square of the quasi-spin

$$[S^2, U] = 0 \tag{177}$$

In this transformation we obtain

$$|\bar{0}\rangle = U |0\rangle \tag{178}$$

By expanding $U|0\rangle$ and by using $S_y = (S_+ - S_-)/2i$ we see that $U|0\rangle$ can also be written as

$$U|0\rangle = \sum_N C_N(\theta) (S_+)^{\frac{N}{2}} |0\rangle \tag{179}$$

where the sum over N extends from $N = 0$ to $N = 2\Omega$.

Up to now θ, or $\bar{v}$ and $\bar{u}$, have not yet been determined. In the BCS theory one imposes the condition

$$\langle \bar{0} | \hat{N} | \bar{0} \rangle = N_0 \tag{180}$$

if we are interested in a nucleus with $N = N_0$. This condition is satisfied if we have

$$\sum_k (2j_k + 1) \bar{v}^2_k = N_0 \tag{181}$$

But since all $\tilde{v}_k$ are equal we obtain

$$\tilde{v}^2 = \frac{N_0}{2\Omega} \tag{182}$$

This fixes the $C_N(\theta)$ unambiguously. If we use U to transform the component S_0 we find:

$$U S_0 U^{-1} = U\left(\frac{\hat{N} - \Omega}{2}\right) U^{-1} = \frac{\hat{\mathcal{N}}_{qp} - \Omega}{2} \tag{183}$$

the action of U is to make the transformations $a^\dagger \to d^\dagger$, $a \to d$. Then we have $\hat{N} \to \hat{\mathcal{N}}_{qp}$, the operator number of quasi particles:

$$\hat{\mathcal{N}}_{qp} = \sum_{jm} d^\dagger_{jm} d_{jm} \tag{184}$$

The right-hand side of Eq. (183) may also be written

$$\frac{\hat{\mathcal{N}}_{qp} - \Omega}{2} = \cos\theta\, S_0 + \sin\theta\, \frac{S_+ + S_-}{2} \tag{185}$$

This transformation, thus, changes the component S_0 into a rotated component S_0'. It transforms also a state having a fixed number of particles into a state having a fixed number of quasi-particles. But because of relation (177), if the state has a given value of the generalized seniority quantum number before the transformation, its value is not affected by the transformation.

We thus can write the transformation of a state having ν particles as

$$\left|\alpha S S_0' = \frac{\nu - \Omega}{2}\right\rangle_\theta = e^{i\theta S} y \left|\alpha S S_0 = \frac{\nu - \Omega}{2}\right\rangle \tag{186}$$

$$= \sum_{\nu'} \mathcal{D}^S_{S_0' S_0}(0, \theta, 0)\left|\alpha S S_0 = \frac{\nu' - \Omega}{2}\right\rangle \tag{187}$$

Expression (187) is just equivalent to expressions (162) or (179). However, the coefficients $C_N(\theta)$ or C_{NN_0} are just taken here as a rotation matrix corresponding to the Euler's angles: $\alpha = 0$, $\beta = \theta$, $\gamma = 0$. According to its expressions the state (186) has ν quasi-particles, it is obtained by rotating a state with ν particles (by replacing in the second-quantized expression of this state any creation operator of a particle by a creation operator of a quasi-particle); the average value of $\hat{N}$ to which it corresponds [9] is obtained by taking

$$\sin^2\frac{\theta}{2} = \frac{N_0 - v_g}{2\Omega - v_g} \tag{188}$$

Its expansion in the N-particle subspace is given by Eq. (187), and finally its generalized seniority is the same as that which corresponds to the states from which we started.

For a given S or v_g we can generate, by starting from different values of ν and using Eq. (186), $(2S+1)$ states having a number of quasi-particles in the limits $-S \leq S'_0 \leq +S$, or

$$v_g \leq \nu \leq 2\Omega - v_g \tag{189}$$

By choosing θ properly as in Eq. (188) we obtain the same average value, N_0, for the number of particles. It is possible to show that not all these states are physical ones [9]. Indeed, if we project out a state like (186) on the space with N_0 particles we find that there is a single state, to one which has

$$\nu = v_g \tag{190}$$

which has a non-zero projection. All the states having $\nu = v_g = 2$, $v_g = 4, \ldots$ $2\Omega - v_g$ quasi-particles are thus completely irrelevant for the problem of N_0 particles which we are considering.

In this way, one understands better the Bogolyubov-Valatin or the quasi-particle method. If we construct the complete basis of states

$$\left| \alpha S = \frac{\Omega - v_g}{2} \quad S'_0 = -S \right\rangle_\theta \tag{191}$$

having v_g quasi-particles, this basis will give the exact energies of the states having an eigenvalue of the generalized seniority quantum number equal to v_g. This, of course, is true only if we use $\mathscr{H}$.

Then a projection on the state having $N = N_0$ gives the exact wave function.

The quasi-particle method is seen to be very convenient for interactions which do not contain any terms not diagonal in the generalized seniority representation.

Since this method is used for all the interactions it is very interesting to see whether these interactions contain large terms which are able to introduce admixtures. This will be done in the following. For more details on the application of the BCS method see Professor Pal's contribution to these Proceedings.

6.   GENERALIZED SENIORITY BREAKING OF TWO-BODY INTERACTIONS

6.1.   The symmetry-breaking terms

We have shown in chapter 2 that a two-body force can be expanded in three terms as follows:

$$W = y_0^0 + y_0^1 + y_0^2 \tag{192}$$

Our first aim is now to carry out such an expansion for a general two-body force and to evaluate the relative magnitude of each of its terms. The answer to this problem has been known for quite a while in the case of $(j)^N$ configurations [13 - 24]. In this case there is no problem about y_0^1 which is proportional to $\hat{N}$ and, therefore, is diagonal in the representation. The only question is to calculate the matrix elements of y_0^2 in terms of the two-body interaction matrix elements. Before giving the results, we must

point out that the knowledge of y_0^2 does not necessarily provide the matrix elements of the seniority-breaking part of the force. Indeed, by considering Eq. (111), we see that some tensor terms and also some vector terms can be diagonal.

This is due to the fact, already pointed previously by Ichimura [25] and Arima and Ichimura [26], that further quantum numbers can be used to classify the operators.

Indeed, if we consider the generators of the symplectic group in 2Ω dimensions: $Sp(2\Omega)$, they can be expressed simply in terms of the operators V_0^0 (ab JM) and only in terms of these operators which are quasi spin scalars. Therefore, the two groups commute. We can classify then the operators according to the direct product $Sp(2\Omega) \otimes SU_2$, where SU_2 is the quasi-spin group. If T is any operator, which could be an irreducible tensor with respect to the quasi-spin rotations, one can expand it, in turn, in terms of irreducible tensors with respect to the transformations of $Sp(2\Omega)$. If $[\sigma] = [\sigma_1 \sigma_2 \ldots \sigma_\Omega]$ is the label of the irreducible representations of $Sp(2\Omega)$ one has then

$$T = \sum_{[\sigma]} T^{[\sigma]} \tag{193}$$

T may contain a scalar part designated by $[00\ldots0]$, which will be diagonal in the generalized seniority representation. Such an expansion can be carried out respectively, for each part of the right-hand side of Eq. (192). It is irrelevant for the first term y_0^0 which may not be a $Sp(2\Omega)$ scalar but which is diagonal since it is a quasi-spin scalar. It is non-trivial for y_0^1 and y_0^2. One finds

$$y_0^1 = y_0^{1[00\ldots0]} + y_0'^1 \tag{194}$$

$$y_0^2 = y_0^{2[00\ldots0]} + y_0'^2 \tag{195}$$

In these two expressions we have isolated only the scalar part under $Sp(2\Omega)$ and we have designated by $y_0'^{1 \text{ or } 2}$ the sums of the other tensors. It can be checked [27] that the expressions for the scalars are

$$y_0^{1\,[00\ldots0]} = \lambda(N - \Omega) = 2\lambda S_0 \tag{196}$$

$$y_0^{2\,[00\ldots0]} = -\overline{G}\sqrt{\frac{2}{3}}\,[\vec{S} \times \vec{S}]_0^2 \tag{197}$$

where $\overline{G}$ and λ are some linear combinations of the matrix elements of the force. Note that these scalar parts are simply identical with the quasi-spin vector and tensor parts of a pairing force, Eq. (111). However, in general, $2\lambda \neq \overline{G}$.

The two-body interaction can now be written in terms of a part which is diagonal in the representation, W_d, and a non-diagonal part as follows:

$$W = W_d + W_{nd} \tag{198}$$

$$W_d = y_0^0 + \lambda(N - \Omega) - \overline{G}\sqrt{\frac{2}{3}}\,(\vec{S} \times \vec{S})_0^2 \tag{199}$$

$$W_{nd} = y_0'^1 + y_0'^2 \tag{200}$$

Equation (199) is similar to the tensor expansion of a pairing force for which $y'^1_0 = y'^2_0 = 0$. This is also the case of the SDI which has the further property $\overline{G} \equiv 0$.

The two terms of W_{nd} are still quasi-spin vectors and tensors, and are, respectively, associated with the selection rules $|\Delta v_g| \leq 2$ and $|\Delta v_g| \leq 4$.

The detailed expressions for the operators y^0_0, y'^1_0, y'^2_0 can be found in Ref.[27]. Let us just discuss in which case one has $y'^2_0 = 0$. By using the notations of Baranger, i.e. with G defined as in expression (12) and F defined as

$$F(abcdJ) = - \sum_{J'} (2J' + 1)W(j_a j_d j_b j_c; J'J) \, G(dabc; J'J) \tag{201}$$

we find that y'^2_0 is expressed only in terms of

$$G^{(2)'}(abcdJ) \equiv \tfrac{1}{3} \left\{ G(abcdJ) - (-1)^{\ell_a + \ell_c} \left[F(abcdJ) + (-1)^{j_c - j_d + J + \ell_c + \ell_d} F(abcdJ) \right] \right\}$$
$$- \tfrac{1}{3} \left[\delta_{ac} \delta_{bd} - \delta_{J0} (-1)^{\ell_a + \ell_c} \sqrt{\Omega_a \Omega_c} \right] \overline{G} \tag{202}$$

where $\overline{G}$, which appears also in Eq.(198), is defined as

$$\overline{G} \equiv \frac{1}{\Omega(1-\Omega)} \sum_{ab} (-1)^{\ell_a + \ell_b} \sqrt{\Omega_a \Omega_b} \left[G(aabb0) - (-1)^{\ell_a + \ell_b} 2F(aabbo) \right] \tag{203}$$

Note that the combination of G and F which appears in $\overline{G}$ is just the same as in the first term of Eq.(202). If this particular combination vanished for any abcd and J, then $G^{(2)'}(abcdJ) = 0$ and $y'^2_0 = 0$. This cancellation happens for all the forces which satisfy $y^2_0 = 0$ like those considered in chapter 3. But now we have a more general criterion if

$$G^{(2)'}(abcdJ) \equiv 0 \tag{204}$$

for all quadruplets abcd and J; we have now a necessary and sufficient condition to cancel the part of the interaction which connects v_g to $v_g \pm 4$.

Note that all the levels inside our space appear through $\overline{G}$. On the other hand, y'^1_0 can be expressed as:

$$y'^1_0 = \sum_a \left[\sum_b \sqrt{\frac{\Omega_b}{\Omega_a}} \, F(aabb0) \right] \left(\hat{N} \frac{\Omega_a}{\Omega} - \hat{N}_a \right) \tag{205}$$

It seems more difficult to annulate the coefficients appearing in Eq.(205). Those are self-energy terms which are important in the Hartree-Fock theory. However, if

$$\sum_b \sqrt{\frac{\Omega_b}{\Omega_a}} \, F(aabb0) = C^{\underline{t}} \tag{206}$$

which incidentally is the case for a SDI, we have now $y'^1_0 = 0$.

We must also mention that the symmetry-breaking terms y'^1_0 and y'^2_0 contribute respectively, to the matrix elements which are non-diagonal as well as those which are diagonal in the generalized seniority representation. Since the term y'^2_0 is associated with the least restrictive selection rules, $|\Delta v_g| \leq 4$, it seems to be the most dangerous and should be considered in more detail. We also must mention that if we introduce a splitting between our single-particle levels, the resulting vector term can, in turn, be expanded according to the symplectic group

$$H_{sm} = \sum_a \epsilon_a \hat{N}_a = \sum_a \epsilon_a \left(\hat{N}_a - \hat{N} \frac{\Omega_a}{\Omega} \right) + \sum_a \frac{\epsilon_a \Omega_a}{\Omega} \hat{N} \tag{207}$$

The first term which is similar to relation (205) is the seniority-breaking term, the second term is obviously diagonal. Note that the symmetry-breaking term can be written

$$\sum_a \hat{N}_a \left[\epsilon_a - \sum_a \frac{\epsilon_a \Omega_a}{\Omega} \right] \tag{208}$$

Its effect will depend on the spreading of the single-particle levels with respect to the average value

$$\bar{\epsilon} = \sum_a \epsilon_a \Omega_a / \Omega \tag{209}$$

Let us just examine the problems which arise owing to Eq.(204). It is much simpler to consider the case of a single j-shell. There we must drop the indices abcd..., and, for example, we have

$$F_J = - \sum_{J'} W(jjjj; J'J) G_{J'} \tag{210}$$

Equation (204) can be written

$$\tfrac{1}{3} [G_J - F_J \{1 + (-1)^J\}] - (1 - \Omega \delta_{J0}) \frac{G_0}{1 - \Omega} = 0 \tag{211}$$

for all J. By using Eq.(210) we can write it in the form

$$\sum_{J'} C_{J'J} G_{J'} = 0 \tag{212}$$

All these equations are not independent. The right number of independent equations has to be found for each j. It is found that these equations are satisfied [13] automatically for $j \leq 7/2$. From $j = 9/2$ on, these relations are no more trivial. For $j = 9/2$ it is known [28] that the only independent condition is

$$- 65 G_2 + 315 G_4 - 403 G_6 + 153 G_8 = 0 \tag{213}$$

This relation is satisfied with a good accuracy by the matrix elements deduced from experiment in the zirconium region. It is independent of G_0. It means that there is only a single independent force which violates the seniority symmetry.

The relations (202) are an extension of these results to the generalized seniority symmetry. One has exactly the same problem: to find the number of independent equations from which the number of interactions violating the symmetry can be deduced. See for this problem Ref.[9, 14].

6.2. Estimate of the symmetry-breaking terms

We now assume that a two-body force is given and that the relation $G^{(2)\prime}(abcd) \approx 0$ is not obeyed. We now want to estimate the effect of this breaking.

The first method is to exploit the separation of H into three parts: $H = H_d + y'^1_0 + y'^2_0$ (the single-particle Hamiltonian can be introduced in H_d and y'^1_0 as well) and to calculate the strength of each part. This is a method which has also been suggested by J. B. French [29] and which has also been used in evaluating the importance of each term in a tensor expansion with respect to SU(3) by Vincent [30]. We define the scalar product of two operators V_1, V_2 by

$$\{V_1 \mid V_2\} = \text{Tr} \{V_1^\dagger V_2\} = \sum_{abcdJM} \langle abJM \mid V_1^\dagger \mid cdJM \rangle \langle cdJM \mid V_2 \mid abJM \rangle \tag{214}$$

If $V_1 = V_2 =$ two body interaction, this gives the norm of W, it can be written in terms of the G'_Js.

$$\{W \mid W\} = \sum_{\substack{abcd \\ J}} (2J+1) \frac{4}{(1+\delta_{ab})(1+\delta_{cd})} \{G(abcdJ)\}^2 \tag{215}$$

The sum over the single-particle states spans the space in which the interaction is defined, for example the (s-d) shell. By replacing W successively by W_d, y'^1_0, y'^2_0 one obtains the norm of each of these operators. One can then compare these norms between them and with the norm of W. If one defines

$$\zeta_1^2 = \{y'^1_0 \mid y'^1_0\} / \{W_d \mid W_d\} \tag{216}$$

$$\zeta_2^2 = \{y'^2_0 \mid y'^2_0\} / \{W_d \mid W_d\} \tag{217}$$

and if

$$\zeta_1^2 \ll 1 \tag{218}$$

and

$$\zeta_2^2 \ll 1 \tag{219}$$

one has then an estimate that v_g is a good quantum number. If only the *second inequality is true, i.e. if there are very small matrix elements*

between v_g and $v_g \pm 4$, the interaction has, in this case, the same symmetry as a S D I or a pairing force in a non-degenerate case.

This evaluation of the norm can be criticized for several reasons, in particular, because the trace is limited to the two-particle states. There is no reason for not considering the traces over spaces with N larger. Also it is a sum of square of matrix elements so that it can probably over-estimate the violation for it does not account for accidental cancellation which can appear because of different signs of the $G^{(2)}$'.

TABLE I.   VALUES OF ζ_1^2 AND ζ_2^2 FOR THE INTERACTIONS LISTED IN THE FIRST COLUMN

See Ref.[27] for more details about the interactions.

	ζ_1^2	ζ_2^2
SDI	0	0
Rosenfeld force	0.380	0.004
Auerbach	0.120	0.036
Argonne	0.007	0.010
Kuo (bare)	0.823	0.010
Wigner force	0.133	0.064
Kuo (polarized core)	1.358	0.355
Pairing + quadrupole	0.125	0.271
Pure quadrupole	0.308	0.669

In Ref.[27] a large number of interactions have been studied corres-ponding to particles in the 1p shell as well as to particles in the shell of the Pb isotopes.   From this reference we extract a few results which are typical of the interactions which were considered.   We will take the case of the Ni region in Table I where all kinds of forces have been considered.

We see that for many interactions ζ_1^2 is large while ζ_2^2 is large in a very few cases, mainly when the quadrupole part of the interaction is en-hanced.   The quadrupole force is indeed that force which has by far the largest $y_0'^2$ term.   In the case of realistic force Kuo (bare) and Kuo (polarized core) it is seen that the inclusion of the polarization of the core increases the non-diagonal part $y_0'^2$ which becomes of the same order as in the case of a pairing plus quadrupole force.   Except in these three cases the magnitude of ζ_2^2 is rather small.   It is then very interesting to examine separately the effect of $y_0'^1$ and of $y_0'^2$ on the properties of the system itself.

7.   INFLUENCE OF THE SYMMETRY-BREAKING TERMS

In the preceding sections we have studied the tensor analysis of a general two-body interaction.   We have discussed the properties of the scalar part of the Hamiltonian, and for any interaction we have carried out the tensor expansion.   We now want to see what are the effects of the symmetry-breaking terms on the properties of the system itself.   We shall consider several possibilities of taking into account the symmetry-breaking terms.

7.1. Exact diagonalization

This procedure can, of course, be used, since our single-particle space is finite, and the many-particle basis which is spanned is also finite. Therefore, we can perform an exact shell-model diagonalization (ESM) which consists of:

    (a) constructing the complete set of states for N particles in the r levels,

    (b) calculating the matrix.elements of H in this basis,

    (c) diagonalizing H.

This process must, of course, be carried out numerically, the techniques to construct the basis and the matrix elements are standard shell-model techniques [13 – 18]. The limitation comes from the dimension of the basis and of the matrices. The main groups which have been using these ideas are the Weizmann Institute group, the Argonne and the Oak Ridge groups. The Oak Ridge code is the best at the moment since it can deal with 600×600 matrices.

Many people all around the world have also been constructing shell-model codes, these codes are, however, much more limited than the last two quoted above.

By fulfilling this program one obtains energies and wave functions and can regard the effect of introducing the symmetry-breaking terms. For the identical-particles case one can take a rather large number of particles into account.

Such a program was first investigated by the Argonne group [18]. They have pointed out that v_g is a very bad quantum number while on the contrary $v = \sum_i v_i$ can be very useful for labelling the lowest eigenstates of a two body interaction.

This can be seen from Table II where the only terms in the interaction violating the symmetry are the single-particle energies which have been taken from experiment (^{207}Pb). The spectrum of ^{205}Pb, on the other hand, can be seen from Fig. 5.

It is seen in this table that while the percentage of $v_g = 1$ is very low for the low-lying states the percentage of $v = 1$ is quite high. This is true more generally, the single-particle energy splitting introduces quite a large mixing. On the other hand, among the states of the even or odd

TABLE II. PERCENTAGE OF $v = 1$ AND $v_g = 1$ IN THE WAVE FUNCTIONS OF AN ESM CALCULATION USING   SDI AND NON-DEGENERATE SINGLE-PARTICLE ORBITS FOR ^{205}Pb (See Ref.[22]).
The states in question are the lowest for a given angular momentum j.

j π	Percentage of v = 1	Percentage of v_g = 1
1/2 -	99	71
3/2 -	91	39
5/2 -	97	40
7/2-	0	0.3
13/2+	98	48
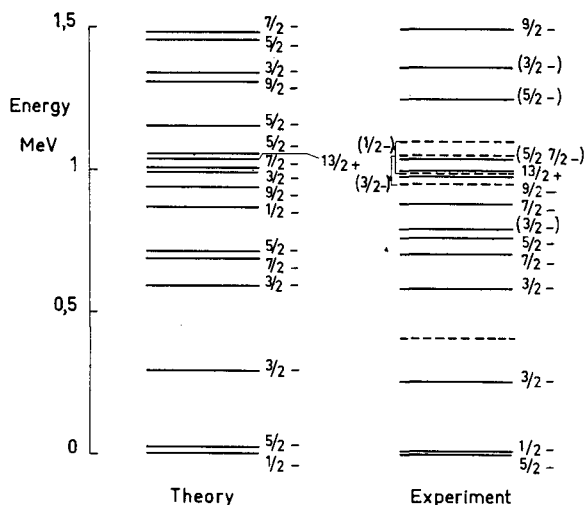
FIG.5. Spectrum of ^{205}Pb, theory and experiment. The theoretical spectrum [22] has been calculated with
S D I and the experimental single-particle spacings of ^{207}Pb. The dashed levels are not well identified.

nuclei, there are always some states which are pure $v = 0$, 1, 2 or even
3 states. We must now look for a study of the violation in an other way
but literally we can assert that v_g is a bad quantum number.

7.2.   The B C S method

An other possibility of calculating the spectra when we have $W_{nd} \neq 0$
will be the use of quasi-particle approximations [3]. These approximations
can be summarized briefly as follows.

(a) Let us define the quasi-particle annihilation and creation opera-
tors as in Eq.(167) and define the rotation operator U with θ_j depending
on the states j as in Eq.(174).

(b) Let us define the vacuum associated with these operators $|\tilde{0}\rangle$ and
consider it to be a trial wave function. The parameters $\bar{u}_j$, $\bar{v}_j$, or equi-
valently θ_j, are then determined by satisfying the two minimization
conditions

$$\delta \langle \tilde{0} | H | \tilde{0} \rangle = 0 \tag{218}$$

$$\langle \tilde{0} | \hat{N} | \tilde{0} \rangle = N_0 \tag{219}$$

These two steps constitute the B C S method or the Bogolyubov-Valatin
method. It defines a new state $|\tilde{0}\rangle$ having, on the average, N_0 particles
which is in a way analogous to the $v_g = 0$ state. When the interaction is
taken purely as W_d, the discussion of chapter 4 has shown that it is a
combination of all the $v_g = 0$ states for all the values of N.

This state can be also written in the B C S form [3]

$$|\tilde{0}\rangle = \pi_{jm}(\bar{u}_j + \bar{v}_j \, (-1)^{j+m} \, a_{jm}^\dagger a_{j-m}^\dagger)|0\rangle \tag{220}$$

The projection of that state onto the subspace having N_0 particles does not have $v_g = 0$. However, if $\theta_j \neq C^t$, one can show that

$$P_{N_0} |\tilde{0}\rangle = C^t \left(\sum_i \frac{\tilde{v}_i}{\tilde{u}_i} \sqrt{2\Omega_i} A_0^{i\dagger} \right)^{\frac{N}{2}} |0\rangle \tag{221}$$

This is identical with a $v_g = 0$ only if $\tilde{v}_i / \tilde{u}_i = C^t$, which implies a very special BCS wave function. This solution is obtained for the operator W_d; however, more generally, if W_{nd} is present, $\tilde{v}_i$ and $\tilde{u}_i$ are not constant.

7.3. Discussion of the BCS method

This method has been applied now for 10 years in nuclear physics and it has been found to be very successful. One has been using $|\tilde{0}\rangle$ or its N_0-projection as approximations to the ground state. We must retain that this BCS wave function
1) has $v = 0$, independently of the $\tilde{v}$ and $\tilde{u}$.
2) does not have $v_g = 0$, but is built in the same way as the $v_g = 0$ wave function, i.e. as a product of pairs.

This method was initiated in the theory of superconductivity where no relationship was set up with the seniority quantum number. Though the method has been used for a long time in nuclear physics, it was not pointed out until recently [26 - 27] that the method is based on the assumption that the term W_d should be much larger than W_{nd}.

If the generalized seniority symmetry is not invoked it is very difficult to understand why expression (221) should be a very good approximation in many cases, and above all why it contains so few parameters.

It is well-known that the complete basis of an exact shell-model calculation can be extremely large. If no particular symmetry is assumed for the Hamiltonian or some of its part, it is very difficult to imagine approximate solutions. To emphasize this point, let us consider only the calculation of 0^+ states in the single-closed-shell isotopes. To simplify the problem, we will consider only the basis having $v = \sum_i v_i = 0$ which is appropriate for a pairing force.

If one considers first ^{62}Ni which has six particles and take only 3 single-particle levels we obtain, for example, nine states with $v = 0$; these states have the form

$$\left| (2p1/2)_{v=0}^{n_1} (2p3/2)_{v=0}^{n_2} (1f5/2)_{v=0}^{n_3} \right\rangle \tag{222}$$

with $n_1 + n_2 + n_3 = 6$.

If we take ^{116}Sn with five subshells the basis is

$$\left| (2d5/2)_{v=0}^{n_1} (1g7/2)_{v=0}^{n_2} (3s1/2)_{v=0}^{n_3} (2d3/2)_{v=0}^{n_4} (1h11/2)_{v=0}^{n_5} \right\rangle \tag{223}$$

with $n_1 + n_2 + \ldots + n_5 = 16$. We then obtain 110 states. This means that in the first case we have nine parameters in the wave functions while we have 110 in the last case!

There is no such freedom in the BCS wave function which has only two parameters for Ni and four parameters in Sn. Since this wave function is still limited to the $v = 0$ subspace we may expect it to be quite a poor

approximation to the real ground state. However, it was found, first by Kerman Lawson and MacFarlane [16] for the pairing force, then by many other authors [18] who used the pairing force or even other interactions, that this wave function is extremely good. In a work on Sn isotopes [7] it was shown that overlaps as large as 0.992 could be obtained by comparing the exact wave function with the N_0-projected BCS state.

Such good overlaps could not be obtained if the real wave function did not have a pair structure as in the BCS state. Such a structure is provided by the part of the interaction diagonal in the generalized seniority representations, i.e. by W_d. It is seen that a possible effect of the symmetry-breaking terms is to keep the memory of this symmetry and just to change the weight of the pairs in the operator which now plays the role of S_+ (Cooper pair).

With this in mind we can say that symmetry is preserved. This is true for single-particle spacings and interaction strengths which are close to the values needed for a reproduction of experimental results. If the spacings (208) are very large the BCS wave function cannot be so good any longer.

It is quite interesting now to see the results for this overlap if we change the interaction and consider forces with quite a large variety of tensor terms $y_0^{1'}$ and $y_0^{2'}$.

This is shown in the Figs 6 and 7. In these figures one sees a clear relationship between the value of the number ζ_2^2 which we have taken as a measure of the symmetry breaking, and the "goodness" of the PBCS wave function. As ζ_2^2 increases the overlap decreases because the tensor term introduces components in the wave functions which are lacking, for example, components having $v_g = 4$, $v_g = 6$ etc.... which are more and more important. A small value of ζ_2^2 or of ζ_1^2 does not necessarily mean that v_g is conserved, it means, however, that the structure of the wave function is that which has been predicted by considering the $v_g = 0$ wave function.

We have, however, to define what we mean by ζ_2^2 being small. By considering the examples [8] of Table III we see that small ζ_2^2 does not mean the same thing for all interactions. The overlap is larger for a pairing force than for Kuo's matrix elements while the ζ_2^2 are the other way round. Also the pairing plus quadrupole force gives approximately the same result for a very different value of the ζ_2^2. The case of the Kuo's interaction can, however, be explained by the large value of ζ_1^2.

The evaluation of ζ_2^2 is, on the one hand, a very clear indication that there is a connection between the tensor part of the force and the structure of the exact wave function. On the other hand, the results of Table III show that it is certainly difficult to define a value of ζ_2^2 for which one can be sure that this structure is fixed. The measurement of the violation by ζ_2^2 certainly gives a rough estimate of the symmetry violation; other criteria have to be studied.

7.4. One-quasi-particle states in odd nuclei

In the quasi-particle theory an elementary excitation can be defined as

$$d_{jm}^\dagger |\bar{0}\rangle \qquad\qquad (224)$$

It carries an angular momentum j with component m. In the quasi-particle
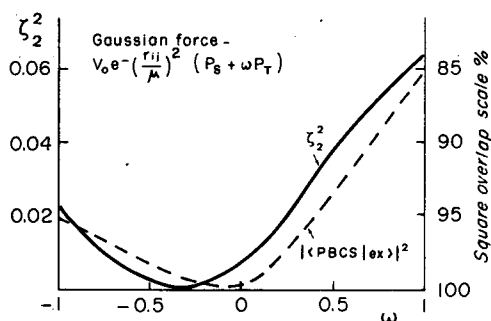
FIG.6. Magnitude of the tensor term, for a Gaussian force, measured by the coefficient ζ_2^2 defined by Eq.(216) of the text and by the overlap $|<\Psi_{exact}\,|\,\Psi_{PBCS}>|^2$.
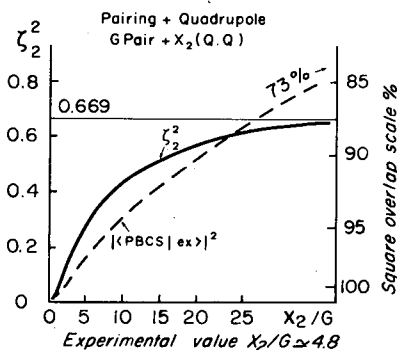
FIG.7. Magnitude of tensor term for a pairing plus quadrupole force as a function of the intensity of the quadrupole part.

formalism, the excitation energy of this state can be calculated [3]. We shall consider here only the structure of the wave function which is implied by definition (224) by studying its N-projection.

Let us introduce the new pair operator

$$\rho_+ = \sum_j{}' \frac{\tilde{v}_j}{\tilde{u}_j} \sqrt{\Omega_j}\, A_0^{j\dagger} \tag{225}$$

the N-projected wave function of the operator (225) is now seen to be

$$a_{jm}^\dagger\,(\rho_+)^{\frac{N-1}{2}}\,|\,0\,\rangle \tag{226}$$

it has a structure similar to the $v_g = 1$ states, Eq.(70). With that in mind we can analyse the structure of the exact wave function of, for example, ^{205}Pb. This is done in Table IV.

We see here that the weights of the seniority-one states are nearly independent of the angular momenta of the hole. Therefore, the concept of a pair holds in this case, too. Owing to the large seniority-conserving part of the two-body force we obtain a very special configuration mixing

TABLE III. EXAMPLES FROM REF.[8]

	ζ_2^2	Projection	ζ_1^2
Pairing + quadrupole	0.271	0.96	0.125
Argonne	0.036	0.95	0.007
Auerbach	0.010	0.97	0.036
Kuo (polarized core)	0.355	0.78	1.358

TABLE IV. STRUCTURE OF ^{206}Pb AND ^{205}Pb

Nucleus	State	$(p1/2)_0^{-2}$	$(f5/2)_0^{-2}$	$(p3/2)_0^{-2}$	$(i13/2)_0^{-2}$	$(f5/2)_0^{-2}$	% v=1	R^2
^{206}Pb	0_1^+	0.794	0.256	0.437	0.161	-0.295		
^{205}Pb	$1/2^-$	-	0.379	0.807	0.202	-0.392	98.9	97.6
	$3/2^-$	0.828	0.141	0.363	0.130	-0.244	91.4	99.0
	$5/2^-$	0.866	0.215	0.301	0.136	-0.249	96.6	98.4
	$13/2^+$	0.815	0.241	0.415	0.150	-0.248	97.8	99.9

Note: First line: seniority-zero components of the ground-state wave function of ^{206}Pb. Other lines: seniority-one components of the lowest states in ^{205}Pb. Eighth column: percentage of seniority one; last column: square overlap, in percent, of the wave function of ^{205}Pb with the ground-state wave function of ^{206}Pb plus a hole in a state j. The interaction used is a S D I [22].

of v = 1 states which is almost independent of the additional hole in the gound state of ^{206}Pb.

Note the pair corresponding to j = 1/2 is not the same. This is due to the fact that the largest component in S_+ corresponds to $(p1/2)^{-2}$. Adding a further hole in the state $(1/2)^{-1}$ is not allowed by the Pauli principle. Therefore, the pair should redistribute itself among the levels in the best possible way. This has been called the blocking effect.

Note also that the $7/2^-$ state is not present in that table although we have taken into account the f7/2 level. Indeed the $7/2^-$ is not found at low energy. Since it is much lower in the potential well it has a higher excitation energy. Therefore the state

$$a_{7/2}(\rho_-)|0\rangle \qquad\qquad (227)$$

should lie higher in Eq.(227); $|0\rangle$ denotes the ground state of the nucleus ^{208}Pb. Therefore, one must use ρ_- instead of ρ_+ where $\rho_- = (\rho_+)^+$. It will then lie near other states having v = 3 and it must interact with them. This state should then be distributed among many other $7/2^-$ levels (see Fig. 8).

Therefore, the concept of a quasi-particle excitation is essentially the same as the concept of generalized seniority-one state. This concept holds with the same accuracy in other nuclei [22] where such an analysis of the structure of the wave function has been made, for example, in ^{59}Ni, ^{211}At. What is necessary for this concept to be valid? The example of ^{205}Pb and of the state $f7/2^-$ shows that it is not sufficient that the two-body interaction contains a large W_d and y'_0^1 is small. We require also that the generalized seniority-one state should be well separated from those of
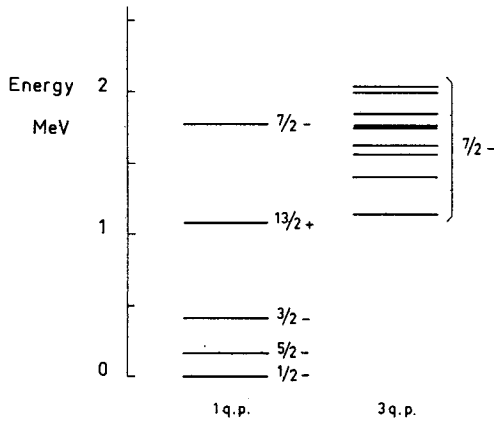
FIG.8.   Comparison of the one-quasi-particle and three-quasi-particle spectrum in ^{205}Pb. On the left-hand side the one-quasi-particle levels are plotted. On the right-hand side, the position of the three-quasi-particle energies calculated at the lowest order for $j = 7/2^-$. It is obvious then that a quasi-particle $7/2^-$ cannot exist. The interaction is a SDI.

generalized seniority three. This is an extra condition which depends on the interaction as well as on the single-particle energies. No work has yet been done on the influence of these two parameters on the overlaps as we have done for the ground-state wave functions. We know, however, that this concept is meaningful since it is so successful when a comparison is made with experiment [10].

7.5.   Several quasi-particle states

In the quasi-particle theory one can construct excited states having any number of quasi-particles. For this purpose one uses exactly the same techniques as for constructing states of a given number of particles. For example, a two-quasi-particle state of angular momentum J can be defined as

$$| (ab)\, JM \rangle = \sum_{m_a m_b} \langle j_a j_b m_a m_b | JM \rangle\, d^+_{am_a} d^+_{bm_b} \, | \tilde{0} \rangle \qquad (228)$$

By allowing the set (ab) to run over all the two-single-particle levels one constructs the complete set of two quasi-particles. This set can be used to diagonalize the total Hamiltonian according to a method called the Tamm-Dancoff method [15]. Let P be the matrix

$$P^{(J)}_{ab,\, cd} = \langle ab\, JM | H | cd\, JM \rangle \qquad (229)$$

of H in this two-quasi-particle space. The eigenvalues of P and its eigenvalues can be taken as approximate eigenvalues and eigenstates of H for the nucleus having N_0 particles. This method has been used with moderate success in the past [33]. From the discussion of chapter 4 we see that this method is exact if $H \equiv W_d$; in this case a diagonalization of P is exactly equivalent to a diagonalization of H in the $v_g = 2$ basis. If $W_{nd} \neq 0$ the method is no longer exact. Projecting out states (228) with the operator P_{N_0} we find

$$P_{N_0} \left| (ab) \, JM \right\rangle = A^+ (ab \, JM) \, S_+^{\frac{N-2}{2}} \left| 0 \right\rangle \tag{230}$$

i.e. the two-quasi-particle states are one broken-pair states (for $J = 0$, a special case, see Ref. [9]).

The Tamm-Dancoff method can be applied to odd nuclei by taking into account $1 + 3 + $ etc... quasi-particles or to even nuclei by taking $0 + 2 + 4 + $ etc... quasi-particles. There a slight generalization of the method is used. The number of quasi-particles is no longer considered to be a good quantum number. This is an idea similar to that of mixing states having $v_g = 1$, 3 etc. or $v_g = 0$, 2, 4 etc... Such methods, more complex than the one-quasi-particle or the two-quasi-particle methods have been applied in the past [34-35].

Another possibility is to operate, for example, directly in the basis (230), i.e. to diagonalize H in a one-broken-pair basis or, more generally, one can use a basis having zero $+ 1 + 2 + $ etc... broken pairs. This method has been developed recently by Lorazo [7, 8].

It is a very interesting question to ask in which case the mixing between states having a different number of broken pairs is important. From the work of Ref. [8] we see that two things play an important role:

(a) the magnitude of W_d, or, separately, of y'^1_0 and y'^2_0.

(b) the unperturbed energy differences of states having a different v_g. For example, for a pairing force, states of different v_g are quite far apart. On the other hand, for a SDI some states having $v_g = 2$ are degenerate with the states having $v_g = 4$ (Fig. 3). In this case, even a small non-diagonal term in the interaction can introduce important admixtures of the two states. The method can, however, be used provided there is not a large admixture between states differing by a large number of broken pairs. In ^{60}Ni, for example, and for the 0^+ excited states, Lorazo has shown that one must include $1 + 2 + 3$ broken-pair states in the lowest excited states. This is as complicated as the exact result in this case. However, if these results were valid for another region, for example, in the Sn-isotope region, it would still be of some interest.

The quasi-particle method is discussed in greater detail in Professor Pal's contribution to these Proceedings.

7.   SUMMARY

In the preceding chapters we have shown that the exact model of a pairing force or of a SDI are very useful for an understanding of the exact methods or the approximations of the shell model. We have considered the symmetry properties of these interactions in greater detail. We have shown that for any general interaction we can isolate a part in the interaction which has this same symmetry, and a part which violates the symmetry. The relative magnitude of these parts have been tentatively estimated as well as the effect on the structure of the wave function. It has been shown that this symmetry-breaking part must be small in order that the approximation method as, e.g. the BCS method can be applied with some confidence.

We should like to point out that, with ζ_1^2 and ζ_2^2, we certainly have a very broad idea of the symmetry breaking. Other ways of measuring it

have to be found in the future. On the other hand, we have found that the symmetry-breaking terms can conserve the structure of the wave functions as well as the elementary-excitation modes of the system with good approximation. Thus, the generalized seniority-zero wave function is a product of pairs, the same as the B C S wave function. This is a very new way of introducing symmetry-breaking effects.

The same kind of discussion has to be made for other symmetry groups, for example, for the SU_3 group, and for deformed nuclei as has also been proposed by French [31]. This remains to be done in the future.

I would like to thank O. Bohigas, B. Lorazo and C. Quesne for their collaboration and for many critical comments during this work.

REFERENCES

[1] GREEN, I.M., MOSZKOWSKI, S.A., Phys. Rev. 139B (1965) 790.

[2] ARVIEU, R., MOSZKOWSKI, S.A., Phys. Rev. 145 (1966) 830.

[3] BELYAEV, S.T., K. danske Vidensk. Selsk. Mat.-fys. Meddr 31 No.11 (1959).

[4] PLASTINO, A., ARVIEU, R., MOSZKOWSKI, S.A., Phys. Rev. 145 (1966) 837.

[5] LETOURNEUX, J., EISENBERG, J.M., Nucl. Phys. 85 (1966) 119.

[6] GLAUDEMANS, P.W.M., WILDENTHAL, B.H., McGRORY, J.B., Phys. Lett.21 (1966) 427.

[7] LORAZO, B., Thèse 3ème cycle (avril 1968) Orsay.

[8] LORAZO, B., Phys. Lett. 29B (1969) 150.

[9] ARVIEU, R., Institut d'Etudes Scientifiques de Cargèse, September 1968, (to be published).

[10] KISSLINGER, L.S., SORENSEN, R.A., K. danske Vidensk. Selsk., Mat.-fys. Meddr, 32 No.9 (1960)
Rev. mod. Phys. 35 (1963) 854.

[11] WONG, S.S.M., DAVIES, R., Phys. Letts 28B (1968) 77.

[12] MORINAGA, H., Phys. Rev. 101 (1956) 254; BRINK, D.M., NASH, G.F., Nucl. Phys. 40 (1963) 608;
BROWN, G.E., C. r. Congr. Int. de Physique Nucléaire, Paris (1964) 129.

[13] DE SHALIT, A., TALMI, I., Nuclear Shell Theory, Academic Press, New York, London (1963).

[14] QUESNE, C., Thèse, Université Libre de Bruxelles (1968).

[15] BARANGER, M., Phys. Rev. 120 (1960) 957.

[16] KERMAN, A.K., LAWSON, R.D., MACFARLANE, M.H., Phys. Rev. 124 (1961) 162.

[17] LAWSON, R.D., MACFARLANE, M.H., Nucl. Phys. 66 (1965) 80.

[18] MACFARLANE, M.H., in Lectures in Theoretical Physics, Univ. of Colorado Press, Boulder (1966) 621.

[19] KERMAN, A.K., Ann. Phys. 12 (1961) 300.

[20] LAWSON, R.D., MACFARLANE, M.H., Nucl. Phys. 66 (1965) 80.

[21] BRINK, D.M., SATCHLER, G.R., Angular Momentum, Clarendon Press, Oxford, 149.

[22] QUESNE, C., BOHIGAS, O., ARVIEU, R. (to be published).

[23] ARVIEU, R., MOSZKOWSKI, S.A., Nucl. Phys. 114 (1968) 161.

[24] RACAH, G., TALMI, I., Physica 18 (1952) 1097; FRENCH, J.B., Nucl. Phys. 15 (1960) 393.

[25] ICHIMURA, M., Progress in Nuclear Physics (to be published).

[26] ARIMA, A., ICHIMURA, M., Prog. Theor. Phys. 36 (1966) 296.

[27] BOHIGAS, O., QUESNE, C., ARVIEU, R., Phys. Letts 26B (1968) 562.

[28] COHEN, S., LAWSON, R.D., MACFARLANE, M.H., SOGA, M., Phys. Letts.10 (1964) 196.

[29] FRENCH, J.B., Phys. Letts 26B (1967) 75.

[30] VINCENT, C.M., Nucl. Phys. A106 (1968) 35.

[31] FRENCH, J.B., Phys. Letts, 26B (1967) 75.

[32] ARVIEU, R., BOHIGAS, O., LORAZO, B., QUESNE, C., in Dubna publication D-3893 (Nuclear
Structure Symp. 1968) 167.

[33] ARVIEU, R., BARANGER, E., VENERONI, M., BARANGER, M., GILLET, V., Phys. Letts 4 (1963) 119.

[34] KUO, T.T.S., BARANGER, E.U., BARANGER, M., Nuclear Phys. 79 (1966) 513.

[35] OTTAVIANI, P.L., SAVOIA, M., SAWICKI, J., TOMASINI, A., Phys. Rev.153 (1967) 1138;
ALZETTA, R., GAMBHIR, Y.K., GMITRO, M., RIMINI, A., SAWICKI, J., WEBER, T., Trieste
IC/68/83.
PAL, M.K., GAMBHIR, Y.K., RAJ, Ram, Phys. Rev. 155 (1967) 1144.

THEORY OF NUCLEAR VIBRATION

M.K. PAL
Saha Institute of Nuclear Physics,
Calcutta, India

Abstract

THEORY OF NUCLEAR VIBRATION.
1. Introduction and outline; 2. General theory of vibration; 3. Derivation of nuclear vibrational
equations; 4. General microscopic theory, quasi-particle mode; 5. Microscopic theory; vibrational
mode; 6. Review of applications of the theory.

1. INTRODUCTION AND OUTLINE

The subject matter of this contribution is the phenomenon of nuclear
vibration. The topic is also discussed in these Proceedings by Z. Szymański,
and G. Alaga. We shall, therefore, avoid going into many of the phenomeno-
logical details, and shall concern ourselves mostly with a microscopic
description of the phenomenon.

The nucleus is a many-body system, consisting of nucleons moving in
an average potential field, and interacting weakly through a residual inter-
action. It is obvious that such a many-body system will have excited states
corresponding to the excitation of one or a few particles. This type of
excitation mode of the nucleus is well-known near closed shells. There is
an altogether different kind of excitation mode of a many-body system – a
mode in which many particles participate in a coherent manner. Such a mode
is well-known in the many-electron problem, where one gets a coherent
plasma mode of oscillation. Similar oscillation modes have also been observed
in nuclei; as a matter of fact, we have a very rich variety here, distinguished
from each other through the angular momentum (J), the parity (π), and the
isospin (T) of the phonon associated with the vibrational mode.

The most important nuclear vibrations, classified in this manner, are:
(1) the giant dipole oscillation ($J^\pi = 1^-$, T = 1), (2) the quadrupole vibration
(2^+, T = 0), and (3) the octupole vibration (3^-, T = 0).

For theoretical purposes it is convenient to classify the vibrational
states according to the type of nuclei to which they belong. In this way we
have the theory of vibration of (1) closed-shell nuclei, (2) spherical non-
closed-shell nuclei, and (3) deformed nuclei, which differ from each other
in some details. The basic concepts, as outlined below, are, however, the
same for all these different cases.

The single-particle level schemes for the three different cases and the
highest occupied level (Fermi level) λ have been shown in Fig. 1.1. In the
case of the closed-shell nucleus the level immediately above λ is separated
from it by a large interval (the spacing between two shells), and hence
excitation of a nucleon from the occupied levels (below and up to the level λ)
to the lowest unoccupied one requires a fairly large amount of energy. The
ground state, therefore, is a fairly good closed-shell state having an occupa-
tion probability P, below and above λ, as depicted in Fig. 1.2a. The state
obtained by exciting a nucleon from an occupied level to an unoccupied level
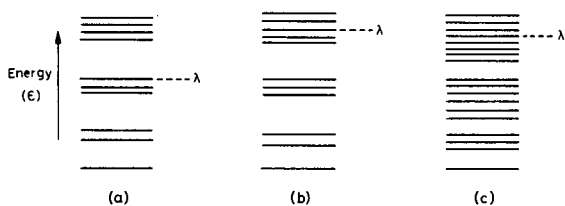
FIG.1.1. Single-particle level schemes in different types of nuclei: (a) closed-shell nuclei, (b) non-closed-shell spherical nuclei, (c) deformed nuclei. The level denotes the highest occupied state.
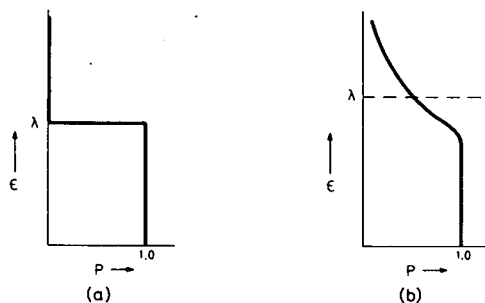
FIG.1.2. Probability of occupation of single-particle states: (a) closed-shell nuclei, (b) non-closed shell spherical and deformed nuclei.

is usually called a state of the one-hole, one-particle (1 hp) type, because in this process of excitation a vacancy (hole) is left in the occupied level and a "particle" is produced, instead, in one of the unoccupied levels. This type of excitation is a possible elementary mode of excitation of a closed-shell nucleus, and such a mode has an energy very nearly equal to the separation of the two shells at the top of the Fermi-sea. However, if we let each of the nucleons in the Fermi-sea get excited in turn above the sea, we have a whole set of 1 hp-type states of the closed-shell nucleus. The question is: can these independent particle modes of the different Fermi-sea nucleons act coherently and build up a collective type of excitation mode? We shall see in this paper that the answer to this question is affirmative, and the resultant coherent state is a vibrational state of the closed-shell nucleus. The exact meaning of the word "vibration" in this context will be made more quantitative as we go along.

Let us now go back to Figs 1.1b, 1.1c, and 1.2b and examine what happens in the case of non-closed-shell spherical and deformed nuclei. The only difference between these two cases is in the nature of the single-particle states. In the case of spherical nuclei [Fig. 1.1b] the states are labelled by the quantum numbers $(n\ell jm)$, and the separation between the major shells is still large. On the other hand, the single-particle states of the deformed nuclei [Fig. 1.1c] are superpositions of several sets of $(n\ell jm)$; for axially symmetric nuclei only m is a good quantum number. In this case, the levels belonging to various major shells also come closer to each other, and can even penetrate into each other for a large deformation. The main point of our interest, at the present moment, is what occurs near the Fermi level λ. In both cases, there are several single-particle energy levels which crowd

together in this energy region. As a consequence, our picture of a sharp
Fermi-sea as the ground state of these nuclei is bound to be rather poor.
Since it costs very little energy to promote a nucleon from the Fermi-sea
to one of these crowded levels immediately above λ, we expect that the ground
state will contain such excitations making the occupation probability of levels
immediately below and above λ depart from their ideal values, 1 and 0,
respectively. This picture of the ground-state having a diffuse single-particle
probability distribution is shown in Fig. 1.2b. Since the ground state is
already somewhat complicated for these nuclei, it is not immediately obvious
what sort of elementary excitations will take place in them. We shall show
in these lectures that it is still possible to find approximately the elementary
excitation modes called "quasi-particles", of such a system. In this approx-
imate theory, the ground state of Fig. 1.2b will be characterized by the
absence of any quasi-particle; the states of odd-mass and even nuclei will
correspond, respectively, to an odd and even number of quasi-particles.
For an even nucleus, the elementary excitation modes of the lowest energies
will thus correspond to a _pair_ of quasi-particles. This is very much analogous
to the hp _pair_ excitation mode of a closed-shell nucleus. Therefore, in a
similar manner one can build up a microscopic theory of vibration correspond-
ing to Fig. 1.2b by the coherent superposition of quasi-particle pair states.
This, in synopsis, is the main idea behind the microscopic theory which we
shall develop in this paper.

The microscopic picture of vibration, as outlined above, apparently
seems rather far-fetched from the classical picture of vibration, which
consists of a certain dynamical variable oscillating as a function of time.
In reality, however, there is an underlying link between these pictures, and
one of our aims in this paper will be to preserve this link as much as possible.
We shall see that the nuclear vibrational state which is a coherent super-
position of many elementary excitation modes of the hole-particle (or pair-
of-quasi-particles) type corresponds to a single-particle density variable
that indeed oscillates with time. The equation of motion for the oscillating
density and the system of linear equations that connect the elementary
excitation modes are exactly identical.

In the papers on Hartree-Fock (HF) theory in these Proceedings, we have
seen that the single-particle density is self-consistently connected to the average
nuclear field. Therefore, the oscillations that we are dealing with can equivalently
be looked upon as oscillations of the average HF-potential. We should keep in mind,
however, that this kind of vibration does not exhaust all the possibilities for a
nucleus. One example of states corresponding to vibrations of an other kind of
dynamical variables is discussed elsewhere in these Proceedings; this is the case
of pairing vibrations, qualitatively described by G. Alaga, and treated in detail
by G. Ripka. The dynamical quantity that vibrates here is the pairing density, or,
equivalently, the pairing potential.

We shall begin by describing several general methods of treating
vibration. All these methods have been applied by various authors in
deriving the equations for nuclear vibrations. Needless to say that the final
equations one derives are independent of the method used. In these lectures
we shall present this derivation in two different ways. The first will be
a time-dependent treatment, and will contain the semi-classical picture
of an oscillating density distribution; the second derivation will be more
formal, and based on the transformation of the Hamiltonian of the many-
body system to a form that clearly shows which is the part responsible for

the vibrations, and then what is left over after such a treatment. The second method, therefore, allows a natural extension, which enables one to incorporate the effects of the residual parts of the Hamiltonian. Such an extension has the consequence of giving rise to anharmonic effects in nuclear vibration. There is ample experimental evidence of such anharmonicity in the nuclear quadrupole vibration.

In the last two lectures we shall describe the application of the theory to the vibrational states in: (1) closed-shell nuclei, (2) spherical non-closed-shell nuclei, and (3) deformed nuclei. A survey of what is to come may not be out of place here.

(1) Closed-shell nuclei: The nuclei that have been treated exhaustively by many authors are ^{16}O, ^{40}Ca, and ^{208}Pb. In all these nuclei, the giant dipole resonance states ($J^\pi = 1^-$, $T = 1$), and the octupole states ($J^\pi = 3^-$, $T = 0$) have been very well reproduced by the theory based on 1 hp type excitations. The agreement of the transition strength in the case of the octupole states is very good, while there are some minor discrepancies for the giant dipole states. The latter states are around 20-25 MeV in the lighter nuclei, while in ^{208}Pb they are in the neighbourhood of 14-15 MeV. It has been found recently that, for these states, the excitation of a nucleon to the continuum states is also important; an extension of the kind of theory which we shall describe here, so as to incorporate the effect of the continuum states are described by C. Mahaux in his contribution to these Proceedings. The octupole states are very strongly collective, have a large E3-transition probability to the ground state, and are very low-lying in energy. The type of theory which we shall derive is very much suited for a description of these two features. For a time, there were many calculations on the 2^+, $T = 0$ states in closed-shell nuclei using the same method based on 1 hp-excitations. However, it is now conclusively established that it is difficult to get a low-lying 2^+ state by this method. Experimentally also, the low-lying 2^+ states of the closed-shell nuclei are found to have very little collective vibrational character – the E2-transition strength connecting such a state to the ground state is rather small. The most enigmatic state in the closed-shell nuclei (and also many spherical even nuclei) is the low-lying 0^+ state. In the early calculations on the vibrational states, a 1 hp-type character was also unsuccessfully attributed to this state. However, the experimentally observed small transition strength to the ground state rules out such a treatment of the 0^+ state. In ^{16}O and ^{40}Ca this state has been established to have a deformation, even though the ground states are spherical. ^{208}Pb, however, is a very stable closed-shell nucleus, and does not tend to acquire a deformation in any low-lying excited state. The 0^+ state in this nucleus is now understood to be a member of the chain of levels in the Pb-region connected to each other by the pairing vibration. In ^{16}O and ^{40}Ca, besides the 0^+ state, there are other states which correspond to a deformed shape.

(2) Spherical non-closed shell nuclei: In contrast to the closed-shell nuclei, these nuclei have a strongly collective quadrupole vibrational level (2^+), as their first excited state. The octupole level (3^-) has also been observed in many of these nuclei. The main points of interest in these nuclei now centre around the group of excited states above the first excited 2^+. For an ideal harmonic quadrupole vibrator one should expect the two-phonon triplet (0^+, 2^+, 4^+) at roughly double the energy of the first 2^+. Experimental data on most of these nuclei depart from this ideal situation. There is no

regularity in the order and magnitude of the splitting in energy of the triplet; sometimes a member of the triplet may be missing; more often there are several extra levels in the vicinity of the triplet. For an ideal harmonic vibrator the second 2^+ level should decay to the first 2^+ by an E2 (no M1) transition, and there should be no cross-over transition to the ground state. The quadrupole moment of the first excited state (2^+) should also be zero under the ideal circumstances. In many cases there is considerable departure from all these idealized expectations. All these properties of the spherical non-closed shell nuclei are, at the present time, a challenge to the theorist. In this paper, we shall develop a theory for these vibrational nuclei, based on the excitation of quasi-particle pairs; extension of the formalism to include four quasi-particle excitations will also be considered. Such an extended theory will be applied to several nuclei and the fit to the experimental data will be discussed. The situation will be seen to be not yet very satisfactory. Of special importance amongst these nuclei are those which belong to the transitional regions. A word of explanation is needed about this nomenclature. It is well known that nuclei in several mass regions have a deformed equilibrium shape. Amongst the nuclei along the stability line there are three such well-marked regions: (a) s-d shell nuclei below ^{28}Si, (b) rare-earth nuclei in the mass-range $145 \leqslant A \leqslant 185$, and (c) nuclei of the actinide region having $A \geqslant 226$. Besides these nuclei, there are other regions off the stability line where equilibrium deformation is expected and has been found in several cases: these are the neutron-deficient regions with both Z and N lying in the interval 28 to 50 or from 50 to 82, and the neutron-rich region for $28 < Z < 50$ and $50 < N < 82$. The spherical nuclei at both ends of these regions of deformation are said to belong to the transitional region. For these nuclei, the departure from an ideal vibrator or rotator is considerable. We shall leave these special nuclei out of consideration in this paper; K. Kumar's paper later in this course will be mainly devoted to them.

　　(3) Deformed nuclei: In these nuclei the levels near the ground state belong to a rotational band. However, they exhibit excited states of the vibrational type, the most important ones being the quadrupole β- and γ-vibrational states, and the octupole vibrational states. In deformed nuclei the phonon of the vibration does not, strictly speaking, have a definite angular momentum; yet it is customary to talk of these vibrational states as "quadrupole" or "octupole" in keeping with a semiclassical picture of the shape oscillation of the nucleus starting from an equilibrium prolate spherical shape. When the prolate spheroid remains a prolate spheroid, and only its degree of deformation changes in course of the oscillation, we have the β-vibration; the projection quantum number is zero for such a vibration, and hence the lowest state of this type is 0^+. Similarly, when the prolate spheroid keeps its deformation parameter the same, but acquires a littly bit of a triaxial shape during the course of oscillation we have a γ-vibration with projection quantum number and parity equal to 2^+, which turns out to be the lowest γ-vibrational state. When the deformed shape during the oscillation is of the octupole type, we may have states with projection 0^-, 1^-, 2^-, 3^-, all of which comprise the octupole vibrational states. In this paper, we shall be very sketchy about the vibrational states of deformed nuclei. Detailed references will be given at the end to the original work by Soloviev et al.

2.   GENERAL THEORY OF VIBRATION
2.1.   Elementary treatment by Schrödinger equation

If the force acting on a body, when the body is displaced from its position of equilibrium, is proportional to its displacement and is directed towards its equilibrium position, then the motion executed by the body under such a force of restitution is a harmonic oscillation about its point of equilibrium. This is the classical definition of harmonic vibration. If the displacement is α, and C the so-called "spring constant" then the potential energy is given by

$$V(\alpha) = \frac{1}{2}\,C\alpha^2$$

while the kinetic energy, in terms of the mass parameter B, is

$$T = \frac{1}{2}\,B\dot{\alpha}^2$$

The dot on the top of α denotes time-derivative. The momentum π is given by

$$\pi = \frac{\partial T}{\partial \dot{\alpha}} = B\dot{\alpha}$$

and hence the Hamiltonian of the oscillator is

$$H(\alpha, \pi) = T + V(\alpha) = \frac{\pi^2}{2B} + \frac{1}{2}C\alpha^2 \tag{2.1}$$

Classically, the oscillatory motion has a frequency ω, given by

$$\omega = \left(\frac{C}{B}\right)^{\frac{1}{2}} \tag{2.2}$$

To quantize the motion of the oscillator, one has to require the usual canonical commutation rule:

$$[\alpha, \pi] = i\hbar \tag{2.3}$$

In the Schrödinger representation we have

$$\pi = -i\hbar\,\frac{\partial}{\partial \alpha}$$

and hence the equation of motion, the standard Schrödinger equation, is given by

$$H\phi(\alpha) = E\phi(\alpha)$$

or

$$\left(-\frac{\hbar^2}{2B}\frac{\partial^2}{\partial \alpha^2} + \frac{1}{2}C\alpha^2\right)\phi(\alpha) = E\phi(\alpha) \tag{2.4}$$

This equation, as is well known, has well-behaved solutions for the following eigenvalues of energy:

$$E_n = \left(n + \frac{1}{2}\right)\hbar\omega, \quad n = 0, 1, 2, \dots. \tag{2.5a}$$

and the corresponding wave function $\phi_n(\alpha)$ is given by

$$\phi_n(\alpha) = H_n(\alpha/b)\, e^{-\frac{1}{2}\alpha^2/b^2} \tag{2.5b}$$

where the harmonic oscillator parameter

$$b = (\hbar/B\omega)^{\frac{1}{2}}$$

makes the co-ordinate α dimensionless, and H_n is the Hermite polynomial. All this is very standard and given in any elementary textbook on quantum mechanics.

The difficulty of applying this straightforward method to the phenomenon of nuclear vibration is the following: the nucleus is a many-body system, and hence it is difficult to identify the variable α for nuclear vibration. Several workers tried to identify such collective vibrational co-ordinates in terms of the co-ordinates of the individual nucleons, but this fundamental program is almost impossible to carry out except for certain simplified two-dimensional models. In a less fundamental approach one may take the variable α to be one or few deformation parameters, specifying the shape of the nuclear surface or equivalently that of the average potential V (see section 3 for details). The task that remains after this is to obtain an expression for V as a function of α, and T as a function of $\dot{\alpha}$. The latter defines the mass parameter B, and the former defines the spring constant C for small vibrations about the equilibrium shape. To understand the last statement let us take a general potential energy function $V(\alpha)$ and expand it in a Taylor series about the equilibrium point α_0. For simplicity, let us shift the origin to α_0, and keep on denoting $\alpha-\alpha_0$ by the old variable α. Then

$$V(\alpha) = V(0) + \left(\frac{dV}{d\alpha}\right)_0 \alpha + \frac{1}{2}\left(\frac{d^2V}{d\alpha^2}\right)_0 \alpha^2 + \dots \tag{2.6}$$

where the zeros imply that the quantities have to be evaluated at the equilibrium point. From the definition of equilibrium, $V(\alpha)$ has a minimum at α_0 and hence $(dV/d\alpha)_0$ is zero. Thus

$$V(\alpha) = V(0) + \frac{1}{2}C\alpha^2 + \dots. \tag{2.7a}$$

where

$$C = \left(\frac{d^2V}{d\alpha^2}\right)_0 \tag{2.7b}$$

Therefore, to this order of approximation, we obtain a harmonic vibration. The inclusion of higher terms in the expansion (2.6) makes the vibration anharmonic.

The program outlined above can be carried out for some models. One such case will be described in section 3. In general, it is difficult to cast the mathematics in the above form if one wants to work with a very general type of many-body Hamiltonian.

2.2. Commutator method

A. In its simplest form this method consists of looking for an operator $Q^\dagger$, whose commutator with the Hamiltonian H is a numerical multiple of itself, i.e.,

$$[H, Q^\dagger] = \hbar\omega Q^\dagger \qquad (2.8)$$

where $\hbar\omega$ is a number. This equation automatically guarantees (take the Hermitean conjugate and reverse the sign)

$$[H, Q] = -\hbar\omega Q \qquad (2.9)$$

Without any loss of generality we may assume $\hbar\omega$ to be positive; because, if it is not, then $-\hbar\omega$ is, and hence all that is necessary is to reverse the roles of Q and $Q^\dagger$.

Now, if Ψ is an eigenfunction of H belonging to the eigenvalue E then Eq. (2.8) guarantees that $Q^\dagger\Psi$ is also an eigenfunction of H belonging to the eigenvalue $E + \hbar\omega$. The proof follows:
Given

$$H\Psi = E\Psi$$

Eq. (2.8) ensures

$$HQ^\dagger\Psi - Q^\dagger H\Psi = \hbar\omega Q^\dagger\Psi$$

or

$$H(Q^\dagger\Psi) - E(Q^\dagger\Psi) = \hbar\omega Q^\dagger\Psi$$

or

$$H(Q^\dagger\Psi) = (E + \hbar\omega)(Q^\dagger\Psi)$$

which proves the required result. In a similar manner, one can prove, with the help of Eq. (2.9),

$$H(Q\Psi) = (E - \hbar\omega)(Q\Psi)$$

Thus $Q^\dagger$ acts as the step-up operator for energy, and Q as the step-down operator. In particular, if Ψ_0 denotes the ground state of H, then

$$Q\Psi_0 = 0 \qquad (2.10)$$

because $Q\Psi_0$ would have to have an energy lower than that of the ground state by $\hbar\omega$, which is, by definition of the ground state, impossible.

It is clear that the method, described so far, is applicable to any Hamiltonian, and not necessarily to that of an oscillator. We have found that for any general Hamiltonian if $Q^\dagger$, as defined by Eq. (2.8), exists, the spectrum of H is given by

$$E_n = E_0 + n\hbar\omega, \quad n = 0, 1, 2, \ldots \tag{2.11}$$

Clearly, it is impossible to know what E_0 is without specifying the Hamiltonian H in detail.

B. We now generalize the commutator method in the following manner. Suppose we have found a set of operators $A_i^\dagger$ ($i = 1, 2, \ldots, N$) which satisfy

$$[H, A_i^\dagger] = \sum_{j=1}^{N} M_{ji} A_j^\dagger = (\widetilde{M}A^\dagger)_i \tag{2.12}$$

for each $i = 1, 2, \ldots, N$. M is a numerical matrix and $\widetilde{M}$ is its transposed. Can we then say anything about the spectrum of H?

To answer this question we first diagonalize the matrix M, and find its eigenvalues ϵ_α ($\alpha = 1, 2, \ldots, N$) and the $X^{(\alpha)}$, corresponding eigenvectors X^α, having components $X_2^{(\alpha)}, \ldots, X_N^{(\alpha)}$. By definition

$$\sum_{j=1}^{N} M_{ij} X_j^{(\alpha)} = \epsilon_\alpha X_i^{(\alpha)}, \quad i = 1, 2, \ldots, N \tag{2.13}$$

Let us now construct the following operators with these eigenvectors:

$$Q_\alpha^\dagger = \sum_{i=1}^{N} X_i^{(\alpha)} A_i^\dagger, \quad \alpha = 1, 2, \ldots, N \tag{2.14}$$

We substitute Eqs (2.12) and (2.13) into the following commutator and obtain:

$$[H, Q_\alpha^\dagger] = \sum_{i=1}^{N} X_i^{(\alpha)} [H, A_i^\dagger]$$

$$= \sum_{j=1}^{N} \left\{ \sum_{i=1}^{N} M_{ji} X_i^{(\alpha)} \right\} A_j^\dagger$$

$$= \epsilon_\alpha \sum_{j=1}^{N} X_j^{(\alpha)} A_j^\dagger = \epsilon_\alpha Q_\alpha^\dagger \tag{2.15}$$

Comparing this expression with results proved in subsection A, we conclude that in the present case there is a set of step-up operators $Q_\alpha^\dagger$, $\alpha = 1, 2, \ldots, N$, which step up the energy by ϵ_α. The corresponding Hermitian conjugate operators Q_α will step down the energy by ϵ_α, and acting on the ground state Ψ_0 of H they will produce a zero result:

$$Q_\alpha \Psi_0 = 0, \quad \alpha = 1, 2, \ldots, N \tag{2.16}$$

Below we demonstrate a simple application of this method for solving the harmonic-oscillator problem, defined by the Hamiltonian (2.1). Using the canonical commutation relation (2.3) we obtain

$$[H, \alpha] = -\frac{i\hbar}{B}\pi \tag{2.17a}$$

$$[H, \pi] = i\hbar C\alpha = i\hbar B\omega^2\alpha \tag{2.17b}$$

These equations can be compared with the general system of linear relations defined by Eq. (2.12). Therefore, as proved there, we diagonalize the transposed of the coefficient matrix:

$$M = \begin{pmatrix} 0 & i\hbar B\omega^2 \\ -\frac{i\hbar}{B} & 0 \end{pmatrix} \tag{2.18}$$

The eigenvalues ϵ are solutions of the secular equation

$$0 = \begin{vmatrix} -\epsilon & i\hbar B\omega^2 \\ -\frac{i\hbar}{B} & -\epsilon \end{vmatrix} = \epsilon^2 - (\hbar\omega)^2$$

or

$$\epsilon = \pm\hbar\omega \tag{2.19}$$

Let us recall our earlier statement in subsection A that we would like to associate the positive quantity $\hbar\omega$ with the operator $Q^\dagger$. Hence, we consider the case of $\epsilon = +\hbar\omega$, and look for the corresponding $Q^\dagger$. According to the result proved earlier in this subsection we require, for this purpose, the corresponding eigenvector of (2.18). Denoting this vector by

$$X = \begin{pmatrix} X_1 \\ X_2 \end{pmatrix}$$

we obtain from

$$MX = \hbar\omega X$$

the result:

$$i\hbar B\omega^2 X_2 = \hbar\omega X_1$$

or

$$X_2 = -\frac{i}{B\omega} X_1$$

Absorbing X_1 in the overall normalization constant N of the vector we, therefore, obtain

$$Q^\dagger = N\left(\alpha - \frac{i}{B\omega}\pi\right)$$

in accordance with the general result (2.14). We choose the normalization constant N to be $(B\omega/2\hbar)^{\frac{1}{2}}$, which makes $Q^\dagger$ dimensionless and guarantees the following boson commutation rule for Q and $Q^\dagger$:

$$[Q, Q^\dagger] = 1 \qquad\qquad (2.20)$$

The final expressions for Q and $Q^\dagger$ are given by

$$Q^\dagger = \sqrt{\frac{B\omega}{2\hbar}}\left(\alpha - \frac{i}{B\omega}\pi\right) \qquad\qquad (2.21a)$$

$$Q = \sqrt{\frac{B\omega}{2\hbar}}\left(\alpha + \frac{i}{B\omega}\pi\right). \qquad\qquad (2.21b)$$

One can verify Eq. (2.20) by the straightforward use of Eqs (2.21a, b) and (2.3).

In this simple example we have an explicit form for H, given by Eq. (2.1), and it is possible to find E_0, and hence a complete expression for E_n as follows. Using Eqs (2.21a, b) and (2.3), we can show in a straightforward manner that

$$H = \hbar\omega\left(Q^\dagger Q + \frac{1}{2}\right) \qquad\qquad (2.22)$$

Since $Q\Psi_0 = 0$, we obtain from Eq. (2.22)

$$H\Psi_0 = \frac{1}{2}\hbar\omega\,\Psi_0$$

i.e.

$$E_0 = \frac{1}{2}\hbar\omega$$

Therefore

$$E_n = \left(n + \frac{1}{2}\right)\hbar\omega$$

according to the general result (2.11). This result agrees with Eq. (2.5a) as it should.

The general method described in this subsection is very well suited for the treatment of the nuclear Hamiltonian. In view of the general nature of this method it is capable of yielding both the single "quasi-particle"-type as well as the "vibrational"-type solutions of the many-body Hamiltonian. We shall see later on in this paper that H is very conveniently expressed in the second-quantized form. If we use the single-particle creation operators and the destruction operators for $A_i^\dagger$

in the general relation (2.12) then, in general, one does <u>not</u> get a set of linear relations connecting these quantities. The application to the nuclear "quasi-particle" mode, therefore, relies on <u>approximations</u> that reduce these commutators to a set of linear relations for the single-particle creation and destruction operators. In the same way, if one uses the 1 hp creation operators, or the quasi-particle pair creation operators for the $A_i^\dagger$, and introduces suitable approximations to obtain a set of linear relations like (2.12) then the resultant $Q^\dagger$ operators give rise to the so-called vibrational states. It is clear that in both cases we have approximations, and hence in practical applications to nuclei one will have to worry about calculating the corrections, too. We emphasize, therefore, that the general method as described here does not give <u>exact</u> results when applied to the nuclear many-body Hamiltonian, unlike the simple example of the harmonic vibrator, where it produced exact results because the linear relations (2.17a, b) were exact in this latter case.

2.3. Time-dependent treatment

It is possible to rewrite the method of section 2.2B by using a time-dependent formalism. Since one is always prone to picture vibration as the time-dependent oscillatory motion of some dynamical variable, there is a general feeling that the abstract commutator method becomes more physical and more understandable when cast in the new language. Since we want to talk in terms of time-dependent dynamical variables, it will be convenient to use the Heisenberg representation. In this representation the time-independent operator Ω for <u>any</u> dynamical variable of the Schrödinger representation changes to a time-dependent operator $\hat{\Omega}$, defined by

$$\hat{\Omega} = e^{-\frac{i}{\hbar}Ht} \Omega \, e^{\frac{i}{\hbar}Ht} \tag{2.23}$$

which satisfies the following equation of motion:

$$i\hbar \frac{\partial \hat{\Omega}}{\partial t} = [\hat{H}, \hat{\Omega}] \tag{2.24}$$

Of course, the definition (2.23) tells us that $\hat{H}$ and H are the same. If we now require the time-dependence of $\hat{\Omega}$ to be of an oscillatory type, i.e. proportional to $\exp(-i\epsilon t/\hbar)$, then Eq.(2.24) reduces to

$$\epsilon\hat{\Omega} = [\hat{H}, \hat{\Omega}] \tag{2.25}$$

Now let us apply such an equation of motion to H and a set of $A_i^\dagger$ satisfying Eq.(2.12). Because of the unitary nature of the transformation (2.23), it is easy to see that Eq.(2.12) ensures

$$[\hat{H}, \hat{A}_i^\dagger] = \sum_{j=1}^{N} M_{ji} \hat{A}_j^\dagger \tag{2.26}$$

with the same matrix M. Therefore, we have the following set of equations of motion for the time-dependent variables $\hat{A}_i^\dagger$:

$$i\hbar \frac{\partial}{\partial t} \hat{A}_i^\dagger \equiv [\hat{H}, \hat{A}_i^\dagger] = \sum_{j=1}^{N} M_{ji} \hat{A}_j^\dagger = \epsilon \hat{A}_i^\dagger \qquad (2.27)$$

From what has been described above, the equality implied by the last step holds only if $\hat{A}_i$ has an oscillatory time dependence $\exp(-i\epsilon t/\hbar)$. The system of equations (2.27) for $i = 1, 2, \ldots, N$ describe an eigenvalue problem for the matrix M; the eigenvalues define the permitted frequencies ($\hbar^{-1}\epsilon$) of vibration of the dynamical variables. The eigenvectors $X^{(\alpha)}$, $\alpha = 1, 2, \ldots, N$ define a new set of dynamical variables

$$\hat{Q}_\alpha^+ = \sum_{i=1}^{N} X_i^{(\alpha)} \hat{A}_i^\dagger \qquad (2.28)$$

which are, in classical language, the normal co-ordinates of vibration. The allowed frequencies $\omega_\alpha = h^{-1}\epsilon$ are the frequencies of the normal modes of vibration. The time-dependent motion of the old variables $\hat{A}_i^\dagger$, $i = 1, 2, \ldots, N$ were coupled to each other through the matrix M in Eq. (2.27), while the time-dependent motion of the new variables $\hat{Q}_\alpha^\dagger$, the normal co-ordinates, are uncoupled from each other. The following uncoupled equation, satisfied by $Q_\alpha^\dagger$,

$$i\hbar \frac{\partial}{\partial t} \hat{Q}_\alpha^\dagger = \epsilon_\alpha Q_\alpha^\dagger, \quad \alpha = 1, 2, \ldots, N \qquad (2.29)$$

can be easily verified from Eqs (2.27), (2.28) and the definition (2.13) for the eigenvalues of M.

There is a slight lack of rigour in what we have stated under Eq. (2.27). The set of linear equations

$$\sum_{j=1}^{N} M_{ji} x_j = \epsilon x_i, \quad i = 1, 2, \ldots, N \qquad (2.30)$$

can be interpreted as the eigenvalue equations for the matrix M only if the elements $X_1, X_2, \ldots, X_N$ of the eigenvector are scalar numbers. In Eq. (2.27), the quantities playing the role of the elements of the eigenvector were $A_1^\dagger$, $A_2^\dagger$, $\ldots$, $A_N^\dagger$, which were operators. To make our interpretation rigorous we have, therefore, to replace, by some clever device, the operators in Eq. (2.27) by some scalar numbers without spoiling the validity of these equations. The simplest way to do this is to take the matrix elements of this set of equations between two eigenstates $\langle \Psi |$ and $| \Psi_0 \rangle$ of the Hamiltonian H, belonging to the eigenvalues E and E_0, respectively. Then we easily obtain

$$\sum_{j=1}^{N} M_{ji} \langle \Psi | \hat{A}_j^\dagger | \Psi_0 \rangle = \epsilon \langle \Psi | \hat{A}_i^\dagger | \Psi_0 \rangle \qquad (2.31a)$$

which is exactly identical with Eq. (2.30) with the definition

$$x_i = \langle \Psi | \hat{A}_i^\dagger | \Psi_0 \rangle \qquad (2.31b)$$

This quantity gives us the transition amplitude from the state Ψ_0 to the state Ψ through the action of the operator $\hat{A}_i^+$; it can also be interpreted as the probability amplitude of the basis state $A_i^+|\Psi_0\rangle$ in the excited nuclear state $|\Psi\rangle$. The quantity ϵ can be further interpreted by tracing back its origin in Eq. (2.31a), via Eq. (2.27) as follows:

$$\epsilon\langle\Psi|\hat{A}_i^\dagger|\Psi_0\rangle = i\hbar\frac{\partial}{\partial t}\langle\Psi|\hat{A}_i^\dagger|\Psi_0\rangle$$

$$= i\hbar\frac{\partial}{\partial t}\langle\Psi|e^{-\frac{i}{\hbar}Ht}A_i e^{\frac{i}{\hbar}Ht}|\Psi_0\rangle$$

$$= i\hbar\left\{\frac{\partial}{\partial t}\,e^{-\frac{i}{\hbar}(E-E_0)t}\right\}\langle\Psi|A_i|\Psi_0\rangle$$

$$= (E-E_0)e^{-\frac{i}{\hbar}(E-E_0)t}\langle\Psi|A_i|\Psi_0\rangle$$

$$= (E-E_0)\langle\Psi|e^{-\frac{i}{\hbar}Ht}A_i e^{\frac{i}{\hbar}Ht}|\Psi_0\rangle = (E-E_0)\langle\Psi|\hat{A}_i|\Psi_0\rangle$$

Thus, ϵ is the difference in energy between the two nuclear states Ψ and Ψ_0. The above result would have also followed by writing $i\hbar(\partial\hat{A}_i^\dagger/\partial t)$ as $[H, \hat{A}_i^\dagger]$ which is equal to $(\hat{H}\hat{A}_i^\dagger - \hat{A}_i^+\hat{H})$, and then letting $\hat{H}(=H)$ of the two terms operate on the left on $\langle\Psi|$ and on the right on $|\Psi_0\rangle$, respectively.

Now, the set of Eqs (2.31a) is trivially satisfied if all the amplitudes $\langle\Psi|\hat{A}_i^\dagger|\Psi_0\rangle$, $i = 1, 2, \ldots, N$ for given Ψ and Ψ_0 are identically zero. Non-trivial values of these amplitudes correspond to the eigenvectors of $\tilde{M}$ belonging to the various eigenvalues of the latter. Thus, we conclude that we obtain a set of non-trivial amplitudes connecting two nuclear states Ψ_0 and Ψ only if these states differ in energy through an eigenvalue of $\tilde{M}$, which incidentally is the energy of a vibrational quantum. Pairs of nuclear states differing in energy by two or more vibrational quanta will all have the transition amplitudes, $\langle\Psi|\hat{A}_i^\dagger|\Psi_0\rangle$, equal to zero.

It is obvious that the same type of interpretation could have been given also to the time-independent Eqs (2.12), by taking matrix elements between $\langle\Psi|$ and $|\Psi_0\rangle$. The matrix element of the commutator $[H, A_i^\dagger]$ $\equiv (HA_i^\dagger - A_i^\dagger H)$ then brings in $(E-E_0)\langle\Psi|A_i^\dagger|\Psi_0\rangle$ in the manner explained above. We finally get the same set of equations as (2.31a) and (2.31b) with the time-dependent operators replaced everywhere by the corresponding time-independent ones.

3. DERIVATION OF NUCLEAR VIBRATIONAL EQUATIONS

3.1. Phenomenological Vibrational Model

This model is an example of a case where it is possible to carry out the program mentioned at the end of section 2.1 in a straightforward manner. The model is based on the assumption that nuclear vibration consists of the oscillatory motion of a well-defined sharp nuclear surface. If R_0 is the equilibrium value of the nuclear radius, then the radial co-ordinate $R(\theta, \phi)$ of a point on the nuclear surface in the direc-

tion (θ, ϕ) at any given time during the oscillatory motion of the surface is given by the general multiple expansion:

$$R(\theta, \phi) = R_0 \left\{ 1 + \sum_{\lambda=0}^{\infty} \sum_{\mu=-\lambda}^{\lambda} \alpha^*_{\lambda\mu}(t) Y^\lambda_\mu(\theta, \phi) \right\} \tag{3.1}$$

where Y^λ_μ is the normalized spherical harmonic of order λ and projection μ. The time-dependent quantities $\alpha^*_{\lambda\mu}(t)$ define the deformation of the surface; when these quantities oscillate with time, each point on the nuclear surface also performs the same oscillatory motion according to Eq. (3.1).

Taking a hydrodynamical model of the nucleus it is possible to derive the expressions of the kinetic and potential energies of the vibration to the lowest order in $\dot{\alpha}_{\lambda\mu}$ and $\alpha_{\lambda\mu}$. These expressions are given by Alaga in these Proceedings, and have the following forms:

$$T = \frac{1}{2} \sum_{\lambda\mu} B_\lambda |\dot{\alpha}_{\lambda\mu}|^2 \tag{3.2a}$$

$$V = \frac{1}{2} \sum_{\lambda\mu} C_\lambda |\alpha_{\lambda\mu}|^2 \tag{3.2b}$$

The mass parameter B_λ has an explicit expression in terms of the density of the nuclear fluid, while the spring constant C_λ is determined by the surface tension of the nuclear fluid and the Coulomb repulsion of the nuclear charge. As a matter of fact, these two basic properties of nuclei compete with each other in determining C_λ. When the nucleus departs from its equilibrium spherical shape, its surface area increases, and hence the energy due to surface tension also increases; the Coulomb energy of the deformed drop, however, is lower than that of the spherical liquid drop and therefore this effect gives a negative contribution to C_λ. For small deformations, the surface tension term is larger than the Coulomb term and C_λ turns out to be positive. Therefore, according to section 2.1, the Hamiltonian defined by (3.2a, b) describes a set of uncoupled vibrators, each $\alpha_{\lambda\mu}$ behaving as a vibrator co-ordinate.

3.2. Time-dependent microscopic theory

In the introduction we mentioned that the microscopic picture of nuclear vibration is based on the oscillations of the one-body density of the nucleons moving in the average nuclear field and interacting with each other through a residual interaction. The average potential is connected self-consistently with the density, and hence any oscillation in the density generates a response on the average potential, and vice versa. In determining the equations of nuclear vibration in our time-dependent microscopic theory we shall make the following basic steps: we shall apply an oscillatory perturbation on the average potential V, and then determine its response on the one-body density by the standard time-dependent perturbation theory. The self-consistent change in the potential generated by this change of density is then put equal to the perturbation in the average potential from

which we started. Clearly, when this equation is satisfied the nuclear
oscillation induced by the perturbation will be sustained. We shall see
that this condition gives us a set of equations determining the frequencies
of the normal modes of vibration of the nucleus.

A. Basic Definitions

To carry out the program outlined above we shall need the basic
definitions of the one-body density ρ, the average self-consistent potential
V, and a few basic properties of the perturbed density function. Some
of these definitions are given in the papers on Hartree-Fock (HF) calcula-
tions in these Proceedings. We will briefly recapitulate them for the
sake of completeness.

In the equilibrium HF state Ψ_0 of the nucleus a set of single-particle
states of V are occupied by the nucleons. These will be denoted by the
letters h, h', ..., etc. ("h" for "hole" states). The states which are unoccu-
pied above the Fermi level will be denoted by the symbols p, p', ..., etc.
("p" for "particle" states). Whenever we want to designate the hole and
particle states together by a single symbol, we shall then use the letters
i, j, k, ℓ, ... All these Latin letters, therefore, stand for the self-
consistent single-particle states of the HF potential. In the HF-work,
the basic quantities ρ, V, etc. are defined usually with respect to a set
of basis single-particle states (usually the harmonic-oscillator states).
For these states we shall always use the Greek letters α, β, ..., etc.

(i) Having defined these conventions, let us now write down the de-
finition of the HF-potential V:

$$\langle \alpha | V | \beta \rangle = \sum_h (\alpha h | v | \beta h) \tag{3.3}$$

where

$$(\alpha h | v | \beta h) = \langle \alpha h | v | \beta h \rangle - \langle \alpha h | v | h \beta \rangle \tag{3.4}$$

The rounded-bracket matrix element of the two-body potential v, acting
between a pair of nucleons, consists of the direct minus the exchange
matrix elements; the pointed-bracket matrix elements of Eq.(3.4) are
the ordinary two-body matrix elements, i.e.

$$\langle \alpha h | v | \beta h \rangle = \int d^3 r_1 \int d^3 r_2 \, \phi_\alpha^*(\vec{r}_1) \phi_h^*(\vec{r}_2) v(\vec{r}_1 - \vec{r}_2) \phi_\beta(\vec{r}_1) \phi_h(\vec{r}_2)$$

(ii) Any self-consistent single-particle state is calculated as a linear
sum of the basis states. Thus,

$$| i \rangle = \sum_\alpha X_\alpha^{(i)} | \alpha \rangle \tag{3.5}$$

Using this kind of an expression for $| h \rangle$ in Eq.(3.3) one obtains

$$\langle \alpha | V | \beta \rangle = \sum_{\gamma, \delta} (\alpha\gamma | v | \beta\delta) \sum_{h} X_{\gamma}^{(h)*} X_{\delta}^{(h)}$$

$$= \sum_{\gamma, \delta} (\alpha\gamma | v | \beta\delta) \langle \delta | \rho | \gamma \rangle \qquad (3.6)$$

where

$$\langle \delta | \rho | \gamma \rangle = \sum_{h}' X_{\gamma}^{(h)*} X_{\delta}^{(h)} \qquad (3.7a)$$

Expression (3.7a) defines the one-body density ρ, and Eq.(3.6) connects the HF-potential with it. In this form, the density ρ appears like an obscure mathematical quantity. We shall derive below several alternative forms of the density operator, and show, in particular, that its co-ordinate-space representation is, indeed, related to the probability density of elementary quantum mechanics.

(iii) According to Eq.(3.5), written for $|h\rangle$, we have

$$X_{\delta}^{(h)} = \langle \delta | h \rangle, \quad X_{\gamma}^{(h)*} = \langle h | \gamma \rangle$$

Hence, Eq.(3.7a) yields

$$\langle \delta | \rho | \gamma \rangle = \sum_{h} \langle \delta | h \rangle \langle h | \gamma \rangle$$

that is,

$$\rho = \sum_{h}' |h\rangle\langle h| \qquad (3.7b)$$

From the orthonormality of the states $|h\rangle$, $|h'\rangle$, etc. we immediately obtain

$$\rho^2 = \sum_{h,h'} |h\rangle\langle h|h'\rangle\langle h'| = \sum_{h}' |h\rangle\langle h| = \rho \qquad (3.8)$$

This is a very important property of the density operator, and will be used later.

(iv) Equation (3.7b) also gives us very easily the matrix elements of ρ in the HF-representation:

$$\langle h | \rho | h' \rangle = \langle h | \sum_{h''}' |h''\rangle\langle h''| h' \rangle$$

$$= \langle h | h' \rangle = \delta_{h,h'} \qquad (3.9a)$$

and

$$\langle h | \rho | p \rangle = \langle p | \rho | p' \rangle = 0 \qquad (3.9b)$$

in a similar manner. These results also are very useful.

(v) In the co-ordinate-space representation ρ yields

$$\langle \vec{r} | \rho | \vec{r}' \rangle = \sum_h \langle \vec{r} | h \rangle \langle h | \vec{r}' \rangle$$

$$= \sum_h \phi_h(\vec{r}) \phi_h^*(\vec{r}') \qquad (3.10a)$$

where ϕ with the appropriate label stands for the self-consistent single-particle wave function. The diagonal component $\langle \vec{r} | \rho | \vec{r} \rangle$ will be denoted, for brevity, by $\rho(\vec{r})$, and it is clearly given by

$$\rho(\vec{r}) \equiv \langle \vec{r} | \rho | \vec{r} \rangle = \sum_h | \phi_h(\vec{r}) |^2 \qquad (3.10b)$$

In this form the connection of ρ with the single-particle probability density becomes obvious. The many-body HF state Ψ_0 contains several occupied single-particle states. Each such state h contributes, according to elementary quantum mechanics, the probability density $| \phi_h(\vec{r}) |^2$. A summation over all the occupied states in Eq.(3.10b), therefore, yields, as expected, the one-body density operator corresponding to the HF-state Ψ_0.

(vi) Ψ_0 is a determinantal state with rows (or columns) labelled by the occupied single-particle states h, h', ..., etc. and the columns (or rows) labelled by particle co-ordinates $\vec{r}_1$, $\vec{r}_2$, ..., etc. It is very easy to obtain the expectation value for this state of a single-particle-type operator $\sum_{I=1}^{A} \delta(\vec{r} - \vec{r}_I)$, where the summation runs over all the nucleons. According to the standard result:

$$\langle \Psi_0 | \sum_{I=1}^{A} \Omega_I | \Psi_0 \rangle = \sum_h \langle h | \Omega | h \rangle$$

where Ω is any one-body operator, we obtain

$$\langle \Psi_0 | \sum_{I=1}^{A} \delta(\vec{r} - \vec{r}_I) | \Psi_0 \rangle = \sum_h \int \phi_h^*(\vec{r}_I) \, \delta(\vec{r} - \vec{r}_I) \, \phi_h(\vec{r}_I) \, d^3 r_I$$

$$= \sum_h | \phi_h(\vec{r}) |^2 \equiv \rho(\vec{r}) \qquad (3.10c)$$

The last equality follows from Eq.(3.10b). Equation (3.10c) shows us
how to obtain the single-particle density $\rho(\vec{r})$ at any point $\vec{r}$, when the
many-body state Ψ_0 is known. Actually, this definition is more general
than the earlier ones in this section, because it can be used for any
general many-body state Ψ_0 which is not necessarily a single determinant.

   (vii) The same result can be rewritten in a different manner. Let
us consider the product $\Psi_0(\vec{r}, r_2, r_3, \ldots, r_A) \Psi_0^*(\vec{r}, r_2, \ldots, r_A)$ and carry
out an integration over the co-ordinates $r_2, r_3, \ldots, r_A$, i.e. the co-
ordinates of all the nucleons, leaving aside the first. The result of this
integration will leave us with a function of $\vec{r}$ which we can take to be the
definition of $A^{-1}\rho(\vec{r})$. As a matter of fact, such a definition of $\rho(\vec{r})$ and

Eq.(3.10c) (i.e. in terms of the matrix element of $\sum\limits_{I=1}^{A} \delta(\vec{r} - \vec{r}_I)$) are

identical. For a single determinantal state it is very easy to establish
this fact. We write this new definition as follows:

$$A^{-1}\rho(\vec{r}) = \int d^3r_2 \ldots \int d^3r_A \ \Psi_0(\vec{r}, \vec{r}_2, \vec{r}_3, \ldots, \vec{r}_A) \ \Psi_0^*(\vec{r}, \vec{r}_2, \vec{r}_3, \ldots, \vec{r}_A).$$

$$= \int d^3r_2 \ldots \int d^3r_A \ \langle \vec{r}, \vec{r}_2, \ldots, \vec{r}_A | \Psi_0 \rangle \langle \Psi_0 | \vec{r}, \vec{r}_2, \ldots, \vec{r}_A \rangle$$

$$= \langle \vec{r} | \{\text{Trace}_{2,\ldots,A} | \Psi_0 \rangle \langle \Psi_0 | \} | \vec{r} \rangle \tag{3.11}$$

The integrals can clearly be interpreted as the trace of a matrix for
$| \Psi_0 \rangle \langle \Psi_0 |$ in the co-ordinate representation; this is indicated in the
final step of Eq.(3.11). Thus,

$$\rho = A \ \text{Trace}_{2,\ldots,A} \ | \Psi_0 \rangle \langle \Psi_0 | \tag{3.12}$$

and the general non-diagonal matrix element of ρ in the co-ordinate
space is clearly given by

$$\langle \vec{r} | \rho | \vec{r}' \rangle = \langle \vec{r} | \{A \ \text{Trace}_{2,\ldots,A} | \Psi_0 \rangle \langle \Psi_0 | \} | \vec{r}' \rangle$$

$$= A \int d^3r_2 \ldots \int d^3r_A \langle \vec{r}, \vec{r}_2, \ldots, \vec{r}_A | \Psi_0 \rangle \langle \Psi_0 | \vec{r}', \vec{r}_2 \ldots, \vec{r}_A \rangle \tag{3.13}$$

The meaning of the two factors in the integrand of Eq.(3.13) is obvious.
The first factor denotes a many-body wave function with the particle
co-ordinates $\vec{r}$, $\vec{r}_2$, $\ldots$, $\vec{r}_A$, while the second factor denotes the complex
conjugate of the wave function of the same many-body state but this time
the particle co-ordinates are $\vec{r}'$, r_2, $\ldots$, r_A; that is, only the co-ordinates
of the first particle are different, while the co-ordinates of the remaining
particles 2, $\ldots$, A are the same in the two many-body wave functions. We
should like to emphasize once again that the definitions (3.10c), (3.11),
(3.12) and (3.13) are very general and valid for any general many-body
state Ψ_0, which is not necessarily a single determinant. When Ψ_0 has

the special form of a single determinant, all these definitions degenerate to the simpler definitions of ρ given by Eqs (3.7a, b) and (3.10a, b).

(viii) There is yet another definition of ρ in terms of the creation and destruction operators, which is valid for any general many-body state Ψ_0, and whose identity with the earlier definitions in the case of HF single-determinantal state Ψ_0 is easy to prove. This definition is given by

$$\langle \beta | \rho | \alpha \rangle = \langle \Psi_0 | C_\alpha^\dagger C_\beta | \Psi_0 \rangle \tag{3.14}$$

where $C_\alpha^\dagger$ is the creation operator for the state α, and C_β is the destruction operator for the state β. To prove its equivalence with the earlier definitions for the HF Ψ_0, we write down the following equation which is obviously equivalent to Eq. (3.5):

$$C_i^\dagger = \sum_\alpha X_\alpha^{(i)} C_\alpha^\dagger \tag{3.15a}$$

Since the states $| \alpha \rangle$ and the states $| i \rangle$ both form complete sets within the subspace chosen for the HF-calculation, the relation (3.5) can be inverted to yield

$$| \alpha \rangle = \sum_i X_\alpha^{(i)*} | i \rangle$$

and hence the corresponding equivalent relation:

$$C_\alpha^\dagger = \sum_i X_\alpha^{(i)*} C_i^\dagger \tag{3.15b}$$

Substituting expression (3.15b) for $C_\alpha^\dagger$, and the Hermitian conjugate relation (with α replaced by β)

$$C_\beta = \sum_j X_\beta^{(j)} C_j \tag{3.15c}$$

in the definition (3.14) we obtain

$$\langle \beta | \rho | \alpha \rangle = \langle \Psi_0 | \sum_{i,j} X_\alpha^{(i)*} X_\beta^{(j)} C_i^\dagger C_j | \Psi_0 \rangle$$

In order that $C_j | \Psi_0 \rangle$ be non-vanishing for the HF-state, j must be one of the states h occupied in Ψ_0, because we cannot otherwise destroy this state from Ψ_0. For the same reason the quantity $\langle \Psi_0 | C_i^\dagger$ is non-vanishing (this is the Hermitian conjugate of $C_i | \Psi_0 \rangle$) only if i is an occupied state in Ψ_0. So, we replace $C_i^\dagger C_j$ by $C_h^\dagger C_{h'}$, and then use $C_h^\dagger C_{h'} = - C_{h'} C_h^\dagger + \delta_{hh'}$. The term $C_{h'} C_h^\dagger | \Psi_0 \rangle$ produces zero, because if we create the state h through $C_h^\dagger$ we violate the Pauli exclusion principle. Thus,

$$\langle \beta | \rho | \alpha \rangle = \sum_{h,h'} \delta_{hh'} X_\alpha^{(h)*} X_\beta^{(h')} \langle \Psi_0 | \Psi_0 \rangle$$

$$= \sum_h X_\alpha^{(h)*} X_\beta^{(h)}$$

Note that this result agrees with Eq.(3.7a), and proves our earlier statement.

(ix) We next write the definition of the one-body potential, given by Eqs (3.3) and (3.4), in the co-ordinate space. The right-hand side of (3.3) is given by

$$\sum_h \int d^3 r_1 \int d^3 r_2 \, \phi_\alpha^*(\vec{r}_1) \phi_h^*(\vec{r}_2) v(\vec{r}_1 - \vec{r}_2) [\phi_\beta(\vec{r}_1) \phi_h(\vec{r}_2) - \phi_h(\vec{r}_1) \phi_\beta(\vec{r}_2)]$$

$$= \int d^3 r_1 \, \phi_\alpha^*(\vec{r}_1) V_D(\vec{r}_1) \phi_\beta(\vec{r}_1) - \int d^3 r_1 \int d^3 r_2 \, \phi_\alpha^*(\vec{r}_1) V_E(\vec{r}_1, \vec{r}_2) \phi_\beta(\vec{r}_2) \quad (3.16)$$

where the one-body potential V_D, associated with the direct term, is <u>local</u> and is given by

$$V_D(\vec{r}_1) = \sum_h \int \phi_h^*(\vec{r}_2) v(\vec{r}_1 - \vec{r}_2) \phi_h(\vec{r}_2) d^3 r_2 = \int d^3 r_2 v(\vec{r}_1 - \vec{r}_2) \rho(\vec{r}_2) \qquad (3.17a)$$

while the potential V_E, associated with the exchange term, is <u>non-local</u> and given by

$$V_E(\vec{r}_1, \vec{r}_2) = \sum_h \phi_h^*(\vec{r}_2) v(\vec{r}_1 - \vec{r}_2) \phi_h(\vec{r}_2) = v(\vec{r}_1 - \vec{r}_2) \langle \vec{r}_1 | \rho | \vec{r}_2 \rangle \qquad (3.17b)$$

The expressions (3.17a, b) have been written down by a direct comparison of both sides of Eq.(3.16), and then substituting the definitions (3.10a, b) for the matrix elements of ρ. Thus, the local part of the density operator gives rise to the local part of the HF-potential, and the non-local part of the density generates the non-local part of the HF-potential.

(x) Finally, we consider some important properties of the density operator describing the nucleus when it is no longer in an equilibrium condition. This is the situation when the nucleus vibrates. Such a ρ will be time-dependent, and we denote it by $\hat{\rho}$. If the departure from the equilibrium condition is small (i.e. if we restrict ourselves to small oscillations) then we can obviously make an expansion of $\hat{\rho}$ by taking the equilibrium ρ as the reference point. Thus, up to the second order of smallness, we have

$$\hat{\rho} = \rho + \hat{\rho}^{(1)} + \hat{\rho}^{(2)} + \ldots \qquad (3.18)$$

We have put a "hat" on the top of all time-dependent quantities. The equilibrium value ρ is time-independent and hence

$$\frac{\partial \rho}{\partial t} = 0 \qquad (3.19)$$

$\hat{\rho}^{(1)}$ and $\hat{\rho}^{(2)}$ are, respectively, first- and second-order quantities compared to ρ. Since

$$\hat{\rho}^2 = \hat{\rho}$$

we obtain from Eq.(3.18)

$$\rho^2 + [\rho\hat{\rho}^{(1)} + \hat{\rho}^{(1)}\rho] + [\rho\hat{\rho}^{(2)} + \hat{\rho}^{(2)}\rho + \{\hat{\rho}^{(1)}\}^2] = \rho + \hat{\rho}^{(1)} + \hat{\rho}^{(2)}$$

On the left-hand side, we have grouped together and enclosed in square brackets the first-order quantities, and also the second-order quantities. Since $\rho^2 = \rho$, the zero-order quantities on the two sides are equal. Next we equate first-order quantities from both sides and obtain

$$\rho\hat{\rho}^{(1)} + \hat{\rho}^{(1)}\rho = \hat{\rho}^{(1)} \qquad (3.20a)$$

Similarly, equating the second-order quantities we obtain

$$\rho\hat{\rho}^{(2)} + \hat{\rho}^{(2)}\rho + \{\hat{\rho}^{(1)}\}^2 = \hat{\rho}^{(2)} \qquad (3.20b)$$

We first consider the consequences of Eq.(3.20a). Let us take its matrix elements in the HF-representation, and use the properties (3.9a,b). We thus obtain

$$\langle h|\hat{\rho}^{(1)}|h'\rangle = \sum [\langle h|\rho|i\rangle\langle i|\hat{\rho}^{(1)}|h'\rangle + \langle h|\hat{\rho}^{(1)}|i\rangle\langle i|\rho|h'\rangle]$$

$$= \langle h|\rho|h\rangle\langle h|\hat{\rho}^{(1)}|h'\rangle + \langle h|\hat{\rho}^{(1)}|h'\rangle\langle h'|\rho|h'\rangle$$

$$= 2\langle h|\hat{\rho}^{(1)}|h'\rangle$$

Therefore,

$$\langle h|\hat{\rho}^{(1)}|h'\rangle = 0 \qquad (3.21a)$$

Similarly,

$$\langle p|\hat{\rho}^{(1)}|p'\rangle = 0 \qquad (3.21b)$$

But

$$\langle h|\hat{\rho}^{(1)}|p\rangle = \langle h|\rho|h\rangle\langle h|\hat{\rho}^{(1)}|p\rangle + \langle h|\hat{\rho}^{(1)}|p\rangle\langle p|\rho|p\rangle$$

$$= \langle h|\hat{\rho}^{(1)}|p\rangle$$

which is an identity. Thus Eq.(3.20a) does not give us any non-trivial information about $\langle h|\hat{\rho}^{(1)}|p\rangle$. And, in general,

$$\langle h|\hat{\rho}^{(1)}|p\rangle \neq 0, \qquad \langle p|\hat{\rho}^{(1)}|h\rangle \neq 0 \qquad (3.21c)$$

We next study the matrix elements of $\hat{\rho}^{(2)}$ in the HF-representation using Eq.(3.20b). For our future purposes it will suffice if we study only two special types of matrix elements:

(1) $\langle h|\hat{\rho}^{(2)}|h\rangle = \langle h|\rho|h\rangle\langle h|\hat{\rho}^{(2)}|h\rangle + \langle h|\hat{\rho}^{(2)}|h\rangle\langle h|\rho|h\rangle + \langle h|\{\hat{\rho}^{(1)}\}^2|h\rangle$

or

$$\langle h| \hat{\rho}^{(2)} |h \rangle = - \langle h| \{\hat{\rho}^{(1)}\}^2 |h \rangle$$

$$= - \sum_p \langle h| \hat{\rho}^{(1)} |p \rangle \langle p| \hat{\rho}^{(1)} |h \rangle \tag{3.22a}$$

(2) $\langle p| \hat{\rho}^{(2)} |p \rangle = \langle p| \rho |p \rangle \langle p| \hat{\rho}^{(2)} |p \rangle + \langle p| \hat{\rho}^{(2)} |p \rangle \langle p| \rho |p \rangle + \langle p| \{\hat{\rho}^{(1)}\}^2 |p \rangle$

or

$$\langle p| \hat{\rho}^{(2)} |p \rangle = \langle p| \{\hat{\rho}^{(1)}\}^2 |p \rangle$$

$$= \sum_h \langle p| \hat{\rho}^{(1)} |h \rangle \langle h| \hat{\rho}^{(1)} |p \rangle \tag{3.22b}$$

In writing the last steps of Eqs (3.22a) and (3.22b) we have made use of the properties (3.21a, b, c) of the matrix elements of $\hat{\rho}^{(1)}$.

B. Self-consistent oscillation of HF-potential

    Having introduced all these definitions and basic properties, we shall now carry out the program sketched in the beginning of section 3.2.
    Let us denote the time-dependent perturbation of the HF-potential by $\hat{\lambda}$. For the entire nucleus the perturbation is obtained by summing over all the nucleons:

$$\hat{H}_1 = \sum_{I=1}^{A} \hat{\lambda}_I \tag{3.23a}$$

Since $\hat{\lambda}$ has to be Hermitian, we assume its time dependence to be of the form

$$\hat{\lambda} = \lambda e^{-i\omega t} + \lambda^* e^{i\omega t} \tag{3.23b}$$

and hence the corresponding $\hat{H}_1$ is given by

$$\hat{H}_1 = H_1 e^{-i\omega t} + H_1^* e^{i\omega t} \tag{3.23c}$$

where

$$H_1 = \sum_{I=1}^{A} \lambda_I \tag{3.23d}$$

It will be clear from the following derivation that we do not require any explicit knowledge of the operator λ for an investigation of the normal modes of vibration of the nucleus.
    Before the oscillatory potential was applied, our grand state wave function was given by

$$\Psi_0 e^{-\frac{i}{\hbar} W_0 t}$$

where W_0 is the energy of this stationary state. Denoting the unperturbed nuclear Hamiltonian by H we have

$$i\hbar \frac{\partial}{\partial t} \left\{ \Psi_0 e^{-iW_0 t/\hbar} \right\} = H \Psi_0 e^{-iW_0 t/\hbar} = W_0 \Psi_0 e^{-iW_0 t/\hbar} \qquad (3.24)$$

If the other excited states of the Hamiltonian are denoted by Ψ_n with energy W_n, n = 1, 2, ... etc., the perturbed ground state wave function $\Psi(t)$ can be expanded in terms of Ψ_0 and the entire set of Ψ_n, as follows:

$$\Psi(t) = a_0(t) \Psi_0 e^{-iW_0 t/\hbar} + \sum_{n=1}^{\infty} a_n(t) \Psi_n e^{-iW_n t/\hbar} \qquad (3.25)$$

At t = 0, when the perturbation (3.23c) is applied, $a_0(t=0) = 1$, and $a_n(t=0) = 0$. As time goes on the quantities $a_n(t)$ build up at the cost of $a_0(t)$. As is well known from elementary quantum mechanics, the value of $a_n(t)$ can be determined to various orders of the time-dependent perturbation theory. We shall use the results up to the first order in the perturbation (see any textbook on quantum mechanics) and write

$$\Psi(t) = \Psi_0 e^{-iW_0 t/\hbar} + \sum_{n=1}^{\infty} a_n^{(1)}(t) \Psi_n e^{-iW_n t/\hbar} \qquad (3.26a)$$

where

$$\dot{a}_n^{(1)}(t) = -\frac{i}{\hbar} \langle \Psi_n | \hat{H}_1(t) | \Psi_0 \rangle e^{-iW_{n0} t/\hbar} \qquad (3.26b)$$

and

$$W_{n0} = W_n - W_0 \qquad (3.26c)$$

The superscript i on a_n denotes that this is the expression in first-order perturbation theory, and the dot overhead denotes the time derivative.

To carry out the time integration in Eq.(3.26b) we have to make use of the explicit form (3.23c) for $\hat{H}_1(t)$, and the boundary condition $a_n^{(1)}(t) = 0$ at t = 0. Thus

$$a_n^{(1)}(t) = -\left\{ \langle \Psi_n | H_1 | \Psi_0 \rangle \frac{e^{-\frac{i}{\hbar}(W_{n0} - \hbar\omega)t}}{W_{n0} - \hbar\omega} + \langle \Psi_n | H_1^* | \Psi_0 \rangle \frac{e^{\frac{i}{\hbar}(W_{n0} + \hbar\omega)t}}{W_{n0} + \hbar\omega} \right\}$$

$$(3.27)$$

Equations (2.26a) and (3.27) represent the solution for the perturbed ground-state wave function in the lowest order of the perturbation theory.

We shall next calculate the density $\hat{\rho}$ for the state $\Psi(t)$ by using the general definition (3.13) and replacing Ψ_0 by Ψ. It is clear from Eq.(3.26a) and

$$\langle \vec{r} | \hat{\rho} | \vec{r}' \rangle = A \int d^3 r_2 \cdots \int d^3 r_A \langle \vec{r}, \vec{r}_2, ..., \vec{r}_A | \Psi(t) \rangle \langle \Psi(t) | \vec{r}', \vec{r}_2, ..., \vec{r}_A \rangle$$

$$(3.28a)$$

that the lowest-order term of $\hat{\rho}$ is the equilibrium density ρ corresponding
to the unperturbed state Ψ_0. The first-order term $\hat{\rho}^{(1)}$ corresponds to the
cross-product between the Ψ_0 term and the Ψ_n terms of Eq. (3.26a). Thus

$$\langle \vec{r} | \hat{\rho}^{(1)} | \vec{r}' \rangle = A \int d^3r_2 ... \int d^3r_A \sum_{n=1}^{\infty} \left\{ e^{iW_{n0}t/\hbar} \, a_n^{(1)*}(t) \langle \vec{r}, \vec{r}_2 ..., \vec{r}_A | \Psi_0 \rangle \right.$$

$$\left. \times \langle \Psi_n | \vec{r}', \vec{r}_2 .. \vec{r}_A \rangle + e^{-iW_{n0}t/\hbar} \, a_n^{(1)}(t) \langle \vec{r}, \vec{r}_2 ... \vec{r}_A | \Psi_n \rangle \langle \Psi_0 | \vec{r}', \vec{r}_2, ... \vec{r}_A \rangle \right\}$$

$$(3.28b)$$

Our next task is to compute the change in the average potential generated
by this $\hat{\rho}^{(1)}$, and then finally we have to equate the result with expression
(3.23b) for self-consistency. This computation is actually better carried
out with expression of $\hat{\rho}^{(1)}$ in the HF-representation, rather than in the
co-ordinate space representation (3.28b). However, if we decide to
consider only the local part $\hat{\rho}^{(1)}(\vec{\gamma})$, and hence only the local part of V
in achieving self-consistency, then the computation using co-ordinate-
space representation is not difficult. Such an approximate calculation,
however, is quite instructive in its physical content, and hence we shall
do such a model calculation before undertaking the exact self-consistent
treatment.

C. A local model for the microscopic theory

We have shown in Eq. (3.10c) that the local part of the density can
be represented in a very simple way as the matrix element of a δ-function
between the many-body state. For $\vec{r} = \vec{r}'$ the definition (3.28a) and such
a definition are equivalent. Therefore, we start from

$$\langle \vec{r} | \hat{\rho} | \vec{r} \rangle \equiv \hat{\rho}(\vec{r}) = \langle \Psi(t) | \sum_{I=1}^{A} \delta(\vec{r} - \vec{r}_I) | \Psi(t) \rangle \qquad (3.29)$$

Using Eq. (3.26a), we obtain, as before, the lowest-order term of $\hat{\rho}(\vec{r})$
to be the equilibrium density $\rho(\vec{r})$ corresponding to Ψ_0. The first-order
quantities are given by

$$\hat{\rho}^{(1)}(\vec{r}) = \sum_{n=1}^{\infty} \left\{ a_n^{(1)*}(t) \, e^{iW_{n0}t/\hbar} \langle \Psi_n | \sum_{I=1}^{A} \delta(\vec{r} - \vec{r}_I) | \Psi_0 \rangle \right.$$

$$(3.30)$$

$$\left. + a_n^{(1)}(t) \, e^{-iW_{n0}t/\hbar} \langle \Psi_0 | \sum_{I=1}^{A} \delta(\vec{r} - \vec{r}_I) | \Psi_n \rangle \right\}$$

Since, by definition, Ψ_n ($n = 1, ..., \infty$) $\neq \Psi_0$, and the operator
$\sum_{I=1}^{A} \delta(\vec{r} - \vec{r}_I)$ is a one-body type operator, Ψ_n differs from Ψ_0 only in

the state of one nucleon and not more. That is to say, Ψ_n in Eq. (3.30) is a 1hp-type state with reference to the ground state Ψ_0. Once again, the standard result for a 1hp state and <u>any</u> one-body operator $\sum_{I=1}^{A} \Omega_I$ is given by

$$\langle \Psi_{hp} | \sum_{I=1}^{A} \Omega_I | \Psi_0 \rangle = \langle p | \Omega | h \rangle$$

and, hence, in our case

$$\langle \Psi_{hp} | \sum_{I=1}^{A} \delta (\vec{r} - \vec{r}_I) | \Psi_0 \rangle = \int d^3 r_I \; \phi_p^*(\vec{r}_I) \; \delta (\vec{r} - \vec{r}_I) \; \phi_h (\vec{r}_I)$$

$$= \phi_p^* (\vec{r}) \; \phi_h (\vec{r}) \qquad\qquad (3.31)$$

Therefore, our expression for $\hat{\rho}^{(1)} (\vec{r})$ reduces to

$$\hat{\rho}^{(1)} (\vec{r}) = \sum_{h, p} \left\{ a_{hp}^{(1)} {}^* (t) \; e^{i W_{hp0} t/\hbar} \; \phi_h (\vec{r}) \; \phi_p^* (\vec{r}) \; + \text{complex conjugate} \right\} (3.32)$$

With this local part of the time-dependent density we get the time-dependent change in the one-body potential from Eq. (3.17a). Let us denote this by $\Delta V (\vec{r}_1)$. Thus

$$\Delta V (\vec{r}) = \int d^3 r' \; V (\vec{r} - \vec{r}') \; \hat{\rho}^{(1)} (\vec{r}') \qquad\qquad (3.33)$$

where $\hat{\rho}^{(1)} (\vec{r}')$ is given by Eq. (3.32).

We have to equate this expression with our initial perturbation of the average potential. To keep the model simple, we no longer take a general $\hat{\lambda}$, but make the following prescription for determining a convenient form for it: We assume that during the course of vibration, as the nucleus gets deformed, its surface co-ordinate R in the direction (θ, ϕ) is defined by an equation independent of ϕ:

$$R (\theta) = R_0 \left\{ 1 + \beta (t) \; Y_0^2 (\theta) \right\} \qquad\qquad (3.34)$$

this is a very special case of the general expression (3.1) with $\lambda = 2$ and $\mu = 0$ only. This actually means that the nuclear surface is a spheroid with its symmetry axis along the Z-axis of our co-ordinate system. $\beta (t)$ is a simpler notation for $\alpha_{20} (t)$. We further assume that each spherical surface of radius r_0 inside the nucleus also gets deformed to a spheroidal surface having the same deformation parameter $\beta (t)$. That is to say, the co-ordinate $r (\theta, \phi)$ of a point on this smaller spheroid is also given by

$$r (\theta) = r_0 \left\{ 1 + \beta (t) \; Y_0^2 (\theta) \right\} \qquad\qquad (3.35)$$
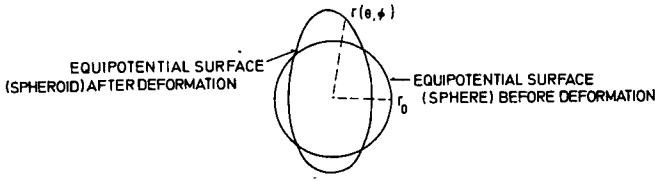
FIG.3.1. Equipotential surfaces.

The average potential V for the equilibrium spherical nucleus is spherically symmetric, i.e. the equipotential surfaces are spheres. We assume that an equipotential surface of radius r_0 gets deformed to a spheroidal surface, during vibration, given by expression (3.35). The situation is shown in Fig.3.1. It is quite reasonable to take the potential everywhere on the deformed equipotential surface to have the same value as it had on the spherical equipotential surface before deformation. Therefore, the potential $\bar{V}$ after deformation at r is given by the old potential V at r_0:

$$\bar{V}(r) = V(r_0) \tag{3.36}$$

But, according to Eq. (3.35), we have for small deformation β

$$r_0 = r \left\{ 1 + \beta(t) Y_0^2(\theta) \right\}^{-1}$$

$$\simeq r - r\beta(t) Y_0^2(\theta)$$

We use this value of r_0 in Eq. (3.36) and make a Taylor expansion:

$$\bar{V}(r) = V(r) - r \frac{dV}{dr} \beta(t) Y_0^2(\theta) \tag{3.37a}$$

Hence, according to this prescription, the perturbation in the average potential is given by

$$\hat{\lambda} = \bar{V}(r) - V(r) \tag{3.37b}$$

$$= -r \frac{dV}{dr} Y_0^2(\theta) \beta(t)$$

It is usual, in this model, to assume the equilibrium potential V to be either a square-well of radius R_0 and depth V_0 or the harmonic-oscillator potential $(1/2) C r^2$. In these two cases $r\, dV/dr$ is given by

$$r \frac{dV}{dr} = V_0 R_0 \delta(r - R_0) \qquad \text{(square-well)} \tag{3.38a}$$

$$= C r^2 \qquad\qquad \text{(harmonic oscillator)} \tag{3.38b}$$

We shall use here the second form, and write

$$\hat{h} = - C r^2 Y_0^2 (\theta) \beta (t)$$

$$= - C Q_0 (\vec{r}) \left\{ \beta e^{-i\omega t} + \beta^* e^{i\omega t} \right\} \tag{3.39}$$

where

$$Q_0 (\vec{r}) = r^2 Y_0^2 (\theta) \tag{3.40a}$$

and

$$\beta (t) = \beta e^{-i\omega t} + \beta^* e^{i\omega t} \tag{3.40b}$$

This completes our prescription for the perturbation in the average potential.

As mentioned earlier, we require expression (3.39) to be equal to expression (3.33) for self-consistency. The algebra will be simple if we introduce some more simplifications in our model: let us assume that the two-nucleon potential $V(\vec{r} - \vec{r}')$ of Eq. (3.33) be separable and given by

$$v(\vec{r} - \vec{r}') = - \chi Q_0 (\vec{r}) Q_0 (\vec{r}') \tag{3.41}$$

where $\vec{r}$ and $\vec{r}'$ are the co-ordinates of the two interacting nucleons, and χ is the strength of this quadrupole-type interaction. With this assumption (3.33) simplifies to

$$\Delta V (\vec{r}) = - \chi Q_0 (\vec{r}) \int d^3 r' Q_0 (\vec{r}') \hat{\rho}^{(1)} (\vec{r}')$$

Equating this expression with expression (3.39) we obtain

$$\beta e^{-i\omega t} + \beta^* e^{i\omega t} = C^{-1} \chi \int d^3 r' Q_0 (\vec{r}') \hat{\rho}^{(1)} (\vec{r}') \tag{3.42a}$$

Comparing expression (3.39) with our general expression (3.23b) we conclude

$$h = h^* = - C \beta Q_0 (\vec{r}) \tag{3.43}$$

We use this expression for h and h^* in the general equation (3.27) for $a_{hp}^{(1)} (t)$ and obtain

$$a_{hp}^{(1)} (t) = C \langle p | Q_0 | h \rangle \left\{ \frac{\beta^* e^{i\omega t}}{W_{hp0} - \hbar\omega} + \frac{\beta e^{-i\omega t}}{W_{hp0} + \hbar\omega} \right\} e^{i W_{hp0} t/\hbar} \tag{3.44}$$

where we have used the standard result for a one-body type operator

and replaced $\left\langle \Psi_{hp} \left| \sum_{I=1}^{A} Q_0(\vec{r}_I) \right| \Psi_0 \right\rangle$ by $\langle p | Q_0 | h \rangle$. Substituting Eq. (3.44) in Eq. (3.32) we obtain

$$\hat{\rho}^{(1)}(\vec{r}) = C \sum_{h,p} \langle p | Q_0 | h \rangle^* \left\{ \frac{\beta e^{-i\omega t}}{W_{hp0} - \hbar\omega} + \frac{\beta^* e^{i\omega t}}{W_{hp0} + \hbar\omega} \right\} \phi_h(\vec{r}) \phi_p^*(\vec{r})$$

$$+ \text{ complex conjugate.}$$

From Eq. (3.42a) and this expression we now obtain

$$\beta e^{-i\omega t} + \beta^* e^{i\omega t} = \sum_{h,p} \chi \, |\langle h | Q_0 | p \rangle|^2 \left\{ \left(\frac{\beta e^{-i\omega t}}{W_{hp0} - \hbar\omega} + \frac{\beta^* e^{i\omega t}}{W_{hp0} + \hbar\omega} \right) \right.$$

$$+ \text{ complex conjugate}$$

$$= (\beta e^{-i\omega t} + \beta^* e^{i\omega t}) \, 2 \chi \sum_{h,p} \frac{W_{hp0} \, |\langle h | Q_0 | p \rangle|^2}{W_{hp0}^2 - (\hbar\omega)^2}$$

or

$$\frac{1}{2\chi} = \sum_{h,p} \frac{W_{hp0} \, |\langle h | Q_0 | p \rangle|^2}{W_{hp0}^2 - (\hbar\omega)^2} \qquad (3.45)$$

This equation determines the frequencies of vibration ω. A graphical solution for $\hbar\omega$ from this equation is very instructive. The quantities W_{hp_0} (= $W_{hp} - W_0$) are the energies of the 1hp states with respect to the ground state. Usually, these energies are taken from the experimental data. In Fig.3.2 the squares of these energies correspond to the points 1, 2, 3, ... etc. on the abscissa. We denote the right-hand side of Eq. (3.45) by $F(\omega^2)$ and plot this as a function of $(\hbar\omega)^2$ in the diagram. Whenever $\hbar\omega$ approaches any of the W_{hp0} from left the
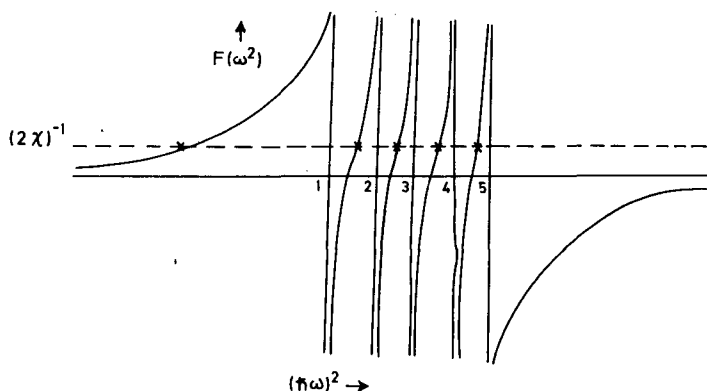
FIG. 3.2. Graphical solution for the vibrational frequencies.

function goes to $+\infty$ because $(W_{hp0} - \hbar\omega)$ for $\hbar\omega < W_{hp0}$ is positive; as soon as we cross over to the right of the energy W_{hp0}, the function $F(\omega^2)$ is still infinitely large but it goes to $-\infty$ because now $(W_{hp0} - \hbar\omega)$ is negative. In between, any two consecutive vertical lines passing through two consecutive values of W_{hp0}, the function $F(\omega^2)$ can, therefore, behave only as the curved lines shown in the diagram. However, below the lowest W_{hp0} and above the highest W_{hp0} the function has to behave differently. The function goes to zero when $(\hbar\omega)^2 \to \mp\infty$ as shown in the figure. The dashed horizontal line represents $1/2\chi$. Hence, the allowed values of $\hbar\omega$ are the points where this dashed line cuts the curves for $F(\omega^2)$. These points are marked with crosses in the diagram. It is clear that there are two types of solutions for $\hbar\omega$: (i) those falling in between the lowest and highest W_{hp0}, and (ii) the single solution to the left of the lowest W_{hp0}. It is clear that the location of this solution is very sensitive to the strength χ of the quadrupole potential. If χ is very small then the dashed line $(2\chi)^{-1}$ is very high up, and hence this solution is very close to the lowest hp state. If, on the other hand, χ is very strong, the dashed curve is very near the abscissa, and hence it may meet $F(\omega^2)$ curve even on the negative side of $(\hbar\omega)^2$. This solution, therefore, corresponds to an imaginary frequency for a very strong quadrupole potential, and hence is completely unphysical. In an indirect way such a situation tells us that the assumed ground state is not really stable under deformation. Finally, for a moderately strong χ, the lowest solution is obtained at a small positive value of $(\hbar\omega)^2$. This situation is said to correspond to a collective vibrational state, a state that is pushed down a lot from the unperturbed hp states.

D. RPA equations of nuclear vibration

We now go back to Eq. (3.28b) of subsection B, and proceed to carry out the procedure mentioned below that equation. Without going into the details of determinantal algebra (taking Ψ_0 to be the HF-determinant and Ψ_n a determinant of the 1hp type), it is possible to simplify the results of the integration in (3.28b) by analogy with the result (3.31) for the diagonal component of ρ. For $\vec{r} = \vec{r}'$, $A \int d^3r_2 \ldots \int d^3r_A$ in the first term of Eq. (3.28b) had led to expression (3.31). By analogy, we expect for $\vec{r} \neq \vec{r}'$, the result $\phi_p^*(\vec{r}')\phi_h(\vec{r})$ because the single-particle state p is present in $\langle \Psi_{hp} |$, while the state h is contained in $|\Psi_0\rangle$, and hence ϕ_p^* must appear with $(\vec{r}')$ while ϕ_h appears with $(\vec{r})$. By a similar analogy, the second term of the right-hand side of Eq. (3.28b) should give rise to $\phi_p(\vec{r})\phi_h^*(\vec{r}')$. Finally,

$$\langle \vec{r} \,|\hat{\rho}^{(1)}|\, \vec{r}'\rangle = \sum_{h,p} \left\{ e^{iW_{hp0}t/\hbar}\; a_{hp}^{(1)*}(t)\,\phi_h(\vec{r})\phi_p^*(\vec{r}') + e^{-iW_{hp0}t/\hbar}\; a_{hp}^{(1)}(t)\phi_p(\vec{r})\phi_h^*(\vec{r}') \right\}$$

$$= \langle \vec{r}\,|\sum_{h,p}\left\{ e^{iW_{hp0}t/\hbar}\; a_{hp}^{(1)*}(t)\,|h\rangle\langle p| + e^{-iW_{hp0}t/\hbar}\; a_{hp}^{(1)}(t)\,|p\rangle\langle h|\right\}|\vec{r}'\rangle$$

Therefore, as an operator, $\hat{\rho}^{(1)}$ is given by

$$\hat{\rho}^{(1)} = \sum_{h,p} \left\{ e^{i W_{hp0} t/\hbar} a_{hp}^{(1)*}(t) |h\rangle\langle p| + e^{-i W_{hp0} t/\hbar} a_{hp}^{(1)}(t) |p\rangle\langle h| \right\}$$

$$(3.46)$$

This expression enables us to evaluate the matrix elements of $\hat{\rho}^{(1)}$ in the HF-representation. Only non-vanishing matrix elements are of the hole-particle type and are clearly given by

$$\langle p|\hat{\rho}^{(1)}|h\rangle = e^{-i W_{hp0} t/\hbar} a_{hp}^{(1)}(t)$$

$$(3.47)$$

$$= -\left\{ \frac{\langle \Psi_{hp}|H_1|\Psi_0\rangle}{W_{hp0} - \hbar\omega} e^{-i\omega t} + \frac{\langle \Psi_{hp}|H_1^*|\Psi_0\rangle}{W_{hp0} + \hbar\omega} e^{+i\omega t} \right\}$$

The matrix element $\langle h|\hat{\rho}^{(1)}|p\rangle$ is just the complex conjugate of this expression. In the final step of Eq. (3.47) we have already substituted from Eq. (3.27) for $a_{hp}^{(1)}(t)$. Next use for H_1 and H_1^* the expression given by (3.23d) and write their matrix elements between $\langle \Psi_{hp}|$ and $|\Psi_0\rangle$ from standard results:

$$\langle p|\hat{\rho}^{(1)}|h\rangle = -\left\{ \frac{\langle p|\text{λ}|h\rangle}{W_{hp0} - \hbar\omega} e^{-i\omega t} + \frac{\langle p|\text{λ}^*|h\rangle}{W_{hp0} + \hbar\omega} e^{i\omega t} \right\}$$

$$(3.48a)$$

$$= -(X_{hp} e^{-i\omega t} + Y_{hp}^* e^{i\omega t})$$

where we have used the abbreviated notations:

$$X_{hp} = \frac{\langle p|\text{λ}|h\rangle}{W_{hp0} - \hbar\omega}$$

$$(3.49a)$$

and

$$Y_{hp}^* = \frac{\langle p|\text{λ}^*|h\rangle}{W_{hp0} + \hbar\omega}$$

$$(3.49b)$$

Therefore, the complex conjugate of Eq. (3.48a) further yields

$$\langle h|\hat{\rho}^{(1)}|p\rangle = -(Y_{hp} e^{-i\omega t} + X_{hp}^* e^{i\omega t})$$

$$(3.48b)$$

We use Eqs (3.48a, b), together with the definition (3.6) for the self-consistent potential, to compute the self-consistent change in the average potential (ΔV) generated by the change in density $\hat{\rho}^{(1)}$. We have

$$\langle p \,|\, \Delta \hat{V} \,|\, h \rangle = \sum_{i, i'} (p\,i \,|\, v \,|\, h\,i') \langle i' \,|\, \hat{\rho}^{(1)} \,|\, i \rangle$$

$$= \sum_{h', p'} [\, (p\,h' \,|\, v \,|\, h'p') \langle p' \,|\, \hat{\rho}^{(1)} \,|\, h' \rangle + (p\,p' \,|\, v \,|\, h\,h') \langle h' \,|\, \hat{\rho}^{(1)} \,|\, p' \rangle\,]$$

$$= - \sum_{h', p'} [\, (p\,h' \,|\, v \,|\, h\,p') \left\{ X_{h'p'} \, e^{-i\omega t} + Y^*_{h'p'} \, e^{i\omega t} \right\}$$

$$+ (p\,p' \,|\, v \,|\, h\,h') \left\{ Y_{h'p'} \, e^{-i\omega t} + X^*_{h'p'} e^{i\omega t} \right\} \tag{3.50a}$$

We have to equate this with the matrix element between $\langle p|$ and $|h\rangle$ of the perturbation $\hat{\lambda}$ we had started with. The latter is given, according to Eqs (3.23b), (3.49a) and (3.49b), by the following expression:

$$\langle p \,|\, \hat{\lambda} \,|\, h \rangle = \langle p \,|\, \lambda \,|\, h \rangle \, e^{-i\omega t} + \langle p \,|\, \lambda^* \,|\, h \rangle \, e^{i\omega t}$$

$$\tag{3.50b}$$

$$= (W_{hp0} - \hbar\omega) \, X_{hp} \, e^{-i\omega t} + (W_{hp0} + \hbar\omega) \, Y^*_{hp} \, e^{i\omega t}$$

Equating expressions (3.50a) and (3.50b) we actually obtain two sets of equations, one set coming from the coefficients of exp $(-i\omega t)$:

$$(W_{hp0} - \hbar\omega) \, X_{hp} = - \sum_{h'p'} [\, (p\,h' \,|\, v \,|\, h\,p') \, X_{h'p'} + (p\,p' \,|\, v \,|\, h\,h') \, Y_{h'p'} \,]$$

$$\tag{3.51a}$$

and the other set of equations from the coefficients of exp $(+i\omega t)$:

$$(W_{hp0} + \hbar\omega) \, Y^*_{hp} = - \sum_{h'p'} [\, (p\,p' \,|\, v \,|\, h\,h') \, X^*_{h'p'} + (p\,h' \,|\, v \,|\, h\,p') \, Y^*_{h'p'} \,]$$

or

$$(W_{hp0} + \hbar\omega) \, Y_{hp} = - \sum_{h'p'} [\, (p\,p' \,|\, v \,|\, h\,h')^* \, X_{h'p'} + (p\,h' \,|\, v \,|\, h\,p')^* \, Y_{h'p'} \,]$$

$$\tag{3.51b}$$

Equations (3.51a) and (3.51b) together provide us with a set of coupled linear equations for the unknown amplitudes X_{hp} and Y_{hp}. Values of $\hbar\omega$ for which this system of equations yields non-trivial solutions for these amplitudes, are the normal frequencies of vibration. This system of equations is'known, in the literature, as the "random-phase-approximation (RPA)" equations for vibration. The name has a historical origin in a set of similar equations derived for the plasma oscillation mode of an electron gas with the assumption that the excitation amplitudes of a pair of electrons corresponding to different momentum transfers have a completely random phase with respect to each other.

It is easy to rewrite the system of Eqs (3.51a, b) in terms of matrices by introducing the following definitions of the two matrices A and B:

$$A_{hp, h'p'} = W_{hp0}\, \delta_{hh'}\, \delta_{pp'} - (p\,h'\,|v|\,p'\,h)$$ (3.52a)

and

$$B_{hp, h'p'} = (p\,p'\,|v|\,h\,h')$$ (3.52b)

Each hp-state defines a row or column of these matrices. In view of the definition (3.4) of the rounded-bracket matrix element, we have interchanged with a reversal of sign the ordering of h and p' in the two-body matrix element occurring in Eq. (3.52a), as compared with the original ordering in Eqs (3.51a, b). We also introduced the notation of a column vector X whose elements are X_{hp}, and a similar column vector Y whose elements are Y_{hp}. Then it is easy to verify that Eqs (3.51a, b) can be replaced by the following matrix equation:

$$\begin{pmatrix} A & B \\ B^* & A^* \end{pmatrix} \begin{pmatrix} X \\ Y \end{pmatrix} = \hbar\omega \begin{pmatrix} X \\ -Y \end{pmatrix}$$ (3.53)

We denote the matrix on the left-hand side by M:

$$M = \begin{pmatrix} A & B \\ B^* & A^* \end{pmatrix}$$ (3.54)

It is clear from the definitions (3.52a, b) that A is Hermitian, and B symmetric. Using these properties we have

$$M^+ = \begin{pmatrix} A^+ & \tilde{B} \\ B^+ & \tilde{A} \end{pmatrix} = \begin{pmatrix} A & B \\ B^* & A^* \end{pmatrix} = M$$ (3.55a)

that is, M is a Hermitian matrix. However, one must notice that Eq. (3.53), because of the presence of the minus sign with Y on the right-hand side, is not an eigenvalue equation for the matrix M.

Since Eq. (3.53) contains the following two matrix equations:

$$AX + BY = \hbar\omega X$$ (3.56a)

$$B^* X + A^* Y = -\hbar\omega Y$$ (3.56b)

we can easily rewrite the second equation as

$$- B^* X - A^* Y = \hbar\omega Y$$ (3.56c)

and then replace the set (3.56a, b) by the set (3.56a, c). The latter can then be written as

$$M' \begin{pmatrix} X \\ Y \end{pmatrix} = \hbar\omega \begin{pmatrix} X \\ Y \end{pmatrix} \tag{3.57a}$$

with

$$M' = \begin{pmatrix} A & B \\ -B^* & -A^* \end{pmatrix} \tag{3.57b}$$

Let us notice now Eq. (3.57a) is indeed the eigenvalue equation of the new matrix M'. But because there are minus signs in the second line of M', one can easily verify that it is <u>not a Hermitian matrix</u>. Thus the RPA equations represent the eigenvalue problem for a non-Hermitian matrix.

Several important mathematical properties of this matrix will now be written down:

(i) The Hermitian matrix M has real eigenvalues. It is possible to prove (see the Appendix to this section) that these real eigenvalues are positive definite, if our equilibrium state Ψ_0 corresponds to a minimum of energy as a function of the deformation. From this property of the eigenvalues of M, it is then possible to derive that <u>the eigenvalues of the RPA matrix M' are real</u>. This proof will be also given in the Appendix.

(ii) Equations (3.57a, b) are equivalent to Eqs (3.56a, c). Let us take the complex conjugate of the latter, keeping in mind that $\hbar\omega$ is real, and we obtain

$$A^*X^* + B^*Y^* = \hbar\omega X^*$$

$$- BX^* - AY^* = \hbar\omega Y^*$$

By reserving the sign we rewrite these equations as

$$AY^* + BX^* = -\hbar\omega Y^*$$

$$-B^*Y^* - A^*X^* = -\hbar\omega X^*$$

The last two equations can be clearly written in matrix form as

$$M' \begin{pmatrix} Y^* \\ X^* \end{pmatrix} = -\hbar\omega \begin{pmatrix} Y^* \\ X^* \end{pmatrix} \tag{3.58}$$

This establishes the second property which we wanted to prove: The eigenvalues of M' occur in pairs $\pm\hbar\omega$; if $\begin{pmatrix} X \\ Y \end{pmatrix}$ is a vector for eigenvalue $\hbar\omega$ then $\begin{pmatrix} Y^* \\ X^* \end{pmatrix}$ is, according to Eq. (3.58), an eigenvector belonging to the eigenvalue $-\hbar\omega$.

(iii) A third property, which also follows from the positive definiteness of the eigenvalues of M, is given by

$$\hbar\omega \; (\,|\, X\,|^2 - |\, Y\,|^2) \geq 0$$

i.e. in more detail,

$$\hbar\omega \sum_{h,\, p} (\,|\, X_{hp}\,|^2 - |\, Y_{hp}\,|^2) \geq 0 \qquad (3.59)$$

This property provides us with a convenient normalization of the eigen-vector $\begin{pmatrix} X \\ Y \end{pmatrix}$. For a positive energy $\hbar\omega$, the summation in relation (3.59) is positive definite, and hence we can normalize the corresponding eigenvectors to

$$\sum_{h,\, p} (\,|\, X_{hp}\,|^2 - |\, Y_{hp}\,|^2) = 1 \qquad (3.60)$$

For a negative energy $\hbar\omega$, the corresponding normalization is to minus unity. According to the property (ii) stated above, X for a negative energy solution is Y* for the corresponding positive energy solution, and Y for the same negative energy solution is X* for the corresponding positive energy solution. Hence, the normalization of a negative-energy solution is automatically guaranteed once we assure the normalization (3.60) for the positive-energy solution.

A detailed interpretation of the RPA-equations, and amplitudes will be given later in these lectures, after we have derived the same equations by an alternative method. Some of the proofs left out above are given in the following Appendix.

APPENDIX TO SECTION 3

A.1. Condition for a HF-minimum and the positive definiteness of M

If the equilibrium HF-state corresponds to a genuine minimum point on energy-versus-deformation curve, then the ground-state energy, after the perturbation has been introduced, must, by definition, be larger than the equilibrium HF-energy. We shall calculate the change in energy and require that it be positive.

The expression for the ground-state energy is given by

$$\langle H \rangle = \sum_h \langle h | T | h \rangle + \frac{1}{2} \sum_{h,h'} (hh' | v | hh') \qquad (3.61)$$

If we use an arbitrary representation (3.5) and the defining equation (3.7a), then this expression can be easily rewritten in a more convenient and general form:

$$\langle H \rangle = \sum_{\alpha,\beta} \langle \alpha | T | \beta \rangle \langle \beta | \rho | \alpha \rangle + \frac{1}{2} \sum_{\alpha,\beta,\gamma,\delta} (\alpha\beta | v | \gamma\delta) \langle \delta | \rho | \beta \rangle \langle \gamma | \rho | \alpha \rangle \qquad (3.62)$$

If we use the equilibrium value of ρ in this expression, we obtain the equilibrium value of the ground-state energy. On the other hand, using the perturbed density:

$$\hat{\rho} = \rho + \hat{\rho}^{(1)} + \hat{\rho}^{(2)} + \ldots$$

in the same expression we obtain the energy of the perturbed state. We denote the latter by $\langle \hat{H} \rangle$ and obtain

$$\langle \hat{H} \rangle = \sum_{\alpha,\beta} \langle \alpha | T | \beta \rangle \langle \beta | \{ \rho + \hat{\rho}^{(1)} + \hat{\rho}^{(2)} \} \alpha \rangle$$

$$+ \frac{1}{2} \sum_{\alpha,\beta,\gamma,\delta} (\alpha\beta | v | \gamma\delta) \langle \delta | \{ \rho + \hat{\rho}^{(1)} + \hat{\rho}^{(2)} \} | \beta \rangle \langle \gamma | \{ \rho + \hat{\rho}^{(1)} + \hat{\rho}^{(2)} | \alpha \rangle \qquad (3.63)$$

We have used, up to second-order, terms in $\hat{\rho}$, and hence shall be satisfied by evaluating $\langle \hat{H} \rangle$ to second order. The zero-order term in Eq.(3.63) comes from ρ everywhere, and hence exactly agrees with the equilibrium value $\langle H \rangle$, as given by Eq.(3.62). We will write explicitly the first- and second-order terms of Eq.(3.63). Denoting the order by the corresponding superscripts we have

$$\langle \hat{H}^{(1)} \rangle = \sum_{\alpha,\beta} \langle \alpha | T | \beta \rangle \langle \beta | \hat{\rho}^{(1)} | \alpha \rangle + \sum_{\alpha,\beta,\gamma,\delta} (\alpha\beta | v | \gamma\delta) \langle \delta | \rho | \beta \rangle \langle \gamma | \hat{\rho}^{(1)} | \alpha \rangle$$
$$\qquad (3.64)$$

In writing the potential energy term in Eq.(3.64) we notice that there are two first-order terms: $\langle \delta | \hat{\rho}^{(1)} | \beta \rangle \langle \gamma | \rho | \alpha \rangle$ and $\langle \delta | \rho | \beta \rangle \langle \gamma | \hat{\rho}^{(1)} | \alpha \rangle$. Because of the summation over $\alpha, \beta, \gamma, \delta$ these two terms lead to identical results. We have, therefore, kept one of these factors in Eq.(3.64) and have cancelled the factor $1/2$ in (3.63) with the factor of 2 which we acquired from the identity of the two terms. In a similar manner, we collect the second-order terms of the type $\rho \hat{\rho}^{(2)}$, $\hat{\rho}^{(2)} \rho$ and $\hat{\rho}^{(1)} \hat{\rho}^{(1)}$ from Eq.(3.63) and obtain

$$\langle \hat{H}^{(2)} \rangle = \sum_{\alpha, \beta} \langle \alpha | T | \beta \rangle \langle \beta | \hat{\rho}^{(2)} | \alpha \rangle,$$

$$+ \sum_{\alpha, \beta, \gamma, \delta} (\alpha \beta | v | \gamma \delta) \langle \delta | \rho | \beta \rangle \langle \gamma | \hat{\rho}^{(2)} | \alpha \rangle$$

$$+ \frac{1}{2} \sum_{\alpha, \beta, \gamma, \delta} (\alpha \beta | v | \gamma \delta) \langle \delta | \hat{\rho}^{(1)} | \beta \rangle \langle \gamma | \hat{\rho}^{(1)} | \alpha \rangle \qquad (3.65)$$

We shall first simplify Eq. (3.64) and show that this first-order change in energy is zero. First insert the definition of the HF potential V from Eq. (3.6) in the second term of Eq. (3.64) and obtain

$$\langle \hat{H}^{(1)} \rangle = \sum_{\alpha, \beta} \langle \alpha | T | \beta \rangle \langle \beta | \hat{\rho}^{(1)} | \alpha \rangle + \sum_{\alpha, \gamma} \langle \alpha | V | \gamma \rangle \langle \gamma | \hat{\rho}^{(1)} | \alpha \rangle$$

$$= \sum_{\alpha, \beta} \langle \alpha | (T + V) | \beta \rangle \langle \beta | \hat{\rho}^{(1)} | \alpha \rangle$$

Notice that this form is actually a trace of $(T + V) \hat{\rho}^{(1)}$ in our arbitrary representation α, β, ... etc. Since the trace is invariant with respect to representation, we examine this expression in the HF-representation, where the HF single-particle Hamiltonian $(T + V)$ is diagonal, and $\rho^{(1)}$, as proved earlier, has only matrix elements connecting a hole state with a particle state. In the HF-representation

$$\langle \hat{H}^{(1)} \rangle = \sum_{i,j} \langle i | (T + V) | j \rangle \langle j | \hat{\rho}^{(1)} | i \rangle$$

$$= \sum_{i,j} \epsilon_i \delta_{ij} \langle j | \hat{\rho}^{(1)} | i \rangle = 0 \qquad (3.66)$$

because the requirement δ_{ij} is contradictory to the property of $\hat{\rho}^{(1)}$ just now mentioned, and makes $\langle j | \hat{\rho}^{(1)} | i \rangle$ vanish. Here ϵ_i is the energy of the HF-state i.

We next examine the second-order expression (3.65). Once again use the definition (3.6) and obtain

$$\langle \hat{H}^{(2)} \rangle = \sum_{\alpha, \beta} \langle \alpha | (T + V) | \beta \rangle \langle \beta | \hat{\rho}^{(2)} | \alpha \rangle$$

$$+ \frac{1}{2} \sum_{\alpha, \beta, \gamma, \delta} (\alpha \beta | v | \gamma \delta) \langle \delta | \hat{\rho}^{(1)} | \beta \rangle \langle \gamma | \hat{\rho}^{(1)} | \alpha \rangle$$

Now we use the HF-representation, together with the properties (3.21a, b, c) and (3.22a, b). This gives for the first line of $\langle \hat{H}^{(2)} \rangle$

$$\sum_h \langle h | (T + V) | h \rangle \langle h | \hat{\rho}^{(2)} | h \rangle + \sum_p \langle p | (T + V) | p \rangle \langle p | \hat{\rho}^{(2)} | p \rangle$$

$$= \sum_{h,p} (\epsilon_p - \epsilon_h) \langle h | \hat{\rho}^{(1)} | p \rangle \langle p | \hat{\rho}^{(1)} | h \rangle$$

where $(\epsilon_p - \epsilon_h) = W_{hp0}$ is the energy of the unperturbed hole-particle state with respect to the ground-state energy W_0. Combining this with the second line of $\langle \hat{H}^{(2)} \rangle$ we obtain the final expression:

$$\langle \hat{H}^{(2)} \rangle = \sum_{h,p} W_{hp0} \langle h | \hat{\rho}^{(1)} | p \rangle \langle p | \hat{\rho}^{(1)} | h \rangle$$

$$+ \frac{1}{2} \sum_{h,p} \sum_{h'p'} [(p'p|v|h'h) \langle h | \hat{\rho}^{(1)} | p \rangle \langle h' | \hat{\rho}^{(1)} | p' \rangle$$

$$+ (h'h|v|p'p) \langle p | \hat{\rho}^{(1)} | h \rangle \langle p' | \hat{\rho}^{(1)} | h' \rangle$$

$$+ (h'p|v|p'h) \langle h | \hat{\rho}^{(1)} | p \rangle \langle p' | \hat{\rho}^{(1)} | h' \rangle$$

$$+ (p'h|v|h'p) \langle p | \hat{\rho}^{(1)} | h \rangle \langle h' | \hat{\rho}^{(1)} | p' \rangle] \tag{3.67}$$

The results (3.66) and (3.67) have an interesting physical meaning. We notice that when we disturb the nucleus from its equilibrium, the first-order change in density cannot generate any first-order change in energy. The lowest-order change in energy is given by Eq.(3.67) and it is quadratic in the density fluctuation $\hat{\rho}^{(1)}$. This has a classical analogy in terms of what happens to a vibrator. Off equilibrium, the vibrator has an energy which is quadratic in the vibrator co-ordinate. Therefore, Eq.(3.67) can be used, with suitable models, to compute the spring constant of nuclear vibration. It will be an interesting exercise for the student to try this program for the model described in section 3C.

We introduce the following simplified notation:

$$\langle p | \hat{\rho}^{(1)} | h \rangle = x_{hp}$$

and hence

$$\langle h | \hat{\rho}^{(1)} | p \rangle = x_{hp}^*$$

since $\hat{\rho}^{(1)}$ is Hermitian. Using definitions (3.52a,b), Eq.(3.67) can be written as

$$\langle \hat{H}^{(2)} \rangle = \frac{1}{2} \sum_{h,p} \sum_{h'p'} [x_{hp}^* A_{hp,h'p'} x_{h'p'} + x_{hp} A_{hp,h'p'}^* x_{h'p'}^*$$

$$+ x_{hp}^* B_{hp,h'p'} x_{h'p'}^* + x_{hp} B_{hp,h'p'}^* x_{h'p'}]$$

$$\equiv \frac{1}{2} (x^* \; x) \begin{pmatrix} A & B \\ B^* & A^* \end{pmatrix} \begin{pmatrix} x \\ x^* \end{pmatrix} \tag{3.68}$$

where x and x^* are vectors having components x_{hp} and x^*_{hp}, respectively. The condition for a genuine HF-minimum then guarantees expression (3.68) being greater than zero, i.e.

$$(x^*\ x)\ M\begin{pmatrix}x\\x^*\end{pmatrix} > 0 \qquad\qquad (3.69)$$

If $\begin{pmatrix}x\\y\end{pmatrix}$ is any eigenvector M having eigenvalue m then

$$Ax + By = mx$$

and

$$B^*x + A^*y = my \qquad\qquad .$$

Since the eigenvalue m of the Hermitian matrix M is real we get, by taking the complex conjugate of these two equations,

$$Ay^* + Bx^* = my^*$$

$$B^*y^* + A^*x^* = mx^*$$

As a matrix equation we, therefore, have

$$M\begin{pmatrix}y^*\\x^*\end{pmatrix} = m\begin{pmatrix}y^*\\x^*\end{pmatrix}$$

Thus, each eigenvalue of M is, at least, doubly degenerate. The existence of an eigenvector $\begin{pmatrix}x\\y\end{pmatrix}$ automatically ensures the existence of another $\begin{pmatrix}y^*\\x^*\end{pmatrix}$, as proved above. Any linear combination of these two vectors will also be an eigenvector of M belonging to the same eigenvalue. Thus, in particular,

$$\begin{pmatrix}x + y^*\\y + x^*\end{pmatrix}\ \text{and}\ \begin{pmatrix}(x - y^*)i\\-i(y - x^*)\end{pmatrix} \qquad\qquad (3.70)$$

are eigenvectors belonging to the same eigenvalue. Both of these vectors have the form of the special vector appearing in inequality (3.69). Because of the different signs in the two vectors (3.70) one of them at least, will be non-vanishing. Therefore, we have proved with the aid of inequality (3.69), where x is arbitrary, that for every eigenvalue m of the matrix M, there is, at least, one eigenvector in the special form of expression (3.69), which shows that each eigenvalue of M is positive definite.

A.2. Eigenvalues of M' are real

The result proved above will enable us to show that the eigenvalues of M' are real. From definition (3.53), if we use an eigenvector $\begin{pmatrix}X\\Y\end{pmatrix}$ of M' belonging to the eigenvalue $\hbar\omega$, we have

$$(X^*\ Y^*)\ M\begin{pmatrix}X\\Y\end{pmatrix} = \hbar\omega\ (X^*\ Y^*)\begin{pmatrix}X\\-Y\end{pmatrix}$$

$$= \hbar\omega\ (|X|^2 - |Y|^2) \qquad\qquad (3.71)$$

But all the eigenvalues of the matrix M being real and positive definite, the left-hand side which is the expectation value of M for an arbitrary state (i.e. not an eigenstate of M) must also be real and positive definite. Therefore,

$$\hbar\omega(|X|^2 - |Y|^2) = \text{real and} \geq 0 \qquad (3.72)$$

Since the quantity enclosed in the parentheses is real, we prove that $\hbar\omega$, the eigenvalue of M', is real. The inequality in (3.72) then requires that

$$|X|^2 - |Y|^2 > 0 \quad \text{when} \quad \hbar\omega > 0$$

$$< 0 \quad \text{when} \quad \hbar\omega < 0 \qquad (3.73)$$

4. GENERAL MICROSCOPIC THEORY − QUASI-PARTICLE MODE

4.1. Basic concept of quasi-particles

In this section we shall derive a general microscopic theory of nuclear states in a manner that will make it applicable to all the three cases mentioned in the introductory section. The second-quantized version of the many-body Hamiltonian, which will be used for this purpose, is given by

$$H = \sum_{\alpha,\beta} \langle \alpha | T | \beta \rangle c_\alpha^\dagger c_\beta + \frac{1}{2} \sum_{\alpha,\beta,\gamma,\delta} \langle \alpha\beta | v | \gamma\delta \rangle c_\alpha^\dagger c_\beta^\dagger c_\delta c_\gamma \qquad (4.1)$$

where $c_\alpha^\dagger$, c_β, etc. are the creation and destruction operators for a set of single-particle basis states. The factor $1/2$ in front of the second term has to be changed to $1/4$ if we want to use the rounded-bracket matrix element $(\alpha\beta | v | \gamma\delta)$ in formula (4.1) defined by Eq.(3.4). However, it is not necessary to do this. The form (4.1) automatically gives rise to the direct-minus-exchange terms of the two-body potential in actual calculations.

The destruction operator used above has the following important property: the physical vacuum state $|0\rangle$ does not contain any nucleons by definition, and hence it should be impossible to destroy any nucleon from this state, that is,

$$c_\beta |0\rangle = 0 \quad \text{for all } \beta \qquad (4.2)$$

To generalize this concept, let us first examine what happens for the HF-state, i.e., the situation depicted in Figs 1.1a and 1.2a. The HF-state $|\Psi_0\rangle$ contains a set of occupied single-particle states h, h',.... etc. and hence it is impossible to create another particle in an occupied state h without violating the Pauli exclusion principle. Therefore,

$$c_h^\dagger |\Psi_0\rangle = 0 \quad \text{for all h occupied in } \Psi_0 \qquad (4.3a)$$

The state $|\Psi_0\rangle$ does not contain any of the unoccupied single-particle

states p, p', ..., etc. and hence it should be impossible to destroy any such state from $|\Psi_0\rangle$

$$c_p|\Psi_0\rangle = 0 \text{ for all p unoccupied in } \Psi_0 \qquad (4.3b)$$

If we now define a new destruction operator for the self-consistent single-particle states by the following relation:

$$b_i = c_i^\dagger \text{ when } i = h, \text{ i.e. any of the occupied states,}$$

$$= c_i \text{ when } i = p, \text{ i.e. any of the unoccupied states,} \qquad (4.4)$$

then Eqs (4.3a,b) can be combined and written as

$$b_i|\Psi_0\rangle = 0 \text{ for all i} \qquad (4.5)$$

Now, notice the formal similarity between Eqs (4.2) and (4.5). We can, therefore, interpret the HF-state $|\Psi_0\rangle$ as the vacuum state for the new objects whose destruction operators are defined by Eqs (4.4). These new objects are created by the operators which are Hermitian conjugate to the operators (4.4), that is, by

$$b_i^\dagger = c_i \text{ when } i \text{ is any of the occupied states,}$$

$$= c_i^\dagger \text{ when } i \text{ is any of the unoccupied states.} \qquad (4.6)$$

We call these new objects the "quasi-particles" and the Hartree-Fock state Ψ_0 plays the role of the vacuum for these quasi-particles. The quasi-particle states are certainly distinct from the particle states we started with, because Ψ_0 does contain a lot of particle states, even though it does not contain any quasi-particle. As a matter of fact, the quasi-particle in the present example is either a "hole" in the HF-state or a "particle" above the occupied states in $|\Psi_0\rangle$. This is a consequence of definition (4.6), the first line of which says that if we destroy a particle state in the Fermi sea (i.e. the set of occupied states), and thereby create a "hole", in that state, this operation becomes equivalent to the creation of a "quasi-particle"; on the other hand, the second line of definition (4.6) gives us another alternative way of getting a quasi-particle, i.e. by creating a "particle" above the Fermi sea.

In the general microscopic theory to be described here, it is our aim to obtain a ground state in the more complicated cases (b) and (c) of Fig.1.1 and (b) of Fig.1.2, which also satisfies a property like Eq.(4.5). Since the probability distribution near the top of the Fermi sea in Fig.1.2b is very much spread out, in this more general case we cannot speak of a pure "hole" state inside the Fermi sea, or a pure "particle" state above the Fermi sea. Hence, the quasi-particle will obviously lose the simple definitions (4.4) and (4.6). The main object of the theory is to find the quasi-particles suitably

so that the ground state in the more general situation can also behave as a vacuum state for these quasi-particles.

4.2. Quasi-particle transformation of the Hamiltonian

Even without writing down the quasi-particle operators explicitly, it is possible to derive a general form for the transformed Hamiltonian. For this purpose, we only assume that a ground state exists which is a vacuum state for the quasi-particles, and that there exists a transformation from the particle creation and destruction operators to the corresponding operators for the quasi-particles.

According to the Wick's theorem which holds for any product of a set of creation and destruction operators, we can write the following identities:

$$c_\alpha^\dagger c_\beta = \; : c_\alpha^\dagger c_\beta : \; + \langle c_\alpha^\dagger c_\beta \rangle \tag{4.7}$$

$$c_\alpha^\dagger c_\beta^\dagger c_\delta c_\gamma = \; : c_\alpha^\dagger c_\beta^\dagger c_\delta c_\gamma :$$

$$+ \; : c_\alpha^\dagger c_\beta^\dagger : \langle c_\delta c_\gamma \rangle \; + \langle c_\alpha^\dagger c_\beta^\dagger \rangle \; : c_\delta c_\gamma :$$

$$+ \; : c_\alpha^\dagger c_\gamma : \langle c_\beta^\dagger c_\delta \rangle \; + \langle c_\alpha^\dagger c_\gamma \rangle \; : c_\beta^\dagger c_\delta :$$

$$- \; : c_\alpha^\dagger c_\delta : \langle c_\beta^\dagger c_\gamma \rangle \; - \langle c_\alpha^\dagger c_\delta \rangle \; : c_\beta^\dagger c_\gamma :$$

$$+ \langle c_\alpha^\dagger c_\beta^\dagger \rangle \langle c_\delta c_\gamma \rangle \; + \langle c_\alpha^\dagger c_\gamma \rangle \langle c_\beta^\dagger c_\delta \rangle \; - \langle c_\alpha^\dagger c_\delta \rangle \langle c_\beta^\dagger c_\gamma \rangle \tag{4.8}$$

In these expressions $\langle \; \rangle$ denotes an expectation value with respect to the ground state Ψ_0 which is the vacuum state of the quasi-particles. This is usually called the contraction of the pair of operators enclosed by the pointed brackets. The symbol : : denotes the normal product of the operators appearing in between the dots. To evaluate the normal product one has, first of all, to express all particle creation and destruction operators in terms of the quasi-particle creation and destruction operators, and then permute all the quasi-particle destruction operators to the right of all the quasi-particle creation operators: the sign has to be plus or minus, depending on the even or odd nature of the permutation needed. Since we have not yet defined our transformation from the particle operators to the quasi-particle operators we shall have to keep the normal products in their symbolic forms, for the time being. The explicit evaluation of the contractions will also involve substituting the particle operators by the quasi-particle operators and then simplifying the expression with the help of the basic property of the ground state, i.e. that a quasi-particle destruction operator produces zero on it. This explicit evaluation also has to wait, for the time being. We proceed transforming our Hamiltonian (4.1) with the standard results (4.7) and (4.8). Even though we have merely quoted these standard results, the enterprising reader may already have discovered the rules of the game on his own. The rule is first to write down the normal product of the whole expression (the first terms of expressions (4.7) and (4.8)); then contract

all possible pairs of operators and multiply by the normal product of any operator that may be left (this gives the second term of expression (4.7) and the second, third and fourth lines of Eq.(4.8)); continue the contraction process with an additional pair and multiply by the normal product of any operator that may be left (this gives the last line of Eq.(4.8)); stop when all the operators have been contracted pairwise. In each term, take the sign as plus or minus depending on the even or odd nature of the permutation of operators that has taken place in the particular term with respect to the ordering of the operators on the left-hand side. This explains the minus sign in the fourth line and the last term of Eq.(4.8).

We substitute the expressions (4.7) and (4.8) in the original Hamiltonian (4.1). There will be terms containing only contractions, and hence these terms represent a pure number. We shall denote this part of H by H_0 (zero denotes that there are no operators in this part of H). Then, there will be a second set of terms which will contain the normal product of a pair of operators. Such terms will be denoted by H_2 (2 denotes that there are two operators in it). Finally, we shall have a part H_4 coming from the first line of Eq.(4.8). We shall write these different parts of H one after another. First,

$$
H_0 = \sum_{\alpha,\beta} \langle \alpha | T | \beta \rangle \langle c_\alpha^\dagger c_\beta \rangle + \frac{1}{2} \sum_{\alpha,\beta,\gamma,\delta} \langle \alpha\beta | v | \gamma\delta \rangle \left[\langle c_\alpha^\dagger c_\beta^\dagger \rangle \langle c_\delta c_\gamma \rangle \right.
$$
$$
\left. + \langle c_\alpha^\dagger c_\gamma \rangle \langle c_\beta^\dagger c_\delta \rangle - \langle c_\alpha^\dagger c_\delta \rangle \langle c_\beta^\dagger c_\gamma \rangle \right]
$$

(4.9)

Since γ, and δ are summation symbols we can interchange them in the last term, which then becomes

$$
-\frac{1}{2} \sum_{\alpha,\beta,\gamma,\delta} \langle \alpha\beta | v | \delta\gamma \rangle \langle c_\alpha^\dagger c_\gamma \rangle \langle c_\beta^\dagger c_\delta \rangle
$$

This term then can be combined with its predecessor to give

$$
\frac{1}{2} \sum_{\alpha,\beta,\gamma,\delta} (\alpha\beta | v | \gamma\delta) \langle c_\alpha^\dagger c_\gamma \rangle \langle c_\beta^\dagger c_\delta \rangle
$$

(4.10)

Notice the appearance of the rounded-bracket matrix element from the direct-minus-exchange terms. If we use definition (3.14) for the density operator (which was valid for any general ground-state wave function Ψ_0), and definition (3.6) for the self-consistent potential V, then the kinetic energy term of expression (4.9) and the last two terms (given by expression (4.10)) give rise to

$$
\sum_{\alpha,\beta} \langle \alpha | T | \beta \rangle \langle \beta | \rho | \alpha \rangle + \frac{1}{2} \sum_{\alpha,\beta,\gamma,\delta} (\alpha\beta | v | \gamma\delta) \langle \gamma | \rho | \alpha \rangle \langle \delta | \rho | \beta \rangle
$$
$$
= \sum_{\alpha,\beta} \langle \alpha | (T + \tfrac{1}{2} V) | \beta \rangle \langle \beta | \rho | \alpha \rangle
$$

(4.11)

This expression agrees with expression (3.62), which was the ground-state energy for a HF-state. In the present case, H_0 is, indeed, the energy of the ground state because the terms H_2 and H_4 of the Hamiltonian will contain normal products of operators in which the quasi-particle destruction operators, by definition, appear on the right, and hence they produce zero operating on the ground state Ψ_0. We notice that the present expression for the energy of the ground state, which is more general than the HF-state, contains an extra term, i.e. the term $\langle c_\alpha^\dagger c_\beta^\dagger \rangle \langle c_\delta c_\gamma \rangle$ of Eq.(4.9). To study the consequence of this term we introduce the following definition of the pairing density κ:

$$\kappa_{\delta\gamma} = \langle c_\delta c_\gamma \rangle \qquad (4.12a)$$

such that

$$\kappa_{\beta\alpha}^* = \langle c_\alpha^\dagger c_\beta^\dagger \rangle = \langle c_\beta c_\alpha \rangle^* \qquad (4.12b)$$

Since the destruction operators anticommute with each other, we have

$$\kappa_{\gamma\delta} = \langle c_\gamma c_\delta \rangle = -\langle c_\delta c_\gamma \rangle = -\kappa_{\delta\gamma} \qquad (4.12c)$$

We, therefore, write the extra term of Eq.(4.9) as

$$\frac{1}{2} \sum_{\alpha,\beta,\gamma,\delta} \langle \alpha\beta | v | \gamma\delta \rangle \kappa_{\beta\alpha}^* \frac{1}{2} (\kappa_{\delta\gamma} - \kappa_{\gamma\delta})$$

$$= \frac{1}{4} \sum_{\alpha,\beta,\gamma,\delta} (\alpha\beta | v | \gamma\delta) \kappa_{\beta\alpha}^* \kappa_{\delta\gamma} \qquad (4.13)$$

In writing the last step we have interchanged γ and δ in the term with $\kappa_{\gamma\delta}$, thereby picking up the rounded-bracket matrix element of x with the direct minus exchange. Now, we introduce the further definition of a pairing potential:

$$\Delta_{\alpha\beta} = \frac{1}{2} \sum_{\gamma,\delta} (\alpha\beta | v | \gamma\delta) \kappa_{\delta\gamma} \qquad (4.14)$$

and then expression (4.13) simplifies to

$$\frac{1}{2} \sum_{\alpha,\beta} \Delta_{\alpha\beta} \kappa_{\beta\alpha}^* \qquad (4.15)$$

Adding expression (4.15) to expression (4.11) we obtain the final formula for the ground-state energy H_0, as given by Eq.(4.9),

$$H_0 = \sum_{\alpha,\beta} \{ \langle \alpha | (T + \tfrac{1}{2} V) | \beta \rangle \langle \beta | \rho | \alpha \rangle + \tfrac{1}{2} \Delta_{\alpha\beta} \kappa_{\beta\alpha}^* \} \qquad (4.16)$$

We next collect, by expressions (4.7) and (4.8), all terms of Eq.(4.1) which contain the normal product of a pair. Thus,

$$
H_2 = \sum_{\alpha, \beta} \langle \alpha | T | \beta \rangle : c_\alpha^\dagger c_\beta : + \frac{1}{2} \sum_{\alpha, \beta, \gamma, \delta} \langle \alpha\beta | v | \gamma\delta \rangle \, [: c_\alpha^\dagger c_\beta^\dagger : \langle c_\delta c_\gamma \rangle
$$

$$
+ \langle c_\alpha^\dagger c_\beta^\dagger \rangle : c_\delta c_\gamma : + \; : c_\alpha^\dagger c_\gamma : \langle c_\beta^\dagger c_\delta \rangle + \langle c_\alpha^\dagger c_\gamma \rangle : c_\beta^\dagger c_\delta :
$$

$$
- : c_\alpha^\dagger c_\delta : \langle c_\beta^\dagger c_\gamma \rangle - \langle c_\alpha^\dagger c_\delta \rangle : c_\beta^\dagger c_\gamma :]
\qquad (4.17)
$$

Since $\langle \alpha\beta | v | \gamma\delta \rangle = \langle \gamma\delta | v | \alpha\beta \rangle$, straightforward interchange of summation labels will verify that the first two terms in the potential energy are Hermitian conjugates of each other. Similarly, since $\langle \beta\alpha | v | \delta\gamma \rangle = \langle \alpha\beta | v | \gamma\delta \rangle$, the next two terms in the potential energy can be proved to be equal to one another; for the same reason, the last two terms of Eq.(4.17) are also equal. Furthermore, by the interchange of summation labels the last term can be converted to $- \langle \alpha\beta | v | \delta\gamma \rangle \langle c_\alpha^\dagger c_\gamma \rangle : c_\beta^\dagger c_\delta :$. Taken with the corresponding positive term in Eq.(4.17) we thus obtain the rounded-bracket matrix element of v. As far as the first term in the potential energy is concerned, we can get the rounded-bracket matrix element by replacing $\kappa_{\delta\gamma}$ with $(\frac{1}{2})(\kappa_{\delta\gamma} - \kappa_{\gamma\delta})$ and then using the trick that went into Eq.(4.13). With all these simplifications, Eq.(4.17) will read

$$
H_2 = \sum_{\alpha, \beta} \langle \alpha | T | \beta \rangle : c_\alpha^\dagger c_\beta : + \sum_{\alpha, \beta, \gamma, \delta} (\alpha\beta | v | \gamma\delta) \langle \delta | \rho | \beta \rangle : c_\alpha^\dagger c_\gamma :
$$

$$
+ \frac{1}{4} \sum_{\alpha, \beta, \gamma, \delta} [(\alpha\beta | v | \gamma\delta) \, \kappa_{\delta\gamma} : c_\alpha^\dagger c_\beta^\dagger : \; + \text{Hermitian conjugate}]
$$

Once again, using the definitions of V and Δ, we get

$$
H_2 = \sum_{\alpha, \beta} \langle \alpha | (T + V) | \beta \rangle : c_\alpha^\dagger c_\beta : + \frac{1}{2} \sum_{\alpha, \beta} \{ \Delta_{\alpha\beta} : c_\alpha^\dagger c_\beta^\dagger : \; + \text{Hermitian conjugate} \}
\qquad (4.18)
$$

Finally, the expression for H_4, which comes from the $: c_\alpha^\dagger c_\beta^\dagger c_\delta c_\gamma :$ term of Eq.(4.8). From (4.1) it is given by

$$
H_4 = \frac{1}{2} \sum_{\alpha\beta\gamma\delta} \langle \alpha\beta | v | \gamma\delta \rangle : c_\alpha^\dagger c_\beta^\dagger c_\delta c_\gamma :
$$

$$
= \frac{1}{4} \sum_{\alpha\beta\gamma\delta} (\alpha\beta | v | \gamma\delta) : c_\alpha^\dagger c_\beta^\dagger c_\delta c_\gamma :
\qquad (4.19)
$$

The last step follows after writing $c_\delta c_\gamma = (\frac{1}{2})(c_\delta c_\gamma - c_\gamma c_\delta)$ and then making interchange of the summation indices γ, δ in the negative term.

4.3. Self-consistent Hartree-Fock and Hartree-Fock-Bogolyubov theory

We have now come to a stage where we can try to determine the ground state Ψ_0 by minimizing H_0, which is the expectation value of the Hamiltonian with respect to this state. For this purpose, let us first note the structure of the pairing density (4.12a) and the pairing potential (4.14). In Eq.(4.12a) we are starting with the ground state Ψ_0 on the right, destroying two particles in states γ and δ, and then trying to reach the state Ψ_0 again on the left. Such a quantity can clearly be non-vanishing only if Ψ_0 contains wave functions with different number of particles. If number conservation of particles holds strictly true for Ψ_0, then after $c_\delta c_\gamma$ has operated on it we reach a state of a nucleus having two nucleons less, and hence the overlap of a number conserving $\langle \Psi_0 |$ with $c_\delta c_\gamma |\Psi_0\rangle$ is zero.

Therefore, for simplicity, let us first consider a ground-state wave function Ψ_0 for which conservation of the number of particles is strictly valid. The terms containing the pairing potential in Eqs (4.16) and (4.18) are then absent. As far as the determination of Ψ_0 is concerned, we may apply the variational principle, and require that

$$\overline{H}_0 = \sum_{\alpha,\beta} \langle \alpha | (T + \tfrac{1}{2} V) | \beta \rangle \langle \beta | \rho | \alpha \rangle \tag{4.20}$$

be minimized. In the parts on HF-theory in this paper, we have seen that this is exactly what the HF-program does. We recall that the solution to this variational problem is as follows: We define a set of single-particle states

$$| i \rangle = \sum_\alpha X_\alpha^{(i)} | \alpha \rangle, \quad \text{or} \quad c_i^\dagger = \sum_\alpha X_\alpha^{(i)} c_\alpha^\dagger \tag{4.21a}$$

and then the variational parameters $X_\alpha^{(i)}$ that make $\overline{H}_0$ a minimum satisfy

$$\sum_\beta \langle \alpha | (T + V) | \beta \rangle X_\beta^{(i)} = \epsilon_i X_\alpha^{(i)} \tag{4.21b}$$

This system of equations for the determination of $X_\alpha^{(i)}$ are the HF-equations, and they have to be solved self-consistently, because V already contains ρ, which, in its turn, contains the unknown coefficients $X_\alpha^{(i)}$ (see Eqs (3.6 and (3.7a)).

If, however, we want to minimize the complete H_0, with the pairing-potential term included, we know a variational state Ψ_0, in which the number of particles is conserved, will not be adequate. We, therefore, consider a generalized variational state Ψ_0, which contains a superposition of the wave functions of nuclei having different numbers of nucleons. If we want to apply such a theory to a given nucleus, then, of course, we shall have to carry out the variational calculation on H_0, subject to the constraint that the average value of the number of nucleons in the state Ψ_0 be equal to the given number of nucleons of the nucleus under consideration. As is well

known, the constraint in a variational problem is specified in terms of a Lagrange multiplier. Therefore, instead of minimizing $\langle \Psi_0 | H | \Psi_0 \rangle$, i.e. H_0 of Eq. (4.16), we have to minimize in this case $\langle \Psi_0 | (H - \lambda \hat{N}) | \Psi_0 \rangle$ where λ is the Lagrange multiplier and $\hat{N}$ is the operator for the total number of nucleons:

$$\hat{N} = \sum_{\alpha} c_\alpha^\dagger c_\alpha$$

If we had transformed $H - \lambda \hat{N}$ instead of H into H_0, H_2 and H_4, then it is clear from the form of $\hat{N}$, i.e.

$$\hat{N} = \sum_{\alpha} c_\alpha^\dagger c_\alpha = \sum_{\alpha} \{ \langle c_\alpha^\dagger c_\alpha \rangle + : c_\alpha^\dagger c_\alpha : \} \qquad (4.22)$$

that the term $-\lambda \hat{N}$ would have contributed a term to H_0 and a term to H_2, leaving H_4 unaltered. In analogy to the kinetic-energy term, it is obvious that these extra terms will be obtained be replacing the operator T by $T - \lambda \mathbf{1}$, where $\mathbf{1}$ is the unity operator, in both H_0 and H_2. We write these expressions for $H_0(\lambda)$ and $H_2(\lambda)$ from Eqs (4.16) and (4.18), together with the recipe mentioned just now:

$$H_0(\lambda) = \sum_{\alpha,\beta} \{ \langle \alpha | (T - \lambda \mathbf{1} + \tfrac{1}{2} V) | \beta \rangle \langle \beta | \rho | \alpha \rangle + \tfrac{1}{2} \Delta_{\alpha\beta} \kappa^*_{\beta\alpha} \} \qquad (4.23a)$$

$$H_2(\lambda) = \sum_{\alpha,\beta} \langle \alpha | (T - \lambda \mathbf{1} + V) | \beta \rangle : c_\alpha^\dagger c_\beta : + \tfrac{1}{2} \sum_{\alpha,\beta} [\Delta_{\alpha\beta} : c_\alpha^\dagger c_\beta^\dagger : \qquad (4.23b)$$

$$+ \text{Hermitian conjugate}]$$

In analogy to the transformation (4.21a) we now use a generalized transformation:

$$b_i^\dagger = \sum_{\alpha} x_\alpha^{(i)} c_\alpha^\dagger + \sum_{\alpha} y_\alpha^{(i)} c_\alpha \qquad (4.24)$$

where the coefficients $x_\alpha^{(i)}$ and $y_\alpha^{(i)}$ are the variational parameters. These operators $b_i^\dagger$ are the creation operators for our quasi-particles and will be completely determined when the minimization program for $H_0(\lambda)$ is carried out. This procedure gives rise, in analogy to the HF-case, to a set of coupled equations for the variational parameters, which once again will have to be solved self-consistently. This self-consistent method of finding the quasi-particles is called the Hartree-Fock-Bogolyubov (HFB) method, and the quasi-particle equation (4.24) is called the HFB-quasi-particle transformation. The self-consistent equations of this method are shown in the Appendix to this section. An observant reader may have already noticed that the HFB-transformation equation (4.24) is, indeed, based on the concept of particle-number non-conservation in the states. The first part of

$b_i^\dagger$ adds a particle, while the second part removes a particle, operating
on any state; thus $b_i^\dagger$ produces wave functions of different number of nucleons
acting on any wave function.

Here, in the main body of this paper, we shall follow, instead of the
fully self-consistent HFB-procedure, a two-step minimization program of
$H_0(\lambda)$ which we shall now describe.

4.4. Simple pairing theory of the BCS-type

In this simplified theory, as the first step of minimizing $H_0(\lambda)$ we shall
omit the pairing potential term of Eq.(4.23a). The resultant minimization
program is clearly identical with what we have done earlier in connection
with Eq.(4.20). The only difference now is the extra term $-\lambda\, 1$. But the
diagonalization problem of $(T+V)$, as shown in Eq.(4.21b), is really not
changed by this extra term. The eigenvectors of $(T+V)$ and $(T+V-\lambda\,1)$
are obviously the same, only the energies are shifted from ϵ_i to $\epsilon_i - \lambda$.
Therefore, at this stage of dealing with $H_0(\lambda)$ we have the set of single-
particle self-consistent states of Eq.(4.21b) and the corresponding energies
$(\epsilon_i - \lambda)$. At the next step of dealing with $H_0(\lambda)$ we use the states $|i\rangle$ as the
basis and rewrite it as

$$H_0(\lambda) = \sum_{i,j} \langle i|(T - \lambda\,1 + \tfrac{1}{2}V)|j\rangle\langle j|\rho|i\rangle + \frac{1}{2}\sum_{i,j} \Delta_{ij}\kappa_{ji}^* \qquad (4.25)$$

where

$$\langle j|\rho|i\rangle = \langle c_i^\dagger c_j\rangle \qquad (4.26a)$$

$$\kappa_{ij} = \langle c_i c_j\rangle \qquad (4.26b)$$

$$\Delta_{ij} = \frac{1}{2}\sum_{k,\ell}(ij|v|k\ell)\kappa_{\ell k} \qquad (4.26c)$$

and

$$\langle i|V|j\rangle = \sum_{k,\ell}(ik|v|j\ell)\langle \ell|\rho|k\rangle \qquad (4.26d)$$

We then do a fresh minimization for $H_0(\lambda)$ using a quasi-particle trans-
formation that is much simpler than the Eq.(4.24). This simpler trans-
formation which we are going to introduce soon, is called the BCS-(Bardeen,
Cooper, Schriffer) transformation, after the name of the people who first
applied a similar transformation to the theory of superconductivity of
metals.

To prepare the ground for the BCS-transformation let us first examine
the characteristics of the self-consistent single-particle states $|i\rangle$. In a
spherical nucleus, such a state is specified by the quantum numbers ℓ, j
and m, and also the number of nodes n in the radial wave function. All the

states having same $(n\,\ell\,j)$ but different $m\,(=-j,\ldots,+j)$ are degenerate. The state $|n\,\ell\,jm\rangle$ has a time-reversed partner which is given by

$$(-1)^{j-m}\,|n\,\ell\,j,\,-m\rangle \qquad (4.27)$$

We shall denote these two partner states, in shorthand notation, as $|i\rangle$ and $|\bar{i}\rangle$; sometimes $|\bar{i}\rangle$ will also be written as $s_i|-i\rangle$, where s_i is the phase factor of expression (4.27) and $|-i\rangle$ stands for the same quantum numbers $(n\,\ell\,j)$ as in $|i\rangle$ but the projection quantum number reversed in sign. In a more general situation when the single-particle states correspond to a non-spherical V, $|i\rangle$ or $|\bar{i}\rangle$ are not as simple as above. But a state $|i\rangle$ in this more complicated case can still be expanded in terms of states of the type $|n\,\ell\,jm\rangle$:

$$|i\rangle = \sum_{n\,\ell\,jm} x^{(i)}_{n\,\ell\,jm}\,|n\ell\,jm\rangle \qquad (4.28a)$$

In this case the time-reversed partner $|\bar{i}\rangle$ is obtained by using Eq.(4.27) for every term in the summation:

$$|\bar{i}\rangle = \sum_{n\,\ell\,jm} x^{(i)}_{n\ell jm}(-1)^{j-m}\,|n\,\ell\,j,\,-m\rangle \qquad (4.28b)$$

If V has a spheroidal symmetry then m is a good quantum number, and there is no summation over m in Eqs (4.28a,b), and the states $|i\rangle$ and $|\bar{i}\rangle$ have m and $-m$ respectively as a labelling quantum number. Even in a more complicated case like Eq.(4.28b) we shall denote $|\bar{i}\rangle$ symbolically as $s_i\,|-i\rangle$. The result that is of most importance to us about the time-reversed partner $|\bar{i}\rangle$ is the following.

Let us carry out a second time reversal on the state (4.27). This clearly gives

$$|\bar{\bar{i}}\rangle = (-1)^{j-m}(-1)^{j+m}\,|n\ell j,\,+m\rangle = -|n\ell\,jm\rangle = -|i\rangle \qquad (4.29a)$$

Similarly, for the more complicated state (4.28b) also, we obtain

$$|\bar{\bar{i}}\rangle = \sum_{n\,\ell\,jm} x^{(i)}_{n\ell jm}(-1)^{j-m}(-1)^{j+m}\,|n\,\ell jm\rangle = -|i\rangle \qquad (4.29b)$$

In both the cases the minus sign is a consequence of the phase factor $(-1)^{2j}$, where $2j$ is always an odd integer. This explicit general result (4.29a,b) tells us that our symbolic quantity s_i has the following property:

$$s_{-i} = -s_i \qquad (4.29c)$$

The steps in proving this important result is as follows: by definition

$$|\bar{i}\rangle = s_i\,|-i\rangle$$

and hence

$$|\bar{\bar{i}}\rangle = s_i s_{-i} |+i\rangle$$

or, by comparison with Eqs (4.29a, b),

$$s_i s_{-i} = -1$$

which is the same as Eq.(4.29c).

In a HF-calculation for even nuclei, a state $|i\rangle$ is usually found to be degenerate with its time-reversed partner $|\bar{i}\rangle = s_i |-i\rangle$. Let us examine now the consequence of creating a particle in the single-particle state $|i\rangle$, and destroying its time-reversed partner $|\bar{i}\rangle$. The first process is achieved by the operator $c_i^\dagger$, while the second process is generated by the operator $s_i c_{-i}$. It is known from the angular momentum property of the second-quantized operators that, under a rotation of the co-ordinate system, the operator $c_{n\ell jm}^\dagger$ and the operator $(-1)^{j-m} c_{n\ell j, -m}$ both transform with the same rotation matrix:

$$c_{n\ell jm}^\dagger \rightarrow \sum_{m'} \mathscr{D}_{mm'}^{(j)} c_{n\ell jm'}^\dagger \qquad (4.30a)$$

$$\{(-1)^{j-m} c_{n\ell j, -m}\} \rightarrow \sum_{m'} \mathscr{D}_{mm'}^{(j)} \{(-1)^{j-m'} c_{n\ell j, -m'}\} \qquad (4.30b)$$

Equation (4.30a) can be taken as a definition, because $c_{n\ell jm}^\dagger$ produces the state $|n\ell jm\rangle$ and this state transforms with $\mathscr{D}_{mm'}^{(j)}$ under rotation. It is left to the reader as an exercise to prove that relation (4.30b) is a consequence of relation (4.30a). All that is necessary is to take the Hermitian conjugate of relation (4.30a), and then use some standard properties of the $\mathscr{D}$-functions.

Using these basic properties, and the expansions (4.28a, b), it is straightforward to establish that $c_i^\dagger$ and $s_i c_{-i}$ behave similarly under rotation. Therefore, instead of using the most general HFB-transformation of (4.24), we now use the simplified BCS-transformation given by

$$b_i^\dagger = u_i c_i^\dagger - v_{-i} s_i c_{-i} \qquad (4.31)$$

The choice of the minus sign in the second term simply defines our phase convention for v_{-i}. One can create a particle in state i only if it is empty, and one can destroy a particle from a certain state only if it is occupied. Therefore, u_i must be the probability amplitude of getting the state i empty (probability of non-occupation), while v_{-i} must be the probability amplitude for occupation of the corresponding time-reversed state. By definition, therefore,

$$u_i^2 + v_i^2 = 1 = u_{-i}^2 + v_{-i}^2 \qquad (4.32)$$

because the total probability of non-occupation plus occupation plus occupation of any state i or -i must be unity. Equation (4.31) automatically gives the quasi-particle destruction operator

$$b_i = u_i c_i - v_{-i} s_i c^\dagger_{-i} \qquad (4.33a)$$

or

$$s_i b_{-i} = +v_i c^\dagger_i + s_i u_{-i} c_{-i} \qquad (4.33b)$$

where we have used the property (4.29c).

It is clear from definition (4.31) that this formal expression could be used even in the HF-case. There, however, u_i and v_i have known values:

$$\begin{aligned}
u_i &= 1 \text{ for a particle state,}\\
&= 0 \text{ for a hole state,}\\
v_i &= 1 \text{ for a hole state,}\\
&= 0 \text{ for a particle state.}
\end{aligned} \qquad (4.34)$$

That is to say, in the HF-case, even if we formally write two terms in expression (4.31), usually one or the other survives. There will be exceptions to this rule whenever we encounter the following situations in the HF-ground state: (1) a state i is unoccupied but its time-reversed partner is occupied; in this case, both terms in expression (4.31) will be present; (2) the second case is the opposite where i is occupied and its time-reversed partner unoccupied; then both terms in expression (4.31) vanish. These exceptional situations usually never happen in even nuclei, in which either both $|i\rangle$ and $|\bar{i}\rangle$ are occupied or unoccupied.

In the cases depicted in Figs 1.1a and b and the occupation probability and non-occupation probability of states near the Fermi surface are non-vanishing fractional quantities, and hence both terms in the BCS-transformation (4.31) survive. Therefore, in such cases the transformation (4.31) indeed gives rise to nucleon number non-conservation, and hence it is able to take into account the consequences of the pairing potential in $H_0(\lambda)$ and $H_2(\lambda)$.

We now require that the quasi-particle operators behave as fermions. Thus, the fermion-anticommutation properties

$$\left\{ b_i, b_j \right\} = \left\{ b^\dagger_i, b^\dagger_j \right\} = 0 \qquad (4.35a)$$

and

$$\left\{ b_i, b^\dagger_j \right\} = \delta_{ij} \qquad (4.35b)$$

will have to be ensured. From Eq.(4.31) we have

$$\left\{ b^\dagger_i, b^\dagger_j \right\} = \left\{ (u_i c^\dagger_i - v_{-i} s_i c_{-i}), (u_j c^\dagger_j - v_{-j} s_j c_{-j}) \right\}$$

$$= -\delta_{i,-j} \, u_i v_{-j} s_j - \delta_{-i,j} \, v_{-i} u_j s_i$$

$$= (+u_i v_i - u_{-i} v_{-i}) s_i$$

We have used here the standard anticommutation rules of $c_i^\dagger$, c_j etc. In the HF-case, this result is always zero, because a state is either occupied or unoccupied and hence either u or v for any state has to be zero. But in the more general BCS-case anticommutation demands

$$u_i v_i = u_{-i} v_{-i} \qquad (4.36a)$$

Next we apply Eq. (4.35b) together with Eqs (4.33a) and (4.31). This gives

$$\delta_{ij} \equiv \left\{ b_i, b_j^\dagger \right\} = \left\{ (u_i c_i - v_{-i} s_i c_{-i}^\dagger), (u_j c_j^\dagger - v_{-j} s_j c_{-j}) \right\}$$

$$= u_i u_j \delta_{ij} + v_{-i} v_{-j} s_i s_j \delta_{-i, -j}$$

$$= (u_i^2 + v_{-i}^2) \delta_{ij}$$

Thus, the requirement is

$$u_i^2 + v_{-i}^2 = 1 \qquad (4.36b)$$

Taking Eq. (4.36b) together with Eq. (4.32) we prove

$$v_i^2 = v_{-i}^2 \text{ and } u_i^2 = u_{-i}^2 \qquad (4.37)$$

Thus, a state i and its time-reversed partner $\bar{i}$ must have the same value for their occupation probability and non-occupation probability. Then Eq. (4.36a) requires either

$$u_i = u_{-i}, \ v_i = v_{-i} \qquad (4.38a)$$

or

$$u_i = -u_{-i}, \ v_i = -v_{-i} \qquad (4.38b)$$

We will choose the phase convention of Eqs (4.38a). The statement underlined above is usually taken as an assumption to start with, in which case one writes v_i instead of v_{-i} in the BCS-transformation (4.31) from the very beginning. The present approach is more physical and rigorous. Now that we have proved Eqs (4.38a), we shall not use a negative subscript any longer in the defining equations (4.31) and (4.33b) which become

$$b_i^\dagger = u_i c_i^\dagger - v_i s_i c_{-i} \qquad (4.39a)$$

and

$$s_i b_{-i} = -v_i c_i^\dagger - u_i s_i c_{-i} \qquad (4.39b)$$

It is easy to invert these relations with the help of Eq. (4.32). One then obtains

$$c_i^\dagger = u_i b_i^\dagger + v_i s_i b_{-i} \qquad (4.40a)$$

and hence

$$c_i = u_i b_i + v_i s_i b_{-i}^\dagger \tag{4.40b}$$

We are now fully equipped to go back to the equations (4.25) and (4.26a, b, c) and do the minimization of $H_0 (\lambda)$, treating u_i and v_i as the variational parameters subject to the constraint $u_i^2 + v_i^2 = 1$. We shall use the basic definition

$$b_i \, | \, \Psi_0 \rangle = 0 \text{ for all i} \tag{4.41}$$

and evaluate Eqs (4.26a) and (4.26b) with the help of Eqs (4.40a, b). Thus

$$\langle j | \rho | i \rangle = \langle \Psi_0 | (u_i b_i^\dagger + v_i s_i b_{-i}) (u_j b_j + v_j s_j b_{-j}^\dagger) | \Psi_0 \rangle$$

$$= \langle \Psi_0 | b_{-i} b_{-j}^\dagger | \Psi_0 \rangle \, v_i v_j s_i s_j \tag{4.42a}$$

$$= \delta_{ij} \, v_i^2$$

and

$$\kappa_{ij} = \langle \Psi_0 | (u_i b_i + v_i s_i b_{-i}^\dagger) (u_j b_j + v_j s_j b_{-j}^\dagger) | \Psi_0 \rangle$$

$$= \langle \Psi_0 | b_i b_{-j}^\dagger | \Psi_0 \rangle \, u_i v_j s_j \tag{4.42b}$$

$$= \delta_{i, -j} \, u_j v_j s_j$$

In simplifying the expressions (4.42a, b) we have used definition (4.41) and its Hermitian conjugate, and then the anticommutator $\{b_i, b_j^\dagger\} = \delta_{ij}$, i.e. $b_i b_j^\dagger = - b_j^\dagger b_i + \delta_{ij}$.

Using the above expression of κ_{ij}, we obtain, for the pairing potential of (4.26c), the following result:

$$\Delta_{ij} = \frac{1}{2} \sum_{k, l}{}' (i\,j \, | \, v \, | \, k\,l) \, u_k v_k s_k \, \delta_{k, -l}$$

$$= \frac{1}{2} \sum_k (i\,j \, | \, v \, | \, k, \bar{k}) \, u_k v_k$$

It is easy to show from the time-reversal invariance of the two-body potential v that in the above expression the state j must be the time-reversed partner of i. Thus

$$\Delta_{ij} = \frac{1}{2} \delta_{j, \bar{i}} \sum_k (i, \bar{i} \, | \, v \, | \, k, \bar{k}) \, u_k v_k \tag{4.42c}$$

Similarly from relations (4.42a) and (4.26d)

$$\langle i \mid V \mid j \rangle = \sum_k (i\,k \mid v \mid j\,k)\, v_k^2 \tag{4.42d}$$

Inserting expressions (4.42a, b, c, d) into Eq. (4.25) we obtain

$$H_0(\lambda) = \sum_i \langle i \mid (T \dashv \lambda\,\mathbf{1}) \mid i \rangle\, v_i^2 + \frac{1}{2} \sum_i \Delta_{i,\bar{i}}\, u_i v_i$$

$$+ \frac{1}{2} \sum_i \langle i \mid V \mid i \rangle\, v_i^2 \tag{4.43a}$$

$$= \sum_i \langle i \mid (T - \lambda\,\mathbf{1}) \mid i \rangle\, v_i^2 + \frac{1}{4} \sum_{i,k} (i,\bar{i} \mid v \mid k, \bar{k})\, u_k v_k u_i v_i$$

$$+ \frac{1}{2} \sum_{i,k} (i\,k \mid V \mid i\,k)\, v_i^2 v_k^2 \tag{4.43b}$$

We now minimize expression (4.43b) by requiring

$$\frac{\partial H_0(\lambda)}{\partial v_a} = 0$$

for each a, using

$$u_a^2 = 1 - v_a^2$$

or

$$\frac{\partial u_a}{\partial v_a} = -\frac{v_a}{u_a}$$

in carrying out the differentiation. We thus obtain

$$2(\epsilon_a - \lambda)\, v_a + \frac{1}{2} \sum_k (a,\bar{a} \mid v \mid k, \bar{k})\, u_k v_k \frac{\partial}{\partial v_a} (u_a v_a)$$

$$= 2(\epsilon_a - \lambda)\, v_a + \Delta_{a,\bar{a}} \left\{ u_a - \frac{v_a^2}{u_a} \right\}$$

$$= 2 u_a^{-1} \left[(\epsilon_a - \lambda)\, u_a v_a + \frac{1}{2} \Delta_{a,\bar{a}} (u_a^2 - v_a^2) \right] = 0$$

or, since u_a^{-1} is non-vanishing,

$$(\epsilon_a - \lambda) \, u_a v_a + \frac{1}{2} \, \Delta_{a,\bar{a}} \, (u_a^2 - v_a^2) = 0 \qquad (4.44)$$

In view of $u_a^2 + v_a^2 = 1$, we can easily solve this equation by putting

$$\cos \theta_a = v_a \, , \qquad \sin \theta_a = u_a$$

Equation (4.44) then yields

$$(\epsilon_a - \lambda) \sin 2 \theta_a = \Delta_a \cos 2 \theta_a$$

or

$$\tan 2 \theta_a = \frac{\Delta_a}{\epsilon_a - \lambda}$$

or

$$2 u_a v_a = \sin 2 \theta_a = \frac{\Delta_a}{\sqrt{(\epsilon_a - \lambda)^2 + \Delta_a^2}} \quad \text{and} \quad \cos 2 \theta_a \equiv u_a^2 - v_a^2 = \frac{\epsilon_a - \lambda}{\sqrt{(\epsilon_a - \lambda)^2 + \Delta_a^2}}$$

$$(4.45)$$

In these equations we have defined

$$\Delta_a = - \Delta_{a, \bar{a}} \qquad\qquad (4.46)$$

$$= - \frac{1}{2} \sum_k (a, \bar{a} \, | v | \, k, \bar{k}) \, u_k v_k$$

which is a positive quantity in virtue of the special matrix element of v being attractive. This matrix element of v which takes a <u>paired</u> state (a state and its time-reversed partner) to another paired state is called the <u>pairing</u> matrix element of the potential. Using the second relation (4.45) with $u_a^2 + v_a^2 = 1$ we obtain

$$u_a^2 = \frac{1}{2} \left[1 + \frac{\epsilon_a - \lambda}{E_a} \right], \quad v_a^2 = \frac{1}{2} \left[1 - \frac{\epsilon_a - \lambda}{E_a} \right] \qquad (4.47)$$

where

$$E_a = \sqrt{(\epsilon_a - \lambda)^2 + \Delta_a^2} \qquad\qquad (4.48)$$

Similarly, substituting the first relation (4.45) into Eq. (4.46) we obtain

$$\Delta_a = - \frac{1}{4} \sum_k (a, \bar{a} \, | v | \, k, \bar{k}) \, \frac{\Delta_k}{E_k} \qquad (4.49)$$

Furthermore, from Eq. (4.42a) we have

$$\sum_i \langle i | \rho | i \rangle \equiv \langle \Psi_0 | \sum_i c_i^\dagger c_i | \Psi_0 \rangle \equiv \langle \Psi_0 | \hat{N} | \Psi_0 \rangle = \sum_i {}' v_i^2$$

where $\hat{N}$ is the total-number operator. According to our earlier stipulation, this expression should be equated to the given number of nucleons (A, say) in the nucleus which we want to calculate. Thus,

$$A = \sum_a v_a^2 = \frac{1}{2} \sum_a \left[1 - \frac{\epsilon_a - \lambda}{E_a} \right] \tag{4.50}$$

Equations (4.49) and (4.50) are a system of coupled non-linear equations (due to definition (4.48) of E_a) in the unknown quantity λ and the set of Δ_a. The total number of the latter depends upon the total number of single-particle states admitted in the calculation. These equations can be solved for the unknown quantities, starting with a <u>given</u> two-body potential. Only a very special type of matrix elements, namely the pairing matrix elements, of the potential are, however, relevant at this stage of the calculation. Knowing λ and the Δ'_as it is then trivial to compute the occupation probabilities of the various states (v_a^2) from Eqs (4.47) and the energies E_a from Eq. (4.48).

To help the reader in his assimilation of facts we mention that the key equations in the long derivation given above are: 1) Equation (4.39a, b) defining the quasi-particle transformation, (2) Eqs (4.47) which determine the transformation coefficients u_a and v_a in the quasi-particle, (3) Eq. (4.48) which determines E_a, (4) Eqs (4.49) and (4.50) whose solutions determine λ and the set of Δ_a. As a matter of fact, one has to start the computation by solving these equations and then go to the equations mentioned in 1) to 3) for the determination of the various quantities.

Treatment of $H_2(\lambda)$ and interpretation of E_a

We shall next show that the minimization of $H_0(\lambda)$ has a very interesting consequence on $H_2(\lambda)$ of Eq. (4.23b). First, we rewrite this equation in terms of the HF-representation, in which the first term $T - \lambda \mathbb{1} + V$ is diagonal and Δ has non-vanishing elements of the type $\Delta_{i\bar{i}}$. Therefore,

$$H_2(\lambda) = \sum_i (\epsilon_i - \lambda) : c_i^\dagger c_i : + \frac{1}{2} \sum_i [\Delta_{i,\bar{i}} s_i : c_i^\dagger c_{-i}^\dagger : \tag{4.51}$$

$$+ \text{ Hermitian conjugate}]$$

We proceed to an evaluation of the normal products from their definition and Eqs (4.40a, b). Thus,

$$: c_i^\dagger c_i : = : (u_i b_i^\dagger + v_i s_i b_{-i})(u_i b_i + v_i s_i b_{-i}^\dagger) :$$

$$= u_i^2 b_i^\dagger b_i - v_i^2 b_{-i}^\dagger b_{-i} + u_i v_i s_i (b_i^\dagger b_{-i}^\dagger + b_{-i} b_i) \tag{4.52a}$$

Only in one term, i.e. in $v_i^2 b_{-i} b_{-i}^\dagger$ we had to take the destruction operator to the right of the creation operator through <u>one</u> permutation, and hence this term has a minus sign. With a similar algebra we obtain

$$: c_i^\dagger c_{-i}^\dagger : = : (u_i b_i^\dagger + v_i s_i b_{-i}) (u_i b_{-i}^\dagger - v_i s_i b_i) :$$

$$= u_i^2 b_i^\dagger b_{-i}^\dagger - v_i^2 b_{-i} b_i - u_i v_i s_i (b_i^\dagger b_i + b_{-i}^\dagger b_{-i})$$

(4.52b)

Using Eqs (4.52a, b) in Eq. (4.51) we get

$$H_2 (\lambda) = H_{11} (\lambda) + H_{20} (\lambda) + H_{02} (\lambda)$$ (4.53)

where the two subscripts denote, respectively, the number of <u>quasi-particle</u> creation and destruction operators. Thus, picking up the appropriate terms from Eqs (4.52a, b) we obtain

$$H_{11} (\lambda) = \sum_i (\epsilon_i - \lambda) (u_i^2 b_i^\dagger b_i - v_i^2 b_{-i}^\dagger b_{-i}) - \sum_i \Delta_{i,\bar{i}} u_i v_i (b_i^\dagger b_i + b_{-i}^\dagger b_{-i})$$

(4.54)

We can simplify this expression further by noting that ϵ_i and ϵ_{-i}, the energy for the time-reversed state, are equal. Hence, by changing i to -i in the summation of the term $b_{-i}^\dagger b_{-i}$, we obtain the first term simplified to

$$\sum_i (\epsilon_i - \lambda) (u_i^2 - v_i^2) b_i^\dagger b_i$$ (4.55a)

Let us do similar tricks with $b_{-i}^\dagger b_{-i}$ occurring with the pairing potential. Here $\Delta_{i\bar{i}} \equiv s_i \Delta_{i, -i}$ changes to $s_i \Delta_{-i, i}$ when $-i \to i$. The latter is equal to $-s_i \Delta_{-i, i} \equiv -\Delta_{\bar{i}, i}$. However, according to the definition (4.42c) $-\Delta_{\bar{i}, i} = \Delta_{i, \bar{i}}$. Therefore, under $-i \to i$, the term $b_{-i}^\dagger b_{-i} \Delta_{i, \bar{i}}$, simply changes to $\Delta_{i, \bar{i}} b_i^\dagger b_i$. Therefore, the second term of Eq. (4.54) simplifies to

$$-2 \sum_i \Delta_{i, \bar{i}} u_i v_i b_i^\dagger b_i$$ (4.55b)

Adding expressions (4.55a, b) we obtain

$$H_{11} (\lambda) = \sum_i [(\epsilon_i - \lambda)(u_i^2 - v_i^2) - 2\Delta_{i, \bar{i}} u_i v_i] b_i^\dagger b_i$$

$$= \sum_i [(\epsilon_i - \lambda) \cos 2\theta_a + \Delta_i \sin 2\theta_i] b_i^\dagger b_i$$ (4.56)

$$= \sum_i E_i b_i^\dagger b_i$$

In simplifying this expression we have used the first line of Eq. (4.46), and Eqs (4.45) and (4.48).

In a similar manner we pick up the appropriate terms from Eqs (4.52a, b), put them into formula (4.51) and obtain

$$H_{20}(\lambda) + H_{02}(\lambda) = \sum_i (\epsilon_i - \lambda)\, u_i v_i\, s_i\ (b_i^\dagger b_{-i}^\dagger + b_{-i}\, b_i)$$

$$+ \frac{1}{2} \sum_i [\Delta_{i,\bar{1}}\, s_i\ (u_i^2\, b_i^\dagger b_{-i}^\dagger - v_i^2 b_{-i}\, b_i)$$

$$\text{+ Hermitian conjugate]}$$

$$= \sum_i \left[(\epsilon_i - \lambda)\, u_i v_i + \frac{1}{2}\, \Delta_{i,\bar{1}}\, (u_i^2 - v_i^2) \right] s_i\ (b_i^\dagger b_{-i}^\dagger + b_{-i}\, b_i) \tag{4.57}$$

Let us compare the quantity enclosed in square brackets with the expression occurring in the minimization condition (4.44). They are exactly identical. Hence the minimization condition <u>automatically</u> guarantees that expression (4.57) is zero:

$$H_{20}(\lambda) + H_{02}(\lambda) \equiv 0 \tag{4.58}$$

This is the interesting consequence to which we have alluded earlier. We can now summarize the transformed Hamiltonian:

$$H = H_0(\lambda) + \sum_i E_i\, b_i^\dagger b_i + H_4(\lambda) \tag{4.59a}$$

where $H_0(\lambda)$ and $H_4(\lambda)$ are given by expressions (4.43a) and (4.19), respectively. The term $H_0(\lambda)$ is the ground-state energy and simplifies to the following expression when we use the expression for $u_i v_i$ from formulas (4.45):

$$H_0(\lambda) = \sum_i \langle i \mid T - \lambda\, \mathbf{1} + \frac{1}{2}\, V \mid i \rangle\, v_i^2 - \frac{1}{4} \sum_i \frac{\Delta_i^2}{E_i} \tag{4.59b}$$

and

$$\langle i \mid V \mid i \rangle = \sum_k (i\, k \mid v \mid i\, k)\, v_k^2 \tag{4.59c}$$

The second term of the Hamiltonian (4.59a), which is the sole survivor of $H_2(\lambda)$, obviously represents the energy of single quasi-particles. This can be seen as follows:

For the time being, let us neglect $H_4(\lambda)$, and consider a state having one quasi-particle, i.e. a state $b_k^\dagger |\Psi_0\rangle$. The energy of this state is given by

$$\langle \Psi_0 | b_k \left\{ H_0(\lambda) + \sum_i E_i b_i^\dagger b_i \right\} b_k^\dagger | \Psi_0 \rangle$$

$$= H_0(\lambda) \langle \Psi_0 | b_k b_k^\dagger | \Psi_0 \rangle + \sum_i E_i \langle \Psi_0 | b_k b_i^\dagger b_i b_k^\dagger | \Psi_0 \rangle \qquad (4.60)$$

$$= H_0(\lambda) + E_k$$

The trick of carrying out the algebra here is to permute the destruction operators to the extreme right by using the anticommutator relations, and then dropping terms in which a destruction operator sits next to $|\Psi_0\rangle$, or a creation operator sits next to $\langle \Psi_0 |$. The energy of the state Ψ_0 is $H_0(\lambda)$, and the energy of the state having one quasi-particle in state k in addition to Ψ_0 is found to be $H_0(\lambda) + E_k$. Therefore, the natural interpretation of E_k is that it is the energy carried by the single quasi-particle.

The term $H_4(\lambda)$ actually contains the interaction between quasi-particles, and a proper calculation of the consequences of $H_4(\lambda)$ is the major task of the general microscopic theory. The development so far has led us only to independent quasi-particle excitations of the nucleus. The treatment of $H_4(\lambda)$ will give rise to other modes of excitation. This will be done in the next section.

Interpretation of λ

The quantity λ used in the theory is called chemical potential and it has the following interpretation. Let us consider the expression (4.47) for v_a^2, the occupation probability of a state. The fact that it is the occupation probability can be verified by evaluating $\langle \Psi_0 | c_a^\dagger c_a | \Psi_0 \rangle$; the result is indeed v_a^2 as demonstrated by Eq. (4.42a). Now, expression (4.47) reveals the following facts:

$$\begin{array}{lll}
\text{(i)} & \text{when } \epsilon_a < \lambda, & v_a^2 = 0.5 \\
\text{(ii)} & \text{when } \epsilon_a > \lambda, & v_a^2 = 0.5 \\
\text{(iii)} & \text{when } \epsilon_a = \lambda, & v_a^2 = 0.5
\end{array}$$

Let us now look at the curve of Fig.1.2b. The occupation probability of deep-down states is ≈ 1, which also follows from relation (4.47) by making ϵ_a very small, i.e. $\epsilon_a - \lambda \approx -\lambda$ and $E_a \approx \lambda$. As ϵ_a becomes comparable to λ, according to relation (4.47), v_a^2 starts decreasing from 1 and approaches 0.5 for $\epsilon_a \to \lambda$. On the other side of λ, ϵ_a decreases below 0.5 and eventually reaches zero, according to relation (4.47) when $\epsilon_a \to \infty$. Thus λ is the single-particle energy, on both sides of which the occupation probability departs significantly from the ideal HF-values. It, therefore, belongs to the same energy region where the Fermi level

would have belonged if we had ignored the existence of close-lying levels near the Fermi surface and had allowed the nucleons to go to the lowest available states. The quantity λ is, therefore, very often loosely called the Fermi level.

Interpretation of the quantities Δ_a

From the expression of the quasi-particle energy E_a, it is clear that even if the HF-energy ϵ_a of the state a coincides with the Fermi level λ, there is a minimum value of E_a which is given by the positive quantity Δ_a, which owes its origin entirely to the pairing matrix elements of the two-body potential. For reasons to be explained later, in the quasi-particle theory, the even nuclei, are associated with a ground state Ψ_0, which behaves as the quasi-particle vacuum, and the excited states of such nuclei are taken to have 2, 4, ..., etc. quasi-particles. The lowest excited states of such nuclei have at least two quasi-particles, and hence an energy which is, at least, twice the parameter Δ. These parameters are, therefore, called the energy-gap parameters, the gap being roughly half of the energy difference between the ground state and the first set of excited states of even nuclei. However, one must keep in mind the interaction term $H_4(\lambda)$ of the Hamiltonian. As we have stated qualitatively in the introduction, the interaction between pairs of quasi-particles may build up collective effects, and produce a coherent state that may very well differ markedly in energy from the unperturbed energies of the quasi-particle pair. If that happens then, of course, the observed first excited state of an even nucleus will not show a very pronounced energy gap with respect to the ground state.

The odd nuclei in this theory are associated with odd numbers of quasi-particles, the lowest states being 1 and 3 quasi-particle-type states. All the one-quasi-particle states have a minimum energy Δ, and hence the levels near the ground state of odd nuclei are never expected to show an energy gap with respect to the ground state.

Special pairing force

In our derivation of the quasi-particles we used a general potential but we saw that the special BCS-transformation picked up only the pairing part of it in the fundamental energy-gap equations of the theory. For this reason, sometimes the entire theory is worked out with a model two-body potential, called the pairing potential (not to be confused with our earlier Δ_{ij}, which was certainly not the two-body potential). This idealized potential is defined to have non-vanishing matrix elements of the following type with a constant magnitude:

$$(a, \bar{a} \mid v_p \mid b, \bar{b}) = -G \qquad (4.61)$$

In the special case of spherical single-particle states we have

$$(-1)^{j-m} (jm; j, -m \mid v_p \mid j'm'; j', -m') (-1)^{j'-m'} = -G \qquad (4.62)$$

In this second form the pairing potential has the important property of

being non-vanishing only for the two-body $J = 0$ state. To prove this statement we proceed as follows:

$$(j_1 j_2 \, J \, M \, | \, v_p \, | \, j_1' j_2' \, J' \, M')$$

$$= \sum_{\substack{m_1 m_2 \\ m_1' m_2'}} \begin{bmatrix} j_1 & j_2 & J \\ m_1 & m_2 & M \end{bmatrix} \begin{bmatrix} j_1' & j_2' & J' \\ m_1' & m_2' & M' \end{bmatrix} (j_1 \, m_1 , \, j_2 \, m_2 \, | \, v_p \, | \, j_1' \, m_1' , \, j_2' \, m_2')$$

$$= - G \sum_{\substack{m_1 m_2 \\ m_1' m_2'}} \begin{bmatrix} j_1 & j_2 & J \\ m_1 & m_2 & M \end{bmatrix} \begin{bmatrix} j_1' & j_2' & J' \\ m_1' & m_2' & M' \end{bmatrix} \delta_{j_1 j_2} \, \delta_{m_2, -m_1} \, \delta_{j_1' j_2'} \, \delta_{m_2', -m_2}$$

$$\times \, (-1)^{j_2 - m_1} \, (-1)^{j_1' - m_1'}$$

$$= - G \sum_{m_1} (-1)^{j_1 - m_1} \begin{bmatrix} j_1 & j_1 & J \\ m_1 & -m_1 & 0 \end{bmatrix} \sum_{m_1'} (-1)^{j_1' - m_1'} \begin{bmatrix} j_1' & j_1' & J' \\ m_1' & -m_1' & 0 \end{bmatrix}$$

$$\times \, \delta_{M0} \, \delta_{M'0} \, \delta_{j_1 j_2} \, \delta_{j_1' j_2'}$$

In this expression $\begin{bmatrix} j_1 & j_2 & J \\ m_1 & m_2 & M \end{bmatrix}$ is a Clebsch-Gordan coefficient, and we have merely used the definition (4.62) for the non-vanishing matrix elements of v_p. The summation in the final step can be carried out with the standard orthogonality property of the Clebsch-Gordan coefficients. The result is given by

$$\sum_m \begin{bmatrix} j & j & J \\ m & -m & 0 \end{bmatrix} (-1)^{j-m} = \sum_m \begin{bmatrix} j & j & J \\ m & -m & 0 \end{bmatrix} (-1)^{j-m} \begin{bmatrix} j & 0 & j \\ m & 0 & m \end{bmatrix}$$

$$= \sum_m \begin{bmatrix} j & j & J \\ m & -m & 0 \end{bmatrix} \begin{bmatrix} j & j & 0 \\ m & -m & 0 \end{bmatrix} \sqrt{(2j + 1)} \qquad (4.63a)$$

$$= \delta_{J0} \, \sqrt{2j + 1}$$

The extra Clebsch-Gordan coefficient introduced in the derivation is identically equal to unity. Using this standard result, we finally have

$$(j_1 j_2 \, J \, M \, | \, v_p \, | \, j_1' j_2' \, J' \, M') = - \delta_{j_1 j_2} \, \delta_{j_1' j_2'} \, \delta_{M0} \, \delta_{M'0} \, \delta_{J0} \, G \times \sqrt{(2j_1 + 1)(2j_1' + 1)}$$

$$(4.63b)$$

For the special pairing force (4.61) or (4.62), the energy gap equations (4.49) become very simple. We have, according to relation (4.61),

$$\Delta_a = + \frac{G}{4} \sum_k \frac{\Delta_k}{E_k}$$

Since the summation on the right-hand side is independent of the state a, it is clear that Δ_a now is actually independent of a; there is only one energy gap Δ for all the single-particle states. <u>There is only one gap equation</u>, and that is

$$\Delta = \frac{G}{4} \sum_k \frac{\Delta}{E_k}$$

or

$$1 = \frac{G}{4} \sum_k \frac{1}{\sqrt{(\epsilon_k - \lambda)^2 + \Delta_k^2}} \tag{4.64}$$

One has to solve only this equation and Eq. (4.50) simultaneously.

<u>The ground-state wave function</u>

Finally, we wish to show that a ground-state wave function satisfying

$$b_i \, |\Psi_0\rangle = 0 \text{ for all i} \tag{4.65}$$

actually exists, and it can be constructed in terms of the particle creation operators as follows:

$$|\Psi_0\rangle = \prod_k \left\{ u_k + v_k \, s_k \, c_k^\dagger \, c_{-k}^\dagger \right\} |0\rangle \tag{4.66}$$

where $|0\rangle$ is the vacuum state for the particle operators and satisfies

$$c_i \, |0\rangle = 0 \text{ for all i} \tag{4.67}$$

To show that $|\Psi_0\rangle$ satisfies Eq. (4.65), we write

$$b_i = u_i \, c_i - v_i \, s_i \, c_{-i}^\dagger$$

and let it operate from the left on state (4.66). It is clear that c_i and $c_i^\dagger$ can be commuted past all the factors in state (4.66) for which $k \neq i$. When we encounter the factor $k = i$, we shall have to examine what happens to it when b_{-i} operates on it from the left. We have

$$(u_i^2 c_i - v_i \, s_i \, c_{-i}^\dagger) \, (u_i + v_i \, s_i \, c_i^\dagger \, c_{-i}^\dagger)$$

$$= u_i \, c_i - u_i \, v_i \, s_i \, c_{-i}^\dagger + u_i \, v_i \, s_i \, c_i \, c_i^\dagger \, c_{-i}^\dagger - v_i^2 \, c_{-i}^\dagger \, c_i^\dagger \, c_{-i}^\dagger \tag{4.68}$$

The last term is zero because it contains two $c_{-i}^\dagger$ and hence violates the Pauli exclusion principle. The first term can be commuted past all

other factors which are $k \neq i$, and eventually it operates on $|0\rangle$ and produces zero according to Eq. (4.67). The third term can be written as

$$u_i v_i s_i c_{-i}^\dagger + u_i v_i s_i c_i^\dagger c_{-i}^\dagger c_i$$

where we have used $\{c_i, c_i^\dagger\} = 1$. The first term here cancels with the second term of Eq. (4.68), and the second term produces zero acting on the state $|0\rangle$. Thus we have established the property (4.65) for our ground-state wave function (4.66).

This wave function clearly contains states of 0, 2, 4, 6, ... , etc. particles, when all the factors are multiplied out. The process of fixing λ in the calculation ensures that the strength of the A-particle wave function in this superposition will have a maximum. Because of this form of Ψ_0, it is necessary that we restrict the quasi-particle ground state Ψ_0 to the description of the ground state of an even nucleus. Once we let $b_i^\dagger = u_i c_i^\dagger - v_i s_i c_{-i}$ operate on Ψ_0, the new wave function $b_i^\dagger |\Psi_0\rangle$ clearly becomes a superposition of 1, 3, 5, ... , etc. particles. This is the reason why odd nuclei are described in terms of an odd number of quasi-particle excitation. In the same way an even number of quasi-particle operators operating on Ψ_0, always generates a wave function having a superposition of an even number of nucleons. Thus, in this theory the excited states of even nuclei are associated with an even number of quasi-particle excitations.

Special case of spherical nuclei

We have shown earlier that a lot of simplification takes place if one uses the special pairing force of constant strength G. Even without this special approximation about the two-body force, the general equations (4.49) take a simpler form for spherical nuclei. For such nuclei the single-particle states are of the type $(n \ell j m)$. For simplicity we keep the $(n \ell)$ quantum understood in the following derivation. For spherical nuclei it is physically not possible to make any special choice of the z-axis, all directions in space being equivalent for them. Therefore, we know that the quantities u_a, v_a, E_a, Δ_a, etc. cannot depend on the projection quantum number m_a of the state a. We keep this fact in mind and write Eq. (4.49) as follows:

$$\Delta_j = -\frac{1}{4} \sum_{j', m'} (-1)^{j-m} (jm; j, -m |v| j', m'; j', -m') (-1)^{j'-m'} \frac{\Delta_{j'}}{E_{j'}} \quad (4.69)$$

We replace in this expression the two-body states by the corresponding angular-momentum coupled states, i.e.,

$$|j'm'; j', -m'\rangle = \sum_{J'} \begin{bmatrix} j' & j' & J' \\ m' & -m' & 0 \end{bmatrix} |j' j' J' 0\rangle \quad (4.70a)$$

In the exchange term of the matrix element in (4.69) we will have the state

$$
\left| j', -m'; j'm' \right\rangle = \sum_{J'} \begin{bmatrix} j' & j' & J' \\ -m' & m' & 0 \end{bmatrix} \left| j'j'J'0 \right\rangle
$$

$$
= - \sum_{J'} \begin{bmatrix} j' & j' & J' \\ m' & -m' & 0 \end{bmatrix} (-1)^{J'} \left| j'j'J'0 \right\rangle
$$

(4.70b)

In the final step we have used a standard symmetry relation of the Clebsch-Gordan coefficient. Using Eqs (4.70a) and (4.70b) we have

$$
(jm; j,-m \left| v \right| j'm'; j',-m') \equiv
$$

$$
\left\langle jm; j,-m \left| v \right| j'm'; j',-m' \right\rangle - \left\langle jm; j,-m \left| v \right| j',-m'; j'm' \right\rangle
$$

$$
= \sum_{J} \begin{bmatrix} j & j & J \\ m & -m & 0 \end{bmatrix} \begin{bmatrix} j' & j' & J' \\ m' & -m' & 0 \end{bmatrix} \left\langle jjJ0 \left| v \right| j'j'J0 \right\rangle \{1 + (-1)^{J}\}
$$

Here we have used the property of the potential v which requires J to be equal to J'. The last factor tells us that J must be an even integer, which in turn guarantees the antisymmetry of the state on the right-hand side (it is known that the antisymmetric states of two equivalent nucleons in the same $n\ell j$-orbit can have only even J-values). Therefore, we replace the factor $1/2 \{1+(-1)^{J}\}$ times the two-body matrix element by

$$
(jjJ0 \left| v \right| j'j'J0)
$$

where the rounded bracket, as usually, denotes the matrix element with respect to <u>antisymmetric</u> two-body angular-momentum coupled states. When these expressions are used in relation (4.69) we obtain

$$
\Delta_j = -\frac{1}{2} \sum_{j',m'} (-1)^{j-m} (-1)^{j'-m'} \begin{bmatrix} j' & j' & J \\ m' & -m' & 0 \end{bmatrix} \begin{bmatrix} j & j & J \\ m & -m & 0 \end{bmatrix} (jjJ0 \left| v \right| j'j'J0) \frac{\Delta_{j'}}{E_{j'}}
$$

In this expression the summation over m' can be carried out immediately by using the standard result (4.63a). Thus,

$$
\Delta_j = -\frac{1}{2} (-1)^{j-m} \begin{bmatrix} j & j & 0 \\ m & -m & 0 \end{bmatrix} \delta_{J0} \sum_{j'} (jjJ0 \left| v \right| j'j'J0) \sqrt{(2j'+1)} \frac{\Delta_{j'}}{E_{j'}}
$$

(4.71)

$$
= -\frac{1}{2} \sum_{j'} \sqrt{\frac{2j'+1}{2j+1}} (jjJ=0, M=0 \left| v \right| j'j'J=0, M=0) \frac{\Delta_{j'}}{E_{j'}}
$$

In obtaining the final expression we have substituted $(-1)^{j-m} (2j+1)^{-1/2}$ for the special Clebsch-Gordan coefficient. Thus, we find that for a spherical nucleus, even though we have a set of $\triangle_j$'s that are coupled through Eq. (4.71), the part of the interaction potential v which is responsible for this coupling is merely the interaction in the two-body state of angular momentum $J = 0$.

APPENDIX TO SECTION 4

Hartree-Fock-Bogolyubov Equations

In this appendix we give the derivation of the Hartree-Fock-Bogolyubov (HFB)-equations. These are the equations satisfied by the transformation coefficients $x_\alpha^{(i)}$ and $y_\alpha^{(i)}$ of Eq. (4.24) in the text. One possible way of arriving at these equations is to minimize expression (4.23a) for the ground-state energy. A much simpler derivation can be obtained by posing the problem in the following way: We want for our Hamiltonian (4.1) an excitation mode of the type (4.24) which is a linear superposition of the creation and destruction operators $c_\alpha^\dagger$ and c_α. According to the results of section 2.2.B, the existence of such a mode requires that the commutators of all the $c_\alpha^\dagger$ and c_α with the Hamiltonian (4.1) give rise to a linear sum of these operators. If such results can be proved, then the quasi-particle operators $b_i^\dagger$ can be constructed from all the $c_\alpha^\dagger$ and c_α according to relation (2.14). This is the program which we shall follow here.

By straightforward algebra and using standard anticommutation rules, we obtain

$$[c_\alpha^\dagger c_\beta, c_\mu^\dagger] = c_\alpha^\dagger c_\beta c_\mu^\dagger - c_\mu^\dagger c_\alpha^\dagger c_\beta$$

$$= \delta_{\beta\mu} c_\alpha^\dagger - (c_\alpha^\dagger c_\mu^\dagger + c_\mu^\dagger c_\alpha^\dagger) c_\beta$$

$$= \delta_{\beta\mu} c_\alpha^\dagger \tag{4.72a}$$

and

$$[c_\alpha^\dagger c_\beta^\dagger c_\delta c_\gamma, c_\mu^\dagger] = c_\alpha^\dagger c_\beta^\dagger [c_\delta c_\gamma, c_\mu^\dagger]$$

$$= c_\alpha^\dagger c_\beta^\dagger (c_\delta c_\gamma c_\mu^\dagger - c_\mu^\dagger c_\delta c_\gamma)$$

$$= c_\alpha^\dagger c_\beta^\dagger (\delta_{\gamma\mu} c_\delta - c_\delta c_\mu^\dagger c_\gamma - c_\mu^\dagger c_\delta c_\gamma)$$

$$= c_\alpha^\dagger c_\beta^\dagger (\delta_{\gamma\mu} c_\delta - \delta_{\delta\mu} c_\gamma) \tag{4.72b}$$

Using these results with expression (4.1) we obtain

$$[H, c_\mu^\dagger] = \sum_\alpha \langle \alpha | T | \mu \rangle c_\alpha^\dagger + \frac{1}{4} \sum_{\alpha\beta\gamma\delta} (\alpha\beta | v | \gamma\delta) c_\alpha^\dagger c_\beta^\dagger (\delta_{\gamma\mu} c_\delta - \delta_{\delta\mu} c_\gamma)$$

$$= \sum_\alpha \langle \alpha | T | \mu \rangle c_\alpha^\dagger + \frac{1}{2} \sum_{\alpha\beta\gamma} (\alpha\beta | v | \mu\gamma) c_\alpha^\dagger c_\beta^\dagger c_\gamma \tag{4.73}$$

An interchange of the summation indices γ and δ in the $\delta_{\delta\mu}c_\gamma$ term will easily convince the reader that this term is equal to the $\delta_{\gamma\mu}c_\delta$ term. This accounts for the factor of $\frac{1}{2}$ in the final step of Eq.(4.73).

The exact result (4.73) tells us that the commutator of $c_\mu^\dagger$ with the Hamiltonian does not give rise to a linear sum of single destruction and single creation operators only. According to our earlier statement, such a linear sum is a prerequisite for having a quasi-particle excitation mode of the type (4.24). Therefore, we conclude that the quasi-particle mode is an approximate mode of the Hamiltonian H, and the approximation necessary for this purpose will now be discussed.

In analogy with the results contained in Eqs (4.7) and (4.8), we can write the following exact expression:

$$c_\alpha^\dagger c_\beta^\dagger c_\gamma = \ :c_\alpha^\dagger c_\beta^\dagger c_\gamma: + \langle c_\beta^\dagger c_\gamma \rangle c_\alpha^\dagger - \langle c_\alpha^\dagger c_\gamma \rangle c_\beta^\dagger + \langle c_\alpha^\dagger c_\beta^\dagger \rangle c_\gamma \qquad (4.74)$$

The first term, by definition, contains three operators and cannot be reduced to single creation or destruction operators. On the other hand, the remaining terms in Eq.(4.74) are linear in the operators, $c_\alpha^\dagger$, c_γ, etc. Thus, the required approximation for the quasi-particle mode is to neglect the first term in Eq.(4.74). This approximation is often referred to as the linearization of Eq.(4.73).

With the linearization approximation, therefore, Eq.(4.73) reduces to

$$[H, c_\mu^\dagger] = \sum_\alpha \langle \alpha | T | \mu \rangle \ c_\alpha^\dagger + \frac{1}{2} \sum_{\alpha\beta\gamma} (\alpha\beta | v | \mu\gamma) \{\langle c_\beta^\dagger c_\gamma \rangle c_\alpha^\dagger - \langle c_\alpha^\dagger c_\gamma \rangle c_\beta^\dagger\}$$

$$+ \frac{1}{2} \sum_{\alpha\beta\gamma} (\alpha\beta | v | \mu\gamma) \langle c_\alpha^\dagger c_\beta^\dagger \rangle c_\gamma$$

$$= \sum_\alpha \langle \alpha | T | \mu \rangle \ c_\alpha^\dagger + \sum_{\alpha\beta\gamma} (\alpha\beta | v | \mu\gamma) \langle c_\beta^\dagger c_\gamma \rangle c_\alpha^\dagger$$

$$+ \frac{1}{2} \sum_{\alpha\beta\gamma} (\alpha\beta | v | \mu\gamma) \langle c_\alpha^\dagger c_\beta^\dagger \rangle c_\gamma \qquad (4.75)$$

Once again, we have used the trick of interchanging the summation indices α and β to show that the term involving $-\langle c_\alpha^\dagger c_\gamma \rangle c_\beta^\dagger$ is equal to the term containing $\langle c_\beta^\dagger c_\gamma \rangle c_\alpha^\dagger$; hence the final step (4.75) follows. We next use the definition (3.6) for V, and the definition (4.14) for Δ, and rewrite Eq.(4.75) as follows:

$$[H, c_\mu^\dagger] = \sum_\alpha \langle \alpha | (T + V) | \mu \rangle \ c_\alpha^\dagger + \sum_\alpha \Delta_{\mu\alpha}^* c_\alpha \qquad (4.76)$$

Since we are discussing a particle-number non-conserving theory, for reasons explained in the text, we should actually have worked with the Hamiltonian $H(\lambda) = H - \lambda \sum_\alpha c_\alpha^\dagger c_\alpha$ instead of H. According to (4.72a) the

extra term in $H(\lambda)$ contributes $-\lambda\,\delta_{\alpha\mu}c_\mu^\dagger$ to the commutator, and hence we finally obtain

$$[H(\lambda), c_\mu^\dagger] = \sum_\alpha \langle\alpha|(T-\lambda\,\mathbb{1}+V)|\mu\rangle\,c_\alpha^\dagger + \sum_\alpha \Delta_{\mu\alpha}^* c_\alpha$$

$$= \sum_\alpha \langle\mu|(T-\lambda\,\mathbb{1}+V)|\alpha\rangle^*\,c_\alpha^\dagger + \sum_\alpha \Delta_{\mu\alpha}^* c_\alpha \qquad (4.77a)$$

Here we have used the hermiticity of the operator $(T-\lambda\mathbb{1}+V)$.

    To obtain a closed system of linear equations like (2.12) we also need the commutator of $H(\lambda)$ with c_μ, which is easily obtained by taking the Hermitian conjugate of Eq.(4.77a) and reversing the sign, because $[H(\lambda),\ c_\mu] \equiv (H(\lambda)c_\mu - c_\mu H(\lambda)) = (c_\mu^\dagger H(\lambda) - H(\lambda)c_\mu^\dagger)^\dagger = -[H(\lambda),\ c_\mu^\dagger]^\dagger$. Therefore,

$$[H(\lambda),\ c_\mu] = -\sum_\alpha \Delta_{\mu\alpha}c_\alpha^\dagger - \sum_\alpha \langle\mu|(T-\lambda\,\mathbb{1}+V)|\alpha\rangle\,c_\alpha \qquad (4.77b)$$

    We now compare the set of Eqs (4.77a,b) with Eq.(2.12). Let us assume that we have N creation operators $c_\alpha^\dagger$ and N destruction operators c_α at our disposal. These 2N operators here play the role of N operators $A_i^\dagger$ (i = 1, 2, ... , N) of Eq.(2.12). In the present case, the matrix $\widetilde{M}$ can be written with the help of Eqs (4.77a,b), as follows:

$$\widetilde{M} = \begin{pmatrix} (T-\lambda\,\mathbb{1}+V)^* & \Delta^* \\ -\Delta & -(T-\lambda\mathbb{1}+V) \end{pmatrix} \qquad (4.78a)$$

This is clearly a $2N \times 2N$ matrix, and each of the submatrices, Δ, Δ^*, $(T-\lambda\,\mathbb{1}+V)$, and $(T-\lambda\,\mathbb{1}+V)^*$ are $N \times N$ matrices. According to section 2.2.B, our immediate task is to diagonalize M. The latter can be obtained from Eq.(4.78a) by interchanging the rows and columns and then taking the transposed of each submatrix. Remembering that $\widetilde{\Delta} = -\Delta$, and $\Gamma^\dagger = \Gamma$, i.e., $\widetilde{\Gamma} = \Gamma^*$, where $\Gamma = (T-\lambda\mathbb{1}+V)$, we obtain

$$M = \begin{pmatrix} T-\lambda\,\mathbb{1}+V & \Delta \\ -\Delta^* & -(T-\lambda\,\mathbb{1}+V)^* \end{pmatrix} \qquad (4.78b)$$

From the properties of the matrices Γ and Δ, stated above, one can show that M is a Hermitian matrix. While taking the Hermitian conjugate of M, one has to interchange first the rows and columns in Eq.(4.78b), and then take the Hermitian conjugate of each submatrix.

    This Hermitian matrix has real eigenvalues. Let us consider the eigenvector $\begin{pmatrix} x^{(i)} \\ y^{(i)} \end{pmatrix}$ corresponding to the eigenvalue E_i. Each of the quan-

tities $x^{(i)}$ and $y^{(i)}$ consists of N elements of the type $x_{\alpha}^{(i)}$, $y_{\alpha}^{(i)}$, etc. Writing out the eigenvalue equation in details we obtain

$$M \begin{pmatrix} x^{(i)} \\ y^{(i)} \end{pmatrix} = E_i \begin{pmatrix} x^{(i)} \\ y^{(i)} \end{pmatrix} \qquad (4.79a)$$

or

$$\Gamma x^{(i)} + \Delta y^{(i)} = E_i x^{(i)} \qquad (4.79b)$$

$$-\Delta^* x^{(i)} - \Gamma^* y^{(i)} = E_i y^{(i)} \qquad (4.79c)$$

If we take the complex conjugate of these two equations, and reverse their signs throughout, remembering that $E_i^* = E_i$, we obtain

$$\Gamma y^{(i)*} + \Delta x^{(i)*} = -E_i y^{(i)*}$$

$$-\Delta^* y^{(i)*} - \Gamma^* x^{(i)*} = -E_i x^{(i)*}$$

which are equivalent to

$$M \begin{pmatrix} y^{(i)*} \\ x^{(i)*} \end{pmatrix} = -E_i \begin{pmatrix} y^{(i)*} \\ x^{(i)*} \end{pmatrix} \qquad (4.80)$$

Therefore, the eigenvalues of the matrix (4.78b) occur in $\pm$ pairs. Given the vector for a positive eigenvalue, the vector for the corresponding negative eigenvalue can be obtained easily through the relationship expressed by Eqs (4.79a) and (4.80).

Let us consider a positive eigenvalue E_i, and the corresponding eigenvector as appearing in Eq.(4.79a). According to Eqs (2.14) and (2.16) we can construct the step-up operator

$$b_i^\dagger = \sum_{\alpha} (x_{\alpha}^{(i)} c_{\alpha}^\dagger + y_{\alpha}^{(i)} c_{\alpha}) \qquad (4.81a)$$

and its Hermitian conjugate

$$b_i = \sum_{\alpha} (y_{\alpha}^{(i)*} c_{\alpha}^\dagger + x_{\alpha}^{(i)*} c_{\alpha}) \qquad (4.81b)$$

These operators have the following properties:

$$H b_i^\dagger |\Psi_0\rangle = (E_0 + E_i) b_i^\dagger |\Psi_0\rangle \qquad (4.82a)$$

and

$$b_i |\Psi_0\rangle = 0 \qquad (4.82b)$$

where $|\Psi_0\rangle$ is the ground state of H having energy E_0. The state $b_i^\dagger |\Psi_0\rangle$ which has an energy E_i above the ground state is a one-quasi-particle state, the quasi-particle being in a state i. The operator b_i is the destruction operator for a quasi-particle, and Eq.(4.82b) guarantees that the ground state $|\Psi_0\rangle$ does not contain any quasi-particle to start with. Notice that the eigenvector corresponding to $-E_i$, as given by Eq.(4.80), would have led, according to Eq.(2.14), to the linear combination (4.81b); therefore, in general, the linear combination (4.81b), operating on any eigenstate of H, gives rise to another eigenstate with energy stepped down by $-E_i$. This further confirms the interpretation of the operator b_i as the destruction operator of a quasi-particle of energy E_i. In general, the $2N \times 2N$ matrix M yields 2N eigenvalues, of which N will be positive, and the remaining N, the negative partners of the positive set. The linear combinations like (4.81a) for the N positive eigenvalues have an interpretation as N different quasi-particle creation operators, while similar linear combinations (4.81b) corresponding to the negative eigenvalues give the destruction operators for the same set of N quasi-particles.

Written out in detail Eqs (4.79b,c) for the quasi-particle transformation coefficients read as follows:

$$\sum_\beta \{\langle \alpha |\Gamma| \beta\rangle x_\beta^{(i)} + \Delta_{\alpha\beta} y_\beta^{(i)}\} = E_i x_\alpha^{(i)} \qquad (4.83a)$$

$$\sum_\beta \{\Delta_{\alpha\beta}^* x_\beta^{(i)} + \langle \alpha |\Gamma^*| \beta\rangle y_\beta^{(i)}\} = -E_i y_\alpha^{(i)} \qquad (4.83b)$$

These equations are called the Hartree-Fock-Bogolyubov (HFB) equations. Their appearance as linear equations is rather deceptive, because, by definition, the matrix elements of Γ and Δ contain the density and the pairing matrix, respectively, and the latter are quadratic in the transformation coefficients themselves. In close analogy to the HF-case, the HFB-equations also require a self-consistent treatment for the properties of Γ and Δ stated above. We now proceed to a derivation of the expressions for the density and pairing matrix elements, such that the self-consistent method can be described in detail.

We first write down the following orthogonality properties of the eigenvectors of the Hermitian matrix M. The orthogonality of an eigenvector of positive eigenvalue E_i and another of negative eigenvalue $-E_j$ is expressed, according to Eqs (4.79a) and Eq.(4.80), by

$$(y^{(i)} \quad x^{(j)}) \begin{pmatrix} x^{(i)} \\ y^{(i)} \end{pmatrix} = 0$$

or

$$\sum_\alpha (y_\alpha^{(j)} x_\alpha^{(i)} + x_\alpha^{(j)} y_\alpha^{(i)}) = 0 \qquad (4.84a)$$

Similarly, the scalar product of two eigenvectors, belonging to two different positive eigenvalues E_i and E_j is also zero. However, if $E_i = E_j$, i.e. if we consider the scalar product of an eigenvector of positive eigenvalue with itself, the result can be normalized to unity. Thus

$$\begin{pmatrix} x^{(j)*} & y^{(j)*} \end{pmatrix} \begin{pmatrix} x^{(i)} \\ y^{(i)} \end{pmatrix} = \delta_{ij}$$

or

$$\sum_\alpha (x_\alpha^{(j)*} x_\alpha^{(i)} + y_\alpha^{(j)*} y_\alpha^{(i)}) = \delta_{ij} \qquad (4.84b)$$

It is trivial to verify from the definitions (4.81a,b) and the anticommutator relations of $c_\alpha^\dagger$, c_β, etc. that the summation on the left-hand side of Eq.(4.84a) is equal to $\{b_j, b_i\}$ and that in Eq.(4.84b) is equal to $\{b_j^\dagger, b_i\}$. Thus, the orthogonality properties (4.84a,b) of the eigenvectors of M automatically guarantee that the quasi-particles also satisfy fermion anticommutation properties:

$$\{b_j, b_i\} = 0, \quad \{b_j^\dagger, b_i\} = \delta_{ij} \qquad (4.84c)$$

Equations (4.84a,b) further guarantee the following result:

$$\begin{pmatrix} x & y \\ y^* & x^* \end{pmatrix} \begin{pmatrix} x & y \\ y^* & x^* \end{pmatrix}^\dagger = \begin{pmatrix} x & y \\ y^* & x^* \end{pmatrix} \begin{pmatrix} x^\dagger & \tilde{y} \\ y^\dagger & \tilde{x} \end{pmatrix} = \begin{pmatrix} xx^\dagger + yy^\dagger & x\tilde{y} + y\tilde{x} \\ y^*x^\dagger + x^*y^\dagger & y^*\tilde{y} + x^*\tilde{x} \end{pmatrix} = \begin{pmatrix} \mathbb{1} & 0 \\ 0 & \mathbb{1} \end{pmatrix}$$

$$(4.85)$$

In this equation we have treated x and y as matrices having elements $x_\alpha^{(i)}$ and $y_\alpha^{(i)}$ where i stands for the index specifying the row, and α specifies the column.

Notice that the transformation equation (4.81a,b) can be written as

$$\begin{pmatrix} b^\dagger \\ b \end{pmatrix} = \begin{pmatrix} x & y \\ y^* & x^* \end{pmatrix} \begin{pmatrix} c^\dagger \\ c \end{pmatrix} \qquad (4.86)$$

Here $b^\dagger$ and b stand for columns having elements $b_i^\dagger (i = 1, 2, \ldots, N)$ and $b_i (i = 1, 2, \ldots, N)$. Similarly, $c^\dagger$ and c also stand for columns having elements $c_\alpha^\dagger (\alpha = 1, 2, \ldots, N)$ and $c_\alpha (\alpha = 1, 2, \ldots, N)$. It is clear from Eq.(4.85) that the inverse of this equation is given by

$$\begin{pmatrix} c^\dagger \\ c \end{pmatrix} = \begin{pmatrix} x & y \\ y^* & x^* \end{pmatrix}^\dagger \begin{pmatrix} b^\dagger \\ b \end{pmatrix} = \begin{pmatrix} x^\dagger & \tilde{y} \\ y^\dagger & \tilde{x} \end{pmatrix} \begin{pmatrix} b^\dagger \\ b \end{pmatrix}$$

i.e.

$$c^\dagger = x^\dagger b^\dagger + \tilde{y} b$$

or

$$c_\alpha^\dagger = \sum_i (x^\dagger)_{\alpha i} b_i^\dagger + (\tilde{y})_{\alpha i} b_i$$

$$= \sum_i (x_\alpha^{(i)*} b_i^\dagger + y_\alpha^{(i)} b_i) \qquad (4.87a)$$

Hence

$$c_\alpha = \sum_i (x_\alpha^{(i)*} b_i^\dagger + x_\alpha^{(i)} b_i) \tag{4.87b}$$

Equations (4.87a,b) and (4.82b) now enable us to calculate the density and pairing matrices. In a straightforward manner, using Eq.(4.84c) whenever necessary, we obtain

$$\langle \alpha | \rho | \beta \rangle = \langle \Psi_0 | c_\beta^\dagger c_\alpha | \Psi_0 \rangle = \sum_i y_\beta^{(i)} y_\alpha^{(i)*} \tag{4.88a}$$

and

$$\kappa_{\delta\gamma} = \langle \Psi_0 | c_\delta c_\gamma | \Psi_0 \rangle = \sum_i x_\delta^{(i)} y_\gamma^{(i)*} \tag{4.88b}$$

These expressions, together with the definitions (3.6) for V and Eq.(4.14) for Δ, completely determine the HFB-equations (4.83a,b).

A practical procedure for solving the HFB-equations self-consistently is as follows: (1) First, solve the HF-problem self-consistently. (2) Start the HFB-solutions with a value of the chemical potential in the neighbour-hood of the highest filled HF-level; the starting density matrix elements are also taken from the HF-results. Take some kind of guess values for the pairing density $\kappa_{\delta\gamma}$. (3) Find V and Δ from the starting ρ, κ and the given two-body matrix elements. Diagonalize the HFB-matrix M. (4) Recalculate ρ and κ from the eigenvectors. Repeat the entire procedure until the matrix elements of ρ and κ in two successive iterations are the same to the desired degree of accuracy. (5) Check with the final self-consistent eigenvectors whether the equation for the chemical potential

$$A = \sum_\alpha \langle \alpha | \rho | \alpha \rangle = \sum_i | y_\alpha^{(i)} |^2 \tag{4.89}$$

is satisfied or not. Here, A is the number of nucleons in the nucleus which we want to calculate. In general, Eq.(4.89) will not be satisfied at this stage of calculation. (6) Change the value of λ suitably, and repeat the entire procedure until Eq.(4.89) is satisfied to the desired accuracy.

A complete HF-, and HFB-type calculation for a heavy nucleus is still computationally intractable on most of the present-day electronic computers if we wish to keep all the nucleons in achieving the self-consistency. In most practical calculations, therefore, one omits the core-nucleons in the filled major shells, and does the self-consistent calculation only for the outer nucleons in the valence major shell. In such calculations, the matrix element $\langle \alpha | T | \beta \rangle$ of the kinetic energy is to be replaced, for obvious reasons, by $\epsilon_\alpha \delta_{\alpha\beta}$ where ϵ_α is the single-particle energy of a single nucleon in state α outside the closed major shells. The quantity A of Eq.(4.89) then stands for the number of nucleons in the valence shell.

Transformation of $H_2(\lambda)$

The diagonalization of the HFB-matrix M, and the resultant quasi-particle transformation (4.81a,b), automatically reduce the expression (4.23b) of $H_2(\lambda)$ to a very simple form. The necessary mathematics takes a very elegant form if we introduce the operators $d_I^\dagger$ (I = 1, 2, ... N, N + 1, ..., 2N), defined in the following manner:

$$d_\alpha^\dagger = c_\alpha^\dagger \qquad\qquad (4.90a)$$

and

$$d_{\alpha+N}^\dagger = c_\alpha \qquad\qquad (4.90b)$$

where

$$\alpha = 1, 2, \ldots, N$$

It is clear from this definition that $d_I^\dagger d_J$, where I and J = 1, 2, ..., 2N, consist of four different types of terms:

$$d_\alpha^\dagger d_\beta = c_\alpha^\dagger c_\beta$$

$$d_\alpha^\dagger d_{\beta+N} = c_\alpha^\dagger c_\beta^\dagger$$

$$d_{\alpha+N}^\dagger d_\beta = c_\alpha c_\beta \qquad\qquad (4.91a)$$

$$d_{\alpha+N}^\dagger d_{\beta+N} = c_\alpha c_\beta^\dagger$$

In these expressions both α, β extend over the range 1, 2, ..., N. In a similar manner, the matrix M of Eq.(4.78b) has the following four types of matrix elements:

$$M_{\alpha\beta} = \langle \alpha | (T - \lambda \mathbb{1} + V) | \beta \rangle, \quad M_{\alpha,\beta+N} = \Delta_{\alpha\beta}$$

$$M_{\alpha+N,\beta} = -\Delta_{\alpha\beta}^*, \qquad M_{\alpha+N,\beta+N} = -\langle \alpha | (T - \lambda \mathbb{1} + V) | \beta^* \rangle$$

$$(4.91b)$$

With the help of Eqs (4.91a,b) we can, therefore, rewrite expression (4.23b) as follows:

$$H_2(\lambda) = \frac{1}{2} \sum_{I,J} M_{IJ} : d_I^\dagger d_J : \qquad\qquad (4.92)$$

We have used here the identity $: c_\alpha c_\beta^\dagger : = - : c_\beta^\dagger c_\alpha :$

If we recall the definitions of the matrices x and y, given under Eq.(4.85), then it is easy to verify that the eigenvalue equations (4.83a,b) can be written in the following matrix form:

$$M \begin{pmatrix} \tilde{x} & y^\dagger \\ \tilde{y} & x^\dagger \end{pmatrix} = \begin{pmatrix} \tilde{x} & y^\dagger \\ \tilde{y} & x^\dagger \end{pmatrix} \begin{pmatrix} \mathscr{E} & 0 \\ 0 & -\mathscr{E} \end{pmatrix} \qquad (4.93)$$

where $\mathscr{E}$ is a diagonal matrix whose elements are given by E_i. We denote the matrix involving $\tilde{x}$, $\tilde{y}$, etc. by $U^\dagger$. It can be easily shown from the orthogonality and completeness of the eigenvectors that U is a unitary matrix. Hence we write (4.93 as

$$M = U^\dagger \mathbb{E} U$$

where $\mathbb{E}$ is the diagonal matrix in Eq.(4.93). Therefore

$$M_{IJ} = \sum_{K=1}^{2N} U_{IK}^\dagger \mathbb{E}_K U_{KJ} = \sum_{k=1}^{N} E_k (U_{Ik}^\dagger U_{kJ} - U_{I,k+N}^\dagger U_{k+N,J}) \qquad (4.94)$$

We substitute expression (4.94) into relation (4.92), and simplify the expression with the help of the following results:

$$\sum_{I=1}^{2N} U_{Ik}^\dagger d_I^\dagger = \sum_{\alpha=1}^{N} (U_{\alpha k}^\dagger d_\alpha^\dagger + U_{\alpha+N,k}^\dagger d_{\alpha+N}^\dagger) = \sum_{\alpha=1}^{N} (x_\alpha^{(k)} c_\alpha^\dagger + y_\alpha^{(k)} c_\alpha) = b_k^\dagger \qquad (4.95a)$$

Similarly

$$\sum_{J=1}^{2N} U_{kJ} d_J = \sum_{\alpha=1}^{N} (U_{\alpha J} d_\alpha + U_{\alpha+N,J} d_{\alpha+N}) = \sum_{\alpha=1}^{N} (x_\alpha^{(k)*} c_\alpha + y_\alpha^{(k)*} c_\alpha^\dagger) = b_k \qquad (4.95b)$$

and

$$\sum_{I=1}^{2N} U_{I,k+N}^\dagger d_I^\dagger = b_k \qquad (4.95c)$$

$$\sum_{J=1}^{2N} U_{k+N,J} d_I = b_k^\dagger \qquad (4.95d)$$

In view of the identity

$$: b_k b_k^\dagger : = - : b_k^\dagger b_k : = - b_k^\dagger b_k$$

we have the final result

$$H_2(\lambda) = \sum_{k=1}^{N} E_k b_k^\dagger b_k \qquad (4.96)$$

As in the simple BCS-case, we notice that $H_2(\lambda)$ represents the single quasi-particle part of the Hamiltonian, and the terms in it having two quasi-particle creation or destruction operators have disappeared automatically.

Minimization of $H_0(\lambda)$

The discussions on the HFB-procedure will be complete if we can show that this method minimizes $H_0(\lambda)$, the ground-state energy.

For this purpose, we first introduce, in analogy with the $N \times N$ density matrix

$$\langle \alpha | \rho | \beta \rangle = \langle c_\beta^\dagger c_\alpha \rangle$$

the following $2N \times 2N$ matrix R:

$$\langle I | R | J \rangle = \langle d_J^\dagger d_I \rangle \qquad (4.97)$$

With the help of expressions (4.91a), it is easy to see that R has the following structure:

$$R = \begin{pmatrix} \rho & -\kappa \\ \kappa^* & \mathbb{1} - \rho^* \end{pmatrix} \qquad (4.98)$$

Under the transformation (4.81a,b) the matrices ρ and κ transform as follows:

$$\langle \alpha | \rho | \beta \rangle \to \langle b_j^\dagger b_i \rangle \equiv 0$$

and

$$\kappa_{\alpha\beta} \to \langle b_i b_j \rangle \equiv 0$$

The vanishing of these expressions is a consequence of Eq.(4.82b). Thus, the matrix R undergoes the following transformation

$$R \to R' = \begin{pmatrix} 0 & 0 \\ 0 & \mathbb{1} \end{pmatrix}$$

It was proved by Eq.(4.85) that the quasi-particle transformation from $c^\dagger$, c to $b^\dagger$, b is unitary. Hence the algebraic identity

$$R'^2 = R'$$

guarantees

$$R^2 = R \qquad (4.99)$$

This equation is the analogue of $\rho^2 = \rho$ for the density matrix.

We next split up the matrix M of Eq.(4.78b) into two parts:

$$M = \mathscr{I} + M' \qquad (4.100a)$$

where

$$\mathscr{I} = \begin{pmatrix} T - \lambda \mathbb{1} & 0 \\ 0 & -T + \lambda \mathbb{1} \end{pmatrix} \qquad (4.100b)$$

and

$$M' = \begin{pmatrix} V & \Delta \\ -\Delta^* & -V^* \end{pmatrix} \qquad (4.100c)$$

Then the ground-state energy $H_0(\lambda)$ of (4.23a) can be written in the following form

$$H_0(\lambda) = \tfrac{1}{2} \text{ Trace } [(\mathscr{I} + \tfrac{1}{2} M')R] - \tfrac{1}{2} \text{ Trace } (T - \lambda \mathbb{1} + \tfrac{1}{2} V) \qquad (4.101)$$

To arrive at Eq.(4.101) one has to make use of (1) the hermiticity of ρ and V, such that Trace $V\rho$ = Trace $V^*\rho^*$, and (2), the hermiticity of the two-body potential which will lead to Trace $\Delta\kappa^*$ = Trace $\Delta^*\kappa$.

In the variational treatment of $H_0(\lambda)$, we shall have to vary R (i.e. vary ρ and κ) subject to the constraint (4.99) and then find out the condition for minimization. This procedure is comparable to what one does in the HF-case. In the latter case, the ground-state energy is given by

$$(H_0)_{HF} = \sum_{\alpha, \beta} \langle \alpha | T + \tfrac{1}{2} V | \beta \rangle \langle \beta | \rho | \alpha \rangle$$

$$= \text{ Trace } (T + \tfrac{1}{2} V) \rho \qquad (4.102)$$

and we are required to minimize this expression with respect to variations $\delta\rho$ subject to the constraint $\rho^2 = \rho$. We shall carry out this simple HF-minimization first; the minimization condition of Eq.(4.101) will then be considered as a straightforward generalization.

Writing out $\langle \alpha | V | \beta \rangle$ in terms of the density matrix, we have

$$(H_0)_{HF} = \sum_{\alpha\beta} \langle \alpha | T | \beta \rangle \rho_{\beta\alpha} + \sum_{\alpha\beta\gamma\delta} (\alpha\beta | v | \gamma \delta) \rho_{\delta\beta} \rho_{\gamma\alpha}$$

The equation of constraint is given by

$$\rho^2 = \rho$$

The element $\alpha\gamma$ of this matrix equation is given by

$$\sum_{\beta} \rho_{\alpha\beta} \rho_{\beta\gamma} - \rho_{\alpha\gamma} = 0$$

We multiply this equation by a Lagrange multiplier $\mu_{\gamma\alpha}$ and then sum over

all values of α and γ. Subtracting the resultant expression from $(H_0)_{HF}$ we have the final expression to be minimized:

$$\sum_{\alpha,\beta} \langle \alpha | T | \beta \rangle \, \rho_{\beta\alpha} + \sum_{\alpha\beta\gamma\delta} (\alpha\beta | v | \gamma\delta) \rho_{\delta\beta} \rho_{\gamma\alpha} - \sum_{\alpha,\gamma} \mu_{\gamma\alpha} \left[\sum_{\beta} \rho_{\alpha\beta} \rho_{\beta\gamma} - \rho_{\alpha\gamma} \right]$$

Therefore, the condition of minimization is given by

$$0 = \sum_{\alpha,\beta} \langle \alpha | T | \beta \rangle \, \delta\rho_{\beta\alpha} + \sum_{\alpha\beta\gamma\delta} (\alpha\beta | v | \gamma\delta) \, [\rho_{\delta\beta} \delta\rho_{\gamma\alpha} + \delta\rho_{\delta\beta} \rho_{\gamma\alpha}]$$

$$- \sum_{\alpha\gamma} \mu_{\gamma\alpha} \left[\sum_{\beta} \delta\rho_{\alpha\beta} \delta\rho_{\beta\gamma} + \delta\rho_{\alpha\beta} \rho_{\beta\gamma} - \delta\rho_{\alpha\gamma} \right]$$

We make use of the definition of V, and equate the coefficient of $\delta\rho_{\beta\alpha}$ of this expression to zero. The final condition is, thus, given by

$$\langle \alpha | T | \beta \rangle + \langle \alpha | V | \beta \rangle - \langle \alpha | \mu\rho | \beta \rangle - \langle \alpha | \rho\mu | \beta \rangle + \langle \alpha | \mu | \beta \rangle = 0$$

or

$$T + V + \mu - (\mu\rho + \rho\mu) = 0$$

Taking the commutator with ρ we rewrite this expression as

$$[(T+V), \rho] + [\mu, \rho] - (\mu\rho + \rho\mu)\rho + \rho(\mu\rho + \rho\mu) = 0$$

Since $\rho^2 = \rho$, the terms involving μ cancel exactly, and the condition of HF-minimization finally simplifies to

$$[(T+V), \rho] = 0 \qquad\qquad (4.103)$$

In the HF-procedure, this is achieved through the self-consistent diagonalization of the HF Hamiltonian $T + V$. In the resultant HF representation $(T+V)$ is a diagonal matrix with elements ϵ_i, and ρ is also a diagonal matrix having elements 1 for the occupied states, and 0 for the unoccupied states. The two diagonal matrices $(T+V)$ and ρ commute, and hence the minimization condition (4.103) is satisfied.

The generalization of this procedure to the HFB-case is straightforward. The variation in R does not produce any change in the second term of Eq. (4.101), and hence the expression to be minimized is given by (taking into consideration the equations of constraint)

$$\sum_{I,J} \langle I | \mathcal{G} | J \rangle \langle J | R | I \rangle + \frac{1}{2} \sum_{I,J} \langle I | M' | J \rangle \langle J | R | I \rangle$$

$$- \sum_{I,J} \mu_{JI} \left[\sum_{K} \langle I | R | K \rangle \langle K | R | J \rangle - \langle I | R | J \rangle \right]$$

Mathematics, very similar to what has been done above, finally leads to the minimization condition:

$$[(\mathscr{I} + M'), R] = 0$$

or

$$[M, R] = 0 \qquad (4.104)$$

We have already shown above that the HFB-diagonalization of M automatically ensures the diagonal form R' for the matrix R. Thus Eq.(4.104) is satisfied.

5. MICROSCOPIC THEORY − VIBRATIÓNAL MODE

5.1. General expression of the quasi-particle interaction

In the last section we started transforming the many-body Hamiltonian, and showed that a part of it represents the ground-state energy (H_0), and another part represents energy of single quasi-particles (H_{11}). What remains of the Hamiltonian after this, is the term H_4 of Eq.(4.19). In view of its importance in building up collective vibrational states, we shall devote this section entirely to the treatment of this particular term, which actually represents the interaction between quasi-particles.

We had seen in the previous section that a BCS-type quasi-particle transformation, given by Eqs (4.39a,b), where u_i and v_i are both non-vanishing and computed from Eqs (4.47), describe the case of nuclei having a diffuse Fermi surface. Such a quasi-particle is partly a "hole" and partly a "particle". On the other hand, we also found that the same transformation equations can be formally used to describe the quasi-particles also in a nucleus having a sharp Fermi sea (i.e. a closed-shell nucleus, or a nucleus where the HF-calculation produces a large energy gap between the occupied and unoccupied single-particle states). In this case, however, we must remember to put special values of u_i and v_i, namely $u_i = 1$ and $v_i = 0$ if i is an unoccupied (i.e. a "particle") state, while $u_i = 0$ and $v_i = 1$ if i is an occupied (i.e. a "hole") state. In other words, the quasi-particles here are either pure "particle" or pure "hole" states.

Keeping this fact in mind, we shall write down the general expression for H_4 with the substitutions (4.40a,b), and then apply the same formal expression with the appropriate values of u_i and v_i to describe both types of nuclei mentioned above.

Since the BCS-transformation was done with HF-type single-particle states, we first rewrite H_4 of Eq.(4.19) in the HF-representation:

$$H_4 = \frac{1}{4} \sum_{i,j,k,\ell} (ij|v|k\ell): c_i^\dagger c_j^\dagger c_\ell c_k : \qquad (5.1)$$

We have to substitute from Eqs (4.40a,b) and then permute in each term the destruction operators to the right of the creation operators; finally,

the appropriate sign of each term has to be incorporated according to the rules of forming normal products described under Eq. (4.8). It is clear from Eqs (4.40a,b) that there will be one term in expression (5.1) which contains four quasi-particle creation operators, and one term having four desctruction operators. These terms have obviously the coefficients $u_i u_j v_k v_\ell$ and $v_i v_j u_k u_\ell$ respectively. We shall denote these terms by H_{40} and H_{04} where, as usually, the two subscripts specify the number of creation and destruction operators, respectively. The following expressions are easily obtained:

$$H_{40} = \frac{1}{4} \sum_{ijk\ell} (ij|v|\bar{k}, \bar{\ell}) u_i u_j v_\ell v_k \, b_i^\dagger b_j^\dagger b_\ell^\dagger b_k^\dagger \qquad (5.2a)$$

H_{04} = Hermitian conjugate of H_{40}. $\qquad (5.2b)$

Here a state with a bar on top denotes the corresponding time-reversed state, i.e. $|\bar{k}\rangle = s_k |-k\rangle$ where s_k is the phase-factor appearing in Eqs (4.40a,b). Since k, ℓ are summation indices we had made the legitimate replacements $k \rightarrow -k$, and $\ell \rightarrow -\ell$ in obtaining expression (5.2a).

In a similar manner, it is clear from Eqs (4.40a,b) that there will be four terms in expression (5.1) having one quasi-particle destruction operator, and three creation operators (H_{31}); the number of terms with the roles of destruction and creation operators reversed (H_{13}) is also four. It is possible to relabel the summation indices in the various terms of H_{31} and H_{13} and then obtain the final expressions:

$$H_{31} = \frac{1}{2} \sum_{ijk\ell} [u_i u_j v_k u_\ell (ij|v|\bar{k}, \ell) + u_i v_j v_k v_\ell (i, \bar{\ell}|v|\bar{j}, \bar{k})] b_i^\dagger b_j^\dagger b_k^\dagger b_\ell \qquad (5.2c)$$

H_{13} = Hermitian conjugate of H_{31} $\qquad (5.2d)$

The last set of terms contained in expression (5.1) have two quasi-particle creation and two quasi-particle destruction operators (H_{22}). Their total number is six, but once again a relabelling of the summation indices can be done to write H_{22} in the following compact form:

$$H_{22} = \frac{1}{2} \sum_{ijk\ell} [(u_i u_j u_k u_\ell + v_i v_j v_k v_\ell) \tfrac{1}{2}(ij|v|k\ell)$$

$$- (u_i v_j u_k v_\ell + v_i u_j v_k u_\ell)(j, \bar{k}|v|\ell, \bar{i})] b_i^\dagger b_j^\dagger b_k b_\ell \qquad (5.2e)$$

As a matter of fact, if we compare expression (5.2e) with the second term of expression (4.1), we are at once struck by their similarity. Such a comparison leads us to an interpretation of the expansion enclosed in square brackets as $\langle ij|v_q|k\ell\rangle$, where v_q is the effective interaction potential between two quasi-particles. Such a clear identification of the other terms, (5.2a-d), as the interaction between quasi-particles, is not very obvious, because these terms do not conserve the number of quasi-particles while (5.2e) does. Expression (4.1) conserves the

number of particles, and hence the formal similarity is evident only for the term (5.2e) which conserves the number of quasi-particles.

5.2. Application to the HF-case

5.2.1. Diagrammatic representation of the interaction

By the HF-case here we mean those nuclei where a HF-type ground state having a sharp Fermi sea is a good description. The quasi-particles are either pure holes or pure particles. The coefficients u_i, v_i, etc. in expressions (5.2a-e) will now tell us whether a given state has to be a hole or a particle. For example, in the term H_{40} of (5.2a), the factors $u_i u_j$ and $v_\ell v_k$ tell us that i, j are particle states and k, ℓ are hole states. Therefore, $b_i^\dagger b_j^\dagger b_\ell^\dagger b_k^\dagger$ occurring in this expression describe the creation of two hole-particle pairs. In the matrix element of v, the state on the right is the initial state, and that on the left is the final state. Hence the hole state k is going to particle state i, while the hole state ℓ is going to the particle state j, as a result of the two-body interaction. The appearance, in the two-body matrix element, of a time-reversed state corresponding to a hole has its origin in the transformation property under rotation described by Eq. (4.30b).

All these facts can be described by a diagram in which a dashed horizontal line can be taken to represent v, and solid lines moving towards or away from points to represent the various states. To distinguish between holes and particles, we attach an arrow to a line and make the conventions described in Fig. 5.1. The diagrams (a) and (b)

FIG. 5.1. Particle and hole states (see text).

have upward arrows and are taken to represent particle states, while (c) and (d) having downward arrows represent hole states. For particles, an arrow moving away from a point, as in (a), denotes creation at that point, while an arrow moving towards a point, as in (b) represents destruction of the particle at that point. In the case of holes, the convention is just the opposite: diagram (c) having a hole-line moving towards a point denotes the creation of the hole, while (d) with a hole line moving away from a point denotes the destruction of the hole.

Keeping these conventions in mind we describe the interaction term H_{40} by Fig. 5.2. Notice that the sense of the arrows indeed tells us that the state k is going to i, and the state ℓ is going to j, as described in the first paragraph of this subsection. According to (a) and (c) of Fig. 5.1 we indeed have in Fig. 5.2 the creation of the hole k and ℓ, and creation of the particles i and j. Each "hen track" in Fig. 5.2 corresponds to a "hole-particle" pair, and the diagram corresponds to the creation of two such pairs, as described in the above mentioned paragraph.

In a similar manner the Hermitian conjugate of H_{40}, i.e. H_{04} of (5.2b) describes the destruction of two hole-particle pairs, and is represented by Fig. 5.3.
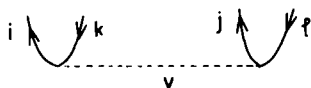
FIG. 5.2.   Interaction H_{40}.
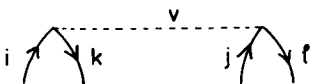
FIG. 5.3.   Interaction H_{04}.
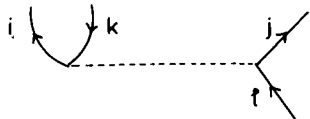
FIG. 5.3a.   The first term of H_{31}.

We next examine H_{31}. There are two terms in expression (5.2c), and the u, v coefficients in the first term tell us that it corresponds to the creation of two particles (i, j) and a hole (k) and the destruction of a particle (ℓ). The matrix element of v appearing in this term tells us that k is going to i and ℓ is going to j. Thus the diagram is given by Fig. 5.3a. The diagram makes it obvious that this term represents the interaction of a hole-particle pair with a particle. In the same manner the reader can convince himself with a little exercise that the second term of H_{31} represents the interaction of a hole-particle pair with a hole state. Drawing similar diagrams for H_{13} of (5.2d) and their appropriate interpretation are also left as an exercise to the reader.

Finally, we consider the expression H_{22} of Eq. (5.2e). There are three different types of terms in it. The first type comes from the $u_i u_j u_k u_\ell$ term of the first line. Clearly, all the states i, j, k, ℓ are required to be particle states, of which i and j are created and k, ℓ destroyed (because of $b_i^\dagger b_j^\dagger b_\ell b_k$). Taking proper recognition of the two-body matrix elements we can easily draw Fig. 5.4. This diagram represents the interaction between two particles, and hence it is usually called the "particle-particle" interaction term. In a similar manner, we examine the second term in the first line of Eq. (5.2e), where the v-coefficients tell us that i, j, k, ℓ are all hole states. This term, there-fore, represents a "hole-hole" interaction, and is given by the diagram of Fig. 5.5. The third type of term in H_{22} corresponds to the second line of Eq. (5.2e). From arguments similar to what has been repeated above several times, we conclude that this term corresponds to the inter-action between a hole and a particle and is represented by the diagram of Fig. 5.6.

Finally, we must point out that we have followed here a convention of drawing only one diagram corresponding to an antisymmetric (rounded bracket) matrix element v. Many authors split up such a matrix element explicitly into the direct and the exchange parts and represent these processes by separate diagrams. To give an example, let us consider the hole-particle term, which contains the matrix element $(j, \bar{k}| v | \ell, i)$ $\equiv \langle j, \bar{k}| v | \ell, \bar{i} \rangle - \langle j, \bar{k}| v | \bar{i}, \ell \rangle$. The direct term will still correspond to a diagram 5.6, while in the exchange term state i goes to j, and state ℓ goes to k. Hence if we decide to draw a separate diagram for the exchange process then it looks like Fig. 5.7. People following the con-vention of drawing the diagram 5.6 for the direct part of the hole-particle

FIG. 5.4. The particle-particle interaction term of H_{22}.
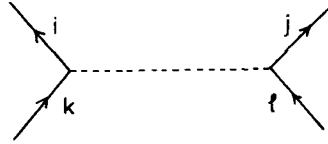
FIG. 5.5. The hole-hole interaction term of H_{22}.

FIG. 5.6. The hole-particle interaction term of H_{22}.
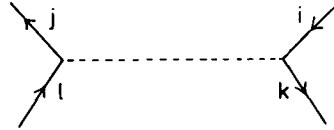
FIG. 5.7. An explicit diagram for the exchange part
of the hole-particle interaction.
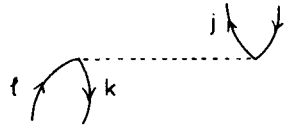
interaction, and the separate diagram 5.7 for the exchange part of the
same interaction refer to these diagrams as the "ladder" and "hen-track"
diagrams, respectively. These nomenclatures are based on obvious
visual similarities.

5.2.2. Tamm-Dancoff calculation for 1h-1p states

A look at the expresssions (5.2a-e) will convince the reader that
except for H_{40}, all other parts of the interaction Hamiltonian contain a
destruction operator for quasi-particle (in the present case a quasi-particle
is either a "hole" or a "particle") to the extreme right. Thus operating
on the ground state $|\Psi_0\rangle$ only the H_{40} part can produce a non-vanishing
result; as a matter of fact the discussion of section 5.2.1 tells us that
the result is a 2h-2p-type state. Therefore, when the interaction is
switched on, the ground state acquires an admixture of 2h-2p-type states
in the lowest approximation. What is important is that there is no term
in the interaction Hamiltonian that can mix a 1h-1p-type state into $|\Psi_0\rangle$.
This well-known result of the HF-theory has been derived in several
possible ways by different lecturers in this course.

The 1h-1p-type states represent excited states of the Hamiltonian,
and it follows from our unperturbed Hamiltonian: $H_0 + H_{11}$ that such a
two quasi-particle state has an unperturbed energy $E_h + E_p$ where E_h
and E_p are given by Eq.(4.55a), and not by Eq.(4.48). This is because
the last term of Eq.(4.54) is zero for the HF-theory, the product uv
vanishing for both occupied and unoccupied states. Keeping in mind the
special values of u, v for the hole and particle states, we have from
Eq.(4.55a)

$$E_h = -(\epsilon_h - \lambda) = \lambda - \epsilon_h \qquad (5.3a)$$

and

$$E_p = \epsilon_p - \lambda \qquad (5.3b)$$

where λ is the energy of the Fermi level. These results actually follow from common sense if we remember that a particle state is above the Fermi level, while a hole state is below it. Finally, from Eqs (5.3a,b), we have the unperturbed energy of a 1h-1p-type state, given by

$$E_h + E_p = \epsilon_p - \epsilon_h \qquad (5.4)$$

All the 1h-1p-type states that are obtained by lifting a nucleon across one major shell, have their unperturbed energies (5.4) lying within a few MeW of each other. The unperturbed energies of the 2h-2p-type states are, on the other hand, roughly double of this value.

We next examine what happens to the 1h-1p-type states when the interaction H_4 is switched on. It is clear from the expression (5.2e) of H_{22} that the hole-particle interaction part of it can give a non-vanishing matrix element connecting the 1h-1p states with each other. Similarly, the term H_{31} of (5.2c) can produce a non-vanishing matrix element between a 1h-1p-type state and 2h-2p-type state. The easiest way to see this is that H_{31} has one destruction operator to its extreme right, and hence the state it operates on must have at least one quasi-particle; the 1h-1p-type states each has 2 quasi-particles and hence meets this criterion. Furthermore, H_{31} creates three quasi-particles after destroying one, that is, it produces 2 additional quasi-particles; 2h-2p states have 4 quasi-particles, while 1h-1p states have 2, and hence after the production of 2 additional quasi-particles the 1h-1p state changes naturally to a 2h-2p state. This kind of argument, even though elementary, has been given here in details once for all, so that a new student of this subject can understand the logic behind similar statements to be made in the future without repeating the reasons.

According to the perturbation theory, therefore, the effect of the interaction is to produce a ground state and a set of excited states of the following structure:

$$|\Psi_0\rangle \rightarrow |\Psi_0'\rangle = |\Psi_0\rangle + \sum_{hp;\,h'p'} f_{hp,\,h'p'}\,|\Psi(hp;h'p')\rangle \qquad (5.5a)$$

$$|\Psi(hp)\rangle \rightarrow |\Psi'(hp)\rangle = |\Psi(hp)\rangle + \sum_{h'p'} g_{hp;h'p'}\,|\Psi(h'p')\rangle \qquad (5.5b)$$

We have written here only the lowest-order perturbation terms. The hole-particle indices in parentheses following a Ψ specify the hole-particle excitations present in that particular basis state. The quantities f and g contain, according to perturbation theory, the appropriate matrix element of H_4 in the numerator and an energy-denominator which is equal to $(E_h + E_p + E_{h'} + E_{p'})$ for f and $(E_{h'} + E_{p'} - E_h - E_p)$ for g. Since the energy-denominator of g is much smaller than that of f, we can consider an approximate treatment of f in the following manner: we neglect any modification of the ground-state through the interaction, but consider the ad-

mixture of the 1h-1p type states with each other. A calculation based
on this point of view is called the Tamm-Dancoff Approximation (TDA).

As a matter of fact, the energy-denominator $(E_{h'} + E_{p'} - E_h - E_p)$ can,
in principle, even vanish when the energies $E_{h'} + E_{p'}$ and $E_h + E_p$ are
accidentally degenerate. At any rate, all the 1h-1p-type states across
a given major shell, as mentioned earlier, form a near-degenerate bunch
of levels and hence their admixture can be better taken into account by a
matrix diagonalization (degenerate perturbation theory), rather than a
perturbation treatment like (5.5b). The calculation in the TDA, therefore,
consists of setting up the matrix of the hole-particle part of H_{22} in the
1h-1p space, adding the unperturbed energies along the diagonal, and
then diagonalizing the resultant Hamiltonian matrix. We proceed to write
down the expression for a typical matrix element.

The two terms in the hole-particle part of Eq. (5.2e) correspond to
the following two possibilities:

(1) $u_i v_j u_k v_\ell$ term: i = particle, j = hole;
$$\phantom{(1) u_i v_j u_k v_\ell \text{ term: }} k = \text{particle, } \ell = \text{hole.} \qquad (5.6a)$$

(2) $v_i u_j v_k u_\ell$ term: i = hole, j = particle;
$$\phantom{(2) v_i u_j v_k u_\ell \text{ term: }} k = \text{hole, } \ell = \text{particle.} \qquad (5.6b)$$

We want the matrix element of these terms connecting the hole-particle
state $b_p^\dagger b_h^\dagger | \Psi_0 \rangle$ with another, $\langle \Psi_0 | b_{h'}^\dagger b_{p'}^\dagger$. In the usual shell-model nota-
tion these states are denoted by $|\bar{h}^{-1}p\rangle$ and $|\bar{h}'^{-1} p'\rangle$ respectively.
Notice that, according to (4.39a) the hole creation operator $b_h^\dagger$ corresponds
to $s_h c_{-h} \equiv c_{\bar{h}}$, and hence it corresponds to a vacancy in the shell-model
state $\bar{h}$ (and not h). This fact accounts for the equivalent shell-model no-
tations mentioned above. We record these correspondences for future use

$$|\bar{h}^{-1}p\rangle = b_p^\dagger b_h^\dagger | \Psi_0 \rangle \qquad (5.7a)$$

$$\langle \bar{h}'^{-1} p'| = \langle \Psi_0 | b_{h'} b_{p'} \qquad (5.7b)$$

We now take the operator $b_i^\dagger b_j^\dagger b_\ell b_k$ from Eq. (5.2e) and easily arrive
at the following results:

$$b_\ell b_k |\bar{h}^{-1}p\rangle = b_\ell b_k b_p^\dagger b_h^\dagger | \Psi_0 \rangle$$
$$= (\delta_{kp} \delta_{\ell h} - \delta_{kh} \delta_{\ell p}) | \Psi_0 \rangle \qquad (5.8a)$$

$$\langle \bar{h}'^{-1}p'| b_i^\dagger b_j^\dagger = \langle \Psi_0 | b_{h'} b_{p'} b_i^\dagger b_j^\dagger$$
$$= \langle \Psi_0 | (\delta_{ip'} \delta_{jh'} - \delta_{ih'} \delta_{jp}) \qquad (5.8b)$$

In deriving these results we have made use of the anticommutators of
the creation and destruction operators to permute the destruction opera-
tors on to $|\Psi_0\rangle$ and the creation operators on to $\langle \Psi_0 |$ both of which are
zero according to (4.5). When we multiply Eq. (5.8b) and (5.8a), the
requirements (5.6a) and (5.6b) tell us that two terms out of the four are
non-vanishing. Thus, putting Eqs (5.8b), (5.8a), (5.6a,b) and (5.2e) together
we finally obtain

$$\langle \overline{h}^{\prime -1}p^{\prime}|H_{22}|\overline{h}^{-1}p\rangle = -\frac{1}{2}\sum_{i,j,k,\ell}(\delta_{kp}\delta_{\ell h}\delta_{ip^{\prime}}\delta_{jh^{\prime}} + \delta_{kh}\delta_{\ell p}\delta_{ih^{\prime}}\delta_{jp^{\prime}})(j,\overline{k}|v|\ell,\overline{i})$$

Using the time-reversal invariance of v, we can easily convince our-
selves that the two terms in this expression are equal, and the final
result is given by

$$\langle \overline{h}^{\prime -1}p^{\prime}|H_{22}|\overline{h}^{-1}p\rangle = -(p^{\prime},\overline{h}|v|p,\overline{h}^{\prime}) \tag{5.9}$$

It has been already mentioned that between the same two states the un-
perturbed part, $(H_0 + H_{11})$, of the Hamiltonian, gives, according to (5.4),

$$\langle \overline{h}^{\prime -1}p^{\prime}|(H_0 + H_{11})|\overline{h}^{-1}p\rangle = \delta_{hh^{\prime}}\delta_{pp^{\prime}}(\epsilon_p - \epsilon_h) \tag{5.10}$$

Equations (5.9) and (5.10) enable us to set up the matrix of the
Hamiltonian, in the TDA, using the 1h-1p-type states as basis. In practical
calculations the particle and hole energies, ϵ_p and ϵ_h, are taken from
experimental data; the harmonic-oscillator states are used for p, h etc.
along with some form for the two-body potential V to calculate the matrix
elements (5.9). However, the observed states in nuclei have good total
angular momentum J, and isospin T, and hence instead of evaluating
(5.9) one evaluates

$$\langle (h^{\prime -1}p^{\prime})JT|H_{22}|(h^{-1}p)JT\rangle \tag{5.11}$$

where the symbols h', p', h, p etc. do not contain any longer the projection
quantum numbers, and hence the time-reversed symbol on top of h, h'
are no longer necessary. Moreover, the total projection quantum numbers
M and M_T have not been written in expression (5.11) explicitly, because
the matrix-elements of v are actually independent of these quantum numbers.
The details of this angular-momentum coupling are given in the appendix to this
section.

For the two-body potential v one can either take well-behaved Yukawa,
Gaussian etc. forms with adjustable range, depth, and exchange-dependence.
The adjustable parameters can be fixed partly from other shell-model type
spectroscopic calculations, and also from the TDA calculation itself. In
more recent work, effective matrix elements of realistic two-body potentials
like the Hamada-Johnston and Yale potentials have also been used. There
was one historical stage of these calculations when the use of schematic
model potentials for v was also quite fashionable. Such schematic calcula-
tions did throw some light on the origin of coherence of one of the states
that result from the TDA-diagonalization. Some details of this type of
work are given in the Appendix mentioned above.

Finally, a few words about the choice of the 1h-1p basic states. It
is clear that for a practical computation we have to limit the number of
such states to a reasonable magnitude. The lifting of a nucleon through
one major shell produces a change of parity, and hence such 1h-1p states
have odd parity. Therefore, for the calculation of odd-parity states, like
the octupole 3^-, T = 0, and giant dipole 1^-, T = 1 states, it is reasonable
to truncate the 1h-1p basis to the subspace of excitations across one major
shell only. In the case of the even-parity states the situation is not so

unambiguous. Such states can be obviously produced by lifting one nucleon across two major shells or two nucleons across one major shell. Both these types will have more or less the same unperturbed energy. Hence the formulas which we have given here, for the 1h-1p-type states only, are not adequate for the treatment of even-parity excited states in closed-shell nuclei. An intelligent reader will be able to derive the matrix elements of H_{22} for the 2h-2p-type states and those of H_{31}, connecting a 1h-1p state with a 2h-2p-type state. We would however, like to make the general remark here that very often the even-parity states of closed-shell nuclei can have 4h-4p-type structure also, and then the question of a possible deformation of such states becomes very important. To sum up: the theory of the even-parity states of closed-shell nuclei is rather difficult and involved through the presence of 2h-2p, 4h-4p states, and the possibility of deformation; at the present time such theories are in a rather unsatisfactory state.

It is interesting to compare the TDA-matrix element of the Hamiltonian, which is a sum of (5.9) and (5.10), with the expression (3.52a) of the A-matrix, that occurred in our earlier RPA derivation. As a matter of fact $W_{hp0} \equiv (W_{hp} - W_0)$ is indeed equal to (5.10), while the second term of A is equal to $\langle h'^{-1}p' | H_{22} | h^{-1}p \rangle$, according to our new notations. The slight difference from (5.9), where $\bar{h}$ and $\bar{h}'$ occur instead of h and h', is really not significant. It has been mentioned earlier that we must do the angular momentum coupling in (5.9). Because of our present choice, $b_h^\dagger \equiv s_h c_{-h}$, the hole state $b_h^\dagger | \Psi_0 \rangle$ transforms as an angular momentum state j_h with projection m_h; this fact reveals itself in the occurrence of the following Clebsch-Gordan coefficient in the states of expression (5.11):

$$| (h^{-1}p)JM \rangle = \sum_{m_h, m_p} \begin{bmatrix} j_h & j_p & J \\ m_h & m_p & M \end{bmatrix} b_{j_p m_p}^\dagger \, b_{j_h m_h}^\dagger | \Psi_0 \rangle \qquad (5.12)$$

Here the operator, $b_{j_h m_h}^\dagger = (-1)^{j_h - m_h} c_{j_h, -m_h}$, occurs along with the first column $j_h m_h$ of the Clebsch-Gordan coefficient. On the other hand, we could have done the same angular momentum coupling by using $c_{j_h m_h}$ as the operator, together with a phase-factor $(-1)^{j_h - m_h}$ and the column $j_h, -m_h$ in the Clebsch-Gordan coefficient. In writing (3.52a) the vacancy was taken to be in the states $(j_h m_h)$ and $(j_{h'} m_{h'})$, rather than in the time-reversed states. Thus with the expression (3.52a) the angular momentum coupling has to be done according to the second alternative mentioned above. However, in view of the summation over m_h in (5.12) it really does not matter which of the two alternative notations we follow in doing the angular momentum coupling. Thus in the angular momentum coupled expressions (3.52a) and (5.9) give identical results.

5.2.3. Alternative derivations of the TDA-equations

There are various alternative ways of deriving the TDA-equations. We shall describe two such methods in this subsection.

(1) Commutator method with linearization

In this method we evaluate the commutator of H with $b_p^\dagger b_h^\dagger$. Being a number H_0 commutes with it. We next evaluate the following commutator:

$$[b_i^\dagger b_i \, , \, b_p^\dagger b_h^\dagger] \equiv b_i^\dagger [b_i \, , \, b_p^\dagger b_h^\dagger]$$

Since

$$b_i b_p^\dagger b_h^\dagger = \delta_{ip} b_h^\dagger - b_p^\dagger b_i b_h^\dagger$$

$$= \delta_{ip} b_h^\dagger - \delta_{ih} b_p^\dagger + b_p^\dagger b_h^\dagger b_i$$

we have

$$[b_i \, , b_p^\dagger b_h^\dagger] = \delta_{ip} b_h^\dagger - \delta_{ih} b_p^\dagger \tag{5.13}$$

Therefore,

$$[b_i^\dagger b_i \, , \, b_p^\dagger b_h^\dagger] = \delta_{ip} b_i^\dagger b_h^\dagger - \delta_{ih} b_i^\dagger b_p^\dagger$$

and hence

$$[H_{11}, b_p^\dagger b_h^\dagger] \equiv \sum_i E_i [b_i^\dagger b_i \, , b_p^\dagger b_h^\dagger]$$

$$= (E_p + E_h) b_p^\dagger b_h^\dagger \tag{5.14}$$

$$= (\epsilon_p - \epsilon_h) b_p^\dagger b_h^\dagger$$

Finally, as a step towards evaluating the commutator with the hole-particle part of H_{22} we evaluate, with the help of (5.13), the result

$$[b_i^\dagger b_j^\dagger b_\ell b_k \, , \, b_p^\dagger b_h^\dagger] = b_i^\dagger b_j^\dagger [b_\ell b_k \, , b_p^\dagger b_h^\dagger]$$

$$= b_i^\dagger b_j^\dagger \{ b_\ell [b_k, b_p^\dagger b_h^\dagger] + [b_\ell, b_p^\dagger b_h^\dagger] b_k \}$$

$$= b_i^\dagger b_j^\dagger \{ \delta_{kp} b_\ell b_h^\dagger - \delta_{kh} b_\ell b_p^\dagger + \delta_{\ell p} b_h^\dagger b_k - \delta_{\ell h} b_p^\dagger b_k \}$$

$$= b_i^\dagger b_j^\dagger \{ \delta_{kp} \delta_{\ell h} - \delta_{kh} \delta_{\ell p} + \delta_{kh} b_p^\dagger b_\ell - \delta_{kp} b_h^\dagger b_\ell$$

$$+ \delta_{\ell p} b_h^\dagger b_k - \delta_{\ell h} b_p^\dagger b_k \} \tag{5.14}$$

We are finally going to use the trick mentioned in the last paragraph of section 2.3. When $|\Psi_0 \rangle$ stands to the right of expression (5.14), the last four terms obviously produce zero. Therefore, in the subsequent steps, we keep only the first two terms of expression (5.14) and obtain from Eqs (5.2e) and (5.6a, b)

$$[H_{22}, b_p^\dagger b_h^\dagger] = -\frac{1}{2} \sum_{i,j} \{ u_i v_j b_i^\dagger b_j^\dagger (j, \bar{p} | v | h, \bar{i}) - v_i u_j b_i^\dagger b_j^\dagger (j, \bar{h} | v | p, \bar{i}) \}$$

$$= -\frac{1}{2} \sum_{h'p'} b_{p'}^\dagger b_{h'}^\dagger \{ (h', \bar{p} | v | h, \bar{p}') + (p', \bar{h} | v | p, h') \}$$

$$= - \sum_{h'p'} (p', \bar{h} | v | p, \bar{h}') b_{p'}^\dagger b_{h'}^\dagger \tag{5.15}$$

Once again we have used the time-reversal invariance of v to equate the
two matrix elements; furthermore, we have taken note of the fact that
$u_i v_j$ in the first term requires i to be a particle state (p') and j to be a
hole state (h'), while $v_i u_j$ in the second term imposes just the opposite
requirement. In the second term $b_{p'}^\dagger b_{h'}^\dagger$ has been rearranged to $- b_{p'}^\dagger b_{h'}^\dagger$.
The procedure described under Eq. (5.14) of putting $|\Psi_0\rangle$ to the right
and $\langle \Psi|$ to the left of the commutator, has enabled us to throw away
terms which are not linear in the 1h-1p creation operators $b_{p'}^\dagger b_{h'}^\dagger$. There-
fore, this procedure is usually called the method of linearization. Notice
that the commutator method of diagonalizing a Hamiltonian, described in
section 2 succeeds only if it is possible to obtain a closed system of
linear equations connecting a given set of operators. This has been
achieved in Eq. (5.15). Putting (5.14) and (5.15) together, we are once
again led, according to the general derivation of Sec. 2, to the diagonaliza-
tion of the same hole-particle matrix of the Hamiltonian that we described
in the previous subsection.

(2) Quasi-boson method:

In this method we first introduce the operators $A_{hp}^\dagger$ which create a
hole-particle pair:

$$A_{hp}^\dagger = b_p^\dagger b_h^\dagger \tag{5.16a}$$

The Hermitian conjugate of this operator destroys a hole-particle pair and
is given by

$$A_{hp} = b_h b_p \tag{5.16b}$$

It can be easily verified from the anticommutators of b_h, b_p, $b_h^\dagger$, $b_p^\dagger$ etc.
that

$$A_{hp}^\dagger = - A_{ph}^\dagger, \qquad A_{hp} = - A_{ph} \tag{5.16c}$$

and

$$[A_{hp}, A_{h'p'}] = [A_{hp}^\dagger, A_{h'p'}^\dagger] = 0 \tag{5.17a}$$

The commutator of a pair destruction operator with a pair creation
operator can be similarly worked out with the help of Eq. (5.13). We
obtain

$$[A_{hp}, A_{h'p'}^\dagger] = [b_h b_p, b_{p'}^\dagger b_{h'}^\dagger]$$

$$= b_h [b_p, b_{p'}^\dagger b_{h'}^\dagger] + [b_h, b_{p'}^\dagger b_{h'}^\dagger] b_p$$

$$= b_h b_{h'}^\dagger \delta_{pp'} - b_{p'}^\dagger b_p \delta_{hh'}$$

$$= \delta_{hh'} \delta_{pp'} - b_{h'}^\dagger b_h \delta_{pp'} - b_{p'}^\dagger b_p \delta_{hh'} \tag{5.17b}$$

Introducing the short-hand notation

$$\hat{N}_{i'i} \equiv b_{i'}^\dagger b_i \tag{5.18}$$

we rewrite Eq.(5.17b) as follows:

$$[A_{hp}, A^{\dagger}_{h'p'}] = \delta_{hh'}\delta_{pp'} - \delta_{pp'}\hat{N}_{h'h} - \delta_{hh'}\hat{N}_{p'p} \qquad (5.19)$$

Once again, if we use this commutator with the $|\Psi_0\rangle$ on its right then the last two terms produce zero and we obtain

$$[A^{\dagger}_{hp}, A^{\dagger}_{h'p'}]\,|\Psi_0\rangle = \delta_{hh'}\delta_{pp'}\,|\Psi_0\rangle \qquad (5.20)$$

Therefore, as long as we have the state $|\Psi_0\rangle$ to the right, the creation and destruction operators of the hole-particle pairs satisfy the commutation relations (5.17a) and (5.20) which are just the commutation relations satisfied by a set of boson operators. The operators A_{hp}, $A^{\dagger}_{h'p'}$ etc. are called quasi-boson operators; the adjective 'quasi' here is a reminder to the fact that (5.20) is not an exact operator equation for the commutator, its validity being restricted to the presence of $|\Psi_0\rangle$ to the right.

The commutor of these quasi-boson operators with the operator $\hat{N}_{i'i}$ of (5.18) is also straightforward to derive. We have, using (5.13), the result:

$$[\hat{N}_{i'i}, A^{\dagger}_{hp}] = [b^{\dagger}_{i'}b_i , b^{\dagger}_p b^{\dagger}_h]$$

$$= b^{\dagger}_{i'}[b_i , b^{\dagger}_p b^{\dagger}_h]$$

$$= \delta_{ip} b^{\dagger}_{i'} b^{\dagger}_h - \delta_{ih} b^{\dagger}_{i'} b^{\dagger}_p$$

$$= \delta_{ip} A^{\dagger}_{hi'} + \delta_{ih} A^{\dagger}_{ih'p} \qquad (5.21a)$$

From the Hermitian conjugate of this equation we have

$$[\hat{N}_{ii'} , A_{hp}] = - (\delta_{ih} A_{i'p} + \delta_{ip} A_{hi'}) \qquad (5.21b)$$

The next step in the derivation is to evaluate the commutator of $A^{\dagger}_{hp}$ with the part of the Hamiltonian that is treated by the TDA. The part H_0 gives zero to the commutator; the parts H_{11} and the hole-particle part of H_{22} are rewritten below in terms of the new operators:

$$H_{11} = \sum_i E_i \hat{N}_{ii} \qquad (5.22a)$$

and

$$\text{Hole-particle part of } H_{22} = -\frac{1}{2}\sum_{h'p';\,h''p''}\{(h'\bar{p}''|v|h''\bar{p}')A^{\dagger}_{h'p'}A_{h''p''}$$

$$+ (p'\bar{h}''|v|p''\bar{h}')A^{\dagger}_{p'h'}A_{p''h''}\}$$

$$= -\sum_{h'p'\,h''p''}(p'\bar{h}''|v|p''\bar{h}')A^{\dagger}_{h'p'}A_{h''p''} \qquad (5.22b)$$

We have used here the time-reversal invariance of v and Eq.(5.16c).

The commutators are now easy to evaluate with the help of Eqs (5.17a), (5.19) and (5.21a). Once again, we shall multiply the commutator by $|\Psi_0\rangle$ from the right and $\langle\Psi|$ from the left in accordance with the trick described in section 2.3, and hence the simpler result (5.20), instead of (5.19) can be used. In this way, we have

$$[H_{11}, A_{hp}^\dagger] = (E_h + E_p)A_{hp}^\dagger = (\epsilon_p - \epsilon_h)A_{hp}^\dagger \qquad (5.23a)$$

and

$$[H_{22}, A_{hp}^\dagger] = -\sum_{h'p'} (p'\bar{h}|v|p\bar{h}') A_{h'p'}^\dagger \qquad (5.23b)$$

These equations are identical with Eqs (5.14) and (5.15). Thus the linearization in the method described earlier is equivalent to using the quasi-boson commutation rule (5.20), instead of the exact result (5.19). Once again, when we multiply the commutators from right by $|\Psi_0\rangle$ and from the left by $\langle\Psi|$, Eqs (5.23a) plus (5.23b) become a system of linear equations for the amplitudes $\langle\Psi|A_{hp}^\dagger|\Psi_0\rangle$ with all possible h, p admitted in the calculation. The solution to this system of equations is obtained by diagonalizing the TDA matrix in the hp-space. The amplitudes $\langle\Psi|A_{hp}^\dagger|\Psi_0\rangle$ are given by the elements of the eigenvector, and they clearly correspond to the amplitude of the basic hole-particle states present in the expansion of the excited state $|\Psi\rangle$.

5.2.4. RPA calculation for 1h-1p states

It is clear from the previous two subsections that the TDA calculation diagonalizes only a limited part of the interaction. The improvement over the TDA could be achieved in two possible ways: (i) bring in states with larger number of hp pairs, or at least 2h-2p pairs. Then as mentioned earlier the part H_{31} and H_{13} become effective in connecting 1h-1p states with 2h-2p states and vice versa; there is a second important consequence, i.e. H_{40} connects the state $|\Psi_0\rangle$ with 2h-2p states, and H_{04} has the opposite effect. Therefore, according to this approach one must set up the matrix in the space of $|\Psi_0\rangle$ all the 1h-1p states, and 2h-2p states. $|\Psi_0\rangle$ does not mix directly with the 1h-1p states but does so through the intermediary of the 2h-2p states. Such a calculation is usually called the 'Higher Tamm-Dancoff Approximation' (HTDA). One has to exercise care in constructing the 2h-2p states in such a calculation, because $A_{hp}^\dagger A_{h'p'}^\dagger|\Psi_0\rangle$ for all h, p and h', p' are not non-trivial states; whenever $h = h'$ and $p = p'$ such basic states do not exist due to Pauli principle (that is, due to the anticommutation of Fermion operators). While considering angular momentum coupling in these operators one has to take care that one keeps only states in which (hh) and (pp) couple to even values of J for $T = 1$ and odd values of J for $T = 0$, where J and T are the resultant angular momentum and isospin of the two holes or the two particles. (2) In the second method of improving upon the TDA, one does not have to introduce explicitly the states with higher number of hp pairs. But the effect of 2h-2p pairs or higher number hole-particle pairs in the ground state is indirectly taken into account in this type of calculation. In other words, this method allows us to take into account the

effect of the correlation in the ground state. We shall, in this subsection, describe this method.

To understand the basic principle let us write down the structure of the correlated ground state. In the lowest order of approximation this is given by Eq. (5.5a). In a similar manner let us consider what happens to the mixed 1h-1p states of the TDA in the next higher approximation when they mix with the 2h-2p states. For simplicity we write a mixed 1h-1p TDA state as $\Psi(1h\text{-}1p)$. This state changes to $|\Psi'\rangle$, given by

$$|\Psi'\rangle = |\Psi(1h\text{-}1p)\rangle + \sum_{h'p'h''p''} \bar{f}_{h'p',h''p''} |\Psi(h'p'; h''p'')\rangle \qquad (5.24)$$

It is clear from Eqs (5.5a) and (5.24) that the amplitude $\langle\Psi'|A^\dagger_{hp}|\Psi_0\rangle$ is large and of the order of unity. Because of the second term (which re-presents correlation in the ground state) in Eq. (5.5a) an amplitude of the type $\langle\Psi'|A_{hp}|\Psi'_0\rangle$ is also non-vanishing and arises through the con-nection of $\Psi(hp, h'p')$ of Eq. (5.5a) with $\Psi(1h\text{-}1p)$ of Eq. (5.24) via the pair-destruction operator. Such an amplitude is clearly of the order of $f_{hp,h'p'}$, i.e. of first order of smallness compared to $\langle\Psi'|A^\dagger_{hp}|\Psi'_0\rangle$. In the same manner, it is clear from Eqs (5.5a) and (5.24) that an amplitude of the type $\langle\Psi'_0|\hat{N}_{i'i}|\Psi'_0\rangle$ is quadratic in f, while $\langle\Psi'|\hat{N}_{i'i}|\Psi'_0\rangle$ is bilinear in f and $\bar{f}$. Both of these amplitudes are, therefore, of second-order of smallness compared with the large amplitude $\langle\Psi'|A^\dagger_{hp}|\Psi'_0\rangle$, and one order smaller compared with $\langle\Psi'|A_{hp}|\Psi'_0\rangle$. Therefore, the natural extension of the TDA method is to construct a set of equations in which the amplitudes $\langle\Psi'|A^\dagger_{hp}|\Psi'_0\rangle$ and $\langle\Psi'|A_{hp}|\Psi'_0\rangle$ are retained while amplitudes of the type $\langle\Psi'|\hat{N}_{i'i}|\Psi'_0\rangle$ are neglected. For simplicity in our notation we shall omit, from now on, the primes on the corrected ground and excited states, and keep on denoting them by the old notations Ψ_0 and Ψ.

The algebraic procedure, once again, is to evaluate the commutator of H with $A^\dagger_{hp}$, and sandwich the result between $\langle\Psi|$ and $|\Psi_0\rangle$. From the resultant expression one has to drop all the terms that are of a smaller order of magnitude than the amplitude $\langle\Psi|A_{hp}|\Psi_0\rangle$. To re-cognize quickly such terms which will be ignored in the end, we carry out the following book-keeping type of work with the suppression of the hole-particle subscripts on all $A^\dagger$ and A operators. The operators carry either two hole or two particle labels, and these will also be suppressed. One exception will be made in the case of the hole-hole and particle-particle part of H_{22} [the first line of Eq. (5.2e)], where the subscripts will be explicitly retained at $A^\dagger$ and A because in this case these operators will carry two particle or two hole labels, as distinguished from $A^\dagger_{hp}$ or A_{hp}.

The terms H_{40} and H_{04}, as given by Eqs (5.2a,b), have the following structure:

$$H_{40} \rightarrow A^\dagger A^\dagger \qquad (5.25a)$$

$$H_{04} \rightarrow AA \qquad (5.25b)$$

Similarly H_{31} and H_{13} of (5.2c, d) have the schematic composition

$$H_{31} \to A^\dagger \hat{N} \tag{5.25c}$$

$$H_{13} \to \hat{N} A \tag{5.25d}$$

The hole-particle part of H_{22} was already explicitly written down in Eq.(5.22b) and it has the following structure:

$$H_{22} \text{ (hole-particle)} \to A^\dagger A \tag{5.25e}$$

In contrast to this, the hole-hole and particle-particle part of H_{22} [the first line of Eq.(5.2e)] has the appearance

$$H_{22} \text{ (hole-hole)} \to A_{h_1 h_2} A_{h_3 h_4} \tag{5.25f}$$

$$H_{22} \text{ (particle-particle)} \to A_{p_1 p_2} A_{p_3 p_4} \tag{5.25g}$$

We next use the commutators (5.19) and (5.21e), and obtain from the following schematic expressions from relations (5.25 a-e):

$$[H_{40}, A^\dagger] \to 0 \tag{5.26a}$$

$$[H_{04}, A^\dagger] \to A + \hat{N} A + A \hat{N} \tag{5.26b}$$

$$[H_{31}, A^\dagger] \to A^\dagger A^\dagger \tag{5.26c}$$

$$[H_{13}, A^\dagger] \to A^\dagger A + \hat{N} + \hat{N} \hat{N} \tag{5.26d}$$

$$[H_{22}(\text{hole-particle}), A^\dagger] \to A^\dagger + A^\dagger \hat{N} \tag{5.26e}$$

To evaluate the commutator of relation (5.25f, g) with $A^\dagger$, a little extra work is required. First we have to evaluate the commutators of $A_{h_3 h_4}$ and $A_{p_3 p_4}$ with $A_{hp}^\dagger$, which can be done in a manner analogous to expression (5.17b). This work is left to the reader as an exercise. Finally, one obtains

$$[H_{22} \text{ (hole-hole)}, A^\dagger] \to A^\dagger \hat{N} \tag{5.26f}$$

$$[H_{22} \text{ (particle-particle)}, A^\dagger] \to A^\dagger \hat{N} \tag{5.26g}$$

If we now put $\langle \Psi |$ to the left, and $| \Psi_0 \rangle$ to the right of relations (5.26a-g), we obtain, besides the amplitudes $\langle \Psi | A^\dagger | \Psi_0 \rangle$ and $\langle \Psi | A | \Psi_0 \rangle$, the following types of quantities: $\langle \Psi | \hat{N} | \Psi_0 \rangle$, $\langle \Psi | \hat{N} \hat{N} | \Psi_0 \rangle$, $\langle \Psi | \hat{N} A | \Psi_0 \rangle$, $\langle \Psi | A \hat{N} | \Psi_0 \rangle$, $\langle \Psi | A^\dagger \hat{N} | \Psi_0 \rangle$, $\langle \Psi | A^\dagger A | \Psi_0 \rangle$, and $\langle \Psi | A^\dagger A^\dagger | \Psi_0 \rangle$. It has been already remarked under Eq.(5.24) that $\langle \Psi | \hat{N} | \Psi_0 \rangle$ is of smaller order than $\langle \Psi | A | \Psi_0 \rangle$. To examine the other amplitudes which are bilinear in the operators $A^\dagger$, A or $\hat{N}$, we follow the practice of introducing a complete set of states $\sum_n | \Psi_n \rangle \langle \Psi_n |$ in between the two operators. As a demonstration of the type of arguments that will follow this procedure,

let us consider the case of $\langle \Psi | A^\dagger \hat{N} | \Psi_0 \rangle$. After the introduction of the intermediate states this term yields

$$\langle \Psi | A^\dagger \hat{N} | \Psi_0 \rangle = \sum_n \langle \Psi | A^\dagger | \Psi_n \rangle \langle \Psi_n | \hat{N} | \Psi_0 \rangle \tag{5.27}$$

Recall that by our choice of notation the present Ψ_0 is actually the same as $\Psi_0^!$ of Eq. (5.5a), and in the latter equation the first term represents the state with no hole or particle. Thus, the second factor $\langle \Psi_n | \hat{N} | \Psi_0 \rangle$ of (5.27) gets a non-vanishing contribution only from the second term of relation (5.5a), and with the choice of the two-hole two-particle states for Ψ_n. Therefore, this factor of (5.27) is already linear in the f-coefficients of (5.5a), and hence of the same order as $\langle \Psi | A | \Psi_0 \rangle$. The other factor $\langle \Psi | A^\dagger | \Psi_n \rangle$ of Eq. (5.27) under the same circumstances (i.e. for Ψ_n equal to a two-hole two-particle state) is extremely small (in fact zero in the lowest approximation) because Ψ is predominantly linear combination of one-hole one-particle type states. Thus the term $A^\dagger \hat{N}$ in the commutator of H with $A_{hp}^\dagger$ can be ignored in comparison with the $A^\dagger$ and A terms. In the same manner, it is possible to argue that all the other bilinear terms in $A^\dagger$, A, $\hat{N}$, with the exception of $\langle \Psi | A \hat{N} | \Psi_0 \rangle$ and $\langle \Psi | A^\dagger A^\dagger | \Psi_0 \rangle$, can be ignored. We will see below that the contribution of $\langle \Psi | A \hat{N} | \Psi_0 \rangle$ is kept in the RPA-theory, while $\langle \Psi | A^\dagger A^\dagger | \Psi_0 \rangle$ is usually ignored.

Going back to relations (5.26a-g) we, therefore, conclude that in the RPA derivation only the commutator with H_{04} and the $A^\dagger$ term in the commutator of H_{22} (hole-particle) need be worked out in details. As a matter of fact, the latter term has already been evaluated carefully in the TDA-theory; hence all we need to do here in detail is to evaluate expression (5.26b) in detail.

For this purpose, we go back to relation (5.2b) and write this expression as

$$H_{04} = -\frac{1}{4} \sum_{h''p''h'p'} (p'' p' | v | \overline{h}' \overline{h}'') A_{h'p'} A_{h''p''}$$

$$= \frac{1}{4} \sum_{h''p''h'p'} (p'' p' | v | \overline{h}'' \overline{h}') A_{h'p'} A_{h''p''} \tag{5.28}$$

Next we evaluate its commutator with $A_{hp}^\dagger$ using (5.19). If we decide to keep only the terms containing one A operator, we omit the last two terms of (5.19) and obtain

$$[H_{04}, A_{hp}^\dagger] = \frac{1}{2} \sum_{h'p'} (pp' | v | \overline{hh}') A_{h'p'} \tag{5.29}$$

This result is, however, not quite right. The factor $1/2$ will actually be absent in a more careful derivation. The source of this error lies in the use of the quasi-boson commutation relation [the first term of Eq. (5.19)]. As a matter of fact if we had used the entire expression (5.19),

we would have obtained terms having the structure of the last two terms of Eq. (5.26b). We will show below that the terms of the type $\langle \Psi | A\hat{N} | \Psi_0 \rangle$ have some $\langle \Psi | A | \Psi_0 \rangle$ concealed in them.

The terms that have to be added to the right hand side of Eq. (5.29) are obtained from Eq. (5.28) and the last two terms of Eq. (5.19). These are given by

$$-\frac{1}{4} \sum_{h'p'} \sum_{h''p''} (p''p' | v | \bar{h}'' \bar{h}') [A_{h'p'}(\delta_{pp''} \hat{N}_{hh''} + \delta_{hh''} \hat{N}_{pp''})$$

$$+ (\delta_{pp'} \hat{N}_{hh'} + \delta_{hh'} \hat{N}_{pp'}) A_{h''p''}] \tag{5.30}$$

Let us examine the first term, $A_{h'p'} \hat{N}_{hh''} \equiv b_{h'} b_{p'} b_h^\dagger b_{h''}$. When we insert $\langle \Psi |$ and $| \Psi_0 \rangle$ to the left and right and $\sum | \Psi_n \rangle \langle \Psi_n |$ in the middle, it appears that this term is always of a smaller order of magnitude than $\langle \Psi | A_{h'p'} | \Psi_0 \rangle$, because of the second factor $\langle \Psi_0 | b_h^\dagger b_{h''} | \Psi_0 \rangle$ [we are here considering the case $\Psi_n = \Psi_0$]. It is, however, not very apparent that there is a possibility of obtaining a non-vanishing result for the case $\Psi_n = \Psi$, as well. To see this, all that we need is to rewrite, by permuting operators,

$$A_{h'p'} \hat{N}_{hh''} = b_{h'} b_{p'} b_h^\dagger b_{h''} = -b_{h'} b_h^\dagger b_{p'} b_{h''} = b_{h'} b_h^\dagger b_{h''} b_{p'}$$

With the choice $\Psi_n = \Psi$, this expression yields $\langle \Psi | b_{h'} b_h^\dagger | \Psi \rangle \langle \Psi | b_{h''} b_{p'} | \Psi_0 \rangle$. The first factor is large when $h = h'$ (actually equal to $\delta_{hh'}$, when Ψ is normalized to unity), while the second factor is the amplitude $\langle \Psi | A_{h''p'} | \Psi_0 \rangle$. This establishes the assertion we made above regarding the concealed presence of $\langle \Psi | A | \Psi_0 \rangle$ in $\langle \Psi | A\hat{N} | \Psi_0 \rangle$. The second term of expression (5.30) can also be handled similarly to yield an amplitude of the type $\langle \Psi | A | \Psi_0 \rangle$. A similar attempt with the third and fourth terms, however, will fail to yield anything. In all this derivation we have to make the consistent assumption that $\langle \Psi | \hat{N} | \Psi_0 \rangle$, which is the probability of getting a particle or a hole in the excited state is an order of magnitude smaller than $\langle \Psi | A^\dagger | \Psi_0 \rangle$. The details of the algebra indicated above, to be applied to the first two terms of expression (5.30), are left here as an exercise. With this extra contribution, one finally obtains

$$[H_{04}, A_{hp}^\dagger] = \sum_{h'p'} (pp' | v | \bar{h}\bar{h}') A_{h'p'} \tag{5.32}$$

Collecting relations (5.23a, b) and (5.32) together we have

$$[H, A_{hp}^\dagger] = (\epsilon_p - \epsilon_h) A_{hp}^\dagger - \sum_{h'p'} (p'\bar{h} | v | p\bar{h}') A_{h'p'}^\dagger + \sum_{h'p'} (pp' | v | \bar{h}\bar{h}') A_{h'p'}$$

$$\tag{5.33a}$$

Taking the Hermitian conjugate and reversing the sign one obtains immediately

$$[H, A_{hp}] = -(\epsilon_p - \epsilon_h) A_{hp} + \sum_{h'p'} (p\bar{h}' | v | p'\bar{h}) A_{h'p'} - \sum_{h'p'} (\bar{h}\bar{h}' | v | pp') A_{h'p'}^\dagger$$

$$\tag{5.33b}$$

In the usual way the system of equations (5.33a, b) give rise to a set of linear equations for the amplitudes $\langle \Psi | A_{hp}^\dagger | \Psi_0 \rangle \equiv \kappa_{hp}$ and $\langle \Psi | A_{hp} | \Psi_0 \rangle$ $\equiv y_{hp}$. The matrix to be diagonalized is clearly of the form (3.57b), with the following definitions of A and B:

$$A_{hp;h'p'} = (\epsilon_p - \epsilon_h) \delta_{hh'} \delta_{pp'} - (p\bar{h}' | v | p'\bar{h}) \tag{5.34a}$$

$$B_{hp;h'p'} = (pp' | v | \bar{h}\bar{h}') \tag{5.34b}$$

Except for the phase-factor, and sign of the projection quantum numbers of the hole-states, these definitions agree with definitions (3.52a, b). This slight difference in the hole-states originates, as mentioned earlier in the TDA-derivation, from the definition $b_h^\dagger = s_h c_{-h}$. The statements made earlier about angular-momentum coupling are also true in the present case. The details of the coupling are given in the Appendix to this section.

5.3.   Theory of vibration in the BCS case

The treatment of the quasi-particle interaction given in section 5.1 in the case of a BCS-type nucleus is now a straightforward generalization of what we have already done in section 5.2.

A.   Definitions

In analogy to the hole-particle pair and number operators of section 5.2 we now introduce the quasi-particle pair and number operators:

$$A_{mn}^\dagger = b_n^\dagger b_m^\dagger, \qquad A_{mn} = b_m b_n, \qquad \hat{N}_{mn} = b_m b_n \tag{5.35}$$

Using the basic anticommution rules we obtain

$$[b_i, b_n^\dagger b_m^\dagger] = \delta_{in} b_m^\dagger - \delta_{im} b_n^\dagger \tag{5.36}$$

By a straightforward application of relation (5.36) we then derive the following commutator relations:

$$
\begin{aligned}
[A_{ij}, A_{mn}^\dagger] &= [b_i b_j, b_n^\dagger b_m^\dagger] \\
&= b_i [b_j, b_n^\dagger b_m^\dagger] + [b_i, b_n^\dagger b_m^\dagger] b_j \\
&= \delta_{jn} b_i b_m^\dagger - \delta_{jm} b_i b_n^\dagger + \delta_{in} b_m^\dagger b_j - \delta_{im} b_n^\dagger b_j \\
&= \delta_{jn} b_i b_m^\dagger - \delta_{jm} b_i b_n^\dagger + \delta_{in} \hat{N}_{mj} - \delta_{im} \hat{N}_{nj} \tag{5.37a}
\end{aligned}
$$

$$
\begin{aligned}
&= (\delta_{im} \delta_{jn} - \delta_{in} \delta_{jm}) + \delta_{jm} \hat{N}_{ni} - \delta_{jn} \hat{N}_{mi} \\
&\quad + \delta_{in} \hat{N}_{mj} - \delta_{im} \hat{N}_{nj}
\end{aligned}
\tag{5.37b}
$$

The quasi-boson approximation consists of dropping all the terms containing the number operator in expression (5.37b). In this approxima-

tion we have, by virtue of the Kronecker deltas inside parantheses in (5.37b):

$$[A_{ij}, A_{ij}^\dagger] = 1 \qquad\qquad [A_{ij}, A_{ji}^\dagger] = -1 \qquad\qquad (5.38)$$

From definition (5.35) we have

$$A_{ji}^\dagger = -A_{ij}^\dagger$$

and hence the two equations (5.38) are, in fact, the same. Therefore, in spite of the two terms with the Kronecker deltas in expression (5.37b), the operators A_{ij}, $A_{ij}^\dagger$ indeed behave as boson operators in the above approximation.

In an analogous manner we derive the following commutator:

$$[N_{ij}, A_{mn}^\dagger] = \delta_{jn} A_{mi}^\dagger - \delta_{jm} A_{ni}^\dagger \qquad\qquad (5.39)$$

Finally, we write down the obvious results:

$$[A_{ij}^\dagger, A_{mn}^\dagger] = [A_{ij}, A_{mn}] = 0 \qquad\qquad (5.40)$$

B. TDA-equations

In the manner of section 5.2 we evaluate the commutator of the pair creation operator $A_{mn}^\dagger$ with H_{11} and H_{22}. Using the commutator (5.39), we obtain:

$$[H_{11}, A_{mn}^\dagger] = \sum_i E_i [\hat{N}_{ii}, A_{mn}^\dagger] = (E_m + E_n) A_{mn}^\dagger \qquad\qquad (5.41)$$

where E_m is the energy of the quasi-particle m.

The operator in H_{22} is clearly $A_{ji}^\dagger A_{\ell k}$, and its commutator with $A_{mn}^\dagger$, according to the quasi-boson commutation relation, is given by

$$[A_{ji}^\dagger A_{\ell k}, A_{mn}^\dagger] = A_{ji}^\dagger [A_{\ell k}, A_{mn}^\dagger]$$

$$= A_{ji}^\dagger (\delta_{\ell m} \delta_{kn} - \delta_{\ell n} \delta_{km}) \qquad\qquad (5.42)$$

Using the commutator (5.42) together with the coefficient in relation (5.2e) we obtain:

$$[H_{22}, A_{mn}^\dagger] = \frac{1}{2} \sum_{ij} \left[\left(u_i u_j u_m u_n + v_i v_j v_m v_n \right) \left(ij \mid v \mid nm \right) \right.$$

$$+ u_i v_j \left\{ u_n v_m \left(j\bar{n} \mid v \mid m\bar{1} \right) - u_m v_n \left(j\bar{m} \mid v \mid n,\bar{1} \right) \right\}$$

$$\left. + v_i u_j \left\{ u_m v_n \left(j, \bar{n} \mid v \mid m',\bar{1} \right) - u_n v_m \left(j\bar{m} \mid v \mid n\bar{1} \right) \right\} \right] A_{ij}^\dagger \dots$$

$$(5.43)$$

By interchanging the labels i, j and using $A_{ji}^{\dagger} = -A_{ij}^{\dagger}$ together with the time-reversal invariance of the matrix elements of v, we can easily establish that (i) the first term in the last line of Eq.(5.43) is equal to the second term in the second line, and (ii) the first term in the second line is equal to the second term of the third line. Therefore, we retain the second terms in the second and third lines of (5.43) and remove the factor of 1/2 for these two lines. Thus,

$$[H_{22}, A_{mn}^{\dagger}] = \sum_{ij} \left[\left(u_i u_j u_m u_n + v_i v_j v_m v_n \right) \frac{1}{2} \left(ij \mid v \mid mn \right) \right.$$

$$\left. + \left(u_i v_j u_m v_n + v_i u_j v_m u_n \right) \left(j\overline{m} \mid v \mid n\overline{i} \right) \right] A_{ij}^{\dagger} \qquad (5.44)$$

Equations (5.41) and (5.44) give rise to a linear set of equations for the amplitudes $\langle \Psi \mid A_{ij}^{\dagger} \mid \Psi_0 \rangle$. The matrix to be diagonalized, therefore, is the coefficient matrix on the right-hand side of Eq.(5.44) together with the quasi-particle pair energies $(E_m + E_n)$ of expression (5.41) along the leading diagonal. As in the hole-particle case of section 5.2 this TDA-calculation is identical with the diagonalization of the unperturbed Hamiltonian plus the quasi-particle interaction in the space of all quasi-particle pair states of the type $A_{mn}^{\dagger} \mid \Psi_0 \rangle$. Finally, in perfect analogy with the TDA-theory of section 5.2, the use of the quasi-boson commutation rule in writing down Eq.(5.42) is justified by the fact that the remaining terms of expression (5.37b) produce zero when the BCS state $\mid \Psi_0 \rangle$ sits to the right.

C. RPA-equations

As in section 5.2, the part H_{40} of the quasi-particle interaction can mix four quasi-particle states into the BCS ground state $\mid \Psi_0 \rangle$. The two quasi-particle excited states described above can also mix with the four quasi-particle states via H_{31}. A higher TDA-calculation can, therefore, be done by mixing zero, two and four quasi-particle states. An alternative way to treat the effect of correlation in the BCS ground state is the RPA method, which admits of two types of amplitudes $\langle \Psi \mid A_{mn}^{\dagger} \mid \Psi_0 \rangle$, and $\langle \Psi \mid A_{mn} \mid \Psi_0 \rangle$, Ψ_0 being the correlated ground state.

By arguments similar to those presented in section 5.2 one can show that the RPA-treatment, in the present case also, requires the evaluation of only one more commutator, namely that of H_{04} with $A_{mn}^{\dagger}$, in details.

According to expression (5.2b) the expression for H_{04} is given by

$$H_{04} = \frac{1}{4} \sum_{ijk\ell} (k, \ell \mid v \mid ij)\, u_i u_j v_\ell v_k\, A_{k\ell} A_{ji} \qquad (5.45)$$

As in section 5.2, if we keep only the quasi-boson terms of (5.37b), we obtain.

$$[H_{04}, A_{mn}^{\dagger}] = \frac{1}{2} \sum_{k\ell} (k\ell \mid v \mid nm)\, (u_m u_n v_k v_\ell + v_m v_n u_k u_\ell)\, A_{k\ell} \qquad (5.46a)$$

This, however, is not the correct result because the other terms in

Eq. (5.37b) give rise to terms in the commutator of the type $A\hat{N}$ and $\hat{N}A$ of which the former yields some extra $A_{k\ell}$ type terms in the final result. Terms of the type $\hat{N}A$, on the other hand, yield $\langle\Psi|\hat{N}|\Psi\rangle\langle\Psi|A|\Psi_0\rangle$ which is smaller, in order of magnitude, than $\langle\Psi|A|\Psi_0\rangle$, because the factor $\langle\Psi|\hat{N}|\Psi\rangle$, which represents the probability of getting a <u>given</u> quasi-particle in the excited state Ψ must be very small compared with unity (Ψ being a coherent superposition of many quasi-particle pair states in the lowest approximation). Therefore, we write only the extra terms in the above commutator of the type $A\hat{N}$, and show how these terms lead to some extra contribution of the type $A_{k\ell}$:

$$\frac{1}{4}\sum_{ijk\ell}(\bar{k}\,\bar{\ell}\mid v\mid ij)\,u_i u_j v_\ell v_k\,A_{k\ell}\left\{\delta_{jm}\,\hat{N}_{ni}-\delta_{jn}\,\hat{N}_{mi}+\delta_{in}\,\hat{N}_{mj}-\delta_{im}\,\hat{N}_{nj}\right\}$$

The first term of expression (5.46b), for example, yields, when the summation indices k and ℓ, in turn, are equal to n, the following result:

$$A_{k\ell}\,\hat{N}_{ni}=b_k b_\ell b_n^\dagger b_i \rightarrow \delta_{\ell n}\,b_k b_i+\delta_{kn}\,b_i b_\ell \qquad (5.46c)$$

Notice that, when $\ell=n$, k is necessarily not equal to ℓ or n (because if $k=\ell$, $b_k b_\ell\equiv 0$), and hence b_k can be taken to the right of $b_n^\dagger$; the same observation holds for the case $k=n$, when b_ℓ can be taken to the right of $b_n^\dagger$ without trouble. As a matter of fact in (5.46c) we have substituted $b_\ell b_n^\dagger$ and $b_k b_n^\dagger$ in the two cases by $\delta_{\ell n}$ and δ_{kn} and omitted the other terms $-b_n^\dagger b_i$ and $-b_n^\dagger b_k$. These terms, together with the other two destruction operators, have the structure $\hat{N}A$, and we have already argued that they lead to terms smaller in order of magnitude than $\langle\Psi|A|\Psi_0\rangle$. The type of work carried out in relation (5.46c) can be repeated for all the terms in expression (5.46b) which then yields a new set of $A_{k\ell}$ terms. Adding these to Eq. (5.46a) we obtain finally

$$[H_{04},\,A_{mn}^\dagger]=\sum_{k,\,\ell}\left[\frac{1}{2}\,(\bar{k}\,\bar{\ell}\mid v\mid nm)\,(u_m u_n v_k v_\ell+v_m v_n u_k u_\ell)\right.$$

$$\left.+(\bar{k}\,\bar{n}\mid v\mid \ell m)\,u_m v_n v_k u_\ell-(\bar{k}\,\bar{m}\mid v\mid \ell n)\,v_m u_n v_k u_\ell\right]A_{K\ell}$$

$$(5.47)$$

Eqs (5.41), (5.44) and (5.47) together give the commutator $[H,\,A_{mn}^\dagger]$ in the RPA approximation. The commutator $[H,\,A_{mn}]$ can then be written down by taking the Hermitian conjugate and reversing the sign. Together, they provide us with the required system of linear equations for the amplitudes $\langle\Psi|A_{k\ell}^\dagger|\Psi_0\rangle$ and $\langle\Psi|A_{k\ell}|\Psi_0\rangle$. Once again the task of angular-momentum coupling is tackled in the Appendix.

APPENDIX TO SECTION 5

Angular-momentum coupling in the hole-particle calculation

Let us forget about the coupling of isospin for the time being, and consider the angular-momentum coupled states (5.12). Using relations (5.7a, b) and (5.9) along with this expression we obtain

$$\langle (h'^{-1} p') \, J M \, | \, H_{22} | \, (h^{-1}p) \, J M \rangle = \sum_{m_h, m_p m'_h, m'_p} \sum \begin{bmatrix} j_h & j_p & J \\ m_h & m_p & M \end{bmatrix} \begin{bmatrix} j_{h'} & j_{p'} & J \\ m_{h'} & m_{p'} & M \end{bmatrix}$$

$$\times \, \langle \bar{h}'^{-1} \, p' \, | \, H_{22} | \, \bar{h}^{-1} \, p \rangle \tag{5.48}$$

$$= - \sum_{m_h m_p m'_h m'_p} \sum \begin{bmatrix} j_h & j_p & J \\ m_h & m_p & M \end{bmatrix} \begin{bmatrix} j_{h'} & j_{p'} & J \\ m_{h'} & m_{p'} & M \end{bmatrix} (p' \, \bar{h} \, | \, v \, | \, p, \bar{h}')$$

The matrix element of v is now explicitly written using the j and m quantum numbers, remembering that $| \bar{h} \rangle = (-1)^{j_h - m_h} \, | j_h, -m_h \rangle$. Finally, we do the angular-momentum coupling in the matrix element. In this way,

$$(p' \, \bar{h} \, | \, H_{22} | \, p \bar{h}') = (j_{p'} m_{p'}; j_{h'}, -m_h \, | \, H_{22} | \, j_p m_p; j_{h'}, -m_{h'}) \, (-1)^{j_h - m_h} \, (-1)^{j_{h'} - m_{h'}}$$

$$= \sum_{J', M'} (-1)^{j_h - m_h + j_{h'} - m_{h'}} \, \begin{bmatrix} j_{p'} & j_h & J' \\ m_{p'} & -m_h & M' \end{bmatrix} \begin{bmatrix} j_p & j_{h'} & J' \\ m_p & -m_{h'} & M' \end{bmatrix} (j_{p'} j_h J' \, | \, v \, | \, j_p j_{h'} J')$$

$$\tag{5.49}$$

The symbols enclosed in square brackets in Eqs (5.48) and (5.49) are the Clebsch-Gordan coefficients. In Eq. (5.48), the quantum number M being given, only two of the summation symbols are independent; they satisfy $m_h + m_p = m_{h'} + m_{p'} = M$. Similarly, in Eq. (5.49) the summation over M' is actually redundant because M' is required to be equal to $m_{p'} - m_h = m_p - m_{h'}$. The two-body matrix element in Eq. (5.49) is actually independent of M' because H_{22} is a scalar, and hence we have omitted M' in this matrix element. Substituting expression (5.49) in Eq. (5.48), and using angular-momentum algebra (the details are left to the reader) to carry out the summation of the product of four Clebsch-Gordon coefficients over the two independent magnetic quantum numbers, we obtain

$$\langle (h'^{-1} p') \, JM | H_{22} | (h^{-1}p) \, JM \rangle = - (-1)^{j_h + j_{h'} + j_p + j_{p'}} \sum_{J'} (2J' + 1) W(j_h j_p j_{p'} j_{h'}; JJ')$$

$$\times \, (j_h j_{p'} J' \, | \, v \, | \, j_{h'} j_p J')$$

Here W is Racah's six j-symbol.

The result, with the isospin coupling, can be similarly derived, and is almost obvious from relation (5.50). We simply quote it below

$$\langle (H'^{-1} p')\, J\, M;\; T\, M_T \, | H_{22} | \, (h^{-1}p)\, J\, M;\; T\, M_T \rangle$$

$$= -(-1)^{j_h + j_{h'} + j_p + j_{p'}} \sum_{T'J'} (2\,J'+1)(2T'+1)\, W\,(j_h\, j_p\, j_{p'}\, j_{h'};\; JJ')\; W\,(\tfrac12\tfrac12\tfrac12\tfrac12;\; TT')$$

$$\times\; (j_h\, j_{p'}, J'\, T' \,|\, v \,|\, j_{h'}\, j_p\, J'\, T')$$

$$(5.51)$$

So, given the two-nucleon matrix elements of v, one can easily carry out the summation shown in Eq. (5.51) and obtain the hole-particle matrix elements. Because of their very frequent occurrence in nuclear structure theory, the following special symbols are generally used:

$$G^{\cdot}(a\,b\,c\,d;\,J\,T) \equiv (a\,b\,J\,T \,|\, v \,|\, c\,d\,J\,T) \qquad\qquad (5.52a)$$

$$F\,(a\,b\,c\,d;\,J\,T) \equiv \langle (a^{-1}b)\, J\,T \,|\, H_{22} | \,(c^{-1}d)\, J\,T \rangle \qquad\qquad (5.52b)$$

G can be calculated, either by taking a well-behaved v, or, in the case of a 'realistic' two-nucleon potential, by assuming that it is equal to the reaction matrix elements calculated by a Brueckner-like theory.

By following the above coupling procedure, one can easily show that the right-hand side of Eq. (5.10) remains unchanged when we use the coupled states [as appearing on the left-hand side of Eq. (5.51)] on the left-hand side of this equation. Therefore, the diagonalization to be done is that of the F-matrix of definition (5.52b) with the hole-particle energies $(\epsilon_p - \epsilon_h)$ along the main diagonal.

We would be led to the same conclusion if we had used the more sophisticated equations (5.23a, b). We first introduce the angular momentum coupled pair-creation operators:

$$A^\dagger\,(h\,p\,J\,M;\; T\,M_T) = \sum_{m_h m_p}\; \sum_{\mu_h \mu_p} \begin{bmatrix} j_h & j_p & J \\ m_h & m_p & M \end{bmatrix}\begin{bmatrix} \tfrac12 & \tfrac12 & T \\ \mu_h & \mu_p & M_T \end{bmatrix} b^\dagger_{j_p m_p \mu_p}\; b^\dagger_{j_h m_h \mu_h}$$

$$(5.53)$$

where μ_h and μ_p are the projection of isospin for the hole and the particle. In defining $b^\dagger_{j_h m_h \mu_h}$ we shall now introduce an extra phase due to isospin, i.e. $b^\dagger_{j_h m_h \mu_h} = (-1)^{j_h - m_h} (-1)^{\tfrac12 - \mu_h}\, C_{j_h, -m_h;\; \tfrac12, -\mu_h}$ where C is the destruction operator for a state specified by the subscripts.

Let is now introduce the Clebsch-Gordon coefficients of Eq. (5.53) in Eq. (5.23a, b) and carry out the indicated summation. That produces $[H,\; A^\dagger\,(h\,p\,J\,M;\; T\,M_T)]$ on the left-hand side. On the right-hand side of Eq. (5.23a), the same procedure produces $A^\dagger\,(h\,p\,J\,M;\; T\,M_T)$, provided, of course, the energies ϵ_p, ϵ_h are independent of the projection

quantum numbers (true for spherical nuclei). On the right-hand side of
Eq. (5.23b), this procedure yields the right-hand side of Eq. (5.48),
multiplied by $A^\dagger$ (h' p' J M; T M_T), with two analogous Clebsch-Gordon
coefficients containing isospin. The rest of the procedure consists of
using (5.49), with of course the inclusion of isospin, and obviously the
final result will be F (h p h' p' ; J T) multiplied by $A^\dagger$ (h' p' J M; T M_T).
We write all these results finally

$$[H, \ A^\dagger (h\,p\,J\,M; \ T\,M_T)] = (\epsilon_p \ - \ \epsilon_h) \ A^\dagger (h\,p\,J\,M; \ T\,M_T)$$

$$(5.54)$$

$$+ \ \sum_{j_h, j_{p'}} F \ (h\,p\,h'\,p' ; \ J\,T) \ A^\dagger (h'\,p'\,J\,M; \ T\,M_T)$$

Introducing $\langle \Psi |$ and $| \Psi_0 \rangle$ to the left and right we obtain the system of
linear equations for the amplitudes $\langle \Psi | A^\dagger (h' p' J M, T M_T) | \Psi_0 \rangle$. The
coefficient matrix to be diagonalized is clearly the hole-particle matrix
F with $(\epsilon_p - \epsilon_h)$ along the diagonal.

We next move on to the angular momentum coupling in the RPA-
equations (5.33a, b). The first line of Eq. (5.33a) will obviously lead to
Eq. (5.54) because this line is nothing but the TDA equation. To tackle
the second line we introduce the operator A (h p J M; T M_T), which is
just the Hermitian conjugate of Eq. (5.53):

$$A \ (h\,p\,J\,M; \ T\,M_T) = \sum_{m_h, m_p} \sum_{\mu_{h'}, \mu_p} \begin{bmatrix} j_h & j_p & J \\ m_h & m_p & M \end{bmatrix} \begin{bmatrix} \tfrac{1}{2} & \tfrac{1}{2} & J \\ \mu_h & \mu_p & M_T \end{bmatrix} b_{j_h m_h \mu_h} \ b_{j_p m_p \mu_p}$$

$$(5.55)$$

While indicating some of the steps in this angular momentum coupling,
we shall first omit the isospin coupling, which can be introduced into the
final result by analogy. As a result of the coupling $A^\dagger$ (h p J M) on the
left-hand side of Eq. (5.33a) we obtain on the right-hand side for the
second line

$$\sum_{j_{h'}, j_{p'}} \sum_{m'_h m'_p} \sum_{m_h m_p} \begin{bmatrix} j_h & j_p & J \\ m_h & m_p & M \end{bmatrix} (p\,p' \,| \,v \,| \,\bar{h}\,\bar{h}') \ A_{h'p'} \qquad (5.56a)$$

Using definition (5.55) in the reverse direction, we obtain (with the
omission of isospin) the following identity:

$$A_{h'p'} = \sum_{J'} \begin{bmatrix} j_{h'} & j_{p'} & J' \\ m_{h'} & m_{p'} & M' \end{bmatrix} A \ (h'\,p'\,J'\,M') \qquad (5.56b)$$

Since, on the left hand side we have already coupled $A^\dagger_{hp}$ to J M, only
the term J' = J and M' = -M in the above sum will contribute to the final
result (because H is scalar). H times $A^\dagger$ (h p J M) transforms as a

tensor of rank J and component M. The part of Eq. (5.56b) that has similar transformation property actually corresponds to $J' = J$, $M' = -M$. The opposite sign of the projection quantum number is due to the fact that $A (h'p'J'M')$ is the destruction operator, while $A^\dagger (hpJM)$ is a creation operator. Using only this particular term of (5.56b) in (5.56a) we obtain

$$\sum_{J'} \sum_{j_{h'}j_{p'}} \sum_{m_h'm_p'} \sum_{m_h m_p} \begin{bmatrix} j_h & j_p & J \\ m_h & m_p & M \end{bmatrix} \begin{bmatrix} j_{h'} & j_{p'} & J \\ m_h' & m_p' & -M \end{bmatrix} \begin{bmatrix} j_p & j_{p'} & J' \\ m_p & m_{p'} & M' \end{bmatrix} \begin{bmatrix} j_h & j_{h'} & J' \\ -m_h & -m_{h'} & M' \end{bmatrix}$$

$$\times \; (-1)^{j_h - m_h} \; (-1)^{j_{h'} - m_{h'}} \; (j_p j_{p'} J' \mid v \mid j_h j_{h'} J') \; A (h'p'J, -M)$$

$$(5.56c)$$

The third and fourth Clebsch-Gordan coefficients and the summation over J' in this expression have resulted from the replacement of the matrix element of v in (5.56a) by the angular-momentum coupled matrix elements of v in (5.56c). The phase-factors have resulted from the $\bar{h}$ and $\bar{h}'$ in (5.56a). Once again, M' is not independent, and only two of the magnetic quantum number summations in expression (5.56c) are independent. Let us carry these summations out by standard algebra and use the earlier definition of the F-matrix to obtain for expression (5.56c):

$$\sum_{j_{h'} j_{p'}} F (hpp'h'; J) (-1)^{j_{h'} + j_{p'} - J} (-1)^{J + M} A (h'p'J, -M) \qquad (5.56d)$$

The extension, to include isospin coupling, is obvious. The result obtained in this way has to be added to Eq. (5.54) to produce the final equation for RPA:

$$[H, A^\dagger (hpJM; TM_T)] = (\epsilon_p - \epsilon_h) A^\dagger (hpJM; TM_T)$$

$$+ \sum_{j_{h'} j_{p'}} \Big\{ F (hph'p'; JT) A^\dagger (h'p'JM; TM_T) + F (hpp'h'; JT) (-1)^{j_{h'} + j_{p'} - J - T}$$

$$\times \; (-1)^{J + M + T + M_T} A (h'p'J, -M; T, -M_T) \Big\} \qquad (5.57)$$

The equivalent of the phase-factor $(-1)^{j_{h'} + j_{p'} - J}$, appearing in Eq. (5.56d) in the case of isospin coupling is $(-1)^{\frac{1}{2} + \frac{1}{2} - T}$; this phase explains the change in the overall minus sign of (5.56d) to a plus sign of the corresponding term in Eq. (5.57), and the appearance of the phase-factor $(-1)^{j_{h'} + j_{p'} - J - T}$. The other phase-factor $(-1)^{J + M + T + M_T}$ along with the $A (h'p'J, -M; T, -M_T)$ gives the precise transformation property under rotation to this term, identical to that of $A^\dagger (hpJM; TM_T)$. This phase-factor is similar to the $(-1)^{j_h - m_h}$ occurring with $C_{j_h, -m_h}$ which makes the rotational transformation of the latter equivalent with that of $C^\dagger_{j_h, m_h}$.

Equation (5.57) enables one to write down the expression for
$[H, A(hpJ, -M; T, -M_T)] (-1)^{J+M+T+M_T}$ with the help of its Hermitian
conjugate. Thus

$$(-1)^{J+M+T+M_T}[H, A(hpJ, -M; T, -M_T)] = -(\epsilon_p - \epsilon_h) A(hpJ, -M; T, -M_T)(-1)^{J+M+T+M_T}$$

$$- \sum_{j_{h'}, j_{p'}} \left\{ F(hph'p'; JT) A(h'p'J, -M; T, -M_T) (-1)^{J+M+T+M_T} \right. \tag{5.58}$$

$$\left. + F(hpp'h'; JT) (-1)^{j_{h'}+j_{p'}-J-T} A^\dagger(h'p'J, -M; T, -M_T) \right\}$$

In the usual way, Eqs (5.57) and (5.58) give rise to a set of linear
equations for the amplitudes $\langle \Psi | A^\dagger (hpJM; TM_T) | \Psi_0 \rangle$ and
$\langle \Psi | A(hpJ, -M; T, -M_T) | \Psi_0 \rangle (-1)^{J+M+T+M_T}$. The matrix to be dia-
gonalized can be identified from these equations and is given by

$$M' = \begin{pmatrix} E+F & \bar{F} \\ -\bar{F} & -E-F \end{pmatrix} \tag{5.59a}$$

where E and $\bar{F}$ are matrices defined by

$$E_{hp; h'p'} = (\epsilon_p - \epsilon_h) \delta_{hh'} \delta_{pp'} \tag{5.59b}$$

$$\bar{F}(hph'p'; JT) = F(hpp'h'; JT) (-1)^{j_{h'}+j_{p'}-J-T} \tag{5.59c}$$

It is easy to establish that the matrix M' of (5.59a) has all the properties
of M', defined by Eq. (3.57b). Deonting the amplitudes with $A^\dagger$ and A by
X_{hpJT} and Y_{hpJT}, it then follows that these amplitudes satisfy the
properties (3.58), (3.59) and (3.60).

Angular-momentum coupling in the quasi-particle calculation

The angular-momentum coupling in the equations of section 5.3 is
also fairly straightforward. We shall specifically deal with the case
of spherical nuclei where the coefficients u_j, v_j etc. are independent
of the projection quantum number. The quasi-particle energies also
have the same property. In most applications of this theory the quasi-
particle pair is taken to be either a pair of proton or a pair of neutron
quasi-particles. This is because the special BCS type transformation,
we are considering, treats only the $J=0$ part of the two-nucleon inter-
action (which is the strong force only for a pair of protons, or a pair of
neutrons; for an n-p pair the interaction in $J=1$, $T=0$ state is stronger
than that in the $J=0$, $T=1$ state) at the stage of producing the independent
quasi-particles. Since a pair of proton or neutron quasi-particles will
always have $T=1$, the latter is a redundant quantum number, and it is

necessary and sufficient just to couple the angular momenta j_m, j_n of
the pair of quasi-particles.

We introduce the following obvious definitions:

$$A^\dagger (m\,n\,J\,M) = \sum_{\mu\nu} \begin{bmatrix} m & n & J \\ \mu & \nu & M \end{bmatrix} b^\dagger_{n\nu}\, b^\dagger_{m\mu} \qquad (5.60a)$$

and

$$A (m\,n\,J\,M) = \sum_{\mu\nu} \begin{bmatrix} m & n & J \\ \mu & \nu & M \end{bmatrix} b_{m\mu}\, b_{n\nu} \qquad (5.60b)$$

Following a procedure similar to what was adopted above for the hole-
particle case, and using the definitions (5.60a, b) one obtains easily
(the details are left to the reader) from the Eqs (5.41), (5.44) and (5.47):

$$[H_{11}, A^\dagger(m\,n\,J\,M)] = (E_m + E_n)\, A^\dagger (m\,n\,J\,M) \qquad (5.61a)$$

$$[H_{22}, A^\dagger (m\,n\,J\,M)] = \sum_{(a,b)} [\,(u_a u_b u_m u_n + v_a v_b v_m v_n)\, G\,(m\,n\,a\,b;\,J)$$

$$+ (v_n u_b u_m v_n + u_a v_b v_m u_n)\, F\,(m\,n\,b\,a;\,J)\,(-1)^{a+b-J}$$

$$- (u_a v_b u_m v_n + v_a u_b v_m u_n)\, F\,(m\,n\,a\,b;\,J)\,\Big] A^\dagger(a\,b\,J\,M)$$

$$\qquad (5.61b)$$

$$[H_{04}, A^\dagger(m\,n\,J\,M)] = -\sum_{(a,b)} [\,(u_a u_b v_m v_n + v_a v_b u_m u_n)\, G\,(a\,b\,m\,n;\,J)$$

$$- (u_a v_b u_n v_m + v_a u_b v_n u_m)\, F\,(a\,b\,m\,n;\,J)$$

$$+ (v_a u_b u_n v_m + u_a v_b v_n u_m)\, F(b\,a\,m\,n;\,J)\,(-1)^{a+b-J}\,]$$

$$\times\ (-1)^{J+M} A\,(a\,b\,J,\,-M) \qquad (5.61c)$$

In Eqs (5.61b, c) the summation (a, b) implies that it has to be carried
out over a particular pair (a, b) only once, and not twice as a, b and b, a.
To achieve this result we have used obvious symmetry relations between
$A^\dagger(a\,b\,J\,M)$, $A^\dagger(b\,a\,J\,M)$ and $A\,(a\,b\,J,\,-M)$ and $A\,(b\,a\,J,\,-M)$, following from
the property of the Clebsch-Gordon coefficient in Eqs (5.60a, b). Similar
symmetry relation between $G\,(a\,b\,m\,n;\,I)$ and $G\,(b\,a\,m\,n;\,I)$ has also been
used. Equations (5.61 a, b, c), added together, give $[H, A^\dagger(m\,n\,J\,M)]$.
As in the hole-particle case we are led to the diagonalization of a matrix
like M' of Eq. (5.59a), in which F (h p h' p' ; J T) and $\bar{F}$ (h p h' p' ; J T) are
replaced respectively by the expressions enclosed in square brackets
in Eqs (5.61b) and (5.61c). Similarly the diagonal matrix elements of $\mathscr{E}$,

instead of being given by (5.59b), are given by $(E_m + E_n)$ as appearing in (5.61a). The eigenvectors of the matrix M' now determine the amplitudes X_{mnJ} and Y_{mnJ} where $X_{mnJ} = \langle \Psi | A^\dagger(m\,n\,J\,M) | \Psi_0 \rangle$ and $Y_{mnJ} = (-1)^{J+M} \langle \Psi | A(m\,n\,J, -M) | \Psi_0 \rangle$.

Calculations using schematic models for the two-body potential
_____

Some general features of the theory of vibration, as worked out here, can be very elegantly demonstrated by using schematic models for the two-body potential.

The oldest model of this type is the δ-function potential. Without giving the details of the derivation, we quote below the G-matrix elements of the δ-function potential:

$$G(a\,b\,c\,d; J\,T) = - V_s^e \mathscr{I}(a\,b\,c\,d) \tfrac{1}{2} \left\{ 1 + (-1)^J \Pi \right\} g(a\,b\,J)\, g(c\,d\,J) \text{ for } T = 1$$

$$(5.62a)$$

$$= - V_t^e \mathscr{I}(a\,b\,c\,d) \left[f(a\,b\,J)\, f(c\,d\,J) + \tfrac{1}{2} \left\{ 1 - (-1)^J \Pi \right\} g(abJ)g(cdJ) \right]$$

$$\text{for } T = 0 \qquad (5.62b)$$

Here $- V_s^e$ and $- V_t^e$ are the depths of the δ-function potential in the singlet-even and triplet-even two-nucleon states. The δ-function potential, by definition, acts only when the two nucleons are coincident in space, and hence only when they have a spatially symmetric (consequently 'even') state. This accounts for the non-occurrence of the odd-state potential depth in Eqs (5.62a, b). The quantity $\mathscr{I}(a\,b\,c\,d)$ is the radial integral, which is actually a single integral by virtue of the δ-function:

$$\mathscr{I}(a\,b\,c\,d) = \int_0^\infty r_1^2 dr_1 \int_0^\infty r_2^2 dr_2\, R_a(r_1) R_b(r_2) \frac{\delta(r_1 - r_2)}{r_1^2} R_c(r_1) R_d(r_2)$$

$$= \int_0^\infty r^2 dr\, R_a(r) R_b(r) R_c(r) R_d(r) \qquad (5.63)$$

The function R(r) is the radial wave function of the single nucleon in the state labelled by the subscripts. In Eq. (5.62a, b) the quantity Π is either +1 or -1 depending on the even or odd parity of the two-nucleon states $|a\,b\,J\,T\rangle$, or equivalently $|c\,d\,J\,T\rangle$. The factors $f(a\,b\,J)$ and $g(a\,b\,J)$ are given by

$$f(a\,b\,J) = \left\{ \frac{(2a+1)(2b+1)}{(2J+1)} \right\}^{\tfrac{1}{2}} (-1)^{a+b} \begin{bmatrix} a & b & J \\ \tfrac{1}{2} & \tfrac{1}{2} & 1 \end{bmatrix} \qquad (5.64a)$$

$$g(a\,b\,J) = \left\{ \frac{(2a+1)(2b+1)}{2J+1} \right\}^{\tfrac{1}{2}} (-1)^{a - \tfrac{1}{2} + \ell_a} \begin{bmatrix} a & b & J \\ \tfrac{1}{2} & -\tfrac{1}{2} & 0 \end{bmatrix} \qquad (5.64b)$$

where ℓ_a is the orbital-angular-momentum quantum number for the state a.

$\vdots$

The hole-particle matrix elements F, corresponding to the above G, can be worked out from Eqs (5.52b) and (5.51). Once again we only quote the final results, leaving the details to the reader:

$$F(h\,p\,h'\,p'\,;JT) = C_T\,\overline{f}\,(h\,p\,J)\,\overline{f}\,(h'\,p'\,J) + C_T'\,\,\overline{g}\,(h\,p\,J)\,\overline{g}\,(h'\,p'\,J) \tag{5.65a}$$

where

$$\overline{f}\,(h\,p\,J) = (-1)^{\ell_h}\,f\,(h\,p\,J) \tag{5.65b}$$

$$\overline{g}\,(h\,p\,J) = (-1)^{\ell_h}\,g\,(h\,p\,J) \tag{5.65c}$$

$$C_{T=0} = -\tfrac{1}{4}\,\mathscr{I}(h\,p\,h'\,p')\,\left\{2\,V_t^e + (-1)^J\,\Pi\,(V_t^e + 3\,V_s^e)\right\} \tag{5.65d}$$

$$C_{T=0}' = \tfrac{1}{4}\,\mathscr{I}(h\,p\,h'\,p')\,(3\,V_s^e - V_t^e) \tag{5.65e}$$

$$C_{T=1} = \tfrac{1}{4}\,\mathscr{I}(h\,p\,h'\,p')\,\left\{2\,V_t^e + (-1)^J\,\Pi\,(V_t^e - V_s^e)\right\}\,, \tag{5.65f}$$

$$C_{T=1}' = \tfrac{1}{4}\,\mathscr{I}(h\,p\,h'\,p')\,(V_t^e + V_s^e) \tag{5.65g}$$

From the symmetry property of the Clebsch-Gordon coefficients in Eqs (5.64a, b) and the definitions (5.65b, c) one obtains

$$\overline{f}\,(p'\,h'\,J) = (-1)^{\ell_{h'} + \ell_{p'} + h' + p' - J}\,\overline{f}\,(h'\,p'\,J) \tag{5.66a}$$

and

$$\overline{g}\,(h'\,h'\,J) = -(-1)^{\ell_{h'} + \ell_{p'}}\,(-1)^{h' + p' + \ell_{h'} + \ell_{p'}}\,\overline{g}\,(h'\,p'\,J) = -(-1)^{h' + p'}\,\overline{g}\,(h'\,p'\,J) \tag{5.66b}$$

Using these expressions, together with Eqs (5.65a) and (5.59c), we easily prove

$$\overline{F}\,(h\,p\,h'\,p'\,;J\,T) = C_T\,\Pi\,(-1)^T\,\overline{f}\,(h\,p\,J)\,\overline{f}(h'\,p'\,J) - C_T'\,(-1)^{J+T}\,\overline{g}(h\,p\,J)\,\overline{g}\,(h'\,p'\,J) \tag{5.67}$$

The schematic model can be further simplified by following either of two assumptions: (i) the Brown-Bolsterli assumption – the radial integral (5.63) is independent of the single-particle quantum numbers; (2) Moszkowski's surface-delta interaction — assume that the radial part of the δ-function potential is such that it is non-vanishing only at the nuclear surface, $r_1 = r_2 = R_0$, where R_0 is the nuclear radius. This implies that in the radial-integral (5.63) we have an additional factor $\delta\,(r - R_0)$, and the integral then reduces to $R_0^2\,R_a(R_0)\,R_b(R_0)\,R_c(R_0)\,R_d(R_0)$.

Under either of the above two assumptions the matrix elements (5.262a, b) have the following general form:

$$G_{KL} = \chi_f \, f_K f_L + \chi_g \, g_K g_L \qquad\qquad (5.68a)$$

while the matrix elements (5.65a) or (5.67) have the general form:

$$F_{KL} = \chi_f' \, \bar{f}_K \bar{f}_L + \chi_g' \, \bar{g}_K \bar{g}_L \qquad\qquad (5.68b)$$

$$\bar{F}_{KL} = \bar{\chi}_f \, \bar{f}_K \bar{f}_L + \bar{\chi}_g \, \bar{g}_K \bar{g}_L \qquad\qquad (5.68c)$$

Here, K, L are shorthand notations standing for an angular momentum coupled state like (abJ), while the strengths $\chi \chi'$, $\bar{\chi}$ can be either attractive (negative) or repulsive (positive) depending on the exact values of V_s^e, V_k^e and the value of J, Π and T. These strengths can be easily read off from (5.62a, b), (5.65d-g) and (5.67).

Owing to the factorable nature of Eqs (5.68a-c) the diagonalization of the TDA or RPA matrix can be carried out in a somewhat closed form. To illustrate this let us first diagonalize the TDA-matrix F (a b c d; J T) assuming that the diagonal matrix·$\mathscr{E}$, whose elements are $(\epsilon_p - \epsilon_h)$, is a constant times the unit matrix. The latter can then be left out of the diagonalization, the constant diagonal element simply giving us the reference point for the eigenvalues of F.

The eigenvalue equation in the notation of Eq. (5.68b) is given by

$$\sum_L F_{KL} X_L = E X_K$$

or

$$\sum_L (\chi_f' \, \bar{f}_K \bar{f}_L + \chi_g' \, \bar{g}_K \bar{g}_L) X_L = E X_K \qquad\qquad (5.69)$$

To further simplify matters let us assume that the $\bar{f}$-term is negligible compared to the $\bar{g}$-term. Then

$$\chi_g' \sum_L \bar{g}_K \bar{g}_L X_L \equiv \chi_g' \, \bar{g}_K \left(\sum_L \bar{g}_L X_L \right) X = E X_K \qquad\qquad (5.70a)$$

or

$$X_K = E^{-1} \chi_g' \, C \, \bar{g}_K$$

where

$$C = \sum_L X_L \bar{g}_L = E^{-1} \chi_g' \, C \sum_L (\bar{g}_L)^2 \qquad\qquad \text{[using (5.70a)]}$$

or

$$E = \chi'_g \sum_L (\bar{g}_L)^2$$

This gives us one eigenvalue of the problem; the K-th element of the corresponding eigenvector, X_K, is proportional, according to Eq. (5.70a), to $\bar{g}_K$. The constant of proportionality is fixed by the normalization of the vector. The eigenvector belonging to any other eigenvalue has to be orthogonal to this one. If the K-th element of such a vector is denoted by X'_K we then have

$$0 = \sum_K X_K X'_K = \sum_K \bar{g}_K X'_K \tag{5.71}$$

But the eigenvalue equation for this eigenvector is given by

$$\chi'_g \sum_L g_K g_L X'_L = E' X'_K$$

But the summation $\sum_L \bar{g}_L X'_L$, present on the left-hand side, is zero according to Eq. (5.71). Hence we conclude $E' = 0$. Therefore, according to this model, only one eigenvalue, E of (5.70b), is displaced with respect to the unperturbed position of the hole-particle states (which are degenerate by our assumption about $\mathscr{E}$); all the other eigenvalues E' remain coincident with the unperturbed energy.

An extension can now be made in two ways: (i) Use the unperturbed energy-matrix $\mathscr{E}$ with elements $(\epsilon_p - \epsilon_h)$ which are not constant, (2) use the complete expression (5.69) containing both the $\bar{f}$ and $\bar{g}$ terms.

In the first case we have, denoting $\epsilon_p - \epsilon_h$ by $\mathscr{E}_K$

$$\sum_L \left\{ \mathscr{E}_K \delta_{KL} + \chi'_g \bar{g}_K \bar{g}_L \right\} X_L = E X_K \tag{5.72}$$

or

$$(E - \mathscr{E}_K) X_K = \chi'_g C \bar{g}_K$$

or

$$X_K = \chi'_g C \frac{\bar{g}_K}{E - \mathscr{E}_K} \tag{5.73a}$$

where

$$C = \sum_L \bar{g}_L X_L = \chi'_g C \sum_L \frac{(\bar{g}_L)^2}{E - \mathscr{E}_L} \tag{5.73b}$$

or

$$1 = \chi'_g \sum_L \frac{(\dot{\bar{g}}_L)^2}{E - \mathscr{E}_L}$$

This so-called dispersion equation then determines the energies E.
Knowing E, the corresponding eigenvector is determined up to a
normalization factor by expression (5.73a). A graphical method of
solution, analogous to that described under Eq. (3.45) and delineated
in Fig. 3.2, can be applied to Eq. (5.73b) with very similar results.

Let us now do the second extension by using the entire expression
(5.69). We have, instead of Eq. (5.72), the following equation:

$$\sum_L \left\{ \mathscr{E}_K \delta_{KL} + \chi'_f \bar{f}_K \bar{f}_L + \chi'_g \bar{g}_K \bar{g}_L \right\} X_L = E X_K \tag{5.74}$$

or

$$(E - \mathscr{E}_K) X_K = \chi'_f C_f \bar{f}_K + \chi'_g C_g \bar{g}_K \tag{5.75a}$$

where

$$C_f = \sum_L \bar{f}_L X_L, \quad C_g = \sum_L \bar{g}_L X_L \tag{5.75b}$$

Let us use Eq. (5.75a) to obtain X_K and then use the result in the two
equations (5.75b). That will give two linear homogeneous equations for
C_f and C_g. The determinant of the coefficient matrix, equated to zero,
gives the secular equation for E. This is left to the reader as an
exercise.

The final stage is to solve the eigenvalues and eigenfunctions of
the RPA-matrix (5.59a). In the condensed notation the equations are
given by

$$\sum_L \left\{ (\mathscr{E}_K \delta_{KL} + F_{KL}) X_L + \bar{F}_{KL} Y_L \right\} = E X_K \tag{5.76a}$$

and

$$\sum_L \left\{ -\bar{F}_{KL} X_L - (\mathscr{E}_K \delta_{KL} + F_{KL}) Y_L \right\} = E Y_K \tag{5.76b}$$

We use Eq. (5.68c) for $\bar{F}_{KL}$. By a procedure similar to what has been
demonstrated above, we have

$$(E - \mathscr{E}_K) X_K = (\chi'_f C_f + \bar{\chi}_f D_f) \bar{f}_K + (\chi'_g C_g + \bar{\chi}_g D_g) \bar{g}_K \tag{5.77a}$$

and

$$-(E + \mathscr{E}_K) Y_K = (\bar{\chi}_f C_f + \chi'_f D_f) \bar{f}_K + (\bar{\chi}_g C_g + \chi'_g D_g) \bar{g}_K \qquad (5.77b)$$

where

$$C_f = \sum_L \bar{f}_L X_L, \quad C_g = \sum_L \bar{g}_L X_L \qquad (5.77c)$$

$$D_f = \sum_L \bar{f}_L Y_L, \quad D_g = \sum_L \bar{g}_L Y_L \qquad (5.77d)$$

Once again one has to substitute from Eqs (5.77a, b) for X_L, Y_L, into Eqs (5.77c, d) to obtain a set of four linear homogeneous equations in C_f, C_g, D_f and D_g. The secular determinant equation of the coefficient matrix determines E.

In the two practical cases, namely the case of giant dipole resonance (J = 1, Π = -1 and T = 1), and octupole vibration (J = 3, Π = -1 and T = 0), the above equations are considerably simplified. As an illustration let us consider the latter case, for which, according to Eqs (5.67) and (5.65a), we have

$$F_{KL} + \bar{F}_{KL} = 2 C'_T \bar{g}_K \bar{g}_L \qquad (5.78a)$$

$$F_{KL} + \bar{F}_{KL} = 2 C_T \bar{f}_K \bar{f}_L \qquad (5.78b)$$

Similar simplifications occur in the case of giant-dipole resonance as well. It is now advantageous to add and subtract (5.76a, b) and use $Z_K^{(+)} = X_K + Y_K$ and $Z_K^{(-)} = X_K - Y_K$. We thus have

$$E Z_K^{(+)} = \sum_L \left\{ E_K \delta_{KL} + 2 C_T \bar{f}_K \bar{f}_L \right\} Z_L^{(-)} \qquad (5.79a)$$

and

$$E Z_K^{(-)} = \sum_L \left\{ E_K \delta_{KL} + 2 C'_T \bar{g}_K \bar{g}_L \right\} Z_L^{(+)} \qquad (5.79b)$$

Let us substitute for $Z_K^{(+)}$ from expression (5.79a) into (5.79b), and vice versa. If we introduce the notations:

$$\mathscr{G}^{(-)} = \sum_L \bar{f}_L Z_L^{(-)}, \quad \mathscr{G}^{(+)} = \sum_L \bar{g}_L Z_L^{(+)} \qquad (5.80)$$

we obtain easily:

$$Z_K^{(+)} = 2(E^2 - \mathscr{E}_K^2)^{-1} \left\{ C'_T \mathscr{G}^{(+)} \bar{g}_K + C_T \mathscr{G}^{(-)} \bar{f}_K \right\} \tag{5.81a}$$

$$Z_K^{(-)} = 2(E^2 - \mathscr{E}_K^2)^{-1} \left\{ C_T \mathscr{G}^{(-)} \bar{f}_K + C'_T \mathscr{G}^{(+)} \bar{g}_K \right\} \tag{5.81b}$$

Substituting expressions (5.81a, b) back into Eqs (5.80) we obtain two linear homogeneous equations in $\mathscr{G}^{(-)}$ and $\mathscr{G}^{(+)}$, and then the solution proceeds as usual. The final dispersion equation for E is exactly similar to Eq. (3.45), in as much as it contains $(\mathscr{E}_K^2 - E^2)$ in the denominator. The task of obtaining this equation is left to the reader as an exercise.

Schematic model for the quasi-particle calculation

To be able to apply the factorable schematic model to Eqs (5.61a-c), we must first of all verify that the products of u_a, v_b etc. also factorize automatically. In the usual way introduce

$$X_{ab} = \langle \Psi | A^\dagger (a\,b\,J\,M) | \Psi_0 \rangle$$

$$Y_{ab} = (-1)^{J+M} \langle \Psi | A(a\,b\,J, -M) | \Phi_0 \rangle$$

$$Z_{ab}^{(+)} = X_{ab} + Y_{ab}, \qquad Z_{ab}^{(-)} = X_{ab} - Y_{ab}$$

Multiply $[H, A^\dagger (m\,n\,J\,m)]$, which is the sum of Eqs (5.61a-c) by $\langle \Psi |$ and $| \Psi_0 \rangle$, and write the result in terms of the amplitudes X and Y, as defined above. Let us carry out similar things with the equation for $[H, A(m\,n\,J\,M)]$ and add and subtract these two equations and finally obtain the following equations satisfied by $Z^{(\pm)}$:

$$E\, Z_{mn}^{(+)} = (E_m + E_n)\, Z_{mn}^{(-)} + \sum_{(a,b)} H(m\,n\,a\,b\,J)\, Z_{ab}^{(-)} \tag{5.82a}$$

$$E\, Z_{mn}^{(-)} = (E_m + E_n)\, Z_{mn}^{(+)} + \sum_{(a,b)} K(m\,n\,a\,b\,J)\, Z_{ab}^{(+)} \tag{5.82b}$$

where

$$H(m\,n\,a\,b\,J) = G(m\,n\,a\,b\,J)\,(u_m u_n + v_m v_n)(u_a u_b + v_a v_b)$$

$$- \left\{ F(m\,n\,a\,b\,J) + (-1)^{a+b-J}\, F(m\,n\,b\,a\,J) \right\}(u_m v_n - v_m u_n)(u_a v_b - v_a u_b)$$

$$\tag{5.82c}$$

$$K(m\,n\,a\,b\,J) = G(m\,n\,a\,b\,J)(u_m u_n - v_m v_n)(u_a u_b - v_a v_b)$$

$$- \left\{ F(m\,n\,a\,b\,J) - (-1)^{a+b-J} \; F(m\,n\,b\,a\,J) \right\}(u_m v_n + v_m u_n)(u_a v_b + v_a u_b)$$

$$(5.82d)$$

Equations (5.82c, d) demonstrate that the factor involving the u, v co-efficients do factorize out automatically. Therefore, if we adopt the factorable forms of the F and G matrix elements given earlier for the schematic model we can once again obtain solutions of Eqs (5.82a, b) by the same procedure.

As explained earlier, we consider in this theory either a pair of proton quasi-particles or a pair of neutron quasi-particles, for which isospin T is identically 1. Using T = 1 in Eqs (5.59c) and (5.67) we obtain

$$\bar{F}(m\,n\,a\,b\,J) \equiv - (1)^{a+b-J} \; F(m\,n\,b\,a\,J)$$

$$= - c \; \Pi \bar{f}(m\,n\,J)\,\bar{f}(a\,b\,J) + c'\,(-1)^J \; \bar{g}(m\,n\,J)\,\bar{g}(a\,b\,J)$$

Here we have suppressed the subscript T = 1 on c and c'. Using this expression in the case of the quadrupole vibration (J = 2, Π = +1), for example, we have

$$F(m\,n\,a\,b\,J) + (-1)^{a+b-J} \; F(m\,n\,b\,a\,J) = 2\,c\,f(m\,n\,J)\,f(a\,b\,J) \qquad (5.83a)$$

$$F(m\,n\,a\,b\,J) - (-1)^{a+b-J} \; F(m\,n\,b\,a\,J) = 2\,c'\,\bar{g}(m\,n\,J)\,\bar{g}(a\,b\,J) \qquad (5.83b)$$

While applying the schematic model in this case, usually an excuse is given to ignore the G(m n a b J) term in Eqs (5.82c, d). If this is per-mitted then it is immediately clear that Eqs (5.82a, b) become exactly similar to Eqs (5.79a, b); the only difference is that in the present case we have factors like $\bar{f}(a\,b\,J)(u_a v_b - v_a u_b)$ and $\bar{g}(a\,b\,J)(u_a v_b + v_a u_b)$ instead of $\bar{f}(a\,b\,J)$ and $\bar{g}(a\,b\,J)$.

Another type of schematic model that has been used in this calcula-tion is based on the use of a multipole type two-body potential:

$$V_{12} = \chi_K \Omega_1^K \cdot \Omega_2^K$$

where χ_K is the strength of the potential of multipolarity K. The operator Ω^K for the ith nucleon (i = 1 and 2 in the above expression for V_{12}), is given by

$$\Omega_q^K = r_i^K Y_q^K(\theta_i, \phi_i)$$

where (r_i, θ_i, ϕ_i) are the co-ordinates of the i-th nucleon, and Y_q^K is the normalized spherical harmonic. In particular, the multipole

potentials corresponding to K = 2 (quadrupole) and K = 3 (octupole) have been extensively used for treating the quadrupole and octupole vibrational states respectively. The schematic model of this type makes the further approximations: (i) the G-type matrix elements can be ignored compared with the F-type matrix elements, and (2) in working out the F-matrix element the direct part can be ignored compared with the exchange part. Use the definition (5.50) for the F-matrix element and replace $(a n \mid V \mid m b)$ by the exchange term, i.e. $-\langle a n \mid V \mid b m \rangle$; then apply the standard result of Racah algebra to write down $-\langle a n \mid \Omega^K \cdot \Omega^K \mid b m \rangle$ explicitly, and to carry out the summation of the product of two W-functions over J'. In this way one obtains, in the present schematic model, the F-matrix element of the multipole potential of order K, given by

$$F (m n a b J) = \delta_{KJ} \, \chi_J \, \bar{g}' (m n J) \, \bar{g}' (a b J) \qquad (5.84a)$$

where

$$g' (a b J) = (4\pi)^{-\frac{1}{2}} \, \bar{g} (a b J) \int_0^\infty r^2 dr \, R_a (r) \, r^K \, R_b (r) \qquad (5.84b)$$

Thus the quadrupole and the octupole potentials give non vanishing matrix elements in J = 2 and J = 3 states respectively. Using the definitions (5.84a, b) and the fact that G will be ignored in comparison to F, we obtain from Eqs (5.82c, d)

$$H (m n a b J) = - \left\{ 1 - (-1)^J \right\} \chi_J \, \bar{g}'_1 (m n J) \, \bar{g}'_1 (a b J) \qquad (5.85a)$$

$$K (m n a b J) = - \left\{ 1 + (-1)^J \right\} \chi_J \, \bar{g}'_2 (m n J) \, \bar{g}'_2 (a b J) \qquad (5.85b)$$

where

$$g'_1 (a b J) = g' (a b J) (u_a v_b - v_a u_b), \quad g'_2 (a b J) = g' (a b J) (u_a v_b + v_a u_b) \qquad (5.85c)$$

It is clear from Eqs (5.85a, b) that H = 0 and K $\neq$ 0 for J = 2 (quadrupole vibration), while the reverse is true for the octupole state. In the case of the quadrupole vibration, for example, the Eqs (5.82a, b) then reduce to

$$E Z^{(+)}_{mn} = (E_m + E_n) Z^{(-)}_{mn} \qquad (5.85d)$$

$$E Z^{(-)}_{mn} = (E_m + E_n) Z^{(+)}_{mn} - 2 \chi_J g'_2 (m n J) \sum_{(a,b)} g'_2 (a b J) Z^{(+)}_{ab} \qquad (5.85e)$$

Substituting from the first equation into the second we obtain

$$\left\{ E^2 - (E_m + E_n)^2 \right\} Z^{(-)}_{mn} = - 2 \chi_J \mathscr{C}^{(+)} \bar{g}'_2 (m n J) \qquad (5.86a)$$

where

$$\mathscr{G}^{(+)} = \sum_{(a,b)} g'_2 \, (a \, b \, J) \, E \, Z^{(+)}_{ab} = \sum_{(a,b)} \bar{g}'_2 \, (a \, b \, J) \, (E_a + E_b) \, Z^{(-)}_{ab} \qquad (5.86b)$$

Solve Eq. (5.86a) for $Z^{(-)}_{mn}$ and substitute this solution for $Z^{(-)}_{ab}$ in expression (5.86b). This yields the dispersion equation for the energy E:

$$1 = -2 \chi_J \sum_{(a,b)} \left\{ E^2 - (E_a + E_b)^2 \right\}^{-1} (E_a + E_b) \left\{ \bar{g}'_2 \, (a \, b \, J) \right\}^2 \qquad (5.87)$$

Once again, note the close correspondence of this equation with Eq. (3.45).

Calculation of transition probability

Any one-body operator, $\sum_I M^k_q (I)$, where the summation goes over all the particles, is given in the second-quantized notation by

$$\sum_I M^K_q (I) = \sum_{a,b} \langle a \mid M^K_q \mid b \rangle \, c^\dagger_a c_b \qquad (5.88)$$

In the special case of electromagnetic transition M^K_q is the electromagnetic transition operator of multipolarity K and component q. We shall consider only the case of electric multipole transition, in which case $M^K_q = \Omega^K_q = r^K Y^K_q (\theta, \phi)$, the quantities (r, θ, ϕ) being the coordinates of a proton. In general,

$$\langle a \mid \Omega^K_q \mid b \rangle = \begin{bmatrix} b & K & a \\ m_b & q & m_a \end{bmatrix} \langle a \mid\mid \Omega^K \mid\mid b \rangle \qquad (5.89a)$$

This equation defines our convention for the definition of the double-barred reduced matrix element.

We substitute from (4.40a, b) for $c^\dagger_a$ and c_b and write the product as

$$c^\dagger_a c_b = (u_a b^\dagger_a + v_a s_a b_{-a}) (u_b b_b + v_b s_b b^\dagger_{-b})$$

$$= (v^2_a \delta_{ab} + u_a u_b b^\dagger_a b_b + v_a v_b s_a s_b b^\dagger_{-b} b_{-a})$$

$$+ (u_a v_b s_b b^\dagger_a b^\dagger_{-b} + v_a u_b s_a b_{-a} b_b) \qquad (5.89b)$$

To evaluate the transition matrix element between states $\langle \Psi \mid$ and $\mid \Psi_0 \rangle$ we have to substitute expression (5.89b) into Eqs (5.85) with $M^K_q = \Omega^K_q$,

and then multiply the resultant expression from the left and right by
$\langle \Psi |$ and $| \Psi_0 \rangle$ respectively. The last line of (5.89b) then gives rise to
amplitudes of the type $\langle \Psi | A^\dagger | \Psi_0 \rangle$ and $\langle \Psi | A | \Psi_0 \rangle$, the first line of
this equation, on the other hand, gives rise to amplitudes of the type
$\langle \Psi | \hat{N} | \Psi_0 \rangle$ from the second and third terms, which are smaller in
order of magnitude compared with $\langle \Psi | A | \Psi_0 \rangle$, and hence will be con-
sistently neglected as was done earlier in the RPA derivation. The
first term of the first line of Eq. (5.89b) being a scalar number produces
exactly zero when sandwiched <u>between</u> two different states $\langle \Psi |$ and $| \Psi_0 \rangle$.
Therefore, from now on, we work only with the second line of Eq. (5.89b)
and do the angular momentum coupling in each of them. We have

$$b^\dagger_a b^\dagger_{-b} = -b^\dagger_{-b} b^\dagger_a = -\sum_J \begin{bmatrix} a & b & J \\ m_a & -m_b & q \end{bmatrix} A^\dagger (a\,b\,J\,q) \tag{5.89c}$$

$$b_{-a} b_b = \sum_J \begin{bmatrix} a & b & J \\ -m_a & m_b & -q \end{bmatrix} A (a\,b\,J,\,-q) \tag{5.89d}$$

The Clebsch-Gordan coefficient in Eq. (5.89a) guarantees that $q = m_a - m_b$,
and this fact has been utilized in the C.G. coefficients of Eqs (5.89c, d).
The summation in Eq. (5.88) consists of that over m_a, m_b and all other
single-particle quantum numbers collectively designed by a and b. The
sum over m_a, m_b can be carried out easily by picking up the C.G.
coefficients of Eqs (5.89a) and (5.89c, d). A restriction $K = J$ then
automatically appears in the result. Putting everything together we
finally obtain

$$\sum_I \Omega^J_q (I) \equiv \sum_{a,b} \langle a | \Omega^J_q | b \rangle C^\dagger_a C_b$$

$$= -\sum_{a,b} g'(a\,b\,J) \left\{ u_a v_b A^\dagger (a\,b\,J\,q) + v_a u_b (-1)^{J+q} A(a\,b\,J,\,-q) \right\}$$

$$\tag{5.90}$$

In the hole-particle case, because of the uv factors, the first term
is non-vanishing when $a = p$, $b = h$, and the second term is non-vanishing
when $a = h$, $b = p$. We also rewrite $A^\dagger (p\,h\,J\,q)$ as $-(-1)^{h+p-J} A^\dagger (p\,h\,J\,q)$,
which follows from its definition (5.53). Finally we obtain

$$\langle \Psi | \sum_I \Omega^J_q (I) | \Psi_0 \rangle = -\sum_{h,p} \left\{ \bar{g}'(h\,p\,J) Y_{hp} - (-1)^{h+p-J} \bar{g}'(p\,h\,J) X_{hp} \right\}$$

Using Eqs (5.66b) and (5.84b), we have

$$- (-1)^{h+p-J} \bar{g}'(p\,h\,J) = (-1)^J \bar{g}'(h\,p\,J)$$

and hence

$$\langle \Psi | \sum_{I} \Omega_q^J | \Psi_0 \rangle = - \sum_{h,p} \bar{g}' (h\,p\,J) \left\{ Y_{hp} + (-1)^J X_{hp} \right\} \qquad (5.91)$$

In the quasi-particle case we put together the terms a, b and b, a contained in Eq. (5.90), and in the summation count a pair (a, b) only once. In this way we obtain

$$\langle \Psi | \sum_J \Omega_q^J(I) | \Psi_0 \rangle = - \sum_{(a,b)} \bar{g}' (a\,b\,J) \left\{ u_a v_b + (-1)^J v_a u_b \right\} \left\{ X_{ab} + (-1)^J Y_{ab} \right\} \qquad (5.92)$$

As an example, let us consider the quadrupole state with the schematic quadrupole potential model. Then this expression reduces to

$$- \sum_{(a,b)} \bar{g}'_2 (a\,b\,J) Z_{ab}^{(+)} = - \sum_{(a,b)} E^{-1} (E_a + E_b) \bar{g}'_2 (a\,b\,J) Z_{ab}^{(-)} \qquad (5.93)$$

The last step follows from Eq. (5.85d). Although this expression can be evaluated exactly after one has solved the Eqs (5.85d, e), we should like to show here, by some rough work, that this transition probability is indeed very large for the state Ψ that gets pushed down (see Fig. 3.2) by a large amount from the vicinity of the unperturbed states. For this state it will be a fairly good approximation to replace the pair energies $(E_a + E_b)$ by an average value $\mathscr{E}_0$, such that (5.93) becomes

$$\langle \Psi | \sum_I \Omega_q^J(I) | \Psi_0 \rangle = - (\mathscr{E}_0/E) \sum_{(a,b)} \bar{g}'_2 (a\,b\,J) Z_{ab}^{(-)} \qquad (5.94a)$$

while Eq. (5.86a) tells us that $Z_{mn}^{(-)}$ is now proportional to $\bar{g}'_2 (m\,n\,J)$. In terms of an overall normalization constant $\mathscr{N}$, we have

$$Z_{mn}^{(-)} = \mathscr{N} \bar{g}'_2 (m\,n\,J) \qquad (5.94b)$$

where $\mathscr{N}$ is determined according to Eq. (3.60) by

$$1 = \sum_{(m,n)} Z_{mn}^{(+)} Z_{mn}^{(-)} = (\mathscr{E}_0/E) \sum_{(m,n)} \left[Z_{mn}^{(-)} \right]^2 = \mathscr{N}^2 (\mathscr{E}_0/E) \sum_{(m,n)} \left[\bar{g}'_2 (m\,n\,J) \right]^2 \qquad (5.94c)$$

Thus, the transition probability (5.94a) is given by

$$- (\mathscr{E}_0/E) \mathscr{N} \sum_{(a,b)} \left[\bar{g}'_2 (a\,b\,J) \right]^2 \equiv \mathscr{N}^{-1} = \left\{ \frac{\mathscr{E}_0}{E} \sum_{(m,n)} \left[\bar{g}'_2 (m\,n\,J) \right]^2 \right\}^{\frac{1}{2}} \qquad (5.94d)$$

According to Eq. (5.87)

$$E^2 = \mathscr{E}_0^2 - 2\chi_J \mathscr{E}_0 \sum_{(a,b)} \left[\bar{g}_2' (a\,b\,J)\right]^2$$

or

$$(\mathscr{E}_0/E) = \left\{1 - (2\chi_J/\mathscr{E}_0) \sum_{a,b} \left[\bar{g}_2' (a\,b\,J)\right]^2\right\}^{\frac{1}{2}}$$

Substituting this in Eq. (5.94d) we conclude

$$\left| \langle \Psi | \sum_I \Omega_q^J(I) | \Psi_0 \rangle \right| > \left\{\sum_{m,n} \left[\bar{g}_2' (m\,n\,J)\right]^2\right\}^{\frac{1}{2}} \qquad (5.94e)$$

It is interesting to compute the transition probability in the TDA-approximation using the same model, and compare it with the inequality (5.94e). Use Eqs (5.61a, b) with $G = 0$; assuming $(E_m + E_n) \approx \mathscr{E}_0$, one easily obtains

$$(E - \mathscr{E}_0) X_{mn} = -\sum_{a,b} (u_a v_b u_m v_n + v_a u_b v_m u_n) F (m\,n\,a\,b; J) X_{ab}$$

where the summation a, b goes over both (a, b) and (b, a). Use F from Eqs (5.84a, b) and the symmetry relations (5.66b) and $X_{ba} = -(-1)^{a+b-J} X_{ab}$, to rewrite the above equation as

$$(E - \mathscr{E}_0) X_{mn} = -\chi \mathscr{C} \bar{g}_2' (m\,n\,J) \qquad (5.95a)$$

with

$$\mathscr{C} = \sum_{(a,b)} \bar{g}_2' (a\,b\,J) X_{ab} \qquad (5.95b)$$

Therefore,

$$X_{mn} = \mathscr{N}' \, g' (m\,n\,J) \qquad (5.95c)$$

where $\mathscr{N}'$ is a normalization constant and determined by

$$1 = \sum_{mn} X_{mn}^2 = \mathscr{N}'^2 \sum_{mn} \left[\bar{g}_2' (m\,n\,J)\right]^2 \qquad (5.95d)$$

Putting $Y_{ab} = 0$ in Eq. (5.92) we obtain the transition probability in the TDA which is given by (for $J = 2$)

$$\left| \left\langle \Psi \left| \sum_{I} \Omega_q^J(I) \right| \Psi_0 \right\rangle \right| = \sum_{(a,b)} \bar{g}_2'\, (a\, b\, J)\, X_{ab}$$

$$= \mathcal{N}' \sum_{(a,b)} [\,\bar{g}_2'\, (a\, b\, J)]^2 \equiv (\mathcal{N}')^{-1} \tag{5.95e}$$

$$= \left\{ \sum_{(a,b)} \left[\bar{g}_2'\, (a\, b\, J) \right]^2 \right\}^{\frac{1}{2}}$$

In obtaining this result, we successively used Eqs (5.95c) and (5.95d). Thus, the RPA transition probability (5.94e) is larger than the TDA-estimate (5.95e). The TDA-value is already much larger compared with a typical single-particle transition probability by virtue of the summation present in Eq. (5.95e). The same kind of demonstration can be given for the hole-particle case as well; the general result is that the TDA transition matrix element for the state that shows collective type of lowering in energy (pushing up in the case of giant dipole resonance) is already very large compared to the single-particle transition probability, and the RPA produces a further enhancement in this quantity.

6. REVIEW OF APPLICATIONS OF THE THEORY

In this section we shall present a review of some of the calculations based on the theory developed in the preceding pages. The purpose of this entire set of lectures being pedagogic, no attempt will be made to survey the existing literature in a complete and comprehensive manner. The specific applications discussed here, and also the references cited, will be representative and typical of what has been done. The selection of the material does not reflect, in any way, the superiority of any of the publications relative to others that have not been specifically referred to. In conformity with the attitude displayed in the introduction, the material will be subdivided into three categories: (i) Hole-particle states and their coherent superposition in closed-shell nuclei, (ii) quasi-particle states and their coherent superposition in spherical heavy nuclei, where pairing effects are important, and (iii) vibrational states in deformed nuclei, where also the latter effects are quite important. Some more details of the extension of the theory will also be presented in the appropriate context while discussing specific applications.

6.1. Closed-shell nuclei

The nucleus that has been the testing ground of many theoretical calculations is ^{16}O. Some calculations have been done for ^{40}Ca and ^{208}Pb, as well.

The single-particle and single-hole energies needed in the calculation are invariably taken from the neighbouring odd nuclei (e.g. ^{17}O, ^{17}F and ^{15}O, ^{15}N in the case of ^{16}O). In the ^{40}Ca region, there is very serious doubt whether the low-lying levels of the neighbouring odd nuclei can at all be interpreted as single-particle or single-hole levels. To that extent the treatment of ^{40}Ca as a closed-shell nucleus is also doubtful. However, standard hole-particle diagonalization calculations have been done by several authors for this nucleus.

The other necessary ingredient for these calculations is the two-nucleon potential. In the earliest work by Elliott and Flowers the authors used the Rosenfeld exchange mixture with a Yukawa-type radial dependence:

$$v_{12} = \frac{V_0}{3} \, \vec{\tau}_1 \cdot \vec{\tau}_2 \, \{0.3 + 0.7 \vec{\sigma}_1 \cdot \vec{\sigma}_2\} \tag{6.1}$$

where $\vec{\tau}$ and $\vec{\sigma}$ are the isopin and spin operators of the nucleon labelled by the subscript. These authors used the LS-coupling representation for their calculation, and hence the spin-orbit coupling of the shell-model potential, namely $\xi \, \vec{l} \cdot \vec{s}$ was also used explicitly as a part of the interaction while doing the diagonalization. The radial integrals of ξ were, however, chosen to reproduce the experimentally observed single-particle splitting of $d_{5/2}$ and $d_{3/2}$ levels in ^{17}O (^{17}F) and the splitting of the hole levels $p_{3/2}$ and $p_{1/2}$ in ^{15}N (^{15}O).

The schematic δ-function potential described in the Appendix of section 5 has also been used by several authors with various types of exchange dependence. One of the favourite brands is the Soper mixture

$$(0.3 + 0.43 \, P_M + 0.27 \, P_B) \tag{6.2}$$

where P_M and P_B are, respectively, the Majorana and Bartlett exchange operators.

The most extensive calculations have been performed by Gillet and co-workers 2,3 who determined the $\Longleftrightarrow$ potential by least squares fit to several levels. Their potential has a Gaussian shape and is given by

$$V_0 \exp\left\{-\left(\frac{r}{\mu}\right)^2\right\} (W + BP_B + HP_H + MP_M) \tag{6.3a}$$

where P_H is the Heisenberg exchange operator. The values of the various parameters, as determined by the least-squares fit, are given by

$$M - W = 0, \quad M + W - B - H = 0.4, \quad H = 0.4 \tag{6.3b}$$

$$V_0 = -40 \text{ MeV}, \quad \mu/b = 1.0 \tag{6.3c}$$

where b is the harmonic-oscillator parameter, and was chosen to be 1.68 fm from the observed r.m.s. radius of ^{16}O. The four parameters W, M, B, H obey the normalization:

$$W + M + H + B = 1 \tag{6.3d}$$

In recent years, effective shell-model matrix elements of the Tabakin potential, and the hard-core Hamada-Johnston (HJ) potential have also been evaluated. There is one calculation with the Tabakin potential by Vinh-Mau (J. P. Svenne, private communication) on the giant resonance of ^{16}O. G. E. Brown refers to calculation on the same states of ^{208}Pb by using the effective matrix elements of the HJ-potential in the Proceedings of the Dubna Symposium on Nuclear Structure (1968), published by the IAEA.

The structure of the various levels of ^{16}O that has emerged from all these calculations, and also from experimental observations has been summarized in Table 6.1. It is clear from this table that there are many excited levels in this nucleus which are not of the 1 hp type. The experimental evidences on the deformation of some of these states, and their forming several rotational bands are summarized in Fig. 6.1, which has been taken from the work of Carter et al. [4]. Actually, the 1 hp-type calculations that we are describing now do not even apply to the levels of this category.

TABLE 6.1. STATES OBSERVED IN ^{16}O (from Ref.[3])

Energy in MeV	J^{π}	T	Proposed description
6.06	0^+	0	Deformed
6.14	3^-	0	1p-1h
6.92	2^+	0	Rotational on 6.06 MeV state
7.12	1^-	0	1p-1h
8.88	2^-	0	3p-3h
9.59	1^-	0	3p-3h (deformed)
9.85	2^+	0	Deformed
10.36	4^+	0	Rotational on 6.06 MeV state
10.95	0^-	0	1p-1h
11.26	0^+	0	Deformed
11.62	3^-	0	Rotational on 9.59 MeV state
12.43	1^-	0	1p-1h
12.52	2^-	0	1p-1h
12.78	0^-	1	1p-1h
12.96	2^-	1	1p-1h
13.10	1^-	1	1p-1h
13.26	3^-	1	1p-1h
13.98	2^-	0	
16.3	0^-	0	
17.3	1^-	1	1p-1h
19.5	$2^{+,-}$		
22.4	1^-	1	1p-1h
24.5	1^-	1	1p-1h
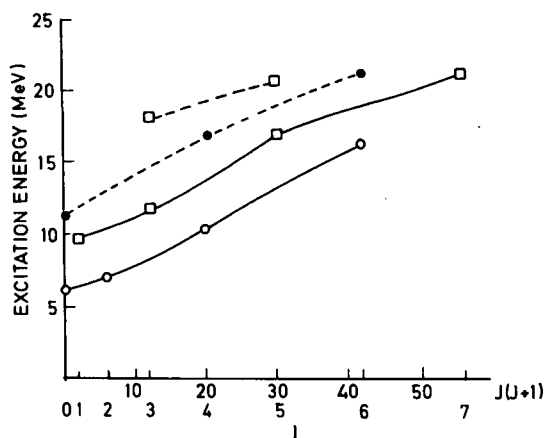
FIG.6.1. Excited states of ^{16}O (Ref. [4]). $\bigcirc$ and $\bullet$ positive-parity levels; $\square$ negative-parity levels.

Leaving them aside we are left with the T = 1 and T = 0 states of $J^\pi = 1^-$, 2^- and 3^-. With the exception of the 2^+ state at 19.5 MeV, all other positive parity states listed in Table 6.1 belong to the rotational bands and need a different kind of treatment. Amongst the most notable deformed odd-parity states are the 9.59 MeV 1^- state, and the 11.62 MeV 3^- state, which are believed to be the first two levels of a rotational band. The other notable odd-parity level that is found, in this table, to be a non-conformist to the 1 hp picture is the 8.88 MeV 2^- state; there is direct experimental evidence that this state cannot be excited in inelastic proton scattering which rules out its having a 1 hp-type structure.

We now discuss the $J^\pi = 1^-$, 2^-, 3^- states of T = 1 and T = 0 that are fairly well described by a 1 hp-type TDA and RPA calculation. The general observations are: (i) the TDA-and RPA-type theories are both equally successful in explaining the observed energies, provided one adjusts the overall strength V_0 of the two-nucleon interaction in the two cases separately; (ii) the agreement in the transition probability is better with the RPA-theory in the cases of the collective 3^- (T = 0), and 1^- (T = 1) states. These states occur at 6.14 MeV (3^-) and 22 MeV-25 MeV (1^-). For the other odd-parity states, which do not show a collective enhancement of the transition probability, there is not much of a difference between the TDA- and RPA-predictions; (iii) finally, the agreement in energy in the hp calculation is somewhat better for the T = 1 states than for the T = 0 states.

There are two important discrepancies in the results of the calculations on dipole states. The experimental situation is shown in Fig. 6.2. Most of the dipole cross-section is found to be located in the energy-range 21 MeV-25 MeV. Theoretically, one gets two strong dipole states in this energy region from the following mechanism: let us think of an idealized dipole state $\vec{D} | \Psi_0 \rangle$, where Ψ_0 is the ground state wave function, and $\vec{D}$ the dipole operator.

$$\vec{D} = \sum_{p=1}^{Z} (\vec{r}_p - \vec{R}) = \frac{N}{A} \sum_{p=1}^{Z} \vec{r}_p - \frac{Z}{A} \sum_{n=1}^{N} \vec{r}_n \qquad (6.4a)$$

Here $\vec{R}$ is the co-ordinate of the centre-of-mass of the nucleus, i.e.
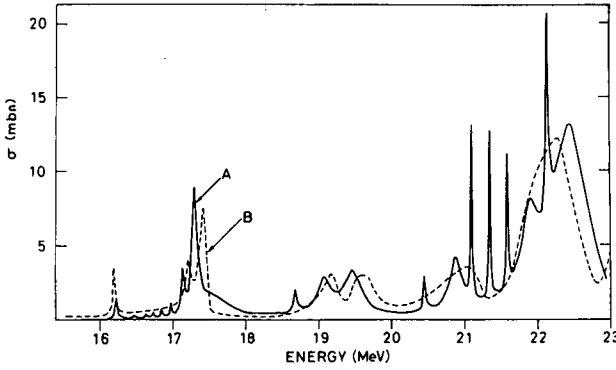
FIG.6.2. Curve A: (γ,n) cross-section on ^{16}O. Curve B: (γ_0, p) cross-section on ^{16}O (for source see Ref.[3]).

$\vec{R} = A^{-1} \sum\limits_{i=1}^{A} \vec{r}_i$; p, and n denote a proton and a neutron; N, Z and A are, respectively, the number of neutrons, protons, and nucleons. In the special case of N = Z (i.e. a case like ^{16}O or ^{40}Ca), expression (6.4a) reduces to

$$\vec{D} = -\frac{1}{2} \sum_{i=1}^{A} \vec{r}_i \tau_3(i) \qquad (6.4b)$$

τ_3 being the third component of isospin of a nucleon. In analogy with the state $\vec{D}|\Psi_0\rangle$, we can also think of an idealized state $\vec{D}_\sigma|\Psi_0\rangle$ where $\vec{D}_\sigma$ is given by

$$\vec{D}_\sigma = -\frac{1}{2} \sum_{i=1}^{A} (\vec{r}_i, \vec{\sigma}_i)^1 \tau_3(i) \qquad (6.4c)$$

where $\vec{\sigma}$ is the nucleon spin operator, and $(\vec{r}, \vec{\sigma}_i)^1$ is the tensor of rank 1 obtained by compounding $\vec{r}$ with $\vec{\sigma}$ (it is actually proportional to $\vec{r}\times\vec{\sigma}$). Acting on the ground state Ψ_0, $\vec{D}_\sigma$ generates a state of total angular momentum J = 1, parity π = -1, and the total intrinsic spin S = 1 [by virtue of the presence of the spin vector $\vec{\sigma}$ in Eq.(6.4c), and the fact that Ψ_0 has S = 0]. We, therefore, refer to the state $\vec{D}_\sigma|\Psi_0\rangle$ as the spin-flip dipole state. It is clear that, if $\vec{D}|\Psi_0\rangle$ is an exact eigenstate of the Hamiltonian then all the dipole transition probability will be exhausted by this state, and all other states, by virtue of their orthogonality with this state, will have zero E1 transition probability. However, in a more realistic situation (i.e. for the exact nuclear Hamiltonian) this idealized state may be shared between several actual states, and then all these states produce a non-vanishing E1 transition probability. In particular, the spin-flip dipole state $\vec{D}_\sigma|\Psi_0\rangle$ can mix fairly well with $D|\Psi_0\rangle$ through the spin-orbit coupling, and then we expect the dipole transition probability to be large for the two states which are mixtures of $\vec{D}|\Psi_0\rangle$ and $\vec{D}_\sigma|\Psi_0\rangle$. This idea of a splitting of the giant dipole resonance into two strong components between 20-25 MeV, was first proposed by Ferrell, and later substantiated by Ferrell,
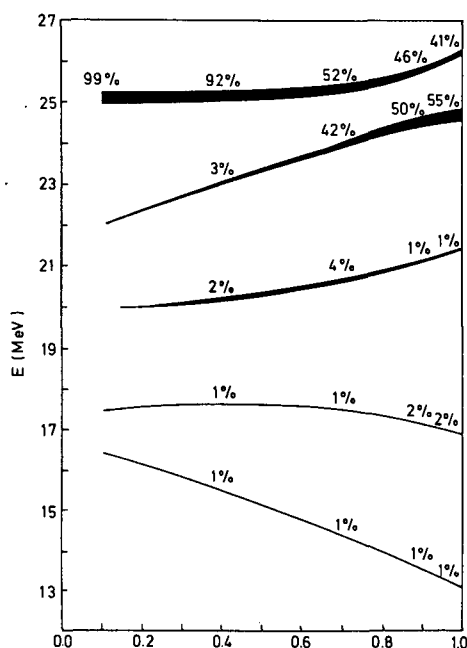
FIG.6.3. Variation of dipole strength as a function of the strength of spin-orbit potential. (Y.C. Lee, Ref.[5]).

TABLE 6.2. RESULTS OF ELLIOTT-FLOWERS AND
SCHEMATIC-MODEL CALCULATIONS

Calculated energy	13.1	17.3	20.4	22.6	25.2
	13.7	17.6	20.0	22.2	25.0
Transition strength (%)	0	1	0	67	32
	1	1	1	68	29

Fallieros and Pal, Pal and Lee, and Lee [5]. Figure 6.3 demonstrates this mechanism of the splitting of the ^{16}O dipole resonance. In the detailed calculations of Ref.[1] and the schematic model calculations of various authors, the splitting into two strong peaks, one around 22 MeV and the other around 25 MeV, was well established. However, one of the discrepancies with experimental data, referred to earlier, has to do with the distribution of the dipole strength between these two levels. The results of the Elliott-Flowers and the schematic-model calculation are shown in Table 6.2. The first and second lines for each datum correspond to Ref.[1] and the schematic model, respectively. The closeness of the two calculations is very obvious. The experimental values of the strength for the energy-region around 22 MeV (the integrated area under the curve) and the region around 25 MeV are of ratio 1:1 rather than of the calculated ratio 2:1.

The other discrepancy referred to earlier concerns the dipole sum rule. We shall first derive the sum rule and then discuss the discrepancy. The

transition strength B(EL) for the multipole transition of order L (in the present case L = 1) is defined to be

$$B_{J_i \to (\alpha J_f)} (EL) = \frac{1}{2J_i + 1} \sum_{M_i M_f} \sum_M |\langle \alpha J_f M_f | \Omega_M^L | J_i M_i \rangle|^2 \qquad (6.5)$$

Here $(J_i M_i)$ are the ground-state angular momentum and its projection; Ω_M^L is the multipole operator, and $(\alpha J_f m_f)$ specify the state that is decaying by the multipole transition. Only two of the summation indices m_i, m_f, M are actually independent. B(EL) is an experimentally measurable quantity, and sum rules can be derived by summing it over all possible states (αJ_f). A more useful sum rule is obtained by weighing expression (6.5) with the energy involved in the transition, i.e. $(E_f - E_i)$ and then carrying out the summation over (αJ_f). In this way

$$\sum_{\alpha J_f} (E_f - E_i) B_{J_i \to (\alpha J_f)}(EL) = \frac{1}{2J_i + 1} \sum_{M_i, M} \sum_{\alpha J_f M_f} (E_f - E_i) |\langle \alpha J_f M_f | \Omega_M^L | J_i M_i \rangle|^2 \qquad (6.6)$$

The left-hand side can be evaluated from experimental data, and the right-hand side can be estimated from theoretical considerations in the following manner. The factor $(E_f - E_i)$ in Eq.(6.6) can be produced automatically out of the commutator of Ω_M^L or Ω_M^{L*} with H. Thus,

$$\sum_{\alpha J_f M_f} (E_f - E_i)|\langle \alpha J_f M_f | \Omega_M^L | J_i M_i \rangle|^2$$

$$\equiv \sum_{\alpha J_f M_f} [\tfrac{1}{2} (E_f - E_i) \langle J_i M_i | \Omega_M^{L*} | \alpha J_f M_f \rangle \langle \alpha J_f M_f | \Omega_M^L | J_i M_i \rangle$$

$$- \tfrac{1}{2}(E_i - E_f) \langle J_i M_i | \Omega_M^{L*} | \alpha J_f M_f \rangle \langle \alpha J_f M_f | \Omega_M^L | J_i M_i \rangle]$$

$$= \frac{1}{2} \sum_{\alpha J_f M_f} [\langle J_i M_i | \Omega_M^{L*} | \alpha J_f M_f \rangle \langle \alpha J_f M_f | (H\Omega_M^L - \Omega_M^L H) | J_i M_i \rangle$$

$$- \langle J_i M_i | (H\Omega_M^{L*} - \Omega_M^{L*}H) | \alpha J_f M_f \rangle \langle \alpha J_f M_f | \Omega_M^L | J_i M_i \rangle]$$

$$= \tfrac{1}{2} \langle J_i M_i | \Omega_M^{L*} [H, \Omega_M^L] - [H, \Omega_M^{L*}] \Omega_M^L | J_i M_i \rangle \qquad (6.7a)$$

The operator H produces E_f and E_i, by definition, when it operates on the states $(\alpha J_f M_f)$ and $(J_i M_i)$. The replacement of $(E_f - E_i)$ and $(E_i - E_f)$ by the commutators is thus explained. In the final step of Eq.(6.7a) we have used the closure relation to carry out the summation over $(\alpha J_f M_f)$. Next we recall that there is a sum over M in Eq.(6.6) and clearly

$$\sum_M [H, \Omega_M^{L*}] \Omega_M^L \equiv \sum_M (-1)^M [H, \Omega_{-M}^L] \Omega_M^L = \sum_M (-1)^M [H, \Omega_M^L] \Omega_{-M}^L$$

$$\equiv \sum_M [H, \Omega_M^L] \Omega_M^{L*} \qquad (6.7b)$$

All we have done here is to relabel the summation index M by -M. Using Eqs (6.7b) and (6.7a) in Eq.(6.6) we finally obtain

$$\sum_{\alpha J_f} (E_f - E_i) B_{J_i \to (\alpha J_f)} \, (EL) = \frac{1}{2 \, (2J_i + 1)} \sum_{M_i, M_f} \langle J_i M_i | [\Omega_M^{L*}, [H, \Omega_M^L]] | J_i M_i \rangle \cdot$$

$$(6.8)$$

If there is no velocity-dependence and space-exchange in the nuclear potential then $[H, \Omega_M^L]$ can be substituted by $[T, \Omega_M^L]$ where T is the kinetic energy operator. In the special case of dipole transition, Ω_M^L is given, according to (6.4a), by

$$\vec{D}_M = \frac{N}{A} \sum_{p=1}^{Z} \vec{r}_M^{(p)} - \frac{Z}{A} \sum_{n=1}^{N} \vec{r}_M(n)$$

where the M-component of any vector $\vec{A}$ is defined to be

$$\vec{A}_0 = A_z, \quad A_{\pm 1} = \mp \frac{1}{\sqrt{2}} (A_x \pm i A_y)$$

The kinetic energy operator T is equal to a sum over all nucleons of the operator $(-\hbar^2/2m) \nabla^2$, m being the nucleon mass. Using the basic commutation relations between the components of momentum and co-ordinate one can easily evaluate $\sum_M [\vec{D}_M^*, [T, D_M]]$, which is equal to $(NZ/A)(\hbar^2/m)$.

Thus the theoretical estimate of the sum rule (6.8), with the approximation of no velocity-dependence and space-exchange in the nuclear potential, is given by

$$\sum_{\alpha J_f} (E_f - E_i) B_{J_i \to (\alpha J_f)} \, (EL) \simeq \frac{NZ}{A} \frac{\hbar^2}{m}$$

$$(6.9)$$

The actual two-nucleon potential contained in H has some velocity dependence and space-exchange. This part of v gives a non-vanishing commutator with D and hence extra contribution to the sum rule (6.9). It is possible to make reasonable estimate of this extra contribution.

    According to the hp-calculation of the giant resonance, we should, therefore, expect that the sum on the left-hand side of the sum rule (6.9) carried over all the dipole states (which are all below 25-26 MeV), should be fairly close to the estimate mentioned above. In practice, the experimental value of the sum is about half of the estimated sum rule if one restricts the sum on the left hand side to states up to about 25-26 MeV. The remaining half of the sum rule is, therefore, contained in rather high-lying states. In the hp-calculation, however, we have no such states. A way out of this discrepancy is to extend the hp-calculation by admitting states with larger number of hp-pairs. Such states will mix with the dipole state, and will be very high-lying in energy. The little bit of transition strength that they acquire in this way, when weighted by the factor $(E_f - E_i)$ can very well account for the transfer of about half of the sum rule to states above 25-26 MeV.

TABLE 6.3. STATES OBSERVED IN ^{40}Ca (from Ref.[3])

Energy (MeV)	J^π	Proposed description
3.35	0^+	Deformed
3.73	3^-	1p-1h
3.90	2^+	Rotational on 3.35 MeV state
4.48	5^-	1p-1h
5.27	3^- or 1^-	3p-3h basis of an odd parity rotational band
5.62	4^+	Rotational on 3.35 MeV state
5.89	1^-	
6.29	3^- ⎫	
6.56	3^- ⎬	Rotational on 5.27 MeV state and 1p-1h
6.94	1^-	1p-1h
7.12	$(\geqq 6^+)$	Rotational on 3.35 MeV state (?)
7.91	4^+	
8.09	2^+	
8.37	5^-	1p-1h or rotational on 5.27 MeV state

The results for ^{40}Ca and ^{208}Pb will be very briefly described now. Table 6.3 lists the states of ^{40}Ca and their structure. The situation is very similar to ^{16}O, namely there are some states which are deformed and some states which can be explained in terms of 1 hp-type configurations. In the case of ^{208}Pb, there are two rather interesting results: (i) The energy of the octupole state (2-6 MeV) can be fairly well reproduced only if one mixes a large number (about 45) of hole-particle configurations having unperturbed energies up to 15 MeV. If, on the other hand, the number of basic states is cut down by restricting to a lower unperturbed energy (of about 6 MeV) the energy of the collective octupole state is very unsatisfactory. This result is shown in Fig.6.4. (ii) The second interesting result concerns the giant dipole state. Experimentally, this collective state occurs in the energy region 13.5-15 MeV. The theoretical calculations using Gillet's potential or the effective potential derived from the Hamada-Johnston potential (reference to G.E. Brown cited earlier) pushes this state only up to about 11 MeV. To achieve a satisfactory result one needs an artificial bolstering-up of the overall strength of the two-nucleon potential by about a factor of two.

6.1.1. Deformed states of closed-shell nuclei

These states need a special treatment, and the theoretical understanding, at the moment, is in a rather unsatisfactory state. Almost all the attempts so far have been restricted to the deformed 0^+ (6.06 MeV) state in ^{16}O.

At one time 1 hp-type calculations were done by several workers on this state. However, it was soon realized that the monopole transition from this state to the ground state had no collective-type enhancement
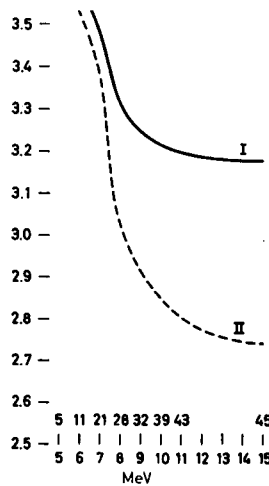
FIG. 6.4. Calculation by Gillet et al. (see Ref. [3]) on the 3⁻ state of ²⁰⁸Pb. The solid and dashed curves are TDA and RPA results respectively.

at all. Therefore, it was surmised for some time that this state consists predominantly of 2 hp-type configurations, although it was rather poorly understood at that stage why the 2 hp-type states should come so low in energy. Then there came a suggestion from Bohr and Mottelson that this state, and the similar low-lying 0^+ state in many other even nuclei, may correspond to a deformed shape of the nucleus. If one looks at the Nilsson single-particle level diagram then one is struck by the fact that as one moves on the positive deformation side, a single-particle level from the upper shell comes down close to the uppermost single-particle level from the lower shell, and thus the gap between major shells gets almost destroyed as a result of the deformation. Since the 6.06 MeV state has to have more than one hp pair, it was suggested that it consists primarily of 2 hp pairs, and the reason the state is so low, is because the 2 hp state tends to acquire a deformation; as soon as the nucleus acquires a deformation, according to the previous statement, very little energy is required to transfer a pair of nucleons from the topmost level of the p-shell to the lowest level of the s-d shell. On the basis of this suggestion, Brown and Green [6] did a phenomenological type of calculation mixing the deformed 2 hp and 4 hp $J = 0$ states with the spherical $J = 0$ state (which has 0 hp pair). They also considered the $J = 2$ state by mixing the deformed 2 hp and 4 hp states. Let us denote the number of the hole-particle pair by N, and denote the various states by $|N, J\rangle$. Then, Brown and Green (BG) have three matrix elements of the nucleon-nucleon potential to deal with:

$$M_1 = \langle 0,0 \,|v|\, 2,0 \rangle, \qquad M_2 = \langle 2,0 \,|v|\, 4,0 \rangle, \qquad M_3 = \langle 2,2 \,|v|\, 4,2 \rangle$$

The hole and particle states of the deformed nuclei are taken to be

$$\text{h-state: } x' |\, p_{3/2}, \tfrac{1}{2} \rangle + y' |\, p_{1/2}, \tfrac{1}{2} \rangle \qquad\qquad\qquad (6.10\text{a})$$

$$\text{p-state: } x |\, d_{5/2}, \tfrac{1}{2} \rangle + y |\, 2s_{1/2}, \tfrac{1}{2} \rangle + z |\, d_{3/2}, \tfrac{1}{2} \rangle \qquad (6.10\text{b})$$

where the second number in each basis state denotes the angular momentum projection. BG take the deformation β for the 2 hp state as $\beta = 0.3$, and $\beta = 0.5$ for the 4 hp state. The values of x, y, z for a given value of the deformation is known from Nilsson's work. For example, for $\beta = 0.3$, one has

$$x = 0.828, \quad . \quad y = 0.537, \quad z = -0.160$$

Actually, for the h-state BG used, instead of the expression given above, the following approximation: it was taken to be a pure $|p_{1/2}, \frac{1}{2}\rangle$ state, but then the matrix elements were multiplied in the end by an overlap factor ($= 0.75$ for $\beta = 0.3$) to take into account the deformation of the state. In this way BG obtained an estimate

$$M_1 = -4.3 \text{ MeV}$$

For the other two matrix elements, M_2 and M_3, very rough estimates, based on SU_3-type wave functions were used:

$$M_2 = -1.8 \text{ MeV}, \quad M_3 = -1.6 \text{ MeV}$$

The unperturbed energies of the states appearing in the matrix elements were also treated as empirically adjustable quantities. Denoting these by $E_J(N)$, the values chosen by BG are

$$E_0(0) = 2.31 \text{ MeV}, \quad E_0(2) = 8.51 \text{ MeV}, \quad E_0(4) = 6.51 \text{ MeV}$$

$$E_2(2) = 10.83 \text{ MeV}, \quad E_2(4) = 7.61 \text{ MeV}$$

The final results obtained are summarized in Table 6.4.

In spite of the highly successful nature of these results, one needs a more fundamental calculation based on less number of empirically determined quantities. The most interesting approach of this kind started with the initial work by Bassichi's and Ripka [7]. These authors consider states of the type (6.10a, b) and determine the coefficients x', y', x, y and z by Hartree-Fock (HF) calculations. The closed-shell ground-state wave function, $|0\rangle$ say, was taken as an inert core, over which 2 hp- and 4 hp-type excitations were allowed to take place. The unperturbed single-particle and single-hole energies (ϵ) were chosen in such a way that a HF calculation yielded the correct single-particle spectrum of ^{17}O and ^{15}O. The two-nucleon interaction (V) used for this purpose was taken to be a well-behaved Gaussian potential with Rosenfeld exchange mixture, the same interaction that had been used earlier in the HF calculations on s-d shell nuclei by other authors. The HF-Hamiltonian Γ for the self-consistent calculation of N-hp states, is defined in the harmonic oscillator representation by

$$\langle n\ell jm\tau_3 | \Gamma | n'\ell'j'm\tau_3 \rangle = \epsilon_{n\ell j}\delta_{nn'}\delta_{\ell\ell'}\delta_{jj'}$$

$$+ \sum_{i=1}^{N}\langle n\ell jm\tau_3; p_i | v | n'\ell'j'm\tau_3; p_i \rangle - \sum_{i=1}^{N}\langle n\ell jm\tau_3; h_i | v | n'\ell'j'm\tau_3; h_i \rangle$$

$$(6.11)$$

where τ_3 is the projection of isosopin; $(n\ell jm)$ is a spin-orbit complex harmonic-oscillator state; p_i and h_i are short-hand notations for the

TABLE 6.4.   SUMMARY OF FINAL RESULTS
In the first column J_n denotes the nth state of angular momentum J.

| State | Energy | Amplitudes of basis states | | |
		N = 0	N = 2	N = 4
0_1^+	0	0.874	0.469	0.130
0_2^+	6.07	-0.262	0.229	0.937
0_3^+	11.36	-0.410	0.853	-0.323
2_1^+	6.92		0.377	0.923
2_2^+	11.52		0.923	-0.377

B(E2) values in units of $e^2 (fm)^4$

| Transition | B(E2) value | |
	Calculated	Experimental
$2_1^+ (6.93$ MeV$) \rightarrow 0_1^+ (0$ MeV$)$	5.3	4.6 ± 1.0
$2_1^+ (6.93$ MeV$) \rightarrow 0_2^+ (6.06$ MeV$)$	103	40
$4_1^+ (10.36$ MeV$) \rightarrow 2_1^+ (6.93$ MeV$)$	152	117 ± 10

quantum numbers of the particle and hole states. In the case of 4-hp
states the determinantal wave function to be considered has the four holes
in the state (6.10a) and its time-reversed state, and the four particles in
the state (6.10b) and its time-reversed state. Such a determinant auto-
matically has a total isospin T = 0. In the case of 2-hp type states this
is not the case and the authors ensured the correct total isospin by suitable
coupling in the determinantal wave functions. There are clearly three pos-
sibilities: 1) the two hole states are coupled to T' = 1, and the two particle
states are coupled to the same isospin, and finally these isospins are coupled
to the total T = 0; the T' = 1 state of two holes or two particles have to
be antisymmetric in the space-spin components, and hence we have only
one possibility, namely the two holes must be in different space-spin states
(the state (6.10a) and its time-reversed) and the two particles must also
be in different space-spin states (the state (6.10b) and its time-reversed).
2) in the case of T' = 0, on the other hand, the space-spin part of the two
holes as well as the two particles must be symmetric, and hence two alter-
natives exist: the possibility mentioned above and also the possibility of
the two holes going to the same state (6.10a) and the two particles going
to the same state (6.10b). Ripka and Bassichis denote these three possi-
bilities for 2-hp states as (a), (b) and (c), respectively.
      The self-consistent energies of the 2-hp type states (cases a, b, c) and
the energy of the 4-hp state are shown as functions of the strength of the

two-body interaction in Fig.6.5, taken from Ref.[7]. These energies cor-
respond to the energies of the intrinsic states. Assuming that each intrinsic
state gives rise to a rotational band, one can find the energy of the observed
0^+ state from the calculated energy of the intrinsic state by subtracting the
value of AJ^2, where the parameter A is obviously related to the moment
of inertia of the deformed intrinsic state. This was calculated by the authors
from the cranking-model expression, and then the energy of the 0^+ state was
obtained from the solid curve marked 4p-h by subtracting $A\langle J^2 \rangle$. The dotted
curve marked E_0 in Fig.6.5 was obtained in this way.
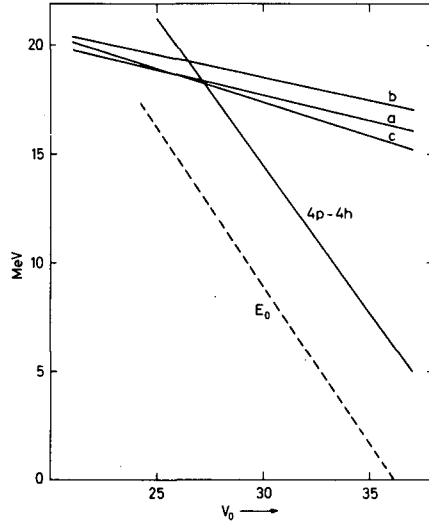
FIG.6.5. Hartree-Fock results (Ref.[7]) for 2-hp
(a,b,c) and 4-hp states in ^{16}O. For further explanation
see text.

It is clear from this diagram that, for suitable values of the interaction
strength, the deformed 4-hp state comes very much below the deformed 2-hp
type states. This explains why the 6.06 MeV state of ^{16}O is predominantly
composed of 4-hp states rather than 2-hp states. The main interest that now
lies in the calculation of this state is whether or not a reasonable two-body
interaction will really push down the 0^+ state to 6.06 MeV. From Fig.6.5,
it is clear that the Ripka-Bassichis potential with a strength around 32 MeV
can do the job. However, it is believed at the present time that more
realistic two-body potentials will not satisfy this criterion too well.

There is an interesting calculation by Banerjee and Stephenson, Jr.[8]
who show that it is likely that the 0^+ state of ^{16}O has a deformed tri-axial
shape, rather than the axially symmetric shape assumed by the previous
workers. The 4-hp-type state in a triaxial HF-potential goes much lower
than the similar state in an axially symmetric potential. Once again there
is the need of doing such calculations with more realistic two-body interaction.

6.2. Spherical vibrational nuclei

6.2.1. Input data

The single-particle energies are usually taken from experimental data
on nuclei with closed shell plus one nucleon in the neighbourhood of the nuclei

being calculated. A smooth variation of these energies with the mass number
(A), of the type A (i.e. inversely proportional to the radius of the nucleus),
is also allowed in many calculations. Wherever experimental data are not
available, one uses theoretical values of the single-particle energies cal-
culated with the Saxon-Woods-type average potential; one set of energies
and wave functions is given by Blomqvist and Wahlborn [9].

The other type of input data concerns the two-body potential. Very
little information was available from shell-model-type calculations. The
potential used in the earliest work by Kisslinger and Sorensen [10] consisted
of the idealized pairing interaction v_p, defined by Eq.(4.63b) and the
schematic quadrupole potential defined by Eq.(5.84a) with K = 2. The
BCS-equations are solved only with v_p to obtain the independent quasi-
particles and the vibrational equations of section 5 are solved only with
the model expression (5.84a). In their first paper dealing with single-
closed-shell nuclei (i.e. nuclei in which either the neutrons or the pro-
tons are in closer shells), these authors used an adiabatic method originally
suggested by Bohr and Mottelson, to obtain the vibrational energy. In the
second paper, dealing with nuclei having both neutrons and protons in un-
filled shells (the unfilled levels of neutrons were, however, much above
those of the protons so that, at the stage of calculating the quasi-particles,
the neglect of the pairing interaction between neutrons and protons could
be justified), these authors used a more sophisticated technique, very much
akin but not exactly analogous to that described in section 5. The strength
of the pairing interaction used in their calculations was obtained by fitting
the odd-even mass difference on the assumption that this is almost entirely
determined by the pairing effect. To elucidate the procedure, let us con-
sider the binding energies (BE) of three neighbouring nuclei and compute

$$BE(Z, N-1) - 2BE(Z, N) + BE(Z, N+1)$$

where the letters in paranthesis denote the proton and neutron numbers of
the nuclei. The nucleus (Z, N) is even-even, while the other two are even-
odd (i.e. odd mass). If one ignores the effect of the residual quasi-particle
interaction this quantity should be equated to $2E_{min}$, where E_{min} is the energy
of the single-neutron quasi-particle state that represents the ground state
of the two odd-mass nuclei. The strength of the pairing force determines
the energy gap and through that the quantity E_{min} and hence a determination
of the former becomes possible in this manner. Kisslinger and Sorensen
found the strength of the pairing force G to be given by (19/A) and (23/A) MeV
in the neighbourhood of Sn and Pb respectively. The strength of the quadrupole
force X was determined by fitting the energy of the first excited 2^+ state.
Instead of treating X as an adjustable parameter for each individual nucleus,
they tried to attribute a smooth A-dependence to this parameter so that the
trend of the 2^+ level of a whole set of nuclei in a particular mass number
region is fairly well reproduced. The final value obtained by these authors
is given by $(5/4\pi) (n+3/2)^2 b^2 X = 110 A^{-1}$ where b is the harmonic oscillator
constant and n is the number of harmonic oscillator quanta associated with
most of the levels (i.e. with the exception of the level that comes down from
the upper shell through the spin orbit coupling) of the unfilled major shell.

In their second paper Kisslinger and Sorensen used equal pairing-force
strength for the neutrons and protons, G_n and G_p. They ignored pairing
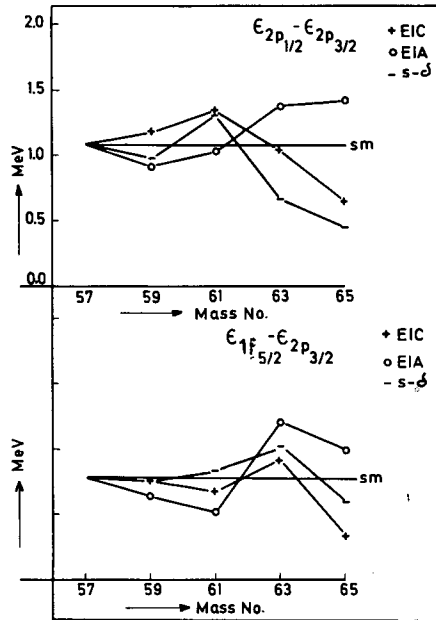
FIG.6.6. Energies of $2p_{1/2}$ and $1f_{5/2}$ single-particle states measured with respect to the $2p_{3/2}$-state, plotted as a function of mass number.

effects between a neutron and a proton from arguments stated earlier. The quadrupole force between two neutrons, two protons and between a neutron and a proton was assumed to have the same strength: $\chi_n = \chi_p = \chi_{np}$. Estimates of these quantities and G_n, G_p were taken from the first paper. In addition, they used a short-range (δ-function-type) potential between a neutron and a proton and considered explicitly the effect of this interaction in changing the proton single-particle energy as the neutron number increases and vice versa. This, in fact, amounts to considering only the contribution of the δ-function potential to the average potential acting on a proton, or a neutron. Apart from this specific change in the single-particle energies with mass number, the smooth A-type dependence of these quantities mentioned earlier and another smooth A-dependent term (to represent the change of spin-orbit coupling effects with A) were also considered. For the details the reader is referred to the Appendix II of the second paper by Kisslinger and Sorensen.

Many of the later workers have used more detailed forms of the two-nucleon potential. Arvieu and co-workers [11] have used a spin-dependent Gaussian potential, whose range depth and the ratio of singlet-to-triplet strengths were treated as parameters in a least-squares fit to the energy levels of odd-mass nuclei. The same potential was then used to predict the 2^+ state of the even nuclei. The work was done in the Sn- and Pb-regions.

In the Ni and Sn regions many different well-behaved central potentials have been used [12,13]. A set of phenomenologically determined two-body matrix elements due to the Argonne group have also been used [12]. Two-body matrix elements, starting from the realistic Hamada-Johnston two-nucleon interaction have been calculated in the Ni-region by Kuo [14] and

in the Sn-region calculated and applied by Gmitro and co-workers [15] . The latter workers have also used the separable non-local Tabakin interaction. In both Refs [14,15] , the effect of excitation of the core-nucleus, in re-normalizing the two-body matrix elements, have been taken into account. Gmitro gives a detailed account of this type of work in these Proceedings.

6.2.2. The inverse-gap-equation method

Gillet and Rho [16] have suggested a new way of supplying the input to the quasi-particle calculation. This is now known as the inverse-gap-equation method. To understand the principle of this approach, let us consider Eq.(4.71) and explicitly pull out the attractive strength $-V_0$ of the potential; denote the rest of the two-body matrix element by $m_0(jj')$ where the subscript refers to the total J. In this manner Eq.(4.71) can be rewritten as

$$\left(\frac{1}{V_0}\right)\Delta_j = \sum_{j'} M_{jj'}\,\Delta_{j'} \tag{6.12a}$$

where

$$M_{jj'} = \frac{1}{2E_{j'}}\sqrt{\frac{2j'+1}{2j+1}}\,m_0(jj') \tag{6.12b}$$

and

$$-V_0\,m_0(jj') = (jjJ = 0, M = 0\,|v|\,j'j'\,J = 0,\ M = 0) \tag{6.12c}$$

If the strength of the potential V_0 is treated as an unknown quantity at the beginning of the calculation and $m_0(jj')$ and E_j for all j and j' are taken to be known, Eq.(4.12a) becomes the eigenvalue–eigenvector equation for the known matrix M of which V_0^{-1} is the eigenvalue and the quantities Δ_j are proportional to the elements of the eigenvector. In general, M will have many eigenvalues; however, the eigenvalue for which the elements of the eigenvector are all real positive quantities will alone serve our purpose because the energy-gap parameters must necessarily be real and positive. Since the matrix elements on the right-hand side of Eq.(6.12c) are attractive, the matrix M is positive definite and by a theorem due to Frobenius, such a matrix has one, and only one, eigenvalue for which the eigenvector has all the elements positive. This theorem guarantees the type of solution we want, and in view of the uniqueness of the latter there is no ambiguity in the method.

It is clear, however, that the quasi-particle energies E_j for all j must be known at the beginning of an IGE calculation. Usually, one assumes that the lowest few levels of the odd-mass nuclei will be very nearly pure single-quasiparticle type states. Therefore, their observed energies can be directly fed as input data for E_j in the IGE method. The results will be unreliable to the extent that this starting hypothesis about the nature of the levels of the odd-mass nuclei goes wrong.

The following check for the consistency of the method is usually applied. We have already remarked that the elements of the special eigenvector of M, in which we are interested, are proportional to the energy gap parameters Δ_j; this is because the system of Eqs (6.12a) for all j form a set of homogeneous equations for the unknown quantities Δ_j and as such remain unaltered through the multiplication of any overall constant, say, ξ. Let us denote the elements of the eigenvector by $\bar{\Delta}_j$ and then $\Delta_j = \xi \, \bar{\Delta}_j$ where ξ has to be determined. For this purpose, one first writes down ($\epsilon_j - \lambda$) from E_j and Δ_j

$$(\epsilon_j - \lambda)^2 + \Delta_j^2 = E_j^2$$

or

$$(\epsilon_j - \lambda) = \pm \{E_j^2 - \Delta_j^2\}^{\frac{1}{2}} = \pm \{E_j^2 - \xi^2 \bar{\Delta}_j^2\}^{\frac{1}{2}} \qquad (6.13)$$

To settle the sign of this expression one has, once again, to take recourse to experimental facts. The information needed is whether or not the occupation probability v_j^2 of the level j as measured in nucleon stripping or pickup experiments exceeds $\frac{1}{2}$. According to the interpretation of λ given in the subsection following Eq.(4.60), we know that ($\epsilon_j - \lambda$) is negative or positive, depending on whether v_j^2 is greater or less than $\frac{1}{2}$, respectively. Having settled the sign in this manner, the expression (6.13) for ($\epsilon_j - \lambda$) becomes specified to the extent of an as yet undetermined ξ. The latter is then determined by using expression (6.13) in Eq.(4.50). Since E_j has to be larger than Δ_j, i.e. $\xi \bar{\Delta}_j$, we conclude that the positive number ξ must be less than ($E_j / \bar{\Delta}_j$). Very often Eq.(4.50) cannot be exactly satisfied with this restriction on ξ. In practice, therefore, one uses the value of ξ, subject to the above restriction, such that the departure of the right-hand side of Eq.(4.50) from the given nucleon number A be a minimum. When ($\epsilon_j - \lambda$) for all the levels have been completely determined in this manner, one can easily calculate the energies ϵ_j of all the single-particle states (not quasi-particle) with respect to one of them, say $\epsilon_{j'}$, to be treated as the reference state. If the whole procedure is repeated for a few odd-mass nuclei in a given region then the values of ϵ_j relative to the reference state can be plotted as a function of the mass number. For the internal consistency of the whole approach we must expect that the dependence on the mass number of this curve be as smooth and as slow as possible. The result of this consistency check for the odd-mass Ni-isotopes are shown in Fig.6.6, taken from the work of Gambhir [17]. The three curves in each diagram labelled EIC, EIA and s-δ correspond to three different sets of two-body matrix elements for the details of which the reader is referred to the original paper. It is clear that the consistency check of the IGE method is rather disturbing, which, in turn, may imply that some of the actual levels of the odd-mass nuclei used in the calculation cannot be interpreted as fairly good one-quasiparticle states.

6.2.3. Salient features of numerical calculations

The IGE method or the straightforward solution of the BCS-equations (as done in Refs [10,11]) both yield a set of values for the quasi-particle

energies E_j and the corresponding transformation coefficients u_j and v_j . With these quantities one then solves the vibrational equation for the even nuclei. The single-quasi-particle energies can be checked against the energy levels of the odd-mass nuclei, while the lowest eigenvalue of the vibrational equation gives the energy of the first 2^+ state of the even nuclei. This general program was carried out in the work of Refs [10, 11] . The B(E2) values were also calculated for the decay of the 2^+-state to the ground state. For the odd-mass nuclei Kisslinger and Sorensen [10] calculated magnetic and quadrupole moments. Expression (5.89b) for any single-particle type operator can be used to evaluate its expectation value in a one-quasi-particle state. Only the first line of this expression contributes, because the second line changes the number of quasi-particles, acting on any state. One can easily verify that the magnetic and quadrupole moment of a single-quasi-particle state will be equal to that of a single-particle state. Thus the quasi-particle theory cannot give any agreement with the observed values of these quantities unless one uses effective gyromagnetic ratios and an effective charge for the nucleon. An understanding of the latter quantities is, how-ever, beyond the capability of a theory that tries to interpret observed ground state of odd-mass nuclei as a one-quasi-particle state. For the magnetic moment, Kisslinger and Sorensen [10] used a δ-function interaction to pro-duce admixture of other shell-model configurations which could then cause additional contribution to the magnetic moment. Switching on of the quasi-particle interaction is not of very much help. This produces a mixture of three-quasi-particle states with the one-quasi-particle state. There is a coherent mixture of two-quasi-particle states which is identified as the vibrational 2^+ state (phonon-state) of the even nucleus. So there is a special three-quasi-particle state that can be looked upon as a single-quasi-particle coupled to the phonon. In the work of Ref.[10] , the admixture of this state to the one-quasi-particle state was taken into consideration. This type of admixture changes the electric quadrupole properties, but does not very much change the magnetic moment. For all the detailed results, the reader is referred to the original papers [10, 11] .

6.2.4. Extension of RPA-work — modified Tamm-Dancoff method

The work reviewed above becomes nearly useless if one attempts to explain the levels above the first 2^+ state in even nuclei and levels above the first few in the odd-mass nuclei. According to the simple RPA-theory, one expects to get states at roughly twice the energy of the calculated 2^+ state which have 2-phonon (i. e. a special admixture of four-quasi-particle states) character. The other two-quasi-particle states which are orthogonal to the one-phonon state also occur in this general neighbourhood of energy. Hence it becomes imperative to develop a theory that allows the admixture of two- and four-quasi-particle states. Since the zero-quasi-particle state is coupled by the part H_{40} of the quasi-particle residual interaction to the four-quasi-particle states, one is led to the diagonalization of the quasi-particle Hamil-tonian in the space of zero, two- and four-quasi-particle states. This proce-dure is usually called the modified Tamm-Dancoff approximation (MTDA) because it is a natural extension of the diagonalization in the two-quasi-particle space which is known by the name TDA. Just as the TDA can be generalized to RPA by allowing both creation and destruction of quasi-particle pairs, the MTDA method can also be generalized by allowing the

destruction of two- and four-quasi-particle states together with their creation. Such a treatment is called Higher Random Phase Approximation (HRPA). For details of these methods the reader is referred to the work of Refs [13, 12]. In the review presented here we shall mention only a few important points of the MTDA-approach.

For the odd-mass nuclei the MTDA-calculation should admix one-, three-, and five-quasi-particle states. In the calculations, done so far, only the admixture of one- and three-quasi-particle states has been taken into account.

One of the important points about the three-, and four-quasi-particle basis states was first pointed out by Sawicki [13] who was also the originator of the movement towards HRPA and MTDA methods and calculations. It is well-known from the shell-model classification of states that allowed anti-symmetric states of three- and four-fermions in the level $(n\ell j)$ span only a subspace of all possible states. The same result is true also for quasi-particles because they are also fermions. Let us consider a three-quasi-particle state of the type $[(b_j^\dagger, b_j^\dagger)^{J'}, b_j^\dagger]_M^J$, where J and M are the total angular momentum and its projection, J' is the angular momentum of the first two quasi-particles; the third quasi-particle has then been coupled to J' to produce the total J. According to our observation above, many such states will identically vanish, and sometimes two or more states with different J' but same J will be linearly dependent on each other. The same kind of observation holds for four quasi-particle states. If we recall our earlier work on TDA then the procedure for deriving the MTDA equations becomes pretty obvious: we will have to evaluate the commutator of H with one- and three-quasi-particle creation operators (in the case of odd nuclei) and two- and four-quasi-particle operators in the case of even nuclei. Since all three-quasi-particle creation operators of the above types and similar four-quasi-particle creation operators are not independent, it is clear that we have to exercise caution in obtaining a set of equations involving a set of non-redundant operators.

In the work of Ref.[12] a complete set of antisymmetric states of three- and four-quasi-particle states have been constructed by standard shell-model methods and the matrix elements of the quasi-particle interaction connecting different states have been obtained by a combination of shell-model and second-quantized techniques.

Sawicki and collaborators [13] followed a somewhat different technique based on the Schmidt orthogonalization procedure to construct their non-redundant set of states.

Another important caution that has to be exercised in this kind of work was also first pointed out by Sawicki [13]. This has to do with the elimination of spurious states. The existence of a spurious 0^+ state in the two-quasi-particle space is fairly well-known to earlier works. This spurious state can be derived in the following way. Consider the effect of the total number operator N operating on the ground state Ψ_0. Since

$$\hat{N} = \sum_a c_a^\dagger c_a = \sum_a v_a^2 + \sum_a (u_a^2 - v_a^2) b_a^\dagger b_a + \sum_a u_a v_a s_a (b_a^\dagger b_{-a}^\dagger + b_{-a} b_a)$$

and $b_a^\dagger b_a$ as well as $b_{-a} b_a$ produce zero acting on Ψ_0, we have

$$\hat{N}|\Psi_0\rangle = \sum_a v_a^2 |\Psi_0\rangle + \sum_a u_a v_a s_a b_a^\dagger b_{-a}^\dagger |\Psi_0\rangle$$

In the quasi-particle theory one equates $\sum_a v_a^2$ with the nucleon number A.
Had there been a strict conservation of the number of nucleons, we there-
fore should have obtained only the first term on the right-hand side. The
second term of this expression, i.e.

$$|\Psi\rangle = \sum_a u_a v_a s_a \, b_a^\dagger b_{-a}^\dagger \, |\Psi_0\rangle$$

is, thus, an entirely spurious state. By doing the angular-momentum coupling
for spherical nuclei, where u_a, v_a do not depend on the projection quantum
number, one can easily show that this represents an angular momentum zero
state.

Any four-quasi-particle state obtained by coupling a two-quasi-particle
state to the above $|\Psi\rangle$ is, therefore, spurious. Similar observation holds
for three-quasi-particle states. There can also be more complicated spurious
states in the four-quasi-particle case; for example, one can examine the
result of $\hat{N}^2$ on Ψ_0 and identify an additional spurious state, and so on. In
the work of Ref.[12], the spurious states arising from $|\Psi\rangle$, as defined above,
have been explicitly projected out. In Ref.[13] the authors have taken care
to eliminate some more spurious states. However, this scheme of obtaining
new spurious states by taking higher powers of N apparently looks like a
never-ending procedure. It seems that the procedure should be better under-
stood before generalizing it too much.

For all the mathematical details and numerical results the reader is
referred to the original papers. Only a few important aspects of the results
will be described below.

Figure 6.7, taken from Sawicki [18], shows the unperturbed energies
of 2-, 4- and 6-quasi-particle states in the Sn and Cd-region. It is clear
that there is considerable overlap between the upper part of the 2qp-spectrum
with the lower part of the 4qp-spectrum, and so on. In the MTDA calculation,
a convenient upper cut-off to the unperturbed energy is usually chosen at the
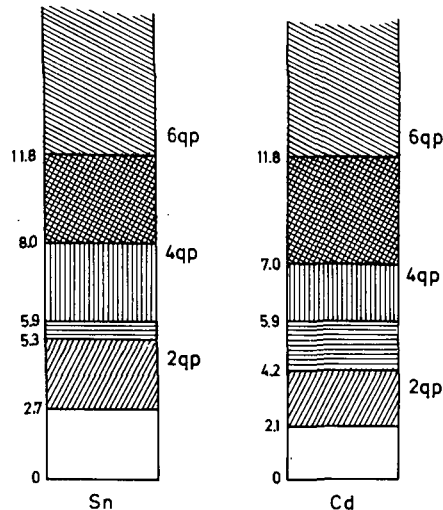
FIG. 6.7. A schematic representation of the bands of the possible two-, four- and six-qp "unperturbed"
excitation energies of IQM in the cases of Sn and Cd appropriate to 0^+, 2^+, 4^+, etc. (energies in MeV).

TABLE 6.5. QUASI-PARTICLE CONTRIBUTION TO THE MAGNETIC
MOMENT IN NUCLEAR MAGNETON. 1_{qp} DENOTES THE VALUE FOR
A SINGLE-QUASI-PARTICLE STATE, AND μ IS THE VALUE
CALCULATED WITH THE QUASI-PARTICLE WAVE FUNCTIONS
HAVING THREE-QUASI-PARTICLE ADMIXTURE. (see Ref.[12])

J^π	1_{qp}	μ			
		A = 59	A = 61	A = 63	A = 65
$1/2^-$	0.64	0.74	0.75	0.68	0.65
$3/2^-$	-1.91	-2.14	-2.22	-2.12	-1.97
$5/2^-$	1.36	1.35	1.36	1.38	1.38

TABLE 6.6. M1-TRANSITION STRENGTH B(M1) IN UNITS OF
SQUARED NUCLEAR MAGNETON (Ref.[12])

Transition	Nucleus	B(M1)	
		MTDA	1_{qp}
$1/2^- \rightarrow 3/2^-$	59	0.91	1.05
	61	0.88	1.02
$3/2^- \rightarrow 1/2^-$	63	2.00	2.05
	65	2.16	2.13

energy at which the 6qp energies start overlapping with the 4qp-energies.
Unless such a cut-off is chosen the number of 4qp-states becomes very large
and one gets energy matrices of terribly large size to diagonalize.

Table 6.5 lists the magnetic moment of several odd-mass nuclei in the
Ni-region, calculated in Ref.[12]. As remarked earlier, the admixture of
the three-quasi-particle states causes very little change in the magnetic
moment; the calculated changes are of the same order of magnitude as the
basic uncertainty of about 0.2 nm (nuclear magneton) inherent in the mag-
netic moment operator itself. Table 6.6 shows similar results for the M1-
transition strength, once again the same observation about the unimportance
of three-quasi-particle admixture is seen to hold. Table 6.7 lists the E2-
transition strength of odd-mass nuclei. Here the MTDA values are some-
times significantly different from the one-quasi-particle values.

Tables 6.8, 6.9 and 6.10 show some of the results of calculation in
Ref.[12] on the even Ni-isotopes. The observed B(E2) values agree well
with the calculated values with a fairly consistent choice of the effective
charge of a nucleon. There are several important features revealed by the
percentage strength of the four-quasi-particle states, shown in brackets
in Table 6.8. In the first place, the first excited 0^+ and 4^+ are never predo-
minantly four-quasi-particle states and hence their interpretation as two-
phonon states is not valid. Such an interpretation is tolerably good only for
the second 2^+-state. In all cases there is a significant admixture of two-

TABLE 6.7. E2- TRANSITION STRENGTH IN UNITS OF $e_{eff}^2 F^4$ WHERE
$F = 10^{-13}$ cm AND e_{eff} IS THE EFFECTIVE CHARGE OF THE NEUTRON
(Ref.[12])

Transition	Interaction	A = 59		A = 61	
		1_{qp}	MTDA	1_{qp}	MTDA
$1/2^- \to 3/2^-$	EIC	6.1	10.8	0.53	3.5
	EIA	6.2	12.9	0.50	6.6
	QQ	6.9	12.4	0.77	2.9
	S-δ	6.6	3.6	0.59	0.19
$5/2^- \to 3/2^-$	EIC	1.5	0.46	0.02	0.32
	EIA	1.6	0.98	0.03	0.16
	QQ	1.6	0.05	0.03	1.55
	S-δ	1.5	3.9	0.02	1.2
		A = 63		A = 65	
$3/2^- \to 1/2^-$	EIC	2.0	1.1	15.5	20.2
	EIA	2.2	0.38	15.6	8.0
	QQ	1.4	0.03	13.3	5.1
	S-δ	2.1	1.9	15.9	2.4
$3/2^- \to 5/2^-$	EIC	0.50	0.87	2.2	1.8
	EIA	0.50	1.7	2.2	3.9
	QQ	0.44	2.9	2.0	3.2
	S-δ	0.49	0.09	2.2	0.78

and four-quasi-particle states; in the phonon language,this is caused by the
anharmonicity of vibration.

Figures 6.8 and 6.9 show the calculated spectra for the Ni and Sn-
isotopes. In the former case, the chi-square value corresponding to the
fit to all the observed levels with the two-body matrix elements determined
by the Argonne group [19] has nearly the same magnitude as achieved by the
direct least squares fit of these authors (i.e. Ref.[19]). In the case of the
Sn-isotopes the model pairing plus quadrupole force was used for the calcu-
lation. It is clear that, although this model is fairly successful for the first
2^+ level, the results for the higher excited states are extremely discouraging.
There is invariably a large gap in the calculated spectra between the first
excited 2^+ level and the next excited level; and after that the calculated levels
are crowded inside too small an energy band. This shortcoming of the re-
sults has been associated conclusively with the inadequacy of the pairing-
plus-quadrupole model interaction.

The numerical results by Sawicki and collaborators, using realistic
two-body matrix elements with core-excitation correction, in the region
of Sn are presented in these Proceedings by Gmitro. Only a very small

TABLE 6.8. CALCULATED ENERGY LEVELS (MeV) OF Ni ISOTOPES. NUMBERS IN PARENTHESES DENOTE PERCENTAGE ADMIXTURE OF FOUR-QUASI-PARTICLE STATES. THE TWO ENTRIES FOR EACH LEVEL CORRESPOND, RESPECTIVELY, TO THE BCS AND IGE VALUES OF UNPERTURBED QUASI-PARTICLE ENERGIES AND OCCUPATION PROBABILITIES (SEE TEXT FOR THE EXPLANATION OF BCS AND IGE). THE STRENGTH OF THE $Q \cdot Q$ INTERACTION, USED IN THE CALCULATION, IS GIVEN BY $\pi^{-1}b^4\chi = 0.097$ WHERE b IS THE OSCILLATOR WELL PARAMETER ($b^2 = \hbar/M\omega$) (Ref.[12])

A	0+			2+			4+		
	EIC	EIA	Q·Q	EIC	EIA	Q·Q	EIC	EIA	Q·Q
58	2.17	2.17	2.31	1.12	1.18	1.28	1.92	2.14	2.23
	2.10	1.99		1.06	1.10		1.90	2.07	
	3.69	3.36	3.32	2.40	2.57	2.09	3.34	3.55	2.97
	3.29	2.90		2.26	2.40		3.24	3.26	
60	2.47 (10.6)	2.45 (11.4)	2.38 (27.7)	1.77 (0.4)	1.78 (0.1)	1.49 (2.3)	2.22 (18.7)	2.62 (5.0)	2.62 (3.1)
	2.47 (11.7)	2.41 (11.2)		1.80 (0.5)	1.75 (0.1)		2.24 (21.5)	2.60 (19.7)	
	3.45 (39.2)	3.11 (60.9)	2.97 (21.6)	2.37 (66.2)	2.38 (83.7)	2.34 (40.0)	2.86 (86.4)	3.00 (97.1)	2.85 (6.4)
	3.41 (38.6)	2.96 (74.8)		2.36 (66.6)	2.21 (91.8)		2.86 (84.2)	2.80 (82.8)	
62	2.50 (11.3)	2.43 (19.4)	2.55 (26.9)	1.83 (2.6)	1.86 (0.4)	1.57 (0.9)	2.19 (33.8)	2.67 (32.9)	2.80 (3.3)
	2.26 (17.2)	1.90 (25.5)		1.82 (4.2)	1.83 (7.5)		2.50 (31.4)	2.80 (4.9)	
	3.22 (47.4)	2.98 (55.6)	2.91 (14.8)	2.29 (74.2)	2.26 (86.7)	2.35 (62.3)	2.80 (71.7)	2.97 (71.5)	2.90 (3.7)
	3.30 (30.4)	2.84 (25.3)		2.26 (49.9)	2.28 (47.8)		2.72 (74.4)	3.04 (95.8)	
64	2.46 (4.1)	2.37 (12.9)	2.66 (10.5)	1.70 (2.2)	1.77 (0.9)	1.52 (1.0)	2.28 (23.1)	2.74 (22.9)	2.72 (1.4)
	2.60 (4.5)	2.28 (19.4)		1.84 (0.4)	1.80 (1.1)		2.50 (8.5)	2.83 (16.7)	
	3.25 (44.2)	3.05 (51.9)	2.86 (15.3)	2.45 (57.7)	2.45 (80.5)	2.45 (64.1)	2.84 (80.7)	3.22 (80.4)	3.01 (4.9)
	3.71 (95.9)	3.17 (67.7)		2.58 (69.5)	2.39 (83.5)		2.88 (92.8)	3.07 (83.0)	

TABLE 6.9. B(E2) VALUES OF Ni ISOTOPES IN UNITS OF $e_{eff}^2 F^4$ WHERE $F = 10^{-13}$ cm, AND e_{eff} = EFFECTIVE CHARGE OF THE NEUTRON. THE COLUMN HEADINGS DENOTE THE VARIOUS E2 TRANSITIONS CONNECTING THE GROUND LEVEL (0), AND EXCITED STATES (J). THE SUBSCRIPT ON ANY EXCITED STATE J HAS THE FOLLOWING MEANING: 2_1, 2_2 DENOTE, RESPECTIVELY, THE FIRST AND SECOND EXCITED STATES OF ANGULAR MOMENTUM J = 2. THE LAST COLUMN GIVES THE QUADRUPOLE MOMENT OF THE 2_1 STATE IN BARNS ($= 10^{-24}$ cm^2). TWO LINES FOR EACH OF EIC, EIA REFER TO BCS AND IGE (Ref.[12])

A	Poten-tial	2_1-0	2_2-0	2_2-2_1	2_2-0_1	0_1-2_1	4_1-2_1	4_1-2_2	$\langle Q \rangle$
60	QQ	72.35	0.43	8.50	0.82	34.72	9.82	0.13	−0.074
	EIC	56.96	0.62	25.41	6.25	0.58	10.88	0.93	−0.051
		57.88	0.74	26.42	5.87	0.67	9.86	0.93	−0.044
	EIA	57.64	0.55	32.26	9.67	3.64	7.70	2.28	−0.047
		66.14	0.15	34.85	7.39	3.59	6.98	2.21	−0.033
62	QQ	85.63	0.073	24.62	0.002	16.96	1.55	1.11	−0.037
	EIC	66.82	0.44	23.07	2.64	1.70	3.86	0.014	−0.029
		56.00	3.14	23.00	0.93	0.73	2.36	0.65	0.025
	EIA	71.38	0.52	33.99	4.29	5.58	3.19	0.91	−0.0007
		45.55	11.31	18.29	1.10	6.34	0.08	0.26	0.064
64	QQ	80.72	0.078	24.40	0.011	4.28	0.04	4.67	0.019
	EIC	59.58	1.77	13.89	0.091	2.40	0.33	0.47	0.023
		63.81	0.022	19.38	0.34	6.09	2.06	0.89	0.055
	EIA	67.97	0.08	23.72	1.81	6.45	0.60	0.004	0.039
		68.10	0.72	25.20	1.45	10.16	0.13	0.071	0.054

part of their results, calculated with the δ-function interaction is presented here in Tables 6.11 and 6.12. These two tables refer to 2^+ and 4^+ states, respectively. The penultimate column in these tables shows the results of simple Tamm-Dancoff calculations using two-quasi-particle states only. The column before that gives the percentage of four-quasi-particle states in the wave functions. The second and third columns give the calculated energies without and with projection of the spurious states. A comparison with the last column, which gives the observed energies, will immediately establish the necessity of the removal of spurious states. For many other important results by this group of workers the reader is referred to the original references and the paper by Gmitro in these Proceedings.

TABLE 6.10. EXPERIMENTAL VALUES OF B(E2) FOR 2_1-0 IN UNITS OF $10^{+2}e^2F^4$. A VALUE OF e_{eff} = 1.35e GIVES EXCELLENT AGREEMENT OF THESE VALUES WITH THE CORRESPONDING RESULTS IN TABLE 6.9 FOR EIC (Ref.[12])

Nucleus	Experiment B(E2) 2_1-0
^{58}Ni	1.46 ± 0.07
^{60}Ni	1.94 ± 0.08
^{62}Ni	1.68 ± 0.08
^{64}Ni	1.74 ± 0.17
^{116}Sn	4.24 ± 0.25
^{118}Sn	4.60 ± 0.27
^{120}Sn	4.40 ± 0.22
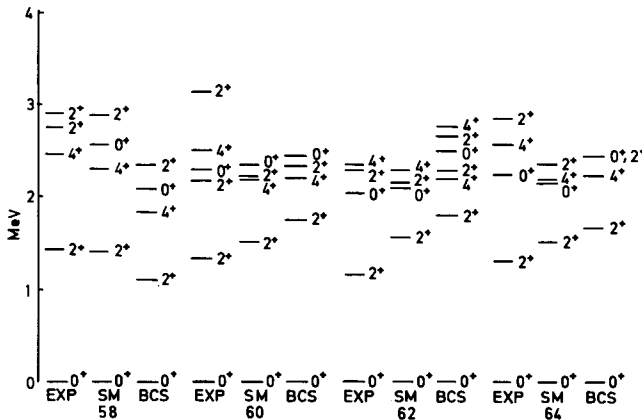
FIG. 6.8.   Energy levels of even Ni isotopes (58-64). EXP: experimental spectra; SM: spectra calculated with EIC matrix elements in Ref.[1]); BCS: spectra calculated by the MTDA method and EIC two-body matrix elements in the present work.

6.3.   Vibrational levels in deformed nuclei

In deformed nuclei the single-particle, as well as single-quasi-particle states are not specified by given angular momentum quantum numbers. In the case of deformation with axial symmetry only the projection quantum number is a good quantum number for these states, while for deformation having no axis of symmetry even this is not true. However, under very general circumstances, a single-particle state of a deformed nucleus and its time-reversed states are usually found to be degenerate. This has been verified, for example, in all the Hartree-Fock-type calculations done up to the present time. So, we take the degeneracy of a quasi-particle state m and its time-reversed state $\bar{m}$, to be granted. Furthermore, we keep in mind the general result (4.29b), namely, $|\bar{\bar{m}}\rangle = -|m\rangle$
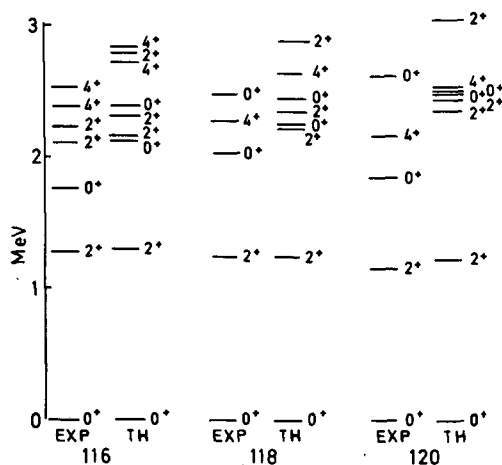
FIG.6.9. Energy levels of even Sn isotopes (116-118). EXP: experimental spectra; TH: spectra calculated with $Q \cdot Q$ interaction.

Since the single-quasi-particle states do not have given angular momenta, we do not do the angular momentum coupling in the quasi-particle pair creation and destruction operators, as we did for spherical nuclei. On the other hand, we use the RPA-equations without this angular-momentum coupling derived in section 5 and embodied in Eqs (5.41), (5.44) and (5.47). Because of the presence of a summation over k, ℓ in Eq.(5.47), we can clearly rewrite the right-hand side changing the summation indices to $\overline{k}, \overline{\ell}$ throughout. The equation for the commutator $[H, A_{mn}]$ which can be derived easily from $[H, A_{mn}^{\dagger}]$ as mentioned under Eq.(5.47), can also be changed to an equation for the commutator $[H, A_{\overline{mn}}]$ where

$$A_{\overline{mn}} = b_{\overline{m}} b_{\overline{n}}$$

In the usual way, we sandwich these equations between $\langle \Psi |$ and $|\Psi_0\rangle$ and define the following amplitudes:

$$Z_{mn}^{(\pm)} = \langle \Psi | (A_{mn}^{\dagger} \pm A_{\overline{mn}}) | \Psi_0 \rangle \tag{6.14}$$

Adding and subtracting the equations for $[H, A_{mn}^{\dagger}]$ and $[H, A_{\overline{mn}}]$ sandwiched between $\langle \Psi |$ and $|\Psi_0\rangle$ we easily obtain the following coupled equations satisfied by the above amplitudes:

$$EZ_{mn}^{(+)} = (E_m + E_n) Z_{mn}^{(-)} + \sum_{(i,j)} [(ij|v|mn) (u_i u_j + v_i v_j) (u_m u_n + v_m v_n)$$

$$- \{(j\overline{m}|v|n\overline{i}) + (i\overline{m}|v|n\overline{j})\} (u_m v_n - v_m u_n) (u_i v_j - v_i u_j)] Z_{ij}^{(-)}$$

$$\tag{6.15a}$$

$$EZ_{mn}^{(-)} = (E_m + E_n) Z_{mn}^{(+)} + \sum_{(i,j)} [ij|v|mn) (u_i u_j - v_i v_j) (u_m u_n - v_m v_n)$$

$$- \{(j\overline{m}|v|n\overline{i}) - (i\overline{m}|v|n\overline{j})\} (u_m v_n + v_m u_n)(u_i v_j + v_i u_j)] Z_{ij}^{(+)} \tag{6.15b}$$

TABLE 6.11. RESULTS FOR THE FOUR LOWEST-LYING 2^+ STATES OF
THE QUASI-PARTICLE SECOND TAMM-DANCOFF (QSTD)
CALCULATIONS [13] FOR EVEN TIN ISOTOPES

$J^{\pi} = 2^+$ A	Level energy (MeV) (case a)		b components (%) (case 2)	OTD levels (MeV)	Observed level energies (MeV)
	(1) No projection	(2) With projection			
116	0.40	1.49	19	1.56	1.291
	1.24	2.05	27	2.62	2.108
	1.42	2.28	42	2.90	2.224
	1.56	2.49	23		
118	-0.06	1.29	14	1.36	1.229
	0.78	1.95	24		
	1.03	2.04	40		
	1.40	2.38	78		
120	-0.41	1.18	12	1.27	1.166
	0.42	1.81	23		
	0.77	2.09	40		
	1.29	2.36	73		
122	-0.66	1.13	10	1.23	1.142
	0.15	1.76	20		
	0.59	2.17	60		
	1.24	2.33	56		
124	-0.85	1.10	8	1.21	1.132
	-0.06	1.74	17		
	0.47	2.19	92		
	1.22	2.39	25		

Here the brackets round the summation symbols i, j denote that a given
pair (i, j) will be counted only once in the summation and not twice as (i, j)
and (j, i).

In conformity with what has been done for spherical nuclei, one can
introduce models for v in order to simplify these general equations. The
usual assumption is to ignore the matrix elements $(ij|v|mn)$ and substitute
the matrix element $(j\bar{m}|v|n\bar{i})$ by a factorable form

TABLE 6.12. RESULTS FOR THE FOUR LOWEST-LYING 4$^+$ STATES OF
THE QSTD CALCULATIONS [13] FOR EVEN TIN ISOTOPES.

$J^\pi = 4^+$ A	Level energy (MeV) (case a)		b components (%) (case 2)	QTD levels (MeV)	Observed level energies (MeV)
	(1) No projection	(2) With projection			
116	1.07	2.15	20	2.44	2.391
	1.74	2.61	23	3.16	2.531
	1.90	2.95	58	3.49	2.803
	2.19	3.01	65	3.75	3.047
118	0.59	1.87	17	2.30	2.278
	1.74	2.81	96		
	2.01	3.12	20		
	2.03	3.37	16		
120	0.27	1.78	15	2.27	2.183
	1.78	2.76	98		
	1.92	3.39	96		
	1.96	3.41	21		
122	0.02	1.74	12	2.25	
	1.83	2.71	99		
	1.87	3.33	98		
	1.93	3.65	64		
124	-0.16	1.75	10	2.22	
	1.79	2.65	99		
	1.84	3.41	99		
	1.94	3.70	88		

$$- (j\overline{m}|v|n\overline{i}) = \sum_\mu \kappa_\lambda \langle j|\Omega_\mu^\lambda|\overline{i}\rangle \langle \overline{m}|\Omega_{\mu^*}^{\lambda*}|n\rangle \qquad (6.16)$$

This expression will follow from a multipole potential of the type

$$V = \kappa_\lambda \sum_\mu \Omega_\mu^\lambda(1)\,\Omega_\mu^{\lambda*}(2) \qquad (6.17a)$$

where 1 and 2 denote nucleon co-ordinates, κ_λ denotes the strength of the interaction and the multipole operator Ω_μ^λ is usually taken to be

$$\Omega_\mu^\lambda(\vec{r}) = r^\lambda Y_\mu^\lambda(\theta, \phi) \tag{6.17b}$$

It is clear that expression (6.16) actually corresponds to the exchange part of the matrix element on the left-hand side when one uses the potential (6.17a).

For the states $|i\rangle$, $|j\rangle$ etc. one can use expansions in terms of basis states $|\alpha\rangle$, $|\beta\rangle$ etc. which are characterized by good angular momentum projection, etc. Thus

$$|i\rangle = \sum_\alpha x_\alpha^i |\alpha\rangle \tag{6.18a}$$

and

$$|\bar{i}\rangle = \sum_\alpha x_\alpha^i (-1)^{j_\alpha - m_\alpha} | -\alpha\rangle \tag{6.18b}$$

where $|-\alpha\rangle$ stands for a set of quantum numbers in which the projection quantum number is $-m_\alpha$. In most applications of the theory, one specifically assumes the existence of an axis of symmetry for the nuclei and hence the state $|i\rangle$ is characterized by a given projection quantum number and the same quantum number goes with all the basic states $|\alpha\rangle$ on the right-hand side of Eq.(6.18a).

The model potential, described by Eq.(16), converts the Eqs (6.15a,b) to equations of the type (6.85d, e). This task is left as a simple exercise to the reader. The solutions of such equations had already been worked out in Eq.(5.87). Usually one takes a sum of quadrupole-plus-octupole-type potential for v. The matrix elements are then obtained from Eq.(6.16) by adding the results for $\lambda = 2$ and $\lambda = 3$. The parity of these multipoles tells us that in the case of $\lambda = 2$, the quasi-particle pair states (m,n), (i,j), etc. that are coupled through Eqs (6.15a, b) have even parity, while in the case of $\lambda = 3$, the pair states have odd parity. Thus, the vibrational equations corresponding to these two multipoles in the potential are completely de-coupled from each other and can be solved separately.

For details of the theoretical derivation and the properties of nuclei calculated, the reader is referred to the work by Soloviev [20]. A few typical results are shown in Figs 6.10, 6.11, 6.12, 6.13 and 6.14. Al-though the general trends are reproduced in these calculations, the model potential used in the work seems to be too restrictive.

6.4. Outlook

In these lectures we have presented a systematic method of calculating vibrational states based on an expansion in terms of number of quasi-particles; in applications the expansion has been cut off at four-quasi-particles for even nuclei and three-quasi-particles for odd-mass nuclei. No investigation has been made into the rapidity of convergence of this ex-pansion. There is an alternative approach based on an expansion in terms
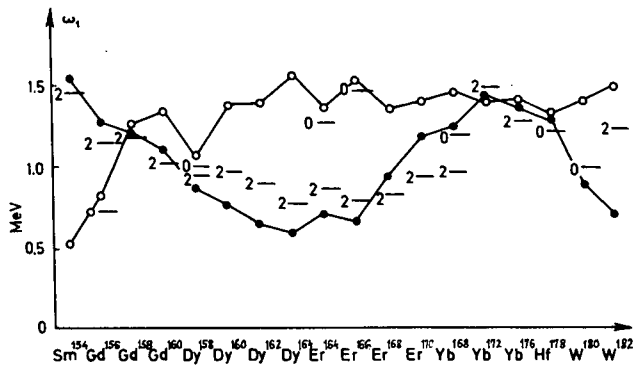
FIG. 6.10.   Energies [20] of first 2^+ and 0^+ excited quadrupole states in the region $154 \leq A \leq 182$, for $\kappa^{(2)} = 10\,A^{-4/3}\hbar\omega_0$, $\kappa^{(2)}_{np} = \kappa^{(2)}$
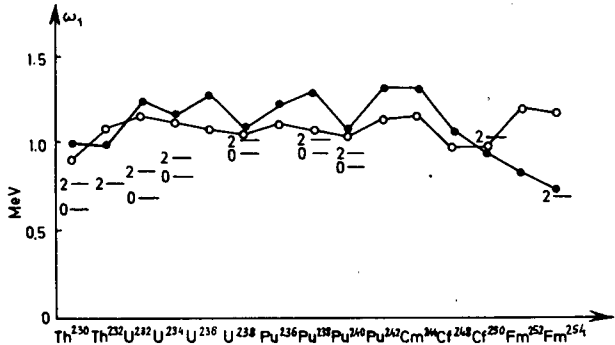
Kπ	exp.	theor.
2^+	2^-	
0^+	-	

FIG. 6.11.   Energies [20] of first 2^+ and 0^+ excited quadrupole states in the region $228 \leq A \leq 254$, for $\kappa^{(2)} = 10\,A^{-4/3}\hbar\omega_0$, $\kappa^{(2)}_{np} = \kappa^{(2)}$.

Kπ	exp.	theor.
2^+	2^-	
0^+	-	

of number of phonons. Some of the pertinent references [21] are given at the end; no specific calculation based on this method is known to the present author.

The groups in Bologna and Trieste (preprint and private communication) are engaged in removing one important deficiency of the method presented here. Since detailed agreement is being sought for the spectra of individual
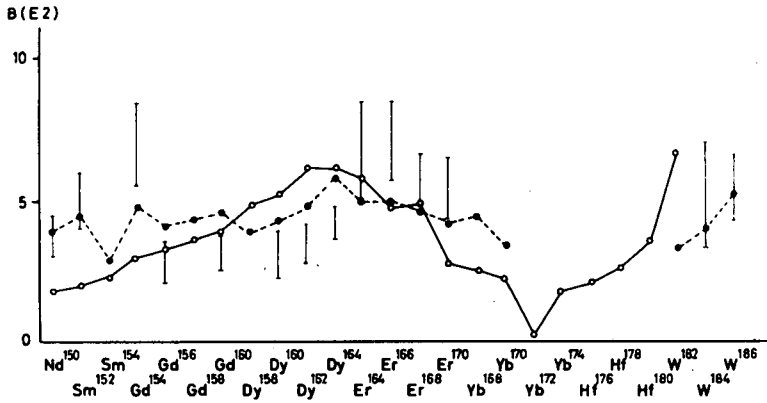
FIG. 6.12. Calculated B(E2) values in single-particle units. Experimental values given with error bars. Theoretical values for $\kappa^{(2)} = 9.5\,A^{-4/3}\,\hbar\dot{\omega_0}$ denoted by ⟋⟍ and for $\omega_0 \approx \omega_1^{\exp}$ by --- ● --- (Ref. [20]).
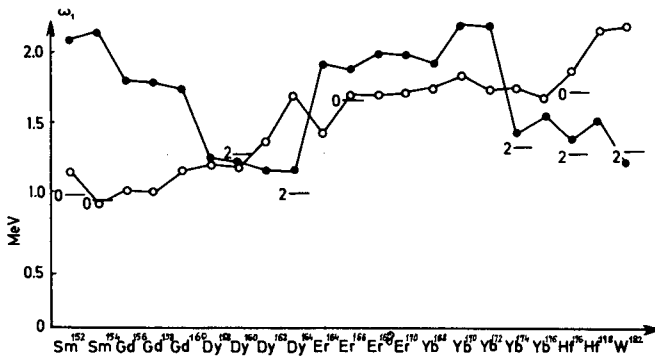
FIG. 6.13. Energies [20] of first 0^- and 2^- excited octupole states in the region $152 \leq A \leq 182$, for $\kappa^{(3)} = 0.00102\,\hbar\dot{\omega_0}$.

Kπ	exp.	theor.
0^-	0^-	⟋▲⟍
2^-	2^-	⟋⟍

nuclei, these authors rightly lay the emphasis on projecting the correct number of particles out of the quasi-particle wave functions.

Klein and collaborators [22] have been working on an alternative theory that conserves the number of particles through the entire formalism.

The major criticism against all these theories is that they are based on a single equilibrium shape of the nucleus. The Kumar-Baranger theory emphasizes the dynamical role that the deformation parameter should play. The Hill-Wheeler method which uses a variational wave function in which an integration has been carried over the deformation parameter has the ability to serve as a bridge between the approach presented here and the dynamical approach that is necessary for a more satisfactory theory.
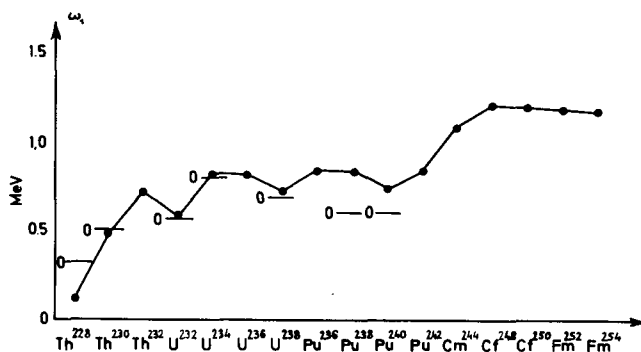
FIG. 6.14.   Energies [20] of first 0^- excited octupole states in the region $228 \leq A \leq 254$, for $\kappa^{(3)} = 0.00052\hbar\omega_0$.

$K\pi$	exp.	theor.
0^-	0^-	

REFERENCES

[1] ELLIOTT, J.P., FLOWERS, B.H., Proc. Roy. Soc. A242 (1957) 57.

[2] GILLET, V., Nucl. Phys. 51 (1964) 410; GILLET, V., SANDERSON, E.A., Nucl. Phys. 54 (1964) 472; GILLET, V., VINH MAU, N., Nucl. Phys. 54 (1964) 321.

[3] GREEN, A.M., "Reports on Progress in Physics", 28 (1965) 113.

[4] CARTER, E.B., MITCHELL, G.E., DAVIS, R.H., Phys. Rev. 133B (1964) 1421.

[5] FALLIEROS, S., FERRELL, R.A., PAL, M.K., Nucl. Phys. 15 (1960) 363; PAL, M.K., LEE, Y.C., Bull. Amer. Phys. Soc. 4 (1959) 407; LEE, Y.C., Ph.D. Thesis of Physics Department, University of Maryland (1963).

[6] BROWN, G.E., GREEN, A.M., Nucl. Phys. 75 (1966) 401.

[7] RIPKA, G., BASSICHIS, W., Phys. Lett. 15 (1965) 320.

[8] STEPHENSON, G.J., Jr., BANERJEE, M.K., Phys. Letters 24B (1967) 209.

[9] BLOMQVIST, I., WAHLBORN, S., Ark. Fys. 16 46 (1959).

[10] KISSLINGER, L.S., SORENSEN, R.A., K. Danske Vidensk. Selsk. Mat.-Fys. Meddr. 32 No.9 (1960); Rev. Mod. Phys. 35 (1963) 853.

[11] ARVIEU, R., BARANGER, E., BARANGER, M., GILLET, V., VENERONI, M., Phys. Letts 4 (1963) 119; ARVIEU, R., VENERONI, M., Phys. Letts 5 (1963) 142; ARVIEU, R., SALUSTI, E., VENERONI, M., Phys. Letts 8 (1964) 334.

[12] PAL, M.K., GAMBHIR, Y.K., RAJ, R., Phys. Rev. 155 (1967) 1144; Phys. Rev. 162 (1967) 1139; Phys. Rev. 163 (1967) 1004.

[13] SAVOIA, M., SAWICKI, J., TOMASINI, A., Nuova Cim. 32 (1964) 991; OTTAVIANI, P.L., SAVOIA, M., SAWICKI, J., TOMASINI, A., Phys. Rev. 153 (1967) 1138; OTTAVIANI, P.L., SAVOIA, M., SAWICKI, J., Phys. Letts 24B (1967) 353; GMITRO, M., HENDEKOVIĆ, J., SAWICKI, J., Phys. Letts 26B (1968) 252.

[14] LAWSON, R.D., MACFARLANE, M.H., KUO, T.T.S., Phys. Letts 22 (1966) 168; KUO, T.T.S., Nucl. Phys. A90 (1967) 199; Phys. Letts 26B (1967) 63; Nucl. Phys. A103 (1967) 71.

[15] GMITRO, M., HENDEKOVIĆ, J., SAWICKI, J., Phys. Rev. 169 (1968) 983; GMITRO, M., RIMINI, A., SAWICKI, J., WEBER, T., Phys. Rev. 175 (1968) 1243.

[16] GILLET, V., RHO, M., Phys. Letts 21 (1966) 82; GILLET, V., GIRAUD, B., RHO, M., Nucl. Phys. A103 (1967) 257.

[17] GAMBHIR, Y.K., Nucl. Phys. A120 (1968) 193.

[18] SAWICKI, J., in 12th Int. Summer Meeting in Physics, Herceg Novi, Yugoslavia (1967) 281.

[19] COHEN, S., LAWSON, R.D., MACFARLANE, M.H., PANDYA, S.P., SOGA, M., Phys. Rev. 160 (1967) 903.

[20] SOLOVIEV, V.G., Atom. Energy Rev. $\underline{3}$ (1965) 117; in Nuclear Structure (Proc. Symp. Dubna, 1968) IAEA, Vienna (1968) 101.

[21] BELYAEV, S.T., ZELEVINSKY, V.G., Nucl. Phys. $\underline{39}$ (1962) 582; SORENSEN, B., Suppl. to J. Phys. Soc. Japan $\underline{24}$ (1968) 588; see the second article for other references.

[22] KLEIN, A., Lectures delivered at the Boulder Summer School of Theoretical Physics, July 1968; and preprint. This article lists all the references by this group of workers.

REALISTIC POTENTIALS IN
NUCLEAR-STRUCTURE CALCULATION

M. GMITRO
Nuclear Research Institute,
Řež, Prague, Czechoslovakia

Abstract

REALISTIC POTENTIALS IN NUCLEAR-STRUCTURE CALCULATION.
  1. Residual interaction; 2. Reaction matrix; 3. Approximations; 4. Model space.

1.   RESIDUAL INTERACTION

The use of simple schematic interactions (like pairing force and
quadrupole-quadrupole force) permits a very simple and fruitful search
for new phenomena in the nuclear structure and clarification of the quali-
tative features of nuclear states. However, in so doing one must not
expect a detailed quantitative description. On the other hand, quite compli-
cated phenomenological potentials widely used recently involve unfavourable
freedom in the choice of adjustable parameters. The same criticism ap-
plies to the "effective-matrix-elements approach" pioneered by Talmi:
two-particle matrix elements themselves were used as parameters of the
theory. To avoid increasing the number of these parameters very much,
only rather limited configuration mixing can be allowed for.

The present notes are devoted to the use in nuclear spectroscopy of the
potentials which were determined from an analysis of the nucleon-nucleon
scattering and deuteron data. Such realistic potentials usually consist of
central, tensor, spin-orbit (L.S. and L.S.)[2] terms together with various
exchange characteristics. In the description of low-energy nuclear pheno-
mena usually only S-, P- and D-states together with $^3S_1$-$^3D_1$ coupling term
are considered.

The change of sign in the $^1S_0$ state phase shift at about 240 MeV in the
free N-N scattering shows that the character of two-nucleon interaction at
short distances is repulsive. According to the technique used for describing
this peculiar character of the interaction, two classes of the realistic po-
tentials can be introduced.

A dynamic description of the repulsion mentioned was chosen in the non-
local separable or velocity-dependent potentials. The best presently avail-
able potential of this type is that of Tabakin [1]. The possibility of the
direct use of this potential in the nuclear structure calculation and in the
H-F procedure should be pointed out.

Static realistic potentials [2,3] are characterized by a repulsive core
of infinite magnitude (hard core) at short distances about $r = c = 0.4$ fm.
Sometimes hard-core repulsion can be replaced by less strong "soft"-core
repulsion. Both hard-core and soft-core potentials produce matrix ele-
ments which are very large (infinite in the case of hard core). Such po-
tentials cannot be applied directly in the nuclear spectroscopy. According
to the reaction-matrix theory, an appropriate modification is to replace
the potential v by the Brueckner reaction matrix t [4].

2.   REACTION MATRIX

Brueckner's method can be illustrated [5] by considering the interaction of two distinguishable particles having a mutual interaction described by a potential v.   The interaction energy

$$\Delta E = E - E_0 \tag{1}$$

defined by the Schrödinger equations

$$H_0 \phi = E_0 \phi \tag{2}$$

and

$$(H_0 + v)\, \Psi = E \Psi \tag{3}$$

can be evaluated by the perturbation methods if the interaction is weak enough.   In the case of a strong repulsive core in the potential, all the matrix elements involved become infinite, and the corresponding perturbation expansion is meaningless.   At the same time, however, ΔE can be finite.   This suggests that we should look for an expansion involving some operator different from the potential v.   For this purpose Eq.(3) can be rewritten in the integral form

$$\Psi = \phi - \frac{Q}{H_0 - E}\, v \Psi \tag{4}$$

where

$$Q = 1 - |\phi\rangle\langle\phi|$$

projects out the state ϕ.   Multiplying Eq.(4) by $(H_0 - E)$, we can check the equivalence of Eqs (3) and (4).   The eigenvalue condition originates in the form

$$\Delta E = \langle \phi | v | \Psi \rangle \tag{5}$$

Introducing an operator Ω which connects the wave functions Ψ and ϕ:

$$\Psi = \Omega \phi \tag{6}$$

a new operator t can be defined

$$t = v \Omega \tag{7}$$

which satisfies the equation

$$t = v - v \frac{Q}{H_0 - E}\, t \tag{8}$$

The energy shift ΔE is then given by

$$\Delta E = \langle \phi \, | \, t \, | \, \phi \rangle \tag{9}$$

For a weak potential v the last formula reduces to the usual perturbation expansion; it gives, however, a solution for the energy shift ΔE in the case of strong potential as well, provided that Eq.(8) is solved exactly or in some approximation.

The main point of this procedure can be seen if the iterative solution

$$t = v - \frac{Q}{e} \, v + v \, \frac{Q}{e} \, v \frac{Q}{e} v - \ldots \tag{10}$$

is examined. From this it is clear that the introduction of the reaction matrix involves re-arrangement of the perturbation series providing summation of the interaction up to all orders. This situation is illustrated in Fig.1, where the wavy line symbolizes the t-matrix, and the dashed line the potential v.
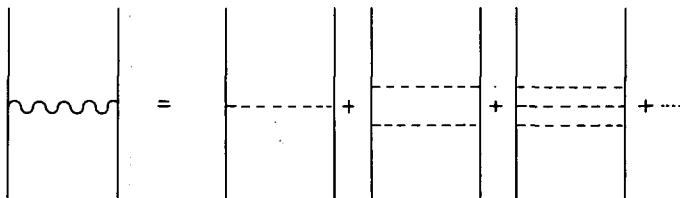
FIG.1. Reaction matrix corresponds to the summation of potential up to all orders.

3. APPROXIMATIONS

For a many-body problem like that of nuclear structure, an equation similar to Eq.(8) is obtained which differs, however, in the energy denominator and the Pauli projector Q.

The main difficulties in the solution of such an equation come from the propagator $P = Q/e$. The idea of the approximation [4] consists in choosing simple forms for P and v which produce at the same time a fairly accurate first approximation to the reaction matrix. From two sets of equations for exact t and approximate t_A matrices

$$P = \frac{Q}{e} \qquad\qquad P_A = \frac{Q_A}{e_A}$$

$$\Omega = 1 - Pt \qquad\qquad \Omega_A^\dagger = 1 - t_A^\dagger P_A^\dagger$$

$$t = v\Omega \qquad\qquad t_A = v_A \Omega_A$$

$$t^\dagger = \Omega^\dagger v^\dagger \qquad\qquad t_A^\dagger = \Omega_A^\dagger v_A^\dagger$$

the formal identity can be written

$$t = t - t_A^\dagger(\Omega + Pt - 1) + (\Omega_A^\dagger + t_A^\dagger P_A^\dagger - 1) t$$

where $\dagger$ stands for Hermitian conjugation. The last equation leads directly to the required relation of the exact and approximate reaction matrices

$$t = t_A^\dagger + \Omega_A^\dagger(v - v_A^\dagger) \, \Omega + t_A^\dagger(P_A^\dagger - P) t \tag{11}$$

3.1. The separation method by Moszkowski and Scott uses the division of the potential into short-range and long-range parts

$$v = v_S \theta(d - r) + v_L \theta(r - d) \qquad \theta(x) = \begin{cases} 1 & \text{if } x > 0 \\ 0 & \text{otherwise} \end{cases} \tag{12}$$

The separation distance d is chosen so that the attractive part of v_S balances the repulsive core. Then what remains is essentially v_L. With an auxiliary reaction matrix constructed for $Q_A = 1$ and $v_A = v_S$, Kuo and Brown [4] found by iterating expression (11) matrix elements of the singlet-even Hamada-Johnston potential

$$(n\ell\, ST | t | n' \ell' \, ST) \approx \delta_{\ell\ell'}\, (n\ell STJ | v_L | n' \ell' STJ) \tag{13}$$

and of the triplet even states of Hamada-Johnston potential:

$$(n\ell\, ST | t | n' \ell' \, ST) \approx (n\ell STJ | v_L - v_{TL} \frac{Q}{e} v_{TL} - t_S \frac{Q}{e} v_{TL} - v_{TL} \frac{Q}{e} t_S | n' \ell' STJ) \tag{14}$$

where v_{TL} stands for the long-range part of the tensor potential.

3.2. The reference spectrum method. When the potential outside of the repulsive core is never attractive (e.g. triplet-odd and singlet-odd Hamada-Johnston potential) the separation method is no longer applicable since it is based on the balance of the attractive and the repulsive parts of the potential. The reference-spectrum method provides a useful approximation in such cases. Two variants of this method correspond to the two single-particle bases which allow the separation of the relative motion and the centre-of-mass motion in the pair states. Plane-waves and harmonic-oscillator functions are these cases.

(a) The nuclear reaction matrix t is expanded in terms of a "reference" reaction matrix

$$t_R = v - v \frac{1}{h^{p.w.} - E_s} t_R \tag{15}$$

if the plane-wave intermediate states, suggested by the nuclear matter theory are considered. E_s is "starting" energy=energy in the initial state.

(b) The ground-state wave function of a bound nucleus is, however, localized. For this reason, intermediate states of a harmonic-oscillator basis were suggested recently [6]. Such an approach can be supported by the preferable cancellation of several important diagrams in energy calculation [6]. Emery, Eden and Sampathar pioneered the use of the harmonic-oscillator basis in the Brueckner theory. We shall call Q_{EE} the approximation to the Pauli projector introduced by these authors. The energy of a two-particle system when written in the individual nucleon $(n_1, \ell_1, n_2, \ell_2)$ quantum numbers, can be simply transformed to the system of relative and centre-of-mass motion:

$$(2n_1 + \ell_1 + 2n_2 + \ell_2)\hbar\omega = (2n + \ell + 2N + \mathscr{L})\hbar\omega \qquad (16)$$

In the case of the ^{16}O nucleus all states with

$$2n_i + \ell_i \leq 1 \qquad (17)$$

are occupied. This corresponds to the x's in Fig.2. The exact Pauli operator restricts scattering to the pair states indicated by circles. Summing conditions (17)

$$2n_1 + \ell_1 + 2n_2 + \ell_2 = 2n + \ell + 2N + \mathscr{L} \leq 2 \qquad (18)$$

too weak a restriction is obtained: all pair states lying above the dashed line are open for the scattering. Emery-Eden's approximation Q_{EE} permits scattering to the states above full line only. The first approximation to the reaction matrix

$$t_R = v - v \frac{Q_{EE}}{h \text{ oscil.} - E_s} t_R \qquad (19)$$

already contains, at least, a part of the Pauli exclusion effects and it is found that the second approximation contributes only a few per cent of t_R.
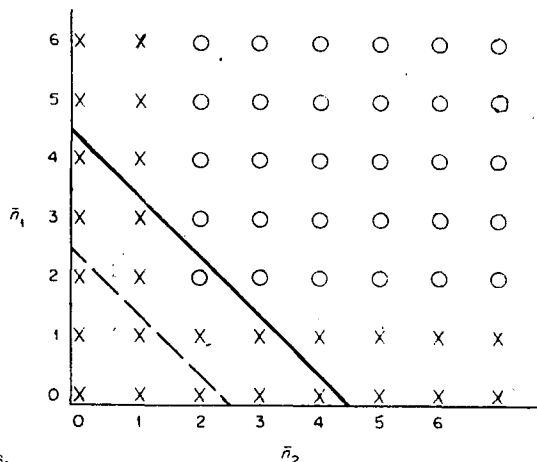
FIG.2. Emery-Eden's approximation for the pair states.

Relation of the exact and approximate reaction matrices is again given by Eq. (11) with $v = v_A$:

$$t = t_R + t_R \left[\frac{Q_A}{e_A} - \frac{Q}{e} \right] t \qquad (20)$$

where Q_A/e_A is taken equal to $1/(h^{p.w.} - E_s)$ or $Q_{EE}/(h^{oscil.} - E_s)$ for the plane wave and harmonic oscillator basis, respectively.

The question of the proper intermediate states remains, however, still open [6,7]. So long as high-lying states are most important in the calculation of the reaction matrix, the plane-wave approximation should be considered more appropriate. Several complications appear, however, in this approach. Actually, since the entire set of single-particle states should be an orthogonal set, the plane-wave states should be orthogonalized to the localized states (occupied and excited) and then these orthogonalized plane waves should be orthogonalized to each other.

4.   MODEL SPACE

We conclude that the realistic nucleon-nucleon potentials can be used in the nuclear structure calculation either directly or in the reaction-matrix approximation. In an alternative approach Elliott et al. [8] derive reduced shell model matrix elements of the two-body nuclear force directly from the experimental phase shifts and found that they are close to the corresponding elements of the Tabakin potential.

A direct correspondence of the matrix elements of realistic potentials to the effective matrix elements extracted from experiments cannot be, however, expected. In standard shell-model calculations with phenomenological nucleon-nucleon potentials or with adjustable reduced matrix elements to be determined from χ^2 fits to selected pieces of data, the effective forces already renormalized for the core-excitation effects are considered. This is by definition not the case with matrix elements of a "bare" realistic potential. Here an explicit consideration of the renormalization processes is necessary. Configuration space of the valence orbitals is clearly too limited and possibilities for including more single particle states into exact diagonalization are strongly restricted by the capacity of present-day computers. The usual approach [4] consists in introducing a model space. Solution Ψ of the Schrödinger equation

$$(H_0 + v)\Psi = E\Psi \qquad (21)$$

can be expanded over unperturbed wave function ϕ_i defined by the equation $H_0 \phi_i = \epsilon_i \phi_i$. In the case of a strong interacting potential v we must expect, however, that such an expansion cannot be limited to a finite number of terms. An infinite series which leads to an infinite matrix diagonalization is meaningless, on the other hand. A model wave function ψ_M can be defined by a finite expansion $\psi_M = \sum_{i=1}^{m} a_i \phi_i$. Then

$$\Psi = \Omega_M \psi_M \qquad (22)$$
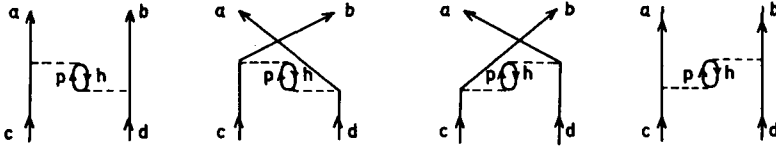
FIG.3.   Second-order bubbles diagrams of core polarization.

where

$$\Omega_M = 1 - \frac{Q_M}{H_0 - E} \, v \, \Omega_M \tag{23}$$

and

$$Q_M = \sum_{i=m+1}^{\infty} |\phi_i\rangle\langle\phi_i|$$

The relations (22)-(23) reduce the problem to a finite-dimensional one. They can be easily checked by utilizing the orthogonality conditions for ϕ_i. The resulting eigenvalue equation reads

$$(H_0 + v\,\Omega_M)\,\psi_M = E\,\psi_M \tag{24}$$

and $v\,\Omega_M$ is called a model interaction. The operator Ω_M provides a generalization of the operator Ω used in the definition of the t-matrix, in the sense that Ω_M includes all the effects of Ω and, in addition, takes care of several intermediate states which were not included in the Ω. Bearing this in mind, we can rewrite Eq.(24) in the form

$$(H_0 + t\,\Omega'_M)\,\psi_M = E\,\psi_M \tag{25}$$

where operator Ω'_M takes care of the intermediate states left out both on the construction of the reaction matrix and of the model space.

Important intermediate states of this type are those of three particles and one hole. Corresponding Feynman diagrams are given in Fig.3. Starting from these diagrams analytic expressions for the core-polarization correction terms can be written directly using the well-known Feynman rules. Historically, these formulae were first derived in the second-quantization formalism [4]. Here, we report a useful modification [9].

Introducing the isotopic spin, we can write

$$\langle\alpha\beta|U|\gamma\delta\rangle = -2\sum_{J'M'T'M_{T'}} G(\text{abcd } J'\,T'\,)\,(j_a j_b m_\alpha m_\beta|J'\,M'\,)$$

$$\times (j_c j_d m_\gamma m_\delta|J'\,M'\,)\,(\tfrac{1}{2}\tfrac{1}{2}t_a t_b|T'\,M_{T'}\,)\,(\tfrac{1}{2}\tfrac{1}{2}t_c t_d|T'\,M_{T'}\,) \tag{26}$$

$$\langle \alpha\,\beta\,|\,U\,|\,\gamma\delta \rangle = -2 \sum_{J''M''T''M_{T''}} F(acdb\,J''T'')\,s_\beta\,s_\gamma(j_a\,j_c\,m_\alpha - m_\gamma\,|\,J''M'')$$

$$\times\,(j_d\,j_b\,m_\delta - m_\beta\,|\,J''M'')\,(-)^{1-t_b-t_c}\,(\tfrac{1}{2}\tfrac{1}{2}\,t_a - t_c\,|\,T''M_{T''})\,(\tfrac{1}{2}\tfrac{1}{2}\,t_d - t_b\,|\,T''M_{T''})$$

$$(27)$$

where $s_\pi \equiv (-)^{j_p - m}\pi$. The symbols $G(abcd\,J'\,T')$ and $F(acdb\,J''T'')$ are just the particle-particle and particle-hole type reduced matrix elements in the notation analogous to that of Baranger [10]. The G, F (abcdJT) satisfy several simple and obvious symmetry relations.

Kuo and Brown [4] have given explicit formulas for the second-order core-polarization corrections for elements with the particle-particle-type vector couplings:

$$\langle ab\,JT\,|\,t(q/e)\,t\,|\,cd\,JT \rangle = N^{ab}_{cd}\,\Delta^{(2)}\,G(abcd\,JT) \qquad (28)$$

Here $N^{ab}_{cd} \equiv -2\,(1+\delta_{ab})^{-\frac{1}{2}}\,(1+\delta_{cd})^{\frac{1}{2}}$ is a normalization constant, and $\Delta^{(2)}\,G(abcd\,JT)$ is the core-polarization correction to the corresponding $G(abcd\,JT)$ computed with the antisymmetrized t operator.

The formula for the correction $\Delta^{(2)}\,F(acdb\,JT)$ to the first-order $F(acdb\,JT)$ coming from the very same second-order diagrams of the core polarization is much simpler because of more natural vector couplings in line with the particle-hole projector in this case.

The transformation from G to F is readily defined as

$$F(acdb\,JT) = -\sum_{J'T'} \hat{J}^{12}\hat{T}^{12}\,W(j_a\,j_b\,j_c\,j_d\,;\,J'\,J)\,W(\tfrac{1}{2}\tfrac{1}{2}\tfrac{1}{2}\tfrac{1}{2}\,;T'\,T)\,G(bacd\,J'T') \qquad (29)$$

where $\hat{J} = (2J+1)^{\frac{1}{2}}$.

Using Eq.(1) of Kuo [4] and performing the transformation of Eq.(29), we easily arrive at the following formula for the second-order core-polarization correction to $F(acdb\,JT)$:

$$\Delta^{(2)}\,F(acdb\,JT) = I(acdb\,JT) + (-)^{J+T}\sum_{J'T'} \hat{J}^{12}\hat{T}^{12} \begin{Bmatrix} j_a & j_c & J \\ j_b & j_d & J' \end{Bmatrix} \begin{Bmatrix} \tfrac{1}{2} & \tfrac{1}{2} & T \\ \tfrac{1}{2} & \tfrac{1}{2} & T' \end{Bmatrix} (-)^{J'+T'}$$

$$(30)$$

$$\times\,[(-)^{j_c+j_d}\,I(adcb\,J'\,T') + (-)^{j_a+j_b}\,I(bcda\,J'T')] + (-)^{j_a+j_b+j_c+j_d}\,I(bdca\,JT)$$

where

$$I(abcd\,JT) = \tfrac{1}{2}\sum_{ph} N^{ah}_{bp}N^{ch}_{dp}\,F(abph\,JT)\,\frac{q}{e}\,F(phcd\,JT)$$

In the above expression the propagator q/e to the left of an element $F(phss'\,JT)$ contains $e \equiv [E^0_p - E^0_h - (E^0_s - E^0_{s'})]$, where h stands for the hole state, p for the particle state of the third (core) nucleon involved, and s, s' belong to the valence shells; E^0_k denotes the single-particle shell-model (Hartree-Fock) energy.

Several simple approximations for the Pauli projector q were used in numerical calculation (q symbolizes three particles). Kuo and Brown [4] approximated q = 1 for A = 18 nuclei, since the complete s-d shell is occupied by two particles only. The energy denominators in their work were conveniently taken as e = 2ℏω because of parity conservation.

Slightly more complicated is the situation in heavy nuclei mainly because of the spin-orbit splitting, which puts single-particle (s.p.) levels of opposite parity close to each other. The former limitation e = 2ℏω is no longer applicable; the energy denominators may be quite small and the calculated corrections sometimes become sensitive to the chosen set of s.p. energies. We found such a situation in the case of tin isotopes [9]. Reliable quantitative fits to the experimental data call for a single-nucleon basis determined with the Hartree-Fock-Bogolyubov self-consistency. Such calculations are, however, not yet available in the region of tin isotopes.

Several semi-empirical sets of the s.p. energies were used in the first paper [9] devoted to the derivation of the effective interaction in the tin region. On a further stage [11], the same renormalization procedure was successfully applied with s.p. energies calculated in the numerical solution of the Schrödinger equation with a Woods-Saxon s.p. potential. Finally, a very simple self-consistent procedure [12] was suggested which preserves the harmonic-oscillator shape of s.p. orbitals (i.e. Hartree-Fock prescription limited to the spherical shape). S.p. energies written in the form

$$\epsilon_s = \langle s |u| s \rangle - \mu_s(\epsilon_t) \tag{31}$$

where

$$\mu_s = \frac{2}{\sqrt{2_s + 1}} \sum_{s'} \sqrt{2j_{s'} + 1} \; F(ss\, s's'J=0, \epsilon_t) \tag{32}$$

can be calculated according to the scheme
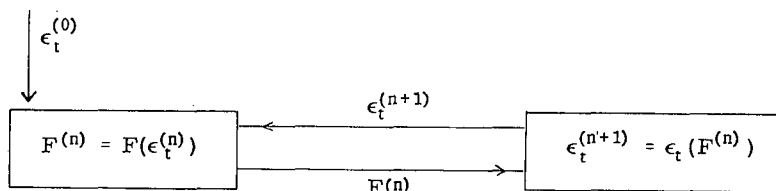
which usually converges very rapidly, in three to five iterations. Spectroscopic results [12] obtained with the mentioned sets of s.p. energies show a reasonable stability.

Core polarization corrections were studied e.g. for p-shell nuclei [13], A = 18 [4,14], A = 20 [15] and A = 21 [16] nuclei and for nickel [4] isotopes in the framework of the shell model; for nickel [17] and tin [9] isotopes with the use of the quasi-particle theories. Examples of such calculations are given in Figs 4-9.
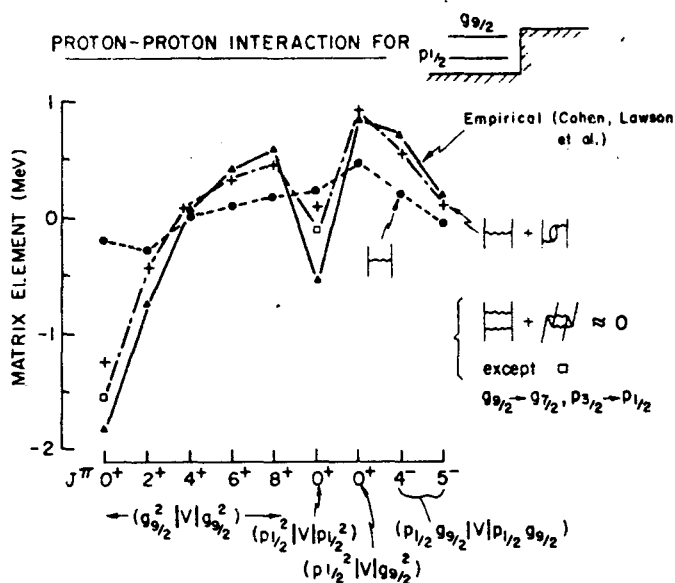
FIG.4. Comparison of calculated and empirical proton-proton matrix elements (Ref. [22]).
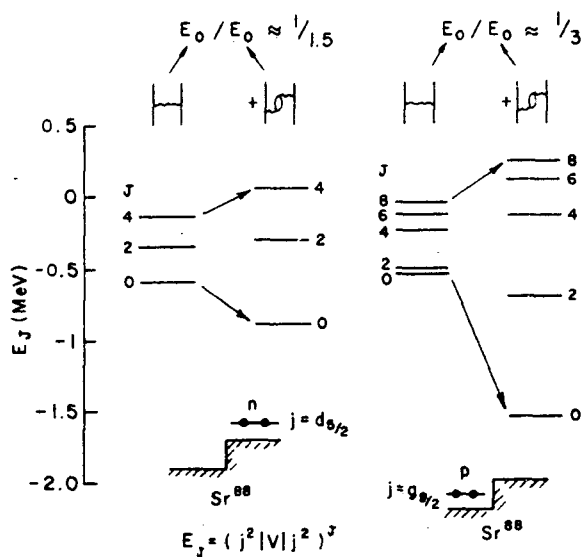
FIG.5. Owing to the core-polarization spectra are "opened", the 0^+ level pushed down, the levels of higher angular momenta up (Ref. [22]).
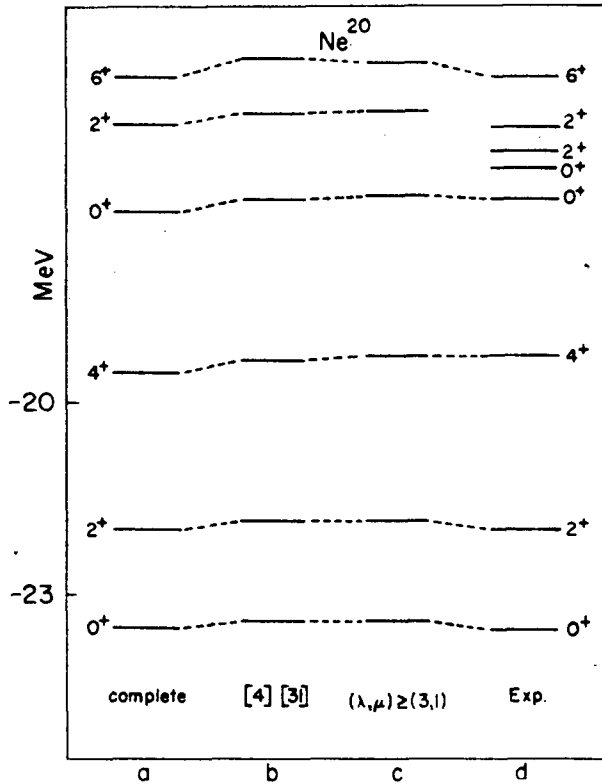
FIG. 6. Energy levels of ^{20}Ne (T = 0) states obtained by using the renormalized Hamada-Johnston potential. Results obtained with complete (column a) SU$_3$-basis for 4 particles in the s-d shell are compared with those obtained in different restricted bases (columns b and c) and with experiment. No such stability was, however, obtained in the case of ^{20}O nucleons (Ref. [15]).
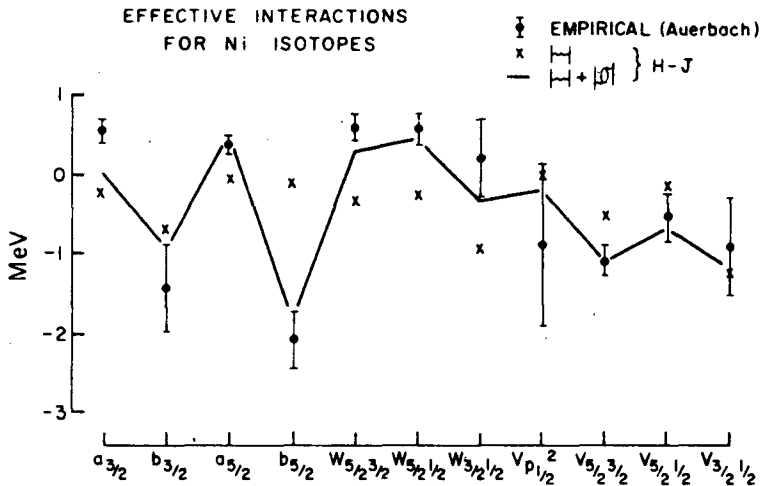
FIG. 7. Comparison of the calculated and empirical matrix elements in the nickel isotopes (Ref. [4]).

    Calculated corrections are generally large and reflect the great im-
portance of the excited configurations of core nucleons in microscopic
spectroscopy with a realistic potential. The effects of the corrections
in question are twofold in the case of superconductive nuclei (e.g. tin
isotopes) in contrast to those in the normal state [9]. In fact, the changes
in the effective pairing force, i.e. in the calculated energy gaps and the
chemical potentials, are even more important than the changes in the
effective residual interaction responsible for the configuration mixing.

    Spectroscopic results obtained with different realistic potentials are
very similar. In particular, we would like to mention here comparison
of the Yale, Reid and Hamada-Johnston potentials in light nuclei [18],
equivalence of Tabakin and Yale potentials in tin isotopes [19] and equiva-
lence of Hamada-Johnston's and Tabakin's potentials found in A = 21
nuclei [16].
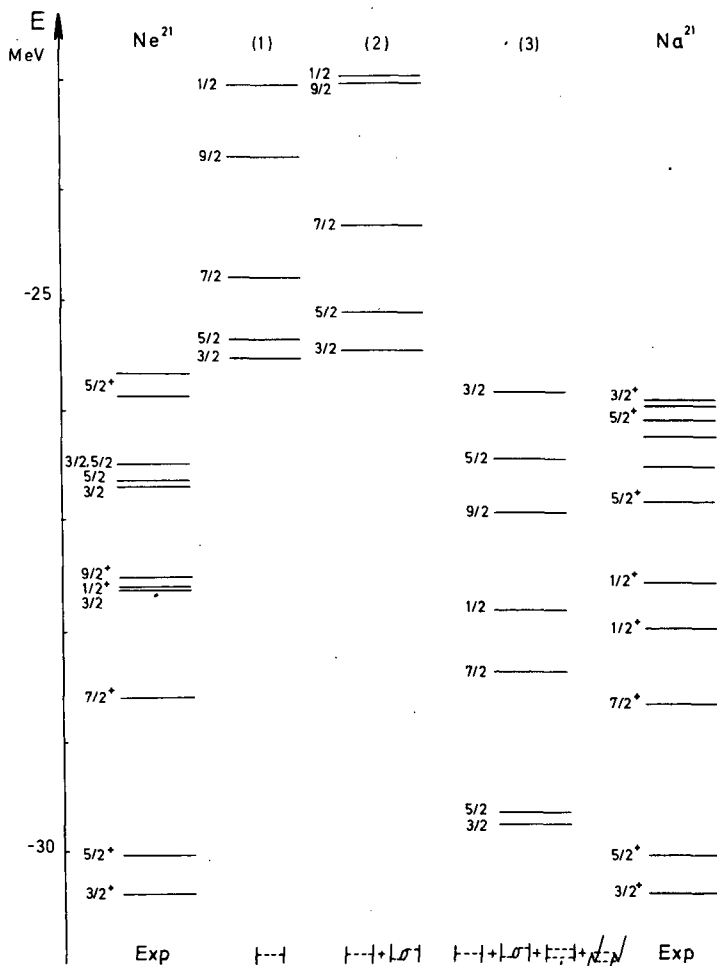
FIG.8.   Energy levels of A = 21 nuclei calculated with Tabakin's realistic potential. Measured spectra
of the ^{21}Ne and ^{21}Na nuclei are given at the sides of the figure (Ref. [16]).
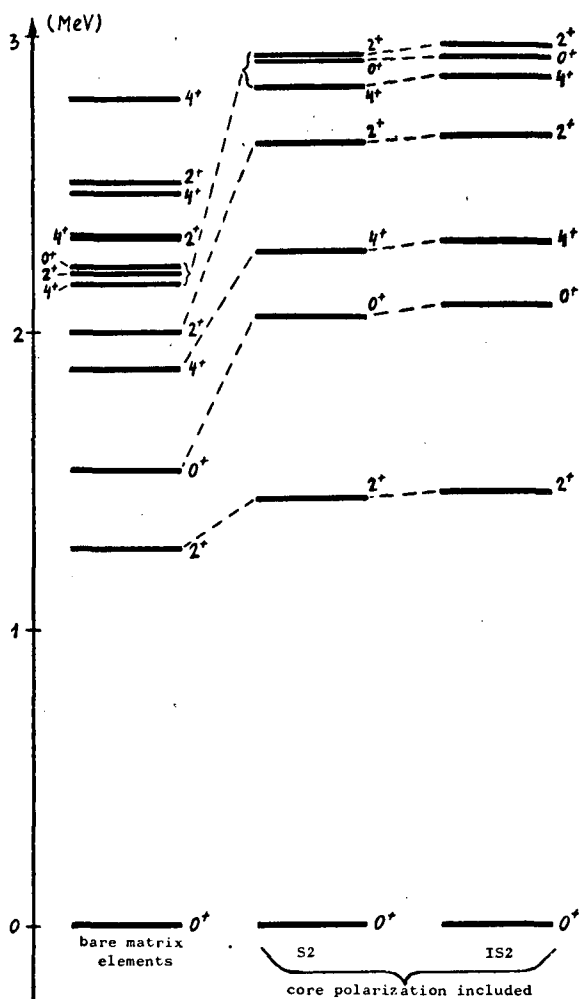
FIG. 9.   Spectrum of the lowest lying 0$^+$, 2$^+$ and 4$^+$ energy levels of ^{116}Sn calculated in the Tamm-Dancoff approximation with the Tabakin potential. Inclusion of the processes which correspond to the different diagrams of Fig. 10 (column IS2) does not change appreciably the renormalized potential (column S2).
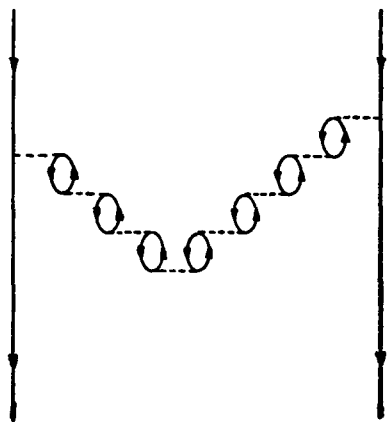
FIG. 10. An example of the RPA-type bubble diagrams in the core-polarization corrections.
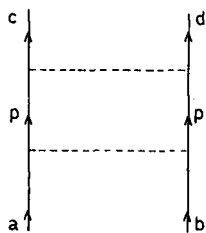
FIG. 11. Two-particle corrections.
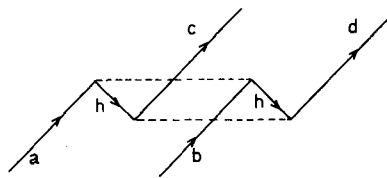
FIG. 12. Two-hole and four-particle corrections.
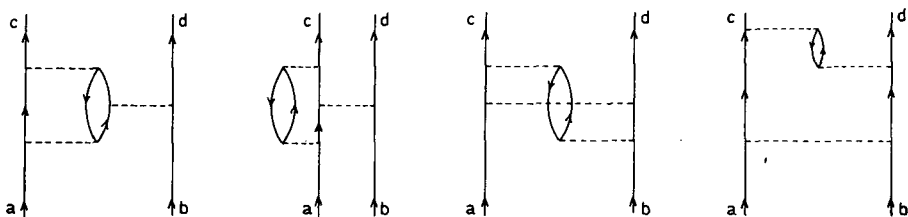
FIG. 13. Examples of the third-order core-polarization corrections.

One wonders naturally about the relative importance of the several processes different from the simplest 3p-1h excitation considered so far. Summing up, we can say that the inclusion of more p-h bubbles, Fig.10 [9] ("exchange of a phonon", in Ref.[20])) leads to negligible corrections only. The two-particle excitations [4,14] of Fig.11, on the other hand, were found to be quite important. The perturbative treatment of the two-hole excitation (Fig.12) is not quite adequate, as has been argued several times [4,14]. However, Kuo and Brown [14] included both 2p and 2h corrections in order to study their relative importance.

The question of how adequate is the limitation to the lowest (second) order in the above-mentioned 3p-1h corrections still remains open. Recent investigations of the problem [21] give some indication that this class of diagrams has to be summed up to all orders (examples of the third-order graphs are shown in Fig.13; we can draw 18 third-order graphs in all). The promising results of several papers based on the second-order contribution, however, give some hope that the higher-order contributions partly cancel, and the resulting correction will not be very different from the second-order terms considered here.

REFERENCES

[1] TABAKIN, F., Annls Phys. (N.Y.) 30 (1964) 51.

[2] HAMADA, T., JOHNSTON, I.D., Nucl. Phys. 34 (1962) 382.

[3] LASSILA, K.E. et al., Phys. Rev. 126 (1962) 881.

[4] KUO, T.T.S., BROWN, G.E., Nucl. Phys. 85 (1966) 40. KUO, T.T.S., Nucl. Phys. A90 (1967) 199.

[5] EDEN, R.J., in Nuclear Reactions, 1, North-Holland, Amsterdam (1959).

[6] BECKER, R.L., MacKELLAR, A.D., MORRIS, B.M., Phys. Rev. 174 (1968) 1264.

[7] CHUN WA WONG, Nucl. Phys. A91 (1967) 399; A104, (1967) 417.

[8] ELLIOTT, J.P. et al., Nucl. Phys. A121 (1968) 241.

[9] GMITRO, M., HENDEKOVIĆ, J., SAWICKI, J., Phys. Rev. 169 (1968) 983.

[10] BARANGER, M., Phys. Rev. 120 (1960) 957.

[11] GMITRO, M., RIMINI, A., SAWICKI, J., WEBER, T., Phys. Rev. 173 (1968).

[12] GMITRO, M., Physics Letts 27B (1968) 616.

[13] HALBERT, E.C. et al., Physics Letts 20 (1966) 657.

[14] KUO, T.T.S., Nucl. Phys. A103 (1967) 71.

[15] FLORES, J., PEREZ, R., Physics Letts 263 (1967) 55.

[16] SOTONA, M., GMITRO, M., PLUHAŘ, Z., TRLIFAJ, L., ICTP preprint IC/69/5.

[17] ALZETTA, R. et al., ICTP preprint IC/69/2.

[18] LYNCH, R.P., KUO, T.T.S., Nucl. Phys. A95 (1967) 561.

[19] GMITRO, M., SAWICKI, J., Physics Letts 26B (1968) 493.

[20] KUO, T.T.S., Physics Letts, 26B (1968) 63.

[21] BARRETT, B.R., KIRSOM, N.W., Physics Letts 27B (1968) 544.

[22] BROWN, G.E., in Nuclear Structure (Proc. Symp. Dubna, 1968), IAEA, Vienna (1968) 563.

EFFECTIVE ELECTROMAGNETIC OPERATORS

A. RIMINI
Istituto di Fisica Teorica,
Università di Trieste, Italy

Abstract

EFFECTIVE ELECTROMAGNETIC OPERATORS.
The fundamental ideas of the theory of effective interactions and electromagnetic operators are reviewed (sections 1 and 2). The advantages and drawbacks of the microscopic and phenomenological determinations of the effective quantities are discussed in section 3. The method of separating core and valence energies is described in section 4. The explicit formulas for the effective em operators are given in section 5. Two calculations concerning tin and nickel isotopes are described in sections 6 and 7, and the results are discussed.

1. INTRODUCTION

An effective electromagnetic (em) operator is an operator which, when used to calculate matrix elements between model wave functions, gives the same results as given by the true em operator between the corresponding true wave functions. Therefore, to get expressions for the effective em operators, it is necessary to know the precise relationship between the model and true wave functions and, in turn, this relationship is connected with the definition of the effective Hamiltonian [1].

Our starting point is the shell-theory Hamiltonian

$$H = H_0 + V \tag{1}$$

where $H_0 = \sum_a \epsilon_a \hat{N}_a$ is a one-body operator. We call V the residual interaction. We divide the levels of H_0 into various groups (see Fig. 1). The core levels are supposed to be filled to a large extent in the nuclear ground and low-lying excited states. The valence levels are partially filled. The nucleons in these levels change essentially their state in going from one low-lying nuclear state to another. The upper levels are supposed to be empty to a large extent. They are further divided into high upper and medium upper levels. The high upper levels are those which can be assumed to be completely empty because a Brueckner-Hartree-Fock calculation has been performed to produce the Hamiltonian (1) or, at any rate, because the two-body potential in V is smooth enough. The medium upper levels are the first few levels beyond the valence region. Just as the topmost core levels, they are often of a non-negligible importance for spectroscopy, but are not included among the valence levels in order to have secular matrices of reasonable dimensions.

We call a Hilbert space complete if it is spanned by all the configurations obtained by putting the nucleons of the given nucleus in the core, valence and medium upper levels. The wave functions obtained by diagonalizing the Hamiltonian (1) in the complete Hilbert space are the
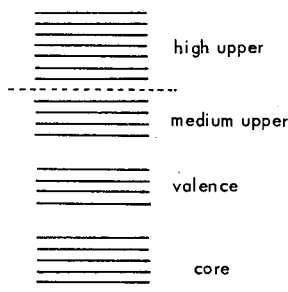
FIG. 1.   Single-particle levels in shell-theory.

true wave functions.   A Hilbert space will be called <u>model</u> Hilbert space
if it is spanned by all the configurations obtained by filling completely the
core levels and putting the remaining nucleons in the valence levels.   This
is the state vector space in which we want to do the spectroscopy of the
low-lying nuclear states by diagonalizing some effective Hamiltonian.   We
shall see how to define this effective Hamiltonian and what is the relation
of its eigenfunctions (the <u>model</u> wave functions) to the true wave functions.
Actually, the Hamiltonian (1) is already an effective Hamiltonian in the
sense of the elimination of the high upper levels, so that ours is a two-step
procedure.   The formal theory of the two steps is the same, but in practice
the important contributions are quite different.   This is precisely the.
reason why a two-step procedure is convenient.   We do not consider here
the first step.

   For an electromagnetic operator, the procedure to get the effective
operator should also consist of two steps.   However, it is usually believed
that the first step, which essentially takes into account the very-short-range
correlations introduced in the nuclear wave functions by the repulsive core
in the free nucleon-nucleon interaction, is not important for the em opera-
tors.   Accordingly, in the second step we shall simply use the operators
corresponding to the interaction of the em field with free nucleons.

2.   SCHRÖDINGER EQUATION AND PERTURBATION EXPANSIONS

   The Schrödinger equation in the complete (as defined above) Hilbert
space is

$$(E - H_0) |\psi\rangle = V|\psi\rangle \tag{2}$$

The wave functions $|\psi\rangle$ are the true wave functions.   Let P be the pro-
jection operator on the model Hilbert space, and Q the projection operator
orthogonal to the complete Hilbert space.   Clearly P and Q commute with
H_0.   In correspondence to any eigenvalue E of Eq. (2) we define an effective
interaction V^{eff} by

$$V^{eff} = V + V \frac{Q}{E - H_0} V^{eff} \tag{3}$$

which is meaningful provided that the operator $(1 - V Q/(E - H_0))^{-1}$ exists.
This is not the case if $P|\psi\rangle = 0$.   From our consideration we exclude

those solutions of Eq. (2) which, clearly, we cannot pretend to describe
within the model Hilbert space. From Eq. (2) it follows

$$V P \left| \psi \right\rangle = \left(1 - V \frac{Q}{E - H_0} \right) V \left| \psi \right\rangle$$

and from Eq. (3)

$$V P \left| \psi \right\rangle = \left(1 - V \frac{Q}{E - H_0} \right) V^{eff} \, P \left| \psi \right\rangle$$

so that, because of the existence of $(1 - V \, Q/(E - H_0))^{-1}$

$$V^{eff} \, P \left| \psi \right\rangle = V \left| \psi \right\rangle \tag{4}$$

It is then easy to see that, if we define the model wave function $\left| \psi_M \right\rangle$ by

$$\left| \psi_M \right\rangle = P \left| \psi \right\rangle \tag{5}$$

it satisfies the Schrödinger-type equation in the model space

$$(E - H_0) \left| \psi_M \right\rangle = P \, V^{eff} \left| \psi_M \right\rangle \tag{6}$$

It differs from an ordinary Schrödinger equation by the fact that the inter-
action $P \, V^{eff} P$ depends on E. Therefore, the solutions $\left| \psi_M \right\rangle$ for different
values of E are not orthogonal because they correspond to different
Hamiltonians. Clearly, this is a consequence of the correspondence (5)
which does not conserve orthogonality.

For the original Schrödinger problem (2), we have substituted an
equivalent problem in the model space through the defining Eq. (3). It is
important to note that from the knowledge of the effective interaction V^{eff}
and of the model wave function $\left| \psi_M \right\rangle$, the knowledge of the true wave
function $\left| \psi \right\rangle$ follows. In fact, if V^{eff} and $\left| \psi_M \right\rangle$ are solutions of Eqs (3) and
(6), we put

$$P \left| \psi \right\rangle = \left| \psi_M \right\rangle, \; Q \left| \psi \right\rangle = \frac{Q}{E - H_0} \, V^{eff} \left| \psi_M \right\rangle \tag{7}$$

It follows that $\left| \psi \right\rangle$ satisfies Eq. (4). Then

$$(E - H_0) \left| \psi \right\rangle = (E - H_0) \left| \psi_M \right\rangle + Q \, V^{eff} \left| \psi_M \right\rangle$$

$$= P \, V^{eff} \left| \psi_M \right\rangle + Q \, V^{eff} \left| \psi_M \right\rangle$$

$$= V^{eff} \left| \psi_M \right\rangle = V \left| \psi \right\rangle$$

It is clear that Eqs (3), (6) and (7) are nothing else than a way of rewriting
Eq. (2).

We can expand Eq. (3) by iteration. We obtain

$$V^{eff} = V + V \frac{Q}{E - H_0} V + V \frac{Q}{E - H_0} V \frac{Q}{E - H_0} V + \dots \tag{8}$$

This series looks like a Brillouin-Wigner perturbative expansion, and, in fact, what we have done is precisely the Brillouin-Wigner perturbation theory for degenerate or quasi-degenerate systems. We can get a diagrammatic representation of the terms in the expansion (8) by inserting complete sets of eigenstates of H_0. If we consider the model interaction $P V^{eff} P$, as given by Eq. (8), we see that it corresponds to our intuitive idea that it should contain all those processes for which the initial and final states are in the model space, while the intermediate states lie outside.

The effective em operator O^{eff} corresponding to the free-nucleon operator O is defined by

$$\langle \psi'_M | O^{eff} | \psi_M \rangle = (\langle \psi' | \psi' \rangle \langle \psi | \psi \rangle)^{-\frac{1}{2}} \langle \psi' | O | \psi \rangle \tag{9}$$

The normalization factor is necessary because Eq. (5) does not allow to normalize both the model and the true wave functions.

In practice, in most cases, one uses the first-order perturbation theory as defined by the truncated expansions

$$P V^{eff} = P V + P V \frac{Q}{E - H_0} V \tag{10a}$$

$$Q V^{eff} = Q V \tag{10b}$$

$$| \psi \rangle = | \psi_M \rangle + \frac{Q}{E - H_0} V | \psi_M \rangle \tag{10c}$$

$$\langle \psi'_M | O^{eff} | \psi_M \rangle$$
$$= \langle \psi'_M | O | \psi_M \rangle + \langle \psi'_M | O \frac{Q}{E - H_0} V | \psi_M \rangle + \langle \psi'_M | V \frac{Q}{E' - H_0} O | \psi_M \rangle \tag{10d}$$

$$O^{eff} = O + O \frac{Q}{E - H_0} V + V \frac{Q}{E' - H_0} O \tag{10e}$$

Later on, we shall discuss the application of this perturbative treatment to the tin and nickel isotopes.

The effective em operators O^{eff} are operators for an η-particle system, η being the number of valence particles. It is obvious that they are not simple one-body operators. For example, using first-order perturbation theory, the last term in Eq. (10e) contains contributions which can be represented by the diagrams of Fig. 2. The labels v, c and u mean valence, core and medium upper, respectively, and the unperturbed ground state of the core is used as a vacuum. Diagrams 2c and 2f give rise to a two-body part in O^{eff}. Let us drop all diagrams of the types 2c and 2f except those which can be re-interpreted as one-body diagrams. These are represented in Fig. 3. Diagrams 3a and 3b are forbidden by the Pauli principle and, in fact, they exactly cancel those contributions from diagrams 2a and 2b which are forbidden because the particle excited from the core is in a state v which is already occupied by same freely propagating valence particle. But this cancellation depends on what the occupied-valence single-particle levels are. Therefore, when we write the operator for an η-particle system O^{eff} as a one-body operator, a new state dependence arises which is of a new kind with respect to the state
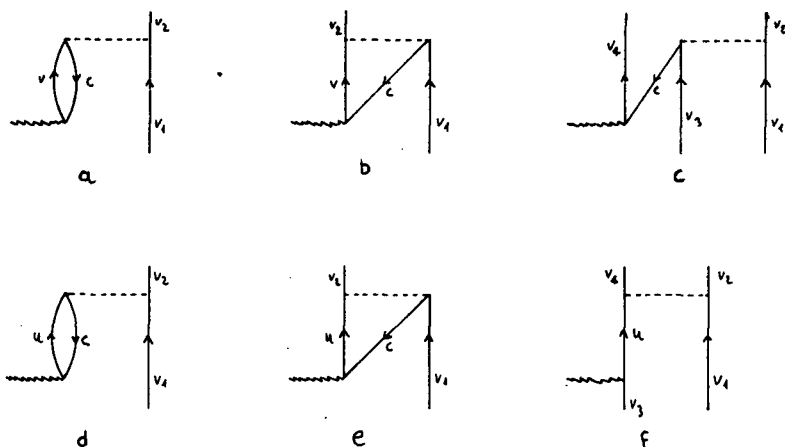
FIG. 2. First-order contributions to the effective electromagnetic operator O^{eff}.
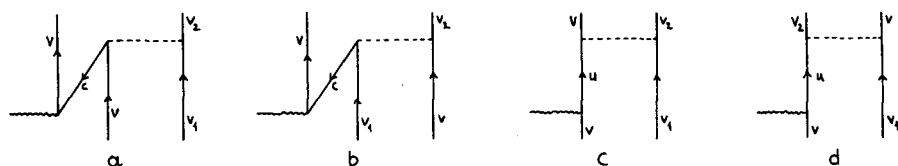
FIG. 3. Particular two-body terms in O^{eff}.
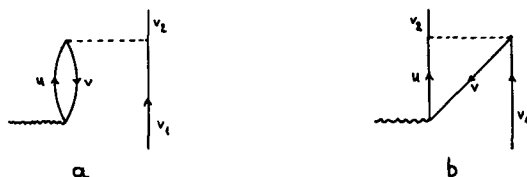
FIG. 4. A different way of drawing diagrams 3c and 3d.

dependence given by the energy denominators. Similarly, the diagrams
3c and 3d, which are usually drawn as in Fig. 4, are state-dependent
because they do not exist if the single-particle state v is empty. Finally,
we note that the one-body operator in O^{eff} depends also on the number of
particles in the valence levels, i. e. on the particular nucleus which we
are treating in the given region.

One can hope, however, that all these troubles are not terribly im-
portant. The two-body terms should be less important than the one-body
ones because they require that two particles are simultaneously in the
conditions to interact with the photon. The state dependence coming from
the energy denominators is weak if the range of the energies of the nuclear
states in which we are interested is small compared with the unperturbed
energy corresponding to the exit from the model space. The state

dependence coming from writing O^{eff} as a one-body operator is weak when the occupation probability of the valence levels is small because in such a case the inhibition of the core-valence processes is small and the valence-upper processes are negligible. When the number of valence particles is large we are usually, because of the pairing effect, in a position to apply the quasi-particle Tamm-Dancoff approximations, according to which the distribution of particles among the valence levels is essentially that of the ground state also for the excited states. Finally, the nucleus dependence is not strong because the core-valence processes are roughly proportional to the unoccupation probability of the valence levels while the valence-upper processes are roughly proportional to the occupation probability. Since one finds that all contributions are coherent, the two effects approximately compensate each other.

What has been said in the last two paragraphs on the effective em operators O^{eff} can be repeated with suitable modifications for the effective interaction in the model space $P\,V^{eff}\,P$.

3. TWO WAYS OF DETERMINING THE EFFECTIVE INTERACTION

There are two possible ways of determining the effective interaction and the effective em operators. One way is to try to calculate them microscopically from the free-nucleon interaction and em operators. Of course, many approximations are necessary in order to simplify the calculations reasonably. These approximations are, first, the neglect of all many-body terms, of any kind of state dependence, of the nucleus dependence in a certain region. Furthermore, even within these limitations, one is compelled to limit the considerations to selected processes, disregarding all the rest in the perturbative expansions.

The alternative to the microscopic calculation is the phenomenological determination. In this type of approach, one looks for an effective interaction which gives the same nuclear energy levels as given by experiment. Then using the model wave functions obtained in this way, one looks for effective em operators which have the same matrix elements as those extracted from experiment. It is obvious that the problem, as formulated above, has an infinite number of solutions. The hope of choosing a physically acceptable solution, i.e. a solution such that the fundamental relation (5) is approximately satisfied, is based on the fact that certain assumptions are made, so that one fits a large number of nuclear levels by adjusting a smaller (possibly much smaller) number of parameters. These assumptions are usually: (a) that $P\,V^{eff}\,P$ is a two-body operator independent of the state and of the particular nucleus in the region we are considering; (b) that the two-body operator in $P\,V^{eff}\,P$ has a definite form containing few parameters. The assumptions contained in (a), as we know, can be valid only as approximations. Assumption (b) could be affected by one's earlier experience in this subject, in which case one would have concealed parameters. Clearly, there is a certain amount of danger of distorting the physical situation, i.e. of getting model wave functions which do not satisfy Eq.(5). The successive phenomenological determination of the effective em operators cannot affect the validity of Eq.(5). Assumptions analogous to (a) and (b) are made for the em operators in order to obtain a significant comparison with experimental data.

The pseudonium calculations have shown that it is possible to succeed in the fitting procedure even when there are true wave functions which have rather small components in the model Hilbert space. This does not necessarily imply that the results are wrong. It only means that, from the success of the fitting procedure, one cannot conclude that the admixtures in the true wave functions from configurations lying outside the model space are small. It would be interesting to know the results of a check of Eq. (5).

The result of our discussion is that the two ways of determining the effective interaction both have troubles, but quite different in character. The main trouble with the microscopic calculations is the possible neglect of important contributions. On the other hand, the main trouble with the phenomenological determination is that the fitting procedure could lead to a result having little to do with the physical situation. The fact that the effective interactions obtained with the two methods generally agree in a satisfactory way [2] is a support for both of them.

4. ENERGY CONSIDERATIONS

The equations which we have written so far cannot be used as they are in the nuclear shell model. In fact, the energies which appear in these equations are the total energies of the system, while in the shell model one has to do with energies relative to the ground state energy of the core. The way of separating the core energy has been shown by Bloch and Horowitz [3]. The method is based on a theorem on the cancellation of classes of diagrams which we shall simply state without proof.

Let ΔE be the energy shift defined by

$$E = E_0 + \Delta E \tag{11}$$

where

$$E_0 = \langle \psi_M | H_0 | \psi_M \rangle \tag{12}$$

The unperturbed energy E_0 can be split into a core and a valence part by writing

$$E_0 = E_{0c} + E_{0v} \tag{13}$$

$$E_{0c} = \langle \psi_M | H_{0c} | \psi_M \rangle, \quad H_{0c} = \sum_{a=core} \epsilon_a \hat{N}_a \tag{14}$$

$$E_{0v} = \langle \psi_M | H_{0v} | \psi_M \rangle, \quad H_{0v} = \sum_{a=valence} \epsilon_a \hat{N}_a \tag{15}$$

If ΔE_c is the ground-state energy shift of the problem of the core alone, then the quantity

$$E_c = E_{0c} + \Delta E_c \tag{16}$$

is just the ground-state energy of the core. The energy shift ΔE can also be split into a part due to the core nucleons, and a part due to the valence

nucleus by using the equation

$$\Delta E = \Delta E_c + \Delta E_v \tag{17}$$

as a definition of ΔE_v.

We now divide the diagrams representing the various terms in the perturbative expansion into three classes:

a) the core diagrams, in which no interaction line is attached to the external lines (we use the unperturbed ground-state of the core as a vacuum, so that the external lines are valence lines);

b) the valence diagrams, in which all interaction lines are connected to external lines;

c) mixed diagrams, all remaining diagrams, in which only a part of the interaction lines is attached to external lines.

Examples of the three classes of diagrams are given in Figs 5a, 5b, and 5c, respectively. Note that no mixed diagram exists in first-order perturbation theory. We now use the algebraic identity

$$\frac{1}{e} = \frac{1}{e_0} + \frac{1}{e_0}(-\delta e)\frac{1}{e} \tag{18}$$

where $e = e_0 + \delta e$, to modify the energy denominators in the core and valence diagrams. Precisely, we put

$$e_0 = E_0 + \Delta E_c - H_0$$

$$\delta e = \Delta E_v$$

for the core diagrams, and

$$e_0 = E_0 + \Delta E_v - H_0$$

$$\delta e = \Delta E_c$$

for the valence diagrams. It can be shown that the contributions from the second term in Eq. (18) exactly cancel the mixed diagrams. We are, therefore, left with the core diagrams (with energy denominators $E_0 + \Delta E_c - H_0$) and the valence diagrams (with energy denominators $E_0 + \Delta E_v - H_0$) only.
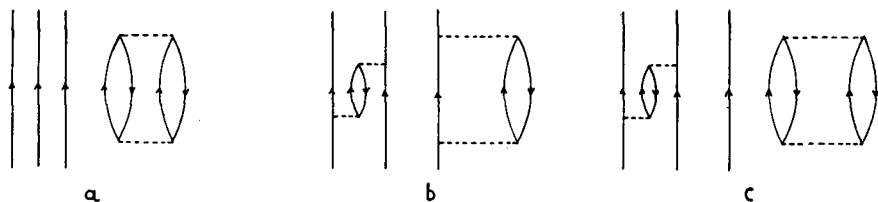
FIG. 5. Examples of core (a), valence (b) and mixed (c) diagrams.

Consider now the contribution of the core diagrams to $V^{eff}P$. These diagrams leave the initial unperturbed model state undisturbed, so that their contribution is a multiple of the identity in the model space. The factor is clearly just ΔE_c, since, apart from the external valence lines, these diagrams form the Brillouin-Wigner expansion for ΔE_c. Therefore

$$V^{eff}P = \Delta E_c P + V_v^{eff} P \tag{19}$$

where $V_v^{eff} P$ contains only the valence diagrams and the energy denominators $E_0 + \Delta E_v - H_0$ are used. Noting that

$$H_0 P = E_{0c}P + H_{0v} \tag{20}$$

and recalling the definitions (11), (13), (17), the Schrödinger equation in the model space (6) can be written

$$(E_v - H_{0v}) |\psi_M\rangle = P V_v^{eff} |\psi_M\rangle \tag{21}$$

where

$$E_v = E_{0v} + \Delta E_v \tag{22}$$

The energy denominators in $V_v^{eff} P$ can conveniently be written

$$E_0 + \Delta E_v - H_0 = E_v - (H_0 - E_{0c}) = E_v - \bar{H}_0 \tag{23}$$

where

$$\bar{H}_0 = - \sum_{a = core} \epsilon_a \hat{N}_a^{holes} + \sum_{a \neq core} \epsilon_a \hat{N}_a , \quad \hat{N}_a^{holes} = 2j_a + 1 - \hat{N}_a \tag{24}$$

Equation (21) is just a shell-model eigenvalue equation, provided that the dependence of $V_v^{eff} P$ on E_v is not too strong.

In first-order perturbation theory, the use of the cancellation theorem is not needed. In fact, since no mixed diagram exists, it is sufficient to neglect ΔE_v and ΔE_c in the energy denominators of the core and valence diagrams, respectively. This is permissible in the domain of validity of first-order theory.

A treatment similar to that given above should be given for the em operators. This is terribly complicated when the general expression (9) is used, but again becomes very simple in first-order theory. In this case all diagrams are "valence" diagrams, and the only thing we have to do is to neglect ΔE_c in the energy denominators. Again these become $E_v - \bar{H}_0$. For more elaborate treatments see Ref.[4].

In what follows we focus our attention on the calculations of the effective em operators and on the use of these in the calculation of observable quantities in practical cases.

5. CALCULATION OF EFFECTIVE EM OPERATORS

The most obvious method of eliminating the state dependence of the energy denominators in first-order theory is to replace the Brillouin-Wigner denominators by Rayleigh-Schrödinger denominators. We note, however, that several variants are possible if the essential condition is fulfilled that the main part in the denominators is the unperturbed energy corresponding to the exit from the model space.

If the energy denominators $E_{0v} - \bar{H}_0$ are used, Eq. (10e) gives, for the one-body part in O^{eff},

$$O_{\beta\alpha}^{eff} = O_{\beta\alpha} - \sum_{\pi\chi} V_{\beta\chi\alpha\pi} \frac{1}{\epsilon_p - \epsilon_n + \epsilon_a - \epsilon_b} O_{\pi\chi} - \sum_{\pi\chi} O_{\chi\pi} \frac{1}{\epsilon_p - \epsilon_n + \epsilon_b - \epsilon_a} V_{\beta\pi\alpha\chi} \quad (25)$$

where $V_{\beta\chi\alpha\pi}$ are the antisymmetrized two-body matrix elements of the interaction. As usual, greek subscripts indicate all single-particle quantum numbers, and the corresponding latin ones indicate the same quantum numbers except the third component of angular momentum. The summations run over the three groups of excitations core-valence, core-upper and valence-upper. Equation (25), however, does not take into account the inhibition of core-valence processes due to the Pauli principle and the inhibition of valence-upper processes since the valence levels are only partially filled. We shall take into account these effects in the simplest way, i. e. by multiplying the contribution from core-valence processes by the average unoccupation probability of the valence levels q and multiplying the contribution from valence-upper processes by the occupation probability 1 - q. One could also use different occupation and unoccupation factors for different valence levels. Owing to the coherence of the various contributions, the results are not very much sensitive to this choice.

Taking into account the rotational properties of the em operator and the interaction, Eq. (25) gives, for valence neutrons,

$$\langle b || O_\lambda^{eff} || a \rangle = \langle b || O_\lambda || a \rangle$$

$$+ 2 \sum_{\substack{pn' \\ (protons)}} \left[\frac{1}{2} \left(F(b\, a\, pn, \lambda\, 0) - F(b\, a\, pn, \lambda\, 1) \right) \frac{1}{\epsilon_p - \epsilon_n + \epsilon_a - \epsilon_b} \right.$$

$$\times \langle p || O_\lambda || n \rangle + \langle h || O_\lambda || p \rangle \frac{1}{\epsilon_p - \epsilon_n + \epsilon_b - \epsilon_a} \frac{1}{2} \left(F(b\, a\, np, \lambda\, 0) \right.$$

$$\left. \left. - F(b\, a\, np, \lambda\, 1) \right) \right] + 2 \sum_{\substack{pn' \\ (neutrons)}} \left[\frac{1}{2} \left(F(b\, a\, pn, \lambda\, 0) + F(b\, a\, pn, \lambda\, 1) \right) \right. \quad (26)$$

$$\times \frac{1}{\epsilon_p - \epsilon_n + \epsilon_a - \epsilon_b} \langle p || O_\lambda || n \rangle + \langle n || O_\lambda || p \rangle \frac{1}{\epsilon_p - \epsilon_n + \epsilon_b - \epsilon_a} \frac{1}{2}$$

$$\left. \times \left(F(b\, a\, np, \lambda\, 0) + F(b\, a\, np, \lambda\, 1) \right) \right]$$

where the reduced matrix elements are defined as in Edmonds [5] and the quantities F are the particle-hole coupled matrix elements of the interaction as defined in Ref. [6]. Equation (26) is to be used in calculations.

6. APPLICATION TO ^{116}Sn

We shall now describe the results of a calculation [7] concerning ^{116}Sn. This nucleus is described, as usually, in terms of a 50 neutrons - 50 protons core. The remaining 16 valence neutrons are distributed among the five valence levels $2s_{5/2}$, $1g_{7/2}$, $3s_{1/2}$, $2d_{3/2}$ and $1h_{11/2}$. The core, valence and medium upper levels include all levels between magic numbers 8 and 126. The smooth force which is used is the Yale-Shakin reaction matrix. The single-particle wave functions are approximated by those of the harmonic oscillator with $\sqrt{\nu} = 0.46$ F^{-1}. The single-particle energies are those given by a reasonable Woods-Saxon potential. Details are given in Ref. [7]. We only quote that the range of the five valence levels $\epsilon_{1h11/2} - \epsilon_{2d5/2}$ is 3.36 MeV, that the gap between core and valence levels $\epsilon_{2d 5/2} - \epsilon_{1g9/2}$ is 4.72 MeV, and the gap between valence and upper levels $\epsilon_{2f 7/2} - \epsilon_{1h11/2}$ is 4.90 MeV. An average occupation probability of the valence neutron levels equal to $\frac{1}{2}$ is assumed in the correction factors for core-valence and valence-upper processes. The effective em operators which are obtained are used, in conjunction with appropriate Q S T D nuclear wave functions, to calculate observable em quantities. The nuclear wave functions follow from an effective interaction derived from the Yale-Shakin force consistently with the method used to get the effective em operators.

The results for the E2-operator e r^2 Y$_{2\mu}$ are given in Table I. This table gives the effective charge matrix, i.e. the matrix of the ratios of the single particle matrix elements of the effective operators to the corresponding matrix elements of the operator which is obtained by assuming a reference effective charge equal to 1 for the valence neutrons. It is seen that the all matrix elements are of the same spin and order of magnitude. They are actually grouped in two clusters: those somewhat higher than 1 and those somewhat smaller than 0.7. The composition of the nine elements of Table I in terms of the contributions of the various groups of transitions is given in Ref. [7]. We only mention that the core-upper transitions contribute a rather large amount (30 - 40% of the total effective charge). The available experimentally measured E2 quantities in ^{116}Sn are the $2_1^+ \rightarrow 0_1^+$ transition probability and the quadrupole moment of the 2_1^+ state. For the B(E2, $2_1^+ \rightarrow 0_1^+$) the experimental values range from 200 to 500 e^{2}F^4, with a most probable value of about 400 e^{2}F^4. The calculated effective operator gives 259.4 e^{2}F^4. For the quadrupole moment, the experimental value is 0.4 ± 0.3 barn and the theoretical value is 0.094 barn, at the lower limit of the experimental error. It is to be noted, however, that the quadrupole moment of the 2_1^+ state is a rather unstable quantity, very

TABLE I. E2 - EFFECTIVE-CHARGE MATRIX FOR TIN

	$3s_{1/2}$	$2d_{3/2}$	$2d_{5/2}$	$1g_{7/2}$	$1h_{11/2}$
$3s_{1/2}$	—	0.6143	0.6757	—	—
$2d_{3/2}$		0.6459	0.6989	1.1636	—
$2d_{5/2}$			0.6521	1.1132	—
$1g_{7/2}$				1.0844	—
$1h_{11/2}$					0.6535

TABLE II. EFFECTIVE MAGNETIC REDUCTION MATRIX FOR TIN

	$3s_{1/2}$	$2d_{3/2}$	$2d_{5/2}$	$1g_{7/2}$	$1h_{11/2}$
$3s_{1/2}$	0.6377	∞	−	−	−
$2d_{3/2}$		0.6972	0.3900	−	−
$2d_{5/2}$			0.6333	∞	−
$1g_{7/2}$				0.4275	−
$1h_{11/2}$					0.5935

sensitive to small components in the nuclear wave function. The theoretical value of B(E2, $2_1^+ \to 0_1^+$) can be considered in good agreement with experiment. It is to be noted that the B(E2) depends quadratically on the effective charge.

The results for the M1-operator are given in Table II in the form of an "effective magnetic reduction matrix". This is the matrix of the ratios of the single-particle matrix elements of the effective operator to the corresponding matrix elements of the "bare" operator due to the magnetic moment of the valence neutrons only. The elements labelled by ∞ are zero in the bare operator because of radial forbiddenness, whereas they are different from zero in the effective operator because this particular selection rule is relaxed by Eq.(26). We see that the contributions from the second and third terms in Eq.(10e), which are all coherent (apart from the contributions due to the proton current which are very small), are of opposite sign with respect to the first term, so that the net effect is that of a reduction of a considerable amount of the bare values. The only available experimentally measured M1-quantity is the magnetic moment of the first excited 5_1^- state. The value given for the giromagnetic ratio is −0.065± 0.005. The theoretical values are −0.1504 if the bare operator is used and −0.0648 if the effective operator is used. We see that the first value is in sharp disagreement with experiment while the second is in excellent agreement.

Further available electromagnetic experimental data on ^{116}Sn concern the inelastic-electron-scattering form factors with excitation of the 2_1^+ and 3_1^- states. Calculating these quantities in the Born approximation (which should be a good one at the energies of the experiment) amounts to calculate the nuclear-matrix elements of the operators $e\, j_2(q\,r)\, Y_{2\mu}$ and $e\, j_3(q\,r)\, Y_{3\mu}$, respectively, q being the momentum transfer. To calculate the corresponding effective operators, Eq.(26) must be used at each value of q. The obtained results are in good agreement with the experimental data for the $0_1^+ \to 2_1^+$ transition, both for the absolute value and for the angular distribution. For the $0_1^+ \to 3_1^-$ transition the angular distribution is again consistent with the experimental data, but the absolute value is too small by a factor about 10 (i.e. a factor 3 for the effective charge). This result is not surprising because the 3_1^- state is known [8] to have important admixtures from core-excited configurations, so that it is outside the domain of validity of the perturbative approach.

Summarizing, one can say that the application of the present theory to ^{116}Sn gives essentially good results both for the E2- and for the M1-cases. It is to be stressed that the calculations involve no adjustable parameter.

7. APPLICATION TO NICKEL ISOTOPES

A treatment similar to that of tin can be used for the nickel isotopes [9]. The assumed core consists of 28 neutrons and 28 protons. The valence neutrons are distributed among the four valence levels $2p_{3/2}$, $1f_{5/2}$, $2p_{1/2}$ and $1g_{9/2}$. The core levels included in the calculation of the effective interaction and em operators are $1p_{3/2}$, $1p_{1/2}$, $1d_{5/2}$, $2s_{1/2}$, $1d_{3/2}$ and $1f_{7/2}$. The upper levels are $1g_{7/2}$, $2d_{5/2}$, $2d_{3/2}$ and $3s_{1/2}$. Since the occupation probability of the valence levels is small, we do not correct for the partial inhibition of the core-valence processes due to the Pauli principle. For the same reason, we do not take into account the valence-upper processes. The energy denominators are simplified, i. e. they are taken equal to the difference between particle and hole single-particle energies. The single-particle wave functions are approximated by those of the harmonic oscillator with a size parameter b = 2.063 F. The single particle energies are chosen to be

$$\epsilon_{1p3/2} = \epsilon_{1p1/2} = \epsilon_{1d5/2} = \epsilon_{2s1/2} = \epsilon_{1d3/2} = -10 \text{ MeV}, \quad \epsilon_{1p7/2} = -5 \text{ MeV},$$

$$\epsilon_{2p3/2} = 0, \quad \epsilon_{1p5/2} = 0.78 \text{ MeV}, \quad \epsilon_{2p1/2} = 1.08 \text{ MeV}, \quad \epsilon_{1g9/2} = 3.5 \text{ MeV},$$

$$\epsilon_{1g7/2} = \epsilon_{2d5/2} = \epsilon_{2d3/2} = \epsilon_{3s1/2} = 10 \text{ MeV}$$

The energies of the lowest three valence levels are obtained from the experimental spectrum of ^{57}Ni. For $\epsilon_{1g9/2}$ several values were tried. The chosen value gave the best results for the 3⁻ states (the remaining states were practically insensitive to $\epsilon_{1g9/2}$). The criterion for the core and

TABLE III. E2 EFFECTIVE-CHARGE MATRIX FOR NICKEL

	$2p_{1/2}$	$2p_{3/2}$	$1f_{5/2}$	$1g_{9/2}$
$2p_{1/2}$	—	0.4694	0.8091	—
$2p_{3/2}$		0.4710	0.8552	—
$1f_{5/2}$			0.8266	—
$1g_{9/2}$				0.5116

TABLE IV. EFFECTIVE MAGNETIC REDUCTION MATRIX FOR NICKEL

	$2p_{1/2}$	$2p_{3/2}$	$1f_{5/2}$	$1g_{9/2}$
$2p_{1/2}$	0.8478	0.4220	—	—
$2p_{3/2}$		0.5262	∞	—
$1f_{5/2}$			0.4121	—
$1g_{9/2}$				0.5216

TABLE V. REDUCED TRANSITION PROBABILITY B(M1, $(5/2^-)_1 \rightarrow (3/2^-)_1$) FOR ^{61}Ni CALCULATED WITH BARE AND EFFECTIVE M1-OPERATORS

	A_{11}	A_{13}	A_{31}	A_{33}	B(M1)	Exp.
bare	0.	-0.012	-0.006	-0.009	7.7×10^{-4}	2.49×10^{-2}
effective	-0.105	0.006	0.002	-0.004	1.02×10^{-2}	

Note: The units are squared nuclear magnetons. Columns labelled A_{11}, A_{13}, A_{31}, and A_{33} give contributions to the transition amplitude due to parts of nuclear states with different numbers of quasi-particles.

upper levels is that of a simple reasonable choice. The only delicate level is $1f_{7/2}$. A smaller value of the $(1f_{7/2})$ - valence energy gap would be probably more realistic since the 2.6 MeV level of ^{57}Ni is indicated as an excitation from the $1f_{7/2}$ shell but, for a significantly smaller value, it would be hard to believe in the adopted procedure of calculating the effective quantities. Essentially, the smallest value for which the adopted procedure is meaningful is chosen, and its consequences are tested. The effective em operators which are obtained are used, together with the consistent appropriate Q S T D nuclear wave functions, to calculate observable em quantities. The obtained E2 effective-charge matrix is given in Table III. It turns out that the elements of this matrix are too small to give the large experimental values of B(E2, $2_1^+ \rightarrow 0_1^+$). Actually an effective charge about 2 would be necessary. This is essentially consistent with what is obtained by other authors with different models and effective interactions. On the other hand the calculated effective charge matrix of Table III has elements equal to about 0.5 or 0.8. Better results could be obtained by modifying the value of $\epsilon_{1p7/2}$, but it seems more reasonable to conclude that the particle-hole theory of the effective E2-operator fails in the frame of the configuration mixing considered here. The most natural thing to do would be to include the excitations from the $1f_{7/2}$ proton level in the configuration mixing. We mention that the comparison between theoretical and experimental values for inelastic electron scattering gives essentially the same results as for transition rates.

The effective M1 reduction matrix is given in Table IV. The reduction effect is rather strong, being near to 50% for all the elements except one which is reduced by 15%. The available experimentally measured M1 data refer to ^{61}Ni and are the magnetic moments of the $(3/2^-)_1$ state (-0.74868 n.m.), the magnetic moment of the $(5/2^-)_1$ state ($\pm$ 0.3 n.m.) and the $(5/2^-)_1 \rightarrow (3/2^-)_1$ transition rate (B(M1, $(5/2^-)_1 \rightarrow (3/2^-)_1$) = 2.4910^{-2} (n.m.)^2). Using the bare M1 operator one gets for the magnetic moments the values -1.75 n.m. and 1.30 n.m. respectively. The effective M1 operator gives -0.93 n.m. and 0.49 n.m. respectively. We see that these values are in considerably better agreement with experiment than the values given by the bare operator. A surprising result is obtained for the B(M1). The theoretical value with the bare operator is 7.710^{-4}(n.m.)^2, in reasonable agreement with the experimental value (remember that the B(M1) depends quadratically on the effective operator). The reason of the enhancement is understood by looking at Table V. It is seen that the result with the bare operator is small because the 1 q.p. - 1 q.p. terms vanish due to radial forbiddenness. On the other hand, the breaking of this selection rule in the effective operator, though small ($\langle 5/2 \| \mu^{eff} \| 3/2 \rangle$ = 0.7668 n.m.) is sufficient to account for the large observed value of B(M1).

Summarizing the results for ^{116}Sn and for the nickel isotopes, one can say that the particle-hole theory of the effective em operators is satisfactory, except in those cases in which the admixtures in the true nuclear wave functions from configurations outside the model space are very large and important. The most important features of this kind of calculations is that they allow us to test the nuclear wave functions on the electromagnetic experimental data without introducing new adjustable parameters.

REFERENCES

[1]   The presentation given here is largely indebted to MACFARLANE, M. H. Lectures given at the International School of Physics "Enrico Fermi", 40th Course, Varenna (1967).

[2]   COHEN, S., LAWSON, R. D., MACFARLANE, M. H., PANDYA, S. P., SOGA, M., Phys. Rev. 160 (1967) 903.

[3]   BLOCH, C., HOROWITZ, J., Nucl. Phys. 8, (1958) 91.

[4]   BRANDOW, B. H., Rev. mod. Phys. 39, (1967) 771.

[5]   EDMONDS, A. R., Angular Momentum in Quantum Mechanics, Princeton University Press (1960).

[6]   GMITRO, M., HENDEKOVIĆ, J., SAWICKI, J., Phys. Rev. 169, (1968) 983.

[7]   GMITRO, M., RIMINI, A., SAWICKI, J., WEBER, T., Phys. Rev. 175, (1968) 1243.

[8]   CLEMENT, D. M., UREY-BARANGER, E., Nucl. Phys. A120, (1968) 25.

[9]   ALZETTA, R., GMITRO, M., RIMINI, A., SAWICKI, J., WEBER, T., ICTP Preprint 69/2.

SECTION III
Nuclear Reactions

SHELL-MODEL DESCRIPTION OF
NUCLEAR REACTIONS

C. MAHAUX
Institute of Mathematics,
University of Liège,
Belgium

Abstract

SHELL-MODEL DESCRIPTION OF NUCLEAR REACTIONS.
1. Introduction; 2. The independent-particle model; 2.1. Introduction; 2.2. Single-particle bound states; 2.3. Single-particle scattering states; 2.4. The scattering function; 2.5. Eigenstates of H_0; 3. Qualitative discussion; 3.1. Resonances and BSEC; 3.2. Role of the residual interaction; 4. The basic equations; 4.1. Reminder of the bound-state problem; 4.2. The scattering problem; 5. The scattering matrix; 6. Giant resonances in light even-even nuclei; 7. Intermediate structure; 7.1. Introduction; 7.2. Doorway states; 7.3. A simple model; 7.4. Average cross-section; 7.5. The fine structure; 7.6. Experimental evidence; 8. The isobaric analogue resonances; 8.1. Introduction; 8.2. Isospin of neutron-excess nuclei and isobaric analogue states; 8.3. Fine structure and neutron decay of IAR; 8.4. The basis states and their mutual coupling; 8.5. Isospin mixing at the IAR; 8.6. Spectroscopic information.

1. INTRODUCTION

These lectures are devoted to the extension of the shell-model to the description of nuclear reactions. We shall, therefore, not deal with the general theory of nuclear reactions, which is independent of the choice of any dynamical model. The restriction to the shell-model is not as limitative as it appears, because of the following reasons: firstly, the main features of the results which will be given below remain unchanged if one replaces the shell-model proper by any model where the exact Hamitonian H is decomposed as the sum of a model Hamiltonian H_0 and a residual interaction V, and where H is diagonalized in a suitably chosen space of functions spanned by the eigenstates of H_0. Secondly, a truly general theory of nuclear reactions does not exist yet, in our opinion. The so-called general theories all imply a number of assumptions. Moreover, these theories become useful only when a dynamical model is introduced. Finally, we believe that the shell-model approach provides a consistent and simple framework for the study of many interesting physical phenomena, like resonance reactions, direct reactions, the giant resonances, the intermediate structure, the isobaric analogue resonances, and the optical model.

In this paper, we can only touch a few of these topics. We shall discuss the extension of the shell-model to the continuum, and its application to the giant resonances, the intermediate structure and the isobaric analogue resonances. We aim neither at generality nor at completeness. Rather, we shall try to emphasize the main physical ideas and results. A detailed and rather complete account of the present state of the shell-model approach to nuclear reactions is given in a recent book by Weidenmüller and the author [1], to which one can refer for more details, or for the application of the theory to other topics. We follow the notations of Ref.[1].

2. THE INDEPENDENT-PARTICLE MODEL

2.1. Introduction

In the present section, we study the independent-particle model, where the residual interaction V is neglected. The Hamiltonian of the model is simply a sum of single-particle Hamiltonians:

$$H_0 = \sum_{n=1}^{A} h_0(n) = \sum_{n=1}^{A} [t(n) + v_0(n)] \qquad (2.1)$$

Here, A is the total number of nucleons of the system, $t(n)$ the kinetic-energy operator for nucleon n, and $v_0(n)$ the single-particle potential. Clearly, v_0 must have a finite depth since we want to describe scattering phenomena. It is usually assumed that $v_0(n)$ is the Hartree-Fock potential for the nucleus with A nucleons. As discussed in the seminars by Vautherin, v_0 is then non-local. For the sake of simplicity (this is by no means restrictive), we shall here take v_0 to have the Woods-Saxon shape, plus a one-body Coulomb potential and a spin-orbit potential:

$$v_0 = V_{cent}(r) + V_{s.o.} \vec{\ell} \cdot \vec{s} + V_{cont} \qquad (2.2)$$

The standard way of choosing v_0 consists in adjusting the parameters of the Woods-Saxon potential to reproduce the experimental values of the single-particle energies, as determined from the adjacent nuclei. This practice is certainly not quite satisfactory and a self-consistent determination of v_0 would probably be preferable. We shall, nevertheless, conform ourselves to the standard procedure, for simplicity.

2.2. Single-particle bound states

There exists a finite number of bound single-particle states in the potential v_0. They are characterized by a principal quantum number n, an orbital angular momentum ℓ, a total angular momentum j and a magnetic quantum number m. We denote the single-particle energies of these bound states by $E_n^{\ell j}$, and the associated normalized single-particle bound states by

$$\frac{1}{r} w_{\ell j}^b (r, k_n^{\ell j}) \mathcal{Y}_{\ell j}^m(\hat{r}) \qquad (2.3)$$

Here, $w_{\ell j}^b$ is the radial part of the wave function, and $\mathcal{Y}_{\ell j}^m(\hat{r})$ is an eigenfunction of the operators $\vec{\ell}^2$, $\vec{j}^2$ and j_z, with eigenvalues $j(j+1)$, $\ell(\ell+1)$ and m, respectively. The bound states are degenerate with respect to the magnetic quantum number m.

Let us give the example of the single-particle states in ^{16}O, by means of which we shall often illustrate the discussion. The single-particle energies are represented in Fig.1. The shaded region represents the continuum set of single-particle energies.
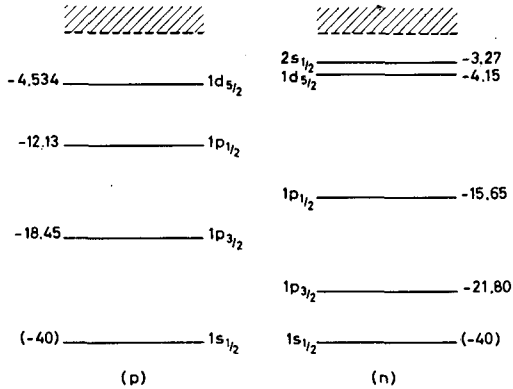
FIG.1.   Neutron and proton single-particle levels in ^{16}O.

2.3. Single-particle scattering states

The scattering eigenstates of h_0 may be characterized by the quantum numbers ℓ, j, m and by the energy E (or the associated wave number k). The single-particle wave function has the same form as (2.3):

$$\frac{1}{r} u_{\ell j}(r, k) \, \mathscr{Y}_{\ell j}^{m} (\hat{r}) \tag{2.4}$$

The $\underline{\text{radial wave function}}$ $u_{\ell r} (r, k)$ is the regular solution of the following differential equation:

$$(E - D_{\ell j}) u_{\ell j} (r, k) = 0 \tag{2.5}$$

Here, the operator $D_{\ell j}$ is defined by

$$D_{\ell j} = - \frac{\hbar^2}{2M} \frac{d^2}{dr^2} + \frac{\hbar^2}{2M} \frac{\ell(\ell+1)}{r^2} + V_{cent} + V_{s.o.} \mathscr{H}_{\ell j} + V_{coul} \tag{2.6a}$$

with

$$\mathscr{H}_{\ell j} = \begin{cases} -(\ell + 1) & \text{for } j = \ell - \frac{1}{2} \\ +\ell & \text{for } j = \ell + \frac{1}{2} \end{cases} \tag{2.6b}$$

We normalize $u_{\ell j}(r, k)$ to a δ-function of the energy:

$$\int_0^{\infty} dr \, u_{\ell j}(r, k) \, u_{\ell j}(r, k') = \delta(E - E') \tag{2.7}$$

The completeness relation reads

$$\sum_n w^b_{\ell j}(r, k^{\ell j}_n) w^b_{\ell j}(r', k^{\ell j}_n) + \int_0^\infty dE\, u_{\ell j}(r, k') u_{\ell j}(r, k) = \delta(r - r')$$

(2.8)

2.4. The scattering function

For large values of kr, we have

$$u_{\ell j}(r, k) = x_{\ell j}(k) O_{\ell j}(r, k) + y_{\ell j}(k) I_{\ell j}(r, k)$$

(2.9)

The functions $O_{\ell j}$ and $I_{\ell j}$ are the outgoing and incoming wave functions, respectively:

$$O_{\ell j} = \exp[i\{kr - \eta \log 2kr - \tfrac{1}{2}\ell\pi + \sigma_0\}]$$

(2.10a)

$$I_{\ell j} = \exp[-i\{kr - \eta \log 2kr - \tfrac{1}{2}\ell\pi + \sigma_0\}]$$

(2.10b)

Here, η is the Coulomb parameter and σ_0 the Coulomb phase shift for $\ell = 0$. The ratio of the amplitude of the outgoing wave to that of the incoming wave is the scattering function $S_{\ell j}$:

$$S_{\ell j}(k) = -\frac{x_{\ell j}(k)}{y_{\ell j}(k)}$$

(2.11)

The conservation of flux implies that $|S_{\ell j}|^2 = 1$. Hence, we can write

$$S_{\ell j}(k) = \exp(2i\delta_{\ell j})$$

(2.12)

The real angle $\delta_{\ell j}$ is the potential scattering phase shift.

In general, $S_{\ell j}(k)$ is a smooth function of k. It can, however, display a strong energy dependence in the vicinity of a single-particle resonance. Then, we can write

$$S_{\ell j}(k) \approx \exp(2i\xi^{\ell j}_n)\left(1 - i\,\frac{\Gamma^{\ell j}_n}{E - \zeta^{\ell j}_n + \tfrac{1}{2}i\Gamma^{\ell j}_n}\right)$$

(2.13)

An example is provided by the $d_{3/2}$ single-particle resonance in the scattering of neutrons by ^{16}O. It occurs at $\zeta^{2\frac{3}{2}}_n = 998$ keV and has a width $\Gamma^{2\frac{3}{2}}_n \approx 97$ keV. We note that if we slightly deepen v_0 for the $d_{3/2}$ states, this single-particle resonance disappears and a $1d_{3/2}$ <u>bound</u> single-particle state appears.

In the absence of residual interaction, the incoming nucleon is scattered elastically by the average single-particle potential. The cross-section is smooth, except for the possible occurrence of single-particle resonances. There exists no possibility for the incoming nucleon to share its energy with the nucleons of the target, and no compound state can be formed. Thus, it is vital to introduce the residual interaction if one wants to describe nuclear resonances. The role of the residual interaction is qualitatively discussed in section 3.

2.5. Eigenstates of H_0

The eigenstates of H_0 are constructed by distributing the A nucleons in single-particle orbitals, and by coupling the individual angular momenta to a given total angular momentum J. The parity π is given by

$$\pi = (-)^{\sum_{i=1}^{A} \ell_i} \tag{2.14}$$

We denote by Φ_n (n = 1, ...,M) the bound eigenstates of H_0 (all nucleons in bound single-particle orbitals). They are called quasi-bound states, or bound states embedded in the continuum (BSEC). We have

$$H_0 \Phi_n = E_n \Phi_n \tag{2.15}$$

We denote by χ_E^c the scattering eigenstates of H_0, with one nucleon in the continuum, i.e. in a single-particle scattering state. The lower index E refers to the energy

$$H_0 \chi_E^c = E \chi_E^c \tag{2.16}$$

The upper index c specifies the state of the (A-1) nucleons of the target, the orbital and total angular momentum of the nucleon in the continuum, the total angular momentum J of the system (and its projection). The explicit form of χ_E^c is the following:

$$\chi_E^c = \mathscr{A}_A \left\{ \frac{1}{r_A} u_{\ell r}(r_A, k_c) \varphi_c \right\} \tag{2.17}$$

Here, $\mathscr{A}_A$ antisymmetrizes with respect to the Ath nucleon and the first (A-1) nucleons, and k_c is the wave number in channel c:

$$\frac{\hbar^2}{2M} k_c^2 = E - \epsilon_c \tag{2.18}$$

ϵ_c is the threshold energy of channel c, i.e. the rest mass of the system target + nucleon. The surface function φ_c is obtained by coupling $\mathscr{Y}_{\ell j}^m(\hat{A})$ to the wave function Ω_c of the target, so that the system has total angular momentum J, projection M.

Let us give an example for the functions Φ_n and χ_E^c. We take the case of ^{16}O (Fig.1). We assume that the wave function of ^{16}O in its ground state is formed by filling the single-particle states $1s_{1/2}$, $1p_{3/2}$, $1p_{1/2}$. We denote this state by $|\Phi_0\rangle$ and take it as reference state, with respect to which we shall count the particles and holes. The state Φ_0 is a quasi-bound state (this terminology is awkward in this case). Another BSEC, which we denote by Φ_1, is obtained by raising a neutron from the $1p_{3/2}$ orbital to the $2s_{1/2}$ state. We have, with the usual notation,

$$\Phi_1 = (2s_{1/2})(1p_{3/2})^{-1} \tag{2.19}$$

According to Fig.1, E_1 is equal to 18.53 MeV (we take E_0 as reference energy). An example of a continuum state χ_E^c is provided by the case where a neutron is scattered by a target ^{15}O. The index c specifies the target state, (for instance, a hole in the $1p_{1/2}$ shell), the orbital angular momentum ($\ell = 0$, for instance) of the neutron, its total angular momentum ($j = 1/2$ in the present example), the total angular momentum of the system ($J = 1$, for instance) and the projection M of the total angular momentum. The latter quantum number is of little physical interest (for unpolarized beams) because the collision matrix is diagonal in M and independent of M. The threshold energy ϵ_c in the present case is $\epsilon_c = 15.65$ MeV. We shall refer to channel c as

$$c = \{(s_{1/2})(1p_{1/2})^{-1}\}_{J=1} \tag{2.20}$$

This example explains the origin of the terminology "bound state embedded in the continuum" used here for the states Φ_n. Indeed, the energy E_1 of Φ_1 is larger than the threshold energy ϵ_c. Hence, the eigenvalue E_1 lies in a continuous spectrum of eigenvalues of H_0. The terminology is derived from pioneering work by Fonda and collaborators [2].

The BSEC Φ_n and the channel functions χ_E^c with one nucleon in the continuum are the only ones which are introduced in the shell-model approach to nuclear reactions. This model was developed by C. Bloch [3]. All wave functions which will be considered are thus linear combinations of the basis functions Φ_n and χ_E^c. In this space of functions, the unit operator is given by

$$1 = \sum_{n=1}^{M} |\Phi_n\rangle\langle\Phi_n| + \sum_{c=1}^{\Lambda} \int_{\epsilon_c'}^{\infty} dE' |\chi_{E'}^c\rangle\langle\chi_{E'}^c| \tag{2.21}$$

3. QUALITATIVE DISCUSSION

3.1. Resonances and BSEC

In section 2.5., we have seen that there exist bound eigenstates of H_0 which lie in the continuous spectrum. Intuitively, we expect that these bound states disappear when the residual interaction is turned on. If the residual interaction is sufficiently weak, we expect that the BSEC will become metastable states with a long life-time, i.e. resonance states. This will be substantiated in the next sections. In the present section,

we discuss qualitatively how the residual interaction allows the population of resonance states.

We consider the example of the BSEC Φ_1 of Eq.(2.1) and of the channel c of Eq.(2.1). In the absence of residual interaction ($V = 0$), the $s_{1/2}$ neutron is scattered by the average potential due to the target ^{15}O. No resonance can occur. In all physical systems, the occurrence of an isolated resonance is associated with the excitation of a normal mode of motion of the system. Let us see how a normal mode of the nucleus ^{16}O, namely the BSEC Φ_1, can be excited by the incoming neutron. If $V \neq 0$, the incoming neutron can interact with the nucleons of the target ^{15}O, and excite them into un-occupied states. In particular, when the kinetic energy of the neutron is equal to 2.88 MeV, the neutron can release 6.15 MeV by falling into the $2s_{1/2}$ orbital. These 6.15 MeV can be used by a neutron of the $(1p_{3/2})$ shell to jump into the hole available in the $(1p_{1/2})$ shell. Thereby, the BSEC Φ_1 is formed via the interaction of the incoming neutron with a neutron of the $(1p_{3/2})$ shell. In turn, the residual interaction V allows the decay of Φ_1 into the channels. Clearly, the neutron in the $(2s_{1/2})$ shell can be re-emitted in channel c by picking 6.15 MeV from a neutron in the $(1p_{1/2})$ state. This is the process of resonant elastic scattering. The state Φ_1 can also decay into other channels. For instance, the neutron in the $(2s_{1/2})$ state can fall in the hole in the $(1p_{3/2})$ shell. Thereby, it liberates 18.53 MeV which can be used by a proton of the $(1p_{1/2})$ shell to escape. This is then the charge exchange resonant reaction ^{15}O(n,p)^{15}N.

According to this simple-minded picture, we expect therefore a resonance to occur at 18.53 MeV excitation energy in ^{16}O. However, we have grossly oversimplified the physical situation, and the role of the residual interaction is much more complex than we have described. This is qualitatively discussed in the next section.

3.2. Role of the residual interaction

In section 3.1, we exhibited one role of the residual interaction, namely that which consists in establishing the connection between the channels and the BSEC. This part of the residual interaction is essential for the occurrence of compound nuclear resonances. It is contained in the first curly brackets of the following equation, derived from Eq.(2.21):

$$
V = \left\{ \sum_{i=1}^{M} \sum_{c=1}^{\Lambda} \int_{\epsilon_c}^{\infty} dE \, |\Phi_i\rangle\langle\Phi_i| V |\chi_E^c\rangle\langle\chi_E^c| \right.
$$

$$
\left. + \sum_{i=1}^{M} \sum_{c=1}^{\Lambda} \int_{\epsilon_c}^{\infty} dE \, |\chi_E^c\rangle\langle\chi_E^c| V |\Phi_i\rangle\langle\Phi_i| \right\}
$$

$$
+ \left\{ \sum_{i=1}^{M} \sum_{j=1}^{M} |\Phi_i\rangle\langle\Phi_i| V |\Phi_j\rangle\langle\Phi_j| \right\}
$$

$$
+ \left\{ \sum_{c=1}^{\Lambda} \sum_{c'=1}^{\Lambda} \int_{\epsilon_c}^{\infty} dE \int_{\epsilon_{c'}}^{\infty} dE' \, |\chi_E^c\rangle\langle\chi_E^c| V |\chi_{E'}^{c'}\rangle\langle\chi_{E'}^{c'}| \right\} \qquad (3.1)
$$

The second curly brackets contain the piece of the residual inter-action which connects the BSEC one to another. This is the part of the residual interaction which is included in the standard bound-state shell-model calculations. It mixes the BSEC with one another. Even when only one BSEC (Φ_1) is present, it shifts the resonance energy by an amount $\langle \Phi_1 | V | \Phi_1 \rangle$ (a few MeV).

The last curly brackets contain that part of the residual interaction which directly connects channel c to channel c'. It is associated to the direct reactions [4,5], and is referred to as direct channel-channel, or direct continuum-continuum coupling. It is only in the absence of direct channel-channel coupling that an explicit algebraic expression can be given for the scattering matrix. In the following, we assume that the direct channel-channel coupling is negligible:

$$\langle \chi_E^c | V | \chi_{E'}^{c'} \rangle = 0 \tag{3.2}$$

This assumption is usually not justified numerically, but is sufficient for our purpose. Various numerical methods to include the direct channel-channel coupling are described in Ref.[1]. The two main methods consist in using perturbation techniques or in transforming the many-body Schrödinger equation into a set of coupled integro-differential equations. Most of the numerical results described below have been obtained by the latter method. Here, we are more interested in obtaining a parametric expression of the S-matrix, in order to study the intermediate structure phenomenon.

4.   THE BASIC EQUATIONS

4.1. Reminder of the bound-state problem

In the standard bound-state shell-model calculations, one diagonalizes the full Hamiltonian H in the space spanned by M bound eigenstates $\Phi_i (i = 1, \ldots, M)$ of H_0. We have the dynamical equations

$$H = H_0 + V \tag{4.1}$$

$$H_0 \Phi_i = E_i \Phi_i, \quad \langle \Phi_i | \Phi_j \rangle = \delta_{ij} \tag{4.2}$$

We want to construct wave functions of the form

$$\Psi_n = \sum_{i=1}^{M} b_n(i) \Phi_i \tag{4.3}$$

in such a way that

$$\langle \Psi_n | H | \Psi_m \rangle = \lambda_n \delta_{nm} \tag{4.4}$$

In other words, we want to diagonalize H in the space of functions $\{\Phi_i\}$, i.e. to construct the eigenstates of the operator

$$\bar{H} = \sum_{i,\,j=1}^{M} |\Phi_i\rangle\langle\Phi_i|H|\Phi_j\rangle\langle\Phi_j| \qquad (4.5)$$

Introducing expression (4.3) into Eq.(4.4), and taking Eqs (4.2) into account, we find that the coefficients $b_n(i)$ fulfill the following set of homogeneous equations:

$$\sum_i [(E_j - \lambda_n)\delta_{ij} + V_{ij}]\,b_n(i) = 0 \qquad (4.6)$$

where

$$V_{ij} = \langle\Phi_i|V|\Phi_j\rangle \qquad (4.7)$$

The energies λ_n of the bound eigenstates of $\bar{H}$ are thus determined by the roots of

$$\det[(E_j - \lambda)\delta_{ij} + V_{ij}] = 0 \qquad (4.8a)$$

The wave functions are given by

$$\psi_j = \sum_{i=1}^{M} \underset{\approx}{Q}_{ni}\,\Phi_i \qquad (4.8b)$$

where $\underset{\approx}{Q}$ is the matrix which diagonalizes the real symmetric matrix

$$E_j\delta_{jk} + V_{jk}$$

4.2. The scattering problem

By analogy with the bound-state problem, we look for a wave function of the form

$$\Psi_E^c = \sum_{n=1}^{M} b_E^c(n)\Phi_n + \sum_{c'=1}^{\Lambda} \int_{\epsilon_{c'}}^{\infty} dE'\,a_E^c(E',c')\chi_{E'}^{c'} \qquad (4.9)$$

and such that we have

$$\langle\Psi_E^c|\Psi_{E'}^{c'}\rangle = \delta_{cc'}\delta(E - E') \qquad (4.10)$$

$$\langle\Psi_E^c|H|\Psi_{E'}^{c'}\rangle = E\delta_{cc'}\delta(E - E') \qquad (4.11)$$

The differences with the bound-state model are the following:
(1) The energy spectrum of H is continuous, above the lowest threshold.
However, we would like to find an equation analogous to Eq.(4.8) which
would determine the resonance energies and widths.
(2) The wave functions Ψ_E^c are characterized not only by the energy, but
also by the boundary condition. This is indicated by the upper index c
which means here that Ψ_E^c has an incoming wave in channel c, only. Hence,
Ψ_E^c has the following asymptotic behaviour (if the radial coordinate r_A
of nucleon A tends towards infinity)

$$\Psi_E^c \propto [\delta_{cc'} I_c(r_A, k_c) - S_{c'c} O_{c'}(r_A, k_{c'})] \varphi_{c'} \qquad (4.12)$$

By definition, $S_{cc'}$ is the cc' element of the <u>scattering matrix</u>. The meaning
of the other symbols has been given in sections 2.4 and 2.5. The relation
between the S-matrix and the cross section is given in the review article
by Lane and Thomas [22]. The expression of $S_{c'c}$ in terms of the coeffi-
cients $b_E^c(i)$ can be found by comparing the asymptotic form of Eq.(4.9)
with Eq.(4.12). We obtain

$$S_{cc'} = \exp(i\delta_c + i\delta_{c'}) \left[\delta_{cc'} - 2i\pi \sum_{j=1}^{M} b_E^c(j) V_j^{c'}(E) \right] \qquad (4.13)$$

where

$$V_j^{c'}(E) = \langle \chi_E^{c'} | V | \Phi_j \rangle \qquad (4.14)$$

We have used assumption (3.2), and the normalization implied by Eq.(4.23)
below.
    Equation (4.11) is equivalent to the following sets of equations

$$\langle \Phi_i | H | \Psi_E^c \rangle = E \langle \Phi_i | \Psi_E^c \rangle \qquad (i = 1, ..., M) \qquad (4.15a)$$

$$\langle \chi_{E'}^{c'} | H | \Psi_E^c \rangle = E \langle \chi_{E'}^{c'} | \Psi_E^c \rangle \qquad (c, c' = 1, ..., \Lambda) \qquad (4.15b)$$

We recall that

$$\langle \Phi_i | \Phi_j \rangle = \delta_{ij}; \quad \langle \chi_E^c | \chi_{E'}^{c'} \rangle = \delta_{cc'} \delta(E - E') \qquad (4.16)$$

Inserting Eq.(4.9) into Eq.(4.15a), and using the definitions (4.7) and (4.14), we obtain

$$(E_i - E)b_E^c(i) + \sum_{j=1}^{M} V_{ij} b_E^c(j) + \sum_{c'=1}^{\Lambda} \int_{\epsilon_{c'}} dE' a_E^c(E', c')$$

$$V_i^{c'}(E') = 0 \qquad (4.17a)$$

Equations (4.9), (4.15b) and (3.2) yield

$$(E' - E)a_E^c(E'; c') + \sum_{j=1}^{M} b_E^c(j) V_j^{c'}(E') = 0 \qquad (4.17b)$$

Equations (4.17a) and (4.17b) are the basic equations of the shell-model approach to nuclear reactions, in the absence of direct continuum-continuum coupling.

4.3. The Lippmann-Schwinger equation

The general solution of Eq.(4.17b) reads

$$a_E^c(E'; c') = A_{cc'} \delta(E - E') + \frac{1}{E - E'} \sum_{j=1}^{M} b_E^c(j) V_j^{c'}(E') \qquad (4.18)$$

The constants $A_{cc'}$ have to be determined from the boundary condition defining Ψ_E^c, which was not yet used. We note that $a_E^c(E'; c')$ occurs in an integral over E' (see Eq.(4.9)), so that we have to specify how we integrate in the vicinity of the singularity at $E' = E$ of the last term in Eq.(4.18). This is a well-known problem of scattering theory. We take the convention that the path of integration passes below the singularity $E' = E$. This amounts to replace E by $E + i\epsilon$ ($\epsilon \to 0$) and to let $\epsilon \to 0$. We recall this convention by writing an upper index + to E. We have

$$\int dE' \frac{f(E'; r)}{E^+ - E'} = \lim_{\epsilon \to 0} \int dE' \frac{f(E'; r)}{E + i\epsilon - E'} = P \int dE' \frac{f(E'; r)}{E - E'} - i\pi f(E; r)$$

$$(4.19)$$

if the range of integration includes $E' = E$. Here, $P\int$ is the principal value integral. If $f(E'; r)$ behaves asymptotically, for large values of r, like $xO(r, k) + yI(r, k)$, the integral (4.18) behaves asymptotically like $O(r, k)$ [6]. Thus, we write

$$a_E^c(E'; c') = \delta_{cc'} \delta(E - E') + \frac{1}{E^+ - E'} \sum_{j=1}^{M} b_E^c(j) V_j^{c'}(E') \qquad (4.20)$$

Equations (4.16) show that

$$b_E^c(i) = \langle \Phi_i | \Psi_E^c \rangle ; \quad a_E^c(E';c') = \langle \chi_{E'}^{c'} | \Psi_E^c \rangle \tag{4.21}$$

From Eqs (4.17a), (4.14) and (4.7), we obtain

$$b_E^c(i) = \frac{1}{E - E_i} \left[\langle \Phi_i | V | \Phi_j \rangle \langle \Phi_j | \right.$$

$$\left. + \sum_{c'=1}^{\Lambda} \int_{\epsilon_{c'}}^{\infty} dE' \langle \Phi_i | V | \chi_{E'}^{c'} \rangle \langle \chi_{E'}^{c'} | \right] \Psi_E^c \rangle \tag{4.22}$$

Equations (4.20), (4.21) and (4.14) yield

$$a_E^c(E';c') = \delta_{cc'}\,\delta(E-E') + \frac{1}{E^+ - E'} \sum_{j=1}^{M} \langle \chi_{E'}^{c'} | V | \Phi_j \rangle \langle \Phi_j | \Psi_E^c \rangle \tag{4.23}$$

Equations (4.9), (4.22) and (4.23) give the following form for Ψ_E^c:

$$\Psi_E^c = \chi_E^c + \sum_{i,j=1}^{M} \frac{1}{E - E_i} | \Phi_i \rangle \langle \Phi_i | V | \Phi_j \rangle \langle \Phi_j | \Psi_E^c \rangle$$

$$+ \sum_{i=1}^{M} \sum_{c'=1}^{\Lambda} \int_{\epsilon_{c'}}^{\infty} dE' \frac{1}{E - E_i} | \Phi_i \rangle \langle \Phi_i | V | \chi_{E'}^{c'} \rangle \langle \chi_{E'}^{c'} | \Psi_E^c \rangle$$

$$+ \sum_{i=1}^{M} \sum_{c'=1}^{\Lambda} \int_{\epsilon_{c'}}^{\infty} dE' \frac{1}{E^+ - E'} | \chi_{E'}^{c'} \rangle \langle \chi_{E'}^{c'} | V | \Phi_i \rangle \langle \Phi_i | \Psi_E^c \rangle \tag{4.24}$$

Remembering that the unit operator is given by Eq.(2.21), and that we made assumption (3.2), we see that Eq.(4.24) is nothing but the Lippmann-Schwinger equation

$$\Psi_E^c = \chi_E^c + \frac{1}{E^+ - H_0} V \Psi_E^c \tag{4.25}$$

When the direct continuum-continuum coupling is not omitted, care must be taken in handling the Lippmann-Schwinger equation (4.25) [1].

5.   THE SCATTERING MATRIX

In the present section, we solve the fundamental equations (4.17a) and (4.20). We recall that the equations hold only if Eq.(3.2) is fulfilled. They do nevertheless contain the essential physical features which are of interest here. We insert Eq.(4.20) in Eq.(4.17a) and obtain

$$\sum_{j=1}^{M} \left[(E - E_j)\delta_{ji} - V_{ij} \sum_{c'=1}^{\Lambda} \int_{\epsilon_{c'}}^{\infty} dE' \; \frac{V_i^{c'}(E')V_j^{c'}(E')}{E^+ - E'} \right] b_E^c(j) = +V_i^c(E) \qquad (5.1)$$

This system of linear equations for the unknowns $b_E^c(j)$ is analogous to Eqs (4.6) of the bound-state problem. The main difference is that the system is now inhomogeneous. This reflects the fact that the energy spectrum is continuous, so that we do not have an eigenvalue problem. We come back to this point below. Let us define the matrix

$$\underset{\approx}{D} = (D_{ij}) \qquad (5.2a)$$

with

$$D_{ij}(E) = (E - E_j)\delta_{ij} - V_{ij} - \sum_{c'=1}^{\Lambda} \int_{\epsilon_{c'}}^{\infty} dE' \; \frac{V_i^{c'}(E')V_j^{c'}(E')}{E^+ - E'} \qquad (5.2b)$$

The solution of Eqs (5.1) reads

$$b_E^c(j) = \sum_{i=1}^{M} (\underset{\approx}{D}^{-1})_{ji} V_i^c(E) \qquad (5.3)$$

Inserting this result in Eq.(4.13), we obtain the expression of the scattering matrix

$$S_{cc'} = \exp(i\delta_c + i\delta_{c'}) \left[\delta_{cc'} - 2i\pi \sum_{i,\,j=1}^{M} V_i^c(E)(\underset{\approx}{D}^{-1})_{ij} V_j^{c'}(E) \right] \qquad (5.4)$$

Let us introduce the complex orthogonal matrix $\mathcal{O}$—which diagonalizes the complex symmetric matrix $\underset{\approx}{D}$:

$$\sum_{j,\,m=1}^{M} \mathcal{O}_{ij} D_{jm} \mathcal{O}_{\ell m} = (E - \mathcal{E}_\ell)\delta_{i\ell} \qquad (5.5)$$

The eigenvalues $\mathcal{E}_{\overline{\ell}}$ are complex:

$$-\mathcal{E}_\ell = \zeta_\ell - \tfrac{1}{2}i\Gamma_\ell \qquad (5.6)$$

The quantities $\mathscr{O}$ and $\mathscr{E}_\ell$ are energy-dependent, because of the last term in Eq.(5.2b). In the absence of single-particle resonances, however, this energy dependence is quite smooth and can safely be neglected. The single-particle resonances can be treated on the same footing as the BSEC Φ_j [1]. We introduce the states

$$\psi_j = \sum_{i=1}^{M} \mathscr{O}_{\overline{ji}} \Phi_i \tag{5.7}$$

and the associated quantities

$$\Gamma_{jc}^{\frac{1}{2}} = (2\pi)^{\frac{1}{2}} \sum_{i=1}^{M} \mathscr{O}_{ji} V_i^c = (2\pi)^{\frac{1}{2}} \langle \chi_E^c | V | \Psi_j \rangle \tag{5.8}$$

Equation (5.4) can be written in the form

$$S_{cc'} = \exp(i\delta_c + i\delta_{c'}) \left[\delta_{cc'} - i \sum_{j=1}^{M} \frac{\Gamma_{jc}^{\frac{1}{2}} \Gamma_{jc'}^{\frac{1}{2}}}{E - \zeta_j + \frac{1}{2}i\Gamma_j} \right] \tag{5.9}$$

We recognize the many-level Breit-Wigner formula. The partial widths are Γ_{jc}, the resonance energies ζ_j and the widths Γ_j. It is possible to show [1] that $\Gamma_j > 0$. Because of the conservation of the trace of a matrix under orthogonal transformations, we have, from Eqs (4.19), (5.5) and (5.6),

$$\sum_{j=1}^{M} \Gamma_j = 2\pi \sum_{j=1}^{M} \sum_{c^+} (V_j^c)^2 = \sum_{j=1}^{M} \sum_{c^+} \Gamma_{jc} \tag{5.10}$$

where the sums over c^+ run over the open channels. In the case of an isolated resonance, Eq.(5.10) yields

$$\Gamma_j = \sum_{c^+=1}^{\Lambda} \Gamma_{jc} \tag{5.11}$$

it is possible to show that the quantities Γ_{jc} are then real. In the case of a narrow but not isolated resonance, we only have the weaker sum rule [1]

$$\Gamma_j = \sum_{c^+=1}^{\Lambda} |\Gamma_{jc}| \tag{5.12}$$

The resonance energies $\mathscr{E}_j$ are the roots of the equation

$$\det \underset{\approx}{D} = D(E) = 0 \tag{5.13}$$

(This equation should be compared with Eq.(4.8a)). At these (complex) energies, the homogeneous system of equations obtained by putting the right-hand side of Eq.(5.1) equal to zero has a non-trivial solution. Hence, the homogeneous Lippmann-Schwinger equation (Eq.(4.25) with $\chi_E^c = 0$ on the right-hand side) has a solution. This means that the Schrödinger equation has a purely outgoing regular solution. This is a "radioactive state" and corresponds to the definition of resonances given by Humblet and Rosenfeld [7].

6. GIANT RESONANCES IN LIGHT EVEN-EVEN NUCLEI

Most of the numerical applications of the formalism described above concern the dipole photonuclear reactions on light even-even nuclei. The giant resonance of ^{16}O has been computed by many authors [1, 8-12], who used different treatments for the continuum-continuum coupling. Recently, the giant resonances of ^{12}C, ^{40}Ca and ^{28}Si were also studied [13]. Since the ground states of these nuclei are 0^+ states with isospin $T = 0$ (at least, within a very good approximation), electric dipole transitions leading to these ground states must come from the $T = 1$ components of 1^- states.

There exists extensive theoretical work on the dipole states in ^{16}O, which we take here as an example. The early calculations used the standard bound-state shell-model, with harmonic oscillator potential wells. We cite the pioneering paper by Elliott and Flowers [14] and the work of Gillet and Vinh Mau [15]. There, the residual interaction is diagonalized among a set of 1p-1h states constructed by putting the particle in the s-d shell, and the hole in the 1p-shell. Since the Coulomb interaction is omitted, the states obtained in this way have pure isospin $T = 1$ or $T = 0$. Gillet and Vinh Mau [15] find $T = 1$ $J^\pi = 1^-$ states ψ_j (see Eq.(4.8b)) at 13.5, 18.1, 19.6, 22.7 and 25.4 MeV excitation energy; $J^\pi = 1^-$, $T = 0$ states occur at 15, 16.7 and 22 MeV. More than 95% of the total dipole transition probability is carried by the states at 22.7 and 25.4 MeV, which we expect, therefore, to lead to prominent bumps in the photonuclear cross-sections, once the effect of the continuum will be included. Experimentally, it is indeed found that two main peaks occur at about 22.3 and 24.8 MeV. The level at 22.7 MeV is mainly a $(1d_{5/2})(1p_{3/2})^{-1}$ configuration; that at 25.4 MeV has the main component $(1d_{3/2})(1p_{3/2})^{-1}$.

The dipole photoabsorption cross-section (γ, c) is proportional to $|M_c(E)|^2$, with

$$M_c(E) = \langle 0 | E1 | \Psi_E^c \rangle \tag{6.1}$$

Here, $|0\rangle$ is the ground state of the target nucleus, E1 the electric dipole operator and Ψ_E^c the wave function (4.9). Hence, the shell-model theory allows the calculation of photonuclear reactions. Most of the calculations described below are based on the coupled-channels method for solving the Lippmann-Schwinger equation (4.25). This method includes the continuum-continuum part of the residual interaction. Since E1 is a sum of one-body operators, only the 1p-1h configurations Φ_i and χ_E^c of Ψ_E^c contribute to $M_c(E)$ (we take $|0\rangle$ as vacuum).
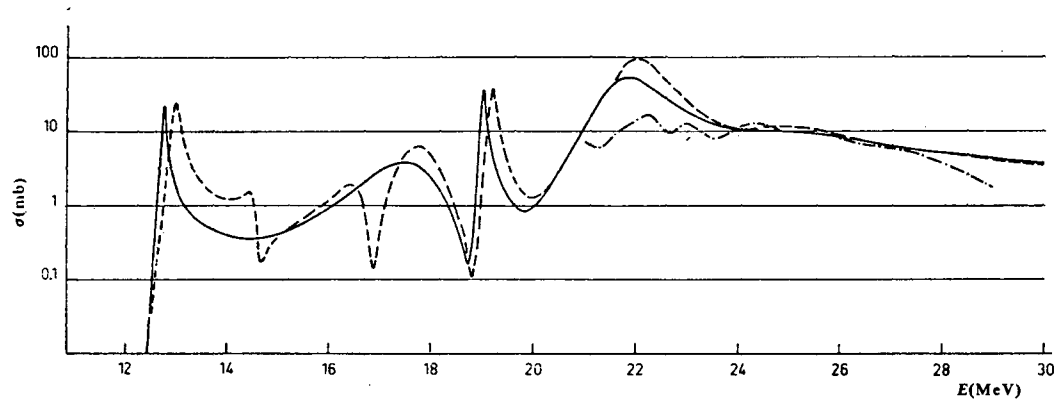
FIG.2. Total $^{16}O(\gamma, p)$ cross-section, including the channels with $(1p_{1/2})^{-1}$ and $(1p_{3/2})^{-1}$ target states. The full curve is the result when no isospin mixing is included. The dashed curve takes isospin mixing into account. The dot- and dash curve represents experimental results (from Raynal et al. [9]).

There exist two types of continuum calculations. In the first case, one neglects the difference between neutron and proton wave functions, for scattering as well as bound single-particle states. The full curve of Fig.2 represents the total $^{16}O(\gamma, p)$ cross-section, computed in this way by Raynal et al.[9]. The dashed curve includes the differences between neutron and proton wave functions. The dot-and-dash curve represents experimental results [16]. We see that the main difference between the dashed and full curves consists in the appearance of strong energy dependences at 14.7 and 16.9 MeV. These are associated with the T = 0 states found by Gillet and Vinh Mau [15] at 15 and 16.7 MeV. Indeed, these states do now have T = 1 admixtures, since the Coulomb interaction is taken into account. Hence, they may also give rise to resonances. We note that the resonance at 14.7 MeV has a peculiar shape. This shape can be interpreted by assuming that the main isospin impurity of this level arises from one continuum wave function χ_E^c [17].

When comparing the theoretical and experimental results, two characteristic features emerge. Firstly, the experimental cross-section is much smaller than the theoretical one. This cannot be remedied by modifying the interaction parameters of the model. It is probably due to the fact that only a few channels are introduced in the calculation, namely those corresponding to $(1p_{1/2})^{-1}$ and $(1p_{3/2})^{-1}$ states of ^{15}O and ^{15}N. At the energy of the giant resonance, many other channels are open. The effect of these channels can be included phenomenologically by taking a complex single-particle potential. This was made by Buck and Hill [8] in the case of ^{16}O, and by Marangoni and Saruis [13] in the cases of ^{12}C and ^{40}Ca, with reasonable success. The second feature is that the experimental curve displays much more structure (i.e. a more complicated energy dependence) than the theoretical one. This is attributed [18] to the influence of 2p-2h excitations, which are not included in the calculation. These unperturbed configurations cannot emit electric dipole radiation to the ground state. However, the residual interaction mixes the 2p-2h with the 1p-1h states, each of the resulting levels being able to produce a resonance in the photonuclear cross-sections. This is related to the intermediate structure phenomenon, which is discussed below.

7. INTERMEDIATE STRUCTURE

7.1. Introduction

The intermediate-structure phenomenon has been one of the fashionable subjects of nuclear reaction theory in the last few years [1, 19, 20]. Much experimental work has also been devoted to the search for intermediate structure. One must admit that the experimental evidence is not very convincing, except perhaps for a few isolated cases (see below) and for the important example of the isobaric analogue resonances. As exhibited by Strutinsky, intermediate structure has also been observed in neutron-induced fission.

The concept of intermediate structure (and of doorway state) is not a new one. Actually, it goes back to the work done by Lane, Thomas and Wigner [21] on the intermediate coupling theory. It has been formulated in a different and more appealing way by Feshbach and his collaborators

[19] following a proposal by Weisskopf [4]. One calls intermediate-structure resonances the bumps of width of several tens keV which some-times appear in cross-sections averaged over several tens keV, in a region of excitation energy where the average width of the compound nuclear resonances is of the order of 1 keV. The expression "inter-mediate structure" expresses the fact that the width of these bumps is much larger than the width of the compound nuclear resonances, and smaller than the width of the giant resonances (a few MeV). There exist several different physical models which can predict the existence of such bumps. Here, we study only one of these models, namely the doorway-state model. Bumps of intermediate width may as well be due to fluctu-ations in the widths of the compound nuclear resonances, for instance [23].

7.2. Doorway states

In their overwhelming majority, the compound nuclear resonances originate from BSEC which are coupled to the channels by the residual interaction. This coupling is expressed by matrix elements of the form

$$V_j^c = \langle \chi_E^c \mid V \mid \Phi_j \rangle \tag{7.1}$$

The fundamental remark of the doorway-state concept is that V_j^c vanishes if Φ_j and χ_E^c differ by more than four quasi-particles, i.e. by the occu-pation numbers of more than four single-particle states. This results from the two- and one-body character of the residual interaction V. This important point is illustrated in Fig.3. There, we assume that the target nucleus Ω_c corresponding to χ_E^c is a doubly closed shell nucleus. The state χ_E^c is thus a one-particle (1p) state (Fig.3a). The state Φ_i represented in Fig.3b has vanishing matrix element V_i^c, because more than one "col-lision" between two nucleons are needed to go from χ_E^c to the BSEC Φ_i of Fig.3b. The BSEC Φ_j shown in Fig.3c may have a non-vanishing V_j^c. Hence, the BSEC with non-vanishing V_j^c are, in this simple example, 2p-1h states. This is no longer true if Ω_c has a complicated structure.

We define a doorway state of a channel c by the property that it has a non-vanishing coupling to the channel wave function χ_E^c. A complicated state of channel c is a BSEC which has vanishing matrix element of the residual interaction with χ_E^c. Let Φ_i be a complicated state and Φ_0 be a doorway state. The state Φ_i can decay to channel c only via the "doorway" Φ_0:

$$\langle \Phi_i \mid V \mid \Phi_0 \rangle \langle \Phi_0 \mid V \mid \chi_E^c \rangle \neq 0 \tag{7.2}$$

We recall that we assumed that the direct channel-channel coupling vanishes. Otherwise, a route different from expression (7.2) would be available for the decay of Φ_i to channel c:

$$\langle \Phi_i \mid V \mid \chi_{E'}^{c'} \rangle \langle \chi_{E'}^{c'} \mid V \mid \chi_E^c \rangle \neq 0 \tag{7.3}$$

This relation uses the fact that the property of being a doorway state is not a property of a BSEC by itself. A given BSEC Φ_i may be a complicated
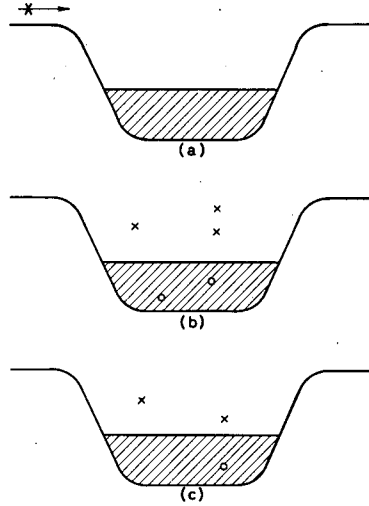
FIG.3. (a) represents the scattering state χ_E^c, (b) a complicated state (3p-2h) for channel c, and (c) a doorway state (2p-1h).

state for channel c, and a doorway state for channel c'. We also note that a linear combination of doorway·states of channel c has a non-vanishing coupling to χ_E^c. Correspondingly, a linear combination of complicated states (of channel c) has vanishing coupling to χ_E^c. Thus, it will be convenient to extend the earlier definitions of complicated and doorway states to linear combinations of BSEC.

7.3. A simple model

In the remaining parts of this section, we study a simple model which contains the essential ingredients of the intermediate structure phenomenon. From the outset, we warn the reader that this model is too simple to be applied to the isobaric analogue resonances, despite claims to the contrary [24]. Nevertheless, the model is quite instructive, because of its simplicity. We assume that only one channel c is open, that the closed channels can be neglected. Thus, we can omit the index c. We include only one doorway state, Φ_0, and N complicated states Φ_j (j = 1, ..., N). We neglect the continuum-continuum coupling, and introduce the following notations (j, k = 0, ... N):

$$[\Gamma^\uparrow(E)]^{\frac{1}{2}} = (2\pi)^{\frac{1}{2}} \langle \Phi_0 | V | \chi_E \rangle, \quad V_{jk} = \langle \Phi_j | V | \Phi_k \rangle \qquad (7.4)$$

$$\epsilon_0 = \langle \Phi_0 | H | \Phi_0 \rangle + P \int_{\epsilon_c}^{\infty} dE' \frac{\Gamma^\uparrow(E')}{2\pi(E-E')} \qquad (7.5)$$

We assume that $\Gamma^\uparrow$ and ϵ_0 are independent of energy in the energy region of interest.

The scattering function is given by Eq.(5.4), which can be given the simple form (i, $= 1$, ..., N)

$$S = \exp(2i\delta) \frac{\det D^*}{\det D} \tag{7.6}$$

where

$$\det D = \begin{vmatrix} E - \epsilon_0 + \frac{1}{2} i\Gamma^\uparrow & V_{0i} \\ \\ V_{0\ell} & (E - E_i)\delta_{i\ell} - V_{i\ell} \end{vmatrix} \tag{7.7}$$

Equation (7.6) exhibits the unitarity of the S-function. Let us diagonalize the Hamiltonian in the space of the complicated states $\{\Phi_i\}$ (i $= 1$, ..., N). We call $\tilde{O}$ the orthogonal matrix which diagonalizes the real symmetric matrix $E_i\delta_{i\ell} + V_{i\ell}$ (i, $\ell = 1$, ..., N). We introduce the definitions

$$\varphi_i = \sum_{\ell=1}^{N} \tilde{O}_{i\ell} \Phi_\ell, \ v_i = \sum_{\ell=1}^{N} \tilde{O}_{i\ell} V_{0\ell} \tag{7.8a}$$

$$\epsilon_\ell \delta_{i\ell} = \sum_{j, m=1}^{N} \tilde{O}_{ij} (E_j \delta_{jm} + V_{jm}) \tilde{O}_{\ell m} \tag{7.8b}$$

Equation (7.6) can thus be written in the form

$$S = \exp(2i\delta) \frac{d^*}{d} \tag{7.9}$$

where

$$d = \begin{vmatrix} E - \epsilon_0 + \frac{1}{2} i\Gamma^\uparrow & v_i \\ \\ v_\ell & (E - \epsilon_\ell)\delta_{i\ell} \end{vmatrix} \tag{7.10}$$

The calculation of the determinant d is straightforward. We find

$$d(E) = \prod_{\ell=1}^{N} (E - \epsilon_\ell) \left[E - \epsilon_0 + \frac{1}{2} i\Gamma^\uparrow - \sum_{j=1}^{N} \frac{v_j^2}{E - \epsilon_j} \right] \tag{7.11}$$

Hence, we have

$$S = \exp(2i\delta) \; \frac{E - \epsilon_0 - \frac{1}{2}i\Gamma^\uparrow - \sum\limits_{j=1}^{N} \dfrac{v_j^2}{E - \epsilon_j}}{E - \epsilon_0 + \frac{1}{2}i\Gamma^\uparrow - \sum\limits_{j=1}^{N} \dfrac{v_j^2}{E - \epsilon_j}} \tag{7.12}$$

If no complicated states were present, the S-function would be given by

$$S^{(0)} = \exp(2i\delta) \; \frac{E - \epsilon_0 - \frac{1}{2}i\Gamma^\uparrow}{E - \epsilon_0 + \frac{1}{2}i\Gamma^\uparrow} \tag{7.13}$$

Then, the cross-section would display a single resonance, of width $\Gamma^\uparrow$. The next sections are devoted to the study of the effect of the existence of N complicated states. We first study the average cross-section, and then the fine structure, i.e. the cross-section which would be measured with a very good energy resolution.

7.4. Average cross-section

We adopt the following definition for the average of a quantity $M(E')$, in the vicinity of E, with an averaging interval I:

$$\langle M(E) \rangle_I = \frac{I}{\pi} \int\limits_{-\infty}^{\infty} dE' \; \frac{M(E')}{(E - E')^2 + I^2} \tag{7.14}$$

The cross-section is given by

$$\sigma = 1 - \mathrm{Re}\, S \tag{7.15}$$

apart from a trivial factor $\pi g_J / k^2$. Its energy average (denoted by $\langle \; \rangle$) is given by

$$\langle \sigma \rangle = 1 - \mathrm{Re}\, \langle S \rangle \tag{7.16}$$

Thus, the average cross-section is given by the average S-function. This is a unique feature of the one open channel model. If more than one channel would be open, the calculation of $\langle \sigma_{cc} \rangle$ would involve that of $\langle |S_{cc}|^2 \rangle$, which is quite difficult.

In section 5.1, we mentioned that S(E) has poles only in the lower-half of the complex E-plane. The value of $\langle S(E) \rangle_I$ can therefore easily be

evaluated by closing the integration contour in Eq.(7.14) along a large semi-circle in the upper half-plane. One finds

$$\langle S(E) \rangle_I = S(E + iI) \tag{7.17}$$

From Eqs (7.17) and (7.12), we obtain

$$\langle S(E) \rangle_I = \exp(2i\delta) \; \frac{E - \epsilon_0 + iI - \tfrac{1}{2}i\Gamma_0 - \displaystyle\sum_{j=1}^{N} \frac{v_j^2}{E - \epsilon_j + iI}}{E - \epsilon_0 + iI + \tfrac{1}{2}i\Gamma_0 - \displaystyle\sum_{j=1}^{N} \frac{v_j^2}{E - \epsilon_j + iI}} \tag{7.18}$$

We note that

$$\left| \langle S(E) \rangle_I \right|^2 < 1 \tag{7.19}$$

This comes from the fact that by averaging one loses the part of the incoming flux which populates the compound states. This part of the flux corresponds to the fluctuating part of the cross-section:

$$\sigma_{\text{flux}} = \langle |S_{cc}|^2 \rangle - |\langle S_{cc} \rangle|^2 \tag{7.20}$$

To calculate the right-hand side of Eq.(7.18), we need the quantity

$$\sum_{j=1}^{N} \frac{v_j^2}{E - \epsilon_j + iI} = \sum_{j=1}^{N} \frac{v_j^2 (E - \epsilon_j) - iI\, v_j^2}{(E - \epsilon_j)^2 + I^2} \tag{7.21}$$

If the quantities ϵ_j and v_j^2 are uniformly distributed on each side of E, the real part of expression (7.21) vanishes. The imaginary part gives, assuming N to be large,

$$-iI \frac{1}{d} \int_{-\infty}^{\infty} \frac{v_j^2}{(E - E')^2 + I^2} dE' = -\frac{i\pi v^2}{d} \tag{7.22}$$

where v^2 denotes the average of the quantities v_j^2, and d the average distance between the energies ϵ_j. Inserting these results in Eq.(7.18), we find

$$\langle S(E) \rangle_I = \exp(2i\delta) \left[1 - i \frac{\Gamma^\uparrow}{E - \epsilon_0 + \tfrac{1}{2} i(\Gamma^\uparrow + \Gamma^\downarrow + 2I)} \right] \tag{7.23}$$

where

$$\Gamma^{\downarrow} = 2\,\frac{v^2}{d} \qquad\qquad (7.24)$$

The quantity $\Gamma^{\downarrow}$ is called the <u>spreading width</u> of the doorway state, while $\Gamma^{\uparrow}$ is the <u>escape width.</u> We see that the effect of the complicated states on the average cross-section is to broaden the resonance due to the doorway state.

7.5. The fine structure

While the average cross-section only displays one resonance of width $(\Gamma^{\uparrow} + \Gamma^{\downarrow} + 2I)$, the cross-section proper has a much more complicated structure. Indeed, the S-function has $N+1$ poles $\mathscr{E}_{\overline{J}}$ given by the roots of (see Eq.(7.11))

$$d(E) = 0 \qquad\qquad (7.25)$$

These $N+1$ resonances are due to the $N+1$ BSEC $\Phi_i\,(i = 0, 1, ..., N)$ included in the model. The states $\Phi_{\ell}\,(\ell = 1, ..., N)$ are not coupled directly to the continuum. Nevertheless, they give rise to resonances because they are coupled to the doorway state Φ_0, which is itself coupled to the channel.

The problem arises of how to parametrize the S-function. Following the same procedure as in section 5.1, we could write it in the form (5.9):

$$S = \exp(2i\delta)\left[1 - i\sum_{n=1}^{N+1} \frac{\mathscr{R}_n}{E - \mathscr{E}_n}\right] \qquad\qquad (7.26a)$$

with

$$\mathscr{E}_n = \zeta_n - \tfrac{1}{2}i\Gamma_n \qquad\qquad (7.26b)$$

Clearly, the quantities ζ_n, Γ_n, real part of $\mathscr{R}_n$, imaginary part of $\mathscr{R}_n$ can display various distribution patterns, depending upon the properties of v_j^2, ϵ_j, ϵ_0 and $\Gamma^{\uparrow}$. A simple result can only be obtained if we make simple assumptions. Henceforth, we often use the <u>picket-fence model,</u> which assumes that all quantities v_j^2 are equal, that all energies ϵ_j are equidistant and that N is infinite. Even in the frame of that simple model, it is found that the quantities $\mathscr{R}_n$ and Γ_n have complicated distributions [25]. It is more convenient to parametrize the S-function in terms of the poles of the K-function, which is defined as follows:

$$S = \exp(2i\delta)\,\frac{1 - iK}{1 + iK} \qquad\qquad (7.27)$$

From Eq.(7.12), we obtain the explicit form of K

$$K = \frac{1}{2} \ \frac{\Gamma^{\uparrow}}{E - \epsilon_0 - \displaystyle\sum_{j=1}^{N} \frac{v_j^2}{E - \epsilon_j}} = \frac{1}{2} \frac{\Gamma^{\uparrow}}{\mathscr{D}} \prod_{j=1}^{N} (E - \epsilon_j) \tag{7.28}$$

The denominator $\mathscr{D}$ of K is the real part of the determinant d. It can be written

$$\mathscr{D}(E) = \begin{vmatrix} E - \epsilon_0 & v_j \\ v_\ell & (E - \epsilon_j)\delta_{j\ell} \end{vmatrix} \tag{7.29}$$

Equation (4.8a) shows that the zeros of $\mathscr{D}$ (and hence the poles of K) are the energies of the bound excited states ψ_n, in a model where the channel wave function would be omitted from the basic set of states. Let us call λ_n $(n = 1, ..., N + 1)$ the roots of

$$\mathscr{D}(E) = 0 \tag{7.30}$$

We can always write

$$K = \sum_{n=1}^{N+1} \frac{a_n^2}{E - \lambda_n} \tag{7.31}$$

It can easily be checked that

$$a_n^2 = \frac{1}{2}\Gamma^{\uparrow}O_{n0}^2 \tag{7.32}$$

where O_{n0} are the elements of the orthogonal matrix which diagonalizes the matrix whose determinant appears in Eq.(7.29). The matrix $\underset{\approx}{Q}$ is analogous to that introduced in Eq.(4.8b). We note that the quantities O_{n0}^2 are related to the BSEC only, and not to the channel. We have (see Eq.(4.8b))

$$\psi_n = \sum_{j=1}^{N} O_{nj}\Phi_j + O_{n0}\Phi_0 \tag{7.33}$$

Hence, O_{n0} measures the probability of finding the doorway configuration Φ_0 in the state Ψ_n. Since $\underset{\approx}{Q}$ is an orthogonal matrix, we have

$$\sum_{n=1}^{N+1} O_{n0}^2 = 1 \tag{7.34}$$

Equations (7.32) and (7.34) show that the following sum rule holds

$$\sum_{n=1}^{N+1} a_n^2 = \tfrac{1}{2} \Gamma^{\uparrow} \tag{7.35}$$

We now study the distribution of the quantities a_n^2. We replace E by $E + iI$ in Eq.(7.27), and use Eq.(7.23). We find

$$\sum_{n=1}^{N+1} \frac{a_n^2}{E - \epsilon_0 + iI} = \frac{1}{2} \frac{\Gamma^{\uparrow}}{E - \epsilon_0 + \frac{1}{2} i(\Gamma^{\downarrow} + 2I)} \tag{7.36}$$

Assuming that the a_n^2's are smoothly distributed, we can replace the summation over n in Eq.(7.36) by an integral:

$$\frac{1}{d} \int_{-\infty}^{\infty} dE' \frac{a^2 (E')}{(E - E') + iI} = \frac{1}{2} \frac{\Gamma^{\uparrow}}{E - \epsilon_0 + \frac{1}{2} i(\Gamma^{\downarrow} + 2I)} \tag{7.37}$$

Taking the imaginary part of Eq.(7.37), and denoting by $\langle a_n^2 \rangle_I$ the average of a_j^2 calculated around E within an energy interval I, we find

$$\langle a_n^2 \rangle = \frac{1}{4\pi} \frac{\Gamma^{\uparrow}(\Gamma^{\downarrow} + 2I)}{(\epsilon_n - \epsilon_0)^2 + \frac{1}{4}(\Gamma^{\downarrow} + 2I)^2} \tag{7.38}$$

We must remember that Eq.(7.38) has been established in the case $I \gg d$. Whenever $\Gamma^{\downarrow} < d$, Eq.(7.38) contains little information concerning the distribution of the quantities a_n^2. In general, however, $\Gamma^{\downarrow} \gg 2I$, and the quantities a_n^2 have a Lorentzian distribution, with width at half-maximum $\Gamma^{\downarrow}$. From Eq.(7.32), we obtain in that case

$$O_{n0}^2 = \frac{\Gamma^{\downarrow}}{(\epsilon_n - \epsilon_0)^2 + \frac{1}{4}(\Gamma^{\downarrow})^2} \tag{7.39}$$

This expression shows the origin of the expression "spreading width" used to designate $\Gamma^{\downarrow}$. This quantity measures the extent of the spreading of the state Φ_0 over the compound levels ψ_n. In the case $\Gamma^{\downarrow} < d$ as well as $\Gamma^{\downarrow} > d$, one can establish the following law, in the frame of the picket-fence model [26]:

$$a_n^2 = \frac{d}{2\pi} \frac{\Gamma^{\downarrow}}{(\epsilon_0 - \epsilon_n)^2 + \frac{1}{4}(\Gamma^{\downarrow})^2 + \frac{d\Gamma^{\downarrow}}{2\pi}} \tag{7.40}$$

We note in passing that the K-matrix parametrization given by Eqs (7.27) and (7.31) is formally very analogous to the R-matrix parametrization [25].

7.6. Experimental evidence

In principle, the analysis of an intermediate-structure resonance in a one-open channel situation would be the following. One computes or measures the average cross-section and sees whether it can be fitted with a Lorentzian. This determines $\Gamma^\uparrow$, $\Gamma^\downarrow$ and ϵ_0, which are the fundamental quantities. Quite often, however, the average cross-section does not display any nice isolated intermediate-structure resonance, and the extraction of $\Gamma^\downarrow$ and $\overline{\Gamma^\uparrow}$ is difficult. In particular, if $\Gamma^\uparrow \ll \Gamma^\downarrow$ (which appears to be the general case), the average cross section barely displays any apparent resonance. Moreover, the whole analysis is meaningful only if the doorway-state model given above applies. This should be checked by looking at the distribution of the fine-structure parameters. If should be possible to fit the distribution of the a_n^2 with Eq.(7.40). This, however, is rarely possible, for several reasons. The detailed experimental data are rarely available. If it is, this generally implies that only a few (about ten) fine-structure peaks exist. This is too little for the statistical assumptions (picket-fence model) to apply. The only two cases which have been examined in detail concern the reaction $^{206}Pb(n,n)^{206}Pb$ [27] and $^{56}Fe(n,n)^{56}Fe$ [28]. The results of these analyses are encouraging but not decisive. More experimental and theoretical work is called for in this field. Fortunately, the isobaric analogue resonances provide a prime example (but not a simple one) of intermediate structure. This is discussed in the next section.

8.   THE ISOBARIC ANALOGUE RESONANCES

8.1. Introduction

It results from section 7 that a doorway state will produce an intermediate-structure resonance only if the following two conditions are fulfilled (among others):

(1) the doorway state is isolated, i.e. the separation between two doorway states is larger than the sum $\Gamma^\uparrow + \Gamma^\downarrow$

(2) the escape width $\Gamma^\uparrow$ is not much smaller than $\Gamma^\downarrow$.

According to crude estimates of $\Gamma^\uparrow$ and $\Gamma^\downarrow$, conditions (1) and (2) are not likely to be fulfilled in general [29]. Hence, intermediate-structure resonances due to doorway states will be observable only if $\Gamma^\downarrow$ is exceptionally small. Looking at the expression (7.24) for $\Gamma^\downarrow$, this implies that v^2 must be exceptionally small, for instance, because of the existence of a selection rule which would considerably reduce the coupling of the doorway state with the complicated states. This is precisely fulfilled in the case of isobaric analogue resonances (for short, IAR). There, the doorway state has approximately pure isospin $T_>$, while the complicated states have approximately pure isospin $T_< = T_> - 1$. Hence, the doorway state is (almost) not coupled to the complicated states by the residual interaction. At the same time, it becomes important to improve the theory to include several refinements. This was first emphasized, in the frame of R-matrix

theory by D. Robson [30]. We cannot aim at a detailed theoretical des-
cription of the IAR. For this, the reader is referred to chapter 13 of
Ref.[1], which is itself largely based upon a paper by Mekjian and
MacDonald [31]. Here, we shall only exhibit the main physical features
of the theory.

8.2. Isospin of neutron-excess nuclei and isobaric analogue states

Let us consider a low-lying excited state of a medium-weight or a
heavy nucleus, with a large neutron excess. We call N the number of
neutrons, Z the number of protons, and denote the nucleus by $^A_Z P$ $(A = Z+N)$.
In a first and crude approximation, the configuration of the nucleus is
that depicted in Fig.4. The shaded area represents the orbitals occupied
by the Z protons, and by the lowest Z neutrons. We have taken, for the
sake of definiteness, the example of the first excited state of $^{93}_{40} Zr$. The
13·excess neutrons occupy the orbitals $1g_{9/2}(10)$, $2d_{5/2}(2)$ and $3s_{1/2}(1)$.
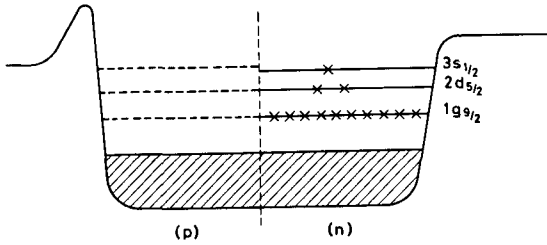
FIG.4. Schematic representation of the configuration of the first excited state of $^{93}_{40} Zr$. The shaded area
corresponds to the core of 40 protons and 40 neutrons.

The bound proton orbital with quantum numbers (n_0, ℓ_0, j_0, m_0) is almost
identical to that of the corresponding bound neutron orbital with same
quantum (n_0, ℓ_0, j_0, m_0). The overlap between the two wave functions is
larger than 0.99, especially for the deeply bound ones. For simplicity
of the discussion, let us assume that these "corresponding" orbitals are
identical. Let us call $\tau(i)$ the isospin operator for nucleon i, and $\tau_+(i)$
the raising operator for nucleon i. The operator τ_+ transforms a proton
$(\tau_z = -\frac{1}{2})$ into a neutron $(\tau_z = +\frac{1}{2})$ in the corresponding orbital. The operator

$$T_+ = \sum_{i=1}^{A} \tau_+(i) \tag{8.1}$$

raises the T_z component of T, and leaves the eigenvalue $T_>(T_>+1)$ of T^2
unchanged. If applied to $^A_Z P$, the operator T_+ gives zero. Indeed, the
neutron orbitals corresponding to the occupied proton orbitals are
completely filled. This means that T_z cannot be increased, i.e. that
$T_z = T_>$. Hence, we have

$$T_> = \frac{1}{2}(N - Z) \tag{8.2}$$

for a nucleus with excess neutron. The isospin purity of the low-lying
states is of the order of 99%.

The operator T_- can be applied to the state $^A_Z P$. It transforms the neutrons into protons, leaving unchanged the quantum numbers of the orbitals. In the example of Fig.4, the application of T_- to $^A_Z P$ yields the following (normalized) state:

$$\Phi_> = (13)^{-\frac{1}{2}} \{ \sqrt{10} \, [(1g_{9/2})_p (1g_{9/2})_n^{-1}]_{J=0}$$

$$+ \sqrt{2} \, [(2d_{5/2})_p (2d_{5/2})_n^{-1}]_{J=0}$$

$$+ [(3s_{1/2})_p (3s_{1/2})_n^{-1}]_{J=0} \} \qquad (8.3)$$

Here, the particle and the hole are taken with respect to $^A_Z P$ as reference state; they are coupled to $J = 0$. The state $\Phi_>$ is an eigenstate of H_0, with eigenvalue

$$E_> = E_P + \Delta_c \qquad (8.4)$$

We denote by E_P the energy of the _parent_ state $^A_Z P$, and by Δ_c the single particle Coulomb energy

$$H_0 | ^A_Z P \rangle = E_P | ^A_Z P \rangle \qquad (8.5)$$

$$H_0 \Phi_> = E_> \Phi_> \qquad (8.6)$$

We note that $\Phi_>$ is an eigenstate of H_0 for a system with $Z+1$ protons and $N-1$ neutrons. It is called the isobaric analogue state (for brevity IAS) of $^A_Z P$. It is a highly excited state of the $(Z+1, N-1)$ nucleus (in our example $^{93}_{41}$Nb). The excitation energy is of the order of 10 MeV in medium-weight nuclei, and 20 MeV in heavy nuclei. Hence, $\Phi_>$ lies in a region of excitation where the density of BSEC Φ_j is extremely large. On the other hand, $\Phi_>$ has a simple structure. It is a linear superposition of 1p-1h states. Therefore, $\Phi_>$ is a doorway state for the channel where a proton is scattered by the target $(Z, N-1)$. The BSEC lying in the vicinity of $\Phi_>$ have the "normal" isospin for the $(Z+1, N-1)$ nucleus, i.e.

$$T_< = T_> - 1 = \frac{N-Z}{2} - 1 \qquad (8.7)$$

Thus, the matrix element of the residual nuclear interaction between $\Phi_>$ and the complicated BSEC Φ_j vanishes. In reality, of course, it is not completely correct to assume that corresponding proton and neutron orbitals are identical, and the above conclusions are only approximately valid. Still, we expect that $\Gamma^\downarrow$ will be particularly small for the doorway state $\Phi_>$, so that we are in ideal conditions to observe intermediate-structure resonances. This is indeed confirmed by the experimental discovery of hundreds of IAR.

8.3. Fine structure and neutron decay of IAR

The IAR are usually observed as pronounced resonances in the elastic scattering of protons. Since they lie at high excitation energy, they are actually intermediate-structure resonances, and we expect to be able to observe a fine structure if the experimental energy resolution is refined. In heavy or even in medium-weight nuclei, the average level spacing of the complicated states is so small that the fine structure cannot be resolved. This is, however, possible in light nuclei. Figure 5 shows the excitation functions of $^{40}Ar(p,p)^{40}Ar$ [32]. The enhancement of the resonance width in the vicinity of a $3/2^-$ IAR at 1.87 MeV is clearly exhibited.
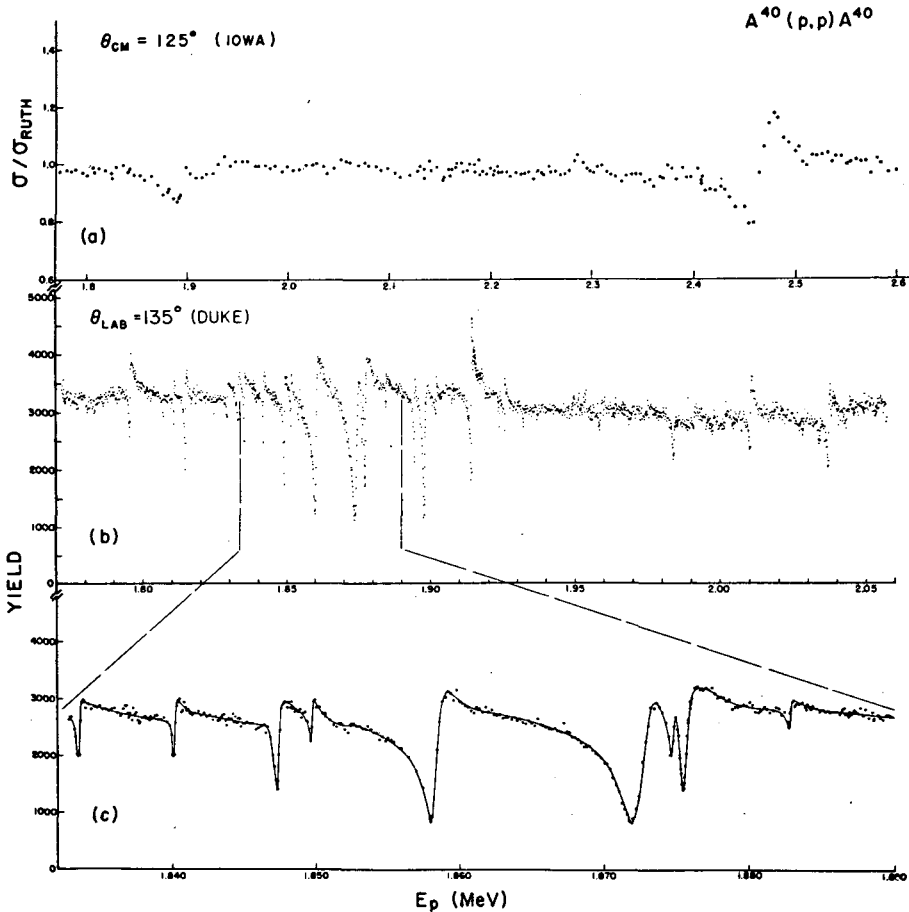
FIG.5. Excitation function of $^{40}Ar(p,p)^{40}Ar$. In (a), the poor energy resolution data are shown, in (b) and (c) the fine structure is displayed (from Ref. [32]).

A plot of the residues a_n^2 of the K-matrix versus λ_n shows that the distribution is not Lorentzian, as Eq.(7.38) would predict. Rather, the distribution of the a_n^2 displays an asymmetric peak, with a vanishing point at about 80 keV above the resonance energy. This characteristic pattern is also found in other cases, and indicates that the model studied in sections 7.3-7.5 is too simple to give a good description of the IAR.

Another interesting characteristic of the IAR is that the (p, n) cross-section displays a resonance. Figure 6 shows the $^{92}_{40}$Zr(p, n)$^{92}_{41}$Nb cross-section in the vicinity of the IAR corresponding to the first excited state of ^{93}Zr (see Fig.4). We see that the resonance peak is asymmetric. If one subtracts the contributions of the angular moments different from the resonating $J^\pi = 1/2^+$, one finds an asymmetric resonance peak which again displays a vanishing point slightly above resonance. The same behaviour is exhibited by many (p, n) cross-sections at the IAR. This suggests that the asymmetries observed in the fine-structure data and in the (p, n) cross-sections have the same origin. In fact, both phenomena involve isospin mixing of the doorway state $\Phi_>$ with the complicated states. This is obvious for the fine structure, and we now show that it is also valid for the (p, n) resonance. The residual nucleus $^{92}_{41}$Nb has isospin 5. Thus, the channel n + ^{92}Nb has isospin 11/2, while the doorway state has isospin $T_> = 13/2$. Hence, neutron decay from $\Phi_>$ is isospin-forbidden, and the (p, n) cross-section can display a resonance only because $\Phi_>$ is mixed with the complicated levels of lower isospin.
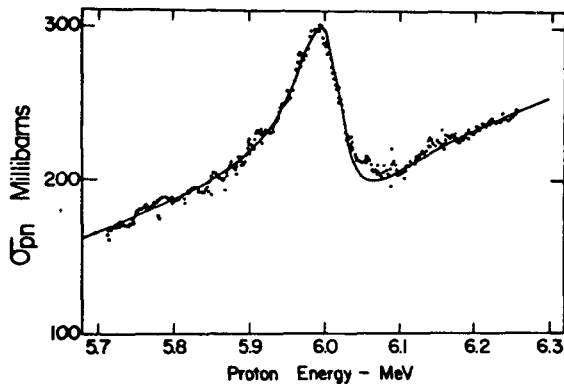
FIG.6. ^{92}Zr(p, n)^{92}Nb cross-section in the vicinity of the IAR corresponding to the parent state represented in Fig.4 (from Ref. [33]).

8.4. The basis states and their mutual coupling

In the present section, we define the set of states which span the space of functions where the full Hamiltonian H will be diagonalized. Several choices are possible. For instance, we might only take the bound state $\Phi_>$ obtained by applying the T_- operator to ^A_ZP, and the channel wave function χ^c_E. This is the so-called Lane model [1]. However, $\Phi_>$ is not an eigenstate of H_0 if corresponding proton and neutron orbitals are not identical. It is therefore more convenient to make a different

choice. Let us first consider the linear space spanned by the 2 $T_>$ one particle-one hole BSEC obtained by applying the T_- operator to $^A_Z P$. We diagonalize H in this restricted subspace. It is then easy to show [35] in a schematic model for instance, that one linear combination of these 1p-1h states, say Φ_0, will have an energy much larger (by about the symmetry energy, i.e. about 10 MeV) than the energy of the $(2T_> - 1)$ other linear combinations. The latter (many of which may be degenerate) are called the anti-analogue states, or configurational states. If the wave functions of single-particle orbitals are identical, Φ_0 is equal to $\Phi_>$. Clearly, Φ_0 must be included among the set of basis states. We diagonalize H among all other bound states orthogonal to Φ_0, i.e. among the BSEC different from the above-mentioned 1p-1h and among the anti-analogue states. This yields states φ_j (j = 1, ..., M). The states φ_j which lie in the vicinity of Φ_0 have almost pure isospin $T_< = T_> - 1$. We introduce the definitions

$$\langle \Phi_0 | H | \Phi_0 \rangle = E_0 \tag{8.8}$$

$$\langle \varphi_j | H | \varphi_k \rangle = \epsilon_j \delta_{jk} \, (j, k = 1, ..., M) \tag{8.9}$$

Finally, we must include the scattering states χ_E^c (c = 1, ..., Λ). Here, c referes to neutron as well as to proton channels. The neutron-channel wave functions have pure isospin $T_<$, but the proton-channel wave function is a mixture of $T_>$ and $T_<$ states. This comes from the fact that the z-component of the isospin of the proton is $-\frac{1}{2}$, and that of the target is $T_> - \frac{1}{2}$.

We now discuss the size of the various matrix elements of the residual interaction. We neglect the residual Coulomb interaction. Still, we must be careful that the residual nuclear interaction does not commute with T^2, because it contains the single-particle potentials, which differ for protons and neutrons by the symmetry potential. Nevertheless, it is possible to show [1] that only that part of V which commutes with T^2 is important. Let us denote by p the proton channels, and by n the neutron channels. The various matrix elements have the following characteristics:

$$\langle \Phi_0 | V | \varphi_j \rangle = v_j : \text{ very small} \tag{8.10a}$$

$$\langle \Phi_0 | V | \chi_E^p \rangle = v_0^p : \text{ normal size} \tag{8.10b}$$

$$\langle \Phi_0 | V | \chi_E^n \rangle = v_0^n : \text{ small} \tag{8.10c}$$

$$\langle \varphi_j | V | \chi_E^p \rangle = v_j^p : \text{ small} \tag{8.10d}$$

$$\langle \varphi_j | V | \chi_E^n \rangle = v_j^n : \text{ small} \tag{8.10e}$$

As we have done before, we neglect the direct channel-channel coupling. The sizes quoted in expression (8.10c) arise from the high isospin purity

of the states $\Phi_0(T_>)$, $\varphi_j(T_<)$ and $\chi_E^n(T_<)$. The smallness of the matrix elements (8.10d) and (8.10e) comes from the fact that the states φ_j are complicated. The very small value of the matrix element (8.10a) is due to both effects. We note that the states φ_j are obtained by diagonalizing H among many BSEC, some of which are doorway states for the proton of the neutron channels (for instance, the one-proton-particle, one-neutron-hole states where the particle and the hole angular momenta are not coupled to $J = 0$). Therefore, the "complicated" states of the IAR are coupled to the channels. This feature, and the smallness of v_j, are the main characteristics of the IAR, as emphasized again in the next section.

8.5. Isospin mixing at the IAR

Since we assume that there exists no direct channel-channel coupling, we can use the equations of section 4. The scattering matrix is given by Eq.(5.4). Let us look at the determinant $D(E)$ of the matrix D in Eqs (5.2b) and (5.4). In the present case, it reads

$$
D(E) = \begin{vmatrix} E - \epsilon_0 + \frac{1}{2} i \Gamma_0 & v_j + \sum_{c=1}^{\Lambda} \int_{\epsilon_c}^{\infty} dE' \dfrac{v_j^c(E') v_0^c(E)}{E^+ - E'} \\[4mm] v_\ell + \sum_{c=1}^{\infty} \int_{\epsilon_c}^{\infty} dE' \dfrac{v_\ell^c(E') v_0^c(E')}{E^+ - E'} & (E - \epsilon_j) \delta_{j\ell} - \sum_{c=1}^{\Lambda} \int_{\epsilon_c}^{\infty} dE' \dfrac{v_j^c(E') v_\ell^c(E')}{E^+ - E'} \end{vmatrix}
$$

$$(8.11)$$

Here, the indices j, $\ell = 1, \ldots, M$, correspond to the complicated states φ_j lying in the vicinity of the energy ϵ_0 of the IAR. We have used the notations (see Eqs (8.8) and (8.9))

$$
\epsilon_0 = E_0 + \sum_{c=1}^{\Lambda} P \int_{\epsilon_c}^{\infty} dE' \frac{[v_0^c(E')]^2}{E - E'}
\tag{8.12}
$$

$$
\Gamma_0 = 2\pi [v_0^c(E)]^2
\tag{8.13}
$$

The main difference between the expression (8.11) and the corresponding expression (7.10) for the simple model is the following. The doorway state Φ_0 is coupled to the complicated state φ_j not only via the matrix element v_j, but also via the quantity

$$
F_{0j}^c = P \int_{\epsilon_c}^{\infty} dE' \frac{v_j^c(E') v_0^c(E')}{E - E'} - i\pi v_j^c(E) v_0^c(E)
\tag{8.14}
$$

Because of relations (8.10b) and (8.10c), the quantities F_{0j}^c are sizeable only when c refers to a proton channel. Because of relations (8.10d) and (8.10e), the quantities (j, $\ell = 1, \ldots, M$)

$$F_{j\ell}^c = \int_{\epsilon_c}^{\infty} dE' \; \frac{v_j^c(E')v_\ell^c(E')}{E^+ - E'} \qquad (8.15)$$

are very small. They do not play any important role in the theory. Thus, the main characteristic feature of the IAR is that the coupling between Φ_0 and φ_j via the proton channel wave functions is larger than (or at least comparable to) the direct coupling. To exhibit the consequences of this property, it is convenient to study the so-called pure external mixing model, where the direct coupling matrix elements are set equal to zero:

$$v_j = 0 \quad \text{(pure external mixing)} \qquad (8.15)$$

Here, we shall only consider the pure external mixing model, in order to exhibit the physical origin of the asymmetries exhibited in section 8.3. We include one proton channel, and Λ neutron channels, which we assume not to be coupled to Φ_0:

$$v_0^n = 0 \qquad (8.16)$$

We use the approximation

$$P \int_{\epsilon_c}^{\infty} dE' \; \frac{v_j^c(E')v_0^c(E')}{E - E'} \approx v_j^c(E)v_0^c(E)f_c(E) \qquad (8.17)$$

The conditions of validity of this approximation are discussed in sections 8.7 and 13.7c of Ref.[1]. It rests upon the fact that the radial dependence of the single-particle scattering wave function $u_c(r, k)$ (see Eq.(2.5)) does not change inside the potential well when the energy $E = \hbar^2 k^2 / 2M$ varies in an energy range of a few MeV. This range is negligible compared to the depth (≈ 50 MeV) of the potential well. Using Eqs (8.15) and (8.17), the basic equations (5.1) become (j = 1, ..., M)

$$(E - \epsilon_j)b_E^P(j) - (f_p - i\pi)v_j^P v_0^P b_E^P(0) - \sum_{n=1}^{\Lambda} (f_n - i\pi)v_j^n \sum_{\ell=1}^{M} v_\ell^n b_E^P(\ell) = v_j^P \qquad (8.18a)$$

$$(E - E_0)b_E^P(0) - (f_p - i\pi) \sum_{m=0}^{M} v_m^P b_E^P(m) = v_0^P \qquad (8.18b)$$

Here, we have written the full scattering wave function in the form

$$\Psi_E^P = \sum_{j=1}^{M} b_E^P \varphi_j + b_E^P(0)\Phi_0 + \sum_{n=1}^{\Lambda} \int_{\epsilon_n}^{\infty} dE' \, a_E^P(E';n)\chi_{E'}^n + \int_{\epsilon_p}^{\infty} dE' \, a_E^P(E';p)\chi_{E'}^P$$

(8.19)

The coefficients $a_E^P(E';c)$ are given by Eq.(4.20):

$$a_E^P(E';c) = \delta_{cp}\delta(E-E') + (E^+ - E')^{-1} \sum_{m=0}^{M} v_m^c b_E^P$$

(8.20)

Taking $E = E_0$ in Eqs (8.18a) and (8.18b), we obtain

$$(E_0 - \epsilon_j) b_{E_0}^P(j) - \sum_{n=1}^{\Lambda} (f_n - i\pi) \sum_{\ell=1}^{M} v_\ell^c b_{E_0}^P(\ell) = 0$$

(8.21)

In general, this system of homogeneous equations for the coefficients $b_{E_0}^P(\ell)$ has no non-trivial solution, so that

$$b_{E_0}^P(\ell) = 0 \qquad (\ell = 1, \ldots, M)$$

(8.22)

We use this result in Eqs (8.20) and (8.19) and find

$$\Psi_{E_0}^P = \chi_{E_0}^P + b_{E_0}^P(0)\left[\Phi_0 + \int_{\epsilon_p}^{\infty} dE' \, (E_0^+ - E')^{-1} \, v_0^P(E')\chi_{E'}^P\right]$$

(8.23)

Let $\Phi_<$ be a normalizable wave function, confined inside the nucleus, and with isospin $T_<$. We can use an approximation analogous to approximation (8.17):

$$P \int_{\epsilon_p}^{\infty} dE' \, (E^+ - E')^{-1} \langle \Phi_< | \chi_{E'}^P \rangle v_0^P(E') \simeq f_p v_0^P(E_0) \langle \Phi_< | \chi_{E_0}^P \rangle$$

(8.24a)

Using this relation in Eq.(8.23), we find

$$\langle \Phi_< | \Psi_{E_0}^P \rangle = \langle \Phi_< | \chi_{E_0}^P \rangle \{1 + (f_p - i\pi)v_0^P b_{E_0}^P(0)\}$$

(8.24b)

Equations (8.18b) and (8.24) yield

$$\langle \Phi_< | \Psi_{E_0}^P \rangle = 0$$

(8.25)

Thus, the full scattering wave function Ψ_E^p has pure isospin $T_>$ in the internal region of the nucleus, at the energy E_0. At E_0, the BSEC φ_j, and the wave functions $\chi_{E'}^n$, are therefore not mixed with Φ_0. Hence, the distribution of the widths of the fine-structure peaks displays a zero at E_0. This zero lies above the resonance energy ϵ_0, because the quantity

$$P \int_{\epsilon_p}^{\infty} dE' \frac{[v_0^p(E')]^2}{E-E'}$$

is usually negative. Indeed, the matrix element $v_0^p(E')$ increases with energy, because of penetration effects.

The elements $S_{cc'}$ of the scattering matrix is proportional to $\langle \chi_E^c | V | \Psi_E^c \rangle$. Since the state $V\chi_E^n$ has pure isospin $T_<$, in our simple example, S_{pn} vanishes at $E = E_0$. More precisely, it can be shown that the (p,n) cross-section σ_{pn} has the shape

$$\sigma_{pn} \propto \frac{(E - E_0)^2}{(E - \epsilon_0)^2 + \frac{1}{4}(\Gamma)^2} \tag{8.26}$$

The expression of Γ is given in Ref.[1].

Whenever the assumptions made above (one open proton channel, pure external mixing, Eq.(8.17), ...) are released, the zero at $E = E_0$ is transformed into a minimum.

8.6. Spectroscopic information

The wave function Φ_0 of the IAS is intimately related to that of the parent state $_Z^A P$. Hence, it can be hoped that spectroscopic information related to $_Z^A P$ can be obtained from the analysis of the IAR. It can be shown that the value of v_0^c (see Eq.(8.19b)) in the proton channels c can be obtained from the measurement of the elastic scattering cross-section in channel c. It is directly connected with the value of the partial width Γ_{0c} obtained from a Breit-Wigner analysis of the IAR. The kind of spectroscopic information obtainable from the IAR is practically identical to that available from (d,p) reactions leading to $_Z^A P$ as residual state. A comparison between the results of the two kinds of experiments can corroborate the validity of the theory of stripping reactions, on the one hand, and of the IAR, on the other hand. The results obtained up to now are very encouraging [1, 34].

As we have stressed in the introduction, these lectures are based on a monograph by H.A. Weidenmüller and the author [1]. We are grateful to H.A. Weidenmüller for many enjoyable discussions.

REFERENCES

[1] MAHAUX, C., WEIDENMÜLLER, H.A., Shell-Model Approach to Nuclear Reactions, North-Holland Publishing Company, Amsterdam (1969).

[2] FONDA, L., NEWTON, R.G., Ann. Phys. (N.Y.) 10 (1960) 490;
FONDA, L., Ann. Phys. 22 (1963) 123;
FONDA, L., GHIRARDI, G.C., Ann. Phys. (N.Y.) 26 (1964) 240.

[3] BLOCH, C., Many-Body Description of Nuclear Structure and Reactions (BLOCH, C., Ed.), Academic Press, New York (1966) 394.

[4] WEISSKOPF, V.F., Phys. Today 14 7 (1961) 18;

[5] HÜFNER, J., MAHAUX, C., WEIDENMÜLLER, H.A., Nuclear Phys. A 105 (1967) 489.

[6] DIRAC, P.A.M., Principles of Quantum Mechanics, 4th edition Oxford University Press, Oxford (1958) 193.

[7] HUMBLET, J., ROSENFELD, L., Nuclear Phys. 26 (1961) 529.

[8] BUCK, B., HILL, A.D., Nuclear Phys. A 95 (1967) 271.

[9] RAYNAL, J., MELKANOFF, M.A., SAWADA, T., Nuclear Phys. A 101 (1967) 369.

[10] SARUIS, A.M., MARANGONI, M., Nucl. Phys. (in press).

[11] BERES, W.P., MACDONALD, W.M., Nuclear Phys. A 91 (1967) 529.

[12] PEREZ, J., MACDONALD, W.M., Phys. Rev. (in press).

[13] MARANGONI, M., SARUIS, A.M., Nucl. Phys. (in press).

[14] ELLIOTT, J.P., FLOWERS, B.H., Proc. Roy. Soc. 242 (1957) 57.

[15] GILLET, V., VINH MAU, N., Nucl. Phys. 54 (1964) 321.

[16] MORRISON, R.C., thesis, Yale University Electron Accelerator Laboratory (1965).

[17] MAHAUX, C., SARUIS, A.M., (to be published).

[18] GILLET, V., MELKANOFF, M.A., RAYNAL, J., Nucl. Phys. A 97 (1967) 631.

[19] FESHBACH, H., KERMAN, A.K., LEMMER, R.H., Ann. Phys. (N.Y.) 41 (1967) 230.

[20] Intermediate Structure in Nuclear Reactions, KENNEDY, H.P., SCHRILS, R., Eds, Univ. of Kentucky Press, Lexington (1968).

[21] LANE, A.M., THOMAS, R.G., WIGNER, E.P., Phys. Rev. 98 (1955) 693.

[22] LANE, A.M., THOMAS, R.G., Rev. mod. Phys. 30 (1958) 257.

[23] MOLDAUER, P.A., Phys. Rev. Letts 18 (1967) 249.

[24] BERES, W.P., DIVADEENAM, M., Phys. Rev. Letts 20 (1968) 1135.

[25] MAHAUX, C., WEIDENMÜLLER, H.A., Nucl. Phys. A 91 (1967) 241.

[26] MACDONALD, W.M., MEKJIAN, A., Phys. Rev. 160 (1967) 730.

[27] LEJEUNE, A., MAHAUX, C., Z. Phys. A 113 (1968) 272.

[28] MONAHAN, J.E., ELWYN, A.J., Phys. Rev. Letts 20 (1968) 1119.

[29] PAYNE, G.L., Phys. Rev. 174 (1968) 1227.

[30] ROBSON, D., Phys. Rev. 137 (1965) B535.

[31] MEKJIAN, A., MACDONALD, W.M., Nucl. Phys. 121 (1968) 385.

[32] KEYWORTH, G.A., KYKER, G.C., Jr., BILPUCH, E.G., NEWSON, H.W., Phys. Letts 20 (1966) 281.

[33] ROBSON, D., FOX, J.D., RICHARD, P., MOORE, C.F., Phys. Letts 18 (1965) 86.

[34] HARNEY, H.L., Nucl. Phys. A 119 (1968) 591.

[35] PINKSTON, W.T., Nucl. Phys. 53 (1964) 643.

THE HARTREE-FOCK APPROXIMATION
IN CO-ORDINATE SPACE

D. VAUTHERIN
Institut de physique nucléaire,
Division de physique théorique,
Orsay, France

Abstract

THE HARTREE-FOCK APPROXIMATION IN CO-ORDINATE SPACE.
 1. The Hartree-Fock integrodifferential system; 2. Method of solution; 3. The two-body effective interaction; 4. Results; 5. Applications to scattering problems; 6. Conclusion.

1. THE HARTREE-FOCK INTEGRO-DIFFERENTIAL SYSTEM

1.1. Introduction

In the last few years techniques have been developed to perform nuclear Hartree-Fock calculations by using a harmonic-oscillator basis. Extended calculations have been done for spherical nuclei [1] as well as for deformed nuclei [2]. The use of this expansion has three main advantages: 1) It requires only the diagonalization of matrices, 2) the matrix method provides a unique framework for a treatment of spherical and deformed nuclei, and 3) the use of the Talmi-Moshinsky transformation greatly simplifies the evaluation of the matrix elements of the Hartree-Fock field. On the other hand, this method has several drawbacks: 1) the amount of numerical work increases drastically with mass number, 2) the convergence of the oscillator expansion, which is well established for light nuclei, seems less reliable for heavy nuclei, and especially for weakly bound states, and 3) this method is unable to reach directly the continuum states of the Hartree-Fock field which are of special interest for scattering problems [3]. In co-ordinate space, the Hartree-Fock wave functions are solutions of a system of coupled integro-partial-differential equations, whose mathematical structure is rather complicated. The two main difficulties are that these equations are non-linear and involve a non-local one-body potential. Up to now, the solution of this system has not been attempted for deformed nuclei, but several calculations are available for spherical nuclei [4-6], including heavy spherical nuclei [7-8].

The aim of these notes is to discuss the properties and the method of solution of the Hartree-Fock integro-differential system for spherical nuclei. The use of the co-ordinate-space representation allows a qualitative understanding of the dependence of the results on the parameters of the two-body interaction. These results will be discussed in section 4. Some applications of the Hartree-Fock techniques to scattering problems will be presented in section 5.

Since the Hartree-Fock equations are derived in Bouten's contribution to these Proceedings [9], it will be simply recalled that, for a given system

of A nucleons interacting via a two-body interaction V, the Hartree-Fock problem is to find a set of A vectors $|i)$, $i = 1, 2, \ldots, A$, such that

$$(i|t|j) + \sum_{k=1}^{A} (ik|\tilde{V}|jk) = e_i\,\delta_{ij} \tag{1}$$

In this equation t denotes the kinetic-energy operator and $\tilde{V}$ is an anti-symmetrized matrix element

$$(ik|\tilde{V}|jk) = (ik|V|jk) - (ik|V|kj) \tag{2}$$

The system of Eqs (1) is equivalent to the following

$$(t + \mathscr{U})|i) = ei|i) \tag{3}$$

where the matrix elements of the potential $\mathscr{U}$ are defined by

$$(i|\mathscr{U}|j) = \sum_{k=1}^{A} (ik|\tilde{V}|jk) \tag{4}$$

The total binding energy E of the system is given by the relation

$$E = \frac{1}{2}\sum_{i=1}^{A}[(i|t|i) + e_i] = \sum_{i=1}^{A}(i|t + \frac{1}{2}\mathscr{U}|i) \tag{5}$$

1.2. The case of doubly-closed-shell nuclei

For doubly-closed-shell nuclei the reduction of angular variables can be carried out and in this case one is left with an integro-differential system involving only the radial co-ordinate r. For this purpose, it is convenient to define the following notations, which are very close to those of Baranger [10]. A single subscript α will be used to define the following set of quantum numbers: the charge q_α, the radial co-ordinate r_α, the orbital and total angular momenta ℓ_α and j_α, and the magnetic quantum number m_α, i.e.

$$\alpha \equiv q_\alpha,\ r_\alpha,\ \ell_\alpha,\ j_\alpha,\ m_\alpha \tag{6a}$$

Following the notations of Baranger, we define

$$a \equiv q_a,\ r_a,\ \ell_a,\ j_a \tag{6b}$$

and letters like s and t will be used to denote the single-particle symmetry type

$$s = q,\ \ell,\ j \tag{6c}$$

Using the basis α, definition (4) of the Hartree-Fock field reads

$$(\alpha \mid \mathcal{U} \mid \gamma) = \sum_{\beta\delta} (\alpha\beta \mid \tilde{V} \mid \gamma\delta)(\delta \mid \rho \mid \beta) \tag{7}$$

where ρ is the one-body density

$$(\delta \mid \rho \mid \beta) = \sum_{i=1}^{A} (\delta \mid i)(i \mid \beta) \tag{8}$$

It is easy to see from Eq.(8) that ρ can be a scalar under rotation in the only case of doubly-closed-shell nuclei. This implies that the one-body density is diagonal in q, ℓ, j and m

$$(\delta \mid \rho \mid \beta) = \delta_{q_\delta q_\beta} \delta_{\ell_\delta \ell_\beta} \delta_{j_\delta j_\beta} \delta_{m_\delta m_\beta} \rho_t (r_\delta , r_\beta) \tag{9}$$

In Eq.(9) t is the symmetry type of both δ and β, and ρ_t is given by

$$\rho_t (r_1 , r_2) = \frac{1}{r_1 r_2} \sum_{n, nt \in A} u_{nt}(r_1) u_{nt}(r_2) \tag{10}$$

assuming that the unknown Hartree-Fock wave functions ϕ_i can be written as

$$\phi_i(\vec{r}, \sigma, \tau) = \frac{1}{r} u_{n_i t_i}(r) \, \mathcal{Y}_{\ell_i j_i m_i}(\Omega, \sigma) \chi_{q_i}(\tau) \tag{11a}$$

i.e. in the α basis

$$(\alpha \mid i) = \delta_{q_\alpha q_i} \delta_{\ell_\alpha \ell_i} \delta_{j_\alpha j_i} \delta_{m_\alpha m_i} u_{n_i t_i}(r_\alpha)/r_\alpha \tag{11b}$$

Since the two-body interaction is invariant under rotations it is convenient to write it in the form

$$(\alpha\beta \mid \tilde{V} \mid \gamma\delta)$$

$$\tag{12}$$

$$= - \sum_{JM} (2\dot{J}+1) F_{\dot{J}} (acdb)(-1)^{j_\alpha - m_\alpha + j_\delta - m_\delta} \begin{pmatrix} j_\alpha & j_\gamma & \dot{J} \\ m_\alpha & -m_\gamma & M \end{pmatrix} \begin{pmatrix} j_\delta & j_\beta & \dot{J} \\ m_\delta & -m_\beta & M \end{pmatrix}$$

The functions $F_{\dot{J}}$ are the same as those of Tarbutton and Davies [11] (except that the principal quantum number n has been replaced by the radial coordinate r) and satisfy the same symmetry relations. Substituting expressions (9) for the one-body density and expression (12) for the matrix elements of the two-body interaction in Eq.(7) one finds that

$$(\alpha \mid \mathscr{U} \cdot \mid \gamma) = \delta_{q_\alpha q_\gamma} \delta_{\ell_\alpha \ell_\gamma} \delta_{j_\alpha j_\gamma} \delta_{m_\alpha m_\gamma} \mathscr{U}_s (r_1, r_2) \tag{13}$$

where $\mathscr{U}_s$ is given by

$$\mathscr{U}_s (r_1, r_2)$$

$$\tag{14}$$

$$= - \sum_t \left(\frac{2j_t + 1}{2j_s + 1} \right)^{\frac{1}{2}} \int r_3^2 dr_3 \, r_4^2 dr_4 \, F_0 (sr_1, sr_2, tr_4, tr_3) \rho_t (r_3, r_4)$$

From relation (14) the Hartree-Fock field is a quadratic function of the unknown radial wave functions $u_{nt}(r)$. On the other hand, the u's are related to the potential by equation (3). Because of relation (13), this equation can be written

$$\frac{\hbar^2}{2m} \left[-u'' + \frac{\ell_t (\ell_t + 1)}{r^2} u \right] + \int_0^{+\infty} \Gamma_t(r, r') u(r') \, dr' = e \, u(r) \tag{15}$$

where we have suppressed the subscript n, t for the sake of simplicity and where

$$\Gamma_t (r_1, r_2) = r_1 r_2 \, \mathscr{U}_t (r_1, r_2) \tag{16}$$

Equations (14) and (15) constitute the radial Hartree-Fock integro-differential system.

Let us note at this point that for a local two-body interaction the function F_0 will contain two δ-functions, which greatly simplify the numerical evaluation of Eq. (14). In the case of a Wigner force

$$V (\mid \vec{r}_1 - \vec{r}_2 \mid) = \sum_k{}' v_k (r_1, r_2) \, P_k (\cos \alpha) \tag{17}$$

one has, for instance,

$$F_0 (sr_1, sr_2, tr_4, tr_3) = - \frac{1}{r_1^2 r_2^2} \sqrt{(2j_s + 1)(2j_t + 1)} \Bigg[\delta(r_1 - r_2) \delta(r_3 - r_4) v_0(r_1, r_3)$$

$$\tag{18}$$

$$- \delta(r_1 - r_3) \delta(r_2 - r_4) \delta_{q_s q_t} (2\ell_s + 1)(2\ell_t + 1) \sum_k \begin{pmatrix} \ell_s & \ell_t & k \\ 0 & 0 & 0 \end{pmatrix}^2 \begin{Bmatrix} \ell_s & j_s & \frac{1}{2} \\ j_t & \ell_t & k \end{Bmatrix}^2 v_k(r_1, r_3) \Bigg]$$

and in this case equation (14) can be written

$$\mathscr{U}_s (r_1, r_2) = \frac{4\pi}{r_1^2} \delta(r_1 - r_2) \int_0^{+\infty} \rho(r_3) v_0(r_1, r_3) \, r_3^2 dr_3$$

$$\tag{19}$$

$$- (2\ell_s + 1) \sum_{kt} \delta_{q_s q_t} (2\ell_t + 1)(2j_t + 1) \begin{pmatrix} \ell_s & \ell_t & k \\ 0 & 0 & 0 \end{pmatrix}^2 \begin{Bmatrix} \ell_s & j_s & \frac{1}{2} \\ j_t & \ell_t & k \end{Bmatrix}^2 v_k(r_1, r_2) \rho_t(r_1, r_2)$$

where ρ is the usual one-body density. In this equation, the first term is a local potential which corresponds to the Hartree term. The second term corresponds to the exchange term.

In the case of tensor and L.S forces similar expressions can be derived from the multipole expansions given in Refs [12] and [13]. For non-local forces the calculation of $\mathscr{U}_s(r_1, r_2)$ from Eq.(14) involves a much larger amount of numerical work. This calculation can be done in principle but only particular cases (a separable s-state interaction and a Green-type interaction, for instance) lead to computations of practicable size.

The asymptotic behaviour of the Hartree-Fock field will be needed in the next section. Unfortunately, there is no room here to discuss it in great detail. In the case of a Gaussian interaction, using Eq.(19) and the asymptotic form of $v_k(r_1, r_2)$ for large r, it can be shown that at large distances the Hartree-Fock field is local and goes to zero as a linear combination of neutron and proton densities. Near the origin one can show that the Hartree-Fock field behaves like a constant.

2. METHOD OF SOLUTION

2.1. Description of the iteration process

The elimination of the average field between Eqs (14) and (15) yields a non-linear system of integro-differential equations. Up to now, the solution of this system has only been obtained by iteration. Let $u_i^{(1)}$ denote a first approximation to the unknown radial wave functions, e.g. harmonic-oscillator or Saxon-Woods wave functions. Inserting these functions into Eq.(14) yields a first approximation $\mathscr{U}_s^{(1)}$ to the Hartree-Fock field. Substituting this value into Eq.(15) yields a new approximation $u_i^{(i)}$ to the radial Hartree-Fock wave functions. This process eventually converges to the exact solution u_i. Starting from Saxon-Woods wave functions we have found that ten to twelve iterations for light nuclei, 20 to 25 for heavy nuclei are sufficient to obtain good convergence.

The computation of the average field from the wave functions by Eq.(14) involves elementary operations only (but they are time-consuming in numerical applications). The solution of Eq.(15) is more difficult. The problem is to find the bound states of a given non-local potential. Several methods have already been proposed [14-16]. The method which we shall describe [6] reduces the non-local Schrödinger equation to a set of local equations. For numerical applications it seems to be a simple and fast method.

2.2. Solution of the non-local Schrödinger equation for bound states

Let us first remark that the non-local Schrödinger equation

$$\frac{\hbar^2}{2m}\left[-u''_\alpha + \frac{\ell_\alpha(\ell_\alpha M)}{r^2} u_\alpha(r)\right] + \int_0^{+\infty} \Gamma(r, r')u_\alpha(r')dr' = e_\alpha u_\alpha(r) \qquad (20)$$

where α now stands for the set (q, n, ℓ, j), is equivalent to the following system

$$
\left\{
\begin{array}{l}
- u_\alpha'' + \dfrac{\ell_\alpha(\ell_\alpha + 1)}{r^2}\, u_\alpha(r) + \dfrac{2m}{\hbar^2}[V_\alpha(r) - e_\alpha]\, u_\alpha(r) = 0 \qquad (21a) \\[4mm]
V_\alpha(r) = \dfrac{1}{u_\alpha(r)} \displaystyle\int_0^{+\infty} \Gamma(r, r')\, u_\alpha(r')\, dr' \qquad (21b)
\end{array}
\right.
$$

The potential $V_\alpha(r)$ is usually called the local equivalent potential corresponding to the state α [17]. We have already mentioned that this potential is regular at the origin and goes to zero for large r as a linear combination of the neutron and proton densities. However, Eq. (21b) shows that this potential will have a pole whenever the radial wave function $u_\alpha(r)$ has a node, so that Eq. (21a) will be a local but generally singular Schrödinger equation. A typical example is shown in Fig. 1·where we have plotted the local equivalent potential of the 2s 1/2 level in ^{40}Ca. Because of non-locality, the integral occurring in Eq. (21b) does not vanish at the node of the radial wave function. As a result the potential has a pole.
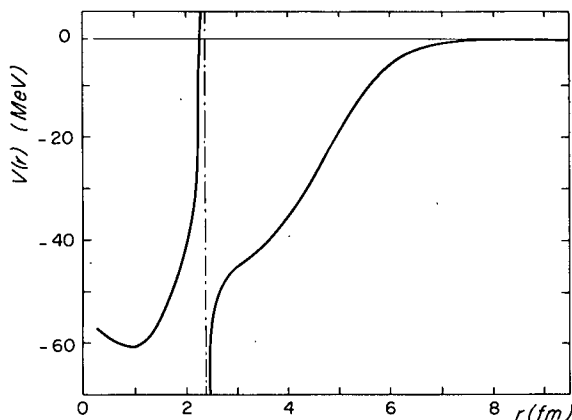
FIG.1.   Local equivalent potential of the 2s1/2 neutron level of ^{40}Ca.

To investigate the difficulties caused by these singularities let us suppose that $V_\alpha(r)$ has a pole at $r = r_0$. In the neighbourhood of r_0 equation (21b) writes

$$
u''(r) + \frac{C}{r - r_0}\, u(r) = 0
$$

Applying Fuchs's theorem [18] one obtains $r(r-1) = 0$ which shows that Eq. (21a) is of the second type. The two linearly independent solutions have the following form near r_0:

$$
u_1(r) = a_1(r - r_0) + a_2(r - r_0)^2 + \cdots
$$

$$
u_2(r) = b_0 + b_1(r - r_0)\, \log |r - r_0| + b_2(r - r_0)^2 + \cdots
$$

From these expansions it is possible to derive an integration formula
analogous to Numerov's formula [15, 19] to integrate the singular Schrödinger
equation (21a). There is, however, a simpler method based on the following
argument [6]. For fixed $\epsilon > 0$, let us define a potential $V_\alpha(\epsilon, r)$ which is
identical to $V_\alpha(r)$ except in the intervals $[r_0 - \epsilon, \ r_0 + \epsilon]$, where r_0 is one of
the singularities of $V_\alpha(r)$. Inside such an interval (we assume that they
do not overlap) $V_\alpha(\epsilon, r)$ is a piece of straight line. Let us denote by $u(\epsilon, r)$
the solution of the Schrödinger equation (we have dropped the index α)

$$- u''(r) + \frac{\ell(\ell+1)}{r^2} \, u(r) + \frac{2m}{\hbar^2} \, [V(\epsilon, r) - e] \, u(r) = 0$$

It can be shown that this function is such that

$$\frac{\partial}{\partial \epsilon} \, u(\epsilon, r) \, \bigg|_{\epsilon = 0} = 0$$

This relation suggests that the solution of the non-local Schrödinger
equation can be approximated by the solution of the system

$$\begin{cases} - u''(r) + \dfrac{\ell(\ell+1)}{r^2} \, u(r) + \dfrac{2m}{\hbar^2} \, [V(\epsilon, r) - e] \, u(r) = 0 & (22a) \\[4mm] V(r) = \dfrac{1}{u(r)} \displaystyle\int_0^{+\infty} \Gamma(r, r') \, u(r') \, dr' & (22b) \end{cases}$$

Since $V(\epsilon, r)$ is regular Eqs (22) can be solved by the following iteration
process

$$\begin{cases} - u''^{(n)}(r) + \dfrac{\ell(\ell+1)}{r^2} \, u^{(n)}(r) + \dfrac{2m}{\hbar^2} \, [V^{(n)}(\epsilon, r) - e_n] \, u^{(n)}(r) = 0 & (23a) \\[4mm] V^{(n+1)}(r) = \dfrac{1}{u^{(n)}(r)} \displaystyle\int_0^{+\infty} \Gamma(r, r') \, u^{(n)}(r') \, dr' & (23b) \end{cases}$$

Eq. (23a) being an ordinary Schrödinger equation which can be solved by
standard techniques. The value of ϵ should not be chosen too small, other-
wise the iteration process would converge only for $u^{(0)}(r)$ very close to the
exact solution. But using as a starting point the solution for $\epsilon = \epsilon_0$ one can
solve again Eqs (22) for $\epsilon = \epsilon_1$ where $\epsilon_1 < \epsilon_0$ and so on ..... In this form
our procedure consists of a double iteration, since one has to iterate Eqs(23)
for each value of ϵ. In fact, this process can be reduced to a single iteration
process by the following formula

$$\begin{cases} - u''^{(n)}(r) + \frac{\ell(\ell+1)}{r^2} u^{(n)}(r) + \frac{2m}{\hbar^2} [V^{(n)}(\epsilon_n, r) - e_n] u^{(n)}(r) = 0 \\ \\ V^{(n+1)}(r) = \frac{1}{u^{(n)}(r)} \int_0^{+\infty} \Gamma(r, r') u^{(n)}(r') dr' \end{cases}$$

where the ϵ's now depend on the iteration number and are chosen such that lim ϵ_n = 0. This shortens considerably the computing time in numerical applications but one must be careful not to let ϵ_n go to zero too rapidly.

To illustrate the convergence with ϵ Table I gives the eigenvalue e corresponding to the proton 2s 1/2 level in ^{40}Ca for various values of ϵ in Eq.(22). The results show that the rate of convergence is very satisfactory.

TABLE I. VARIATION OF THE 2s1/2 EIGENVALUE IN ^{40}Ca OBTAINED BY SOLVING EQS (22) FOR DIFFERENT VALUES OF ϵ. THE NON-LOCAL POTENTIAL IS THE HARTREE-FOCK FIELD OF ^{40}Ca OBTAINED FROM INTERACTION B1 OF Ref.[28].

ϵ	$e_{2s\,1/2}$
0.75	- 19.427
0.35	. - 19.306
0.15	- 19.302
0.05	- 19.301

3.   THE TWO-BODY EFFECTIVE INTERACTION

3.1. Non-singular two-body forces

Several effective interactions suitable for pure Hartree-Fock calcu-lations are now available. These interactions can be classified into two groups which correspond to different approaches to the nuclear problem [20] : i) In the first approach one states that the short-range repulsion of the nucleon-nucleon interaction is not strong enough to invalidate the use of conventional perturbation theory. If this is the case, then the compli-cations of Brueckner theory can be avoided and the simple Hartree-Fock picture should provide a reasonable first-order description of some nuclear properties (such as nuclear radii and densities...). From this point of view, the two-body interaction has to satisfy at least the following require-ments: 1) it must fit the two-body scattering data; 2) nuclear-matter saturation must be obtained approximately in first order with small second-order corrections. Of course, it is far from obvious that there exists a potential satisfying at the same time requirements 1 and 2. To fit the phase shifts and to obtain saturation in nuclear matter, this potential would certainly have some short-range repulsion. The requirement for second-

order corrections to be small is a severe restriction, and for a long time
it has been admitted that two-body data and saturation properties exclude
small second-order corrections. However, a first indication of the contrary
has been given in 1963 with Tabakin's potential [21]. This potential gives a
reasonable fit to the two-body scattering data. In first order saturation is
obtained at $k_F = 1.6$ fm^{-1} with $E/A = -8$ MeV. In second order, E/A has a
minimum of -14.1 MeV at $k_F = 1.8$ fm^{-1}. More recently, Baranger and
co-workers [22] have proposed several interactions which give even smaller
second-order corrections, but in this case the fit to two-body scattering
data is only approximate. Though encouraging these results are not
completely satisfactory (saturation with Tabakin's potential is obtained, for
instance, at too high a density). Moreover, owing essentially to the
extensive development of techniques for treating hard-core potentials
[23, 24], the problem of the existence of a smooth potential has been some-
what neglected in recent years and is still open. ii) The starting point of
the second approach is the observation that the average nuclear field can
be obtained by some Hartree-Fock-like calculations. This average nuclear
field might be the result of the summation of a great number of diagrams,
but one is only interested in parametrizing an "effective" interaction which
would reproduce in first order the result of more elaborated calculations.
Of course, the problem of knowing what diagrams contribute to the effective
interaction is completely left out in this approach. Immediately this fact
introduces strong limitations. In particular, the calculation of higher-order
effects is meaningless in this scope. Also the relationship between the
"effective" interaction and the two-body scattering data is rather obscure.
Some preliminary work has been done by Bethe [25] in order to derive the
parameters of the effective interaction from the reaction-matrix theory.

We shall mention only two interactions belonging to this group. The
first one is that of Skyrme [26], which is a density-dependent effective
interaction. It can be written in the form

$$V(\vec{r}) = (t_0 + t_3 \, \rho(\vec{R})) \, \delta(\vec{r}) + \frac{t_1}{2} \left(\nabla^2 \delta(\vec{r}) + \delta(\vec{r}) \, \nabla^2 \right) + t_2 \vec{\nabla} \delta(\vec{r}) \vec{\nabla}$$

where $\rho(\vec{R})$ denotes the local density at the point $(1/2)(\vec{r}_1 + \vec{r}_2)$. This inter-
action saturates nuclear matter at $k_F = 1.37$ fm with $E/A = -16.8$ MeV. It
also gives a good fit to the experimental binding energies and radii of
several spherical nuclei in a variational calculation using harmonic-
oscillator wave functions.

Other types of effective interactions have been considered, in particular
by Volkov [27] and by Brink and Boeker [28]. Most of these interactions are
local and then well adapted for Hartree-Fock calculations in co-ordinate
space. In the following paragraph, we shall discuss in more detail the
interaction that has been used in most of our calculations.

3.2. The effective interaction B1 of Brink and Boeker [28]

Among other types, Brink and Boeker studied, for different values of
the parameters, interactions which are sums of two Gaussian terms

$$V(r_{12}) = A_1(1 - m_1 + m_1 P_M) \, e^{-(r_{12}/\mu_1)^2} + A_2(1 - m_2 + m_2 P_M) \, e^{-(r_{12}/\mu_2)^2} \quad (24)$$

one of which is attractive and the other one repulsive. Interaction B1 is defined by the following set of parameters

$$\mu_1 = 0.7 \text{ fm} \quad A_1 = 389.5 \text{ MeV} \quad m_1 = -0.529$$

$$\mu_2 = 1.4 \text{ fm} \quad A_2 = -140.6 \text{ MeV} \quad m_2 = 0.4864$$

(25)

These values of the parameters were determined to give in first order nuclear-matter saturation at $k_F = 1.45$ fm^{-1} with $E/A = -15.75$ MeV and the binding energy and density of helium 4. Brink and Boeker also remarked that interaction B1 gives reasonable single-particle energies in ^{16}O. By fitting nuclear matter and helium 4 one hopes that first-order calculations will yield reasonable results for intermediate nuclei. In the following we shall see that this hope will be partly fulfilled.

Let us note that interaction (24) is a particular case of the following one

$$V = \sum_{i=1}^{2} e^{-(r_{12}/\mu_i)^2} [W_i + B_i P_\sigma - H_i P_\tau - M_i P_\sigma P_\tau]$$

(26)

Brink and Boeker were interested only in the properties of $N = Z$ nuclei. In this case, Hartree-Fock calculations involve only linear combinations S and G of the exchange parameters

$$S = 4W + 2B - 2H - M = A(4-5m)$$

$$G = W + 2B - 2H - 4M = A(1-5m)$$

(27)

For instance, the binding energy of helium 4, calculated from harmonic-oscillator wave functions can be written

$$E(1s^4) = 2.25 \hbar\omega + 2 \sum_{i=1}^{2} (S_i - G_i) \lambda_i^3$$

where $\lambda_i = \mu_i / \sqrt{b^2 + \mu^2}$, b denoting the oscillator parameter $\sqrt{\hbar/m\omega}$. In the case of nuclear matter, the binding energy per particle is given by

$$\frac{E}{A} = \frac{3}{10} \frac{\hbar^2}{m} k_F^2 + \frac{1}{\sqrt{\pi}} \left\{ S \frac{x^3}{12} - G \left[\left(\frac{1}{2x} - \frac{1}{x^3} \right) e^{-x^2} - \frac{3}{2x} + \frac{1}{x^3} + \frac{\sqrt{\pi}}{2} \text{erf}(x) \right] \right\}$$

where $x = \mu k_F$ and where we have dropped the index i. The error function is given by

$$\text{erf}(x) = (2/\sqrt{\pi}) \int_0^x \exp(-t^2) dt$$

3.3. Extension of B1 to N ≠ Z systems

For N ≠ Z nuclei the calculation of the average field involves all the exchange parameters in Eq.(26) and the knowledge of S and G is no longer sufficient to determine the interaction. But using the same guiding idea as Brink and Boeker, it is possible to define an extension of B1 to N ≠ Z systems. If the effective interaction has to reproduce approximately the binding energy and densities of spherical nuclei, then it is reasonable to require that it also fits the symmetry-energy coefficient a_τ in nuclear matter. This coefficient is defined by

$$E/A = -a_0 + \alpha^2 a_\tau \qquad \text{where } \alpha = (N-Z)/A$$

In the case of the interaction (26) one has

$$a_\tau = \frac{1}{6} \frac{\hbar^2}{m} k_F^2 + \frac{1}{6\sqrt{\pi}} \left\{ S \frac{x^3}{2} - G \left[\left(x + \frac{1}{x} \right) e^{-x^2} - \frac{1}{x} \right] \right.$$

$$\left. - (2W - B) x^3 + (H + 2M) x (\exp(-x^2) - 1) \right\}$$

where $x = \mu k_F$ and where we have dropped the index i. The quantities S and G are defined by Eq.(27). Since we have four parameters at our disposal to fit the "experimental" value of the symmetry-energy coefficient (28 - 32 MeV [29]), we choose arbitrarily $B_1 = H_1 = 0$, $B_2 = H_2$. We keep the Wigner and Majorana terms as they are defined by Eq.(25), since it can be seen that this procedure leaves the values (27) of the S and G's unchanged. The value of the symmetry-energy coefficient a_τ is given for three different interactions in Table II. Force B1α corresponds to the values (25) of the parameters and is identical to B1. The force B1β gives the best result for the separation energy difference $\Delta = |e_{1h11/2p}| - |e_{1i12/2n}|$ in a self-consistent calculation of ^{208}Pb. Force B1γ reproduces the experimental value of a_τ and gives the best agreement with Coulomb displacement energy in ^{208}Pb (see below).

TABLE II. VALUE OF THE SYMMETRY ENERGY COEFFICIENT a_τ (IN MeV) AS A FUNCTION OF $B_2 = H_2$. THE SEPARATION ENERGY DIFFERENCE Δ BETWEEN NEUTRONS AND PROTONS OBTAINED FROM A SELF-CONSISTENT CALCULATION OF ^{208}Pb IS GIVEN ON THE THIRD LINE.

Force	B1α	B1β	B1γ	exp.
$B_2 = H_2$	0	8.3	26.44	..
a_τ	57.8	49.6	32	28-32
Δ	3.31	-0.57	-5.15	0.66

3.4. The effective two-body spin-orbit force

Since the previous interactions are purely central they cannot give rise to any spin-orbit splitting. A way of obtaining such a splitting is to add to the central force a two-body spin-orbit force

$$V = V_{LS}(|\vec{r}_1 - \vec{r}_2|) \, \vec{L} \cdot \vec{S} \tag{28}$$

where

$$\vec{L} = \vec{r} \times \vec{p}/\hbar, \qquad \vec{S} = \frac{1}{2}(\vec{\sigma}_1 + \vec{\sigma}_2)$$

The contribution of interaction (28) to the Hartree-Fock field is a sum of three terms. The first one is a usual spin-orbit potential $\mathscr{U}(r)\vec{\ell}\cdot\vec{s}$ whose form factor is given by

$$\mathscr{U}(\vec{r}_1) = \int \rho(\vec{r}_2) \, V_{LS}(|\vec{r}_1 - \vec{r}_2|) \left(1 - \frac{\vec{r}_1 \cdot \vec{r}_2}{r_1^2}\right) d\vec{r}_2 \tag{29}$$

In addition to expression (29) one gets two other terms. These terms are generally small and vanish identically for spin-saturated shells (i.e. if both $j = \ell + 1/2$ and $j = 1 - 1/2$ are filled). They will be omitted in the following discussion. Let us now suppose that the range of the two-body spin-orbit force is small as compared to the nuclear size so that $\rho(\vec{r}_2)$ can be replaced by

$$\rho(\vec{r}_2) = \rho(\vec{r}_1) - (\vec{r}_1 - \vec{r}_2) \cdot \vec{\nabla}\rho(\vec{r}_2)$$

in the evaluation of integral (29). Then one obtains the following result (due to Blin-Stoyle [30, 31]) for the contribution of the two-body spin-orbit force to the average nuclear field:

$$\mathscr{U}(r) = \frac{C}{r}\frac{d\rho}{dr}\vec{\ell}\cdot\vec{s} \tag{30}$$

where the constant C is given by

$$C = -\frac{4\pi}{3}\int_0^{+\infty} V_{LS}(\xi)\,\xi^4\,d\xi \tag{31}$$

A rough way of evaluating this constant from the two-body scattering data is to assume that Born's approximation is valid. In this case the phase shift

$$\delta_{LS} = -\frac{m}{\hbar^2}\,k\int_0^{+\infty} j_1^2(kr)\,V_{LS}(r)\,r^2 dr \tag{32}$$

obtained from V_{LS} alone, can be related to the $^3P_-$ phase shifts by the formula [32]

$$\delta_{LS} = \frac{5}{12} \left[\delta(^3P_2) - \frac{3}{5} \delta(^3P_1) - \frac{2}{5} \delta(^3P_0) \right] \qquad (33)$$

Taking the experimental $^3P_-$ phase shifts, Eq.(33) yields an "experimental" value of δ_{LS}. Next assuming for $V_{LS}(r)$ a Gaussian shape one can determine the two parameters V_0 and μ by requiring that Eq.(32) should give the best agreement with the "experimental" value of δ_{LS}. From this procedure one gets

$$V_0 = -202 \text{ MeV} \qquad \mu = 0.8 \text{ fm} \qquad (34)$$

The L-S force is generally assumed to be a triplet-odd interaction. In this case the value of C computed from equation (31) has to be multiplied by a factor of 3/4 which gives

$$C = -\frac{3}{8} \pi^{3/2} \mu^5 V_0 = 2.085 \mu^5 V_0 \simeq 140 \text{ MeV} \times \text{fm}^5 \qquad (35)$$

This value is somewhat too small to explain the splitting of the 1p-levels in ^{16}O satisfactorily. Furthermore, the disagreement is still increased when the exact formula (29) is used. Indeed, a self-consistent calculation of ^{16}O by using interaction B1 and the two-body spin-orbit force (34) yields a spin-orbit splitting which is only half of the observed value (6.15 MeV). Of course, the values (34) of the parameters have been obtained by using Born's approximation, which is not very good. However, more elaborated calculations by Wong [33] show that the single-particle spin-orbit splittings obtained from the LS-force alone are too small and that second-order diagrams involving the tensor force are probably necessary to obtain a good agreement with experimental values. For this reason, we have considered C in Eq.(30) rather as a parameter. Its value has been fitted to the experimental splitting of the 1p-levels in a self-consistent calculation of ^{16}O. The result is C = 176 MeV × fm^5, which has to be compared with the value (35). Although approximation (30) is certainly less accurate for nuclei having spin-unsaturated shells we have used the same value of the constant C for heavy nuclei.

4. RESULTS

4.1. Nuclear radii, densities, electron scattering

The neutron, proton, matter and charge radii obtained from interaction B1β are shown in Table III for several spherical nuclei. The root-mean-square radius r_c of the charge distribution is related to r_p by

$$r_c^2 = r_p^2 + r_{proton}^2, \qquad r_{proton}^2 = 0.64 \text{ fm}^2$$

TABLE III. E/A IS THE TOTAL BINDING ENERGY PER PARTICLE (IN MeV); r_M, r_p, r_n AND r_c ARE, RESPECTIVELY, THE MASS, PROTON, NEUTRON AND CHARGE ROOT-MEAN-SQUARE RADII (IN fm). RESULTS OF OTHER HARTREE-FOCK CALCULATIONS AND EXPERIMENTAL VALUES OF THE ROOT-MEAN-SQUARE CHARGE RADIUS ARE SHOWN IN COLUMNS 6, 7 AND 8.

	E/A	r_M	r_p	r_n	r_c	r_c[41]	r_c[11]	r_c(exp)
^{16}O	-6.05	2.66	2.67	2.65	2.77	2.39	2.67	2.73
^{40}Ca	-6.43	3.40	3.43	3.38	3.52	2.89	3.30	3.50
^{48}Ca	-6.10	3.65	3.51	3.76	3.60	2.79	3.34	3.49
^{90}Zr	-6.28	4.31	4.25	4.37	4.32		4.03	4.30
^{208}Pb	-5.52	5.61	5.44	5.72	5.50		5.14	5.52

Table III also gives some results of other Hartree-Fock calculations and experimental values of r_c. The overall agreement is very good. Let us first note that this agreement has been obtained with a local and density-independent effective interaction. In fact, this agreement is more satis-factory than that obtained with more realistic interactions [1, 11] fitted on two-body data. Because B1 is an effective interaction, our results cannot be considered, however, as a triumph of the Hartree-Fock approximation. They rather indicate that B1 is a quite reasonable parametrization of the effective interaction. Let us also stress that such a good agreement for the radii is not an obvious consequence of the fact that nuclear matter and ^{4}He have been fitted.

When the symmetry energy coefficient a_τ is varied the change in the radii is negligible for ^{16}O and ^{40}Ca, and small for other nuclei. However, important variations occur in the single-particle spectra of $N \neq Z$ nuclei (see Tables IV and VII).

The total densities of ^{16}O and ^{40}Ca are shown in Fig. 2. The shapes of these densities differ largely from Fermi distributions. The density at the centre of ^{40}Ca is almost three times the density at the centre of ^{16}O. This difference is a first illustration of the importance of shell effects. Figure 3 shows the total and proton densities of ^{40}Ca and ^{48}Ca. Since proton levels are deeper in ^{48}Ca than in ^{40}Ca, the proton density has less tail in ^{48}Ca. This effect, however, is not sufficient to obtain the decrease of the mean-square-charge radius observed from ^{40}Ca to ^{48}Ca. The relative variation $\Delta r_c / r_c = [r_c(48) - r_c(40)]/r_c(40)$ is found to be of the order of $+2.5\%$ whereas the experimental value is -0.3%. In ^{90}Zr, whose neutron and proton densities have been plotted in Fig. 4, one still obtains rather large oscil-lations, but a nuclear surface can nevertheless be defined approximately in this case. Figure 5 shows the proton, neutron and total densities of ^{208}Pb. For this nucleus there is no more ambiguity, and one can distinguish a nuclear surface beginning at around 6 fermi. However, the proton density is never really flat and decreases continuously from the centre towards the surface.

TABLE IV.   ROOT-MEAN-SQUARE RADII (IN fm) AND BINDING ENERGIES PER NUCLEON OBTAINED IN ^{208}Pb FROM INTERACTIONS B1α, B1β AND B1γ

	B1α	B1β	B1γ
E/A	-5.40	-5.52	-5.71
r_p	5.43	5.44	5.48
r_n	5.75	5.72	5.68
r_M	5.62	5.61	5.59
r_c	5.49	5.50	5.54

TABLE V.   SINGLE-PARTICLE ENERGIES (IN MeV) OF NEUTRON
LEVELS FOR SEVERAL LOW- AND MEDIUM-MASS NUCLEI.   ROUGH
EXPERIMENTAL VALUES ARE INDICATED IN PARENTHESES.   THE
TWO-BODY INTERACTION IS B1β

Nucleus	^{16}O		^{40}Ca		^{48}Ca		^{90}Zr
1s 1/2	-48.32		-68.04		-66.68		-80.98
1p 3/2	-23.52	(-21.8)	-44.89		-45.72		-61.62
1p 1/2	-17.35	(-15.7)	-41.35		-43.93		-59.96
1d 5/2	- 2.35	(- 4.1)	-23.78	(-22.8)	-25.94	(-16.6)	-43.30
2s 1/2	- 0.18	(- 3.3)	-19.30	(-18.1)	-22.63	(-13.6)	-40.89
1d 3/2	+ 2.83	(+ 0.93)	-17.88	(-15.6)	-22.36	(-13.6)	-40.58
1f 7/2			- 5.17	(-.8.3)	- 7.90	(-10)	-25.96
2p 3/2			- 0.77	(- 6.2)			-21.58
1f 5/2			+ 1.7	(- 2.8)			-21.69
2p 1/2			+ 0.21	(- 4.3)			-19.14
1g 9/2			+ 8.3				- 9.94

TABLE VI.   SINGLE-PARTICLE ENERGIES (IN MeV) OF PROTON
LEVELS

Nucleus	^{16}O		^{40}Ca		^{48}Ca		^{90}Zr
1s 1/2	-44.11	(-44)	-59.43	(-77)	-61.33		-68.96
1p 3/2	-19.64	(-19)	-36.88		-41.42		-51.00
1p 1/2	-13.53	(-12.4)	-33.34	(-32)	-39.05		-49.04
1d 5/2			-16.31	(-14.5)	-22.20	(-19.4)	-33.68
2s 1/2			-11.67	(-10.5)	-16.86	(-15.3)	-30.17
1d 3/2			-10.46	(- 8.3)	-17.74	(-15.6)	-30.33
1f 7/2							-17.00
2p 3/2							-10.97
1f 5/2							-11.94
2p 1/2							- 8.45

TABLE VII. PROTON AND NEUTRON SINGLE-PARTICLE ENERGIES
(IN MeV) OBTAINED FROM INTERACTIONS B1α, B1β, AND B1γ.
OCCUPIED AND UNOCCUPIED STATES ARE SEPARATED BY A
HORIZONTAL LINE (FOR [208]Pb)

Force	B1α		B1β		B1γ	
	Protons	Neutrons	Protons	Neutrons	Protons	Neutrons
1s 1/2	-74.13	-86.83	-72.30	-88.31	-68.83	-91.93
1p 3/2	-61.00	-72.58	-59.20	-74.35	-56.00	-77.68
1p 1/2	-60.14	-71.68	-58.38	-73.48	-55.26	-76.89
1d 5/2	-47.78	-58.81	-46.01	-60.48	-43.00	-63.52
2s 1/2	-45.52	-56.78	-43.84	-58.51	-40.80	-61.70
1d 3/2	-46.36	-57.31	-44.71	-59.09	-41.87	-62.32
1f 7/2	-34.47	-45.07	-32.75	-46.65	-29.87	-49.43
2p 3/2	-30.54	-41.50	-28.92	-43.22	-25.96	-46.23
1f 5/2	-32.26	-42.80	-30.73	-44.57	-28.14	-47.65
2p 1/2	-29.29	-40.30	-27.74	-42.07	-24.86	-45.18
1g 9/2	-21.21	-31.49	-19.55	-32.99	-16.81	-35.52
2d 5/2	-15.44	-26.22	-13.92	-27.88	-11.16	-30.66
1g 7/2	-17.88	-28.14	-16.47	-29.91	-14.09	-32.64
3s 1/2	-12.23	-23.26	-10.79	-24.93	- 8.09	-27.74
2d 3/2	-13.13	-23.97	-11.68	-25.70	- 9.04	-28.61
1h11/2	- 8.25	-18.30	- 6.68	-19.73	- 4.11	-22.02
2f 7/2	- 1.00	-11.69	>0	-13.19	>0	-15.62
1h 9/2	- 3.53	-13.62	- 2.24	-15.34	>0	-18.07
3p 3/2		- 8.03		- 9.40		-11.71
2f 5/2		- 8.64		-10.17		-12.67
3p 1/2		- 6.91		- 8.29		-10.53
1i13/2		- 5.94		- 7.25		- 9.26
2g 9/2		>0		- 0.86		- 3.37
1i11/2		>0		- 1.56		- 4.93

The densities that one would get from a Saxon-Woods potential are
similar to our densities except that they are smoother. For instance, the
density of [208]Pb obtained from a Saxon-Woods potential also has a maximum
at the origin but this maximum is much less pronounced [34].

It has been suggested that the shapes of Hartree-Fock densities are
too singular to give a good fit to the electron scattering data [35]. However,
a calculation of the elastic-electron-scattering cross-section at 250 MeV by
[40]Ca has been made in collaboration with J.B. Bellicard, using the proton
density plotted in Fig.3. The result is represented by the solid line in
Fig.6. The dotted curve corresponds to the best fit obtained from a

Fermi distribution (in fact, most of the experimental points lie on this curve). It can be seen that the agreement is quite fair up to $\theta = 90°$ (which corresponds to a momentum transfer of two inverse fermis approximately).

4.2. Single-particle energies

Single-particle energies and binding energies per nucleon are given for several light and intermediate nuclei in Tables III, V and VI. These results were obtained from interaction $B1\beta$. As mentioned before, the two-body LS-force has been assumed to generate a surface-gradient spin-orbit potential in the Hartree-Fock field, and its magnitude has been fitted in order to reproduce the splitting of the 1p-levels in ^{16}O. When available unoccupied states of the Hartree-Fock potential (bound and unbound) have been given. The calculation of scattering states of the Hartree-Fock field will be described in section 5.
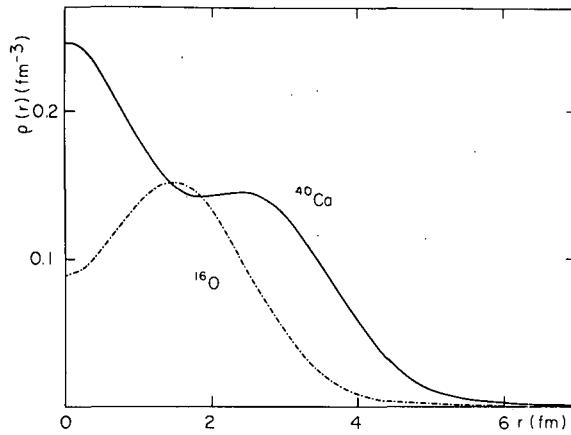
FIG.2.   Matter distributions obtained for ^{16}O and ^{40}Ca from interaction $B1\beta$.
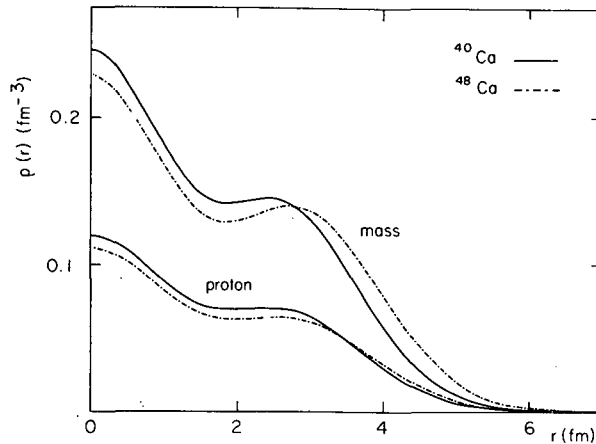
FIG.3. Proton and mass distributions of ^{40}Ca and ^{48}Ca. The two-body interaction is $B1\beta$.
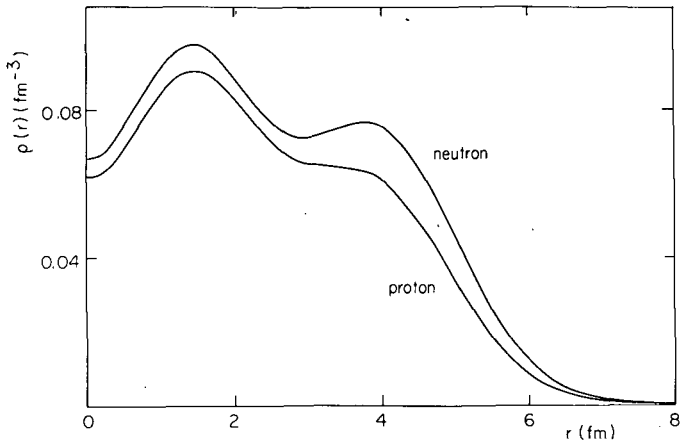
FIG.4. Proton and neutron distributions obtained for ^{90}Zr from interaction B1β.
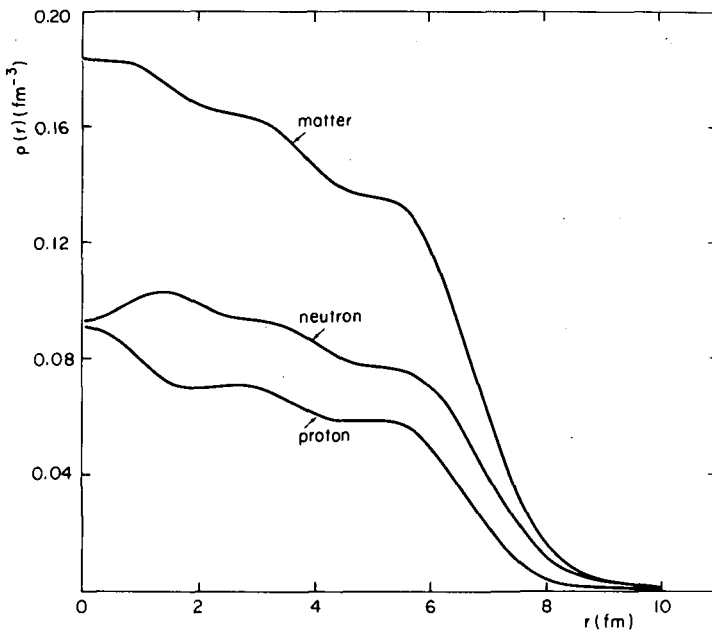
FIG.5. Neutron, proton and mass densities of ^{208}Pb. Interaction is B1α.
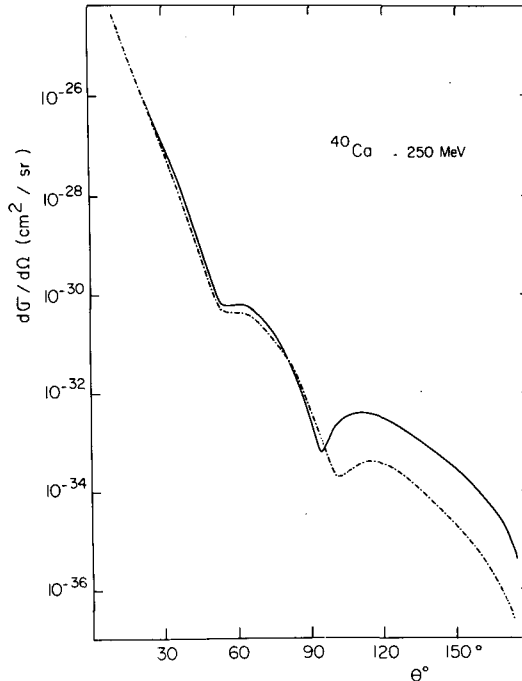
FIG. 6.   Elastic-electron-scattering cross-section at 250 MeV from ^{40}Ca.   The solid line is obtained from the proton Hartree-Fock density of ^{40}Ca corresponding to interaction B1α.   The dotted curve is the best fit to the experimental cross-section given by a 3-parameter Fermi model.

   The single-particle energies of ^{16}O and ^{40}Ca are satisfactory, including the 1d-splitting in calcium.   The main discrepancy is that the gap between occupied and unoccupied states is too large.   In particular, the 2p 1/2 and 1f 5/2 neutron levels of ^{40}Ca are weakly unbound in contrast to what the experimental data suggest.   In ^{48}Ca the energy difference between the 1f 7/2 and 1d 3/2 neutron levels (14.5 MeV) disagrees with the observed value (3.6 MeV).

   The proton and neutron single-particle energies of the bound states of ^{208}Pb (occupied and unoccupied) are given in Table VII for the three different versions of interaction B1 mentioned earlier.   Unfortunately, the comparison with experiment is only possible just below or just above the Fermi surface, while the deepest state is around -90 MeV.   In any case this comparison reveals two major discrepancies.   The first one is that the neutron 1i 13/2 and the proton 1h 11/2 levels are too high.   The other one is that the level density is too small.   These discrepancies are common to all self-consistent calculations [11] including Brueckner-Hartree-Fock calculations [7, 36].   As a consequence of this discrepancy one gets too small a number of bound unoccupied states.   These discrepancies might come either from the interactions that have been used up to date (which, however, are quite different), or, more likely, from higher-order effects such as a coupling with collective modes.   On the other hand, experimental single-particle energies in ^{208}Pb have been fitted quite well using Saxon-Woods

potentials. Let us note, however, that these phenomenological Saxon-Woods well are clearly very far from self-consistency (presumably for any reasonable two-body interaction).

The spin-orbit splittings obtained in ^{208}Pb have the correct order of magnitude. However, one must keep in mind that the surface-gradient formula for the one-body spin-orbit potential is only an approximate way of including a two-body spin-orbit force in Hartree-Fock calculations of heavy nuclei. In fact, there are two spin-unsaturated shells in ^{208}Pb, i.e. (1i 13/2-neutron and 1h 11/2 proton). In this case, the two terms that have been omitted in deriving Blin-Stoyle's formula (30) are no more negligible. Notice that the shape of our density does not limit the contribution of the Thomas spin-orbit term to the surface region. Notice also that increasing the value of the constant C would decrease, at least partially, the discrepancy concerning the neutron-1i 13/2 and proton 1h 11/2-levels.

Although interaction B1 fits, in lowest order, the binding energies of ^{4}He and nuclear matter, the results which we obtain for the binding energies per nucleon are in less satisfactory agreement with experiment than nuclear radii. In ^{16}O, for instance, we get only 6 MeV per nucleon whereas the experimental value is 8 MeV. However, it is clear that, owing to the relation,

$$E = \frac{1}{2} \sum_{i=1}^{A} (t_i + e_i) \tag{36}$$

a Hartree-Fock calculation of ^{16}O cannot fit at the same time the experimental values of the radius, of the total binding energy and of the single-particle energies[1]. Since our calculation gives a good fit to experimental values of the radius and single-particle energies, the total binding energy cannot be in such a good agreement with experiment.

4.3. Local equivalent potentials

An example of a local equivalent potential has already been given in section 1 (Fig. 1). Other examples are shown on Fig. 7 where we have plotted the local equivalent potentials of the s1/2 proton levels in ^{208}Pb. These potentials have been linearly interpolated in the neighbourhood of their poles. They are in fact the potentials $V(\epsilon, r)$ of section II corresponding to $\epsilon = 0.75$ fermi. By comparing the depths of these potentials one immediately remarks the importance of the non-locality of the Hartree-Fock field. We have also indicated by dotted lines on this figure the position of the corresponding single-particle energies. The intersection of such a line with the corresponding potential gives a rough estimate of the radius of the wave function. It can be seen that the ratio of the radii of the 1s and 2s levels is much smaller than it would be in a Saxon-Woods potential. Let us also note that there exists a great similarity between the shapes of the density and of the potentials. For large r, we have already mentioned in

---

[1] In ^{16}O, harmonic-oscillator wave functions approximate quite accurately the Hartree-Fock wave functions so that "experimental" values of the single-particle kinetic energies t_i can be extracted from the experimental radius. When these values, together with the experimental single-particle energies, are inserted into Eq.(36), one gets for the total binding energy E a value which disagrees with experiment.
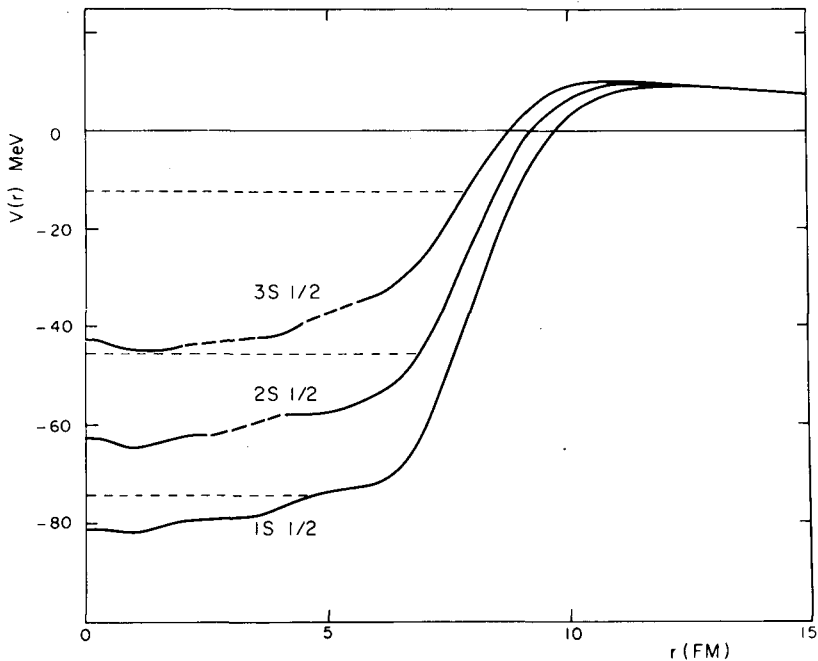
FIG.7.   Local equivalent potentials of the s1/2 proton levels of [208]Pb. The interaction is B1α.

section 1 that the nuclear part of the Hartree-Fock potential is exactly
proportional to the density. Inside the nuclear surface the direct term of
the Hartree-Fock field is exactly given by the convolution product of the
density by the form factor of the two-body interaction. For the exchange
term, this proportionality relation is only approximate (it would be exact
for a zero-range force).

4.4. Overlaps with oscillator wave functions

It is well-known that for light nuclei, harmonic-oscillator wave functions
approximate accurately Hartree-Fock wave functions [1]. In Table VIII we
give the expansions of several neutron wave functions obtained in [208]Pb with
interaction B1α, for two different values of the oscillator parameter b. The
value b = 2.7 fermis gives a maximum overlap of the 1s 1/2 wave function
with oscillator wave functions whereas the value b = 2.4 fermis gives a
maximum overlap for the 1i 13/2 neutron wave function. Since our radius is
a little larger, these two numbers differ slightly from those of Tarbutton
and Davies (2.6 and 2.28 fm, respectively) but the general trend is the same.
In particular, one needs larger b values for low-lying states in spite of the
small value of the radius of the 1s 1/2 wave function. As expected, the
results of Table VII show that it is more difficult to reproduce levels at the
bottom of the well by oscillator wave functions. Although these overlaps are
still rather large they are not as good as for light nuclei. For instance,

TABLE VIII.   OVERLAPS OF SOME ORBITALS WITH OSCILLATOR
WAVE FUNCTIONS FOR TWO VALUES OF THE OSCILLATOR
PARAMETER b. INTERACTION IS B1α

		n = 1	n = 2	n = 3	n = 4	n = 5
b = 2.4	1s 1/2	0.9854	-0.1690	0.0045	0.0162	-0.0027
	2s 1/2	0.1722	0.9683	-0.1635	-0.0642	0.0287
	3s 1/2	0.0250	0.1484	0.9844	-0.0517	-0.0725
	1i13/2	0.9974	-0.0388	-0.0320	-0.0383	-0.0072
b = 2.7	1s 1/2	0.9995	-0.0176	-0.0226	0.0067	0.0010
	2s 1/2	0.0297	0.9893	0.1257	0.0638	-0.0151
	3s 1/2	0.0230	-0.1084	0.9314	0.3429	0.0419
	1i13/2	0.9531	0.2855	0.0454	-0.0650	-0.0589

one can find off-diagonal elements of the order of 40 per cent. As already
noticed by Tarbutton and Davies it seems difficult to reproduce all the wave
functions with only one value of the oscillator parameter.

4.5. Coulomb-displacement energies

Let us recall that the isobaric analogue state is obtained by applying
the isospin lowering operator T_- to the ground state ϕ of a given nucleus.
Since nuclear forces commute with T_- the energy difference between the
analogue state and its parent is just given by the Coulomb-displacement
energy

$$\Delta E_c = \frac{(\phi|T_+ V_c T_-|\phi)}{(\phi|T_+ T_-|\phi)} - (\phi|V_c|\phi)$$

where V_c denotes the Coulomb interaction. If neutron and proton wave
functions are assumed to be identical one obtains the following expression
for ΔE_c:

$$\Delta E_c = \frac{4\pi}{N-Z} \int_0^{+\infty} \left[\rho_n(r) - \rho_p(r) \right] V(r) r^2 dr \qquad (37)$$

where V(r) is the Coulomb potential due to the proton distribution

$$V(r) = \int \rho_p(r') \frac{e^2}{\vec{r} - \vec{r'}} d\vec{r'}$$

TABLE IX.   DIRECT COULOMB DISPLACEMENT ENERGIES ΔE_c(IN MeV).   THE CONTRIBUTION OF EACH (NEUTRON) ORBITAL IS GIVEN SEPARATELY.   LAST COLUMN CORRESPONDS TO UNOCCUPIED PROTON ORBITALS

Force	B1α	B1β	B1γ	B1α (protons)
2f 7/2	19.18	19.22	19.38	19.18
1h 9/2	18.80	18.82	18.88	18.73
3p 3/2	18.87	18.98	19.34	-
2f 5/2	18.88	18.96	19.20	-
3p 1/2	18.55	18.70	19.13	-
1i13/2	17.72	17.75	17.85	-
ΔE_c	18.53	18.58	18.74	-

Actually Eq.(37) corresponds only to the direct term. We have checked that the exchange term is approximately -3% of the direct term.

     Table IX gives for ^{208}Pb the variations of the individual Coulomb-displacement energies

$$\Delta E_c (i) = \int_0^{+\infty} V(r) \, u_i^2(r) \, dr$$

as a function as the neutron orbitals i which contribute to the difference $\rho_n - \rho_p$ in integral (37). The results of column 4 correspond to bound un-occupied proton orbitals. The difference with the results of column 1 is rather small and justifies the approximation made above concerning the identity of neutron and proton wave functions. The result we obtain for the total Coulomb-displacement energy ΔE_c is somewhat smaller than the experimental value 18.87 ± 0.02 MeV [37] (one should, furthermore, sub-tract the exchange term). When one goes from interaction α to γ agree-ment with the experimental value improves. At the same time, the difference $r_n - r_p$ between the neutron and proton r.m.s. radii decreases from 0.32 to 0.20 fm. The present calculation gives for the difference $r_n - r_p$ a smaller value than the shell-model and optical analysis [34, 38]. On the other hand, Nolen, Schiffer and Williams have remarked that a value of r_n can be deduced with a good reliability from the experimental knowledge of r_c and ΔE_c [39]. They first found $r_n - r_p$ = 0.07 ± 0.03 fm [39] and in a very recent analysis $r_n - r_p$ = 0.16 fm [40]. We believe that our results favour also a small $r_n - r_p$ difference in agreement with the analysis of Ref. [39].

5.   APPLICATIONS TO SCATTERING PROBLEMS

5.1.   Potential scattering by the Hartree-Fock field [42]

The solution of the integro-differential system (14, 15) directly yields the angular components $\Gamma_s(r, r')$ of the average nuclear field. From these components one can compute the bound unoccupied states and the scattering states of the Hartree-Fock field. In the case of neutron scattering, the phase shifts $\delta_{\ell j}$ are obtained by solving, for each excitation energy E, the Schrödinger equation

$$\frac{\hbar^2}{2m} \left[-u'' + \frac{\ell(\ell+1)}{r^2} u \right] + \int_0^{+\infty} \Gamma_{\ell j}(r, r') u(r') dr' = E u(r) \qquad (38)$$

and next by matching u(r) to its asymptotic behaviour

$$u(r) \sim kr \left[\cos \delta_{\ell j} \, j_\ell(kr) + \sin \delta_{\ell j} \, n_\ell(kr) \right], \quad \text{where} \quad k = \sqrt{2mE/\hbar^2}$$

Then the total cross-section for potential scattering is given by

$$\sigma(E) = \frac{2\pi}{k^2} \sum_{\ell j} (2j+1) \sin^2 \delta_{\ell j}$$

In the Hartree-Fock approximation unoccupied states of the Hartree-Fock field of the nucleus of mass number A describe excited states of the A+1 nucleon system whereas occupied states describe the excited states of the A-1 nucleus. The phase shifts $\delta_{\ell j}$ then correspond to the potential scattering of a neutron from the closed-shell nucleus of mass number A.

For bound unoccupied states the solution of the non-local Schrödinger equation has been obtained by the method already described in section 2. For continuum states there is only one boundary condition (u(0) = 0) to Eq.(38). In this case, the solution u(r) can be obtained by the more usual iteration procedure [43] in which the inhomogeneous differential equation associated with Eq.(38) is iterated according to

$$\frac{\hbar^2}{2m} \left[-u''^{(n+1)}(r) + \frac{\ell(\ell+1)}{r^2} u^{(n+1)}(r) \right] + \int_0^{+\infty} \Gamma_{\ell j}(r, r') u^{(n)}(r') dr' = E u^{(n+1)}(r) \qquad (39)$$

Starting from an approximation $u^{(0)}(r)$ to the solution of Eq.(38) (for instance a scattering state of a reasonable Saxon-Woods well) Eq.(39) is integrated with the initial values

$$u^{(1)}(0) = 0, \qquad u^{(1)}(h) = u^{(0)}(h)$$

where h denotes the integration step. This procedure yields a new approxi-
mation $u^{(1)}$ to the solution and so on.... In practice, the solution of the
inhomogeneous equation (39) has been obtained by the modified Numerov
method for inhomogeneous equations as described in Ref. [44].

Some neutron single-particle resonance energies have already been
given in Table V. The s and d phase shifts for ^{16}O are shown in Fig. 8.
The rapid increase of the s phase shift is due to the fact that the 2s1/2 level
is only very weakly bound. The d3/2 wave is more rewarding. It resonates
at 2.83 MeV with a 1 MeV width while the experimental d3/2 resonance
occurs at 0.93 MeV with a 94 KeV width. The p and f phase shifts are much
smaller than the s and d ones but are not negligible after 7 MeV.
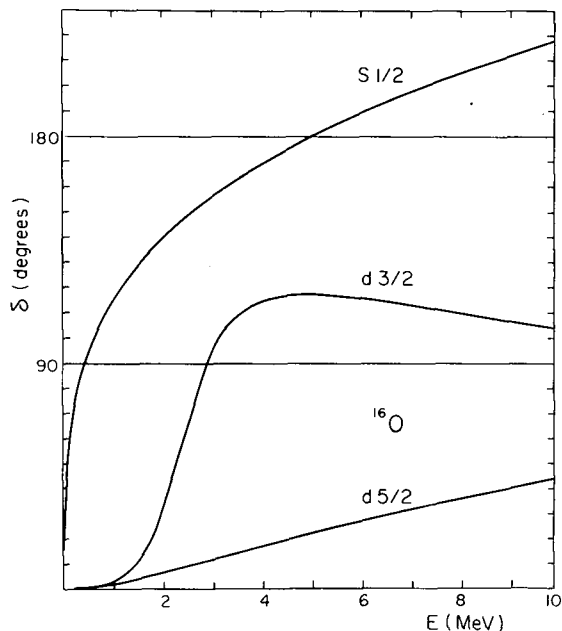
FIG. 8.   Absolute value of s and d phase shifts for ^{16}O. The d3/2 phase shift is positive, the d5/2 and s1/2 ones
are negative.

In Fig. 9 we show the total cross-sections for the elastic scattering of a
neutron from ^{16}O and ^{40}Ca. In both cases the behaviour of the cross-section
near the threshold should be considered with great caution. Indeed, we
have no adjustable parameter at our disposal to match the theoretical
threshold with the experimental one. In ^{16}O the s-wave cross-section
near zero energy is very sensitive to the 2s1/2 binding energy, which could
be easily moved up or down by a small change of the two-body interaction.
This is also true for the p1/2 and f5/2 resonances found in ^{40}Ca near 0.2 and
1.7 MeV respectively (corresponding experimental states are bound).
Indeed it is quite evident that the simple shell model with a single valence
nucleon outside a double closed shell is a very crude model for both ^{17}O
and ^{41}Ca. It may be useful also to recall that we have nothing like an
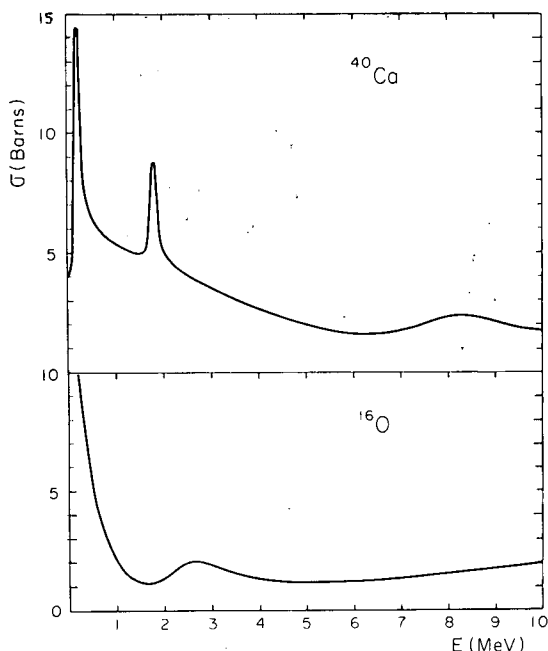
FIG.9.   Total cross-sections for potential scattering of a neutron by the Hartree-Fock fields of ^{16}O and ^{40}Ca.

imaginary part to take account of processes which are not pure elastic poten-
tial scattering. These considerations make the comparison with experi-
mental elastic-scattering data [45, 46] of neutrons from ^{16}O and ^{40}Ca
difficult. Nevertheless, the right order of magnitude is obtained for the
total cross-section if one excludes the region just above threshold.

5.2.   Particle-hole calculations including continuum states in the
Hartree-Fock basis

By computing the scattering states we have achieved the calculation of
the complete Hartree-Fock basis. This basis can be considered as a
starting point for spectroscopy calculations, such as particle-hole calcu-
lations. The advantage of the co-ordinate representation is that it provides
a good spatial description of the Hartree-Fock potential even around its
edge. This is a necessary condition to have good single-particle energies
and wave functions just below zero energy (i.e. for weakly bound unoccupied
state) and above (i.e. for continuum states).

These single-particle energies and wave functions are the necessary
ingredients for the particle-hole calculation (including continuum states
which we shall now discuss briefly. This calculation, made in collaboration
with J. Raynal, is of the same type as that of Ref. [44]. In the calculation
of Ref. [44] the unperturbed Hamiltonian is taken to be a Saxon-Woods poten-
tial whose parameters depend on the orbital angular momentum. We use,
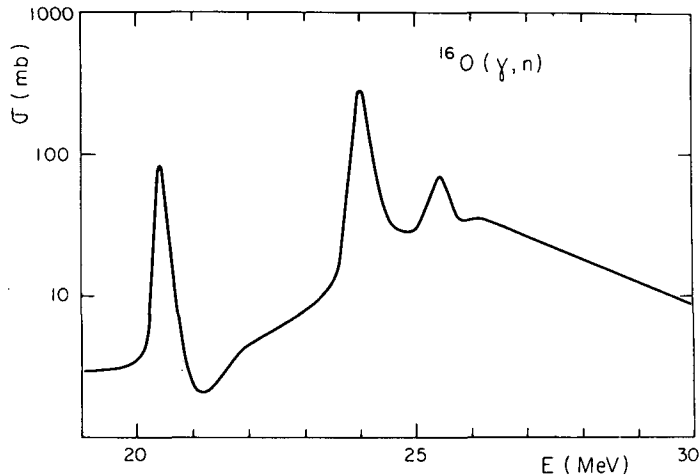
FIG. 10.   Total (γ, n) cross-section obtained for ^{16}O.

instead, the Hartree-Fock Hamiltonian obtained for ^{16}O with interaction B1, which is also used as residual interaction. Of course, the choice of inter-action B1 as particle-hole residual interaction may be disputable. However, Brink and Boeker already observed that in the SU_3 scheme this interaction gives an excitation energy of 27.7 MeV for the dipole state $(J\pi = 1^-)$ in ^{16}O. The result for the $^{16}O(\gamma, n)$ cross-section is shown in Fig. 10. As expected the position of the dipole state is in rather good agreement with the experi-mental value (24 MeV). But the order of magnitude of the cross-section is much too large, as it is in the calculations using phenomenological Saxon-Woods potentials [44, 47, 48].

6.   CONCLUSION

It is certainly significant that the Hartree-Fock field appears to give a reasonable first-order description of single-particle properties obtained from a wide range of experiments, such as electron scattering, low-energy neutron scattering, p-2p reactions, transfer reactions, etc. All our results have been obtained with a local, density-independent interaction which has been fitted to give some properties of nuclear matter and ^4He. Contrary to other calculations [1, 4, 7; 11], no attempt has been made to relate the parameters of this effective interaction to two-body data. It is, however clear, that the results of Hartree-Fock calculations will not be understood completely before this relation itself is not completely understood.

The author wishes to acknowledge the fruitful collaboration of M. Veneroni in all phases of this work. The study of electron scattering from Hartree-Fock densities has been made in collaboration with Dr. J.B. Bellicard, and the calculation of the $^{16}O(\gamma, n)$ cross-section in collaboration with Dr. J. Raynal.

REFERENCES

[1] KERMAN, A.K., SVENNE, J.P., VILLARS, F.M.H., Phys.Rev. 147 (1966) 710;
DAVIES, K.T.R., KRIEGER, S.J., BARANGER, M., Nucl.Phys. 84 (1966) 545.

[2] See, for instance, the review article by RIPKA, G., in Advances in Nuclear Physics, 1 (BARANGER, VOGT, Eds) Plenum Press (1968), where further references can be found.

[3] LEMMER, R.H., VENERONI, M., Phys.Rev. 170 (1968) 883.

[4] BRUECKNER, K.A., LOCKETT, A.M., ROTENBERG, M., Phys.Rev. 121 (1961) 255.

[5] KÖHLER, H.S., Phys.Rev. 138 (1965) 831.

[6] VAUTHERIN, D., VENERONI, M., Phys.Lett. 25B (1967) 175.

[7] MASTERSON, K.S., LOCKETT, A.M., Phys.Rev. 129 (1963) 776.

[8] VAUTHERIN, D., VENERONI, M., Phys.Lett. 29B (1969) 203.

[9] BOUTEN, M., these Proceedings.

[10] BARANGER, M., Phys.Rev. 120 (1960) 957.

[11] TARBUTTON, R.M., DAVIES, K.T.R., Nucl.Phys. A120 (1968) 1.

[12] TALMI, I., Phys.Rev. 89 (1953) 1065.

[13] HOPE, J., LONGDON, L.W., Phys.Rev. 102 (1956) 1124.

[14] BRUECKNER, K.A., GAMMEL, J.L., WEITZNER, H., Phys.Rev. 110 (1958) 431.

[15] HARTREE, D.R., The Calculation of Atomic Structures, John Wiley (1957).

[16] BARTELS, E.C., KERMAN, A.K., MacKELLAR, A., M.I.T. CTP 49 (June, 1968).

[17] PEREY, F.G., in Direct Interactions and Nuclear Reaction Mechanism, (CLEMENTEL, E., VILLI, C. Eds) Gordon and Breach (1958) 125-137.

[18] GOURSAT, E., Cours d'Analyse mathématique Gauthier-Villars (1942) 476.

[19] NUMEROV, B., Publications de l'Observatoire Central Astrophysique Russe 2 (1933) 188.

[20] BHADURI, R.K., THOMUSIAK, E.L., Nucl.Phys. 88 (1966) 353.

[21] TABAKIN, F., Anns Physics, 30 (1964) 51.

[22] NESTOR, C.W., DAVIES, K.T.R., KRIEGER, S.J., BARANGER, M., Nucl.Phys. A113 (1968) 14.

[23] See, for instance, the review article by DAY, B.D., Rev. Mod.Phys. 39 (1967) 719.

[24] WONG, C.W., Nucl.Phys. 91 (1967) 399.

[25] BETHE, H.A., in Nuclear Structure (Proc.Int.Conf.Gatlinburg, 1965) Academic Press (1966);
BETHE, H.A., Phys.Rev. 167 (1968) 879.

[26] SKYRME, T.H.R., Nucl.Phys. 9 (1959) 615.

[27] VOLKOV, A.B., Nucl.Phys. 74 (1965) 33.

[28] BRINK, D.M., BOEKER, E., Nucl.Phys. A91 (1967) 1.

[29] MYERS, W.D., SWIATECKI, J., Nucl.Phys. 81 (1966) 1;
GREEN, A.E.S., Rev. Mod.Phys. 30 (1958) 569.

[30] BLIN-STOYLE, R.J., Phil.Mag. 46 (1955) 973.

[31] LAW, J.B., SPRUNG, D.W.L., Dubna (1968), Dubna publication D-3898, 162.

[32] See, for instance, PRESTON, M.A., Physics of the Nucleus, Addison-Wesley (1962) 107.

[33] WONG, C.W., Nucl.Phys. A108 (1968) 481.

[34] ELTON, L.R.B., Phys.Lett. 26 (1968) 689.

[35] BELLICARD, J.B., BONNIN, P., FROSH, R.F., HOFSTADER, R., MacCARTHY, J.S., UHRHANE, F.J., YEARIAN, M.R., CLARK, B.C., HERMAN, R., RAVENHALL, D.G., Phys.Rev. Lett. 19 (1967) 527.

[36] DAVIES, K.T.R., BARANGER M., TARBUTTON, R.M., KUO, T.T.S., Phys.Rev. 177 (1969) 1519.

[37] BREDIN, D.J., HANSEN, O., LENZ, G., TEMMER, G.M., Phys.Lett. 21 (1966) 677.

[38] GREENLESS, G.W., PYLE, G.J., TANG, Y.C., Phys.Rev.Lett. 17 (1966) 33.

[39] NOLEN, J.A., Jr., SCHIFFER, J.P., WILLIAMS, N., Phys.Lett. 27 (1968) 1.

[40] NOLEN, J.A., Jr., private communication. We are grateful to Dr. Nolen for communicating this result before publication.

[41] KERMAN, A.K., SVENNE, J.P., VILLARS, F.M.H., Ref.[1];
SVENNE, J.P., private communication, and LANDE, A., SVENNE, J.P., (to be published).

[42] VAUTHERIN, D., VENERONI, M., Phys.Lett. 26B (1968) 552.

[43] PEREY, F.G., BUCK, B., Nucl.Phys. 32 (1962) 353.

[44] MELKANOFF, M.A., RAYNAL, J., SAWADA, T., Nucl.Phys. 101 (1967) 369.

[45] LISTER, D., SAYRES, A., Phys.Rev. 143 (1966) 745.
JOHNSON, C.H., FOWLER, J.L., Phys.Rev. 162 (1967) 890.

[46] REBER, J.D., BRANDENBERGER, J.D., Phys.Rev. 163 (1967) 1077.

[47] BUCK, B., HILL, A.D., Nucl.Phys. A95 (1967) 271.

[48] MARANGONI, M., SARIUS, A.M., Phys.Lett. 24B (1967) 218.

HIGH-ENERGY SCATTERING
OF COMPOSITE HADRONS

W. CZYŻ
Institute of Nuclear Physics,
Cracow, Poland

Abstract

HIGH-ENERGY SCATTERING OF COMPOSITE HADRONS.
1. High-energy potential scattering; 2. High-energy, small-angle nuclear scattering; 3. Extension of the model of high-energy scattering.

INTRODUCTION

There is a considerable amount of experimental data available on high-energy elastic scattering of a variety of strongly interacting particles from different targets, and in the next few years one may expect considerably more data to come. A representative selection of more recent experimental data which was subject to an analysis of the type discussed in this paper is given in Refs [1-11]. This collection of data has recently been interpreted theoretically from unified point of view first in the cases of nuclear scattering [12-26, 30] and then extended to the scattering of "more elementary" hadrons (e.g. proton-proton, pion-proton etc. [27, 28, 29].

To introduce the subject in a reasonably systematic way we are going to present the material in three chapters starting with the high-energy potential scattering − the best established aspect of the problem. Then we shall go over to the high-energy nuclear scattering phenomena and discuss the extrapolation of the potential-scattering results to this case. The last chapter will mention some further (very speculative) extrapolation of the model of high-energy nuclear scattering to very high-energy hadron-hadron scattering (e.g. proton-proton scattering).

1. HIGH-ENERGY POTENTIAL SCATTERING

At the beginning we shall follow rather closely an article by Schiff [31], which we recommend as a very nice introduction into the theory of high-energy potential scattering.

First, let us notice that the first-Born-approximation scattering amplitude ($\vec{k}_0, \vec{k}_f$ are the initial and final momenta and $V(\vec{r})$ is the potential)

$$F_{B.A.}(\vec{k}_f, \vec{k}_0) = - \frac{m}{2\pi\hbar^2} \int d^3\vec{r}\, e^{i\vec{q}\cdot\vec{r}}\, V(\vec{r}) \tag{1}$$

is not a useful approximation in the case of scattering of strongly interacting particles. This is so for the following reason. The condition for the Born approximation to be valid is

$$\frac{1}{\hbar v} \left| \int_{-\infty}^{z} dz'\, V(x, y, z') \right| \ll 1 \tag{2}$$

throughout the scattering region. This condition is virtually never satisfied for hadronic interactions. Equation (2) can always be satisfied if $v \to \infty$, which is possible in a non-relativistic approach, in our case, however, $v \to c$ (velocity of light).

We have, therefore, to go beyond the lowest-order approximation. Let us follow the discussion of Ref. [31] and write down the scattering amplitude as an infinite Born series:

$$F(\vec{k}_f \vec{k}_0) = -\frac{1}{4\pi} \sum_{n=1}^{\infty} \int d^3 r_1 \ldots d^3 r_n \, e^{-i\vec{k}_f \cdot \vec{r}_n} \, U(\vec{r}_n) G(\vec{r}_n - \vec{r}_{n-1}) U(\vec{r}_{n-1})$$

$$\times \, G(\vec{r}_{n-1} - \vec{r}_{n-2}) U(\vec{r}_{n-2}) \ldots U(\vec{r}_2) G(\vec{r}_2 - \vec{r}_1) U(\vec{r}_1) e^{i\vec{k}_0 \cdot \vec{r}_1} \tag{3}$$

where $U(\vec{r}) = (2m/\hbar^2) V(\vec{r})$ and $G(\vec{r}) = -(1/4\pi r) \exp(ikr)$ is the Green function of the operator $(\nabla^2 + k^2)$:

$$(\nabla^2 + k^2) G(\vec{r}) = -\delta^{(3)}(\vec{r}) \tag{4}$$

where $k = |\vec{k}_f| = |\vec{k}_0|$. Equation (3) can be represented graphically as a sum of all possible paths which the incident particle can perform inside the region of space where $V(\vec{r}) \neq 0$ (see Fig. 1). (For a classical exposition of the path technique see Ref. [32]). If we assume that $U(\vec{r})$ varies slowly over distances k^{-1} we can show that two classes of graphs give leading contributions to the scattering amplitude (3) (in the limit $k \to \infty$). These are the graphs shown in Fig. 2.

To show this, let us observe that the function $\exp[i(k\rho - \vec{k} \cdot \vec{\rho})]$ oscillates rapidly as $\vec{\rho}$ deviates from the direction of $\vec{k}$. The consequence of this oscillating character is that

$$\int d^3 \rho \, g(\vec{\rho}) \frac{1}{\rho} \exp[i(k\rho - \vec{k} \cdot \vec{\rho})] = \frac{2\pi i}{k} \int_0^{\infty} d\rho \, g(\hat{k}\rho) + O(k^{-2}) \tag{5}$$

The leading contribution to the integral is due to the neighbour-hood of the direction of $\vec{k}$-vector (from the angular region $1 - \cos\theta \lesssim (k\rho)^{-1}$ or $\theta \lesssim (k\rho)^{-\frac{1}{2}}$), provided $g(\vec{\rho})$ varies slowly over distances k^{-1}. We shall understand by the "stationary-phase region" the region of space from which comes the leading contribution to the integral.

One can easily introduce such exponentials into our integral expression for amplitude (3). We can use the identity

$$-\vec{k}_f \cdot \vec{r}_n + \vec{k}_0 \cdot \vec{r}_1 = -\vec{k}_f \cdot \vec{\rho}_{n-1} - \vec{k}_f \cdot \vec{\rho}_{n-2} - \cdots - \vec{k}_f \cdot \vec{\rho}_m$$

$$+ \vec{q} \cdot \vec{r}_m \tag{6}$$

$$- \vec{k}_0 \cdot \vec{\rho}_{m-1} - \cdots - \vec{k}_0 \cdot \vec{\rho}_2 - \vec{k}_0 \cdot \vec{\rho}_1$$

FIG.1.   Graph of the 7th-order scattering.

(a)   (b)
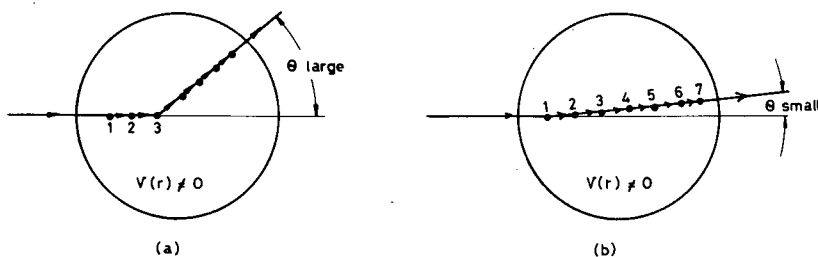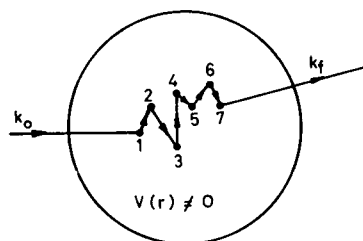
FIG.2.   a) 7th-order graph dominating large-angle scattering;
         b) 7th-order graph dominating small-angle scattering.

where

$$\vec{\rho}_1 = \vec{r}_2 - \vec{r}_1, \quad \vec{\rho}_2 = \vec{r}_3 - \vec{r}_2, \quad \cdots \quad \vec{\rho}_{n-1} = \vec{r}_n - \vec{r}_{n-1} \tag{7}$$

and $\vec{q} = \vec{k}_0 - \vec{k}_f$;   m can be any of the integers $1, 2 \ldots n$.   We can go over from the variables $r_1, r_2, \ldots r_n$ to $\vec{\rho}_1, \vec{\rho}_2, \ldots \vec{\rho}_{n-1}, \vec{r}_m$ (the Jacobian is unity) and obtain

$$\int d^3 r_1 \, d^3 r_2 \ldots d^3 r_n \, e^{-i\vec{k}_f \cdot \vec{r}_n} \, U(\vec{r}_n) G(\vec{r}_n - \vec{r}_{n-1}) \ldots U(\vec{r}_2) G(\vec{r}_2 - \vec{r}_1) U(\vec{r}_1) e^{i\vec{k}_0 \cdot \vec{r}_1}$$

$$= \left(\frac{-1}{4\pi}\right)^{n-1} \int \frac{d^3\rho_1}{\rho_1} \ldots \frac{d^3\rho_{n-1}}{\rho_{n-1}} d^3 r_m \, e^{i\vec{q} \cdot \vec{r}_m} U(\vec{\rho}_{n-1} + \vec{\rho}_{n-2} + \ldots + \vec{r}_m) \, e^{i(k_f\rho_{n-1} - \vec{k}_f \cdot \vec{\rho}_{n-1})}$$

$$\times \, U(\vec{\rho}_{n-2} + \vec{\rho}_{n-3} + \ldots + \vec{r}_m) \ldots e^{i(k_0 \rho_2 - \vec{k}_0 \cdot \vec{\rho}_2)} U(-\vec{\rho}_2 - \vec{\rho}_3 - \ldots - \vec{\rho}_{m-1} + \vec{r}_m)$$

$$\tag{8}$$

$$\times \, e^{i(k_0 \rho_1 - \vec{k}_0 \cdot \vec{\rho}_1)} U(-\vec{\rho}_1 - \vec{\rho}_2 - \ldots - \vec{\rho}_{m-1} + \vec{r}_m)$$

$$\underset{k \to \infty}{=} \left(\frac{-1}{4\pi}\right)^{n-1} \left(\frac{2\pi i}{k}\right)^{n-1} \int d^3 r_m \int_0^\infty d\rho_1 \ldots \int_0^\infty d\rho_{n-1} \, e^{i\vec{q} \cdot \vec{r}_m} U\left(\vec{r}_m + \hat{k}_f(\rho_{n-1} + \ldots + \rho_m)\right)$$

$$\ldots \, U(\vec{r}_m + \hat{k}_f \rho_m) \, U(\vec{r}_m) U(\vec{r}_m - \hat{k}_0 \, \rho_{m-1}) \ldots U\left(\vec{r}_m - \hat{k}_0(\rho_{m-1} + \ldots + \rho_1)\right)$$

where we employed Eq.(5) in the last step. Notice that, in general, to different $\vec{r}_m^{\,!}$ s correspond different stationary-phase regions in the $\vec{\rho}_1 \ldots \vec{\rho}_{n-1}$ space. There are two special cases of great interest which lead to simple expressions for $F(\vec{k}_f \vec{k}_0)$:

    a) all stationary phase-regions corresponding to different $\vec{r}_m$ s are different, and

    b) all stationary phase regions are identical.

Case a) corresponds to graph a) of Fig.2, case b) to graph b) of Fig.2. One can see this as follows.

    The rapidly oscillating exponentials $\exp[i(k\rho_\ell - \vec{k}\cdot\vec{\rho}_\ell)]$ inside the integral (8) $(\vec{\rho}_\ell = \vec{r}_{\ell+1} - \vec{r}_\ell)$ define the direction of propagation from the point $\vec{r}_\ell$ to the point $\vec{r}_{\ell+1}$ about which the phase of the exponential is stationary. If we choose a certain point on the graph as $\vec{r}_m$, the propagation up to this point proceeds along the direction $\hat{k}_0$ and from this point onward in the direction $\hat{k}_f$. So, we obtain the graph a) of Fig.2. Notice that in this case the angle θ between $\hat{k}_0$ and $\hat{k}_f$ has to be large.

    The stationary-phase regions in the $3(n-1)$ space of the ρ-variables corresponding to different $\vec{r}_m$ do not overlap if θ is large enough. Hence one must take the sum of all these contributions, and the amplitude takes the form

$$F^{(a)}(\vec{k}_f \vec{k}_0) = -\frac{1}{4\pi} \sum_{n=1}^{\infty} \sum_{m=1}^{\infty} \left(\frac{-i}{2k}\right)^{n-1} \int_0^{\infty} d\rho_1 \ldots d\rho_{n-1} \int d^3 r_m\, e^{i\vec{q}\cdot\vec{r}_m} U\left(\vec{r}_m + \hat{k}_f(\rho_{n-1} + \ldots + \rho_m)\right)$$

$$(9)$$

$$\ldots U(\vec{r}_m + \hat{k}_f \rho_m)\, U(\vec{r}_m)\, U(\vec{r}_m - \hat{k}_0 \rho_{m-1}) \ldots U\left(\vec{r}_m - \hat{k}_0(\rho_{m-1} + \ldots + \rho_1)\right)$$

Whereas in the cases of small scattering angle θ (graph b)) the stationary-phase regions corresponding to different $\vec{r}_m^{\,!}$ s do overlap almost completely, and one should not sum over the index m as in Eq.(9) (the choice of $\vec{r}_m$ must turn out to be irrelevant in this case, and so it does — see below). In this case, the amplitude is

$$F^{(b)}(\vec{k}_f \vec{k}_0) = -\frac{1}{4\pi} \sum_{n=1}^{\infty} \left(\frac{-i}{2k}\right)^{n-1} \int_0^{\infty} d\rho_1 \ldots d\rho_{n-1} \int d^3 r_m\, e^{i\vec{q}\cdot\vec{r}_m}$$

$$(10)$$

$$\times\, U(\vec{r}_m + \hat{k}_f(\rho_{n-1} + \ldots + \rho_m)) \ldots U\left(\vec{r}_m - \hat{k}_0(\rho_{n-1} + \ldots + \rho_1)\right)$$

    The expressions (9) and (10) can be worked out as follows. Let us first consider expression (9). We shall separately treat the first $m-1$ integrations and then the remaining $n-1-m$. We have

$$\int_0^{\infty} d\rho_1 \ldots d\rho_{m-1}\, U(\vec{r}_m - \hat{k}_0 \rho_{m-1}) \ldots U\left(\vec{r}_m - \hat{k}_0(\rho_m + \ldots + \rho_1)\right)$$

$$= \int_0^{\infty} ds_{m-1} \int_{s_{m-1}}^{\infty} ds_{m-2} \ldots \int_{s_2}^{\infty} ds_1\, U(\vec{r}_m - \hat{k}_0 s_{m-1}) \ldots U(\vec{r}_m - \hat{k}_0 s_1) \quad (11)$$

$$= \int_0^{w_0} dw_{m-1} \int_0^{w_{m-1}} dw_{m-2} \ldots \int_0^{w_3} dw_2 \int_0^{w_2} dw_1 = \frac{1}{(m-1)!} \left[\int_0^{\infty} ds\, U(\vec{r}_m - \hat{k}_0 s)\right]^{m-1}$$

where

$$
w_0 = \int_0^\infty ds\, U(\vec{r}_m - \hat{k}_0 s), \quad w_\ell = \int_{s_\ell}^\infty ds\, U(\vec{r}_m - \hat{k}_0 s), \quad \ell = 1, 2, \ldots m-1
$$

Similarly,

$$
\int_0^\infty d\rho_m \cdots \int_0^\infty d\rho_{n-1}\, U\left(\vec{r}_m + \hat{k}_f(\rho_{n-1}+\ldots+\rho_m)\right) \cdots U(\vec{r}_m + \hat{k}_f \rho_m)
$$

$$
= \int_0^\infty ds_m \int_{s_m}^\infty ds_{m+1} \cdots \int_{s_{n-2}}^\infty ds_{n-1}\, U(\vec{r}_n + \hat{k}_f s_{n-1}) \cdots U(\vec{r}_m + \hat{k}_f s_m) \qquad (12)
$$

$$
= \frac{1}{(n-m)!} \left[\int_0^\infty ds\, U(\vec{r}_m + \hat{k}_f s) \right]^{n-m}
$$

Hence

$$
F^{(a)}(\vec{k}_f \vec{k}_0) = -\frac{1}{4\pi} \sum_{n=1}^\infty \sum_{m=1}^n \int d^3 r_m\, e^{i\vec{q}\cdot\vec{r}_m} U(\vec{r}_m) \left(\frac{-i}{2k}\right)^{n-1} \frac{1}{(m-1)!} \frac{1}{(n-m)!}
$$

$$
\times \left[\int_0^\infty ds\, U(\vec{r}_m - \hat{k}_0 s) \right]^{m-1} \left[\int_0^\infty ds\, U(\vec{r}_m + \hat{k}_f s) \right]^{n-m} \qquad (13)
$$

$$
= -\frac{1}{4\pi} \int d^3 r\, e^{i\vec{q}\cdot\vec{r}} U(\vec{r}) \exp\left\{-\frac{i}{2k}\left[\int_0^\infty ds\, U(\vec{r}-\hat{k}_0 s) + \int_0^\infty ds\, U(\vec{r}+\hat{k}_f s) \right]\right\}
$$

because

$$
\sum_{n=1}^\infty \sum_{m=1}^n X^{n-1} \frac{a^{m-1}}{(m-1)!} \frac{b^{n-m}}{(n-m)!} \equiv \sum_{\ell_1=0}^\infty \frac{1}{(\ell_1)!} a^{\ell_1} \sum_{\ell_2=0}^\infty \frac{1}{(\ell_2)!} b^{\ell_2} (X)^{\ell_1+\ell_2}
$$

Equation 13 is the final expression for the scattering amplitude at large scattering angles (represented by graph a) of Fig. 2).

Let us now consider the graph b) of Fig. 2. In this, case all the different stationary-phase regions overlap. Let us choose the z-axis along the vector $\vec{k}_0$. As, to a very good approximation

$$
\int_0^\infty ds\, U(\vec{r}_m - \hat{k}_0 s) = \int_{-\infty}^{z_m} dz\, U(x_m, y_m, z)
$$

$$
\int_0^\infty ds\, U(\vec{r}_m + \hat{k}_f s) = \int_{z_m}^\infty dz\, U(x_m, y_m, z)
$$

we obtain

$$(e^{i q_z z_m} \approx 1 \text{ here}):$$

$$\dot{F}^{(b)}(\vec{k}_f, \vec{k}_0) = -\frac{1}{4\pi} \sum_{n=1}^{\infty} \left(\frac{-i}{2k}\right)^{n-1} \int_{-\infty}^{+\infty} dx_m \, dy_m \, dz_m \, e^{i(q_x x_m + q_y y_m)}$$

$$\times U(x_m, y_m, z_m) \frac{1}{(n-1)! \, (n-m)!} \left[\int_{-\infty}^{z_m} dz \, U(x_m, y_m, z)\right]^{m-1} \left[\int_{z_m}^{\infty} dz \, U(x_m, y_m, z)\right]^{n-m} \tag{14}$$

(Notice that one cannot perform the exponentiation similarly as before because of the lack of summation over index m). We can perform the summation as follows (b is the impact parameter):

$$\int_{-\infty}^{+\infty} dz_m \, U(b, z_m) \frac{1}{(m-1)! \, (n-m)!} \left[\int_{-\infty}^{z_m} dz \, U(b, z)\right]^{m-1} \left[\int_{z_m}^{\infty} dz \, U(b, z)\right]^{n-m}$$

$$= \frac{\chi^n}{n!} \text{ (it does } \underline{\text{not}} \text{ depend on the index m!).}$$

where we introduced a new variable $\chi(b) = \int_{-\infty}^{+\infty} dz \, U(b, z)$.

So, finally

$$F^{(b)}(\vec{k}_f, \vec{k}_0) = -\frac{1}{4\pi} \frac{2k}{-i} \sum_{n=1}^{\infty} \left(\frac{-i}{2k}\right) \int d^2 b \, e^{i\vec{q}\cdot\vec{b}} \frac{\left[\int_{-\infty}^{+\infty} dz \, U(b, z)\right]^n}{n!}$$

$$= \frac{ik}{2\pi} \int d^2 b \, e^{i\vec{q}\cdot\vec{b}} \left(1 - \exp\left(-\frac{i}{2k} \int_{-\infty}^{+\infty} dz \, U(b, z)\right)\right) \tag{15}$$

From the above considerations we can see that the cases a) and b) follow naturally from the general formula (3) as the two limiting ($k \to \infty$) cases for large-angle a) and small-angle b) scattering. One should remember that the scattering angle must be large (substantially larger than $(kR)^{-\frac{1}{2}}$ where R is the range of the potential) in the case a). Otherwise one cannot introduce the summation over index m in Eq.(9). On the other hand, in case b) the angle θ must be substantially smaller than $(kR)^{-\frac{1}{2}}$ in order to secure large overlapping of all the stationary-phase regions.

Formulas (13) and (15) for large- and small-angle potential scattering were obtained a long time ago [31] and after that, many further developments in the theory of high-energy potential scattering took place [33-37]. We shall not, however, go into these problems further. For our purpose of constructing a crude but realistic model for high-energy collisions of composite strongly interacting particles formulas (13) and (15) (especially

the second one) will be adequate. This is so, because we do not really know
to what extent we can apply the potential-scattering description to such
collisions, hence there is no basis for using some more sophisticated
versions of potential scattering and believe in higher reliability of such
results. The other reason is their simplicity. Any more sophisticated
starting-point formulas are usually impossible to handle in practical cases
of multiple scattering. We shall come back to these problems in the next
chapter.

Let us come back to relations (15) and (13) and define the following
phase shift

$$\chi(b) = -\frac{1}{2k} \int_{-\infty}^{+\infty} dz \; U(b, z) \tag{16}$$

(Notice that $\chi(b)$ does not go to zero as $k \to \infty$ as Eq.(16) might suggest.
U grows linearly with k because it contains the relativistic mass as a
factor, compare Eq.(3)). Then Eq.(15) takes the form

$$F^{(b)}(\vec{k}_f \vec{k}_0) = \frac{ik}{2\pi} \int d^2 b \; e^{i\vec{q}\cdot\vec{b}} \; (1 - \exp[i\chi(b)]) \tag{17}$$

$$= ik \int_0^\infty db \, b \, J_0(qb)(1 - \exp[i\chi(b)] \tag{17'}$$

In Eq.(17') we assume that $\chi(b)$ depends only on the absolute value of $\vec{b}$.
Equations (17) and (17') are a very convenient form of the impact-parameter
representation, where $\vec{b}$ is the so-called impact parameter, which is related
to the angular-momentum quantum number by the following relation (exact
in the limit $k \to \infty$):

$$b \cong \frac{(2\ell + 1)}{2k} \tag{18}$$

As, for $\ell \gg 1$ and $\theta \ll 1$,

$$P_\ell(\cos\theta) \approx J_0\left[\left(\ell + \frac{1}{2}\right)\theta\right] \tag{19}$$

one can see that, in the limit $k \to \infty$, we get Eq.(17) or Eq.(17')) from the
standard partial-wave expansion of the amplitude

$$F(\vec{k}_f \vec{k}_0) = \frac{i}{2k} \sum_{\ell=0}^{\infty} (2\ell + 1)(1 - \exp[i\chi_\ell]) P_\ell(\cos\theta) \tag{20}$$

and Eqs (18) and (19). For more details about the exact relationship
between the impact-parameter (or Fourier-Bessel) representation and
partial-wave expansion see Refs [38, 39].

The amplitude of the large-angle scattering given by Eq.(13) cannot be expressed in terms of $\chi(b)$. It was, however, suggested recently [26] that if we apply Eq.(13) to some intermediate angles we might be able again to use only $\chi(b)$ given by definition (16). We shall not go into the arguments given in Ref. [26] and merely quote the result which says that for

$$\frac{1}{\sqrt{kR}} \ll \theta \ll \frac{1}{R(k-\kappa)} \tag{21}$$

where κ is the momentum of the scattered particle within the range of the potential (hence $\hbar^2 c^2 \kappa^2 + m^2 c^4 = (E-V)^2$),

$$F^{(a)}(\vec{k}_f \vec{k}_0) = -\frac{1}{4\pi} \int d^2 b \int_{-\infty}^{+\infty} dz \, e^{i\vec{q}\cdot\vec{b}} \, U(\vec{b},z) \exp\left(-\frac{i}{2k}\left[\int_{-\infty}^{z} dz' \, U(b,z') + \int_{z}^{+\infty} dz' \, U(b,z')\right]\right)$$

$$\tag{22}$$

$$= \frac{k}{2\pi} \int d^2 b \, e^{i\vec{q}\cdot\vec{b}} \, \chi(b) \, e^{i\chi(b)}$$

If the angular region defined by the inequality (21) does exist one may try to fit small-angle and large-angle scattering by using relations (17) and (22) and assuming that the relations between the small- and large-angle scattering given (through $\chi(b)$) by these two formulas are quite general and can be applied even if there are no potentials involved in the interactions between hadrons.

Unfortunately, we do not yet know how useful formula (22) will turn out to be. We do not know whether, in the region of its applicability, it will be as accurate as formula (17) in the forward direction. However, because of its simplicity, it deserves more thorough investigation.

2.   HIGH-ENERGY, SMALL-ANGLE NUCLEAR SCATTERING

2.1.   Formulation of the model

We are now going to discuss the small-angle, high-energy nuclear scattering, that is to say, scattering of nucleons or anti-nucleons or mesons of any kind from nuclei and we shall also talk about scattering of nuclei from
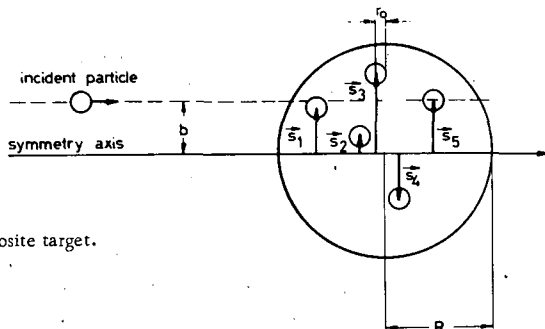
FIG.3.   Geometry of collision with composite target.

nuclei. Hence we shall try to describe, from a unified point of view, high-energy scattering of composite, strongly interacting particles. Since our aim is so general, it is not surprising that our model of high-energy colli-sions will be very crude. Among many other approximations we shall neglect, right from the beginning, the spins of colliding particles. We shall, however, point out some important spin effects without going deeper into these problems.

Let us first deal with small-angle nucleon (meson) scattering from a nucleus. We can picture ourselves such a collision as is shown in Fig. 3.

If we assume that the total interaction between the incident particle (let us call it nucleon) and the nucleus is a sum of individual interactions, we obtain from expression (16)

$$\chi(b) = \sum_{j=1}^{A} \chi_j(\vec{b} - \vec{s}_j) \tag{23}$$

where

$$\chi_j(\vec{b} - \vec{s}_j) = -\frac{1}{2k} \int_{-\infty}^{+\infty} dz \, U_j(\vec{b} - \vec{s}_j, z) \tag{24}$$

One can, therefore, entirely eliminate the potentials since the relation between the j-th phase shift and the j-th amplitude is

$$f_j(\delta) = \frac{ik}{2\pi} \int d^2 b \, e^{i\vec{\delta}\cdot\vec{b}} (1 - e^{i\chi_j(b)}) \tag{25}$$

$$\exp[i\chi_j(\vec{b} - \vec{s}_j)] = 1 - \frac{1}{2\pi ki} \int d^2\delta \, e^{-i\vec{\delta}\cdot(\vec{b}-\vec{s}_j)} f_j(\delta) \tag{25'}$$

and express the total amplitude $F^{(b)}$ of Eq.(17) in terms of the individual amplitudes f_j by employing relations (23) and (25') in Eq.(17). In doing so, we keep the target nucleons in the space positions given by the vectors $\vec{s}_j$. Hence we treat the nucleus as if it were frozen in a certain geometrical configuration. Obviously, if we want to apply this approach to some realistic cases, we should average out the positions of the target nucleons. We shall discuss this problem in more detail later. By expanding

$$\exp\left[i\sum_j \chi_j(\vec{b} - \vec{s}_j)\right]$$

in Eq.(17) we can represent the amplitude as a series of the terms usually called single- double-, triple-, etc. scattering contributions:

$$F^{(b)} = F_1^{(b)} + F_2^{(b)} + \ldots + F_A^{(b)} \tag{26}$$

where A is the number of nucleons in the target and

$$F_1^{(b)}(q) = \sum_j^A f_j(q) \, e^{i\vec{q}\cdot\vec{s}_j}$$

$$F_2^{(b)}(q) = -\frac{1}{2\pi k i} \sum_{j>\ell}^A \int d^2\delta_j \, d^2\delta_\ell \, f_j(\delta_j) f_\ell(\delta_\ell) \, e^{i\vec{\delta}_j\cdot\vec{s}_j + i\vec{\delta}_\ell\cdot\vec{s}_\ell} \, \delta^{(2)}(\vec{q} - \vec{\delta}_j - \vec{\delta}_\ell)$$

$$F_3^{(b)}(q) = \left(\frac{1}{2\pi k i}\right)^2 \sum_{j>\ell>k}^A \int d^2\delta_j \, d^2\delta_\ell \, d^2\delta_k \, f_j(\delta_j) f_\ell(\delta_\ell) f_k(\delta_k)$$

$$\times \, e^{i\vec{\delta}_j\cdot\vec{s}_j + i\vec{\delta}_\ell\cdot\vec{s}_\ell + i\vec{\delta}_k\cdot\vec{s}_k} \, \delta^{(3)}(\vec{q} - \vec{\delta}_j - \vec{\delta}_\ell - \vec{\delta}_k)$$

(27)

- -

$$F_n^{(b)}(q) = \left(\frac{-1}{2\pi k i}\right)^{n-1} \sum_{j_1>j_2>\ldots>j_n} \int d^2\delta_{j_1} \ldots d^2\delta_{j_n} \, f_{j_1}(\delta_{j_1})\ldots f_{j_n}(\delta_{j_n})$$

$$\times \, e^{i\sum_k^n \vec{\delta}_{j_k}\cdot\vec{s}_{j_k}} \, \delta^{(2)}\left(\vec{q} - \sum_k^n \vec{\delta}_{j_k}\right)$$

Let us note the interesting fact that the result (27) can also be obtained without having recourse to any potential-scattering theory, but by assuming (which is a very sound assumption) that the nucleon-nucleon amplitude is almost purely imaginary which means that the elastic scattering is almost purely a shadow of production processes. If we write the nucleon-nucleon amplitude in the Fourier-Bessel representation

$$f(\delta) = \frac{ik}{2\pi} \int d^2 b \, e^{i\vec{\delta}\cdot\vec{b}} \gamma(b) \tag{28}$$

and use the optical theorem

$$\text{Im} \, f(0) = \frac{k\sigma}{4\pi} \tag{29}$$

where σ is the total cross-section, we obtain the relation

$$\sigma = 2 \int d^2 b \, \text{Re} \, \gamma(b) \tag{30}$$

But if the amplitude is purely imaginary we obtain from relation (30)

$$\sigma = 2 \int d^2b \ \gamma(b) \tag{31}$$

From relation (31) it follows that, within such an approximation, one can interpret $\gamma(b)$ as a <u>probability density</u> (we shall call it "profile", hence-forth): $\gamma(b) \, db$ is the probability that something happens to the particle if the collision occurs between b and b+db. If we want to calculate the total profile $\Gamma(b)$ of the target, it is enough to observe that the probability that something happens to the incident particle, and the probability that nothing happens add up to unity:

$$\Gamma(b) + \prod_{j=1}^{A} \left[1 - \gamma_j(\vec{b} - \vec{s}_j) \right] = 1 \tag{32}$$

hence

$$\Gamma(b) = 1 - \prod_{j=1}^{A} \left[1 - \gamma_j(\vec{b} - \vec{s}_j) \right] \tag{33}$$

One can immediately generalize this expression to the case of collisions of two complex nuclei and obtains the following expression for the total profile

$$\Gamma(b) = 1 - \prod_{j=1}^{A} \prod_{k=1}^{B} \left[1 - \gamma_{jk}(\vec{b} - \vec{s}_j^A + \vec{s}_k^B) \right] \tag{34}$$

where A and B are the numbers of nucleons in the colliding nuclei, and the indices j and k run from 1 to A and from 1 to B, respectively.

By expanding expression (33) in powers of γ and employing formula (28) we again obtain series (27). Notice, however, that in such an approach the multiplicity of collisions is not given by the number of γ's involved. For instance, physically, the single-collision contributions are the probabilities that <u>one</u> nucleon is hit but not the remaining A-1 nucleons; hence it is given by the terms of the following type

$$\gamma_1(1 - \gamma_2)(1 - \gamma_3) \dots (1 - \gamma_A) \tag{35}$$

which contains all powers of γ. This is just a problem of interpretation of various terms and does not introduce anything new into the technique of calculating amplitudes.

In the spirit of Ref.[12], to obtain the transition amplitude we first take the two-dimensional Fourier transform of $\Gamma(b)$ and then take its matrix element between the initial and final states[1]:

$$\langle n|F|0 \rangle = \langle n| \frac{ik}{2\pi} \int d^2b \ e^{i\vec{q} \cdot \vec{b}} \ \Gamma(b)|0 \rangle \tag{36}$$

---

[1] That expression (36) — in the case of inelastic scattering — is an expression consistent with the <u>elastic</u>-scattering amplitude follows also from the analysis of the unitarity of our model (compare with Ref.[50]) which shows that one of the most important contributions to the <u>elastic</u> amplitude comes from the <u>inelastic</u> processes represented by expression (36) where n designates an excited state.

We shall work out the matrix element (36) in the general case of nucleus-nucleus scattering (Γ(b) given by expression (34), which can easily be reduced to the nucleon-nucleus case. In all formulas we shall assume that the z-integration — along the direction of the incident-particle momentum — has been performed, and only the "transverse" degrees of freedom are left.

Let us now discuss in greater detail the elastic scattering process. In this case, the initial and the final states are, respectively

$$| 0\rangle = |\ \exp{(i\vec{P}_i^A \cdot \vec{r}_A)}\ \Phi_A(s^{A'})\ e^{i\vec{P}_i^B \cdot \vec{r}_B}\ \Phi_B(s^{B'})\rangle$$

$$\tag{37}$$

$$| n\rangle = |\ \exp{(i\vec{P}_f^A \cdot \vec{r}_A)}\ \Phi_A(s^{A'})\ e^{i\vec{P}_f^B \cdot \vec{r}_B}\ \Phi_B(s^{B'})\rangle$$

Here we have introduced the centre-of-mass vectors of the nuclei A and B,

$$\vec{r}_A = \frac{1}{A} \sum_j \vec{s}_j^A, \quad \vec{r}_B = \frac{1}{B} \sum_k \vec{s}_k^B \tag{38}$$

and the relative co-ordinates

$$\vec{s}_j^{A'} = \vec{s}_j^A - \vec{r}_A, \quad \vec{s}_k^{B'} = \vec{s}_k^B - \vec{r}_B \tag{39}$$

Furthermore, $\vec{P}_i^A$, $\vec{P}_i^B$, $\vec{P}_f^A$, $\vec{P}_f^B$ are the initial and final momenta, and $\Phi_A(s^{A'})$ and $\Phi_B(s^{B'})$ are the internal ground-state wave functions of the colliding nuclei. Notice that they depend on A - 1 and B - 1 co-ordinates, respectively. From Eqs. (36) and (37), we see that the matrix element whose absolute square gives the elastic cross-section is

$$M = \langle \Phi_A(s^{A'}) \Phi_B(s^{B'}) | F' | \Phi_A(s^{A'}) \Phi_B(s^{B'}) \rangle \tag{40}$$

where F' is obtained from the transition operator F (see Eq. (36)) by replacing $s_{j,k}$ by $s'_{j,k}$. In practical calculations, however, it is often very convenient to use wave functions which do not have the c.m. co-ordinates separated out, but which depend rather on the A co-ordinates s_j^A and the B co-ordinates s_k^B. This is an especially convenient procedure if one approximates the ground-state wave function by a product of single-particle wave functions. Let us denote by $\Psi_A(s^A)$ and $\Psi_B(s^B)$ the ground-state wave functions, which are thus, explicitly, functions of the A variables s_j^A and the B variables s_k^B, related to the internal ground-state wave functions $\Phi_A(s^{A'})$ and $\Phi_B(s^{B'})$ by

$$\Psi_A(s^A) = \mathscr{R}_A(r_A)\,\Phi_A(s^{A'})$$

$$\tag{41}$$

$$\Psi_B(s^B) = \mathscr{R}_B(r_B)\,\Phi_B(s^{B'})$$

As we shall show below

$$F(q, s^A; s^B) = F'(q; s^{A'}; s^{B'}) \exp(i\vec{q} \cdot \vec{r}_A - i\vec{q} \cdot \vec{r}_B) \tag{42}$$

Then from Eqs (40-42) it follows that one can use the wave functions without the centre-of-mass dependence factored out (which procedure simplifies calculations considerably), provided an extra correction factor θ is introduced as follows

$$M = \langle \Phi_A \Phi_B | F' | \Phi_A \Phi_B \rangle = \theta(q^2) \langle \Psi_A \Psi_B | F | \Psi_A \Psi_B \rangle \tag{43}$$

where

$$\theta(q^2) = \left[\int d^2 r_A | \mathscr{R}_A(r_A)| \ e^{i\vec{q} \cdot \vec{r}_A} \int d^2 r_B | \mathscr{R}_B(r_B)|^2 \ e^{i\vec{q} \cdot \vec{r}_B} \right]^{-1} \tag{44}$$

In the case of nucleon-nucleus collision this correction factor reduces to

$$\theta_A(q^2) = \left[\int d^2 r_A | \mathscr{R}_A(r_A)|^2 \exp(-i\vec{q} \cdot \vec{r}_A) \right]^{-1} \tag{45}$$

In general, a factorization such as that given in expression (48) cannot be obtained exactly. There is, however, the very important case of the harmonic-oscillator well potential [40], for which the completely anti-symmetrized shell-model wave function of any non-spurious state can be written in the form (41) with

$$\mathscr{R}(r) = (A | \pi^3 R^6)^{1/4} \exp(-A r^2 | 2R^2) \tag{46}$$

where R is the parameter in the Gaussian factor $\exp(-r^2/2R^2)$ which appears in the oscillator wave functions. Hence, provided that the ground-state wave functions of the colliding particles can be approximated adequately by the oscillator-potential wave functions, we have

$$\theta_A(q^2) = \left[\int d^2 r_A | \mathscr{R}_A(r)|^2 \exp(-i\vec{q} \cdot \vec{r}_A) \right]^{-1} = \exp(q^2 R_A^2 /4A) \tag{47}$$

$$\theta_B(q^2) = \left[\int d^2 r_B | \mathscr{R}_B(r)|^2 \exp(i\vec{q} \cdot \vec{r}_B) \right]^{-N} = \exp(q^2 R_B^2 /4B)$$

One should perhaps emphasize at this point that any modification of the oscillator-potential wave functions which introduces factors depending on the relative nucleon-nucleon co-ordinates does not change the correction factors (47). Hence the introduction of correlations, e.g. of the Jastrow

type [41, 15], may be made without any modification of our discussion of the centre-of-mass motion corrections, and Eqs (47) are still correct.

To prove Eq.(42) we use the form (27) of the amplitude operator:

$$F_{\cdot}(q; \vec{s}^A, \vec{s}^B) = \frac{ik}{2\pi} \int d^2b \; e^{i\vec{q}\cdot\vec{b}} \left\{ 1 - \prod_j^A \prod_k^B \left[1 - \frac{1}{2\pi ki} \int d^2\delta_{jk} \right. \right.$$

$$\left. \left. \times e^{-i\vec{\delta}_{jk}\cdot(\vec{b}-\vec{s}_j^A+\vec{s}_k^B)} f_{jk}(\delta_{jk}) \right] \right\}$$

$$= \sum_{jk} \int d^2\delta_{jk} \, \delta^{(2)}(\vec{q}-\vec{\delta}_{jk}) \, e^{i\vec{\delta}_{jk}\cdot(\vec{s}_j^A-\vec{s}_k^B)} f_{jk}(\delta_{jk}) - \frac{1}{2\pi ki} \sum_{j_1 k_1 j_2 k_2} \int d^2\delta_{j_1 k_1} d^2\delta_{j_2 k_2}$$

$$\times \delta^{(2)}(\vec{q}-\vec{\delta}_{j_1 k_1}-\vec{\delta}_{j_2 k_2}) \, e^{i\vec{\delta}_{j_1 k_1}\cdot(\vec{s}_{j_1}^A-\vec{s}_{k_1}^B)+i\vec{\delta}_{j_2 k_2}\cdot(\vec{s}_{j_2}^A-\vec{s}_{k_2}^B)} f_{j_1 k_1}(\delta_{j_1 k_1}) f_{j_2 k_2}(\delta_{j_2 k_2})$$

$$\tag{48}$$

$$+ \left(\frac{1}{2\pi ki}\right)^2 \sum_{j_1 k_1 j_2 k_2 j_3 k_3} \int d^2\delta_{j_1 k_1} d^2\delta_{j_2 k_2} d^2\delta_{j_3 k_3} \delta^{(2)}\!\left(\vec{q}-\vec{\delta}_{j_1 k_1}-\vec{\delta}_{j_2 k_2}-\vec{\delta}_{j_3 k_3}\right)$$

$$\times e^{i\vec{\delta}_{j_1 k_1}\cdot(\vec{s}_{j_1}^A-\vec{s}_{k_1}^B)+i\vec{\delta}_{j_2 k_2}\cdot(\vec{s}_{j_2}^A-\vec{s}_{k_2}^B)+i\vec{\delta}_{j_3 k_3}\cdot(\vec{s}_{j_3}^A-\vec{s}_{k_3}^B)}$$

$$\times f_{j_1 k_1}\!\left(\delta_{j_1 k_1}\right) f_{j_2 k_2}\!\left(\delta_{j_2 k_2}\right) f_{j_3 k_3}\!\left(\delta_{j_3 k_3}\right)$$

Introducing now the internal co-ordinates

$$\vec{s}_j^{A'} = \vec{s}_j^A - \vec{r}_A, \quad \vec{s}_k^{B'} = \vec{s}_k^B - \vec{r}_B \tag{49}$$

we see that the centre-of-mass co-ordinates appear in the exponents in Eq.(48) as

$$\vec{r}_A \cdot \left(\vec{\delta}_{j_1 k_1}+\vec{\delta}_{j_2 k_2}+\vec{\delta}_{j_3 k_3}+\ldots\right) \quad \text{and}$$

$$-\vec{r}_B \cdot \left(\vec{\delta}_{j_1 k_1}+\vec{\delta}_{j_2 k_2}+\vec{\delta}_{j_3 k_3}+\ldots\right)$$

In view of the delta functions in Eq.(48), these expressions become, upon integration, $\vec{r}_A \cdot \vec{q}$ and $-\vec{r}_B \cdot \vec{q}$, from which expression (42) follows.

2.2. Applications

Before discussing any specific case in detail, let us briefly review the experimental material available. First, we should realize that if we want to test the model described above we should, in principle, limit ourselves to the very forward scattering cross-sections. Such data are given in the CERN experiment with 19.3 GeV incident protons [9]. Unfortunately, the energy resolution of this experiment is rather poor (50 MeV in both the incident and outgoing beams) and the measured scattering cross-sections contain a lot of contributions from excitations of nuclear states, and although the same transition-amplitude operators as defined above can be used, one should rather calculate the sum rules than the purely elastic-scattering cross-sections [15, 16, 22]. The Brookhaven experiment [1] satisfies the demands for good energy resolution (the energy resolution is ~ 3 MeV), the angles, however, are not very small. If we calculate the angle $\theta_c \simeq (kR)^{-\frac{1}{2}}$ (which, in the potential scattering, determines the angles where the eikonal approximation is valid: $\theta \ll \theta_c$) taking for R the rms radii of ^{4}He, ^{12}C, ^{16}O nuclei used as targets in Ref. [1] at the incident laboratory momentum $k_{LAB} = 1.7$ GeV/c, we get the numbers shown in Table I.

One should keep in mind, however, that if we introduce into formula (15) the nucleon-nucleus interaction in the form of a sum of nucleon-nucleon interactions

$$U(\vec{b}, z) = \sum_{j=1}^{A} v_j(\vec{b} - \vec{s}_j, z)$$

which results in Eq. (23), the relevant radius determining the stationary-phase regions in formula (3) is the <u>nucleon</u> radius r_0, <u>not</u> the nuclear radius (hence our considerations from chapter 1 are valid under the assumption that the nucleon-nucleon potential does not change appreciably over distances k^{-1}). It would, therefore, seem more appropriate to consider the region of validity of Eq. (15) in nucleon-nucleus collision to be $\theta_c' \approx (kr_0)^{-\frac{1}{2}}$ (given also in Table I) rather than calculated from radii of the target nuclei. To support this point of view let us consider possible limitations imposed on scattering angles by the method of calculating absorption probabilities (Eqs (31)-(34)). There the following criterium of validity could be used: as long as the geometry of screening is not changed we can use the model. That means that $\theta \ll \arctan(r_0/R)$, since r_0 is the radius of the nucleon profile and R is of the order of magnitude of an average nucleon-nucleon distance. In the case of ^{4}He target $r_0/R \approx 2/3$, hence the angle is very large. From this point of view it follows that the tighter the nucleus the better should the model work.

All these <u>qualitative</u> arguments strongly suggest that, if the target is composed of well defined subunits, the high-energy scattering model is probably valid at larger angles than is suggested by the standard criterium $\theta \ll \theta_c \approx (kR)^{-\frac{1}{2}}$ where R is the radius of the target with the corresponding numbers shown in Table I.

In any case, whichever point of view is applied, the ^{16}O target seems to be the best possibility of applying the eikonal approximation, and we shall start by discussing this case as a representative one.

TABLE I.   CALCULATION OF θ_c FOR ^{4}He, ^{12}C, ^{16}O USED AS TARGETS

Target	rms radius (from electron scattering)	θ_c (deg)	θ_c corresponding to the nucleon radius $r_0 = 0.8$ fm (deg)	Position of the first minimum on the measured elastic-scattering cross-section (in laboratory system)
^{4}He	1.6 fm	$\sim 15°$	$\sim 22°$	$\sim 16°$
^{12}C	2.29 fm	$\sim 13°$	$\sim 22°$	$\sim 13°$
^{16}O	2.60 fm	$\sim 12°$	$\sim 22°$	$\sim 10°$

To calculate the p - ^{16}O elastic cross-section from

$$\frac{d\sigma_{el}}{d\Omega} = |\langle 0| F |0\rangle|^2$$

and from expressions (36) and (33), we have to specify the nucleon
"profiles" γ_j, and the ground-state wave function of ^{16}O. The profile can
be obtained from the nucleon-nucleon scattering amplitude using the inverse
transformation of transformation (28). For small momentum transfer we can
re-construct the nucleon-nucleon amplitude from the data (assuming no
spin dependence). The amplitude f, and hence the profile γ, can always be
thought of as proportional to the total cross-section σ:

$$f(\delta) = \frac{[i + \alpha(\delta)]\, k\sigma}{4\pi}\, e(\delta)$$

where $\alpha(\delta)$ is the ratio of the real to the imaginary part of the amplitude
and may depend on the momentum transfer δ, and $e(\delta)$ is a function of the
momentum transfer which, for $\delta = 0$, becomes unity (to satisfy the optical
theorem). In the case of nucleon-nucleon scattering one can, for small
momentum transfers, to a very good accuracy, assume $e(\delta) = \exp(-\frac{1}{2} a\delta^2)$,
where a is the slope of the nucleon-nucleon elastic cross-section. In all
our consideration we shall assume $\alpha^2(\delta) \ll 1$ for all δ and virtually in-
dependent of δ (although one can put various δ-dependences into the calcu-
lations). So, finally we shall parametrize the small-momentum-transfer
nucleon-nucleon-scattering amplitude as follows:

$$f(\delta) = \frac{(i + \alpha)\, k\sigma}{4\pi} \exp\left(-\tfrac{1}{2} a \delta^2\right)$$

Figure 4 shows the experimental data from Ref. [1] against the following
three variants of approximate evaluation of the ground-state expectation
value:

a) Single-particle-density model:

$$\langle 0 | 0\rangle = \prod_{j=1}^{A} \rho(\vec{r}_j)$$

where

$$\vec{\rho}(\vec{r}_j) = \rho(0)\left(1 + \beta \frac{r^2}{R^2}\right)\! \exp\left(-\frac{r^2}{R^2}\right)$$

$$\rho(0) = 4A^{-1}\, \pi^{-3/2}\, R^{-3},\ \beta = \frac{1}{3}\left(\frac{A}{2} - 2\right)$$

where R is the same radius as in Eq. (46).
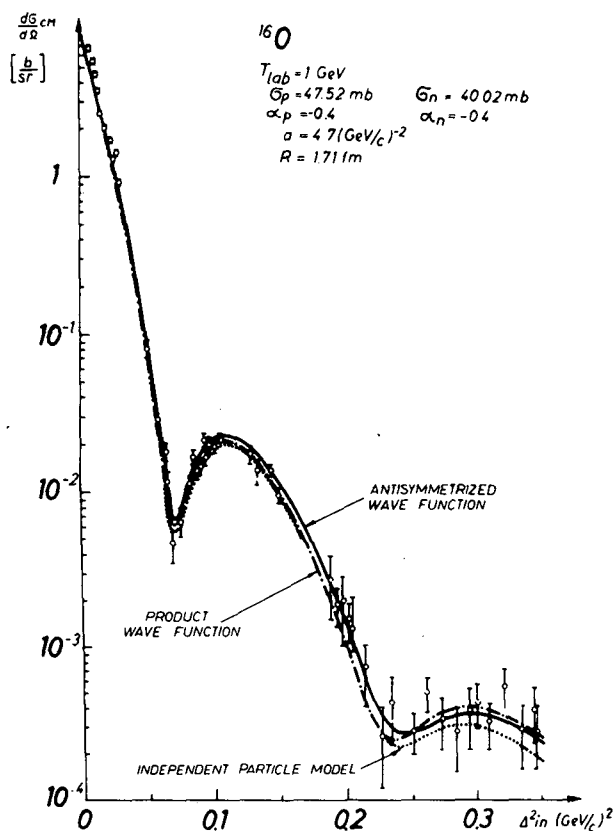
FIG.4.   Proton- ^{16}O elastic-scattering differential cross-section for laboratory kinetic energy
1 GeV (p $\approx$ 1.7 GeV/c). The three curves correspond to the three models of the ground state described in the text. The experimental points are taken from Ref.[1].

b)   Product wave function:

$$|0\rangle = \left| \prod_{j=1}^{A} \varphi_j (\vec{r}_j) \right\rangle$$

where the $\varphi_j(\vec{r}_j)$ are the single-particle states of the oscillator-well shell model:

$$\varphi_0(r) = 2\pi^{-1/4} R^{-3/2} \exp\left(-\frac{r^2}{R^2}\right) Y_{00} \text{ for s-shell}$$

$$\varphi_{1m}(r) = 3^{-1/2} 2^{3/2} \pi^{-1/4} R^{-5/2} r \exp\left(-\frac{r^2}{R^2}\right) Y_{1m} \text{ for p-shell}$$

c) Anti-symmetrized wave function:

$$|0\rangle = |(A!)^{-1/2} \, || \, \varphi_j(\vec{r}_j) \, ||\rangle$$

where $|| \, \varphi_j(\vec{r}_j) \, ||$ denotes the Slater determinant of A single particle functions φ_j.

Before drawing any conclusions from these results, let us stress the fact that the elastic p-^{16}O cross-section is one of the reasonably clean cases to be analysed with formulas (33) and (36): the eikonal approximation is probably reasonably good, the spin of the target is zero, hence, at small angles, the spin-flip part of the p-^{16}O amplitude is negligible (it goes to zero as $\sin(\theta/2)$), and we have then only one amplitude contributing (non-spin-flip): the shape of ^{16}O is quite well known from the electron elastic scattering, hence the parameters in Eqs (47)-(49) are reasonably well established, and finally the ^{16}O nucleus is, most probably, spherical in its ground state; this fact saves us many complications.

Keeping all this in mind we can draw the following conclusions from the results shown in Fig. 4:

1.   The agreement of our model of high-energy scattering with the experimental data is very good. It should be considered as a very strong support of the model.
2.   The only important input concerning the structure of the target is the single-particle density $\rho(r)$ (Eq.(47)). The anti-symmetrization of the ground-state wave function and the correlations resulting from it are unimportant.
3.   If we accept that in the elastic electron scattering from spin-zero nuclei we measure the Fourier transform of the single-particle density $\rho(r)$ (the form factor), this form factor also determines the elastic cross-section for hadron-nucleus scattering. It is a very interesting question as to how general is the relation between the form factors and hadronic cross-sections. With some reservations, it has already been argued [27] that such a relation between, e.g. the nucleon form factors and the nucleon-nucleon cross-sections does indeed exist.

Let us go over to the ^{4}He target [1]. The results of the calculations which are similar to those in the case of ^{16}O are shown in Figs 5 and 6. ^{4}He is also spinless and presumably spherical in its ground state but it is smaller than ^{16}O, hence the diffractive structure lies at larger angles than previously. The interpretation of the elastic p-^{4}He cross-section measured in Brookhaven experiment [1] at the beginning caused many troubles [1, 42] which were resolved by application to p-^{4}He elastic scattering the model presented in these lectures [15].

In Fig. 5 the experimental data of Ref. [1] are plotted against the cross-sections computed from the Gaussian densities: $\rho = \rho_0 \exp(-r^2/R^2)$ assumed for the ground state of ^{4}He. The parameters α (the ratio of the real to the imaginary part of the nucleon-nucleon scattering amplitude) and a (the slope of the nucleon-nucleon elastic cross-section) were varied to show the sensitivity of the results to the parameters of the nucleon-nucleon elastic-scattering amplitude. We can see that the filling of minima depends

FIG.5.   Proton-^{4}He elastic-scattering differential cross-section for laboratory kinetic energy
1 GeV($p \approx 1.7$ GeV/c). The ground state density of ^{4}He was taken in a Gaussian form (see the text). The
experimental points are taken from Ref.[1].

critically on the value of α (the cross-section curve has a zero there if
$\alpha = 0$). It is possible that in future one will be able to employ this fact to
measure α. We shall come to this point later.

Figure 6 supports again the point of view expressed before that the
density of the nuclear matter as given by the charge form factor determines
the hadronic cross-section. The charge form factor of ^{4}He measured
experimentally [43] was used to obtain the p-^{4}He cross-section. We can
see from Fig.6 that the agreement is excellent. One should, however, be
not overoptimistic about such an agreement. First of all, the redundancy
of the centre-of-mass co-ordinate was removed by using the same $\theta(q^2)$
function as before (compare Eq.(47)). We do not know whether this is
consistent with the density measured in Ref.[43] (Equation (47) is correct
only for harmonic-oscillator potential densities). Secondly, many other
effects such as, e.g. spin dependence of the nucleon-nucleon amplitude
were neglected (for such corrections compare Refs [44, 45]). One may
only say that the results of Fig.6 and Refs [44, 45] do not indicate any dis-
agreement with the statement that the density of nuclear matter determines
the p-nucleus cross-section to a very good accuracy.

Figure 7 shows the experimental results and the calculations for p - ^{12}C
scattering. This nucleus is probably deformed in the ground state, and
this fact considerably complicates the calculations. Such calculations are
being done by Leśniak and Wołek [46]; they indicate that the deformation
introduces corrections in the right direction. In calculating the curves of
Fig.7 the ^{12}C nucleus was assumed to be spherical.

$$\frac{d\sigma_{CM}}{d\Omega}$$
in $\frac{b}{sr}$

^{4}He

$$f_j(\rho,\delta) = \frac{(i+\alpha_j)\rho\sigma_j}{4\pi} e^{-\frac{a}{2}\delta^2}$$

$\alpha = -0.4$
$\sigma_n = 40.02\,mb$
$\sigma_p = 47.53\,mb$
$a = 5\,(GeV/c)^{-2}$
$\rho = 1.7\,GeV/c$

Δ^2 in $(GeV/c)^2$

FIG.6. Proton-^{4}He elastic-scattering differential cross-section for laboratory kinetic energy
1 GeV (p $\approx$ 1.7 GeV/c). The curve marked —·—·—·— was computed directly from the ^{4}He charge form factor
found in experiment. For more details see Ref. [15].

Let us say a few words about scattering of protons and pions from
deuterons. There are very many papers on this subject, both experimental
and theoretical (some of the representative references are [4,-7, 13, 14,
19, 30, 44, 45, 47-49). We shall not go into all details of the problem, but
want to stress only a few characteristic points. First of all, the p-d profile
constructed as shown in Eq.(40) works very well if we use the complete
ground-state wave functions of deuteron known to be a superposition of the S-
and D-waves. Recently, some calculations were performed of p-d and
π-d elastic scattering which include the deformation of the ground state of the
deuteron (the existence of the D-state) and some spin effects (the most
important spin effect is the role of spin 1 of the deuteron ground state
[47-49]). Figure 8 illustrates the relative importance of the S- and D-wave
contributions [30]. From the results of Refs [47-49] we can see that there
is a complete agreement between theory and experiment in the case of
elastic scattering of hadrons from deuterons. Let us finally discuss one
amusing aspect of the deuteron case. The scattering amplitude is obtained
trivially from our general formulas (33) and (36) after separating out the

FIG.7. Proton-^{12}C elastic-scattering differential cross-section for laboratory kinetic energy
1 GeV (p $\approx$ 1.7 GeV/c). The curve labelled with (A) has been computed the same way as the curve
—·—·— of Fig.4. The remaining two curves are computed in the "optical limit", see text and Ref.[20]. The
data are taken from Ref.[1].

centre-of-mass motion (which, in the two-body system, can always be done exactly):

$$M = M^{(1)} + M^{(2)} \tag{50}$$

$$= F_d\left(\frac{1}{2}\vec{q}\right)f_n(\vec{q}) + F_d\left(-\frac{1}{2}\vec{q}\right)f_p(\vec{q}) + \frac{i}{2\pi k}\int d^2\lambda \, F_d(\vec{\lambda}) f_n\left(\frac{1}{2}\vec{q} - \vec{\lambda}\right)f_p\left(\frac{1}{2}\vec{q} - \vec{\lambda}\right)$$

where F_d (q) is the deuteron-ground-state form factor and $f_{p,n}$ are the scattering amplitudes from the proton and the neutron. The last term (the so-called double-scattering term: $M^{(2)}$) gives a large momentum-transfer cross-section since the first two decrease with q much faster than the last one. Since F_d is a much more strongly peaked function than $f_{p,n}$ (the deuteron radius is much larger than the nucleon radius) we obtain

$$M^{(2)} \cong \text{const. } f^2\left(\frac{1}{2}\vec{q}\right) \tag{51}$$

If f has the form of the Gaussian given in Eq.(46) we obtain a/2, for the slope of the double scattering term (in the cross-section). Note that, once we assume Eq.(46) to be valid, we obtain the slope a/2 irrespective of the functional form of $F_d(\lambda)$. This is so because the λ and q dependences in
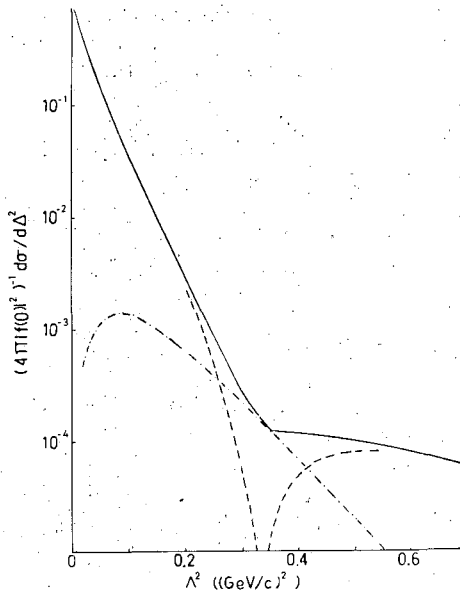
FIG.8. Elastic scattering of pions or protons from deuterons. This figure illustrates how the existence of the D-state combined with spin 1 of the deuteron ground state fill the minimum predicted by the S-state, hence spherically symmetric density. The curves are taken from Ref.[1].

Eq.(50) then factorize. The existing data and the theoretical analysis indicate (see, e.g. Refs [14, 47-49]) that this term has been clearly seen in the recent experiments. But this is essentially a collision of three nucleons (if the incident particle is a nucleon), or one meson and two nucleons (if the incident particle is a meson). This process (or rather its momentum-transfer dependence, as Eq.(51) indicates) virtually does not depend on the ground state of the deuteron and, to a good approximation, can be treated as a collision of three free particles. For example, in nucleon-nucleus collisions one can have multi-particle collisions of the same nature, where many nucleons are pumped into a small region of space and again the momentum-transfer dependence of such processes is such that, virtually, it does not depend on the fact that the nucleons are bound in the nuclei [20].

3. EXTENSIONS OF THE MODEL OF HIGH-ENERGY SCATTERING

In this chapter we shall discuss some limiting and special cases of the formulas presented in the previous chapter. First, we saw from the example of p-^{16}O scattering that the single-particle densities determine the elastic cross-section to a very good accuracy. We shall, therefore, use only single-particle densities in the following discussion.

Let us now quote and discuss some limiting cases of our multiple-scattering formulas (33), (34) and (36) and their possible applications (for more details of this approach see Ref.[20]). Let us consider two composite particles with A and B sub-units, respectively (we may think of them as

being two nuclei). The limit of our formulas (33), (34), and (36) for very large A and B is of particular interest to us. In Ref. [20] it was shown that if both A and B become arbitrarily large then the amplitude M given by

$$M = \Theta(q^2) \frac{ik}{2\pi} \int d^2b \, e^{i\vec{q}\cdot\vec{b}} \left\{ 1 - \int \prod_{\ell=1}^{A} d^2s_\ell^A \, \rho_{A,\ell}(s_\ell^A) \prod_{m=1}^{B} d^2s_m^B \, \rho_{B,m}(s_m^B) \right.$$

$$\left. \times \prod_{j=1}^{A} \prod_{k=1}^{B} \left[1 - \gamma_{jk}\left(\vec{b} - \vec{s}_j^A + \vec{s}_k^B\right) \right] \right\} \tag{52}$$

goes over to the <u>optical-limit</u> amplitude:

$$M^{opt} = \theta(q^2) \frac{ik}{2\pi} \int d^2b \, e^{i\vec{q}\cdot\vec{b}} \left\{ 1 - e^{-\kappa \int d^2s \, d^2s' \, \rho_A(\vec{s}) \gamma(\vec{b} - \vec{s} + \vec{s}') \rho_B(\vec{s}')} \right\} \tag{53}$$

where κ is, in general, a complex constant. In the case of pure absorption κ is real. If we use formula (46) for the sub-unit A-subunit B (hence nucleon-nucleon in the case of nuclear scattering) scattering amplitude, we have the relation:

$$\kappa = \frac{1}{2}(1 - i\alpha) AB\sigma \tag{54}$$

If γ is a very sharply peaked function compared to ρ_A and ρ_B, we obtain

$$M^{opt} = \theta(q^2) \frac{ik}{2\pi} \int d^2b \, e^{i\vec{q}\cdot\vec{b}} \left\{ 1 - e^{-\kappa \int d^2s \, \rho_A(\vec{b}-\vec{s}) \rho_B(\vec{s})} \right\} \tag{55}$$

On the other hand, if we want to consider, e.g. nucleon (meson)-nucleus collision in this limit we should put one of the densities equal to a δ-function and instead of Eq. (55) we have

$$M^{opt} = \theta(q^2) \frac{ik}{2\pi} \int d^2b \, e^{i\vec{q}\cdot\vec{b}} \left\{ 1 - e^{-\kappa \int d^2s \, \rho_A(\vec{s}) \gamma(\vec{b}-\vec{s})} \right\} \tag{56}$$

Figures 7, 9, 10 show that this limit is obtained very quickly, indeed, as A increases.

The results presented in Figs 7, 9, 10 suggest very strongly that the hadronic cross-sections are determined by the hadronic densities of the colliding particles and the complex parameter κ which can be connected with the total cross-section. For instance, if we have purely absorptive processes, hence κ is purely real, it can be determined from the total cross-section as follows:

$$\sigma_T = 4\pi \int_0^\infty db \, b \left\{ 1 - \text{Re} \exp\left[-\kappa \int d^2s \, \rho_A(\vec{s}) \rho_B(\vec{b}-\vec{s}) \right] \right\} \tag{57}$$
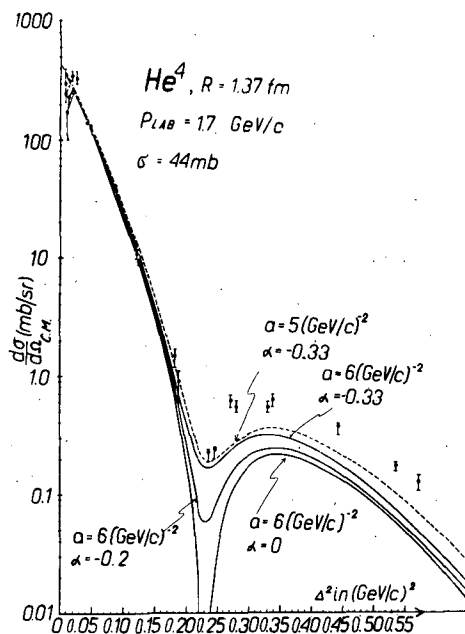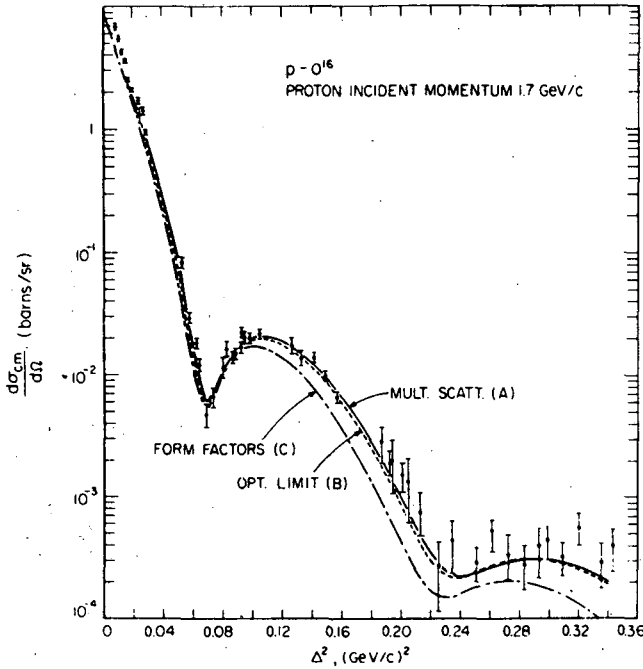
FIG. 9. Proton-^{16}O elastic-scattering differential cross-section for laboratory kinetic energy
1 GeV (p $\approx$ 1.7 GeV/c). The curve (A) has been computed the same way as the curve —·—·— of Fig. 4. The
remaining two curves have been computed in the "optical limit", see text and Ref.[20]. The data are taken
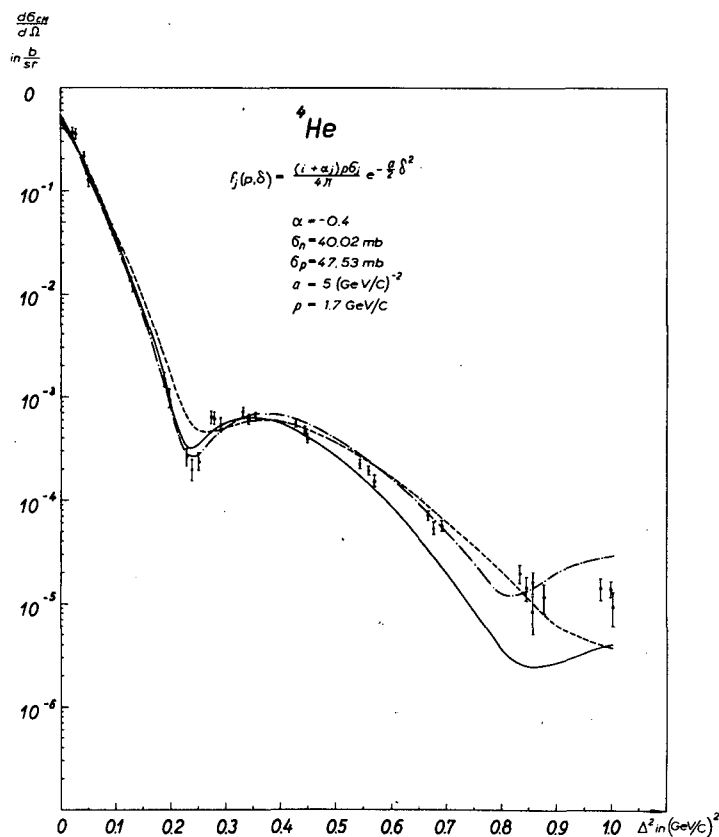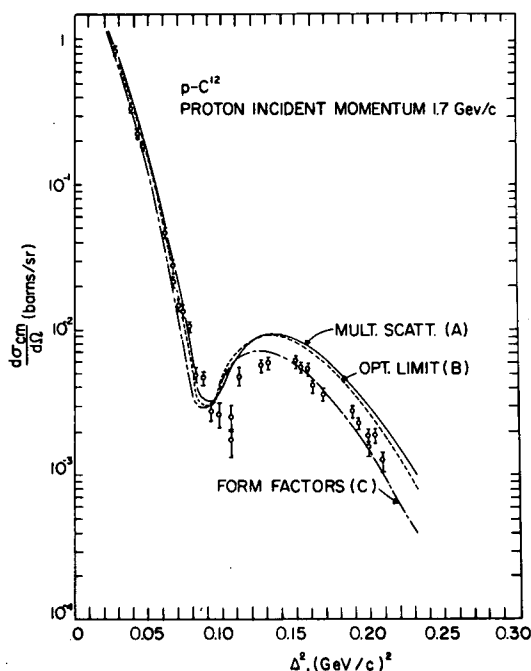from Ref.[1].
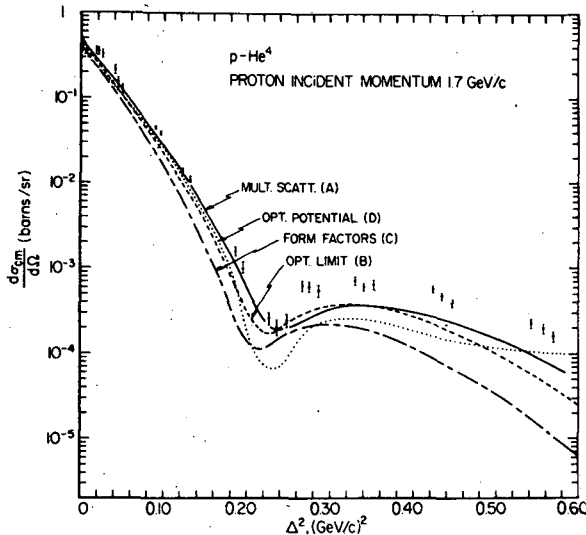
FIG. 10. Proton-^{4}He elastic-scattering differential cross-section for laboratory kinetic energy
1 GeV ($\approx$ 1.7 GeV/c). The curve (A) has been computed from a Gaussian ground-state density. The
remaining two curves have been computed in the "optical limit", see text and Ref. [20]. The data are
taken from Ref.[1].

Since one may hope to determine ρ_A and ρ_B from some other experiments the "pure absorption" (κ real) case might have no free parameters.

Formulas (55) - (57) do not depend on any details of the internal structure of colliding hadrons. It is very tempting, therefore, to use them to calculate elastic scattering of "more elementary" hadrons than nuclei, for instance: nucleon-nucleon or meson-nucleon. Such calculations have already been done (see, e.g. Refs [27-29]) and the results look very encouraging.

All the results presented in Figs 4-10 were obtained with the small-angle scattering formula (17) where the total phase shift was assumed to be the sum of individual phase shifts. This enabled us to introduce the individual amplitudes. In principle, a similar procedure can be applied to the large-angle scattering formula (22) although one obtains rather complex final expressions.

The outcome of the analysis presented in these lectures is that at small scattering angles the "gross features" of the colliding particles determine the elastic cross-sections. The seemingly rich pattern of the differential cross-section does not drastically depend on the details of the target structure. It might, however, be that some information (as, e.g. the ratio of the real to the imaginary) on nucleon-nucleon or meson-nucleon amplitudes can be extracted from the data provided the target nuclei are spherical and spinless.

The most interesting aspect of this analysis is, perhaps, its generality. Hence, it looks as if we really made some progress recently in understanding the phenomena of the elastic scattering of hadrons at high energies.

REFERENCES

[1]   PALEVSKY, H., FRIEDES, J.L., SUTTER, R.J., BENNET, G.W., IGO, G.J., SIMPSON, W.D.,
      PHILLIPS, G.C., CORLEY, D.M., WALL, N.S., STEARNS, R.L., GOTTSCHALK, B., Phys.Rev.Letts,
      18 (1967) 1200. Errata to ^{12}C elastic-scattering data in BNL Report 11360 (to be published).
[2]   BOSCHITZ, E.T., ROBERTS, W.K., VINCENT, J.S., GOTOW, K., GUGELOT, P.C., PERDRISAT, C.F.,
      SWENSON, L.W., Phys.Rev.Letts, 20 (1968) 1116.
[3]   FRIEDES, J.L., Nucl.Phys., A104 (1967) 294; see also CORLEY, D.M., Quasi-Free Scattering of
      1 GeV Protons from ^{12}C and ^{40}C, Thesis, University of Maryland, Department of Physics and
      Astronomy (1968).
[4]   COLEMAN, E., HEINZ, R.M., OVERSETH, O.E., PELLET, D.E., Phys.Rev. Letts, 16 (1966) 761;
      Phys.Rev. 164 (1967) 1655.
[5]   BENNET, G.W., FRIEDES, J.L., PALEVSKY, H., SUTTER, R.G., IGO, G.J., SIMPSON, W.D.,
      PHILLIPS, G.C., STEARNS, R.L., CORLEY, D.M., Phys.Rev.Letts, 19 (1967) 387.
[6]   BRADAMANTE, F., CONETTI, S., FIDECARO, G., FIDECARO, M., GIORGI, M., PENZO, A.,
      PIEMONTESE, L., SAULI, F., SCHIAVON, P., Phys.Letts 28B (1968) 193.
[7]   CHASE, R.C., COLEMAN, E., RHOADES, T.G., FELLINGER, M., GUTMAN, E., LAMB, R.C.,
      SCHROEDER, L.S., Paper submitted to the 14th Int.Conf. High Energy Physics, Vienna (1968).
[8]   JONES, L.W., LONGO, M.I., O'FALLON, J.R., KREISLER, M.N., Neutron-Nuclei Total Cross-
      Section Data at 27 GeV/c, Int.Conf. High Energy Physics, Vienna, (1968).
[9]   BELLETTINI, G., COCCONI, G., DIDDENS, A.N., LILLETHUN, E., MATTHIAE, G., SCANLON, I.P.,
      WETHERELL, A.M., Nucl.Phys. 79 (1966) 609.
[10] ALLABY, J.V., BINON, F., DIDDENS, A.N., DUTEIL, P., KLOVNING, A., MEUNIER, R.,
      PEIGNEUX, J.P., SACHARIDIS, E.J., SCHLÜPMANN, K., SPIGHEL, M., STROOT, J.P.,
      THORNDIKE, A.M., WETHERELL, A.M., Phys.Letts 28B (1968) 67.
[11] For a recent compilation of data on high-energy collisions of hadrons, see, e.g. BELLETTINI, G.,
      Rapporteur's talk, 14th Int.Conf. High-Energy Physics, Vienna (1968).
[12] GLAUBER, R.J., High-Energy Collisions Theory, Lectures in Theoretical Physics, 1, Interscience
      Publishers, New York (1959).

[13] FRANCO, V., GLAUBER, R.J., Phys.Rev. 142 (1966) 1195.

[14] FRANCO, V., COLEMAN, E., Phys.Rev.Letts, 17 (1966) 827.

[15] CZYŻ, W., LEŚNIAK, Phys.Letts, 24B (1967) 227; Phys.Letts, 25B (1967) 319, High-Energy Physics and Nuclear Structure, (ALEXANDER, G., Ed.) North-Holland, Amsterdam (1967).

[16] CZYŻ, W., Medium Energy Nuclear Physics with Electron Linear Accelerators, MIT 1967 Summer Study, 359.

[17] BASSEL, R.H., WILKIN C., Phys.Rev.Letts, 18 (1967) 811; Phys.Rev. 174 (1968) 1179.

[18] FROMANEK, J., TREFIL, J.S., Nucl.Phys. B4 (1968) 165.

[19] ALBERI, G., BERTOCCHI, L., ICTP, Trieste preprint IC/68/99, Phys.Letts 28B (1968) 186.

[20] CZYŻ, W., MAXIMON, L.C., Phys.Letts, 27B (1968) 354, National Bureau of Standards, Report 9933 and Ann.Phys., 52 (1969) 59.

[21] LEŚNIAK, L., WOŁEK, H., Report INP 621/PH, Nucl.Phys. 125A, (1969) 665.

[22] GLAUBER, R.J., High-Energy Physics and Nuclear Structure, (ALEXANDER, G., Ed.) North-Holland, Amsterdam (1967).

[23] LEE, H.K., McMANUS, H., Phys.Rev.Letts, 20 (1968) 337.

[24] CHOU, T.T., Phys.Rev., 168 (1968) 1594.

[25] ROSS, D.K., Phys.Rev. 173 (1968) 1695.

[26] SCHIFF, L.I., Phys.Rev. 176 (1968) 1390.

[27] CHOU, T.T., YANG, C.N., High-Energy Physics and Nuclear Structure, (ALEXANDER, G., Ed.) North-Holland, Amsterdam (1967); Phys.Rev. 170 (1968) 1591; Phys.Rev.Letts, 20 (1968) 1213; Phys.Rev. 175 (1968) 1832.

[28] DURAND, L., LIPES, R., Phys.Rev.Letts 20 (1968) 637.

[29] CHAN HONG-MO, Collissions at High-Energy, Rapporteur's talk, 14th Int.Conf. High-Energy Physics, Vienna (1968). It contains a fairly complete literature on high-energy hadron scattering.

[30] HARRINGTON, D.R., Phys.Rev.Letts 21, (1968) 1496.

[31] SCHIFF, L.I., Phys.Rev. 103 (1956) 443.

[32] FEYNMAN, R.P., Quantum Electrodynamics, Benjamin, New York (1961); Theory of Fundamental Processes, Benjamin, New York (1961), FEYNMAN, R.P., HIBBS, A.R.; Quantum Mechanics and Path Integrals, McGraw-Hill (1965).

[33] SAXON, D.S., SCHIFF, L.I., Nuovo Cim. 6 (1957) 614.

[34] TIEMANN, J.J., Phys.Rev. 109 (1958) 183.

[35] TIEMANN, J.J., Ph.D.Thesis, Stanford University (1960) (unpublished).

[36] BAKER, A., Phys.Rev. 134B (1964) 240.

[37] YENNIE, D.R., BOSS, F.L., RAVENHALL, D.G., Phys. Rev. 137 B (1965) 882.

[38] GOLDBERGER, M.L., WATSON, K.M., Collision Theory, John Wiley and Sons, 617.

[39] COTTINGHAM, W.N., PEIERLS, R.F., Phys.Rev. 137B (1965) 147.

[40] ELLIOT, J.P., SKYRME, T.H.R., Proc.Roy.Soc. London A 232 (1955) 561.

[41] JASTROW, R., Phys.Rev. 98 (1955) 1479.

[42] PALEVSKY, H., in Int.Conf.Nuclear Physics (BECKER, R.L., Ed.) (Gatlinburg, Tennessee, 1966) 1060.

[43] FROSCH, R.F., McCARTHY, J.S., RAND, R.E., YEARIAN, M.R., Phys.Rev. 160 (1967) 874.

[44] FRANCO, V., Phys.Rev.Letts 21 (1968) 1360.

[45] KUJAWSKI, E., SACHS, D., TREFIL, J.S., Phys.Rev.Letts 21 (1968) 583.

[46] LEŚNIAK, L., WOŁEK, H., private communication.

[47] FRANCO, V., GLAUBER, R.J., Phys.Rev.Letts 22 (1969) 370.

[48] ALBERI, G., BERTOCCHI, L., preprint IC/69/14, to be published in Nuovo Cimento.

[49] MICHAEL, C., WILKIN, C., Elastic Pion-Deutron Scattering at High Energies (to be published in Nuclear Physics).

[50] CZYŻ, W., High-Energy Collisions of Hadrons and Nuclei, Lecture delivered at the Inaugural Conference of the European Physical Society, Florence, 8-12 April 1969.

PHOTO- AND ELECTRO-DISINTEGRATION OF NUCLEI AND EXCHANGE CURRENTS*

B. BOSCO
Istituto di Fisica dell' Università,
Cagliari, Sardegna, Italy

Abstract

PHOTO- AND ELECTRO-DISINTEGRATION OF NUCLEI AND EXCHANGE CURRENTS.
1. Introduction; 2. Connection between magnetic dipole photo- and electro-disintegration; 3. The nuclear tensors in the presence of exchange currents; 4. Effect of exchange currents on the relation between photo- and electro-disintegration; 5. Discussion and conclusions.

1. INTRODUCTION

In this paper, we shall try to summarize the results that our group[1] has obtained in the last few years.

The main point of our arguments is the connection between photo- and electro-disintegration of nuclei which has been established some years ago for each multipole [1]. We shall, therefore, review this connection with particular emphasis on the magnetic dipole. The reason is fairly obvious since the Siegert theorem states that exchange-current effects do not contribute to the electric-multipole operators; we must, therefore, look for the magnetic ones.

In fact, what we shall see is that there is a simple proportionality between the cross-sections for the magnetic-dipole disintegration induced by photons and by electrons, the proportionality factor being a definite function of the electron kinematical variables in the absence of exchange currents. When exchange effects are present this proportionality function is multiplied by a factor $(1 + \epsilon)$ where ϵ is determined by the coefficients of the Foldy-Osborn invariants [2]. We shall, therefore, subdivide our discussion into the following three problems:

(a) connection between magnetic dipole photon and electron disintegration,

(b) exchange currents, and

(c) experimental determination of the effects of exchange currents.

2. CONNECTION BETWEEN MAGNETIC-DIPOLE PHOTO- AND ELECTRO-DISINTEGRATION

2.1. The general treatment of the correlation between photo- and electro-disintegration is given elsewhere [3]. Here we shall recall the explicit relation for the magnetic dipole only for the benefit of those

---

who are not familiar with the problem. The matrix element for an electro-
magnetic transition is given by

$$H = \sum_{\mu} \langle \alpha | J_\mu | \alpha' \rangle A_\mu \tag{1}$$

where $\langle \alpha | J_\mu | \alpha' \rangle$ is the matrix element of the nuclear current between
the states $|\alpha\rangle$ and $|\alpha'\rangle$ representing the initial and final states of the
nuclear system. Working in the momentum space — if the transition is
induced by electrons — A_μ is given by

$$A_\mu = \frac{\tilde{u}(p - k^e)\, \gamma_\mu\, u(p)}{k^{e2}} \tag{2}$$

p being the four-momentum of the initial electron, k^e the four-momentum
transfer u and γ_μ the usual spinor and Dirac matrices, respectively.
Because of the conservation laws of the nuclear and electron charges
we have

$$k_\mu^e \langle \alpha | J_\mu | \alpha' \rangle = 0$$

$$K_\mu^e A_\mu = 0 \tag{3}$$

One can therefore rewrite Eq. (1) in the form

$$H = \langle \alpha | \vec{J} | \alpha' \rangle \vec{A}' \tag{4}$$

with

$$\vec{A}' = \vec{A} - \vec{k}^e \frac{\vec{k}^e \cdot \vec{A}'}{k_0^{e2}} \tag{5}$$

with k_0^e the fourth component of the momentum transfer.

The differential cross-section for electro-disintegration is therefore

$$\frac{d^2 \sigma_{e\ell}}{d\Omega_e \, d\Omega_N} = \frac{2\pi}{v_e}\, J_{i\,i'}\, N_{i\,i'}\, \rho_e\, \rho_N \tag{6}$$

In this formula v_e is the velocity of the incoming electrons, ρ_e and ρ_N are
the densities of the final state for electrons and nucleons, respectively,
and

$$J_{i\,i'} = S \langle \alpha | J_i | \alpha' \rangle^* \langle \alpha | J_{i'} | \alpha' \rangle \tag{7}$$

$$N_{i\,i'} = S\, A'_i{}^*\, A_{i'} \tag{8}$$

In Eqs (7) and (8) S means summation over the final spin states and averaging
over the initial ones.

The explicit expression for $N_{ii'}$ is

$$N_{ii'} = \frac{e^2}{2\,m^2\,(k_0^{e^2} - k^{e^2})^2} \left\{ 2\,p_i\,p_{i'} + \frac{1}{2}\,(k^{e^2} - k_0^{e^2})\,\delta_{ii'} \right.$$

$$+ (k_i^e\,k_{i'}^e - p_i\,k_{i'}^e - p_{i'}\,k_i^e) \left(1 - \frac{k^{e^2}}{k_0^{e^2}} + 2\,\frac{\vec{p}\cdot\vec{k^e}}{k_0^{e^2}}\right) \tag{9}$$

$$\left. + \frac{k_i^e\,k_{i'}^e}{k_0^4} \left[2\,(\vec{p}\cdot\vec{k}^e)^2 - 2\,k^{e^2}(\vec{p}\cdot\vec{k}) + \frac{1}{2}\,(k^{e^2} - k_0^{e^2})\,k^{e^2} \right] \right\}$$

The photo-disintegration cross-section is given in terms of the tensor $J_{ii'}$ by the formula

$$\frac{d\sigma_{ph}}{d\Omega_N} = \frac{2\pi}{c} \sum_{pol} \rho_N\,\epsilon_i\,\epsilon_{i'}\,J_{ii'} \tag{10}$$

where $\vec{\epsilon}$ is the photon polarization vector and $\sum\limits_{pol}$ means sum over the photon polarization. There is one remark which one must make at this point: the expression of the nuclear current tensor $J_{ii'}$ which through Eq. (6) and (10) determines both the electron and the photo-disintegration should be computed for the same relative energy of the outgoing particles. Therefore, the momentum of the photon $\vec{k}$ and the three-momentum transfer of the electron $\vec{k}^e$ will in general be different.

    2.2. Now we must construct the tensor $J_{ii'}$. It can be shown that, as a consequence of the Schrödinger equation, in the absence of exchange terms and gauge invariance, the expression for the nucleon current for two-nucleon systems must be written as [4]

$$\vec{j}\,(\vec{k},\vec{r}) = \vec{k} \times (\mu_1\,\vec{\sigma}\,(1) + \mu_2\,\vec{\sigma}\,(2)) \tag{11}$$

where μ_1 and μ_2 are the magnetic moments of nucleons 1 and 2, respectively. $\sigma\,(1)$ and $\sigma\,(2)$ are the Pauli spin operators for the corresponding particles.[2]

    To construct the tensor $J_{ii'}$ we must first compute the matrix element $\langle\alpha\,|\,\vec{j}\,(\vec{k},\vec{r})\,|\,\alpha'\,\rangle$ of the current (11) between the state $|\alpha\rangle$ and $|\alpha'\rangle$.

    For the sake of simplicity, we shall from now on refer to a deuteron as an s-wave bound state only.[3]

    Then our bound state is a $^3S_1$ state and of the two possible continuum states ^1S and ^3S induced by current (11) only the first transition will really occur.[4]

    Using the identity

$$\mu_1\vec{\sigma}\,(1) + \mu_2\,\vec{\sigma}\,(2) = \frac{1}{2}\,(\mu_1 + \mu_2)\,(\vec{\sigma}\,(1) + \vec{\sigma}\,(2) + \frac{1}{2}\,(\mu_1 - \mu_2)\,(\vec{\sigma}\,(1) - \vec{\sigma}\,(2)) \tag{12}$$

---

    [2] On the left-hand side of Eq. (11) we have indicated also the dependence on the variable $\vec{r}$, the relative distance of the two particles. This notation will be useful later on.

    [3] The correction due to the presence of the wave will be discussed in section 5.

    [4] The reason is, as is well known, that the continuum triplet is orthogonal to the bound triplet.

we obtain

$$\langle \alpha | \vec{j} (\vec{k}, \vec{r}) | \alpha' \rangle = S (q^2) \frac{\mu_1 - \mu_2}{2} \vec{k} \times \langle i | \vec{\sigma} (1) - \vec{\sigma} (2) | f \rangle \tag{13}$$

where $|i\rangle$ and $|f\rangle$ are the initial and final spin states, respectively, $\vec{q}$ the relative momentum of the outgoing particles and

$$S (q^2) = \langle \alpha | \alpha' \rangle$$

Definition (7) now gives the nuclear tensor $J_{ii'}$

$$J_{ii'} = |S (q^2)|^2 \left(\frac{\mu_1 - \mu_2}{2} \right)^2 \epsilon_{i\alpha\beta} \epsilon_{i\alpha\mu} \dot{k}_\alpha k_\nu$$

$$\times \frac{1}{2} \sum_{if} \langle f | [\vec{\sigma} (1) - \vec{\sigma} (2)] | i \rangle \langle i | [\vec{\sigma} (1) - \vec{\sigma} (2)] | f \rangle \tag{14}$$

$$= g (q^2) [k^2 \delta_{ii'} - k_i k_{i'}]$$

with

$$g (q^2) = |S (q^2)|^2 (\mu_1 - \mu_2)^2$$

From Eqs (6) and (14) we have

$$\frac{d^2 \sigma_{e\ell}}{d\Omega_e d\Omega_N} = \frac{2\pi}{v_e} \left[k^{e^2} \delta_{ii'} - k_i^e k_{i'}^e \right] g (q^2) N_{ii'} \rho_e \rho_N \tag{15}$$

From Eqs (10 and (14) we get instead

$$\frac{d\sigma_{ph}}{d\Omega_N} = \frac{4\pi}{c} g (q^2) k^2 \rho_N \tag{16}$$

Equations (15) and (16) give us the requested relation between the photo- and the electro-disintegration cross-sections

$$\frac{d^2 \sigma_{e\ell}}{d\Omega_e d\Omega_N} = \frac{c}{2 v_e} \frac{1}{k^2} N_{ii'} \left[k^{e^2} \delta_{ii'} - k_i^e k_{i'}^e \right] \frac{d\sigma_{ph}}{d\Omega_N} \rho_e \tag{17}$$

This equation which can be shown to be valid for the spin part transition of each multipole [5] is the main relation on which our investigation is based.

2.3.   To proceed in our discussion let us summarize the main hypo-thesis on which Eq. (17) rests
    (a) Born approximation in the electromagnetic coupling constant,
    (b) Schrödinger equation, and
    (c) nucleon current contribution only.
We shall discuss points (a) and (b) later on, while now we wish to devote ourselves to point (c).

By nucleon current contribution only, we mean that there are no ex-
change terms in the Schrödinger equation, or which is equivalent in the
spirit of first quantization, no exchange currents.

If we now wish to introduce an exchange current we have two different
approaches which we may follow:

(1) utilization of meson-theory results, and
(2) reliance on the phenomenological work initiated by Sachs [6] and
     extended by Foldy and Osborn [7].

We shall prefer the second path.

Since, however, we are only interested in the magnetic-dipole tran-
sition we do not need to go through to all the labour of the afore-mentioned
works. All we shall need is to recall the underlying principles. In the
spirit of first quantization any interaction Hamiltonian should be expressible
in terms of nucleon spin, isospin and position co-ordinates.

We shall directly construct the interaction Hamiltonian responsible
for the magnetic-dipole transition.

Our two-body problem will still be further simplified by the fact that,
as far as the nucleon part is concerned, we have only the following three
variables: $\vec{\sigma}(1)$ and $\vec{\sigma}(2)$, the spin operators of the two nucleons, and $\vec{r}$,
the relative distance of the two nucleons.

As far as the electromagnetic part is concerned, we begin to observe
that we have only two vectors: $\vec{u}$, which must be identified with $\vec{\epsilon}$ in the
case of photo-disintegration and with $\vec{A}'$ in case of electro-disintegration,
and $\vec{k}$. Furthermore, if the interaction we are constructing has to be a
magnetic dipole, $\vec{u}$ and $\vec{k}$ must form an antisymmetric tensor

$$\vec{u} \times \vec{k} \tag{18}$$

For the nuclear part we must therefore construct all the possible axial
vectors with the three vectors $\vec{r}, \vec{\sigma}(1), \vec{\sigma}(2)$. This problem has been solved
by Foldy and Osborn [8]. There are at maximum seven possible terms

(a) $\vec{\sigma}(1) - \vec{\sigma}(2)$

(b) $\vec{\sigma}(1) \times \vec{\sigma}(2)$

(c) $[\vec{\sigma}(1) \times \vec{\sigma}(2) \cdot \vec{r}]\vec{r}$

(d) $[(\vec{\sigma}(1) - \vec{\sigma}(2)) \cdot \vec{r}]\vec{r}$

(e) $\vec{\sigma}(1) + \vec{\sigma}(2)$

(f) $[(\vec{\sigma}(1) + \vec{\sigma}(2)) \cdot \vec{r}]\vec{r}$

(g) $[\vec{\sigma}(1) \times \vec{r}][\vec{\sigma}(2) \cdot \vec{r}] + [\vec{\sigma}(2) \times \vec{r}][\vec{\sigma}(1) \cdot \vec{r}]$ $\tag{19}$

Let us note that the combinations are chosen such that they have definite
parity under the operation

$$\vec{\sigma}(1) \to \vec{\sigma}(2) \quad \vec{\sigma}(2) \to \vec{\sigma}(1) \quad \vec{r} \to -\vec{r} \tag{20}$$

In fact, expressions (19a), (19b), (19c) and (19d) are changing sign under
operation (20) while the remaining ones do not. Therefore, multiplying

the listed expressions by arbitrary functions of $\vec{r}$ and $\vec{k}$, even or odd in $\vec{r}$, it is easy to construct the requested expressions symmetric or antisymmetric under operation (20).

To complete the treatment we still have to take care of the behaviour under time reversal. In this respect we should observe that expressions (19a), (19d), (19e) and (19f) change sign under time reversal while the remaining ones do not. Furthermore, when they are multiplied by scalar functions of $\vec{k}$ and $\vec{r}$ one must also take into account the effect of time reversal on these functions. In doing this it is important to keep in mind that a scalar function of two vectors $\vec{k}$ and $\vec{r}$ which is even or odd in one vector is also even or odd in the other one. This follows from the fact that a scalar function of two vectors $\vec{k}$ and $\vec{r}$ is a function of the three invariants which one can build with the given two vectors k^2, r^2 and $\vec{k} \cdot \vec{r}$. With these observations in mind it is an easy task to write down the proper combinations which are symmetric or antisymmetric under the operation (20) and which have a definite parity under time inversion (some factor i should be introduced in some term in order to satisfy this last requirement). Then the combination which is symmetric under the operation (20) and invariant (after multiplication by $\vec{u} \times \vec{k}$) under time reversal must be combined with the isotopic operator

$$\tau^x(1)\,\tau^x(2) + \tau^y(1)\,\tau^y(2) \tag{21}$$

to give the current called $j_{t'}$ by Osborn and Foldy. The other combination which is antisymmetric under operation (20) and changes sign under time reversal must be multiplied by the isotopic operator

$$\tau^x(1)\,\tau^y(2) - \tau^y(1)\,\tau^y(2) \tag{22}$$

to give the current j_t.

Since, however, we are only concerned with the space structure of the matrix element we shall not deal with the isospin space any more. This means that in the actual calculations some factor should be added to our expression in order to account for the isotopic-spin matrix element.

In a phenomenological approach like that which we are following these constants can always be incorporated in the parameters of the theory.

3. THE NUCLEAR TENSORS IN THE PRESENCE OF EXCHANGE CURRENTS

We are now in a position to write down the interaction Hamiltonian due to the exchange currents:

$$
\begin{aligned}
H_{\text{int}}^{\text{exch.}} = \vec{u}\cdot\vec{j}^{\,\text{exch.}} =\ & \vec{u}\times\vec{k}\,\{\vec{a}\,(\vec{k},\vec{r})\,[\vec{\sigma}(1) - \vec{\sigma}(2)]\} \\
& + b\,(\vec{k},\vec{r})\,\vec{\sigma}(1)\times\vec{\sigma}(2) + c\,(\vec{k},\vec{r})\,[\vec{\sigma}(1)\times\vec{\sigma}(2)\cdot\vec{r}]\,\vec{r} \\
& + d\,(\vec{k},\vec{r})\,[(\vec{\sigma}(1) - \vec{\sigma}(2)\cdot\vec{r}]\vec{r} + e\,(\vec{k},\vec{r})\,(\vec{\sigma}(1) + \vec{\sigma}(2)) \\
& + f\,(\vec{k},\vec{r})\,[(\vec{\sigma}(1) + \vec{\sigma}(2))\cdot\vec{r}]\,\vec{r} \\
& + g\,(\vec{k},\vec{r})\,[(\vec{\sigma}(1)\times\vec{r})\,(\vec{\sigma}(2)\cdot\vec{r}) + (\vec{\sigma}(2)\times\vec{r})\,(\vec{\sigma}(1)\cdot\vec{r})]\}
\end{aligned} \tag{23}
$$

From this expression we can now write down the nuclear tensor according to the defining Eq. (7).

The only relevant terms are the interference of Eq. (23) with the nucleon current defined by Eq. (11)

$$\vec{j}^N = \frac{1}{2}\, (\mu_p - \mu_n)\, \vec{k} \times (\vec{\sigma}\,(1) - \vec{\sigma}\,(2))$$

We shall designate by $J_{ii'}^{(N,\,a)}$, $J_{ii'}^{(N,\,b)}$ etc. that part of the nuclear tensor which comes from the interference of the nucleon current with the term a), (b) etc. of Eq. (23). To complete these terms let us first recall the following formulas:

(a) $S \langle i | [\vec{\sigma}\,(1) - \vec{\sigma}\,(2)]_q | f \rangle \langle f | [\vec{\sigma}(1) - \vec{\sigma}\,(2)]_m | i \rangle = \frac{2}{3}\,\delta_{qm}$

(b) $S \langle i | [\vec{\sigma}\,(1) - \vec{\sigma}\,(2)]_q | f \rangle \langle f | \sigma_\alpha\,(1)\,\sigma_\beta\,(2) | i \rangle = \frac{2}{3}\, i\epsilon_{q\alpha\beta}$ \hfill (24)

(c) $S \langle i [\vec{\sigma}\,(1) - \vec{\sigma}\,(2)]_q | f \rangle \langle f | [\vec{\sigma}\,(1) + \vec{\sigma}\,(2)] | i \rangle = 0$

where $|i\rangle$ is the initial triplet state, $|f\rangle$ is the final singlet state. S means average over initial spin state and sum over the final spin state.

These formulas are almost obvious. They are derived in the Appendix of the paper by Bosco and Piazza [9].

With the help of Eq. (24) it is easy to see that only the tensor $J_{ii'}^{(N,\,a)}$, $J_{ii'}^{(N,\,b)}$, $J_{ii'}^{(N,\,c)}$, $J_{ii'}^{(N,\,d)}$, $J_{ii'}^{(N,\,g)}$ can be different from zero. Furthermore, the only technical difficulty which still remains is to extract the s-wave part from terms like (c) and (g) which also give rise to higher waves. We shall not discuss this point here but rather give the results:

(a) $J_{ii'}^{(N,\,a)} = \frac{2}{3}\, (\mu_p - \mu_n)\, \mathrm{Re}\, [S^*\,(q^2)\, A\,(\vec{k},\,\vec{q})]\, [k^2\delta_{ii'} - k_i k_{i'}]$

(b) $J_{ii'}^{(N,\,b)} = -\frac{4}{3}\, (\mu_p - \mu_n)\, \mathrm{Im}\, [S^*\,(q^2)\, B\,(\vec{k},\,\vec{q})]\, [k^2\delta_{ii'} - k_i k_{i'}]$

(c) $J_{ii'}^{(N,\,c)} = -\frac{4}{3}\, (\mu_p - \mu_n)\, \mathrm{Im}\, [S^*\,(q^2)\, C^{(1)}\,(\vec{k},\,\vec{q})]\, [k^2\delta_{ii'} - k_i k_{i'}]$ \hfill (25)

(d) $J_{ii'}^{(N,\,d)} = \frac{2}{3}\, (\mu_p - \mu_n)\, \mathrm{Im}\, [S^*\,(q^2)\, D^{(1)}\,(\vec{k},\,\vec{q})]\, [k^2\delta_{ii'} - k_i k_{i'}]$

(g) $J_{ii'}^{(N,\,g)} = 0$

In these equations the symbols have the following meanings:

$$S\,(q^2) = \langle \alpha | \alpha' \rangle$$

$$A\,(\vec{k},\,\vec{q}) = \langle \alpha | a\,(\vec{k},\,\vec{r}) | \alpha' \rangle$$

$$B\,(\vec{k},\,\vec{q}) = \langle \alpha | b\,(\vec{k},\,\vec{r}) | \alpha' \rangle$$

As far as $C^{(1)}(\vec{k},\vec{q})$ and $D^{(1)}(\vec{k},\vec{q})$ are concerned some more details are necessary.

When we in fact wish to compute the matrix elements between $|\alpha\rangle$ and $|\alpha'\rangle$ of the operator appearing in terms like c and d we are faced with the problem of evaluating terms of the structure

$$T_{ms}(\vec{k},\vec{q}) = \langle\alpha|t(\vec{k},\vec{r})\, r_m\, r_s\,|\alpha'\rangle \tag{26}$$

Remembering that $|\alpha\rangle$ depends only on $\vec{r}$ and $|\alpha'\rangle$ on $\vec{r}$ and $\vec{q}$, the most general structure of T_{ms} is from translational invariance considerations, of the form

$$T_{ms}(\vec{k},\vec{q}) = T^{(1)}(\vec{k},\vec{q})\,\delta_{ms} + T^{(2)}(\vec{k},\vec{q})\,k_m q_s$$

$$+ T^{(3)}(\vec{k},\vec{q})\,k_s q_m + T^{(4)}(\vec{k},\vec{q})\,k_s k_m + T^{(5)}(\vec{k},\vec{q})\,q_s q_m$$

From this it is clear that only the isotropic parts of the tensor C_{ms} and D_{ms} give rise to s-waves. This has been indicated by $C^{(1)}(\vec{k},\vec{q})$ and $D^{(1)}(\vec{k},\vec{q})$, respectively.

4.   EFFECT OF EXCHANGE CURRENTS ON THE RELATION BETWEEN PHOTO- AND ELECTRO-DISINTEGRATION

Having written down the nuclear tensors we can now re-derive step by step the relation between the photo-disintegration and the electro-disintegration cross-section of nuclei which has been obtained in Sec. 2.2 in the absence of exchange currents.

In this case we obtain

$$\frac{d^2\sigma_{e\ell}}{d\Omega_e d\Omega_N} = \frac{c}{2v_e}\frac{(1+\epsilon)}{k^2}\,N_{ii'}[\,k^{e2}\,\delta_{ii'} - k_i^e\,k_{i'}^e\,]\frac{d\sigma_{ph}}{d\Omega_N}\,\rho_e \tag{27}$$

where

$$\epsilon = \left\{ \frac{\mathrm{Re}\,[S^*(q^2)\,A(\vec{k}^e,\vec{q})]}{\mathrm{Re}\,[S^*(q^2)\,A(\vec{k},\vec{q})]} + \frac{\mathrm{Im}\,[S^*(q^2)\,B(\vec{k}^e,\vec{q})]}{\mathrm{Im}\,[S^*(q^2)\,B(\vec{k},\vec{q})]} \right.$$

$$\left. + \frac{\mathrm{Im}\,[S^*(q^2)\,C^{(1)}(\vec{k}^e,\vec{q})]}{\mathrm{Im}\,[S^*(q^2)\,C^{(1)}(\vec{k},\vec{q})]} + \frac{\mathrm{Re}\,[S^*(q^2)\,D^{(1)}(\vec{k}^e,\vec{q})]}{\mathrm{Re}\,[S^*(q^2)\,D^{(1)}(\vec{k},\vec{q})]} - 4 \right\} \tag{28}$$

Clearly ϵ is zero if for a given $\vec{q}$, i.e. for a given relative kinetic energy of the outgoing particles we have $\vec{k} = \vec{k}^e$. This is not the case. The other possibility for $\epsilon = 0$ is that the functions $A, B, C^{(1)}$ and $D^{(1)}$ have a trivial dependence upon $\vec{k}$, or are independent of it, at all.

5.   DISCUSSION AND CONCLUSIONS

Let us first remark that in practice Eq. (27) is valid only if there are no d-waves present in the deuteron. Since the effect of these waves is comparable to the effect we are looking for, we should take this fact into

account. This is easily done. In fact, the transition from d-waves will lead to an isotropic angular distribution in the nuclear particles for which a relation can also be established between photo- and electro-disintegration cross-sections. This relation reads [10]

$$\frac{d^2 \sigma_{e\ell}^{(s,d)}}{d\Omega_e d\Omega_N} = \frac{c \rho_e}{2 v_e k^2} N_{ii'} [k^{e^2} \delta_{ii'} - k_i^e k_{i'}^e] \frac{d\sigma_{ph}^{(s,d)}}{d\Omega_N}$$ (29)

Of course, the angular distribution on the left-hand side of Eq. (29) must be considered with respect to $\vec{k}^e$ axis. So once this interference effect between s and d-waves is removed by means of Eq. (29), if we choose a kinematical situation in which only magnetic-dipole transitions are allowed in the electro-disintegration, Eq. (27) will determine ϵ through experiment; thus the importance of the exchange currents.

This kinematical situation can be realized by utilizing the technique of 180° electron scattering as introduced by Barber and Peterson [11]. In this case the ratio of the magnetic to the electric cross-section is of the order of

$$\left(\frac{p_0 + p}{p_0 - p}\right)^2$$

where p_0 and p are the absolute values of the initial and final electron momenta, and therefore it may be increased at will.

Furthermore, there are two more points which we would like to mention. The first point is the dependence of the function A, B, $C^{(1)}$ and $D^{(1)}$ on $\vec{k}$. It can be shown that if this dependence is trivial also the dependence of the quantities $a(\vec{k}, \vec{r})$, $b(\vec{k}, \vec{r})$ etc. [12] on $\vec{r}$ which appear in Eq. (23) is trivial.

The other point is that the treatment discussed here is based on the Born approximation in the electromagnetic coupling constant. Independently of any theoretical consideration we should like to point out that the validity of this approximation can be checked directly on each particular nucleus by measuring the ratio of electron to positron cross-section with the nucleus. Experiments of this kind have already been performed by Herring et al. [13].

REFERENCES

[1] BOSCO, B., QUARATI, P., Nuovo Cim. 33 (1964) 527.
[2] OSBORN, R.K., FOLDY, L.L., Phys. Rev. 79 (1960) 795.
[3] BOSCO, B., QUARATI, P., loc. cit.
[4] SACHS, R.G., Nuclear Theory, Cambridge, Mass. (1953) 232.
[5] BOSCO, B., QUARATI, P., loc. cit.
[6] SACHS, R.G., Phys. Rev. 74 (1948) 433.
[7] OSBORN, R.K., FOLDY, L.L., loc. cit.
[8] OSBORN, R.K., FOLDY, L.L., loc. cit.
[9] BOSCO, B., PIAZZA, A., to be published in Phys. Rev.
[10] BOSCO, B., PIAZZA, A., to be published in Phys. Rev.
[11] PETERSON, G.A., BARBER, W.C., Phys. Rev. 128 (1962) 812.
[12] BOSCO, B., PIAZZA, A., loc. cit.
[13] HERRING, D.F., NASCIMENTO, I.C., WALTON, R.B., SUND, R.E., Phys. Rev. 139 (1965) 562.

.

PART III

Specialized Seminars

NUCLEON-NUCLEON POTENTIAL
WITH A SOFT CORE FOR
THE ISOTOPIC TRIPLET STATE

I. ÚLEHLA, J. BYSTRICKÝ, E. HUMHAL, F. LEHÁR,
V. LELEK, J. WIESNER
Faculty of Mathematics and Physics,
Charles University,
Prague, ČSSR

Abstract

NUCLEON-NUCLEON POTENTIAL WITH A SOFT CORE FOR THE ISOTOPIC TRIPLET STATE.
   A soft-core two-nucleon potential is computed as a superposition of Yukawa potentials. It contains the
central, spin, spin-orbit, quadratic spin-orbit, and tensor terms and depends on the total angular momentum J.
The parameters of the individual terms are given for the isotopic triplet state of the two-nucleon system.

The data of the unique phase-shift analysis of n-p and p-p elastic
scattering in the 0.17 – 310 MeV energy region [1] have been used for the
calculation of the soft-core potential for the isotopic triplet state, i.e.
for singlet even and triplet odd states.

It is obvious that the non-relativistic nucleon-nucleon potential can
be split uniquely into two non-mixing terms (the isotopic singlet and the
isotopic triplet term). In this paper, only the latter term is studied.
Moreover, it is possible to consider independently the singlet even and the
triplet odd state if a suitable representation of the potential is chosen. For
the singlet even state of the two-nucleon system, we have taken the soft-
core potential from our earlier paper [2], while the triplet odd state was
considered in this calculation.

The equation of the two-nucleon relative motion is written in the form

$$\left[\frac{d^2}{dx^2} + k^2 - \frac{j(j+1) - 2a}{x^2} - v \right] u = 0 \tag{1}$$

where

$$x = \mu r, \quad k^2 = \frac{m_N E_{lab}}{2 \mu^2}$$

$$\mu = 0.707 \cdot 10^{13} \text{ cm}^{-1}$$

$$m_N = 937 \text{ MeV} = 4.75 \times 10^{13} \text{ cm}^{-1}$$

The quantity E_{lab} is the energy of the incident particle, j is the total-
angular-momentum quantum number. Furthermore, we have

$$v \equiv v(x, j) = m_N \frac{1}{\mu^2} V(r)$$

where $V(r)$ is the potential energy. For the potential v the following representation [3] has been taken:

$$v(x, j) = v_0(x, j) + v_1(x, j) a + v_2(x, j) b + v_3(x, j) c + v_4(x, j) a^2 \tag{2}$$

$$a \equiv (\vec{S} \cdot \vec{L}) + \frac{S^2}{2}$$

$$b \equiv Z \frac{(\vec{r}\,\vec{S})^2}{r^2} - \frac{S^2}{2} = \frac{1}{3}\left(S_{12} + \frac{S^2}{2}\right)$$

$$c \equiv \frac{S^2}{2}$$

Here, $\vec{L}$ is the orbital momentum, $\vec{S}$ the spin of the system, and S_{12} the symbol of the tensor force.

If p-p scattering is considered, the term

$$V_c = \frac{m_N e^2}{nx} \qquad e^2 = \frac{1}{137}$$

should then be added to the potential (2).

For the singlet state

$$a = b = c = 0, \qquad j = \ell \tag{3a}$$

for the non-mixing triplet state

$$a = 0, \ b = c = 1, \ j = \ell \tag{3b}$$

for the state $^3P_0$

$$a = b = -1, \ c = 1 \tag{3c}$$

and for the coupled triplet state

$$a = \begin{vmatrix} j & 0 \\ 0, & -j-1 \end{vmatrix}, \ b = \frac{1}{2j+1} \begin{vmatrix} 1, & 2\sqrt{j(j+1)} \\ 2\sqrt{j(j+1)}, & -1 \end{vmatrix}, c = \begin{vmatrix} 1 & 0 \\ 0 & 1 \end{vmatrix} \tag{3d}$$

Each of the independent terms $v_i(x, j)$ is taken as the following superposition:

$$v_i(x, j) = \frac{e^{-x}}{x} \sum_{n=0}^{3} [a_n^{(i)} + j(j+1) b_n^{(i)}] \tag{4}$$

$$z = e^{-x}$$

where the expression

$$\sum_{n=0}^{3} [a_n^{(i)} + j(j+1) b_n^{(i)}] z^n = f_i(z, j) \tag{5}$$

represents the correction function to the simple Yukawa potential.

TABLE I. a_n AND b_n COEFFICIENTS FOR n-p ISOTOPIC TRIPLET STATES

Potential term	a_n	b_n
central v_0	$a_0 = -\ 2.06$ $a_1 = \ \ 31.8$ $a_2 = -179.6$ $a_3 = \ \ 212.2$	$b_0 = \ \ 0.183$ $b_1 = \ -4.9$ $b_2 = \ \ 29.9$ $b_3 = -41.9$
spin v_3	3.181 -59.97 288.5 -359.0	- 0.768 14.35 -71.03 97.80
spin orbit v_1	0.581 -21.62 152.5 -334.4	- 0.0461 1.180 -3.932 8.006
quadratic spin-orbit v_4	0.0855 5.418 -51.62 120.0	0.0250 -0.476 1.093 -1.280
tensor v_2	-0.665 33.88 -153.6 277.8	0.615 -9.835 45.68 -69.39

TABLE II. a_n AND b_n COEFFICIENTS FOR p-p ISOTOPIC TRIPLET STATES .

Potential term	a_n	b_n
central v_0	-2.30 40.0 -213.1 245.9	0.160 -4.1 23.1 -30.3
spin v_3	3.421 -68.17 322.0 -392.7	-0.745 13.55 -64.23 86.20

The unknown parameters $a_n^{(i)}$ and $b_n^{(i)}$ of the two-nucleon potential have been computed by the methods described in Ref.[3] to fit the scattering data.

Before doing it, we note that in the singlet state the potential (2) reduces to $v_0(x, j)$ whereas in the triplet state the term $v_0(x, j)$ occurs always in the sum $v_0(x, j) + v_3(x, j)$. That is why the parameters for singlet and triplet states can be computed independently.

Since the phase-shift analysis does not distinguish between p-p and n-p scattering in the triplet states, the Coulomb field (the term v_c) has not been used.

In Table I the coefficients $a_n^{(i)}$ and $b_n^{(i)}$ are given for n-p isotopic triplet states. Table II presents the parameters $a_n^{(i)}$ and $b_n^{(i)}$ for p-p isotopic triplet states in the case in which they differ from the values in Table I.

Note that the coefficients $a_n^{(i)}$ and $b_n^{(i)}$ are dimensionless. When using Eq.(1) we obtain the potential energy $V(r)$ in MeV

$$V(r) = v(x, j) \cdot 20.76 \text{ MeV}$$

In Figs 1-5 the correction functions $f_i(z, j)$ are given for $z \in \langle 1, 0 \rangle$, n-p. Their value at $z = 1$

$$f_i(1, j) = \lim_{x \to 0} x \, v_i(x, j)$$

defines the strength of the potential while the value $f_i(0, j)$ characterizes the behaviour of the potential at large distances.
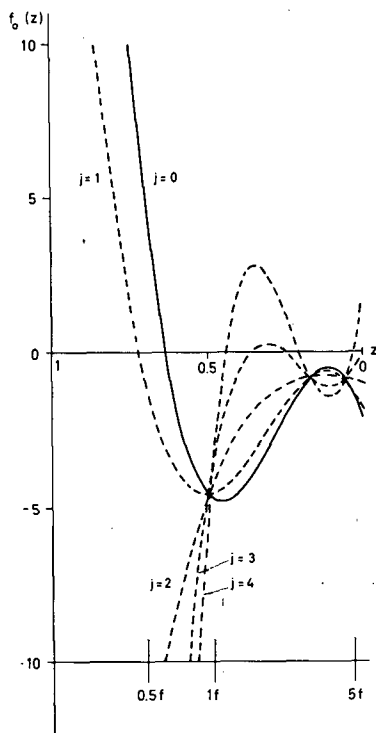
FIG.1.   Correction function $f_0(z, j)$.
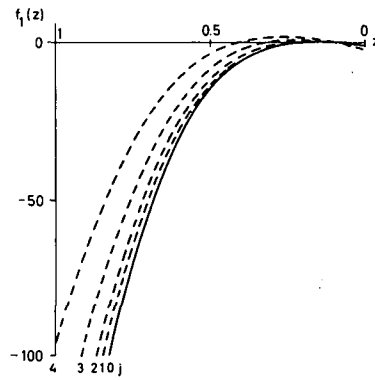
FIG.2. Correction function f_1 (z).
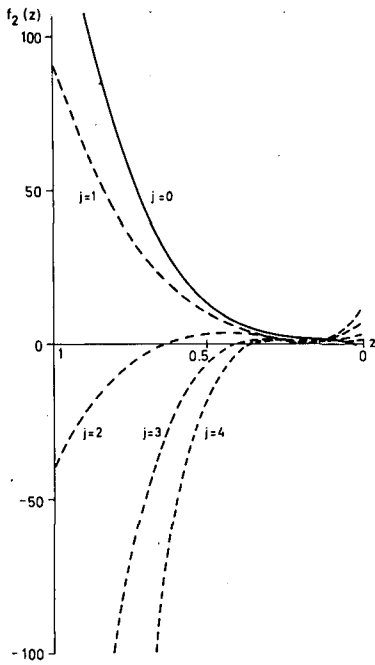
FIG.3. Correction function f_2 (z).
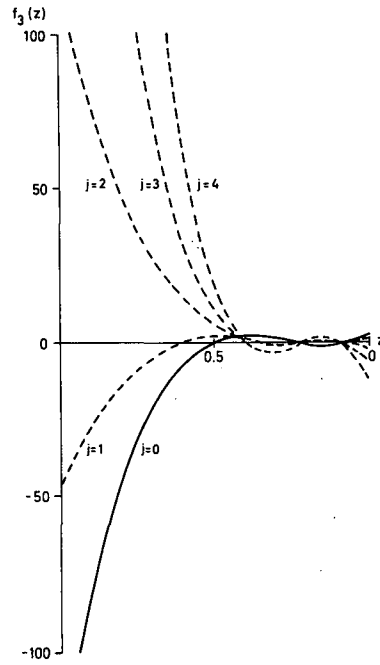
FIG.4. Correction function f_3 (z).
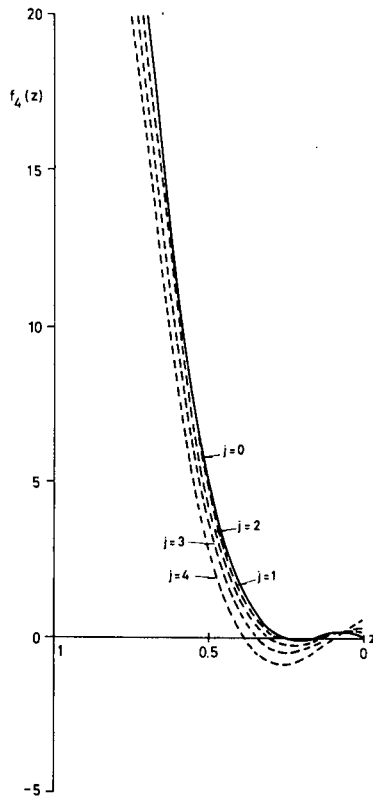
FIG.5.   Correction function $f_4(z)$.
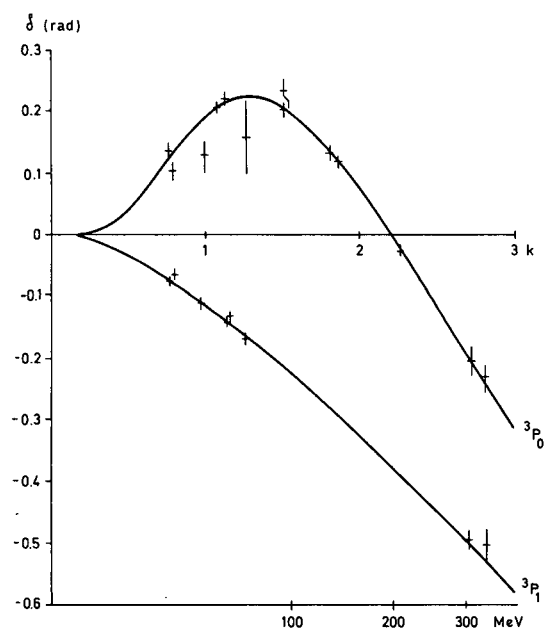
FIG.6.   Comparison of computed
phase-shifts with experimental ones.
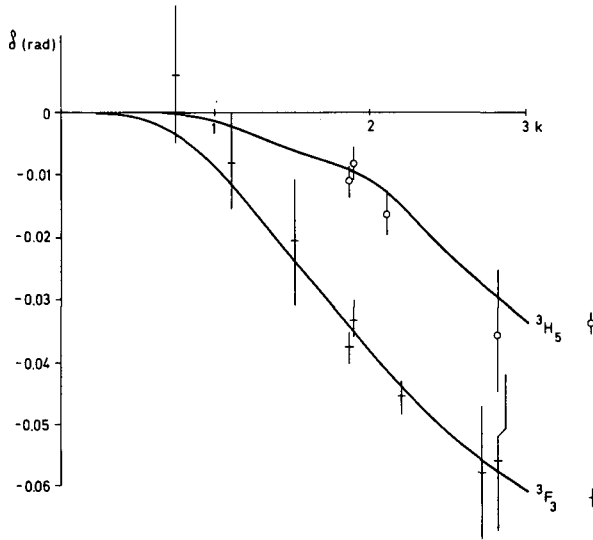
FIG.7.   Comparison of computed phase-shifts with experimental ones.
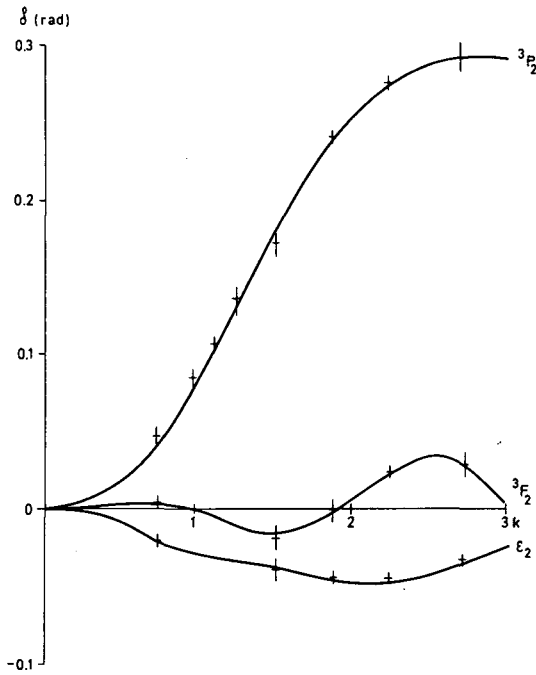
FIG.8.   Comparison of computed phase-shifts with experimental ones.

TABLE III. STRENGTHS AND CORRESPONDING x_0 VALUES

Potential term	0		1		2		3		4	
	f	x_0	f	x_0	f	x_0	f	x_0	f	x_0
central (0)	62.34	0.45	28.91	0.33	-37.96	-	-138.3	1.02	-272.0	0.82
spin (3)	-127.3	0.66	-46.58	0.5	114.8	2.3	357.0	0.97	679.8	0.91
spin orbit (1)	-202.9	3.2	-192.5	3.2	-171.6	1.3	-140.4	0.99	-98.74	0.83
quadratic spin orbit (4)	73.92	-	72.64	1.4	70.8	1.2	66.24	0.96	61.12	
tensor (2)	157.4	3.7	91.53	-	-40.20	0.45	-237.8	0.88	-501.2	1.04
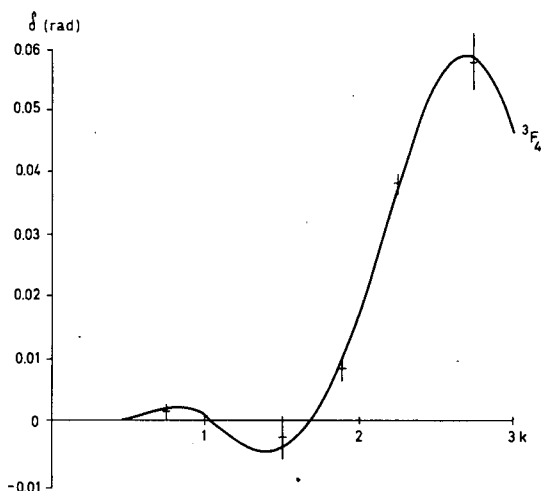
FIG.9. Comparison of computed
phase-shifts with experimental ones.

In Figs 6-9 the computed triplet phase shifts are plotted and compared with all experimental points used from Ref.[1]. The accuracy of the fit satisfies fully the χ^2-criterion.

Conclusions:

It has been shown that the experimental scattering data can be reproduced by a soft-core-type potential. The potential represented by expressions (2), (4), Table I and Table II is a superposition of the Yukawa potentials, i.e. each term, e.g. the spin-orbit term, is composed of four Yukawa potentials. All terms have repulsive and attractive parts but not each of them has a soft core.

The strength $f_i(1, j)$ of the potential term v_i indicates whether the potential is repulsive or attractive near the origin. In Table III the strengths are presented together with the corresponding number x_0. This number is the value of x for which the potential term has its first zero. It shows in which cases one can speak of a soft core. A typical soft-core potential has $x_0 < 0.707$, the others are merely repulsive or attractive near the origin (see also Figs 1 - 5).

The computations were performed on the Elliott-4130 Computer in Prague. The authors are indebted to Z. Janout for valuable discussions on phase-shift analysis.

REFERENCES

[1] KAZARINOV, Yu.M., et al., Preprint JINR P 2241, Dubna (1965);
    ARNDT, R.A., MacGREGOR, M.M., UCRL 12252 (1965);
    NOYES, H.P., Proc. Karlsruhe Conf. (1965);
    BILENKAYA, S.J., et al., Preprint JINR E 2609, Dubna (1966);
    KAZARINOV, Yu. et al., Preprint JINR E-1-2953, Dubna (1966);
    BILENKAYA, S.J., et al., Preprint JINR E-1-3899, Dubna (1968);
    JANOUT, Z., et al., Preprint JINR E-1-3707, Dubna (1968);
    Nucleons and Pions, JINR P-1-3971, Dubna (1968) 48-49.
[2] ULEHLA, I., et al., Proc. Int. Nucl. Phys. Conf. Gatlinburg, (1966).
[3] ULEHLA, I., Czech. J. Phys. 1969 (to be published).

THOMAS-FERMI THEORY OF ATOMIC NUCLEI

J. NÉMETH
Institute for Theoretical Physics,
Roland-Eötvös-University,
Budapest, Hungary

Abstract

THOMAS-FERMI THEORY OF ATOMIC NUCLEI.
A deduction of an integral equation for the density of nuclear matter is given. Its solution gives the energy and the density of nuclei as a function of their mass number.

Let us assume that we know a sufficiently weak effective scalar two-body interaction; we can then determine the energy of the system by the first-order perturbation theory. The Hamiltonian of a finite nucleus can be written as

$$H = \sum_i T_i + \frac{1}{2} \sum_{ij} v_{ij} = \sum_i T_i + \sum_i V_i + \frac{1}{2} \sum_{ij} v_{ij} - \sum_i V_i = H_0 + H_1 \tag{1}$$

where V_1 is the one-particle potential, which determines in zeroth order the single-particle wave functions, and

$$H_1 = \frac{1}{2} \sum_{ij} v_{ij} - \sum_i V_i$$

is small enough. In this case the unperturbed Schrödinger equation has the form

$$H_0 \Phi = \sum_i (T_i + V_i) \Phi = W_0 \Phi \tag{2}$$

and Φ can be written as the antisymmetric product of one-particle wave functions, which are determined by the equations

$$T_i \varphi_i + V_i \varphi_i = E_i \varphi_i \tag{3}$$

The energy of the system in first-order perturbation theory can then be obtained as

$$W = -\frac{\hbar^2}{2m} \sum_i \int \varphi_i^* \nabla^2 \varphi_i d^3 r + \frac{1}{2} \sum_{ij} \int \varphi_i^*(r_1) \varphi_j^*(r_2) v^D(r) \varphi_i(r_1) \varphi_j(r_2) d^3 r_1 d^3 r_2$$

$$+ \frac{1}{2} \sum_{ij} \int \varphi_1^*(r_1) \varphi_j^*(r_2) v^X(r) \varphi_1(r_2) \varphi_j(r_1) d^3 r_1 d^3 r_2 \tag{4}$$

where

$$v^D(r) = v_{even}(r) + v_{odd}(r)$$

$$v^X(r) = v_{even}(r) - v_{odd}(r) \tag{5}$$

In a simple Hartree–Fock theory we minimize this simple energy expression as a function of the density and in this way, we obtain equations determining the ground-state single-particle wave-functions

$$-\frac{\hbar^2}{2m}\nabla^2 \varphi_i(r_1) + \left(\sum_j \int \varphi_j^*(r_2) v^D(r)' \varphi_j(r_2) d^3 r_2\right) \varphi_1(r_1)$$

$$-\int \left(\sum_j \varphi_j^*(r_2) v^X(r) \varphi_j(r_1)\right) \varphi_i(r_2) d^3 r_2 = E_i \varphi_i(r_1) \tag{6}$$

Determining $\varphi_i(r)$ from Eq. (6) instead of Eq. (3) is a better approximation, but, of course, requires a much more complicate calculation since a system of non-linear integral equations has to be solved self-consistently. The harmonic-oscillator wave functions can be used as starting functions, but even in this case further approximations are necessary to solve Eq. (6). With the Thomas–Fermi method one does not want to get the single-particle wave-functions and single-particle energies, but only the density distribution and the total energy of nuclei with a given mass number. If we are content with learning only these very overall properties of nuclei, we may try a much simpler approximation than the HF approximation, i.e. we express the total energy of a nucleus as the function of the density, and minimize it as the function of ρ. In this way we obtain an integral equation for the density to be solved if we get the energy and the density of nuclei as a function of their mass number.

The direct energy term can be expressed very easily as the function of the density. Since $\displaystyle\sum_i |\varphi_i|^2 = \rho$, it can be written as

$$\frac{1}{2}\int \rho(r_1) \rho(r_2) v^D(r) d^3 r_1 d^3 r_2 \tag{7}$$

To express the kinetic and the exchange terms as a function of ρ, we have to use some kind of approximation. For the kinetic energy we use the so-called Thomas–Fermi approximation. For an infinite system the density can be expressed in terms of the Fermi momentum and the kinetic energy in terms of the density. In the following we assume that these relations are also valid for finite nuclei:

$$\rho(r) = \frac{2}{3\pi^2} k_F(r)^3 \tag{8}$$

$$W_{kin} = \frac{3}{5}\frac{\hbar^2}{2m} k_F(r)^2 \rho(r) \tag{9}$$

The above relations are valid in the first order. Weizsäcker [1] has shown, that we can write W_{kin} in a better approximation as

$$W_{kin} = \frac{3}{10} \hbar^2 k_F(r)^2 \rho(r) + \kappa \frac{\hbar^2}{8m} \frac{(\nabla\rho)^2}{\rho} \tag{10}$$

where κ is a constant, depending on the model potential. Weizsäcker used $\kappa = 1$, but Berg and Wilets [2] have shown, that κ changes between 0.1 up to 1, according to the model we use. Bethe [3] has given a detailed justification for expression (9) and he shows that it is valid for not too low densities, i.e. if

$$\rho > 0.15 \, \rho_c$$

The difficulty with the correction term is that we have to make our calculation in a local potential which is probably not good enough. Luckily, however, detailed calculations have shown [4] that the Weizsäcker correction term coming from the kinetic energy is negligible compared to the potential terms proportional to $(\nabla\rho)^2$ and $\Delta\rho$, so we can accept expression (9) in our calculations.

The determination of the exchange term as a function of the density needs some further approximations.

The exchange term can be written as

$$\frac{1}{2} \int \sum_i \varphi_i^*(r_1)\,\varphi_i(r_2) \sum_j \varphi_j^*(r_2)\,\varphi_j(r_1)\,v^X(r)\,d^3r_1\,d^3r_2 \tag{11}$$

Let us expand the φ-s around R, where

$$\vec{r}_1 = \vec{R} + \frac{\vec{r}}{2}, \qquad \vec{r}_2 = \vec{R} - \frac{\vec{r}}{2} \tag{12}$$

The expansion is justified by the fact that $v^X(r)$ is essentially short ranged, being a linear combination of Yukawa potentials

$$\varphi_i^*(r_1)\,\varphi_i(r_2) = \varphi_i^*(R)\,\varphi_i(R) + \frac{1}{2} r\,(\varphi_i(R)\,\Delta\varphi_i^*(R) - \varphi^*(R)\,\Delta\varphi_i(R))$$

$$+ \frac{1}{8} r_m r_n\,[\varphi_i(R)\Delta_{mn}\,\varphi_i^*(R) + \varphi_i^*(R)\Delta_{mn}\,\varphi_i(R) - 2\nabla_m\varphi_i(R)\nabla_n\,\varphi_i^*(R)] \tag{13}$$

If we average over the angle, we obtain v(r) being a central potential,

$$\overline{\varphi_i^*(r_1)\,\varphi_i(r_2)} = |\varphi_i(R)|^2 - \frac{r^2}{6}\,t_i(R) \tag{14}$$

where

$$t_i(R) = -\frac{1}{4}\left[\varphi_i\Delta\varphi_i^* + \varphi_i^*\Delta\varphi_i - 2\nabla\varphi_i\nabla\varphi_i^*\right] \tag{15}$$

is connected with the kinetic energy

$$W_{kin} = \frac{\hbar^2}{2m} \sum_i t_i(R) \tag{16}$$

With the help of Eq.(15), the exchange term can be written as

$$\sum_i \sum_j \int \left[|\varphi_i|^2 - \tfrac{1}{6} r^2 t_i(R) \right] \left[|\varphi_j|^2 - \tfrac{1}{6} r^2 t_j(R) \right] v(r) \, d^3r \, d^3R$$

$$= \int \left[\rho(R)^2 V_1 - \tfrac{1}{3} V_2 \, \rho(R) \sum_i t_i(R) \right] d^3R \tag{17}$$

where

$$V_1 = \int v(r) \, d^3r, \qquad V_2 = \int r^2 v(r) \, d^3r \tag{18}$$

In contrast to the direct term, the exchange term in this approximation is momentum-dependent and local. If we use again the Thomas-Fermi approximation (9), we may express Eq.(17) as a function of ρ:

$$\int V_1 \, \rho(R)^2 d^3R - V_2 \tfrac{1}{5} \int k_F^2(R) \, \rho(R)^2 d^3R \tag{19}$$

If we do not want to use the approximation (18), we may use again an infinite-nuclear-matter analogy. In fininite nuclear matter [3, 4]

$$\rho(r_1 r_2) = \sum_i \varphi_i^*(r_1) \, \varphi_i(r_2) = \frac{e}{\pi^2} \frac{\sin k_F r - k_F r \cos k_F r}{3} \tag{20}$$

and we may evaluate k_F at the point $k_F(R)$. The result is again a local term. Numerical calculations of Lin [3] and Moszkowski [5] with exactly soluble simple models have shown that the exchange term is a momentum-dependent local term in good approximation. The total energy of the system, using expressions (7), (9), and (19) can be written as

$$W = \int F[\rho(R)] \, d^3R + \tfrac{1}{2} \int v^D(r) \, [\rho(r_1) \rho(r_2) - \rho(r_1)^2] \, d^3r_1 d^3r_2 \tag{21}$$

where $\int F(\rho)$ is the energy of the system with constant density, so it is just the infinite-nuclear-matter energy at different densities. We can minimize Eq.(21) as a function of the density, with the subsidiary condition

$$\int \rho \, d\tau = A \tag{22}$$

$$\delta \left(W - E_F \int \rho \, d\tau \right) = 0 \tag{23}$$

$$E_F = \frac{dF(\rho(r_1))}{d\rho} + \int [\rho(r_2) - \rho(r_1)] \, v^D(r) \, d^3r_2 \tag{24}$$

If $\rho = $ const., we have $E_F = dF/d\rho$; this is just the Fermi energy of a particle. The value of $dF/d\rho = w_{nm}$ can be obtained from density-dependent nuclear-matter calculations and knowing $v^D(r)$ we can solve the density equations as the function of the mass number.

Transforming the Thomas-Fermi calculations into Hartree-Fock equations, we may check the validity of our basic approximations. The Hartree-Fock equations (6) can be written as

$$-\frac{\hbar^2}{2m}\nabla^2\varphi_i(r_1) + \left[\int \rho(r_2)v(r)d^3r_2\right]\varphi_i(r_1)$$

$$-\int \rho(r_1 r_2)v(r)\varphi_i(r_2)d^3r_2 = E_i\varphi_i(r_1) \tag{25}$$

Solving the non-linear integral-equation system (25) for φ_i and having used the Thomas-Fermi values for $\rho(r)$ and $\rho(r_1 r_2)$, we can calculate a Hartree-Fock ρ from the

$$\sum_i |\varphi_i|^2 = \rho$$

equation. We can do this iteration until we obtain a good ρ value. With this good φ_i and ρ values we can check the validity of the Thomas-Fermi approximations for the kinetic and the exchange energy and see how good are the results concerning the density and the energy of the system.

In the last few years, the Thomas-Fermi method was developed further by many people, who used the Brueckner theory of finite nuclei [6] instead of effective two-body forces. Recently, Bethe [3] outlined a Thomas-Fermi theory, which made maximum use of nuclear-matter theory. The chief aim was to start from the Brueckner theory of finite nuclei and again transform the energy into a function of density. To do this, the local-density approximation was used, with some modification.

Let us consider a system of an equal number of protons and neutrons, and we shall again neglect the Coulomb interaction. The energy of such a nucleus can be written in the first-order Brueckner approximation as

$$W = \sum_{m < k_F} \langle \phi_m | T | \phi_m \rangle + \frac{1}{2}\sum_{m,n}\langle \phi_m \phi_n | G | \phi_m \phi_n \rangle \tag{26}$$

where the G-matrix satisfies the usual equation

$$\langle \phi_{m'}\phi_{n'} | G | \phi_m \phi_n \rangle = \langle \phi_{m'}\phi_{n'} | v | \phi_m \phi_n \rangle$$

$$-\sum_{ab}\langle \phi_{m'}\phi_{n'} | v | \phi_a \phi_b \rangle \frac{Q(ab)}{E(a)+E(b)-E(m)-E(n)}\langle \phi_a \phi_b | G | \phi_m \phi_n \rangle \tag{27}$$

Here Q is the Pauli operator, E(a), E(b) are the particle energies, E(m), E(n) the hole energies, and $|\phi_m\rangle$, $|\phi_n\rangle$ are the finite single-particle wave functions. Let us separate the two-body forces into a short and long-range part

$$v = v_\ell + v_s \tag{28}$$

The G-matrix can be also separated into two parts

$$G = v_\ell + G' \tag{29}$$

where

$$G' = v_s - v \frac{Q}{e} G \qquad (30)$$

is essentially a short-range operator. We know anyhow that the effect of the G-matrix is

$$G \phi = v \psi = v (\phi - \chi)$$

where χ is the defect wave function, which is large around the repulsive core and falls off to zero very rapidly, and then is negative and of small absolute value: it is well known that the wave function in nuclear matter heals rapidly. Since the largest contributions to G' come from the inside and the surface of the repulsive core, we may assume that it does not depend too much on the long-range behaviour of the wave functions, so we can use a local-density approximation for G'.

Let us consider the interior and the surface of the nucleus. In the interior the density changes slowly, so in Eq.(27) we may use instead of $\phi_m \phi_n$, the plane-wave approximation for G'. At the surface ρ changes rapidly, but here, around the classical turning point, the second derivative of the wave functions is very small such that the substitution

$$\phi_m (r'_1) \phi_n (r'_2) = |m(R)\rangle |n(R)\rangle$$

can be made, namely we expand $\vec{r}'_1$, $\vec{r}'_2$ about $\vec{R}$, and approximate the product with plane waves having the same value at R.

There are, however, two corrections which we have to consider when substituting local density values into the G'-matrix elements. One of the corrections concerns the long-range tensor forces. If we want to use a local density approximation for G', the long-range tensor forces have to be contained in v_ℓ. However, now we want to use for v_ℓ a first-order Born approximation, which is not good enough for a tensor force. Kuo and Brown have shown that into the second-order Born-approximation term for the tensor force we can quite well substitute a first-order Born term of an effective, density-dependent central force. So v_ℓ contains the effective ρ-dependent tensor force, too.

The other correction arises in connection with the energy denominator. From infinite-nuclear-matter calculations we know that the particle energies can be treated as kinetic energies only if the potential energy of the particles is zero in good approximation. The energy denominator (27) contains, however, the whole single-particle energies of finite nuclei instead of those of nuclear matter. It is true,then, that for the G-matrix element of the right-hand side of Eq.(27) we can use plane-wave wave functions, but the difference of finite and infinite single-particle energies has to be taken into account.

Let us define a Thomas-Fermi G-matrix where in the energy denominator we use infinite-nuclear-matter single-particle energies, and a finite one

$$\left. \begin{array}{l} G_{TF} = v - v \dfrac{Q}{e_{TF}} G_{TF} \\[4mm] G_F = v - v \dfrac{Q}{e_F} G_F \end{array} \right\} \qquad (31)$$

$$G_F = G_{TF} + G_{TF} \left(\frac{Q}{e_{TF}} - \frac{Q}{e} \right) G_F = G_{TF} + G_{TF} \frac{Q}{e_{TF}} \Delta e \frac{Q}{e} G_F$$

where

$$\Delta e = e_F - e_{TF} \tag{32}$$

The matrix elements of G_F can then be written as

$$(\phi_m \phi_n \,|\, G_F \,|\, \phi_m \phi_n) = (\phi_m \phi_n \,|\, G_{TF} \,|\, \phi_m \phi_n) + (\chi_{mn}^{TF} \,|\, \Delta e \,|\, \chi_{mn}^F)$$

$$\sim (mn \,|\, G_{TF} \,|\, mn) + (\chi_{mn}^{TF} \,|\, \Delta e \,|\, \chi_{mn}^{TF}) \tag{33}$$

where

$$\chi_{mn} = |\, mn \rangle - \psi_{mn} = \frac{Q}{e} \, G \,|\, mn \rangle$$

is the defect wave function, and Δe, is, in good approximation, just twice the potential energy difference of holes in nuclear matter and finite nuclei. Δe is approximately independent of the momenta:

$$\Delta e \sim - 2\Delta u_{hole} \tag{34}$$

Separating G_F into a short- and a long-range part as we did in Eq. (29), we obtain the matrix elements

$$\langle \phi_m \phi_n \,|\, G_F \,|\, \phi_m \phi_n \rangle \sim \langle \phi_m \phi_n \,|\, v_\ell \,|\, \phi_m \phi_n \rangle$$

$$+ \langle mn \,|\, G'_{TF} \,|\, mn \rangle - 2\Delta u \langle \chi_{mn}^{TF} \,|\, \chi_{mn}^{TF} \rangle \tag{35}$$

The total energy of the nucleus with the Thomas-Fermi approximation for kinetic energy can be written as

$$W = W(\rho)_{NM} + \frac{1}{2} \int v_\ell^D (r \, \rho) \,[\rho (r_1) \rho (r_2) - \rho (r_1)^2] \, d^3 r_1 d^3 r_2$$

$$+ \frac{1}{2} \int v_\ell^X (r \, \rho) \left[|\, \rho (r_1 r_2)|_F^2 - |\, \rho (r_1 r_2)|_{NM}^2 \right] d^3 r_1 d^3 r_2$$

$$- \int \Delta u (R) \, \tau (R) \, d^3 R \tag{36}$$

where

$$\tau(R) = \sum_{nm} \int |\chi_{nm}^{TF}|^2 d^3 r \sim 0.14 \, \rho = \kappa \, \rho \tag{37}$$

from nuclear-matter calculations, and the exchange term is zero for the local approximation. Minimizing Eq. (36) as a function of ρ we obtain

$$E_F = w (\rho) + \int v_\ell^D (r \, \rho) \,[\rho (r_2) - \rho (r_1)] \, d^3 r_2 + \frac{1}{2} \int \frac{\partial v_\ell}{\partial \rho} \,[\rho (r_2) \rho (r_1) - \rho (r_1)^2] \, d^3 r_2$$

$$- \frac{\partial \Delta u}{\partial \rho} \, \kappa \, \rho - \kappa \, \Delta u \tag{38}$$

E_F is the Fermi energy of a finite nucleon, $w(\rho)$ its energy in nuclear matter, so if Δu is roughly independent of the momentum, $E_F - w(\rho) = \Delta u$. Solving Eq.(38) approximately we obtain

$$E_F - w(\rho) = \Delta u = \frac{1}{1+2\kappa} \left\{ \int v_\ell^D(\rho r) [\rho(r_2) - \rho(r_1)] d^3 r_2 \right.$$

$$\left. + \frac{1}{2} \int \frac{\partial v_\ell^D(\rho r)}{\partial \rho} [\rho(r_2)\rho(r_1) - \rho(r_1)^2] d^3 r_2 \right\} \tag{39}$$

Solving Eq.(39), we get the density of the nuclei. Substituting this ρ into the energy

$$W = W_{NM} + \frac{1}{2(1+2\kappa)} \int v_\ell^D(\rho r) [\rho(r_1)\rho(r_2) - \rho(r_1)^2] d^3 r_1 d^3 r_2$$

$$- \frac{\kappa}{2(1+2\kappa)} \int \frac{\partial v_\ell^D(r\rho)}{\partial \rho} [\rho(r_2)\rho(r_1)^2 - \rho(r_1)^3] d^3 r_1 d^3 r_2 .$$

we obtain the energy of nuclei for a given A. From Eq.(40) it is easy to see that the effective forces obtained from this simple Thomas–Fermi approximation are

$$v_{eff}(\rho r) = G(\rho) \delta(\vec{r}) + \frac{1}{1+2\kappa} v_\ell(\rho r) [1 - \delta_{\rho(r_1)\rho(r_2)}]$$

$$- \frac{\kappa}{2(1+2\kappa)} \rho \frac{\partial v_\ell^D}{\partial \rho} [1 - \delta_{\rho(r_1)\rho(r_2)}]$$

where $G(\rho)$ is just the nuclear-matter effective force, i.e. the G-matrix coming from nuclear-matter calculations as a function of density. The concrete mathematical form of the effective forces (41) using as a starting point the Reid soft-core potentials [7] and the nuclear-matter calculations of Sprung [8] and Siemens [9], can be found in Ref.[10].

The integral equation (39) has been solved by Bethe and Németh [11]. The total surface energy of the nuclei, as the function of the mass number, can be written as

$$W_{surf} = 19.6 A^{2/3} + 9A^{1/3}$$

which is in good agreement with the experimental values [19 ± 1 MeV] of different semi-empirical mass formulas. The surface thickness defined by Bethe

$$6 = \frac{\rho_c}{\rho'_{max}} \sim (2 - 2.2) fm$$

changes very slightly with the mass number and is in good agreement with the electron-scattering experiments. The central density of nuclei increases slightly as a function of the mass number.

The calculations can be applied for different proton and neutron numbers including also the Coulomb forces. In this case, instead of Eq.(39),

we obtain two non-linear coupled integral equations, which can be solved by iteration. Such calculations are being done (Ref.[12]).

REFERENCES

[1] WEIZSÄCKER, Z., Physik 96 (1955) 431.

[2] BERG, P., WILETS, Z., Proc. Phys. Soc. A68 (1955) 229.

[3] BETHE, H.A., Phys. Rev. 167 (1968) 879.

[4] NÉMETH, J., BETHE, H.A., Nucl. Phys. A116 (1968) 241.

[5] MOSZKOWSKI, S. (private communication).

[6] BRUECKNER, K.A., GAMMEL, J.L., WEITZNER, H., Phys. Rev. 110 (1958) 431;
    BRUECKNER, K.A., LOCKELT, A.M., ROTENBERG, M., Phys. Rev. 121 (1961) 255.

[7] REID, R., Annls Physics 50 (1968) 411.

[8] SPRUNG, D.W.L., (to be published).

[9] SIEMENS, P., (to be published).

[10] NÉMETH, J., Acta Phys. Hung. (to be published).

[11] BETHE, H.A., NÉMETH, J., (to be published).

[12] NÉMETH, J., (to be published).

OCTUPOLE STATES OF DEFORMED NUCLEI

P. VOGEL*
Nuclear Research Institute,
Řež, Czechoslovakia

Abstract

OCTUPOLE STATES OF DEFORMED NUCLEI.
   1. Introduction; 2. Standard calculations; 3. Results of calculations; 4. The nuclear potential energy as a function of the octupole deformation parameters; 5. Coriolis interaction.

1. INTRODUCTION

In almost all even-even nuclei one can observe a number of low-lying states strongly excited in electric inelastic processes of the low multipole order. A typical spectrum of a spherical nucleus is shown in Fig.1.
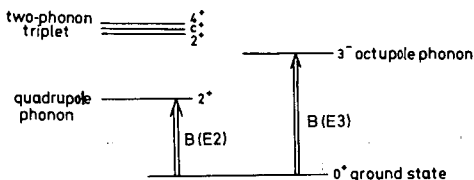
FIG.1.   A typical spectrum of a spherical nucleus.

The low-lying states are called vibrations or phonons. They are characterized by angular-momentum (and sometimes also by spin or isospin) quantum numbers. The measured quantities are the energy ω_λ and the B(Eλ) transition probability.

For a deformed nucleus, the angular momentum is no longer a good quantum number. However, the states may be characterized by a number K – the projection on the symmetry axis. States with +K and -K give rise to a single intrinsic state only. Thus, from the octupole 3⁻ state in the spherical nucleus one obtains a quadruplet $K^\pi = 0^-$, 1^-, 2^-, 3^- in the deformed nucleus.

Even though the total angular momentum of the vibration is not a constant of motion, one may often characterize the vibrations by a parameter λ, which, in the spherical limit, would correspond to the multipole order. λ also determines the parity of the phonon $\pi = (-1)^\lambda$. The numerical value of the deformation parameter is small compared to unity; however, it substantially modifies the wave functions and energies of the nucleons outside filled shells. And since low-energy vibrations are largely associated with such nucleons, the modes with the same λ but different K may have rather different properties.

---

* On leave at Niels Bohr Institute, Copenhagen, Denmark.

The experimental evidence of the octupole states was rather poor until recently. Only $K^\pi = 0^-$ states around $A = 225$ were known (from α-decay). Nowadays, – thanks, primarily, to the systematic measurement of the (d, d') reactions in the group of Professor Elbek in Copenhagen – our knowledge is more complete. In almost each of the even-even rare-earth nuclei several octupole states are known. Unfortunately, the K-numbers are seldom known with certainty.

2. STANDARD CALCULATIONS

We shall not go into the details of the mathematical method used in the usual calculation. It is the quasi-particle RPA and we shall use Professor Pal's contribution to these Proceedings as a reference. What one needs for the actual calculation is the particle-hole spectrum (or the two-quasi-particle spectrum) and the form and parameters of the residual interaction.

To build a 3^- state one needs a particle and a hole (or two quasi-particles) with opposite parities. It is well known that one can divide the possible 3^- particle-hole states into three groups:

"inside shell"	with energy	2Δ
$\Delta N = 1$	-"-	$\hbar\dot\omega_0$
$\Delta N = 3$	-"-	$3\,\hbar\dot\omega_0$

In the $150 \leq A \leq 190$ region there are two strong "inside-shell" transitions, for protons the $d_{5/2} - h_{11/2}$ one and for neutrons the $f_{7/2} - i_{13/2}$ one. When the shell is filled the contribution from the $\Delta N = 3$ and $\Delta N = 1$ states is varied smoothly, while the contributions from 2Δ states can jump from one nucleus to another. For the low-lying vibrations the "inside-shell" states are the most important even if they carry a rather small part of the full transition strength.

When the nucleus is deformed, every sub-shell is split into states with different K. Thus, the energy and strength of the two-quasi-particle state will depend on K, too, the K=0 state being lowest as a rule. This can be understood from classical arguments, i.e. the vibrations with K = 0 are along the polar axis – with the lowest frequency – while those with K = 3 are perpendicular to it – with the highest frequency.

The division of the available states into the three groups mentioned will not be so sharp in the deformed nucleus. And the dimensionality of the problem will grow very much. Thus, we have not much choice in the residual interaction problem. The only force which one can handle is a schematic force with separable matrix elements. Then a diagonalization is not necessary. There are several possible schematic forces; let me mention

octupole-octupole force $\qquad -\kappa\, J_{3\mu}^{*}\ (\vec{r}_1)\, J_{3\mu}\ (\vec{r}_2)$

SDI (surface delta interaction) $\ -F\,\delta\ (\vec{r}_1 - \vec{r}_2)\,\delta\ (\vec{r}_1 - R)$

for both

$$\langle\, a\,b\ |V|\ c\,d\,\rangle = V_{ab}\, V_{cd}$$
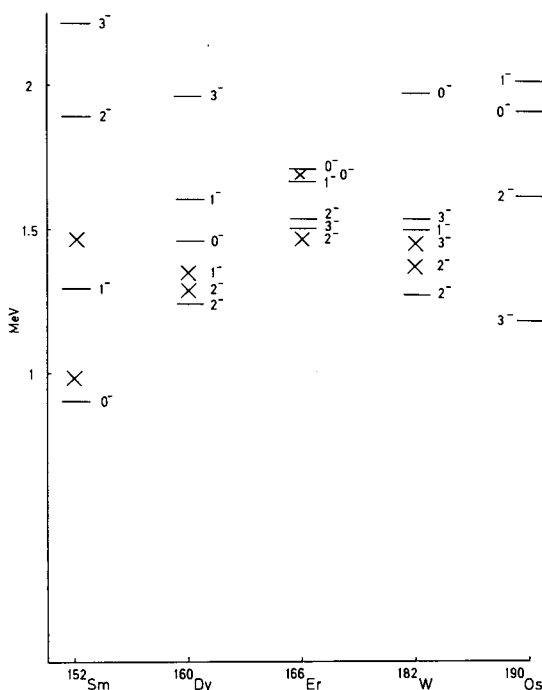
FIG.2. Splitting of the $I^\pi = 3^-$ quadruplet in several rare-earth nuclei (X experimental, —— theory).

3. RESULTS OF CALCULATIONS

Several calculations of octupole-state properties were performed during the last few years with different level schemes and residual interactions. We want to mention studies made by Professor Soloviev's group in Dubna with the octupole-octupole force and those by Professor Faessler et al. with the SDI. All the calculations gave essentially equivalent results.

The theory must explain two main features: the splitting of the octupole quadruplet and the behaviour of the full B(E3) strength. The first quantity is illustrated in Fig.2. For small deformation, one expects

$$\omega_K = \omega_{\text{spherical}} + \epsilon X \langle 32 K 0 \mid 3 K \rangle$$

It seems that X changes sign, when passing from the Sm to Os. In Fig.3 we see a rather good agreement between theory and experiment in the $\Sigma B(E3)$ value. The decrease of the $\Sigma B(E3)$ as well as the be-haviour of X could be connected with the filling of the $h_{11/2}$ proton and $i_{13/2}$ neutron sub-shells. One can give the following simple arguments: When the atomic number A increases from A = 150 to A = 190 there are states (from the mentioned subshells) with larger and larger projections K near the Fermi surface. Therefore, there is less and less possibility of building up the octupole state (decrease of $\Sigma B(E3)$) and the higher K quantum numbers will be more and more preferred (change of splitting).
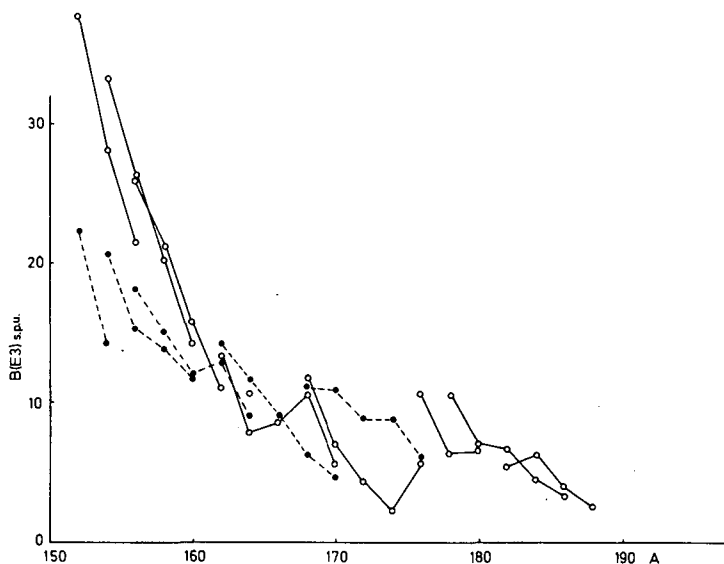
FIG.3.   The ΣB(E3) for the lowest octupole states (---- experimental, ——— theory).

Similar results can be obtained analytically if quadrupole deformation is taken in the perturbation approach.   More detailed comparison of the theory with experiment is shown in Figs 4 - 7. Note the discrepancy in the B(E3) values for $K^\pi = 2^-$ states in the Dy and Er isotopes.

We have not yet mentioned the other characteristic feature of the octupole states.   Their rotational bands are often strongly distorted. Sometimes, they do not follow the $I(I+1)$ rule and if the moment of inertia can be extracted from the experimental energies it is much larger than the J for the ground-state band.

So there are two open (closely related) problems:
1.   The division of the full oscillator strength between states with different K.
2.   The properties of the rotational bands.

One can attack the problems from two sides.   The first possibility is to consider the possible deviations from the picture of the independent harmonic phonons.   Such an assumption is implicitly made by using the RPA-type of calculations.   This approach is discussed in the next paragraph.

4.   THE NUCLEAR POTENTIAL ENERGY AS A FUNCTION OF THE OCTUPOLE DEFORMATION PARAMETER

To approach the problem, the β_2- and β_3-dependence of the potential-energy part of the collective Hamiltonian was calculated. Nuclei with $218 \leq A \leq 232$, i.e. in the beginning of the deformed actinide region, were selected because here maximal deviations from the simple harmonic quadratic dependence could be expected.
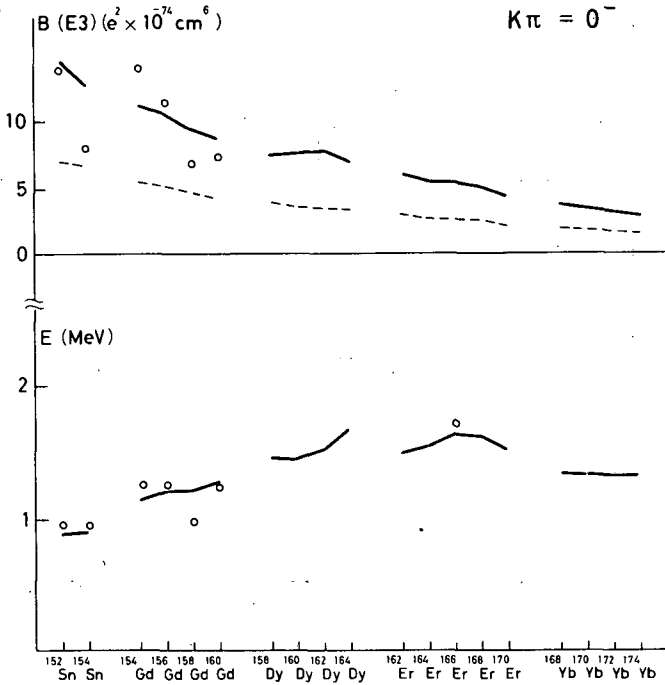
FIG. 4.   Calculated and experimental energies and B(E3) values for $K\pi = 0^-$.

in B(E3)   ——— $e_{eff} = 0.15$,   - - - - $e_{eff} = 0$

in E $\dfrac{0.44}{A^{4/3}}$. $(1 - \dfrac{4}{5} \epsilon)\, \hbar\overset{\circ}{\omega}_0 = \dfrac{0.37}{A^{4/3}} \equiv \kappa$

The energy is of the form

$$\langle H_0 + H_{pair} \rangle \equiv \mathscr{E}(\beta_2, \beta_3) = 2 \sum_s \epsilon_s (\beta_2, \beta_3)\, v_s^2 - \Delta^2/G$$

where $\epsilon_s(\beta_2, \beta_3)$ are the eigenvalues of $H_0(\beta_2, \beta_3)$. In analogy to the
Nilsson potential the nucleons are forced to move in a common potential

$$V = \tfrac{1}{2} M \overset{\circ}{\omega}_0\, r^2 \left(1 + \frac{5}{4\pi}\, (\beta_2^2 + \beta_3^2)\right)$$

$$\otimes \left[1 - 2\beta_2 Y_{20} - 2\beta_3 Y_{30} + 18 \sqrt{\frac{3}{35\pi}}\, \beta_2 \beta_3\, Y_{10} \right]$$

Such a potential conserves the volume and the centre-of-mass position.
In Fig.8 the maps of the potential-energy surfaces for several nuclei
are shown. We see that the minimum is always at $\beta_3 = 0$; this means
that no nuclei with stable octupole deformation exist in this (most
favourable) region. On the other hand, the curves in the figures differ
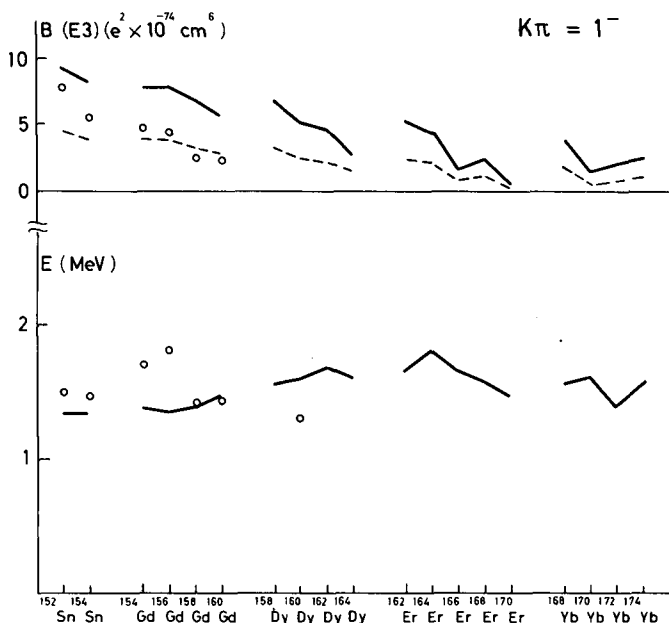
FIG. 5.   Calculated and experimental energies and B(E3) values for $K\pi = 1^-$.
—— $e_{eff} = 0.15$,   ---- $e_{eff} = 0$

$$\frac{0.46}{A^{4/3}} \quad (1 - \frac{3}{5} \epsilon) \hbar\overset{\circ}{\omega}_0 = \frac{0.40}{A^{4/3}} \equiv \kappa$$

from the predictions of the harmonic approximation, i.e. from a system
of ellipses with the axes in the β_2- and β_3-directions.

The "valley" in the β_3-direction is not parallel to the β_3-axis;
this means that there is an interaction between quadrupole and octupole
phonons. The curvature of $\mathscr{E}(\beta_3)$ decreases as β_2 increases, i.e. the
restoring force decreases for larger deformations. All these features
are most strongly pronounced for the transition nuclei. In both spherical
and strongly deformed nuclei the deviations from harmonicity are smaller.
So these calculations form some basis for our discussion today; they
show that in the strongly deformed nuclei the independent octupole
phonons are a good "zero" approximation.

5. CORIOLIS INTERACTION

The other possible reason for the discrepancies mentioned may
lie in the Coriolis interaction. Such an interaction arises inevitably when
a deformation is present. It will cause mixing between different bands
and distortion of the rotational sequences. The Coriolis interaction is of
the well-known form

$$- \frac{\hbar^2}{2\mathscr{J}} (I_+ j_- + I_- j_+)$$
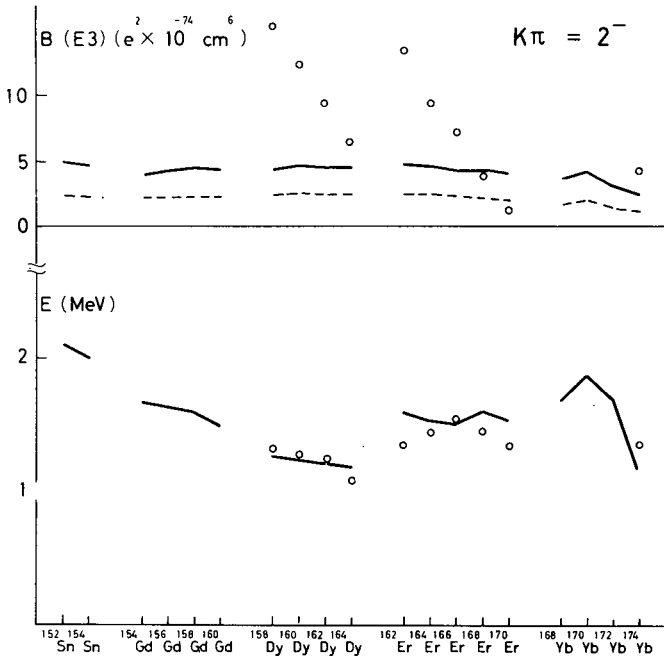
FIG. 6.   Calculated and experimental energies and B(E3) values for $K\pi = 2^-$.
——— $e_{eff} = 0.15$, ---- $e_{eff} = 0$

$$\kappa = \frac{0.45}{A^{4/3}} \ \hbar\overset{\circ}{\omega}_0$$

Thus, to find its influence, one has to know the matrix element of the form

$$M = \langle Q_{K+1} | j_+ | Q_K^+ \rangle$$

To obtain the corresponding formula, the contribution from all processes with phonon K in the initial and phonon K + 1 in the final state and the "field" j_+ acting in between must be summed.

The most important processes are shown in Fig.9. There exist four more of the same order, but probably less important. The corresponding formula for the two mentioned graphs is

$$M = \sum_{1, 2, 3} \langle 1 | j_+ | 2 \rangle \ (\psi_{13}^K \psi_{23}^{K+1} - \varphi_{13}^K \varphi_{23}^{K+1}$$

where ψ_{13}^K, φ_{13}^K are the components of the phonon K for quasi-particles 1, 3 (φ coming from the backward directed graphs).

The influence of the Coriolis interaction will be important if the dimensionless quantity

$$\frac{\hbar^2}{2\mathcal{J}} \ \sqrt{I(I+1)} \ \frac{M}{\omega_K - \omega_{K+1}}$$

is not too small (compared to unity), i.e. M must be larger than unity.
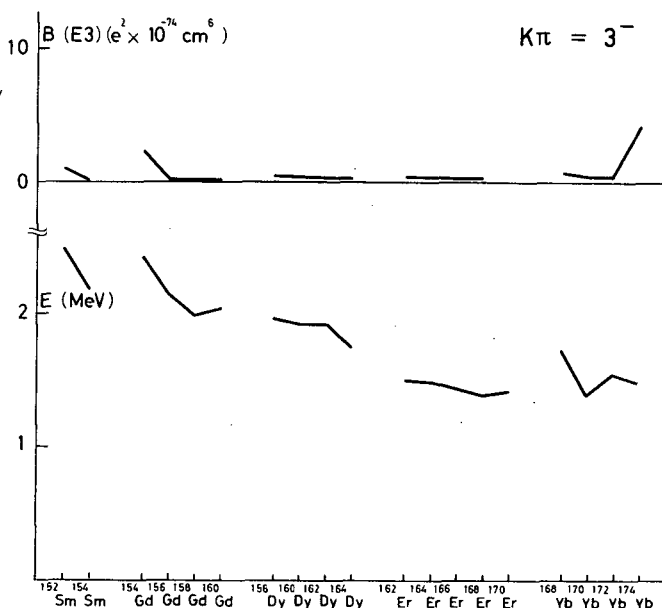
FIG. 7.   Calculated and experimental energies and B(E3) values for $K\pi = 3^-$.

$$\kappa = \frac{0.59}{A^{4/3}} \, \hbar\overset{\bullet}{\omega}_0 = \frac{0.44 \, (1 + \epsilon)}{A^{4/3}} \, \hbar\overset{\bullet}{\omega}_0$$

There is no very transparent reason for any coherence effects in a sum like M. However, one can give some arguments in favour of it. In the spherical nucleus the $Q^+_{\lambda K}$ operator is a spherical tensor (λ, K), therefore, in this limit, the matrix element M is given by

$$M = \sqrt{(\lambda - K) (\lambda + K + 1)}$$

This is a rather large number. However, for a deformed state, $Q^+_{\lambda K} | 0 \rangle$ has no definite angular momentum, and the M can be different from the limiting case. In the limit when both K and K + 1 states are close to the two-quasi-particle ones, the resulting M has nothing to do with the spherical value. They can be large, only if the two states have a common quasi-particle and the matrix element for the other states is not hindered.

With the phonon wave functions already known we have calculated the M for several nuclei. Unfortunately, the program is technically not very simple, and each run needs a considerable amount of computer time. Therefore the results are accumulated rather slowly and only a small part of preliminary data is available now.

However, the first results show that

a)   matrix elements between two collective states are really large, though smaller than the spherical limit;
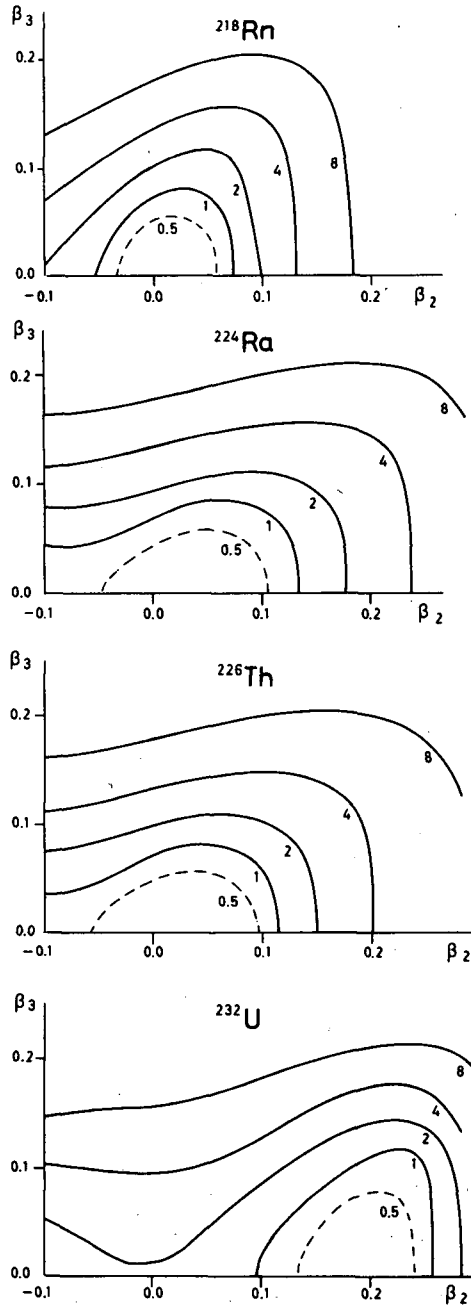
FIG. 8.   The "maps" of the potential energy in the β_2, β_3 plane.
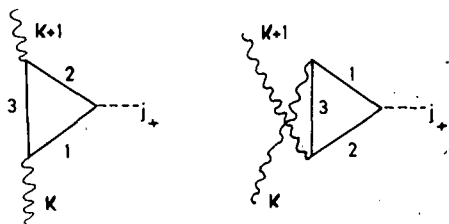
FIG.9.   The most important processes.
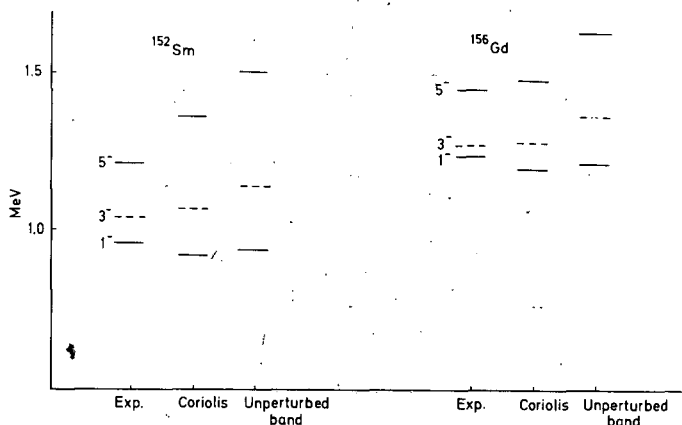
FIG.10.   Effect of the first-order Coriolis interaction on the bands with $K^{\pi} = 0^{-}$ in ^{152}Sm and ^{156}Gd.

b) matrix elements between a collective and non-collective state are about ten times smaller. Therefore, for the analysis of the collective states, only the collective partners are important. The two-quasi-particle ones may cause a slight renormalization of the moment of inertia; and

c) the influence of the Coriolis interaction is the right direction (Fig.10), but not great enough. The mixing of the 3^{-} states is about 15% in ^{152}Sm and 30% in ^{156}Gd.

The remaining discrepancy can probably be attributed to higher-order effects or to neglected graphs (which, however, give zero in the spherical limit). But it is clear already that the Coriolis interaction is rather important for understanding the remaining problems.

BIBLIOGRAPHY

[1] General theory of the vibrations in the "microscopic nuclear model". BOHR, A., MOTTELSON, B., Lectures on Nuclear Structure and Energy Spectra (first volume published).

[2] Experimental data concerning the octupole states. HYDE, E.K., PERLMAN, I., SEABORG, G., The nuclear properties of the heavy elements, New Jersey (1964). ELBEK, B., Tokyo Conference 1967, paper 4.90.

[3] Calculations of the octupole states. SOLOVIEV, V.G., VOGEL, P., KORNEICHUK, A.A., Izv. Akad. Nauk SSSR, ser. fiz. 28, 1599. FAESSLER, A., PLASTINO, A., Nucl. Phys. A116; (1968) 129. NEERGAARD, K., Thesis (unpublished), Copenhagen (1969).

[4] Potential energy as a function of β_3. VOGEL, P., Nucl. Physics A112 (1968) 583.

A MODEL FOR THE ^{28}Si SPECTRUM

J.P. SVENNE
Institut de Physique Nucléaire
Orsay, France

Abstract

A MODEL FOR THE ^{28}Si SPECTRUM.
    The author presents a model which explains all the levels of the ^{28}Si spectrum below 8 MeV. [1]

There seems to be considerable difficulty in understanding the spectrum of ^{28}Si. Though the nuclei at the beginning of the s-d shell exhibit characteristic rotational spectra [1] which are quite easily described as a projection [2] from a deformed intrinsic Hartree-Fock (H.F.) state (as discussed in my papers), this agreement breaks down toward the middle of the shell. In Fig. 1 the experimental spectrum [1] of ^{28}Si is shown along with some theoretical calculations which will be discussed here. In particular, note the poor agreement with the projected H.F. spectrum.

The lowest levels, 0^+, 2^+, 4^+ look somewhat like the beginning of a rotational band, $E_J = A J (J+1)$, but

$$\frac{E(4^+) - E(2^+)}{E(2^+) - E(0^+)} = \frac{4.61 - 1.78}{1.78} = 1.59$$

whereas the $J(J+1)$ law would give $7/3 = 2.33$. The other feature of the ^{28}Si spectrum is the low-lying 0^+ state and the rather complicated structure at around $7-8$ MeV. I will propose here a model which attempts to explain essentially all the levels below 8 MeV. But first let me discuss some of the past work.

Ripka [2] has performed H.F. calculations on ^{28}Si taking ^{16}O as an inert core and using two different effective forces: a Serber and a Rosenfeld force. Then, using the Peierls-Yoccoz [3] projection technique, he calculates the spectrum of rotational levels, according to [1]:

$$E_J = \frac{\int_0^\pi \sin\beta \, d\beta \, d_{kk}^J(\beta) \langle \Psi_k | e^{-i\beta J_y} H | \Psi_k \rangle}{\int_0^\pi \sin\beta \, d\beta \, d_{kk}^J(\beta) \langle \Psi_k | e^{-i\beta J_y} | \Psi_k \rangle} \tag{1}$$

where Ψ_k is the H.F. wave-function of the (oblate) deformed intrinsic state. He finds that the two forces give essentially the same spectrum, even though the single-particle spectra in the two cases are quite different. In particular, the gap between the occupied and unoccupied orbitals in the case of the Serber force is less than $1/2$ that obtained for the Rosenfeld force. But in both cases, the projected spectra are compressed by

---

[1] See the other contribution of Svenne to these Proceedings, and Ref.[2].
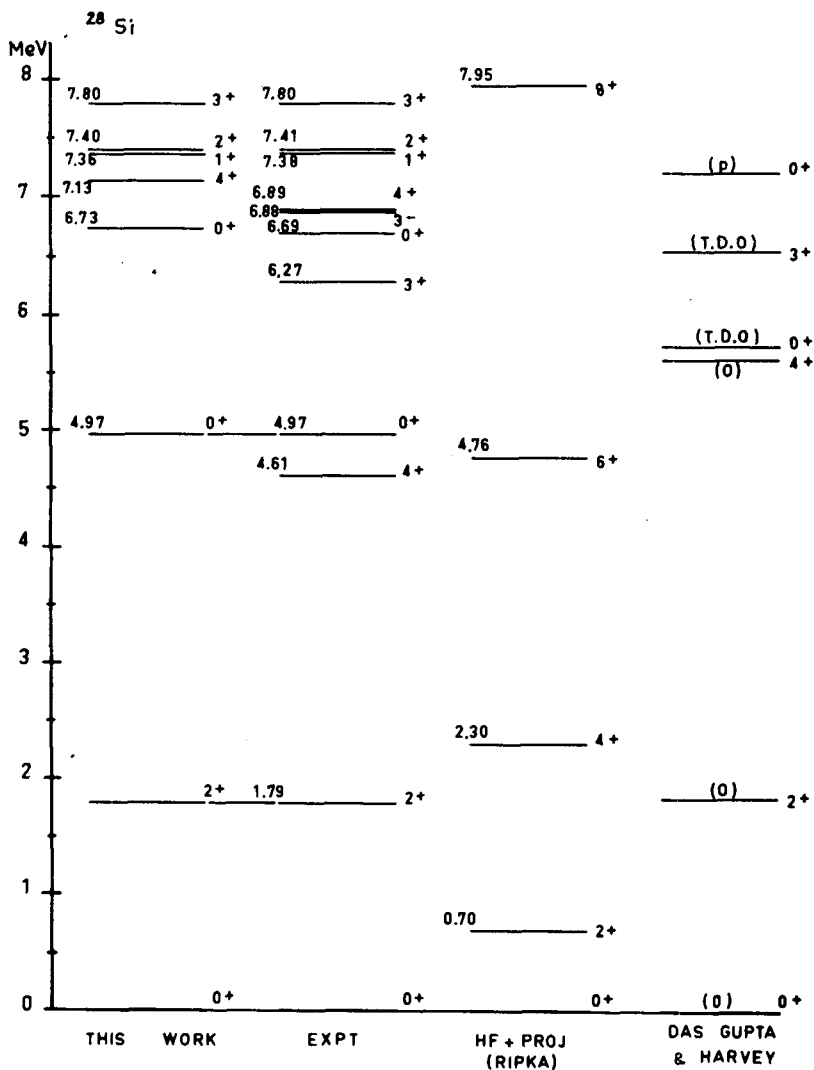
FIG.1.   Comparison of the experimental spectrum of ^{28}Si with theoretical calculations.

about a factor of 2 relative to the experimental ones (see Fig.1).   The
same disagreement is seen if the projection is done on the prolate deformed
solution[2] Ripka suggests that the H.F. solutions obtained for ^{28}Si are too
deformed.   I would like to suggest here that because of the near degeneracy
of the prolate and oblate solutions, the true deformation of ^{28}Si is in neither
one of these two H.F. minima, but somewhere in between, and, in fact,
that the low-energy spectrum of ^{28}Si is dominated by an interaction of these
two minima.

---

[2] Projection from both prolate and oblate solutions has also been done in a recent work of Tewari and
Guillot [Phys. Rev. 177 (1969) 1717], but they also find a spectrum which is too compressed.

A recognition of the need to take into account both the oblate and prolate structures in discussing the low-energy spectrum of ^{28}Si is the work of Das Gupta and Harvey [3]. They explain the ^{28}Si spectrum as an inter-leaving of levels based on the oblate and prolate minima, obtained both by projection from the deformed H.F. minima, and by particle-hole, Tamm-Dancoff calculations on each minimum. They obtain many more of the observed levels, but must multiply, arbitrarily, their calculated spectrum by a factor of two in order to obtain reasonable agreement in the positions of the levels. They cannot satisfactorily explain this factor of two. Perhaps part of the flaw is that they considered the two systems of levels as es-sentially independent, whereas it would be reasonable to expect them to interact rather strongly. This is perhaps inherent in their suggestion towards the end of the paper that ^{28}Si could be expected to be "soft" toward β-vibrations about the oblate minimum.

In fact, vibrations should be possible about either minimum. Follow-ing this approach, Castel and the author [4] have considered a model in-volving vibrations about the two minima, coupled through their quadrupole field. This is merely a simple model and not a serious attempt to explain the spectrum from a microscopic point of view. Free parameters remain which are chosen to fit the spectrum. However, it is a suggestion of a possible direction which a detailed calculation might take, and may also be a simple model by which experimental spectra in other, similar cases might be described.

In an H.F. calculation on ^{28}Si, with a basis consisting of the 1s, 1p, 2s-1d and 1f$_{7/2}$ shells (no inert core), and using the Kuo [5] effective matrix elements, we find an oblate lowest minimum and a local prolate minimum lying 3 MeV higher in energy. These are both, in fact, true minima, stable toward γ-deformations, as we have verified by actual calculations. The spherical solution is also a self-consistent one, but is actually a maximum and lies much higher in energy.

We suggest here that the nucleus can vibrate about either minimum, and that these vibrations can couple through their quadrupole moments. The 0$^+$ ground state is associated with the oblate minimum and the first 2$^+$ state, as a one-phonon state built on it. The second 0$^+$ state at 4.97 MeV is associated with the prolate minimum. Its separation from the ground state is more than the difference in the H.F. minima, since we would expect them to mix and therefore be pushed apart. The one-phonon state built on the prolate "ground state" has no independent existence but is broken down into a multiplet of levels, centred around 7 MeV, because of its strong coupling with the phonon belonging to the oblate state.

We write the Hamiltonian for this model as

$$H = \hbar\omega_1 \sum_m b_m^\dagger b_m + \hbar\omega_2 \sum_m c_m^\dagger c_m + E_0 + H_{int} \qquad (2)$$

Here $b_m^\dagger$ is a boson-creation operator creating a vibration of energy $\hbar\omega_1$ at the lowest minimum and $c_m^\dagger$ a similar operator for the vibration of energy $\hbar\omega_2$ at the other minimum. E_0 is the energy difference between the two minima, and the interaction is written as[3]

---

[3] The simpler choice, $H_{int} = K \sum_m (-)^m b_m^\dagger c_m + H.c.$ is not interesting since, by a change of variables, it breaks down into two uncoupled vibrations.

$$H_{int} = K \sum_M (-)^M Q_{bM} Q_{c-M} \tag{3}$$

Here the quadrupole operator is

$$Q_{bM} = \sum_{m_1 \overline{m}_1} (2m_1 2\overline{m}_1 | 2M) (-1)^{m_1} b^\dagger_{-m_1} b_{\overline{m}_1} . \tag{4}$$

with a similar definition for the C-operators; K is an interaction strength. To calculate the energies of the coupled phonon states, we evaluate the matrix elements of H_{int} in states of one phonon of type b and one of type c, noting that b and c phonons are not, in general, orthogonal states. If we let $(1-\alpha^2)^{\frac{1}{2}}$ denote the overlap between b and c phonons, we obtain the following expression for the energies of the multiplet of levels resulting in this way:

$$\frac{\Delta E_J}{5K} = \alpha^4 (-1)^J \begin{Bmatrix} 2 & 2 & J \\ 2 & 2 & 2 \end{Bmatrix}$$

$$+ \alpha^2 (1-\alpha^2) \left[2(1+(-)^J) \begin{Bmatrix} 2 & 2 & J \\ 2 & 2 & 2 \end{Bmatrix} + 2 + (-1)^J \right] \tag{5}$$

$$+ 2(1-\alpha^2)^2 (1+(-1)^J) \left[1 + \begin{Bmatrix} 2 & 2 & J \\ 2 & 2 & 2 \end{Bmatrix} \right]$$

Clearly, there are 5 levels in the multiplet, $J^\pi = 0^+$, 1^+, 2^+, 3^+, and 4^+. Furthermore, the overlap between the prolate and oblate states is small, i.e.: $\alpha \approx 1$, so that the dominant term in the expression is the α^4-term. Therefore, the relative spacing of the levels is fixed by the 6-j symbol. Only the absolute spacing is adjusted by a choice of K. The small deviation of α from unity enables small shifts of the odd levels relative to the even ones.

We find a very satisfactory agreement to the ^{28}Si spectrum by choosing $\alpha^2 = 0.94$, $K = -0.5$ MeV and $E + \hbar\omega_2 = 7.2$ MeV (see Fig. 1). Some levels are outside of this simple model. First, levels below the prolate "ground state" (the 0^+ at 4.97) should belong entirely to the oblate structure. The 3^- level at 6.88 MeV is probably an octupole vibration which cannot be given by the simple model Hamiltonian of Eq. (2). Finally, the 3^+ at 6.27 is so low that it probably belongs essentially to the oblate structure – there is indication [3], both experimental and theoretical, that it is largely of a single-particle nature, a particle-hole state built on the oblate ground state.

Though the excellent fit obtained here, as opposed to the earlier work, is largely furthered by the adjustable parameters of the model, I must emphasize again that the relative spacing of the multiplet is fixed, independent of our adjustable parameters. Also, we explain all the positive-parity levels in the intermediate energy region 6.5 – 8 MeV whereas the other work could only hope to fit a few of them, and we have a hope of including the others in the same general framework.

In addition, observed transition rates are consistent with this model. In particular, transitions between states belonging to the same structure (prolate or oblate) should be preferred to cross-over transitions. Indeed,

the states at 6.64 MeV (0^+) and 7.80 MeV (3^+) of the multiplet produced by the splitting of the prolate phonon are known [6] to have inhibited transitions to the predominantly oblate $J = 2^+$ state at 1.77 MeV.

I have emphasized that this is a model calculation and should be followed by a more detailed investigation, in particular, a calculation of the parameters K, α from microscopic considerations. A possible way of including the coupling between the two structures from the start, in a self-consistent manner, is to take as a trial function a sum of two (or more) determinants (rather than one as in the usual H.F. method):

$$\Psi = a_1 \Psi_1 + a_2 \Psi_2$$

where Ψ_1 is an oblate and Ψ_2 is a prolate intrinsic function. Such multi-configuration Hartree-Fock calculations have been done in atomic physics and perhaps it is not too early to attempt such a step in nuclear structure calculations [7].

REFERENCES

[1] ENDT, P.M., VAN DER LEUN, C., Nucl. Phys. A105 (1967) 1.
[2] RIPKA, G., Advances in Nuclear Physics, 1, VOGT, E., BARANGER, M., Eds, Plenum Press, N.Y. (1968).
[3] DAS GUPTA, S., HARVEY, M., Nucl. Phys. A94 (1967) 602.
[4] CASTEL, B., SVENNE, J.P., Nucl. Phys. A127 (1969) 141.
[5] KUO, T.T.S., Nucl. Phys. A103 (1967) 71.
[6] ALEXANDER, T.K. et al., in Nuclear Physics (Proc. Conf. Gatlinburg, 1966) Academic Press, New York (1967).
[7] FAESSLER, A., PLASTINO, A., Z. Physik 220 (1969) 88.

COUPLED–CHANNEL CALCULATION
OF THE INTERACTION
OF NUCLEONS WITH THE
COLLECTIVE MODES OF NUCLEI

G. PISENT
Istituto di Fisica dell'Università di Padova,
Padua, Italy

Abstract

COUPLED-CHANNEL CALCULATION OF THE INTERACTION OF NUCLEONS WITH THE COLLECTIVE MODES OF NUCLEI.
1. Introduction; 2. The formalism; 3. The extreme surface coupling model; 4. The collective doorway states.

1. INTRODUCTION

This paper deals with the coupled-channel calculation of the elastic and inelastic interaction between nucleons and "collective" nuclei. The purposes are mainly didactic.

The starting point of the approach is a model Hamiltonian for the description of the target spectrum. The total wave function is then represented by these model wave functions, by suitable truncation of the representation space.

The method has been widely applied in the framework of the macroscopic phenomenological description of the collective target [1 – 4], while only recently have microscopic calculations been made [5 – 6].

A peculiar feature of all these calculations is that the space truncation is usually severe so that manageable differential systems are dealt with. After this the problem may be solved exactly, of course with the aid of a computer. In this connection, the method may be considered to be a generalization of the optical model, in the sense that near the usual average complex potential, the possible excitation (virtual or real) of few internal degrees of freedom of the target are taken into account. It must be finally pointed out that a serious approximation is implicitly introduced since possible exchanges between the incoming nucleon and the target nucleons are neglected.

The principal aim of these notes is to stress the model as a generator of resonances of "intermediate" type, which may be actually seen at low energies if the hypothesis of prominent strong excitation of few collective target levels is fulfilled.

2. THE FORMALISM

Let us summarize briefly the formal content of the method for easy reference[1].

---

[1] For details see, i.e. Tamura [4] and Glendenning [6].

The total Hamiltonian reads:

$$H(\vec{r}, \vec{\xi}) = T(\vec{r}) + H_t(\vec{\xi}) + v(\vec{r}, \vec{\xi}) \tag{1}$$

where T is the kinetic energy of relative motion, H_t the target Hamiltonian and v the interaction potential. The symbol ξ stands for the internal target co-ordinates and will be better defined later, in the framework of a given model.

Let us choose a representation where the orbital angular momentum $\vec{l}$ is coupled with the projectile spin $\vec{s}$, and the sum $\vec{j}$ is coupled with the target spin $\vec{I}$, to give $\vec{J}, M$.

Then, for a given entrance channel $c \equiv I$ (ground state), j, ℓ, the total wave function ψ is expanded as follows:

$$\psi_c^{JM} = \frac{1}{n}\left[u_c^J(r) \,|\, cJM \rangle + \sum_n{}' u_{c_n}^J(r) \,|\, c_n JM \rangle \right] \tag{2}$$

where $c_n \equiv I$ (excited state), j, ℓ labels all channels which are coupled with c, through conservation of parity and total angular momentum.

The projection of the Schrödinger equation on each state $\langle c|, \langle c_m|$ (JM is omitted for the sake of brevity) leads finally to the following system of coupled equations for the radial wave function u(r):

$$(T_c - E + \langle c|V|c\rangle)u_c + \sum_n{}' \langle c|V|c_n\rangle \, u_{c_n} = 0 \tag{3a}$$

$$\langle c_m|V|c\rangle \, u_c + \sum_n{}' \left[\left(T_{c_m} + \epsilon_{c_m} - E \right)\delta_{mn} + \langle c_m|V|c_n\rangle \right] u_{c_n} = 0 \tag{3b}$$

where

$$T_c = \frac{\hbar^2}{2M}\left(-\frac{d^2}{dr^2} + \frac{\ell(\ell+1)}{r^2} \right) \tag{4}$$

and where the target eigenvalues ϵ_{c_m} refer to the ground-state energy.

The next step is a multipole expansion of the potential V, whose elements carry the tensorial character of the interaction, and let the cc' coupling to be effective.

In any case the specification of the target model is necessary at this stage in order to move forward. In the framework of the macroscopic phenomenological collective models (to which we shall refer from now on), a possible procedure is to write

$$V = -(V_0 + iW_0)f(r-R) \tag{5}$$

where f may be, for example, the usual Wood and Saxon form

---

[2] The complications of surface absorption, spin-orbit forces and possible Coulomb interaction are disregarded in this oversimplified example.

$(f(r - R) = \{1 + \exp[r - R) | a]\}^{-1})$ and R is supposed to be angular-dependent according to the deformed or deformable potential assumed.

By multipole expansion of R, and power expansion of f in the coupling constants, one can write down V, separated in diagonal and non-diagonal components:

$$V = V_{spherical} + V_{tensor} \tag{6}$$

A suitable example is obtained by retaining only the quadrupole term in the radius and the linear term in the potential. For an (axially symmetric) deformed nucleus we have:

$$V_{spherical}(\vec{r}) = -(V_0 + iW_0) f(r - R_0), \tag{7a}$$

$$V_{tensor}(\vec{r}, \hat{\xi}) = (V_0 + iW_0) \beta R_0 \sqrt{\frac{4\pi}{5}} \left[\frac{df}{dr}\right]_{R_0} \sum_m V_2^m(\hat{r}) Y_2^{m*}(\hat{\xi}) \tag{7b}$$

where we are able now to specify the co-ordinates $\hat{\xi}$, as the target orientation.

What is interesting to learn from this example is that

1) the expansion in the coupling constant determines the radial dependence of V_{tensor}. In particular, first-order expansion means surface coupling;

2) the multipole expansion fixes the tensorial rank of the interaction, and

3) the details of the target model appear only as a form factor in the target-space component of the V_{tensor} reduced matrix elements (in the given example $\langle I \| \overline{Y}_2 (\hat{\xi}) \| I' \rangle$).

3. THE EXTREME SURFACE COUPLING MODEL (ESCM)

A further schematization may be introduced into the model by assuming for the radial dependence f(r) a square well [7-9]:

$$f(r) = 0 \text{ for } r > R_0; \qquad f(r) = 1 \text{ for } r < R_0 \tag{8}$$

If surface coupling is considered (irrespective of the target model employed), the tensor potential contains a delta function, and the system of equations can be integrated easily.

It is clear that, at this stage of schematization, the model is no longer closely related to the physical picture from which we started. In spite of this, the ESCM can be usefully employed either in the framework of our physical model, at least, in searching first approximate data, or, in a ·more general context, as an exactly soluble surface interaction model. The point is that, in spite of the schematization in the radial form, the model retains entirely its tensorial nature, able to generate resonances of intermediate type.

By means of Eq.(8) the differential system (3) is transformed into the following algebraic system (see Ref.[9]):

$$(Z_c - z_c) u_c + \sum_n \alpha_{cc_n} u_{c_n} = 0 \qquad (9a)$$

$$\alpha_{c_m c} u_c + \sum_n [(Z_{c_m} - \mathcal{L}_{c_m}) \delta_{mn} + \alpha_{c_m c_n}] u_{c_n} = 0 \qquad (9b)$$

Here Z is an effective internal logarithmic derivative where all surface effects other than coupling are included (i.e. spin-orbit forces which have been omitted in Eq.(5)) $\mathcal{L} \equiv S + iP$ is the outgoing wave logarithmic derivative [10] and $\alpha_{cc'}$ are pure geometrical constants related to the matrix elements[3] $\langle c | V_{tensor} | c' \rangle$. The only unknown in Eq.(9) is the open channel external logarithmic derivative z_c which is immediately derived from Eq.(9); namely:

$$z_c = Z_c + \sum_n{}' (-)^n \alpha_{cc_n} \mathscr{D}_{cc_n} / \mathscr{D}_{cc} \qquad (10)$$

with obvious meaning of the determinants $\mathscr{D}$. Once the external logarithmic derivative z_c is known, the calculation of elastic and inelastic cross-sections is straightforward.

Equation (10) is interesting since it realizes in a very easy way (at the price of an oversimplified model), the separation between the entrance channel c and the coupled channels c_n. In particular, one can easily recognize at least in the elastic case and in the weak-coupling limit that the cross-section is composed of single-particle resonances (corresponding to the zeros of the elastic channel function Z_c), together with resonances of intermediate type (in correspondence with the zeros of the closed-channel determinant $\mathscr{D}_{cc}$). These results may be usefully compared with the general properties of the coupled-channel system, which can be deduced by means of Feshbach's approach [11].

4.   THE COLLECTIVE DOORWAY STATES

The physical ideas which underlie the coupled-channel approach, can be interpreted in terms of the doorway-states hypothesis, as formulated by Feshbach [12]. The collective doorway states dealt with in our problem are intended as follows: the incoming nucleon excites the target to a collective level and is captured in a bound orbit around it, having lost part of its energy; afterwards the system may develop towards more complicated structures [13]. In this connection, it seems particularly interesting to apply the model to cases of light targets and low-energy projectiles, where it is reasonably assumed that the excitation of the collective doorway states is the most complicated thing which happens. If this were the case, a simple coupled-channel calculation would be able to describe completely the low-energy cross-section behaviour. Such calculations have been

---

[3] In the particular example of Eq.(7) it is given by

$$\alpha_{cc'} = -\frac{2M}{\hbar'} (V_0 + iW_0) \beta R_0^2 \sqrt{\frac{4\pi}{5}} \langle c | \overline{Y}_2(\hat{r}) \overline{Y}_2(\hat{\xi}) | c' \rangle$$

carried out successfully by many authors [14-19], in the case of the nucleon-^{12}C process. Why is carbon better than other light nuclei? The reasons are the following:

1) The ^{12}C is a strongly deformed nucleus [20] with a high 2^+ excitation energy, so that a wide energy interval is allowed to the incoming nucleon below or not much above the inelastic threshold.

2) The separation energy of a neutron (proton) from ^{13}C (^{13}N) is relatively low, so that by means of the n-^{12}C (p-^{12}C) scattering, one may explore a low-lying region of the ^{13}C (^{13}N) compound system.

Apart from several unresolved details, all the analyses carried out so far [8-11], clearly indicate that both n-^{12}C and p-^{12}C low-energy cross-sections can be satisfactorily explained in terms of single-particle resonances and collective doorway-state resonances.

As to the details of the analysis, we refer, in particular, to the recent papers [18] and [19] devoted to neutron and proton scattering, respectively[4]. Among the still open questions it is worthwhile to mention the problem of the $0^+ - 2^+$ coupling strength, in connection with other kinds of experimental indications (i.e. Coulomb excitation experiments and mean-life measurements [22].

As a final remark we want to underline the obvious fact that both single-particle and intermediate states and both elastic and inelastic cross-sections are here calculated at the same time, from the same potential. This is an important feature of the theory, but leads to understandable fitting difficulties, especially when many partially interfering resonances are dealt with [23]. In this connection, the practical interest of an exactly solvable schematic model (like the ESCM) should be recognized once more.

REFERENCES

[1] CHASE, D.M., WILETS, L., EDMONDS, A.R., Phys. Rev. 110 (1958) 1080.
[2] BUCK, B., Phys. Rev. 130 (1963) 712.
[3] FURNOYA, J., SUGIE, A., Nucl. Phys. 44 (1963) 44;
[4] TAMURA, T., Rev. Mod. Phys. 37 (1965) 679.
[5] FAESSLER, A., GLENDENNING, N.K., PLASTINO, A., Phys. Rev. 159 (1967) 846.
[6] GLENDENNING, N.K., Nucl. Phys. A117 (1968) 49.
[7] YOSHIDA, S., Proc. Phys. Soc. A69 (1956) 668.
[8] RATCLIFF, K.F., AUSTERN, N., Ann. of Phys. 42 (1967) 185.
[9] PISENT, G., ZARDI, F., Nuovo Cim. 53B (1968) 310.
[10] LANE, A.M., THOMAS, R.G., Rev. Mod. Ph. 30 (1958) 257.
[11] FESHBACH, H., Annls Phys. 5 (1958) 357, 19 (1962) 287.
[12] FESHBACH, H., Nuclear Structure Studies with Neutrons, North-Holland (1966) 257.
[13] PISENT, G., ZARDI, F., Nuovo Cim. 48 (1967) 174.
[14] OKAY, S., TAMURA, T., Nucl. Phys. 31 (1962) 185.
[15] EDVI-ILLES, C.A., Proc. Ph. Soc. 81 (1963) 856.
[16] PISENT, G., SARUIS, A.M., Nucl. Phys. 91 (1967) 561.
[17] ROEDER, J.L., Annls Phys. 43 (1967) 382.
[18] REYNOLDS, J.T., SLAVIK, C.J., LUBITZ, C.R., FRANCIS, B.C., Phys. Rev. 176 (1968) 1213.
[19] PASCOLINI, A., PISENT, G., ZARDI, F., Lettere Nuovo Cim. 1 (1969) 643.

---

4 In connection with the p-^{12}C analysis, a recent calculation of A.C.C. Barnard [21] must be also mentioned. This is, however, not directly related to the phenomenological model dealt with here since the hypothesis of free coupling matrix elements has been employed.

[20] FAESSLER, A., SAUER, P.U., STINGE, M.M., Z. Physik 212, 1 (1968).

[21] BARNARD, A.C.L., Phys. Rev. 155 (1967) 1135.

[22] STELSON, P.H., McGOWAN, F.K., Ann. Rev. Nucl. Sc. 13 (1963) 163.

[23] PASCOLINI, A., PISENT, G., ZARDI, F., Nuovo Cim. 61B (1969) 462.

OPTICAL MODEL AND DIRECT REACTIONS

A. AGODI
Istituto di Fisica dell' Università di Catania,
Italy

Abstract

OPTICAL MODEL AND DIRECT REACTIONS.
The presentation of the optical model chosen in this paper permits a study of the relationship between gross structure and fine structure of nuclear cross-sections by starting from any approximate solution of the nuclear many-body problem. In particular, new insights into the theory of direct nuclear reactions are provided.

1. A comparison of the data on nucleon-nucleus scattering with the expectations of a model involving only the observables needed to describe the nucleon-nucleus relative motion was tried quite early in the story of nuclear physics [1].

But the discovery of narrow, closely spaced resonances in the low-energy neutron-nucleus cross-sections [2] ruled out the primitive potential well model and suggested consideration of nucleon-nucleus scattering as a many-particle process. This view was clearly stated by N. Bohr in his famous address [3] to the Copenhagen Academy in 1936. The fact that the observed cross-section turned out to be mainly capture, at resonance, led Bohr to the assumption that the incident neutron, impinging on the target nucleus, quickly shares its energy with many other nucleons through its strong interaction with them: this formation of excited compound states should be, therefore, an intermediate essential step in any neutron-nucleus reaction. The long life-time of excited states, as shown by the width of the resonances, which are several orders of magnitude smaller than predicted by the potential well model, was taken as an indication that the nucleon motions in the compound system were extremely unlikely to produce again a concentration of the energy on one particle, allowing it to escape, and the system to decay into some of the open channels. The close spacing of the resonances was interpreted by assuming that many (or possibly all) target nucleons take part in the process of compound-nucleus formation: level distances of a few eV in systems of nuclear size can occur if a large number of particles are involved in the excitation.

The change from the potential-well to the compound-nucleus model evidently involves a drastic change in the views about the mechanism of neutron-nucleus reactions: in the first case, the mean free path of a neutron in the nucleus is infinite while in the second case it is essentially zero. This drastic change also brings with it the necessity of considering any neutron-nucleus reaction as a many-particle problem, which at the time of Bohr's address was accessible to some kind of statistical treatment, at most.

Considering an isolated narrow resonance, it seemed natural to think of it in terms of an almost stationary state, whose decay, of course, does not depend on its formation: the quantum-mechanical treatment of resonance phenomena was initiated by Breit and Wigner [4] at about the same

time as Bohr proposed the compound-nucleus model of nuclear reactions, and the form which they determined for the "resonating" transition amplitude soon became a standard ingredient in the parametrization and discussion of experimental data.

In the case of closely spaced resonances one has to take into account, at any given energy, the contributions of many overlapping Breit-Wigner amplitudes: for the transition from any initial state $|i'\rangle$ to any final state $|f'\rangle$ the probability amplitude should then read

$$T_{f'i'} = T_{f'i'}^{(0)} + \sum_{\nu} \frac{a_\nu (f', i')}{E - E_\nu} \tag{1}$$

with $T_{f'i'}^{(0)}$ varying only slowly with the energy $E = E_{i'} = E_{f'}$ and with $E_\nu = \operatorname{Re} E_\nu - i\Gamma_\nu/2$. The sum over the index ν is over the compound nucleus resonances whose position and width are, of course, related to $\operatorname{Re} E_\nu$ and Γ_ν, respectively. The $a_\nu(f', i')$ are proportional to the probability amplitude of the process involving the formation of the state $|i'\rangle$ of the compound state $|\nu\rangle$ and then its decay into the state $|f'\rangle$.

To compute the $a_\nu(f', i')$ of Eq. (1), one should be able to solve, at least approximately, the nuclear many-body problem.

There were attempts [5] made to circumvent this difficult condition by assuming that the $a_\nu(f', i')$ should have properties such as to lead to an approximation for the cross-sections consistent with Bohr's qualitative model of nuclear reactions, in particular, with the assumption of independence between formation and decay of the compound nucleus, and accessible to some kind of statistical evaluation, only "ensemble properties" of the $a_\nu(f' i')$ being relevant in that case.

It has been found that assuming a random distribution of the $a_\nu(f' i')$ allows us to obtain independence of formation and decay on the average, the average being carried out over energy intervals containing a suitably large number of levels of given spin and parity [5].

The random distribution of the $a_\nu(f' i')$ can be interpreted by saying that the coupling to the $|i'\rangle$, $|f'\rangle$ states does not select any "special" or "preferred" direction in the space of compound-nucleus states [6].

Now, if the compound-nucleus model of nuclear reactions is valid, this implies, as emphasized above, that the mean free path of nucleons in nuclei is much less than the nuclear dimensions.

If this is true the nucleon-nucleus interaction should affect the relative-motion wave function, e.g. of the neutron-nucleus state as an almost purely imaginary potential [7], and the more so at energies where many overlapping resonances are involved.

Although a potential of this kind gives rise to elastic scattering through shadow diffraction, it turns out that the differential cross-section for such a scattering shows no diffraction maxima, and the total cross-section varies smoothly with energy.

According to what was stated previously, this was expected to be verified experimentally, at least, for the average cross-sections. In contrast to these expectations, by doing measurements of total neutron cross-sections in conditions of poor energy resolution Barshall and coworkers [8] found an oscillatory energy dependence, showing a kind of "resonances" with widths of the order of one or two MeV. They were named "giant

resonances" because their widths are several orders of magnitude larger
than those of the compound nucleus resonances: Feshbach, Porter and
Weisskopf [9] showed that such "giant resonances" are reasonably well
reproduced by a model where the scattering of the neutron is evaluated by
solving a one-body Schrödinger equation with a complex square-well
potential.

There is no natural explanation for such giant resonances in the
compound-nucleus picture.

So we are confronted with the problem of understanding nuclear reactions
such as to explain both the narrow, closely spaced resonances observed
with sufficiently good energy resolution and the giant resonances appearing
in poor resolution experiments. This problem of the relationship between
fine structure and gross structure of nuclear cross-sections has been
carefully studied, by starting from the initial suggestions of Lane, Thomas
and Wigner [10] and, further on, by trying to discover which properties
of the nuclear many-body systems are relevant for a determination of this
relationship [11,12] as revealed by the experiments. Roughly speaking,
what manifests itself here is the single-particle structure of nuclear states,
or, in other words, the existence of preferred directions in the space of
the compound-nucleus states especially those what are coupled to the initial
and/or final nucleon-nucleus states, and so giving rise to deviations from
randomness of the $a_\nu(f' i')$ coefficients of Eq. (1) such as to produce [12]
the giant-resonance behaviour in the transition amplitude, averaged over
a suitably chosen energy interval.

The presentation of the optical model which we shall give here has
been conceived such as to allow a study of the relationship between gross
structure and fine structure of the nuclear cross-sections by starting from
any approximate solution of the nuclear many-body problem.

In particular, it will also provide us with new insights into the theory
of direct nuclear reactions.

As previously mentioned, the giant resonances have been discovered
as a property of neutron-nucleus scattering cross-sections when they were
measured by beams with a rather substantial spread in neutron energies.

Now, from the well known [13] equation

$$\sigma_k^{tot} = \frac{4\pi}{k} \text{ Im } T_{\vec{k}, \vec{k}} \tag{2}$$

usually called the "optical theorem", and linearly relating the total cross-
section σ_k^{tot} to the forward-scattering amplitude $T_{\vec{k}, \vec{k}}$, we obtain by aver-
aging over an energy interval I around $E_k = E$

$$\left\{ \sigma_k^{tot} \right\}_I = \left\{ \frac{4\pi}{k} \text{ Im } T_{\vec{k}, \vec{k}} \right\}_I$$

The precise way in which we carry out the averaging should not be of
any special relevance in the following considerations, so we choose the
definition

$$\left\{ \sigma_k^{tot} \right\}_I = \int_{-\infty}^{\infty} dE_k \, \rho_I(E, E_k) \sigma_k^{tot} \tag{3}$$

with the normalized weighting function

$$\rho_I \, (E, E_k) = \frac{I}{\pi} \, \frac{1}{(E-E_k)^2 + I^2} \tag{4}$$

If in the energy interval I the variation of k is negligibly small, we are allowed to write

$$\left\{ \sigma_k^{tot} \right\}_I = \frac{4\pi}{\mu} \left\{ \mathrm{Im} \, T_{\vec{k}, \vec{k}} \right\}_I \tag{5}$$

We read in Eq. (5) that the mean total cross-section is directly determined by the mean scattering amplitude. For the energy average of the differential elastic scattering cross-section we have

$$\left\{ \frac{d\sigma_{\vec{k}, \vec{k}}}{d\Omega_{\vec{k}'}} \right\}_I = \left\{ \, | \, T_{\vec{k}, \vec{k}} \, |^2 \right\}_I = \left| \left\{ T_{\vec{k}', \vec{k}} \right\}_I \right|^2 + \left[\left\{ | \, T_{\vec{k}', \vec{k}} \, |^2 \right\}_I - \left| \left\{ T_{\vec{k}', \vec{k}} \right\}_I \right|^2 \right] \tag{6}$$

showing that it is determined by the mean scattering amplitude only when the fluctuation term within the square brackets on the right-hand side above is negligible.

The physical meaning of the two terms contributing to the elastic cross-section can be clarified by a time-dependent treatment [14]: the mean amplitude $\{T_{\vec{k}', \vec{k}}\}_I$ describes the scattering of a wave packet of width I around $E_k = E$, as determined by selecting out, in the detection of the scattered particles, only those pass over the target in a time of the order of $1/I$[1]. Of course, if I is substantially larger than a typical compound-nucleus resonance width, such particles cannot correspond to processes involving compound-nucleus formation. The scattering described by $\{T_{\vec{k}', \vec{k}}\}_I$ is commonly termed "shape-elastic". On the other hand, the scattering described by the fluctuation amplitude

$$T_{\vec{k}', \vec{k}}^{fl} = T_{\vec{k}', \vec{k}} - \{T_{\vec{k}', \vec{k}}\}_I \tag{7}$$

in the presence of compound-nucleus processes appreciably varies over energy intervals of the order of the width of the compound-nuclear resonance ($\sim$1 eV at low energies). Hence the particles, whose scattering is described by $T_{\vec{k}', \vec{k}}^{fl}$, stay in the nucleus, by order of magnitude, a million times longer than those of the shape-elastic scattering corresponding to a wave packet of a width of the order of 1 MeV. Of course, if compound-nucleus processes contribute to the elastic scattering the information about them is carried by $T_{\vec{k}', \vec{k}}^{fl}$. When

$$\left\{ \, | \, T_{\vec{k}', \vec{k}}^{fl} \, |^2 \right\}_I = \left\{ | \, T_{\vec{k}', \vec{k}} \, |^2 \right\}_I - \left| \left\{ T_{\vec{k}', \vec{k}} \right\}_I \right|^2 \neq 0$$

then the compound elastic-scattering processes contribute to the average elastic cross-section, Eq. (6).

---

[1] $\hbar = c = 1$ units are used throughout.

Owing to Eq. (5) it follows that the average scattering amplitude $\{T_{\vec{K},\vec{K}}\}_I$ will be affected by the existence of such compound elastic processes, which is manifested by its non-unitarity.

This fact amounts to saying that if a model Hamiltonian can be found describing the nucleon-nucleus average scattering and so determining a scattering amplitude to be compared with $\{T_{\vec{K},\vec{K}}\}_I$, this Hamiltonian must take into account the compound processes as producing a particle loss from the elastic channel. Consequently, such a model Hamiltonian cannot be a self-adjoint operator. In fact, if $|\psi_t\rangle$ is the time-dependent wave packet of nucleon-nucleus states and H_M is the model Hamiltonian, we must have

$$i\frac{\partial}{\nabla t}\,|\psi_t\rangle = H_M|\psi_t\rangle$$

The adjoint equation is

$$-i\frac{\partial}{\partial t}\langle\psi_t| = \langle\psi_t|H_M^\dagger$$

with $H_M^\dagger$ being the adjoint operator to H_M.

It follows

$$i\frac{\partial}{\partial t}\,||\psi_t||^2 = i\frac{\partial}{\partial t}\langle\psi_t|\psi_t\rangle = \langle\psi_t|(H_M - H_M^\dagger)|\psi_t\rangle$$

If then $(\partial/\partial t)||\psi_t||^2 < 0$ is required, to describe a loss of particles, we obtain

$$\langle\psi_t|\,\text{Im}\,H_M\,|\psi_t\rangle < 0 \qquad (8)$$

Since the last equation must hold true for any choice of the wave packet, it follows that $\text{Im}\,H_M = (1/2i)(H_M - H_M^\dagger)$ must be a negative-definite operator.

2. We want now to determine the model operator H_M such as to display its relationship with the original physical Hamiltonian H of the nuclear many-body systems as well as with the selection of processes which it must describe.

To find a proper starting point let us first consider the formal expression [15] of the outgoing wave-scattering eigenstates $\Psi_{0\vec{K}}^{(+)}\rangle$ of the Schrödinger equation for the many-body nuclear system.

$$\Psi_{0\vec{K}}^{(+)}\rangle = \Psi_{0\vec{K}}\rangle + \frac{1}{E_{0k}^{(+)} - H}\,V_{0\vec{K}}^\dagger\rangle \qquad (9)$$

where, if $c_{\vec{K}}^\dagger$ is the creation operator of a neutron in the plane-wave state with momentum $\vec{K}$, $\psi_0\rangle$ is the ground state of a spin-zero target and $c_{\vec{K}}^\dagger\rangle$ a single-nucleon state

$$\Psi_{0\vec{K}}\rangle = c_{\vec{K}}^\dagger\Psi_0\rangle; \quad E_{0k} = E_0 + \omega_k; \quad \omega_k = M + \frac{k^2}{2M}$$

$$(E_0 - H)\Psi_0\rangle = 0; \quad (\omega_k - H)c_{\vec{K}}^\dagger\rangle = 0$$

$$V_{0\vec{K}}^\dagger\rangle = (H - E_{0k})c_{\vec{K}}^\dagger\Psi_0\rangle = ([H, c_{\vec{K}}^\dagger] - \omega_k c_{\vec{K}}^\dagger)\Psi_0\rangle \equiv V_{\vec{K}}^\dagger\Psi_0\rangle$$

To simplify matters, let us neglect the recoil of the target, and consider the asymptotic behaviour of $\langle \Psi_0 c (\vec{r}) \Psi_{0\vec{k}}^{(+)} \rangle$ being proportional to the probability amplitude of finding the neutron-plus-target system in the state $c^{\dagger}(\vec{r}) \Psi_0 \rangle$ when it is in the state $\Psi_{0\vec{k}}^{(+)} \rangle$:

$$\lim_{r \to \infty} \langle \Psi_0 c (\vec{r}) \Psi_{0\vec{k}}^{(+)} \rangle = \lim_{r \to \infty} \left[\langle \Psi_0 c (\vec{r}) c_{\vec{k}}^{\dagger} \Psi_0 \rangle \right.$$

$$\left. + \left(\frac{1}{2\pi} \right)^{3/2} \int d^3\vec{k}' \frac{e^{i\vec{k}' \cdot \vec{r}}}{E_{0k}^{(+)} - E_{0k'}} \left(c_{\vec{k}'} + V_{\vec{k}'} \frac{1}{E_{0k}^{(+)} - H} \right) V_{0\vec{k}}^{\dagger} \rangle \right] \tag{10}$$

$$\sim \left(\frac{1}{2\pi} \right)^{3/2} \left[e^{-i\vec{k} \cdot \vec{r}} - \frac{e^{ikr}}{r} (2\pi)^2 M \langle V_{0\vec{k}'} | \Psi_{0\vec{k}}^{(+)} \rangle \right]$$

where $\vec{k}' = k \, \vec{r}/r$, and use has been made of the following equations:

$$c_{\vec{k}} \frac{1}{z - H} = \frac{1}{z - H - \omega_k} \left[c_{\vec{k}} + V_{\vec{k}} \frac{1}{z - H} \right]$$

$$\lim_{r \to \infty} \int d^3\vec{k}' \frac{e^{i\vec{k}' \cdot \vec{r}}}{E_{0k}^{(+)} - E_{0k'}} F (\vec{k}') \sim - (2\pi)^2 M \frac{e^{ikr}}{r} F (k\frac{\vec{r}}{r})$$

$$\langle \Psi_0 c_{\vec{k}'} V_{\vec{k}}^{\dagger} \Psi_0 \rangle \Big|_{k=k'} = \langle \Psi_0 V_{\vec{k}'} c_{\vec{k}}^{\dagger} \Psi_0 \rangle \Big|_{k=k'}$$

From Eq. (10) it follows that

$$T_{\vec{k}', \vec{k}} = - (2\pi)^2 M \langle V_{0\vec{k}'} | \Psi_{0\vec{k}}^{(+)} \rangle \tag{11}$$

Now let us take the energy average of both sides of Eq. (10); this gives

$$\lim_{r \to \infty} \left\{ \langle \Psi_0 c (\vec{r}) \Psi_{0\vec{k}}^{(+)} \rangle \right\}_I = \lim_{r \to \infty} \langle \Psi_0 c (\vec{r}) \left\{ \Psi_{0\vec{k}}^{(+)} \right\} \rangle_I$$

$$\sim \left(\frac{1}{2\pi} \right)^{3/2} \left[e^{i\vec{k} \cdot \vec{r}} - \frac{e^{ikr}}{r} (2\pi)^2 M \left\{ \langle V_{0\vec{k}'} | \Psi_{0\vec{k}}^{(+)} \rangle \right\}_I \right] \tag{12}$$

$$= \left(\frac{1}{2\pi} \right)^{3/2} \left[e^{i\vec{k} \cdot \vec{r}} + \frac{e^{ikr}}{r} \left\{ T_{\vec{k}', \vec{k}} \right\}_I \right]$$

showing that $\{ T_{\vec{k}', \vec{k}} \}_I$ is the transition amplitude for the scattering processes described by the state $\{ \Psi_{0\vec{k}}^{(+)} \rangle \}_I$. Let us remark that two states $\Psi_{0\vec{k}}^{(+)} \rangle$, $\Psi_{0\vec{k}}'^{(+)} \rangle$ will give rise to the same $T_{\vec{k}', \vec{k}}$ whenever

$$\lim_{r \to \infty} \langle \Psi_0 c (\vec{r}) \Psi_{0\vec{k}}^{(+)} \rangle = \lim_{r \to \infty} \langle \Psi_0 c (\vec{r}) \Psi_{0\vec{k}}'^{(+)} \rangle \tag{13}$$

which is of course satisfied if, for all $\vec{r}$

$$\langle \Psi_0 \, c \, (\vec{r}) \, \Psi_{0\vec{k}}^{(+)} \rangle = \langle \Psi_0 \, c \, (\vec{r}) \, \Psi'^{(+)}_{0\vec{k}} \rangle \tag{14}$$

holds true, i.e. if the states $\Psi_{0\vec{k}}^{(+)} \rangle$, $\Psi'^{(+)}_{0\vec{k}} \rangle$ have the same projection on the subspace spanned by all $c^\dagger (\vec{r}) \Psi_0 \rangle$ states. The parameters symbolized by $\vec{r}$ can be substituted by any complete set of single-particle quantum numbers: the subspace of all $c^\dagger (\vec{r}) \Psi_0 \rangle$ states is the same as that of all $c_{\vec{k}}^\dagger \Psi_0 \rangle$ states. It is the subspace of all neutron-plus-nucleus $c^\dagger \Psi_0 \rangle$ states where the nucleus is in its ground state $\Psi_0 \rangle$.

Let us denote by P_{10} the projection operator on this subspace of the space of the states; Eq. (14) holds true for all $\vec{r}$ if and only if

$$P_{10} \, \Psi_{0\vec{k}}^{(+)} \rangle = P_{10} \, \Psi'^{(+)}_{0\vec{k}} \rangle \tag{15}$$

In particular, by definition

$$P_{10} \, c^\dagger (\vec{r}) \, \Psi_0 \rangle = c^\dagger (\vec{r}) \, \Psi_0 \rangle \tag{16}$$

and consequently, for all $\vec{r}$,

$$\langle \Psi_0 \, c(\vec{r}) \left\{ \Psi_{0\vec{k}}^{(+)} \right\}_I = \langle \Psi_0 c \, (\vec{r}) \, P_{10} \left\{ \Psi_{0\vec{k}}^{(+)} \right\}_I \tag{17}$$

Since P_{10} is independent of E_{0k}, it follows

$$\lim_{r \to \infty} \langle \Psi_0 \, c \, (\vec{r}) \, P_{10} \left\{ \Psi_{0\vec{k}}^{(+)} \right\}_I = \lim_{r \to \infty} \langle \Psi_0 \, c \, (\vec{r}) \left\{ P_{10} \Psi_{0\vec{k}}^{(+)} \right\}_I \tag{18}$$

allowing us to state that $\{T_{\vec{k}', \vec{k}}\}_I$ is also the transition amplitude of the scattering processes described by the state $\{P_{10} \Psi_{0\vec{k}}^{(+)} \rangle\}_I$. Let us stress the point that the latter cannot give rise to outgoing spherical waves in any inelastic channel, since P_{10} projects out asymptotically any state not including the target ground state: only the single-particle quantum numbers, e.g. $\vec{k}$, are allowed to change and so only elastic scattering is possible. But if compound elastic and inelastic processes are present in $\Psi_{0\vec{k}}^{(+)} \rangle$ then there will be a loss of particles from the initial channel, that is from the subspace spanned by all superpositions of $\{c_{\vec{k}}^\dagger \Psi_0 \rangle\}_I$ states.

Owing to Eqs (12) and (18) it is just this loss of particles which produces the non-unitarity of $\{T_{\vec{k}', \vec{k}}\}_I$.

Leaving understood the dependence on the target quantum numbers, the function

$$\varphi_{\vec{k}}^{(+)} (\vec{r}) = \langle \Psi_0 \, c \, (\vec{r}) \left\{ \Psi_{0\vec{k}}^{(+)} \rangle \right\}_I = \langle \Psi_0 \, c \, (\vec{r}) \left\{ P_{10} \Psi_{0\vec{k}}^{(+)} \rangle \right\}_I \tag{19}$$

is a possible definition of a "single-particle" wave function describing the mean elastic scattering in the considered neutron-nucleus channel. Let us remark that Eq. (19) makes precise the physical meaning of $\varphi_{\vec{k}}^{(+)}(\vec{r})$ for all values of $\vec{r}$; whereas the usual optical-model wave functions, generated

from a complex potential well, are only known to assign asymptotically the correct amplitude $\{T_{\vec{K},\vec{K}}\}_I$ to the outgoing spherical waves.

Now if Eq. (19) defines the "optical-model" wave function, what can we say about its corresponding "optical-model" Hamiltonian?

To get the answer let us consider the equation obtained from Eq. (9) after application of P_{10}, by the averaging procedure

$$\left\{ P_{10}\Psi^{(+)}_{0\vec{k}} \right\}_I = \left\{ P_{10}\Psi_{0\vec{k}} \right\}_I + \left\{ P_{10}\frac{1}{E^{(+)}_{0k}-H}\ V^{\dagger}_{0\vec{k}} \right\}_I$$

$$\cong \Psi_{0\vec{k}} + P_{10}\frac{1}{E_{0k}-H+iI}\ V^{\dagger}_{0\vec{k}} \rangle \tag{20}$$

where the variation of $\Psi_{0\vec{k}}\rangle$ and $V^{\dagger}_{0\vec{k}}\rangle = (H-E_{0k})\,c^{\dagger}_{\vec{k}}\Psi_0\rangle$ has been regarded as negligible in the interval I around $E = E_{0k}$ and use has been made of

$$\left\{ \frac{1}{E^{(+)}_{0k}-H} \right\}_I = \frac{1}{E_{0k}-H+iI} \tag{21}$$

Let us now define the projection operator Q_{10} such that

$$P_{10} + Q_{10} = 1$$

and remember the algebraic identities

$$P_{10}\frac{1}{z-H}Q_{10} = P_{10}\frac{1}{z-H}P_{10}HQ_{10}\frac{1}{z-Q_{10}HQ_{10}}$$

$$P_{10}\frac{1}{z-H}P_{10} = \frac{P_{10}}{z-P_{10}HP_{10}-W_{10}(z)} \tag{22}$$

with

$$W_{10}(z) = P_{10}HQ_{10}\frac{1}{z-Q_{10}HQ_{10}}Q_{10}HP_{10} \tag{23}$$

Using these identities we obtain

$$P_{10}\frac{1}{E_{0k}-H+iI}\ V^{\dagger}_{0\vec{k}}\rangle = P_{10}\frac{1}{E_{0k}-H+iI}\ P_{10}\left[(H-E_{0k})\Psi_{0\vec{k}}\rangle \right.$$

$$\left. + W_{10}(E_{0k}+iI)\Psi_{0\vec{k}}\rangle \right]$$

If the interval I can be chosen such that

$$-\operatorname{Im} W_{10}(E_{0k}+iI) \gtrsim I \tag{24}$$

we are allowed to write

$$P_{10}\frac{1}{E_{0k}-H+iI}P_{10} \approx \frac{P_{10}}{E^{(+)}_{0k}-P_{10}HP_{10}-W_{10}(E_{0k}+iI)} \tag{25}$$

and finally

$$\left\{P_{10} \, \Psi_{0\vec{k}}^{(+)} \rangle\right\}_I \cong \Psi_{0\vec{k}} \rangle + \frac{1}{E_{0k}^{(+)} - H_k^{(opt)}} \, (H_k^{(opt)} - E_{0k}) \Psi_{0\vec{k}} \rangle \tag{26}$$

with

$$H_k^{(opt)} = P_{10} \, H \, P_{10} + W_{10} \, (E_{0k} + iI) = H_M \tag{27}$$

From Eq. (26) we find that $\{P_{10} \Psi_{0\vec{k}}^{(+)} \rangle\}_I$ is the outgoing wave solution of

$$(E_{0k} - H_k^{(opt)}) \, \{P_{10} \Psi_{0\vec{k}}^{(+)} \rangle\}_I = 0$$

determined by the "initial state" $\Psi_{0\vec{k}} \rangle \cong \{P_{10} \Psi_{0\vec{k}} \rangle\}_I$. Hence the "optical-model" Hamiltonian $H_k^{(opt)}$ determining $\varphi_{\vec{k}}^{(+)}(\vec{r})$, Eq. (19), is given by Eq. (26). Quite clearly it is a one-body operator

$$H_k^{(opt)} = P_{10} \, H_k^{(opt)} \, P_{10}$$

defined in the space of $c^\dagger \Psi_0 \rangle$ states and producing there only changes in the single-particle quantum numbers labelling $c^\dagger$.

From the definition it is, rather obviously, a non-local energy-dependent operator.

Its imaginary part can be written

$$\frac{1}{2i} \left(H_k^{(opt)} - H_k^{(opt)\dagger} \right) = \text{Im} \, H_k^{(opt)} = \text{Im} \, W_{10} \, (E_{0k} + iI)$$

$$= \text{Im} \int_{\alpha' E'} P_{10} \, H \, |\alpha' E' \rangle \, \frac{1}{E_{0k} - E' + iI} \langle \alpha' E' | \, H \, P_{10}$$

$$= - I \int_{\alpha' E'} P_{10} \, H \, |\alpha' E' \rangle \, \left| \frac{1}{E_{0k} - E' + iI} \right|^2 \langle \alpha' E' | \, H \, P_{10} \tag{28}$$

$$= \left\{ \text{Im} \, W_{10} (E_{0k}^{(+)}) \right\}_I$$

where $\int_{\alpha' E'}$ indicates summation over the discrete and integration over the continuous spectrum of the complete set of $\alpha' E'$ quantum numbers labelling the eigenstates $|\alpha' E' \rangle$ of $Q_{10} H Q_{10}$.

Equation (28) clearly shows that $\text{Im} \, H_k^{(opt)}$ is a negative-definite operator, as we expected on physical grounds.

Also it can be realized easily that, if $\Psi_0 \rangle$ can be approximated with a single Slater determinant $\Psi_0^{(S)} \rangle$ as in the case of a closed shell nucleus, then $P_{10} H P_{10}$ can be represented by the Hartree-Fock Hamiltonian determining $\Psi_0^{(S)} \rangle$ as its lowest eigenstate. From Eq. (23) the determination of W_{10} becomes then a well defined problem. It clearly appears that W_{10}

vanishes with $P_{10} H Q_{10}$: if H only involves, at most, two-body nucleon-nucleon interactions, then $P_{10} H Q_{10}$ can only have matrix elements connecting the space of the $c^\dagger \Psi_0 \rangle$ states to $c^\dagger c^\dagger c \, \Psi_0 \rangle$ states such that $P_{10} c^\dagger c^\dagger c \Psi_0 \rangle = 0$.

The two particle-one hole states satisfying this condition span a sub-space of the space of the states whose elements can be expressed as super-positions of $(1 - P_{10}) c^\dagger c^\dagger c \Psi_0 \rangle$ states: let us denote by P_{21} the projection operator over this space of two particle-one hole states.

If only two-body interactions are present in H, then

$$P_{10} H Q_{10} = P_{10} H P_{21}$$

If, furthermore, $\Psi_0 \rangle \approx \Psi_0^{(s)} \rangle$ we also have

$$P_{10} H P_{21} \approx P_{10}^{(s)} H P_{21}^{(s)}$$

showing the relevance of the so-called core-polarization terms in the residual nucleon-nucleon interaction to get a realistic evaluation of W_{10}. Obviously, any such evaluation will involve an approximation to $Q_{10} / (z - Q_{10} H Q_{10})$; let us just mention here that several such approximations have already been suggested and studied in the literature [16].

If the shell-model approximation for $\Psi_0^{(s)} \rangle$ cannot be regarded as good, a calculation of W_{10} might be carried out by methods similar to those intro-duced [16] to study the matrix elements of the resolvent operator in the nuclear-many problem: a careful treatment of this problem in the case of finite "spherical" nuclei, with a proper substitution of the rotation in-variance to the translation invariance exploited in "infinite"-nuclear-matter studies is not yet available.

If the shell-model approximation is not only good for $|\Psi_0 \rangle$ but also for, at least, a selection of bound states of the neighbouring nuclei with one particle or one hole added to $|\Psi_0 \rangle$, then the core-polarization terms in the nucleon-nucleon interaction give negligibly small matrix elements and the optical-model scattering "essentially" reduces to Hartree-Fock scattering, i.e. to the scattering due to $P_{10} H P_{10} \approx P_{10}^{(s)} H P_{10}^{(s)}$.

Let us remark that if $\chi_{0k}^{(+)} \rangle$ denotes the outgoing wave solution of

$$(E_{0k} - P_{10} H P_{10}) \chi_{0k}^{(+)} \rangle = 0 \tag{29}$$

i.e. if

$$\chi_{0\vec{k}}^{(+)} \rangle = \Psi_{0\vec{k}} \rangle + \frac{1}{E_{0k}^{(+)} - P_{10} H_{10}} (P_{10} H P_{10} - E_{0k}) \Psi_{0\vec{k}} \rangle$$

we can write $T_{\vec{k}',\vec{k}}$ so as to put in evidence the scattering amplitude $T_{\vec{k}',\vec{k}}^{(10)}$ determined by $P_{10} H P_{10}$. We have, in fact

$$\Psi_{0k}^{(+)} \rangle = \Psi_{0\vec{k}} \rangle + \frac{1}{E_{0k}^{(+)} - H} V_{0\vec{k}}^\dagger \rangle$$

$$= \chi_{0\vec{k}}^{(+)} \rangle + \frac{1}{E_{0k}^{(+)} - H} (H - P_{10} H P_{10}) \chi_{0\vec{k}}^{(+)} \rangle \tag{30}$$

$$= \chi_{0\vec{k}}^{(+)} \rangle + \frac{1}{E_{0k}^{(+)} - H} Q_{10} H P_{10} \chi_{0k}^{(+)} \rangle$$

where use has been made of Eq. (29), implying $Q_{10} \chi_{0\vec{k}}^{(+)} \rangle = 0$.

From Eq. (30) we readily obtain, for $E_{0k} = E_{0k'} = E$,

$$\langle V_{0\vec{k}'} | \psi_{0\vec{k}}^{(+)} \rangle = \langle V_{0\vec{k}'} | \chi_{0\vec{k}}^{(+)} \rangle + \langle V_{0\vec{k}'} | \frac{1}{E^{(+)} - H} Q_{10} H \chi_{0\vec{k}}^{(+)} \rangle$$

$$= \langle V_{0\vec{k}'} | \chi_{0\vec{k}}^{(+)} \rangle + \langle V_{0\vec{k}'} | \left(\frac{1}{E^{(+)} - P_{10} H P_{10}} P_{10} H Q_{10} + Q_{10} \right) \frac{1}{E^{(+)} - H} Q_{10} H \chi_{0\vec{k}}^{(+)} \rangle$$

$$= \langle V_{0\vec{k}'} | \chi_{0\vec{k}}^{(+)} \rangle + \langle \chi_{0\vec{k}}^{(-)}, H Q_{10} \frac{1}{E^{(+)} - H} Q_{10} H \chi_{0\vec{k}}^{(+)} \rangle$$

and therefore, with

$$T_{\vec{k}',\vec{k}}^{(10)} = - (2\pi)^2 M \langle V_{0\vec{k}'} | \chi_{0\vec{k}}^{(+)} \rangle \Big|_{k' = k}$$

the decomposition

$$T_{\vec{k}',\vec{k}} = T_{\vec{k}',\vec{k}}^{(10)} - (2\pi)^2 M \langle \chi_{0\vec{k}}^{(-)}, H Q_{10} \frac{1}{E_{0k}^{(+)} - H} Q_{10} H \chi_{0\vec{k}}^{(+)} \rangle \Big|_{k' = k} \tag{31}$$

The second term on the right-hand side of Eq. (31) becomes negligibly small when the "optical-model" scattering reduces to the Hartree-Fock scattering and $\Psi_0 \rangle \approx \psi_0^{(s)} \rangle$.

It is this term which contains the energy dependence of the elastic-scattering amplitude caused by the compound-nucleus resonances. We stress the point that the contribution of this term to the mean scattering amplitude, determined as it is by matrix elements of $P_{21} [1/(E_{0k} - H + iI)] P_{21}$ is as accessible to an approximate evaluation as the real and imaginary parts of the "optical potential", determined through $W_{10} (E_{0k} + iI)$ by matrix elements of $P_{21} [1/(E_{0k} - Q_{10} H Q_{10} + iI)] P_{21}$.

I am inclined to think that instead of computing $[T_{\vec{k}',\vec{k}}]_I$ by first constructing the optical-model potential and then solving the one-body Schrödinger equation, it is perhaps already possible to make use of approximate solutions of the nuclear many-body problem to determine directly

$$\{ T_{\vec{k}',\vec{k}}^{}\}_I = T_{\vec{k}',\vec{k}}^{(10)} - (2\pi)^2 M \langle \chi_{0\vec{k}}^{(-)}, H Q_{10} \frac{1}{E_{0k} - H + iI} Q_{10} H \chi_{0\vec{k}}^{(+)} \rangle \tag{32}$$

The interest of the latter approach can be illustrated by considering, for example, the neutron-nucleus total cross-section in the limit of vanishing k: only $\ell = 0$ waves then contribute, and use of Eq. (2) gives (for spinless nucleons)

$$\lim_{\mu \to 0} \sigma_k^{tot} \sim - \frac{4\pi}{k} \text{Im} \left[\frac{1}{4\pi} \sum_{\ell} (2\pi)^2 M (2\ell + 1) \langle V_{0k\ell} | \psi_{0k\ell}^{(+)} \rangle P_\ell (1) \right]$$

$$\sim - \frac{4\pi}{k} \text{Im} \, \pi M \langle V_{0k0} | \psi_{0k0}^{(+)} \rangle$$

$$\sim - \frac{4\pi}{k} \left[\text{Im} \, \pi M \langle V_{0k0} | \chi_{0k0}^{(+)} \rangle \right.$$

$$\left. + \text{Im} \, (\pi M F) (1 - 2\pi iM k \langle V_{0k0} | \chi_{0k0}^{(+)} \rangle) \right]$$

with

$$F = \left\langle \chi^{(+)}_{0k0} H Q_{10} \frac{1}{E^{(+)}_{0k} - H} Q_{10} H \chi^{(+)}_{0k0} \right\rangle$$

Let a_0 be the scattering length from $P_{10} H P_{10}$:

$$4\pi a_0^2 \sim - \lim_{\mu \to 0} \frac{4\pi}{k} \text{Im} \, \pi M \left\langle V_{0k0} | \chi^{(+)}_{0k0} \right\rangle$$

We have then

$$\lim_{k \to 0} \sigma^{tot}_k \sim 4\pi a_0^2 \left[1 + \frac{2\pi M}{a_0} \text{Re} \, F \right] - \frac{1}{k} (2\pi)^2 M \, \text{Im} \, F$$

and hence

$$\lim_{k \to 0} \left\{ \sigma^{tot}_k \right\}_I \sim 4\pi a_0^2 \left[1 + \frac{2\pi M}{a_0} \left\{ \text{Re} \, F \right\}_I \right] - \frac{1}{k} (2\pi)^2 M \left\{ \text{Im} \, F \right\}_I \qquad (33)$$

The experimental values of R defined as

$$R = + \, | a_0 | \left[1 + \frac{2\pi M}{a_0} \left\{ \text{Re} \, F \right\}_I \right]^{\frac{1}{2}}$$

are known to vary with the target mass number A, around the values $r_0 A^{1/3}$ expected according to the model of the perfectly absorbing target, with a behaviour in rough qualitative agreement with the potential-well predictions. The experimental points show a kind of fine structure superimposed over this average behaviour [8,9,12]: it should be quite interesting to try and see how well this behaviour of R can be explained by computing the values of a_0 and $\{\text{Re} F\}_I$ from any approximate solution of the nuclear many-body problem.

The experimental values of the so-called s-wave strength function $(\tilde{\gamma}/D)$, defined at very low neutron energy by

$$\pi \left(\frac{\tilde{\gamma}}{D} \right) \approx \frac{k^2}{2\pi} \left\{ \sigma^{tot}_k \right\}_I$$

have been found [8,9,12] to exhibit a mean behaviour in rough qualitative agreement with the complex-potential-well calculations. Also here a kind of fine structure has been found superimposed over the mean, whose existence has been suggested [17] to depend on the density of the "doorway states", introduced to explain some aspects of the so-called "intermediate" resonance structure of nuclear reactions.

Assuming only two-body nucleon-nucleon interactions we get from Eq.(33) to lowest order in k,

$$\left(\frac{\tilde{\gamma}}{D} \right) \approx 2\pi k M \left\{ \left\langle \chi^{(+)}_{0k0} H P_{21} \delta (E_{0k} - H) P_{21} H \chi^{(+)}_{0k0} \right\rangle \right\}_I \qquad (34)$$

It is apparent that $(\bar{\gamma}/D)$ depends both on the scattering due to $P_{10} H P_{10}$ through $\chi_{0k_0}^{(+)}\rangle$, and on the spectral density of H in the energy interval I around E_{0k}, reduced in the subspace of the $Q_{10} c^{\dagger} c^{\dagger} c \Psi_0 \rangle$ two-particle-one-hole states, through the coupling of such states to the $\chi_{0k_0}^{(+)}\rangle$.

Equation (34) clearly shows that if the mean behaviour of the s-wave strength function is well approximated by a shell-model calculation then its fine structure will essentially depend on the coupling of the shell-model scattering states to the two-particle-one-hole excitations, and from the mean density of the latter in the energy interval I around E_{0k}.

This confirms the validity of a previous suggestion made by Feshbach [17], and makes it accessible to a more precise verification through evaluation of $(\bar{\gamma}/D)$ using Eq. (34) and approximate solution of the nuclear many-body problem, in the space of the $c^{\dagger}\Psi_0\rangle$ and of the $c^{\dagger}c^{\dagger}c \Psi_0\rangle$ states [18].

Let us again emphasize the feasibility of such calculations and their rather obvious physical interest, arising from the simple relationship between nuclear structure and observable cross-sections.

3. We have presented the optical model, basically, as a theory of the average elastic-scattering amplitudes, the average being over an energy interval of suitably chosen extension: and we have mentioned that the mean scattering amplitude describes those processes which do not involve compound-nucleus formation, because a wave packet extending over an energy interval I cannot give information about processes lasting longer than $1/I$. The same arguments which are employed in discussing the elastic scattering allow us to interpret the average of the general transition matrix element

$$\{T_{f' i'}\}_I = T_{f' i'}^{(D)}$$

as describing direct processes, i.e. not involving compound-nucleus formation and the fluctuation around the average

$$T_{f' i'}^{fl} = T_{f' i'} - \{T_{f' i'}\}_I$$

as describing compound-nucleus processes.

It is well known that in the study of direct reactions the so-called distorted wave Born approximation (DWBA) is usually employed, which amounts to assume

$$\langle V_{f'} | \Psi_{i'}^{(+)} \rangle |_{direct} \approx \langle \tilde{\varphi}_{f'}^{(-)} | V | \varphi_{i'}^{(+)} \rangle \qquad (35)$$

with the states $|\varphi_{i'}^{(+)}\rangle$, $\langle \tilde{\varphi}_{f'}^{(-)}|$ describing the optical-model elastic scattering in the initial and final channels, and V being, in general, an effective interaction operator, determined as a rule, on the basis of heuristic, semi-phenomenological arguments.

It has been shown [18] that, if P_i and P_f are the projection operators on the initial and final channels, i.e. on the subspaces spanned by all $|i'\rangle$ and $|f'\rangle$ states, respectively, then whenever

$$P_i P_f = 0 \qquad (36)$$

the equation

$$\{T_{f'i'}\}_I = T^{(D)}_{f'i'} = - (2\pi)^2 M_f \langle \tilde{\phi}^{(-)}_{f'} | V^{(fi)} | \varphi^{(+)}_{i'} \rangle \tag{37}$$

holds true, with the definitions ($E = E_{i'} = E_{f'}$)

$$|\varphi^{(+)}_{i'}\rangle = \left\{ P_i \ \Psi^{(+)}_{i'} \right\}_I = |i'\rangle + \frac{1}{E^{(+)} - H^{(opt)}_{i'}} V^{(opt)\dagger}_{i'}\rangle$$

$$\langle \tilde{\phi}^{(-)}_{f'}| = \left\{ \langle \Psi^{(-)}_{f'} \ P_f \right\}_I = \langle f'| + \langle V^{(opt)\dagger}_{f'} \frac{1}{E^{(+)} - H^{(opt)}_{f'}} \tag{38}$$

$$V^{(fi)} = P_f H P_i + P_f H Q_f \frac{1}{E + iI - Q_f H Q_f} (Q_i H P_i - W_i)$$

$$W_i = W_i (E + iI) = P_i H Q_i \frac{1}{E + iI - Q_i H Q_i} Q_i H P_i$$

This result has some implications which we want to emphasize.

First: it gives a precise indication about the wave functions and the effective interaction to be employed in the DWBA formula whenever one requires that it must describe just the same processes as the mean transition amplitude. Let us stress the point that the definition of the optical-model scattering states previously constructed starting from the many-body scattering problem, allows us to realize this rather important interdependence of elastic distortions and effective coupling of channels in direct inelastic processes.

Second: if the shell model is a good approximation for the initial and the final channel states then the DWBA gives a good approximation to $\{T_{f'i'}\}_I$.

To show this, let us consider inelastic scattering of neutrons of a closed-shell nucleus. If $\Psi_0 \approx \Psi^{(s)}_0\rangle$ then $P_i \cong P^{(s)}_{10}$. Let us assume that the excited state of the residual nucleus is a superposition of particle-hole excitations so that $P_f \cong P^{(s)}_{21}$.

Of course it is then $P_i P_f \cong P^{(s)}_{10} P^{(s)}_{21} = 0$.

But if the shell model is a good approximation to both the initial and the final states this means that configuration mixing is negligible and, consequently, the $W^{(s)}_{10}$, $W^{(s)}_{21}$ terms in the optical potentials as well as the second term in the definition of $V^{(fi)}$, being of analogous structure, all are negligible.

Therefore, we obtain

$$T^{(D)}_{f'i'} \approx - (2\pi)^2 M_f \langle \chi^{(-)}_{f'} \ P^{(s)}_{21} H P^{(s)}_{10} \chi^{(+)}_{i'} \rangle \approx T^{(DWBA)}_{f'i'} \tag{39}$$

i.e. the effective interaction only involves the so-called core-polarization terms in the residual nucleon-nucleon interaction, and with this V the DWBA is valid.

Let us remark that the core-polarization terms in the residual nucleon-nucleon interaction also determine the direct transition amplitude of a (d, p) or (d, n) reaction from a single-hole nucleus to the ground state of a closed-shell nucleus. From well known properties of stripping and pick-up reactions it follows that in such a case we can explore essentially the "long-range" terms in the interaction, while, for example, study of (n, p) direct reactions on closed-shell nuclei, leaving a particle-hole excitation in the residual nucleus, can give information on the "short-range" terms in the same effective interaction. Remember that this "core-polarization" part of the residual interaction also determines the "optical-model" corrections to the Hartree-Fock scattering and, in particular, the behaviour of the zero-energy s-wave neutron strength function.

As a final remark let me add that in the general case, i. e. when configuration mixing is to be taken into account, the problem of determining $V^{(fi)}$ according to Eq. (38) does not appear more difficult than the proper computation of the optical-model potential. Also in this case we are confronted with the fact that the work needed to compute $V^{(fi)}$ is as difficult and time-requiring as the work needed to directly evaluate the mean transition amplitude from

$$\left\{ \left\langle V_{f'} \middle| \Psi_{i'}^{(+)} \right\rangle \right\}_I = \left\langle V_{f'}^{(P)} \middle| \Psi_{i'}^{(P)(+)} \right\rangle + \left\langle \Psi_{f'}^{(P)(-)} \middle| HQ \frac{1}{E - H + iI} QH \Psi_{i'}^{(P)(+)} \right\rangle \tag{40}$$

where this time P is the projection operator on the combined space of all $|i'\rangle$ and $|f'\rangle$ states (be they orthogonal or not!), Q = 1 - P, and $|\Psi^{(P)(\pm)}\rangle$ are the eigenstates of PHP. The analysis of direct nuclear reactions on the basis of the quantum theory of many-nucleon systems might start from here.

REFERENCES

[1] BETHE, H.A., Phys. Rev. 47 (1935) 747; FERMI, E. et al., Proc. Roy. Soc. A149 (1935) 522; PERRIN, ELSASSER, J. de Phys. 6 (1935) 195.
[2] BJERGE, WESTCOTT, Proc. Roy. Soc. A150 (1935) 709; MOON, TILLMAN, Nature 135 (1935) 904; 136 (1935) 66; SZILARD, Nature 136 (1935) 849, 950; FERMI, E., AMALDI, Ric. Sci. A6 (1935) 544.
[3] BOHR, N., Nature 137 (1936) 344.
[4] BREIT, WIGNER, Phys. Rev. 49 (1936) 519.
[5] BETHE, H.A., Rev. mod. Phys. 9 (1937) 69; BETHE, H.A., PLACZECK, G., Phys. Rev. 51 (1937) 450; LANE, A.M., THOMAS, R.G., Rev. mod. Phys. 30 (1958) 257.
[6] AGODI, A., Proc. SIF Meeting, Bari (1963).
[7] BETHE, H.A., Phys. Rev. 57 (1940) 1125.
[8] BARSCHALL, Phys. Rev. 86 (1952) 431; WALT, BARSCHALL, Phys. Rev. 93 (1954) 1062; OKAZAKI, DARDEN, WALTON, Phys. Rev. 93 (1954) 461; COOK, BONNER, Phys. Rev. 94 (1954) 651.
[9] FESHBACH, PORTER, WEISSKOPF, Phys. Rev. 96 (1954) 448.
[10] LANE, THOMAS, WIGNER, Phys. Rev. 98 (1955) 693.
[11] BLOCH, C., J. Phys. Rad. 17 (1956) 510; Nucl. Phys. 3 (1957) 137; BROWN, G.E., DeDOMINICIS, C.T., Proc. Phys. Soc. A70 (1957) 668; FESHBACH, H., Ann. Rev. Nucl. Sci., 8 (1958) 44.
[12] BROWN, G.E., Revs Mod. Phys. 31 (1959) 893.
[13] MOTT, N.F., MASSEY, H.S.W., The Theory of Atomic Collisions, 3rd ed., Oxford (1965).
[14] FRIEDMAN, WEISSKOPF in "Niels Bohr and the Development of Physics, Pergamon Press, London (1955) 134.
[15] DIRAC, P.A.M., The Principles of Quantum Mechanics, 3rd ed., Oxford (1947) 193-198.

[16] HUGENHOLTZ, Physica 23 (1957) 481; SHAW, G.D., Ann. Phys. 8 (1959) 509; BELL, G.S.,
     SQUIRES, E.J., Phys. Rev. Letters 3 (1959) 96; THOULESS, D., The Quantum Mechanics of
     Many-Body Systems, Acad. Press, N.Y. (1961); BROWN, G.E., Unified Theory of Nuclear Models,
     North Holland, Amsterdam, 1964; MEERON, E., ed. Physics of Many-Particle Systems: Methods
     and Problems 1, Gordon and Breach, New York (1966).

[17] FESHBACH, BLOCK, Ann. Phys. N.Y. 23 (1963) 49; FESHBACH, KERMAN, LEMMER, Ann. Phys. 41
     (1967) 230.

[18] AGODI, A., Suppl. Nuovo Cim. 3 (1965) 1; Proc. 11th Summer Meeting of Nucl. Phys., Herceg-Novi,
     1966 (ŠIPS, L. Ed.) 2, Zagreb (1967) 229-290.

HARTREE-FOCK-BOGOLYUBOV CALCULATIONS

H.H. WOLTER
University of Münster,
Federal Republic of Germany

Abstract

HARTREE-FOCK-BOGOLYUBOV CALCULATIONS.
The author discusses in which way and to what extent pairing correlations affect the nuclear wave function. He finds that for many nuclei in the pf-shell the Hartree-Fock approximation is not valid.

1. INTRODUCTION

The Hartree-Fock-Bogolyubov (HFB) approach to nuclear structure is a unification of two of the most important microscopic theories, the HF- and the BCS-approximations. As in HF, it attempts to compute the parameters of a single-particle model from first principles, and as in BCS it takes into account the pairing correlation, but both of this is done self-consistently.

In this contribution we first want to review the HFB-theory briefly and discuss the possibility of proton-neutron correlations. Then we present results of such calculations in pf-shell nuclei. These calculations seem to indicate that in such nuclei pairing often gives significant improvements over the HF-wave-function.

2. REVIEW OF HFB-THEORY

The derivation of the HFB-equation has been presented by various authors [1, 2]. In it one deals with a linear transformation of a particle basis $c_k^\dagger$ to quasi-particles $a_\alpha^\dagger$

$$a_\alpha^\dagger = \sum_k A_{k\alpha} c_k^\dagger + B_{k\alpha} c_k \tag{1}$$

The ground state is approximated as the vacuum of these quasi-particles

$$a_\alpha \big| \text{HFB} \big\rangle = 0 \tag{2}$$

and the coefficients A and B are determined by a variational principle

$$\delta \big\langle \text{HFB} \big| H' \big| \text{HFB} \big\rangle = 0$$

$$H' = H - \lambda_P \hat{N}_P - \lambda_N \hat{N}_N \tag{3}$$

where H is the true many-body Hamiltonian, and $\hat{N}_P$ and $\hat{N}_N$ are the operators for the particle numbers of the protons and neutrons, respectively. The Lagrange multipliers λ_P and λ_N are adjusted to conserve the mean particle numbers.

The HFB-equations then have the following form

$$\begin{pmatrix} W & \Delta \\ -\Delta^* & -W^* \end{pmatrix} \begin{pmatrix} A^* \\ B^* \end{pmatrix} = E \begin{pmatrix} A^* \\ B^* \end{pmatrix} \tag{4}$$

A and B are the column vectors of the transformation coefficients (1).
W and Δ are matrices with the following meaning:

$$W_{k\ell} = T_{k\ell} - \lambda_k \delta_{k\ell} + \Gamma_{k\ell} \tag{5}$$

where T is the kinetic energy and

$$\Gamma_{k\ell} = \sum_{mn} \langle km | V | \ell n \rangle \rho_{nm} \tag{6}$$

is the Hartree potential, which is the same as in HF-theory.

$$\rho_{k\ell} = \langle c_\ell^\dagger c_k \rangle = \sum_\alpha B_{k\alpha}^* B_{\ell\alpha} \tag{7}$$

is the density matrix. The pairing tensor

$$\kappa_{k\ell} = \langle c_k c_\ell \rangle = \sum A_{k\alpha}^* B_{\ell\alpha} \tag{8}$$

is used to define the pairing potential

$$\Delta_{k\ell} = \frac{1}{2} \sum_{mn} \langle k\ell | V | mn \rangle \kappa_{nm} \tag{9}$$

The matrices κ and Δ are identically zero in the HF-case.

The HFB-equations are non-linear and solved by iterations. Moreover, the Lagrange parameters have to be adjusted during the iteration, to give the particle numbers correctly.

The HFB-theory considers what can be called "static" correlations as opposed to the theory of pairing vibrations [3]. It contains pairing correlations already in the ground state of the nucleus, while in pairing vibrations one builds pairing correlations on the ground state to obtain an excited state.

The HFB-wave-function represents an intrinsic state because the position and the orientation of the potential well are fixed in space. The generality of the intrinsic state is usually restricted by a truncation of the basis and by symmetry restrictions of the transformation (1) because one has to reduce the computational labour and to assume some properties of the intrinsic state. In the calculation reported, the following symmetries are assumed: axial symmetry, time reversal, and parity. Also pairing is restricted to pairing either between protons and protons or between neutrons and neutrons.

The latter is achieved by summing only over protons or only over neutrons in transformation (1). With PP or NN one can only make T = 1 pairs. If one wanted to mix P and N in the quasi-particle transformation, one could get PN correlation with T = 0 and T = 1 pairing. PN-pairing, especially T = 0, may be more important than PP- and NN-pairing for light nuclei, where protons and neutrons are in the same shell. This is suggested by the experimental fact that the ground states of most light nuclei have T = 0 and also by model calculations with PN-pairing [4].

Let us study what PN-pairing means for the HFB-equations. A matrix element of the pairing potential (9) between a P- and an N-state, separated into T = 0 and T = 1 parts, is

$$\Delta_{kP,\ell N} = \frac{1}{4}\sum_{mn} \langle k\ell | V | mn \rangle^{T=0} (\kappa_{nN,mP} - \kappa_{nP,mN}) + \langle k\ell | V | mn \rangle^{T=1}$$

$$\times (\kappa_{nN,mP} + \kappa_{nP,mN}) \tag{10}$$

Let us, for a moment, assume that charge conjugation is a symmetry of the system, i.e. N = Z and no Coulomb force. Then one finds from expression (1)

$$\kappa_{nN,mP} = \kappa_{nP,mN}^{*} \tag{11}$$

Therefore, if κ is real (A and B in expression (1) real), then one only gets T = 1 PN-pairing. If κ is imaginary (e.g. A real, B imaginary), one only has T = 0 pairing. Only in the case of non-trivially complex κ one has both kinds of pairing. This makes the numerical treatment more difficult, but recently a method was proposed, to reduce the general complex HFB-problem to the handling of real matrices [5]. In the following results with PP- and NN-pairing only, the coefficients were taken to be real.

3. EVIDENCE OF PAIRING CORRELATIONS

The calculations, from which the following results are taken, have been performed together with A. Faessler, P.U. Sauer and M.M. Stingl [6-9]. For the nucleon-nucleon interaction we use soft-core semi-realistic potentials like the Brink force [10]. We also include the Coulomb interaction and subtract the kinetic energy of the centre-of-mass motion. The basis consists of all oscillator levels up to the N = 4 main shell. The forces do not have a spin-orbit interaction, which makes detailed comparison with experiment difficult for heavier elements.

Here we are mainly concerned with the effect of pairing correlations. What effects are we looking for? One important consequence of pairing is the energy gap in the single-particle spectrum of even-even nuclei, which is the pairing energy. But one has to distinguish between two kinds of gaps, the HF- and the pairing gap.

In a HF-calculation, the occupied orbitals are separated from the empty ones by a gap, which originates, as can be seen in model calculations [11], from the monopole part of the force. The size of this gap determines the stability of the HF-solution against the residual interaction, especially the pairing correlation.

On the other hand, the pairing gap is determined from the strength of the pairing force. In a usual BCS-calculation, this is a free parameter, but in a microscopic theory the pairing strength is determined from the nucleon-nucleon interaction. If we use a HF-basis, the efficiency of pairing is determined by the size of the HF-gap.

In a HFB-calculation both the average field and the pairing correlation are treated simultaneously, so we cannot see where the HFB-gap comes from. But we can compare with a corresponding HF-calculation. Then, if
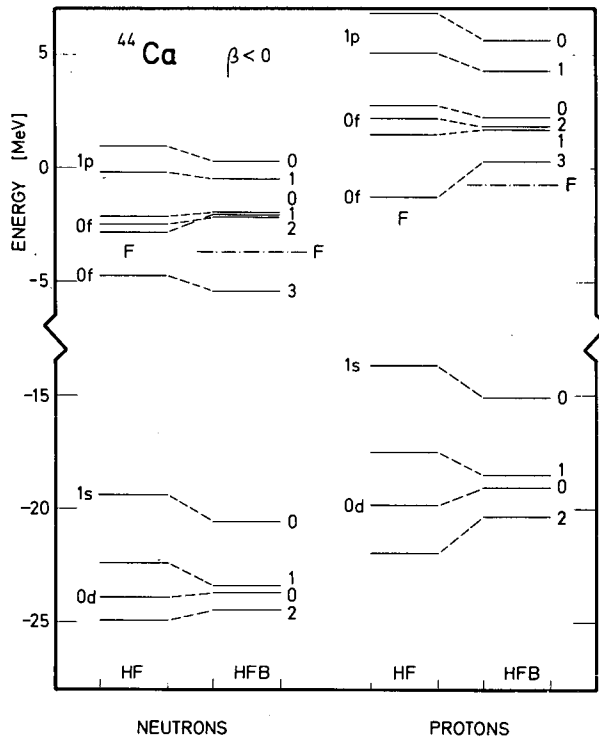
FIG.1.   Single-particle level spectrum of the oblate solution of ^{44}Ca for protons and neutrons in the sd- and pf-shells. The results of a HF- and a HFB-calculation are compared. F indicates the Fermi surface. The levels are labelled on the right by the projection of the angular momentum on the symmetry axis Λ, which is sharp, and on the left by the main component of the spherical-harmonic-oscillator states.

the HF-gap is already large, we expect little change in the wave function by pairing.

It is known that the HF-gap is very large in light nuclei. In HF-calculation it is found to be about 8 MeV in the p and sd-shell [12] and even larger with the Brink force. For such nuclei no pairing correlations are expected. HFB-results reduce to HF ones. Since we are interested here in the effect of pairing, we will not discuss such results. They are generally of the same quality compared to experiment as other HF-calculations.

The situation changes if we consider nuclei in the pf-shell with neutron excess. There the HF-gaps become considerably smaller, and pairing becomes evident. As an example, the single-particle levels of the oblate solution of ^{44}Ca are compared in Fig. 1 for the HF- and the HFB-calculation. The HF-neutron-energy gap is only about 1.8 MeV. In the HFB-calculation, the pairing energy increases the gap to about 3.3 MeV. This widening of the gap is the direct consequence of pairing.

But also all the other single-particle levels change their position, even far below the Fermi surface. This is an indirect consequence of pairing. Pairing makes a nucleus more spherical, because it is a short-range effect. In this case the charge quadrupole moment decreases from 75 fm^2 to 39 fm^2.
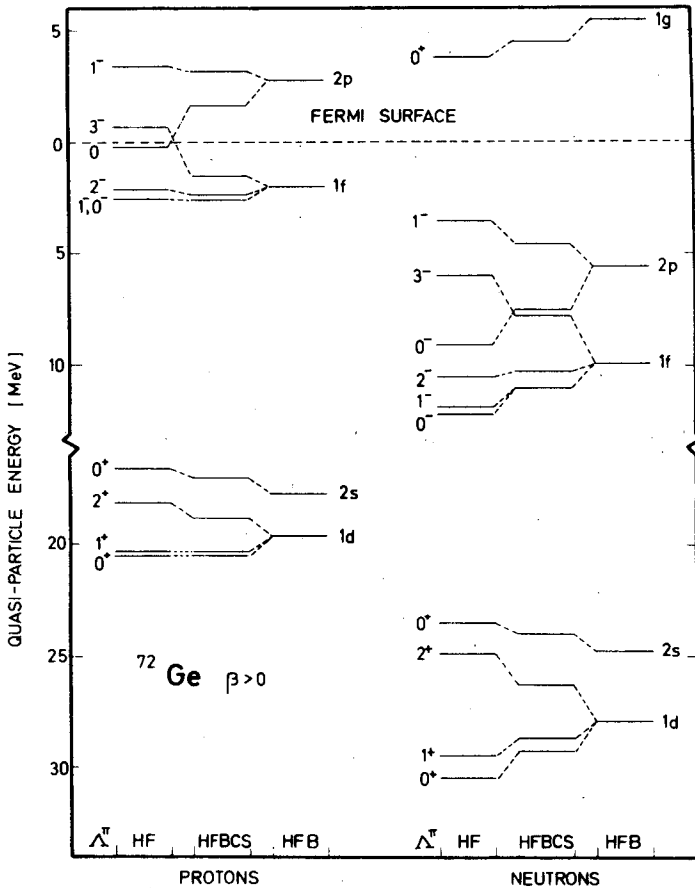
FIG.2.   Single-particle level spectrum for the prolate solution of ^{72}Ge.   Here the HF, the two-step HF-BCS and the HFB-calculations are compared.   The HFB-solution becomes spherical.   Labelling of the levels is similar to that of Fig.1.

Consequently, all the single-particle levels of one shell become more de-generate.   Thus, pairing changes the structure of the self-consistent field considerably.   In these cases it is important to use HFB.

This nucleus is a case of rather strong pairing correlations, as judged from the effect on the wave-function.   But even here, other properties of the nucleus are very insensitive.   The total binding energy of about 300 MeV changes only by about 1 MeV, and the radius is practically unchanged.   This is to be expected, because these are volume effects which will not be affected by a small smearing-out of the Fermi surface.

An even more interesting nucleus is ^{72}Ge.   We get two HF-solutions, a prolate and an oblate one.   Both are well deformed with a quadrupole moment of 129 and -30 fm^2, respectively.   In the HFB-calculation, both solutions become spherical and actually identical.   This is shown for the prolate case in Fig. 2.   There is practically no HF-gap for the protons at the Fermi sur-face, but one of about 5 MeV in the HFB-calculation.   All levels of each

shell become degenerate. The picture for the oblate solution looks quite similar.

In Fig. 2 we also represented the results of an intermediate method between HF and HFB, called HF-BCS. This is a BCS-calculation with the same nucleon-nucleon interaction on the HF-solution. An infinite succession of HF-BCS calculations would be identical to a HFB-calculation up to a unitary transformation. Usually the first two steps, i.e. HF-BCS, already give a very good approximation to HFB. But this is not so in ^{72}Ge. HF-BCS decreases the deformation but both solutions are still different and deformed. Only by simultaneous variation of both degrees of freedom is the spherical solution with the lower energy obtained. Thus, this is an example where it is essential to use the HFB-approach.

To see more clearly the trend of HFB-calculations, the results for some selected nuclei have been collected in Table I. The effect of pairing on the energy, the charge-quadrupole moment and the gaps is shown. For nuclei below ^{40}Ca the gaps are so large that no pairing occurs. But also for heavier nuclei the picture is not unique. There are some where pairing is very important, as in ^{72}Ge or the oblate Ca isotopes, but also other nuclei where pairing is unimportant, as in the prolate Ca isotopes or ^{56}Fe. The effects depend very sensitively on the size of the HF-gap, and we do get rather small HF-gaps for some nuclei in the pf-shell.

It is even possible to give a quantitative estimate in the case of the Brink force. If the HF-gap is below 3 MeV, pairing will be important and increases the gap to about 3 MeV or larger. The force is not very realistic for the description of pf-shell nuclei, because of the lack of spin-orbit force. So the results for special nuclei will certainly change, but we think that the general picture will be the same. It is to be expected that, with spin-orbit force, pairing will even become larger because the spin-orbit force tends to decrease the gaps [12].

TABLE I. EFFECT OF PAIRING CORRELATIONS ON THE BINDING ENERGY (B), CHARGE QUADRUPOLE MOMENT (Q) AND THE PROTON AND NEUTRON ENERGY-GAP PARAMETERS (Δ_P, Δ_N) FOR SOME NUCLEI IN THE sd AND pf SHELLS

Nucleus	B(MeV)		Q(fm²)		Δ_P(MeV)		Δ_N(MeV)	
	HF	HFB	HF	HFB	HF	HFB	HF	HFB
^{16}O sph.	92.90	92.90	0	0	10.7	10.7	10.8	10.8
^{20}Ne prol.	110.1	110.1	54.0	54.0	6.7	6.7	6.6	6.6
^{40}Ca sph.	289.82	289.82	0	0	17.4	17.4	15.8	15.8
^{44}Ca obl.	301.72	302.93	-16.0	-7.9	12.3	15.4	1.8	3.3
^{56}Fe prol.	329.13	329.42	162.5	162.7	5.4	5.5	2.1	3.2
^{72}Ge prol.	434.63	438.70	129.4	0	0.9	4.7	7.3	11.0
^{72}Ge obl.	437.17	438.70	-30.1	0	1.9	4.7	9.4	11.0
^{78}Se prol.	465.88	466.53	51.0	47.6	2.5	2.8	1.7	3.0
^{78}Se obl.	468.10	468.13	-114.4	-112.4	4.4	4.5	2.7	2.9

4. SUMMARY

A study has been made of how and to what extent pairing correlations affect the nuclear wave-function. It is found that for many nuclei in the pf-shell, but not for all, the HF-approximation is not valid. The HF-solution is unstable against pairing correlations. A HFB-calculation does not change the energy very much, but it changes the single-particle spectrum and the deformation significantly. Quantitative comparison of pairing effects with experiment is not so decisive at this stage, because of the force deficiencies. But it is concluded that the general picture of the importance of pairing correlations will persist.

REFERENCES

[1] BARANGER, M., in 1962 Cargèse Lectures in Theoretical Physics (LEVY, M., Ed.), W.A. Benjamin Inc., New York (1963).

[2] FAESSLER, A., in Nuclear Many-Body Problem, Herceg Novi 1967, (MIHAILOVIČ, M.V., ROSINA, M., STRNAD, J., Eds), The Federal Nuclear Energy Commission of Yugoslavia, Beograd (1967).

[3] RIPKA, G., these Proceedings.

[4] GOODMAN, A.L., STRUBLE, G.L., GOSWAMI, A., Phys.Lett. 26B (1968) 260, and preprint.

[5] VUJICIČ, M., HERBUT, F., preprint.

[6] FAESSLER, A., SAUER, P.U., STINGL, M.M., Z.Phys. 212 (1968) 1.

[7] WOLTER, H.H., FAESSLER, A., SAUER, P.U., STINGL, M.M., Nucl.Phys. A116 (1968) 145.

[8] SAUER, P.U., FAESSLER, A., WOLTER, H.H., Nucl.Phys. A125 (1969) 257.

[9] FAESSLER, A., SAUER, P.U., WOLTER, H.H., to be published in Nucl.Phys.

[10] BRINK, D.M., BOEKER, E., Nucl.Phys. A91 (1967) 1.

[11] BAR-TOUV, J., LEVINSON, C.A., Phys.Rev. 153 (1967) 1099.

[12] RIPKA, G., in Advances of Nuclear Physics 1 (BARANGER, M., VOIGT, E., Eds), Plenum Press, New York (1968).

SEPARATION AND PAIRING ENERGIES
IN SPHERICAL NUCLEI

M. BEINER
Institut de Physique Nucléaire,
Division de Physique Théorique,
Orsay, France

Abstract

SEPARATION AND PAIRING ENERGIES IN SPHERICAL NUCLEI.

   Separation energies of nucleons as well as pairing properties are calculated for spherical nuclei and systematically compared with experimental data. The spherical odd-nuclei (Z or $N \gg 15$) are represented by 31 "mean odd-Z nuclei", $(Z, \overline{N}(Z))$, and by 46 "mean odd-N nuclei", $(\widetilde{Z}(N), N)$, $\overline{N}(Z)$ and $\widetilde{Z}(N)$ being real mean values (in general non-integer) associated with any odd number Z and N, respectively. Using a local average potential (depending on few constants) in order to obtain sets of single-particle states and introducing computed realistic pairing matrices in the gap equations we obtain theoretical predictions in good agreement with the corresponding empirical data.

1. INTRODUCTION

   The main aim of these notes is to present and comment on some recent and improved results obtained in the framework of the simplified pairing scheme which was introduced and tested in two previous papers [1].[1]
   Justification of such an intuitive nuclear pairing model and discussion of its relations with the exact Hartree-Bogolyubov theory lie outside the scope of the present report. Even the question whether this model represents some approximation to the first-order H-B treatment of the n-body system (i.e. by neglecting the H_4 terms) cannot really be answered yet. The very last results available from numerical solutions of the H-F equations in co-ordinate space [2] for ^{208}Pb where pairing effects are believed not to be of crucial importance seem to indicate that our pairing model is probably no approximation of the first-order H-B scheme because the mean spacing of the single-particle levels around the Fermi limits is very different in the two approaches. Not so significant are the "bad" eigenvalues of our low-lying subshells which are systematically too high (e.g. - 41 MeV for the 15 neutron state in ^{208}Pb). In fact they do not sensitively influence the final results (chemical potentials as well as quasi-particle excitations).
   We must emphasize that our pairing model neglects, in principle, any reorganization energies (i.e. the mean separation energies (see I) are are directly given by the chemical potentials, λ_p and λ_n, which are somewhat regularized Fermi limits) and fails to predict the total energy of a given nucleus in the usual way. In fact, we are not interested in the total energy which, however, may be accurately computed (up to an additive constant) by integrating the chemical potentials. The necessary integrability condition $\partial_Z \lambda_n = \partial_N \lambda_p$ is actually fairly well satisfied in our model (as a direct consequence of the assumption (2.4)).

---

[1] These two papers are designated by I and II throughout this paper.

For the sake of completeness we briefly mention the principles de-
fining our scheme:
a) Introduction of a phenomenological local average nuclear potential
constructed from specific nuclear properties and providing us with sets of
single-particle states (section 2).
b) Use of suitable forces in order to compute realistic gap matrices
(section 3).
c) Interpretation of the numerical results in the approximation of free
quasi-nucleons (section 4).

2. THE AVERAGE NUCLEAR POTENTIAL

The single-particle states are defined by a local phenomenological
average potential with spherical symmetry.
    A critical analysis of the results given in I and II as well as new
numerical searches and comparisons with experimental data have suggested
two main modifications of our original assumptions (see I). The first
one concerns the radial dependence of the potential and the second the
form of the $\vec{\ell} \cdot \vec{s}$ term.

A) Generalized Woods-Saxon radial dependences

The first modification consists in introducing a somewhat more
flexible potential radial dependence which may be called a generalized
Woods-Saxon form:

$$f(r) \equiv \left(1 + \exp \frac{r - \widetilde{R}}{\alpha_5}\right)^{-\alpha_6} \tag{2.1}$$

(the α_i are numerical constants and the usual Woods-Saxon form is ob-
tained by taking $\alpha_6 = 1$).
Here $\widetilde{R}$ is determined by the condition

$$f(R) = 1/2 \tag{2.2}$$

with

$$R \equiv \alpha_3 A^{1/3} \pm \delta R \qquad \text{(+ sign for protons, - sign for neutrons)} \tag{2.2'}$$

δR is a small correction given by

$$\delta R = \frac{\alpha_2}{2\alpha_1} (C_n - C_p) \tag{2.3}$$

where C_n and C_p are the radii corresponding to the maximum values of
$-\rho_n'(r)$ (or $-\rho_p'(r)$) in the skin region of the density distributions. α_1 and
α_2 are constants making the potential depth a simple linear function of
$(N-Z)/A$ (see below). The two other constants α_5 and α_6 are allowed to
be different for protons and neutrons. Consequently, we shall distinguish
the two probably different radial functions by $f_+(r)$ and $f_-(r)$.

The main terms of the average potentials, $W_{\pm}^{C}(r)$ are then obtained with the help of the radial functions $f_{\pm}(r)$ as follows:

$$W_{\pm}^{C}(r) \equiv - (\alpha_1 \pm \alpha_2 \frac{N-Z}{A}) \ f_{\pm}(r) \qquad \begin{array}{l} + \text{ sign for protons} \\ - \text{ sign for neutrons} \end{array} \qquad (2.4)$$

It should be noted that α_1 and α_2 as well as α_3 are assumed to be the same for protons and neutrons.

B) Phenomenological $\vec{\ell} \cdot \vec{s}$ terms

Our second modification concerns the use of $\vec{\ell} \cdot \vec{s}$ terms directly derived from the above radial functions $f_{\pm}(r)$ (i.e. without (N-Z) dependence, see I):

$$W_{\pm}^{\ell s}(r) \equiv - \alpha_4^{\pm} \frac{1}{r} \ f'_{\pm}(r) \qquad (2.5)$$

We have also tried to introduce in the expression (2.5) the simple two-parameter empirical charge distribution of Hahn, Ravenhall and Hofstadter [3]

$$\rho_{\text{Hof.}}(r) \equiv \rho^0 \left(1 + \exp \frac{r - 1.09 \ A^{1/3}}{0.55} \right)^{-1} \qquad (2.6)$$

instead of $f_{\pm}(r)$. This attempt was misleading. We definitively obtained less satisfactory results (see section 4). (We remind that $\alpha_4^{\pm}$ are numerical constants, i.e. independent of Z and N.)

Furthermore we have also investigated for selected nuclei $\vec{\ell} \cdot \vec{s}$ terms of the following structure:

$$W_{\pm}^{\ell s}(r) \equiv - \alpha_3' \frac{1}{r} \rho'_{\pm}(r) - \alpha_3'' \frac{1}{r} \rho'_{\pm}(r) \qquad (2.7)$$

where $\rho_{+} \equiv \rho_p$ and $\rho_{-} \equiv \rho_n$ are theoretical distributions of protons and neutrons, respectively. The resulting ℓs splittings depends strongly on the principal quantum numbers of ths subshells as well as on Z and N. For example there is no more splitting of the high-lying 3p neutron level for N around 85. It is very difficult to check whether such sophisticated terms (needing iteration process) would represent a general improvement with respect to the simple expression (2.5).

C) Structure of the average potential

For the protons we add the Coulomb potential, $W^{Ch}(r)$, which is calculated including exchange contributions [4] from the empirical charge distributions (2.6) or, if more consistency is desired, from the computed proton distributions. We chose this last option for the theoretical determination of the charge distribution differences for selected pairs of isotopes (see section 2-D), whereas the first and simpler one was used for

the numerical adjustment of the constants α_i. A similar situation occurs
for the term δR (see expression 2.2') and (2.3)): in principle, it should
be computed by using an iteration process, however, for nuclei close to
the stability line its effects can be simulated by taking a value of α_3 1.6%
larger for protons than for neutrons, and it is precisely what we have
done in order to adjust the constants α_i.

Let us now write down explicitly the expressions giving the complete
set of spherical potentials as functions of the nucleon numbers:

$$W_p(r) \equiv -\left(\alpha_1 + \alpha_2 \frac{N-Z}{A} + \alpha_4^+ \frac{\vec{\ell}\cdot\vec{s}}{r}\frac{d}{dr}\right)\left(1 + \exp\frac{r - \tilde{R}^+}{\alpha_5^+}\right)^{-\alpha_6} + W^{Cb}(r)$$

(for protons)

(2.8)

$$W_n(r) \equiv -\left(\alpha_1 - \alpha_2 \frac{N-Z}{A} + \alpha_4^- \frac{\vec{\ell}\cdot\vec{s}}{r}\frac{d}{dr}\right)\left(1 + \exp\frac{r - \tilde{R}^-}{\alpha_5^-}\right)^{-\alpha_6}$$

(for neutrons)

where the $\tilde{R}^{\pm}$ are determined by the conditions

$$\left(1 + \exp\frac{\alpha_3 A^{1/3} \pm (\alpha_2/2\alpha_1)(C_n - C_p) - R^{\pm}}{\alpha_5^{\pm}}\right)^{-\alpha_6^{\pm}} = 1/2$$

(2.9)

The numerical values of our nine constants α were adjusted by
fitting in the independent-nucleon approximation (see Ref. [4]):
a) the empirical nuclear radii,
b) the mean separation energies of protons and neutrons as functions of
Z and N, and
c) the empirical sequence of single-particle levels in selected spherical
odd nuclei.
They are given by:

$$\alpha_1 = 51.6 \text{ MeV}, \quad \alpha_2 = 31.1 \text{ MeV}, \quad \alpha_3 = 1.26 \text{ fm}$$
$$\alpha_4^+ = 36.5 \text{ MeV}\cdot\text{fm}^2, \quad \alpha_5^+ = 0.59 \text{ fm}, \quad \alpha_6^+ = 0.42 \quad (2.10)$$
$$\alpha_4^- = 34.5 \text{ MeV}\cdot\text{fm}^2, \quad \alpha_5^- = 0.54 \text{ fm}, \quad \alpha_6^- = 0.53$$

We shall call W_θ the average potential W for which W^{Cb} is calculated
from the empirical charge distributions and the δR term replaced by
taking different values of α_3 for protons and for neutrons.

D) Distributions of nucleons

Figures 1, 2 and 3 give the calculated distributions of nucleons for
six selected nuclei. The ^{40}Ca, ^{48}Ca and ^{208}Pb distributions are obtained
directly from the above set of average potentials because in such double
magic structures only trivial solutions ($\Delta_j = 0$ for all j) of the gap equa-
tions occur (see section 3-C). The good fit to the empirical r.m.s.
radius of the nuclear charge density will be shown in section 4.

For comparison purposes we have also plotted in Figs 1-3 the em-
pirical charge distributions (2.6).
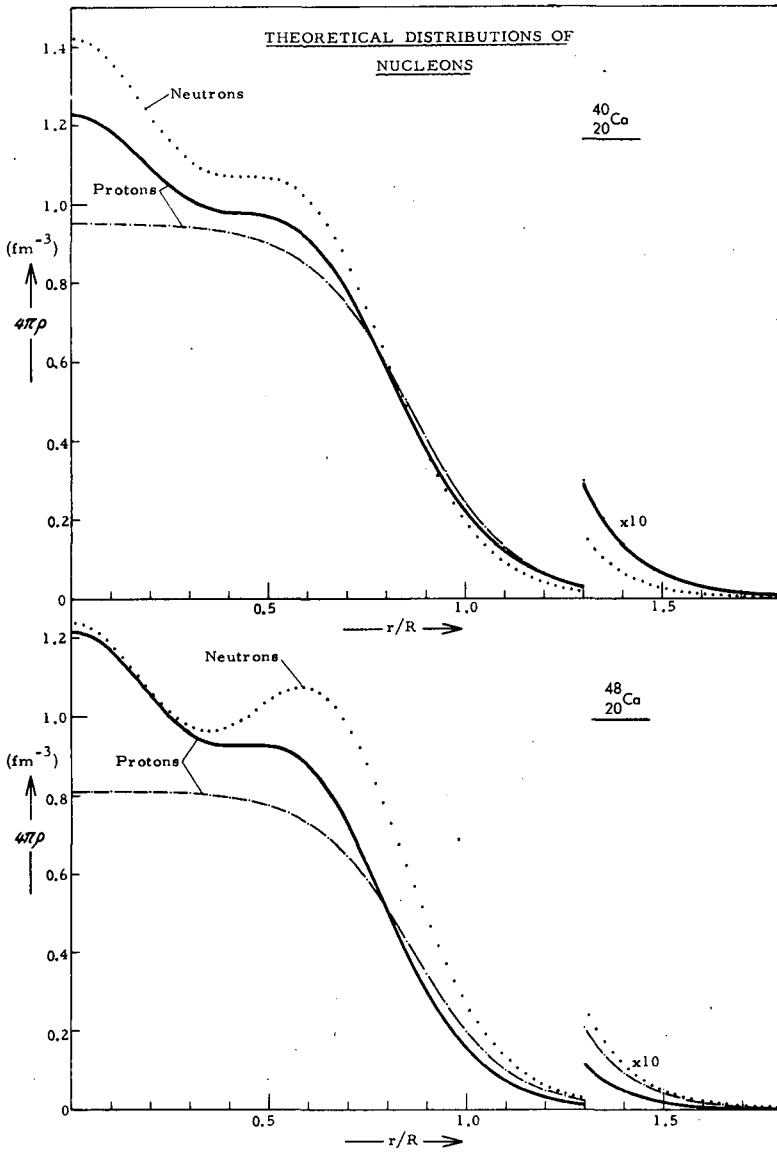
FIG.1.   "Self-consistent" distributions of nucleons in ^{40}Ca and ^{48}Ca, computed from the local average potential W given by Eqs (2.8), (2.9) and (2.10), section 2-C. The mean Stanford two-parameter charge distributions, Eq. (2.6), are also plotted (dotted curves).
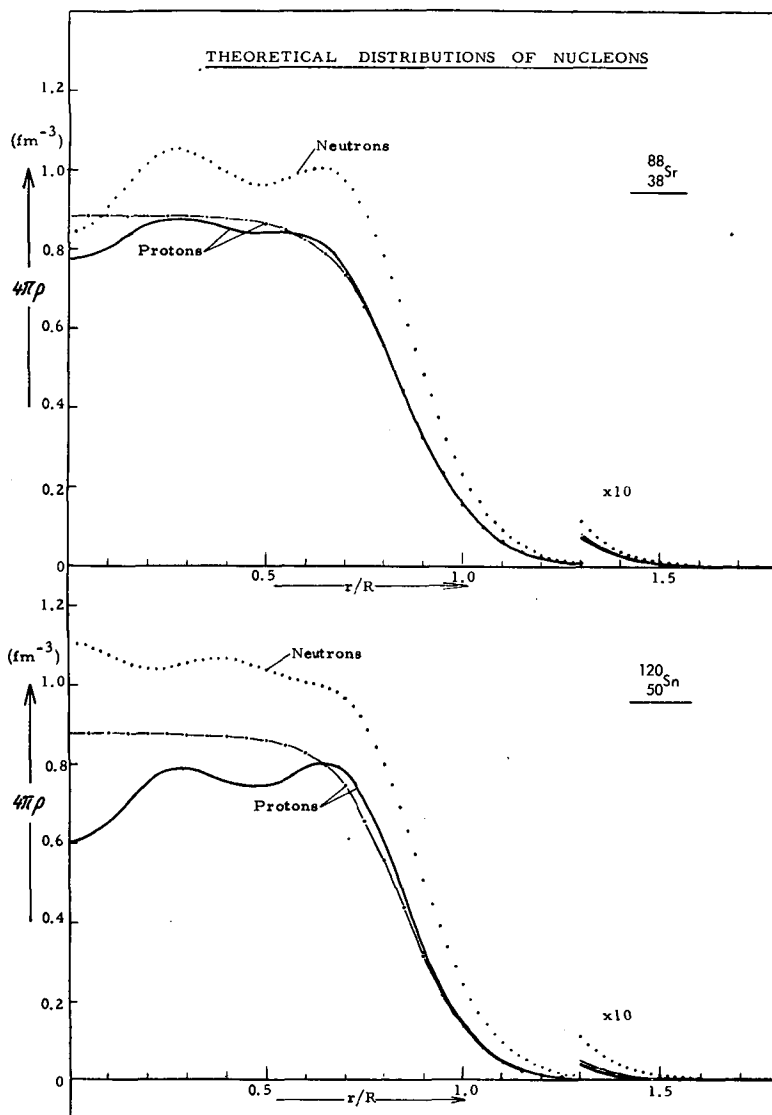
FIG.2. Theoretical distributions of nucleons in $^{88}_{38}$Sr, $^{120}_{50}$Sn, calculated in the BCS framework (diffuse Fermi limits) using (a) the local average potential W^0 (see Sect. 2-C) with α_3(protons) = 1.29 fm and α_3(neutrons) = 1.27 fm (trial values) and (b) the two-body Bonn interaction (see Sect. 3-A). The mean Stanford two-parameter empirical charge distributions, Eq. (2.6), are also plotted (dotted curves).

THEORETICAL DISTRIBUTIONS OF NUCLEONS
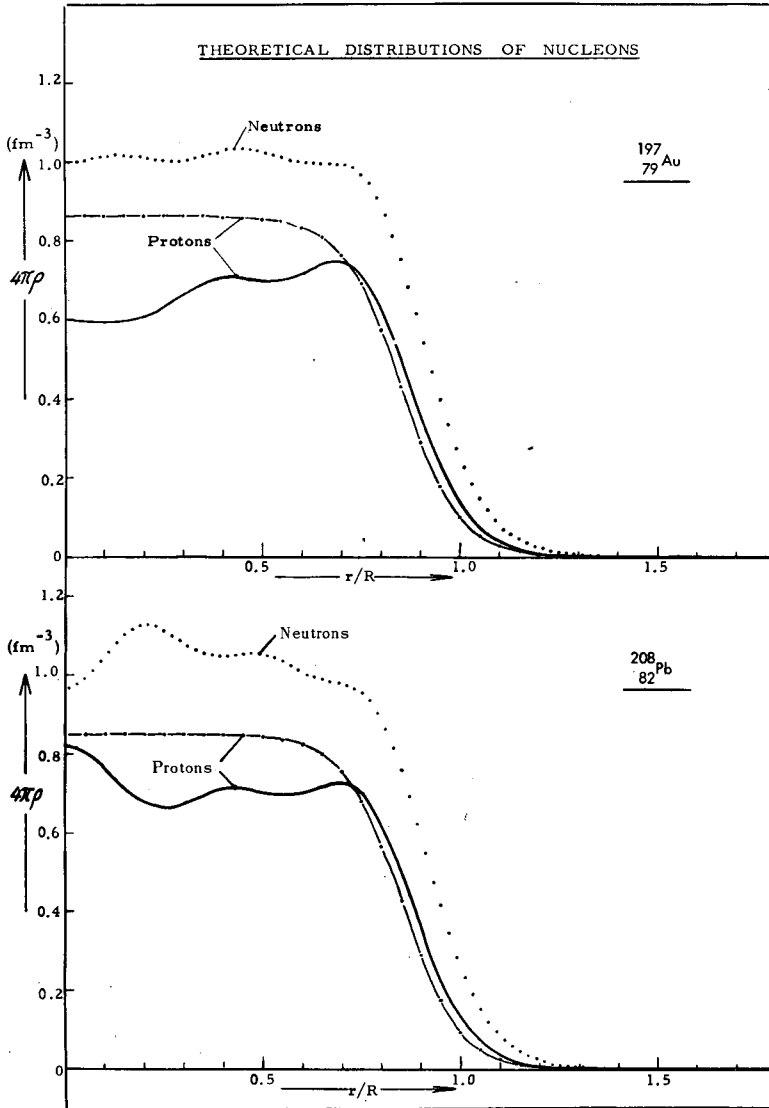
FIG.3. Theoretical distributions of nucleons in $^{197}_{79}$Au, $^{208}_{82}$Pb, calculated in the BCS framework (diffuse Fermi limits) using (a) the local average potential W^0 (see Sect. 2-C) with α_3 (protons) = 1.29 fm and α_3(neutrons) = 1.27 fm (trial values!) and (b) the two-body Bonn interaction (see Sect. 3-A). The mean Stanford two-parameter empirical charge distributions, Eq.(2.6), are also plotted (dotted curves).
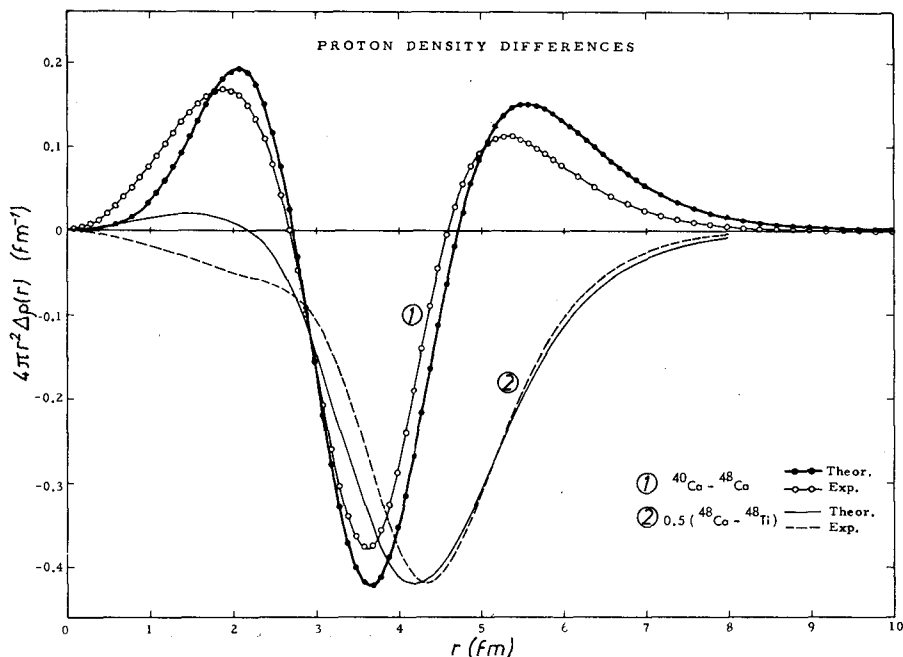
FIG.4.   Theoretical and experimental proton-density differences for the (^{40}Ca - ^{48}Ca) and (^{48}Ca - ^{48}Ti) pairs.

More significant for the adequacy of the average potential structure are the results plotted in Fig.4. We there compare the empirical differences in charge distributions of the (^{40}Ca - ^{48}Ca) and (^{48}Ca - ^{48}Ti) pairs recently determined at Stanford [5] with our predictions. The plotted quantities are the charge distribution differences multiplied by $4\pi r^2/e$. The agreement is surprisingly good if one considers that these computations constitute an independent test for the behaviour of the average potential as a function of Z and N (i.e. the structure of the average potential as well as the numerical constants α_i were not adapted to these last empirical data). It should also be noted that the δR term given by expression (2.3) was exactly worked out in the computation of these differences, a fact which was crucial for the good fit. Finally, it may be worth while noting that the agreement is completely disturbed for the other measured pairs ((^{40}Ca - ^{42}Ca) and (^{40}Ca - ^{44}Ca), see Ref. [5]) for which the theoretical predictions (as consequences of the assumed exact spherical symmetry) are of the type obtained for the (^{40}Ca - ^{48}Ca) spherical pair, i.e. also with two nodes.

E) Single-particle energies

The computations which we have done concern either
a) selected nuclei, or
b) the two classes of spherical odd-Z or odd-N nuclei (Z, N $\geq$ 15).
To reduce the extent of the explicit computations in this last case we define (in the (Z, N)-plane) a middle line of the flow of stable nuclei.
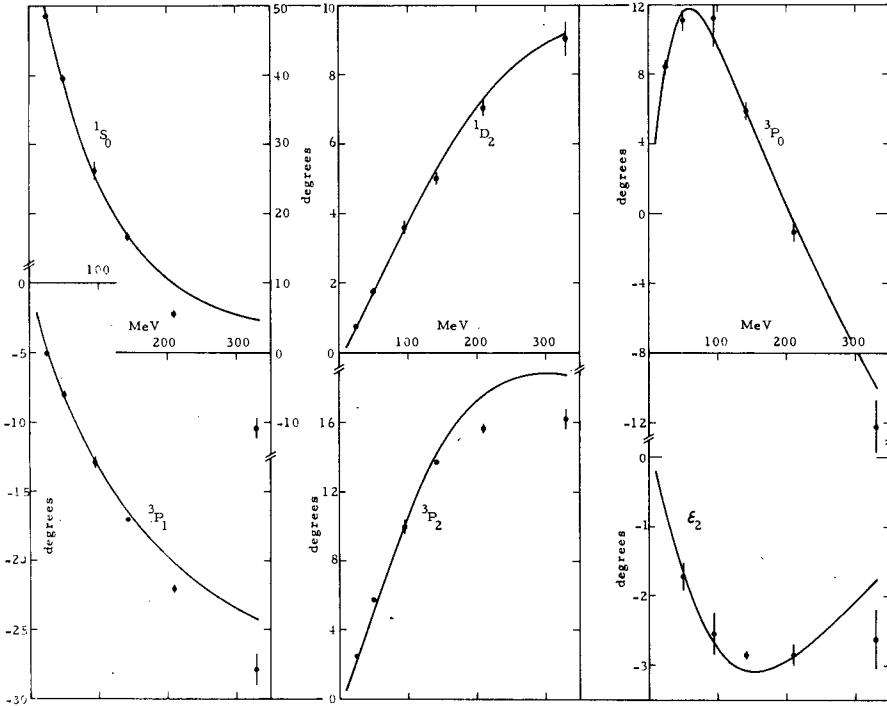
FIG.5. Main even-singlet ($^1S_0$ and $^1D_2$) and odd-triplet ($^3P_0$, $^3P_1$, $^3P_2$ and ϵ_2) phase shifts obtained with the Bonn interaction compared to the results of the single-energy phase-shift analyses of Arndt-MacGregor-Wright ($\blacklozenge$).

This line connects the following isotopes by straight segments:

$$(Z,N) = (0,0),\ (10,11),\ (20,23),\ (30,37),\ (40,52),\ (50,68),\ (60,85),$$
$$(70,102),\ (80,120),\ (90,138),\ (100,156). \tag{2.11}$$

We call "mean odd-Z nuclei" the points $(Z, \bar{N}(Z))$ on this line with (integer) odd Z values ($\bar{N}(Z)$ being in general non-integer) and "mean odd-N nuclei" the points $(\bar{Z}(N), N)$ on this line with (integer) odd N values. This notation will be used throughout this paper. When dealing with such mean odd-nuclei we shall, in general, omit the redundant arguments. For example, $\epsilon_{j_p}(Z)$, $\lambda_p(Z)$ and $G_{j_p j'_p}(Z)$ will designate the single-proton energies, the proton chemical potential and the proton-gap-matrix elements, in mean odd-Z nuclei, respectively. Theoretical properties can be computed directly for such "ideal" nuclei whereas the corresponding experimental data will be obtained by appropriate interpolations (see footnote to section 4-B).

Single proton energies of the mean odd-Z nuclei and single neutron energies of the mean odd-N nuclei are represented by the two sets of curved thin lines in the middle part of Fig.8. The corresponding Fermi limits are indicated by dotted lines (zigzag-lines). One sees that these dotted lines are already a first approximation to the experimental mean

FIG.6. Best adjusted oscillator constants $\hbar\omega_0$ for proton states (full circles) and for neutron states (open circles) in mean odd-Z and odd-N nuclei as defined in section 2-E.

separation energies (defined in Fig.7) represented by the two lines of connected full circles. This adjustment of the Fermi limits to the experimental mean separation energies is the main condition fixing both qualitatively and quantitatively the average potential. The chemical potentials, $\lambda_p(Z)$ and $\lambda_n(N)$, (see section 3-C) are nothing but somewhat regularized Fermi limits. They are represented in Fig.8 by the thick lines connecting open circles.

$$B^{\alpha}(Z,N) \equiv B(Z,N) - \mathcal{E}^{\alpha}(Z,N) \quad Z,N$$

$$B_{\overline{Z}n}(Z,N) \equiv \tfrac{1}{2}\left[B(Z,N+1) - B(Z,N-1) \right] \quad Z,N \qquad \text{(s.c. mean separation energy)}$$

$$\left.\begin{array}{l} B_n^{\alpha}(Z,N) \equiv B^{\alpha}(Z,N) - B(Z,N-1) \\[4pt] \tilde{B}_n^{\alpha}(Z,N) \equiv B(Z,N+1) - B^{\alpha}(Z,N) \end{array}\right\} \; Z\,\text{even},\,N\,\text{odd} \quad \text{(generalized separation energies)}$$

$$\Delta_{nn}(Z,N) \equiv \tfrac{1}{2}\left[B_{\overline{Z}n}(Z,N-1) - B_{\overline{Z}n}(Z,N+1) \right] \; Z,N \;,\; \text{slope of the "surface", } B_{\overline{Z}n}(Z,N)$$

$$\left.\begin{array}{l} \lambda_n = \partial_N E^{HB}(Z,N) \quad \text{(Theorem)} \\[6pt] -E^{HB}(Z,N)\big|_{ee} \sim B(Z,N)\big|_{ee} \\[6pt] \delta_{eo} \sim E_j^{min} \end{array}\right\} \Rightarrow$$

$$\underline{B_n^{\alpha}(Z,N)^{theor.}} = -\int_{N-1}^{N} \lambda_n(N')\,dN' - E_{j\mu}(N) \cdot$$

$$\cong -(\lambda_n(N-\tfrac{1}{2}) + E_{j\mu}) = \tfrac{1}{2}\partial_N\lambda_n - (\lambda_n + E_{j\mu})$$

$$\underline{\tilde{B}_n^{\alpha}(Z,N)^{theor.}} = -\int_{N}^{N+1} \lambda_n(N')\,dN' + E_{j\mu}(N)$$

$$\cong -(\lambda_n(N+\tfrac{1}{2}) - E_{j\mu}) = -\tfrac{1}{2}\partial_N\lambda_n - (\lambda_n - E_{j\mu})$$

$$\underline{B_{\overline{Z}n}(Z,N)^{theor.} = -\lambda_n(Z,N)}$$

pairing energies:

$$P_n \equiv 2\delta_{eo} \sim 2E_j^{min}$$

$$P_n^o \equiv \tilde{B}_n - B_n = P_n - \partial_N\lambda_n$$

FIG. 7. Definitions of the empirical data in which we are interested and basis of their theoretical interpretation.

3. REALISTIC GAP MATRICES

Although the average nuclear potential has been introduced pheno-menologically in our scheme we do not calculate the gap matrices $G_{jj'}$ with some residual interaction but with the full two-nucleon interaction as suggested by the H-B formalism. The gap matrices for spherical nuclei are defined by (see I, Eq. (4.8)):

$$G_{jj'} \equiv \frac{2}{(2\bar{j}+1)(2\bar{j}'+1)} \sum_{\substack{m \\ m'}} (-1)^{\bar{j}+\bar{j}'-m-m'} \langle jm, j-m \,|-V|\, j'm', j'-m' \rangle$$

$$(3.1)$$

FIG. 8. General comparison of pairing and mean separation energies (see section 4-B) in mean odd-Z
nuclei (upper half of the figure) and in mean odd-N nuclei (lower half of the figure). The two sets of
curved thin lines in the middle part of the drawing represent the single proton and neutron energies,
ϵ_{j_p} (Z) and ϵ_{j_n} (N), in the neighbourhood of the Fermi limits indicated by the two dotted lines
(zigzag-lines).

where j is an abbrevation for the principal, orbital and total angular momentum quantum numbers n, ℓ, $\bar{\jmath}$. The $|jm\rangle$ are either the single-proton states or the single-neutron states of our average nuclear potential, and V is the complete two-nucleon interaction.

We shall not discuss here the fundamental problem of the choice of a suitable N-N interaction. This problem has been partly treated in Refs[1] and [2]. As a rule, we have used the interaction (with new, adapted parameters) constructed some years ago in Bonn [1, 6] because we still believe that it is well adapted to our scheme. However, some pairing properties presented in this paper have also been computed with the two-body interactions of Brink-Boeker[7] and of Pires-de Tourreil [8].

Since we consider neutron-neutron and proton-proton pairing we do not need the two T = 0 projections of the interaction. For this reason we just give here the even singlet and odd-triplet projections of the Bonn and Pires-de Tourreil interactions which are both explicitly constructed within the four invariant subspaces of the two-nucleon problem.

A) T = 1 projections of the Bonn interaction

Let us first note that the Bonn interaction only contains reconstructed long-range tails of the Hamada-Johnston potential [9] with energy-independent cut-off radii. It fits the N-N scattering data fairly well up to about 150 MeV (see Fig.5).

a) even-singlet potential

$$V = V_C + V_{LL}\ L_{12}$$

(the tensor and $\vec{L}\cdot\vec{s}$ operators vanish in the even-singlet subspace!)

(3.2)

where L_{12} is the Hamada-Johnston quadratic operator defined by

$$L_{12} \equiv (\vec{\sigma}_1 \cdot \vec{\sigma}_2)\ \vec{L}^2 - \frac{1}{2}\ [\ (\vec{\sigma}_1 \cdot \vec{L})\ (\vec{\sigma}_2 \cdot \vec{L}) - (\vec{\sigma}_2 \cdot \vec{L})\ (\vec{\sigma}_1 \cdot \vec{L})]\qquad (3.3)$$

V_C and V_{LL} are radial functions vanishing for 0 fm $\leq$ r $\leq$ 1.25 fm and given for r > 1.25 fm by

$$V_C = -11.15\ Y\ (1 + 25\ Y)\quad (MeV)$$

$$V_{LL} = -1.62\ ZX^{-2}\ (1 - 2\ Y)\ (MeV)$$

(3.4)

where

$$Y \equiv X^{-1}e^{-X}\ ,\quad X = \mu r,\ \mu = 0.7067\ fm^{-1}$$

$$Z \equiv (1 + 3X^{-1} + 3X^{-2})$$

(3.5)

b) odd-triplet potential

$$V = V_C + V_T S_{12} + V_{LS}\ \vec{L}\cdot\vec{s}\qquad \text{(the } V_{LL} \text{ potential is taken equal to 0)}$$

(3.6)

where S_{12} is the usual tensor operator:

$$S_{12} \equiv 3 \, r^{-2} \, (\vec{\sigma}_1 \cdot \vec{r}) \, (\vec{\sigma}_2 \cdot \vec{r}) - (\vec{\sigma}_1 \cdot \vec{\sigma}_2) \tag{3.7}$$

The V_C, V_T and V_{LS} radial functions vanish for 0 fm $\leq r \leq 0.94$ fm and are given for $r > 0.94$ fm by

$$
\begin{aligned}
V_C &= 3.35 \; Y \; (1 - 0.5 \; YX + 10 \; Y^2 X^{-1}) & \text{(MeV)} \\
V_T &= 3.35 \; Z \; (1 - 0.7 \; YX^{-2} + 0.7 \; Y^2 X) & \text{(MeV)} \\
V_{LS} &= 34.8 \; Y^2 \; (1 - Y \; (4X^{-2} + 3X^{-1})) & \text{(MeV)}
\end{aligned}
\tag{3.8}
$$

We have plotted in Fig.5 the main even-singlet ($^1S_0$ and $^1D_2$) and odd-triplet ($^3P_0$, $^3P_1$, $^3P_2$ and ϵ_2) phase shifts given by the Bonn interaction together with the results of the single-energy phase-shift analyses of Arndt-MacGregor-Wright [10]. This figure shows that we obtain a satisfactory fit to the experimental data up to about 150 MeV. The complete interaction (see I for the T = 0 projections) gives in first order 6.4 MeV binding energy per article in nuclear matter at an equilibrium density corresponding to a Fermi momentum of k_F = 1.55 fm^{-1} [11].

B) T = 1 projections of the Pires-de Tourreil interaction

This interaction is also based upon the Hamada-Johnston operator basis. However, the hard core is suppressed and the Yukawa-type radial functions are replaced by Gaussians. This interaction gives 8 MeV binding energy per particle in nuclear matter at k_F = 1.48 fm^{-1} (together with small second-order contributions) and a satisfactory fit to the N-N scattering data up to 330 MeV.

a) even-singlet potential

It has the structure given by the foregoing formulas (3.2) and (3.3). The V_C and V_{LL} radial functions are now sums of two Gaussians and read (with r measured in fm):

$$
\begin{aligned}
V_C &= 500 \; e^{-(r/0.61)^2} - 190 \; e^{-(r/1.10)^2} & \text{(MeV)} \\
V_{LL} &= -20 \; e^{-(r/0.79)^2} + 0.02 \; e^{-(r/4.85)^2} & \text{(MeV)}
\end{aligned}
\tag{3.9}
$$

b) odd-triplet potential

$$V = V_C + V_T S_{12} + V_{LS} \; \vec{L} \cdot \vec{s} + V_{LL} \; L_{12} \tag{3.10}$$

with

$$
\begin{aligned}
V_C &= 75 \; e^{-(r/1.05)^2} - 55 \; e^{-(r/1.10)^2} \\
V_T &= 20 \; e^{-(r/1.44)^2} - 10 \; e^{-(r/0.80)^2} \\
V_{LS} &= -110 \; e^{-(r/0.92)^2} \\
V_{LL} &= -10 \; e^{-(r/0.80)^2} + 0.06 \; e^{-(r/3.0)^2}
\end{aligned}
\tag{3.11}
$$

C) Numerical solution of the gap equations

Let us recall the structure of the gap equations (see II, section 4) which we want to solve numerically for our two sequences of mean odd-nuclei (see 2-E):

$$\Delta_{j'} = 1/2 \sum_{j} (\bar{j} + 1/2) \frac{G_{jj'}}{E_j} \Delta_j \tag{3.12}$$

with

$$E_j \equiv +\sqrt{(\epsilon_j - \lambda)^2 + \Delta_j^2} \tag{3.13}$$

and

$$\lambda = \frac{P - \sum_{j} (\bar{j} + 1/2)(1 - \epsilon_j / E_j)}{\sum_{j} (\bar{j} + 1/2)/E_j} \qquad (P = Z \text{ or } N, \text{ odd}) \tag{3.14}$$

The summations extend over all proton subshells (for the computation of (proton) properties of mean odd-Z nuclei) or over all neutron subshells. The gap matrix elements $G_{jj'}$ and the single-particle energies ϵ_j are the input data while the physically interesting unknowns are the chemical potential λ and the quasi-particle excitations E_j (Δ_j has no direct physical meaning). We have, therefore, to insert in the above equations the following values (see 2-E), either:

$$G_{jj'} = G_{j_p j'_p}(Z), \quad \epsilon_j = \epsilon_{j_p}(Z) \qquad P = Z$$

or:

$$G_{jj'} = G_{j_n j'_n}(N), \quad \epsilon_j = \epsilon_{j_n}(N) \qquad P = N$$

Our first task is, thus, the numerical determination of the gap-matrix elements $G_{j_p j'_p}(Z)$ and $G_{j_n j'_n}(N)$ defined by expression (3.1).

This may be done, to a good approximation, in the following relatively simple way. For any given mean odd-Z or odd-N nuclei we expand the radial part of the single-proton or neutron states $|jm\rangle$ of the average potential W^0 (see 2-C) with respect to the ortho-normal system of oscillator wave functions and we determine an oscillator constant $\hbar\omega_0$ which maximizes the following weighted sum (all the α_j are positive numbers ≤ 1)

$$S \equiv \sum_{j_1}^{j_2} a_j / E_j^0 \tag{3.15}$$

where the a_j are the main expansion coefficients of the states $|jm\rangle$, and E_j^0 are quasi-particle excitations computed with some approximate gap matrix. The summation extends over a great number of subshells around the Fermi limit (see Table I). It turns out that the so computed $\hbar\omega_0$ does not significantly depend on the E^0 values and on the number of expanded subshells and that the mean value $\bar{a}$ of the main expansion coefficients a_j is close to unity (see Table I). It is then allowed to replace

TABLE I. BEST ADJUSTED OSCILLATOR CONSTANTS $\hbar\omega_0$ FOR THE TWO SEQUENCES OF MEAN ODD-N NUCLEI AND MEAN ODD-Z NUCLEI (See Section 3.C and Eq. (2.11))

N	R (fm)	$\hbar\omega_0$ (MeV)	$\bar{a}$	n_1	n_2	Z	R (fm)	$\hbar\omega_0$ (MeV)	$\bar{a}$	n_1	n_2
15	3.81	11.38	0.981	8	0	15	4.04	10.40	0.975	9	0
17	3.97	11.09	0.973	9	0	17	4.22	10.28	0.984	9	0
19	4.12	11.01	0.982	9	0	19	4.38	10.15	0.988	9	0
21	4.25	10.72	0.986	10	0	21	4.54	9.89	0.991	10	0
23	4.38	10.63	0.991	10	0	23	4.69	9.78	0.994	10	0
25	4.49	10.48	0.992	11	0	25	4.84	9.64	0.995	10	0
27	4.60	10.31	0.994	11	0	27	4.97	9.47	0.996	11	0
29	4.70	0.89	0.987	12	0	29	5.10	9.12	0.996	11	0
31	4.80	9.67	0.976	13	0	31	5.23	8.97	0.994	12	0
33	4.90	9.62	0.981	13	0	33	5.35	8.79	0.990	13	0
35	4.99	9.48	0.975	14	0	35	5.47	8.67	0.990	13	0
37	5.08	9.39	0.981	14	0	37	5.58	8.52	0.992	13	0
39	5.16	9.29	0.984	14	0	39	5.69	8.38	0.992	13	0
41	5.24	9.22	0.987	15	0	41	5.80	8.27	0.992	14	0
43	5.32	9.12	0.988	15	0	43	5.90	8.14	0.991	14	0
45	5.39	9.06	0.990	15	1	45	6.00	8.08	0.991	15	1
47	5.47	8.97	0.991	15	1	47	6.10	7.96	0.990	15	1
49	5.54	8.87	0.991	15	1	49	6.20	7.84	0.989	15	1
51	5.61	8.61	0.992	15	1	51	6.29	7.70	0.989	15	1
55	5.74	8.40	0.975	15	3	53	6.38	7.60	0.988	15	1
59	5.87	8.25	0.963	15	4	55	6.47	7.50	0.986	15	1
63	5.99	8.13	0.973	15	4	57	6.56	7.39	0.986	15	1
67	6.10	8.01	0.978	15	4	59	6.64	7.27	0.985	15	1
71	6.21	7.93	0.980	15	7	61	6.72	7.16	0.984	15	1
75	6.32	7.84	0.982	15	7	63	6.80	7.06	0.983	15	1
79	6.42	7.73	0.984	15	7						
81	6.47	7.68	0.985	15	7						
83	6.52	7.57	0.986	15	7	77	7.33	6.45	0.975	15	4
89	6.66	7.47	0.987	15	7	79	7.40	6.35	0.974	15	4
						81	7.47	6.24	0.972	15	4
						83	7.54	6.41	0.968	15	4
115	7.21	6.93	0.972	15	13	85	7.61	6.35	0.968	15	4
119	7.29	6.86	0.974	15	14	87	7.67	6.29	0.974	15	6
123	7.37	6.78	0.977	15	14						
125	7.40	6.74	0.979	15	14						
127	7.44	6.75	0.979	15	14						
129	7.48	6.73	0.981	15	14						
133	7.55	6.69	0.982	15	14						

R : average nuclear potential radius
$\bar{a}$: mean value of the main expansion coefficients
n_1: number of expanded subshells
n_2: number of not expanded low-lying subshells

in expression (3.1) the $|jm\rangle$ wave functions by those of the best adjusted oscillators and the extent of the numerical computations is once more considerably reduced. Figure 6 shows the two sets of oscillator constants for the mean odd-Z and odd-N nuclei.

Using the Moshinsky transformation the explicit computation of the gap matrices is now carried out, and one finds that the gap matrix is a sum of two matrices, G^{es} and G^{ot}, the first one giving the contribution of the even-singlet projection of the interaction and the second one

that of the odd-triplet projection (see II, formulas (3.3') and (3.5 to 3.9)).
Finally the system of coupled gap equations (3.12) and (3.14) is solved
numerically by iterations.

D) Pairing contributions of low- and high-lying subshells

The first problem which arises if one considers the summations in
Eqs (3.12) and (3.14) is obviously the pairing contributions of the low-
and high-lying subshells. We have investigated this question and shall
briefly review the results. To test the contributions of the low-lying
subshells in a representative case we have selected a heavy mean odd-N
nucleus presenting large pairing effects. We chose N = 115 (see Fig.8).
Using the Bonn interaction (see section 3-A) and the single-neutron states
of the average potential (2.8) we have successively omitted from the total
pairing contribution of 29 bounded subshells the contributions of the 1, 2,
3, ..., 11 first subshells of the following "canonical" neutron subshell
sequence:

$$1s1/2 - 1p3/2 - 1p1/2 - 1d5/2 - 2s1/2 - 1d3/2 - 1f7/2 - 2p3/2 -$$
$$2p1/2 - 1f5/2 - 1g9/2 - 2d5/2 - 3s1/2 - 2d3/2 - 1g7/2 - 1h11/2 - ...$$

$$(3.16)$$

i.e. the contributions from the 2, 6, 8, 14, 16, 20, 28, 32, 34, 40 and
50 more bounded neutrons.

We obtained the following corresponding decreases (given in %) of
$E_{j_n}^{min}$ (in this case $E_{13/2+}$ and of the mean quadratic deviation ΔN of the
neutron number N (see II, section 4):

$$0,5, \ 0.7, \ 1.5, \ 3.0, \ 3.7, \ 4.4, \ 6.7, \ 8.1, \ 8.9, \ 11.9, \ 14.8\%,$$
and   0.1, 0.4, 0.5, 0.9, 1.1, 1.4, 2.1, 2.5, 2.7, 3.3, 4.3%

We see that these contributions are small, but not very small. In fact,
they are probably overestimations of the actual contributions because
(as already stated) our low-lying subshells (as those of any local average
potential normalized to give a fair account of the Fermi limits assuming
small reorganization energies) are energetically too high. Anyway it is
simpler and well justified to avoid an arbitrary cut-off starting in all cases
the summations with the 1s subshell. A somewhat more ambiguous
situation holds for the upper sum limit. It is certainly justified to ex-
tend the summation over all high-lying bounded subshells ($\epsilon_j < 0$). How-
ever, no negligible contributions must be expected from quasi-bounded
subshells ($\epsilon_j \geq 0$, but smaller than the sum of the centrifugal and Coulomb
walls) and even from the continuum.

We have not tried to solve accurately this interesting problem which
will probably lead to tedious computations. We shall only give here the results
of a first check concerning this question. We choose a light mean odd-N
nucleus (N = 19, $\hbar\omega_0 = 11$ MeV) with energy centred in the fourth bounded
shell (1f + 2p) with ~ 3 MeV. We add the three next oscillator shells
(1g + 2d + 3S), (1h + 2f + 3p) and (1i + 2g + 3d + 4s) at 8, 19 and 30 MeV,
respectively, neglecting the $\vec{\ell} \cdot \vec{s}$ splitting. Taking successively 0, 1, 2

and 3 shells more into the summation, we obtain for $E_{j_n}^{min}$ (in this case $E_{3/2^+}$) and ΔN the following values:

$$E_{3/2^+} = 1.54,\ 1.70,\ 1.742\ \text{and}\ 1.754\ \text{MeV}$$

$$\Delta N\quad = 1.50,\ 1.56,\ 1.580\ \text{and}\ 1.584$$

In these model estimations, the contribution of the first added shell at 8 MeV is not negligible, but the convergence is fast. Taking now into account all bounded and quasi-bounded subshells, i.e. adding to the 10 bounded subshells the unique quasi-bounded $1g9/2$ subshells at 4 MeV, we obtain:

$$E_{3/2^+} = 1.64\ \text{MeV}\quad \text{and}\quad N = 1.53$$

To use a realistic and simple prescription we have decided to extend systematically the summations in Eqs (3.12) and (3.14) over all bounded and quasi-bounded subshells.

E) Pairing effects of the different parts of the two-body force

Before presenting systematical results obtained with the complete $T = 1$ Bonn interaction (including the Coulomb force), let us finally discuss the relative importance of the different parts of this interaction.

Although additivity holds in setting up the gap matrix (see II, section 3) but is lost in the pairing effects (see the structure of the gap equations), it is more convenient to use a characteristic pairing property (as, for example, $2\ E_j^{min}$ which is the theoretical value corresponding to the usual empirical pairing energy (see Fig.7)) in order to determine the relative importance of the different parts of the interaction. Comparing, thus, pairing energies calculated with the complete and the truncated Bonn interaction (see section 3-A) we can state that

a) the even-singlet central term is the unique part of the interaction giving constructive pairing effects,

b) the L_{12} term has negligible pairing effects (less than 1%),

c) the complete nuclear odd-triplet interaction reduces, on the average, by 8.2% and by 7.3% the neutron and proton pairing energies, respectively, and

d) the Coulomb interaction reduces on the average, by 20% the proton-pairing energies.

4. RESULTS AND COMMENTS

We are now ready to present and comment on our general results.

A) Nuclear radii and Coulomb displacement energies

Table II shows a summary of the experimental r.m.s. charge radius [12] together with the computed characteristics of the distributions of protons and neutrons, $\rho_p(r)$ and $\rho_n(r)$, respectively.

TABLE II. MAIN CHARACTERISTICS OF THEORETICAL DISTRIBUTIONS
OF NUCLEONS $\rho_p(r)$ AND $\rho_n(r)$[a]

| Nucleus | Experimental r.m.s. charge radius (fm) | Computed characteristics (fm) | | | | | | |
| | | Protons | | | | Neutrons | | |
		$\langle r^2 \rangle^{1/2}$	C_p^-	C_p	C_p^+	$\langle r^2 \rangle^{1/2}$	C_p^-	C_n	C_n^+
8 ^{16}O	2.71 - 2.75	2.74	1.59	2.32	3.31	2.58	1.60	2.28	3.20
8 ^{18}O	2.77	2.67	1.62	2.33	3.30	2.90	1.75	2.50	3.49
12 ^{24}Mg	2.91 - 2.98	3.13	1.99	2.80	3.87	2.94	2.03	2.78	3.74
13 ^{27}Al	2.91 - 2.98	3.15	2.13	2.93	3.97	3.04	2.21	2.96	3.92
14 ^{28}Si	3.04	3.22	2.21	3.02	4.07	3.05	2.22	2.98	3.93
15 ^{31}P	3.07	3.26	2.26	3.13	4.19	3.16	2.32	3.16	4.13
16 ^{32}S	3.12 - 3.33	3.34	2.26	3.22	4.30	3.15	2.34	3.17	4.13
b 20 ^{40}Ca	3.50	3.47	2.65	3.47	4.51	3.29	2.68	3.44	4.38
b 20 ^{42}Ca	3.53	3.45	2.69	3.50	4.53	3.41	2.80	3.56	4.52
b 20 ^{44}Ca	3.53	3.44	2.74	3.54	4.55	3.51	2.91	3.67	4.63
b 20 ^{48}Ca	3.49	3.44	2.81	3.60	4.59	3.67	3.11	3.85	4.82
22 ^{46}Ti	3.57	3.58	2.86	3.67	4.70	3.50	2.93	3.69	4.64
b 22 ^{48}Ti	3.60	3.57	2.89	3.69	4.71	3.59	3.04	3.79	4.75
22 ^{50}Ti	3.57	3.56	2.92	3.71	4.72	3.66	3.15	3.89	4.85
23 ^{51}V	3.57 - 3.59	3.62	2.89	3.77	4.79	3.66	3.16	3.90	4.85
24 ^{52}Cr	3.66	3.68	3.04	3.84	4.86	3.65	3.17	3.90	4.85
26 ^{54}Fe	3.72	3.78	3.16	3.95	4.98	3.65	3.19	3.92	4.87
26 ^{56}Fe	3.74 - 3.85	3.77	3.18	3.97	4.98	3.75	3.20	4.02	5.00
27 ^{59}Co	3.76 - 4.01	3.80	3.26	4.04	5.05	3.82	3.25	4.12	5.12
28 ^{58}Ni	3.79 - 3.93	3.85	3.30	4.07	5.09	3.74	3.23	4.04	5.01
28 ^{60}Ni	3.82 - 3.84	3.84	3.31	4.08	5.09	3.82	3.27	4.13	5.13
38 ^{88}Sr	4.06 - 4.14	4.22	3.82	4.67	5.71	4.32	4.09	4.85	5.82
49 ^{115}In	4.49 - 4.50	4.60	4.43	5.22	6.23	4.70	4.50	5.37	6.38
50 ^{116}Sn	4.50 - 4.55	4.63	4.46	5.25	6.25	4.70	4.50	5.37	6.38
50 ^{120}Sn	4.57 - 4.64	4.64	4.49	5.28	6.28	4.79	4.62	5.48	6.50
50 ^{124}Sn	4.60 - 4.67	4.65	4.53	5.32	6.31	4.87	4.73	5.58	6.60
51 ^{122}Sb	4.63 - 4.67	4.67	4.52	5.32	6.32	4.81	4.66	5.52	6.53
79 ^{197}Au	5.28 - 5.32	5.47	5.59	6.41	7.41	5.61	5.77	6.61	7.63
82 ^{208}Pb	5.39 - 5.55	5.52	5.71	6.52	7.53	5.71	5.93	6.78	7.80
83 ^{209}Bi	5.17 - 5.54	5.56	5.74	6.55	7.56	5.71	5.94	6.79	7.80

[a] $C^- < C < C^+$ are those radii for which $-\rho'(C) = \max$ and $\rho'(C^-) = \rho'(C^+) = \frac{1}{2} \rho'(C)$. For the calculations resumed in this table the Coulomb potential was calculated from the empirical charge distribution (2.6) and the δR term (2.3) was replaced by two different values for α_4 ($\alpha_4 = 1.27$ for protons, and $\alpha_4 = 1.25$ for neutrons).

[b] For these five isotopes exact calculations were performed (i.e. the Coulomb potential was calculated from the theoretical proton distributions and the δR term was rigorously computed by using an iteration process).

C_p and C_n are defined by (see 2-A)

$$-\rho'_p (C_p) = \text{maximum} \quad \text{and} \quad -\rho'_n (C_n) = \text{maximum} \qquad (4.1)$$

while C_p^- and C_p^+, for example, are those radii ($C_p^- < C_p < C_p^+$) for which

$$\rho'_p(C_p^-) = \rho'_p(C_p^+) = \frac{1}{2} \rho'_p (C_p) \qquad (4.2)$$

The good fit to the experimental r.m.s. charge radius (in particular, the truely reproduced (N-Z) dependences) confirms once more the adequacy of the relatively simple structure of the average potential (see section 2-C).

For (Z = N) nuclei the r.m.s. proton radius is greater than the r.m.s. neutron radius whereas for nuclei close to the stability line the reverse situation holds. However, the difference between the two r.m.s. radii is always small and does not exceed 0.23 fm (^{18}O, ^{48}Ca and ^{124}Sn).

In the case of a two-parameter (c, z) Fermi distribution

$$\rho(r) = \rho^0 \left(1 + \exp \frac{r - c}{z}\right)^{-1} \tag{4.3}$$

one has

$$C = c, \quad C^+ - C = C - C^- \quad \text{and} \quad C^+ - C = 3.52 \, z = 0.80 \, t.$$

Taking the mean t value, t = (2.4 ± 0.3) fm, one obtains
$\langle C^+ - C^- \rangle^{\text{exp.}} = (1.92 \pm 0.24)$ fm whereas our theoretical values are
$\langle C_p^+ - C_p^- \rangle = 1.82$ fm and $\langle C_n^+ - C_n^- \rangle = 1.77$ fm.

Much more significant is the asymmetry of $\rho'(r)$ around r = C. We obtain:

$$\langle C_p^+ - C_p^- \rangle = 1.02 \text{ fm}, \quad \langle C_p - C_p^- \rangle = 0.80 \text{ fm};$$

$$\langle C_n^+ - C_n^- \rangle = 0.98 \text{ fm}, \quad \langle C_n - C_n^- \rangle = 0.79 \text{ fm}$$

with a very small dispersion of the individual values (see Table II). In this connection we believe that a three-parameter distribution of the type we have called a generalized Woods-Saxon form

$$\rho(r) = \rho^0 \left(1 + \exp \frac{r - \alpha_1}{\alpha_2}\right)^{-\alpha_3} \tag{4.4}$$

which well describes such an asymmetry without relating it to the be-haviour of the central density (as does the usual three-parameter Fermi distribution), would be better.

Finally, we obtain for the Coulomb displacement energy in ^{208}Pb estimated to be

$$\Delta E_C = \frac{4\pi}{N-Z} \int_0^\infty [\rho_n(r) - \rho_p(r)] \, W^{Cb}(r) \, r^2 dr \tag{4.5}$$

the following value: $\Delta E_C = 18.25$ MeV ($\Delta E_C^{\text{exp.}} = 18.98 \pm 0.02$ MeV) (see Ref. [2], section 4).

B) Separation and pairing energies

These energies represent our main results. Let B(N.Z) and $\epsilon^\alpha(Z, N)$ be the ground-state total binding energy or excitation energy of the state $|\alpha\rangle$ in the nucleus (Z, N). They determine completely the experimental data in which we are interested: the mean separation energy, the gene-ralized separation energies, the slope of the mean-separation-energy surface, and the pairing energy, which we have all defined in the upper
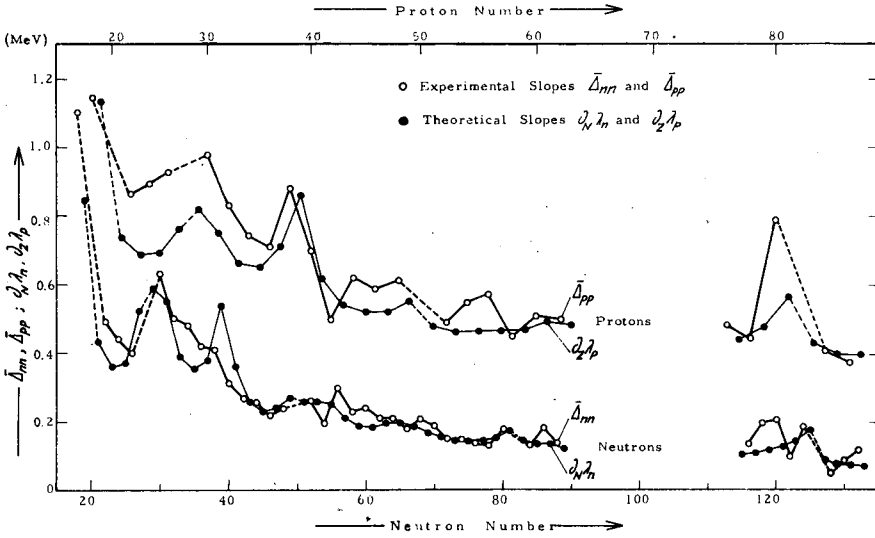
FIG.9. Experimental and theoretical slopes of the $B_{\overline{2p}}$ (Z,N) and $B_{\overline{2n}}$ (Z,N) surfaces (see Fig.7 as well as Eqs (4.6) and (4.7)).

and lower parts of Fig.7 for the neutron case. Symmetrical formulas have to be used for the proton case. Systematic surveys of some of these experimental data are given in Refs [1, 4, 13 - 15]. In the middle part (a) of Fig.7 we define and illustrate (also for the neutron case) the correspondence between these data and the theoretical values: λ (chemical potential) and E_j (quasi-particle-excitation energies). Let us note that we assume pure proton-proton and neutron-neutron pairing, i.e. that the ground state of an even-even nucleus is approximated by the product of two BCS wave functions, one for the protons and the other for the neutrons. The mean odd-Z and odd-N nuclei will thus be described as one quasi-proton or one quasi-neutron systems, the expectation values of the nucleon operators being taken equal to $(Z, \overline{N}(Z))$ and $(Z(\overline{N}), N)$, respectively. $E^{HB}(Z,N)$ is the total Hartree-Bogolyubov energy of the nucleus (Z,N). Dropping all the arguments we put together the formula which we shall use for the theoretical interpretation of the empirical data :

$$B_{\overline{2p}}^{th.} = -\lambda_p, \quad B_p^{\alpha th.} = \tfrac{1}{2} \cdot \partial_Z \lambda_p - (\lambda_p + E_{j_p(\alpha)}), \quad \Delta_{pp}^{th.} = \partial_Z \lambda_p$$
$$\text{and } \overline{P}_p^{th.} = 2E_{j_p}^{min} \tag{4.6}$$

$$B_{\overline{2n}}^{th.} = -\lambda_n, \quad B_n^{\alpha th.} = \tfrac{1}{2} \, \partial_N \lambda_n - (\lambda_n + E_{j_n(\alpha)}), \quad \Delta_{nn}^{th.} = \partial_N \lambda_n$$
$$\text{and } \overline{P}_n^{th.} = 2E_{j_n}^{min} \tag{4.7}$$

Figures 8 and 9 show for the two complete sequences of mean odd-nuclei the comparison between experimental and theoretical values of
a) the pairing and mean separation energies (Fig.8), and
b) the slopes of the $B_{\overline{2p}}$ (Z,N) and $B_{\overline{2n}}$ (Z,N) surfaces (Fig.9).

FIG.10. Generalized separation energies in $^{207}_{82}$Pb, $^{209}_{82}$Pb, $^{207}_{81}$Tl and $^{209}_{83}$Bi (see Fig.7 as well as Eqs(4.6) and (4.7)).

Experimental and theoretical generalized separation energies of four heavy nuclei (^{207}Pb, ^{209}Pb, ^{207}Tl and ^{209}Bi) are plotted in Fig.10.

Finally, Tables III and IV give the numerical values of the experimental and theoretical "functions" plotted in Fig.8, their differences as well as some additional information concerning the assignments of the low-lying states of odd nuclei.

Although the numerical parameters α_i are independent of Z and N the good agreement extends over the whole domain of spherical nuclei ($15 \leq Z \leq 87$ and $15 \leq N \leq 131$) and is thus really quite impressive.

Let $\langle \bar{P}_p \rangle$ be, for example, the mean experimental proton pairing energy for the complete sequence of mean odd-Z nuclei. We obtain for the mean difference between experimental and theoretical values:

a) $\langle B_{\overline{2p}} + \lambda_p \rangle$ = 0.02 MeV)
) (adjustment of α_1 and α_2!)
b) $\langle B_{\overline{2n}} + \lambda_n \rangle$ = 0.06 MeV)

c) $\langle \bar{P}_p - 2E_{j_p}^{min} \rangle$ = 0.50 MeV or 18.5% of $\langle \bar{P}_p \rangle$

d) $\langle \bar{P}_n - 2E_{j_n}^{min} \rangle$ = -0.01 MeV or -0.3% of $\langle \bar{P}_n \rangle$

with the following corresponding mean deviations of the individual differences:

TABLE III. PROPERTIES OF SPHERICAL ODD-Z NUCLEI

		Experimental data					Theoretical predictions						
Z	$\bar{N}$	$B_{\overline{2p}}$ (MeV)	$\frac{1}{2}\bar{P}_p$ (MeV)	$j_<^\pi$	$j_>^\pi$	n	$-\lambda_p$ (MeV)	$\delta\lambda$ (MeV)	$E_{j_p}^{min}$ (MeV)	δE (MeV)		j^π	
15	17.0	9.10	1.37	$1/2^+$	$(=)^a$	(1)	9.96	-0.86	1.29	0.08	$1/2^+$	$3/2^+$	$5/2^+$
17	19.4	8.73	1.57	$3/2^+$	$=^b$	1	9.24	-0.51	1.21	0.36	$3/2^+$	$1/2^+$	$7/2^+$
19	21.8	8.88	1.62	$3/2^+$	$=$	3	9.53	-0.65	1.29	0.33	"	"	"
21	24.4	8.46	2.09	$7/2^-$	$=$	(3)	7.72	0.74	1.11	0.98	$7/2^-$	$3/2^-$	$3/2^+$
23	27.2	8.84	1.80	$7/2^-$	$=$	(3)	8.44	0.40	1.06	0.74	"	"	"
25	30.0	9.13	1.55	$5/2^-$			9.06	0.07	1.04	0.51	"	"	$1/2^-$
27	32.8	8.95	1.53	$7/2^-$	$=$	(2)	9.51	-0.56	1.07	0.46	"	"	"
29	35.6	7.90	1.17	$3/2^-$	$=$	5	7.94	-0.04	1.00	0.17	$3/2^-$	$1/2^-$	$5/2^-$
31	38.5	7.85	1.32	$3/2^-$	$=$	1	7.88	-0.03	1.22	0.10	"	$5/2^-$	$1/2^-$
33	41.5	7.97	1.68	$3/2^-$	$=$	1	8.03	-0.06	1.36	0.32	$5/2^-$	$3/2^-$	$1/2^-$
35	44.5	7.94	1.64	$3/2^-$	$=$	1	8.30	-0.36	1.31	0.33	"	$1/2^-$	$3/2^-$
37	47.5	8.07	1.45	$5/2^-$	$=$	1	8.47	-0.40	1.34	0.11	$1/2^-$	$5/2^-$	"
39	50.5	7.93	1.11	$1/2^-$	$=$	2	8.34	-0.41	1.07	0.04	"	"	$9/2^+$
41	53.6	7.86	1.52	$9/2^+$	$(=)$	(2)	7.93	-0.07	1.08	0.44	$9/2^+$	$1/2^-$	$3/2^-$
43	57.6	8.20	1.66	$9/2^+$	$(=)$	(1)	8.14	-0.06	1.03	0.63	""	"	"
45	60.0	8.20	1.50	$7/2^+$			8.36	-0.16	0.99	0.51	"	"	"
47	63.2	8.17	1.52	$1/2^-$	$=$	(2)	8.55	-0.38	0.97	0.55	"	"	"
49	66.4	8.20	1.56	$9/2^+$	$=$	2	8.68	-0.48	0.99	0.57	"	"	"
51	69.7	6.74	1.31	$(5/2^+)$	$=$	(4)	5.95	0.79	0.94	0.37	$5/2^+$	$7/2^+$	$1/2^+$
53	73.1	6.94	1.21	$5/2^+$	$=$	2	6.14	0.80	1.07	0.14	"	"	"
55	76.5	6.73	1.11	$5/2^+$	$7/2^+$	0	6.33	0.40	1.16	-0.05	"	"	"
57	79.9	6.56	1.20	$(5/2^+)$	$7/2^+$	0	6.51	0.05	1.28	-0.08	"	"	"
59	83.3	6.66	1.34	$5/3^+$	$7/2^+$	0	6.61	0.05	1.29	0.05	"	"	"
61	86.7	6.69	1.40	$7/2^+$	$=$	2	6.63	0.06	1.31	0.09	"	"	$11/2^-$
63	90.1	6.77	1.48	$5/2^+$	$(=)$	(1)	6.58	0.19	1.40	0.08	"	$11/2^-$	$7/2^+$
77	114.6	6.24	1.00	$3/2^+$	$=$	2	6.60	-0.36	1.14	-0.14	$3/2^+$	$1/2^+$	$11/2^-$
79	118.2	6.54	0.89	$3/2^+$	$=$	(2)	6.50	0.04	0.98	-0.09	$1/2^+$	$3/2^+$	"
81	121.8	6.12	0.66	$1/2^+$	$=$	3	6.29	-0.17	0.73	-0.07	"	"	"
83	125.4	4.31	0.87	$9/2^-$	$=$	1	4.28	0.03	0.87	0.0	$9/2^-$	$7/2^-$	$13/2^+$
85	129.0	4.56	0.98	$(9/2^-)$	$(=)$	(1)	4.29	0.27	0.87	0.11	"	"	"
87	132.6	(5.05)	1.00	?	?	?	4.29	(0.76)	0.90	0.10	"	"	"

[a] ( ) *indicates that an experimental value is only a probable one.*

[b] = indicates the (horizontal) repetition of the last tabulated value.

Note: $\bar{N}$ is a mean neutron number associated with every odd-Z thus defining a mean odd-Z nuclei (Z, $\tilde{N}(Z)$) on our middle line (see section 2.E, in particular expression (2.11)). $B_{\overline{2p}} \equiv B_{\overline{2p}}(Z, N(Z))$ is the linear interpolation between the two proton mean separation energies $B_{\overline{2p}}(Z, N^-)$ and $B_{\overline{2p}}(Z, N^+)$ see Fig. 7), N^- and N^+ being the two even integers immediate neighbours of N(Z). $\bar{P}_p$ is a weighted average value of the proton pairing energies $P_p(Z, N)$ (see Fig. 7) over all even N isotopes (Z, N). $j_<^\pi$ and $j_>^\pi$ represent the assignments of the ground states of the two odd-Z nuclei (Z, N$^-$) and (Z, N$^+$), respectively, while n gives the length of the common sequence of ground and excited states in (Z, N$^-$) and (Z, N$^+$). $-\lambda_p$ is the theoretical value of $B_{\overline{2p}}$, $\delta\lambda$ being the difference ($B_{\overline{2p}} - (-\lambda_p)$) and $E_{j_p}^{min}$ is the theoretical value of $1/2\ \bar{P}_p$, δE being the difference ($1/2\ \bar{P}_p - E_{j_p}^{min}$) (see expression (4.6)). Finally, j^π gives the assignments of the ground and two first excited states in mean odd-Z nuclei.

TABLE IV. PROPERTIES OF SPHERICAL ODD-N NUCLEI (SEE CAPTION OF TABLE III AND REVERSE THE ROLES OF PROTONS AND NEUTRONS)

N	Z	Experimental data					Theoretical predictions						
		$\bar{B}_{2p}$ (MeV)	$\frac{1}{2}\bar{P}_n$ (MeV)	$j^\pi_<$	$j^\pi_>$	n	$-\lambda_n$ (MeV)	$\delta\lambda$ (MeV)	$E^{min}_{j_n}$ (MeV)	δE (MeV)	j^π		
15	13.38	8.87	1.65	1/2+	= b	(2)a	10.08	-1.21	1.58	0.07	1/2+	3/2+	5/2+
17	15.00	9.02	1.90	3/2+	=	2	9.75	-0.73	1.68	0.22	3/2+	1/2+	7/2-
19	16.67	9.14	2.00	3/2+	=	1	10.21	-1.07	1.63	0.37	"	"	"
21	18.33	8.45	1.76	7/2-	=	3	8.73	-0.28	1.39	0.37	7/2-	3/2-	3/2+
23	20.00	9.53	1.75	7/2-			9.45	0.08	1.29	0.46	"	"	"
25	21.43	9.92	1.61	7/2-	5/2-	. 0	9.94	-0.02	1.30	0.31	"	"	1/2-
27	22.86	10.13	1.57	7/2-	=	(3)	10.21	-0.08	1.51	0.06	"	"	"
29	24.29	9.06	1.23	3/2-	=	(5)	0.03	0.03	1.30	-0.07	3/2-	1/2-	7/2-
31	25.71	8.57	1.44	3/2-	1/2-	0	8.78	-0.21	1.49	-0.05	"	"	5/2-
33	27.14	8.50	1.54	3/2-	=	1	8.74	-0.24	1.75	-0.21	5/2-	"	3/2-
35	28.57	8.65	1.67	1/2-	5/2-	0	8.96	-0.31	1.61	0.06	"	"	"
37	30.00	8.63	1.72	5/2-			9.19	-0.56	1.63	0.09	1/2-	5/2-	"
39	31.33	8.66	1.70	1/2-	=	1	9.18	-0.52	1.57	0.13	"	"	"
41	32.67	8.88	1.71	9/2+	5/2+	0	8.81	0.07	1.35	0.36	9/2+	1/2-	5/2-
43	34.00	8.95	1.66	1/2			8.98	-0.03	1.27	0.39	"	"	"
45	35.33	9.14	1.62	7/2+	=	2	9.19	-0.05	1.20	0.42	"	"	5/2+
47	36.67	9.35	1.54	9/2+	(=)	(3)	9.42	-0.07	1.19	0.35	"	"	"
49	38.00	9.77	1.43	9/2+	=	(3)	9.58	0.19	1.20	0.23	"	5/2+	1/2-
51	39.33	7.56	0.82	5/2+	· =	2	7.42	0.14	0.92	-0.10	5/2+	1/2+	7/2+
53	40.63	7.71	0.90	5/2+	=	(2)	7.42	0.29	1.02	-0.12	"	"	"
55	41.88	7.68	1.01	5/2+	=	1	7.41	0.27	1.28	-0.27	"	"	"
57	43.63	7.61	1.29	1/2+	5/2+	0	7.46	0.15	1.58	-0.29	5/2+	7/2+	1/2+
59	44.37	7.70	1.33	1/2+	5/2+	0	7.57	0.13	1.55	-0.22	7/2+	1/2+	5/2+
61	45.62	7.75	1.37	5/2+	=	2	7.72	0.03	1.56	-0.19	"	"	"
63	46.88	7.74	1.36	5/2+	1/2+	0	7.86	-0.12	1.74	-0.38	1/2+	7/2+	3/2+
65	48.12	7.83	1.30	1/2+	=	1	7.94	-0.11	1.76	-0.46	"	3/2+	7/2+
67	49.37	7.87	1.35	1/2+	=	1	8.03	-0.16	1.76	-0.41	3/2+	11/2-	1/2+
69	50.59	7.99	1.45	1/2+	=	(3)	8.11	-0.12	1.55	-0.10	11/2-	3/2+	"
71	51.77	8.12	1.35	3/2+	1/2+	0	8.21	-0.09	1.42	-0.07	"	" "	"
73	52.94	8.12	1.33	1/2+	=	(2)	8.32	-0.20	1.33	0.0	"	"	"
75	54.12	8.11	1.25	1/2+	(=)	(1)	8.44	-0.33	1.28	-0.03	"	"	"
77	55.30	8.18	1.20	3/2+	(1/2)	(0)	8.55	-0.37	1.26	-0.06	"	"	"
79	56.48	8.32	1.12	3/2+	(=)	(1)	8.65	-0.33	1.25	-0.13	"	"	"
81	57.65	8.17	0.85	3/2 +	=	3	8.71	-0.54	1.28	-0.43	11/2-	3/2+	1/2+
83	58.82	6.58	0.92	7/2-	=	2	6.07	0.51	0.79	0.13	7/2-	3/2-	9/2-
85	60.00	6.65	0.94	7/2-			6.10	0.55	0.85	0.09	"	9/2-	3/2-
87	61.18	6.64	1.13	5/2-	7/2-	0	6.15	0.49	0.96	0.17	"	"	"
115	77.22	7.04	1.05	(9/2-)	(1/2-)	0	7.34	-0.34	1.29	-0.24	13/2+	5/2-	3/2-
117	78.34	7.13	0.98	1/2-	=	1	7.44	-0.31	1.25	-0.27	5/2-	13/2+	"
119	79.45	7.15	0.83	(3/2-)	1/2-	0	7.47	-0.32	1.15	-0.32	"	1/2-	"
121	80.56	7.19	0.78	3/2-	(5/2-)	0	7.48	-0.29	1.06	-0.28	1/2-	5/2-	"
123	81.67	7.31	0.79	5/2-	=	1	7.46	-0.15	0.85	-0.06	"	"	"
125	82.78	7.14	0.46	1/2-	=	1	7.39	-0.25	0.63	-0.17	"	"	"
127	83.89	5.24	0.79	9/2+	(=)	1	5.08	0.14	0.67	0.12	9/2+	11/2-	15/2-
129	85.00	5.46	0.77	(9/2+)	?	(1)	5.14	0.32	0.71	0.06	"	"	"
131	86.11	5.62	0.91	?	?	?	5.21	0.41	0.76	0.15	"	"	"

a ( ) indicates that an experimental value is only a probable one.
b = indicates the (horizontal) repetition of the last tabulated value.

a) 0.27 · (0.42, 0.57) MeV or 3.6% of $\langle B_{\overline{2p}} \rangle$

b) 0.24 (0.41, 0.30) MeV or 3.0% of $\langle B_{\overline{2n}} \rangle$

c) 0.56   MeV or 20.5% of $\langle \bar{P}_p \rangle$

d) 0.40   MeV or 15.8% of $\langle \bar{P}_n \rangle$

The values 0.42 and 0.41 are obtained using $\rho_{\text{Hof.}}(r)$ instead of $f_{\pm}(r)$ in the $\vec{\ell}\cdot\vec{s}$ term with new adjusted $\alpha_4^{\pm}$ (see 2-B). They demonstrate the inadequacy of deriving the phenomenological $\vec{\ell}\cdot\vec{s}$ term from smooth radial functions having the range of the empirical charge distributions. Of course this conclusion does not prejudice the use of computed nucleon densities in $\vec{\ell}\cdot\vec{s}$ terms (see expression (2.7)). However, it becomes very difficult to justify such a more sophisticated treatment experimentally. The mean deviations 0.57 and 0.30 MeV characterize results based upon the average potential. The relatively large one originates from unsuitable radial dependence of the proton potential (too short potential tails) and from wrong (N-Z) dependence of the $\ell\cdot s$ splitting intensity.

Whereas the mean differences $\langle B_{2p} + \lambda_p \rangle$ and $\langle B_{\overline{2n}} + \lambda_n \rangle$ have no particular meaning (adjustment of α_1 and α_2 (see expression (2.4)) those of $\langle \overline{P}_p - 2E_{j_p}^{\min} \rangle$ and $\langle \overline{P}_n - 2E_{j_n}^{\min} \rangle$ are very significant. They depend sensitively on the level density as well as on the two-body interaction, and it is really interesting to obtain the above results without any arbitrary renormalizations. However, one notices a definitively less satisfactory fit to $\overline{P}_p$ (Z) than to $\overline{P}_n$ (N), owing to the Coulomb interaction which notably reduces the theoretical proton pairing energies (see section 3-E). We have not yet found any compensations to this effect which does not seem to occur actually.

The mean deviations obtained are fairly small (in particular, those of the mean separation energies) and indicate that we also well reproduce some typical variations with Z or N of the empirical data (see Fig.8). The largest discrepancies occur for the pairing energies in the regions of theoretically isolated subshells with high j values ($21 \leq Z, N \leq 27$ and $41 \leq Z, N \leq 49$).

The results shown in Fig.9 nicely conform that our simple model works. In fact, they are not trivial, the important Coulomb asymmetry as well as some sensitive subshell effects being fairly well reproduced. Furthermore the relation:

$$\partial_N \lambda_p = \partial_Z \lambda_n \quad \text{(nothing but } \partial_{NZ}^2 E^{HB}(Z, N) = \partial_{ZN}^2 E^{HB}(Z, N),$$

$$\text{see Fig.7)}$$

(4.8)

is automatically satisfied in our model as a direct consequence of the symmetry of the expression (2.4).

Finally, let us briefly comment on the results shown in Fig.10. The mean discrepancy between theoretical and empirical generalized separation energies (absolute values) amounts to 0.21 MeV in ^{207}Pb (13 levels), 0.19 MeV in ^{209}Pb (7 levels), 0.66 MeV in ^{207}Tl (5 levels) and 0.17 MeV in ^{209}Bi (5 levels) (compare with Rost's results [16]). Thus, a local, suitably normalized average potential really seems to yield reasonable subshell density in the neighbourhood of the Fermi limits, which still remains the most disturbing well-known fact (see Introduction and Ref. [2]). Anyway the good fit to the levels of well-measured heavy nuclei strongly suggests to investigate super heavy spherical structures using the same set of numerical constants α_i (see expressions (2.10)) which successfully determine average potentials for the complete range of spherical nuclei known so far. We have not yet achieved results of computations along these lines and thus we just give a preliminary result: the only possible

candidate to be found for a spherical double-magic structure is $^{298}_{114}X_{184}$ with

$$\epsilon_{j_p} \ (2f7/2) = -4.30 \text{ MeV}; \quad \epsilon_{j_p} \ (2f5/2) = -2.47 \text{ MeV}$$

$$\epsilon_{j_n} \ (3d3/2) = -5.96 \text{ MeV}; \quad \epsilon_{j_n} \ (2h11/2) = -3.68 \text{ MeV}$$

Before drawing any conclusions, let us say a few words about the pairing properties of other N-N interactions.

C) Pairing effects of different interactions .

Since the good simultaneous fit to the experimental separation and pairing energies is probably not of accidental nature, it may be interesting to test the pairing effects of other N-N interactions just using the "best" sets of single-particle energies as well as oscillator constants which we have constructed. This procedure is obviously not self-consistent. However, it is actually the best way of doing something in this field without entering into tedious calculations. It is now very convenient (see section 3-C) to use once again the E_j^{min} values in order to compare the pairing effects of different two-body forces, and we put together the main results of these last investigations:

a)   For 4 groups of odd-Z isotones (N = 28, Z = 21-27; N = 50, Z = 37-43; N = 82, Z = 55-63; N = 126, Z = 81-87) and for 3 groups of odd-N isotopes (Z = 28, N = 29-37; Z = 50, N = 63-75; Z = 82, N = 119-129) the Bonn and Brink-Boeker B1, C1, L4, B4, C4 and L1 (see Ref. [7]) interactions successively give the following results:

$$\langle E_{j_p}^{min} \rangle = 1.05; \ 1.91, \ 2.28, \ 1.21, \ 1.66, \ 2.20, \text{ and } 1.60 \text{ MeV, respectively}$$

$$\langle E_{j_n}^{min} \rangle = 1.26; \ 18.0, \ 2.27, \ 0.87, \ 1.21, \ 1.87, \text{ and } 0.96 \text{ MeV, respectively}$$

whereas the corresponding experimental values are

$$\langle \tfrac{1}{2} P_p \rangle = 1.24 \text{ MeV} \quad \text{and} \quad \langle \tfrac{1}{2} P_n \rangle = 1.17 \text{ MeV}$$

The dispersion of the results obtained with the different kinds of the Brink-Boeker effective interaction should be noted, C1 giving the largest pairing effects in the proton as well as in the neutron case.

b)   For the two complete sequences of mean odd-Z and mean odd-N nuclei we obtain, by using successively Pires-de Tourreil [8], Bonn and Brink-Boeker C1 interactions:

$$\langle 2E_{j_p}^{min} \rangle / \langle \bar{P}_p \rangle = 0.50, \ 0.82, \text{ and } 1.74, \text{ respectively}$$

$$\langle 2E_{j_n}^{min} \rangle / \langle \bar{P}_n \rangle = 0.65, \ 1.00, \text{ and } 1.88, \text{ respectively}$$

The Pires-de Tourreil interaction thus clearly gives small pairing effects because the level density which we are using probably represents an upper limit of the actual density.

Finally, it may be worth while also comparing the corresponding chemical potentials in regions where they notably depend on the pairing
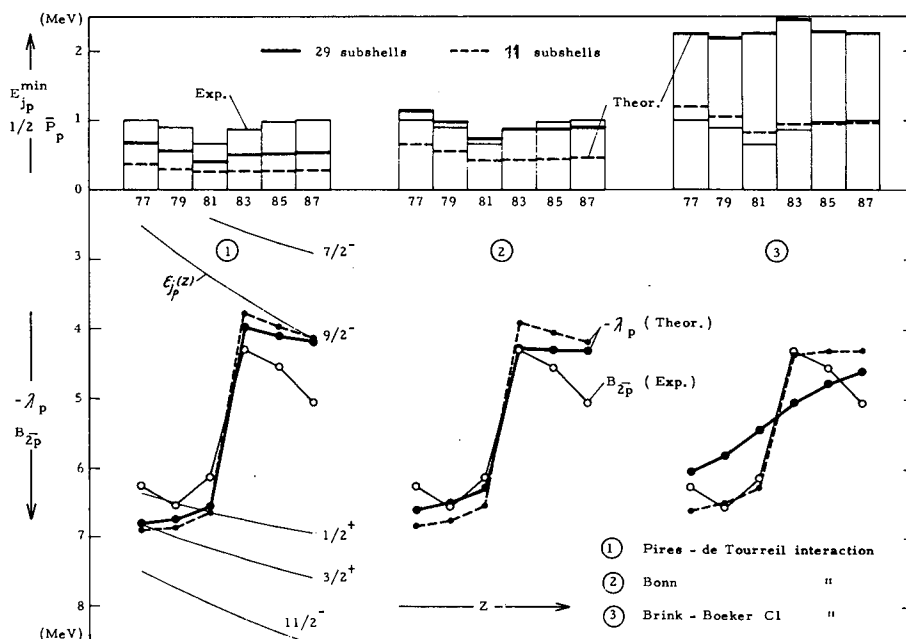
FIG. 11.   Pairing properties of mean odd-Z nuclei in the lead region, calculated with different N-N interactions.

intensity, i.e. in the immediate neighbourhood of magic numbers. Figure 11 illustrates the results for mean odd-Z nuclei in the lead region ($77 \leqq Z \leqq 87$). The three cases (designated by 1, 2 and 3) just correspond to the above three interactions while the 11 subshell calculations neglect the contributions of the 11 low-lying proton subshells 1s1/2 to 1g9/2 as well as those of the 7 high-lying proton subshells 2g9/2 - 1j15/2 - 1i11/2 - 3d5/2 - 2g7/2 - 3d3/2 and 4s1/2. Thus, using the single-proton energies of our average potential we find that (see Fig. 11):

a) In the first case (Pires-de Tourreil interaction fitting the N-N scattering data up to 330 MeV):

No fit can be obtained, neither to $B_{\overline{2p}}$ nor to $\overline{P}_p$.

b) In the second case (Bonn interaction containing long-range tails and fitting the N-N scattering data only up to 150 MeV):

A simultaneous fit to $B_{\overline{2p}}$ and to $\overline{P}_p$ is directly obtained.

c) In the third case (Brink-Boeker C1 effective interaction fitting in first-order nuclear matter and binding energy as well as density of $_2^4$He):

A simultaneous fit to $B_{\overline{2p}}$ and to $\overline{P}_p$ is only obtained if the interaction is renormalized suitably (dropping of low- and high-lying subshells).

5. CONCLUSION

Our simple pairing model nicely reproduces a relatively wide range of experimental data. In particular, in the neighbourhood of the Fermi limits our average potentials give realistic sets of single-proton and

neutron states needed in nuclear shell-model calculations. However, from a more fundamental point of view, the situation is not satisfactory since we actually do not know whether this model represents some approximation to the first-order Hartree-Bogolyubov treatment of the N-body problem.

REFERENCES

[1] BLEULER, K., BEINER, M., de TOURREIL, R., Nuovo Cim. 52B (1967) 45 and 149.
[2] VAUTHERIN, D., these Proceedings.
[3] HAHN, B., RAVENHALL, D.G., HOFSTADTER, R., Phys. Rev. 101 (1956) 1131.
[4] BEINER, M., Forschungsberichte des Landes Nordrhein-Westfalen, No.1407 (1964).
[5] FROSCH, R.F., HOFSTADTER, R., MacCARTHY, J.S., NÖLDIKE, G.K., VAN OOSTRUM, K.J.,
       YEARIAN, M.R., CLARK, B.C., HERMAN, R., RAVENHALL, D.G., Phys. Rev. 174 (1968) 1380.
[6] ERKELENZ, K., Thesis, Bonn 1967.
[7] BRINK, D.M., BOEKER, E., Nucl. Phys. A91 (1967) 1.
[8] PIRES, P., de TOURREIL, R., private communication.
[9] HAMADA, T., JOHNSTON, I., Nucl. Phys. 34 (1962) 382.
[10] MacGREGOR, M.H., ARNDT, R.A., WRIGHT, R.M., UCRL 70075 (Part X) (1968).
[11] de TOURREIL, R., private communication.
[12] LANDOLT-BÖRNSTEIN, Numerical Data and Functional Relationships in Science and Technology,
       New Series, Group I, Band 2, Nuclear Radii; see Table 2.1.
[13] BEINER, M., BLEULER, K., Nucl. Phys. 22 (1961) 589.
[14] ZELDES, N., GRONAU, M., LEV, A., Nucl. Phys. 63 (1965) 1.
[15] BLEULER, K., BEINER, M., ERKELENZ, K., SCHNEIDER, R., Ark. f. Fysik 36 (1967) 385.
[16] ROST, E., Phys. Lett. 26B (1968) 184.

MICROSCOPIC DERIVATION OF THE OPTICAL POTENTIAL

N. VINH-MAU
Institut de Physique Nucléaire,
Division de Physique Théorique,
Orsay, France

Abstract

MICROSCOPIC DERIVATION OF THE OPTICAL POTENTIAL.
This paper is an attempt to determine an optical potential from the microscopic many-body theory taking into account all the effects of antisymmetrization.

From the shell model, we know that the interaction of a particle with the remaining particles in the nucleus can be well represented by a single-particle potential. Then, one can suppose that this assumption holds for the scattering of a nucleon by a nucleus. This interaction of the incident particle with the nucleus can be represented by means of a single-particle potential which is called the optical potential and must be complex to take into account all inelastic processes [1]. The optical model has been extensively used in a phenomenological way. Assuming the validity of the model, one postulates a given form (local or non-local) for the optical potential [2], depending on parameters which are adjusted to reproduce the experimental data.

Then from a theoretical point of view, an interesting problem has to be solved: how can this optical potential be derived from many-body theory? Several attempts [3] have been made but they do not take properly into account the identity of the $(A+1)$ nucleons of the total system composed of the incident nucleon and the target nucleus of mass number A. Furthermore, either the Fermi gas model or the shell model are used to describe the target nucleus.

In the work reported here, we have tried to determine an optical potential from the microscopic many-body theory taking into account all the effects of the antisymmetrization. For such a program the Green's functions are a very powerful tool. A first attempt has been made in collaboration with N.V. Giai and G. Sawicki [4], but we did not get far enough through the hierarchy of Green's functions and finally performed our calculation of the Fourier transform of optical potential with an "anti-symmetrized" Feshbach's formula. In the same approximation, with M. Bruneau [5], we have looked at the properties of such an optical potential for 14-MeV nucleons scattered by calcium 40. But we shall see later on that this treatment of antisymmetrization is not justified.

Let us consider a system of $(A+1)$ interacting particles represented by

$$H = \sum_{i=1}^{A+1} T_i + \sum_{i<j=1}^{A+1} V(ij)$$

and look for the eigenstates $|\alpha\rangle$ of H:

$$H|\alpha\rangle = E|\alpha\rangle$$

We must find an equivalent system of one particle in a single-particle potential $\mathscr{V}$ such that all the observables calculated for this equivalent system would be identical with those of the initial problem.

Let us call $|0\rangle$ the true ground state of the A system and $\Psi^\dagger(\vec{r})$ the field operator in Schrödinger representation, which creates a particle in $\vec{r}$. The optical-model wave function for elastic scattering is by definition

$$\varphi(\vec{r}) = \langle 0|\psi(\vec{r})|\alpha\rangle$$

$\varphi(\vec{r})$ satisfies an integral equation [6] which can be written as

$$\varphi(\vec{r}) = \varphi_0(\vec{r}) + \int\int d^3\vec{r}' \, d^3\vec{r}'' G_1^{(0)}(\vec{r}, \vec{r}'; E) \sum (\vec{r}', \vec{r}''; E)\varphi(\vec{r}'') \qquad (1)$$

where $\varphi_0(\vec{r})$ is the free-particle wave function and $G_1(\vec{r}, \vec{r}'; E)$ is the Fourier transform of the one-particle Green's function:

$$G_1(r, r'; t - t') = -i\langle 0|T[\psi(\vec{r}, t)\psi^\dagger(\vec{r}', t')]|0\rangle \qquad (2)$$

$G_1^{(0)}(\vec{r}, \vec{r}'; E)$ is the Fourier transform of the free-particle Green's function and $\Sigma(\vec{r}', \vec{r}''; E)$ is the mass operator defined by the integral equation of G_1:

$$G_1(\vec{r}, \vec{r}_0; t - t_0) = G_1^{(0)}(\vec{r}, \vec{r}_0; t - t_0) - \int\int\int\int d\vec{r}' \, d\vec{r}'' \, dt' \, dt'' \qquad (3)$$

$$G_1^{(0)}(\vec{r}, \vec{r}'; t - t') \sum (\vec{r}', \vec{r}''; t' - t'')G_1(\vec{r}'', \vec{r}_0; t'' - t_0)$$

Eq.(1) is the Lippman-Schwinger equation of motion for a particle in a non-local potential which is by definition the optical potential $\mathscr{V}(\vec{r}, \vec{r}'; E)$:

$$\mathscr{V}(\vec{r}, \vec{r}'; E) = -\sum{}^i (\vec{r}, \vec{r}'; E)$$

$$= -\int_{-\infty}^{+\infty} e^{iE(t-t')} \sum (\vec{r}, \vec{r}'; t - t')d(t - t') \qquad (4)$$

E being the energy of the (A + 1) system.

This optical potential defined through the mass operator is non-local, depends on energy and is related to the mass operator of the one-particle Green's function for the A-system.

To derive Σ, two equivalent methods can be employed. Σ can be directly expanded in perturbative theory and in terms of Feynman diagrams; considering all the possible graphs to each order, one has to select some of them which can be resumed and calculated. Nevertheless, this is a very delicate work, although perhaps shorter and more elegant [7], and we have preferred to use dynamical equations for Green's functions as far as we could.

For the n-particle Green's function, the generalization of definition (2) is:

$$G_n(x_1...x_n; x'_1...x'_n) = (-i)^n \langle 0 | T[\psi(x_1)..\psi(x_n)\psi^\dagger(x'_n)..\psi^\dagger(x'_1)] | 0 \rangle \tag{5}$$

From the equations of field operator $\psi(x)$ and $\psi^\dagger(x)$, the dynamical equations of G_n can be derived [8]:

$$\left(i\frac{\partial}{\partial t_1} + \frac{\hbar^2}{2m}\Delta_1 \right) G_n(x_1...x_n; x'_1...x'_n) = \sum_{i-1}^{n} \delta^4(x_1 - x'_i)(-1)^{i-1}$$

$$G_{n-1}(x_2...x_n; x'_1...x'_{i-1} x'_{i+1}...x'_n) - i\int d^4 x_{n+1} U(x_1 - x_{n+1}) \tag{6}$$

$$G_{n+1}(x_1...x_{n+1}; x'_1...x_{n+1})$$

where $x^\dagger_{n+1} = (\vec{r}_{n+1}, t+0)$ and $U(x_1 - x_{n+1}) = V(\vec{r}_1 - \vec{r}_{n+1})\delta(t_1 - t_{n+1})$.

For $n=1$, the integral form of Eq.(1) gives us G_1 in terms of $G_1^{(0)}$ and G_2. Comparing Eqs (6) and (3), we obtain the following expression for Σ:

$$\sum(x, x') = i\int d^4 x_1, d^4 x_2 U(x - x_1)G_2(x, x_1; x_2 x_1^\dagger)G_1^{-1}(x_2 x') \tag{7}$$

assuming the existence of the inverse of G_1:

$$\int d^4 x_1 G_1(x; x_1)G_1^{-1}(x_1; x') = \delta^4(x-x') \tag{8}$$

From now on, all integrations will be implicitly understood each time where we have repeated variables.

In Eq.(7), the dynamical Eq.(6) may be used for G_2, and involves now G_1 and G_3.

Here we stop the hierarchy of Green's functions by assuming that G_3 is a sum of products $G_1 G_2$. That is equivalent to saying that we take into account the correlations between a pair of particles, neglecting the

correlations between this pair and the third particle. Taking care of double counting of graphs, this yields the following expansion of G_3 [9]:

$$G_3(x_3, x_1, x_4; x_2, x_1^\dagger, x_4^\dagger) = G_1(x_1; x_1^\dagger)G_2(x_3, x_4; x_2 x_4^\dagger)$$

$$-G_1(x_1; x_2)G_2(x_3, x_4; x_1, x_4^\dagger) - G_1(x_1; x_4)G_2(x_3, x_4; x_2 x_1)$$

$$+G_1(x_3; x_2)G_2'(x_1, x_4; x_1^\dagger, x_4^\dagger) - G_1(x_3; x_1)G_2'(x_1 x_4; x_2 x_4^\dagger) \qquad (9)$$

$$+G_1(x_3; x_4)G_2(x_1 x_4; x_2 x_1^\dagger) + G_1(x_4; x_4^\dagger)G_2'(x_3 x_1; x_2 x_1^\dagger)$$

$$+G_1(x_4; x_2)G_2'(x_3, x_1; x_1^\dagger x_4) - G_1(x_4; x_1)G_2'(x_3 x_1; x_2 x_4)$$

where

$$G_2' = G_2(x_3, x_1; x_2 x_4) - (G_1(x_3; x_2)G_1(x_1; x_4) - G_1(x_3; x_4)G_1(x_1; x_2))$$

Inserting expressions (9) and (6) for $n = 2$ into expression (7) and using relation (8), we obtain Σ in pair-correlation approximation:

$$\sum(x, x') = i\, U(x, x_1)G_1(x_1; x_1^\dagger) - i\, U(x, x')G_1(x; x')$$

$$+ U(x, x_1)G_1(x; x_1)U(x', x_2)G_2'(x_1 x_2; x_1^\dagger x_2^\dagger) + U(x, x_1)G_1(x, x_2)$$

$$U(x', x_2)G_2'(x_2 x_1; x_1^\dagger x') + U(x, x_1)G_1(x, x_3)U(x_3, x_4)\,[-G_1(x_1; x_4)$$

$$G_2(x_3, x_4; x_2 x_1) - G_1(x_3; x_1)G_2'(x_1 x_4; x_2 x_4^\dagger) + G_1(x_3''; x_4)$$

$$G_2'(x_1, x_4; x_2 x_1^\dagger) + G_1(x_4; x_4^\dagger)G_2'(x_3 x_1; x_2 x_1^\dagger) - G_1(x_4; x_1)$$

$$G_2'(x_3 x_1; x_2 x_4')]\, G_1^{-1}(x_2; x') \qquad (10)$$

The first two terms of expansion (10) correspond to the well-known Hartree-Fock potential, the two next terms are easily interpreted since they contain hole-particle and one-particle Green's functions. For the remaining terms, we shall make a further approximation: in each term there appears a two-particle Green's function containing two equal-time arguments associated with two annihilation operators or with one creation and one annihilation operator. We assume that in our expansion of Σ, we allow only ladder graphs and replace these G_2 by the particle-particle propagator or by the particle-hole propagator designated by G_{II} .

In the ladder approximation, G_2 and G_{II} obey the following simple integral equations [10]:

If t_1, $t_2 < t'_1$, t'_2 or t_1, $t_2 > t'_1$, t'_2:

$$G_2(x_1, x_2; x'_1 x'_2) = G_1(x_1 x'_1)G_1(x_2 x'_2) - G(x_1, x'_2)G(x_2 x'_2)$$

$$+ i \int d^4x_3 d^4x_4 d^4x'_3 d^4x'_4 \, G_1(x_1 x_3)G_1(x_2 x_4)\langle x_3 x_4 | \overline{V} | x'_3 x_4 \rangle$$

$$G_2(x'_3 x'_4; x'_1 x'_2) \tag{11}$$

If t_1, $t'_2 < t_2$, t'_1 or t_1, $t'_2 > t_2$, t'_1:

$$G_{II}(x_1, x_2; x'_1, x'_2) = G_1(x_1; x'_1)G_1(x_2; x'_2) + i \int d^4x_3 d^4x_4$$

$$d^4x'_3 d^4x'_4 G_1(x_1, x_3)G_1(x_4, x'_2) \langle x_3 x'_4 | \overline{V} | x'_3 x_4 \rangle G_{II}(x'_3, x_2; x'_1 x'_4) \tag{12}$$

where $\overline{V}$ is the antisymmetrized operator. Equations (11) and (12) are given in the general case of a non-local potential.

Using Eqs (11) and (12) in formula (10), we get Σ where now the G_2 and G_{II} propagators must be calculated in the ladder approximation:

$$\sum(x, x') = i U(x, x_1)G_1(x_1; x_1^\dagger) - i U(x, x')G_1(x; x')$$

$$+ U(x, x_1)U(x', x_2)[G_1(x; x')G'_{II}(x_1 x_2; x_1^\dagger x_2^\dagger)$$

$$+ G_1(x; x_2)G'_{II}(x_2 x_1; x_1^\dagger x') + G_1(x_1, x_2)G'_{II}(x, x_2; x_1, x')$$

$$- G_1(x_1; x')G'_{II}(x x_2; x_1 x_2) - G_1(x_2 x_1)G_2(x x_1; x' x_2) \tag{13}$$

From expression (13) it is easy to draw the corresponding dia-grammatic expansion of Σ (Fig.1).

In fact, the calculated expression of Σ involves more terms than given in formula (13) — one of them is represented in Fig.2 — but they are already contained in the previous expansion if the single propagators are approximated by Hartree-Fock propagators.

From this expansion of the optical potential, some interesting features can be concluded:

1) since, from each graph including the R.P.A. states, the corresponding unperturbed graph must be subtracted, only collective states will contribute to $\mathcal{V}$;

2) the weak-coupling approximation to nucleon-scattering on nuclei would correspond to graphs a) and b) without subtraction. All other terms are a consequence of our completely antisymmetrized derivation of $\mathcal{V}$;
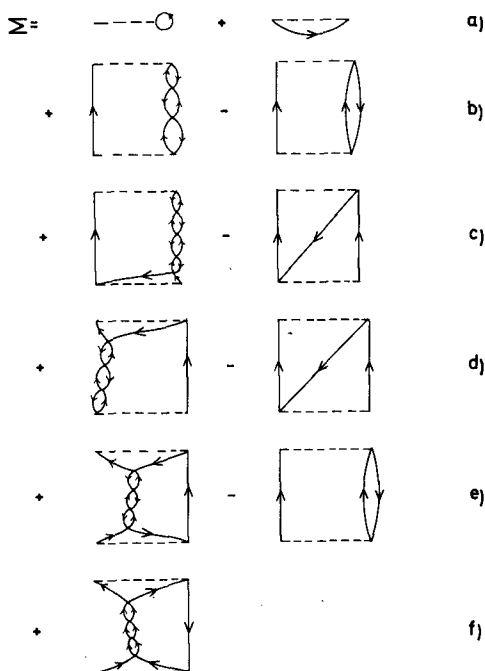
FIG.1.   Diagrammatic expansion of Σ in the ladder approximation.   Arrows in the same direction represent the ladder expansion of the particle-particle generator, arrows in opposite directions that of the hole-particle generator.
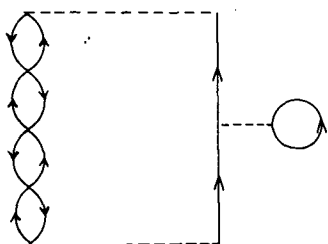
FIG.2.   One type of graph in Σ already contained in Fig. 1b.

3) the optical potential calculated in Refs (4) and (5) corresponds to graphs a), b), c), d), and e) but without subtraction of the unperturbed graphs. Furthermore the graph f) was omitted.

For the calculation of $\mathscr{V}$, we must define the following amplitudes:

$$\chi_{ij}^{(n)} = \langle \psi_n(A) | a_i^\dagger a_j | \psi_0(A) \rangle$$

$$\chi_{k\ell}^{(N)} = \langle \psi_N(A+2) | a_k^\dagger a_\ell^\dagger | \psi_0(A) \rangle \qquad (14)$$

$$x_{k\ell}^{(M)} = \langle \psi_M(A-2) | a_k a_\ell | \psi_0(A) \rangle$$

where i, j are particle-hole or hole-particle states, $k\ell$ are both either particle states, or hole-states. In the ladder approximation, the χ's are eigenstates of the RPA equations, the X and x's are eigenstates of an equivalent system of equations obtained directly from Eq.(11) [11], i.e.:

$$\left(\epsilon_k + \epsilon_\ell - E_N\right) X^{(N)}_{k\ell} + \frac{1}{2} \sum_{mn} \langle k\ell \,|\bar{V}|\, mn \rangle X^{(N)}_{mn} + \frac{1}{2} \sum_{m'n'} \langle k\ell \,|\bar{V}|\, m'n' \rangle X^{(N)}_{m'n'} = 0$$

(15)

$$\left(\epsilon_k + \epsilon_{\ell'} - E_N\right) X^{(N)}_{k'\ell'} - \frac{1}{2} \sum_{mn} \langle k'\ell' \,|\bar{V}|\, mn \rangle X^{(N)}_{mn} - \frac{1}{2} \sum_{m'n'} \langle k'\ell' \,|\bar{V}|\, m'n' \rangle X^{(N)}_{m'n'} = 0$$

in expression (15) k, ℓ are unoccupied states in the Hartree-Fock ground state of the A nucleus and $k'\,\ell'$ are occupied states, and

$$E_N = E_N(A+2) - E_0(A)$$

The x obey the same equations where E_N is replaced by $-E_M = E_0(A) - E_M(A-2)$.

In terms of the amplitudes (14), the optical potential $\mathscr{V}(r, r'; E)$ may be calculated as the Fourier transform of $\Sigma(x, x')$ given by expression (13):

$$\mathscr{V}(\vec{r},\,\vec{r}'\,;E) = V_{H.F.}(\vec{r},\vec{r}') + \sum_{ijk\ell} \left[\sum_{\lambda_{occ}} \left(\sum_n \frac{\chi^{(n)}_{ij}\,\chi^{(n)}_{k\ell}}{E - \epsilon_\lambda + E_n - i\eta} - \frac{n_j(1-n_i)\delta_{ik}\,\delta_{j\ell}}{E - \epsilon_\lambda + \epsilon_i - \epsilon_j - i\eta} \right) \right.$$

$$+ \sum_{\lambda_{unocc}} \left(\sum_n \frac{\chi^{(n)}_{ij}\,\chi^{(n)}_{k\ell}}{E - \epsilon_\lambda - E_n + i\eta} - \frac{n_j(1-n_i)\delta_{ik}\,\delta_{j\ell}}{E - \epsilon_\lambda - \epsilon_i + \epsilon_j + i\eta} \right) \left. \right] \int d^3\vec{r}_1\, \varphi^*_j(\vec{r}_1)V(\vec{r},\vec{r}_1)[1 - \vec{P}]$$

$$\varphi_\lambda(\vec{r})\varphi_i(\vec{r}_1) \int d^3\vec{r}_2\, \varphi^*_\lambda(\vec{r}')\varphi^*_\ell(\vec{r}_2)[1 - \overleftarrow{P}]\, V(\vec{r}',\vec{r}_2)\varphi_\ell(\vec{r}_2) + \sum_{\lambda_{occ}\,N(A+2),\,ijk\ell} \sum$$

$$\frac{X^{(N)}_{ji}X^{(N)}_{\ell k}\varphi^*_k(\vec{r}')\varphi_i(\vec{r})}{E + \epsilon_\lambda - E_N + i\eta} \int d^3\vec{r}_1\, \varphi^*_\lambda(\vec{r}_1)V(\vec{r},\vec{r}_1)\varphi_j(\vec{r}_1) \int d^3\vec{r}_2\, \varphi^*_\ell(\vec{r}_2)V(\vec{r}',\vec{r}_2)\varphi_\lambda(\vec{r}_2)$$

$$+ \sum_{\substack{\lambda_{unocc.}\\M(A-2)\\ijk\ell}} \frac{x^{(M)}_{k\ell}x^{(M)}_{ij}\varphi^*_k(\vec{r}')\varphi_i(\vec{r})}{E + \epsilon_\lambda + E_M - i\eta} \int d^3\vec{r}_1\, \varphi_j(\vec{r}_1)\varphi^*_\lambda(\vec{r}_1)V(\vec{r},\vec{r}_1) \int d^3\vec{r}_2\, \varphi_\lambda(\vec{r}_2)\varphi^*_\ell(\vec{r}_2)V(\vec{r}',\vec{r}_2)$$

(16)

where $\begin{cases} n_j = 1 \text{ if } j \text{ is an occupied state} \\ \quad = 0 \text{ if } j \text{ is an unoccupied state} \end{cases}$

$\overleftarrow{P}$ and $\overrightarrow{P}$ are operators exchanging two particles and acting, respectively, on the left- or the right-hand side.

All the energies are referred to the energy of the ground state of the A-nucleus; then E is just the energy of the incident particle.

For simplicity, we have used a formalism that is independent of spin and isospin but the generalization of expression (16) is straightforward.

Our $\mathscr{V}$ has been obtained in a completely antisymmetrized theory and in the ladder approximation. For a given A-nucleus, $\mathscr{V}$ must be calculated in the following coherent way:

1) a realistic nucleon-nucleon potential, V, must be used all through the calculation;

2) the Hartree-Fock single particle states have to be calculated;

3) from these Hartree-Fock states, the RPA states of the A-system and the states of the (A + 2) - and (A - 2) - systems have to be derived;

4) expression (16) directly yields the corresponding optical potential.

Although this program is well defined and, in principle, straightforward, the primary steps 2) and 3) need quite a long time. We thought it to be interesting to proceed first to a rougher calculation by using given intermediate n, N and M states. This will give us a first idea of what can be learnt from such a derivation of the optical potential. The following simplifications could be considered:

1) the real part of the optical potential is certainly dominated by the Hartree-Fock potential when the energy of the incident particle is not too high, and we consider only the imaginary part of the optical potential;

2) when Im $\mathscr{V}$ is concerned, expression (16) is much simplified since only a limited number of intermediate states will contribute, i.e.:

a) the RPA states with $E_n < E$ for which we use the states quoted in the literature;

b) the lowest states of the (A + 2)- system. This last property allows us to approximate the graph (1.f) by its lowest term, using the harmonic-oscillator states for single particles.

c) none of the states of the (A - 2)- system since E_M is always positive;

3) in formula (16), V will be replaced by a zero-range interaction. Here we lose the coherence of our derivation of $\mathscr{V}$, but to minimize this inconvenient feature, a δ-force can be used with the exchange mixture used in the determination of the RPA states.

4) for positive-energy states of single particles, plane waves will be used.

This preliminary program has been carried out for the scattering of 8, 10, 12 and 14 MeV-nucleons on calcium 40. The detailed results will be published elsewhere. Formula (16) has been transformed to express $\mathscr{V}$ as a function of $\rho = |\vec{r} - \vec{r}'|$, $R = r + r'$ and θ the angle between $\vec{\rho}$ and $\vec{R}$. The part of Im $\mathscr{V}$ which is independent of θ would correspond to the non-local optical potential used by Perey and Buck. The calculated Im $\mathscr{V}$ reproduces the gross features of this phenomenological potential in the sense that, as a function of R, Im $\mathscr{V}$ behaves as a mixture of volume and surface absorption.

This first test of a derivation of $\mathscr{V}$ is encouraging and could be considered as a test of the phenomenological optical potentials. Nevertheless, before going to a more realistic calculation, we intend to go on with our simplifying approximations and look at the validity of the usual assumption about the θ-independence of $\mathscr{V}$—or at the energy dependence of the imaginary potential.

REFERENCES

[1] FERNBACH, S., SERBER, R., TAYLOR, T.B., Phys. Rev. 75 (1949) 1352;
     FESHBACH, H., PORTER, C.E., WEISSKOPF, V.F., Phys. Rev. 90 (1953) 166 and 96 (1954) 448.
[2] BEYSTER, J.R., WALT, M., SALMI, E.W., Phys. Rev. 104 (1956) 1319;
     BJORKLUND, F.E., FERNBACH, S., Phys. Rev. 109 (1958) 1295;
     TAYLOR, T.B., Phys. Rev. 92 (1953) 831; PEREY, F., BUCK, B., Nucl. Phys. 32 (1962) 353.
[3] WATSON, K.M., Phys. Rev. 89 (1958) 575; BRUECKNER, K.A., LOCKETT, A.M., ROTENBERG, M.,
     Phys. Rev. 121 (1961) 255;
     FRAHN, W.E., LEMMER, R.H., Nuovo cim. 5 (1967) 1567;
     FESHBACH, H., Annls Physics 5 (1958) 357; LEMMER, R.H., MARIS, Th.A., TANG, Y.C., Nucl.
     Phys. 12 (1959) 618.
[4] GIAI, N.V., SAWICKI, J., VINH MAU, N., Phys. Rev. 141 (1966) 913.
[5] BRUNEAU, M., VINH MAU, N., Proc. 60th Birthday Prof. R.E. Peierls, Birmingham (1967).
[6] BELL, J.S., SQUIRES, E.J., Phys. Rev. Letts 3 (1959) 96;
     BELL, J.S., Lectures on the Many-Body Problem (CAIANIELLO, E.R., Ed.) Academic Press, New York
     (1962).
[7] BLOCH, C., private communication.
[8] see, for example, KADANOFF, L.P., BAYM, G., Quantum Statistical Mechanics (1962).
[9] MARTIN, P.C., SCHWINGER, J., Phys. Rev. 115 (1959) 1342.
[10] see, for example, NOZIERES, P., Le Problème à N, corps (1963).
[11] These equations in their most general form were derived first by FUKUDA, N., IWAMOTO, F.,
     SAWADA, K., Phys. Rev. 135A (1964) 932;
     RIPKA, G., PADJEN, R., preprint Saclay (1969).

THE SYMMETRY ENERGY OF NUCLEI AND ITS ASTROPHYSICAL APPLICATIONS

J. NÉMETH
Roland-Eötvös-University,
Budapest, Hungary

Abstract

THE SYMMETRY ENERGY OF NUCLEI AND ITS ASTROPHYSICAL APPLICATIONS.
Nuclear-matter concepts and calculations are used to explain the structure and the evolution of neutron stars.

The semi-empirical mass formula of atomic nuclei is a function of the neutron and of the proton number

$$B = -c_1 A + c_2 A^{2/3} + c_3 \frac{(N-Z)^2}{A} - c_4 \frac{(N-Z)^2}{A^{4/3}} + c_5 \frac{Z^2}{A^{1/3}} + \frac{c_6 \delta}{A^{0.55}} \tag{1}$$

where c_1, c_2, c_3, c_4, c_5 and c_6 are constants, and the first term is the volume term, the second term the surface energy, the third term the symmetry energy, the fourth term the surface-symmetry energy, the fifth term the Coulomb energy, and the last term the pairing energy. Minimizing B as a function of Z with a given A, we can determine the most favourable proton-neutron number concentration relation. The Pauli principle favours nuclei with equal proton and neutron numbers, and the effect of the Coulomb energy modifies this relation by reducing the number of protons.

If we want to determine the symmetry energy of very large or infinite systems, we have to use nuclear-matter calculations.

Nuclear-matter calculations consider a system with an equal number of neutrons and protons, neglecting the Coulomb energy and every kind of surface effects. In this way, we obtain the volume energy term in the semi-empirical mass formula. For determining the symmetry energy, we have to consider an infinite system of neutrons and protons, neglect the Coulomb interaction between protons and calculate the energy as a function of the neutron and the proton number. If we assume that $x = (N-Z)/A$ is a small quantity, and expand the energy as a function of x, the term proportional to x^2 is the symmetry energy. If we want to determine the energy of a neutron star, we have to make the opposite approximation, namely that $y = Z/A$ is small.

The Hamiltonian of the system can be written as

$$H = \sum T_i + \tfrac{1}{2} \sum v_{ij} = H_0 + H_1 \tag{2}$$

If H_1 is a small quantity, we can use perturbation theory to determine the energy. The unperturbed wave function is just the antisymmetrized product

of plane-wave single-particle wave functions. In the first-order Born approximation, the energy of the system is

$$W = \sum_i \langle i | T | i \rangle + \tfrac{1}{2} \sum_{ij} [\langle ij | v | ij \rangle - \langle ij | v | ji \rangle] \qquad (3)$$

The $|ij\rangle$ two-particle wave functions have a space-, spin- and isospin-dependent part. The Pauli principle requires that for $T = 0$, $S = 1$ or $T = 1$, $S = 0$ the space part be symmetric, and for $T = 0$, $S = 0$ or $T = 1$, $S = 1$ the space part be antisymmetric. If $N = Z$, the probability of these states is $3/16$, $3/16$, $1/16$ and $9/16$, respectively, so that the energy is given by

$$W_{pot} = \tfrac{1}{2} \sum_{k_i k_j} 16 \, [\langle k_i k_j | v | k_i k_j \rangle - \tfrac{1}{4} \langle k_i k_j | v | k_j k_i \rangle] \qquad (4)$$

where k_i is the wave number of the plane-wave wave functions. Thus, we obtain a momentum-dependent effective interaction

$$W_{pot} = \tfrac{1}{2} \sum_{k_i k_j} \int 16 \, v(r) \, [1 - \tfrac{1}{4} e^{-2i \vec{k} \cdot \vec{r}}] \, d^3 r_1 d^3 r_2 = \tfrac{1}{2} \sum_{k_i k_j} V(k) \qquad (4a)$$

where $\vec{k}_i - \vec{k}_j = 2\vec{k}$.

If the numbers of neutrons and protons are not equal, we have to split up expression (4) into a neutron-neutron, neutron-proton and proton-proton interaction part

$$W_{pot} = \tfrac{1}{2} \sum_0^{k_N} \sum_0^{k_N} V_{NN}(k) + \tfrac{1}{2} \sum_0^{k_P} \sum_0^{k_P} V_{PP}(k) + \sum_0^{k_N} \sum_0^{k_P} V_{NP}(k) \qquad (5)$$

where

$$V_{NN}(k) = \sum_{sm_s} V(sm_s, \; T = 1, \; T_z = 1, \; k) \qquad (6a)$$

$$V_{NP}(k) = \tfrac{1}{2} \sum_{sm_s} [V(sm_s, \; T = 1, \; T_z = 0, \; k) + V(sm_s, \; T = 0, \; T_z = 0, \; k)] \qquad (6b)$$

Let us examine a very simple case, when $V(k)$ is a second-order polynomial of

$$V_{NN} = -a + b \, \frac{k^2}{k_F^2}, \quad V_{PP} = -a + b \frac{k^2}{k_F^2}$$

$$V_{NP} = \tfrac{1}{2} \left[-(a + \alpha) + (\beta + b) \frac{k^2}{k_F^2} \right] \qquad (7)$$

The total potential energy of the nucleus is then

$$W_{pot} = c \left[-\frac{a}{18} (k_N^2 + k_P^2) + \frac{b}{60 k_F^2} (k_N^8 + k_P^8) - \frac{a + \alpha}{18} k_N^3 k_P^3 + \frac{\beta + b}{120 k_F^2} (k_N^2 + k_P^2) k_N^3 k_P^3 \right]$$

$$= c k_F^6 \left[-\frac{(3a + \alpha)}{18} + \frac{(3b + \beta)}{60} \right] + c k_F^6 x^2 \left[-\frac{(a - \alpha)}{18} + \frac{3b - \beta}{54} \right] + c k_F^6 x^4 \frac{\beta}{729} \qquad (8)$$

It is easy to see from Ref.[10] that the effects of ¹S and ³S forces add up in the first term and are subtracted in the symmetry-energy term so that the potential-energy contribution to the symmetry energy is less than to the first-order term, and its sign is positive. The kinetic energy adds a positive term to both orders, so that in the first-order term it has the opposite sign to the potential energy and, the same sign, in the symmetry energy term.

In the case of a pure neutron gas the potential energy of the system will be

$$(W_{pot})_N = -\frac{kc}{18}k_N^6 + \frac{bc}{60k_F^2}k_N^8 = c\left[-\frac{2a}{9} + \frac{2^{2/3}b}{15}\right]k_F^6 \qquad (9)$$

If the even singlet and triplet forces are equal ($\alpha = 3a$, $\beta = 3b$) we obtain the last result, while for nuclear matter

$$(W_{pot})_{NM} = ck_F^6\left[-\frac{3a}{9} + \frac{6}{10}\right] \qquad (10)$$

which in itself is already a·larger negative value than expression (9). Taking into account that $\alpha \gg a$, and that the kinetic energy is higher for a pure neutron gas than for nuclear matter, it is easy to understand why the neutron gas is not bounded.

The above calculations are only valid if the two-body potentials are small and then they can be treated perturbatively. Since we know that for realistic nuclear forces these conditions are not fulfilled, we have to introduce the many-body scattering matrix called G

$$G = v - v\frac{Q}{e}G \qquad (11)$$

where Q is the Pauli operator and e is the difference of particle and hole single-particle energies. In the Brueckner approximation, the energy of a nucleus in first order can be written as

$$W_{pot} = \frac{1}{2}\sum_0^{k_N}\sum_0^{k_N}(k_mk_n|G_{NN}|k_mk_n) + \frac{1}{2}\sum_0^{k_P}\sum_0^{k_P}(k_mk_n|G_{PP}|k_mk_n)$$
$$+ \sum_0^{k_P}\sum_0^{k_N}(k_mk_n|G_{NP}|k_mk_n) \qquad (12)$$

where G_{NN} is the neutron-neutron, G_{PP} the proton-proton and G_{NP} the neutron-proton interaction contribution to the G matrix. We can again express the G matrix elements as a function of the relative momentum. Nuclear-matter calculations give the G elements for $k_N = k_P$, and it is also easy to determine G_{NN} for $Z = 0$ (i.e. for a pure neutron gas). Comparing the matrix elements for these two extreme cases [1, 2] it is easy to see that the approximation of Brueckner and Dąbrowski [3], i.e.

$$G_{NN}(k_Nk_Pk) \sim G_{NN}(k_Nk_Nk) \qquad (13)$$

is justified in the region of nuclear–matter densities. A similar approximation is, of course, valid for the proton–proton interaction. The unlikeparticle–interaction treatment is somewhat less justified, but it seems reasonable to assume that the Brueckner approximation is also valid in this case:

$$G_{NP}(k_N k_P k) \sim G_{NP}(k_A k_A k) \tag{14}$$

where

$$2k_A^2 = k_N^2 + k_P^2 \tag{15}$$

In view of expression (11) it is clear that this approximation is rather good in the case of the energy denominator; the Pauli operator would, however, give somewhat more complex results.

With the approximations (13)–(14) we may expand the G matrix element around its average density value:

$$G_{NN}(k_N k) = G_{NN}(k_F k) + \frac{dG_{NN}}{dk_N}\bigg|_{k_N = k_F}(k_N - k_F) + \frac{1}{2}\frac{d^2 G_{NN}}{dk_N^2}\bigg|_{k_N = k_F}(k_N - k_F)^2 + \ldots \tag{16}$$

and a similar approximation is valid for G_{NP}, G_{PP}. Knowing the G matrix elements as a function of the density, we can determine $G_{NN}(k_N k)$ from expression (16) and in this way the total energy of the nucleus can be written as

$$\frac{W_{pot}}{A} = \epsilon_0 (T = 1) + \epsilon_0 (T = 0) + x^2 [\epsilon_2 (T = 1) + \epsilon_{2R} (T = 1)$$

$$+ \epsilon_2 (T = 0) + \epsilon_{2R} (T = 0)] + O(x^4) \tag{17}$$

where ϵ_R always means the rearrangement contribution arising from the fact that the effective potentials, i.e. the G matrix elements, depend on the density. The $T = 1$ and $T = 0$ terms have the same signs in the zeroth order and opposite signs in the second order. $\epsilon_2 (T = 1)$ and $\epsilon_{2R} (T = 1)$ have opposite signs and the relative importance of $\epsilon_{2R} (T = 1)$ increases rapidly with the density; at nuclear–matter density they are almost the same. The leading term in the symmetry energy is the $\epsilon_2 (T = 0)$ term, and the rearrangement contributions are an order of magnitude smaller altogether, because they are small and $\epsilon_{2R} (T = 1)$ and $\epsilon_{2R} (T = 0)$ have different signs, so they partly cancel each other.

Detailed calculations of Bethe and Németh [4] based on the nuclear-matter calculation of Sprung [1] give a symmetry energy

$$E_{sym} \simeq 18 + 13 \text{ MeV} = 31 \text{ MeV} \tag{18}$$

where the first term comes from the potential and the second from the kinetic energy. Relation (18) is in very good agreement with the results of the semi-empirical mass formula $E_{sym} \sim 30$ MeV ± 1 MeV. The rearrangement contribution to the potential energy is less than 1 MeV, which

shows that it is really almost negligible. Brueckner and Dąbrowski got
a larger contribution for the rearrangement energy, because they used
a Gammel-Thaler potential in their calculations, which overestimates the
$T = 1$ forces, so that the cancellation of the rearrangement terms is not
so far-reaching.

The coefficient of the x^4 term is very small, this shows that the semi-
empirical mass formula is a very good approximation even for extremely
neutron-abundant nuclei.

If we minimize β as a function of the relative proton number, it is
easy to see that the neutron excess is not too large, even in the case of
the heaviest nuclei, $x \sim 0.25$ for $A \sim 250$. Nuclei with larger relative
neutron number are not stable against β-decay, and a pure neutron gas
turns out to be unbounded.

In spite of these stability considerations which are valid for the
elements of our surroundings, astrophysicists firmly believe that there
are some stellar objects which consist mostly of neutrons. This belief
is strictly based on theoretical considerations, and, up to now, is not
supported by entirely conclusive experimental evidence. In the last few
years, every now and then, research workers found stellar objects which
seemed to be neutron stars.

The reason why we believe in the existence of neutron stars can be
understood if we consider the main stages of stellar evolution.

A star is considered to be a gas sphere in hydrodynamical equilibrium.
An equilibrium stage can only be reached if the forces acting on any part
of the system are balanced, and if the radiative energy loss is compensated
for somehow. Pressure and gravitational attraction have to balance one
another, as a result of the first requirement. In ideal-gas approximation,
this means that, since the pressure is proportional to the temperature,
gravitational contraction of the system increases its temperature. The
second requirement means that when the heated gas radiates, this radiative
energy loss has to be compensated for somehow if there is no other source of
energy gain than gravitational contraction.

The largest part of the universe consists even now of hydrogen, so
that, at birth, the galaxies were probably consisting of very rare proton
and electron gas clouds. By gravitational attraction these large bulks
were heated up slowly. Angular-momentum conservation required gravita-
tional contraction to produce pancake shapes, later on, the big bulk broke
up into smaller parts. The stars are born in this way.

When the core temperature of the star reaches 10^7 degrees, building-
up of heavier nuclei starts. The first step is the $4H \rightarrow He$ process, where
four protons go over into a He state. During the hydrogen-burning period,
the radiative energy loss of the star is covered by the nuclear-energy
sources so the temperature does not increase further. However, when
the core's hydrogen supply is exhausted, further gravitational contraction
will occur until the temperature is high enough for heavier elements to
burn. The beginning of a new nuclear reaction process stops gravitational
contraction for a while.

There are two possible ways in which this process of evolution can
be ended. In stars with mass less than 1.5 solar masses the terminating
mechanism is due to the electrons. As the density increases, the electron
gas becomes degenerate because of the Pauli principle. Above a critical
density the pressure can be expressed as

$$p \sim K \, \rho_e^{5/3}$$

so it is no longer sensitive to temperature. The temperature loses its controlling role, and the system will cool down when it radiates, without compensating contraction. These very dense, slowly, cooling objects are called white dwarfs.

If the mass of the star is large enough, it does not become degenerate so easily and owing to the higher temperature – needed to balance the larger weight – every kind of nuclear reaction can take place. These stars finish up with a core consisting mainly of iron nuclei. The very high radiative energy loss can then be compensated for only by gravitational contraction. The outer layers and the core itself will contract very fast, increasing the temperature of the core. In a very short time the iron elements transform by dissociation or fusion into all the elements of the periodical system. This means that the energy loss of the star has already two sources. The energy loss can be compensated for only by gravitational contraction, and, at this stage, the equilibrium state of the star will be overturned. · The enormous energy output of the core reaches the outer layers, either by neutrino processes, or by shock waves or any other kind of mechanism, and somehow explodes the star. The final result of a supernova explosion is always a very dense small star, with a density approximately equal to that of nuclear matter; its mass is about a tenth of its original mass.

If an electron gas is dense enough, an electron–proton pair transforms into a neutron. Increasing the density of the system the protons of the nuclei transform more and more into neutrons and, finally, the neutron-abundant nuclei dissolve into neutrons. If the mass of the residual system is not higher than once or twice the solar mass, the pressure of the neutron gas compensates the gravitational pressure and the star reaches an equilibrium state again. If the original mass of the star was larger than ten times the solar mass, such an equilibrium state cannot occur and according to our present knowledge, the only possibility for the star is further gravitational contraction.

As this short survey of stellar evolution has shown, neutron stars are the final states of stars with 2 – 10 times of solar mass. The question which arises naturally is: how can we observe these neutron stars? Their energy can be stored up initially in thermal, vibrational, rotational or magnetic form. It turns out that the thermal energy content diminishes rapidly, the vibrational energy is probably also dissipated quite fast. The calculations differ according to different nuclear theories, but even the most extreme results yield a very short time. So it seems that direct observation of hot neutron stars is rather hopeless.

In 1962 a new possibility of observation was opened for astrophysics when, for the first time, astronomical observations were performed from rockets. The rockets went above the atmosphere and so were able to observe X-ray radiation. In the last few years, they could identify some of the X-ray sources with optical objects. The two most important objects are the Sco XR 1 and the Crab Nebula. The Crab Nebula is the remnant of a supernova explosion in our galaxy which took place in 1054. It is a very strange cloud, which radiates almost equally in the radio, visible and X-ray domains; all these radiations are polarized. ·This can only be explained if we assume that the radiation is some kind of synchrotron

radiation. The electrons emitting X-ray radiation have to have 10^4 eV
energies. The life-time of electrons against synchrotron X-ray radiation
is very short, less than a year, so that there has to be a pumping mechanism
in the system which supplies these very high-energy electrons continuously.
It was a very natural assumption that the electrons gain their energy in
some fashion from the neutron star, invisibly hidden somewhere in the
middle of the Nebula, which was created in the supernova explosion.

   Melrose and Cameron considered the possibility [5] of Shklovsky's
model [6] being valid in the case of the Crab Nebula, i.e. the neutron star
increases its mass at the expense of a binary companion. It attracts mass
at its surface by its very strong gravitational field, and a high-energy
surface bremsstrahlung is created, which is absorbed by the photosphere
and re-emitted in the X-ray domain. There is an upper limit to the rate
at which material falls on the star's surface because of radiation stress,
and so there is also an upper limit for the resulting luminosity of radiation.
If there is an extra blob of matter falling toward the star, luminosity will
increase, at the same time also the radiative stress will increase, which
will slow down the rate of material falling on the surface until the equi-
librium state is reached again. In this way we can get wisps in luminosity.
The equilibrium maximum luminosity corresponds to 10^{38} erg/sec, which
is the same value of energy as that required for synchrotron radiation of
X-rays. Wisps were also observed in the radiation of the Crab Nebula,
3 - 4 times a year. The radiation of the Crab Nebula might be one of the
indirect ways how a neutron star can become visible. Long ago it dissi-
pated its energy, but its enormous gravitational field makes it possible to
produce some kind of radiation.

   An other interesting phenomenon which can be caused by neutron
stars was observed last year. Astrophysicists observed pulsating radio-
sources, which emit electromagnetic radiation over a wide frequency
range (between 40 and 2700 MHz) with a pulse duration of $\sim$ 50 ms and with
a period $0.25 - 1.34$ s. The surprising features are this very short period,
the very systematic repetition of the period time, and the very irregular
behaviour of the pulse amplitudes. The fact that the sign is so short means
that it has to come from a very massive but small object, because radia-
tion starting from different parts of the object has to reach the observer
within pulse duration. The only known small stellar objects are neutron
stars and white dwarfs. There were different theories concerning the
reason of this radiation such as two neutron stars rotating about one another,
vibrating white dwarfs, rotating neutron stars with magnetic field, etc.
However, it seems that the period of a vibrating white dwarf cannot be
shorter than 1 sec, so, at this moment, the most probable explanation is
the rotating-neutron-star model.

   A possible model for pulsar radiation based on a rotating neutron star
was suggested by Gold [7]. The basic idea is that the emission derives its
energy from the rotational energy of the star, and is the result of rela-
tivistic effects in a co-rotating magnetosphere. In the vicinity of a rotating
star, with a magnetic field, there exists a co-rotating magnetosphere.
This co-rotation ceases at a certain distance at which external influences
begin to dominate. In the case of a fast-rotating neutron star, where the
surface field is strong, the distance at which this co-rotation ceases
may be close to that at which co-rotation would happen almost with velocity
of light. From the surface of the star material this relativistically moving

plasma emits radiation which is flung out into this magnetosphere; it reaches high velocities and is strong enough to overcome the magnetic forces. The period of the pulsation is equal to the rotation period of the star. The pulse length within this period is connected with the geometry of the radiation region. Asymmetries in the radiation could arise because the field or the charged plasma cloud is not axially symmetric.

Gold's theory was supported by some experimental facts discovered in the last half year. If the above picture is correct, one may find a slight but steady slowing down of the repetition frequencies. The shortest period times have to belong to the youngest neutron stars. The shortest period time known up to now is that of the Crab pulsar, which is very likely the youngest of any of the pulsars. Astrophysicists were able to observe a slowing down of the pulse rate too. The rate of slow-down is one part in 2400 per year. These facts furthered the development of the rotating-neutron-star model [8]. The agreement between theory and experimental facts is surprisingly good.

All the above conclusions concerning the possibility of observing neutron stars, as the cooling-down rate of the star, the inertial momenta of a rotating star, the surface radiation of a star with strong gravitational field increasing its energy, etc., depend strongly on the structure and consistency of the star. The cooling-down of a star occurs mainly through ν evaporation, e.g. $e^- + p \rightarrow n + \nu$, $n \rightarrow p + e^- + \bar{\nu}$. These are the so-called URCA processes and their probability depends on the structure of the star. The most important thing is the proportion of the protons in a neutron star. Other interesting questions are the clustering of neutrons and protons, the neutron abundance of nuclei in a star, the superfluidity of the system, etc.

As we have mentioned, if the density of a star increases, also the kinetic energy of the electrons increases. If the energy of an electron at the Fermi surface is ϵ_f, then at a density where the relationship

$$M_e c^2 + \epsilon_f^{(e)} + M_{Z,A} c^2 \gtrless M_{Z-1,A} c^2 \tag{19}$$

holds, the nucleus may capture an electron, and a proton and an electron transform into a neutron. In this way the relative neutron number in the nuclei increases. A further increase of the density dissolves these nuclei; we then get a neutron gas around the nuclei. These neutrons can be absorbed by heavier nuclei in this way creating heavier elements than iron. Increasing the density even more, all the heavier nuclei dissolve and we are confronted with a neutron gas, with a small proton and electron gas admixture. That is probably the stage in which the remnant of a supernova explosion remains and which is called a neutron star.

The exact structure of a neutron star is hard to determine. At the surface, where the density is small, there are neutron-abundant nuclei, but we do not know which ones. In the middle of the star this clustering of nucleons ceases and their density is approximatively constant. The density estimates where this clustering stops are only speculative, it is probably around the $0.5 - 0.75$ nuclear-matter density. Better nuclear-physical calculations are needed to determine it more exactly.

It is relatively easy to determine the proton density in the case of a neutron star without clustering. In a first approximation we may neglect all gravitational and electromagnetic effects, and we can determine the

energy of the system as the sum of nuclear energy and the energy of the relativistic electron gas, and minimize it as a function of relative proton number.

The energy of the relativistic electron gas can be written as

$$W_e = \frac{m_e^4 c^5}{24\pi^2 \hbar^3} [6x^3 \sqrt{x^2+1} + 3x\sqrt{x^2+1} - \text{arc sh}\, x]$$

(20)

where

$$x = (3\pi^2 \rho_e)^{1/3} \frac{\hbar}{m_e c} = (3\pi^2 \rho)^{1/3} \frac{\hbar}{m_e c} \left(\frac{Z}{A}\right)^{1/3}$$

(21)

and we used the fact that the electron density ρ_e is equal to the proton density. If the density of the electron gas is high enough, we have

$$W_e \sim \frac{3}{4} A (3\pi^2 \rho)^{1/3} \left(\frac{Z}{A}\right)^{4/3} \hbar c \sim 4 \times 10^{-11} \rho^{1/3} \left(\frac{Z}{A}\right)^{1/3} Z$$

(22)

The energy of the nucleon system at low densities is just the rest mass of the nucleons and their kinetic energy

$$W_n = M_n c^2 A + (M_p - M_n) c^2 Z + 10^{-24} \rho^{2/3} \frac{(Z^{5/3} + N^{5/3})}{A^{2/3}}$$

(23)

and the last term is negligibly small. Minimizing the total energy

$$W = W_n + W_e$$

(24)

as a function of the proton number we get

$$\frac{W}{A} = -1.2 \frac{Z}{A} + 4 \times 10^{-11} \rho^{1/3} \left(\frac{Z}{A}\right)^{4/3} - 1.2 + 5.3 \times 10^{-11} \rho^{1/3} \left(\frac{Z}{A}\right)^{1/3} = 0$$

(25)

$$\frac{Z}{A} \rho \sim 10^{31} \text{ cm}^{-3}$$

The electron–proton system goes over into a neutron state only when $Z < A/2$, namely when $\rho > (2-3) \times 10^{31}$ cm^{-3}. The relative proton number reaches its minimum around 10^{-3} times nuclear–matter density, so around 10^{35} cm^{-3}. In this case $Z/A \sim 10^{-4}$. At higher densities the above expression for W_n is not valid any more and the number of protons increases again because of nuclear interaction.

There were many calculations performed concerning the determination of the energy of a nucleon system where the number of neutrons is much larger than the number of protons. The simplest calculations used the semi–empirical mass formula, which is, of course, not reliable enough. More precise calculations took into account some effective interactions among nuclei and the best calculations use the nuclear many–body approximations just as in the case of nuclear–matter calculations. From relation (12) we can determine the total energy of a system where $N \gg Z$,

assuming now that $y = Z/A$ is small instead of x. The result can be written as [2]:

$$\frac{W_n}{A} = a_0(\rho) + a_1(\rho)\frac{Z}{A} + a_{5/3}(\rho)\left(\frac{Z}{A}\right)^{5/3} + a_2(\rho)\left(\frac{Z}{A}\right)^2 \qquad (26)$$

where a_0, a_1, $a_{5/3}$, a_2 are given functions of ρ depending on the models used in the calculation. The calculations are meaningful from $0.01\ \rho_{nm}$ up to $2\rho_{nm}$ because at higher densities the effect of repulsive core becomes too important and the nuclear many-body technique is not applicable any more. At nuclear-matter densities a_0 is about $9-13$ MeV, which means that a pure neutron gas is not bounded. The minimizing proton density is for $10^{-2}\ \rho_{nm}$ about 0.4%, for nuclear-matter density about 5-6%, and at twofold nuclear-matter density about 7%; this shows that the effect of nuclear forces and the Pauli principle favouring equal numbers of protons and neutrons partly compensates for the effect of electron gas.

The determination of the relative proton number in case of clustering is a much more difficult problem and needs detailed nuclear-physical calculations. First, the most favoured clustered nuclei have to be determined, and then we have to calculate their energy in a surrounding neutron gas. Unfortunately, the surface-symmetry energy plays a very important role in this case, so we have to deal with different neutron and proton densities and density distributions inside these nuclei.

Another interesting question is the superfluidity of the neutron and proton system inside the star since this phenomenon influences the cooling-down rate. It may be also important for the determination of the moments of inertia of the whole star. The neutron gas is probably not superfluid since its density is about nuclear-matter density, but the question has not yet been answered definitely for the proton gas. Another interesting question is the muon and hyperon creation probability in these stars. Some calculations have been made, but static equilibrium calculations are not enough as the dynamics of the processes has to be examined, too. Rough calculations show that muon creation becomes important at about nuclear-matter density and hyperon creation at about ten times nuclear-matter densities.

REFERENCES

[1] SPRUNG, D.W.L., to be published.

[2] NÉMETH, J., SPRUNG, D.W.L., Phys. Rev. (to be published).

[3] BRUECKNER, K.A., DĄBROWSKI, J., Phys. Rev. 134B (1964) 772.

[4] BETHE, H.A., NÉMETH, J., to be published.

[5] MELROSE, D.B., CAMERON, A.G.W., Can. J. of Physics 46 (1968) 472.

[6] SHKLOWSKY, I.S., Astrophys. J. 148 (1967) 11.

[7] GOLD, T., Nature 218 (1968) 731.

[8] GOLD, T., Nature 221 (1969) 25.

FACULTY AND PARTICIPANTS

DIRECTORS

G. Alaga*   Institute "Rudjer Bošković", Zagreb   Yugoslavia

L. Fonda*   Istituto di Fisica, Trieste   Italy

LECTURERS AND SEMINAR LECTURERS

A. Agodi   Istituto di Fisica   Italy
                             Catania, Italy

R. Arvieu   Institut de Physique Nucléaire   France
                             Orsay, France

M. Beiner   Institut de Physique Nucléaire   Switzerland
                             Orsay, France

K. Bleuler**   Institut für Theoretische Kernphysik   Switzerland
                             Bonn, Federal Republic of Germany

A. Bohr   Niels Bohr Institute   Denmark
                             Copenhagen, Denmark

B. Bosco   Istituto di Fisica   Italy
                             Cagliari, Sardegna, Italy

M. Bouten   Centre d' Etude de l' Energie Nucléaire   Belgium
                             Mol-Donk, Belgium

P. von Brentano   Max-Planck Institute for Physics   Federal Republic
                             Heidelberg, Federal Republic of Germany   of Germany

D.M. Brink   Department of Theoretical Physics   Australia
                             University of Oxford, England

G. Caglioti**   CCR Euratom   Italy
                             Ispra, Varese, Italy

B. Carminati**   Istituto di Fisica   Italy
                             Trieste, Italy

N. Cindro   Institute "Rudjer Boškovic"   Yugoslavia
                             Zagreb, Yugoslavia

---

* Also lectured.
** The contribution of this lecturer is not published in these Proceedings.

R. Coveyou**	IAEA Vienna, Austria	USA
W. Czyz	Institute of Nuclear Physics Cracow 23, Poland	Poland
J. Dąbrowski	Institute for Nuclear Research Warsaw, Poland	Poland
W.E. Frahn	Physics Department University of Cape Town Rondebosch, South Africa	Federal Republic of Germany
M. Gmitro	Nuclear Research Institute Řež, Prague, Czechoslovakia	Czechoslovakia
W. Good**	IAEA Vienna, Austria	USA
M. Jean	Institut de Physique Nucléaire Orsay, France	France
J. Kumar**	Niels Bohr Institute Copenhagen, Denmark	USA
A. Landé**	Niels Bohr Institute Copenhagen, Denmark	USA
K. Lathrop**	Los Alamos Scientific Laboratory New Mexico, USA	USA
C. Mahaux	Institute of Mathematics University of Liège Belgium	Belgium
M.V. Mihailović**	Nuclear Institute "J. Stefan" Ljubljana, Yugoslavia	Yugoslavia
M.K. Pal	Saha Institute of Nuclear Physics Calcutta, India	India
G. Pisent	Istituto di Fisica Padua, Italy	Italy
N. Raisić**	Institute "Boris Kidrič" Belgrade, Yugoslavia	Yugoslavia
M. Rho**	Commissariat à l'Energie Atomique Saclay, France	Korea
R. Ricci**	Istituto di Fisica Padua, Italy	Italy
G.P. Ripka	Commissariat à l'Energie Atomique Saclay, France	France

---

* Also lectured.

** The contribution of this lecturer is not published in these Proceedings.

I. Šlaus	Institute "Rudjer Bošković" Zagreb, Yugoslavia	Yugoslavia
V. Soloviev**	JINR, Dubna Moscow, USSR	USSR
J.M. Soper	Atomic Energy Research Establishment, Harwell, Didcot, Berks., England	UK
B.I. Spinrad**	IAEA Vienna, Austria	USA
V. Strutinsky**	Niels Bohr Institute Copenhagen, Denmark	USSR
J.P. Svenne	Institut de Physique Nucléaire Orsay, France	Canada
Z. Szymański	Institute for Nuclear Research Warsaw, Poland	Poland
I. Talmi	The Weizmann Institute of Science Rehovoth, Israel	Israel
Y. Tchernilin**	IAEA Vienna, Austria	USSR
D. Vautherin	Institut de Physique Nucléaire Orsay, France	France
N. Vinh-Mau (Mrs.)	Institut de Physique Nucléaire Orsay, France	France
P. Vogel	Niels Bohr Institute Copenhagen, Denmark	Czechoslovakia
H. Wolter	University of Münster Federal Republic of Germany	Federal Republic of Germany
R. Żelazny**	Institute for Nuclear Research Swierk, Warsaw, Poland	Poland

EDITOR

A.M. Hamende	International Centre for Theoretical Physics Trieste	Italy

PARTICIPANTS

U. Abbondanno	Istituto di Fisica Trieste, Italy	Italy
F. Accinni	Centro Informazioni Studi Esperienze Milano, Italy	Italy

---

* Also lectured.
** The contribution of this lecturer is not published in these Proceedings.

G. Adam	Technische Hochschule	Austria
	Vienna, Austria	
S. Ahn	Physikalische Abteilung der Technischen Hochschule	Korea
	München, Federal Republic of Germany	
G. Alberi	Istituto di Fisica	Italy
	Trieste, Italy	
R. Alzetta	Istituto di Fisica	Italy
	Trieste, Italy	
M. Asghar	Laboratoire de Physique Nucléaire	Pakistan
	Le Haut Vigneau, 33 Gradignan	
	France	
C. Avilez-Valdez	Instituto de Fisica	Mexico
	Universidad Nacional Autónoma de México	
	Mexico DF, Mexico	
H. Baier	Österr. Studiengesellschaft für Atomenergie	Austria
	Reaktorzentrum Seibersdorf	
	Seibersdorf, Austria	
M. Baldo	Istituto di Fisica	Italy
	Catania, Italy	
M. Behar	Department of Physics	Argentina
	University of Buenos Aires	
	Argentina	
R. Barjon	Institut des Sciences Nucléaires	France
	Grenoble, France	
F. Beonio-Brocchieri	CCR Euratom	Italy
	Ispra, Varese, Italy	
N. Bijedić	Institute "Boris Kidrič"	Yugoslavia
	Belgrade, Yugoslavia	
R.B. Blanco	Philippines Atomic Energy Commission	Philippines
	Manila, Philippines	
S. Boffi	Istituto di Fisica	Italy
	Pavia, Italy	
V. Boffi	Comitato Nazionale per l'Energia Nucleare	Italy
	Bologna, Italy	
M.L. Bogdanović (Miss)	Institute "Boris Kidrič"	Yugoslavia
	Belgrade, Yugoslavia	
D. Bollacasa	Centro Informazioni Studi Esperienze	USA
	Milano, Italy	
G. Bonsignori	Istituto di Fisica	Italy
	Bologna, Italy	

N. Büget (Mrs.)	Middle East Technical University Ankara, Turkey	Turkey
C. Carles	Laboratoire de Physique Nucléaire Le Haut-Vigneau, 33 Gradignan France	France
F. Catara	Istituto di Fisica Catania, Italy	Italy
U. Cattani	Istituto Superiore di Sanità Rome, Italy	Italy
S. Chatraphorn	Office of Atomic Energy Bangkhen, Bangkok Thailand	Thailand
I-T. Cheon	Research Institute for Fundamental Physics Kyoto, Japan	Korea
C. Ciofi degli Atti	Istituto Superiore di Sanità Rome, Italy	Italy
D. Clement	Institute for Theoretical Physics Tübingen, Federal Republic of Germany	Federal Republic of Germany
E. Coffou	Institute "Rudjer Bošković" Zagreb, Yugoslavia	Yugoslavia
M. Copić	Nuclear Institute "J. Stefan" Ljubljana, Yugoslavia	Yugoslavia
M. Cristu	Institute of Atomic Physics Bucharest, Romania	Romania
J. Cugnon	Institute of Physics University of Liège Belgium	Belgium
F. Cvelbar	Nuclear Institute "J. Stefan" Ljubljana, Yugoslavia	Yugoslavia
O.B. Dabbousi	College of Petroleum and Minerals Dhahran, Saudi Arabia	Syrian Arab Republic
D.J. De Frenne	Natuurkundig Laboratorium Gent, Belgium	Belgium
A. De Pinho	Instituto de Fisica Universidade Católica Rio de Janeiro, Brazil	Brazil
M. Dost	Max-Planck Institute for Physics Heidelberg, Federal Republic of Germany	Federal Republic of Germany
L. Drigo	Istituto di Fisica Padua, Italy	Italy

B. Eman	Institute "Rudjer Bošković" Zagreb, Yugoslavia	Yugoslavia
D. Engelhardt	Institut des Sciences Nucléaires Grenoble, France	Federal Republic of Germany
K. Erkelenz	Institut für Theoretische Kernphysik Bonn, Federal Republic of Germany	Federal Republic of Germany
M. Fellah	Institut d'Etudes Nucléaires Algiers, Algeria	Algeria
J.A. Flores	Instituto de Fisica Mexico DF, Mexico	Mexico
A.C. Fubini	Laboratorio FNA CSN Casaccia Rome, Italy	Italy
I. Gabrielli	Istituto di Fisica Trieste, Italy	Italy
G.J. Garcia	Department of Physics University of Buenos Aires, Argentina	Argentina
R. Giacomich	Istituto di Fisica Trieste, Italy	Italy
P. Goldschmidt	Belgonucléaire, Société Belge pour l'Industrie Nucléaire, S.A. 35 Rue des Colonies Brussels, Belgium	Belgium
J. Grabowski	Institute for Theoretical Physics University of Warsaw Poland	Poland
L. Granata	Istituto di Fisica Trieste, Italy	Italy
M. Gravost	Institut des Sciences Nucléaires Grenoble, France	France
A. Grossmann	Centre de Physique Théorique Marseille, France	USA
L. Grünbaum	Institut für Theoretische Kernphysik der Technischen Hochschule Darmstadt Federal Republic of Germany	Federal Republic of Germany
M. Grypeos	Department of Physics University of Surrey Guildford, England	Greece
I. Guiasu (Mrs.)	Institute for Atomic Physics Bucharest, Romania	Romania

V.K. *Gupta*	Department of Physics University of Delhi India	India
P.R. Haensel	Institute for Theoretical Physics Warsaw, Poland	Poland
M.Y.M. Hassan	Physics Department Cairo University United Arab Republic	United Arab Republic
K.L.G. Heyde	Institute for Nuclear Science University of Gent Belgium	Belgium
P.P. Hraskó	Central Research Institute for Physics Budapest, Hungary	Hungary
B. Hrastnik	Institute "Rudjer Bošković" Zagreb, Yugoslavia	Yugoslavia
K. Ilakovac	Institute "Rudjer Bošković" Zagreb, Yugoslavia	Yugoslavia
L. Ixaru	Institute for Atomic Physics Bucharest, Romania	Romania
S. Joffily	Centro Brasileiro de Pesquisas Fisicas Rio de Janeiro, Brazil	Brazil
D. Justin	Nuclear Institute "J. Stefan" Ljubljana, Yugoslavia	Yugoslavia
G. Kernel	Nuclear Institute "J. Stefan" Ljubljana, Yugoslavia	Yugoslavia
H.J. Kreuzer	Institut für Theoretische Kernphysik Bonn, Federal Republic of Germany	Federal Republic of Germany
F. Krmpotić	Facultad de Ciencias Exactas Universidad Nacional de la Plata Argentina	Argentina
H. Kunaish	Physics Department University of Damascus Syrian Arab Republic	Syrian Arab Republic
M. Lagonegro	Istituto di Fisica Trieste, Italy	Italy
A.C. Lejeune	Institute of Physics University of Liège Belgium	Belgium
R. Leonardi	Istituto di Fisica Bologna, Italy	Italy
L. Lesniak	Institute of Nuclear Physics Craców, Poland	Poland

S. Lie	Department of Physics University of Oslo Norway	Norway
E.K. Lin	Institute of Physics National Tsing Hua University Hsinchu, Taiwan Republic of China	China
P.O. Lipas	Research Institute for Theoretical Physics University of Helsinki Finland	Finland
U. Lombardo	Istituto di Fisica Catania, Italy	Italy
V. Lopac	Institute "Rudjer Bošković" Zagreb, Yugoslavia	Yugoslavia
V.C. Lukyanov	JINR, Dubna Moscow, USSR	USSR
D. Ma	Institute of Nuclear Energy Research Atomic Energy Council Lung-Tan, Taiwan Republic of China	China
R. Mach	Nuclear Research Institute Řež, Prague, Czechoslovakia	Czechoslovakia
A.R. Małecki	Institute of Nuclear Physics Craców, Poland	Poland
L.A. Malov	JINR, Dubna Moscow, USSR	USSR
V. Manfredi	Istituto di Fisica Padua, Italy	Italy
N. Mankoč (Miss)	Nuclear Institute "J. Stefan" Ljubljana, Yugoslavia	Yugoslavia
M. Marangoni (Mrs.)	Comitato Nazionale per l'Energia Nucleare Bologna, Italy	Italy
V.S. Mathur	Department of Physics Banaras Hindu University Varanasi, India	India
E. Menapace	Comitato Nazionale per l'Energie Nucleare Bologna, Italy	Italy
M. Michelini	Laboratorio Fisica e Calcolo Reattori CNEN, Casaccia Rome, Italy	Italy
I.N. Mikhailov	JINR, Dubna Moscow, USSR	USSR

G. Moschini	Istituto di Fisica Padua, Italy	Italy
M. Motta	Comitato Nazionale per l'Energia Nucleare Bologna, Italy	Italy
J. Németh-Dörnyei (Mrs.)[*]	Roland Eötvös University Budapest, Hungary	Hungary
P.R. Oliva	Laboratorio FNA CSN Casaccia Rome, Italy	Italy
V. Paar	Institute "Rudjer Bošković" Zagreb, Yugoslavia	Yugoslavia
D. Pal (Mrs.)	Saha Institute of Nuclear Physics Calcutta, India	India
V.R. Pandharipande	Tata Institute of Fundamental Research Bombay, India	India
A. Pascolini	Istituto di Fisica Padua, Italy	Italy
G. Pauli	Istituto di Fisica Trieste, Italy	Italy
M. Pavelescu	Institute for Atomic Physics Bucharest, Romania	Romania
T. Persi	People's University Pula, Yugoslavia	Yugoslavia
Z. Pluhař	Department of Theoretical Physics Faculty of Technical & Nuclear Physics Prague, Czechoslovakia	Czechoslovakia
G. Poiani	Istituto di Fisica Trieste, Italy	Italy
M. Potokar	Nuclear Institute "J. Stefan" Ljubljana, Yugoslavia	Yugoslavia
F. Premuda	Centro di Calcolo del CNEN Bologna, Italy	Italy
P. Quentin	Commissariat à l'Energie Atomique Saclay, France	France
V. Rado	Laboratorio FNA CSN Casaccia Rome, Italy	Italy
J. Ralarosy	Nuclear Research Centre Strasbourg, France	France

[*] Also lectured.

G. Reffo	Centro di Calcolo del CNEN Bologna, Italy	Italy
G. Remy	Nuclear Research Centre Strasbourg, France	France
J. Richert	Nuclear Research Centre Strasbourg, France	France
T.M.H. Rihan	Physics Department Atomic Energy Establishment Cairo, UAR	United Arab Republic
A. Rimini [*]	Istituto di Fisica Trieste, Italy	Italy
M. Rosina	Nuclear Institute "J. Stefan" Ljubljana, Yugoslavia	Yugoslavia
V.K. Samaranayake	Department of Mathematics University of Ceylon Colombo, Ceylon	Ceylon
A. Scalia	Istituto di Fisica Catania, Italy	Italy
D. Schütte	Institut für Theoretische Kernphysik Bonn, Federal Republic of Germany	Federal Republic of Germany
G. Sena	Laboratorio FNA CSN Casaccia Rome, Italy	Italy
W. Senghaphan	Department of Physics Chulalongkorn University Bangkok, Thailand	Thailand
H. Sen Gupta	Physics Department Dacca University Pakistan	Pakistan
M.A.H. Sharaf	Faculty of Science Cairo University Giza, UAR	United Arab Republic
L. Šips	Institute "Rudjer Bošković" Zagreb, Yugoslavia	Yugoslavia
B. Slavov	Faculty of Physics Sofia University Bulgaria	Bulgaria
A. Soenoto	Istituto di Fisica Teorica Naples, Italy	Indonesia
M. Stefanon	Comitato Nazionale per l'Energia Nucleare Bologna, Italy	Italy

[*] Also lectured.

B. Stepančić	Institute "Boris Kidrič" Belgrade, Yugoslavia	Yugoslavia
W. Stepień-Rudzka (Mrs.)	Institute for Theoretical Physics University of Warsaw Poland .	Poland
J. Theobald	Central Bureau for Nuclear Measurements (EURATOM) Geel, Belgium	Federal Republic of Germany
G. Tornielli	Istituto di Fisica Padua, Italy	Italy
T. Trombetti	Centro di Calcolo del CNEN Bologna, Italy	Italy
W-C. Tung (Mrs.)	Institute of Nuclear Energy Research Atomic Energy Council Lung-Tan, Taiwan Republic of China	China
I. Úlehla*	Department of Theoretical Physics Faculty of Mathematics and Physics Prague, Czechoslovakia	Czechoslovakia
J. Vujaklija	Institute "Boris Kidrič" Belgrade, Yugoslavia	Yugoslavia
T. Weber	Istituto di Fisica Trieste, Italy	Italy
C-Y. Wong	Niels Bohr Institute Copenhagen, Denmark	China
C. Yalcin	Middle East Technical University Ankara, Turkey	Turkey
C.T. Yap	Department of Physics University of Singapore Singapore	Singapore
D. Yeboah-Amankwah	Physics Department University of Ghana Accra, Ghana	Ghana
A. Zepeda Dominguez	Department of Physics Centro de Investigación y de Estudios Avanzados Mexico DF, Mexico	Mexico
J. Žofka	Nuclear Research Institute Řež, Prague, Czechoslovakia	Czechoslovakia
L. Zuffi (Mrs.)	Centro di Calcolo del CNEN Bologna, Italy	Italy

---

* Also lectured.

IAEA SALES AGENTS AND BOOKSELLERS

Orders for Agency publications can be placed with your bookseller or any of the addresses listed below:

ARGENTINA
Comisión Nacional de
Energía Atómica
Avenida del Libertador 8250
Buenos Aires

AUSTRALIA
Hunter Publications
23 McKillop Street
Melbourne, C.1

AUSTRIA
Publishing Section
International Atomic Energy Agency
Kärntner Ring 11
P.O. Box 590
A-1011 Vienna

BELGIUM
Office International
de Librairie
30, Avenue Marnix
Brussels 5

CANADA
Queen's Printer for Canada
International Publications
Ottawa, Ontario

C.S.S.R.
S.N.T.L.
Spolena 51
Nové Mesto
Prague 1

DENMARK
Ejnar Munksgaard Ltd.
6 Norregade
DK-1165 Copenhagen K

FRANCE
Office International de
Documentation et Librairie
48, Rue Gay-Lussac
F-75 Paris 5e

HUNGARY
Kultura
Hungarian Trading Company
for Books and Newspapers
P.O. Box 149
Budapest 62

INDIA
Oxford Book & Stationery Comp.
17, Park Street
Calcutta 16

ISRAEL
Heiliger & Co.
3, Nathan Strauss Str.
Jerusalem

ITALY
Agenzia Editoriale Commissionaria
A.E.I.O.U.
Via Meravigli 16
I-20123 Milan

JAPAN
Maruzen Company, Ltd.
P.O. Box 5050,
100-31 Tokyo International

MEXICO
Librería Internacional, S.A.
Av. Sonora 206
México 11, D.F.

NETHERLANDS
Martinus Nijhoff N.V.
Lange Voorhout 9
P.O. Box 269
The Hague

PAKISTAN
Mirza Book Agency
65, Shahrah Quaid-E-Azam
P.O. Box 729
Lahore - 3

POLAND
Ars Polona
Centrala Handlu Zagranicznego
Krakowskie Przedmiescie 7
Warsaw

ROMANIA
Cartimex
3-5 13 Decembrie Street
P.O. Box 134-135
Bucarest

SPAIN
Librería Bosch
Ronda Universidad 11
Barcelona - 7

SWEDEN
C.E. Fritzes Kungl. Hovbokhandel
Fredsgatan 2
Stockholm 16

SWITZERLAND
Librairie Payot
Rue Grenus 6
CH-1211 Geneva 11

U.S.S.R.
Mezhdunarodnaya Kniga
Smolenskaya-Sennaya 32-34
Moscow G-200

U.K.
Her Majesty's Stationery Office
P.O. Box 569
London S.E.1

U.S.A.
UNIPUB, Inc.
P.O. Box 433
New York, N.Y. 10016

YUGOSLAVIA
Jugoslovenska Knjiga
Terazije 27
Belgrade

IAEA Publications can also be purchased retail at the United Nations Bookshop at United Nations Headquarters, New York, from the news-stand at the Agency's Headquarters, Vienna, and at most conferences, symposia and seminars organized by the Agency.

In order to facilitate the distribution of its publications, the Agency is prepared to accept payment in UNESCO coupons or in local currencies.

Orders and inquiries from countries not listed above may be sent to:

Publishing Section
International Atomic Energy Agency
Kärntner Ring 11
P.O. Box 590
A-1011 Vienna, Austria